Flat Dilatometer Testing

Edited by

R. A. Failmezger
In-Situ Soil Testing, L.C., Lancaster, Virginia, USA

J. B. Anderson
University of North Carolina at Charlotte
Charlotte, North Carolina

Cover design: Noelle Brinley

Proceedings from the Second International Conference
on the Flat Dilatometer, Washington, D.C., April 2-5, 2006

BACK

TABLE OF CONTENTS

BACK

PREFACE

The Flat Dilatometer measures the insitu stiffness, strength, and stress history parameters of soil for better site characterization, reducing overall project cost and improving design reliability. It also gives the engineer nearly continuous depth-profiles of these important soil properties. Both researchers and practitioners have complemented the accuracy and breadth of the Dilatometer, now in wide spread use throughout the world.

Dr. Silvano Marchetti invented the Flat Dilatometer in 1975. He performed tests at ten well-documented research sites and developed empirical correlations with classical soil properties. In 1980, he published a classic paper presenting those correlations, many of which are still routinely used today. In 1981, Marchetti traveled to the United States on sabbatical and worked with Drs. John Schmertmann and David Crapps. While they were initially skeptical of Dr. Marchetti's invention, the impressive accuracy of the results won them over.

In 1983, a small group of engineers convened in Edmonton, Canada to present their findings at the "First International Conference on the Flat Dilatometer." In April 2006, over two decades later, we met again to share experiences and new developments in the use, implementation, and application of the DMT to geotechnical engineering.

This book is organized by the conference themes:

- Case studies of projects using dilatometer tests,
- Correlations and comparisons with other lab or insitu tests,
- New testing developments (seismic and other instrumentation),
- Theoretical and numerical evaluations of the DMT, and
- Applications in difficult geomaterials

The editors thank the authors for submitting numerous well-researched technical papers. We thank the following technical committee members for their careful and thorough review of the papers. Their efforts improved the quality of the papers.

J. Anderson, USA	A. Huang, Taiwan	J. Powell, UK
J. Benoit, USA	S. Hossain, USA	J. Reese, USA
P. Bullock, USA	M. Jamiolkowski, Italy	G. Sallfors, Sweden
R. Coutinho, Brazil	P. Lambe, USA	J. Schmertmann, USA
D. Crapps, USA	J. Logar, Slovenia	F. Schnaid, Brazil
N. Cruz, Portugal	D. Marchetti, Italy	W. Steiner, Switzerland
M. Devincenzi, Spain	S. Marchetti, Italy	W. Van Impe, Belgium
M. Fahey, Australia	P. Mayne, USA	A. Viana da Fonseca
R. Failmezger, USA	Z. Mlynarek, Poland	S. Wissa, Egypt
H. Giacheti, Brazil	P. Monaco, Italy	
R. Gupta, USA	A. Penna, Brazil	

R. A. Failmezger, J. B. Anderson
Editors

BACK

BACKGROUND OF THE FLAT DILATOMETER

Origin of the Flat Dilatometer

Marchetti S.
University of L'Aquila, Italy

Keywords: Origin, Flat Dilatometer, DMT, Laterally loaded piles

ABSTRACT: This Note tells the story of the origin of the Flat Dilatometer

1 ORIGIN OF THE FLAT DILATOMETER

I have been requested by the Organizers of this Conference to tell the story of the origin of the Flat Dilatometer.

Regretfully, I have to transfer the blame of having introduced one more in situ device (in the forest of the existing ones) to two dearest persons, Mike Jamiolkoski and my wife, Eleonora.

Mike, in my first months of profession with him, gave me many assignments where the problem of laterally loaded piles was often central (he had even advised me, before, to choose my thesis at Imperial College on this topic, which I did). Soon I realized that, despite some helpful tables by Terzaghi and others, I ended up choosing design moduli essentially based on my mood that day. This made me uncomfortable, because good engineering requires a modulus "unemotional" and linked to measurements.

My wife had the fault of snatching me, in August 1974, from my beloved table covered by papers on piles, dragging me to the Alassio Riviera. On the beach there are, of course, many beach umbrellas oscillating under the breeze. Observing their base, the question came by itself : Would it be possible to conceive a mechanism to force, in the embedded part of the pole, some curvature and measure the reaction that the soil opposes to such deformation?

The rest of the story – seven steps leading from the beach umbrella to the DMT - is described in a 1977 Note (Proc. Spec. Session No. 10 of the 9th ICSMFE in Tokyo). An excerpt of such contribution and the original figures of the steps are reproduced below.

It is singular that for many years after his conceivement, much of the research and use of the DMT was attracted by the evaluation of design parameters (in particular Su, M and OCR). It was only some 15 years later (Robertson et al. 1987, Marchetti et al. 1991) that DMT methods for laterally loded piles were developed. The two methods are still used today and generally predict well the behaviour of laterally loaded piles.

As a conclusion, DMT is a tool that was stimulated by two persons who are not the person telling this story. Moreover DMT is mostly used for purposes other than the original one !

2 EXCERPT FROM SPECIALTY SESSION 10 OF THE TOKYO 1977 9TH ICSMFE: THE EFFECT OF HORIZONTAL LOADS ON PILES

Devices for in situ Determination of Soil Modulus Es – by S. Marchetti, Faculty of Engineering, L'Aquila University.

……different devices were examined (Figs. a to g) :

(a) ***Small diameter short penetration pipe*** : Es can be worked out by the ratio load/deflection. However this system can supply only Es values near ground surface.

(b) ***Small diameter pipe, with an internal jack producing inflection of an embedded pile portion***. The shortcoming is that, if the pipe has to be robust enough to withstand driving forces, almost the totality of the inflecting action is absorbed by the pipe, so obscuring the influence of soil deformability.

(c) ***Pipe of elliptical cross section***: by pumping a fluid into the pipe, measured changes of diameter enable soil deformability evaluation. Same shortcoming as (b). Also corrugated shapes as (d) have the same shortcoming.

BACK

(e,f) The conclusion was that ***two members, having separate tasks***, were necessary: the first one to carry driving forces, the second one to provide an easily expandable element.

(g) ***This "Flat dilatometer" was finally chosen***; the circular shape of the membrane makes easier mechanical construction and test interpretation. In situ tests with (g) closely duplicate (although in different scale) the load sequence induced on soil by driven piles subsequently subjected to lateral loads: to the penetration stage follows the stage in which the points at contact are displaced horizontally, all in the same direction. Correlations between E_S and soil modulus determined by dilatometer should be more direct than other existing correlations.

REFERENCES

Robertson, P.K., Davies, M.P. & Campanella, R.G. (1987). "Design of Laterally Loaded Driven Piles Using the Flat Dilatometer". Geot. Testing Jnl, Vol. 12, No. 1, Mar., 30-38.

Marchetti, S., Totani, G., Calabrese, M. & Monaco, P. (1991). "P-y curves from DMT data for piles driven in clay". Proc. 4th Int. Conf. on Piling and Deep Foundations, DFI, Stresa, Vol. 1, 263-272.

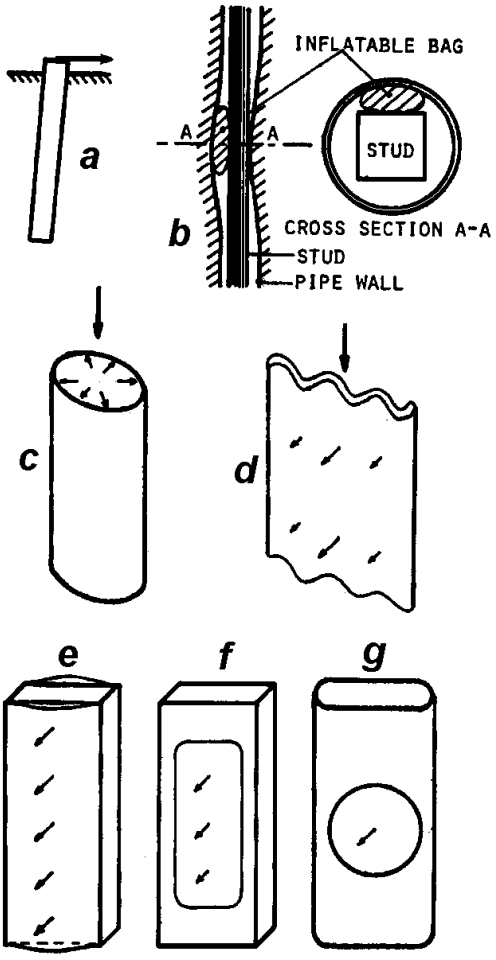

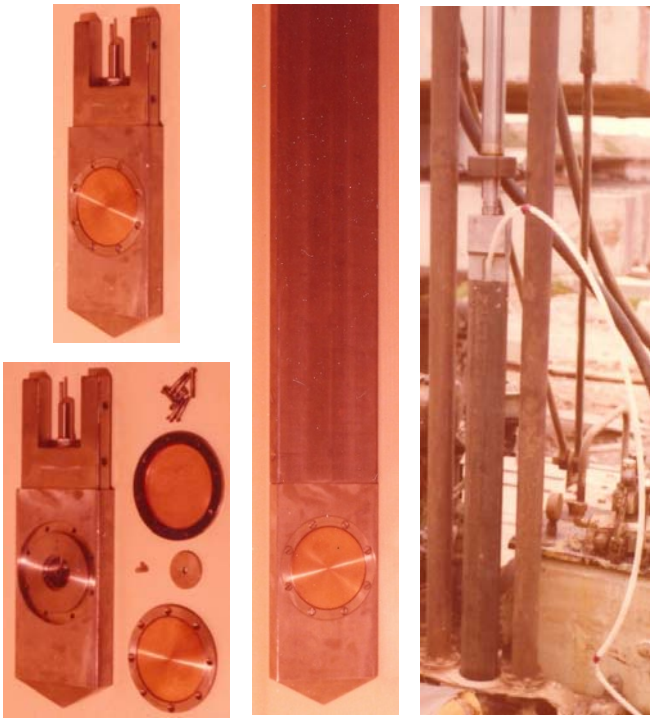

Version 1974 of the blade.

The membranes are made out of copper. The tip has a cuspidal shape. There are two membranes, one on each face. The push rods had initially a rectangular cross section (not easy to mount and to join). The tubings were coaxial, so the exhaust found its way up to the surface through the annular interspace.

Version 1975 of the blade.
The membrane is made out of steel. The push rods are circular.

Current version of the blade.

Brief History of the Flat Plate Dilatometer in North America

David K. Crapps, P.E., Ph.D.
GPE, Inc., Gainesville, Florida

Keywords: dilatometer, history

Abstract: This paper summarizes the development of the flat plate dilatometer in North America.

1. EARLY DEVELOPMENT

The dilatometer and dilatometer test (DMT) were developed in Italy by Dr. Silvano Marchetti. This paper provides a brief history of the dilatometer in North America

Prof. Marchetti fabricated the first dilatometer blade in 1974 at the L'Aquila University in Italy, over 30 years ago. Dr. Marchetti briefly described the dilatometer in 1975 at the ASCE Specialty Conference at Raleigh, North Carolina (see Marchetti (1975)). In 1980 he published a paper in ASCE that is still widely used as a primary reference for the DMT.

2. INTRODUCTION INTO UNITED STATES

Dr. Marchetti corresponded with Dr. John H. Schmertmann (formerly Professor of Geotechnical Engineering at the University of Florida) and encouraged him to include the dilatometer in his research and consulting practice. Preliminary DMT correlations looked promising. However, Dr. Schmertmann remained somewhat skeptical. This soon changed as explained subsequently.

Dr. Schmertmann retired from teaching and joined the author in 1978 to form Schmertmann & Crapps, Inc. to provide geotechnical consulting services. Dr. Marchetti provided equipment to Dr. Schmertmann for evaluation purposes in 1979. The author, assisted by Mr. William Whitehead (then a technician at the University of Florida (UF)), ran the first dilatometer tests in the United States at the University of Florida.

3. FIRST DMT USERS IN NORTH AMERICA

Within a short time after the first UF trial tests, Dr. Schmertmann received a consulting assignment to evaluate the consolidation characteristics of a clay layer beneath proposed cooling towers for a power plant in North Florida. The opinions meant the difference between a contractor bidding the project with a pile foundation or a shallow ring foundation. Dilatometer tests, made in August 1979, showed that the clay layer was overconsolidated, settlement would be within allowable limits and that a shallow foundation would be adequate. The contractor was the successful bidder. Several weeks after bidding the project, the contractor received the results of conventional consolidation tests which confirmed the conclusions made from the dilatometer results. Dr. Schmertmann and the author were both pleased with this first practical application of the dilatometer in the United States. They were enthused then and remain so many years later.

Schmertmann & Crapps, Inc. completed over 1,000 DMT tests during the soils investigation for the Sunshine Skyway Bridge across Tampa Bay, Florida. This was the first use of the DMT on a large project in the United States. The Sunshine Skyway Bridge is a 6.4 km (4 miles) long bridge with a 365.8 m (1,200 feet) main span, then a world record for cable stayed concrete bridges.

Mr. Ron Innis of Mobile Augers and Research, LTD and Mr. Jack Hayes of Site Investigation Services, LTD were the first users of the DMT in Canada. They were also very enthusiastic about the DMT. Mobile Augers and Research, LTD sponsored

BACK

the First International Conference on the Flat Dilatometer in Edmonton, Alberta, Canada on February 4, 1983 (see Mobile Augers and Research (1983). Mr. Hayes presented a paper at the first conference (see Hayes (1983)).

4. EARLY RESEARCH IN NORTH AMERICA

Dr. Marchetti came to the University of Florida in Gainesville, Florida as a Visiting Professor in the Fall of 1980 and remained until early summer of 1981. Dr. Marchetti presented a paper on the dilatometer to the Florida Section of ASCE on September 12, 1980. The first dilatometer research in the United States was at the University of Florida under the direction of Dr. Marchetti. By February 1983, research was also actively underway at Clarkson University (Potsdam, NY) and the University of British Columbia. Purdue University, Louisiana State University, North Carolina State University and Carleton University in Ottawa, Canada followed soon thereafter (see Schmertmann (1983)).

5. PROMOTION OF DMT IN NORTH AMERICA

Dr. John H. Schmertmann headed an S&C research project sponsored by the Federal Highway Administration (FHWA) and the Pennsylvania Department of Transportation (see Schmertmann (1983)) which provided a report used by many as a manual for the DMT and its practical applications. The FHWA later sponsored a project to develop an updated manual for the DMT (see Briaud and Miran (1992). The intent of both these projects was to encourage the use of the DMT in the United States.

GPE, Inc., a sister of company of Schmertmann & Crapps, Inc., worked with Dr. Marchetti to provide an outlet for the dilatometer in North America. The author assisted Dr. Marchetti in preparing the first English version of a manual for the DMT (see Marchetti and Crapps (1981)). GPE, Inc., located in Gainesville, Florida still markets the DMT in North America.

6. US STANDARDS & GROWTH

In 1986 a "Suggested Method for Performing the Flat Dilatometer Test" was published by ASTM (see Schmertmann (1986)). Dr. Paul Bullock (then with Schmertmann & Crapps, Inc. and with the University of Florida at the time of its adoption) worked intently with ASTM Subcommittee 18.02 to establish a standard for the dilatometer. The suggested method was revised and the dilatometer standard (D6635) became official in 2002 (see ASTM (2002).

Growth in the use of the dilatometer in North America has been steady; but, slow when one considers the wealth of information provided by the DMT at a reasonable cost. Dr. Marchetti's web site (see www. marchetti-dmt.it) shows that there are presently about 210 users world-wide with about one-third of them in the North America. Several hundred technical papers have been written about the DMT. Dr. Marchetti's web site also has key references of interest concerning the dilatometer.

REFERENCES

ASTM (2002), Standard Test Method D6635-01, American Society for Testing and Materials, The standard test for performing the Flat Dilatometer Test (DMT), 14 pp.

Briaud, Jean-Louis and Miran, Jerome (1992), "THE FLAT DILATOMETER TEST", Report No. FHWA-SA-91-044, Federal Highway Administration, Office of Technology Applications, Washington, DC (February 1992).

Hayes, John A., "Case Histories Involving the Dilatometer", *Proceedings*, FIRST INTERNATIONAL CONFERENCE ON THE FLAT DILATOMETER, Edmonton, Alberta, Canada, February 4., pages 21-39.

Marchetti, Silvano. (1975), "A NEW IN SITU TEST FOR THE MEASUREMENT OF HORIZONTAL SOIL DEFORMABILITY", Volume II, ASCE, Raleigh, 1975 Specialty Conference on In Situ Measurement of Soil Properties, pp. 255-259, June 1-4.

Marchetti, Silvano. (1980), "In Situ Tests by Flat Dilatometer", GT3, March, p. 299.

Marchetti, S. and Crapps, D. K. (1981), "Flat Dilatometer Manual", internal report of GPE, Inc.,

distributed to purchasers of the DMT equipment.

Mobile Augers and Research, LTD (1983), *Proceedings*, FIRST INTERNATIONAL CONFERENCE ON THE FLAT DILATOMETER, Edmonton, Alberta, Canada, February 4., 134 pages.

Schmertmann, John H. (1983), "THE PAST PRESENT AND FUTURE OF THE FLAT DILATOMETER", *Proceedings*, FIRST INTERNATIONAL CONFERENCE ON THE FLAT DILATOMETER, Edmonton, Alberta, Canada, February 4, pages 13-18.

Schmertmann, John H. (1988), "GUIDELINES FOR USING THE CPT, CPTU AND MARCHETTI DMT FOR GEOTECHNICAL DESIGN", Volume III, "DMT TEST METHODS AND DATA REDUCTION", Report No. FHWA-PA-024+84-24 (183 pp) and Volume IV, "DMT DESIGN METHODS AND EXAMPLES", Report No. FHWA-PA-025+84-24 (135 pp), U.S. Department of Transportation, Federal Highway Administration, Washington, D.C. and PA Dept. of Transportation, Office of Research & Special Studies, Harrisburg, PA, March.

International Society for Soil Mechanics and
Geotechnical Engineering (ISSMGE)

The Flat Dilatometer Test (DMT) in Soil Investigations

Report of the ISSMGE
Technica1 Committee 16
on
Ground Property Characterisation from In-situ Testing

2001

The Flat Dilatometer Test (DMT) in soil investigations
A Report by the ISSMGE Committee TC16

Marchetti S., Monaco P., Totani G. & Calabrese M.
University of L'Aquila, Italy

ABSTRACT: This report presents an overview of the DMT equipment, testing procedure, interpretation and design applications. It is a statement on the general practice of dilatometer testing and is not intended to be a standard.

FOREWORD

This report on the flat dilatometer test is issued under the auspices of the ISSMGE Technical Committee TC16 (Ground Property Characterization from In-Situ Testing).

It was authored by the Geotechnical Group of L'Aquila University (Italy), with additional input from other members of the Committee.

The first outline of this report was discussed at the TC16 meeting in Atlanta – ISC '98 (April 1998).

The first draft was presented and discussed at the TC16 meeting in Amsterdam – 12th ECSMGE (June 1999).

Members of the Committee and other experts were invited to review the draft and provide comments. These comments have been taken into account and incorporated in this report.

AIMS OF THE REPORT

This report describes the use of the flat dilatometer test (DMT) in soil investigations. The main aims of the report are:

- To give a general overview of the DMT and of its design applications
- To provide "state of good practice" guidelines for the proper execution of the DMT
- To highlight a number of significant recent findings and practical developments.

This report is not intended to be (or to originate in the near future) a Standard or a Reference Test Procedure (RTP) on DMT execution.

Efforts have been made to preserve similarities in format with previous reports of the TC16 and other representative publications concerning in situ testing.

The content of this report is heavily influenced by the experience of the authors, who are responsible for the facts and the accuracy of the data presented herein.

Efforts have been made to keep the content of the report as objective as possible.

Occasionally subjective comments, based on the authors experience, have been included when considered potentially helpful to the readers.

SECTIONS OF THIS REPORT

PART A – PROCEDURE AND OPERATIVE ASPECTS

1. BRIEF DESCRIPTION OF THE FLAT DILATOMETER TEST
2. DMT EQUIPMENT COMPONENTS
3. FIELD EQUIPMENT FOR INSERTING THE DMT BLADE
4. MEMBRANE CALIBRATION
5. DMT TESTING PROCEDURE
6. REPORTING OF TEST RESULTS
7. CHECKS FOR QUALITY CONTROL
8. DISSIPATION TESTS

PART B – INTERPRETATION AND APPLICATIONS

9. DATA REDUCTION AND INTERPRETATION
10. INTERMEDIATE DMT PARAMETERS
11. DERIVATION OF GEOTECHNICAL PARAMETERS
12. PRESENTATION OF DMT RESULTS
13. APPLICATION TO ENGINEERING PROBLEMS
14. SPECIAL CONSIDERATIONS
15. CROSS RELATIONS WITH RESULTS FROM OTHER IN SITU TESTS

BACKGROUND AND REFERENCES

BACKGROUND

The flat dilatometer test (DMT) was developed in Italy by Silvano Marchetti. It was initially introduced in North America and Europe in 1980 and is currently used in over 40 countries.

BACK

The DMT equipment, the test method and the original correlations are described by Marchetti (1980) "In Situ Tests by Flat Dilatometer", ASCE Jnl GED, Vol. 106, No. GT3. Subsequently, the DMT has been extensively used and calibrated in soil deposits all over the world.

BASIC DMT REFERENCES / KEY PAPERS

Various international standards and manuals are available for the DMT. An ASTM Suggested Method was published in 1986. A "Standard Test Method for Performing the Flat Plate Dilatometer" is currently being published by ASTM (2001). The test procedure is also standardized in the Eurocode 7 (1997). National standards have also been developed in various countries (e.g. Germany, Sweden). A comprehensive manual on the DMT was prepared for the United States Department of Transportation (US DOT) by Briaud & Miran in 1992. Design applications and new developments are covered in detail in a state of the art report by Marchetti (1997). A list of selected comprehensive DMT references is given here below.

STANDARDS

ASTM D6635-01 (2001). Standard Test Method for Performing the Flat Plate Dilatometer. Book of Standards Vol. 04.09.

Eurocode 7 (1997). Geotechnical design - Part 3: Design assisted by field testing, Section 9: Flat dilatometer test (DMT).

MANUALS

Marchetti, S. & Crapps, D.K. (1981). "Flat Dilatometer Manual". Internal Report of G.P.E. Inc.

Schmertmann, J.H. (1988). Rept. No. FHWA-PA-87-022+84-24 to PennDOT, Office of Research and Special Studies, Harrisburg, PA, in 4 volumes.

US DOT - Briaud, J.L. & Miran, J. (1992). "The Flat Dilatometer Test". Departm. of Transportation - Fed. Highway Administr., Washington, D.C., Publ. No. FHWA-SA-91-044, 102 pp.

STATE OF THE ART REPORTS

Lunne, T., Lacasse, S. & Rad, N.S. (1989). "State of the Art Report on In Situ Testing of Soils". Proc. XII ICSMFE, Rio de Janeiro, Vol. 4.

Lutenegger, A.J. (1988). "Current status of the Marchetti dilatometer test". Special Lecture, Proc. ISOPT-1, Orlando, Vol. 1.

Marchetti, S. (1997). "The Flat Dilatometer: Design Applications". Proc. Third International Geotechnical Engineering Conference, Keynote lecture, Cairo University, 28 pp.

CONFERENCES, SEMINARS, COURSES

Several conferences, seminars and courses have been dedicated to the DMT. The most important are mentioned here below.

- First International Conference on the Flat Dilatometer, Edmonton, Alberta (Canada), Feb. 1983.
- One-day Short Course on the DMT held by S. Marchetti in Atlanta (GA), USA, in connection with the First International Conference on Site Characterization (ISC '98), Apr. 1998.
- International Seminar on "The Flat Dilatometer and its Applications to Geotechnical Design" held by S. Marchetti at the Japanese Geotechnical Society, Tokyo, Feb. 1999.

DMT ON THE INTERNET

Key papers on the DMT can be downloaded from the bibliographic site: http://www.marchetti-dmt.it

PART A

PROCEDURE AND OPERATIVE ASPECTS

1. BRIEF DESCRIPTION OF THE FLAT DILATOMETER TEST

The flat dilatometer is a stainless steel blade having a flat, circular steel membrane mounted flush on one side (Fig. 1).

The blade is connected to a control unit on the ground surface by a pneumatic-electrical tube (transmitting gas pressure and electrical continuity) running through the insertion rods. A gas tank, connected to the control unit by a pneumatic cable, supplies the gas pressure required to expand the membrane. The control unit is equipped with a pressure regulator, pressure gage(s), an audio-visual signal and vent valves.

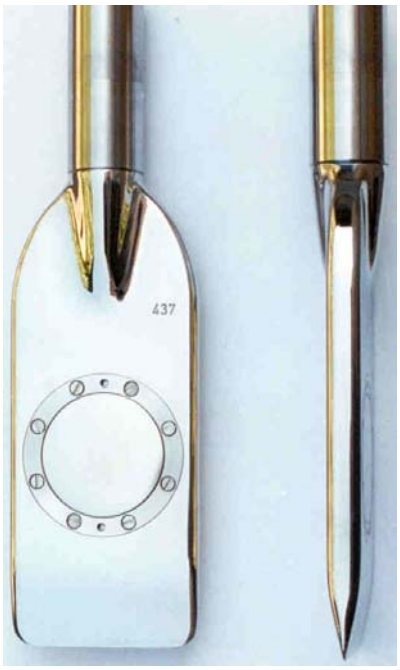

Fig. 1. The flat dilatometer - Front and side view

BACK

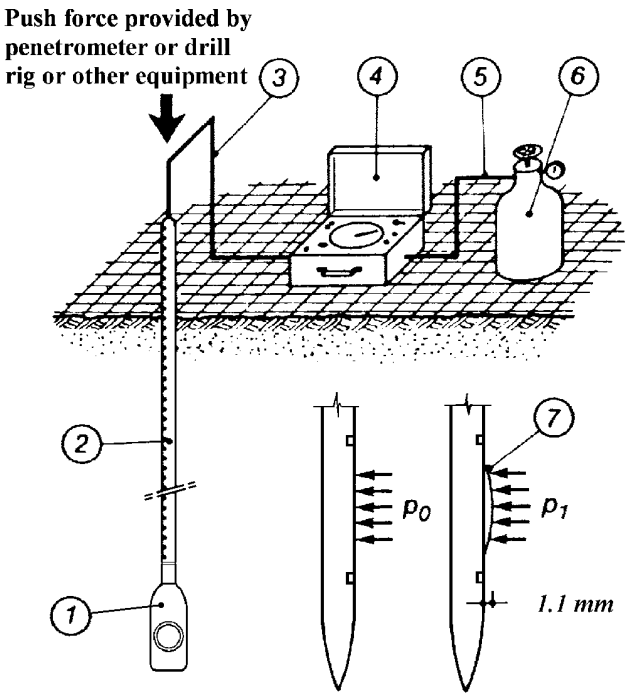

1. Dilatometer blade	4. Control box
2. Push rods (eg.: CPT)	5. Pneumatic cable
3. Pneumatic - electric cable	6. Gas tank
7. Expansion of the membrane	

Fig. 2. General layout of the dilatometer test

The blade is advanced into the ground using common field equipment, i.e. push rigs normally used for the cone penetration test (CPT) or drill rigs. Push rods are used to transfer the thrust from the insertion rig to the blade.

The general layout of the dilatometer test is shown in Fig. 2. The test starts by inserting the dilatometer into the ground. Soon after penetration, by use of the control unit, the operator inflates the membrane and takes, in about 1 minute, two readings:

1) the *A*-pressure, required to just begin to move the membrane against the soil ("lift-off")
2) the *B*-pressure, required to move the center of the membrane 1.1 mm against the soil.

A third reading *C* ("closing pressure") can also optionally be taken by slowly deflating the membrane soon after *B* is reached.

The blade is then advanced into the ground of one depth increment (typically 20 cm) and the procedure for taking *A*, *B* readings is repeated at each depth.

The pressure readings *A*, *B* must then be corrected by the values ΔA, ΔB determined by calibration, to take into account the membrane stiffness, and converted into p_0, p_1.

The *field of application* of the DMT is very wide, ranging from extremely soft soils to hard soils/soft rocks. The DMT is suitable for sands, silts and clays, where the grains are small compared to the membrane diameter (60 mm). It is not suitable for gravels. However the blade is robust enough to cross gravel layers of about 0.5 m thickness.

Due to the balance of zero pressure measurement method (null method), the DMT readings are highly accurate even in extremely soft - nearly liquid soils. On the other hand the blade is very robust (can safely withstand up to 250 kN of pushing force) and, if the thrust provided by the rig is sufficient, can penetrate even soft rocks. Clays can be tested from c_u = 2-4 kPa up to 1000 kPa (marls). The range for moduli *M* is from 0.4 MPa up to 400 MPa.

2. DMT EQUIPMENT COMPONENTS

The basic equipment for dilatometer testing consists of the components shown in Fig. 2.

2.1 DILATOMETER BLADE

2.1.1 Blade and membrane characteristics

The nominal dimensions of the blade are 95 mm width and 15 mm thickness. The blade has a cutting edge to penetrate the soil. The apex angle of the edge is 24° to 32°. The lower tapered section of the tip is 50 mm long. The blade can safely withstand up to 250 kN of pushing thrust.

The circular steel membrane is 60 mm in diameter. Its normal thickness is 0.20 mm (0.25 mm thick membranes are sometimes used in soils which may cut the membrane). The membrane is mounted flush on the blade and kept in place by a retaining ring.

2.1.2 Working principle

The working principle of the DMT is illustrated in Fig. 3 (see also the photo in Fig. 4). The blade works as an electric switch *(on/off)*. The insulating seat prevents electrical contact of the sensing disc with the underlying steel body of the dilatometer. The sensing disc is stationary and is kept in place press-fitted inside the insulating seat. The contact is signaled by an audio/visual signal. The sensing disc is grounded (and the control unit emits a sound) under one of the following circumstances:

1) the membrane rests against the sensing disc (as prior to membrane expansion)
2) the center of the membrane has moved 1.1 mm into the soil (the spring-loaded steel cylinder makes contact with the overlying sensing disc).

There is no electrical contact, hence no signal, at intermediate positions of the membrane.

When the operator starts increasing the internal pressure (Fig. 3), for some time the membrane does not move and remains in contact with its metal

BACK

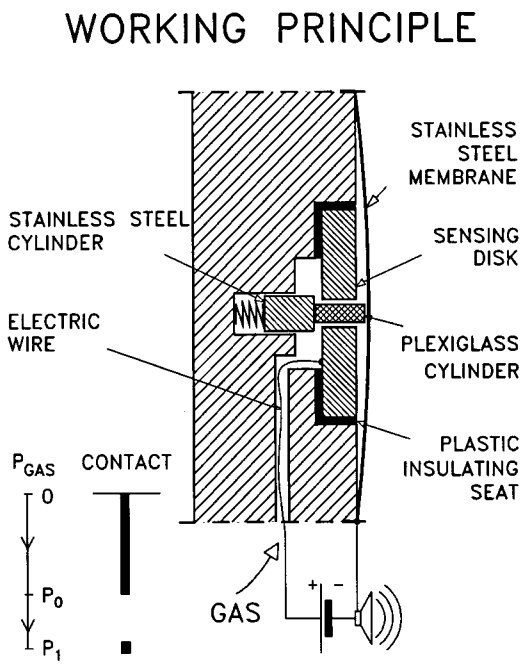

Fig. 3. DMT working principle

Fig. 4. Particular of the DMT blade

support (signal *on*). When the internal pressure counterbalances the external soil pressure, the membrane initiates its movement, losing contact with its support (signal *off*). The interruption of the signal prompts the operator to read the "lift-off" *A*-pressure (later corrected into p_0). The operator, without stopping the flow, continues to inflate the membrane (signal *off*). When the movement of the membrane center reaches 1.1 mm, the spring-loaded steel cylinder touches (and grounds) the bottom of the sensing disc, reactivating the signal. The reactivation of the signal prompts the operator to read the "full expansion" *B*-pressure (later corrected into p_1).

The top of the sensing disc carries a 0.05 mm feeler having the function to improve the definition of the lift-off of the membrane, i.e. the instant at which the electrical circuit is interrupted.

The fixed-displacement system insures that the membrane expansion will be 1.10 mm ± 0.02 mm, since the operator cannot vary or regulate such distance. Only calibrated quartz (once plexiglas) cylinders (height 3.90 ± 0.01 mm) should be used to insure accuracy of the prefixed movement.

NOTE: Remarks on the DMT working principle

– The membrane expansion is not a load controlled test - apply the load and observe settlement - but a displacement controlled test - fix the displacement and measure the required pressure. Thus in all soils the central displacement (and, at least approximately, the strain pattern imposed to the soil) is the same.
– The membrane is not a measuring organ but a passive separator soil-gas. The measuring organ is the gage at ground surface. The accuracy of the measurements is that of the gage. The zero offset of the gage can be checked at any time, being at the surface. A low range pressure gage can be used, e.g. in very soft soils, to increase accuracy to any desired level.
– The method of pressure measurement is the balance of zero (null method), providing high accuracy.
– The blade works as an electric switch *(on/off)*, without electronics or transducers.
– Given the absence of delicate or regulable components, no special skills are required to operate the DMT.

2.2 CONTROL UNIT

2.2.1 Functions and components

The control unit on ground surface is used to measure the *A, B (C)* pressures at each test depth.

The control unit (Fig. 5) typically includes two pressure gages, a pressure source quick connect, a quick connect for the pneumatic-electrical cable, an electrical ground cable connection, a galvanometer and audio buzzer signal (activated by the electric switch constituted by the blade) which prompt when to read the *A, B (C)* pressures, and valves to control gas flow and vent the system.

Fig. 5. Control unit

2.2.2 Pressure gages

The two pressure gages, connected in parallel, have different scale ranges: a low-range gage (1 MPa), self-excluding when the end of scale is reached, and a high-range gage (6 MPa). The two-gage system ensures proper accuracy and, at the same time, sufficient range for various soil types (from very soft to very stiff).

According to Eurocode 7 (1997), the pressures should be measured with a resolution of 10 kPa and a reproducibility of 2.5 kPa, at least for pressures lower than 500 kPa. Gages should have an accuracy of at least 0.5 % of span.

In case of discrepancy between the two gages, replace the malfunctioning gage or correct as appropriate. In case of single-gage (old control units), the gage should be periodically calibrated.

Though the control unit is encased in an aluminium carrying case, it should be handled with care to avoid damaging the gages.

2.2.3 Gas flow control valves

The valves on the control unit panel permit to control the gas flow to the blade.

The *main valve* provides a positive shutoff between the gas source and the control unit-blade system. The *micrometer flow valve* is used to control the rate of flow during the test. It also provides a shutoff between the source and the DMT system (anyway, if the control unit is left unattended for some time, it is advisable to close the *main valve* and to open the *toggle vent valve*). The *toggle vent valve* allows the operator to vent quickly the system pressure to the atmosphere. The *slow vent valve* allows to vent the system slowly for taking the *C*-reading.

2.2.4 Electrical circuit

The electrical circuitry in the control unit has the scope of indicating the *on/off* condition of the blade-switch. It provides both a visual galvanometer and an audio buzzer signal to the operator. The buzzer is *on* when the blade is in the short circuit condition, i.e. membrane collapsed against the blade or fully expanded. The buzzer is *off* when between these two positions. The transitions from buzzer *on* to *off* (at lift-off) and then *off* to *on* (at the end of expansion) are the prompts for the operator to take respectively the *A* and *B* pressure readings.

A 9-Volt battery supplies electrical power to the wire inside the pneumatic-electrical cable. The power is returned at the ground cable jack if the blade is in the short circuit condition.

A test button permits to check the vitality of the battery and the operation of the galvanometer and buzzer. Note that this button simply shorts across the control unit portion of the circuit and hence provides no information about the status of the blade, the pneumatic-electrical cable or the ground cable. If annoyed by the sound during test delays, the operator may disable the buzzer. However, quieting the buzzer involves the risk of missing to switch it on again, then missing the prompts to take the readings and overinflating the membrane.

2.3 PNEUMATIC-ELECTRICAL CABLE

The pneumatic-electrical (p-e) cable provides pneumatic and electrical continuity between the control unit and the dilatometer blade. It consists of a stainless steel wire enclosed within nylon tubing with special metal connectors at either end. Two different cable types are normally used (Fig. 6):

- *Non-extendable cable:* this cable has an insulated male metal connector for the DMT blade on one end, and a non-insulated quick-connect for attachment to the control unit on the other end. The cable length (a working length at the surface should also be accounted for) limits the maximum sounding depth: once the test depth is such that all the cable is inside the soil, the cable cannot be extended and the test must be stopped. This inconvenience is balanced by the simplicity of the cable and its lower cost.
- *Extendable cable:* by using an extendable cable, the operator may connect additional cable(s) as needed during the sounding. The female terminal of such cable (insulated) cannot fit directly into the corresponding quick connector in the control unit. Therefore a *cable leader* (or *short connector cable*) permitting such a connection must be used in conjunction with this cable. This short adaptor is removed when a new cable is added. Though slightly more complex, this type of cable provides the operator with greater flexibility.

The proper type and length of cable should be chosen based on the anticipated sounding depth. For ease of handling and to minimize pressure lag in the entire system, it is recommended to use the shortest length practical.

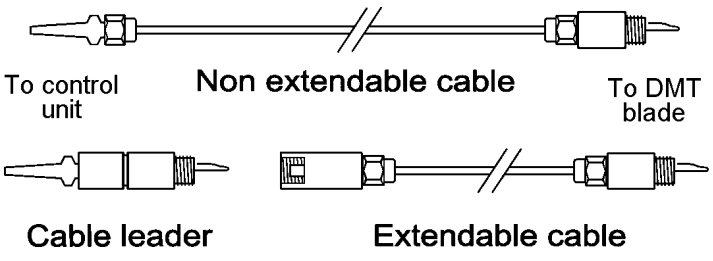

Fig. 6. Types of pneumatic-electrical cables

BACK

Short cables are easier to handle, but require junctions. Junctions normally work well and do not represent a problem as long as care is exercised to avoid particles of soils getting into the conduits.

To keep contaminants out, the terminals and connectors must always be protected with caps when disconnected.

The metal connectors are electrically insulated from the inner wire to prevent a short circuit in the ground and sealed by washers to prevent gas leakage.

The cables and terminals are not easily repairable in the field.

2.4 GAS PRESSURE SOURCE

The pressure source is a gas tank equipped with a pressure regulator, valves and pneumatic tubing to connect to the control unit.

The pressure regulator (suitable to gas type) must be able to supply a regulated output pressure of at least 7-8 MPa.

When testing in most soils the output pressure is set at 3-4 MPa. In very hard soils the output pressure is further increased (without exceeding the high-range gage capacity).

Any non flammable, non corrosive, non toxic gas may be used. Compressed nitrogen or compressed air (scuba tanks) are most generally used.

Gas consumption increases with applied pressure (*A*, *B* readings) and test depth (cable length). In "average" soils a scuba size tank (≈ 0.6 m high), initially at 15 MPa, contains gas to perform approximately 70-100 m of "standard" sounding (≈ one day of testing). In general, it is more economical and efficient to have a large tank (≈ 1.5 m high) when more than one day of testing is anticipated.

2.5 ELECTRICAL GROUND CABLE

The ground cable provides electrical continuity between the push rods and the control unit. It returns to the control unit the simple *on/off* electrical power carried to the blade by the pneumatic-electrical cable.

3. FIELD EQUIPMENT FOR INSERTING THE DMT BLADE

3.1 PUSHING EQUIPMENT

The dilatometer blade is advanced into the ground using common field equipment.

The blade can be pushed with a cone penetrometer rig or with a drill rig (Fig. 7).

The penetration rate is usually 2 cm/s as in the CPT (for DMT rates from 1 to 3 cm/s are acceptable, see Eurocode 7 1997).

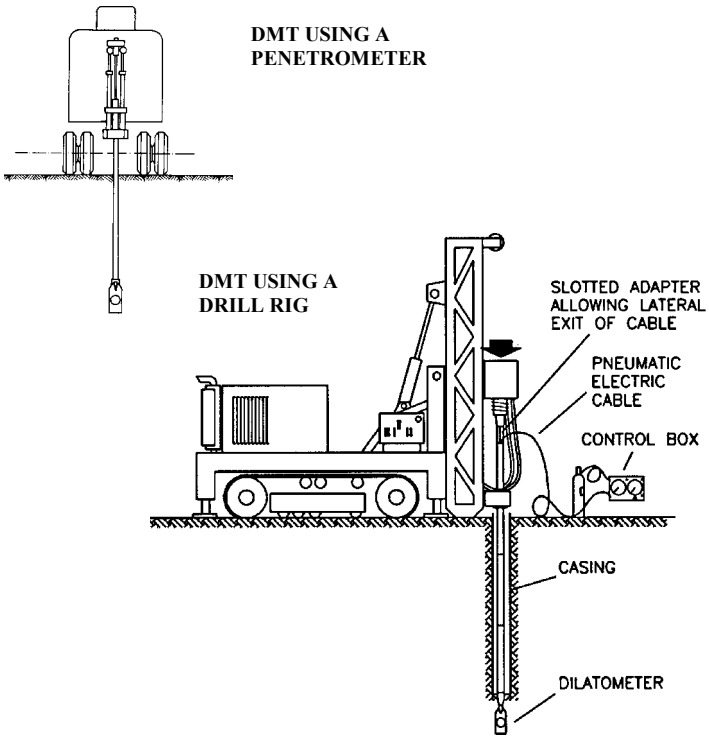

Fig. 7. Equipment for inserting the DMT blade

The DMT can also be driven, e.g. using the SPT hammer and rods, but statical push is by far preferable.

Heavy truck-mounted penetrometers are incomparably more efficient than drill rigs. Moreover the soil provides lateral support to the rods (which is not the case in a borehole). Pushing the blade with a 20 ton penetrometer truck is most effective and yields the highest productivity (up to 80 m of sounding per day).

Drill rigs or light rigs may be used only in soft soils or to very short depths. In all other cases (especially in hard soils) light rigs may be inadequate and source of problems. However drill rigs may be necessary in soils containing occasional boulders or hard layers, where the obstacle-destroying capability will permit to continue the test past the obstacle.

When the DMT sounding is resumed after preboring, the initial test results, obtained in the zone of disturbance at hole bottom (≈ 3 to 5 borehole diameters), should be regarded with caution.

When the DMT is performed inside a borehole, the diameter of the borehole (and casing, if required) should be as small as possible to minimize the risk of buckling (possibly 100-120 mm).

In all cases the penetration must occur in "fresh" (not previously penetrated) soil. The minimum recommended distance from other nearby DMT (or CPT) soundings is 1 m (25 borehole diameters from unbackfilled/uncased borings).

NOTE: Possible problems with light rigs
Possible problems with light rigs (such as many SPT rigs) are:
- Light rigs have typically a pushing capacity of only 2 tons, hence refusal is found very soon (not rarely at 1-2 m depth).
- Often there is no collar near ground surface (i.e. no ground surface side-guidance of the rods).
- Often there is a hinge-type connection in the rods just below the pushing head, which permits excessive freedom and oscillations of the rods inside the hole.
- The distance between the pushing head of the rig and the bottom of the hole is several meters, hence the free/buckling length of the rods is high. In some cases the loaded rods have been observed to assume a "Z" shape.
- Oscillations of the rods may cause wrong results. In case of short penetration in hard layers it was occasionally observed that the "Z" shape of the rods suddenly reverted to the opposite side. This is one of the few cases in which the DMT readings may be instrumentally incorrect: oscillations of the rods cause tilting of the blade, and the membrane is moved without control close to/far from the soil.

NOTE: Pushing vs driving
Various researchers (US DOT 1992, Schmertmann 1988) have observed that "hammer-driving alters the DMT results and decreases the accuracy of correlations", i.e. the insertion method does affect the test results, and static penetration should be preferred.

According to ASTM (1986), in soils sensitive to impact and vibrations, such as very loose sand or very sensitive clays, dynamic insertion methods can significantly change the test results compared to those obtained using a static push. In general, structurally sensitive soils will appear conservatively more compressible when tested using dynamic insertion methods. In such cases the engineer may need to check such dynamic effects and, possibly, calibrate and adjust test interpretation accordingly. US DOT (1992) recommends that, if the driving technique is used, as a minimum 2 soundings be performed side by side, one by pushing and one by driving. This would give a site/soil specific correlation, which would allow to get back to the parameters obtained from correlations based on the pushing insertion (with added imprecision, however).

According to Eurocode 7 (1997), driving should be avoided except when advancing the blade through stiff or strongly cemented layers which cannot be penetrated by static push.

3.2 PUSH RODS

While in principle any kind of rod can be used, most commonly CPT rods or drill rig rods are employed.

A friction reducer is sometimes used. However the consequent reduction in rod friction is moderate, because of the multi-lobate shape of the cavity produced in the penetrated soil by the blade-rod system.

If used, the friction reducer should be located at least 200 mm above the center of the membrane (Eurocode 7 1997).

NOTE: Use of stronger rods
Many heavy penetrometer trucks performing DMT are today also equipped with rods much stronger than the common 36 mm CPT rods. Such stronger rods are typically 44 to 50 mm in diameter, 1 m length, same steel as CPT rods (yield strength > 1000 MPa).

A very suitable and convenient type of rod is the commercially available 44 mm rod used for pushing 15 cm^2 cones.

The stronger rods have been introduced since the rods are "the weakest element in the chain" when working with heavy trucks and the current high strength DMT blades, able to withstand a working load of approximately 250 kN.

The stronger rods have several advantages:
- Capability of penetrating through cemented layers/obstacles.
- Better lateral stability against buckling in the first few meters in soft soils or when the rods are pushed inside an empty borehole.
- Possibility of using completely the push capacity of the truck.
- Reduced risk of deviation from the verticality in deep tests.
- Drastically reduced risk of loosing the rods.

Obvious drawbacks are the initial cost and the heavier weight. Also, their use may not be convenient in OC clay sites because of the increased skin friction.

3.3 ROD ADAPTORS

The DMT blade is connected to the push rods by a *lower adaptor* (Fig. 8).

The most common adaptor has its top connectable to CPT rods, its bottom connectable to the DMT blade (ending cylindrical male M27x3mm).

If rods other than CPT rods are used, specific adaptors need to be prepared (see Fig. 8).

An *upper slotted adaptor* is also needed to allow lateral exit of cable, otherwise pinched by the pushing head.

BACK

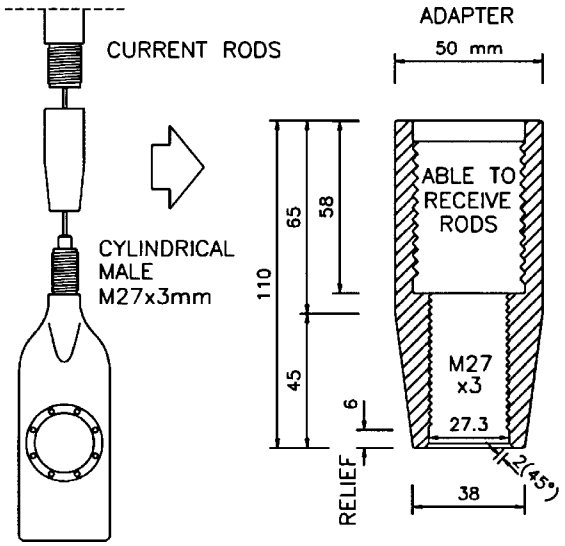

Fig. 8. Lower adaptor connecting the DMT blade to the push rods

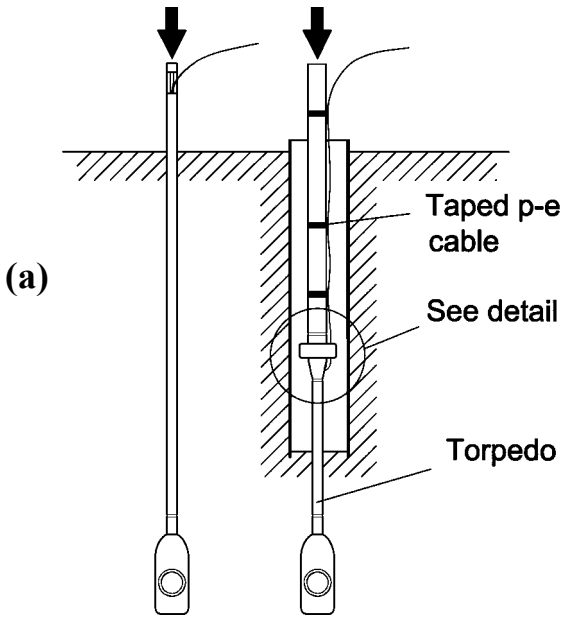

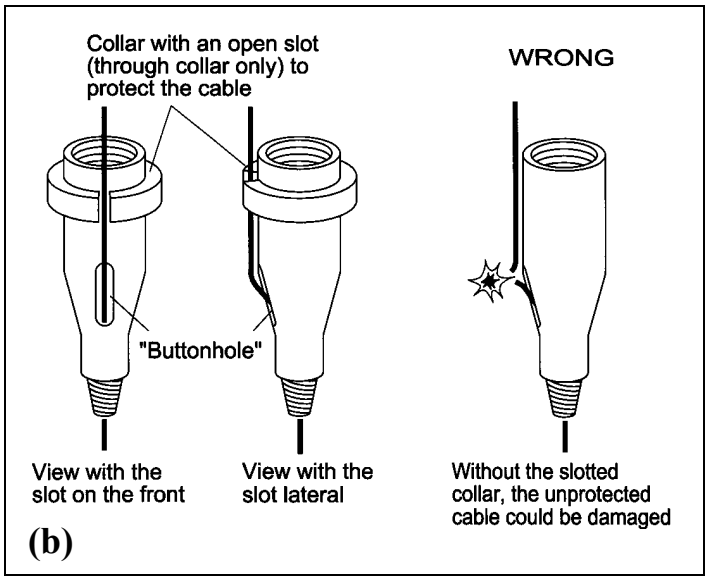

Fig. 9. (a) Possible exits of the cable from the rods (b) Intermediate slotted adaptor joining the upper push rods to the torpedo-like bottom assembly of blade and rods

When using a CPT truck, a DMT sounding normally starts from the ground surface, with the tube running inside the rods (Fig. 9a, left).

When testing starts from the bottom of a borehole, the pneumatic-electrical (p-e) cable can either run all the way up inside the rods, or can exit laterally from the rods at a suitable distance above the blade (Fig. 9a, right). In this case an additional *intermediate slotted adaptor* is needed to permit egress of the cable (Fig. 9a, right). Above this point the cable is taped to the outside of the rods at 1-1.5 m intervals up to the surface.

The torpedo-like bottom assembly in Fig. 9a is composed by the blade, 3 to 5 m (generally) of rods and the *intermediate slotted adaptor*. The "torpedo" is pre-assembled and then mounted at the end of the rods each time. The "torpedo" arrangement speeds production, since it is easier to handle the upper rods, in this case free from the cable.

Since the unprotected cable is vulnerable, the *intermediate slotted adaptor* needs a special collar (Fig. 9b). The collar has a vertical channel for the cable and has a diameter larger than the upper rods so as to insure a free space between the upper rods and the casing. The operator should not allow the slotted adaptor and the exposed cable to penetrate the soil, thus limiting the test depth to the length of rods threaded at the bottom.

4. MEMBRANE CALIBRATION

4.1 DEFINITIONS OF ΔA AND ΔB

The calibration procedure consists in obtaining the ΔA and ΔB pressures necessary to move the membrane to the A and B positions in absence of soil. ΔA and ΔB would be zero if the membrane had an infinitesimal thickness. ΔA and ΔB are then used to correct the A, B readings.

Note that in air, under atmospheric pressure, the free membrane is in an intermediate position between the A and B positions, because the membranes have a slight natural outward curvature (Fig. 10).

ΔA is the external pressure which must be applied to the membrane, in free air, to collapse it against its seating (i.e. A-position). ΔB is the internal pressure which, in free air, lifts the membrane center 1.1 mm from its seating (i.e. B-position).

Various aspects related to the membrane calibration are described in detail by Marchetti (1999) and Marchetti & Crapps (1981).

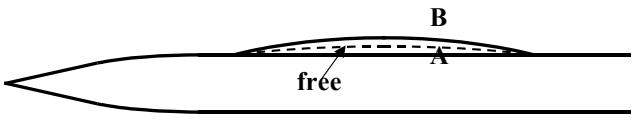

Fig. 10. Positions of the membrane (free, *A* and *B*)

NOTE: Meaning of the term "calibration"
The membrane calibration is not, strictly speaking, a *calibration*, since the term calibration usually refers to the scale of a measuring instrument. The membrane, instead, is a passive separator gas/soil and not a measuring instrument. Actually the membrane is a "tare" and the "calibration" is in reality a "tare determination".

4.2 DETERMINATION OF ΔA AND ΔB

ΔA and ΔB can be measured by a simple procedure using a syringe to generate vacuum or pressure.

During the calibration the high pressure from the bottle should be excluded from the pneumatic circuit by closing the *main valve* on the control unit panel.

To obtain ΔA: quickly pull back (almost fully) the piston of the syringe, in order to apply the maximum vacuum possible (the vacuum causes an inward deflection of the membrane similar to that resulting from the external soil pressure at the start of the test). Hold the piston for sufficient time (at least 5 seconds) for the vacuum to equalize in the system. During this time the buzzer signal should become active. Then slowly release the piston and read ΔA on the low-range gage (gage vacuum reading at which the buzzer stops, i.e. *A*-position). Note this negative pressure as a positive value (e.g. a vacuum of 15 kPa should be reported as ΔA = 15 kPa). The correction formula for p_0 (Eq. 1 in Section 9.2) is already adjusted to take into account that a positive ΔA is a vacuum.

To obtain ΔB: push slowly the piston into the syringe and read ΔB on the low-range gage when the buzzer reactivates (i.e. *B*-position).

Repeat this procedure several times to have a positive check of the values being read.

Membrane corrections ΔA, ΔB should be measured before a sounding, at the end of a sounding, and whenever the blade is removed from the ground.

ΔA, ΔB are usually measured, as a check, in the office before moving to the field. However the initial ΔA, ΔB to be used are those taken just before the sounding (though the difference is generally negligible).

The calibration values of an undamaged membrane remain relatively constant during a DMT sounding. Comparison of before/after values provides a useful indication on the condition of the membrane. E.g. a large difference should prompt a membrane change. Therefore, the calibration procedure is a good indicator of the equipment condition, and consequently of the quality of the data.

4.3 ACCEPTANCE VALUES OF ΔA AND ΔB

Acceptance values of ΔA, ΔB are indicated in Eurocode 7 (1997).

- The initial ΔA, ΔB values must be in the following ranges: ΔA = 5 to 30 kPa, ΔB = 5 to 80 kPa. If the values of ΔA, ΔB obtained before inserting the blade into the soil fall outside the above limits, the membrane shall be replaced before testing.
- The change of ΔA or ΔB between the beginning and the end of the sounding must not exceed 25 kPa, otherwise the test results shall be discarded.

Typical values of ΔA, ΔB are: ΔA = 15 kPa, ΔB = 40 kPa.

ΔA, ΔB values also indicate when it is time to replace a membrane. An old membrane needs not to be replaced as long as ΔA, ΔB are in tolerance.

Indeed an old membrane is preferable, in principle, to a new one, having more stable and lower ΔA, ΔB. However, in case of bad wrinkles, scratches, etc. a membrane should be changed even if ΔA, ΔB are in tolerance (though ΔA, ΔB are not likely to be in tolerance if the membrane is in a really bad shape).

4.4 CONFIGURATIONS DURING THE CALIBRATION

The membrane calibration (determining ΔA, ΔB) can be performed in two configurations.

1) The first configuration (*blade accessible*, Fig. 11) is adopted e.g. at the beginning of a sounding, when the blade is still in the hands of the operator.

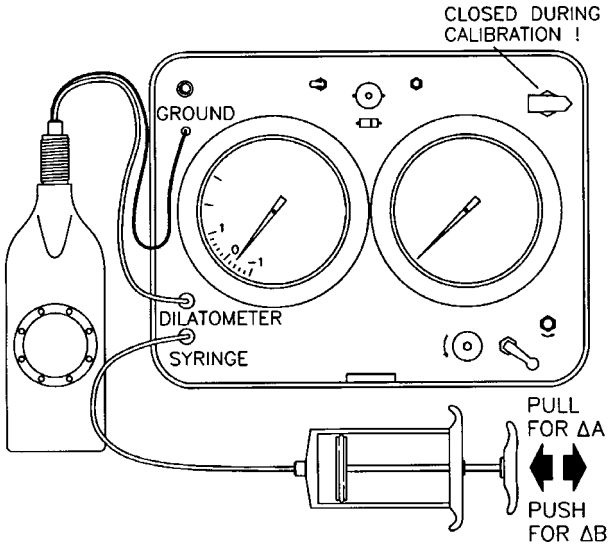

Fig. 11. Layout of the connections during membrane calibration (blade accessible)

BACK

The operator will then use the *short calibration cable*, or the *short calibration connector*.

2) The second configuration (*blade not readily accessible*) is used when the blade is under the penetrometer, and is connected to the control unit as during current testing (Fig. 12) with cables of normal length (say 20 to 30 m).

The calibration procedure is the same. The only difference is that, in the second case, due to the length of the DMT tubings, there is some time lag (easily recognizable by the slow response of the pressure gages to the syringe). Therefore, in that configuration, ΔA, ΔB must be taken slowly (say 15 seconds for each determination).

4.5 Exercising the membrane

The exercising operation is to be performed whenever a new membrane is mounted. A new membrane needs to be "exercised" in order to stabilize ΔA, ΔB values (obtain ΔA, ΔB values which will remain constant during the sounding).

The exercising operation simply consists in pressurizing the blade in free air at about 500 kPa for a few seconds two or three times.

If the membrane exercising is performed with the blade submerged in water, it is possible to verify blade airtightness.

After exercising, verify that ΔA, ΔB are in tolerance: ΔA = 5 to 30 kPa (typically 15 kPa), ΔB = 5 to 80 kPa (typically 40 kPa).

4.6 Importance of accurate ΔA and ΔB

The importance of accurate ΔA, ΔB measurements, especially in soft soils, is pointed out by Marchetti (1999). Inaccurate ΔA, ΔB are virtually the only potential source of DMT instrumental error. Since ΔA, ΔB are used to correct all A, B of a sounding, any inaccuracy in ΔA, ΔB would propagate to all the data.

The importance of ΔA, ΔB in soft soils derives from the fact that, in the extreme case of nearly liquid clays, or liquefiable sands, A and B are small numbers, just a bit higher than ΔA, ΔB. Since the correction involves differences between similar numbers, accurate ΔA, ΔB are necessary in such soils.

ΔA, ΔB must be, as a rule, measured before and after each sounding. Their average is subsequently used to correct all A, B readings. Clearly, if the variation is small, the average represents ΔA, ΔB reasonably well at all depths. If the variation is large, the average may be inadequate at some depths. In fact, in soft soils, the operator can be sure that the test results are acceptable only at the end of the sounding, when, checking ΔA, ΔB final, he finds that they are very similar to ΔA, ΔB initial.

In medium to stiff soils ΔA, ΔB are a small part of A and B, so small inaccuracies in ΔA, ΔB have negligible effect.

NOTE: How ΔA, ΔB can go out of tolerance
In practice the only mechanism by which ΔA, ΔB can go out of tolerance is *overinflating the membrane* far beyond the B-position. Once overinflated, a membrane requires excessive suction to close (ΔA generally > 30 kPa), and even ΔB may be a suction.

5. DMT TESTING PROCEDURE

5.1 Preliminary checks and operations before testing

Select for testing only blades respecting the tolerances (have available at least two). Similarly, use only properly checked pieces of equipment.

Pre-thread the pneumatic-electrical (p-e) cable through a suitable number of push rods and the adaptors. During this operation keep the cable terminals protected from dirt with the caps.

Wrench-tighten the cable terminal to the blade. Connect the blade to the bottom push rod (with interposed the *lower adaptor*). Avoid excessive twists in the cable while making the connections.

Insert the electrical ground cable plug into the "ground" jack of the control unit. Clip the other end (electrical alligator clip) to the *upper slotted adaptor* or to one of the push rods (not to the metal frame of the rig, which may be not in firm electrical contact with the rods).

The connections should be as indicated in Fig. 12 (but do not open the valve of the bottle yet!).

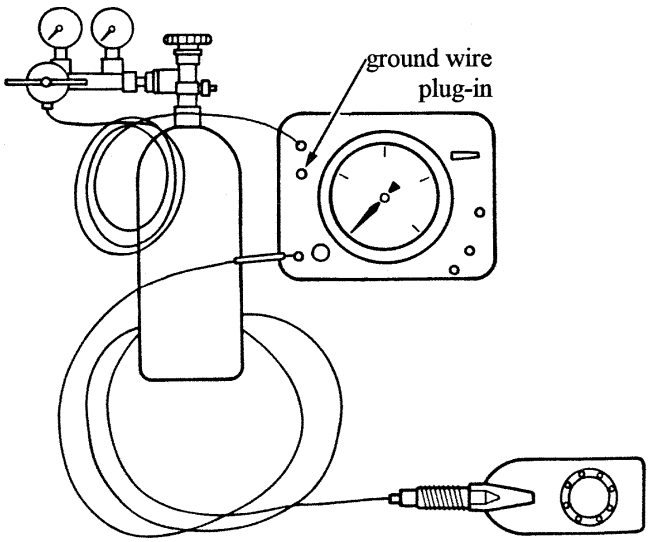

Fig. 12. Layout of the connections during current testing

BACK

Check the electrical continuity and the switch mechanism by pressing the center of the membrane. The signal should activate. If not, make the appropriate repair.

Record the zero of the gage Z_M (reading of the gage for zero pressure) by opening the *toggle vent valve* and read the pressure while tapping gently on the glass of the gage.

Perform the calibration as described in detail in Section 4.

With the gas tank valve closed, connect the pressure regulator to the tank. Set the regulated pressure to zero (fully unscrew the regulating lever).

Connect the pneumatic cable from the gas tank regulator to the control unit female quick connector marked "pressure source".

Make sure that: the *main valve* is closed, the *toggle vent valve* is open and the *micrometer flow valve* is closed.

Open the tank valve. Set the regulator so that the pressure supplied to the control unit is about 3 MPa (this pressure can be later increased if necessary).

Open the *main valve*. (This valve normally remains always open during current testing. During current testing the operator only uses the *micrometer flow valve* and the *vent* valves).

5.2 STEP-BY-STEP TEST PROCEDURE (*A, B, C* READINGS)

The DMT test consists in the following sequence of operations.

1) The DMT operator makes sure that the *micrometer flow valve* is closed and the *toggle vent valve* open, then he gives the go-ahead to the rig operator (the two operators should position themselves in such a way they can exchange control and visual communication easily).
2) The rig operator pushes the blade vertically into the soil down to the selected test depth, either from ground surface or from the bottom of a borehole. During the advancement the signal (galvanometer and buzzer) is normally *on* because the soil pressure closes the membrane. (The signal generally starts at 20 to 40 cm below ground surface).
3) As soon as the test depth is reached, the rig operator releases the thrust on the push rods and gives the go-ahead to the DMT operator.
4) The DMT operator closes the *toggle vent valve* and slowly opens the *micrometer flow valve* to pressurize the membrane. During this time he hears a steady audio signal or buzzer on the control unit. At the instant the signal stops (i.e. when the membrane lifts from its seat and just begins to move laterally), the operator reads the pressure gage and records the first pressure reading *A*.
5) Without stopping the flow, the DMT operator continues to inflate the membrane (during this phase signal is *off*) until the signal reactivates (i.e. membrane movement = 1.1 mm). At this instant the operator reads at the gage the second pressure reading *B*. After mentally noting or otherwise recording this value, he must do the following four operations:
   1 - Immediately open the *toggle vent valve* to depressurize the membrane.
   2 - Close the *micrometer flow valve* to prevent further supply of pressure to the dilatometer (these first two operations prevent further expansion of the membrane, which may permanently deform it and change its calibrations, and must be performed quickly after the *B*-reading, otherwise the membrane may be damaged).
   3 - Give the rig operator the go-ahead to advance one depth increment - generally 20 cm (during penetration the *toggle vent valve* must remain open to avoid pushing the blade with the membrane expanded).
   4 - Write the second reading *B*.

Repeat the above sequence at each depth until the end of the sounding. At the end of the sounding, when the blade is extracted, perform the final calibration.

If the *C*-reading is to be taken, there is only one difference in the above sequence. In Step 5.1, after the *B* reading, open the *slow vent valve* instead of the fast *toggle vent valve* and wait (approximately 1 minute) until the pressure drops approaching the zero of the gage. At the instant the signal *returns* take the *C*-reading. Note that, in sands, the value to be expected for *C* is a low number, usually < 100-200 kPa, i.e. 10 or 20 m of water.

NOTE: Frequent mistake in C-readings
As remarked in DMT Digest Winter 1996 (edited by GPE Inc., Gainesville, Florida), several users have reported poor *C*-readings, mostly due to improper technique. The frequent mistake is the following. After *B*, i.e. when the slow deflation starts, the signal is *on*. After some time the signal stops (from *on* to *off*). The mistake is to take the pressure at this inversion as *C*, which is incorrect (at this time the membrane is the *B*-position). The correct instant for taking *C* is some time later, when, completed the deflation, after say 1 minute, the membrane returns to the "closed" *A*-position, thereby contacting the supporting pedestal and reactivating the signal.

BACK

NOTE: Frequence of C-readings

(a) Sandy sites

In sands ($B \geq 2.5\ A$) *C*-readings may be taken sporadically, say every 1 or 2 m, and are used to evaluate u_0 (equilibrium pore pressure). It is advisable to repeat the *A*-*B*-*C* cycle several times to insure that all cycles provide similar *C*-readings.

(b) Interbedded sands and clays

If the interest is limited to finding the u_0 profile, then *C*-readings are taken in the sandy layers ($B \geq 2.5\ A$), say every 1 or 2 m.

When the interest, besides u_0, is to discern free-draining layers from non free-draining layers, then *C*-readings are taken at each test depth.

NOTE: Electrical connections during testing

The rig operator should never disconnect the ground cable (e.g. to add a rod which requires to remove the electrical alligator) while the DMT operator is taking the readings and anyway not before his go-ahead indication.

NOTE: Expansion rate

Pressures *A* and *B* must be reached slowly.

According to the Eurocode 7 (1997), the rate of gas flow to pressurize the membrane shall be such that the *A*-reading is obtained (typically in 15 seconds) within 20 seconds from reaching the test depth and the *B*-reading (expansion from *A* to *B*) within 20 seconds after the *A*-reading. As a consequence, the rate of pressure increase is very slow in weak soils and faster in stiff soils.

The above time intervals typically apply for cables lengths up to approximately 30 m. For longer cables the flow rate may have to be reduced to allow pressure equalization along the cable.

During the test, the operator may occasionally check the adequacy of the selected flow rate by closing the *micrometer flow valve* and observing how the pressure gage reacts. If the gage pressure drops in excess of 2 % when closing the valve (ASTM 1986), the rate is too fast and must be reduced.

NOTE: Time required for the test

The time delay between end of pushing and start of inflation is generally 1-2 seconds. The complete test sequence (*A*, *B* readings) generally requires about 1 minute. The total time needed for obtaining a "typical" 30 m profile (if no obstructions are found) is about 3 hours. The *C*-reading adds about 45 seconds to 1 minute to the time required for the DMT sequence at each depth.

NOTE: Depth increment

A smaller depth increment (typically 10 cm) can be assumed, even limited to a single portion of the DMT sounding, whenever more detailed soil profiling is required.

NOTE: Test depths

The test depths should be recorded with reference to the center of the membrane.

NOTE: Thrust measurement

Some Authors or existing standards (Schmertmann 1988, ASTM 1986, ASTM 2001) recommend the measurement of the thrust required to advance the blade as a routine part of the DMT testing procedure.

The specific aim of this additional measurement is to obtain q_D (penetration resistance of the blade tip). q_D permits to estimate K_0 and Φ in sand according to the method formulated by Schmertmann (1982, 1983).

Measuring q_D directly is highly impractical. One way of obtaining q_D is to derive it from the thrust force, measurable by a properly calibrated load cell.

The preferable location of such load cell would be immediately above the blade to exclude the rod friction (however the lateral friction on the blade has still to be detracted). Even this cell location is impractical and not presently adopted except for research purposes, so that the load cell, when used, is generally located above the ground surface.

Practical alternative methods for estimating q_D are indicated in ASTM (1986): (a) Measure the thrust at the ground surface and subtract the estimated parasitic rod friction above the blade. (b) Measure both the thrust needed for downward penetration and the pull required for upward withdrawal: the difference gives an estimate of q_D. (c) If values of the cone penetration resistance q_c from adjacent CPT are available, assume $q_D \approx q_c$ (e.g. ASTM 1986, Campanella & Robertson 1991, ASTM 2001).

6. REPORTING OF TEST RESULTS ("FIELD RAW DATA")

A typical DMT field data form is shown in Fig. 13.

Besides the field raw data, the test method should be described, or the reference to a published standard indicated.

7. CHECKS FOR QUALITY CONTROL

7.1 CHECKS ON HARDWARE

7.1.1 Blade

Membrane corrections tolerances

Verify that all blades available at the site are within tolerances (initial ΔA = 5 to 30 kPa, initial ΔB = 5 to 80 kPa).

BACK

Typical: 0.15 0.40

FIRM (max characters no.=32)	BLADE No. ↓	ΔA (bar) 0.05-0.20	ΔB (bar) 0.20-0.80	(1) Δmm	Membrane Aspect (2)
CUSTOMER (32)	Start				
JOB (32)	Z_E= (3)				
SITE (32)	Z_E=				
REMARK (32)	Z_E=				

TEST NAME (12) DATE (20)

Absol. elev.(optional) _____ m Z_{water} (necess.) ____ m or ☐ > Z_{final}

Zero of gauge _____ bar γ_{top} _____ t/m³ (default 1.75)

(1) Coaxiality error (L square)

(2) Elastic, overinflated, wrinkled, snapping, scratched, etc.

(3) Depth reached from extracted blade

☐ Rig ☐ Penetrometer

Diameter of rod behind the blade _____

TEST STOPPED BECAUSE → REFUSAL ☐ MEMBRANE † ☐ Z =$Z_{prefixed}$ ☐

OPERATOR _____

0	A	B	C	6				12				18				24			
2				2				2				2				2			
4				4				4				4				4			
6				6				6				6				6			
8				8				8				8				8			
1				7				13				19				25			
2				2				2				2				2			
4				4				4				4				4			
6				6				6				6				6			
8				8				8				8				8			
2				8				14				20				26			
2				2				2				2				2			
4				4				4				4				4			
6				6				6				6				6			
8				8				8				8				8			
3				9				15				21				27			
2				2				2				2				2			
4				4				4				4				4			
6				6				6				6				6			
8				8				8				8				8			
4				10				16				22				28			
2				2				2				2				2			
4				4				4				4				4			
6				6				6				6				6			
8				8				8				8				8			
5				11				17				23				29			
2				2				2				2				2			
4				4				4				4				4			
6				6				6				6				6			
8				8				8				8				8			

Fig. 13. Typical DMT field data form - (1 bar = 100 kPa)

BACK

Sharpness of electrical signal
Using the syringe (in the calibration configuration) apply 10 or more cycles of vacuum-pressure to verify sharpness of the electrical signal at the *off* and *on* inversions. If the signal inversions are not sharp, the likely reason is dirt between the contacts and the blade must be disassembled and cleaned.

Airtightness
Submerge the blades under water and pressurize them at 0.5 MPa.

Elevations of sensing disc, feeler and quartz (once plexiglas) cylinder
These checks are executed using a special "tripod" dial gage (Fig. 14). The legs of the tripod rest on the surrounding plane and the dial gage permits to measure the elevations above this plane. Their values should fall within the following tolerances:

Sensing disc - Nominal elevation above the surrounding plane: 0.05 mm. Tolerance range: 0.04-0.07 mm.

Feeler - Nominal elevation above the sensing disc: 0.05 mm. Tolerance range: 0.04-0.07 mm.

Quartz cylinder - Only calibrated quartz (once plexiglas) cylinders (height 3.90 ± 0.01 mm) should be used to insure accuracy of the prefixed movement. Therefore checking the elevation of the top of the quartz cylinder is redundant. However such elevation can be checked, and should be in the range 1.13-1.18 mm above the membrane support plane.

Sensing disc extraction force (the sensing disc must be stationary inside the insulating seat)
The disc should fit tightly, thanks to the lateral gripping force, inside the insulating seat. The extraction force should be, as a minimum, equal to the weight of the blade so that, if the sensing disc is lifted, the blade is lifted too without falling.

If the coupling becomes loose (disc free to move) then the gripping force should be increased. One quick fix can be the insertion, while reinstalling the disc, of a small piece of plastic sheet laterally (not on the bottom).

Conditions of the penetration edge of the blade
In case of severe denting of blade's edge, straighten the major undulations, then sharpen the edge using a file.

Coaxiality between blade and axis of the rods
With the *lower adaptor* mounted on the blade, place the inside edge of an L-square against the side of the adaptor. Note the distance from the penetration edge of the blade to the side of the L-square. Turn the blade 180° and repeat the measurement. The difference between the two distances should not exceed 3 mm (corresponding to a coaxiality error of 1.5 mm).

Fig. 14. "Tripod" dial gage

Blade planarity
Place a 15 cm ruler against the face of the blade parallel to its long side. The "sag" between the ruler and blade should not exceed 0.5 mm (to be checked with a flat 0.5 mm feeler gage).

Check the blade for electrical continuity
If the calibration has been carried out without irregularities in the expected electrical signal, the calibration itself already proves that the electrical function of the blade is working properly.

Additional electrical checks can be carried out with the membrane removed (but with the quartz cylinder in its place) using a continuity tester. The open blade should respond electrically as follows:

- Continuity between the metal tubelet located in the blade neck and the sensing disc
- Continuity between the above metal tubelet and the blade body when the quartz cylinder is lifted
- No continuity (insulation) between the metal tubelet and blade body if the quartz cylinder is depressed (continuity in this case would mean that the blade is in short circuit).

A recommended check just before mounting the membrane is the following:

- Press 10 times or more on the quartz cylinder to insure that the *on* and *off* signal inversions are sharp and prompt.

Sensing disc, underlying cavity and elements inside cavity must be perfectly clean
The parts of the instrument inside the membrane (disc, spring, metal cylinder, cylinder housing) must be kept perfectly clean (e.g. blowing each piece with compressed air) to insure proper electrical contacts.

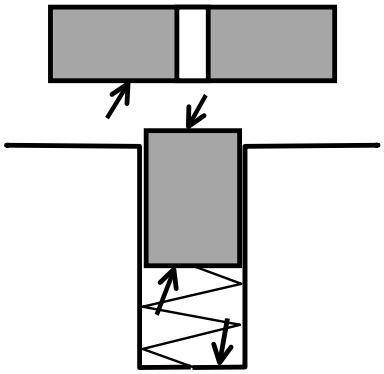

Fig. 15. Electrical contact points to be kept clean to avoid membrane overinflation

A complete guide for disassembling and cleaning the blade can be found in Marchetti & Crapps (1981) and Schmertmann (1988).

In particular, the critical electrical contact points (highlighted in Fig. 15) should be perfectly free from dirt/grains/tissue. If not, the defective electrical contact may cause *severe and costly inconveniences*.

In fact electrical malfunctioning will result in no *B*-signal. In absence of *B*-signal, the operator will keep inflating, eventually overexpanding the membrane beyond ΔA, ΔB tolerances, in which case the test results will be rejected.

The risk of absence of *B*-reading can be reduced by the following check: before starting a sounding, repeat the calibration (ΔA, ΔB) 10 times or more, to make sure that the *B*-signal is regular and sharp.

7.1.2 Control unit

Check the control unit for electrical operation

- Press the test button with the audio switch *on*. The galvanometer and buzzer should activate.
- Connect with an electric wire the inside of the "ground" jack with the female quick connector marked "dilatometer". The galvanometer and buzzer should activate.

Check the control unit for gas leakage

This check is carried out on the control unit alone (cables and blade disconnected). Close the *vent* valves, open the *main valve* and the *micrometer flow valve*. Pressurize the control unit to the maximum gage range. Close the *main valve* to avoid further pressure supply. Observe the gages for leaks.

7.1.3 Pneumatic-electrical cables

Check the cables for mechanical integrity

Inspect the entire length to determine if the tubing is pinched or broken.

Check the cables for electrical operation

Check by a continuity tester both electrical continuity and electrical insulation between the terminals and the inner wire. The male quick connectors should be in contact with the inner wire, while the metal terminals should be insulated from the wire.

Check the cables for gas leakage

Plug with the special female closed-ended terminal the blade terminal of the cable and connect the other end of the cable to the control unit. Use the control unit to pressurize the cable to 4-6 MPa. Then close the *micrometer flow valve*. Observe the gage for any loss in pressure. A leak can be localized by immersing the cable and fittings in water.

7.2 CHECKS ON TEST EXECUTION

- Verify that *A* is reached in ≈ 15 seconds (within 20 seconds), *B* in ≈ 15 seconds (within 20 seconds) after *A*.
- The change of ΔA or ΔB before/after the sounding must not exceed 25 kPa, otherwise the test will be rejected.
- The *C*-reading, when taken, should be obtained in 45 to 60 seconds after starting the deflation following *B*.

NOTE: Accuracy of DMT measurements

The prefixed displacement is the difference between the height of the quartz (once plexiglas) cylinder and the thickness of the sensing disc. These components are machined to 0.01 mm tolerance, and their dimensions cannot be altered by the operator. Likely change in dimensions of such components due to even large temperature variation is much less than 0.01 mm. Hence the displacement will be 1.10 mm ± 0.02 mm.

The pressure measurements are balance of zero measurements (null method), providing high accuracy. The accuracy of the pressure measurements is the accuracy of the gages in the control unit.

Since the accuracy of both measured pressure and displacement is high, the instrumental accuracy of the DMT results is also high, and operator independent. Accuracy problems can only arise when the following two circumstances occur simultaneously: (a) The soil is very soft. (b) The operator has badly overinflated the membrane, making ΔA, ΔB uncertain.

NOTE: Reproducibility of DMT results

The high reproducibility of the test results is a characteristic of the DMT unanimously observed by many investigators.

It has been noted that "peaks" or other discontinuities in the profiles repeat systematically if one performs more than one sounding, therefore they are not due to a random instrumental deviation, but reflect soil variability.

BACK

Even in sand, which is usually considered inherently variable, the DMT has been found to give repeatable profiles.

NOTE: Automatic data acquisition for DMT and "research" dilatometers

While the mechanical DMT is the type most commonly used today, various users have developed automatic data acquisition systems. These systems are outside the scope of this report. Only a few comments are given below.

Automatic data acquisition is not as indispensable as in other in situ tests (e.g. CPT/CPTU), since the DMT generates only a few measurements per minute, that the operator can easily write in the dead time between the operations.

Automatic acquisition does not speed the test or increase productivity or accuracy. Rather, automatic recording is often requested nowadays mostly for *quality control checks*, easier when everything is recorded.

"Research" dilatometers, involving blades instrumented with various types of sensors, are outside the scope of this report. The interested reader is referred to Boghrat (1987), Campanella & Robertson (1991), Fretti et al. (1992), Huang et al. (1991), Kaggwa et al. (1995), Lutenegger & Kabir (1988), Mayne & Martin (1998).

One interesting finding obtained by testing with different instrumented blades is that the pressure-displacement relationship, between A and B, is almost linear.

8. DISSIPATION TESTS

In low permeability soils (clays, silts) the excess pore water pressure induced by the blade penetration dissipates over a period of time much longer than required for the DMT test. In these soils it is possible to estimate the in situ consolidation/flow parameters by means of dissipation tests.

A DMT dissipation test consists in stopping the blade at a given depth, then monitoring the decay of the total contact horizontal stress σ_h with time. The flow parameters are then inferred from the rate of decay.

The DMT dissipation method recommended by the authors is the DMT-A method (Marchetti & Totani 1989, ASTM 2001). Other available methods are the DMT-C method (Robertson et al. 1988) and the DMT-A_2 method (ASTM 2001). The interpretation is covered in Section 11.4.1.

Dissipation tests are generally performed during the execution of a standard DMT sounding, stopping the blade at the desired dissipation depth. After the dissipation is completed, the sounding is resumed following the current test procedure. In this case, the time required for the entire DMT sounding includes the time for the dissipations.

Dissipation tests can be time consuming and are generally performed only when information on flow properties is especially valuable. In very low permeability clays, a dissipation can last 24 hours or more. In more permeable silty layers, the dissipation may last hours, if not minutes.

Dissipation tests can also be performed separated from DMT soundings, by means of one or more blades pushed and left in place at the desired depths. This permits to carry out DMT soundings and dissipations simultaneously, with considerable time saving.

The dissipation depths are decided in advance, based on earlier DMT profiles or other available soil information.

It should be noted that DMT dissipations are not feasible in relatively permeable soils (e.g. silty sands), whose permeability is such that most of the dissipation occurs in the first minute. Hence most of the dissipation curve is missed, because the first reading cannot be taken in less than 10-15 seconds from start. Clearly DMT dissipations are not feasible in sand and gravel.

8.1 DMT-A DISSIPATION METHOD

The DMT-A method (Marchetti & Totani 1989) consists in stopping the blade at a given depth, then taking a timed sequence of A-readings. Note that only the A-reading is taken, avoiding the expansion to B. The operator deflates the membrane by opening the *toggle vent valve* as soon as A is reached (this method is also called "A & deflate" dissipation).

Procedure:

1) Stop the penetration at the desired dissipation depth and immediately start a stopwatch. The time origin ($t = 0$) is the instant at which pushing is stopped. Then, without delay, *slowly* inflate the membrane to take the A-reading. As soon as A is reached, immediately vent the blade. Read at the stopwatch the elapsed time at the instant of the A-reading and record it together with the A-value.
2) Continue to take additional A-readings to obtain reasonably spaced points for the time-dissipation curve. A factor of 2 increase in time at each A-reading is satisfactory (e.g. 0.5, 1, 2, 4, 8, 15, 30 etc. minutes after stopping the blade). For each A-reading record the exact stopwatch time (which has not necessarily to coincide with the above values).

3) Plot in the field a preliminary *A–log t* diagram. Such diagram has usually an S-shape. The dissipation can be stopped when the *A–log t* curve has flattened sufficiently so that the contraflexure point is clearly identified (the time at the contraflexure point t_{flex} is used for the interpretation).

8.2 DMT-A_2 DISSIPATION METHOD

The DMT-A_2 method (described in ASTM 2001) is an evolution of the DMT-C method (Robertson et al. 1988, see also details in Schmertmann 1988 and US DOT 1992).

The DMT-C method consists in performing, at different times, one cycle of readings *A-B-C* and plotting the decay curve of the *C*-readings taken at the end of each cycle.

The DMT-C method relies on the assumption that p_2 (corrected *C*-reading) is approximately equal to the pore pressure u in the soil facing the membrane. Then the method treats the p_2 vs time curve as the decay curve of u (hence p_2 after complete dissipation should be equal to u_o).

The assumption $p_2 = u$ has been found to be generally valid for soft clays, not valid for OC clays. Thus the DMT-C method should be used with caution.

In 1991 (DMT Digest 12) Schmertmann found that a better approximation of the u decay can be obtained in the following way. Perform first one complete cycle *A-B-C* (only one cycle), then take only *A*-readings (called by Schmertmann *"A_2"*) at different times, without performing further *A-B-C* cycles.

The procedure for DMT-A_2 is very similar to the one previously described for the DMT-A dissipation, with the following differences:

1) The readings taken and used to construct the decay curve are the A_2-readings rather than the *A*-readings.
2) The dissipation is stopped after making at least enough measurements to find t_{50} (time at 50 % of *A*-dissipation). If time permits, the test is continued long enough for the dissipation curve to approach its eventual asymptote at 100 % dissipation A_{100}. Ideally $A_{100} = u_0$ when corrected.

PART B

INTERPRETATION AND APPLICATIONS

9. DATA REDUCTION AND INTERPRETATION

9.1 INTERPRETATION IN TERMS OF SOIL PARAMETERS

The primary way of using DMT results is to interpret them in terms of common soil parameters.

The parameters estimated by DMT can be compared and checked vs the parameters obtained by other tests, and design profiles can be selected. This methodology ("design via parameters") is the current practice in engineering applications.

"Direct" DMT-based methods are limited to some specific applications (e.g. axially loaded piles, *P-y* curves for laterally loaded piles).

9.2 DATA REDUCTION / INTERMEDIATE AND COMMON SOIL PARAMETERS

The basic DMT data reduction formulae and correlations are summarized in Table 1.

Field readings *A*, *B* are corrected for membrane stiffness, gage zero offset and feeler pin elevation in order to determine the pressures p_0, p_1 using the following formulae:

$$p_0 = 1.05\ (A - Z_M + \Delta A) - 0.05\ (B - Z_M - \Delta B) \quad (1)$$

$$p_1 = B - Z_M - \Delta B \quad (2)$$

where

ΔA, ΔB = corrections determined by membrane calibration

Z_M = gage zero offset (gage reading when vented to atmospheric pressure) – For a correct choice of Z_M see Note on next page.

The corrected pressures p_0 and p_1 are subsequently used in place of *A* and *B* in the interpretation.

The original correlations (Marchetti 1980) were obtained by calibrating DMT results versus high quality parameters obtained by traditional methods. Many of these correlations form the basis of today interpretation, having been generally confirmed by subsequent research.

The interpretation evolved by first identifying three "intermediate" DMT parameters (Marchetti 1980):

– the material index I_D
– the horizontal stress index K_D
– the dilatometer modulus E_D

then relating these intermediate parameters (not directly p_0 and p_1) to common soil parameters.

BACK

SYMBOL	DESCRIPTION	BASIC DMT REDUCTION FORMULAE	
p_0	Corrected First Reading	$p_0 = 1.05\ (A - Z_M + \Delta A) - 0.05\ (B - Z_M - \Delta B)$	Z_M = Gage reading when vented to atm. If ΔA & ΔB are measured with the same gage used for current readings A & B, set $Z_M = 0$ (Z_M is compensated)
p_1	Corrected Second Reading	$p_1 = B - Z_M - \Delta B$	
I_D	Material Index	$I_D = (p_1 - p_0) / (p_0 - u_0)$	u_0 = pre-insertion pore pressure
K_D	Horizontal Stress Index	$K_D = (p_0 - u_0) / \sigma'_{v0}$	σ'_{v0} = pre-insertion overburden stress
E_D	Dilatometer Modulus	$E_D = 34.7\ (p_1 - p_0)$	E_D is NOT a Young's modulus E. E_D should be used only AFTER combining it with K_D (Stress History). First obtain $M_{DMT} = R_M E_D$, then e.g. $E \approx 0.8\ M_{DMT}$
K_0	Coeff. Earth Pressure in Situ	$K_{0,DMT} = (K_D / 1.5)^{0.47} - 0.6$	for $I_D < 1.2$
OCR	Overconsolidation Ratio	$OCR_{DMT} = (0.5\ K_D)^{1.56}$	for $I_D < 1.2$
c_u	Undrained Shear Strength	$c_{u,DMT} = 0.22\ \sigma'_{v0}\ (0.5\ K_D)^{1.25}$	for $I_D < 1.2$
Φ	Friction Angle	$\Phi_{safe,DMT} = 28° + 14.6°\ \log K_D - 2.1°\ \log^2 K_D$	for $I_D > 1.8$
c_h	Coefficient of Consolidation	$c_{h,DMTA} \approx 7\ cm^2 / t_{flex}$	t_{flex} from A-log t DMT-A decay curve
k_h	Coefficient of Permeability	$k_h = c_h\ \gamma_w / M_h$ ($M_h \approx K_0\ M_{DMT}$)	
γ	Unit Weight and Description	(see chart in Fig. 16)	
M	Vertical Drained Constrained Modulus	$M_{DMT} = R_M E_D$ if $I_D \le 0.6$ $R_M = 0.14 + 2.36 \log K_D$ if $I_D \ge 3$ $R_M = 0.5 + 2 \log K_D$ if $0.6 < I_D < 3$ $R_M = R_{M,0} + (2.5 - R_{M,0}) \log K_D$ with $R_{M,0} = 0.14 + 0.15\ (I_D - 0.6)$ if $K_D > 10$ $R_M = 0.32 + 2.18 \log K_D$ if $R_M < 0.85$ set $R_M = 0.85$	
u_0	Equilibrium Pore Pressure	$u_0 = p_2 = C - Z_M + \Delta A$	In free-draining soils

Table 1. Basic DMT reduction formulae

The intermediate parameters I_D, K_D, E_D are "objective" parameters, calculated from p_0 and p_1 using the formulae shown in Table 1.

The interpreted (final) parameters are common soil parameters, derived from the intermediate parameters I_D, K_D, E_D using the correlations shown in Table 1 (or other established correlations).

The values of the in situ equilibrium pore pressure u_0 and of the vertical effective stress σ'_{v0} prior to blade insertion must also be introduced into the formulae and have to be known, at least approximately.

Parameters for which the DMT provides an interpretation (see Table 1) are:

- vertical drained constrained modulus M (all soils)
- undrained shear strength c_u (in clay)
- in situ coefficient of lateral earth pressure K_0 (in clay)
- overconsolidation ratio OCR (in clay)
- horizontal coefficient of consolidation c_h (in clay)
- coefficient of permeability k_h (in clay)
- friction angle ϕ (in sand)
- unit weight γ and soil type (all soils)
- equilibrium pore pressure u_0 (in sand).

Correlations for clay apply for $I_D < 1.2$. Correlations for sand apply for $I_D > 1.8$.

The constrained modulus M and the undrained shear strength c_u are believed to be the most reliable and useful parameters obtained by DMT.

NOTE: Gage zero offset Z_M

In all the formulae containing Z_M enter $Z_M = 0$ (even if $Z_M \neq 0$) *if* ΔA, ΔB are measured by the *same gage* used for the current A, B readings (this is the normal case today, using the dual-gage control unit).

The reason is that the Z_M correction is already accounted for in ΔA, ΔB (this compensation can be verified readily from the algebra of the correction formulae for A, B). Hence entering the real Z_M would result, incorrectly, in applying twice the correction to A, B.

In general, if ΔA, ΔB and the current A, B readings are not measured by the same gage, the value of Z_M to be input in the equations should be the zero offset of the gage used for reading A & B minus the zero offset of the gage used for reading ΔA & ΔB.

NOTE: Correction formula for p_0

Eq. 1 for p_0 (back-extrapolated contact pressure at zero displacement) derives from the assumption of a linear pressure-displacement relationship between 0.05 mm (elevation of the feeler pin above sensing disc) and 1.10 mm (Marchetti & Crapps 1981).

NOTE: Sign of ΔA, ΔB corrections
Although the actual ΔA-pressure is negative (vacuum), it simulates a positive soil pressure. Consequently it is recorded and introduced in the p_0 formula as a positive number when it is a vacuum (which is the normal case). Eq. 1 is already adjusted to take into account that a positive ΔA is a vacuum. ΔB is normally positive.

NOTE: Selecting the "average" ΔA, ΔB to calculate p_0, p_1 (for a detailed treatment of this topic see Marchetti 1999)
Selecting the average ΔA, ΔB from the before/after ΔA, ΔB values must be done by an experienced technician. While performing the average, the entity of ΔA, ΔB and their variations during the sounding will also give him an idea of the care exercised during the execution.

If the test has been regular (e.g. the membrane has not been overinflated, and the Eurocode 7 tolerances for ΔA, ΔB have not been exceeded), the before/after values of ΔA, ΔB are very close, so that their arithmetic average is adequate.

If ΔA or ΔB vary more than 25 kPa during a sounding, the results, according to the Eurocode 7 (1997), should be discarded. However, if the soil is stiff, the results are not substantially influenced by ΔA, ΔB, and using typical ΔA, ΔB values (e.g. 15 and 40 kPa respectively) generally leads to acceptable results.

NOTE: Comments on the 3 intermediate parameters
The three intermediate parameters I_D, K_D, E_D are derived from two field readings. Clearly, only two of them are independent (the DMT is a two-parameter test). I_D, K_D, E_D have been introduced because each one of them has some recognizable physical meaning and some engineering usefulness.

10. INTERMEDIATE DMT PARAMETERS

10.1 MATERIAL INDEX I_D (SOIL TYPE)

The material index I_D is defined as follows:

$$I_D = \frac{p_1 - p_0}{p_0 - u_0} \qquad (3)$$

where u_0 is the pre-insertion in situ pore pressure.

The above definition of I_D was introduced having observed that the p_0 and p_1 profiles are systematically "close" to each other in clay and "distant" in sand.

According to Marchetti (1980), the soil type can be identified as follows:

clay	$0.1 < I_D < 0.6$
silt	$0.6 < I_D < 1.8$
sand	$1.8 < I_D < (10)$

In general, I_D provides an expressive profile of soil type, and, in "normal" soils, a reasonable soil description. Note that I_D sometimes misdescribes silt as clay and vice versa, and of course a mixture clay-sand would generally be described by I_D as silt.

When using I_D, it should be kept in mind that I_D is not, of course, the result of a sieve analysis, but a parameter reflecting mechanical behavior (some kind of "rigidity index"). For example, if a clay for some reasons behaves "more rigidly" than most clays, such clay will be probably interpreted by I_D as silt.

Indeed, if one is interested in mechanical behavior, sometimes it could be more useful for his application a description based on a mechanical response rather than on the real grain size distribution. If, on the other hand, the interest is on permeability, then I_D should be helpfully supplemented by the pore pressure index U_D (see Section 11.4.4).

10.2 HORIZONTAL STRESS INDEX K_D

The horizontal stress index K_D is defined as follows:

$$K_D = \frac{p_0 - u_0}{\sigma'_{v0}} \qquad (4)$$

where σ'_{v0} is the pre-insertion in situ overburden stress.

K_D provides the basis for several soil parameter correlations and is a key result of the dilatometer test.

The horizontal stress index K_D can be regarded as K_0 amplified by the penetration. In genuinely NC clays (no aging, structure, cementation) the value of K_D is $K_{D,NC} \approx 2$.

The K_D profile is similar in shape to the *OCR* profile, hence generally helpful for "understanding" the soil deposit and its stress history (Marchetti 1980, Jamiolkowski et al. 1988).

10.3 DILATOMETER MODULUS E_D

The dilatometer modulus E_D is obtained from p_0 and p_1 by the theory of elasticity (Gravesen 1960). For the 60 mm diameter of the membrane and the 1.1 mm displacement it is found:

$$E_D = 34.7\ (p_1 - p_0) \qquad (5)$$

E_D in general should not be used as such, especially because it lacks information on stress history. E_D should be used only in combination with K_D and I_D.

The symbol E_D should not evoke special affinity with the Young's modulus E' (see Section 11.3.2).

11. DERIVATION OF GEOTECHNICAL PARAMETERS

11.1 STRESS HISTORY / STATE PARAMETERS

11.1.1 Unit weight γ and soil type

A chart for determining the soil type and unit weight

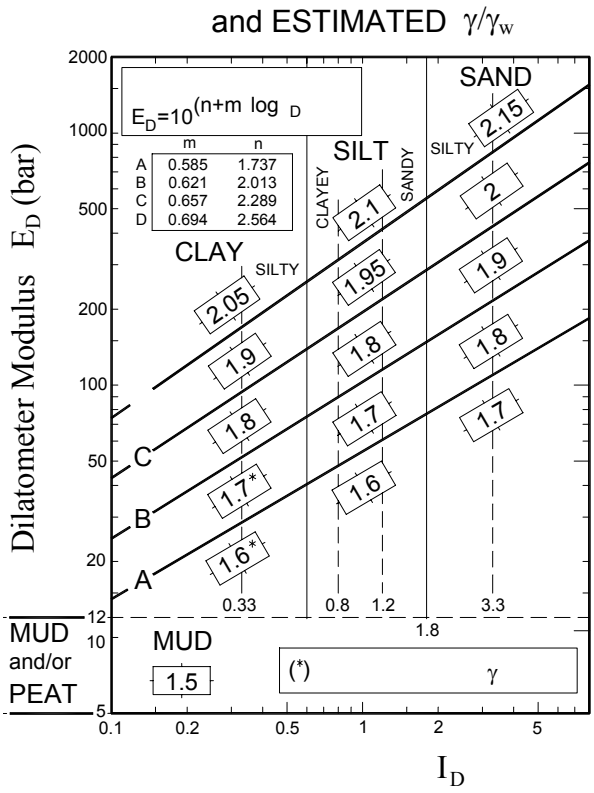

Fig. 16. Chart for estimating soil type and unit weight γ (normalized to $\gamma_w = \gamma$ water) - Marchetti & Crapps 1981 - (1 bar = 100 kPa)

γ from I_D and E_D was developed by Marchetti & Crapps 1981 (Fig. 16).

Many Authors (e.g. Lacasse & Lunne 1988) have presented modified forms of such table, more closely matching local conditions. However the original chart is generally a good average for "normal" soils. On the other hand, the main scope of the chart is not the accurate estimation of γ, but the possibility of constructing an approximate profile of σ'_{v0}, needed in the elaboration.

11.1.2 Overconsolidation ratio *OCR*

11.1.2.1 *OCR* in clay

The original correlation for deriving the overconsolidation ratio *OCR* from the horizontal stress index K_D (based on data only for uncemented clays) was proposed by Marchetti (1980) from the observation of the similarity between the K_D profile and the *OCR* profile:

$$OCR_{DMT} = (0.5\ K_D)^{1.56} \qquad (6)$$

Eq. 6 has built-in the correspondence $K_D = 2$ for $OCR = 1$ (i.e. $K_{D,NC} \approx 2$). This correspondence has been confirmed in many genuinely NC (no cementation, aging, structure) clay deposits.

The resemblance of the K_D profile to the *OCR* profile has also been confirmed by many subsequent comparisons (e.g. Jamiolkowski et al. 1988).

Research by Powell & Uglow (1988) on the *OCR*-K_D correlation in several UK deposits showed some deviation from the original correlation. However their research indicated that:

- The original correlation line (Eq. 6) is intermediate between the UK datapoints.
- The datapoints relative to each UK site were in a remarkably *narrow band*, *parallel* to the original correlation line.
- The narrowness of the datapoints band for each site is a confirmation of the remarkable resemblance of the *OCR* and K_D profiles, and the *parallelism* of the datapoints for each site to the original line is a confirmation of its slope.

The original *OCR*-K_D correlation for clay was also confirmed by a comprehensive collection of data by Kamei & Iwasaki 1995 (Fig. 17), and, theoretically, by Finno 1993 (Fig. 18).

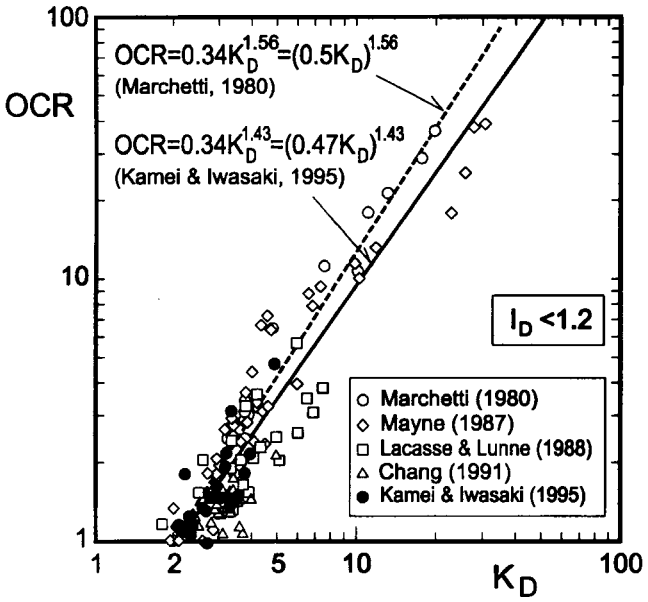

Fig. 17. Correlation K_D-*OCR* for cohesive soils from various geographical areas (Kamei & Iwasaki 1995)

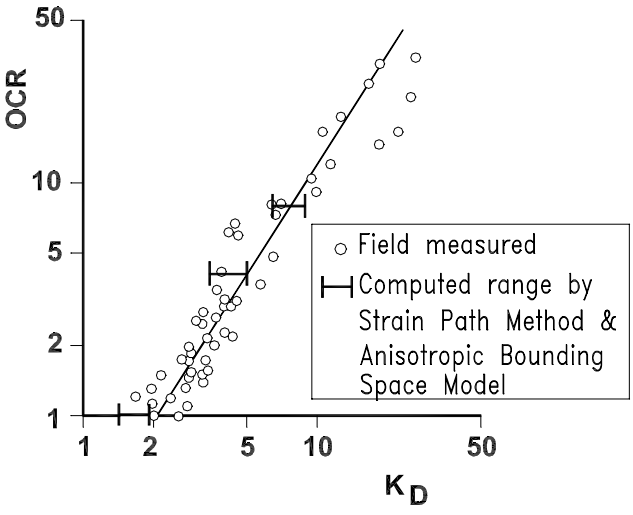

Fig. 18. Theoretical K_D vs *OCR* (Finno 1993)

A confirmation of $K_D \approx 2$ in genuine NC clays comes from recent slip surface research (Totani et al. 1997). In fact: (a) In all the layers where sliding was confirmed by inclinometers, it was found $K_D \approx 2$. (b) The clay in the remolded sliding band has certainly lost any trace of aging, structure, cementation, i.e. such clay is a good example of genuine NC clay.

Thus $K_D \approx 2$ appears the lower bound value for $K_{D,NC}$. If a geologically NC clay has $K_D > 2$, any excess of K_D above 2 indicates the likely existence of aging, structure or cementation.

Cemented-aged-structured clays (for brevity called below "cemented clays")

The original *OCR*-K_D correlation for uncemented clays established by Marchetti (1980) was presented as non applicable to cemented clays. However various researchers have attempted to develop correlations also in cemented clays.

It cannot be expected the existence of a unique *OCR*-K_D correlation valid for all cemented clays, because the deviation from the uncemented correlation depends on the (variable) entity of the cementation and the consequent (variable) excess of K_D above 2. Therefore, in general, datapoints for cemented clays should be kept separated, without attempting to establish a unique average correlation for both cemented and uncemented clays.

Practical indications for estimating *OCR* in various clays

- The original *OCR*-K_D correlation (Eq. 6) is a good base for getting a first interpretation of the *OCR* profile (or, at least, generally accurate information on its shape).
- In general the K_D profile is helpful for "understanding" the stress history. The K_D profile permits to discern NC from OC clays, and clearly identifies shallow or buried desiccation crusts. The K_D profile is often the first diagram that the engineer inspects, because from it he can get at a glance a general grasp on the stress history.
- In NC clays, the inspection of the K_D profile permits to distinguish genuine NC clays ($K_D \approx 2$, constant with depth) from cemented NC clays ($K_D \approx 3$ to 4, constant with depth, e.g. Fucino, Onsøy). In these clays any excess of K_D compared with the "floor" value $K_D \approx 2$ provides an indication of the intensity of cementation/structure/aging. However the NC condition can be easily recognized (despite $K_D > 2$), because K_D does not decrease with depth as typical in OC deposits.
- In cemented OC clays the inspection of the K_D profile does not reveal cementation as clearly as in NC clays (though the cementation shows up in the form of a less marked decrease of K_D with depth). In cemented clays the geological *OCR* will be overpredicted by Eq. 6.
- Highly accurate and detailed profiles of the in situ *OCR* can be obtained by calibrating OCR_{DMT} versus a few high quality oedometers (in theory even one or two - see Powell & Uglow 1988). Since *OCR* is a parameter difficult and costly to obtain, for which there are not many measuring options, the possibility of projecting via K_D a large number of high quality data appears useful.
- Stiff fissured OC clays. It is found that in non fissured OC clays the K_D profiles are rather smooth, while in fissured OC clays the K_D profiles are markedly seesaw-shaped. Such difference indicates that fissures are, to some extent, identified by the low points in the K_D profiles. The sensitivity of K_D to fissures may be useful in studies of fissure pattern. Note that the K_D s in the fissures of an OC clay are still considerably > 2, in fact fissures are not, in general, slip surfaces - characterized by $K_D = 2$ (see Section 13.4).

11.1.2.2 *OCR* in sand

The determination (even the definition) of *OCR* in sand is more difficult than in clay. *OCR* in sand is often the result of a complex history of preloading or desiccation or other effects. Moreover, while *OCR* in clay can be determined by oedometers, sample disturbance does not permit the same in sand. Therefore some approximation must be accepted.

A way of getting some information on *OCR* in sand is to use the ratio M_{DMT}/q_c. The basis is the following:

- Jendeby (1992) performed DMTs and CPTs before and after compaction of a loose sand fill. He found that before compaction (i.e. in nearly NC sand) the ratio M_{DMT}/q_c was 7-10, after compaction (i.e. in OC sand) 12-24.
- Calibration chamber (CC) research (Baldi et al. 1988) comparing q_c with M, both measured on the CC specimen, found the following ratios M_{cc}/q_c: in NC sands 4-7, in OC sands 12-16.
- Additional data in sands from instrumented embankments and screw plate tests (Jamiolkowski 1995) indicated a ratio (in this case E'/q_c): in NC sands 3-8, in OC sands 10-20.
- The well documented finding that compaction effects are felt more sensitively by M_{DMT} than by q_c (see Section 13.5) also implies that M_{DMT}/q_c is increased by compaction/precompression (see Fig. 42 ahead).

BACK

Hence *OCR* in sands can be approximately evaluated from the ratio M_{DMT}/q_c, using the following indicative values as a reference: M_{DMT}/q_c = 5-10 in NC sands, M_{DMT}/q_c = 12-24 in OC sands.

An independent indication of some ability of K_D to reflect *OCR* in sand comes from the crust-like K_D profiles often found at the top of sand deposits, very similar to the typical K_D profiles found in OC desiccation crusts in clay.

11.1.3 In situ coefficient of lateral earth pressure K_0

11.1.3.1 K_0 in clay

The original correlation for K_0, relative to uncemented clays (Marchetti 1980), is:

$$K_0 = (K_D / 1.5)^{0.47} - 0.6 \qquad (7)$$

Various Authors (e.g. Lacasse & Lunne 1988, Powell & Uglow 1988, Kulhawy & Mayne 1990) have presented slightly modified forms of the above equation. However the original correlation produces estimates of K_0 generally satisfactory, especially considering the inherent difficulty of precisely measuring K_0 and that, in many applications, even an approximate estimate of K_0 may be sufficient.

In highly cemented clays, however, the Eq. 7 may significantly overestimate K_0, since part of K_D is due to the cementation.

Example comparisons of K_0 determined by DMT and by other methods at two research sites are shown in Fig. 19 (Aversa 1997).

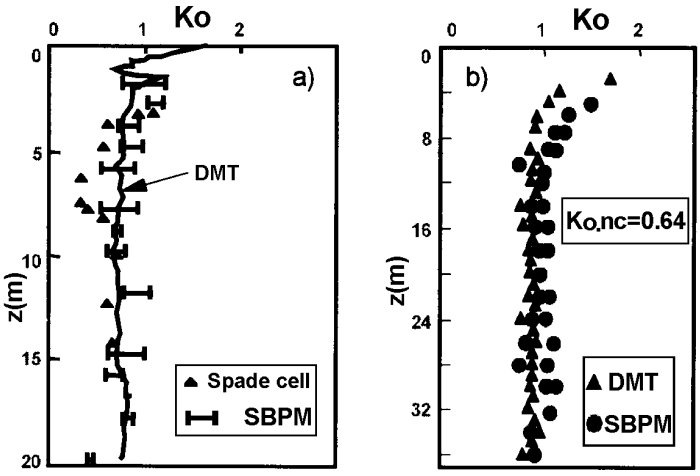

Fig. 19. K_0 from DMT vs K_0 by other methods at two clay research sites (Aversa 1997) (a) Bothkennar, UK (Nash et al. 1992) (b) Fucino, Italy (Burghignoli et al. 1991)

11.1.3.2 K_0 in sand

The original K_0-K_D correlation was obtained by interpolating datapoints relative mostly to clay. The very few (in 1980) datapoints relative to sands seemed to plot on the same curve. However, subsequent sand datapoints showed that a unique correlation cannot be established, since such correlation in sand also depends on ϕ or D_r.

Schmertmann (1982, 1983), based on CC results, interpolated through the CC datapoints a K_0-K_D-ϕ correlation equation (the lengthy fractionlike equation reported as Eq. 1 in Schmertmann 1983 or Eq. 6.5 in US DOT 1992). Such equation is the analytical equivalent of Fig. 10 in Schmertmann (1983), containing, in place of a unique K_0-K_D equation, a family of K_0-K_D curves, one curve for each ϕ. Since ϕ is in general unknown, Schmertmann (1982, 1983) suggested to use also the Durgunoglu & Mitchell (1975) theory, providing an additional condition q_c-K_0-ϕ, if q_c (or q_D) is also measured. He suggested an iterative computer procedure (relatively complicated) permitting the determination of both K_0 and ϕ. A detailed description of the method can be found in US DOT (1992).

To facilitate calculations, Marchetti (1985) prepared a K_0-q_c-K_D chart in which ϕ was eliminated, by combining the Schmertmann (1982, 1983) K_0-K_D-ϕ relation with the Durgunoglu & Mitchell (1975) q_c-K_0-ϕ relation. Such chart (reported as Fig. 6.4 in US DOT 1992) provides K_0, once q_c and K_D are given.

Baldi et al. (1986) updated such K_0-q_c-K_D chart by incorporating all subsequent CC work. Moreover the chart was converted into simple algebraic equations:

$$K_0 = 0.376 + 0.095\ K_D - 0.0017\ q_c/\sigma'_{v0} \qquad (8)$$

$$K_0 = 0.376 + 0.095\ K_D - 0.0046\ q_c/\sigma'_{v0} \qquad (9)$$

Eq. 8 was determined as the best fit of CC data, obtained on artificial sand, while Eq. 9 was obtained by modifying the last coefficient to predict "correctly" K_0 for the natural Po river sand.

In practice the today recommendation for K_0 in sand is to use the above Eqns. 8 and 9 with the following values of the last coefficient: -0.005 in "seasoned" sand, -0.002 in "freshly deposited" sand (though such choice involves some subjectivity).

While this is one of the few methods available for estimating K_0 in sand (or at least the shape of the K_0 profile), its reliability is difficult to establish, due to scarcity of reference values.

Cases have been reported of satisfactory agreement (Fig. 20, Jamiolkowski 1995). In other cases the K_0 predictions have been found to be incorrect as absolute values, though the shape of the profile appears to reflect the likely K_0 profile. The uncertainty is especially pronounced in cemented sands (expectable, due to the additional unknown

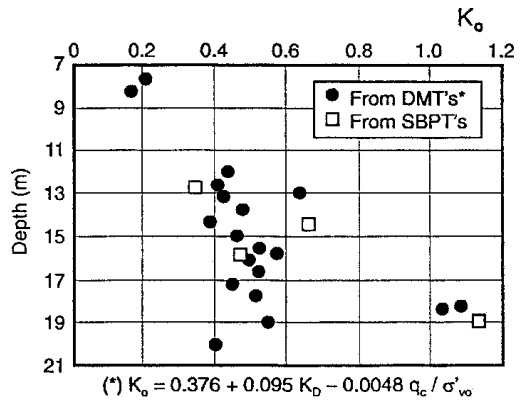

Fig. 20. K_0 from DMTs and SBPTs in natural Ticino sand at Pavia (Jamiolkowski 1995)

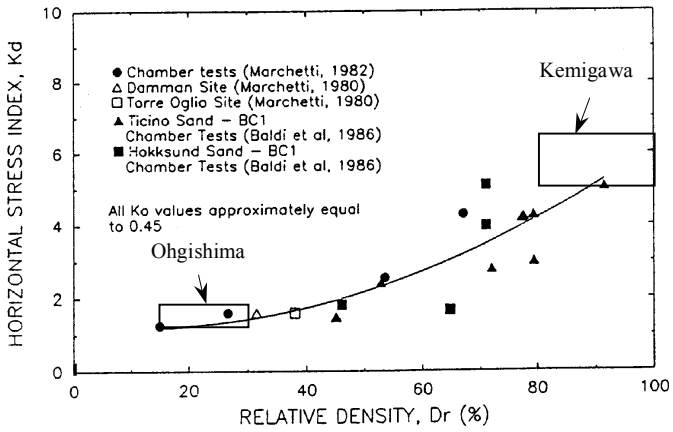

Fig. 21. Correlation K_D-D_r for NC uncemented sands (after Reyna & Chameau 1991, also including Ohgishima and Kemigawa datapoints obtained by Tanaka & Tanaka 1998)

"cementation"). An inconvenience of the method is that it requires both DMT and CPT and proper matching of correspondent K_D and q_c.

11.1.4 Relative density D_r (sand)

In NC uncemented sands, the recommended relative density correlation is the one shown in Fig. 21 (Reyna & Chameau 1991), where D_r is derived from K_D. This correlation is supported by the additional K_D-D_r datapoints (also included in Fig. 21) obtained by Tanaka & Tanaka (1998) at the Ohgishima and Kemigawa sites, where D_r was determined on high quality samples taken by the freezing method.

In OC sands, and in cemented sands, Fig. 21 will overpredict D_r, since part of K_D is due to the overconsolidation and cementation, rather than to D_r. The amount of the overprediction is difficult to evaluate at the moment.

11.2 STRENGTH PARAMETERS

11.2.1 Undrained shear strength c_u

The original correlation for determining c_u from DMT (Marchetti 1980) is the following:

$$c_u = 0.22\ \sigma'_{v0}\ (0.5\ K_D)^{1.25} \qquad (10)$$

Eq. 10 has generally been found to be in an intermediate position between subsequent datapoints presented by various researchers (e.g. Lacasse & Lunne 1988, Powell & Uglow 1988). Example comparisons between $c_{u\,DMT}$ and c_u by other tests at two research sites are shown in Figs. 22 and 23.

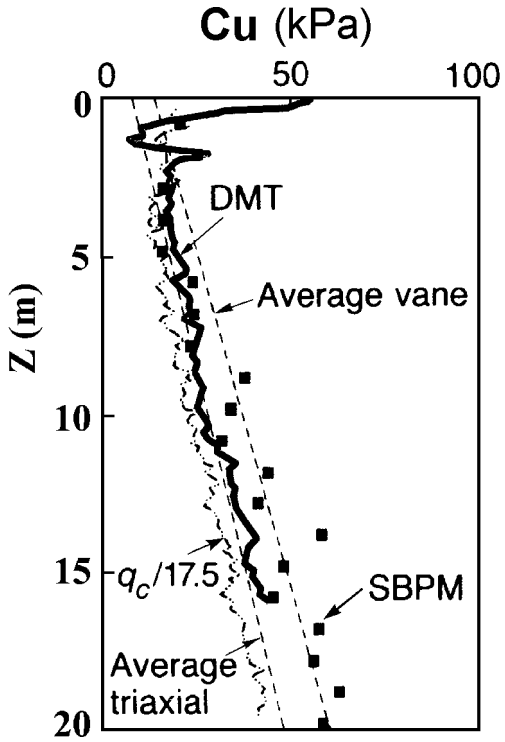

Fig. 22. Comparison between c_u determined by DMT and by other tests at the National Research Site of Bothkennar, UK (Nash et al. 1992)

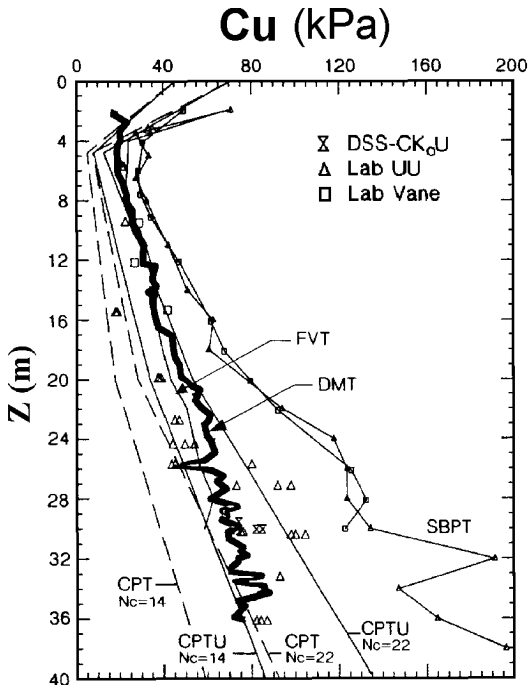

Fig. 23. Comparison between c_u determined by DMT and by other tests at the National Research Site of Fucino, Italy (Burghignoli et al. 1991)

BACK

Experience has shown that, in general, $c_{u\,DMT}$ is quite accurate and dependable for design, at least for everyday practice.

11.2.2 Friction angle Φ (sand)

Two methods are currently used today for estimating ϕ from DMT (see also Marchetti 1997).

The first method (Method 1) provides simultaneous estimates of ϕ and K_0 derived from the pair K_D and q_D (Method 1a) or from the pair K_D and q_c (Method 1b). The second method (Method 2) provides a *lower bound* estimate of ϕ based only on K_D.

Method 1a (ϕ from K_D, q_D)
This iterative method, developed by Schmertmann (1982, 1983), described in Section 11.1.3.2 relative to K_0 in sand, permits the determination of both K_0 and ϕ.

Method 1b (ϕ from K_D, q_c)
This method (Marchetti 1985) first derives K_0 from q_c and K_D by Eqns. 8 and 9, as indicated in Section 11.1.3.2 (K_0). Then uses the theory of Durgunoglu & Mitchell (1975), or its handy graphical equivalent chart in Fig. 24, to estimate ϕ from K_0 and q_c.

Method 2 (ϕ from K_D)
Details on the derivation of the method can be found in Marchetti (1997). ϕ is obtained from K_D by the following equation:

$$\phi_{safe,DMT} = 28° + 14.6° \, log\, K_D - 2.1° \, log^2 K_D \quad (11)$$

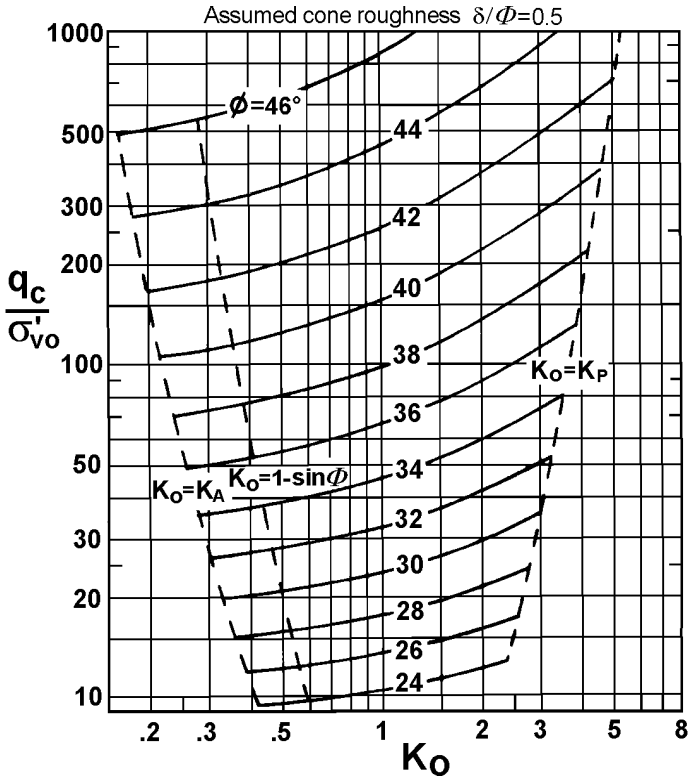

Fig. 24. Chart q_c-K_0-ϕ – graphical equivalent of the Durgunoglu & Mitchell theory (worked out by Marchetti 1985)

As already noted, ϕ from Eq. 11 is intended to be not the "most likely" estimate of ϕ, but a *lower bound* value (typical entity of the underestimation believed to be 2° to 4°). Obviously, if more accurate reliable (higher) values of ϕ are available, then such values should be used.

It should be noted that in cemented sands it is difficult to separate the two strength parameters *c*-ϕ, because there is an additional unknown.

11.3 Deformation parameters

11.3.1 Constrained modulus *M*

The modulus *M* determined from DMT (often designated as M_{DMT}) is the vertical drained confined (one-dimensional) tangent modulus at σ'_{v0} and is the same modulus which, when obtained by oedometer, is called $E_{oed} = 1/m_v$.

M_{DMT} is obtained by applying to E_D the correction factor R_M according to the following expression:

$$M_{DMT} = R_M \, E_D \quad (12)$$

The equations defining $R_M = f(I_D, K_D)$ (Marchetti 1980) are given in Table 1. The value of R_M increases with K_D. I_D has a lesser influence on R_M. Hence R_M is *not* a unique proportionality constant.

R_M varies mostly in the range 1 to 3.

Since E_D is an "uncorrected" modulus, while M_{DMT} is a "corrected" modulus, deformation properties should in general be derived from M_{DMT} and not from E_D.

Experience has shown that M_{DMT} is highly reproducible. In most sites M_{DMT} varies in the range 0.4 to 400 MPa.

Comparisons both in terms of M_{DMT}–$M_{reference}$ and in terms of predicted vs measured settlements have shown that, in general, M_{DMT} is reasonably accurate and dependable for everyday design practice.

M_{DMT} is to be used in the same way as if it was obtained by other methods (say a good quality oedometer) and introduced in one of the available procedures for evaluating settlements.

Example comparisons between M_{DMT} and *M* from high quality oedometers at two research sites are shown in Figs. 25 and 26.

NOTE: Necessity of applying the correction R_M to E_D

- E_D is derived by loading the soil distorted by the penetration.
- The direction of loading is horizontal, while *M* is vertical.
- E_D lacks information on stress history, reflected to some extent by K_D. The necessity of stress history for the realistic assessment of settlements has been emphasized by many researchers (e.g. Leonards & Frost 1988, Massarsch 1994).

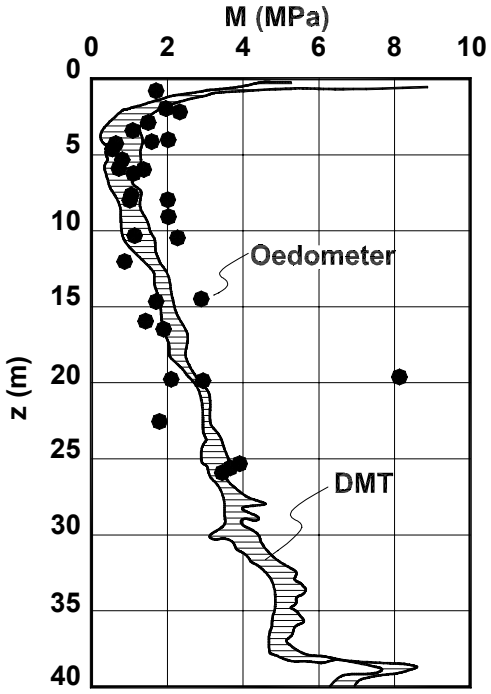

Fig. 25. Comparison between *M* determined by DMT and by high quality oedometers, Onsøy clay, Norway (Lacasse 1986)

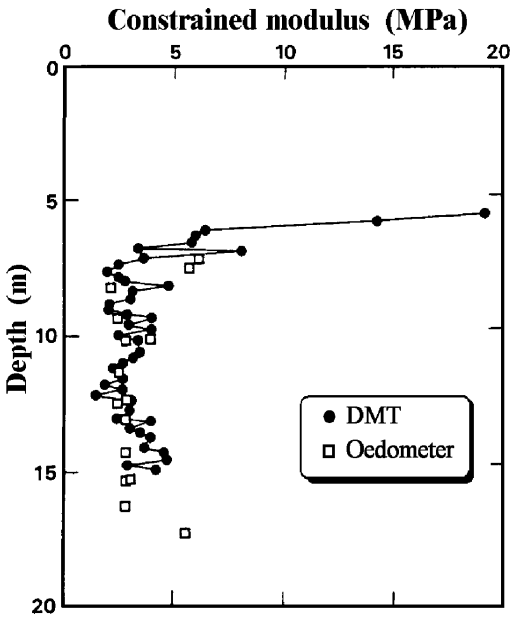

Fig. 26. Comparison between *M* determined by DMT and by high quality oedometers, Komatsugawa site, Japan (Iwasaki et al. 1991)

– In clays, E_D is derived from an undrained expansion, while M is a drained modulus. (For more details on this specific point see Marchetti 1997).

11.3.2 Young's modulus *E′*

The Young's modulus E' of the soil skeleton can be derived from M_{DMT} using the theory of elasticity equation:

$$E' = \frac{(1+\nu)(1-2\nu)}{(1-\nu)} M \qquad (13)$$

(e.g. for a Poisson's ratio ν = 0.25-0.30 one obtains $E' \approx 0.8\ M_{DMT}$).

The Young's modulus E' should not be derived from (or confused with) the dilatometer modulus E_D.

11.3.3 Maximum shear modulus G_0

No correlation for the maximum shear modulus G_0 was provided by the original Marchetti (1980) paper.

Subsequently, many researchers have proposed correlations relating DMT results to G_0.

A well documented method was proposed by Hryciw (1990). Other methods are summarized by Lunne et al. (1989) and in US DOT (1992).

Recently Tanaka & Tanaka (1998) found in four NC clay sites (where $K_D \approx 2$) $G_0/E_D \approx 7.5$. They also investigated three sand sites, where they observed that G_0/E_D decreases as K_D increases. In particular they found G_0/E_D decreasing from ≈ 7.5 at small K_D (1.5-2) to ≈ 2 for $K_D > 5$.

Similar trends in sands had been observed e.g. by Sully & Campanella (1989) and Baldi et al. (1989).

11.4 Flow characteristics and pore pressures

11.4.1 Coefficient of consolidation c_h

The method recommended by the authors for deriving c_h from DMT dissipations is the DMT-A method (Marchetti & Totani 1989, ASTM 2001). Another accepted method (ASTM 2001) is the DMT-A_2 method.

The test procedures - and some information on their origin - are described in Section 8.

In all cases the dissipation test consists in stopping the blade at a given depth, then monitoring the decay of the contact pressure σ_h with time. The horizontal coefficient of consolidation c_h is then inferred from the rate of decay.

Note that, as shown by piezocone research, the dissipation rate is governed in most cases predominantly by c_h rather than by c_v, which is the reason why c_h is the target of these procedures.

<u>c_h from DMT-A dissipation</u>

Interpretation of the DMT-A dissipations for evaluating c_h (Marchetti & Totani 1989):

– Plot the *A–log t* curve
– Identify the contraflexure point in the curve and the associated time (t_{flex})
– Obtain c_h as

$$c_{h,\,OC} \approx 7\ \text{cm}^2 / t_{flex} \qquad (14)$$

BACK

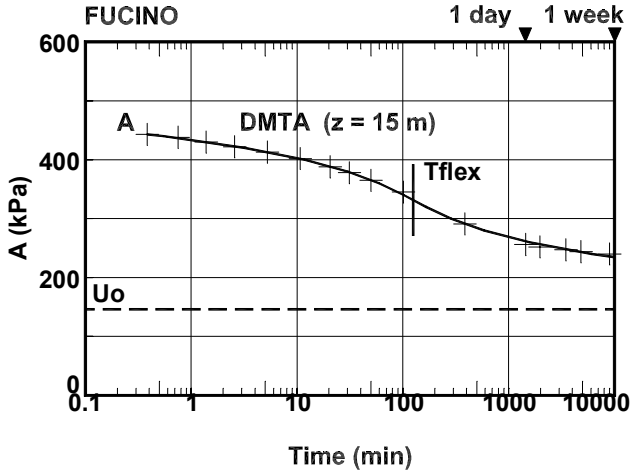

Fig. 27. Example of DMT-A decay curve

It should be noted that c_h from Eq. 14 refers to the soil behavior in the OC range. A c_h value several times lower should be adopted for estimating the settlement rate in a problem involving loading mainly in the NC range.

Comments on the origin of Eq. 14 are given in one of the Notes below.

An example of DMT-A decay curve (Fucino clay) is shown in Fig. 27.

c_h from DMT-A_2 dissipation

Basically the DMT-A_2 method (that can be considered an evolution of the DMT-C method) infers c_h from t_{50} determined from the A_2-decay dissipation curve. c_h is calculated from t_{50} by using an equivalent radius for the DMT blade and a time factor T_{50} obtained from the theoretical solutions for CPTU.

A detailed description of the method for interpreting the DMT-C dissipations can be found in Robertson et al. (1988), Schmertmann (1988) and US DOT (1992). The DMT-A_2 dissipation can be interpreted in the same way as the DMT-C, with the only difference that the readings A_2 are used in place of the readings C.

A detailed description of the method for interpreting DMT-A_2 dissipations can be found in ASTM 2001.

NOTES

- The DMT-A method does not require the knowledge of the equilibrium pore pressure u_o, since it uses as a marker point the contraflexure and not the 50 % consolidation point.
- The use of t_{flex} in the DMT-A method is in line with the recent suggestions by Mesri et al. (1999), advocating the preferability of the "inflection point method" for deriving c_v from the oedometer over the usual Casagrande or Taylor methods.
- The DMT-A dissipation test is very similar to the well-established "holding test" by pressuremeter. For such test the theory is available. It was developed by Carter et al. (1979), who established theoretically the S-shaped decay curve of the total contact pressure σ_h vs time (hence the theoretical time factor T_{flex} for the contraflexure point). A similar theory is not available yet for the decay σ_h vs time in the DMT blade, whose shape is more difficult to model. However, since the phenomenon is the same, the theory must have a similar format. The link $7\ cm^2$ between c_h and t_{flex} in Eq. 14 was determined by experimental calibration. (Determining $7\ cm^2$ by calibration is similar to determining $T_{50} = 0.197$, in the Terzaghi theory of 1-D consolidation, by field calibration rather than by mathematics). As to *fixity*, in the case of the DMT blade the *fixity* during the holding test is inherently insured, being the blade a solid object.
- Case histories presented by Totani et al. (1998) indicated that the c_h from DMT-A are in good agreement (or "slower" by a factor 1 to 3) with c_h backfigured from field observed behavior.
- The DMT-A_2 method (and the DMT-C method) rely on the assumption that the contact pressure A_2 (or C), after the correction, is approximately equal to the pore pressure u in the soil facing the membrane. Such assumption is generally valid for soft clays, but dubious in more consistent clays. (The DMT-A method, differently, does not rely on such assumption).
- The problem of filter smearing or clogging does not exist with the DMT membrane, because the membrane is anyway a non draining boundary, and what is monitored is a *total* contact stress.

11.4.2 Coefficient of permeability k_h

Schmertmann (1988) proposes the following procedure for deriving k_h from c_h:

- Estimate M_h using $M_h = K_0 M_{DMT}$, i.e. assuming M proportional to the effective stress in the desired direction
- Obtain $k_h = c_h \gamma_w / M_h$ (15)

11.4.3 In situ equilibrium pore pressure by *C*-readings in sands

The DMT, though non provided with a pore pressure sensor, permits, in free-draining granular soils ($B \geq 2.5\ A$), the determination of the pre-insertion ambient equilibrium pore pressure u_0. Since analysis of the DMT data depends on the in situ effective stress, water pressure is an important and useful information.

The reason why the DMT closing pressure (*C*-reading) closely approximates u_0 in sand (e.g. Campanella et al. 1985) is the following. During inflation, the membrane displaces the sand away from the blade. During deflation the sand has little tendency to rebound, rather tends to remain away from the membrane, without applying effective pressure to it ($\sigma'_h = 0$, hence $\sigma_h = u_0$). Therefore, at closure, the only pressure on the membrane will be u_0 (see sandy layers in Fig. 28).

This mechanism is well known to pressuremeter investigators, who discovered long ago that the contact pressure, in a disturbed pressuremeter test in sand, is essentially u_0.

In clay the method does not work because, during deflation, the clay tends to rebound and apply to the membrane some effective stresses. Moreover, in general, $u > u_0$ due to blade penetration. Hence $C > u_0$.

u_0 in sand is estimated as p_2:

$$u_0 \approx p_2 = C - Z_M + \Delta A \qquad (16)$$

(the gage zero offset Z_M is generally taken = 0, more details in Section 9.2).

Before interpreting the *C*-reading the engineer should insure that the operator has followed the right procedure (Section 5.2), in particular has not incurred in the frequent mistake highlighted in Section 5.2. Note that, in sands, the values expected for *C* are low numbers, usually < 100 or 200 kPa, i.e. 10 or 20 m of water.

C-readings typically show some experimental scatter. It is therefore preferable to rely on a p_2 profile vs depth, rather than on individual measurements, to provide a pore water pressure trend.

If the interest is limited to finding the u_0 profile, then *C*-readings are taken in the sandy layers ($B \geq 2.5\ A$), say every 1 or 2 m. When the interest, besides u_0, is to discern free-draining layers from non free-draining layers, then it is recommended to take *C*-readings routinely at each test depth (see next Section).

More details about the *C*-reading can be found in Marchetti (1997) and Schmertmann (1988).

11.4.4 Discerning free-draining from non free-draining layers - Index U_D

In problems involving excavations, dewatering, piping/blowup control, flow nets etc. the identification of free-draining/non free-draining layers is important. For such identification, methods based on the DMT *C*-reading (corrected into p_2 by Eq. 16) have been developed (see Lutenegger & Kabir's 1988 Eq. 2, or Schmertmann's 1988 Eq. 3.7).

The basis of the methods making use of the *C*-reading (or p_2) is the following. As discussed in the previous Section, in free-draining layers $p_2 \approx u_0$. In layers not free-draining enough to reach $\Delta u \approx 0$ in the first minute elapsed since insertion, some excess pore pressure will still exist at the time of the *C*-reading, hence $p_2 > u_0$.

Therefore: $p_2 = u_0$ indicates a *free-draining* soil, while $p_2 > u_0$ indicates a *non free-draining* soil (Fig. 28).

Index U_D

Based on the above, the pore pressure index U_D was defined by Lutenegger & Kabir (1988) as:

$$U_D = (p_2 - u_0) / (p_0 - u_0) \qquad (17)$$

In free-draining soils, where $p_2 \approx u_0$, $U_D \approx 0$. In non free-draining soils, p_2 will be higher than u_0 and U_D too.

The example in Fig. 29 (Benoit 1989) illustrates how U_D can discern "permeable" layers ($U_D = 0$), "impermeable" layers ($U_D = 0.7$) and "intermediate permeability" layers (U_D between 0 and 0.7), in agreement with B_q from CPTU.

Note that U_D, while useful for the above scope, cannot be expected to offer a scale over the full range of permeabilities. In fact beyond a certain *k* the test will be drained anyway, below a certain *k* the test will be undrained anyway (see Note on next page).

In layers recognized by U_D as non free-draining, quantitative evaluations of c_h can be obtained e.g. using the DMT dissipations described earlier.

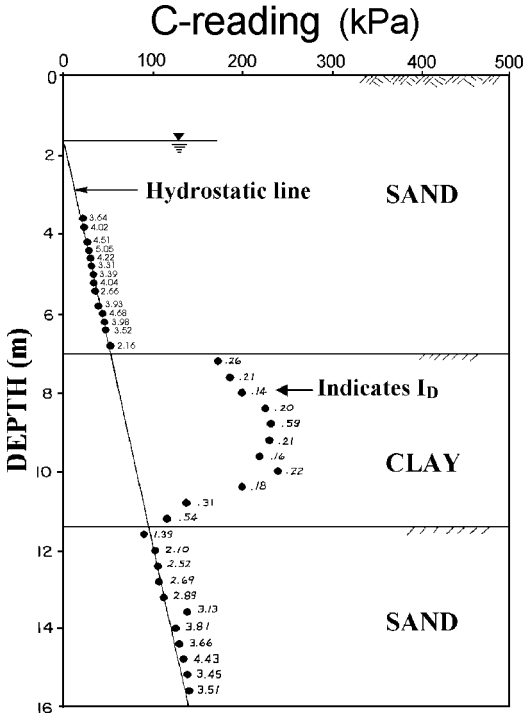

Fig. 28. Use of *C*-readings for distinguishing free-draining from non free-draining layers (Schmertmann 1988)

BACK

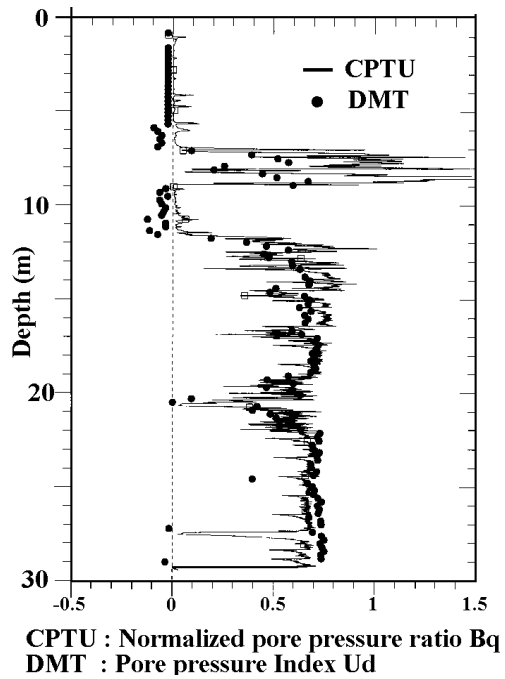

Fig. 29. Use of U_D for discerning free-draining layers (U_D = 0) from non free-draining layers (Benoit 1989)

In layers recognized by U_D as free-draining, the DMT dissipations will not be performed (the DMT dissipations are not feasible if most of the dissipation occurs in the first minute, because readings cannot be taken in the first ≈ 15 sec).

NOTE: Drainage conditions during the test
In a clean sand the DMT is a perfectly drained test. Δu is virtually zero throughout the test, whose duration (say 1 minute) is sufficient for any excess to dissipate. In a low permeability clay the opposite is true, i.e. the test is undrained and the excesses do not undergo any appreciable dissipation during the normal test.

It should be noted that, for opposite reasons, the *u* values in the soil surrounding the blade are constant with time during the test in both cases. In permeable soils everywhere $u = u_0$. In impermeable soils the pore pressures do not dissipate.

There is however a *niche* of soils (in the silts region) for which 1 minute is insufficient for full drainage, but sufficient to permit some dissipation. In these *partial drainage* soils the data obtained can be misleading to an unaware user. In fact the reading *B*, which follows *A* by say 15 seconds, is not the "proper match" of *A*, because in the ≈ 15 seconds from *A* to *B* some excess has been dissipating and *B* is "too low", with the consequence that the difference *B-A* can also be very low and so the derived values I_D, E_D, *M*. In such soils I_D will possibly end up in the extreme left hand of its scale (I_D = 0.1 or less) and *M* will also possibly be far too low. Fortunately the sites where this behavior - recognizable by frequent values of I_D = 0.1 or less - has been encountered (e.g. Drammen, Norway) are less than 1 % of the investigated sites.

To be sure, in case of very low I_D and *M* there is some ambiguity, because the low values of *B-A* could just be the normal response of a low permeability very soft clay. The ambiguity can be solved with the help of *C*-readings (or U_D). If the U_D values in the "low *B-A*" layers are intermediate between those found in the free-draining layers and those found in the non free-draining layers, than the above interpretation of *partial drainage* is presumably correct.

Of course the *partial drainage* explanation can also be verified by means of laboratory sieve analysis or permeability tests. In practice, if the *partial drainage* explanation of the low *B-A* is confirmed, all results dependent from *B-A* (recognizable by very depressed I_D troughs) have to be ignored.

12. PRESENTATION OF DMT RESULTS

Fig. 30 shows the recommended graphical format of the DMT output. Such output displays four profiles: I_D, *M*, c_u and K_D. Experience has shown that these four parameters are generally the most significant group to plot (for reliability, expressivity, usefulness). Note that K_D, though not a common soil parameter, has been selected as one to be displayed as generally helpful in "understanding" the site history, being similar in shape to the *OCR* profile. It is also recommended that the diagrams be presented side by side, and not separated. It is beneficial for the user to see the diagrams together.

The graphical output contains only the main profiles. The numerical values of these and other parameters are listed in the tabular output normally accompanying the graphical output (see example in Fig. 31).

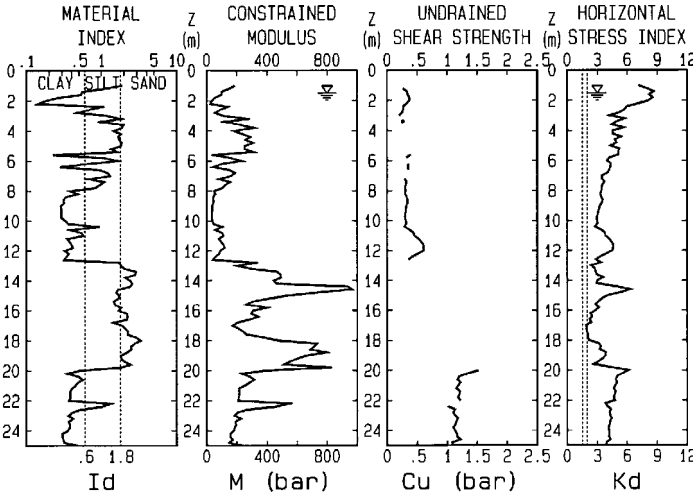

Fig. 30. Recommended graphical presentation of DMT results - (1 bar = 100 kPa)

SOIL TEST — D M T : D3 - 4 OCT 1989 — Reg 1003
LIVORNO HARBOUR — NEW QUAY — WATERTABLE m 1.5

Reduction formulae according to ASCE Geot.Jnl.,Mar. 1980, Vol.109, 299-321
NOTE : OCR = ''relative OCR''. OCR below often reasonable. Accuracy can be improved if precise OCR values are available. Then factorize all OCR below by the ratio OCRreference/OCR

Po = Corrected A reading bar
P1 = Corrected B reading bar
Gamma = Bulk unit weight/GammaH2O (-)
Sigma'= Effective overb. stress bar
U = Pore pressure bar
Id = Material Index (-)
Kd = Horizontal stress index (-)
Ed = Dilatometer modulus bar

INTERPRETED GEOTECHNICAL PARAMETERS
Ko = In situ earth press. coeff. (-)
Ocr= Overconsolidation ratio (-)
Phi= Safe floor value of friction angle (-)
M = Constrained modulus (at Sigma') bar
Cu = Undrained shear strength bar

Z (m)	Po	P1	Gamma	Sigma'	U	Id	Kd	Ed	Ko	Ocr	Phi	M	Cu	DESCRIPTION
1.00	1.2	3.5	1.80	0.17	0.00	1.89	7.1	85			39	186		SILTY SAND
1.20	1.6	3.4	1.70	0.21	0.00	1.09	7.9	66	1.6	8.6		150	0.26	SILT
1.40	2.1	3.2	1.70	0.24	0.00	0.56	8.6	43	1.7	9.8		100	0.33	SILTY CLAY
1.60	2.2	3.3	1.70	0.26	0.01	0.53	8.2	43	1.6	9.0		98	0.34	SILTY CLAY
1.80	2.4	3.0	1.60	0.28	0.03	0.27	8.5	23	1.7	9.6		55	0.37	CLAY
2.00	2.4	2.8	1.60	0.29	0.05	0.18	8.2	16	1.6	9.0		36	0.37	CLAY
2.20	2.2	2.5	1.50	0.30	0.07	0.15	7.1	12	1.5	7.3		25	0.32	MUD
2.40	1.9	3.8	1.70	0.31	0.09	1.02	6.0	70	1.3	5.5		139	0.27	SILT
2.60	2.0	3.2	1.70	0.32	0.11	0.68	5.7	47	1.3	5.2		90	0.27	CLAYEY SILT
2.80	1.9	2.7	1.60	0.34	0.13	0.48	5.2	31	1.2	4.4		57	0.25	SILTY CLAY
3.00	1.6	3.4	1.70	0.35	0.15	1.19	4.3	66	1.0	3.3		110	0.20	SILT
3.20	2.2	6.0	1.80	0.36	0.17	1.81	5.7	140			38	276		SILTY SAND
3.40	2.0	3.8	1.70	0.38	0.19	0.96	4.9	66	1.1	4.0		118	0.26	SILT
3.60	2.0	5.4	1.80	0.39	0.21	1.97	4.5	128			37	224		SILTY SAND
3.80	2.5	6.8	1.90	0.41	0.23	1.87	5.6	159			38	312		SILTY SAND
4.00	2.2	5.0	1.70	0.43	0.25	1.45	4.6	105			37	183		SANDY SILT
4.20	2.3	5.9	1.80	0.44	0.26	1.85	4.5	136			37	238		SILTY SAND
4.40	2.7	6.8	1.80	0.46	0.28	1.67	5.4	152			38	289		SANDY SILT
4.60	2.5	6.4	1.70	0.47	0.30	1.73	4.7	144			37	258		SANDY SILT
4.80	2.7	7.2	1.90	0.49	0.32	1.89	4.9	167			37	306		SILTY SAND
5.00	2.5	6.5	1.80	0.50	0.34	1.82	4.4	148			36	253		SILTY SAND
5.20	3.1	6.7	1.80	0.52	0.36	1.37	5.2	136			37	253		SANDY SILT
5.40	3.1	7.6	1.80	0.53	0.38	1.65	5.1	167			37	310		SANDY SILT
5.60	3.2	3.8	1.70	0.55	0.40	0.23	5.1	23	1.2	4.3		42	0.39	CLAY
5.80	2.8	5.4	1.70	0.56	0.42	1.10	4.2	97	1.0	3.2		160	0.32	SILT
6.00	2.7	6.6	1.80	0.58	0.44	1.69	4.0	144			36	233		SANDY SILT
6.20	3.1	4.6	1.70	0.59	0.46	0.61	4.4	58	1.1	3.4		96	0.35	CLAYEY SILT
6.40	3.1	3.8	1.70	0.61	0.48	0.28	4.3	27	1.0	3.3		44	0.35	CLAY
6.60	3.1	5.6	1.70	0.62	0.50	0.97	4.2	93	1.0	3.2		152	0.35	SILT
6.80	3.1	6.2	1.70	0.63	0.52	1.23	4.0	117			36	187		SANDY SILT
7.00	2.8	5.7	1.70	0.65	0.54	1.31	3.5	109			35	159		SANDY SILT
7.20	2.9	4.4	1.70	0.66	0.56	0.69	3.5	58	0.88	2.4		83	0.29	CLAYEY SILT
7.40	3.1	5.8	1.70	0.68	0.58	1.08	3.7	101	0.93	2.6		154	0.32	SILT
7.60	3.0	5.3	1.70	0.69	0.60	0.95	3.5	85	0.89	2.4		124	0.31	SILT
7.80	3.0	5.0	1.70	0.70	0.62	0.83	3.4	74	0.88	2.3		105	0.30	SILT
8.00	3.1	4.0	1.70	0.72	0.64	0.39	3.4	35	0.87	2.3		49	0.31	SILTY CLAY
8.20	3.1	4.2	1.70	0.73	0.66	0.48	3.3	43	0.85	2.2		58	0.30	SILTY CLAY
8.40	3.2	4.0	1.70	0.74	0.68	0.33	3.4	31	0.86	2.3		43	0.32	SILTY CLAY
8.60	3.4	4.2	1.70	0.76	0.70	0.31	3.6	31	0.90	2.4		45	0.34	CLAY
8.80	3.4	4.2	1.70	0.77	0.72	0.31	3.5	31	0.88	2.4		44	0.34	CLAY
9.00	3.3	4.0	1.70	0.79	0.74	0.29	3.3	27	0.84	2.1		37	0.32	CLAY
9.20	3.3	4.0	1.70	0.80	0.76	0.29	3.2	27	0.82	2.1		36	0.31	CLAY
9.40	3.3	4.0	1.70	0.81	0.77	0.29	3.1	27	0.81	2.0		35	0.31	CLAY
9.60	3.3	4.0	1.70	0.83	0.79	0.29	3.0	27	0.79	1.9		35	0.30	CLAY
9.80	3.3	4.0	1.70	0.84	0.81	0.30	3.0	27	0.77	1.8		34	0.30	CLAY
10.00	3.4	4.2	1.70	0.85	0.83	0.33	3.0	31	0.78	1.9		39	0.31	CLAY
10.20	3.5	4.4	1.70	0.87	0.85	0.36	3.0	35	0.79	1.9		45	0.32	SILTY CLAY
10.40	3.3	5.6	1.70	0.88	0.87	0.94	2.8	85	0.74	1.7		104	0.29	SILT
10.60	3.9	5.0	1.70	0.90	0.89	0.39	3.3	43	0.85	2.2		59	0.37	SILTY CLAY

Fig. 31. Example of numerical output of DMT results - (1 bar = 100 kPa)

All input data, in particular the uncorrected field readings A and B and the calibration values ΔA and ΔB, must always be reported, either in a separate document or as added columns in the above tabular output.

BACK

Figs. 32 and 33 show examples of DMT results in predominantly NC and OC sites. The condition NC or OC is clearly identified by K_D (K_D in the vertical band between the two dashed lines (K_D = 1.5-2) in NC sites, higher K_D in OC sites).

13. APPLICATION TO ENGINEERING PROBLEMS

As mentioned earlier, the primary way of using DMT results is "design via parameters".

This Section provides some details on the use of DMT in some specific applications.

13.1 SETTLEMENTS OF SHALLOW FOUNDATIONS

Predicting settlements of shallow foundations is probably the No. 1 application of the DMT, especially in sands, where undisturbed sampling and estimating compressibility are particularly difficult.

Settlements are generally calculated by means of the one-dimensional formula (Fig. 34):

$$S_{1-DMT} = \sum \frac{\Delta\sigma_v}{M_{DMT}} \Delta z \qquad (18)$$

with $\Delta\sigma_v$ generally calculated according to Boussinesq and M_{DMT} constrained modulus estimated by DMT.

It should be noted that the above formula, being based on linear elasticity, provides a settlement *proportional* to the load, and is unable to provide a non linear prediction. The predicted settlement is meant to be the *settlement in "working conditions"* (i.e. for a safety factor Fs = 2.5 to 3.5).

13.1.1 Settlements in sand

Settlements analyses in sand are generally carried out using the 1-D elasticity formula (in 1-D problems, say *large* rafts or embankments) or the 3-D elasticity formula (in 3-D problems, say *small* isolated footings).

However, based on considerations by many Authors (e.g. Burland et al. 1977), it is recommended to use the 1-D formula (Eq. 18) in *all* cases. The reasons are illustrated in detail by Marchetti (1997).

In case it is opted for the use of the 3-D formulae, E' can be derived from M using the theory of elasticity, that, for ν = 0.25, provides $E' = 0.83\ M$ (a factor not very far from unity). Indeed M and E' are often used interchangeably in view of the involved approximation.

13.1.2 Settlements in clay

Eq. 18 is also recommended for predicting settlements in clay. The calculated settlement is the *primary* settlement (i.e. net of immediate and secondary), because M_{DMT} is to be treated as the average E_{oed} derived from the oedometer curve

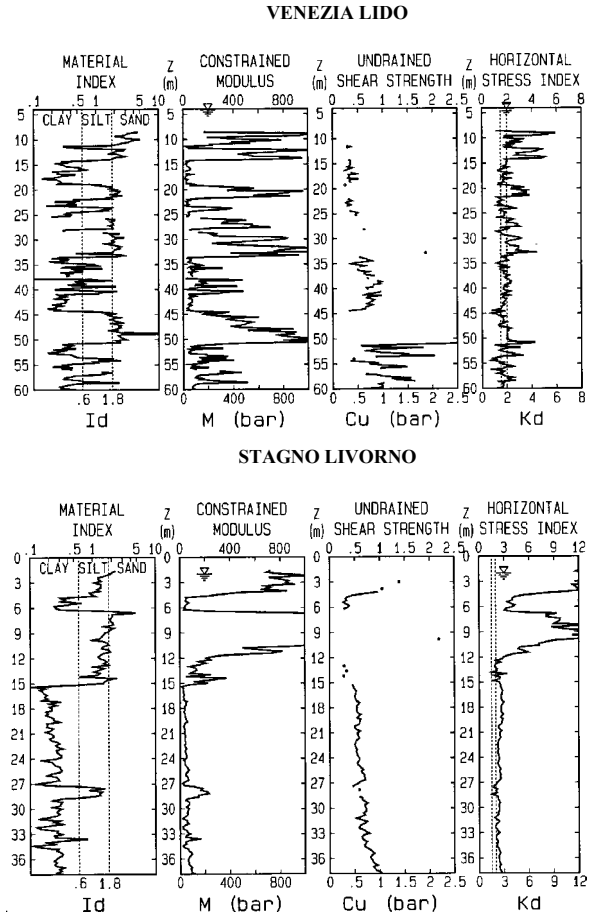

Fig. 32. Examples of DMT results in NC sites ($K_D \approx 2$) - (1 bar = 100 kPa)

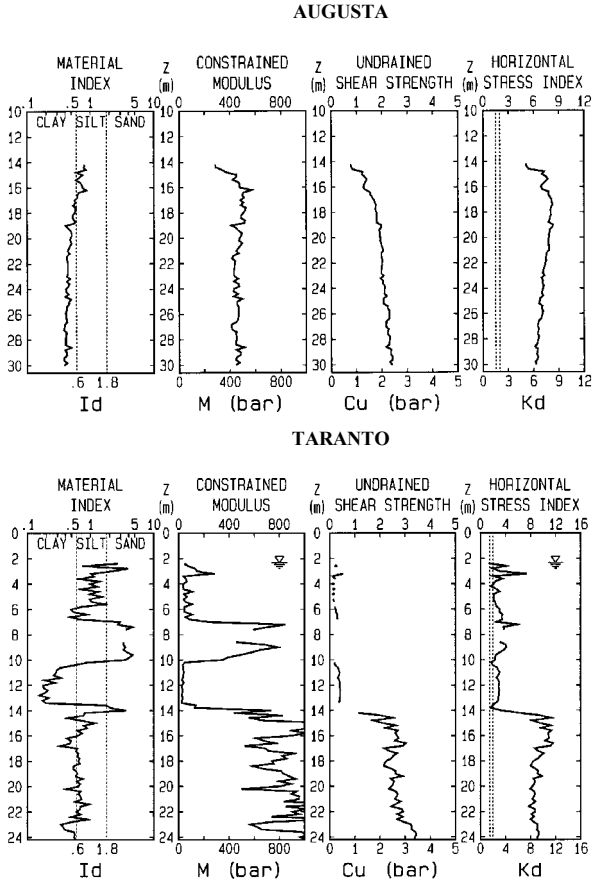

Fig. 33. Examples of DMT results in OC sites ($K_D >> 2$) - (1 bar = 100 kPa)

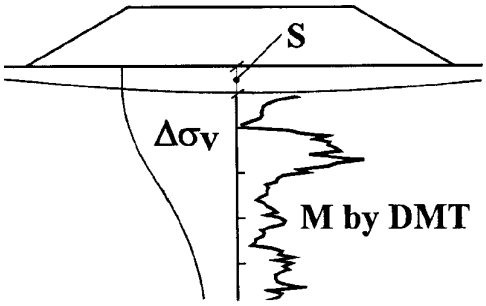

$$S = \sum \frac{\Delta\sigma_v}{M} \cdot \Delta Z$$

Fig. 34. Recommended settlement calculation

in the expected stress range.

It should be noted that in some highly structured clays, whose oedometer curves exhibit a sharp break and a dramatic reduction in slope across the preconsolidation pressure p'_c, M_{DMT} could be an inadequate average if the loading straddles p'_c. However in many common clays, and probably in most natural sands, the M fluctuation across p'_c is mild, and M_{DMT} can be considered an adequate average modulus.

In 3-D problems in OC clays, "according to the book", the Skempton-Bjerrum correction should be applied. Such correction in OC clays is often in the range 0.2 to 0.5 (<<1). However considering that:

– The application of the Skempton-Bjerrum correction is equivalent to reducing $S_{I\text{-}DMT}$ by a factor 2 to 5
– Terzaghi & Peck's book states that in OC clays "the modulus from even good oedometers may be 2 to 5 times smaller than the in situ modulus"

these two factors approximately cancel out.

Therefore it is suggested to adopt as *primary* settlement (even in 3-D problems in OC clays) directly $S_{I\text{-}DMT}$ from Eq. 18, *without* the Skempton-Bjerrum correction (while adopting, if applicable, the rigidity and the depth corrections).

13.1.3 Comparison of DMT-calculated vs observed settlements

Many investigators have presented comparisons of observed vs DMT-predicted settlements, reporting generally satisfactory agreement.

Schmertmann (1986) reports 16 case histories at various locations and for various soil types. He found an average ratio calculated/observed settlement ≈ 1.18, with the value of that ratio mostly in the range 0.75 to 1.3.

Fig. 35 (Hayes 1990) confirms the good agreement for a wide settlement range. In such figure the band amplitude of the datapoints (ratio between maximum and minimum) is approximately 2. Or the observed settlement is within ± 50 % from the DMT-predicted settlement.

Similar agreement has been reported by others (Lacasse & Lunne 1986, Skiles & Townsend 1994, Steiner et al. 1992, Steiner 1994, Woodward & McIntosh 1993, Failmezger et al. 1999, Didaskalou 1999, Pelnik et al. 1999).

13.2 AXIALLY LOADED PILES

13.2.1 Driven piles

13.2.1.1 The DMT-σ_{hc} method for piles driven in clay

The DMT-σ_{hc} method (Marchetti et al. 1986) was developed for the case of piles driven in clays. The method is based on the determination of σ'_{hc} (effective horizontal stress against the DMT blade at the end of the reconsolidation). Then a ρ factor is applied to σ'_{hc}, and the product is used as an estimate of the pile skin friction ($f_s = \rho\ \sigma'_{hc}$).

The DMT-σ_{hc} method has conceptual roots in the theories developed by Baligh (1985). However, in practice, the method has two drawbacks:

(a) In clays, the determination of σ'_{hc} can take considerable time (the reconsolidation around the blade in low permeability clays can take many hours, if not one or two days), which makes the σ'_{hc} determination expensive (especially in offshore investigations).
(b) The ρ factor has been found to be not a constant, but a rather variable factor (mostly in the range 0.10 to 0.20). Therefore, until methods for

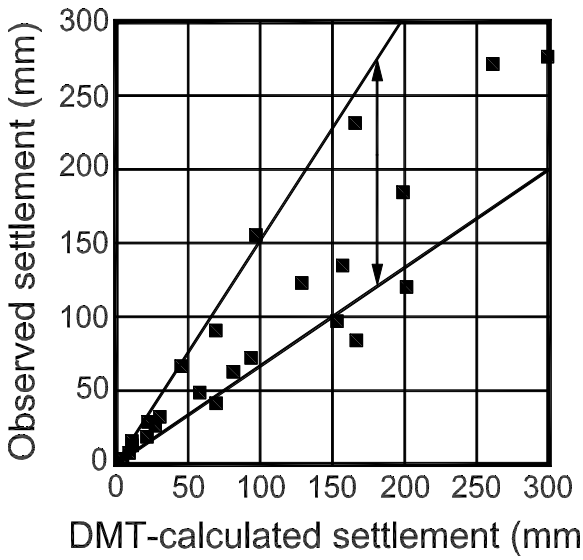

Fig. 35. Observed vs DMT-calculated settlements (Hayes 1990)

BACK

more reliable estimates of ρ are developed, the uncertainty in f_s is too wide. Nevertheless, in important jobs, the method could helpfully be used to supplement other methods, e.g. for getting information on the shape of the f_s profile, or for estimating a lower bound value of f_s using ρ = 0.10.

13.2.1.2 Method by Powell et al. (2001 b) for piles driven in clay

Powell et al. (2001 b) developed a new method for the design of axially loaded piles driven in clay by DMT. The method was developed based on load tests on about 60 driven or jacked piles at 10 clay sites in UK, Norway, France and Denmark, as part of an EC Brite EuRam Project.

This method predicts the pile skin friction q_s from the material index I_D and $(p_1 - p_0)$. The recommended design formulae for skin friction in clay (both tension and compression piles) are:

$I_D < 0.1$ $\quad q_s/(p_1 - p_0) = 0.5$ (19)

$0.1 < I_D < 0.65$ $\quad q_s/(p_1 - p_0) = -0.73077\, I_D + 0.575$ (20)

$I_D > 0.65$ $\quad q_s/(p_1 - p_0) = 0.1$ (21)

A slightly *modified* form of the above equations was proposed for predicting q_s of *compression piles only*:

$I_D < 0.6$ $\quad q_s/(p_1 - p_0) = -1.1111\, I_D + 0.775$ (22)

$I_D > 0.6$ $\quad q_s/(p_1 - p_0) = 0.11$ (23)

For the upper parts of the pile where $h/R > 50$ (h = distance along the pile upwards from the tip, and R = pile radius), in both cases the above values should be multiplied by 0.85.

The pile unit end resistance q_p is evaluated as:

$$q_p = k_{di}\ p_{1e} \quad (24)$$

where p_{1e} is the *equivalent* p_1 (a suitable average beneath the base of the pile) and k_{di} is the "DMT bearing capacity factor". For closed ended driven piles the recommended values for k_{di} are:

for $E_D > 2$ MPa $\quad k_{di} = 1.3$ (25)

for $E_D < 2$ MPa $\quad k_{di} = 0.7$ (26)

For open ended piles multiply these values by 0.5.

The criteria for the variation of k_{di} with soil type need to be established from a larger database to establish the transition at $E_D = 2$ MPa.

Based on comparisons with the measured capacity of a large number of piles, Powell et al. (2001 a & b) conclude that the *general* shaft resistance method for all piles *(both tension and compression)* shows good potential for use in design, and performs at least as well as other methods currently available.

The *modified* method for estimating q_s for *compression piles only* based on DMT (Eqns. 22 - 23) was found to predict more accurately the observed shaft capacity of compression piles, q_p being derived as above (Fig. 36). This modified method based on DMT was found to outperform other methods investigated for compression piles (Powell et al. 2001 a).

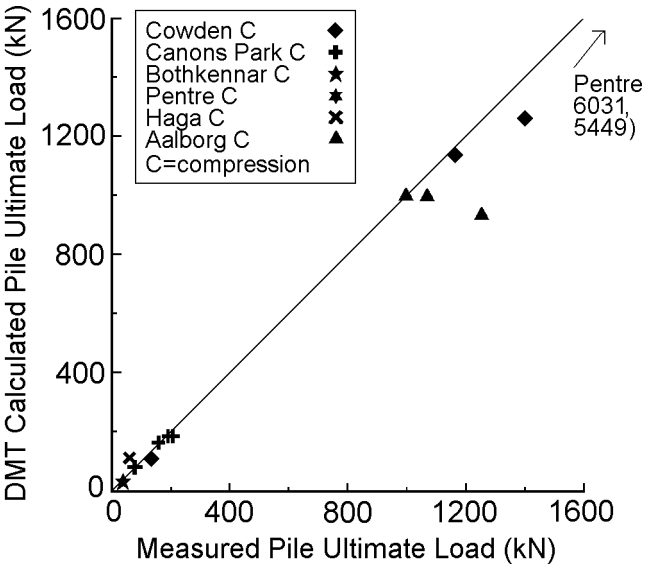

Fig. 36. Predicted vs measured ultimate pile capacity using the DMT compression pile method (Powell et al. 2001 a)

13.2.1.3 Horizontal pressure against piles driven in clay during installation

Totani et al. (1994) report a finding of practical interest to engineers having to decide the thickness of the shell of mandrel-driven piles in clay. The paper describes measurements of σ_h (total) on a pile 57 m long, 508/457 mm in diameter, driven in a slightly OC clay. The pile was instrumented with 8 total pressure cells. Cells readings (σ_h against the pile) were taken during pauses in driving. The σ_h values were found at each depth virtually equal to p_0 determined by a normal DMT.

This finding is in accordance to theoretical findings by Baligh (1985), predicting σ_h independent from the dimensions of the penetrating object (these results suggest independence of σ_h even from the shape).

13.2.1.4 Low skin friction in calcareous sand

Some calcareous sands are known to develop unusually low skin friction, hence very low lateral pile capacity.

DMTs performed in calcareous sands (Fig. 37) have indicated unusually low K_D values. This suggests: (a) The low f_s in these sands is largely due to low σ'_h. (b) The low K_D in calcareous sands is a possible useful warning of low skin friction.

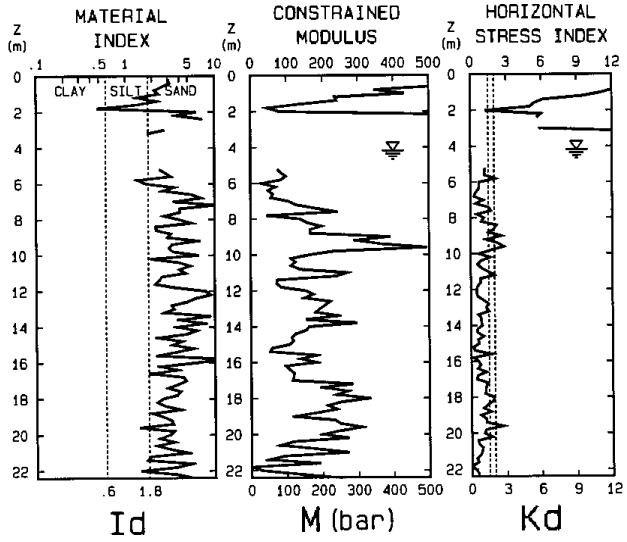

Fig. 37. DMT results in the Plouasne (Brittany) calcareous sand (K_D << 2) - (1 bar = 100 kPa)

13.2.2 Screw piles

Peiffer (1997) developed a method for estimating the skin friction of Atlas screw piles based on p_0 from DMT.

The DMT is run in the usual way, but is performed next to the pile (one diameter away from the shaft) *after* its execution.

This method is intermediate between a real design method and a pile load test. It is not a pre-execution design method, because the skin friction is estimated after the pile has been executed. Nor is it a load test, because the skin friction is estimated not by loading the pile, but from DMT-determined properties of the after-pile-installation soil, in accord with the widely recognized notion that pile capacity largely depends on execution, besides soil type.

13.2.3 Bored piles

No special DMT-based methods have been developed for the design of bored piles, which is generally carried out via soil parameters.

However the method developed by Peiffer (1997) for skin friction on screw piles (perform DMT in the soil surrounding the pile, see above Section) is in principle applicable also to bored piles.

13.2.4 Monitoring pile installation effects

The DMT has also been used extensively by Ghent investigators (Peiffer & Van Impe 1993, Peiffer et al. 1993, Peiffer et al. 1994, De Cock et al. 1993) for *comparing soil changes caused by various pile installation methods*. For instance De Cock et al. (1993) describe the use of before/after DMTs to verify, in terms of K_D, the installation effects of the Atlas pile (Fig. 38).

13.3 LATERALLY LOADED PILES

Methods have been developed for deriving *P-y* curves from DMT results. For the single pile the authors recommend the methods developed by Robertson et al. (1987) and by Marchetti et al. (1991). Note that all methods address the case of first time monotonic loading.

13.3.1 Robertson et al. (1987) method (clays and sands)

The Robertson method is an adaptation of the early methods (Skempton ε_{50} - Matlock 1970 cubic parabola approach) estimating the *P-y* curves from soil properties obtained in the laboratory. In the Robertson method such "laboratory soil properties" are inferred from DMT results. Then the method continues in the same way as the Matlock method.

A detailed description of the step-by-step procedure to derive the *P-y* curves from DMT, both for sands and clays, can be found in Robertson et al. (1987), or in US DOT (1992).

Validations of the Robertson method by Marchetti et al. (1991) indicated, for various cases, remarkably good agreement between predicted and observed behavior.

13.3.2 Marchetti et al. (1991) method (clays)

Marchetti et al. (1991) developed further the Robertson method for clay, eliminating from the correlation chain the tortuous step of estimating by DMT the "laboratory soil properties", and evolved a procedure for deriving the *P-y* curves directly from DMT data (in clays).

The *P-y* curve at each depth is completely defined by a hyperbolic tangent equation having the

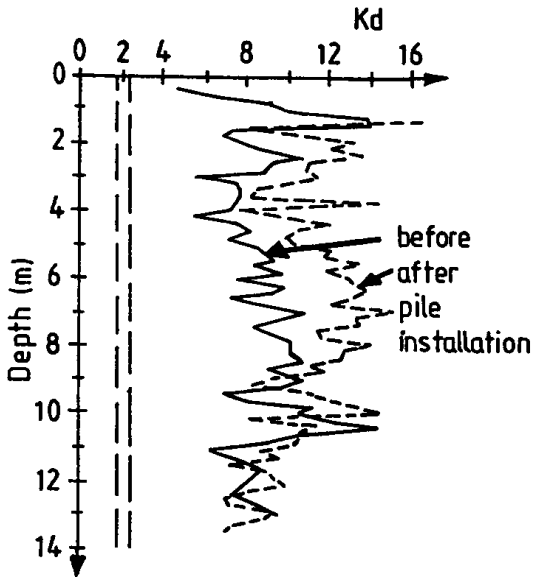

Fig. 38. Before/after DMTs for comparing installation effects of various piles (here an Atlas pile) - DeCock et al. (1993)

BACK

non-dimensional form:

$$\frac{P}{P_u} = \tanh\left(\frac{E_{si} \cdot y}{P_u}\right) \quad (27)$$

with

$$P_u = \alpha \cdot K_1 \cdot (p_0 - u_0) \cdot D \quad (28)$$

$$E_{si} = \alpha \cdot K_2 \cdot E_D \quad (29)$$

$$\alpha = \frac{1}{3} + \frac{2}{3} \cdot \frac{z}{7 \cdot D} \leq 1 \quad (30)$$

where

P_u = ultimate lateral soil resistance [F/L]
E_{si} = initial tangent "soil modulus" [F/L^2]
α = non-dimensional reduction factor for depths less than $z = 7\,D$ (α becomes 1 for $z = 7\,D$)
p_0 = corrected first DMT reading
u_0 = in situ pore pressure
D = pile diameter
z = depth
K_1 = empirical soil resistance coefficient: $K_1 = 1.24$
K_2 = empirical soil stiffness coefficient:

$$K_2 = 10 \cdot (D / 0.5\ \text{m})^{0.5}$$

The authors had several occasions to compare the behavior of laterally loaded test piles with the behavior predicted by the Marchetti et al. (1991) method. They found an amazingly good agreement between observed and predicted pile deflections.

A number of independent validations (NGI, Georgia Tech and tests in Virginia sediments) have indicated that the two methods provide similar predictions, in good agreement with the observed behavior.

It has been noted that DMT provides data even at shallow depths, i.e. in the layers dominating pile response.

13.3.3 Laterally loaded pile groups

A method was developed by Ruesta & Townsend in 1997. The method, based on the results of a large-scale load test on a 16 piles group, derives the *P-y* curves from DMT/PMT.

13.4 DETECTING SLIP SURFACES IN OC CLAY SLOPES

Totani et al. (1997) developed a quick method for detecting active or old slip surfaces in OC clay slopes, based on the inspection of the K_D profiles. The method is based on the following two elements:

(a) The sequence of sliding, remolding and reconsolidation (illustrated in Fig. 39) generally creates a remolded zone of nearly normally consolidated clay, with loss of structure, aging or cementation.

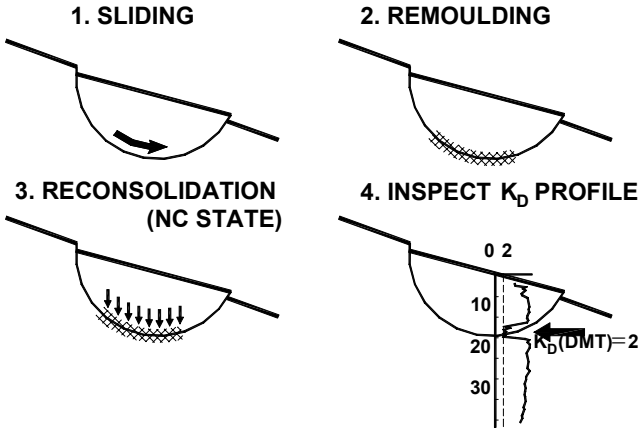

Fig. 39. DMT-K_D method for detecting slip surfaces in OC clay slopes

(b) Since in NC clays $K_D \approx 2$, if an OC clay slope contains layers where $K_D \approx 2$, these layers are likely to be part of a slip surface (active or quiescent).

In essence, the method consists in identifying zones of NC clay in a slope which, otherwise, exhibits an OC profile, using $K_D \approx 2$ as the identifier of the NC zones. Note that the method involves searching for a specific numerical value ($K_D = 2$) rather than for simply "weak zones", which could be detected just as easily also by other in situ tests.

The method was validated by inclinometers or otherwise documented slip surfaces (see Fig. 40).

The "K_D method" provides a faster response than inclinometers in detecting slip surfaces (no need to

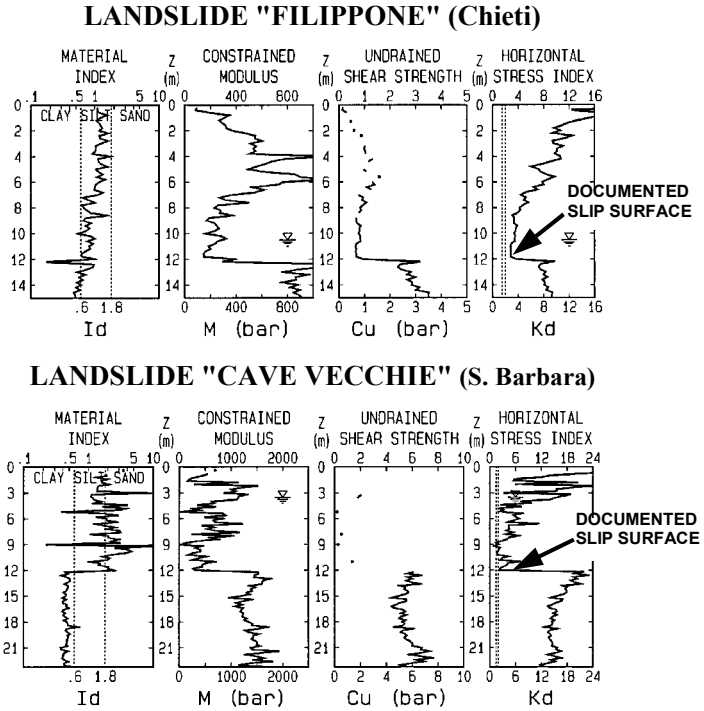

Fig. 40. Examples of $K_D \approx 2$ in documented slip surfaces in two OC clay slopes - (1 bar = 100 kPa)

wait for movements to occur). Moreover, the method enables to detect even possible quiescent surfaces (not revealed by inclinometers), which could reactivate e.g. after an excavation.

On the other hand, the method itself, unlike inclinometers, does not permit to establish if the slope is moving at present and what the movements are. In many cases, DMT and inclinometers can be used in combination (e.g. use K_D profiles to optimize location/depth of inclinometers).

13.5 MONITORING DENSIFICATION / K_0 INCREASE

The DMT has been used in several cases for *monitoring soil improvement*, by comparing DMT results before and after the treatment (see e.g. Fig. 41). Compaction is generally reflected by a brisk increase of *both* K_D and M.

Schmertmann et al. (1986) report a large number of before/after CPTs and DMTs carried out for monitoring dynamic compaction at a power plant site (mostly sand). The treatment increased substantially both q_c and M_{DMT}. The increase in M_{DMT} was found to be approximately *twice* the increase in q_c.

Jendeby (1992) reports before/after CPTs and DMTs carried out for monitoring the deep compaction produced in a loose sand fill with the "vibrowing". He found a substantial increase of both q_c and M_{DMT}, but M_{DMT} increased at a faster rate (nearly *twice*, see Fig. 42), a result similar to the previous case.

Pasqualini & Rosi (1993), in monitoring a vibroflotation treatment, noted that the DMT clearly

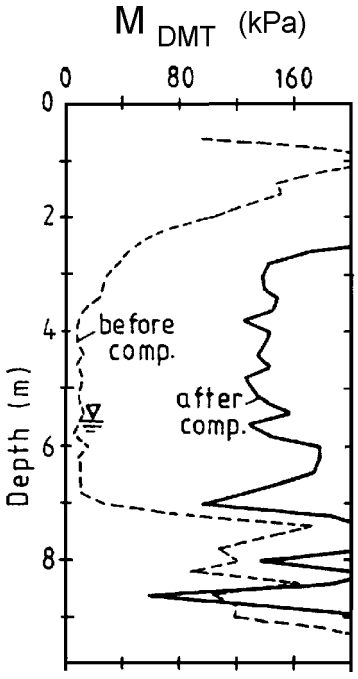

Fig. 41. Before/after DMTs for compaction control (resonant vibrocompaction technique, Van Impe et al. 1994)

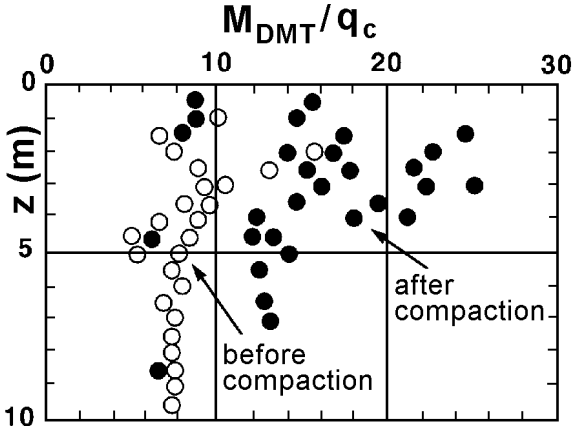

Fig. 42. Ratio M_{DMT}/q_c before/after compaction of a loose sand fill (Jendeby 1992)

detected the improvement even in layers marginally influenced by the treatment, where the benefits were undetected by CPT.

All the above results concurrently suggest that the DMT is sensitive to changes of stresses/density in the soil and therefore is well suited to detect the benefits of the soil improvement (in particular increased σ_h and increased D_r).

An interesting consideration by Schmertmann et al. (1986) is that, since treatments are often aimed at reducing settlements, it would be more rational to base the control and set the specifications in terms of minimum M rather than of minimum D_r.

Stationary DMT as pressure sensing elements

DMT blades have also been used to sense variations in stress state/density using them not as penetration tools, but as stationary spade cells. In this application DMT blades are inserted at the levels where changes are expected, then readings (only A) are taken with time. Various applications of this type have been reported. Peiffer et al. (1994) show (Fig. 43)

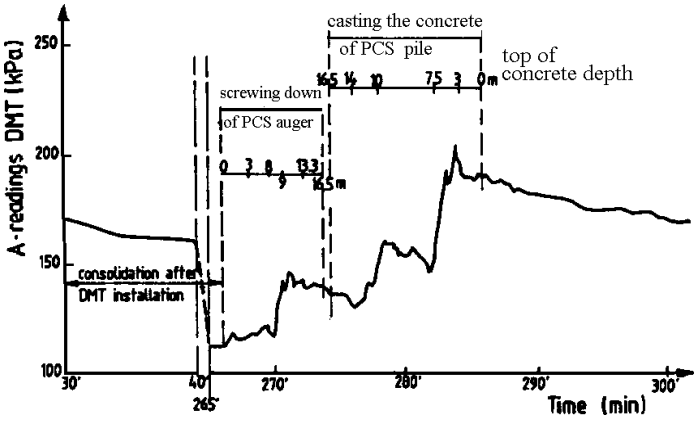

Fig. 43. Stationary DMT blades left in place to feel stress variations caused by the nearby installation of a screw pile (Peiffer et al. 1994)

BACK

representative results of such application, where a DMT blade was left in the soil waiting for the installation of a PCS auger pile. The clear distance between the blade and pile face was 1 pile diameter. Sufficient time was allowed for stabilization of the *A*-reading before the pile insertion.

Fig. 43 shows that the *A*-readings reflected clearly the reconsolidation, the screwing of the piles and the casting of the concrete.

It should be noted, however, that DMT blades used as stationary pressure cells, while able to detect stress *variations*, do not provide *absolute* estimates of the stresses before and after installation, in contrast with before/after continuous DMTs. Moreover each stationary blade can provide information only at one location.

13.6 MONITORING SOIL DECOMPRESSION

The DMT has been used not only to feel the increase, but also the *reduction of density or horizontal stress*.

Peiffer and his colleagues, as mentioned in Section 13.2.4, used the DMT to monitor the decompression caused by various types of piles.

Some investigators (e.g. Hamza & Richards 1995 for Cairo Metro works) have used before/after DMTs to get information on stress changes in the *decompressed* volume of soil behind diaphragm walls.

13.7 SUBGRADE COMPACTION CONTROL

Some experience exists on the use of DMT for evaluating the suitability of the compacted ground surface (i.e. the subgrade soil) to support the road superstructure (subbase, base, pavements).

Borden (1986), based on laboratory work on A-2-4 to A-7-5 soils, tentatively suggested to estimate CBR % (corrected, unsoaked) as:

$$\text{CBR \%} = 0.058\ E_D\ (\text{bar})^{-0.475} \qquad (31)$$

(1 bar = 100 kPa)

Marchetti (1994) describes the use of DMT as a fast acceptance tool for the subgrade compaction in a road in Bangladesh. The procedure was the following:

- Perform a few preliminary DMTs in the *accepted* subgrade (i.e. satisfying the contract specifications)
- Draw an average profile through the above M_{DMT} profiles and use it as an acceptance profile (Fig. 44).

The acceptance M_{DMT} profile could then be used as an economical production method for quality control of the compaction, with only occasional verifications by the originally specified methods (Proctor, laboratory/in situ CBR and plate load tests).

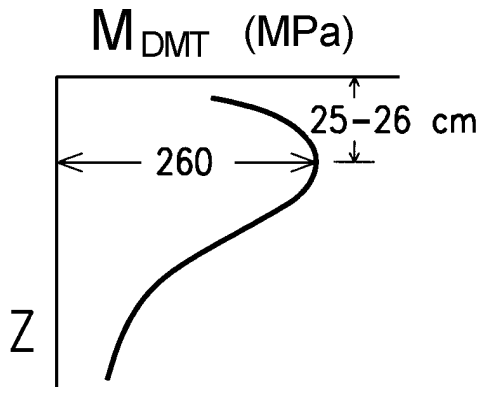

Fig. 44. Example of M_{DMT} acceptance profile for verifying subgrade compaction (Marchetti 1994)

Interestingly, all the after-compaction M_{DMT} profiles had the typical *shape* of the profile shown in Fig. 44, with the maximum M_{DMT} found almost invariably at 25-26 cm depth.

Cases have been reported of after-construction checks with the blade penetrating directly through asphalt.

It can be noted that many today's methods of pavement design make use of moduli rather than other parameters. Hence the availability of the M_{DMT} profiles may be of some usefulness.

13.8 LIQUEFACTION

Fig. 45 summarizes the available knowledge for evaluating sand liquefiability by DMT. The curve currently recommended to estimate the cyclic resistance ratio (*CRR*) from the parameter K_D is the curve by Reyna & Chameau (1991). Such curve is based for a significant part on their curve K_D-D_r (relative to NC sands) shown in Fig. 21.

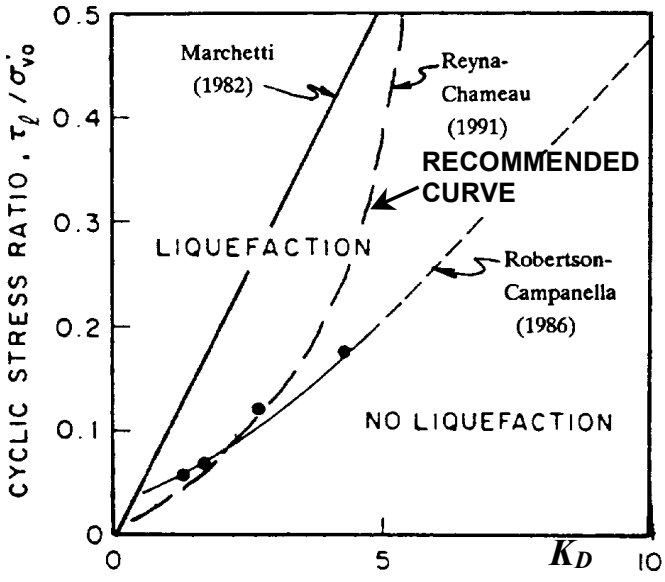

Fig. 45. Recommended curve for estimating *CRR* from K_D (Reyna & Chameau 1991)

This K_D-D_r correlation has been confirmed by additional datapoints obtained by Tanaka & Tanaka (1998) at the sites of Ohgishima and Kemigawa, where D_r was determined on high quality frozen samples.

Once *CRR* has been evaluated from Fig. 45, it is used in liquefaction analysis with the methods developed by Seed (a detailed step-by-step procedure can be found in US DOT 1992).

The high sensitivity of K_D in monitoring densification suggests that K_D may be a sensitive parameter also for sensing sand liquefiability.

In fact a liquefiable sand may be regarded as a sort of "negatively compacted" sand, and it appears plausible that the DMT sensitivity holds in the positive and negative range.

Fig. 45, in combination with the available experience (see Marchetti 1997), suggests that a clean sand (natural or sandfill) is adequately safe against liquefaction (M = 7.5 earthquakes) for the following K_D values:

- Non seismic areas: $K_D > 1.7$
- Low seismicity areas ($a_{max}/g = 0.15$): $K_D > 4.2$
- Medium seismicity areas ($a_{max}/g = 0.25$): $K_D > 5.0$
- High seismicity areas ($a_{max}/g = 0.35$): $K_D > 5.5$

13.9 USE OF DMT FOR FEM INPUT PARAMETERS

Various approaches have been attempted so far.

(a) Use the simplest possible model (linear elastic) assigning to the Young's modulus $E' \approx 0.8\ M_{DMT}$. An example of such application is illustrated by Hamza & Richards (1995).

(b) Model the dilatometer test by a finite elements (FEM) computer program by adjusting the input parameters until the DMT results are correctly "predicted". This approach has the shortcoming of requiring many additional (unknown) parameters.

(c) Another more feasible approach, in problems where linear elasticity is known to give inadequate answers (e.g. settlements outside diaphragm walls), is to check preliminarly the set of intended FEM parameters as follows. Predict for a case of simple loading the settlement by DMT (generally predicting well such settlements - see Section 13.1). Then repeat for the same loading case the settlement prediction by FEM. The comparison of the two predicted settlements may help in the final choice of the FEM parameters.

(d) Other approaches try to identify an "equivalent representative average" DMT strain, with the intent of producing a point in the G-γ degradation curve.

14. SPECIAL CONSIDERATIONS

14.1 DISTORTIONS CAUSED BY THE PENETRATION

Fig. 46 compares the distortions caused in clay by conical tips and by wedges (Baligh & Scott 1975). The deformed grids show that distortions are considerably lower for wedges.

Davidson & Boghrat (1983) observed, using a stereo photograph technique, the strains produced in sand by CPT tips and by DMT blades. The strains in the sand surrounding the cone were found to be considerably higher.

14.2 PARAMETER DETERMINATION BY "TRIANGULATION"

In situ tests represent an "inverse boundary conditions" problem, since they measure *mixed* soil responses rather than *pure* soil properties. In order to isolate *pure* soil properties, it is necessary a "triangulation" (a sort of matrix inversion).

The "triangulation" is possible if more than one response has been measured.

The availability of two independent responses by DMT permits some elementary form of response combination. E.g. M_{DMT} is obtained using both p_0 and p_1.

It may be remarked that one of the two responses, p_0 (hence K_D), reflects stress history, a factor often dominating soil behavior (e.g. compressibility, liquefiability).

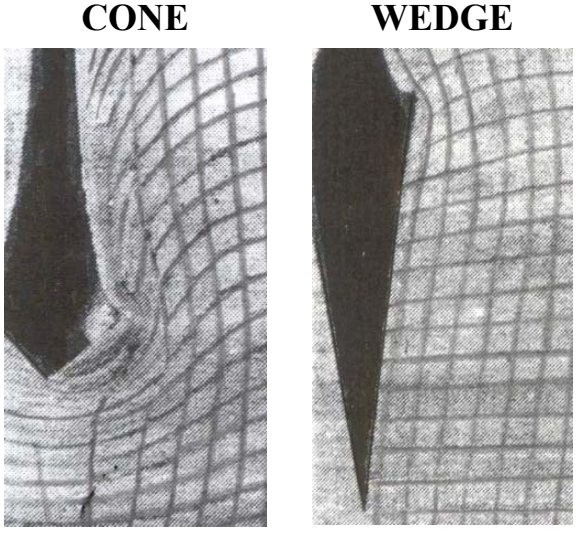

Fig. 46. Deformed grids by Baligh & Scott (1975)

BACK

14.3 ARCHING AND SENSITIVITY TO σ_h

Hughes & Robertson (1985) analyzed the horizontal stresses against the CPT sleeve in sands. They showed that at the level of the conical tip σ_h reaches very high values, while, behind the tip, σ_h undergoes an enormous stress reduction.

The penetration of the cone creates an annular zone of high residual stresses, at some distance from the sleeve. The resulting stiff annulus of precompressed sand is a *screen limiting* σ_h *at interface*, while the enormous unloading *makes undetermined* σ_h. This mechanism may be viewed as a form of an arching phenomenon.

A "plane" tip (DMT width/thickness ratio ≈ 6) should largely reduce arching and improve the possibility of sensing σ_h. Also the stress reduction after the wedge is considerably smaller due to the streamlined shape in the transition zone.

14.4 COMPLEXITY OF THE THEORETICAL MODELS

The DMT is more difficult to model than axisymmetric tips for at least two reasons:

1) The penetration of the DMT blade is a truly three-dimensional problem, in contrast with the two-dimensional nature of penetration of axisymmetric tips
2) The DMT is made of two stages:
   - Stage 1. Insertion.
   - Stage 2. Expansion. Moreover expansion is not the continuation of Stage 1.

A consequence of 1) and 2) is that theoretical solutions have been developed so far only for the first stage (insertion). Solutions have been worked out by Huang (1989), Whittle & Aubeny (1992), Yu et al. (1992), Finno (1993).

15. CROSS RELATIONS WITH RESULTS FROM OTHER IN SITU TESTS

15.1 RELATIONS DMT/PMT

Some information exists about relations between DMT and pressuremeter (PMT) results. Cross relations could help DMT users to apply the design methods developed for PMT.
Preliminary indications, in clays, suggest:

$$p_0 / p_L \approx 0.8,\ p_1 / p_L \approx 1.2 \quad (32)$$

(Schmertmann 1987)

$$p_1 / p_L \approx 1.25,\ E_{PMT} \approx 0.4\ E_D \quad (33)$$

(Kalteziotis et al. 1991)

where p_L = limit pressure from PMT.

Ortigao et al. (1996) investigated the Brasilia porous clay by Menard PMT, Plate Loading Tests (PLT) and DMT. As Kalteziotis, they found that E_{PMT} was less than half E_D and also E_{PLT}. They explained such low PMT moduli with disturbance in the pressuremeter boring. After careful correction of the PMT field curve, E_{PMT} were similar to E_D and E_{PLT}.

Similar ratios (about 1/2) between PMT moduli and DMT moduli are quoted by Brown & Vinson (1998).

Dumas (1992) reports good agreement between settlements calculated with PMT and with DMT.

Contributions on DMT/PMT have also been presented by Lutenegger (1988), Sawada & Sugawara (1995), Schnaid et al. (2000).

15.2 RELATIONS DMT/CPT

As previously mentioned (Section 11.1.2.2), existing data suggest, in sand, the following broad cross relations:

$$M_{DMT}/q_c = 5\text{-}10 \quad \text{in NC sands} \quad (34)$$

$$M_{DMT}/q_c = 12\text{-}24 \quad \text{in OC sands} \quad (35)$$

15.3 RELATIONS DMT/SPT

According to Schmertmann (1988), the estimation of N_{SPT} from DMT would be "a gross misuse of the DMT data ... any such correlation depends on soil type and is probably site specific and perhaps also rig specific".

As a broad indication, Schmertmann (1988) cites the following relation, based on data from a number of US sites:

$$N_{SPT} = M_{DMT}\ (\text{MPa}) / 3 \quad (36)$$

Tanaka & Tanaka (1998) based on data from three sandy sites (Tokyo and Niigata areas) indicate:

$$N_{SPT} = E_D\ (\text{MPa}) / 2.5 \quad (37)$$

Blowcount SPT vs DMT

A limited number of parallel data, obtained in cases where the DMT was driven with the SPT equipment in gravels and silts, indicated very similar values of N_{SPT} and N_{DMT} (number of blows per 30 cm blade penetration).

SUMMARY

The Flat Dilatometer Test (DMT) is a push-in type in situ test quick, simple, economical, highly reproducible.

It is executable with a variety of field equipment.

It provides estimates of various design parameters/information (M, c_u, soil stratigraphy, deposit history).

One of the most fitting application is investigating the in situ soil compressibility for settlements prediction.

Interpretations and applications described by various Authors include:

- Compaction control
- Sensing the effects of pile installations (increase/ decrease of D_r and σ_h)
- Liquefiability of sands
- Verify if a slope contains slip surfaces
- Axially loaded piles in cohesive soils
- Laterally loaded piles
- Pavement subgrade compaction control
- Coefficient of consolidation and permeability of clays
- Phreatic level in sands
- Help in selecting FEM input parameters.

REFERENCES

ASTM Subcommittee D 18.02.10 - Schmertmann, J.H., Chairman (1986). "Suggested Method for Performing the Flat Dilatometer Test". ASTM Geotechnical Testing Journal, Vol. 9, No. 2, June, 93-101.

ASTM D6635-01 (2001). "Standard Test Method for Performing the Flat Plate Dilatometer". Book of Standards Vol. 04.09.

Aversa, S. (1997). "Experimental aspects and modeling in design of retaining walls and excavations" (in Italian). Proc. IV Nat. Conf. of the Geotechn. National Research Council Group, Perugia, Oct., Vol. II, 121-207.

Baldi, G., Bellotti, R., Ghionna, V. & Jamiolkowski, M. (1988). "Stiffness of sands from CPT, SPT and DMT – A critical review". ICE Proc. Conf. Penetration Testing in the UK, Univ. of Birmingham, July, Paper No. 42, 299-305.

Baldi, G., Bellotti, R., Ghionna, V., Jamiolkowski, M. & Lo Presti, D.C.F. (1989). "Modulus of Sands from CPT's and DMT's". Proc. XII ICSMFE, Rio de Janeiro, Vol. 1, 165-170.

Baldi, G., Bellotti, R., Ghionna, V., Jamiolkowski, M., Marchetti, S. & Pasqualini, E. (1986). "Flat Dilatometer Tests in Calibration Chambers". Proc. In Situ '86, ASCE Spec. Conf. on "Use of In Situ Tests in Geotechn. Engineering", Virginia Tech, Blacksburg, VA, June, ASCE Geotechn. Special Publ. No. 6, 431-446.

Baligh, M.M. (1985). "Strain path method". ASCE Jnl GE, Vol. 111, No. GT9, 1108-1136.

Baligh, M.M. & Scott, R.F. (1975). "Quasi Static Deep Penetration in Clays". ASCE Jnl GE, Vol. 101, No. GT11, 1119-1133.

Benoit, J. (1989). Personal communication to S. Marchetti.

Boghrat, A. (1987). "Dilatometer Testing in Highly Overconsolidated Soils". Technical Note, ASCE Journal of Geotechn. Engineering, Vol. 113, No. 5, May, 516.

Borden, R.H., Aziz, C.N., Lowder, W.M. & Khosla, N.P. (1986). "Evaluation of Pavement Subgrade Support Characteristics by Dilatometer Test". Proc. 64th Annual Meeting of the Transportation Res. Board, June, TR Record 1022.

Brown, D.A. & Vinson, J. (1998). "Comparison of strength and stiffness parameters for a Piedmont residual soil". Proc. First Int. Conf. on Site Characterization ISC '98, Atlanta, GA, Apr., Vol. 2, 1229-1234.

Burghignoli, A., Cavalera, L., Chieppa, V., Jamiolkowski, M., Mancuso, C., Marchetti, S., Pane, V., Paoliani, P., Silvestri, F., Vinale, F. & Vittori, E. (1991). "Geotechnical characterization of Fucino clay". Proc. X ECSMFE, Florence, Vol. 1, 27-40.

Burland, J.B., Broms, B.B. & De Mello, V.F.B. (1977). "Behavior of foundations and structures". Proc. IX ICSMFE, Tokyo, Vol. 2, 495-546.

Campanella, R.G. & Robertson, P.K. (1991). "Use and Interpretation of a Research Dilatometer". Canad. Geotechn. Journal, Vol. 28, 113-126.

Campanella, R.G., Robertson, P.K., Gillespie, D.G. & Grieg, J. (1985). "Recent Developments in In-Situ Testing of Soils". Proc. XI ICSMFE, S. Francisco, Vol. 2, 849-854.

Carter, J.P., Randolph, M.F. & Wroth, C.P. (1979). "Stress and pore pressure changes in clay during and after the expansion of a cylindrical cavity". Int. Jnl Numer. Anal. Methods Geomech., Vol. 3, 305-322.

Davidson, J. & Boghrat, A. (1983). "Displacements and Strains around Probes in Sand". Proc. ASCE Spec. Conf. on "Geotechnical Practice in Offshore Engineering", Austin, TX, Apr., 181-203.

De Cock, F., Van Impe, W.F. & Peiffer, H. (1993). "Atlas screw piles and tube screw piles in stiff tertiary clays". Proc. BAP II, Ghent, 359-367.

Didaskalou, G. (1999). "Comparison between observed and DMT predicted settlements of the Hyatt Regency Hotel shallow foundation on a compressible silt in Thessaloniki". Personal communication to S. Marchetti.

Dumas, J.C. (1992). "Comparisons of settlements predicted by PMT and DMT in a silty-sandy soil in Quebec". Personal communication to S. Marchetti.

Durgunoglu, H.T. & Mitchell, J.K. (1975). "Static Penetration Resistance of Soils, I - Analysis, II - Evaluation of the Theory and Implications for Practice". ASCE Spec. Conf. on "In Situ Measurement of Soil Properties", Raleigh, NC, Vol. 1.

Eurocode 7 (1997). Geotechnical design - Part 3: Design assisted by field testing, Section 9: Flat dilatometer test (DMT). Final Draft, ENV 1997-3, Apr., 66-73. CEN - European Committee For Standardization.

Failmezger, R.A., Rom, D. & Ziegler, S.B. (1999). "Behavioral Characteristics of Residual Soils. SPT? - A Better Approach to Site Characterization of Residual Soils using other In-Situ Tests". ASCE Geot. Special Pub. No. 92, Edelen, Bill, ed., ASCE, Reston, VA, 158-175.

Finno, R.J. (1993). "Analytical Interpretation of Dilatometer Penetration Through Saturated Cohesive Soils". Geotéchnique, 43, No. 2, 241-254.

Fretti, C., Lo Presti, D. & Salgado, R. (1992). "The Research Dilatometer: In Situ and Calibration Chamber Test Results". Riv. Italiana di Geotecnica, 26, No. 4, 237-243.

BACK

Gravesen, S. (1960). "Elastic Semi-Infinite Medium Bounded by a Rigid Wall with a Circular Hole". Laboratoriet for Bygninsteknik, Danmarks Tekniske Højskole, Meddelelse No. 10, Copenhagen.

Hamza, M. & Richards, D.P. (1995). "Correlations of DMT, CPT and SPT in Nile Basin Sediment". Proc. XI Afr. Conf. SMFE, Cairo, 437-446.

Hayes, J.A. (1990). "The Marchetti Dilatometer and Compressibility". Seminar on "In Situ Testing and Monitoring", Southern Ont. Section of Canad. Geot. Society, Sept., 21 pp.

Hryciw, R.D. (1990). "Small-Strain-Shear Modulus of Soil by Dilatometer". ASCE Jnl GE, Vol. 116, No. 11, Nov., 1700-1716.

Huang, A.B. (1989). "Strain-Path Analyses for Arbitrary Three Dimensional Penetrometers". Int. Jnl for Num. and Analyt. Methods in Geomechanics, Vol. 13, 561-564.

Huang, A.B., Bunting, R.D. & Carney, T.C. (1991). "Piezoblade Tests in a Clay Calibration Chamber". Proc. ISOCCT-1, Clarkson Univ., Potsdam, NY, June.

Hughes, J.M.O. & Robertson, P.K. (1985). "Full displacement pressuremeter testing in sand". Canad. Geot. Jnl, Vol. 22, No. 3, Aug., 298-307.

Iwasaki, K., Tsuchiya, H., Sakai, Y. & Yamamoto, Y. (1991). "Applicability of the Marchetti Dilatometer Test to Soft Ground in Japan". Proc. GEOCOAST '91, Yokohama, Sept., 1/6.

Jamiolkowski, M. (1995). "Opening address". Proc. Int. Symp. on Cone Penetration Testing CPT '95, Swedish Geot. Soc., Linköping, Vol. 3, 7-15.

Jamiolkowski, M., Ghionna, V., Lancellotta, R. & Pasqualini, E. (1988). "New Correlations of Penetration Tests for Design Practice". Proc. ISOPT-1, Orlando, FL, Vol. 1, 263-296.

Jendeby, L. (1992). "Deep Compaction by Vibrowing". Proc. Nordic Geotechnical Meeting NGM-92, Vol. 1, 19-24.

Kaggwa, W.S., Jaksa, M.B. & Jha, R.K. (1995). "Development of automated dilatometer and comparison with cone penetration test at the Univ. of Adelaide, Australia". Proc. Int. Conf. on Advances in Site Investig. Practice, ICE, London, Mar.

Kalteziotis, N.A., Pachakis, M.D. & Zervogiannis, H.S. (1991). "Applications of the Flat Dilatometer Test (DMT) in Cohesive Soils". Proc. X ECSMFE, Florence, Vol. 1, 125-128.

Kamey, T. & Iwasaki, K. (1995). "Evaluation of undrained shear strength of cohesive soils using a Flat Dilatometer". Soils and Foundations, Vol. 35, No. 2, June, 111-116.

Kulhawy, F. & Mayne, P. (1990). "Manual on Estimating Soil Properties for Foundation Design". Electric Power Research Institute, Cornell Univ., Ithaca, NY, Report No. EL-6800, 250 pp.

Lacasse, S. (1986). "In Situ Site Investigation Techniques and Interpretation for Offshore Practice". Norwegian Geotechnical Inst., Report 40019-28, Sept.

Lacasse, S. & Lunne, T. (1986). "Dilatometer Tests in Sand". Proc. In Situ '86, ASCE Spec. Conf. on "Use of In Situ Tests in Geotechn. Engineering", Virginia Tech, Blacksburg, VA, June, ASCE Geotechn. Special Publ. No. 6, 686-699.

Lacasse, S. & Lunne, T. (1988). "Calibration of Dilatometer Correlations". Proc. ISOPT-1, Orlando, FL, Vol. 1, 539-548.

Leonards, G.A. & Frost, J.D. (1988). "Settlements of Shallow Foundations on Granular Soils". ASCE Jnl GE, Vol. 114, No. 7, July, 791-809.

Lunne, T., Lacasse, S. & Rad, N.S. (1989). "State of the Art Report on In Situ Testing of Soils". Proc. XII ICSMFE, Rio de Janeiro, Vol. 4, 2339-2403.

Lutenegger, A.J. (1988). "Current status of the Marchetti dilatometer test". Special Lecture, Proc. ISOPT-1, Orlando, FL, Vol. 1, 137-155.

Lutenegger, A.J. & Kabir, M.G. (1988). "Dilatometer C-reading to help determine stratigraphy". Proc. ISOPT-1, Orlando, FL, Vol. 1, 549-554.

Marchetti, S. (1980). "In Situ Tests by Flat Dilatometer". ASCE Jnl GED, Vol. 106, No. GT3, Mar., 299-321.

Marchetti, S. (1982). "Detection of liquefiable sand layers by means of quasi static penetration tests". Proc. 2nd European Symp. on Penetration Testing, Amsterdam, May, Vol. 2, 689-695.

Marchetti, S. (1985). "On the Field Determination of K_0 in Sand". Discussion Session No. 2A, Proc. XI ICSMFE, San Francisco, Vol. 5, 2667-2673.

Marchetti, S. (1994). "An example of use of DMT as a help for evaluating compaction of subgrade and underlying embankment". Internal Techn. Note, Draft.

Marchetti, S. (1997). "The Flat Dilatometer: Design Applications". Proc. Third International Geotechnical Engineering Conference, Keynote lecture, Cairo University, Jan., 421-448.

Marchetti, S. (1999). "On the calibration of the DMT membrane". L'Aquila Univ., Unpublished report, Mar.

Marchetti, S. & Crapps, D.K. (1981). "Flat Dilatometer Manual". Internal Report of G.P.E. Inc.

Marchetti, S. & Totani, G. (1989). "C_h Evaluations from DMTA Dissipation Curves". Proc. XII ICSMFE, Rio de Janeiro, Vol. 1, 281-286.

Marchetti, S., Totani, G., Calabrese, M. & Monaco, P. (1991). "P-y curves from DMT data for piles driven in clay". Proc. 4th Int. Conf. on Piling and Deep Foundations, DFI, Stresa, Vol. 1, 263-272.

Marchetti, S., Totani, G., Campanella, R.G., Robertson, P.K. & Taddei, B. (1986). "The DMT-σ_{hc} Method for Piles Driven in Clay". Proc. In Situ '86, ASCE Spec. Conf. on "Use of In Situ Tests in Geotechn. Engineering", Virginia Tech, Blacksburg, VA, June, ASCE Geotechn. Special Publ. No. 6, 765-779.

Massarsch, K.R. (1994). "Settlement Analysis of Compacted Granular Fill". Proc. XIII ICSMFE, New Delhi, Vol. 1, 325-328.

Matlock, H. (1970). "Correlation for Design of Laterally Loaded Piles in Soft Clay". Proc. II Offshore Technical Conf., Houston, TX, Vol. 1, 577-594.

Mayne, P.W. & Martin, G.K. (1998). "Seismic flat dilatometer test in Piedmont residual soils". Proc. First Int. Conf. on Site Characterization ISC '98, Atlanta, GA, Apr., Vol. 2, 837-843.

Mesri, G., Feng, T.W. & Shahien, M. (1999). "Coefficient of Consolidation by Inflection Point Method". ASCE Jnl GGE, Vol. 125, No. 8, Aug., 716-718.

Nash, D.F.Y., Powell, J.J.M. & Lloyd, I.M. (1992). "Initial investigations of the soft clay test site at Bothkennar". Geotéchnique, 42, No. 2, 163-181.

Ortigao, J.A.R., Cunha, R.P. & Alves, L.S. (1996). "In situ tests in Brasilia porous clay". Canad. Geot. Jnl, Vol. 33, No. 1, Feb., 189-198.

Pasqualini, E. & Rosi, C. (1993). "Experiences from a vibroflotation treatment" (in Italian). Proc. Annual Meeting of the Geotechn. National Research Council Group, Rome, Nov., 237-240.

Peiffer, H. (1997). "Evaluation and automatisation of the dilatometer test and interpretation towards the shaft bearing capacity of piles". Doctoral Thesis, Ghent University.

Peiffer, H. & Van Impe, W.F. (1993). "Evaluation of pile performance based on soil stress measurements - Field test program". Proc. BAP II, Ghent, 385-389.

Peiffer, H., Van Impe, W.F., Cortvrindt, G. & Bottiau, M. (1993). "Evaluation of the influence of pile execution parameters on the soil condition around the pile shaft of a PCS-pile". Proc. BAP II, Ghent, 217-220.

Peiffer, H., Van Impe, W.F., Cortvrindt, G. & Bottiau, M. (1994). "DMT Measurements around PCS-Piles in Belgium". Proc. XIII ICSMFE, New Delhi, Vol. 2, 469-472.

Pelnik, T.W., Fromme, C.L., Gibbons, Y.R. & Failmezger, R.A. (1999). "Foundation Design Applications of CPTU and DMT Tests in Atlantic Coastal Plain Virginia". Transp. Res. Board, 78th Annual Meeting, Jan., Washington, D.C.

Powell, J.J.M., Lunne, T. & Frank, R. (2001 a). "Semi-Empirical Design Procedures for axial pile capacity in clays". Proc. XV ICSMGE, Istanbul, Aug., Balkema.

Powell, J.J.M., Shields, C.H., Dupla, J.C. & Mokkelbost, K.H. (2001 b). "A new DMT method for the design of axially loaded driven piles in clay soils". Submitted for publication.

Powell, J.J.M. & Uglow, I.M. (1988). "The Interpretation of the Marchetti Dilatometer Test in UK Clays". ICE Proc. Conf. Penetration Testing in the UK, Univ. of Birmingham, July, Paper No. 34, 269-273.

Reyna, F. & Chameau, J.L. (1991). "Dilatometer Based Liquefaction Potential of Sites in the Imperial Valley". Proc. 2nd Int. Conf. on Recent Advances in Geot. Earthquake Engrg. and Soil Dyn., St. Louis, May.

Robertson, P.K. & Campanella, R.G. (1986). "Estimating Liquefaction Potential of Sands Using the Flat Plate Dilatometer". ASTM Geotechn. Testing Journal, Mar., 38-40.

Robertson, P.K., Campanella, R.G., Gillespie, D. & By, T. (1988). "Excess Pore Pressures and the Flat Dilatometer Test". Proc. ISOPT-1, Orlando, FL, Vol. 1, 567-576.

Robertson, P.K., Davies, M.P. & Campanella, R.G. (1987). "Design of Laterally Loaded Driven Piles Using the Flat Dilatometer". Geot. Testing Jnl, Vol. 12, No. 1, Mar., 30-38.

Ruesta, F. & Townsend, F.C. (1997). "Evaluation of Laterally Loaded Pile Group at Roosvelt Bridge". Jnl ASCE GGE, 123, 12, Dec., 1153-1161.

Sawada, S. & Sugawara, N. (1995). "Evaluation of densification of loose sand by SBP and DMT". Proc. 4th Int. Symp. on Pressuremeter, May, 101-107.

Schmertmann, J.H. (1982). "A method for determining the friction angle in sands from the Marchetti dilatometer test (DMT)". Proc. 2nd European Symp. on Penetration Testing, ESOPT-II, Amsterdam, Vol. 2, 853-861.

Schmertmann, J.H. (1983). "Revised Procedure for Calculating K_o and OCR from DMT's with $I_D > 1.2$ and which Incorporates the Penetration Measurement to Permit Calculating the Plane Strain Friction Angle". DMT Digest No. 1. GPE Inc., Gainesville, FL.

Schmertmann, J.H. (1986). "Dilatometer to compute Foundation Settlement". Proc. In Situ '86, ASCE Spec. Conf. on "Use of In Situ Tests in Geotechn. Engineering", Virginia Tech, Blacksburg, VA, June, ASCE Geotechn. Special Publ. No. 6, 303-321.

Schmertmann, J.H., Baker, W., Gupta, R. & Kessler, K. (1986). "CPT/DMT Quality Control of Ground Modification at a Power Plant". Proc. In Situ '86, ASCE Spec. Conf. on "Use of In Situ Tests in Geotechn. Engineering", Virginia Tech, Blacksburg, VA, June, ASCE Geotechn. Special Publ. No. 6, 985-1001.

Schmertmann, J.H. (1987). "Some interrelationship with p_0 in clays". DMT Digest No. 9, Item 9A, Schmertmann Ed., May.

Schmertmann, J.H. (1988). "Guidelines for Using the CPT, CPTU and Marchetti DMT for Geotechnical Design". Rept. No. FHWA-PA-87-022+84-24 to PennDOT, Office of Research and Special Studies, Harrisburg, PA, in 4 volumes with the 3 below concerning primarily the DMT: Vol. I - Summary (78 pp.); Vol. III - DMT Test Methods and Data Reduction (183 pp.); Vol. IV - DMT Design Method and Examples (135 pp.).

Schmertmann, J.H. (1991). "Pressure Dissipation Tests. A-B-C vs A_2 vs A". DMT Digest No. 12, Section 12C, Schmertmann Ed., Dec.

Schnaid, F., Ortigao, J.A.R., Mantaras, F.M, Cunha, R.P. & MacGregor, I. (2000). "Analysis of self-boring pressuremeter (SBPM) and Marchetti dilatometer (DMT) tests in granite saprolites". Canad. Geot. Jnl, Vol. 37, 4, Aug., 796-810.

Skiles, D.L. & Townsend, F.C. (1994). "Predicting Shallow Foundation Settlement in Sands from DMT". Proc. Settlement '94 ASCE Spec. Conf., Texas A&M Univ., Geot. Spec. Publ. No. 40, Vol. 1, 132-142.

Steiner, W. (1994). "Settlement Behavior of an Avalanche Protection Gallery Founded on Loose Sandy Silt". Proc. Settlement '94 ASCE Spec. Conf., Texas A&M Univ., Geot. Spec. Publ. No. 40, Vol. 1, 207-221.

Steiner, W., Metzger, R. & Marr, W.A. (1992). "An Embankment on Soft Clay with an Adjacent Cut". Proc. ASCE Conf. on Stability and Performance of Slopes and Embankments II, Berkeley, CA, 705-720.

Sully, J.P. & Campanella, R.G. (1989). "Correlation of Maximum Shear Modulus with DMT Test Results in Sand". Proc. Proc. XII ICSMFE, Rio de Janeiro, Vol. 1, 339-343.

Tanaka, H. & Tanaka, M. (1998). "Characterization of Sandy Soils using CPT and DMT". Soils and Foundations, Japanese Geot. Soc., Vol. 38, No. 3, 55-65.

Terzaghi, K. & Peck, R.B. (1967). "Soil Mechanics in Engineering Practice". John Wiley & Sons, NY.

Totani, G., Calabrese, M., Marchetti, S. & Monaco, P. (1997). "Use of in situ flat dilatometer (DMT) for ground characterization in the stability analysis of slopes". Proc. XIV ICSMFE, Hamburg, Vol. 1, 607-610.

Totani, G., Calabrese, M. & Monaco, P. (1998). "In situ determination of c_h by flat dilatometer (DMT)". Proc. First Int. Conf. on Site Characterization ISC '98, Atlanta, GA, Apr., Vol. 2, 883-888.

Totani, G., Marchetti, S., Calabrese, M. & Monaco, P. (1994). "Field studies of an instrumented full-scale pile driven in clay". Proc. XIII ICSMFE, New Delhi, Vol. 2, 695-698.

US DOT - Briaud, J.L. & Miran, J. (1992). "The Flat Dilatometer Test". Departm. of Transportation - Fed. Highway Administr., Washington, D.C., Publ. No. FHWA-SA-91-044, Feb., 102 pp.

Van Impe, W.F., De Cock, F., Massarsch, R. & Menge', P. (1994). "Recent Experiences and Developments of the Resonant Vibrocompaction Technique". Proc. XIII ICSMFE, New Delhi, Vol. 3, 1151-1156.

Whittle, A.J. & Aubeny, C.P. (1992). "The effects of installation disturbance on interpretation of in situ tests in clay". Proc. Wroth Memorial Symp. Predictive Soil Mechanics, Oxford, July, 742-767.

Woodward, M.B. & McIntosh, K.A. (1993). "Case history: Shallow Foundation Settlement Prediction Using the Marchetti Dilatometer". ASCE Annual Florida Sec. Meeting - Abstract & Conclusions.

Yu, H.S., Carter, J.P. & Booker, J.R. (1992). "Analysis of the Dilatometer Test in Undrained Clay". Proc. Wroth Memorial Symp. Predictive Soil Mechanics, Oxford, July, 783-795.

BACK

CASE STUDIES OF PROJECTS USING DILATOMETER TESTS

Prediction of P-y Curves from Dilatometer Tests Case Histories and Results

J. B. Anderson
Department of Civil Engineering, University of North Carolina Charlotte, Charlotte, NC, USA

F.C. Townsend
Department of Civil and Coastal Engineering, University of Florida, Gainesville, FL, USA

B. Grajales
URS Corporation, Tampa, FL, USA

Keywords: dilatometer, pile, drilled shaft, lateral load test

ABSTRACT: The p-y method made popular by Reese (1983) has become the de facto method for the analysis of deep foundation systems under lateral loading. This approach has been implemented in computer programs such as FB-MultiPier and LPILE. Both codes include typical p-y curves based on soil parameters, but also allow the input of custom user defined curves. Based on original work by Roberston et al. (1989), p-y curves were generated based on dilatometer soundings at sites where lateral load tests were performed. The sites and tests include:

1) Roosevelt Bridge - Stuart, Florida: single pile and pile group load tests

2) US17 Bypass - Wilmington, North Carolina: single pile and pile/drilled shaft group load tests

3) Rio Puerto Nuevo - San Juan, Puerto Rico: steel pipe pile load tests

4) Salt Lake City International Airport – Utah: single pile and pile group load tests

5) East Pascagoula River Bridge - Mississippi: pile/drilled shaft group load test

6) Auburn NGES - Opelika Alabama: multiple drilled shaft and pile group load tests

The p-y curves were implemented in the program FB-MultiPier to predict the results of a lateral load test at each site. The paper documents the dilatometer sounding data and associated p-y curves. For each load test, the general geometry is presented and the actual load test data is plotted with the dilatometer based predictions.

1 INTRODUCTION

The p-y method, made popular by Reese (1983), is commonly used in the analysis of deep foundations (piles or drilled shafts) under lateral load. The computer programs LPILE (Ensoft, 2005) and FB-MultiPier (Florida BSI, 2005), the standard tools for lateral substructure analysis, include the p-y method. While normalized p-y curves developed from limited research sites are included both programs, it is most useful to develop custom p-y curves derived from insitu soil tests at the project site.

The dilatometer test (DMT) was developed by Marchetti (1980). The DMT is conducted by pushing a flat blade with a laterally inflatable disc to a test depth, then inflating the disc into the soil using gas pressure. The disc moves 1.1 mm laterally, thereby performing an insitu small strain "lateral load test" (figure 1). Thus, logically, the results of the DMT test have been used to develop p-y curves for soil, including those by Robertson et al. (1989) and Gabr and Borden (1988).

Validating of p-y curves generated from any method is accomplished by simulating a full pile or drilled shaft load test using software such as LPILE or FB-MultPier. In this paper, six load tests are examined where DMT tests were performed prior to foundation installation. In the following discussion, each case history is detailed with The DMT sounding data, pile load tests details, derived p-y curves, and comparison of load test and computer based simulation.

BACK

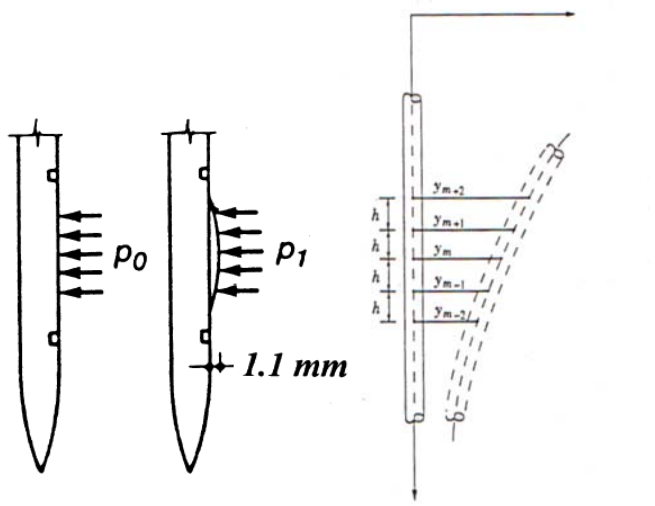

Figure 1 DMT Inflation versus Pile Lateral Loading.

2 SOIL STRUCTURE INTERACTION WITH P-Y CURVES

As previously mentioned, the dilatometer test produces one millimeter of lateral deformation; therefore, there are no increments of pressure with which to develop a load-deformation curve. Therefore, a "hybrid method" using the properties determined from the dilatometer indices are used in conjunction with a parabolic function to develop p-y curves. For this case history, curves determined from dilatometer tests were developed based on the method presented by Robertson et al. (1989).

For cohesive soils a cubic parabolic p-y curve was suggested:

$$\frac{P}{P_u} = 0.5\left(\frac{y}{y_c}\right)^{0.33} \quad (1)$$

$$y_c = \frac{23.67 S_u D^{0.5}}{F_c E_D} \quad (2)$$

where y_c is the reference deflection, Su is the undrained strength of the soil, D is the pile diameter, F_c is a factor ≈ 10, and E_D is the dilatometer modulus. The evaluation of the ultimate lateral resistance Pu is given as:

$$P_u = N_p S_u D \quad (3)$$

At considerable depths Np ≈ 9, but near the surface it reduces to a range of 2 - 4; accordingly,

$$N_p = 3 + \frac{\sigma_{vo}'}{S_u} + \left(J\frac{x}{D}\right) \quad < 9.0 \quad (4)$$

and x = depth, σ_{v0}' = effective stress at depth x, and J = 0.5 (soft clay) to 0.25 (stiff clay).

For cohesionless soils, the same cubic parabola, equation (1) is used, where P_u is from Reese et al. (1974) and Murchison and O'Neill (1984) and is the lesser of:

$$P_u = \sigma_{v0}'[D(K_p - K_a) + xK_p \tan\phi' \tan\beta] \quad (5)$$

$$P_u = \sigma_{v0}' D[K_p{}^3 + 2K_a K_p{}^2 \tan\phi' - \tan\phi' - K_a] \quad (6)$$

and

$$\beta \text{ is } 45^o + \frac{\phi'}{2} \quad (7)$$

And y_c is:

$$y_c = \frac{4.17 \sin\phi' \sigma_{v0}'}{E_D F_\phi (1 - \sin\phi')} D \quad (8)$$

where F_ϕ is an empirical factor equal to 1 for cohesionless soil.

Data from a dilatometer soundings at the each test site was reduced using the computer program "Dilly" (GPE Inc., 1993) to get values for ϕ or S_u and E_D for the p-y curves.

3 CASE HISTORIES

In this section, each case history will be briefly introduced. It is the intent of the authors to provide enough information on the case history that the reader may be able to generate p-y curves and perform his or her own analysis. Therefore, the complete DMT sounding, p-y curves generated, pile properties, load test geometry, and the results of the simulation by the author are included at the end of the paper.

3.1 *Roosevelt Bridge - Stuart, Florida*

A submerged 4 by 4 free-head pile group of 760 mm prestressed concrete piles was laterally loaded as part of a test program for the construction of a new bridge over the St. Lucie River by the Florida Department of Transportation. An additional load test on pile 9, one of the piles from the group, was performed by pushing the pile in the opposite direction from the group load test. (Ruesta, and Townsend, 1997).

The soil profile at Roosevelt consisted of layers of loose sand over cemented sand, both with shell fragments.

3.2 *US 17 Bypass – Wilmington North Carolina*

The test program was funded by the NCDOT and NCHRP for a new US 17 bridge over the NE Cape Fear River near Wilmington, NC. At Test Area 2, a 915mm diameter concrete cylinder pile with a wall thickness of 152mm and embedded length of 26.4m was laterally loaded against a 762mm square prestressed concrete pile embedded 27.6 m.

The soil profile at the Wilmington Bypass site was comprised of two zones of sand: a loose alluvial fine sand layer over a dense fine sand known as the Pee Dee formation.

3.3 *Rio Puerto Nuevo, San Juan, Puerto Rico*

The test program consisted of pushing apart two 1219mm with a 19mm thick wall open ended steel pipe piles separated by approximately 7.6m as part of a test program for a cantilever wall system by the US Army Corps of Engineers – Jacksonville District. One pile was driven to elevation -13.1m (short pile), while the other to elevation -19.7m (long pile). Two static load tests were performed on the piles. The first "pre-excavation" test was performed with the ground surface at elevation +0.7m. Subsequently, a cofferdam was installed and the soil excavated to elevation – 5m, "post-excavation", to simulate planned dredging in front of the wall. The post excavation load test was considered in this study.

The subsurface profile at Puerto Nueveo was predominantly clay with some trace fine sands.

3.4 *Salt Lake City International Airport - Utah*

The project consisted of four lateral load tests; two static tests and two StatNAMIC. One of the static tests was performed upon a single pile and the other upon a free-head pile group. According to Peterson (1996), the single pile test, analyzes in this discussion, was performed to obtain the row-multipliers in order to normalize the pile group results. A sheet pile wall was used as reaction.

The soil profile at this site consists of interbedded layers of sand and clay, however, the predominant soil type in the critical depth for lateral analysis was clay.

3.5 *East Pascagoula River Bridge - Mississippi*

The test program consisted of a submerged group of two 2100mm drilled shafts spaced at 3 diameters, which reacted against a group of 6 762mm prestressed concrete piles. Both groups were embedded into 2.4-m thick concrete caps and subjected to static and StatNAMIC lateral loadings (Anderson and Townsend, 1999). For this analysis of the drilled shafts p-y multipliers of 0.8 (leading) and 0.4 (trailing) and for the piles (Ruesta and Townsend, 1997) were used.

Soils at Pascagoula were interbedded layers of sand and clay.

3.6 *Auburn NGES - Opelika, Alabama*

Six 915mm drilled shafts were laterally loaded as part of a static and Statnamic test program for Alabama DOT and FHWA project at Auburn University. Shaft 2 in the SW was analyzed for this study (Anderson at al., 1999) (Brown and Vinson, 1998).

The soil at the Auburn site is characteristic of the Piedmont geological province of the southeastern United States. These soils are derived from weathering of metamorphic rocks, predominantly gneisses and schists of and are composed of micaceous sandy silts.

4 DISCUSSION

Each of the load tests were simulated using FB-Pier, the earlier generation of the program that is currently distributed at FB-MultPier. The structural details of each pile or drilled shaft were collected including the shape, reinforcing details, strength, and modulus. FB-MultiPier includes a full non-linear structural model that accounts for cracked and yielding sections. As the structural models are well developed, the focus of this discussion will attribute quality of fit to soil parameters.

The load tests can be separated into several categories. The prominent groups to consider are piles and drilled shafts and cohesionless and cohesive soils. Of the six tests, two are on drilled shafts (Pascagoula and Auburn) and the remaining four are piles (Roosevelt, Wilmington, Puerto Nuevo, and Salt Lake City). The soils represented, three are predominantly cohesionless (Roosevelt, Wilmington, and Auburn), and three have significant cohesive soils (Pascagoula, Puerto Nuevo, and Salt Lake City).

When comparing the load test simulations between drilled shafts and piles, it does not appear that DMT p-y curves work better for drilled shafts or piles.

Considering the difference between cohesive and cohesionless soils, the data suggest that predictions in cohesionless materials are better than those in cohesive materials.

Within the piles, two were prestressed concrete and two were pipe piles. Predictions among the piles may show slightly better prediction for concrete piles versus steel pipe. However, this may be affected by the cohesionless versus cohesive behavior discussed previously.

5 SUMMARY AND CONCLUSION

Six deep foundation load tests were simulated using p-y curves generated from DMT tests. The six tests represent foundation types including drilled shafts, concrete piles, and steel pipe piles. In addition, half

BACK

of the tests were performed in cohesionless soil and the remainder in cohesive soils. From these analyses, the following conclusions are drawn:

1) DMT generated p-y curves provide a better model for cohesionless soils than cohesive
2) There is little difference between the goodness of predictions for DMT p-y curves for piles and drilled shafts.
3) DMT p-y curves may better suited for concrete piles over pipe piles.

It should be noted that these conclusions have been drawn from limited case histories. The author continues to collect case studies of lateral load tests with DMT and other insitu tests for verification of these methods.

6 ACKNOWLEDGEMENTS

Access to load test data was essential to the research this paper was based on. Individuals and agencies that shared data include:

Paul Bullock – Schmertmann and Crapps
Dan Brown – Auburn University
Florida Department of Transportation
Scott Hidden – North Carolina Department of Transportation
Mike Muchard and Don Robertson – Applied Foundation Testing
Kyle Rollins – Brigham Young University
Kimberly Spoor and Pauline Smith – US Army Corps of Engineers Jacksonville District

7 REFERENCES

Anderson, J.B., and Townsend, F.C. (1999). "Validation of P-y Curves from Pressuremeter Tests at Pascagoula Mississippi," Proc., XI Panamerican Conference on Soil Mechanics and Geotechnical Engineering, August.

Anderson, J. B., Grajales, B., Townsend, F. C. and Brown, D., (1999). "Validation of P-y Curves from Pressuremeter and Dilatometer Tests at Auburn, Alabama," Behavioral Characteristics of Residual Soils, ASCE GSP 92, Bill Edelen ed., American Society of Civil Engineers, pp 77-87.

Brown, D.A. and J. Vinson (1998). "Comparison of Strength and Stiffness Parameters for a Piedmont Residual Soil," Proc., 1st Int'l Conf. on Site Characterization - ISC'98, pp. 1229-1234, Atlanta, Ga., April.

Ensoft, INC. (2005). LPILE Plus 3 for Windows-A Program for the Analysis of Piles and Drilled Shafts Under Lateral Loads, http://www.ensoftinc.com , December.

Florida Bridge Software Institute (2005). FB-MultiPier version 4.03, http://bsi-web.ce.ufl.edu/, December.

Gabr, M. A. and Borden, R.H. (1988). "Analysis of Load Deflection Response of Laterally Loaded Piers Using DMT", Proceedings of the 1st International Conference on Penetration Testing ISOPT-1, Orlando, FL. Vol 1, 513-520.

GPE Inc. (1993). Marchetti Dilatometer, Data Reduction "Dilly" Basic Program, Gainesville, Florida.

Marchetti, S. (1980). "In Situ Test by Flat Dilatometer", Proceedings of American Society of Civil Engineers, ASCE Journal of the Geotechnical Engineering Division, 106 (GT3), pp. 299-321, March.

Peterson, K. T. (1996) Static and Dynamic Lateral Load Testing of a Full-Scale Pile Group in Clay, M.S. Theses, Brigham Young University, Provo, December.

Robertson, P. K., Davies, M. P., and Campanella, R. G. (1989). "Design of Laterally Loaded Driven Piles Using the Flat Dilatometer," Geotechnical Testing Journal, GTJODJ, Vol. 12, No. 1, pp. 30-38, March.

Reese, L. C. (1983). "Behavior of Piles and Pile Groups Under Lateral Load," a manual prepared for the U.S. Department of Transportation, Federal Highway Administration, Office of Research, Washington, D.C.

Ruesta, P. F. and Townsend F. C. (1997). "Evaluation of Laterally Loaded Pile Group at Roosevelt Bridge," Journal of Geotechnical and Geoenvironmental Engineering , Vol. 123, issue 12, pp. 1153-1161, Dec.

BACK

DILATOMETER DATA LISTING & INTERPRETATION (BASED ON THE 1988 DILATOMETER MANUAL) SNDG. NO. DMT-1
University of Florida
JOB FILE: Roosevelt Bridge FILE NO. : UF1995
LOCATION: Vicinity of Pier 16
SNDG.BY : Pedro, FCT, Ed SNDG.DATE: November 1995
ANAL.BY : J.B. Anderson ANAL.DATE: 27 Dec 05

ANALYSIS PARAMETERS: LO RANGE =40.00 BARS ROD DIAM. = 3.57 CM BL.THICK. = 15.0 MM SU FACTOR = 1.00
SURF.ELEV. = -2.00 M LO GAGE 0 = 0.05 BARS FR.RED.DIA. = 4.78 CM BL.WIDTH = 96.0 MM PHI FACTOR = 1.00
WATER DEPTH = 0.00 M HI GAGE 0 = 0.00 BARS LIN.ROD WT. = 6.50 KGF/M DELTA-A = 0.20 BARS OCR FACTOR = 1.00
SP.GR.WATER = 1.000 CAL GAGE 0 = 0.05 BARS DELTA/PHI = 0.50 DELTA-B = 1.50 BARS M FACTOR = 1.00
MAX SU ID = 0.60 SU OPTION = MARCHETTI MIN PHI ID = 1.20 OCR OPTION= MARCHETTI K0 FACTOR = 1.00
UNIT CONVERSIONS: 1 BAR = 1.019 KGF/CM2 = 1.044 TSF = 14.51 PSI 1 M = 3.2808 FT

Z (M)	THRUST (KGF)	A (BAR)	B (BAR)	C (BAR)	P0 (BAR)	P1 (BAR)	P2 (BAR)	U0 (BAR)	GAMMA (T/M3)	SVP (BAR)	KD	ID	UD	ED (BAR)	K0	SU (BAR)	QD (BAR)	PHI (DEG)	SIGFF (BAR)	PHIO (DEG)	PC (BAR)	OCR	M (BAR)	SOIL TYPE
0.25		0.39	2.85	0.55	1.35			0.025	0.02	-0.025	-21.50	1.51	0.00	28.									0.	SANDY SILT
0.50		0.54	4.05	0.65	2.55			0.049	1.70	-0.028	-21.44	3.17	0.00	66.									0.	SILTY SAND
0.75		0.58	4.85	0.65	3.35			0.074	1.70	-0.011	-53.35	4.67	0.00	94.									0.	SAND
1.00		0.80	5.45	0.85	3.95			0.098	1.70	0.006	118.95	4.11	0.00	107.									521.	SAND
1.25		0.53	3.85	0.65	2.35			0.123	1.70	0.024	22.38	3.23	0.00	59.									193.	SILTY SAND
1.50		1.15	6.85	1.15	5.35			0.147	1.80	0.042	23.92	4.19	0.00	146.									485.	SAND
1.75		0.92	6.05	0.95	4.55			0.172	1.70	0.060	12.88	4.64	0.00	125.									342.	SAND
2.00		0.75	4.45	0.85	2.95			0.196	1.70	0.077	8.44	3.21	0.00	73.									171.	SILTY SAND
2.25		1.07	5.25	1.15	3.75			0.221	1.70	0.095	9.77	2.81	0.00	90.									224.	SILTY SAND
2.50		1.18	5.45	1.25	3.95			0.245	1.70	0.112	9.00	2.68	0.00	94.									225.	SILTY SAND
2.75		1.34	6.85	1.35	5.35			0.270	1.80	0.130	8.29	3.71	0.00	139.									324.	SAND
3.00		1.53	6.85	1.55	5.35			0.294	1.80	0.150	8.37	3.03	0.00	132.									309.	SILTY SAND
3.25		1.53	6.85	1.55	5.35			0.319	1.80	0.169	7.26	3.09	0.00	132.									293.	SILTY SAND
3.50		1.58	7.85	1.55	6.35			0.343	1.80	0.189	6.39	3.97	0.00	167.									351.	SAND
3.75		2.99	13.45	2.75	11.95			0.368	1.90	0.210	11.35	3.86	0.00	319.									836.	SAND
4.00		11.94	33.45	11.15	31.95			0.393	2.15	0.235	45.75	1.93	0.00	722.									2844.	SILTY SAND
4.25		6.13	23.45	5.55	21.95			0.417	2.00	0.261	19.63	3.20	0.00	569.									1786.	SILTY SAND
4.50		2.71	19.65	2.15	18.15			0.442	1.90	0.285	5.99	9.38	0.00	555.									1141.	SAND
4.75		6.39	24.85	5.75	23.35			0.466	2.00	0.308	17.16	3.33	0.00	611.									1839.	SAND
5.00		5.57	19.65	5.15	18.15			0.491	2.00	0.333	14.01	2.79	0.00	451.									1272.	SILTY SAND
5.25		7.18	29.45	6.35	27.95			0.515	2.00	0.357	16.34	3.70	0.00	749.									2222.	SAND

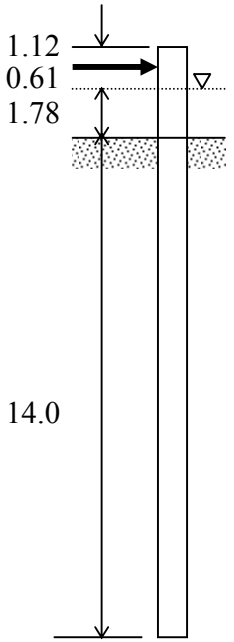

Length: 17.5m
Type: Square, Prestressed
Width: 762mm Void Diameter: 457mm
Void:
Material Properties:
Concrete:
f'_c = 44.8 MPa
E_c = 31.5 GPa
Steel:
f_y = 275.7 MPa
E_s = 200 GPa

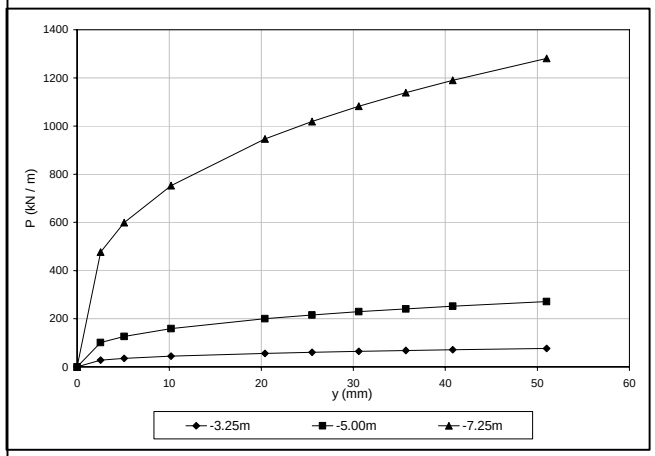

P-y Curves for Roosevelt Bridge

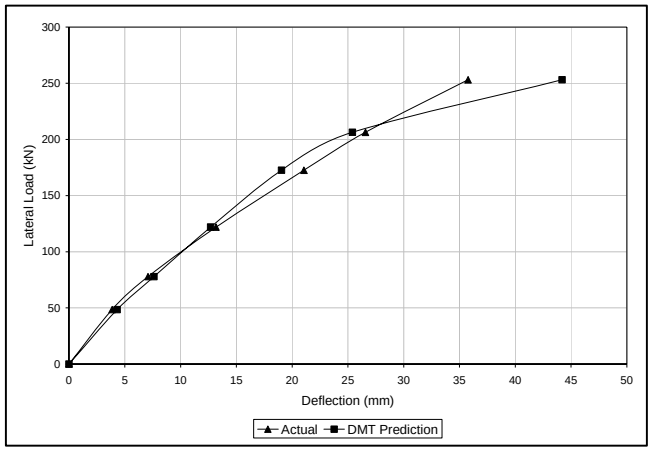

Simulation Results for Roosevelt Bridge

Figure 1Roosevelt Bridge Load Test

BACK

DILATOMETER DATA LISTING & INTERPRETATION (BASED ON THE 1988 DILATOMETER MANUAL) SNDG. NO. DMT-1

University of Florida
JOB FILE: Wilmington Bypass- NCDOT FILE NO. : UF 1998-1
LOCATION: 38+55 34.5 L
SNDG.BY : Brian, Andrew, Norb, Cory, Tom SNDG.DATE: 6 January 99
ANAL.BY : J.B. Anderson ANAL.DATE: 27 Dec 05

ANALYSIS PARAMETERS:
SURF.ELEV. = -1.46 M | LO RANGE =40.00 BARS | ROD DIAM. = 4.44 CM | BL.THICK. = 15.0 MM | SU FACTOR = 1.00
WATER DEPTH = 0.00 M | HI GAGE 0 = 0.00 BARS | FR.RED.DIA. = 5.71 CM | BL.WIDTH = 96.0 MM | PHI FACTOR = 1.00
SP.GR.WATER = 1.000 | CAL GAGE 0 = 0.00 BARS | LIN.ROD WT. = 6.25 KGF/M | DELTA-A = 0.19 BARS | OCR FACTOR = 1.00
MAX SU ID = 0.60 | SU OPTION = MARCHETTI | DELTA/PHI = 0.50 | DELTA-B = 0.42 BARS | M FACTOR = 1.00
MIN PHI ID = 1.20 | OCR OPTION= MARCHETTI | K0 FACTOR = 1.00
UNIT CONVERSIONS: 1 BAR = 1.019 KGF/CM2 = 1.044 TSF = 14.51 PSI 1 M = 3.2808 FT

Z (M)	THRUST (KGF)	A (BAR)	B (BAR)	C (BAR)	P0 (BAR)	P1 (BAR)	P2 (BAR)	U0 (BAR)	GAMMA (T/M3)	SVP (BAR)	KD	ID	UD	ED (BAR)	K0	SU (BAR)	QD	PHI (DEG)	SIGFF (BAR)	PHIO (DEG)	PC (BAR)	OCR	M (BAR)	SOIL TYPE
0.83		0.80	4.20		0.85	3.78		0.081	1.70	0.069	11.15	3.81	0.00	102.									265.	SAND
1.33		1.00	4.40		1.05	3.98		0.131	1.70	0.103	8.90	3.18	0.00	102.									244.	SILTY SAND
1.83		0.80	3.40		0.89	2.98		0.180	1.70	0.138	5.16	2.94	0.00	73.									139.	SILTY SAND
2.33		4.80	12.80		4.62	12.38		0.229	1.80	0.174	25.17	1.77	0.00	269.									908.	SANDY SILT
2.83		1.60	4.20		1.69	3.78		0.278	1.70	0.211	6.69	1.48	0.00	73.									153.	SANDY SILT
3.33		0.60	3.20		0.69	2.78		0.327	1.70	0.246	1.48	5.74	0.00	73.									62.	SAND
3.83		0.80	2.40		0.94	1.98		0.376	1.70	0.280	2.02	1.84	0.00	36.									36.	SILTY SAND
4.33		1.00	2.80		1.13	2.38		0.425	1.60	0.312	2.26	1.77	0.00	43.									47.	SANDY SILT
4.83		1.50	2.20		1.69	1.78		0.474	1.50	0.339	3.58	0.08	0.00	3.	0.90	0.15					0.84	2.5	5.	MUD
5.33		1.40	2.80		1.55	2.38		0.523	1.60	0.366	2.81	0.81	0.00	29.	0.74						0.62	1.7	35.	CLAYEY SILT
5.83		1.60	3.00		1.75	2.58		0.572	1.60	0.395	2.98	0.70	0.00	29.	0.78						0.74	1.9	36.	CLAYEY SILT
6.33		2.70	9.00		2.61	8.58		0.621	1.90	0.432	4.59	3.01	0.00	207.									378.	SILTY SAND
6.83		3.80	12.00		3.61	11.58		0.670	1.90	0.476	6.17	2.71	0.00	277.									573.	SILTY SAND
7.33		4.80	15.00		4.51	14.58		0.719	1.90	0.520	7.28	2.66	0.00	349.									775.	SILTY SAND
7.83		5.60	17.40		5.23	16.98		0.768	2.00	0.567	7.87	2.63	0.00	408.									932.	SILTY SAND
8.33		5.60	15.80		5.31	15.38		0.817	2.00	0.616	7.29	2.24	0.00	349.									772.	SILTY SAND
8.83		7.80	23.80		7.22	23.38		0.867	2.00	0.665	9.55	2.54	0.00	561.									1379.	SILTY SAND
9.33		8.20	27.00		7.48	26.58		0.916	2.00	0.714	9.19	2.91	0.00	663.									1608.	SILTY SAND

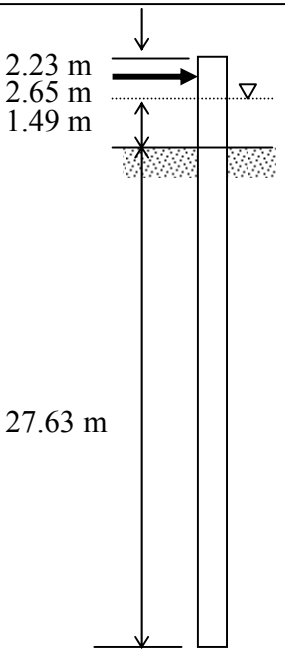

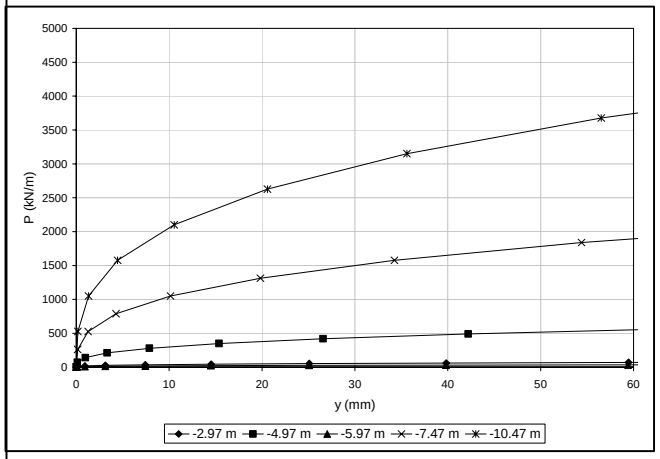

P-y Curves for Wilmington

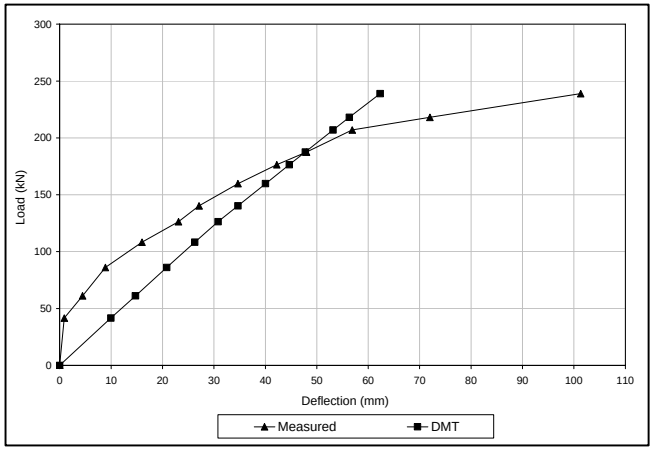

Simulation Results for Wilmington

Length: 34m
Type: Square Prestressed
Width: 762mm
Void Diameter: 424.2mm
Material Properties:
Concrete:
f'_c = 41.8 MPa
E_c = 30.4 GPa
Steel:
f_y = 275.7 MPa
E_s = 200 GPa

Figure 2 Wilmington Bypass Load Test

BACK

DILATOMETER DATA LISTING & INTERPRETATION (BASED ON THE 1988 DILATOMETER MANUAL) SNDG. NO. DMT-1
University of Florida
JOB FILE: Rio Puerto Nueveo Project - USACOE Jax FILE NO. : UF 1998-1
LOCATION: CB-59
SNDG.BY : Anderson, Townsend, Guzman, Spoor SNDG.DATE: 10 March 98
ANAL.BY : J.B. Anderson ANAL.DATE: 27 Dec 05

ANALYSIS PARAMETERS: LO RANGE =40.00 BARS ROD DIAM. = 4.44 CM BL.THICK. = 15.0 MM SU FACTOR = 1.00
SURF.ELEV. = 0.00 M LO GAGE 0 = 0.00 BARS FR.RED.DIA. = 5.71 CM BL.WIDTH = 96.0 MM PHI FACTOR = 1.00
WATER DEPTH = 2.68 M HI GAGE 0 = 0.00 BARS LIN.ROD WT. = 6.25 KGF/M DELTA-A = 0.11 BARS OCR FACTOR = 1.00
SP.GR.WATER = 1.000 CAL GAGE 0 = 0.00 BARS DELTA/PHI = 0.50 DELTA-B = 0.97 BARS M FACTOR = 1.00
MAX SU ID = 0.60 SU OPTION = MARCHETTI MIN PHI ID = 1.20 OCR OPTION= MARCHETTI K0 FACTOR = 1.00
UNIT CONVERSIONS: 1 BAR = 1.019 KGF/CM2 = 1.044 TSF = 14.51 PSI 1 M = 3.2808 FT

Z (M)	THRUST (KGP)	A (BAR)	B (BAR)	C (BAR)	P0 (BAR)	P1 (BAR)	P2 (BAR)	U0 (BAR)	GAMMA (T/M3)	SVP (BAR)	KD	ID	UD	ED (BAR)	K0	SU (BAR)	QD (BAR)	PHI (DEG)	SIGFF (BAR)	PHIO (DEG)	PC (BAR)	OCR	M (BAR)	SOIL TYPE
5.49		1.70	3.80		1.76	2.83		0.276	1.60	0.586	2.53	0.72	0.00	37.	0.68						0.85	1.4	41.	CLAYEY SILT
6.10		1.10	2.40		1.20	1.43		0.336	1.50	0.619	1.39	0.27	0.00	8.	0.37	0.09					0.35	0.6	7.	MUD
6.71		1.60	3.70		1.66	2.73		0.395	1.60	0.652	1.94	0.85	0.00	37.	0.53						0.62	1.0	32.	CLAYEY SILT
7.32		1.70	3.70		1.76	2.73		0.455	1.60	0.688	1.90	0.74	0.00	34.	0.52						0.64	0.9	28.	CLAYEY SILT
7.92		1.90	4.30		1.94	3.33		0.514	1.60	0.723	1.98	0.97	0.00	48.	0.54						0.71	1.0	42.	SILT
8.53		2.30	5.50		2.30	4.53		0.574	1.70	0.762	2.27	1.29	0.00	77.									81.	SANDY SILT
9.14		3.10	6.60		3.09	5.63		0.634	1.70	0.804	3.05	1.04	0.00	88.	0.80						1.56	1.9	116.	SILT
9.75		2.40	5.40		2.41	4.43		0.694	1.70	0.846	2.03	1.17	0.00	70.	0.55						0.87	1.0	65.	SILT
10.36		3.70	6.60		3.72	5.63		0.754	1.70	0.888	3.34	0.64	0.00	66.	0.86						1.98	2.2	91.	CLAYEY SILT
10.97		4.00	7.80		3.97	6.83		0.814	1.80	0.933	3.39	0.90	0.00	99.	0.87						2.12	2.3	140.	SILT
11.58		3.30	6.30		3.31	5.33		0.873	1.70	0.978	2.50	0.83	0.00	70.	0.67						1.38	1.4	77.	CLAYEY SILT
12.19		3.60	6.40		3.62	5.43		0.933	1.70	1.019	2.64	0.67	0.00	63.	0.70						1.57	1.5	72.	CLAYEY SILT
12.80		3.70	6.90		3.70	5.93		0.993	1.70	1.061	2.55	0.82	0.00	77.	0.68						1.55	1.5	87.	CLAYEY SILT
13.41		6.40	10.40		6.36	9.43		1.053	1.80	1.106	4.80	0.58	0.00	106.	1.13	0.73					4.34	3.9	186.	SILTY CLAY
13.94		7.00	11.90		6.92	10.93		1.105	1.80	1.148	5.07	0.69	0.00	139.	1.17						4.89	4.3	251.	CLAYEY SILT
15.85		9.80	14.60		9.72	13.63		1.292	1.90	1.307	6.45	0.46	0.00	136.	1.38	1.24					8.12	6.2	278.	SILTY CLAY
16.46		11.60	17.40		11.47	16.43		1.352	1.90	1.361	7.44	0.49	0.00	172.	1.52	1.55					10.56	7.8	378.	SILTY CLAY
17.07		11.00	16.60		10.88	15.63		1.412	1.90	1.415	6.69	0.50	0.00	165.	1.42	1.41					9.32	6.6	344.	SILTY CLAY
17.68		11.20	16.00		11.12	15.03		1.472	1.90	1.469	6.57	0.40	0.00	136.	1.40	1.43					9.40	6.4	281.	SILTY CLAY
18.29		13.20	17.40		13.15	16.43		1.532	1.90	1.523	7.63	0.28	0.00	114.	1.55	1.79					12.30	8.1	253.	CLAY

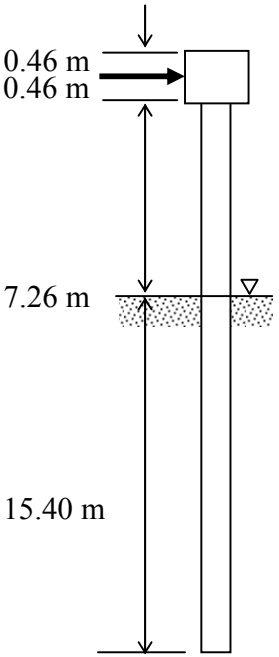

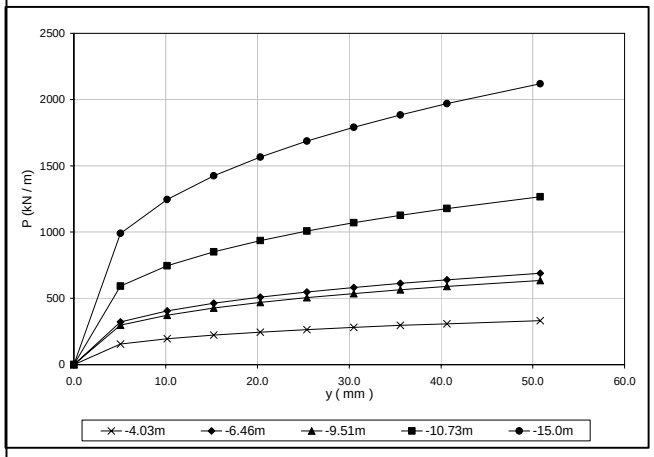

P-y Curves for Puerto Nuevo

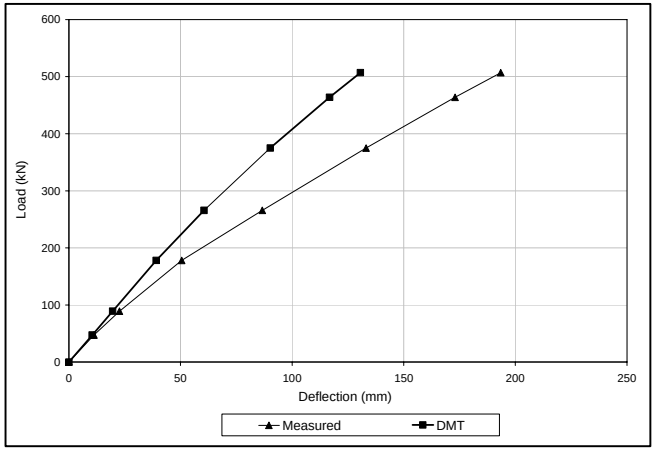

Simulation Results for Puerto Nuevo

Length: 23.35m
Type: Steel Pipe
Diameter: 1219 mm
Thickness: 19.1 mm
Material Properties:
Steel:
f_y = 275.7 MPa
E_s = 200 GPa
Cap Concrete:
f'_c = 27.7 MPa
E_c = 24.86 GPa

Figure 3 Puerto Nuevo Load Test

BACK

DILATOMETER DATA LISTING & INTERPRETATION (BASED ON THE 1988 DILATOMETER MANUAL) SNDG. NO. DMT-SE
University of Florida
JOB FILE: Salt Lake City FILE NO. : SLC
LOCATION: BYU Load Test Site
SNDG.BY : ??? SNDG.DATE: November 1995
ANAL.BY : J.B. Anderson ANAL.DATE: 27 Dec 05

ANALYSIS PARAMETERS: LO RANGE =40.00 BARS ROD DIAM. = 3.57 CM BL.THICK. = 15.0 MM SU FACTOR = 1.00
SURF.ELEV. = 0.00 M LO GAGE 0 = 0.00 BARS FR.RED.DIA. = 4.78 CM BL.WIDTH = 96.0 MM PHI FACTOR = 1.00
WATER DEPTH = 2.44 M HI GAGE 0 = 0.00 BARS LIN.ROD WT. = 6.50 KGF/M DELTA-A = 0.16 BARS OCR FACTOR = 1.00
SP.GR.WATER = 1.000 CAL GAGE 0 = 0.01 BARS DELTA/PHI = 0.50 DELTA-B = 0.62 BARS M FACTOR = 1.00
MAX SU ID = 0.60 SU OPTION = MARCHETTI MIN PHI ID = 1.20 OCR OPTION= MARCHETTI K0 FACTOR = 1.00
UNIT CONVERSIONS: 1 BAR = 1.019 KGF/CM2 = 1.044 TSF = 14.51 PSI 1 M = 3.2808 FT

Z (M)	THRUST (KGP)	A (BAR)	B (BAR)	C (BAR)	P0 (BAR)	P1 (BAR)	P2 (BAR)	U0 (BAR)	GAMMA (T/M3)	SVP (BAR)	KD	ID	UD	ED (BAR)	K0	SU (BAR)	QD (BAR)	PHI (DEG)	SIGFF (BAR)	PHIO (DEG)	PC (BAR)	OCR	M (BAR)	SOIL TYPE
1.68		2.00	6.20		2.00	5.59		0.000	1.70	0.339	5.90	1.80	0.00	125.									249.	SANDY SILT
1.83		2.25	5.55		2.29	4.94		0.000	1.70	0.364	6.30	1.15	0.00	92.	1.36						2.18	6.0	188.	SILT
1.98		2.05	5.25		2.10	4.64		0.000	1.70	0.389	5.40	1.21	0.00	88.									167.	SANDY SILT
2.13		1.50	4.90		1.54	4.29		0.000	1.70	0.414	3.72	1.79	0.00	95.									149.	SANDY SILT
2.29		2.45	6.45		2.46	5.84		0.000	1.70	0.441	5.58	1.37	0.00	117.									227.	SANDY SILT
2.44		8.30	16.40		8.10	15.79		0.000	1.95	0.468	17.33	0.95	0.00	267.	2.56						13.58	29.0	806.	SILT
2.59		7.05	15.50		6.84	14.89		0.015	1.95	0.482	14.16	1.18	0.00	279.	2.27						10.21	21.2	791.	SILT
2.74		10.00	22.50		9.58	21.89		0.029	1.95	0.496	19.28	1.29	0.00	427.									1333.	SANDY SILT
2.90		17.00	34.00		16.36	33.39		0.045	2.10	0.512	31.88	1.04	0.00	591.	3.61						38.45	75.1	2126.	SILT
3.05		14.00	27.00		13.56	26.39		0.060	2.10	0.528	25.57	0.95	0.00	445.	3.19						28.12	53.3	1509.	SILT
3.20		4.40	8.05		4.43	7.44		0.075	1.80	0.542	8.03	0.69	0.00	105.	1.60						4.74	8.7	238.	CLAYEY SILT
3.35		2.15	4.50		2.24	3.89		0.089	1.70	0.553	3.89	0.77	0.00	57.	0.97						1.56	2.8	88.	CLAYEY SILT
3.51		2.25	4.35		2.35	3.74		0.105	1.70	0.564	3.99	0.62	0.00	48.	0.98						1.66	2.9	75.	CLAYEY SILT
3.66		1.65	3.30		1.78	2.69		0.120	1.60	0.573	2.89	0.55	0.00	32.	0.76	0.20					1.02	1.8	39.	SILTY CLAY
3.81		1.35	2.95		1.48	2.34		0.134	1.60	0.582	2.31	0.64	0.00	30.	0.62						0.73	1.3	30.	CLAYEY SILT
3.96		1.20	2.90		1.32	2.29		0.149	1.60	0.591	1.99	0.82	0.00	34.	0.54						0.59	1.0	29.	CLAYEY SILT
4.11		0.90	3.50		0.98	2.89		0.164	1.70	0.601	1.36	2.34	0.00	66.									56.	SILTY SAND
4.27		5.20	19.00		4.72	18.39		0.180	2.00	0.614	7.39	3.01	0.00	474.									1061.	SILTY SAND
4.42		15.50	34.50		14.76	33.89		0.194	2.10	0.630	23.14	1.31	0.00	664.									2187.	SANDY SILT
4.57		12.50	30.00		11.83	29.39		0.209	2.10	0.646	18.00	1.51	0.00	609.									1862.	SANDY SILT
4.72		13.00	29.50		12.38	28.89		0.224	2.10	0.662	18.37	1.36	0.00	573.									1762.	SANDY SILT
4.88		13.50	31.50		12.81	30.89		0.239	2.10	0.679	18.51	1.44	0.00	627.									1934.	SANDY SILT
5.03		11.00	27.00		10.41	26.39		0.254	2.10	0.695	14.60	1.57	0.00	555.									1585.	SANDY SILT
5.18		10.50	25.50		9.96	24.89		0.269	2.10	0.712	13.62	1.54	0.00	518.									1447.	SANDY SILT
5.33		8.00	20.00		7.61	19.39		0.284	1.95	0.727	10.08	1.61	0.00	409.									1025.	SANDY SILT
5.49		8.50	21.00		8.08	20.39		0.299	1.95	0.742	10.50	1.58	0.00	427.									1087.	SANDY SILT
5.64		10.00	25.50		9.43	24.89		0.314	2.10	0.757	12.05	1.69	0.00	536.									1436.	SANDY SILT
5.79		13.00	32.00		12.26	31.39		0.329	2.10	0.773	15.44	1.60	0.00	664.									1933.	SANDY SILT
5.94		15.00	35.50		14.18	34.89		0.343	2.10	0.789	17.54	1.50	0.00	718.									2179.	SANDY SILT
6.10		12.50	32.00		11.73	31.39		0.359	2.10	0.806	14.11	1.73	0.00	682.									1927.	SANDY SILT
6.25		14.50	31.50		13.86	30.89		0.374	2.10	0.822	16.40	1.26	0.00	591.									1754.	SANDY SILT
6.40		10.50	22.00		10.13	21.39		0.389	1.95	0.838	11.64	1.16	0.00	391.	2.02						13.06	15.6	1032.	SILT
6.55		3.50	8.60		3.45	7.99		0.403	1.80	0.850	3.59	1.49	0.00	157.									237.	SANDY SILT
6.71		2.70	6.20		2.73	5.59		0.419	1.70	0.862	2.68	1.23	0.00	99.									120.	SANDY SILT
6.86		3.50	5.10		3.63	4.49		0.434	1.70	0.873	3.66	0.27	0.00	30.	0.92	0.41					2.24	2.6	44.	CLAY
7.01		3.50	5.10		3.63	4.49		0.448	1.70	0.883	3.60	0.27	0.00	30.	0.91	0.41					2.21	2.5	43.	CLAY
7.16		3.55	5.15		3.68	4.54		0.463	1.70	0.893	3.60	0.27	0.00	30.	0.91	0.41					2.23	2.5	43.	CLAY
7.32		4.00	6.05		4.11	5.44		0.479	1.70	0.904	4.01	0.37	0.00	46.	0.99	0.47					2.68	3.0	72.	SILTY CLAY
7.47		3.80	5.50		3.92	4.89		0.494	1.70	0.914	3.75	0.28	0.00	34.	0.94	0.44					2.44	2.7	50.	CLAY
7.62		5.20	11.00		5.12	10.39		0.508	1.80	0.925	4.98	1.14	0.00	183.	1.16						3.84	4.2	331.	SILT
7.77		3.60	8.40		3.57	7.79		0.523	1.80	0.937	3.25	1.39	0.00	146.									206.	SANDY SILT
7.92		5.30	10.50		5.25	9.89		0.538	1.80	0.949	4.96	0.99	0.00	161.	1.16						3.92	4.1	290.	SILT
8.08		9.00	21.00		8.61	20.39		0.553	1.95	0.963	8.37	1.46	0.00	409.									951.	SANDY SILT
8.23		9.50	21.50		9.11	20.89		0.568	1.95	0.977	8.74	1.38	0.00	409.									969.	SANDY SILT
8.38		7.50	20.00		7.08	19.39		0.583	2.00	0.991	6.56	1.89	0.00	427.									898.	SILTY SAND
8.53		8.10	22.50		7.59	21.89		0.598	2.00	1.006	6.95	2.05	0.00	496.									1073.	SILTY SAND
8.69		12.00	28.00		11.41	27.39		0.613	2.10	1.022	10.56	1.48	0.00	555.									1415.	SANDY SILT
8.84		9.00	23.50		8.48	22.89		0.628	2.00	1.038	7.57	1.83	0.00	500.									1118.	SILTY SAND
8.99		17.00	41.00		16.01	40.39		0.643	2.10	1.053	14.59	1.59	0.00	846.									2418.	SANDY SILT

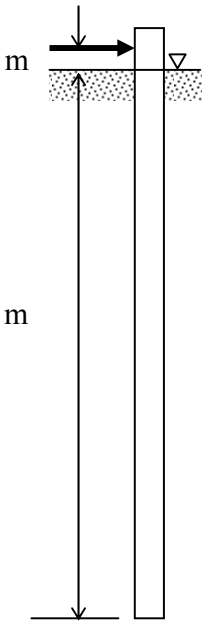

Length: 7.85m
Type: Closed End Concrete Filled Pipe
Diameter: 305mm
Thickness: 9.5mm
Material Properties
Concrete:
f'_c = 18.6 MPa
E_c = 17.2 GPa
Steel:
f_y = 275.7 MPa
E_s = 200 GPa

Figure 4a Salt Lake City Load Test

BACK

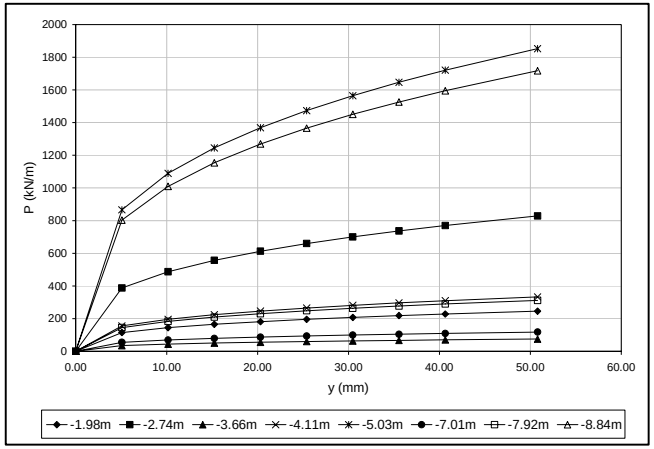

P-y Curves for Salt Lake City

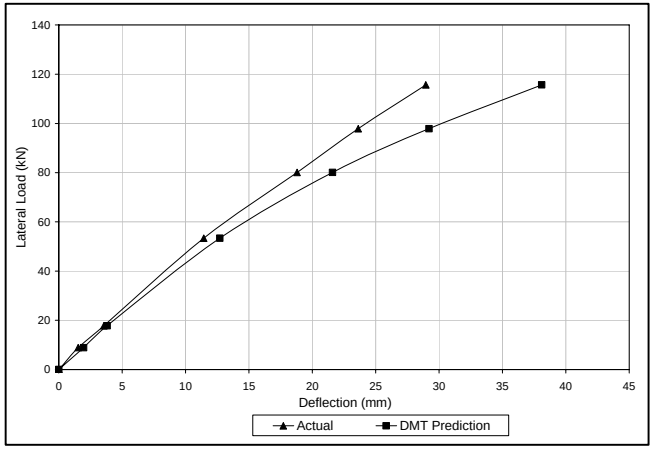

Simulation Results for Salt Lake City

Figure 4b Salt Lake City Load Test continued

BACK

DILATOMETER DATA LISTING & INTERPRETATION (BASED ON THE 1988 DILATOMETER MANUAL) SNDG. NO. DMT-1
Schmertmann & Crapps, Inc.
JOB FILE: Pascagoula Load Test Program FILE NO. : 970
LOCATION: Sta. 250+12, Offset 103' LT C.L.
SNDG.BY : C.Kohlhof,T.Esin/S&C;W.Watkins/SES SNDG.DATE: 03 Sep 97 to 05 Sep
ANAL.BY : T.Esin ANAL.DATE: 09 Sep 97

ANALYSIS PARAMETERS: LO RANGE =10.00 BARS ROD DIAM. = 4.44 CM BL.THICK. = 14.6 MM SU FACTOR = 1.00
SURF.ELEV. = -5.15 M LO GAGE 0 =-0.01 BARS FR.RED.DIA. = 5.34 CM BL.WIDTH = 95.8 MM PHI FACTOR = 1.00
WATER DEPTH = 0.00 M HI GAGE 0 = 0.15 BARS LIN.ROD WT. = 6.27 KGF/M DELTA-A = 0.23 BARS OCR FACTOR = 1.00
SP.GR.WATER = 1.034 CAL GAGE 0 =-0.01 BARS DELTA/PHI = 0.50 DELTA-B = 0.46 BARS M FACTOR = 1.00
MAX SU ID = 0.60 SU OPTION = MARCHETTI MIN PHI ID = 1.20 OCR OPTION= MARCHETTI K0 FACTOR = 1.00
UNIT CONVERSIONS: 1 BAR = 1.019 KGF/CM2 = 1.044 TSF = 14.51 PSI 1 M = 3.2808 FT

Z (M)	THRUST (KGP)	A (BAR)	B (BAR)	C (BAR)	P0 (BAR)	P1 (BAR)	P2 (BAR)	U0 (BAR)	GAMMA (T/M3)	SVP (BAR)	KD	ID	UD	ED (BAR)	K0	SU (BAR)	QD (BAR)	PHI (DEG)	SIGFF (BAR)	PHIO (DEG)	PC (BAR)	OCR	M (BAR)	SOIL TYPE
5.76	314.	2.98	6.98		3.04	6.52		0.584	1.78	0.051	48.24	1.41	0.00	121.	6.14		3.6	31.3	0.08	24.0	23.35	457.8	481.	SANDY SILT
6.07	391.	2.48	5.22	0.76	2.61	4.76	0.99	0.616	1.78	0.074	27.04	1.08	0.19	75.	3.29						4.28	58.1	257.	SILT
6.27	684.	1.95	4.73		2.08	4.27		0.636	1.78	0.088	16.31	1.52	0.19	76.	2.04		18.2	41.2	0.15	36.5	2.63	29.8	226.	SANDY SILT
6.85	905.	1.57	7.09	0.44	1.56	6.63	0.67	0.695	1.88	0.134	6.47	5.87	-0.03	176.	0.74		28.3	44.0	0.23	40.4	0.55	4.1	373.	SAND
7.16	2726.	3.12	12.20	0.49	2.94	11.58	0.72	0.727	1.98	0.161	13.76	3.91	-0.00	300.	1.43		83.3	46.7	0.28	43.7	2.47	15.3	840.	SAND
7.44	3868.	4.42	16.65	0.53	4.08	16.03	0.76	0.755	1.98	0.187	17.80	3.59	0.00	415.	1.92		116.6	46.6	0.32	43.9	4.98	26.6	1263.	SAND
7.77	4150.	1.96	14.60	0.54	1.60	13.98	0.77	0.788	1.88	0.216	3.76	15.24	-0.02	430.									709.	SAND
8.07	2400.	1.29	7.70	0.51	1.23	7.24	0.74	0.819	1.78	0.239	1.74	14.47	-0.19	208.									204.	SAND
8.37	895.	2.88	6.92	0.60	2.94	6.46	0.83	0.849	1.78	0.261	8.01	1.68	-0.01	122.	1.14		23.5	38.2	0.42	35.1	2.29	8.8	279.	SANDY SILT
8.68	602.	2.99	4.42	2.20	3.18	3.96	2.43	0.881	1.68	0.282	8.16	0.34	0.67	27.	1.62	0.36					2.53	9.0	62.	CLAY
8.98	273.	3.26	4.76	2.46	3.45	4.30	2.69	0.911	1.78	0.303	8.39	0.34	0.70	30.	1.65	0.40					2.83	9.4	68.	CLAY
9.29	144.	3.28	4.75	2.42	3.47	4.29	2.65	0.943	1.78	0.325	7.77	0.32	0.68	28.	1.57	0.39					2.70	8.3	64.	CLAY
9.59	288.	3.47	5.06	2.64	3.65	4.60	2.87	0.973	1.78	0.347	7.72	0.35	0.71	33.	1.56	0.41					2.86	8.2	73.	SILTY CLAY
9.90	288.	3.34	5.08	2.47	3.52	4.62	2.70	1.005	1.78	0.370	6.79	0.44	0.67	38.	1.43	0.38					2.49	6.7	80.	SILTY CLAY
10.20	370.	3.78	5.35	2.66	3.97	4.89	2.89	1.035	1.78	0.392	7.48	0.32	0.63	32.	1.53	0.45					3.07	7.8	71.	CLAY
10.51	448.	4.15	6.15	2.73	4.31	5.69	2.96	1.066	1.78	0.414	7.84	0.42	0.58	48.	1.58	0.50					3.49	8.4	107.	SILTY CLAY
10.81	514.	4.56	6.62	3.09	4.72	6.16	3.32	1.097	1.78	0.436	8.31	0.40	0.61	50.	1.64	0.57					4.02	9.2	115.	SILTY CLAY
11.12	576.	4.85	7.12	3.18	5.00	6.66	3.41	1.128	1.78	0.459	8.44	0.43	0.59	58.	1.65	0.61					4.34	9.4	134.	SILTY CLAY
11.42	607.	5.23	7.80	3.34	5.37	7.34	3.57	1.159	1.88	0.482	8.72	0.47	0.57	68.	1.69	0.67					4.80	9.9	162.	SILTY CLAY
11.73	838.	5.82	8.92	3.32	5.93	8.46	3.55	1.190	1.88	0.508	9.33	0.53	0.50	88.	1.76	0.77					5.61	11.0	213.	SILTY CLAY
12.03	792.	5.18	7.18	3.68	5.34	6.72	3.91	1.221	1.78	0.532	7.76	0.33	0.65	48.	1.56	0.64					4.40	8.3	107.	CLAY
12.34	838.	4.85	7.08	2.65	5.00	6.62	2.88	1.252	1.78	0.554	6.77	0.43	0.43	56.	1.43	0.56					3.71	6.7	118.	SILTY CLAY
12.64	833.	4.29	6.62	2.30	4.44	6.16	2.53	1.283	1.78	0.576	5.48	0.55	0.40	60.	1.24	0.45					2.77	4.8	113.	SILTY CLAY
12.90	3580.	5.63	22.05	1.06	5.08	21.43	1.29	1.309	2.08	0.599	6.30	4.33	-0.01	567.	0.77		107.0	43.0	1.01	41.5	2.57	4.3	1190.	SAND
13.25	4300.	6.45	9.30	4.82	5.58	8.59	5.05	1.345	1.88	0.632	8.70	0.38	0.71	70.	1.63	0.82					5.81	9.2	161.	SILTY CLAY
13.56	4100.	4.62	25.35	1.11	3.86	24.73	1.34	1.376	1.98	0.659	3.76	8.42	-0.01	724.	0.36		130.6	44.8	1.12	43.6	0.71	1.1	1196.	SAND
13.86	4250.	5.62	14.85	1.03	5.43	14.23	1.26	1.406	1.98	0.687	5.86	2.19	-0.04	305.	0.69		128.7	43.4	1.16	42.2	2.44	3.6	613.	SILTY SAND
14.17	4750.	5.85	11.75	2.83	5.83	11.13	3.06	1.438	1.88	0.714	6.15	1.21	0.37	184.	0.71		143.9	43.7	1.21	42.6	2.69	3.8	372.	SANDY SILT
14.47	4900.	5.61	16.65	1.11	5.33	16.03	1.34	1.468	1.98	0.740	5.22	2.77	-0.03	371.	0.57		151.5	44.2	1.26	43.2	1.86	2.5	715.	SILTY SAND
14.78	6950.	5.67	26.75	1.20	4.89	26.13	1.43	1.500	2.08	0.771	4.40	6.27	-0.02	737.	0.25		223.0	47.2	1.34	46.3	0.46	0.6	1317.	SAND
15.08	4950.	5.49	9.80	3.27	5.54	9.34	3.50	1.530	1.88	0.799	5.02	0.95	0.49	132.	1.16						3.36	4.2	239.	SILT
15.39	6700.	4.57	17.45	1.33	4.20	16.83	1.56	1.562	1.98	0.826	3.19	4.79	-0.00	438.	0.03		218.4	47.9	1.44	47.1	0.01	0.0	661.	SAND
15.69	6250.	6.03	10.40	4.10	6.08	9.78	4.33	1.592	1.88	0.852	5.27	0.82	0.61	128.	1.21						3.86	4.5	238.	CLAYEY SILT
15.99	3200.	7.50	9.80	5.73	7.65	9.34	5.96	1.623	1.88	0.877	6.87	0.28	0.72	59.	1.44	0.90					6.01	6.9	124.	CLAY
16.30	1373.	9.45	13.20	6.52	9.53	12.58	6.75	1.654	1.98	0.904	8.71	0.39	0.65	106.	1.69	1.25					8.98	9.9	249.	SILTY CLAY
16.60	1430.	7.17	9.45	5.05	7.32	8.99	5.28	1.684	1.88	0.931	6.05	0.30	0.64	58.	1.33	0.82					5.24	5.6	115.	CLAY
16.91	1605.	6.54	8.51	4.52	6.71	8.05	4.75	1.716	1.88	0.957	5.22	0.27	0.61	47.	1.20	0.70					4.27	4.5	85.	CLAY
17.21	2073.	8.70	13.05	3.47	8.75	12.43	3.70	1.746	1.98	0.983	7.13	0.52	0.28	128.	1.48	1.06					7.14	7.3	275.	SILTY CLAY
17.52	2068.	8.45	12.15	5.51	8.54	11.53	5.74	1.778	1.88	1.010	6.69	0.44	0.59	104.	1.42	1.01					6.65	6.6	217.	SILTY CLAY
17.82	2037.	5.71	7.72	4.40	5.87	7.26	4.63	1.808	1.78	1.034	3.93	0.34	0.69	48.	0.97	0.53					2.97	2.9	74.	CLAY
18.13	2068.	6.14	8.49	4.52	6.29	8.03	4.75	1.840	1.88	1.058	4.20	0.39	0.65	60.	1.02	0.59					3.37	3.2	97.	SILTY CLAY
18.26	3395.	6.34	9.90	3.89	6.43	9.44	4.12	1.853	1.88	1.069	4.28	0.66	0.50	105.	1.04						3.50	3.3	171.	CLAYEY SILT
18.36	11500.	7.21	30.30	1.67	6.33	29.68	1.90	1.863	2.08	1.078	4.14	5.23	0.01	810.									1405.	SAND
23.39	3400.	3.88	9.85	1.90	3.83	9.43	2.12	2.373	1.88	1.545	0.94	3.83	-0.17	194.	0.26		114.4	39.5	2.53	39.3	0.61	0.4	165.	SAND
23.54	3950.	7.11	27.10	2.11	6.37	26.52	2.33	2.389	2.08	1.559	2.55	5.06	-0.01	699.	0.46		122.2	39.1	2.54	39.0	2.06	1.3	919.	SAND
23.69	3700.	5.84	25.05	2.05	5.14	24.47	2.27	2.404	1.98	1.574	1.74	7.07	-0.05	671.	0.36		119.1	39.2	2.57	39.1	1.24	0.8	657.	SAND
24.00	2600.	6.46	9.80	5.15	6.54	9.38	5.37	2.435	1.88	1.601	2.57	0.69	0.71	98.	0.69						2.36	1.5	110.	CLAYEY SILT
24.30	772.	7.51	12.00	4.31	7.55	11.42	4.53	2.466	1.88	1.626	3.12	0.76	0.41	134.	0.81						3.26	2.0	177.	CLAYEY SILT
24.61	364.	7.72	11.45	4.14	7.79	10.87	4.36	2.497	1.88	1.652	3.21	0.58	0.35	107.	0.83	0.66					3.45	2.1	142.	SILTY CLAY
24.91	6000.	8.35	29.60	2.29	7.55	29.02	2.51	2.528	2.08	1.680	2.99	4.28	-0.00	745.	0.44		186.9	41.3	2.79	41.3	2.22	1.3	1081.	SAND
25.22	7400.	7.76	28.10	2.29	7.00	27.52	2.51	2.559	2.08	1.712	2.60	4.62	-0.01	712.	0.32		236.8	43.0	2.88	43.1	1.31	0.8	946.	SAND
25.52	5950.	8.26	26.60	2.25	7.60	26.02	2.47	2.590	2.08	1.743	2.88	3.67	-0.02	639.	0.43		185.4	41.1	2.89	41.1	2.23	1.3	906.	SAND
25.82	5100.	5.82	17.10	2.30	5.52	16.52	2.52	2.620	1.98	1.772	1.63	3.80	-0.03	382.	0.29		166.3	40.8	2.93	40.9	1.01	0.6	354.	SAND
26.13	5000.	4.89	17.00	2.35	4.54	16.42	2.57	2.651	1.98	1.801	1.05	6.27	-0.04	412.	0.21		167.5	41.1	2.98	41.2	0.55	0.3	350.	SAND
26.43	6150.	5.25	20.10	2.37	4.77	19.52	2.59	2.682	1.98	1.829	1.14	7.07	-0.04	512.	0.17		205.7	42.4	3.06	42.5	0.39	0.2	435.	SAND
26.74	4950.	5.03	17.60	2.40	4.66	17.02	2.62	2.713	1.98	1.858	1.05	6.34	-0.05	429.									365.	SAND
27.04	4200.	10.20	20.90	2.82	9.76	20.32	3.04	2.744	2.03	1.886	3.72	1.51	0.04	367.	0.65		119.6	37.2	3.03	37.4	4.89	2.6	566.	SANDY SILT
27.35	3000.	9.30	12.20	0.00	9.41	11.62	0.22	2.775	1.88	1.914	3.47	0.33	-0.38	77.	0.88	0.84					4.52	2.4	108.	CLAY
27.65	1229.	11.20	15.35	8.30	11.08	14.77	8.52	2.806	1.98	1.941	4.27	0.45	0.69	128.	1.03	1.10					6.33	3.3	208.	SILTY CLAY
27.96	1157.	10.35	13.30	9.75	10.29	12.72	9.97	2.837	1.88	1.968	3.79	0.33	0.96	84.	0.95	0.96					5.33	2.7	127.	CLAY
28.26	1178.	9.25	11.95	8.23	9.38	11.37	8.45	2.868	1.88	1.993	3.27	0.31	0.86	69.	0.84	0.81					4.28	2.1	94.	CLAY
28.57	1193.	8.80	11.25	7.65	8.94	10.67	7.87	2.899	1.88	2.019	2.99	0.29	0.82	60.	0.78	0.73					3.78	1.9	76.	CLAY
28.87	1543.	9.05	11.80	0.00	9.17	11.22	0.22	2.929	1.88	2.043	3.06	0.33	-0.43	71.	0.80	0.76					3.96	1.9	91.	CLAY
29.18	1749.	9.40	13.90	5.22	9.43	13.32	5.44	2.961	1.88	2.069	3.13	0.60	0.38	135.	0.81						4.16	2.0	176.	CLAYEY SILT
29.48	1610.	11.00	14.85	8.75	10.90	14.27	8.97	2.991	1.98	2.096	3.77	0.43	0.76	117.	0.94	1.02					5.64	2.7	176.	SILTY CLAY
29.79	1641.	13.20	18.90	8.31	13.01	18.32	8.53	3.023	1.98	2.124	4.70	0.53	0.55	184.	1.11	1.36					8.06	3.8	318.	SILTY CLAY
30.09	1924.	13.20	18.05	8.32	13.05	17.47	8.54	3.053	1.98	2.152	4.64	0.44	0.55	153.	1.10	1.36					8.01	3.7	263.	SILTY CLAY
30.40	1800.	12.05	17.15	8.40	11.89	16.57	8.62	3.085	1.98	2.181	4.04	0.53	0.63	163.	0.99	1.15					6.52	3.0	255.	SILTY CLAY
30.70	1698.	10.70	14.35	9.00	10.61	13.77	9.22	3.115	1.88	2.207	3.39	0.42	0.81	110.	0.87	0.94					5.04	2.3	153.	SILTY CLAY
31.01	1610.	13.70	17.10	10.80	13.62	16.52	10.86	3.147	1.98	2.235	4.69	0.28	0.74	101.	1.11	1.43					8.44	3.8	173.	CLAY
31.31	1965.	13.60	17.70	10.00	13.49	17.12	10.22	3.177	1.98	2.263	4.56	0.35	0.68	126.	1.09	1.39					8.18	3.6	214.	SILTY CLAY
31.54	2505.	14.70	20.00	10.05	14.53	19.42	10.11	3.200	1.98	2.284	4.96	0.43	0.61	170.	1.15	1.56					9.42	4.1	302.	SILTY CLAY

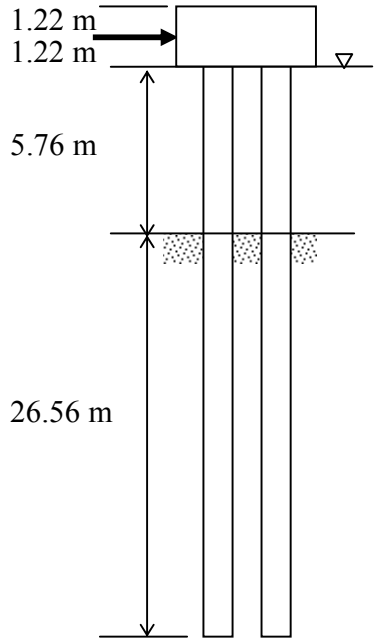

Length: 33.5m
Type: Drilled Shaft Group
Diameter: 2134 mm
Material Properties:
Concrete:
f'_c = 33.1 MPa
E_c = 27.2 GPa
Steel:
f_y = 275.7 MPa
E_s = 200 GPa

Reinforcement Details:
48 # 14 bars above elevation –7.6 m
24 # 14 bars below elevation –7.6 m
76 mm clear cover.

Figure 5a Pascagoula Load Test

BACK

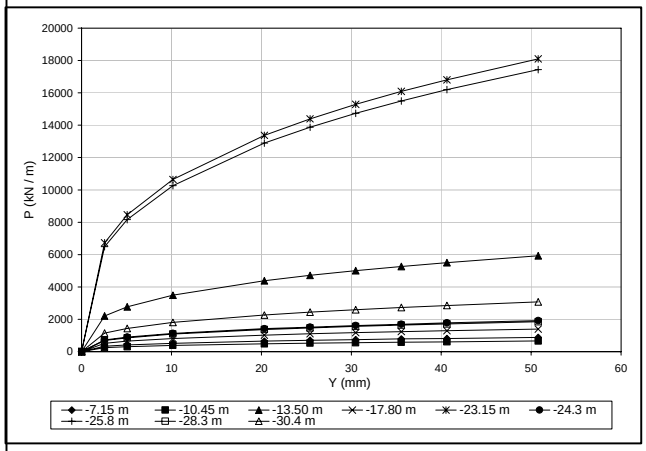

P-y Curves for Pascagoula

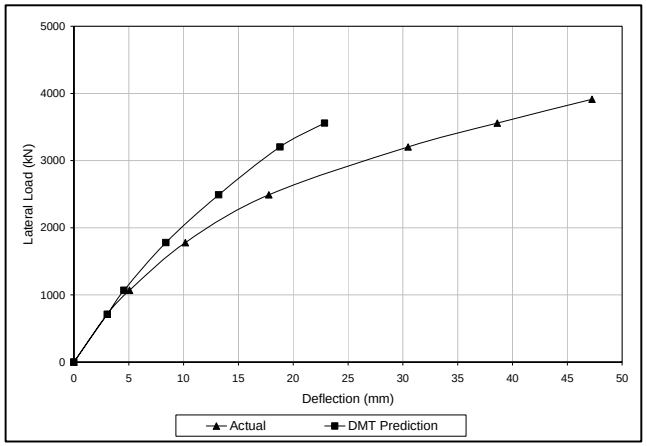

Simulation Results for Pascagoula

Figure 5b Pascagoula Load Test Continued

BACK

DILATOMETER DATA LISTING & INTERPRETATION (BASED ON THE 1988 DILATOMETER MANUAL)
University of Florida
JOB FILE: Auburn Spring Villa NGES
LOCATION: Spring Villa Site
SNDG.BY : ???
ANAL.BY : J.B. Anderson

SNDG. NO. DMT-2
FILE NO. : AU-2
SNDG.DATE: August 1996
ANAL.DATE: 15 Dec 05

ANALYSIS PARAMETERS: LO RANGE =40.00 BARS ROD DIAM. = 3.57 CM BL.THICK. = 15.0 MM SU FACTOR = 1.00
SURF.ELEV. = 0.00 M LO GAGE 0 = 0.00 BARS FR.RED.DIA. = 4.78 CM BL.WIDTH = 96.0 MM PHI FACTOR = 1.00
WATER DEPTH = 2.44 M HI GAGE 0 = 0.00 BARS LIN.ROD WT. = 6.50 KGF/M DELTA-A = 0.16 BARS OCR FACTOR = 1.00
SP.GR.WATER = 1.000 CAL GAGE 0 = 0.00 BARS DELTA/PHI = 0.50 DELTA-B = 0.62 BARS M FACTOR = 1.00
MAX SU ID = 0.60 SU OPTION = MARCHETTI MIN PHI ID = 1.20 OCR OPTION= MARCHETTI K0 FACTOR = 1.00
UNIT CONVERSIONS: 1 BAR = 1.019 KGF/CM2 = 1.044 TSF = 14.51 PSI 1 M = 3.2808 FT

Z (M)	THRUST (KGP)	A (BAR)	B (BAR)	C (BAR)	P0 (BAR)	P1 (BAR)	P2 (BAR)	U0 (BAR)	GAMMA (T/M3)	SVP (BAR)	KD	ID	UD	ED (BAR)	K0	SU (BAR)	QD (BAR)	PHI (DEG)	SIGFF (BAR)	PHIO (DEG)	PC (BAR)	OCR	M (BAR)	SOIL TYPE
0.30		2.70	8.70		2.60	8.08		0.000	1.90	0.055	47.25	2.11	0.00	190.									755.	SILTY SAND
0.60		4.90	10.10		4.84	9.48		0.000	1.80	0.109	44.21	0.96	0.00	161.	4.30						13.70	125.1	629.	SILT
1.20		5.10	11.40		4.98	10.78		0.000	1.80	0.215	23.13	1.16	0.00	201.	3.02						9.82	45.6	662.	SILT
1.50		4.10	9.40		4.03	8.78		0.000	1.80	0.268	15.03	1.18	0.00	165.	2.35						6.24	23.2	475.	SILT
1.80		3.70	8.25		3.67	7.63		0.000	1.80	0.321	11.42	1.08	0.00	137.	2.00						4.87	15.2	361.	SILT
2.10		3.80	8.15		3.78	7.53		0.000	1.80	0.374	10.10	0.99	0.00	130.	1.85						4.68	12.5	326.	SILT
2.40		3.80	8.05		3.79	7.43		0.000	1.80	0.427	8.86	0.96	0.00	126.	1.70						4.36	10.2	301.	SILT
2.70		3.60	7.35		3.61	6.73		0.026	1.80	0.455	7.88	0.87	0.00	108.	1.58						3.86	8.5	245.	CLAYEY SILT
3.00		3.30	6.95		3.32	6.33		0.055	1.80	0.478	6.82	0.92	0.00	105.	1.44						3.24	6.8	221.	SILT
3.30		2.85	6.70		2.86	6.08		0.084	1.70	0.501	5.54	1.16	0.00	112.	1.25						2.45	4.9	214.	SILT
3.60		3.55	7.25		3.56	6.63		0.114	1.80	0.523	6.60	0.89	0.00	106.	1.41						3.37	6.4	222.	CLAYEY SILT
3.90		4.70	8.40		4.71	7.78		0.143	1.80	0.546	8.37	0.67	0.00	106.	1.64						5.09	9.3	247.	CLAYEY SILT
4.20		3.95	7.55		3.97	6.93		0.173	1.80	0.570	6.66	0.78	0.00	103.	1.42						3.72	6.5	215.	CLAYEY SILT
4.50		4.40	8.45		4.40	7.83		0.202	1.80	0.593	7.07	0.82	0.00	119.	1.47						4.25	7.2	256.	CLAYEY SILT
4.80		3.65	7.25		3.67	6.63		0.232	1.80	0.617	5.57	0.86	0.00	103.	1.25						3.05	4.9	196.	CLAYEY SILT
5.10		3.70	7.25		3.72	6.63		0.261	1.80	0.640	5.40	0.84	0.00	101.	1.23						3.02	4.7	190.	CLAYEY SILT
5.40		3.70	6.90		3.74	6.28		0.290	1.80	0.664	5.19	0.74	0.00	88.	1.19						2.94	4.4	162.	CLAYEY SILT
5.70		4.05	8.85		4.01	8.23		0.320	1.80	0.687	5.37	1.14	0.00	146.	1.22						3.21	4.7	276.	SILT
6.00		4.25	9.50		4.19	8.88		0.349	1.80	0.711	5.40	1.22	0.00	163.									308.	SANDY SILT
6.30		4.15	8.60		4.13	7.98		0.379	1.80	0.735	5.10	1.03	0.00	134.	1.18						3.17	4.3	245.	SILT
6.60		4.80	9.95		4.74	9.33		0.408	1.80	0.758	5.72	1.06	0.00	159.	1.28						3.90	5.1	309.	SILT
6.90		5.00	9.80		4.96	9.18		0.438	1.80	0.782	5.78	0.93	0.00	146.	1.29						4.10	5.2	286.	SILT
7.20		6.05	11.50		5.98	10.88		0.467	1.80	0.805	6.84	0.89	0.00	170.	1.44						5.49	6.8	360.	CLAYEY SILT
7.50		5.85	12.50		5.72	11.88		0.497	1.80	0.829	6.30	1.18	0.00	214.	1.36						4.96	6.0	437.	SILT
7.80		4.55	11.80		4.39	11.18		0.526	1.80	0.852	4.53	1.76	0.00	236.									412.	SANDY SILT
8.10		7.25	21.25		6.75	20.63		0.555	2.00	0.879	7.05	2.24	0.00	482.									1049.	SILTY SAND

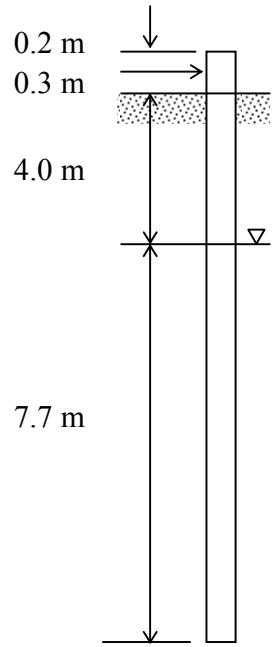

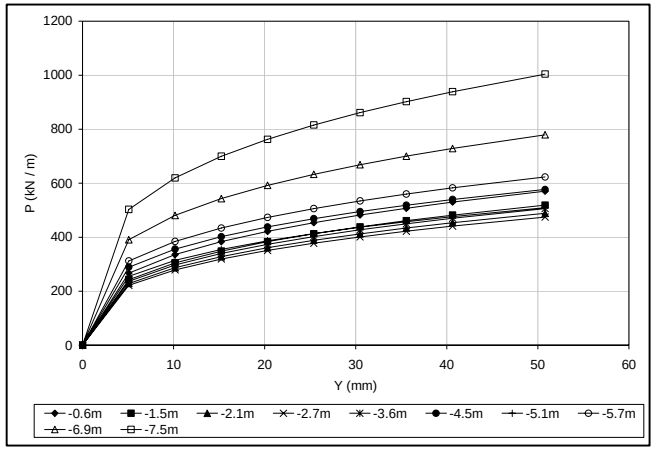

P-y Curves for Auburn

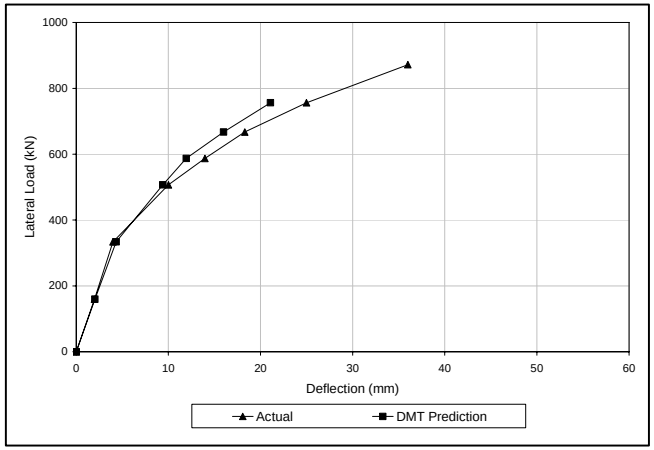

Simulation Results for Auburn

Length: 12m
Type: Drilled Shaft
Diameter: 915 mm
Material Properties
Concrete:
f'_c = 33.1 MPa
E_c = 27.7 GPa
Steel:
f_y = 275.7 MPa
E_s = 200 GPa

Reinforcement Details: 12 #11 Bars
76mm clear cover

Figure 6 Auburn Load Test

BACK

Embankment design with DMT and CPTu: prediction and performance

M. Arroyo
Department of Geotechnical Engineering and Geosciences, UPC, Barcelona, Spain

T. Mateos.
Iberinsa, Madrid, Spain

Keywords: CPTu, DMT, settlement, deformability, stiffness, deltaic, embankments

ABSTRACT: Ongoing enlargement of the Barcelona Airport at Prat de Llobregat required a major road access redesign. Major earthworks were necessary both for preloading purposes and to build the final motorway embankments. Accurate settlement prediction was necessary, and it was largely based on "in situ" tests. DMT was the basic tool to predict final settlements, while CPTu provided the necessary information to evaluate consolidation times. The motorway embankments are now approaching completion. Several instrumented sections have been employed for the detailed monitoring of settlements. Instrumentation-revealed settlements are presented and compared with those predicted at the design stage. Comments are made on the adequacy or else of the several hypothesis employed for design.

1 INTRODUCTION

Barcelona is the second largest city in Spain. The Llobregat delta plain is located just south of Barcelona and is the location of our study. It hosts an expanding population, a large number of basic infrastructures, important industrial areas as well as several natural reserves and tourist resorts.

1.1 *Geological setting*

The geological structure of Llobregat delta is similar to other Mediterranean deltas. A wedge of low plasticity silty and clayey deposits, increasing to a thickness of 60 m near the shoreline, overlies a deep sandy and gravelly aquifer and is overlaid by a roughly 10 m thick, well-graded, medium-dense sand layer. A superficial thin deposit of alluvial and marshy clays sometimes occurs on top. A detailed CPT-based stratigraphic and sedimentological analysis of Llobregat delta is presented by Devincenzi et al. (2004).

The water table is located in the upper sand, generally at 1 to 1.5 m depth. These sands are highly permeable with equivalent permeability of 10^{-2} cm/s. On several isolated spots the sands had been quarried, being generally replaced by uncontrolled fills.

1.2 *Local geotechnical practice*

Past experience in the area clearly indicates that the main foundation problem appears as a consequence of the medium to high compressibility of the intermediate silts and clays. The upper sand offers a fairly good foundation level, but large settlements may ensue when the load extent is such that silts and clays are also affected.

The depth of the lower aquifer makes any attempt to support foundations using piles non-feasible. Apart from that, the lower aquifer is also a vital water resource of the area, and stringent environmental rules severely limit its perforation by piled foundations. On the other hand the frequent presence sandy layers within the silty and clayey levels, generally results in a relatively fast consolidation. These circumstances make preloading a sensible choice in many instances (e.g. Alonso et al. 2000, Gens & Lloret, 2003).

Settlement evaluation requires an estimate of soil stiffness. The critical silty and clayey layers present great sampling difficulties, partly due to the presence of finely interbedded sandy layers. There-fore intact sample recovery is problematic and laboratory measurements of "in situ" stiffness are scarce and probably biased. For large projects, large instrumented load tests have been employed to overcome the ensuing uncertainty.

The traditional "in situ" measurement in the area was SPT. Since the early 90's CPTu testing has become common practice. Pressuremeter testing is also

BACK

sometimes performed. There was no previous large-scale experience of DMT testing.

Figure 1. Projected enlargement of El Prat airport (Barcelona). A solid line encloses the motorway project area.

2 EMBANKMENT DESIGN

2.1 *Project description*

The new terminal building of Barcelona Airport will serve up to 25 million passengers per year (Fig. 1). The road access to this new terminal is de-signed as a 8-lane motorway. This motorway flies over a relocated 6-lane motorway, a major flood de-fence waterway, railway access to the airport and various minor roads.

These many obstacles force the motorway into heights of 12 m and above for more than 2 km. A number of large embankments alternate with several bridges and caisson type structures. The expected schedule for work completion is less than 3 years and the construction sequence may include several successive enlargements.

It was clear from the onset that the width and length of the embankment loads wouls cause large settlements. Embankment settlement was important "per se" and also because of its possible influence on old or recently built structures

It was also anticipated that structural loads, even if smaller than those induced by the earthworks, would cause settlements unacceptable for good structural performance. Preloading was the obvious solution. However, the preloaded embankments were subjected to a strict schedule, since the material available for earthworks was very scarce, and needed for the motorway embankments.

Within these project constraints, estimating the magnitude and rate of embankment induced settlement became a critical design issue.

2.2 *Site investigation*

The site investigation program included rotary coring, laboratory tests, DMT and piezocone probes. The resulting stratigraphic picture fell well within expectations. In the project area the mean depth of the lower aquifer was 40 m. A roughly 30 m thick intermediate layer of silts and clay appeared between the upper sands and the lower aquifer. In some places the upper sand had been replaced by uncontrolled fills.

More details from the site investigation program and the results obtained might be found in Arroyo et al. (2004).

2.3 *Design approach*

As expected, sampling problems were pervasive on the softest layers, resulting on very few quality samples to obtain stiffness with. SPT values were numerous, but also deemed too unreliable and approximate to be employed as a design tool. Therefore, the general design approach relied mostly on in-situ probes. DMT probes were selected as the basic tool to evaluate settlement magnitude, while CPTu data were mostly used to ascertain set-tlement rate.

The DMT-based settlement evaluation procedure was pretty standard. The method (Marchetti, 2001) involves approximating a 1-D integral of deformation using an expression like

$$S = \int_E^H \varepsilon(z)dz \approx \sum_{z_i=E}^{z_i=H} \frac{\Delta\sigma_v(z_i)}{M_D(z_i)}\Delta z \qquad (1)$$

The formula uses two depth-dependent distributions, that of constrained moduli, $M_D(z)$, obtained from a DMT test and an incremental stress distribution $\Delta\sigma_v$ (z). The latter was obtained from elastic closed-form solutions; this process involved some extra approximations, particularly considering the highly contrasted stiffness profile. The S value thus obtained corresponds to a drained, long-term, post-consolidation, settlement

The above procedure can be easily generalised to account for consolidation. To do so, $\Delta\sigma'_v$ (z,t), a time-dependent effective incremental stress distribution is used in (1). This distribution is computed by means of

$$\Delta\sigma'_v(z,t) = \Delta\sigma_v(z)U\left(\frac{tc_v}{H^2}\right) \qquad (2)$$

where U represents a consolidation degree given by the classical Terzaghi 1-D theory. Apart from time, t, U depends on the vertical consolidation coefficient, c_v, and the distance to a free draining surface, H. These two values were obtained using the CPTu probes.

Piezocone dissipation tests were interpreted following Teh & Houlsby (1991) to obtain horizontal

consolidation coefficients (c_h). Some results from laboratory oedometric tests on the most fine-grained layers were also available. In Figure 2 both datasets are plotted together, revealing large differences between field and laboratory results.

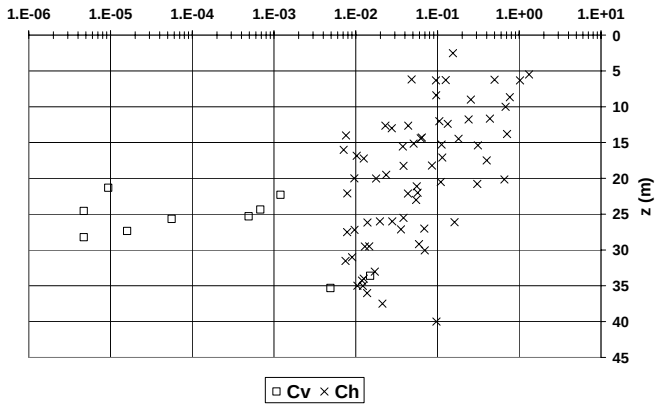

Figure 2. Consolidation coefficients obtained from field (Ch) and laboratory data (Cv).

Admittedly, such differences are not uncommon (Schnaid, 2005), but they still leave ample room for choice. In this case, and based on previous load test results in the area (Alonso et al. 2000), a unique c_v of $4*10^{-3}cm^2/s$ was chosen for the silty and clayey deposits. The upper sands were considered as free draining.

The choice of a drainage distance value, H, is of greater consequence to the computation than that of the consolidation coefficient. In our case the H value to employ in (2) was directly based on piezocone logs. A depth-dependent H(z) was selected inspecting the excess pore pressure log of the piezocone. This resulted in H(z) distributions for each piezocone, an example of which is shown in Figure 3. The selection procedure had a deliberately conservative bias, intended to roughly compensate possible lateral discontinuities of the draining layers.

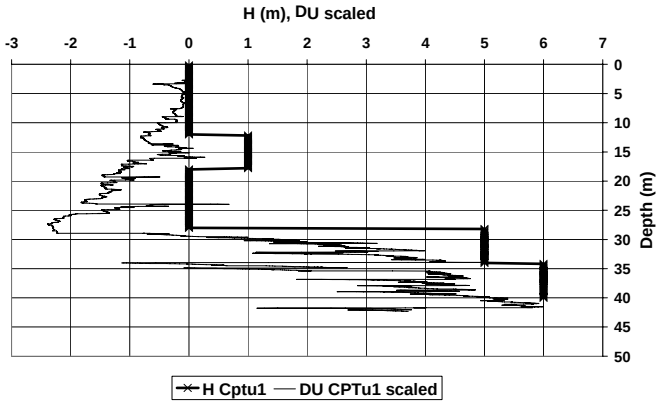

Figure 3 Excess pore pressure log (scaled) and interpreted undrained average distances, H.

Two final aspects of the design approach are worth mentioning. One is that, initially, a relatively small amount of secondary consolidation was also taken into account, since there were some reports pointing to its importance (Alonso et al. 2000). Secondary consolidation was conspicuously absent from the monitoring measurements, and therefore the "predicted" results in this paper have been removed of these extra settlements. The second aspect is that a performance-based relation between CPTu and DMT (Arroyo et al., 2004) was employed to supplement the lack of direct DMT data on some emplacements. None of the cases described in the following lacked direct DMT data, and therefore none is analyzed using such relation.

3 CASE STUDY DESCRIPTION

Results from three monitored case studies, including five different embankments will now be presented.

The first case study corresponds to three closely spaced pre-loading embankments, located in an area where the geotechnical profile is fairly typical of the Llobregat delta average.

The second case study corresponds to a permanent embankment, located in an area where the site investigation revealed an important layer of very soft mud.

The third case study corresponds to an embankment located in an area where the upper sand layer was replaced by made ground.

3.1 *Case study 1*

Three embankments (P-10, P-10s, and P-10m) were built nearby to pre-load the area of construction of a box culvert and two overpasses.

Preload embankment P-10 was the largest. It has an irregular plan area, with length of about 100 m at the top and an average width of about 50 m. The maximum embankment height was 12.75 m and it was constructed in 78 days.

Preload embankment P-10s was approximately square in plan, with 50 m per side. It was raised to 11.85 m and the construction lasted 150 days. Preload embankment P-10m was also square in plan, with a 40 m side. It was raised to 12.20 m in a 60 day period.

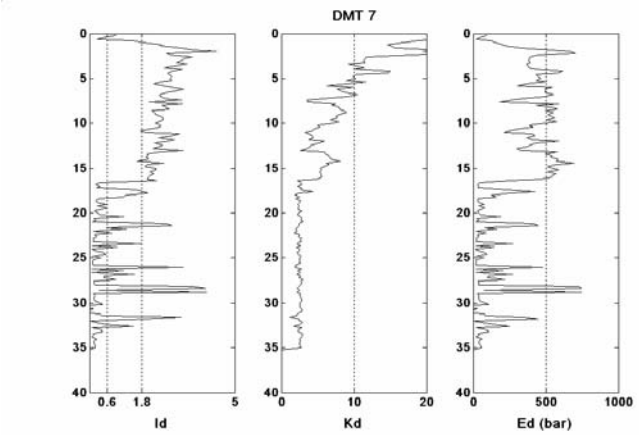

Figure 4: Typical DMT profile at Case 1 location

Settlement evaluations for embankments P-10 and P-10s were both based on the results of dilatometer DMT7 and piezocone CPTu7. Settlement evaluation for embankment P-10m was based instead on tests DMT14s and CPTu14s. An example of the DMT profiles obtained in the area is shown in Figure 4. The upper sand layer is clearly visible.

The three preload embankments were monitored with settlement plates, plus horizontal and vertical inclinometers. In Figure 5 the instrumentation outlay for embankment P10m is illustrated. The arrangement for the other embankments was very similar.

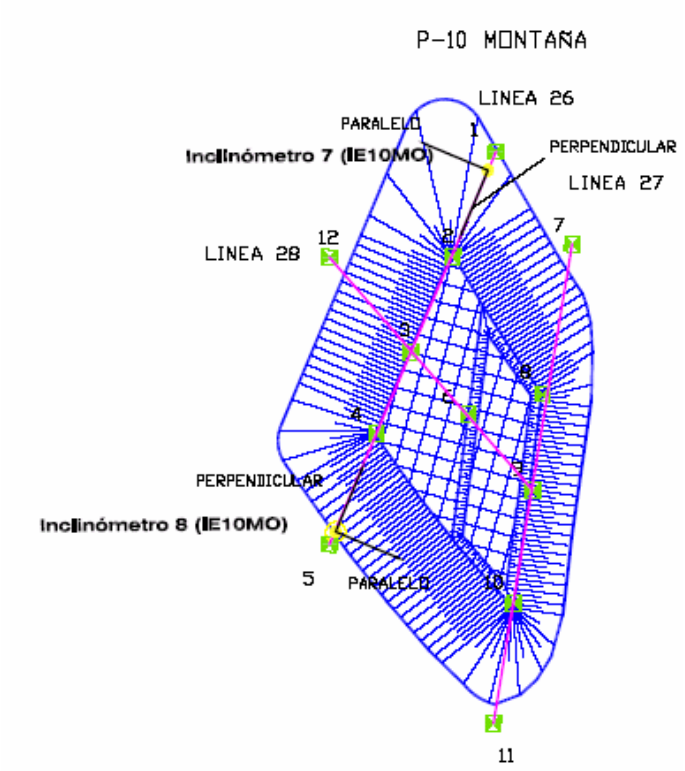

Figure 5. Instrumentation outlay for embankment P10m

3.2 *Case study 2*

This is a permanent embankment, 12 m high, 80 m wide and 190 m long, located on the main axis of the motorway. Construction started in April 2005 and, while not yet finished, had attained a height of 4.5 m at the time of writing. Embankment is being monitored using settlement plates, horizontal and vertical inclinometers and an extensometer.

Soil investigation at the embankment location initially included two dilatometers (DMT4 and DMT5). They revealed softer than average silt layers. As a consequence of the large embankment load, the dilatometer settlement evaluation indicated an average of 2.5 m of long term settlement. The extra volume of material required to compensate such settlement was not negligible, and it seemed convenient to confirm the dilatometric results by performing another sounding. Test repeatability was good and the prediction of large settlements was confirmed. It is noteworthy that the accompanying piezocone (CPTu4) would have not given enough indication of such a large deformability.

An example DMT profile at this case is shown in figure 6. The very soft layers below the upper sands are clearly visible.

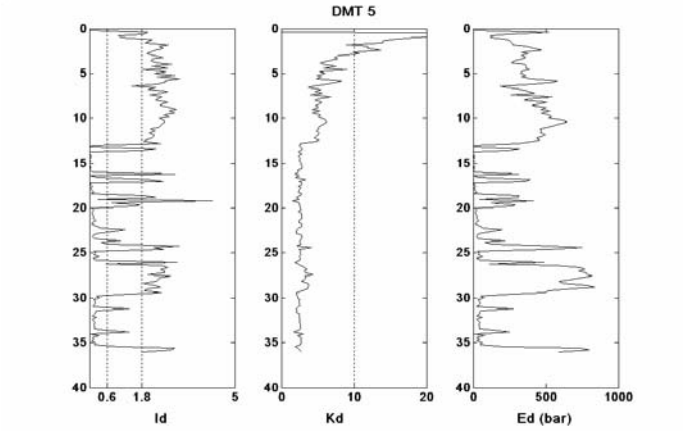

Figure 6. Typical DMT profile at Case 2 location

3.3 *Case study 3*

The third case study corresponds to an area where the upper sand layer had been replaced by uncontrolled fills. Both rotary drilling and in-situ tests detected the presence of the fills, whose thickness varied between 4 and 8 m.

The piezocone and dilatometer results in that layer were unreliable, erratic and frequently lacking pressure readings (Figure 7).

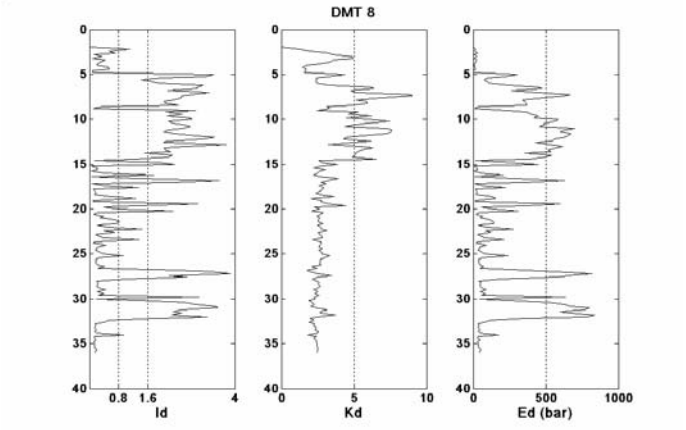

Figure 7. Typical DMT results at case 3 location. Estimated fill thickness at this point: 6 m.

A large culvert box structure is planned in the area, and preloading was necessary to ensure acceptable settlements. A preloading embankment, 11 m high, 17 m wide and of 120 m long, was constructed in 10 weeks.

As shown in Figure 8, the preload embankment was monitored using settlement plates, horizontal and vertical inclinometers and an extensometer. However, this extensometer was only operative for a month, since it was damaged early after the start of construction operations.

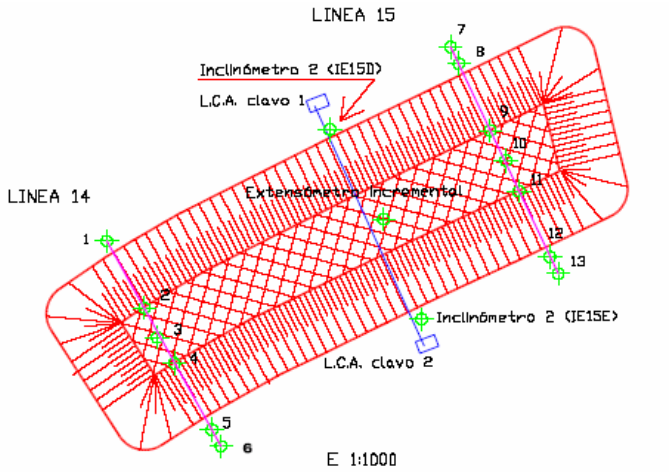

Figure 8. Instrumentation outlay for Case 3. LCA indicates an horizontal inclinometer. Numbers 1 to 13 indicate settlement plates.

4 RESULTS

4.1 *Case study 1*

In Figure 9 the settlement evolution predicted along the centerline of embankment P10 is compared with the settlement measured by a plate located there. Initially, the computations had assumed a very fast construction, i.e. quasi-instantaneous load application. In practice, it took over two months for the embankment to reach its maximum height of about 12 m. When the real load history is taken into account the predicted settlement agreed very well with the measured settlement.

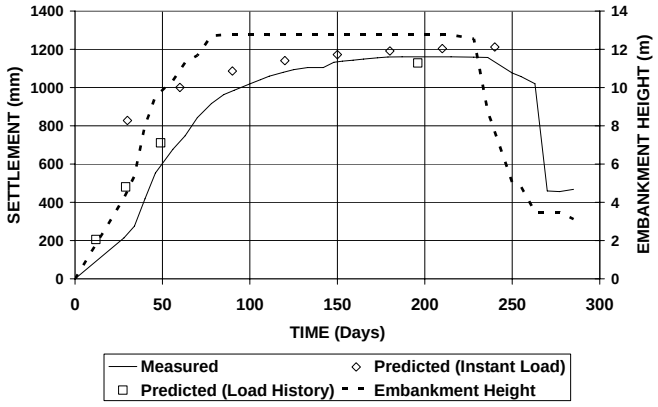

Figure 9. Time-history of embankment loading, measured and predicted settlements for P10 (Case 1).

The settlement seemed to stabilize after 150 days. The final consolidation settlement value measured has an excellent agreement with that predicted with the DMT. Similar results were obtained with the other two nearby embankments, P10m and P10s as shown in Figure 10.

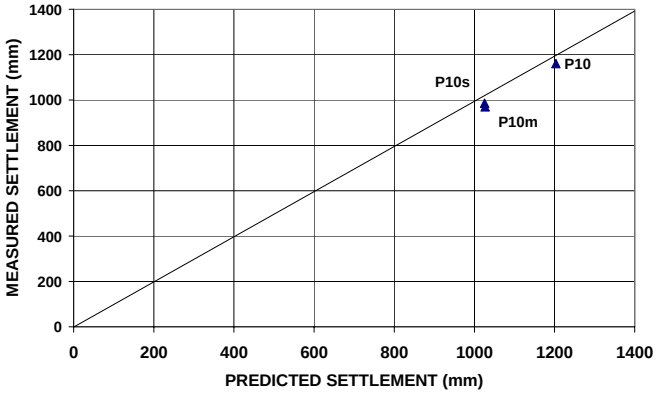

Figure 10. Predicted vs measured settlement at the end of consolidation at embankment centerline

4.2 *Case study 2*

As explained above, this embankment has not yet reached its design height. In Figure 11 the load history is plotted alongside the measured settlement at a plate located at the embankment centerline. The figure includes the measured settlement at the top of a nearby extensometer and the DMT-predicted settlement history. The prediction was obtained taking into account the load history of the embankment.

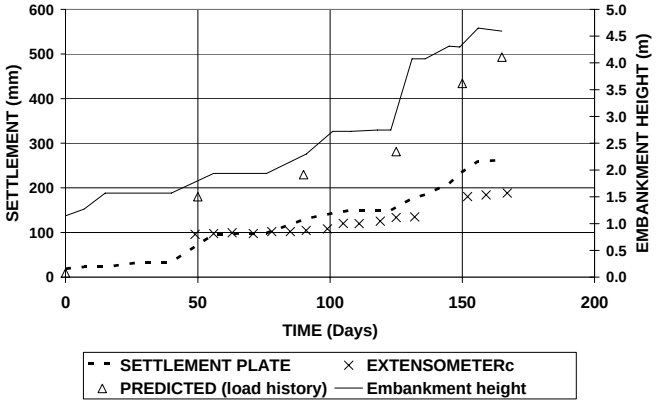

Figure 11: Time history of loading, measured and predicted settlements for Case 2.

It is fairly clear that the settlement prediction here obtained is too conservative, nearly double of that measured by the settlement plates. Some insight into the sources of this error might be obtained by looking in more detail at the DMT prediction.

Such a detail is provided, in principle, by the extensometric readings. In fact, the extensometric readings available in this case pose some problems of their own, like their late start or their divergence from the plate readings, visible in Figure 11. Notwithstanding these difficulties a comparison is attempted in Figure 12 for the settlements measured as a response to the loading step of approximately 1.5 m made 125 days after the construction started.

The comparison shows that there are two main causes for the divergence between measured and predicted settlements. The first is the greater depth of the upper rigid layer at the extensometer location:

BACK

16 m vs 12 m for the assumed profile. The second cause is the larger settlements predicted for the deeper clayey layers. It remains yet to be seen if the prediction error is due here to a DMT-based underestimate of the operative drained moduli or to a CPTu-based overestimate of the settlement rate.

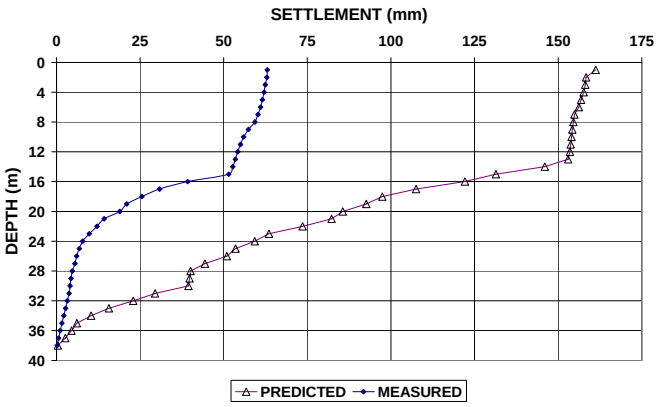

Figure 12. Settlement vs depth distributions predicted and measured in case 2. Prediction made by DMT-CPTu method for a load step of 1.5 m at 125 days.

4.3 *Case study 3*

In this case, as in case 1, the preload history is complete. Figure 13 shows that both load and settlements were almost level for a period of nearly 100 days. The figure presents measurements obtained with different instruments: two different settlement plates, an horizontal inclinometer (LCA in Figure 8) and an extensometer. There are important variations in the measurements of the to different instruments. This may be partly attributed to the different thickness of fills present alongside the embankment.

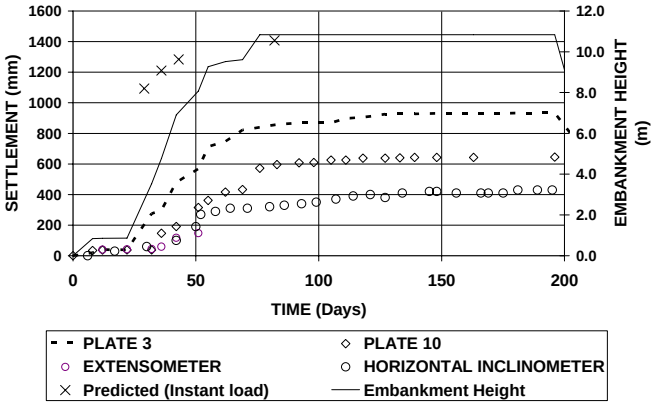

Figure 13. Time-history of embankment loading, measured and predicted settlements for Case 2.

However variable the fill thickness was, it is clear that a large part of the discrepancy between measures and prediction may be attributed to the conservative characterization of the fill at the design stage. The poor results of the DMT measurements in the fill were compensated with a very conservative estimate of the fill operative modulus. This is clear in Figure 14, where the 5 upper meters of fill contribute almost half of the surface settlement.

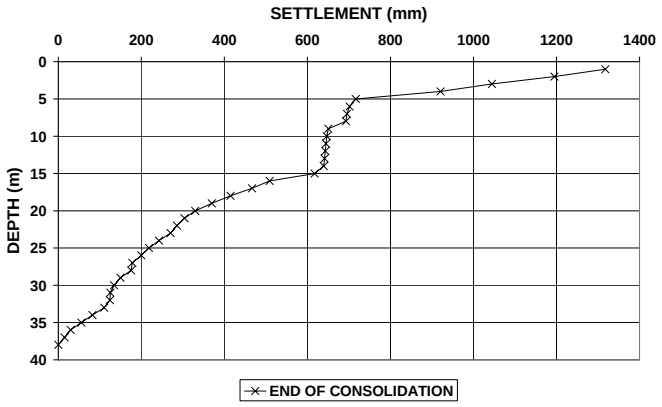

Figure 14. Depth distribution of the predicted consolidation settlement for Case 3.

As shown in figure 13, the extensometer present in this case failed quickly, only after nearly 50 days of embankment construction. At that stage the accumulated settlement measured by the instrument is shown in figure 15.

The extensometer readings do not suggest there is a fundamental change in stiffness between made ground and soil as assumed in design. If this error is removed from the DMT-prediction shown in Figure 14, the final settlement value estimated would have compared much better with the settlement plate measurements (600 to 900 mm, Figure 13).

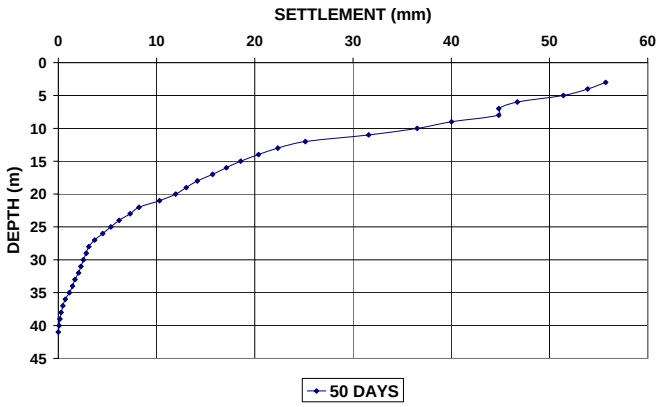

Figure 15. Last valid reading of the extensometer in Case 3.

4.4 *Other aspects*

None of the previous cases had included piezometers within the monitoring measurements. That decision was partly based on the generally poor performance of these instruments on the Llobregat delta area. In fact, measurements taken with vibrating wire piezometers in other embankments of the project were always unable to register any excess porepressure.

5 SUMMARY AND CONCLUSIONS

This paper has presented results from several embankment loads on a deltaic area where large settlements have been measured. These measurements have been compared with settlement predictions

made with DMT and CPTu. Three cases were presented.

In the first case consolidation is complete and the ground profile is regular and did not include any large pockets of very soft mud or made ground. The end of consolidation DMT-predicted settlement fits almost perfectly with the measurements. The CPTu-based prediction of consolidation is acceptable.

In the second case the ground profile is more varied, due to the presence of pockets of very soft mud. The settlement prediction seems over conservative. Since consolidation is not yet complete, it is not possible to determine if the measured settlements will continue to increase until they more closely match the DMT or CPTu predictions.

The emplacement of the third case is full of fill of varying thickness. The preload embankment completed its settlement, attaining a lower final settlement than that predicted with the "in situ" probes. The prediction error can be mostly attributed to an incorrect characterization of the fill, partly due to failing "in situ" measurements.

In balance, it may be said that the combination DMT-CPTu has proved itself a very useful instrument for settlement prediction in this deltaic area.

ACKNOWLEDGEMENTS

The authors gratefully acknowledge the permission of AENA to use the data presented in this work.

REFERENCES

Alonso, E., Gens, A. & Lloret, A. 2000. *Precompression design for secondary settlement reduction*. *Gèotechnique*, 50,6, 645-656.

Arroyo, M, Mateos, M.T., Devicenzi, M., Gómez-Escoubes, R. & Martínez, J.M. (2004) CPT-DMT performance-based correlation for settlement design, *ISC'2 International Symposium on Site Characterization Porto 2004, Viana da Fonseca et al. (eds)* Millpress, 1605-1611

Devincenzi, M., Colas, S., Casamor, J.L. Canals, M., Falivene, O. & Busquets, P. 2004. *High resolution stratigraphic and sedimentological analysis of Llobregat delta –Barcelona– from CPT/CPTu Tests*. Proc. 2nd International Conference on Geotechnical Site Characterization ISC-2, Porto.

Gens, A. & Lloret, A. 2003. *Monitoring a preload test in soft ground, Field measurements in Geomechanics.* Myrvoll (ed.) Swets & Zeitlinger, Lisse. 53-59.

Lunne, T., Robertson, P.K. & Powell, J.J.M. 1997. *Cone Pentration Testing in geotechnical practice*. Blackie Academic & Professiona, London, U.K.

Marchetti, S. 2001. *The flat dilatometer. Applications to geotechnical design*. 18th Conferencia geotecnica Torino

Marchetti, S. 1997. *The flat dilatometer. Keynote lecture.* 3rd geotechnical engineering conference, Cairo University.

Mayne, P.W. 2002. *Equivalent CPT method for calculating shallow foundation settlements in the Piedmont residual soils based on the DMT constrained modulus approach.* At http://www.ce.gatech.edu/~geosys/Faculty/Mayne/papers/

Mayne, P.W. 1998. *Commentary on Marchetti flat dilatometer correlations in soils*. *ASTM Geotechnical Testing Journal*, 21, 3, 222-239.

Schnaid, F. (2005) Geo-characterisation and properties of natural soils by in situ tests, Proc. XVI ICSMGE Osaka, Vol.1, 3-45

Teh, C.I. & Houlsby, G.T. (1991) An analytical study of the cone penetration test in clay. Geotechnique, 41(1): 17-34

BACK

Assessment of the stability of a century-old water supply dam in north-central Pennsylvania

Robert W. Bruhn, P.E.
GAI Consultants, Inc. 385 E. Waterfront Drive, Homestead (Pittsburgh), Pennsylvania 15220, email: r.bruhn@gaiconsultants.com

Thomas A. Gower, P.G.
GAI Consultants, Inc. 385 E. Waterfront Drive, Homestead (Pittsburgh), Pennsylvania 15220, email: t.gower@gaiconsultants.com

Richard M. Ruffolo
GAI Consultants, Inc. 385 E. Waterfront Drive, Homestead (Pittsburgh), Pennsylvania 15220, email: r.ruffolo@gaiconsultants.com

Kim R. Benjamin
Bradford City Water Authority, 28 Kennedy Street, Bradford, Pennsylvania 16701, email:bcwa@atlanticbb.net

Keywords: dilatometer, borehole shear test, stability, earth dam, case study

ABSTRACT: The Bradford No.3 Dam, located a few miles west of the City of Bradford, Pennsylvania, is a 47-foot high earth embankment that was constructed as a water supply impoundment in the late Nineteenth Century and is still used for that purpose today. Although the dam has served its purpose admirably over the past hundred years, its stability had not been formally evaluated nor had the potential for overtopping. This prompted a detailed assessment of the dam pursuant to upgrading the structure to meet state regulatory requirements. The consequent drilling and testing program to establish the types and properties of the embankment and foundation soils revealed soft zones within the embankment that were evidenced by Standard Penetration Test N-values near zero, accompanied by settlement of the drilling tools under their own weight. Difficulties experienced in procuring and testing representative "undisturbed" embankment samples prompted a program of dilatometer and borehole shear testing to more reliably define and characterize the soils. These in-place tests contributed greatly to a rational assessment of the stability of the dam embankment and to the design of cost-effective rehabilitation measures that are expected to extend the life of the dam for decades to come.

1. INTRODUCTION

The Bradford No.3 Dam has for over one hundred years impounded the flows of Marilla Brook to form the Marilla Reservoir, a twenty-acre lake that supplies water to the City of Bradford and provides recreational opportunities for fishing, canoeing, and hiking. The lake is located approximately two miles west of the City of Bradford in McKean County, situated in the Allegheny National Forest Region of north-central Pennsylvania, just south of the New York state line.

Owned and operated by the Bradford City Water Authority, the dam is a diaphragm-earth embankment structure that impounds approximately 500-acre-feet of water at normal pool (Figure 1). It was constructed in 1898-99 by a local contractor and placed in service in 1900. The Pennsylvania Division of Dam Safety classifies the dam as a "B-1", High Hazard "1" structure, the B-1 classification pertaining to dams that are 40-feet or more in height and the High Hazard "1" classification to structures whose sudden failure could result in substantial loss of life and excessive economic losses.

The dam has performed commendably over its first century of service. Maintenance has so far involved relatively minor issues, such as improving drainage in wet areas immediately downstream of the toe of dam, locally resetting stone on the upstream face of the dam, replacing wood planks in the spillway apron, and the like. Even so, no documentation concerning the stability of the dam was known to exist, and, given the age of the structure, none may ever have existed. Also, the spillway was undersized by today's standards, creating the possibility according to recent projections that the embankment might someday be overtopped (al-

Figure 1 Bradford No.3 Dam at Spillway

though so far that has never happened). These circumstances, along with recent attention to a wet zone and a localized surficial slip on the downstream face of the embankment prompted the Bradford City Water Authority, at the request of the Pennsylvania Division of Dam Safety, to assess the stability of the dam and to design and implement rehabilitation measures to bring the dam into compliance with current standards of the Commonwealth of Pennsylvania. The first writers' firm was contracted by the Authority to perform the assessment, design rehabilitation measures, and prepare the necessary technical specifications and drawings.

2. BACKGROUND ON THE DAM

The Bradford No.3 Dam is a 47-foot high, 770-foot long diaphragm-earth embankment, whose embankment faces slope at 2.H:1V (downstream) and 2.5H:1V (upstream), with the topmost six feet of the upstream face steepening to 1.5H:1V.

The spillway is a 58.6-foot wide stone masonry weir located near the left abutment, with a crest elevation approximately six feet below the top of the earth embankment. The principal outlet works consist of a 16-inch cast iron water supply line and a 20-inch diameter cast iron drawdown, or discharge, pipe. Control valves are located in a small building at the downstream toe of the dam.

An 1898 drawing provides the only information available concerning the internal structure of the dam. It indicates that the dam embankment was built of soil derived from a borrow area at the upstream end of the reservoir and, according to 19th Century boring logs, was founded on alluvial deposits of gravel, sand, and clay. "Selected" soil of specification no longer known was used to construct the core of the dam as well as the 8 to 20 foot thick wedge of soil forming the lower half of the upstream face. The core is 60-feet wide at foundation level narrowing to 12 feet at the top of the dam. Within the core is a stone masonry diaphragm (a two to six foot thick wall, narrowing to the top, and constructed of sandstone blocks and Portland cement mortar) that is located along the longitudinal centerline of the dam. It extends to within six feet of the top of the dam embankment and to a depth of nine feet below the original ground surface in an 8 to 12 foot wide trench at the base of the dam. Undifferentiated earth fill was used to construct the shell of the dam. Specifications for fill placement and compaction are unknown.

The upstream face of the dam is armored with tabular slabs of sandstone that have been laid side-by-side, edge-to-edge on the sloping embankment face. Rip rap is reportedly present on the upstream face of the dam at the toe but is out of view below pool level.

The 1898 drawing shows no drainage blanket beneath the embankment downstream of the core.

3. INITIAL SUBSURFACE INVESTIGATION

To achieve a better understanding of site conditions, a traditional subsurface investigation was undertaken that consisted of:

a) Drilling a series of test borings through the embankment and into the foundation, terminating in the alluvial deposits 15 to 25 feet below the base of the embankment, and including borings at the top, at mid-slope, and at the downstream toe of the dam arranged along an uphill-downhill line through the highest embankment section.

b) Conducting Standard Penetration Tests [ASTM D-1586] on a continuous basis along with pocket penetrometer tests on any soils that exhibited cohesive characteristics.

c) Collecting "undisturbed" Shelby tube samples of soil for laboratory testing.

d) Installing piezometers in the test borings.

The drilling investigation was conducted in the summer of 2003 while the reservoir was at normal pool. Drilling began with a boring (B-3-1) at the top of the dam, five feet downstream of the masonry cutoff wall. As the boring was advanced, SPT values at or near zero were recorded at certain depths, accompanied by the drill tools settling under their own weight. The initial boring was terminated at 20 foot depth, 50 feet above the target elevation, while plans for further drilling were reevaluated in light of the soft soil conditions and possible implications concerning embankment stability.

Drilling subsequently resumed with a second boring (B-3-1A) being advanced from the top of the dam near the first boring. The second boring was, in effect, an extension of the first and was augered without sampling to the bottom elevation of the first boring and then advanced with continuous SPTs through the remainder of the embankment and into the foundation soils. The embankment soils encountered in B-3-1A were similar to those in B-3-1 – certain intervals being soft to very soft. Soils encountered in this boring near the base of the dam just downstream of the masonry core wall were characterized by the field geologist as "mud."

Additional borings were drilled on the downstream face of the dam by securing the drill rig by cable to a second rig positioned at the top of the dam as a deadman. This drilling revealed embankment soils that were generally similar to those of the top-of–dam borings, although less frequently as soft.

4. MATERIAL PROPERTIES

Laboratory tests conducted on a series of SPT and Shelby tube samples showed the embankment soils to include clay with sand [CL], clayey sand [SC-SM], silty sand with gravel [SM], and silty gravel with sand [GM]. Distinctions between certain embankment zones shown on the 1898 drawing were somewhat blurred, however, there being no apparent difference between the "selected material" of the central core and the undifferentiated material forming the rest of the embankment.

A representative profile of Standard Penetration Test N-values is presented in Figure 2. The N-value is defined as the number of blows required to drive a standard split barrel sampler a distance of 12 inches into the soil using a 140-pound hammer dropping through a height of 30 inches. Corresponding pocket penetrometer values are also presented in Figure 2. The penetrometer values provide a rough estimate of Qu, the unconfined compressive strength, and in turn the undrained shear strength Su of a cohesive soil.

Profiles of Su estimates from the top-of-dam borings showed a predominance of soft to very soft material (Su $\leq$ 0.5 ksf). Mid-slope and toe borings showed a greater proportion of soils of medium consistency (0.5ksf $\leq$ Su $\leq$ 1ksf). On the basis of the penetrometer tests, the mean value of Su was found to be 0.59 ksf, and the median value, 0.5 ksf.

Laboratory direct shear tests conducted on Shelby tube samples of soil yielded effective friction angles of 33 to 37 degrees and effective cohesion values of 0.476 ksf to 1.34 ksf. These values were regarded as suspiciously high, but were the only results available from the "undisturbed" samples that were collected.

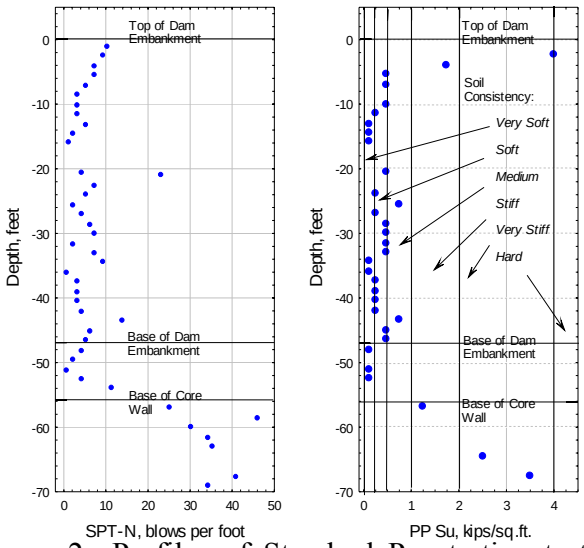

Figure 2 Profiles of Standard Penetration test N-values (left) and Pocket Penetrometer Estimates of undrained Shear Strength (right) for Top-of-Dam Test Borings B-3-1 and B-3-1A (combined)

5. SEEPAGE ANALYSES

The normal pool of Marilla Reservoir is approximately six feet below the top of the dam embankment, and the tail water is downhill of the embankment toe.

A wet zone observed on the downstream face of the dam during the site investigation – an area where surficial slippage was also noted - was recognized as an outbreak of seepage from the reservoir that extended approximately 30 feet upslope from the toe at the mid-section of the embankment and tapered off towards each abutment. Its presence was consistent with no drainage blanket being located beneath the embankment downstream of the core and was expected on the basis of piezometer readings and seepage analyses performed using Seep/W software (Geo-Slope International, Inc).

6. STABILITY ANALYSES

The Pennsylvania Division of Dam Safety requires a factor of safety of no less than 1.5 against failure of the downstream dam face (as does the Corps of Engineers (2003)) for the case of long-term steady state seepage at normal pool.

The Corps of Engineers (2003) has commented on the challenges of assessing the stability of existing dams: "There is danger in relying too heavily on slope stability analyses for existing dams. Appropriate emphasis must be placed on the often difficult task of establishing the true nature of the behavior of the dam through field investigations and research into the historical design, construction records, and observed performance of the embankment. In many instances monitoring and evaluation of instrumentation are the keys to a meaningful assessment of stability. Nevertheless, stability analyses are essential for evaluating remedial measures that involve changes in dam cross sections."

The Bradford No.3 Dam analysis was to provide, in addition to an assessment of existing embankment stability, a baseline for: 1) designing stabilization measures, such as a buttress, in the event that the factor of safety of the existing embankment was unsatisfactory, and 2) determining how far the reservoir pool must be lowered on an interim basis to achieve an acceptable factor of safety while stabilization measures were being designed. Emptying the reservoir in its entirety was to be avoided given its function as a water supply and fish habitat.

The effective stress stability analysis subsequently performed was based on the laboratory-determined effective strength parameters and the pore pressures determined from a steady state seepage analysis. The

Morgenstern-Price method, implemented with Slope/W software (Geo-Slope International, Inc.), indicated a factor of safety of 1.84 of the downstream face of the existing embankment under steady state seepage/normal pool conditions. This was suspected to be a serious overestimate of the factor of safety and to reflect the difficulties of procuring representative samples of the soft to very soft embankment soils, transporting them, and testing them in the laboratory.

For comparison, a total stress analysis of the existing embankment was also performed, with the core and flanking soils being assigned undrained shear strengths between 0.5 ksf and 0.59 ksf, as had been estimated from pocket penetrometer tests. This analysis yielded a factor of safety of between 1 and 1.2 for the downstream face of the dam. Considering the steepness of the downstream face, the undesirable seepage condition on the face, and known low strength zones within the embankment, the results of the total stress analysis were considered more plausible than those of the effective stress analysis.

It was concluded that: 1) the traditional subsurface investigation, which had involved Shelby tube sampling and laboratory testing along with Standard Penetration and Pocket Penetrometer Tests, as are customary for projects of this type and size in this region of the United States, had yielded unreliable and/or contradictory estimates of embankment shear strength and factors of safety, and 2) a supplementary field investigation involving more sophisticated in-place testing was required to reliably determine the strength parameters essential for the effective stress stability analyses, which were needed to assess interim drawdown requirements and to design long term stabilization measures.

7. SUPPLEMENTARY INVESTIGATION

The supplementary field investigation included two dilatometer soundings and three borehole shear tests conducted from the top of the dam near where the first test borings had been drilled. All of the in-place tests were performed at the direction of the writers by In-Situ Soil Testing using downhole equipment temporarily mounted on the drilling contractor's rig, which served as a reaction platform.

7.1 *Dilatometer Soundings*

The flat dilatometer is a steel blade having a thin circular expandable steel membrane mounted on one face. The blade is advanced vertically into the ground by means of push rods, which transfer the thrust from the insertion rig to the blade. (The hydraulic system of a drill rig was used in this case to push the blade, Figure 3). The blade is connected to a control unit on the ground surface by a pneumatic-electrical tube. At regular depth intervals (generally every 8 inches) penetration is stopped and the membrane is inflated by use of compressed gas. Two pressure readings are taken at each depth:

P_o = pressure required to just begin to move the membrane against the soil ("lift-off" pressure)

P_i = pressure required to move the center of the membrane 1.1 mm against the soil.

This process provides an essentially continuous profile of soil properties with depth.

The dilatometer soundings, through correlations such as presented by Marchetti (1980) and ISSMGE

Figure 3 Dilatometer Test in progress at the top of the dam

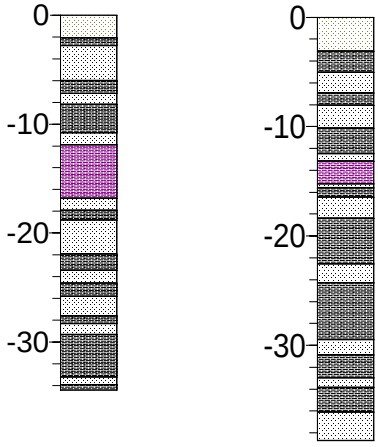

Figure 4 Soil Layering Delineated by Top-of-Dam Dilatometer Soundings D-3-1 (left) and D-3-2 (right). Light-toned layers are cohesionless soils; dark-toned layers are cohesive soils. Vertical axis is in feet.

(2001), differentiated cohesionless layers from cohesive, quantified the effective friction angles of the cohesionless layers, and quantified the undrained shear strengths of the cohesive layers. Of particular significance are the following points:

- Soil Layers. Cohesive layers within the dam embankment alternate with cohesive layers. The cohesive layers were found to range from 0.5 feet to 5 feet in thickness, and to average 2 feet. The cohesionless layers were found to range from 0.35 to 3.2 feet in thickness, and to average 1.6 feet (Figure 4). No correlation of layers is evident between soundings. The layering is thought to reflect the construction methods used a century ago when horse and mule-drawn equipment was used to place the embankment fill (Figure 5), and rudimentary pavements of cohesionless soils were alternated with soft, low permeability cohesive soils to enable the construction equipment to cross the embankment without bogging down. The dilatometer soundings indicate that the embankment consists of approximately 56 percent cohesive soils and 44 percent cohesionless soils.

Figure 5 Bradford Dam No.3 (circa 1898) under construction

- Effective Friction Angle of Cohesionless Soil Layers. The drained friction angle was found to range between 26 and 42 degrees, with a mean value of approximately 34 degrees (Figure 6). These values are based on the correlation of Marchetti presented in ISSMGE (2001):

  $N_{safe,DMT} = 28^o + 14.6^o \log K_D - 2.1^o \log^2 K_D$,

  where K_D is the horizontal stress index.
- Undrained Shear Strength of Cohesive Layers. Su values of the cohesive layers ranged from 0.15 ksf to 0.7 ksf. The mean value was approximately 0.28 ksf (Figure 7). These values are based on the correlation of Marchetti (1980):

  $S_u = 0.22\ \Phi\rho_{vo}\ (0.5K_D)^{1.25}$,

  where $\Phi\rho_{vo}$ is the vertical effective stress prior to blade insertion and K_D is as above.

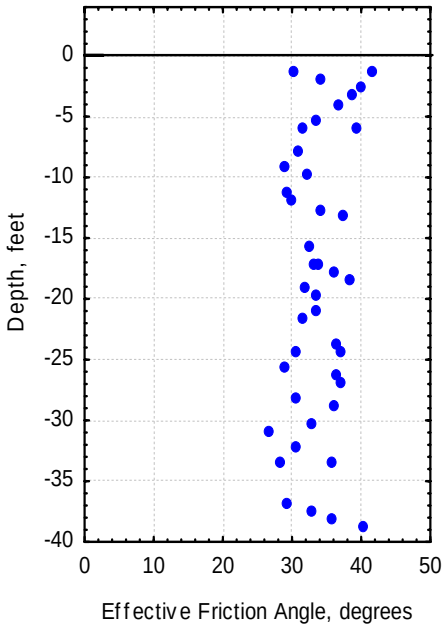

Figure 6 Profile of Effective (Drained) Friction Angle Values for the Cohesionless Soil Layers as determined from dilatometer soundings

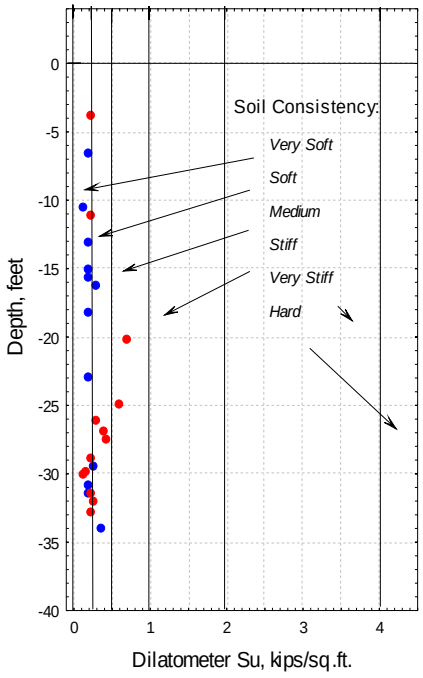

Figure 7 Profile of Undrained Shear Strength Values for the Cohesive layers as determined from dilatometer soundings

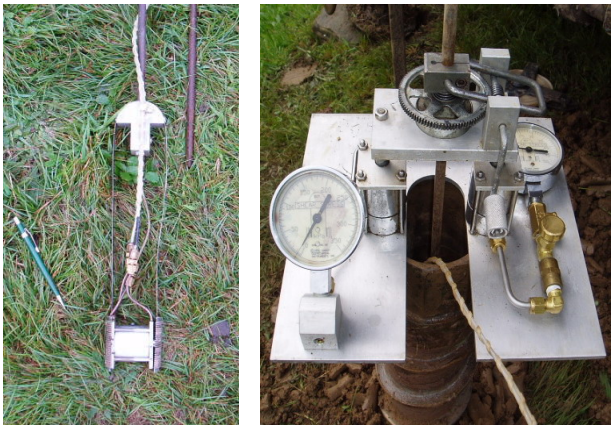

Figure 8 Borehole Shear Device – downhole component (left); components at collar of boring (right)

7.2 *Borehole Shear Testing*

The borehole shear test is essentially a direct shear test that is performed downhole to determine the effective strength parameters of a cohesive soil (Handy, 2002). The borehole is augered by conventional means to a depth approximately 18 inches above the test interval. A Shelby tube is then pushed through the test interval to create a smooth side wall. Upon extraction of the tube, the cylindrically-shaped borehole shear device is lowered to the test depth and a normal stress is applied to the borehole sidewall by two opposed, hydraulically-activated platens (Figure 8). The soil is allowed to consolidate under the normal stress and is then sheared by pulling the expanded BST device axially upward to at a sufficiently slow rate to limit the development of excess pore pressure within the soil. The BST is performed in a stepwise manner at each test depth, so as to define a Mohr envelope from the shear stress values at slippage at progressively higher levels of effective normal stress.

Of particular significance are the following points:

- All three borehole shear tests, which were performed at depths of 10 ft., 15 ft., and 30 ft. below the top of dam and within intervals identified by dilatometer testing to be cohesive, yielded similar results.
- These three tests yielded values of effective friction angle between 17.2 and 25.2 degrees and cohesion between 0.122 and 0.269 ksf. Taken together, these tests suggest an effective friction angle of 20.7 degrees and an effective cohesion of 0.196 ksf to be representative of the cohesive soils (Figure 9).

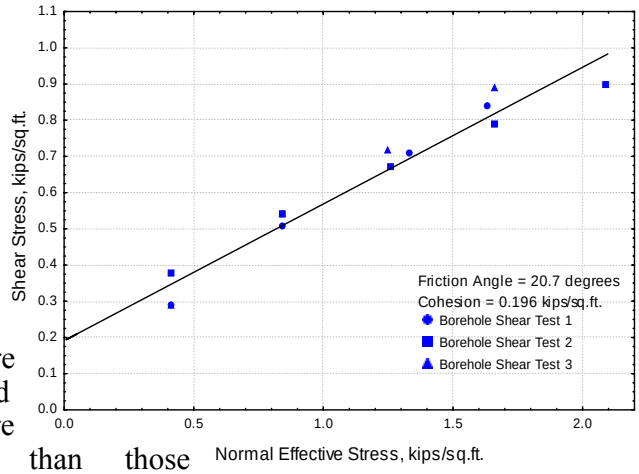

The BST-derived strength parameter values are considered far more plausible than those obtained from the laboratory direct shear tests on so-called "undisturbed" Shelby tube samples, which are suspected to have been disturbed or to reflect the presence of granular soils that may inadvertently have been incorporated into the samples or to be otherwise non-representative.

Figure 9 Mohr Envelope developed from Borehole Shear Testing conducted in cohesive soil intervals within top-of-dam borings

7.3 *Refined Estimate of Effective Strength Parameters and Revised Factor of Safety*

For the purposes of further stability analyses, a value of 25 degrees was assigned to the effective friction angle and 0.110 ksf to the effective cohesion of the soils that comprise the dam embankment. These values represent a weighted average of the effective strength parameters of the cohesionless and cohesive soil layers interpreted from the dilatometer and borehole shear tests.

Using these values, the factor of safety of the downstream face of the existing dam was computed to be 1.05 for the steady state seepage/normal pool condition. The refined stability analysis provided a basis for the interim drawdown strategy implemented while the rehabilitation measures were being designed as well as a basis for the design of stabilization measures, which include a downstream buttress, an internal drainage system and overtopping protection consisting of roller compacted concrete.

8. CONCLUSIONS

The field and laboratory methods commonly employed in investigations of slope stability in northern Appalachia – soil borings with Standard Penetration and Pocket Penetrometer Tests, Shelby tube sampling, and laboratory testing – produced results that were contradictory and/or unreliable in the case of the Bradford No.3 Dam.

A subsequent, more refined program of field investigation that included dilatometer and borehole

BACK

shear testing played an invaluable role in characterizing the soils that compose the dam embankment – in differentiating cohesionless soil layers from cohesive and in quantifying their respective effective strength parameters. This enabled the stability of the existing embankment to be evaluated in a manner that could confidently be used as a basis for the design of stabilization measures.

Neither the dilatometer nor the borehole shear test is in common use in projects of this type and size in the northern Appalachian Region. Their future use is to be recommended when customary methods of soil characterization prove inadequate.

9. ACKNOWLEDGEMENTS

This paper was written with the approval of the Bradford City Water Authority, whose kind assistance and cooperation during this project are gratefully acknowledged. The assistance of the Authority's consultant, Bankson Engineers of Indianola, Pennsylvania, is also acknowledged. The opinions expressed are those of the GAI authors, who take responsibility for the technical content of this paper.

10. REFERENCES

Corps of Engineers, 2003, "Engineering and Design, Slope Stability", Manual EM 1110-2-1902, Department of the Army, Washington, D.C., October 31, 2003.

Handy, R.L., 2002, "Borehole Shear Test", Handy Geotechnical Instruments, Inc., Madrid, Iowa.

ISSMGE, 2001, "The Flat Dilatometer Test (DMT) in Soil Investigations", Report of the ISSMGE Technical Committee 16 on Ground Property Characterization from In-situ Testing, International Society for Soil Mechanics and Geotechnical Engineering

Marchetti, S., 1980, "In-Situ Test by Flat Dilatometer", ASCE Journal of the Geotechnical Engineering Division, Vol 106, No.GT3, March, pp.299-321.

Influence of stress state and seasonal variability in a DMT campaign for a tunnel project in a porous tropical Brazilian clay

R.P. Cunha & A.P. Assis & C.R.B. Santos
Dept. of Civil and Environmental Engineering, University of Brasília, Brasília-DF, Brazil

F.E.R. Marques
Dept. of Civil Engineering, Faculty of Science and Technology, University of Coimbra, Portugal

Keywords: tropical clay, seasonal variability, stress state, in situ testing, tunnel design

ABSTRACT: The paper presents a discussion of the effect of field stress state modifications on the geotechnical predicted Marchetti DMT parameters, via results from a test located inside the settlement basin of the excavation (Location A) and from a location free from the interferences caused by the excavation (Location B) of a tunnel in the city of Brasília, Brazil. These results showed that the soil of Location A has suffered significant reductions in the values of the geotechnical predicted parameters, when compared to similar values from the other location (Location B). This situation should somehow be considered in tunnel design projects, and field-testing programs, for areas with similar conditions as the one presented herein. In fact, the difference of predicted results from one location to the other can be appreciable, although distinct (different magnitudes) are observed from one parameter to the other. The paper also presents a discussion of the effect of seasonal variations on the DMT predicted geotechnical parameters. To achieve that, two field-testing campaigns were carried out, the first during the wet (rainy) season of the year and the second during dry season. Surprisingly, it was noticed that seasonality didn't cause important modifications in the DMT predicted results (at least no appreciable *engineering* differences), indicating that field-testing campaigns for underground or tunnel design projects can be organized and carried out at any time of the year.

1 INTRODUCTION

Great part of the Federal District of Brazil, where its capital Brasília is located, presents a meta-stable porous and collapsible soil, commonly known as the Brasilia "porous clay". This soil is constituted by a superficial layer of silty clay that, when submitted to stress alterations or water content variations (or both), suffers a considerable volume change and structural breakdown. This phenomenon is defined as "soil collapse", and it was visibly observed during the underground construction works that took place in this city some recent years ago – in particular within the superficial settlement basin (or influence zone) of the excavated tunnel of this major governmental enterprise. Of course, this was caused during tunnel construction by the associated effects of stress state and humidity changes (wet versus dry seasons) that took place, respectively, internally and externally to the natural soil layers of this city.

Therefore, a jointed research project between Brazil and Portugal was established, with the aim to study these effects and its prediction or detection via *in situ* testing. This common project has produced an on going PhD (Marques 2005), a MSc thesis (Santos 2003) and an international paper in the recent ISC´2 Conference (Marques et al. 2004), and it was conducted with field tests in the Brasilia porous clay, in areas within and outside the influence zone of the already existing underground tunnel, and at different times of the year, i.e., during wet and dry seasons, as will be detailed next.

As presented by Marques et al. (2004), the Brasilia metro has a total length of 42 km, which has been built using several construction methods. About 6.8 km of those were built in tunnel (D_{eq} = 9.6 m), excavated in a layer of porous clay with collapsible characteristics, using the NATM. The on going PhD thesis has the purpose of better understanding the particular behavior of the Brasilia porous clay for further numerical simulations of the tunnel construction, using the Finite Element Method. The geotechnical characterization of the soil affected by the tunnel excavation was made via in situ testing as well as via an extensive program of laboratory tests that included oedometric and drained triaxial tests. In this paper, however, only the DMT results are presented, given the focus of the present international Conference.

BACK

Since the porous clay is generally in an unsaturated field condition, suction is a very important factor in its behavior. Once its known that suction varies with soil water content, the study tried to evaluate the effect of moisture content changes on soil behavior (hence on in situ testing) during distinct time (or season) of the year, as already commented before. For such, field works were divided in two stages. One of them was carried out during the rainy season (October-March) and the other when the soil water content was lower (dry season, April-September).

The investigation also evaluated the effect of the tunnel excavation on the behavior of the surrounding soil, because it was foreseen that this particular tunnel excavation would induce soil collapse. Thus, in both stages (rainy and dry seasons), identical in situ tests were accomplished in two locations. One of those was defined in the lateral of the tunnel (Location A), inside of the area affected by the excavation works. The other location was in the same cross section, but at a sufficient far away distance to be out of the subsidence basin (hence, located 75 m apart from the tunnel axis, i.e., Location B). These testing locations were defined as close as possible to the instrumented section of this tunnel (which, by the way, has served to other University of Brasília theses).

Details of the Brasília porous clay have already been extensively published elsewhere (Cunha et al. 1999, Marques et al. 2004) and will not be again presented herein. It will however be briefly commented next just to aid the unaware reader to visualize its main characteristics.

2 MAIN SITE CHARACTERISTICS

The Brazilian capital Brasília and its neighboring areas (Federal District) are located in the Central Plateau of Brazil, as presented in Figure 1. This district has a total area of 5814 km^2 and is limited in the north by the 15°30' parallel and in the south by the 16°03' parallel. The University of Brasília (UnB) campus is located within the city of Brasília in its "north wing", portrayed in this figure by an "airplane" shape like form. The tunnel is also located in this same city, however at its "south wing", as portrayed in Figure 1.

Within the Federal District extensive areas (more than 80 % of the total area) are covered by a weathered latosoil of the tertiary-quaternary age. This latosoil has been extensively subjected to a laterization process and it presents a variable thickness throughout the District, varying from few centimeters to around 40 meters. There is a predominance of the clay mineral caulinite, and oxides and hydroxides of iron and aluminum. The variability of the characteristics of this latosoil depends on several factors, such as the topography, the vegetal cover, and the parent rock. In localized points of the Federal District the top latosoil overlays a saprolitic/residual soil with a strong anisotropic mechanical behavior and high (SPT) penetration resistance, which originated from a weathered, folded and foliate slate, the typical parent rock of the region. In other points this latosoil overlays a thick layer of metamorphic rocks, known as "metarithimitics" (sandstones, claystones, etc.). This latter case is the case found in the location of the studied conducted herein. The thickness of the top latosoil is evaluated as around 24 m according to SPT results at site.

The surficial latosoil is locally known as the Brasília "porous" clay, being geotechnically constituted by sandy clay with traces of silt, forming a lateritic horizon of low unit weight and high void ratio, as well as an extremely high coefficient of collapse. Although these characteristics vary from site to site at this city, its main geotechnical characteristics are generally similar. These characteristics are illustrated in Table 1, obtained from a comprehensive site and laboratory investigation program at the UnB research site. In the particular area of the tunnel, Locations A and B, the soil has similar (but slight distinct) geotechnical values as those of Table 1, as already presented by Marques et al. (2004).

Table 1. Main geotechnical values for the Brasília porous clay (Cunha et al. 1999)

Parameter	Units	Range of Values
Sand percentage	%	12-27
Silt percentage	%	8-36
Clay percentage	%	80-37
Moisture content	%	20-34
Nat. unit weight	kN/m^3	17-19
Degree of saturation	%	50-86
Void ratio	--	1.0-2.0
Liquid limit	%	25-78
Plasticity limit	%	20-34
Plasticity index	%	5-44
Young Modulus	MPa	2-14
Drained Cohesion	kPa	10-34
Drained Friction angle	degrees	25-33
Coefficient of Collapse	%	0-12
Coef. earth pressure	--	0.4-0.6
Coef. of permeability	cm/s	10^{-6}-10^{-3}

Figures 2 and 3, in the next page, respectively present the specific area of the in situ tests (Locations A and B) and their position in relation to the tunnel cross section and its (superficial) measured settlement deployment basin (with a maximum settlement at tunnel centerline of 16.8 cm, this section).

BACK

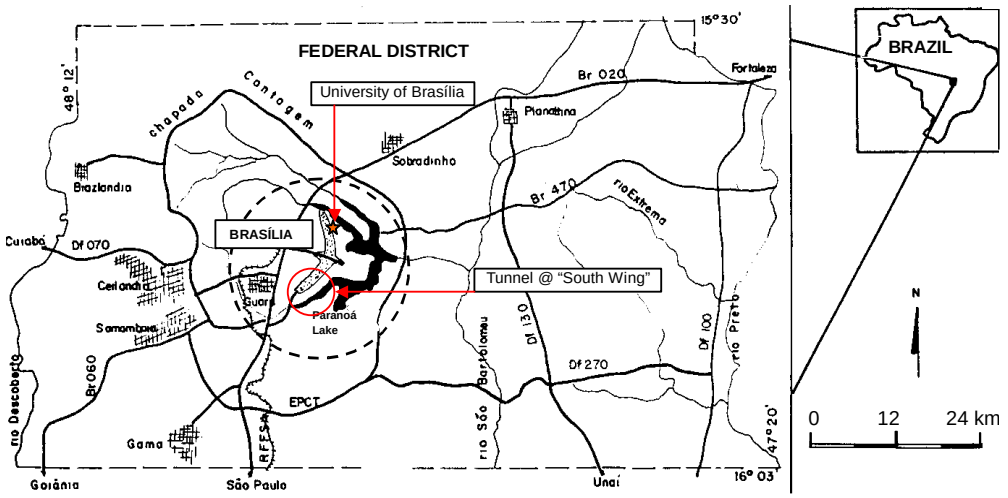

Figure 1. Location map of Brasília city and tunnel position

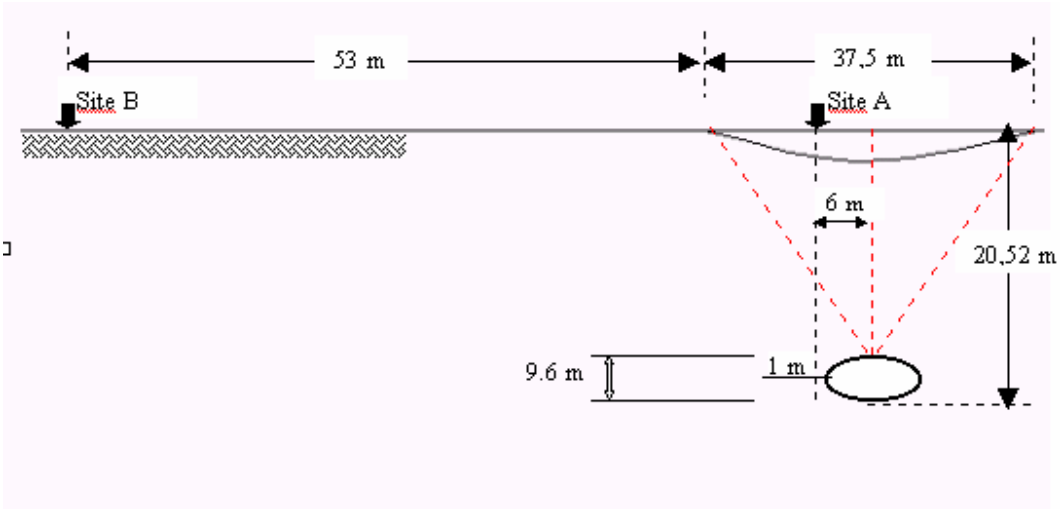

Figure 2. Locations A and B in relation to tunnel axis and settlement basin

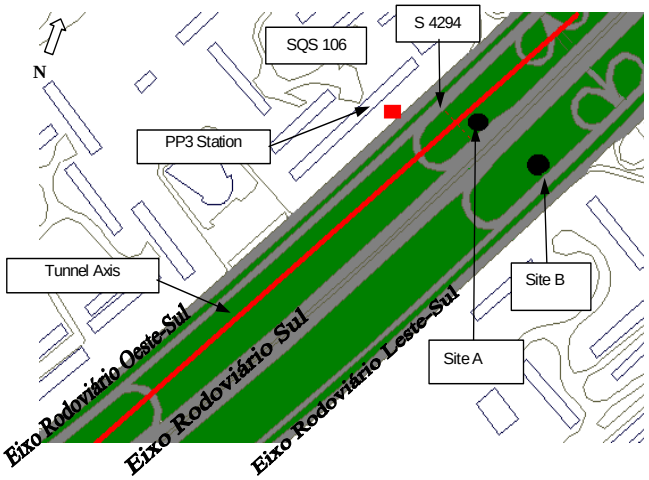

Figure 3. Specific in situ testing areas and tunnel S 4294 cross section

3 DMT RESULTS

3.1 *Stress state influence on results (A vs. B)*

In order to study the influence of the stress state of the soil into DMT corrected (by calibration values) and interpreted results (standard empirical correlations) a set of DMT tests was carried out at each distinct site location, A and B. Site A was chosen to be within the displacement basin of the tunnel, at around 1 m from the tunnel's face (6 m from its centerline). Site B on the other hand was chosen to be at around 67 m from the tunnel's face (72 m from its centerline), where it is believed that the soil is unaffected by the tunnel's overall displacement vectors and stress changes. Figure 2 clearly depicts both site locations A and B.

The DMT tests were carried out in distinct membrane positions in relation to the tunnel's longitudinal axis. In this particular sub item it is solely presented the results for the tests in which the

membrane was positioned at 45° to the tunnel's longitudinal axis, but the results are valid for all positions tested in this research. Although not shown herein, it can be said that the main difference between distinct membrane positions was related to the sensitivity of the DMT obtained results, i.e., the closer is the membrane to a perpendicular position in regard to the tunnel's long. axis (parallel to the horizontal displacement vectors) the higher is the sensitivity of the DMT obtained results to the tunnel's stress changes around the soil.

As observed before, the study was carried out for the two main seasons of Brasília city, i.e., wet and dry seasons. It is noticed in Figure 4 that during the wet season there was a slight increase in the soil's water content in relation to those of the dry season. This increase was higher for the upper portions of the strata, and tends to disappear as deeper we go into the profile.

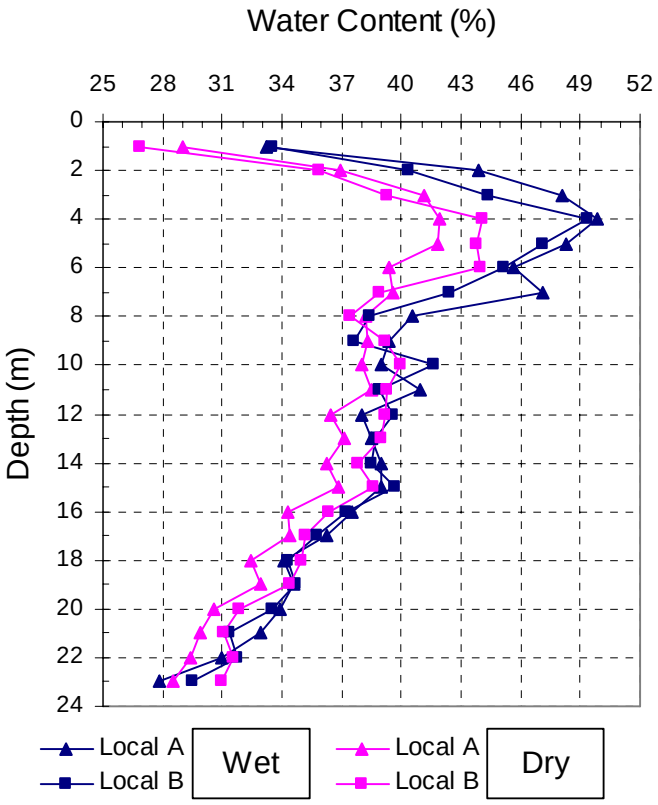

Figure 4. Water content variation at each location and season

Therefore, two sets of DMT results for p_0 and p_1 pressures were obtained, each respectively for sites A and B at wet and dry seasons.

From this set of results it was noticed that there seams to be three distinct geotechnical layers, herein defined as layers I, II and III, although the strata can be considered as "homogeneous" in pedological terms. This was noticed to be more pronounced in Site A, although some layer discretization is also possible in Site B. Most probably, distinct laterization and pedogenetic processes that have occurred distinctively along the profile during the geological times give the difference in results. These layers are depicted in Figure 5.

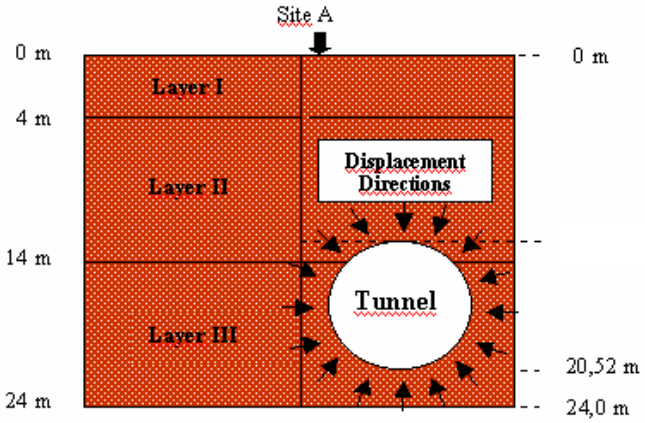

Figure 5. Distinct soil layers idealized for the profile

Figures 6 and 7 present the DMT p_0 and p_1 results for both dry and wet seasons, while Figures 8 and 9 present interpreted results for K_0 (Lunne et al. 1990) and M (Marchetti 1980) solely for wet season.

From these figures it can be noticed:

- There seems to be a much larger influence of the stress state relief during wet rather than dry season, and in particular more concentrated to layer III. It is believed that this was caused by the proximity of the tunnel's face to the testing positions in this particular layer, and by the fact that, during dry season, there is another effect taking place and influencing the results;
- There seems, therefore, that during dry season there is also the variable (along profile) influence of suction in the obtained DMT raw and interpreted results. This effect tends to "mask" the stress state effects, decreasing differences between results from sites A and B. This is clearly noticed by a close comparison between these figures;
- There also seems to be some influence of the stress state relief in layer I, where the settlement basin is located (Site A). This influence was also noticed to be more pronounced during wet rather than dry season, for the same aforementioned reasons. It reveals that, from the three distinct layers of the profile, only the intermediate (4-14 m) one was not influenced by displacement vectors and stress change variations caused by the presence of the tunnel.

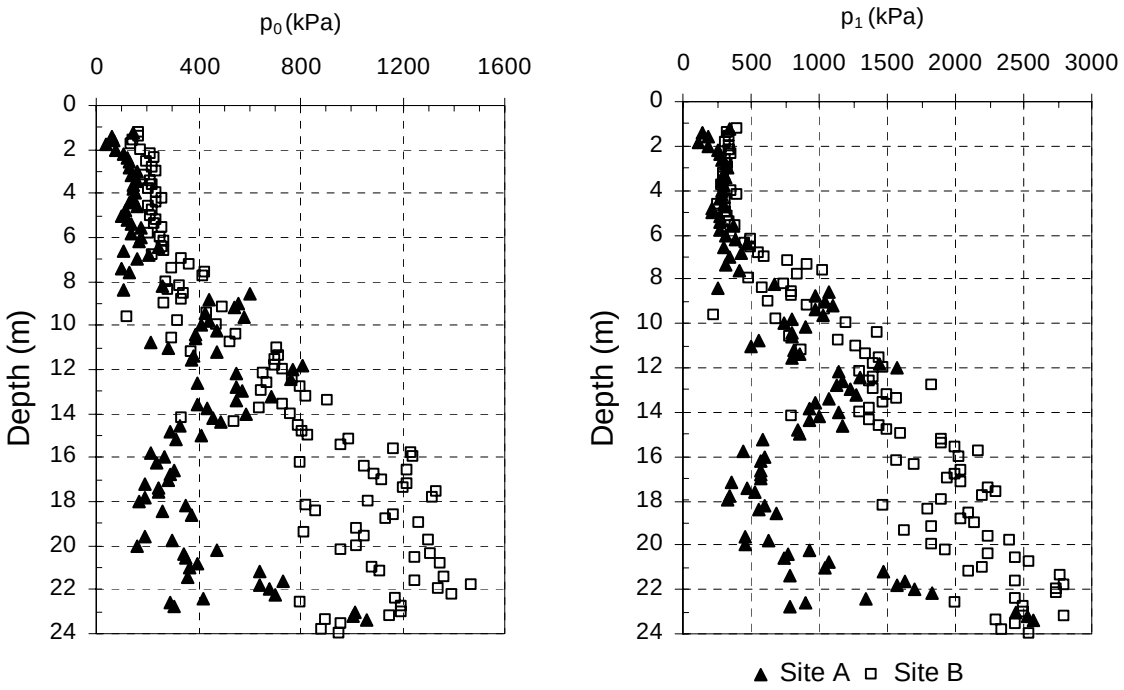

Figure 6. DMT p_0 and p_1 results for wet season

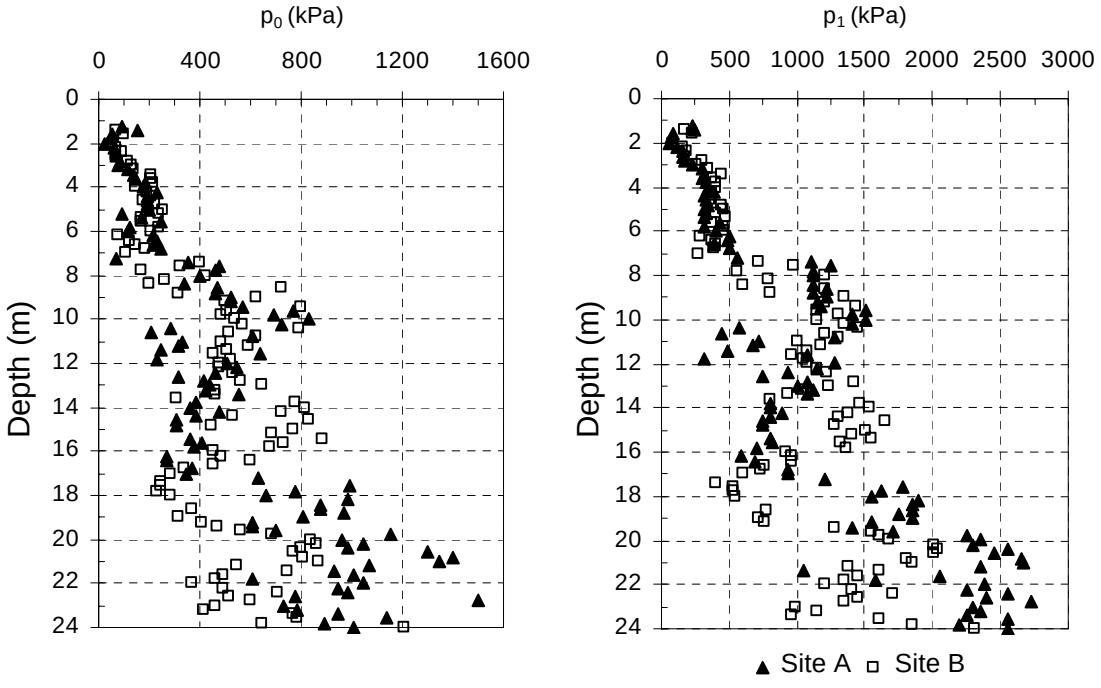

Figure 7. DMT p_0 and p_1 results for dry season

BACK

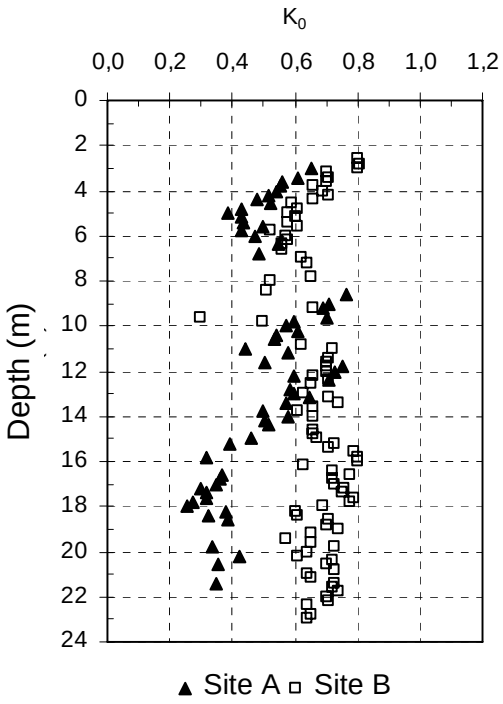

Figure 8. DMT interpreted K_0 results at distinct locations (wet season)

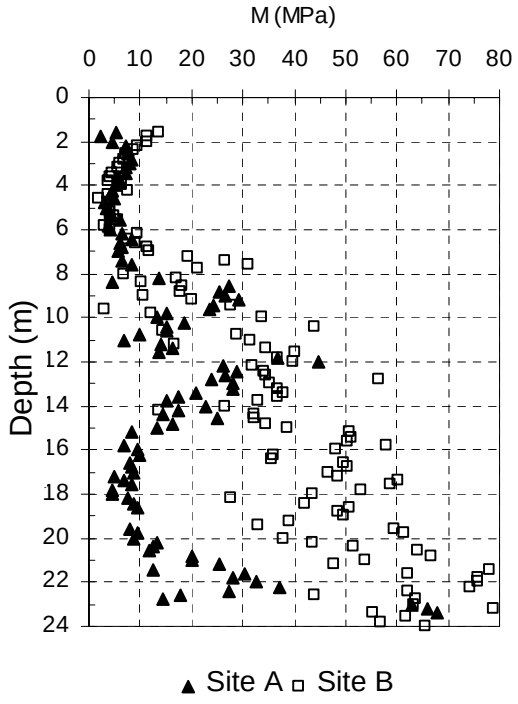

Figure 9. DMT interpreted M results at distinct locations (wet season)

- There seems to be the same stress state influence in both interpreted K_0 and M results, also concentrated for layers I and III. In terms of K_0 (coeff. of stress state at rest) the average decrease of values from Site B to A was respectively 50 and 24%, for layers III and I, denoting higher stress state influence at points closer to the tunnel's face. For layer II this average decrease was only 5%, which is negligible considering possible natural stratigraphic variations from one site to another. In terms of the M (constrained modulus) parameter the average values of decrease were respectively 72 and 30% for layers III and I, whereas for layer II this decrease was in the range of 19% (in this case not so negligible, but lower than the other layers).

3.2 *Seasonal variability influence on results (wet vs. dry season)*

In order to study the influence of the seasonal variability on the obtained DMT corrected (by calibration values) and interpreted results, it was applied herein the same procedures as applied before. That means, the direct comparison of initial and intermediate DMT parameters as well as interpreted, via empirical correlations, geotechnical values.

For the sake of simplicity, and given the fact that all the comparisons have similar trends, it will be presented herein only the comparison between the K_0 and M values derived at Site A respectively at wet and dry seasons. In this particular case the DMT membrane was located parallel to the tunnel's longitudinal axis, but, as already commented before, this set of comparative results express similar trends and conclusions as those obtained in other (not shown) data from this same site.

Figures 10 and 11 respectively show the results for K_0 and M, at distinct seasons. From these figures it can be said:

- The average difference of values for all the profile from K_0 results at wet and dry seasons was in the range of 9%, with slight lower values for the dry season. This comparison, therefore, indicates that the influence of the moisture content variation from one season to another was not enough to induce appreciable variations, or a perceptible "trend", in the obtained DMT initial, intermediate and empirically derived parameters. This is perhaps related to the fact that, indeed, soil moisture variations from one season to another was not appreciable (see Figure 4), and its influence was lower than the influence of other factors (as stratigraphy);

- Similar results were obtained for M. In this case the average difference was in the range of 30% (however with large scatter), with slight lower values for the dry season. Again the same aforementioned observations can be applied here;

It is believed that the large scatter of data for all the comparisons presented in this sub item are primordially related to stratigraphic differences of the tropical soil tested in each season. Although the site was the same (Site A) there was a distance difference between the geographic points tested from one season to another. This could, perhaps, indicate the non-expected trend of slight lower geotechnical values obtained for the dry rather than the wet season (which was not initially expected). Suction has influenced the results, given the average soil´s moisture content variation from one season to another. It however did not appear to be enough to produce a clear trend in the comparisons from wet to dry seasons.

Given the discussion of sub item 3.1 it is also observed that suction effects were solely markedly noticed to "mask" the difference of results from one site to another, i.e., to approximate DMT results from site A to B (hence decreasing stress state effects) during dry season. During the wet season this approximation of values was not noticed, as observed before.

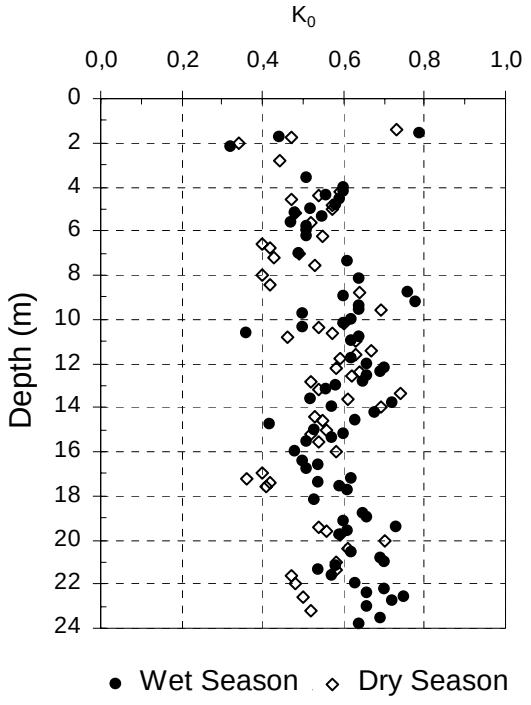

Figure 10. DMT interpreted K_0 results at distinct seasons (site A)

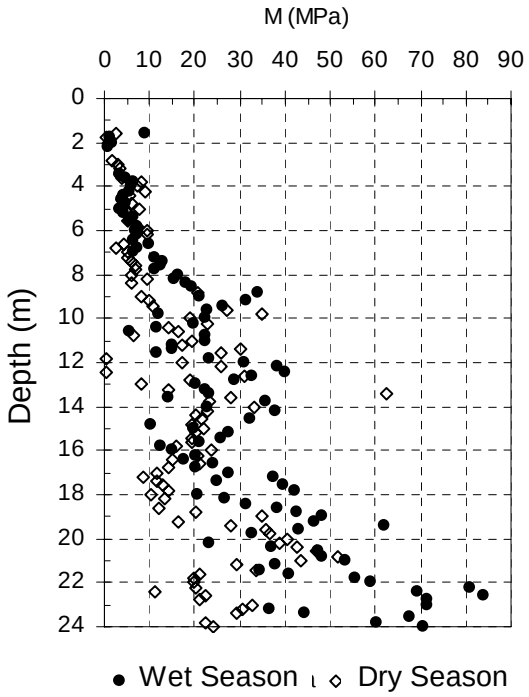

Figure 11. DMT interpreted M results at distinc seasons (site A)

4 CONCLUSIONS

This study has emphasized the importance of a better understanding of the effects of stress and suction (indirectly measured by the soil's moisture content) generated around tunnels constructed in tropical soils, and their influence into the derived soil's parameters.

Although limited, the study has indicated initial points and preliminary conclusions of value, which still have to be tested against future numerical analyses with the data and site characteristics presented in this paper.

It is initially concluded that the excavation of the tunnel influences the state of stress in soil layers around it. It was noticed that the DMT empirically interpreted geotechnical values have substantially decreased from a point close to the tunnel's face in relation to another point in an area unaffected by the tunnel's excavation. Besides, this influence was hindered by suction effects, i.e., it could not be clearly noticed during the dry season of the year, as observed with tests during the wet season.

This therefore indicates that the stress state influence around the tunnel, given its construction, should somehow be incorporated into DMT interpre-

tative correlations, at least for tunnel projects in soil deposits of this particular type.

The influence of soil's suction or moisture content variation, from one season to another, has shown to be limited because for tests at similar site location (close or distant to tunnel's face) there was no appreciable difference in the results of the DMT empirically interpreted values. The observed large data scatter at the same site appears to be related to stratigraphic differences of this tropical soil.

This therefore tends to indicate that in situ testing programs can be carried out at any season of the year for soil deposits of this particular type.

ACKNOWLEDGEMENTS

The authors would like to express their gratitude to WRJ Engenharia Ltda. for the field tests carried out herein, and to the Brazilian Sponsorship Governmental Organization CNPq for the financial support and scholarship provided herein.

REFERENCES

Cunha, R.P., Jardim, N.A. & Pereira, J.H.F. 1999. In Situ Characterization of a Tropical Porous Clay via Dilatometer Tests. *Geo-Congress 99 on Behavorial Characteristics of Residual Soils*, ASCE Geotechnical Special Publication 92, Charlotte, pp. 113-122.

Lunne, T., Powell, J.J.M., Hauge, E.A., Uglow, I.M. & Mokkelbost, K.H. 1990. Correlation of dilatometer readings to lateral stress. *Proc. 69th Annual Meeting of the Transportation Research Board*, Washington.

Marchetti, S. 1980. In situ tests by flat dilatometer. *Journal of Geotechnical Engineering*, ASCE, 106 (GT3), pp. 299-321.

Marques, F.E.R. 2005. Behavior of superficial tunnels excavated in porous soils – the case of Brasília/DF underground. *Ph.D. Thesis*. Faculty of Sciences and Technology, University of Coimbra. (On Going Thesis).

Marques, F.E.R., Almeida e Sousa, J., Santos, C.B., Assis, A.P. & Cunha, R.P. 2004. In-situ geotechnical characterisation of the Brasilia porous clay. *Proceedings ISC-2 on Geotechnical and Geophysical Site Characterization*, Porto, Vol. 2, pp. 1301-1309.

Santos, C.R.B. 2003. Influence of stress state modification and seasonality in the geotechnical parameters via in situ testing in the Brasília porous clay. *M.Sc. Thesis*. University of Brasília, Department of Civil and Environmental Engineering, 118 p. (In Portuguese).

Use of dilatometer testing for design of a large diameter steel water main

Roger A. Failmezger, P.E.
In-Situ Soil Testing, L.C., 173 Dillin Drive, Lancaster, Virginia, USA, 22503, email:insitusoil@prodigy.net

Somba Ndeti, P.E.
Thomas L. Brown Associates, P.C., 7280 Baltimore-Annapolis Boulevard, Glen Burnie, Maryland, 21061, email: sndeti@tlbinc.net

Keywords: Dilatometer, compaction, aging, soil-structure interaction

ABSTRACT: Large diameter steel water mains rely on the soil's support to maintain their shape and allow them to perform as intended. Dilatometer tests were used to evaluate the soil's stiffness for a finite element design. During the evaluation of an existing water main, we discovered that the natural soil, which had a lower dry unit weight than the compacted backfill, had constrained deformation moduli that were about four times higher than the backfill.

1 INTRODUCTION

To meet the water needs in the Maryland suburbs of Washington, D.C., the Washington Suburban Sanitary Commission (WSSC) sends large quantities of water through 72 to 120 inch (1.83 to 3.05 m) diameter water mains that parallel the capital beltway (Interstate I-495). A section of 84-inch (2.13 m) diameter water main near Central Avenue was not performing as intended, and a flexible steel pipe was designed to replace the existing prestressed concrete pipe. The geotechnical investigation included evaluating the existing water main and designing the replacement water main.

2 COMPACTION

Compaction specifications require the contractor to compact structural fill to a specified effort based on either standard or modified Proctor tests. While these specifications make it relatively easy for a trained technician to monitor the placement of fill, they do not assess the deformation characteristics of the fill. Soil type is usually more important to the soil's performance than the compactive effort, but it is often overlooked in compaction specifications. For example, sands will usually be stiffer than clays with similar compactive efforts. Dilatometer tests should be used to evaluate the deformation properties of compacted fills that are significantly thick and do not contain much gravel.

3 TEST PIT EXCAVATION

A large test pit was excavated along the existing prestressed concrete water main. Soil samples were collected and used for laboratory standard Proctor and soil classification tests. The soil was classified as a light brown, medium to fine sand with some silt. The pipe backfill was the same soil type as the adjacent natural soil.

In-place density tests were performed in the backfill and adjacent natural soil and are summarized on Table 1. As shown on that table, the pipeline backfill was compacted to higher unit weights and to lower void ratios than the natural soil.

Parameter	Number of Data Points	Average	Standard Deviation	Range
BACKFILL:				
Total Unit Weight (pcf)	10	118.6	4.9	111.0 to 128.6
(kN/m^3)		18.63	0.77	17.4 to 20.2
Dry Unit Weight (pcf)	10	96.8	4.8	91.4 to 108.3
(kN/m^3)		15.21	0.75	14.4 to 17.0
Moisture Content (%)	10	22.5	1.8	18.7 to 25.7
Void Ratio*	10	0.75	0.08	0.56 to 0.84
Percent Compaction (%)	10	90.1	4.4	85.2 to 100.5
NATURAL SOIL:				
Total Unit Weight (pcf)	7	111.9	4.9	107.2 to 120.0
(kN/m^3)		17.58	0.77	16.8 to 18.9
Dry Unit Weight (pcf)	7	91.7	3.9	88.0 to 98.5
(kN/m^3)		14.41	0.61	13.8 to 15.5
Moisture Content (%)	7	22.2	7.3	14.8 to 32.1
Void Ratio*	7	0.84	0.08	0.71 to 0.91

*Void ratio computed using an assumed specific gravity equal to 2.7

Table 1: Statistical summary of field density test data

BACK

4 DILATOMETER TESTS IN PIPE BACKFILL

During our testing the pipe was in service and had an internal water pressure of 180 psi (1241 kPa). Based on the drawings for the existing concrete pipeline, we staked out the approximate locations of the pipe's centerline and springline from the state highway fence line. However, we needed to precisely locate the springline. We attached a ¾-inch (19 mm) schedule 40 PVC pipe to the discharge of our drill rig pump and jetted vertical holes at locations perpendicular to the pipe's centerline. Jetting refusal occurred when the concrete pipe was encountered. The horizontal distances from our reference centerline stake and the jetting refusal depths were recorded. When the probing hole was just beyond the springline, however, we lost the return water at 14.0 feet (4.3 m). We believe at this depth the water went into the gravel bedding of the pipe, and we were confident that we were within the backfill of the pipe.

We performed a dilatometer sounding 4.0 feet (1.2 m) north of that probe hole and parallel to the state highway fence. Dilatometer tests were performed at approximately 0.5 meter intervals within the backfill. The dilatometer membrane faced the pipe.

5 DILATOMETER TESTS IN NATURAL SOIL

Eleven (11) dilatometer test soundings were performed along the pipeline alignment in the natural soil. Tests were done at 0.5 meter intervals with the membrane facing the pipe. The constrained deformation moduli from the tests in both the backfill and natural soil are shown on Figure 1.

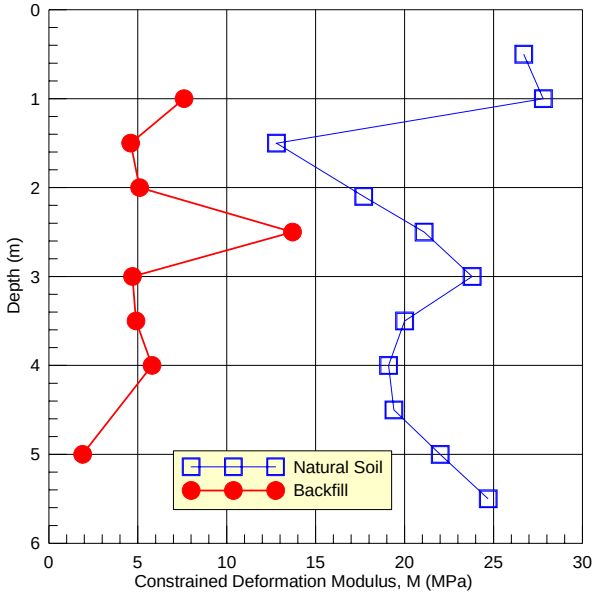

Figure 1: Comparison of constrained deformation moduli in natural soil and backfill

As shown in Figure 1, the constrained deformation moduli values were up to 4 times higher for the natural soil than the backfill. However, as shown in Table 1 the void ratios for the backfill were significantly lower than the natural soil. We believe that the better deformation moduli in the natural soil are due to its aging, stress history and cementation.

6 STEEL PIPE FINITE ELEMENT METHOD FOR DESIGN

Steel pipe is a flexible system that relies on the surrounding soil for support. Without adequate lateral support, the pipe will become egg-shaped and not perform as intended. The structural engineers used the constrained deformation modulus of the soil in their finite element analyses for this soil-structure interaction design. They determined that the soil needed to have a constrained modulus of at least 10 MPa to provide adequate support.

Based on the first phase explorations with dilatometer tests, we identified two areas where the soil was inadequate. A second phase of dilatometer tests was conducted to delineate those areas better. In the inadequate zones, the design recommended that the natural soil be excavated one pipe diameter on each side of the springline and replaced with compacted backfill. The specifications required that existing soil not be reused as backfill, but that concrete sand (ASTM C-33 gradation) be used and be compacted to 95% of the maximum dry unit weight determined from a standard Proctor test.

7 CONCLUSIONS

1. The dilatometer is needed to evaluate the constrained deformation modulus for the finite element method of design for flexible steel pipelines.
2. The percentage of compaction is not a good indicator of the soil's deformation properties.
3. Natural soils through their aging, stress history and cementation can have higher deformation moduli than fills consisting of the same soil type that are compacted to higher dry unit weights.

8 REFERENCES

Marchetti, Silvano, "In Situ Tests by Flat Dilatometer," Journal of the Geotechnical Engineering Division, ASCE, Vol. 106, No. GT3, March 1980, pp. 299-321.

Schmertmann, John H., "Measure and use of the Insitu Lateral Stress," The Practice of Foundation Engineering, The Department of Civil Engineering, Northwestern University, 1985, pp. 189-213.

Schmertmann, John H., “The Mechanical Aging of Soils,” Journal of Geotechnical Engineering, ASCE, Vol. 117, No. 9, September, 1991, pp. 1288-1330.

BACK

Settlement analyses from dilatometer test data justify supporting parking garage on spread footings

Roger A. Failmezger
In-Situ Soil Testing, L.C., 173 Dillin Drive, Lancaster, Virginia, 22503, email: insitusoil@prodigy.net
Robert J. Niber
Whitlock Dalrymple Poston & Associates, Inc., 8832 Rixlew Lane, Manassas, Virginia 20109, email: rniber@wdpa.com

Keywords: Settlement, dilatometer, parking garage

ABSTRACT: For heavily loaded structures, the cost of the foundation system can be quite large. Therefore, owners seek the most economical foundation that will safely support the structure's loads. Because the dilatometer is a calibrated static deformation test, data from these tests will accurately predict the amount of settlement that is likely to occur. Its accuracy enables the engineer to use probability design charts to explain the probability of success in simplistic terms to the owner and contractor. Consequently, they can make informed decisions regarding risk as demonstrated in this case study.

1 INTRODUCTION

A 6-level, precast concrete, parking garage was planned overlying approximately 35 to 50 feet (10 to 15 m) of residual soils further underlain by weathered metamorphic bedrock. A preliminary foundation design study based on six (6) soil test borings recommended the parking structure be founded on drilled piers (caissons) bearing on the weathered rock or on shallow spread foundations using a reduced soil bearing pressure to control settlement. Prior to construction, the design/build contractor retained Whitlock Dalrymple Poston & Associates, Inc. (WDP) and In-Situ Soil Testing, LC to re-evaluate the foundation design alternates and settlement potential; consequently, six (6) dilatometer test (DMT) soundings were performed. Settlement analyses were performed for varying column loads (850 to 2000 kips [3780 to 8900 kN]) using the closest DMT sounding. Probability analyses were done to evaluate the risk of settlement exceeding the owner's desired maximum value of 1 inch [25 mm] total settlement and 0.5 inch [12.5 mm] differential settlement criteria. The owner and contractor accepted the calculated risk and the parking garage was supported on shallow spread footings using allowable soil bearing pressures of 6,000 psf and 8,000 psf [287 to 383 kPa]. This foundation redesign saved the project about $200,000 to $300,000.

2 PREVIOUS GEOTECHNICAL INVESTIGATION

The parking garage is about 200 feet by 400 feet [61 by 122 m] in plan view. Six soil test borings were performed to depths of 50 to 60 feet [15 to 18 m] at the corners and the middle of the long sides. Geologically, the site contained residual soils overlying decomposed metamorphic rock of the Sykesville Formation. Limited laboratory tests performed on random soil samples indicated the residual soils contain approximately 52 to 81% silt/clay fraction and 19 to 48% sand. The liquid limits were less than 45, and the plasticity index was less than 7.

The results from the soil test borings are summarized in the Table 1. A Central Mine Equipment (CME) automatic standard penetration test hammer was used to drive the split spoon sampler. Notably, the correction of the raw N-values to N_{60}-values (Skempton, 1986) is quite significant due to the high efficiency of the automatic hammer (Schmertmann, 1984). Additionally, the split spoon barrel that was used could accommodate liners, but liners were not used. This correction increased the N_{60}-values by 20%. Robertson (2004) shows that the resistance of the soil for N-values exceeding 50 blows per foot is no longer linear. In soils with an N-value of 100 their CPT tip resistance was only 10 to 20% higher than the tip resistance for soils with an N-value of 50.

Soil Test Boring Number	Nearest Dilatometer Sounding	Elevation	Uncorrected N-value	N_{60}-value
B-1	D-5	380-361 Below 361	21 - 41 > 50	34 - 78 > 50
B-2	D-4	380 - 354 Below 354	7 - 12 21 - 28	11 - 22 40 - 53
B-3	D-1	380 - 350 350- 335 Below 335	7 - 15 27- 62 > 50	11 - 26 > 50 > 50
B-4	D-6	380 - 349 Below 349	22 - 42 > 50	41 - 80 > 50
B-5	D-3	380 - 370 370- 355 Below 355	20 - 31 32 - 61 > 50	32 - 44 > 50 > 50
B-6	D-2	380 - 366 366 - 348 Below 348	6 - 26 24 - 52 > 50	9 - 37 41 - 93 > 50

Table 1: Summary of SPT N-values at site

Based on the SPT N-value results, the initial geotechnical engineer preliminarily recommended using an allowable bearing pressure of 3 to 4 ksf [144 to 192 kPa] for footings near Borings B-2 and B-3 and 6 to 8 ksf [288 to 384 kPa] elsewhere. Alternatively, drilled piers into the weathered rock were recommended.

3 DILATOMETER RESULTS

Six (6) dilatometer test soundings were performed near the soil borings shown on Table 1 but about 30 feet [9 m] closer to the center of the parking garage. Tests were performed at 20-cm depth intervals until penetration refusal occurred, which ranged from 7.8 to 14.8 m. The results of the tests are plotted on Figures 1 to 3.

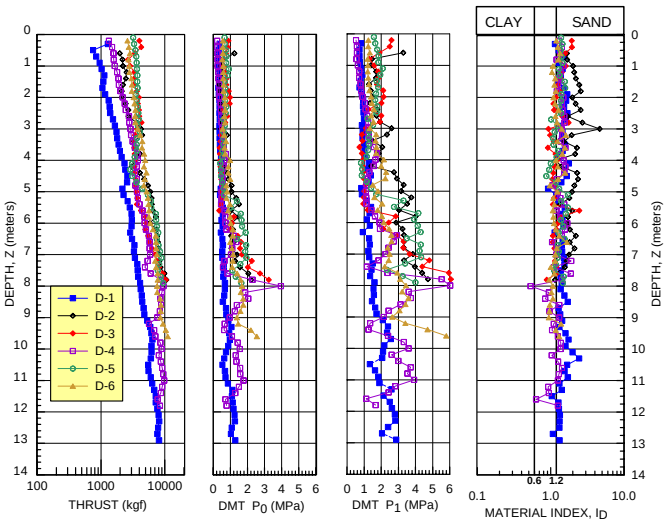

Figure 1: Summary of dilatometer results for soundings D-1 to D-6

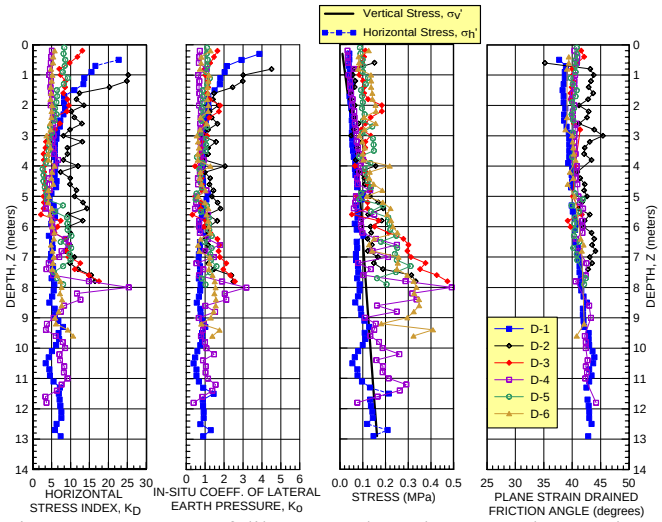

Figure 2: Summary of dilatometer lateral stress and strength parameters for soundings D-1 to D-6

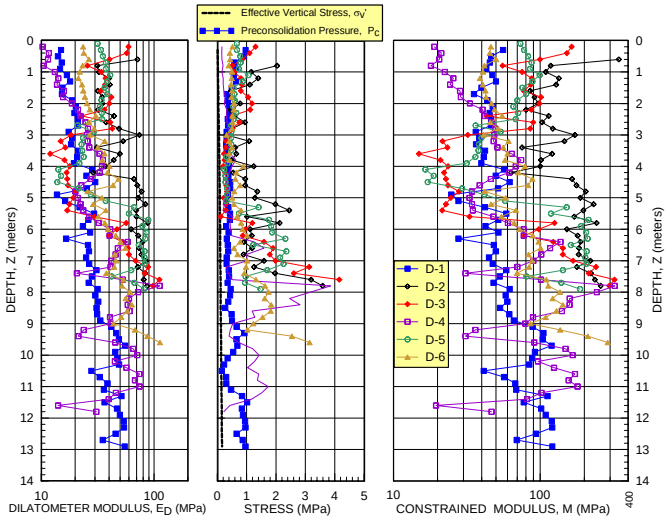

Figure 3: Summary of dilatometer modulus parameters for soundings D-1 to D-6

As indicated by the dilatometer test results, the residual soils are overconsolidated to highly overconsolidated. Their strengths and stiffness generally improve with depth as the chemical weathering decreases. The dilatometer soil classification (I_D) correlates well with the laboratory test results.

4 SETTLEMENT ANALYSES

The structural engineer provided the various loads for each column. We overlaid six zones that corresponded to our six dilatometer test sounding locations on the structural plan sheet. We performed settlement analyses using Schmertmann's (1986) ordinary and special methods. The ordinary method is simply the stress increase multiplied by the layer thickness divided by the constrained deformation modulus. The special method considers the preconsolidation pressure and uses the recompression modulus for stress less than the preconsolidation pressure and the virgin modulus for stress above the

BACK

preconsolidation pressure. However, if the stress increase is less than the preconsolidation pressure, the special method does not adjust the constrained modulus from the dilatometer correlations and uses the same modulus as the ordinary method. Because the residual soils were, in general, overconsolidated, there was little difference in the settlement predictions between the ordinary and special methods. We initially sized the footings based on an applied soil bearing pressure of 10 ksf [479 kPa]. However, the resulting settlements exceeded the strict tolerable total settlement criterion of 1 inch [25 mm] that was established for the parking garage by the owner. We recomputed the settlement for footings sized based on an applied bearing pressure of 8 ksf [383 kPa]. For the footings near Sounding D-1, an applied bearing pressure of 6 ksf [287 kPa] was used for design to keep the settlements within acceptable tolerance. The results of our analyses are presented in Table 2.

Column Load (kips/kN)	Footing Width (ft/m)	Applied Bearing Pressure (ksf/kPa)	Sounding	Predicted Settlement (inch/mm)
850/3780	10.5/3.2	7.71/369	D-5	0.24/6.1
850/3781	10.5/3.2	7.71/369	D-6	0.37/9.4
1000/4448	13/4	5.92/283	D-1	0.70/17.8
1000/4448	11/3.4	8.26/396	D-2	0.33/8.4
1400/6227	15/4.6	6.22/298	D-1	0.84/21.3
1400/6227	13/4	8.28/397	D-2	0.38/9.7
1400/6227	13/4	8.28/397	D-3	0.57/14.5
1400/6227	13/4	8.28/397	D-4	0.82/20.8
1400/6227	13/4	8.28/397	D-5	0.40/10.2
1400/6227	13/4	8.28/397	D-6	0.51.13.0
1500/6672	16/4.9	5.86/281	D-1	0.84/21.3
1500/6672	13.5/4.1	8.23/394	D-2	0.38/9.7
1500/6672	13.5/4.1	8.23/395	D-5	0.42/10.7
1500/6672	13.5/4.1	8.23/396	D-6	0.53/13.5
2000/8896	18/5.5	6.17/296	D-1	0.98/24.9
2000/8896	16/4.9	7.81/374	D-2	0.41/10.4
2000/8896	16/4.9	7.81/375	D-3	0.72/18.3
2000/8896	16/4.9	7.81/376	D-4	0.89/22.6
2000/8896	16/4.9	7.81/377	D-5	0.50/12.7
2000/8896	16/4.9	7.81/378	D-6	0.57/14.5

Table 2: Summary of settlement analyses used for design

5 PROBABILITY ANALYSES

Failmezger et al. (2004) discovered that the average value of settlement and its standard deviation have linear relationships with risk provided that the probability distribution curve is bell-shaped. The average value of settlement can be easily computed from the values in Table 2. The computed standard deviation from the values in Table 2 represents the standard deviation due the subsurface heterogeneity (spatial standard deviation). There is also some uncertainty as to how well Schmertmann's method predicts settlement based on dilatometer test data. Based on Schmertmann's and Hayes' case study data bases, the coefficient of variation, which equals the standard deviation divided by the average, is 0.18 (Failmezger and Bullock, 2004). This value is low, demonstrating the accuracy of the design method. There may be other sources of uncertainty that contribute to the overall standard deviation. In our case, we considered that there was a lack of dilatometer soundings in the analyses as an additional source of uncertainty. If the contributory sources of uncertainty are considered to be independent of each other, then the overall standard deviation is the square root of the sum of each standard deviation squared. In Table 3, we show the computations for the average and overall standard deviations.

		(inch)	(mm)
Average Settlement		0.57	14.48
Spatial Standard Deviation		0.22	5.48
Method Coefficient of Variation =	0.18	(Failmezger, 2004)	
Method Standard Deviation		0.10	2.61
Intangible Coefficient of Variation =	0.20	(Lack of Soundings)	
Intangible Standard Deviation		0.11	2.90
Overall Standard Deviation		0.26	6.72

Table 3: Summary of average and overall standard deviation computations

After determining the average and overall standard deviation, one simply plots those x-y values (standard deviation = 6.72, average settlement = 14.48 mm) on the settlement design summary figure as shown below.

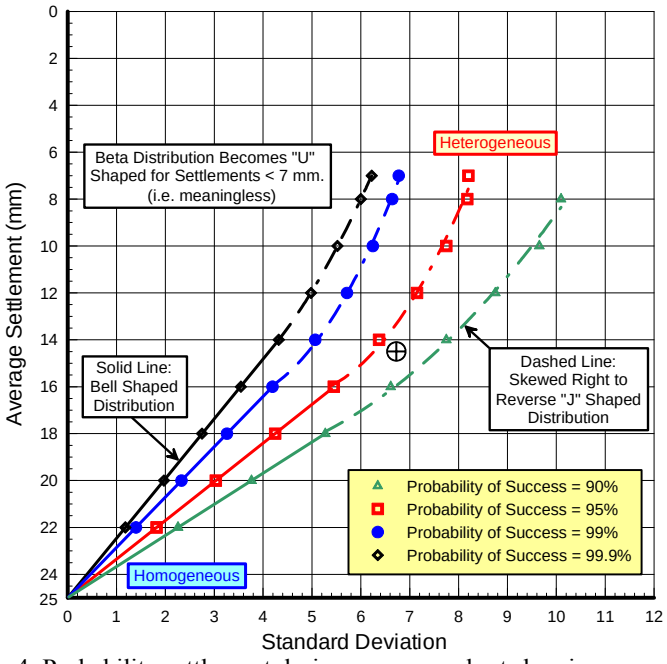

Figure 4: Probability settlement design summary chart showing probability of success for the foundation design for this site

As one can readily observe from Figure 4, the probability of success for this design was 93%. The owner and design/build contractor agreed that this foundation design sufficiently addressed their concerns, tolerable settlement criteria, and was subsequently approved for construction.

6 CONCLUSIONS

1. Settlement analyses based on dilatometer test data can be used to accurately size spread footings for structures.
2. Schmertmann's dilatometer design method is accurate enough to enable the engineer to assess risk using probability analyses.
3. The probability analyses and design chart enabled the owner and design/build contractor to understand the project risk and make an informed decision regarding the foundation design.

7 REFERENCES

Burland, J. B. and Burbridge, M. C., 1985, "Settlement of Foundations on Sand and Gravel", Proc., Inst. of Civ. Engrs, Part 1, 78, 1325-1381.

Duncan, J. Michael, April 2000, "Factors of Safety and Reliability in Geotechnical Engineering", ASCE Journal of Geotechnical and Geoenvironmental Engineering, Vol 126, No. 4, pp. 307-316.

Failmezger, Roger A., 2001, Discussion of "Factors of Safety and Reliability in Geotechnical Engineering", ASCE Journal of Geotechnical and Geoenvironmental Engineering, Vol 127, No. 8, pp. 703-704.

Failmezger, Roger A., Bullock, Paul J., 2004, "Individual foundation design for column loads", International Site Characterization '02, Porto, Portugal, pp. 1439-1442.

Failmezger, Roger A., Bullock, Paul J., Handy, Richard L., 2004, "Site Variability, Risk, and Beta", International Site Characterization '02, Porto, Portugal, pp. 913-920.

Hayes, J.A., August 1986, "Comparison of flat dilatometer in-situ test results with observed settlement of structures and earthwork", Proceedings 39th Geotechnical Conference, Ottawa, Ontario, Canada.

Marchetti, S., March 1980, "In situ tests by flat dilatometer, Journal of the Geotechnical Engineering Division, ASCE, Vol. 106, No. GT3, pages 299-321.

Robertson, Peter K., June 2004, "In-situ testing update, with emphasis on the CPT and its application for geotechnical practice," ASCE, Pittsburgh Section Geotechnical Group

Schmertmann, J.H., September 1984, Discussion of "Reproducible SPT Hammer Force with an Automatic Free Fall SPT Hammer System" by C.O. Riggs, N.O. Schmidt, and C.L. Rassieur, Geotechnical Testing Journal, American Society for Testing and Materials, Philadelphia, PA, pp. 167-168.

Schmertmann, J. H., June 1986, "Dilatometer to compute foundation settlement", Proceedings, ASCE Specialty Conference, In-Situ '86, VPI, Blacksburg, Virginia, pages 303-321.

Skempton, A.W. (1986), "Standard penetration test procedures and the effects in sands of overburden pressure, relative density, particle size, ageing, and overconsolidation", Geotechnique 36, No.3, pp. 425-447.

DMT testing for redesign using shallow foundations

Roger Failmezger
In-Situ Soil Testing, L.C., 173 Dillin Drive, Lancaster, Virginia 22503, email: insitusoil@prodigy.net

Paul Till
Hardin-Kight Associates, Inc., 12515 Caterpillar Lane, Bishopville, Maryland 21813, email: PTillHKA@aol.com

Keywords: Dilatometer, standard penetration test, settlement, case studies

ABSTRACT: Yes, the United States has far too many lawyers, and geotechnical engineers worry about their liability. But, when geotechnical engineers recommend costly foundation solutions because they don't have accurate enough data, we are making inexcusable errors and are not serving the owner's needs. Dilatometer tests provide engineers with high quality data so that they can make good foundation design decisions. Presented in this paper are several case studies showing how dilatometer tests and analyses resulted in much more economical foundation design solutions than in the originally proposed solutions.

1 INTRODUCTION

Engineers in the U.S. often use standard penetration testing as the only method of investigating a project site. Laboratory consolidation testing is routinely omitted either due to too small of a testing fee or sands that are difficult to sample. Because of the high uncertainty in defining and understanding the deformation characteristics of the soil, the engineer becomes overly conservative with his design. Unfortunately, many engineers are often reluctant to ask the owner to pay for additional investigations after they know that they need them to do good design. Faced with expensive foundation recommendations that the owner is not sure he needs, the owner will lose confidence in the first engineer and often ask another engineer to redesign the foundation. As the second engineers, we performed subsurface investigations using dilatometer tests to characterize the deformation characteristics of the soils better and provide much more economical yet safe designs.

2 REVIEW OF SPT SETTLEMENT PREDICTION

2.1 *SPT Procedure*

The standard penetration test (SPT) is a dynamic penetration test that strains the soil to much higher levels than what structures impose on the underlying soil (Figure 1). Correlations between the dynamic penetration response of the soil and the soil's static deformation modulus are poor. There is further uncertainty in correlation coefficients when trying to extrapolate the deformation modulus from a high strain test to a medium strain loading condition.

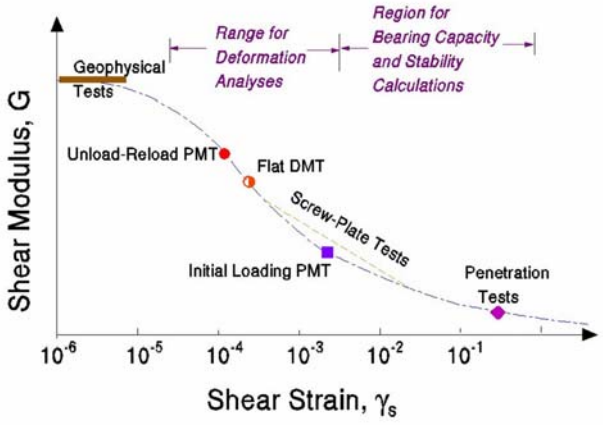

Figure 1: Strain levels imposed by DMT and other in-situ tests (Mayne, 2001)

While the applied hammer energy of the SPT can vary from 30 to 95% of the potential energy of 4200 in-lbf [48260 kgf-mm] (30-inch drop times 140 lbf hammer), it is rarely calibrated. The test is operator dependent. Higher quality operators provide more repeatable results. The uncertainty from measurement noise (test repeatability) can be as high as 45 to 100% (Schmertmann, 1978; Kuhawy, 1996).

Much research for the SPT was performed in the 1940s-1960s using mud rotary drilling methods and donut and safety hammers. Instrumentation had not been developed then to measure the applied hammer

energy. Researchers believe the applied hammer energies were about 55 to 60% of the potential energy. Skempton (1986) proposed correcting the SPT N-value to an N_{60}-value, representing a 60% applied hammer energy. However, even today it has been rare to find N_{60} values shown on boring logs in the U.S.

Many newer SPT drill rigs use automatic hammers. Many of these hammers, provided that they are well maintained, consistently deliver 90 to 95% of the SPT potential energy. Without making the N_{60} correction, the N-value from the automatic hammer will be about 2/3 of the N-value from a safety hammer.

In the 1940s-1960s the inner diameter of the barrel of the SPT spoon was the same as the tip. Today, the inner barrel has an inside diameter that is larger than the tip inside diameter, which allows liners to be inserted in the barrel. Without liners, the frictional resistance along the inside of the spoon is greatly reduced. While the reduction in resistance depends on soil conditions, Skempton (1986) suggests that an average reduction of 20% occurs.

When a borehole is made using hollow-stem augers, the pre-existing geostatic stresses are removed. When a borehole is made using mud rotary drilling, about half of the pre-existing geostatic stresses are removed. Reductions in the pre-existing geostatic stresses soften or loosen the soils and result in lower N-values.

With today's methods and without the N_{60} correction, the uncorrected N-values can be ½ of the N-value measured during the 1940s-1960s. Yet, geotechnical engineers will often use their uncorrected N-values with the design methods from that era. As a result, they are misled into believing the soils are much weaker than they actually are.

2.2 *SPT Design Methods for Settlement*

In sands Burland and Burbridge (1985) developed the following equation to predict settlement using the SPT:

$$S = B^{0.75} \{1.7/(N_{60AVG})^{1.4}\}(q-2/3\sigma_{vo}')$$

where S= predicted settlement (mm),
B= footing width (m),
q = applied bearing pressure (kPa),
σ_{vo}' = initial effective vertical stress at the base of the footing level (kPa),
and N_{60AVG} = average SPT blow count within a depth of $B^{0.75}$ meters beneath the footing.

Their case study database revealed the following graph (Figure 2) of predicted and measured settlement.

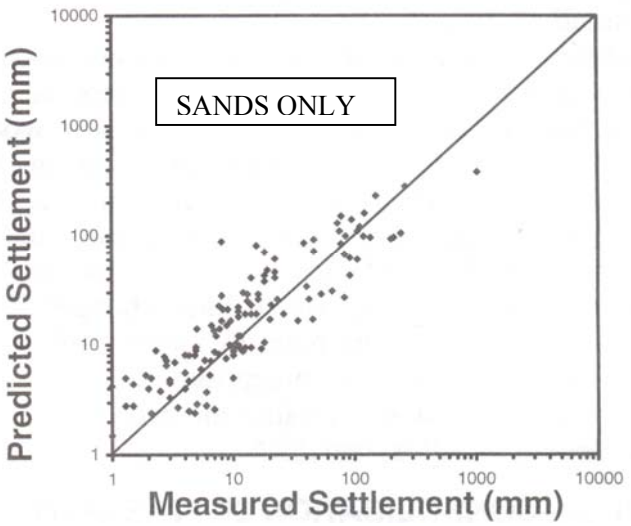

Fiure 2: Predicted vs. Measured Settlement from SPT in Sands Only (Burland and Burbridge (1985).

Based on the Burland and Burbridge (1985) equation, Duncan (2000) presented a settlement example that showed that an average settlement of 0.3 inches [7.6 mm] was required for the structure to have less than 1.0 inch [25 mm] of settlement. Duncan (2000) showed that the coefficient of variation (standard deviation/average value) was 0.67 for the Burland and Burbridge (1985) method. Failmezger (2001) showed that when measurement noise (test repeatability) and spatial (site subsurface variability) are considered in addition to the method error, the average settlement such that settlement would not likely exceed 1.0 inch [25 mm] is less than 0.3 inches [7.6 mm].

Engineers may use other design charts or correlations to predict settlement in sands and even other soil types. SPT tests in clay and residual soils destroy the soil structure and will often result in low "N" values that may only be representative of remolded properties instead of intact properties. The accuracy with these methods will be even less than the Burland and Burbridge (1985) method.

In summary, settlement predictions based on SPT are too inaccurate to be used for design.

3 REVIEW OF DMT SETTLEMENT PREDICTION

Schmertmann (1986) developed his ordinary and special methods for computing settlement of a structure or embankment. The ordinary method is simply the increase stress multiplied by the layer thickness divided by the constrained deformation modulus. In his special method the modulus is adjusted to account for whether the increase stress occurs below the preconsolidation pressure (highly overconsolidated soil), above the preconsolidation pressure (normally consolidated soil) or starts below the preconsolidation pressure and then exceeds it (lightly

overconsolidated soil). Generally, settlement prediction from the ordinary method is within 10% of the special method. Using his 16 case studies, Schmertmann (1986) had an average predicted to measured ratio of 1.18 with a standard deviation of 0.38. If the predictions where the dilatometer blade was driven and where tests were performed in quick clayey silts are excluded from the data set, the average predicted to measured ratio reduces to 1.07 with a standard deviation of 0.22.

From dilatometer test data, Hayes (1986) computed settlement at 5 sites using Schmertmann's (1986) methods. From his case studies with the ordinary method, the average predicted to measured ratio was 1.02 with a standard deviation of 0.14 and for the special method, the average predicted to measured ratio was 1.06 with a standard deviation of 0.25. If we use all the case study data and exclude the data for the quick clayey silts and driven DMT data, the average predicted to measured ratio is 1.06 and its standard deviation is 0.18. A summary graph (Figure 3) from these researchers is shown below:

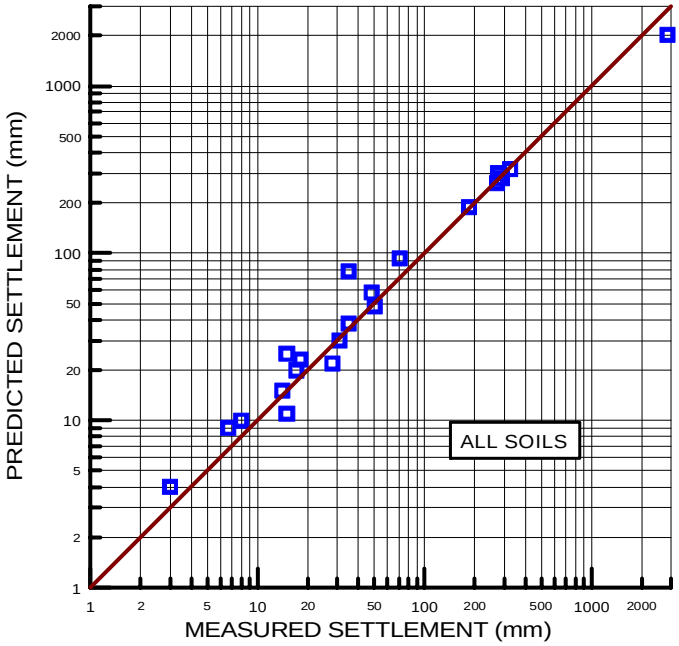

Figure 3: Predicted vs. Measured Settlement from DMT in All Soils (adapted from Schmertmann, 1986) and Hayes, 1986)

4 CASE STUDIES

Five case studies are presented below that demonstrate the value of using dilatometer test data for design. In each case the redesign saved the owners between US $200,000 and US $800,000. Each building is performing to the satisfaction of the owners. A summary of the original design and the redesign based on dilatometer testing is shown in Table 1.

Site	Column Load (kips/kN)	First Engineer's Recommended		DMT Redesign Recommendation	
		Bearing Capacity (psf/kPa)	Predicted Settlement (inches/mm)	Bearing Capacity (psf/kPa)	Predicted Settlement (inches/mm)
Westminister Village	90 [400]	1000 [48]	1 to 4 [25-100]	1500 [72]	< 1.0 [<25]
Walmart Store at Ocean Landing Shopping Center	60 to 160 [267 to 712]	1000 [48]	2.5 [64]	2000 [96]	0.5 [13]
Old Town Crescent	250 [1112]	3000 [144]	3 [75]	5000 [239]	< 0.5 [<13]
Fox Run Village - Novi, Michigan	300 [67]	2000 [96]	3 to 5 [75-125]	4000 [192]	< 1.0 [<25}
Monarch Landing - Naperville, Illinois	200 [45]	2000 [96]	> 1 [>25]	6000 [287]	< 1.0 [<25]

Table 1: Summary of Foundation Redesign Case Studies

4.1 *Westminister Village*

In the first geotechnical investigation program, soil test borings showed 7 to 13 feet [2.1 to 4.0 m] of sand underlain by a soft to medium stiff clay. One laboratory consolidation test was performed on an "undisturbed" clay sample. The stress-strain curve from that test was rather flat indicating that the sample was disturbed. The geotechnical engineer predicted settlements between 1 and 7 inches [25 and 178 mm] for shallow spread footings and recommended pile foundations.

We performed dilatometer tests near the two boring locations where the clay was the softest and thickest. The results of the dilatometer tests are presented in Figure 4. We redesigned the building to be supported on shallow spread footings and conventional ground supported floor slabs. We predicted settlements of about 0.5 inches [12.7 mm].

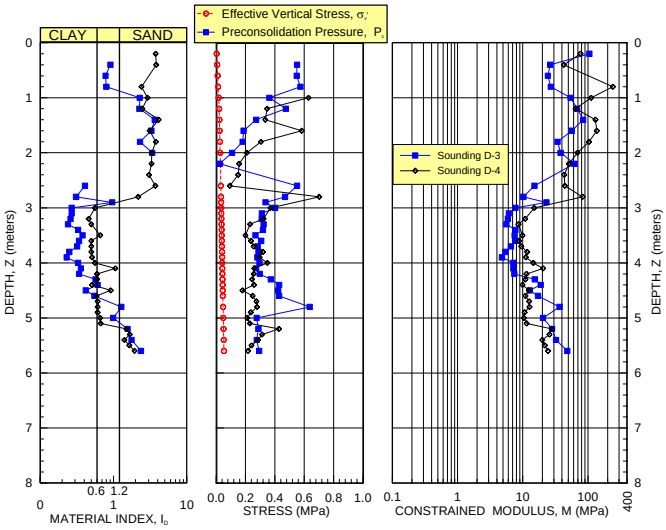

Figure 4: Summary of dilatometer results from Westminister Village

4.2 *Ocean Landing Shopping Center--Walmart Store*

For the Walmart Store site, the first geotechnical engineer performed soil test borings that showed sand with an underlying near surface organic silt and clay layer. Based on a consolidation test from an undisturbed Shelby tube sample, the engineer predicted 2.5 inches [64 mm] of settlement. The engineer recommended pile foundations to support the column and slab loads.

We performed 13 dilatometer test soundings within the footprint of the building. Representative results are presented on Figure 5. We predicted settlement to be between 0.25 and 0.75 inches [6.4 and 19.1 mm].

To verify our settlement predictions, an embankment load test was performed (Figure 6). The fill height was 8 feet [2.4 m], which imposed the same stress on the organic layer that the proposed footings would impose. Piezometers and settlement points were installed within the embankment. Under the load, a settlement of 0.5 inches [12.7 mm] occurred rapidly and excess pore pressures dissipated quickly.

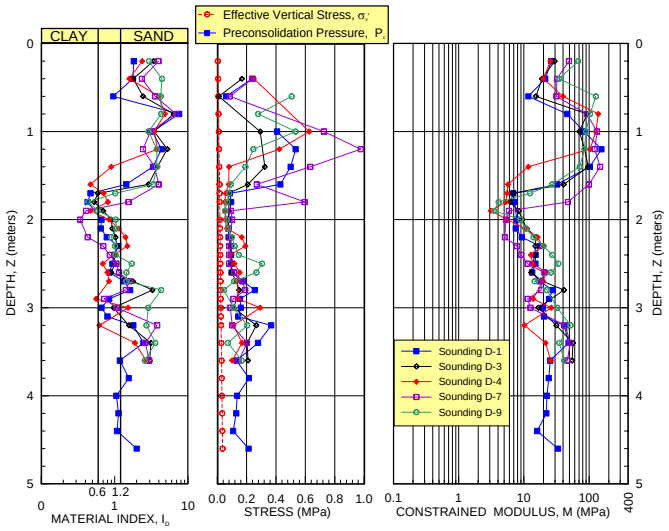

Figure 5: Summary of dilatometer tests from Ocean Landing Shopping Center

Figure 6: Embankment load test setup

At an adjacent site, without the benefit of dilatometer test data, the geotechnical engineer recommended using stone columns to support a similarly loaded structure. We investigated the adjacent parcel on the other side to this center parcel with dilatometer tests. The boring logs show that all three sites have similar geologic conditions. The two sites where dilatometer tests were performed were successfully designed using conventional spread footings, while we believe the center site was overdesigned at an additional cost of US $750,000.

4.3 *Old Town Crescent*

Based on standard penetration tests, the first geotechnical engineers found a loose silty fine sand between 12 and 22 feet [3.7 and 6.7 m]. Groundwater was about 5 feet [1.6 m] deep. They recommended

using shallow spread footings with an allowable bearing pressure of 1500 psf [72 kPa].

Settlement predictions based on SPT are very inaccurate even in sands (Failmezger, 2001). As the second geotechnical engineer, we performed dilatometer test soundings at the corners and center of the proposed building. Those DMT results are summarized on Figure 7. Because the structure also had a 1-level underground garage, we considered the removal of 960 psf [46 kPa] of overburden as well as no overburden removal in our settlement analyses. The design column load was 250 kips [1110 kN]. With the overburnen removal and with a design bearing pressure of 5000 psf [240 kPa], our settlement predictions were less than 0.25 inches [6.4 mm]. Without the overburden removal, our settlement predictions were between 0.2 and 1.1 inches [5.1 and 27.9 mm].

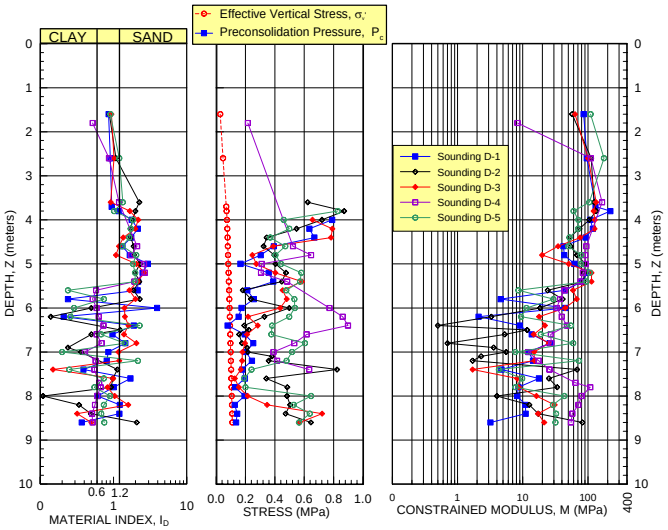

Figure 7: Summary of dilatometer tests from Old Town Crescent

4.4 *Fox Run Village*

The first geotechnical engineer recommended a mat foundation for the proposed 3 to 4 story residential retirement buildings. From the standard penetration test results, the first engineer concluded that the clays at the site were soft. One building was under construction and the two other buildings (Nos. 2.3 and 3.1) had their building pads graded when we were hired to reevaluate the first engineer's recommendations.

We performed dilatometer test soundings for Buildings 2.3 and 3.1 and one dilatometer sounding adjacent to the constructed mat foundation. For Buildings 2.3 and 3.1, we predicted settlements of less than 1.0 inch [25 mm] for the design column load of 300 kips [1334 kN] using an applied bearing stress of 4 ksf [191 kPa]. For the building with an existing mat foundation, we found that the clays were softer there. Here the foundations needed an applied bearing pressure of 1.7 ksf [81 kPa] to keep settlements less than 1.0 inch [25 mm].

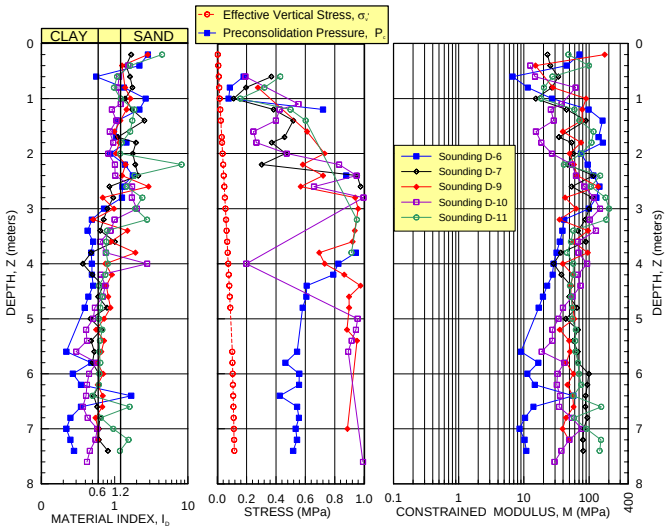

Figure 8: Summary of dilatometer tests from Fox Run Village

4.5 *Monarch Landing*

The first geotechnical engineer performed 62 soil test borings and 21 test pits as their subsurface exploration plan. They recommended supporting the building, which had design interior column loads of 1500 kips [6672 kN] on spread footing using an allowable bearing pressure of 3000 psf [144 kPa].

We performed 15 dilatometer test soundings at the site to reevaluate their design. While the depth intervals for the dilatometer tests were generally 20 cm, in areas where softer clays were found we used depth intervals of 10 cm to define those clays better. Where the clays were too soft to provide adequate support, the close interval test spacing helped us to determine how deep to undercut those clays and replace them with compacted structural fill. We found that the allowable bearing pressure could be 6000 psf [287 kPa] and the resulting settlements would be less than 1.0 inch [25 mm].

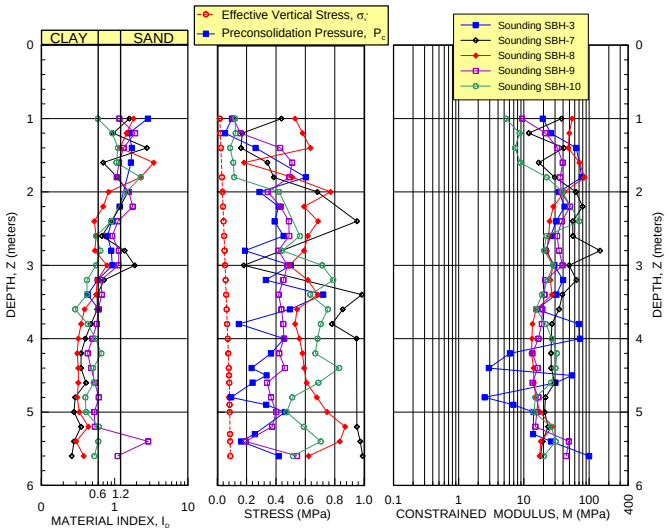

Figure 9: Summary of dilatometer tests from Monarch Landing

5 CONCLUSIONS

1. Today engineers' biggest mistakes are recommending a costly foundation solution without adequate data to prove that this solution is necessary.
2. Standard penetration test data should never be used to predict foundation settlements for any soil.
3. Accurate settlement predictions can be made using dilatometer test data.
4. The dilatometer is not an expensive in-situ test, and the appropriate interpretation of the testing data can save quite a lot of money in the foundation design, as presented in the five case studies.

6 REFERENCES

Burland, J. B. and Burbridge, M. C., (1985), "Settlement of Foundations on Sand and Gravel", Proc., Inst. of Civ. Engrs, Part 1, 78, 1325-1381.

Duncan, J. M. (2000), "Factors of Safety and Reliability in Geotechnical Engineering", ASCE Journal of Geotechnical and Geoenvironmental Engineering, Vol 126, No. 4, pp. 307-316.

Failmezger, R. A., (2001), Discussion of "Factors of Safety and Reliability in Geotechnical Engineering", ASCE Journal of Geotechnical and Geoenvironmental Engineering, Vol 127, No. 8, pp. 703-704.

Failmezger, R. A. and Bullock, P. J., (2004), "Individual foundation design for column loads", International Site Characterization '02, Porto, Portugal, pp. 1439-1442.

Hayes, J.A., (1986), "Comparison of flat dilatometer in-situ test results with observed settlement of structures and earthwork", Proceedings 39th Geotechnical Conference, Ottawa, Ontario, Canada.

Marchetti, S., (1980), "In situ tests by flat dilatometer, Journal of the Geotechnical Engineering Division, ASCE, Vol. 106, No. GT3, pages 299-321.

Mayne, P. W. (2001). Keynote: "Stress-Strain-Strength-Flow Parameters from Enhanced In-Situ Tests", Proceedings, International Conference on In-Situ Measurement of Soil Properties & Case Histories (In-Situ 2001), Bali, Indonesia, 27-47.

Schmertman, J. H. (1978), "Use the SPT to Measure Dynamic Soil Properties? – Yes, But..!", Dynamic Geotechnical Testing, ASTM STP 654, American Society for Testing and Materials, pp. 341-355.

Schmertmann, J. H., (1986), "Dilatometer to compute foundation settlement", Proceedings, ASCE Specialty Conference, In-Situ '86, VPI, Blacksburg, Virginia, pages 303-321.

Skempton, A. W. (1986), "Standard penetration test procedures and the effects in sands of overburden pressure, relative density, particle size, ageing, and overconsolidation", Geotechnique 36, No.3, pp. 425-447.

BACK

The Use of Dilatometer and In-Situ Testing to Optimize Slope Design

E. Farouz & J.-Y. Chen
Senior Geotechnical Engineer and Geotechnical Engineer, CH2M HILL, Inc., Herndon, Virginia, U.S.A.

R. A. Failmezger
President, In-Situ Soil Testing, L.C., Lancaster, Virginia, U.S.A, email: insitusoil@prodigy.net

Keywords: dilatometer, cone penetrometer, finite-element analyses, slope stability

ABSTRACT: Finite-element analyses can accurately model soil's response to loading conditions. However, without realistic geotechnical parameters to model the stress-strain and strength characteristics of soils, its accuracy diminishes. This paper discusses use of finite-element analyses with the computer program, PLAXIS, to evaluate long-term performance of cut slopes at the Virginia Route 288 project, near Richmond, Virginia, USA. The 9-meter high cut slopes are located near an area with a history of slope failures.
Limit-equilibrium slope stability analyses based on the conventional subsurface investigation approach using borings and overly-conservative soil parameters derived from Standard Penetration Test results and back-analyses of historical slope failures near this area, indicated that the cut slopes will be stable at a slope ratio of 5-horizontal-to-1-vertical (5H:1V). Using the finite-element analyses with soil parameters developed based on the results of dilatometer tests (DMT) and piezo-cone penetrometer tests (CPTU), the cut slopes were found to be stable at a slope ratio of 3H:1V. The slope has been observed over the past 4 years and found to be stable, with no sign of distress.

1 INTRODUCTION

The Virginia 288 PPTA (Public Private Transportation Act) project was approved for construction in December 2000, and construction started in April 2001. The project includes construction of approximately 17 miles of new highway with 23 bridges and overpasses. The project design team, led by CH2M HILL, was asked to reduce the cost of a cut slope within a segment of the project designated as "Cut C." Cut C is located along the Virginia Route 288 mainline, immediately south of the James River. Documented historical slope failures near this area of the project led to conservative slope design in Cut C. The cut slopes were originally recommended to be at a slope ratio as flat as 5H:1V, including a drainage blanket. A proposal by the contractor initiated the study presented in this paper to re-evaluate the cut slope stability. Results of this study led to a more reasonable and cost-saving design. The general location of this project is shown in Figure 1.

Figure 1. Site Location Map of the Virginia Route 288 Project

2 PROJECT GEOLOGY

The project is located in the Piedmont Physiographic Province of Central Virginia. The region is characterized by complexly folded and faulted igneous and metamorphic rocks of Late Precambrian to Paleozoic age (Wilkes, 1988) below Triassic-aged coal measures, shales, and interbedded sandstones and shales. Geologic literature for the Midlothian Quadrangle of Virginia reports that a Tertiary-aged gravelly terrace deposit is present at the cut slope location, south of the James River flood plain and north of Bernard's Creek (Goodwin, 1970). This material is composed mostly of coarse gravel, with clayey sand beds inter-layered with the gravel. The

matrix of the formation is predominately sand with varying amounts of clay.

3 PROJECT DESCRIPTION

The cut slope extends approximately between Virginia Route 288 mainline stations 158+20 and 161+00 and is entirely within the limits of Cut C, which extends from station 153+00 to station 163+00. The original designer of this roadway cut slope recommended a slope ratio as flat as 5H:1V at some cuts. The design included a drainage blanket. A schematic design cross-section is presented in Figure 2.

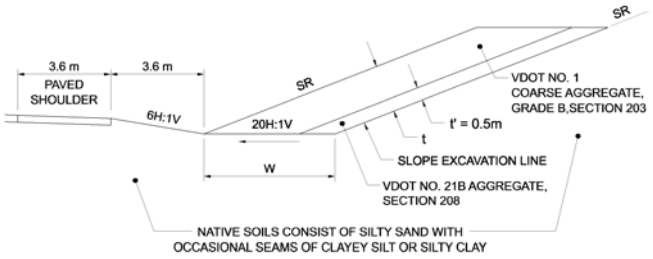

Slope Ratio (SR) (Location Used)	Blanket Width (w) (meters)	Recommended Blanket Thickness (t) (meters)
2H:1V (Bridge)	8.0	3.5
2H:1V (Roadway)	6.0	2.7
3H:1V (Bridge)	6.0	1.9
3H:1V (Roadway)	5.5	1.7
4H:1V (Roadway)	4.0	1.0
5H:1V (Roadway)	2.5	0.5

Notes: Width (w) is horizontal dimension; Thickness (t) is perpendicular to slope.

Figure 2. Original Schematic Design Cross-Section of the Cut Slope (after HDR Engineering, Inc., 1999)

Groundwater levels in the Cut C area along Route 288, indicated by borings and monitoring wells, are summarized in Table 1. Generally, groundwater between stations 154+00 and 163+00 is observed to be near or above the finished grade. At maximum, groundwater is approximately 4 to 5 meters above the finished grade between station 155+00 and 160+00.

Table 1. Summary of Measured Groundwater Levels in Cut C Area (after HDR Engineering, Inc., 1999)

Station	Cut Depth (m)	Ground-water Elevation (m)	Ground-water Depth from Surface (m)	*Groundwater Height above Finished Cut (m)
153	2	Dry	3	-1
154	5	58	6	-1
155	8	61	3	5
156	10	62	5	5
157	8	60	4	4
158	9	60	5	4
159	8	60	3	5
160	6	59	2	4
161	4	56	1	3
162	5	54	3	2
163	2	52	3	-1

* Note that negative values indicate groundwater table below the finished cut.

Because geotechnical properties of soils are generally site-specific even within the same geological formation, in-situ testing was performed and slope stability re-evaluated upon the contractor's proposal to increase the slope ratio and avoid using a drainage blanket, to save valuable construction dollars. Based on the study presented hereafter, the cut slope is found to be stable at a slope ratio of 3H:1V.

4 IN-SITU TESTING

The in-situ testing program consisted of both dilatometer tests (DMT) and piezo-cone penetrometer tests (CPTU), which are near-continuous soil profiling techniques, to delineate subsurface stratigraphy and soil properties. The CPTU data require a good estimate of correlation coefficients to determine strength and deformation parameters. These coefficients depend on the geologic formation and can be site-specific.

The Marchetti dilatometer test is a calibrated static deformation test. The thrust to push the DMT blade, the lift-off pressure, p_0, and the pressure at full expansion, p_1, are measured. These measurements are used to compute the Marchetti indices: I_D, K_D, and E_D. These independent indices are used to compute other soil parameters through triangulation (two variables to get a third variable). Vertical constrained deformation modulus, M, was calculated using Marchetti's (1980) correlation. This modulus is obtained after combining the dilatometer modulus, E_D, with the horizontal stress index, K_D, which is an indicator of stress history, and I_D, which is a soil classification index based on its mechanical behavior. Schmertmann's (1982) method, which used the thrust measurement, for determining the drained friction angle in the cohesionless soils was used.

In this study, in-situ testing including three CPTUs, designated as PZ-1, PZ-2, and PZ-3, and four DMTs, designated as DT-1, DT-2, DT-3, and DT-4, were performed at selected locations shown in Figure 3. DT-1, DT-2, and PZ-1 are located at the top of the cut slope on the south-bound-lane (SBL) side of the highway and DT-3, DT-4, and PZ-2 are located at the bottom of the cut slope on the SBL side. PZ-3 is an additional CPTU located at the top of the cut slope on the north-bound-lane (NBL) side of the highway. At the time of testing, the slope had already been cut close to the planned finished elevation, at a slope ratio of 3H:1V, without obvious distress.

Typical CPTU and DMT results from this study are presented in Figures 4 and 5, respectively. These results were obtained at testing locations PZ-1 and DT-1, shown in Figure 3. Interpreted DMT strength and deformation parameters from testing at DT-1 are

presented in Figures 6 and 7, respectively. Testing results consistently show that soils within the cut slope are primarily sandy soils with occasional seams of clayey silt or silty clay, which correlates well with geological literature (e.g., Goodwin, 1970).

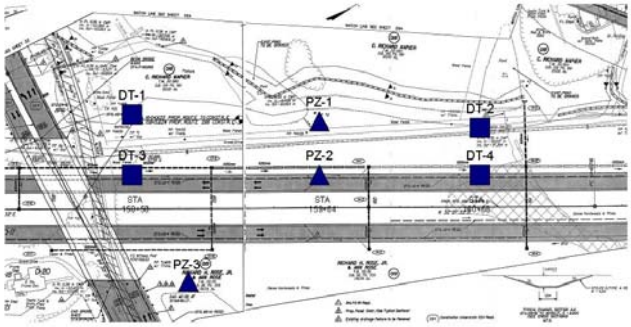

Figure 3. In-Situ Testing Locations

From the DMT results obtained at DT-1, a stiffer sandy soil layer is observed at a depth between 0 and 2 meters below the top of slope, as indicated by the higher thrust required to push the dilatometer blade and the higher M. Below a depth of 4 meters from the top of slope, the stiffness of sandy soils generally increases with increasing depth. For example, between a depth of 4 and 9 m in DT-1, constrained modulus (M) increases from 200 to 900 bars. The drained friction angle (ϕ') of the sandy soils is generally greater than 37 degrees (ranging between 37 and 47 degrees) under the plane-strain condition. The drained friction angle under triaxial compression (ϕ'_{TC}) is averaging 38 degrees. Also, sandy soil deposits within the slope are generally overconsolidated, with an overconsolidation ratio (OCR) decreasing with increasing depth.

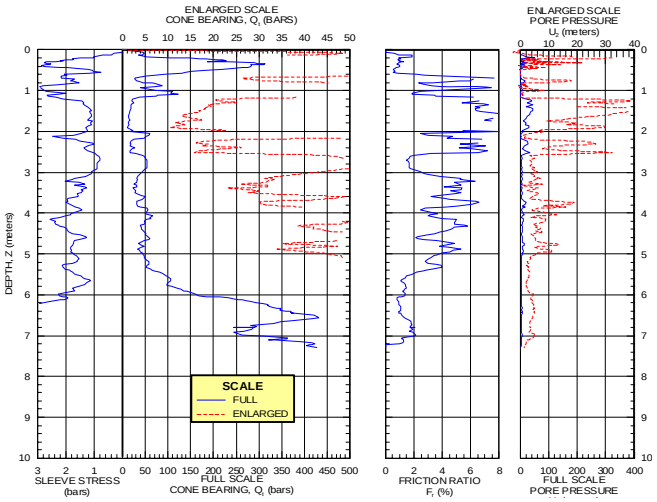

Figure 4. CPTU Results Obtained at Testing Location PZ-1

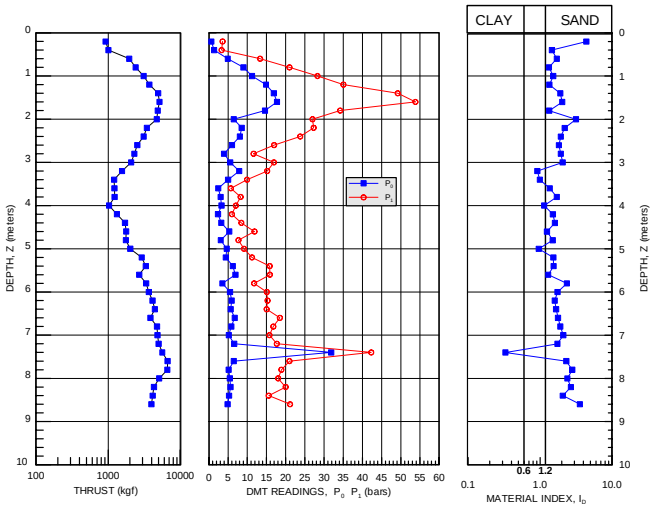

Figure 5. DMT Results Obtained at Testing Location DT-1

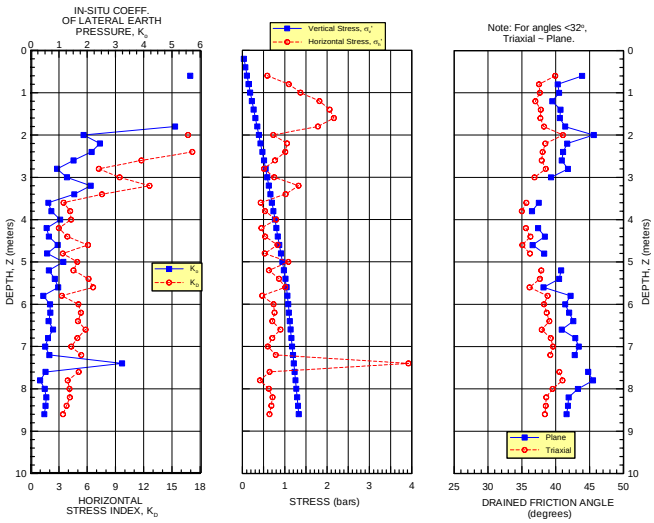

Figure 6. Interpreted DMT Strength Parameters from Testing Results Obtained at DT-1

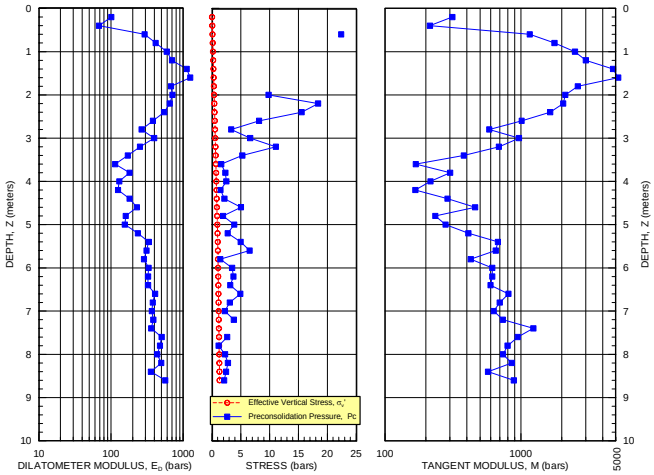

Figure 7. Interpreted DMT Deformation Parameters from Testing Results Obtained at DT-1

5 STABILITY ANALYSES

Slope stability analyses using a finite-element based computer program, PLAXIS (Brinkgreve and Vermeer, editors, 1998), were executed to evaluate the cut slope performance. A cross-section at the SBL side of Virginia Route 288 mainline station 158+20 was analyzed. This cross-section represents one of the deepest cut sections along this slope. The cut depth is approximately 9 m, with a revised slope ratio of 3H:1V. The top of the slope is at an elevation of 65 m above mean sea level (MSL) and the bottom of the slope is at an elevation of 56 m above MSL. The top of bedrock is at an approximate elevation of 50 m above MSL (4 m below the bottom of cut). A single soil type was used for soils above the rock, which is assumed as fixity in the model. This cut section was analyzed under the following groundwater conditions:

1) Normal groundwater condition, with the groundwater level at an elevation of 60 m above MSL (4 m above the bottom of cut).
2) The worst-case groundwater condition with the groundwater level at an elevation of 65 m above MSL (corresponding to a fully-saturated cut slope).

In the model, the cut was excavated in three steps. Each cut step involved removal of soil of 3-m vertical thickness in accordance with the 3H:1V slope ratio, during a 2-month period. Groundwater drawdown characteristics were modeled with the groundwater flow module in PLAXIS during each cut step, such that effective stress within the cut slope can be estimated more accurately.

Soil behavior was modeled using the hardening soil model presented in Table 2, with various strength, deformation, and groundwater flow parameters. Strength and deformation parameters were considered the most critical ones for this particular cut slope with regard to its stability, and the DMT results were used to develop these parameters. CPTU results were used to confirm that variation of soil properties within the slope profile was small and a single soil type can reasonably represent the slope behavior. Sources or correlations where these parameters were developed are presented in Table 2 and discussed hereafter.

1) Moist and Saturated Unit Weights: The moist unit weight was estimated from the DMT results, and matched up well with the data in HDR Engineering, Inc. (1999). Therefore, both moist and saturated unit weights are the same as those in HDR Engineering, Inc. (1999).
2) Strength Parameters: Drained cohesion was assumed to be zero for a sandy soil. The drained friction angle was the minimum friction angle (37 degrees) under the plane-strain condition, indicated by DMT results. The correlation between friction angle and dilatancy angle was presented by Bolton (1986). As an order of magnitude estimate, the dilatancy angle was estimated to be: $\varphi = \phi' - 30$ degrees.
3) Deformation Parameters: The oedometer modulus was assumed to be the constrained modulus at a depth of 6 m. As a result, the reference pressure is the effective horizontal stress at a depth of 6 m. An at-rest earth pressure coefficient of 0.9, indicated by the DMT results, was used to estimate the effective horizontal stress. The Young's modulus (E) can be estimated from constrained modulus (M) and Poisson's ratio (υ) by: $E = M(1+\upsilon)(1-2\upsilon)/(1-\upsilon)$. The Poisson's ratio was determined to be 0.29 from the drained friction angle under triaxial compression (ϕ'_{TC}), using the relationship presented in Kulhawy and Mayne (1990): $\upsilon = 0.1 + 0.3\ (\phi'_{TC} - 25 \text{ degrees})/(20 \text{ degrees})$. The power (m) for stress-dependent stiffness was assumed to be 0.5 for dense sand, according to Janbu (1963).
4) Hydraulic Conductivity and Void Ratio: The hydraulic conductivity for dense sand with occasional seams of clayey silt or silty clay was interpreted from the guidelines in Terzaghi et al. (1996). Anisotropy was assumed in hydraulic conductivity such that the ratio between horizontal and vertical hydraulic conductivity is 1.5. The initial void ratio was assumed to be 0.5 for a typical dense sand matrix presented in Terzaghi et al. (1996).

The ϕ-c reduction procedure in PLAXIS was performed to evaluate the stability of this cut slope. The factors of safety calculated from the ϕ-c reduction procedure under the normal and worst-case groundwater conditions are 2.2 and 1.2, respectively. Limit-equilibrium slope stability analyses were also performed to check the cut slope stability. The factors of safety calculated from limit-equilibrium analyses under normal and worst-case groundwater conditions are 1.3 and 1.1, respectively. These factors of safety are lower than the ones obtained from finite-element analyses because a horizontal straight-line phreatic surface broken by the slope was assumed in the limit-equilibrium analyses, while groundwater drawdown was modeled with assigned groundwater heads (as the boundary conditions) and hydraulic conductivity of soils in the finite-element analyses. As shown in Figure 8, groundwater drawdown in sandy soils increases the mean effective stress, and thus increases the shear strength of soils and factors of safety of the slope.

Table 2. Soil Parameters Developed from In-Situ Testing and Used in the Finite-Element Analyses

Soil Properties	Value	Unit	Source
Moist Unit Weight, γ	18.9	kN/m^3	Estimated from DMT results.
Saturated Unit Weight, γ_{sat}	20.2	kN/m^3	HDR Engineering, Inc. (1999).
Cohesion, c'	0	kPa	Assumed for the drained condition.
Drained Friction Angle, ϕ'	37	degrees	Estimated from DMT results.
Dilatancy Angle, φ	7	degrees	Bolton (1986).
Oedometer Modulus, E_{oed}	57000	kPa	Estimated from DMT results.
Secant Young's Modulus, E_{50}	45000	kPa	Estimated based on E_{oed} and Poisson's ratio.
Power, m	0.5	-	Janbu (1963).
Reference Pressure, p^{ref}	100	kPa	Estimated from DMT results.
Horizontal Permeability, k_x	1.5E-04	cm/sec	Terzaghi, Peck, and Mesri (1996).
Vertical Permeability, k_y	1.0E-04	cm/sec	Terzaghi, Peck, and Mesri (1996).
Initial Void Ratio, e_{init}	0.5	-	Terzaghi, Peck, and Mesri (1996).

The incremental shear strain calculated from the ϕ-c reduction procedure is a good indication of the most-critical failure surface of the slope. Under the normal groundwater condition, the incremental shear strain contours are presented in Figure 9. As shown in Figure 9, the most critical failure surface is influenced by groundwater drawdown and presence of the bedrock (assumed as fixity in the model). These two factors contribute to the overall stability of this cut slope.

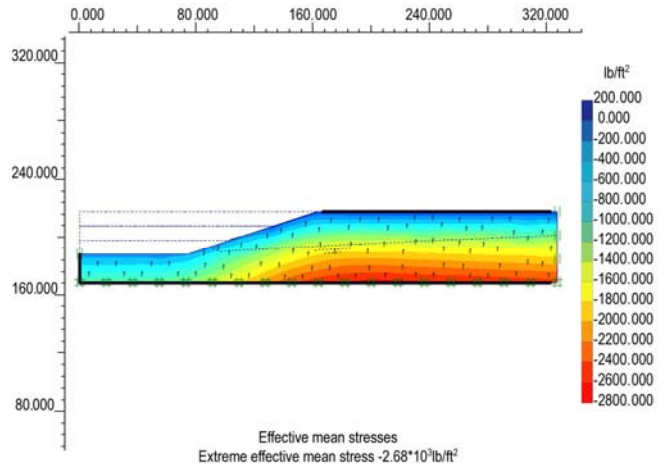

Figure 8. Influence of Groundwater Drawdown on the Mean Effective Stress within the Slope [X-axis and y-axis show PLAXIS coordinates in feet.]

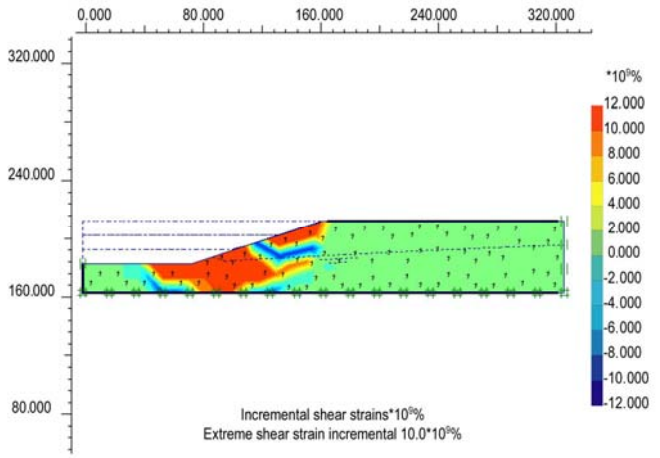

Figure 9. Incremental Shear Strain Contours Showing the Most-Critical Failure Surface of the Slope [X-axis and y-axis show PLAXIS coordinates in feet.]

As a result of the in-situ testing program and analyses using more realistic soil parameters from such testing, this cut slope was determined to be stable at a slope ratio of 3H:1V, without a drainage blanket. The saving of construction spending compared with an original 5H:1V slope with a drainage blanket, along both the NBL and SBL sides of the roadway, was approximately half a million dollars, which was significantly more than the cost of the in-situ testing program and more refined analyses.

6 CONCLUSIONS

The following conclusions can be drawn from the project described herein.

1) Geotechnical properties of soils are site-specific and, under certain circumstances, in-situ testing offers the best measure to characterize various strength and deformation parameters of soils in place. The proper selection of geotechnical properties of soils can reduce overall project cost.
2) In-situ testing is best performed by a specialist who has knowledge of the geology and soil behavior of the site, such that soil parameters can be more accurately estimated.
3) The finite-element analysis can more accurately model the state of stress, stress-dependent deformability and strength, and groundwater characteristic within an earth structure. However, such analysis requires more soil parameters than a conventional limit-equilibrium slope stability analysis. In-situ testing is considered the best way to obtain these soil parameters, especially within a sandy soil deposit where sampling and laboratory testing are more difficult and costly.

REFERENCES

Bolton, M. D. (1986). "The Strength and Dilatancy of Sands," Geotechnique, Vol. 36, No. 1, pp. 65-78.

Brinkgreve, R. B. J. and P. A. Vermeer, editors (1998). "PLAXIS Finite Element Code for Soil and Rock Analyses Version 7," Computer Program Manual, A. A. Balkema, Rotterdam, Netherlands.

Goodwin, B. K. (1970). "Report of Investigation 23 Geology of the Hylas and Midlothian Quadrangles, Virginia," Virginia Division of Mineral Resources, Charlottesville, VA.

HDR Engineering Inc. (1999). "Route 288 State Project 0288-072-104, PE101, Powhatan County, Virginia, Geotechnical Engineering Report for Roadway Design," Pittsburgh, PA.

Janbu, J. (1963). "Soil Compressibility as Determined by Oedometer and Triaxial Tests," Proc. ECSMFE Wiesbaden, Vol. 1, pp. 19-25.

Kulhawy, F. H. and P. W. Mayne (1990). "Manual on Estimating Soil Properties for Foundation Design," EL-6800 Research Project 1493-6, Final Report Prepared for Electric Power Research Institute, Palo Alto, CA.

Marchetti, S. (1980). "In Situ Tests by Flat Dilatometer," ASCE Journal of Geotechnical Engineering Division, March 1980, pp. 299-321.

Schmertmann, J. H. (1982). "A Method for Determining the Friction Angle in Sands from the Marchetti Dilatometer (DMT)," Proceeding of the Second European Symposium on Penetration Testing, Amsterdam, pp. 853-861.

Terzaghi, K., R. B. Peck, and G. Mesri. (1996). "Soil Mechanics in Engineering Practice," John Wiley & Sons, Inc., New York, 549 pp.

Wilkes, G. P. (1988). "Mining History of the Richmond Coalfield of Virginia," Virginia Department of Mines, Minerals & Energy, Charlottesville, VA.

Flat Dilatometer Testing in Brazilian Tropical Soils

Heraldo L. Giacheti & Anna S. P. Peixoto
São Paulo State University, Unesp-Bauru, Brazil

Giuliano De Mio
Golder Associates Brasil and University of São Paulo, USP-São Carlos, Brazil

David de Carvalho
University of Campinas, Unicamp-Campinas, Brazil

Keywords: site characterization, tropical soils, DMT, interpretation

ABSTRACT: Flat dilatometer tests were carried out at three relatively well-studied tropical research sites in the state of São Paulo, Brazil. Test results are presented and interpreted according to the traditional approach for site characterization of conventional soils. The results were compared to laboratory and others in situ tests. Soil description in terms of grain size distribution had to be confirmed with soil sampling. Correlations to estimate geotechnical parameters have to consider soil genesis. In this manner, some adjustment is necessary, especially for the soils with higher clay content. In tropical soils this approach appears to be an interesting way to achieve all requirements for an appropriate site characterization based on DMT testing.

1 INTRODUCTION

Flat dilatometer test (DMT) has been used by the geotechnical community as a logging tool to estimate geotechnical parameters for most soil conditions. Besides stratigraphic information, the DMT allows the estimative of geotechnical parameters based on correlations developed for soils from Europe and North America.

Tropical soils exhibit a unique mechanical behavior due to their genesis and partially saturated condition. The properties of these soils are very dependent on the degree of weathering and there are only a few DMT data available on tropical soils.

DMT test results from three relatively well-studied tropical research sites in the state of São Paulo, Brazil, are presented and interpreted according to the traditional approach developed for conventional soils. The results were compared to available reference soil parameters determined based on laboratory and others in situ tests. Preliminary findings are presented and briefly discussed.

2 TROPICAL SOILS

Tropical soils are formed predominantly by chemical alteration of the rock and they have peculiar behavior that cannot be explained by the principles of classical soil mechanics.

The term tropical soil includes both lateritic and saprolitic soils. Saprolitic soils are necessarily residual and retain the macro fabric of the parent rock. Lateritic soils can be either residual or transported and are distinguished by the occurrence of laterization process, which is enriching a soil with iron and aluminum and their associated oxides, caused by weathering in regions which are hot, acidic, and at least seasonally humid. Following laterization, high concentration of oxides and hydroxides of iron and aluminum bonds support a highly porous structure. Saprolitic soil has structural or chemical bonding retained from the parent rock. The contribution of this cementation to the soil stiffness depends on the strain level the soil will experience. Differences between the mechanical behaviors of the mature (lateritic) and young (saprolitic) soils have been reported for both natural and compacted condition. For tropical soils it is also necessary to identify their genetic characteristics since their properties are strongly dependent on the degree of weathering.

3 DESCRIPTION OF SITES AND TESTS

3.1 *Sites*

Research sites located at three University *campus*: Unesp (Bauru), Unicamp (Campinas) and USP (São Carlos), in the state of São Paulo, Brazil, were studied (Figure 1). At the site in Bauru, the subsoil is a sandy soil. The top 13 m has lateritic soil behavior. The soil at the Campinas Site has a clayey texture and is composed of two distinct layers: porous lateritic clay overlaying a silty clay of non-lateritic behavior, both derived from weathering of Diabase rock. At the site in São Carlos, the subsoil is clayey

fine sand with two well-defined layers; Cenozoic sediments of lateritic behavior overlaying the residual soil derived from sandstone with non-lateritic behavior. The MCT Classification System (Mini, Compacted, Tropical) proposed by Nogami and Villibor (1981) for tropical soils was used to define and classify the soil with regards to its lateritic behavior.

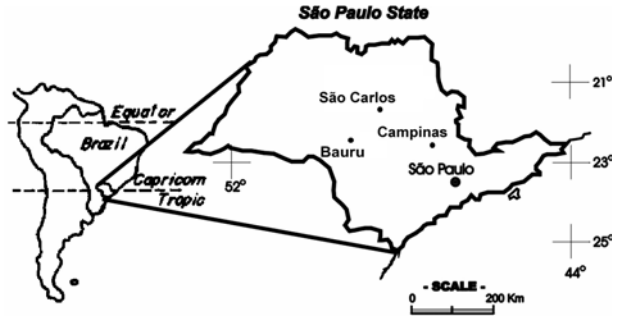

Figure 1. Cities where research sites are located.

3.2 *Tests*

Marchetti (1997) describes the flat dilatometer, which consists of a steel blade with a thin, expandable, circular steel membrane mounted on one face (Figure 2). The blade is connected, by an electro-pneumatic tube, running through the insertion rods, to a control unit on the surface. Marchetti (1997) also describes the test procedure which starts by inserting the dilatometer into the ground. By use of a control unit with a pressure regulator, a gauge and an audio signal, the operator determines the p_o-pressure required to just begin to move the membrane and p_1-pressure required to move it 1.1 mm into the ground. The blade is then advanced into the ground of one depth increment, typically 200 mm, using common field equipment.

According to Marchetti et al. (2001), the primary way of using DMT results is to interpret them in terms of common soil parameters and this methodology ("*design via parameters*") opens the door to a wide variety of engineering applications.

DMT interpretation starts with the calculation of three intermediate parameters (I_D, K_D and E_D). The Material Index $I_D = (p_1-p_o)/(p_o-u_o)$ is calculated to identify soil type, where u_o is the hydrostatic pore pressure. In general, I_D provides an expressive profile of soil type and, in "normal" soils a reasonable soil description (Marcheti et al., 2001). The Horizontal Stress Index $K_D = (p_1-p_o)/(\sigma'_{vo})$ where σ'_{vo} is the pre-insertion in situ overburden stress, provides the basis for several soil parameters correlations and is the key result of the dilatometer test (Marcheti et al., 2001). The dilatometer modulus (E_D) is obtained from p_0 and p_1 by the theory of elasticity and it is found that $E_D = 34.7\ (p_1 - p_0)$. E_D in general should not be used as such, especially because it lacks information on stress history (Marchetti et al., 2001). The strength and deformability soil parameters can be obtained from published empirical correlations.

DMT tests were carried out at each site in order to obtain pioneering data for this type of test in these reasonably well-known sites. One field logging with the DMT was carried out in each research site pushing the dilatometer blade into the ground with a heavy truck-mounted penetrometer at a penetration rate of about 20 mm/s. The calibration procedure to obtain ΔA and ΔB pressures, necessary to overcome membrane stiffness, was done before each profile. A-Pressure and B-Pressure were recorded every 200 mm during all the tests and p_o and p_1 pressures were calculated. The subsoil at all the sites is mostly partially saturated, so C-Pressure was not recorded.

A comprehensive site characterization program including SPT, SPT-T, CPT, SCPT and Cross-hole tests were carried out at each site. Ménard Pressuremeter Test (PMT) was also carried out at the Bauru Site. Sample pits were excavated to retrieve disturbed and undisturbed soil blocks in all the sites. These blocks were tested in the laboratory to characterize the soil and to determine mechanical properties.

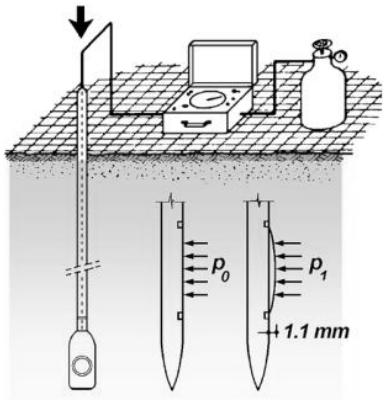

Figure 2. General layout of the dilatometer test (*www.marchetti-dmt.it/pagespictures/testlayout.htm*).

4 TEST RESULTS AND DISCUSSION

DMT tests results in terms of p_o, p_1, I_D, K_D and E_D are presented in Figures 3, 4 and 5, respectively for Bauru, Campinas and São Carlos sites. Grain size distribution and stratigraphic characterization based on various SPT soundings carried out at the sites to identify and classify the soils are also presented.

As DMT testing does not provide soil samples, soil type can be identified based on the I_D parameter. Total unit weight can be estimated by using the Marchetti and Crapps (1981) chart, which relates I_D and E_D (Figure 6). The I_D, K_D and E_D parameters were interpreted using classical or standard empirical correlations. The derived geotechnical parameters were then compared to reference laboratory ones from tests on undisturbed block samples or from those obtained via in situ tests. This comparison allowed establishing preliminary bases to interpret DMT tests on these soils.

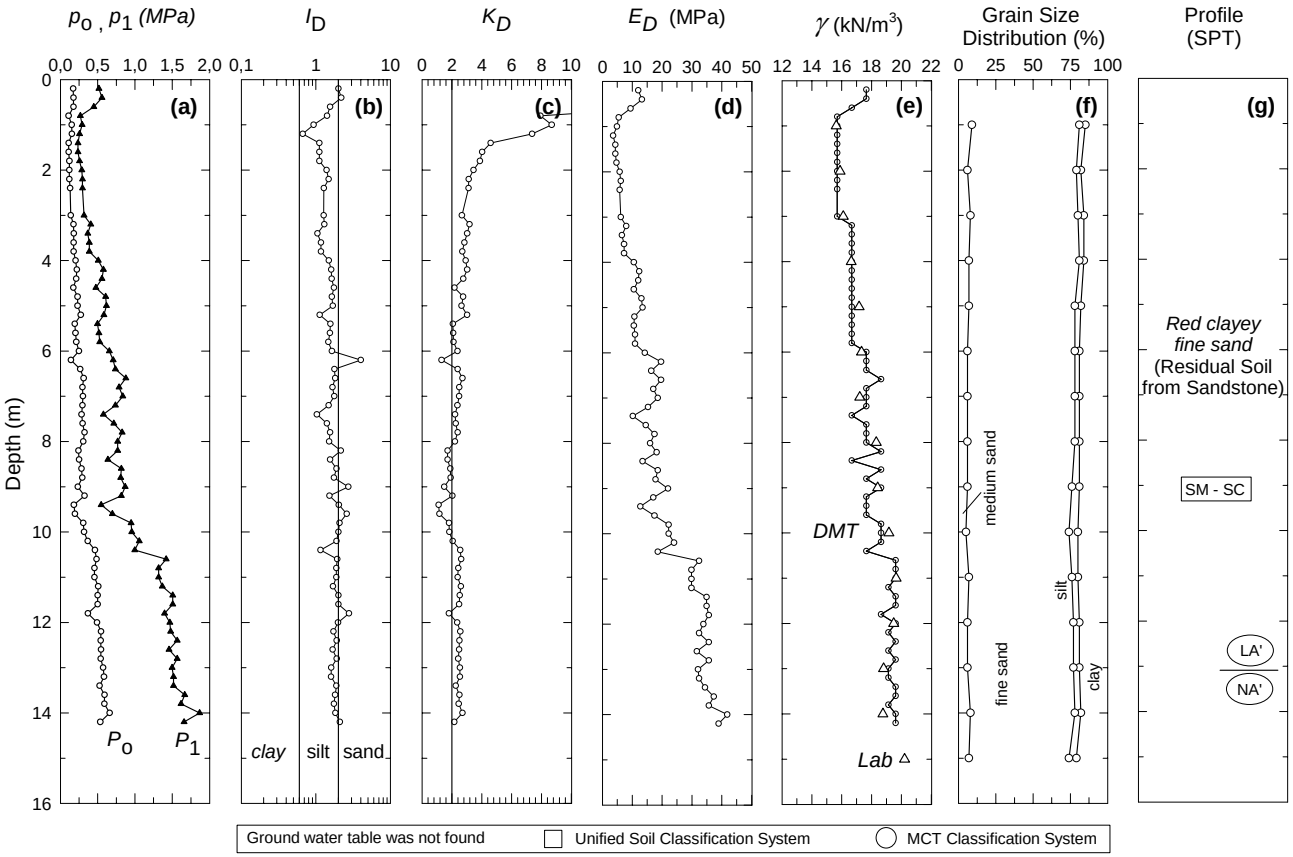

Figure 3. DMT test results; total unit weight, grain size distribution and SPT profile for Bauru Site.

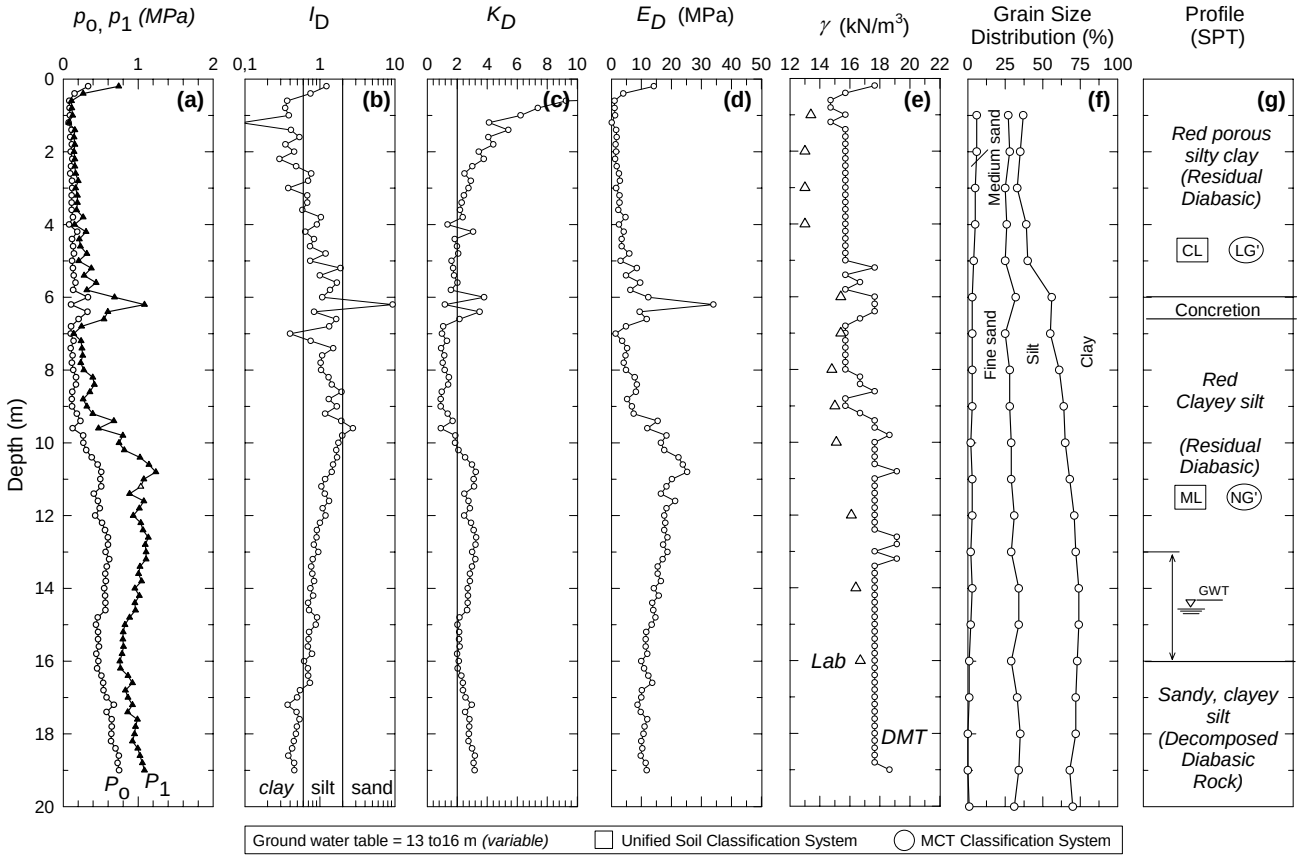

Figure 4. DMT test results; total unit weight, grain size distribution and SPT profile for Campinas Site.

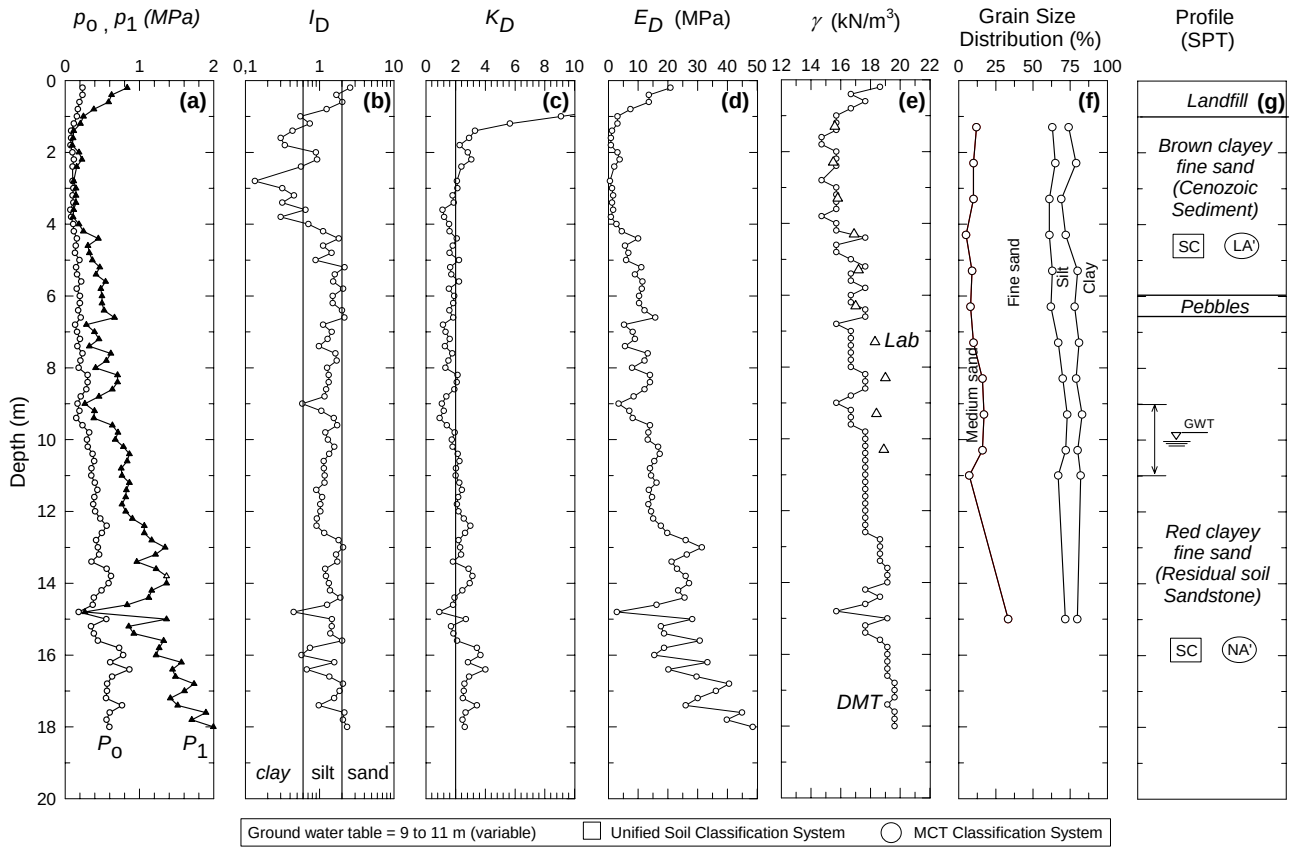

Figure 5. DMT test results; total unit weight, grain size distribution and SPT profile for São Carlos Site.

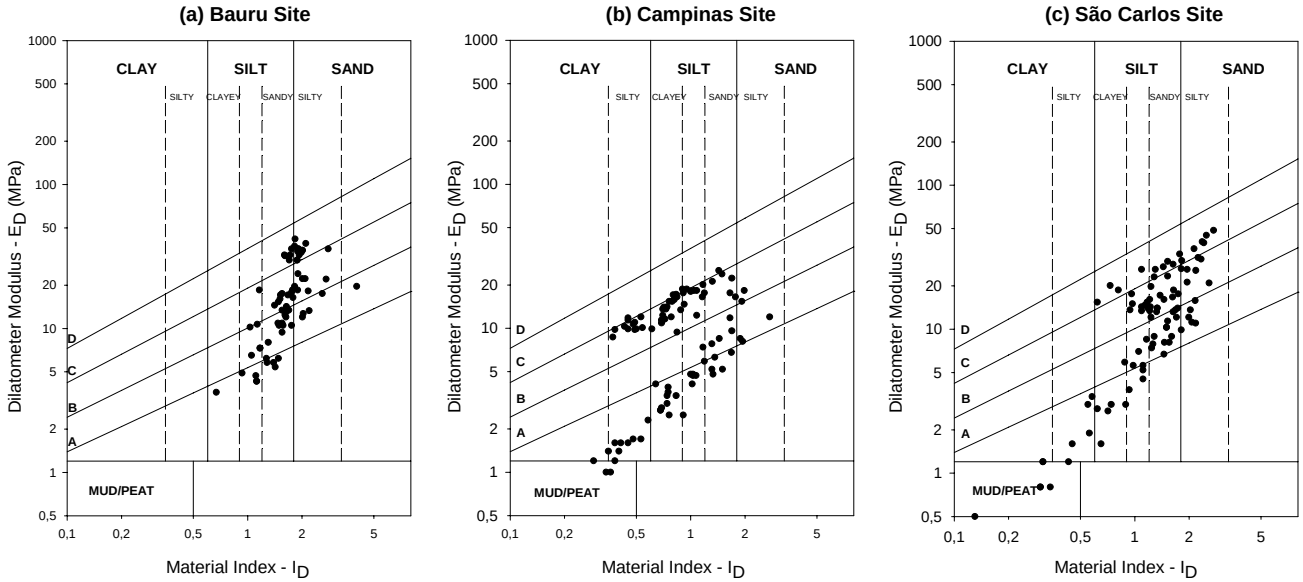

Figure 6. Testing data position on the schematic DMT soil classification chart, proposed by Marchetti and Crapps (1981) for each research site. (a) Bauru Site (b) Campinas Site (c) São Carlos Site.

4.1 *Bauru Site*

4.1.1 *Soil classification*

For the Bauru Site the I_D parameter indicates that the soil basically behaves as a sandy silt up to 9.2 m depth and silty sand between 9.4 to 14.2 m depth (Figure 3.b). The soil texture determined based on grain size distribution is a clayey fine sand, as can be seen in the Figure 3.f.

As pointed out by Marchetti et al. (2001), the I_D is not a result of a sieve analysis but it is a parameter that reflects mechanical behavior and this parameter indicates that a mixture of clay-sand would generally

be described as silt. This is what happened for this particular site.

Results from Standard Penetration Test with Torque Measurements (SPT-T) indicates that T/N ratio for the top 13 m is almost constant within an average value of 0.7, defining the boundaries of two different layers at that depth (Giacheti et al., 1999). MCT classification system separated lateritic (LA') from non-lateritic (NA') soils at the same depth (Figure 3.g). CPT tests carried out at this site also indicate that cone tip resistance (q_c) and friction ratio (R_f) are different at the same two layers identified by MCT and SPT-T tests. Unfortunately DMT test stopped at a depth of 14.2 m , so no conclusion can be drawn regarding this aspect because there are not sufficient testing data in the non-lateritic soil layer (below 13 m depth).

Total unit weight (γ) of the soil estimated, based on material index I_D and dilatometer modulus E_D using Marchetti and Crapps (1981) chart (Figure 6.a) are in close agreement with those obtained from undisturbed samples, as presented in Figure 3.e. DMT testing results, for this particular site, were able to estimate soil density.

4.1.2 *Geotechnical soil parameters*

PMT tests were carried out at the Bauru Site quite close to the DMT test. Figure 7.b presents Dilatometer Modulus (E_D) together with Ménard PMT modulus (E_{pmt}). This figure shows that despite the existence of just a pair of tests, E_D was similar to E_{pmt} values up to about 11 m depth. E_{pmt} was almost half E_D after that depth. Ortigão et al. (1996) investigated the Brasilia porous clay and found that E_{pmt} was less than half E_D. They explain the low PMT modulus with soil disturbance and after careful correction of the PMT field curves, E_{pmt} was similar to E_D.

Another interesting application of DMT test is to estimate the coefficient of lateral earth pressure (K_o). Original correlation proposed by Marchetti (1980) was developed for clayey soils. Marchetti (1985) prepared a K_o chart for sand. Such chart provides K_o for given values of cone tip resistance (q_c) and K_D. Baldi et al. (1986) updated this chart and it was converted into the following algebraic equation for sandy soils:

$$K_o = 0.376 + 0.095\ K_D - 0.0017\ q_c/\sigma'_{vo} \qquad (1)$$

Figure 7.b presents K_o curves estimated based on DMT test results using Marchetti (1980) original correlation and Baldi et al. (1986) correlation (equation 1) as well as K_o values interpreted based on PMT test results. K_o from PMT is equal to 3.5 at 0.5 m of depth, 1.3 at 1.5 m depth and it assumes an almost constant value equal to 0.8 up to about 8 m depth. For this part of the soil profile K_o predicted from DMT results using Marchetti (1980) correlation closely matched PMT K_o values. Below 8 m depth, K_o interpreted based on PMT test results assumed an almost constant value equal to about 0.5, which could be computed by Jaky (1948) formula for a friction angle (ϕ) of 30°. DMT K_o curve calculated using Baldi et al. (1986) better matches the other part of the soil profile, between 8 to 14 m depth.

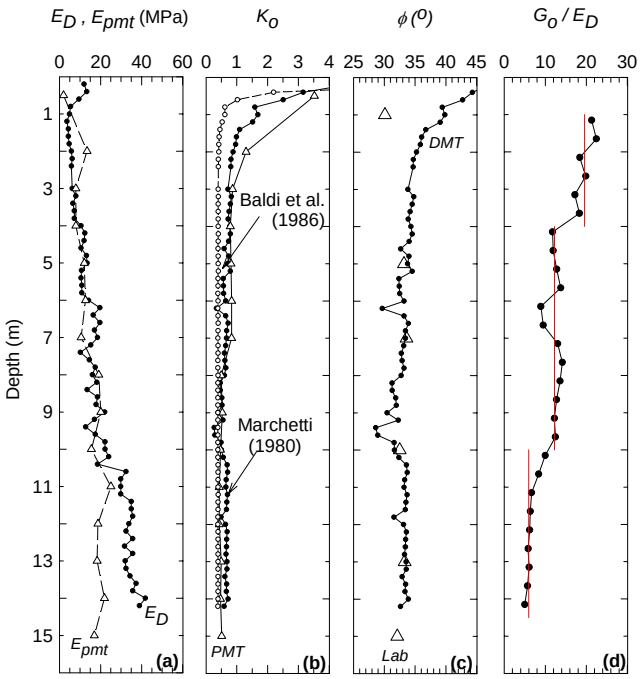

Figure 7. Estimated parameters from DMT test for the Bauru Site and results from other tests.

The reference friction angle for this site was determined by direct shear tests under consolidated drained condition (CD) on undisturbed soil samples at its natural soil content. The correlation adopted to estimate friction angle (ϕ) based on DMT test results is presented by Marchetti (1997), where the ϕ is obtained from K_D by the following equation:

$$\phi = 28 + 14.6 \log K_D - 2.1 \log^2 K_D \qquad (2)$$

Figures 7.c presents the comparison of reference (lab) and predicted (DMT) friction angles. The estimated DMT friction angle was quite good for the soil below 5 m depth. In this case, average estimated ϕ angle was equal to the average measured ϕ angle of about 32°. For the 5 m topsoil, the ϕ angle was determined just for the sample collected at 1 m depth and it was 30°. The interpretation of DMT test results yielded to a ϕ angle 8° higher than the measured one.

Shear wave velocity determined with cross-hole seismic tests and total unit weight determined with undisturbed soil samples collected in a sample pit excavated at the site were used to calculate maximum shear modulus (Go) based on elastic theory.

The Go/E_D values *versus* depth are also presented at the Figure 7.d**.** The criteria used to select E_D to calculate this ratio was averaging three E_D values over 0.6 m intervals. It is interesting to note at the Figure 7.d that Go/E_D ratio tends to decrease with depth, which indicates that Go/E_D ratio tends to increase with soil evolution. Three average Go/E_D ratios were presented; between 1 to 4 m depth it was 20, between 4 to 10 m depth it was 12 and between 10 to 14.5 m depth it was 6 (Figure 7.d).

4.2 *Campinas Site*

4.2.1 *Soil classification*

The I_D parameters for this site are presented in Figure 4.b. The top 6 m red porous silt clay, which is classified as LG soil at the MCT classification system, presented an I_D of silt clay or clayey silt. DMT was able to identify the concretion at 6 to 6.5 m depth and classified it as a sand material. The layer between 6.5 to 16 m depth is a clayey silt, residual soil from dibasic rock, and it was described by the DMT as different materials, changing from the upper to the lower part as a sandy silt, to silt and to clayey silt. The last layer, a sandy clayey silt (decomposed Diabasic rock), was identified by DMT as a silty clay.

For this site, the I_D parameter was not able to describe the soil based on the grain size distribution but the DMT response identified soils with distinct behavior. Marchetti et al. (2001) already emphasized that the I_D is not to describe the soil in terms of grain size distribution since this parameter reflects mechanical behavior. The DMT test results identified layers with distinct behavior at this site but the DMT was not able to separate the boundaries of lateritic and saprolitic soils.

The estimated total unit weight (γ) for the Campinas Site using Marchetti and Crapps (1981) chart (Figure 6.b) based on DMT data was much higher (γ between 16 to 20 kN/m^3) than the values obtained in the laboratory (γ between 13 to 16 kN/m^3), as can be seen in Figure 4.e, especially for the red porous silty clay layer.

4.2.2 *Geotechnical soil parameters*

DMT constrained modulus (M) derived from the original correlation proposed by Marchetti (1980) is compared with laboratory values from oedometer tests (Figures 9.a$_2$). The oedometer tests were carried out with undisturbed soil samples at natural soil content up to a maximum load of 800 kPa. It can be seen in Figure 9.a$_2$ that the original Marchetti's correlation is quite promising for the soil from Campinas Site since M estimated from DMT is in relatively close agreement with M determined based on oedometer, basically for all testing data.

The correlations for drained materials were preferentially adopted to estimate strength parameters for the unsaturated red porous silty clay from the Campinas Site, which has high void ratio and high permeability. This approach was also assumed by Cunha et al. (1999) to interpret DMT tests for a porous clay from Brasilia. The reference friction angle was determined with consolidated undrained triaxial tests (CU) carried out on undisturbed soils samples at the natural moisture content. Figures 8.b presents the comparison of reference (lab) and predicted (DMT) friction angles. The estimated DMT friction angles using Marchetti (1997) correlation (equation 2) were higher than those obtained from triaxial tests. The red porous silty clay layer presented an average friction angle equal to 30.5^o based on triaxial tests and the estimated DMT friction angle has an average value equal to 34.5^o. This difference is even higher for the clayey silt layer, where the triaxial average friction angle was 20.2^o and the average predicted DMT friction angle was 32.5^o.

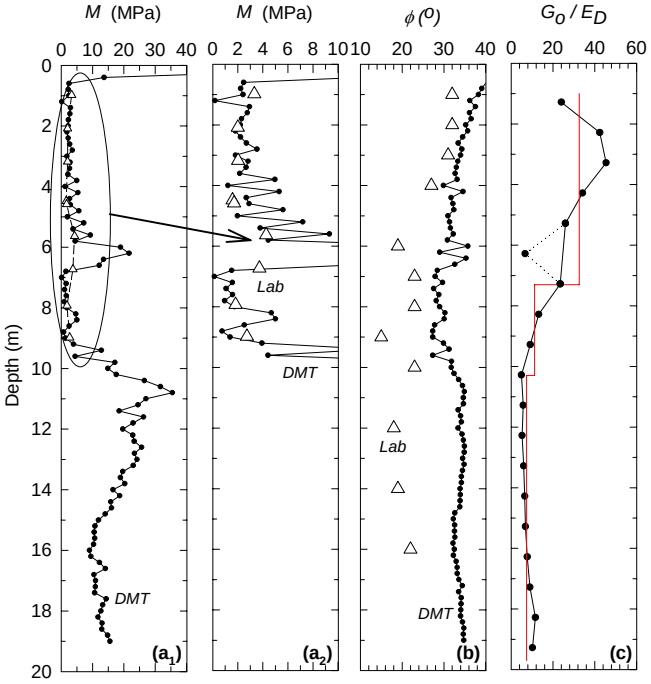

Figure 8. Estimated parameters from DMT test for Campinas Site and results from other tests.

Seismic piezocone test results from the Campinas Site allowed calculation of maximum shear modulus (Go). The Go/E_D values *versus* depth are also presented at the Figure 8.c and this ratio was calculated using the same criteria already presented for the Bauru Site. It also can be seen in Figure 8.c, that lateritic soil layer achieves a higher Go/E_D ratio, which decreases with depth and follows the same trend of Go/E_D ratio observed for the Bauru Site. Three average Go/E_D ratios were calculated for the Campinas Site. This ratio was 33 between 1 to 7 m depth (the lateritic soil layer), 11 between 7 to 10 m depth and 7 between 10 to 19.5 m depth.

4.3 *São Carlos Site*

4.3.1 *Soil classification*

At the Cenozoic sediment, between 1 to 6 m depth, the I_D parameter identified two distinct soils at this layer (Figure 5.b); a clayey soil (clayey silt or silty clay) between 1.0 to about 4.0 m depth and a silt material (silty sand or sandy silt), between 4.0 to 6.0 m depth. DMT test was not sensitive to the stone line, which was identified by the SPT and some CPT tests between 6.0 to 6.5 m depth. The I_D parameter identified the residual soil; red clayey fine sand as a soil that behaves as silt; sometimes it is more a sandy silt and other times it is more silty sand.

At this particular site the DMT response was not able to identify exactly the changes in the soil behavior since it did not separate the boundaries of lateritic and saprolitic soils. It is also interesting to point out that at the site in São Carlos, Robertson et al. (1986) classification chart identifies the red clayey fine sands (residual soil from sandstone), as clays with a SBT=3 (Giacheti et al., 2003). DMT identified this material as silty soils. Marchetti et al. (2001) affirmed that the I_D is not a result of a sieve analysis but it is a parameter that reflects mechanical behavior and a clayey sand can behave as a silty soil.

Total unit weight of the soil estimated based on material index (I_D) and dilatometer modulus (E_D) using Marchetti and Crapps (1981) chart (Figure 6.c) are in reasonable agreement with those obtained from undisturbed samples, as presented in Figure 5.e, especially for the Cenozoic sediment (up to about 6 m depth).

4.3.2 *Geotechnical soil parameters*

DMT constrained modulus (M) derived from the original correlation proposed by Marchetti (1980) is compared with laboratory values from oedometer tests. The oedometer tests were carried out with undisturbed soil sample at natural soil content up to a maximum load of 800 kPa. It can be seen in Figure 9.a_2 that the original Marchetti's correlation is promising for the clayey fine sand from the São Carlos Site since M estimated from DMT is in relatively close agreement with M from oedometer tests for the samples collected at 1.4, 3.0, 7.0 and 8.4 m depth. Just for the samples collected at 4.6 m depth, M from DMT was almost twice M from oedometer test.

Machado (1998) carried out a comprehensive laboratory study on the soil from the São Carlos Site considering its unsaturated condition. Drained triaxial tests (CD_{sat}) over saturated soil samples as well as multistage triaxial tests with controlled suction were carried out on undisturbed block samples colleted at 2, 5 and 8 m depth. It was concluded that the soil behaves as cohesive-frictional material with the cohesion varying with suction. Friction angle was not dependent on suction and it can be assumed equal to effective friction angle determined based on consolidated drained triaxial test results. Figures 9.b presents the comparison of reference (lab) and predicted (DMT) friction angles. Machado (1998) considered an average ϕ angle equal to 30° for the Cenozoic sediment and the average estimated DMT ϕ angle for this layer was about 32°. For the residual soil, measured ϕ angle was 26° at 8 m depth and estimated ϕ angle was around 30°, based on Marchetti (1997) correlation (equation 2).

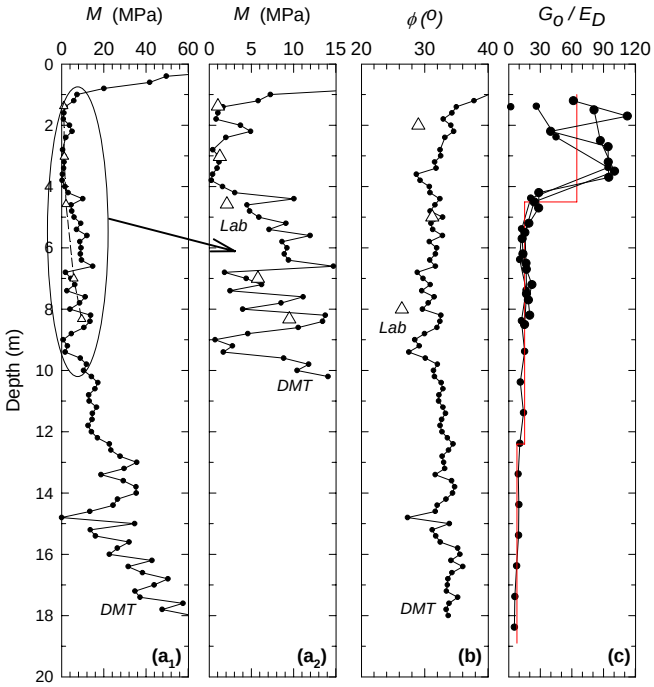

Figure 9. Estimated parameters from DMT test for São Carlos Site and results from other tests.

Seismic piezocone and cross-hole test results from the São Carlos Site allowed calculation of maximum shear modulus (Go) up to about 19 m depth. Shear wave velocities (Vs) calculated with the SCPT tests were in close agreement with Vs calculate with cross-hole seismic tests for this site (Giacheti et al, 2006). The Go/E_D ratio *versus* depth is presented at the Figure 9.c and this ratio was calculated using the same criteria already presented for the Bauru Site. It can be seen in this figure that the lateritic soil has a higher Go/E_D ratio (with some scatter) also for this site, and it tends to decrease with depth, following the same trend of Go/E_D ratio observed for the Bauru and Campinas sites. Three average Go/E_D ratios were calculated for São Carlos Site: 65, between 1 to 4.5 m depth; 15, between 4.5 to 12.5 m depth and 8, between 12.5 to 19 m depth.

5 FINAL REMARKS

This paper presents pioneer DMT tests carried out at three experimental research sites in Brazil and the initial experience and interpretation on this test with "non-classical" geotechnical materials.

The I_D parameter was able to identify changes and the boundaries of soil layers in terms of DMT soil behavior, but it was unable to separate the boundaries of lateritic and saprolitic soils. The I_D parameter was not appropriate to identify soil texture since mixtures of sand and clay or sand, silt and clay were identified as silt or silty soils. For tropical soil, the soil description in terms of grain size distribution has to be confirmed with soil samples, which can also be used to help identifying genetic characteristics of the soils, since they affect soil behavior. At the moment, in Brazil, SPT has been currently used together with DMT to provide samples. Another option is to use a soil sampler from the direct-push technology. DMT can govern the depths from where to recover samples and the same equipment that pushes the probe can also push the soil sampler.

The estimated total unit weight based on DMT test was quite good for the Bauru Site, reasonable for the São Carlos Site and inadequate for the Campinas Site.

At the Bauru Site DMT Modulus (E_D) was similar to PMT modulus (E_{pmt}) up to about 11 m depth and E_{pmt} was almost half E_D after that depth. It is interesting to note that the lateritic soil layer ends close to this depth (between 12 to 13 m depth), based on MCT Classification System, SPT-T and CPT test interpretation. For this site, K_o predicted from DMT using Marchetti (1980) correlation basically matched PMT K_o values up to 8 m depth. Below this depth, DMT K_o curve calculated using Baldi et al. (1986) correlation better matched PMT K_o values, which could be estimated using Jaky (1948) formula.

DMT constrained modulus (M) derived from the original correlation proposed by Marchetti (1980) seems to be quite promising for the São Carlos and Campinas Sites.

The estimated strength parameters for the studied soils assumed drained expansion of the DMT membrane even for clayey soils, because their high permeability and unsaturated condition. The estimated DMT friction angle based on Baldi et al. (1986) correlation was quite good for the soil below 5 m depth in the Bauru Site, reasonable for the São Carlos Site and has to be adjusted for the Campinas Site.

Findings from research on the dynamic behaviour of tropical soils have shown that lateritic soils behave differently from saprolitic soils. Go/E_D ratio was calculated for all the sites and it was higher at the lateritic soil layer tending to decrease as the soil is less developed. It follows the same trend of Go/q_c presented by Schnaid et al. (1998), Giacheti et al. (1999) and Giacheti et al. (2006) for tropical soils. Relating low strain modulus to an ultimate strength parameter or a high strain modulus appears to be an interesting approach to help characterize tropical soils since the low strain modulus from seismic tests reflects the weakly cemented structure of lateritic soils while the penetration or a higher strain modulus breaks down all cementation.

6 ACKNOWLEDGEMENTS

The authors acknowledge the financial support from *Fundação de Amparo à Pesquisa do Estado de São Paulo* (FAPESP) and from *Conselho Nacional de Desenvolvimento Científico e Tecnológico* (CNPq).

7 REFERENCES

Baldi, G., Bellotti, R., Ghionna, V., Jamiolkowski, M., Marchetti, S. and Pasqualini, E. (1986). Flat Dilatometer Tests in Calibration Chambers. Proc. In Situ '86, ASCE Spec. Conf. on Use of In Situ Tests in Geotechn. Eng., Virginia Tech, Blacksburg, USA, ASCE GSP. No. 6, 431-446.

Cunha, R. P., Jardim, N. A. and Pereira, J. H. F. (1999). In Situ Characterization of a Tropical Porous Clay via Dilatometer Tests. Geo-Congress 99 on Behavorial Characteristics of Residual Soils, ASCE GSP 92, Charlotte, pp. 113-122.

Giacheti, H. L., Ferreira, C. V. and Carvalho, D. (1999). In-situ testing methods for characterization of Brazilian tropical soils, Proc. XI PCSMGE, Brazil, V. 1, p. 307-314.

Giacheti, H. L.; De Mio, G. and Peixoto, A. S. P. (2006). Cross-hole and Seismic CPT Tests in a Tropical Soil Site, Proc. ASCE Conference, Atlanta/USA, accepted paper.

Giacheti, H. L.; Marques, M. E. M and Peixoto, A. S. P. (2003). Cone Penetration Testing on Brazilian Tropical Soils. Proc. XII PCSMGE, USA, v. 1, p. 397-402.

http://www.marchetti-dmt.it/pagespictures/testlayout.htm. Visited in Oct, 2005, 15th.

Jaky, J. (1948). Earth pressure in soils. Proc. 2nd. ICSMFE, Rotterdan, V. 1, p. 103-107.

Machado, S.L. (1998). Aplicações de conceitos de elastoplasticidade a solos não saturados, Tese de doutorado, EESC-USP, São Carlos/SP, Brazil. 360 p.

Marchetti S., Monaco P., Totani G. and Calabrese M. (2001). The Flat Dilatometer Test (DMT) in Soil Investigations, TC16 Report. Proc. IN SITU 2001, Intnl. Conf. on In situ Measurement of Soil Properties, Indonesia, 41 pp.

Marchetti, S (1980). In Situ Tests by Flat Dilatometer, Journal of the Geotechnical Engineering Division, asce, V-106, nº GT3, pp. 299-321.

Marchetti, S. (1985). On the Field Determination of K_0 in Sand. Discussion Session No. 2A, Proc. XI ICSMFE, USA, V. 5. p. 2667-2673.

Marchetti, S. (1997). The Flat Dilatometer: Design Applications. Proc. 3rd International Geotechnical Engineering Conference, Keynote Lecture, Cairo University, p. 421-448.

Marchetti, S. and Crapps, D.K. (1981). Flat Dilatometer Manual. Internal Report of GPE Inc., Gainesville. USA.

Nogami, J. S. and Villibor, D. F. (1981). Uma nova classificação de solos para finalidades rodoviárias, Anais do Simpósio Brasileiro de Solos Tropicais em Engenharia, COPPE/UFRJ, Rio de Janeiro/RJ/Brasil, V. 1, p. 30-41.

Ortigão, J.A.R., Cunha, R.P. and Alves, L.S. (1996). In Situ Tests in Brasília Porous Clay. Canadian Geotechnical Journal. V. 33. p. 189-198.

Schnaid, F.; Consoli, N.C. and Averbeck, J. H. (1988). Aspects of cone penetration in natural weakly-cemented deposits, ISC´98 Conference, V.2, p. 1159-1163.

Dilatometer experience in the Charleston, South Carolina region

Edward L. Hajduk, PE
Senior Geotechnical Engineer, WPC Inc., Mt Pleasant, SC, USA

Jiewu Meng, PhD.
Geotechnical Project Manager, WPC Inc., Mt Pleasant, SC, USA

William B. Wright, PE
Senior Geotechnical Engineer and CEO, WPC Inc., Mt Pleasant, SC, USA

Kenneth J. Zur
Geotechnical Project Manager, WPC Inc., Mt Pleasant, SC, USA

Keywords: dilatometer, standard penetration test, cone penetration test, classification, liquefaction, settlement

ABSTRACT: The soil stratigraphy in the Charleston, SC area present ideal conditions for conducting soil explorations using insitu testing methods. The overburden soils in this region typically consist of Pleistocene marine deposits of loose to medium dense sands and very soft to firm clays and silts. The relative loose/soft nature of the overburden soils, coupled with the high seismic design issues of the region, often lead to liquefaction and/or settlement concerns during site geotechnical explorations.

Within the past ten years, traditional soil borings with the Standard Penetration Test (SPT) used for site geotechnical explorations in the region have been replaced or augmented with insitu testing methods. The most common insitu testing methods are flat blade dilatometer testing (DMT) and piezocone cone penetration testing (CPTu). As a result of the insitu testing methods, refined geotechnical analyses can be performed and improved foundation solutions can be implemented.

The following paper presents six case histories in the Charleston, SC area where SPT soil borings, flat blade dilatometer tests, and piezocone penetration testing were performed. Comparisons of the soil classifications, liquefaction susceptibility, and other geotechnical analyses at these sites were conducted to evaluate the different soil exploration methods. These comparisons have shown that the flat blade dilatometer accurately classifies soils in the region and the test provides insitu soil data that allow for more refined geotechnical analyses than those performed using soil boring SPT and/or CPTu data.

1 INTRODUCTION

In the Charleston, South Carolina region, insitu testing is increasingly being used to perform subsurface investigations. Within the last ten years, flat blade dilatometer (DMT) and piezocone penetration testing (CPTu) have supplemented or supplanted traditional soil test borings and the standard penetration test (SPT). The amount of insitu testing is dependent on a variety of factors, such as cost, availability of the testing equipment, accessibility of the site, and size/complexity of the project. Within the last few years, insitu testing is almost used exclusively for smaller projects in the area.

Charleston, South Carolina lies within the Lower Coastal Plain geological province of the Atlantic Ocean coast. The near surface "overburden" soils consist primarily of Pleistocene deposits of the Quaternary Period. These Pleistocene formations generally consist of sand and clay deposits with varying amounts of shells and occasional organics. Beneath the "overburden" soils lies a highly calcareous soil stratum called the Cooper Group, known locally as the Cooper Marl Formation. The Cooper Marl Formation is a marine deposit of late Eocene to Oligocene Periods that underlies a significant portion of the Charleston Area. These soil formations are ideal for insitu testing, since they generally lack stiff/hard soils and/or rock formations that prevent penetration of standard DMT and CPTu tests.

The speed, cost, and amount of data from insitu testing, coupled with the need for increased geotechnical data caused by increases in the magnitude of the design earthquake within the relevant building codes, has driven the expanded use of insitu testing in the region. However, published comparisons of the various subsurface testing methods within the Charleston, SC region are scarce. Therefore, geotechnical engineers must rely on experience and judgment when using these various test methods.

The following paper presents comparisons of DMT with SPT and CPTu data from six (6) project sites in the Charleston, SC area with respect to soil classification, main testing result parameters (i.e. DMT E_D, SPT N and CPTu q_t values), liquefaction analysis, and settlement analysis.

2 CASE HISTORIES

Data from six (6) case histories (i.e. project sites) in the Charleston, SC area where DMT was performed adjacent to traditional soil test borings with SPT (hereafter referred to as SPT) and/or CPTu was complied. The DMT at these sites was conducted in accordance with ASTM D6635-01. The CPTu testing was conducted in accordance with ASTM D5778-95 (2000). The SPT was conducted in accordance with ASTM D1586-99. SPT N values were corrected to N_{60} values using the procedures described by Skepton (1986).

From the six (6) case histories, ten (10) DMT-CPTu test comparisons and nine (9) DMT-SPT test comparisons were conducted. Table 1 presents a summary of the case histories and the relevant subsurface testing data from each. Figure 1 presents the project site locations relative to the Charleston, SC area. Figures 2 and 3 present typical results of subsurface tests relative to the soil profile determined from the SPT for case histories 1 and 5, respectively.

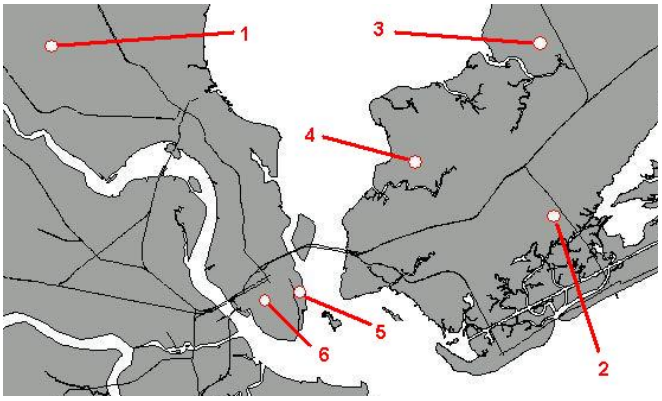

Figure 1. Subsurface Testing Project Site Locations Relative to the Charleston, SC Area.

Table 1. Case History Summary.

Case	Location	DMT[1]	Depth[2] (m)	CPTu[1]	Depth[2] (m)	Dist.[3] (m)	SPT[1]	Depth[2] (m)	Dist.[3] (m)
1	Charleston, SC	11	6.4	12	5.9	23	11	6.1	3
		18	7.4	17	6.0	23	18	6.1	3
2	Mt Pleasant, SC	5	13.7	10	6.3	30	4	6.1	30
		11	13.7	12	6.4	30	7	12.2	30
3	Mt. Pleasant, SC	2	7.5	1	7.2	12	NA	NA	NA
4	Mt. Pleasant, SC	2	6.3	1	12.1	12	NA	NA	NA
5	Charleston, SC	1	36.0	1	37.8	3	3	40.1	3
		2	35.8	3	36.6	3	2	40.1	3
		3	36.6	NA	NA	3	1	36.6	3
6	Charleston, SC	4	9.1	3	18.1	18	2	22.9	18
		5	10.3	3	18.1	18	1	22.9	18

NOTES:
1. Number assigned to DMT (a.k.a. D), CPTu (a.k.a. C), or SPT (a.k.a. B).
2. Depth of test below existing ground surface.
3. Distance from DMT.

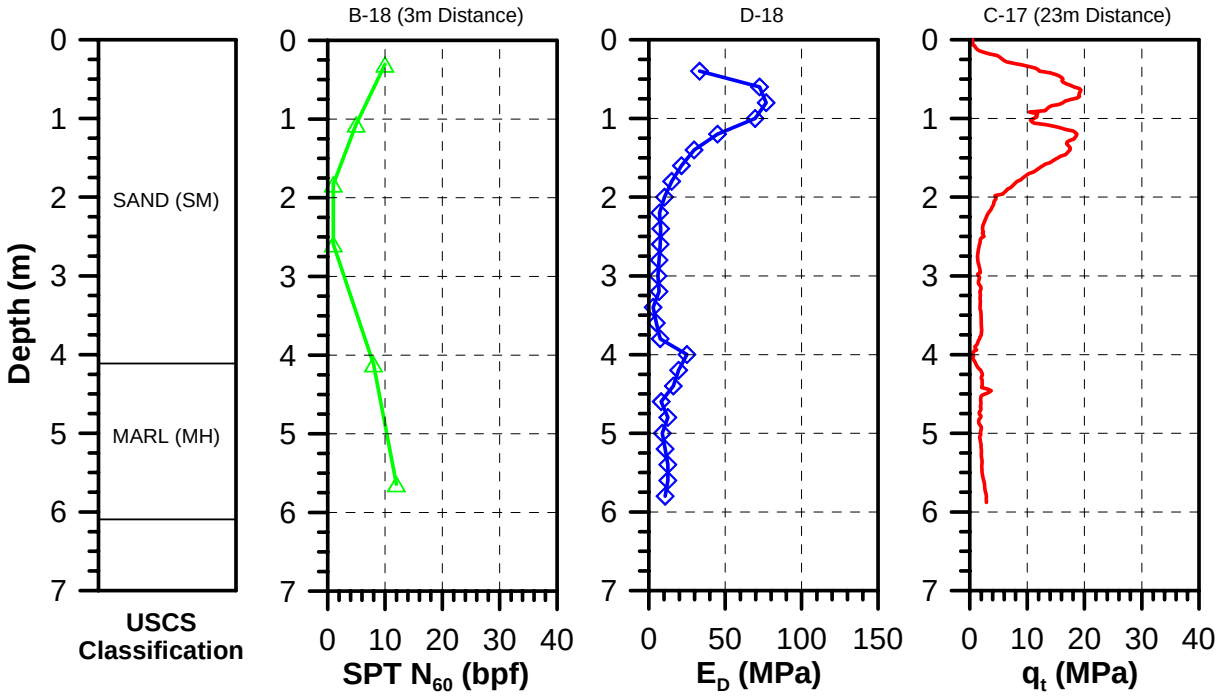

Figure 2. Comparison of Subsurface Testing Data (SPT N_{60}, E_D, and q_t) with USCS Classification for Case History 1.

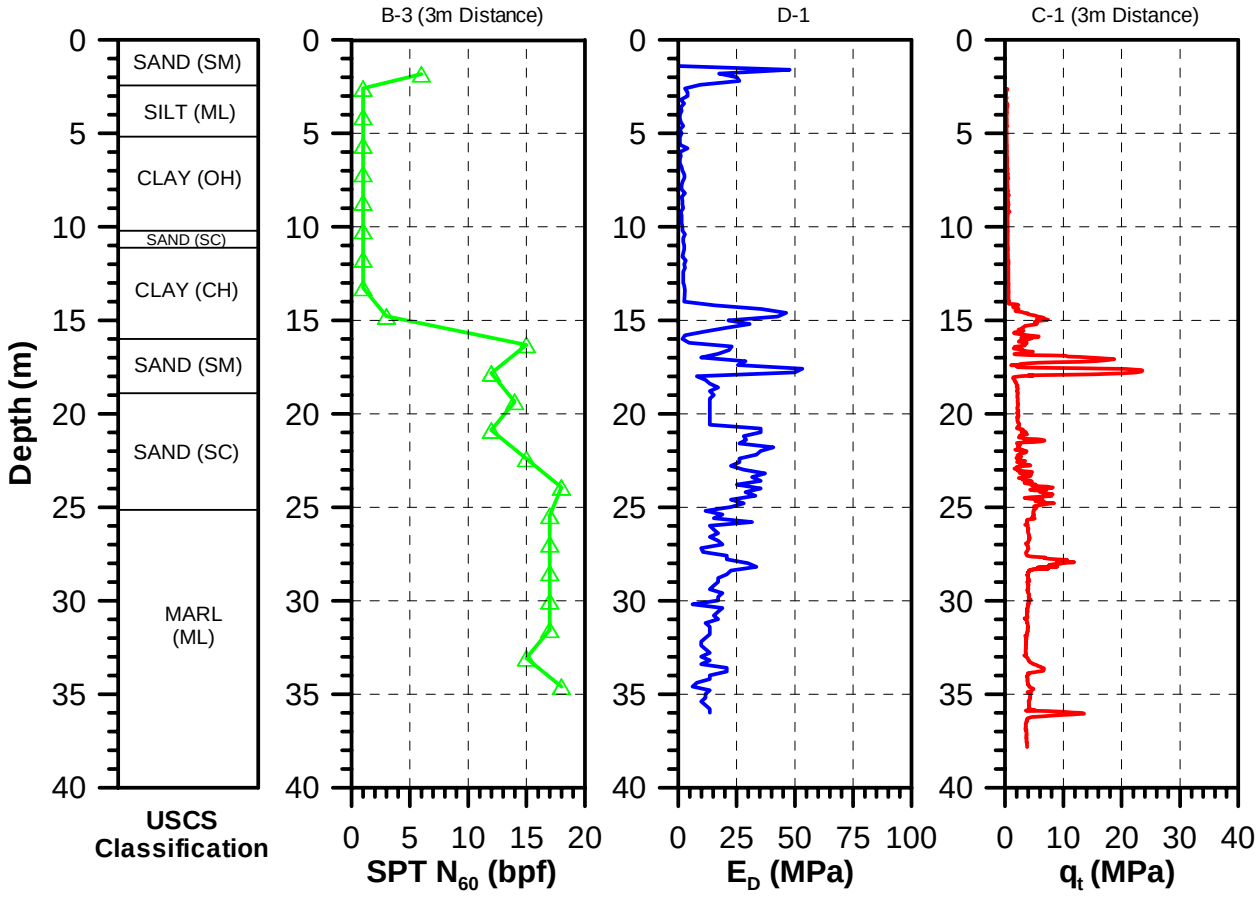

Figure 3. Comparison of Subsurface Testing Data (SPT N_{60}, E_D, and q_t) with USCS Classification for Case History 5.

Each site was relatively level within the limits of the subsurface testing (i.e. the ground surface did not vary in elevation more than 0.15m (6 inches) between test locations). However, ground surface elevation measurements were not taken. Therefore, no attempt was made to correlate the depths of the various subsurface tests with elevation. The small variance in elevation was deemed to not significantly affect the comparison of the three subsurface testing methods.

To minimize the effects of changes in soil stratigraphy during the test comparisons, only projects where the DMT, CPTu, and/or SPT were within

30m (100ft) were used. Furthermore, data from the other available subsurface tests not presented in this paper were examined to determine if the site soil profiles were sufficiently uniform to allow for test distances greater than 3m (10ft) to be used in this study.

3 SOIL CLASSIFICATION

Soil classification using the DMT for this study was done using the Material Index (I_D) and the relationships presented by Marchetti (1980). A summary of soil classification using I_D presented by Marchetti (1980) is shown in Table 2.

Soil classification using the DMT is based on mechanical behavior of the soil and not grain size and therefore is better termed a soil behavior classification. In general, I_D provides an expressive profile of soil type, and, in "normal" soils, a reasonable soil description. Note that I_D sometimes misdescribes silt as clay and vice versa. A mixture of sands and clays would generally be described by I_D as silt (Marchetti et al., 2001).

Table 2. Soil Classification Based on I_D (Marchetti, 1980).

Soil Type	Material Index (I_D) Range	
Peat/Sensitive Clays	<0.10	
Clay	0.10	0.30
Silty Clay	0.30	0.60
Clayey Silt	0.60	0.90
Silt	0.90	1.20
Sandy Silt	1.20	1.80
Silty Sand	1.80	3.30
Sand	<3.30	

Soil classification of soil samples collected via SPT was conducted in accordance with the Unified Soil Classification System (USCS). Refer to ASTM D2487-00 for additional details concerning the USCS.

A comparison of the USCS soil classifications at the SPT locations compared to the DMT soil behavior classifications at the same depth is presented in Figure 4.

Soil classification using the CPTu data was conducted based on the methods developed by Robertson et al. (1986) and Robertson (1990). Soil classification using CPTu data, as with the DMT, is based on mechanical behavior of the soil and is better categorized as a soil behavior classification.

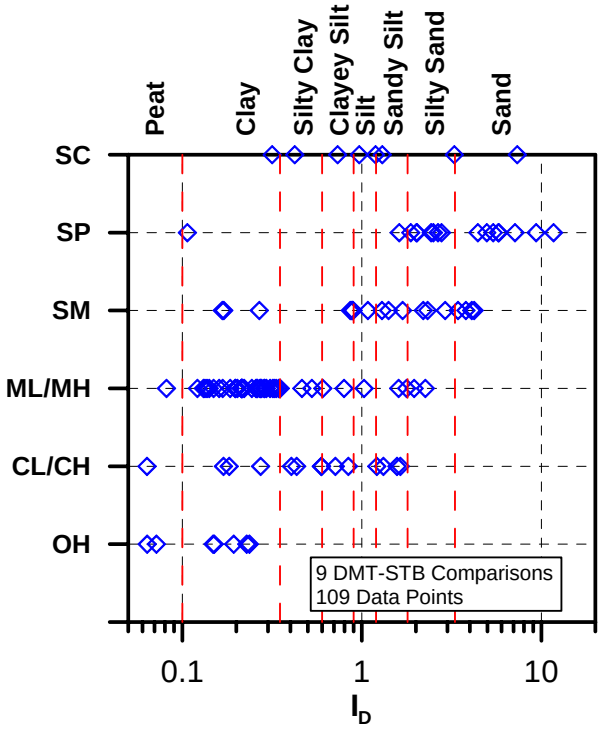

Figure 4. Comparison of USCS and DMT Soil Classifications.

As shown in Figure 4, the DMT and USCS soil classifications are in good overall agreement, with cohesionless soils (i.e. sands) and cohesive soils (i.e. clays and silts) groups generally aligning with each other. Soils classified as silts according to the USCS are generally classified as clays by the DMT. Although the DMT is known to mis-classify clays and silts (Marchetti et al., 2001), the majority of this mis-classification is due to a local soil strata known as the Cooper Marl Formation (CMF). Although the CMF typically classified according to the Unified Soil Classification System as a low plasticity sandy silt (ML) or sandy clay (CL), its USCS classification can range between CH, CL, MH, ML, SM, or SC.

The additional scatter between the USCS and DMT soil classifications is most likely due to differences between the methods. As previously stated, the DMT classifies soils not by grain size but by mechanical behavior.

Comparisons of the CPTu and DMT soil behavior classifications at the same depth is presented in Figure 5 for the Roberston et al. (1986) classification method and Figure 6 for the Robertson (1990) classification method, respectively.

As with the USCS-DMT soil classification comparison, the CPTu-DMT soil behavior comparisons in general show good overall agreement between cohesionless soils (i.e. sands) and cohesive soils (i.e. clays and silts) groups. However, a wide range of scatter exists between the soil behavior correlations between the two CPTu classifications methods and

the DMT classification. This is clearly illustrated in the CPTu soil behavior classification for sand to silty sand in Figure 5. The correlating DMT soil behavior classification ranges from peat/sensitive clays to sand, with a relatively even distribution of data points across the various DMT classifications. These differences are most likely based on differences in the testing methods; i.e. CPTu classification is based primarily on vertical penetration resistance while the DMT is a horizontal expansion into the soil.

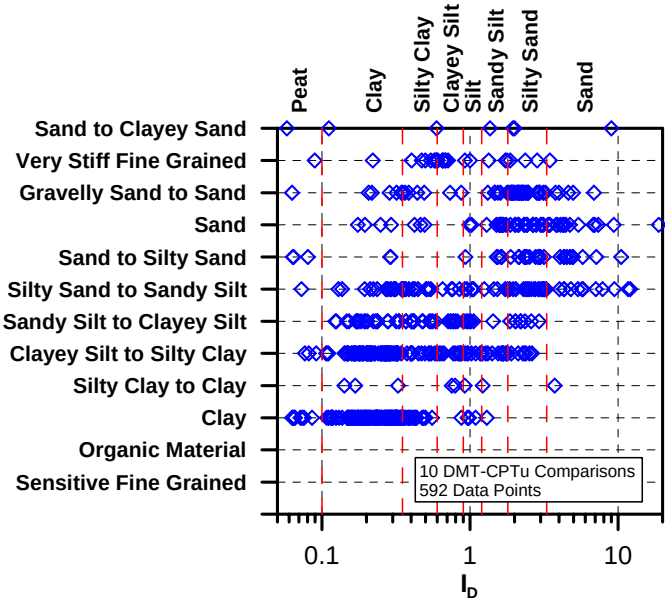

Figure 5. Comparison of CPTu Robertson et al. (1986) and DMT Soil Behavior Classifications.

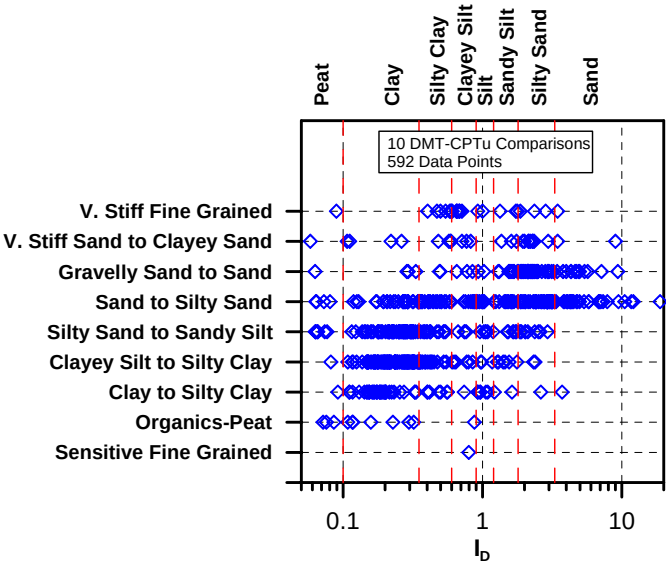

Figure 6. Comparison of CPTu Robertson (1990) and DMT Soil Behavior Classifications.

4 MAIN TEST RESULTS COMPARISON

Comparisons were made between main testing result parameters for each subsurface test; i.e. the DMT dilatometer modulus (E_D), SPT N_{60} value, and the CPTu corrected tip resistance (q_t). These testing results are generally the main parameters used in majority of design methodologies for the three test methods.

A qualitative comparison between the three main testing parameters in Figures 2 and 3 shows excellent correlations with depth. General trends in soil stiffness are observed within all three testing parameters. Quantitative comparisons were also conducted to examined relationships between the three testing parameters. A comparison of E_D and SPT N_{60} values is presented in Figure 7, while Figure 8 presents E_D vs. q_t. Within Figures 7 and 8, the results are divided into the three main soil behavior classifications from the DMT based on I_D data: clays ($I_D < 0.6$), silts ($0.6 \leq I_D \leq 1.8$), and sands ($I_D > 1.8$).

As shown in Figure 7, the E_D vs. SPT N_{60} comparisons shows general correlations between the two parameters for the three soil behavior types, although a wide range of scatter is observed for the three soil groups. In addition, the correlations vary in magnitude between the soil types (e.g. E_D (MPa) = $1.08N_{60}$ for clays, $2.65N_{60}$ for silts).

A comparison of Tanaka and Tanaka (1999) E_D-N_{60} correlation in sands is also presented in Figure 7. The current data set shows a significant amount of scatter, while the Tanaka and Tanaka (1999) data noted good general agreement between the parameters. Tanaka and Tanaka (1999) had a D_{50} varying between 0.2mm to 0.4 mm, which is the same general range of sand particles found within the Charleston, SC region. Since the soil particle size between the two correlations is the same, the differences in the correlations are due to other factors not examined in this paper.

As shown in Figure 8, no clear relationships exist between E_D and q_t for the three soil groups.

5 LIQUEFACTION ANALYSIS COMPARISON

Due to its past earthquake history and changes/updates in the relevant building codes, the design earthquake in the Charleston, SC area has peak ground accelerations (PGA) ranging from 0.30g to 0.45g. Given the relatively loose nature of the overburden sandy soils in the region and these high PGA values, liquefaction is a major concern in the Charleston, SC area. Therefore, insitu testing methods should have an accepted design methodology for assessing the potential for liquefaction for them to be effectively used in the region. The lack of an effective and accepted liquefaction potential analysis procedure could prevent a test method from being used in the region.

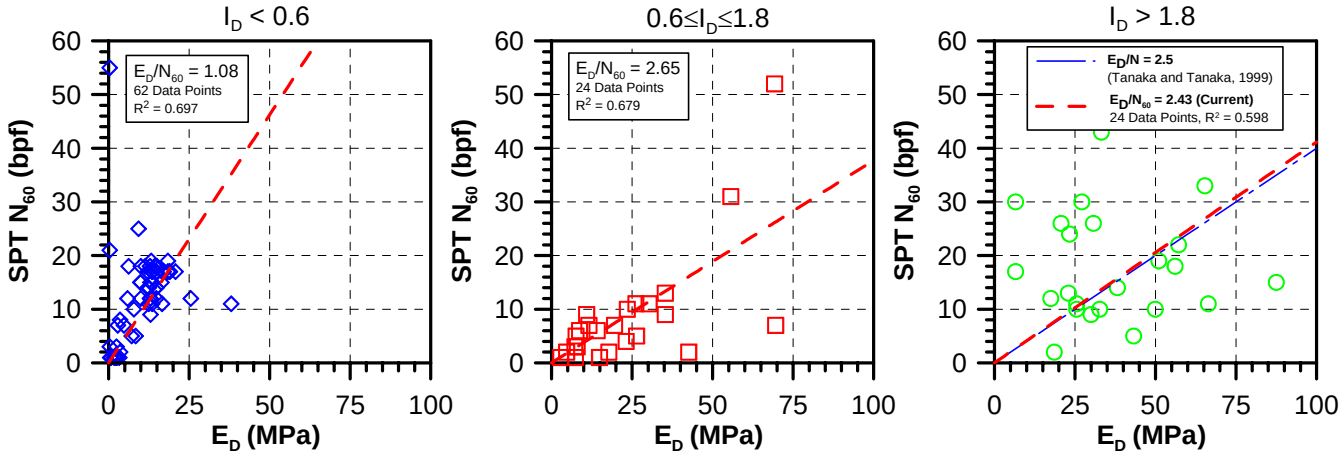

Figure 7. Comparison of Dilatometer Modulus (E_D) and SPT N_{60} Values.

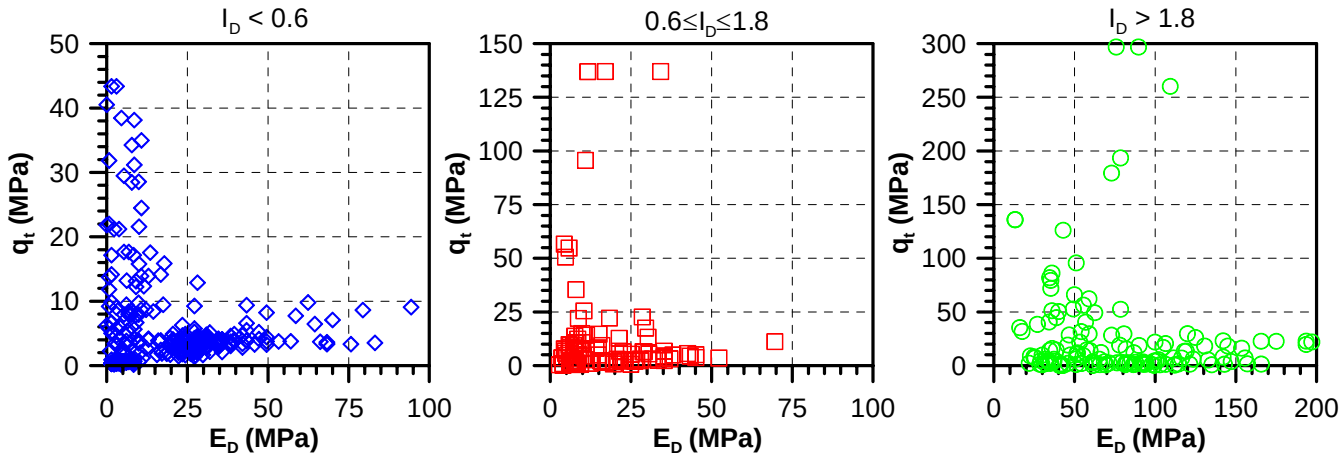

Figure 8. Comparison of Dilatometer Modulus (E_D) and CPTu Corrected Tip Resistance (q_t).

Liquefaction potential analysis via subsurface testing has been examined by a variety of researchers. In general, these analyses consist of comparing the seismic demand on the soil generated by the design earthquake (i.e. the cyclic stress ratio or CSR) to the capacity of the soil to resist liquefaction (i.e. the cyclic resistance ratio or CRR).

Liquefaction potential analysis comparisons were made for two (2) of the project sites. A design earthquake with a peak horizontal acceleration of 0.4 g and earthquake moment magnitude of 7.3 was used in our analysis. These parameters are typical for a design earthquake in the Charleston, SC area based on local building codes. The methods for evaluating liquefaction potential detailed by Youd and Idriss (2001) were used for the SPT and CPTu data. The methodology presented by Monaco et al. (2005) was used to evaluate the DMT data. The results of the liquefaction potential analyses are shown in Figures 9 and 10 for Case Histories 1 and 5, respectively.

As shown in Figures 9 and 10, the CRR's evaluated with the CPT and DMT are consistent to some extent in the sandy soils as encountered. However, the DMT is highly effective in demonstrating the liquefaction potential in the Cooper Marl Formation, which is a highly cemented silt and is unlikely to liquefy to the design earthquake. The SPT and CPTu analyses indicate that these layers would liquefy.

6 SETTLEMENT ANALYSIS COMPARISON

Settlement analysis comparisons for shallow foundations were made between the three (3) subsurface test methods at five (5) of the project sites. These sites have predominantly near surface sandy soils. The other two sites were not selected for settlement analysis due to large deposits of soft cohesive soils, which made them unsuitable for shallow foundations. Deformation estimates for the DMT, CPT, and SPT were conducted using the procedures described by Marchetti et al. (2001), Schmertmann (1978), and Burland and Burbidge (1985), respectively. In the analyses, an allowable soil contact pressure of 100 kPa and a square footing of 3 m were used. This allowable soil contact pressure and footing size are typical for commercial buildings in the area. A summary of the various settlement analyses results is presented in Table 3.

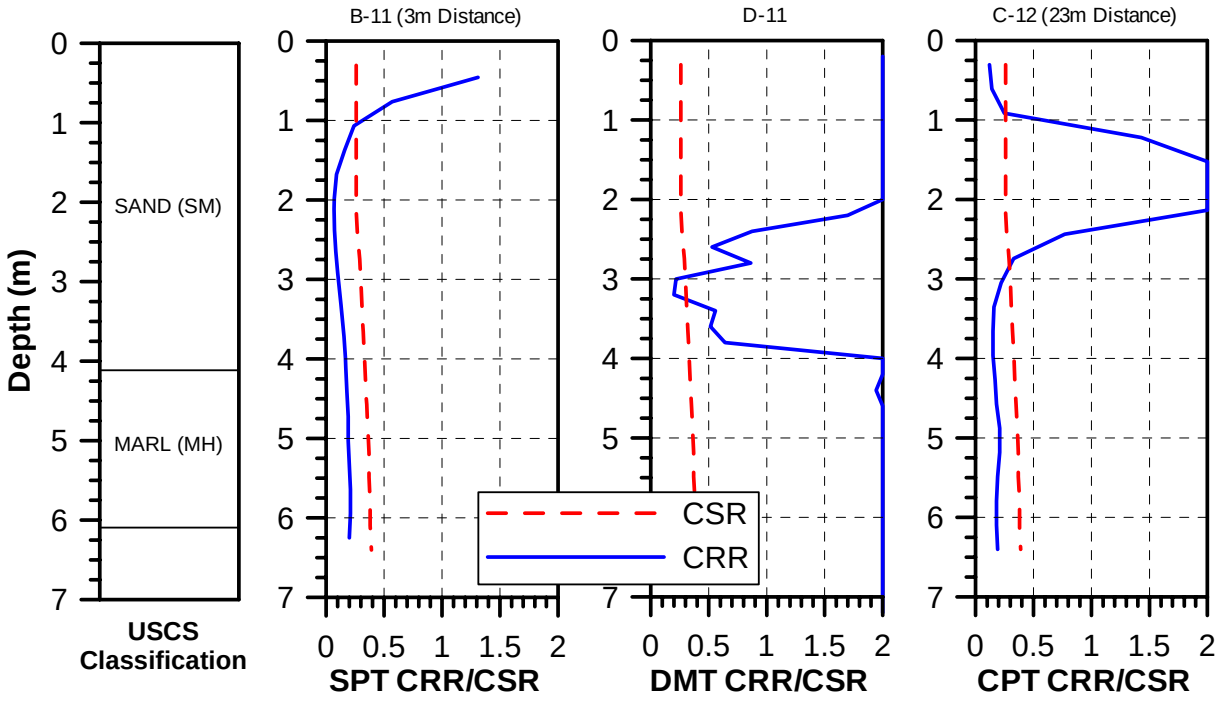

Figure 9. Comparison of Liquefaction Potential Analyses for Case History 1.

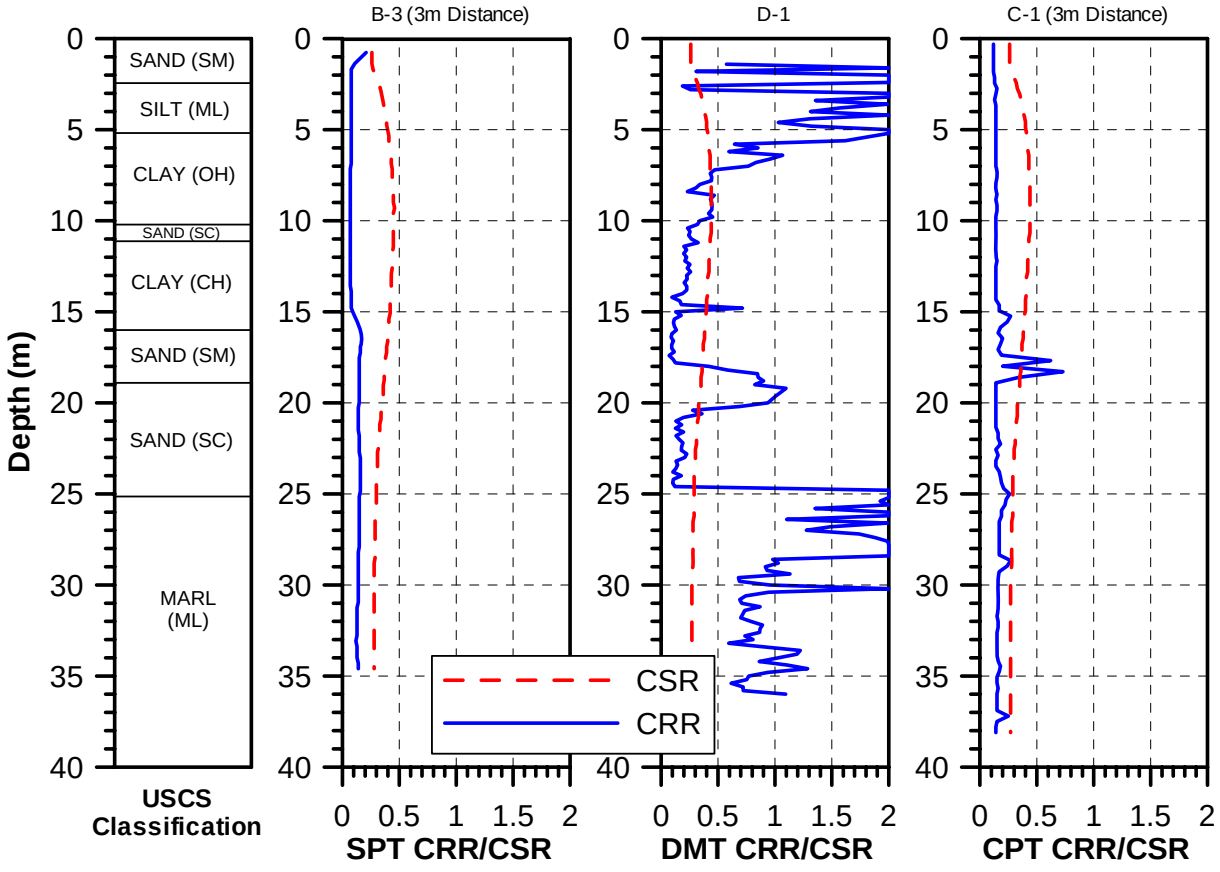

Figure 10. Comparison of Liquefaction Potential Analyses for Case History 5.

As shown in Table 3, the settlement estimates from the CPTu are in close agreement with those from the SPT. The settlements from the DMT are on the order to 2.3 to 4.4 times less than the CPTu/SPT measurements. Although limited data exists between DMT predicted and observed settlements in the Charleston, SC area, DMT settlement estimates are commonly preferred due to their past agreement in the technical literature (e.g., Lacasses and Lunne (1986), Hayes (1990), Woodward and McIntosh (1993)).

Table 3. Settlement Analysis Summary.

Case	Calculated Settlement (cm)		
	DMT	CPT	SPT
1	1.1	2.5	2.5
2	0.4	1.7	1.8
3	2.7	7.1	NA

7 CONCLUSIONS - RECOMMENDATIONS

DMT, SPT, and CPTu subsurface testing data from six (6) project sites in the Charleston, SC were presented. Comparison of the data from these sites showed the following:

Soil classifications between the three insitu tests showed overall general agreement between the major soil types (i.e. cohesionless and cohesive soils). Significant scatter was observed in the comparisons for more detailed soil classifications (e.g. silty sands) within the three test methods. However, given the major difference in the insitu testing methods (i.e. vertical penetration for the CPTu and horizontal expansion for the DMT), differences can and should be expected for soil behavior classifications from these tests.

General correlations exist between E_D and N_{60} values for the Charleston, SC area. However, significant scatter exists within these correlations. When coupled with the limitations of SPT design methodologies, we recommend the use of E_D directly instead of correlating to N_{60} values.

No correlations exist between E_D and q_t for the Charleston, SC area.

Settlement estimates for shallow foundations calculated using the DMT in the Charleston, SC area are considerably less than those calculated by CPTu and SPT methods. The DMT is commonly used for settlement calculations in the region based on the known limitations of the SPT and CPTu methods and past research showing good correlations between DMT estimates and observed settlements.

The DMT effectively evaluates the potential for liquefaction in sandy soils in the Charleston, SC area when compared to SPT and CPT analyses. In addition, the DMT shows that the Cooper Marl Formation is not susceptible to liquefaction, while the other two test types in general show a potential for liquefaction in this soil layer.

Based on the above conclusions and presented data comparisons, the DMT is shown to be an effective insitu testing tool in the Charleston, SC area.

REFERENCES

ASTM D1586-99 (2005). “Standard Test Method for Penetration Test and Split-Barrel Sampling of Soils”. Book of Standards Vol. 04.08

ASTM D2487-00 (2005). “Standard Classification of Soils for Engineering Purposes (Unified Soil Classification System)”. Book of Standards Vol. 04.08

ASTM D5778-95(2000) (2005). “Standard Test Method for Performing Electronic Friction Cone and Piezocone Penetration Testing of Soils”. Book of Standards Vol. 04.09

ASTM D6635-01 (2005) "Standard Test Method for Performing the Flat Plate Dilatometer". Book of Standards Vol. 04.09

Burland, J.B. and Burbidge, M.C. (1985). “Settlement of Foundations on Sand and Gravel,” Proceedings, Institute of Civil Engineers, Part I, Vol. 7, pp1325-1381.

Hayes, J.A. (1990). “The Marchetti Dilatometer and Compressibility”. Southern Ontario Section of the Canad. Geotechn. Society. Seminar on "In Situ Testing and Monitoring".

Lacasse, S. and Lunne, T. (1986). "Dilatometer Tests in Sand". Proceedings of the ASCE Specialty Conference In Situ 86: Use of In Situ Tests in Geotechnical Engineering, Blacksburg, 1263-80, ASCE.

Marchetti S., Monaco P.,Totani G. & Calabrese M. (2001). "The Flat Dilatometer Test (DMT) in Soil Investigations". A Report by the ISSMGE Committee TC16. Proc. IN SITU 2001, Inter. Conf. On In situ Measurement of Soil Properties, Bali, Indonesia, May 2001, 41 pp.

Monaco, P, Marchetti, S., Totani, G., and Calabrese, M. (2005). "Sand liquefiability assessment by Flat Dilatometer Test (DMT)", Proc. 16th ICSMGE Engineering, Osaka, Japan.

Robertson, P.K. (1990) Soil classification using the cone penetration test”. Canadian Geotechnical Journal, 27 (1), 151-8.

Robertson, P.K., Campenalla, R.G., Gillespie, D. and Grieg, J. (1986). “Use of piezometer cone data”, Proceedings of the ASCE Specialty Conference In Situ 86: Use of In Situ Tests in Geotechnical Engineering, Blacksburg, 1263-80, ASCE.

Skemptom, A.W. (1986) “Standard Penetration Test Procedures, and the effects of sands of overburden pressure, relative, density, particle size, ageing, and overconsolidation” Geotechnique, Vol. 36, No. 3, 425-447.

Tanaka, H. & Tanaka, M. (1998). "Characterization of Sandy Soils using CPT and DMT". Soils and Foundations, Japanese Geotechnical Society, Vol. 38, No. 3, 55-65.

Schmertmann, J.H. (1978). Guidelines for CPT: performance and design. *Report FHWA-TS-78-209*, Federal Highway Administration, Washington DC, 145 p.

Woodward, M.B. and McIntosh, K.A. (1993). "Case history : Shallow Foundation Settlement Prediction Using the Marchetti Dilatometer", ASCE Annual Florida Sec. Meeting

Youd, T.L. and Idriss, I.M. (2001). "Liquefaction resistance of soils: Summary report from the 1996 NCEER and 1998 NCEER/NSF workshops on evaluation of liquefaction resistance of soils." *J. Geotech. And Geoenvir. Engrg.*, ASCE, 127(4), 297-313.

BACK

Flat Plate Dilatometer Correlations in the Coastal Plain in Maryland

Eric M. Klein, P. E.
Rummel, Klepper & Kahl, L.L.P. 81 Mosher Street, Baltimore, Maryland 21217

Abhijit Bathe
Rummel, Klepper & Kahl, L.L.P. 81 Mosher Street, Baltimore, Maryland 21217

Keywords: In Situ Testing, Dilatometer, Coastal Plain, Potomac Clays, Laboratory Testing, Case Study

ABSTRACT: To design the retaining wall for widening the outer loop of the Capital Beltway (I-495) several CPT and DMT probes and Shelby tube samples were obtained. Construction of this wall will require cutting about 35-ft (10.7 m) into the Monmouth and Potomac Formations: two over consolidated silt and clay formations. To determine the subsurface conditions including stress history, several UU and CIU triaxial compression tests and one-dimensional consolidation tests were performed. This paper discusses experience gained using laboratory test results and already published correlations for CPT and DMT tests for two geologic formations of the Atlantic Coastal Plain and recommends areas for future research.

1 INTRODUCTION

1.1 *Project Description*

The traffic on the existing six-lane Woodrow Wilson Bridge has exceeded the traffic planned when the bridge was designed, so the bridge will have to be replaced. The replacement bridge will be a twelve-lane structure that will carry both loops of the Capital Beltway (I-495/95) over the Potomac River. As part of this work several interchanges need to be improved and the Capital Beltway (I-495/95) approaching the new bridge needs to be widened. The outer loop of I-496/95 near the MD 210 interchange will be widened requiring about 70-ft (21.3 m) outside the existing roadway. The roadway in this area is a cut area with side slopes of 2(H):1(V). Roughly parallel to and south of the beltway are two ramps connecting southbound I-295 with southbound MD 210 and northbound MD 210 with northbound I-295. These ramps are supported by a 15-ft (4.57 m) high Mechanically Stabilized Embankment (MSE) that is situated on top of a 2(h):1(v) slope that slopes down to the outer loop of the beltway.

To provide space to add more lanes to the outer loop, the proposed construction will consist of replacing this slope with a new retaining wall: Structure 6B. This wall will be about 1880-ft (573 m) long and will typically be about 25-ft (7.62 m) high, but the portion of the wall closest to the existing MSE will be about 33-ft (10.06 m) high. Two bridges will span over Structure 6B. Structure 1 will be a multi-span bridge that will connect northbound MD 210 with the inner loop of the beltway and Structure 2 that will be a two span bridge to provide local access to a nearby national park.

To build Structure 6B it will be necessary to use top down construction to avoid undermining the existing MSE wall supporting the two ramps of I-295. The ramps can not be closed during construction, so all construction will need to be from below the existing slope. Excavation will extend below the groundwater level; therefore, ground water will need to be controlled.

At the eastern end of the project it is proposed to replace the bridge that carries the beltway over Livingstone Road, a local road. The new bridge, Structure 4, will be wider to support the additional lanes and longer to provide better pedestrian passage under the bridge. In this area, the beltway is supported on an embankment and it is proposed to widen the embankment using a retaining wall, since there is no additional space for a wider slope.

1.2 *Geologic Setting*

According to USGS (1964) the project site is located in the Atlantic Coastal Plain Physiographic Province. The coastal plain consists of a wedge of sedimentary deposits that thickens to the southeast. The top of crystalline rock is mapped at a depth of about 600-ft (180 m) below sea level, and dips gradually. The overlying sedimentary formations dip progressively less. The formations described below are based the mapping units described in USGS (1964) and the symbols are the Washington Metropolitan Area Transit Administration (WMATA) generalized strata descriptions.

The Sunderland Formation [T] typically consists of varicolored boulders, cobbles, gravels and silty sands deposited in stream valley and estuarine deposits that were placed during an interglacial period in the Pleistocene Epoch. Typically, the silty T1 material overlies the more granular deposits of the T2 layer. This stratum overlies the C stratum or where the C is not present the M stratumThe SPT N-values ranged from 4 to 100/3-inches, but most of the larger SPT N-values were exaggerated due to gravel and cobbles.

The Chesapeake Group [C] typically consists of dark gray to light gray, olive diatomaceous silt and clay and fine yellow sand deposited during the Miocene Epoch. In this area, it is relative thin and was not observed in all the borings. This formation consisted of CL and ML with some samples of SM and CH.

The Monmouth Formation [M] consists of very fine black sand with mica and glauconite with weathering rust-brown. This was deposited during the Upper Cretaceous Period and unconformably overlies the Potomac Group. The M material consisted predominately of CL and ML with occasional CH and SM samples encountered. In this area little C stratum was encountered and it was difficult to differentiate between the C and the M. The SPT N-values in the C/M stratum ranged from 3 to 38 bpf and averaged 13-bpf. The moisture content ranged from 12 to 43-percent and averaged 30-percent. The liquid limit ranged from 23 to 52 and the PI ranged from 4 to 25.

The Patapsco Formation and Arundel Clay [P1] is the uppermost formations of the Potomac Group. The Patapsco Formation consists of the dark gray, maroon, and varicolored clays with micaceous sand deposited during the Upper Cretaceous Period. The Arundel Clay consists of red and brown clay, and these two units are often mapped togther. The P1 stratum consisted predominately of CL and CH with some seams of SC.

There were various thicknesses of fill that were typically associated with construction of the existing I-295 ramps.

For the most part, the T-1 and T-2 were too dense for either the CPT or DMT to penetrate, so these materials were pre-augered and no in situ testing was obtained from these strata. The CPT and DMT could penetrate a fair distance into the P1, but would often encounter refusal on a dense sand layer.

2 SUBSURFACE EXPLORATION

2.1 *Soil Borings and Laboratory Testing*

The field work used to design Structure 6B consisted of drilling twenty-nine Standard Penetration Test (SPT) borings, four Cone Penetration Test (CPT) probes, five flat plate dilatometer (DMT) probes, and three groundwater monitoring wells. The SPT borings were drilled in four phases in September 2001, November 2001, April 2002 and August 2005. Typically, soil samples were obtained using the SPT method, but in addition several Shelby tube samples were obtained to conduct laboratory testing.

The laboratory testing for Structure 6B consisted of consolidation tests, CIUC-triaxial compression tests with pore pressure measurement, and UU-triaxial compression tests. In addition, several index and classification tests were performed on Shelby tube and split spoon samples PCC (2002 B and 2005A).

For Structure 4 the subsurface exploration program consisted of drilling four SPT borings. Two of the SPT borings were drilled in January 2002, and two of the SPT borings were drilled in August 2005 PCC (2002B) and PCC (2005B).

2.2 *DMT Soundings*

The DMT soundings for Structure 6B were performed in February to March 2002. The DMT probes nearby Structure 4 were performed January 2001, PCC (2002A and 2002B).

The DMT testing was performed in accordance with ASTM subcommittee 18.02 “Suggested Method for Performing the Flat Plat Dilatometer Tests”. The test consisted of pushing the dilatometer blade into the soil with the hydraulic ram of a truck mounted rig. During penetration the operator measured the thrust needed to advance the blade. At the desired test depth, the operator used gas pressure to expand the membrane located on one side of the blade. The operator measured and recorded the pressure required to expand the membrane into the soil at two preset deflections. The membrane was then deflated, advanced to the next test depth and the process repeated.

Where the DMT blade could not be advanced, the DMT hole was pre-augered using hollow stem augers of a drill rig to advance through the hard zones. After pre-augering, the DMT was performed at regular intervals of about 30-cm or 1-ft to the final sounding depth.

The equipment used was purchased from GPE, Inc. and included a standard control unit having 40-bar (580-psi) capacity pressure gage and Marchetti dilatometer tip with a “hard” membrane.

2.3 *CPT Soundings*

The CPT soundings for Structure 6B were obtained in two phases in October 2001 for Bridge No. 1 and again in December 2001, PCC (2002A and 2002B).The two CPT probes for Structure 4 were obtained in January 2002, PCC(2002B).

The CPT soundings were performed using a 20-ton truck mounted CPT rig. The piezocone, a 10-ton subtraction cone was pushed by twin hydraulic rams capable of developing 45-kips of down feed force and 60-kips of pullout force. Where the CPT probe could not be advanced the CPT hole was pre-augered by a drill rig.

3 TEST RESULTS

3.1 *Summary of Results*

Tables 1 and 2 summarize undrained shear strength, S_u, and initial elastic modulus, E_i, as determined using the CU and UU-triaxial tests and the preconsolidation stress Pc as determined from the one-dimensional consolidation test from Structures 6 and 4 at the MD 210 interchange, respectively.

Figure 1a relates the stress history at Structure 6 with elevation and compares the results of the laboratory testing and DMT correlations. Figure 1b relates the stress history at Structure 6 with elevation and compares the laboratory test results with the CPT soundings. Figure 1c compares the stress history at Structure 4 using the laboratory test results and the CPT soundings. Figures 2a to 2c illustrate the relationship of undrained shear strength with elevation. The separate graphs are based on the proximity the each boring and CPT/DMT sounding to each other. Figure 3 compares the E_i elastic modulus obtained from the DMT with that obtained from the UU and CU triaxial tests.

Table 1. Summary of Laboratory Test Results Structure 006

Boring	Depth (ft)	USCS	S_u(tsf)	Ei (tsf)	Pc (tsf)
2-S-006-18	32	CL	1.22	235	5.5
	33	CL	1.43	400	-
	34	CL	1.79	375	-
2-S-006-19	40	CL	0.73	150	-
	41	CL	2.41	227	-
	42	CL	3.17	850	-
2-S-006-A1	29	CL	0.95	107	10
	39	ML	2	425	11
2-S-006-A3	49	CL	0.66	500	7
	69[1]	CL	2.76	135	16
2-S-006-A4	54	CL	0.96	133	5
	66	CL	3.06	345	-
	67	CL	3.62	340	-
	68	CL	4.36	350	-
	74[1]	CH	2.61	574	10

Note 1: These two samples are P1 stratum, all others are M stratum.

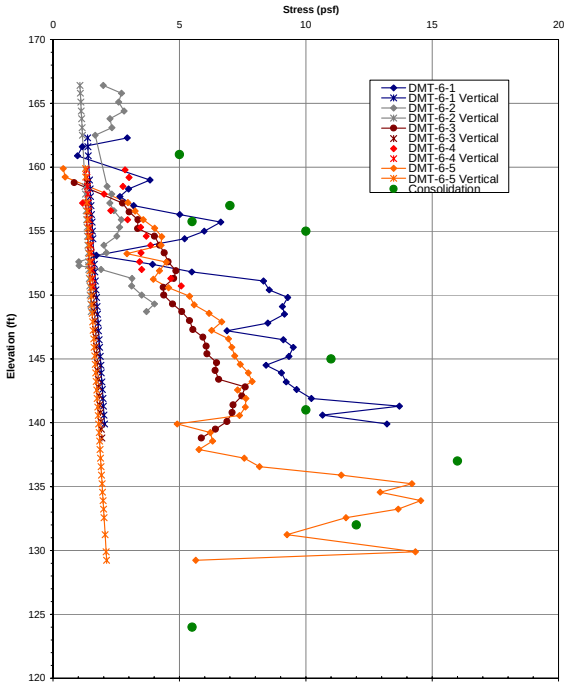

Figure 1a – Stress History (Structure 006B)

Table 2. Summary of Laboratory Test Results Structure 004

Table 2 - Summary of Laboratory Test Results Structure 4

Boring	Depth (ft)	USCS	S_u(tsf)	E_i (tsf)	Pc (tsf)
2-S-030-2	42	CL	3.54	469	
2-S-004-3	47	ML	1.55	219	
	48	ML	2.77	589	
	49	ML	3.11	539	
	53	SM	1.77	174	12
	61	SM	2.29	251	5.5
2-S-004-4	30	CL	2.43	360	
	31		2.51	485	

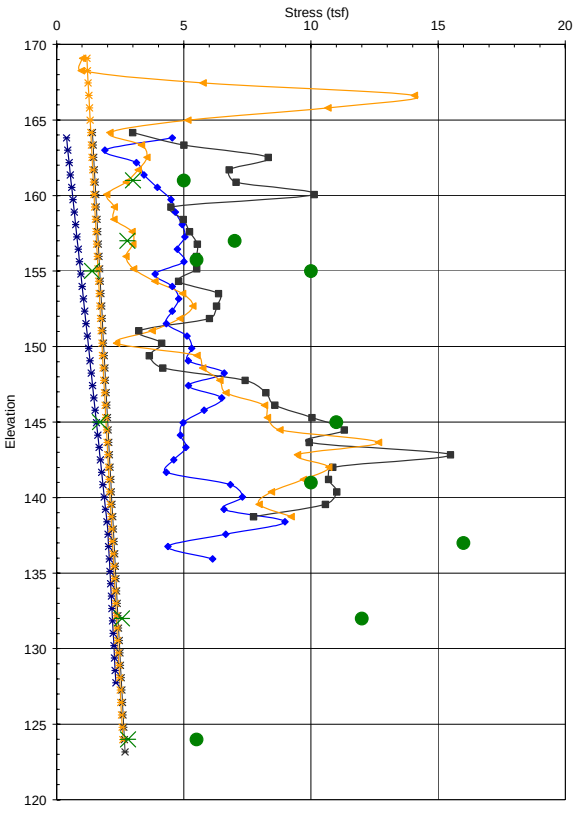

Figure 1b. Stress History CPT Results (Structure 006B)

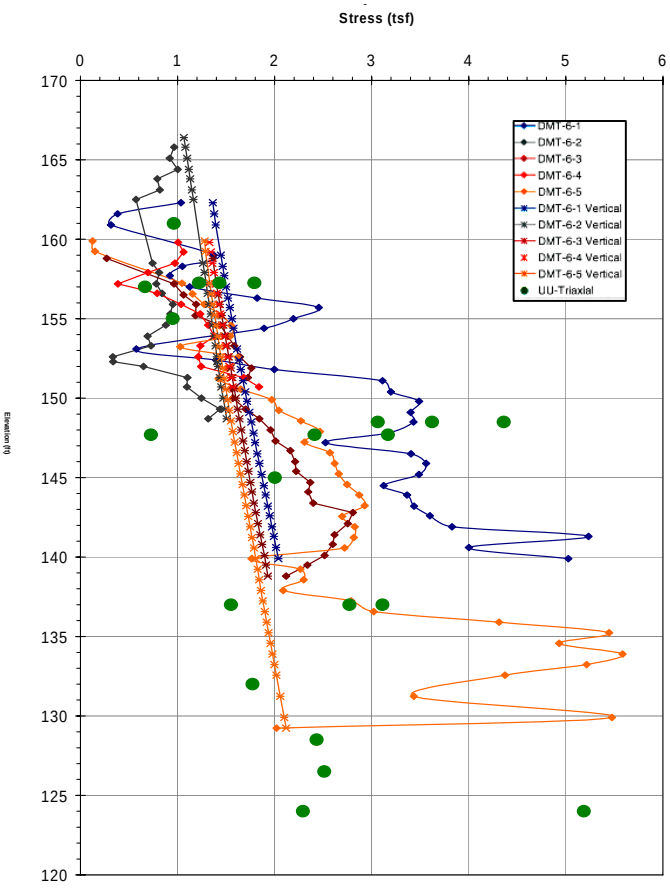

Figure 2a. Undrained Shear Strength DMT Results STR 006B M Layer

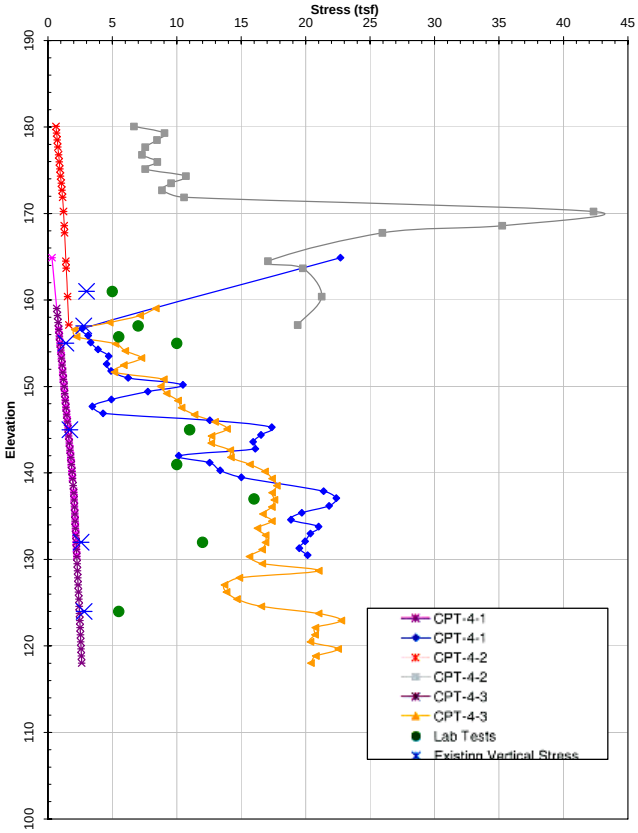

Figure 1c. Stress History CPT Results (Structure 004)

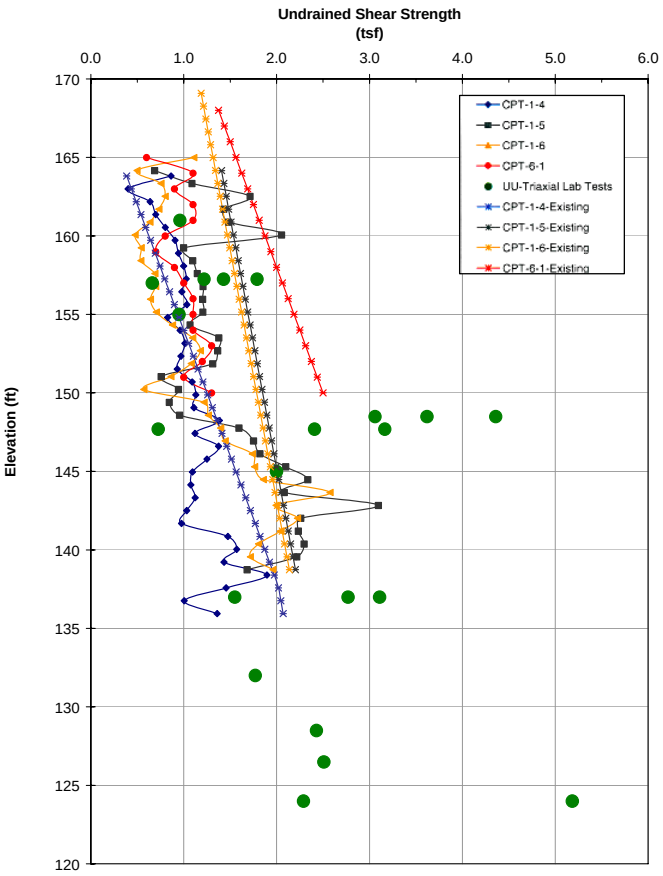

Figure 2b. Undrained Shear Strength CPT Results (Str 006)

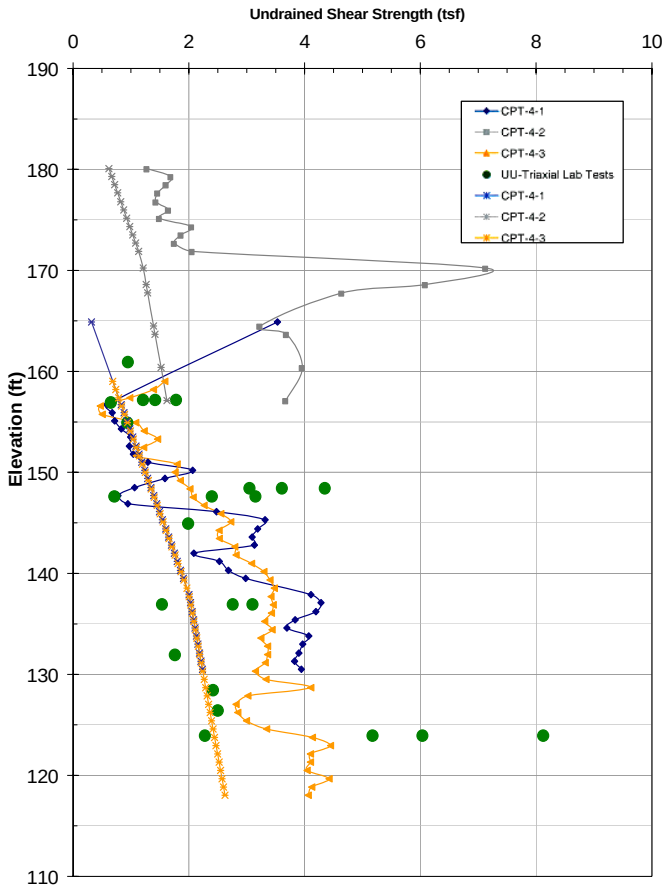

Figure 2c. Undrained Shear Strength CPT
Str 004 M Layer

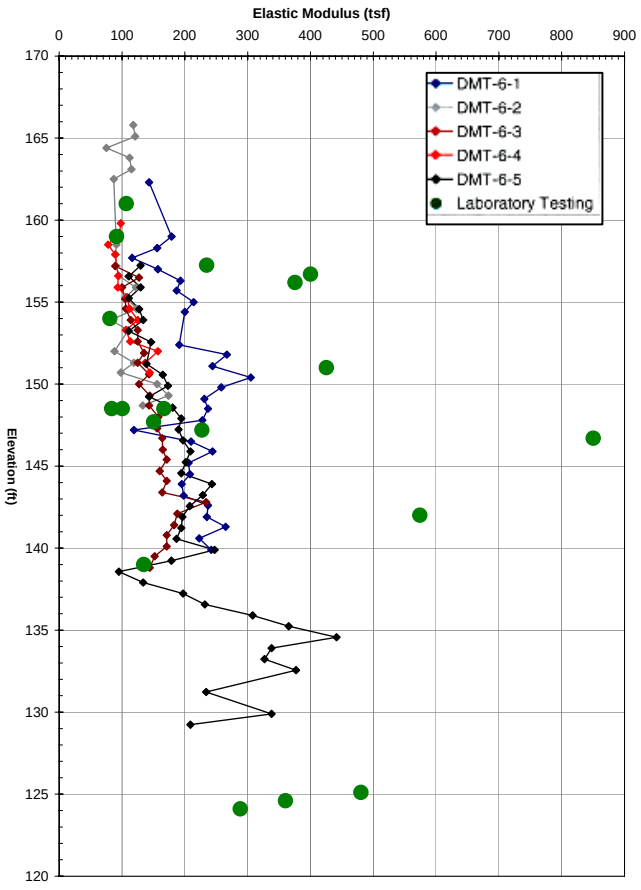

Figure 3a. Tangent Modulus, E_1 and DMT Modulus, E_D
Structure 006B

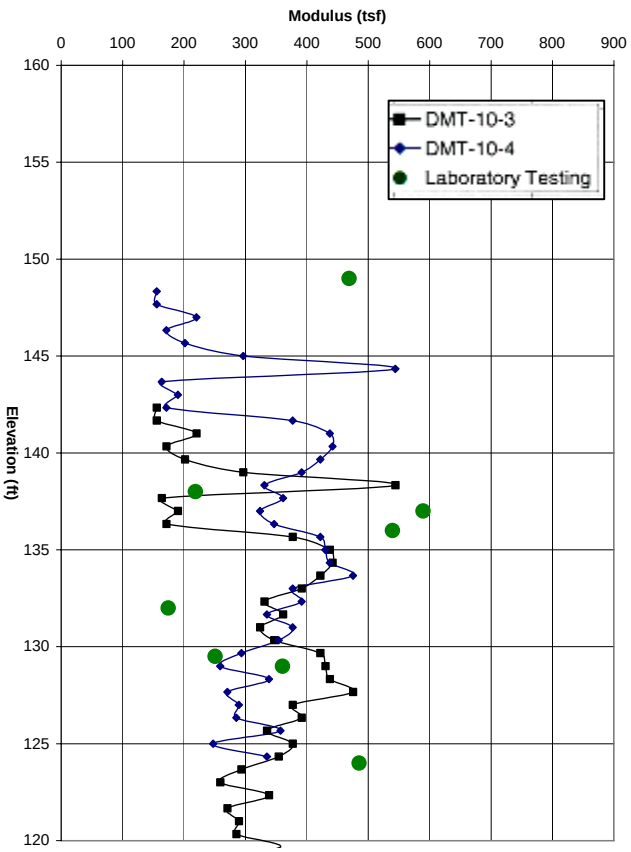

Figure 3b. Tangent Modulus, E_1 and DMT Modulus, E_D
Structure 004

In general the results of the DMT and CPT were consistent with the laboratory testing and with each other. The results were significantly improved when the CPT and DMT data were modified based on laboratory test results and more accurate groundwater readings to more accurately determine the vertical effective stress. Initially, the in situ testing operator made an estimate concerning the unit weights of the soils the groundwater regime. Once the laboratory tests were completed, the in situ parameters were re-evaluated with the updated soils information. In general, this seemed to improve the agreement between the laboratory test results and the in situ testing. In several cases, even after the in situ test results were revised, the preconsolidation estimated by the in situ tests was underestimated, but not enough to effect any engineering recommendations significantly. To estimate the preconsolidation stress from the laboratory test results, both the conventional, Casagrande method and the work-energy method (FHWA 2002) were used along with engineering judgment to reconcile the two methods (note that the axes in Figure 50 of FWHA 2002 are reversed). Several of the soil samples were disturbed slightly, and it is possible that the interpreted preconsolidation stresses from the laboratory testing might not be representative of the actual in situ conditions.

In Figure 3a, some of the modulus values are significantly larger than the in situ tests and some of the

BACK

other laboratory tests. These results are from CIUC-triaxial tests and the results with excessively large values are from specimen with large confining stresses.

3.2 DMT Correlations

Marchetti proposed the original correlation for deriving OCR from the horizontal stress index K_D from the observation of the similarity between the K_D profile and the OCR profile.

$$OCR_{DMT} = (0.5\ K_D)^{1.56} \quad (1)$$

The above equation is in correspondence that $K_D = 2$ for OCR = 1 and has been confirmed in non cemented aging clay deposits. The Horizontal Stress Index K_D is a function of the vertical effective stress, σ'_{vo}; pore pressure, u_o and corrected A-pressure. p_o.

$$K_D = \frac{p_0 - u_0}{\sigma'_{vo}} \quad (2)$$

The preconsolidation stress is then estimated by multiplying the OCR by the effective vertical stress.

The original correlation developed by Marchetti for determining the undrained shear strength, s_u, from DMT,

$$s_u = 0.22\ \sigma'_{vo}\ (0.5\ K_D)^{1.25} \quad (3)$$

These correlations were found to provide consistent results for both the M and the P1 strata as shown in Figure 1, and are consistent with the results obtained from the CPT as shown in Figure 2.

Two different values of elastic modulus are used, the initial tangent modulus, E_i, and the modulus at 25% of strength, E_{25}. Either E is obtained by applying a correction factor F to E_D according to the following expression:

$$E = (F)E_D \quad (4)$$

F is a function of both I_D and K_D. Table 6.2 in FHWA (1992) presents values of F. This is not a unique proportionality constant and mostly ranges from 1 to 3, but for cohesive soils is reported to be 10 to derive E_i. Figure 3 illustrates the relationship between E_D as obtained from the DMT and the initial tangent modulus, E_i, obtained from UU and CU testing. In the figures E_i, was compared to E_D because it compared more favorably to the laboratory tests than M_{DMT}, E_{25} or other relationships as presented in FHWA (1992). There was some difficulty is obtaining an accurate initial tangent modulus from some of the laboratory tests due to some sample disturbance and settling in of the test apparatus, so some engineering judgment was used in establishing E_i. For the overconsolidated clay soils encountered an F value of 1 to less that 1 seemed to be the best fit.

3.3 CPT Correlations

The Young's modulus for clay can be estimated by using figures in FHWA (1992) which shows the variation of E_u / s_u as a function of stress level. The undrained shear strength must first be determined. It is often estimated using the tip resistance, q_c and the effective vertical stress σ'_{vo}.

$$s_u = \frac{(q_c - \sigma_{vo})}{N_k} \quad (9)$$

The cone factor, Nk, is empirical and it should be correlated for each project. There are also other methods to estimate s_u using the pore pressure measurements. For this project several values of Nk ranging from 10 to 18 were used estimate he undrained shear strength. For both fine-grained strata, Nk = 16 seemed to best fit the data. To estimate the OCR, the s_u must first be determined and the s_u/σ_{vo} determined. Several charts are presented in FHWA (1992).

4 CONCLUSIONS

When using in situ testing techniques such as the DMT and CPT it is very important to understand how the correlations with soil parameters are obtained. For example, nearly all the correlations depend on knowing the vertical effective stress. Although a rough guess of 125-pcf (7.8 kg/m^3) is usually close to the actual unit weight, once laboratory testing is obtained, however, significantly different in situ test results often may be obtained. It is often instructive to use a range of values of unit weights as well as other constants to establish a potential range of parameters. An item affecting the effective vertical stress is the location of the groundwater level. The operator in the field should measure the depth to water or at least cave in at the time of testing. Groundwater levels typically change with time, so obtaining a water reading from a nearby boring or well a few days before or later is usually not sufficient, unless, of course, it is all that is available. The engineer should also be aware of the entire groundwater regime or regimes to accurately determine the existing vertical effective stress at each

point of a test. Perched water can significantly affect the estimated vertical effective stress.

Several constants such as the cone factor are empirical, and can be varied from site to site and even for different geologic formations on the same site. Several values should be experimented with and compared to the laboratory test data to obtain a good fit with the data.

Often using both DMT and CPT will provide a range of values that can be compared to each other. This can be beneficial in situations where good laboratory testing is unavailable or a wide range of values are obtained. One of the often overlooked benefits of using CPT and DMT is the large number of data points available. This allows the engineer to evaluate likely ranges of soil parameters and select a Factor of Safety (FS) or β-value of a risk based analysis is being used that will result in a cost effective design.

The results of these tests at this site tend to support the correlations as presented, but care should be exercised by the engineer designing with in situ testing. In situ testing should not be considered a black box; it is recommended that in addition to hard copy test results, the electronic results be submitted to the engineer by the in situ testing consultant. This way the engineer can compare and plot results of different test methods and develop site specific correlations or constants using the published correlation relationships as well as adjust the vertical effective stress to be consistent with laboratory test results.

In addition to foundation design, in situ testing is often used in the design of top down retaining walls and cut slopes. The stress paths of the soils in these conditions are significantly different from that used in the traditional and standardized UU and CU triaxial test methods. Additional correlations should be developed for such unloading conditions particularly to estimate shear strength and elastic modulus parameters. This could improve the results from numerical modeling, retaining wall design and slope stability evaluations.

REFERNCES

FHWA (1992), “The Flat Plate Dilatometer Test”, FHWA-SA-91-044, February

FHWA (1992), “The Cone Penetrometer Test”, FHWA-SA-91-043, February

FHWA (2002), “Geotechnical Engineering Circular No. 5 Evaluation of Soil and Rock Properties”, FHWA-IF-02-034, April

PCC (2001A), “Geotechnical Data Report No. 4 Woodrow Wilson Replacement Bridge Project Maryland Section, I-95/MD 210 Interchange,” Maryland State highway Administration, August.

PCC (2002A), “Geotechnical Data Report No. 9 Woodrow Wilson Replacement Bridge Project Maryland Section, I-95/MD 210 Interchange,” Maryland State highway Administration, September

PCC (2002B), “Geotechnical Data Report No. 10 Woodrow Wilson Replacement Bridge Project Maryland Section, I-95/MD 210 Interchange,” Maryland State highway Administration, September.

PCC (2005A), “Geotechnical Data Report No. 14 Woodrow Wilson Replacement Bridge Project Maryland Section, I-95/MD 210 Interchange, Contract MB-4, Retaining Wall Number 6B” Maryland State highway Administration.

PCC (2005B), “Geotechnical Data Report No. 15 Woodrow Wilson Replacement Bridge Project Maryland Section, I-95/MD 210 Interchange, Contract MB-4, Retaining Wall Number 6B, Retaining Wall Number 30, Bridge Number 4” Maryland State highway Administration.

USGS (1964) “Geology and Groundwater-Water Resources of Washington, D.C. and Vicinity; Geological Survey Water Supply Paper 1776”

Flat Plate Dilatometer and Ko-Blade Correlations in the Coastal Plain in Delaware

Eric M. Klein, P. E.
Rummel, Klepper & Kahl, L.L.P. 81 Mosher Street, Baltimore, Maryland 21217

Jessica Gorske
Rummel, Klepper & Kahl, L.L.P. 81 Mosher Street, Baltimore, Maryland 21217

Keywords: In Situ Testing, Dilatometer, Ko Blade, Cone Penetration Test, Coastal Plain, Potomac Clays, Laboratory Testing, Case Study

ABSTRACT: To design retaining walls for new interchange ramps connecting SR1/SR7/I-95 in northern Delaware several CPT, DMT and Ko-blade probes and Shelby tube samples were obtained. Construction of this wall will require cutting about 22-ft (6.7-m) into the Potomac Formation: an overconsolidated silt and clay formation. To determine the subsurface conditions including stress history, several UU and CIU triaxial compression tests and one-dimensional consolidation tests were performed. This paper discusses experience gained using laboratory test results and already published correlations for CPT and DMT tests for this geologic formation of the Atlantic Coastal Plain.

1 INTRODUCTION

1.1 *Project Description*

Traffic in the project area often experiences significant delays during peak hour and holiday travel. As part of the program to improve traffic flow the interchange connecting SR1, SR7 and I-95 will be improved. The existing ramp that connects north bound SR1 to northbound I-95 is in a cut section and it is proposed to relocate the ramp as much as 150-ft (45.7 m) to the east. To avoid encroaching excessively into the mall parking lot, retaining walls will be used to support the mall parking lot. The retaining wall to the right of the ramp will be about 2610-ft (796 m) long and will be about 18-ft (5.49 m) high. Also, to provide room to widen the south bound lanes of SR-1 another retaining wall will be built on the west side of the interchange. This wall will be 970-ft (295 m) long and 22-ft (6.7 m) high. A new flyover ramp is proposed to connect south bound I-95 with south bound SR1/7. The exit ramp from I-95 will require widening the interstate roadway to the northwest. To reduce the foot-print of the ramp retaining walls will be cut into the existing side slopes. Most of the new flyover will be structure, but a portion of it will be supported on an embankment. The embankment will be as high as 45-ft (13.7 m)

1.2 *Geologic Setting*

According to Woodruff and Thompson (1972) the project site is located in the Atlantic Coastal Plain Physiographic Province. The coastal plain consists of a wedge of sedimentary deposits that thickens to the southeast from the edge of the Piedmont. The top of crystalline rock is mapped at a depth of about 150-ft (24 m) below sea level, and dips to the southeast at about 90-ft/mile (17 m/km).

The Potomac Formation consists mostly of silts and clays with interbedded seams and lenses of sands and gravels. The Potomac Formation consists of the dark gray, maroon, and varicolored clays with micaceous sand deposited during the Cretaceous Period. This stratum consisted predominately of CL and CH with some seams of SC. The moisture content typically ranged from 16 to 26 percent, averaging 21 percent; the liquid limit typically ranged from 29 to 57, averaging 42; and the plasticity index typically ranged from 17 to 27, averaging 21. The lower portion of this formation is mostly coarse grained, but it is difficult to develop correlations across large areas. Typically, the highest elevation of this deposit is near El 100 (El 30.5 m), but about 6-miles (9.6 km) to the west of the project site deposits at El 270 (El 82.3 m) are mapped.

The Columbia Formation typically consists of varicolored silty sand and gravel deposited unconformably over the underlying Cretaceous age deposits during the Pleistocene Epoch. It is believed that this formation was deposited during the late Wisconsin or early Sangamon ages by straight to meandering, shallow but wide streams. It is not mapped in the southern portion of the interchange and is mapped as being as thick as 40-ft (12.2 m) in the northern portion of the interchange. The borings generally tended to confirm this general stratigra-

phy. This material consisted mostly of SM and SC with some GM noted in road cuts. There were various thicknesses of fill that were typically associated with construction of the existing I-95 ramps and the nearby mall.

2 SUBSURFACE EXPLORATION

2.1 *Soil Borings and Laboratory Testing*

The field work consisted of drilling 206 Standard Penetration Test (SPT) borings, twenty-seven Cone Penetration Test (CPT) probes, twenty-five flat plate dilatometer (DMT) probes, two Ko-blade probes, and thirty-one groundwater monitoring wells. The subsurface exploration work was performed from October 2004 to March 2005. Typically, soil samples were obtained using the SPT method, but in addition several Shelby tube samples were obtained to conduct laboratory testing.

The laboratory testing consisted of consolidation tests, direct shear tests, CU-triaxial compression tests with pore pressure measurement, unconfined compression tests, and UU-triaxial compression tests. In addition, several index and classification tests were performed on Shelby tube and split spoon samples DelDOT (2005A).

2.2 *DMT Probes*

The DMT testing was performed in accordance with ASTM subcommittee 18.02 "Suggested Method for Performing the Flat Plat Dilatometer Tests". The test consisted of pushing the dilatometer blade into the soil with the hydraulic ram of a truck mounted rig. During penetration the operator measured the thrust needed to advance the blade. At the desired test depth, the operator used gas pressure to expand the membrane located on one side of the blade. The operator measured and recorded the pressure required to expand the membrane into the soil at two preset deflections. The membrane was then deflated, advanced to the next test depth and the process repeated.

Where the DMT blade could not be advanced, the DMT hole was pre-augered using hollow stem augers of a drill rig to advance through the hard zones. After pre-augering, the DMT was performed at regular intervals of about 30-cm or 1-ft to the final sounding depth.

The equipment used was purchased from GPE, Inc. and included a standard control unit having 40-bar (580-psi) capacity pressure gage and Marchetti dilatometer tip with a "hard" membrane.

2.3 *CPT Probes*

The CPT soundings were performed using a 20-ton truck mounted CPT rig. The piezocone, a 10-ton subtraction cone was pushed by twin hydraulic rams capable of developing 45-kips of down feed force and 60-kips of pullout force. Where the CPT probe could not be advanced the CPT hole was pre-augered by a drill rig.

2.4 *Ko-Blade Probes*

The Ko-Blade soundings were continuously pushed using a 20-ton truck mounted CPT rig. The Ko-blade consists of a steel blade with four thicknesses or steps of 7.5, 6, 4.5 and 3 mm. At each step is a membrane that can be inflated and it is connected to a direct reading gauge. At the test depth system the thinnest portion of the blade is inserted and the horizontal stress measured. The blade is then advanced and the horizontal stress is measured at the same depth using the next thickest step. The process is repeated for each of the four steps at a given test depth. The log of pressure is plotted against the blade thickness and the plot is then extrapolated to zero thickness. This pressure is the in situ horizontal stress.

3 TEST RESULTS

3.1 Summary of Results

Figure 1 and Table 1 compares the results from the two Ko-blade and the two closest DMT probes IDMT-9 and 10. Below a depth of about 15-ft (4.57 m) the Ko values from all four probes are in very close agreement and seem to converge on a value of about 1.0 below a depth of 20-ft (6.1 m). Assuming a φ-angle of about 15^{o} and an average OCR of about 3 this is not unreasonable based on the Jaky equation. At depths shallower than 15-ft (4.57 m) the Ko blade results indicate the Ko value is as much as twice the Ko values obtained from the DMT probes. The OCR of the soils at depths less than 15-ft (4.57 m) generally ranges from about 9 to over 100 except in IDMT-10 where there seems to be a softer zone with an OCR of about 4 near a depth of 10-ft (3.05 m). The OCR below a depth of 15-ft (4.57 m) generally declined smoothly from about 10 to about 3 or 4 with depth. In this area, the Columbia Formation was absent and the soils encountered in these four probes are thought to be the Potomac Formation.

The large OCR values near the surface can probably be accounted for by erosion, desiccation, the impact of previous construction equipment, and the effects of animals and plant roots as well as secondary effects of ageing. Figure 2b illustrates the relationship between depth below ground surface and

the lateral stress as obtained by both the K_o blade and the DMT. As with the K_o value there is fair agreement below depths of about 15-ft. If the lateral stress is extrapolated to zero, then the estimated depth of erosion is about 40-ft (12.2 m). Using the estimated OCR values from the lower 20-ft (6.1 m) of the probes, the estimated overburden eroded away ranged from about 50 to 70-ft (15.7 to 21.3 m).

Figure 2 illustrates the relationship of undrained shear strength with elevation. The separate graphs are based on the proximity the each boring and CPT/DMT probe to each other. Figure 3 relates the Stress history with elevation and compares the results of the laboratory testing, CPT correlations and DMT correlations. Figure 4 compares the E_i elastic modulus obtained from the DMT with that obtained from the UU and CU triaxial tests.

Table 1. Ratio of Horizontal Stresses as measured by Ko-blade and DMT

Depth (ft)	Ko-9/DMT-9	Ko-10/DMT-10
1.3	1.4	10.9
1.6	2.1	3.8
2.0	4.2	3.2
4.6	3.6	1.5
4.9	3.8	2.2
11.5	3.5	2.1
11.8	1.7	2.2
14.4	2.4	1.9
14.8	2.6	2.6
15.1	3.3	No DMT
15.4	3.3	No DMT
17.4	1.1	No DMT
17.7	1.3	2.1
21.0	1.2	2.8
21.3	1.1	1.9
21.7	1.1	2.0
24.3	0.6	1.2
24.6	1.1	0.7
24.9	0.8	0.9
27.6	0.9	0.7
27.9	0.9	0.8
28.2		0.9

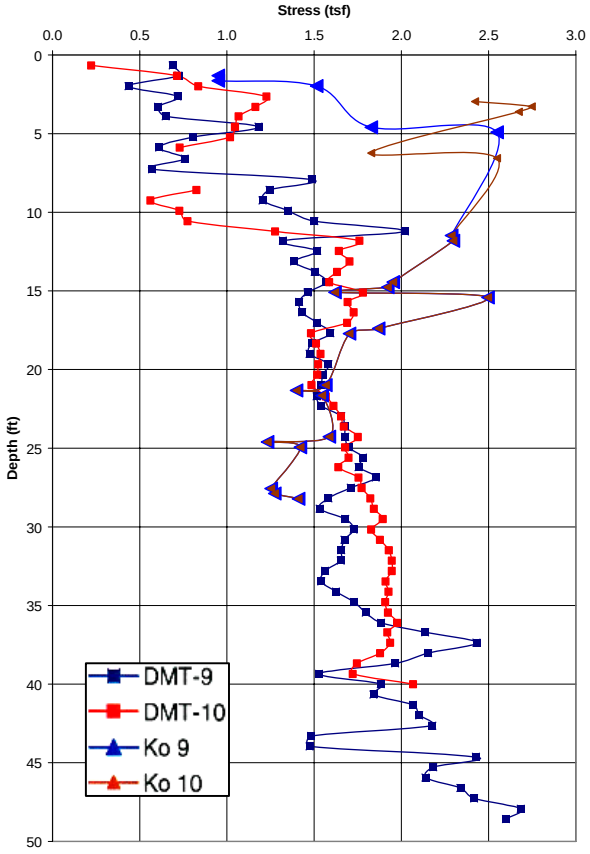

Figure 1a. IDMT – 9&10 In Situ Lateral Stress Coefficient

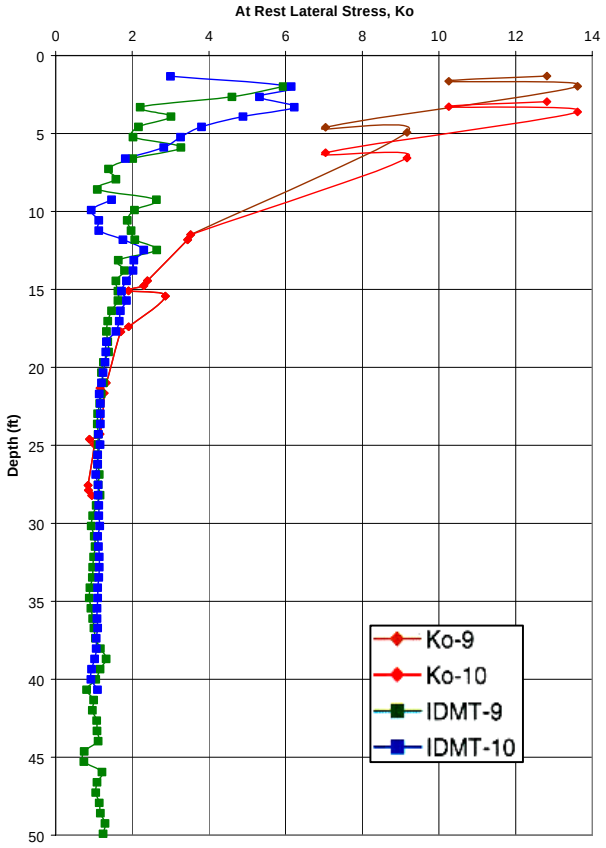

Figure1b. IDMT 9 & 10 Lateral Stresses

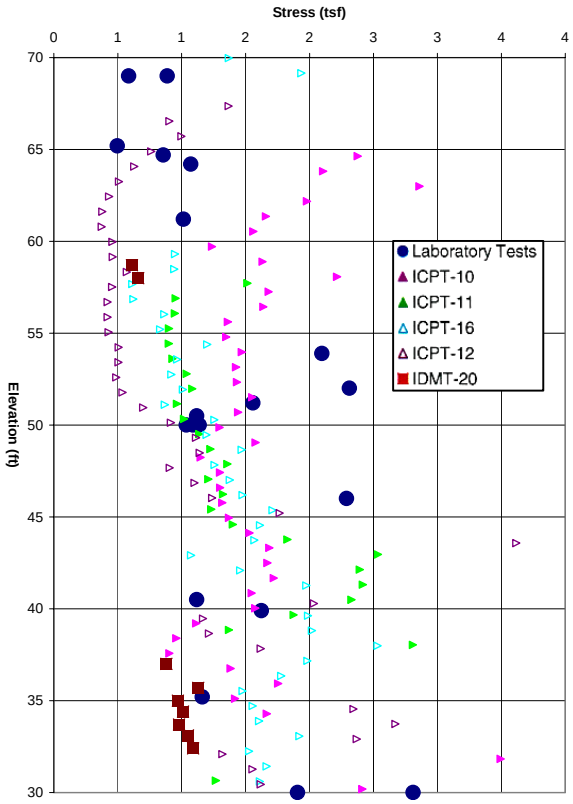

Figure 2a. IDMT-17 Undrained Shear Strength

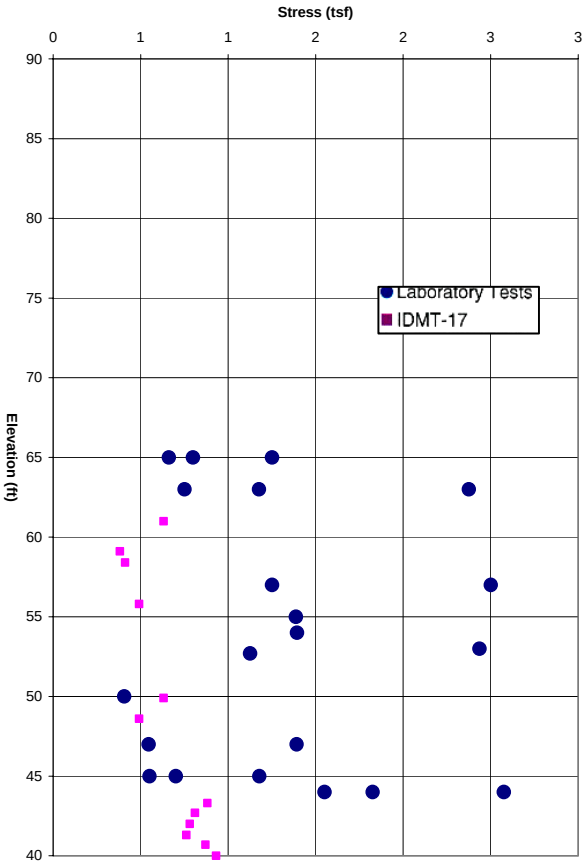

Figure 2b. IDMT-20 Undrained Shear Strength

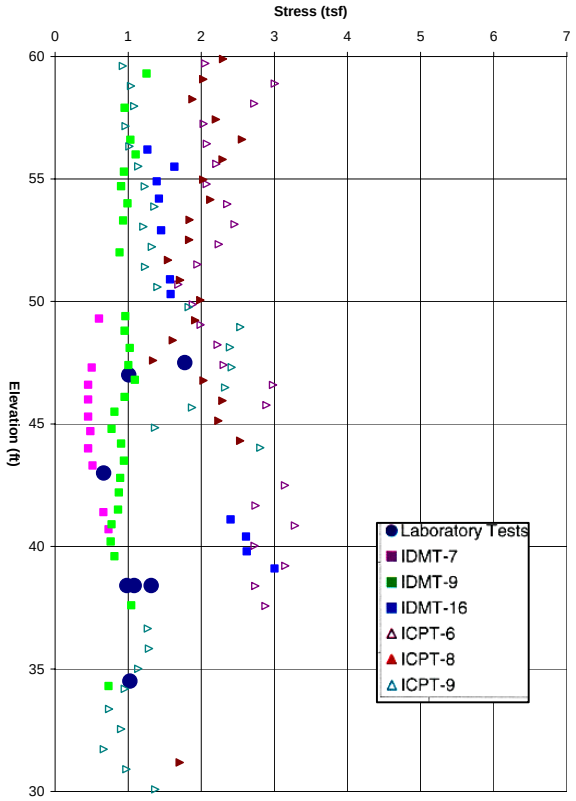

Figure 2c. IDMT-7, 9 & 16 - Undrained Shear Strength

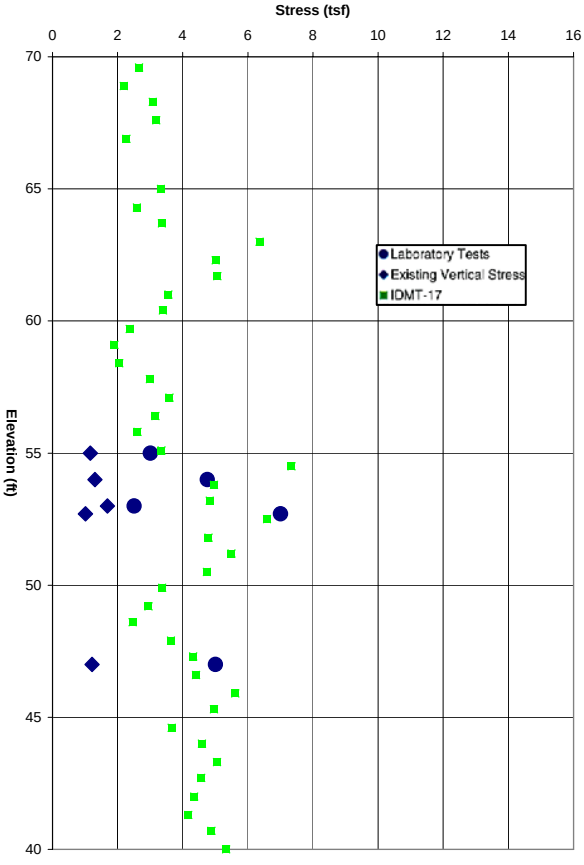

Figure 3a. IDMT-17 Stress History

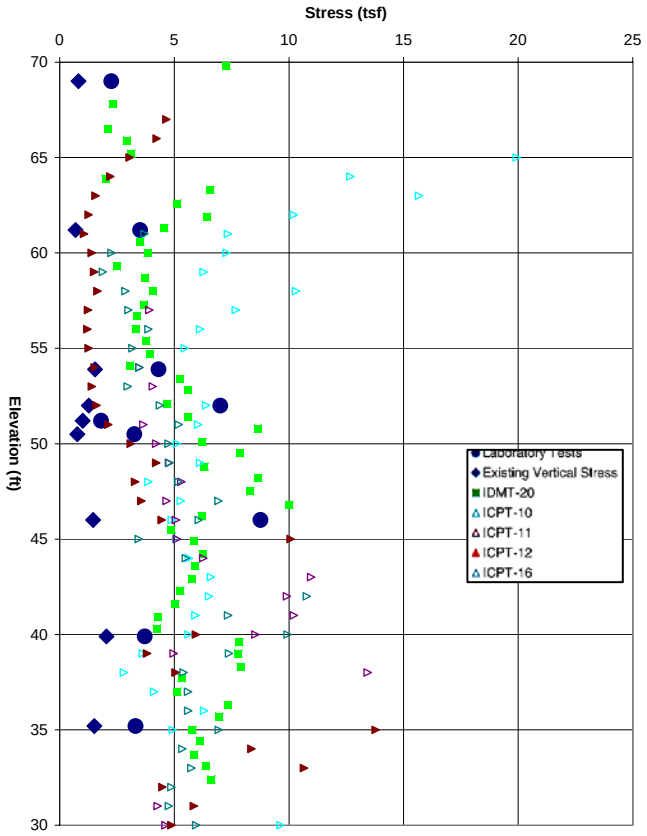

Figure 3b. IDMT-20 Stress History

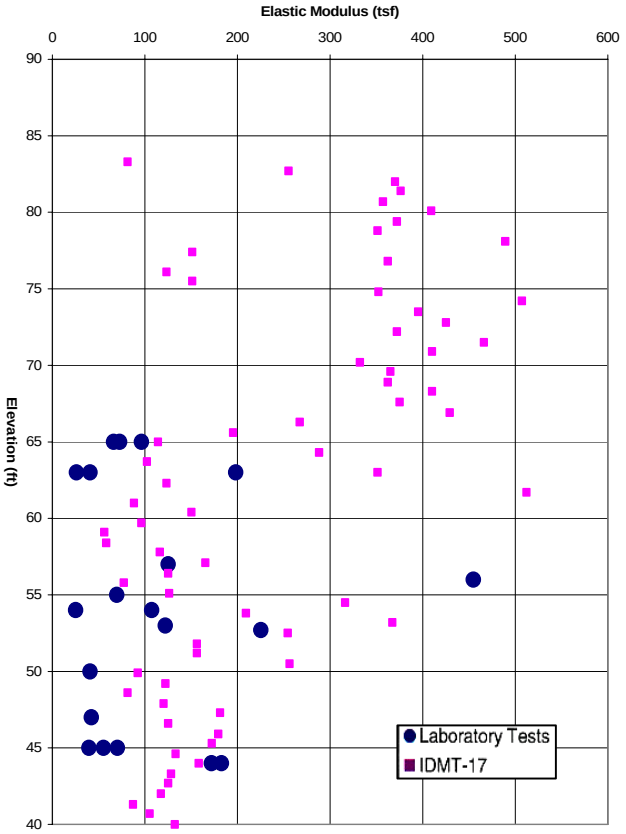

Figure 4a. IDMT-17 Tangent Modulus, E_i and DMT Modulus E_D

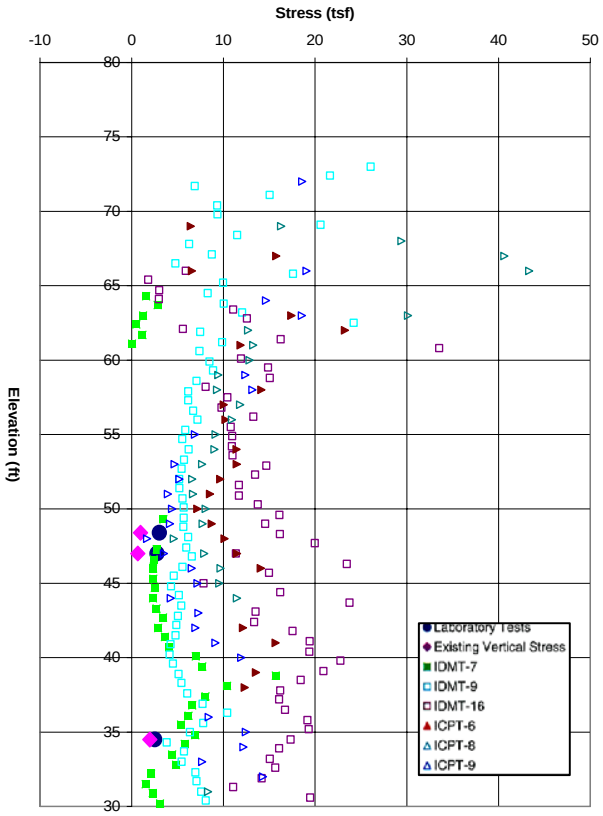

Figure 3c. IDMT-IDMT 7, 9 & 16 Stress History

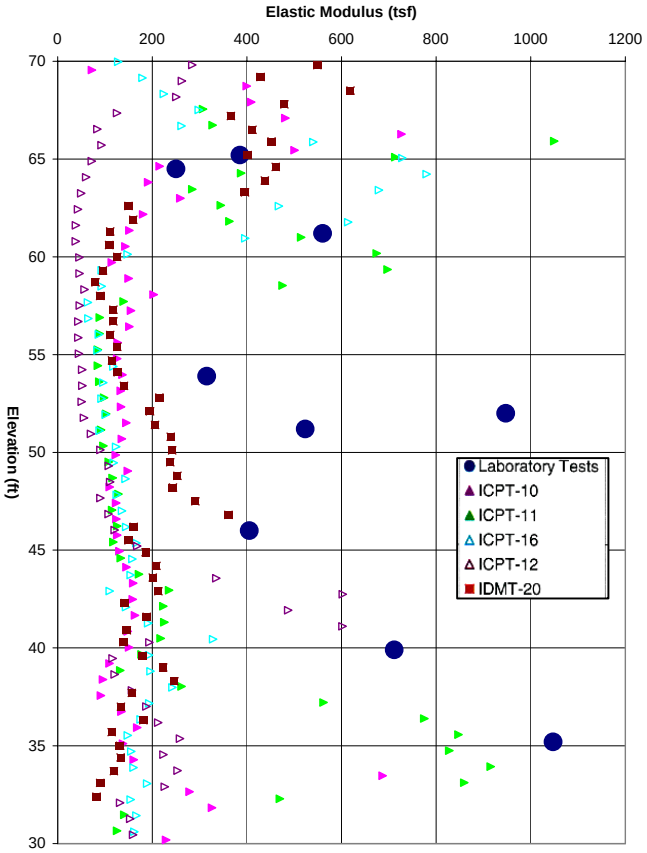

Figure 4b. IDMT-20 Tangent Modulus, E_i and DMT Modulus E_D

BACK

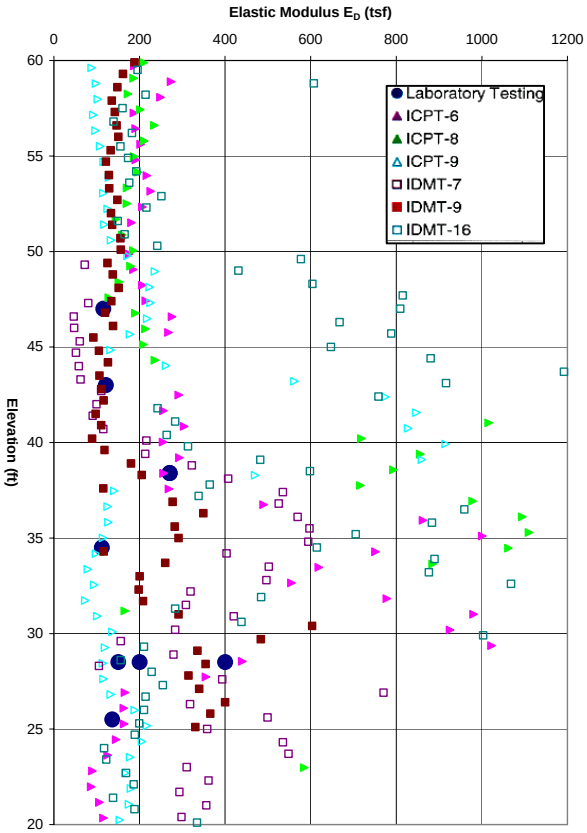

Figure 4b. IDMT-7, 9 & 16
Tangent Modulus, E_i and DMT Modulus E_D

3.2 DMT Correlations

FHWA (1992) recommends that the at rest lateral stress coefficient, K_o, for fine-grained soils be estimated from the DMT by:

$$K_0 = 0.68\ K_D^{0.54} \textit{ for } s_u/\sigma'_{vo} > 0.8 \qquad (1)$$

$$\text{or} \quad K_0 = 0.34\ K_D^{0.54} \textit{ for } s_u/\sigma'_{vo} < 0.5 \qquad (2)$$

The K_o on the other hand is more nearly directly measured and can be used in granular materials and not just fine-grained soils. Below depths of about 15-ft there seems to be little difference between the two methods, but at shallower depths the DMT correlations result in much smaller estimates of the horizontal stress as compared to the K_o-Blade.

Marchetti proposed the original correlation for deriving OCR from the horizontal stress index K_D from the observation of the similarity between the K_D profile and the OCR profile.

$$OCR_{DMT} = (0.5\ K_D)^{1.56} \qquad (3)$$

The above equation is in correspondence that $K_D = 2$ for OCR = 1 and has been confirmed in non cemented aging clay deposits. The Horizontal Stress Index K_D is a function of the vertical effective stress, σ'_{vo}; pore pressure, u_o and corrected A-pressure, p_o.

$$K_D = \frac{p_0 - u_0}{\sigma'_{vo}} \qquad (4)$$

The preconsolidation stress is then estimated by multiplying the OCR by the effective vertical stress.

The original correlation developed by Marchetti for determining the undrained shear strength, s_u, from DMT,

$$s_u = 0.22\ \sigma'_{vo}\ (0.5\ K_D)^{1.25} \qquad (5)$$

These correlations were found to provide consistent results for soils as shown in Figure 1, and are consistent with the laboratory test results and the results obtained from the CPT.

Two different values of elastic modulus are used, the initial tangent modulus, E_i, and the modulus at 25% of strength, E_{25}. Either E is obtained by applying a correction factor F to E_D according to the following expression:

$$E = (F)E_D \qquad (6)$$

F is a function of both I_D and K_D. Table 6.2 in FHWA (1992) presents values of F. This is not a unique proportionality constant and mostly ranges from 1 to 3, but for cohesive soils is reported to be 10 to derive E_i. Figure 4 illustrates the relationship between E_D as obtained from the DMT and the initial tangent modulus, E_i, obtained from UU and CU testing. In the figures E_i, was compared to E_D because it compared more favorably to the laboratory tests than M_{DMT}, E_{25} or other relationships as presented in FHWA (1992). There was some difficulty is obtaining an accurate initial tangent modulus from some of the laboratory tests due to some sample disturbance and settling in of the test apparatus, so some engineering judgment was used in establishing E_i. For the overconsolidated clay soils encountered an F value of 1 to less that 1 seemed to be the best fit.

3.3 CPT Correlations

The Young's modulus for clay can be estimated by using figures in FHWA (1992) which shows the variation of E_u / s_u as a function of stress level. The

undrained shear strength must first be determined. It is often estimated using the tip resistance, q_c and the effective vertical stress σ'_{vo}.

$$s_u = \frac{(q_c - \sigma_{vo})}{N_k} \quad (7)$$

The cone factor, Nk, is empirical and it should be correlated for each project. There are also other methods to estimate s_u using the pore pressure measurements. For this project several values of Nk ranging from 10 to 18 were used estimate he undrained shear strength. For both fine-grained strata, Nk = 16 seemed to best fit the data. To estimate the OCR, the s_u must first be determined and the s_u/σ_{vo} determined. Several charts are presented in FHWA (1992).

4 CONCLUSIONS

When using in situ testing techniques such as the DMT and CPT it is very important to understand how the correlations with soil parameters are obtained. For example, nearly all the correlations depend on knowing the vertical effective stress. Although a rough guess of 125-pcf (7.8 kg/ m^3) is usually close to the actual unit weight, once laboratory testing is obtained, however, significantly different in situ test results may be obtained. It is often instructive to use a range of values of unit weights as well as other constants to establish a potential range of parameters. One of the most important factors affecting the effective vertical stress is the location of the groundwater level. The operator in the field should measure the depth to water or at least cave in at the time of testing. Groundwater levels typically change with time, so obtaining a water reading from a nearby boring or well a few days before or later is usually not sufficient, unless, of course, it is all that is available. The engineer should also be aware of the entire groundwater regime or regimes to accurately determine the existing vertical effective stress at each point of a test. Perched water can often lead to an error in estimating the vertical effective stress.

Several constants such as the cone factor for the CPT are empirical, and can be varied from site to site and even for different geologic formations on the same site. Several values should be experimented with and compared to the laboratory test data to obtain a good fit with the data.

Often using both DMT and CPT will provide a range of values that can be compared to each other. This can be beneficial in situations where good laboratory testing is unavailable or a wide range of values are obtained. One of the often overlooked benefits of using CPT and DMT is the large number of data points available. This allows the engineer to evaluate likely ranges of soil parameters and select a Factor of Safety (FS) or β-value of a risk based analysis is being used that will result in a cost effective design. The results of these tests at this site tend to support the correlations as presented, but care should be exercised by the engineer designing with in situ testing. In situ testing should not be considered a black box; it is recommended that in addition to hard copy test results, the electronic results be submitted to the engineer by the field operator. This way the engineer can plot results of different test methods and develop site specific correlations or constants using the published correlations as well as adjust the vertical effective stress to be consistent with laboratory test results.

Additional research is still required for in situ testing. Specifically, the unloading characteristics of soils are poorly understood and correlated with either the DMT or the CPT. Since a common use of either method of in situ testing is excavation support structures and retaining walls a better understanding of the relationship of the unloading characteristics would lead to more economical and safer designs for support of excavations. In urban areas and with increasing frequency in suburban area such designs are of increasing importance.

In heavily overconsolidated soils the Ko-Blade tends to provide estimates that are much larger than the DMT. At lower elevations, however, there seemed to be very good agreement with the DMT, the Ko-Blade and the Jaky equation.

REFERNCES

FHWA (1992), “The Flat Plate Dilatometer Test”, FHWA-SA-91-044, February

FHWA (1992), “The Cone Penetrometer Test”, FHWA-SA-91-043, February

DelDOT (2005A), “Delaware Turnpike Improvements Geotechnical Data Report No. 2 Final, August 26, 2005.

Woodruff, K. D. & Thompson, A. M., (1972) “Geology of the Newark Area, Delaware, Geologic Map Series No. 3” Delaware Geological Survey

Spoljaric, Nenad (1972), “Geology of the Fall Zone in Delaware” RI 19, Delaware Geological Survey

Jordan, Robert R. (1983), “Stratigraphic Nomenclature of Nonmarine Cretaceous Rocks of Inner Margin of Coastal Plain in Delaware and Adjacent States” RI 37, Delaware Geological Survey

Woodruff, K. D., Miller, J. C., Jordan, R. R., Spoljaric, N., Pickett. T. E. “Geology and Groundwater, University of Delaware, Newark, Delaware” RI 18, Delaware Geological Survey

Dilatometer Use in Geotechnical Investigations

John P. Marshall, P.E. & Robert A. O'Berry
Marshall Engineering, Inc.
3161 Solomons Island Road, Suite 2
Edgewater, Maryland 21037
email: marshallengineering@gmail.com

Keywords: Dilatometer, settlement, standard penetration test, investigation

ABSTRACT: The authors describe their considerations in determining when to use the dilatometer in their geotechnical investigations, either in combination with Standard Penetration Test (SPT) borings or without the former, and the results when they are used. Most of their studies are in the Chesapeake Bay area where Coastal Plain soils predominate the profile. Many of the soils are soft/medium stiff Clays (CL) or loose/medium dense Sands (SC-SM) with "N" values from below 10 to the low teens. In cases where the proposed building will have high loads, such as multi-story structures, limiting settlement to acceptable amounts based on current methods using SPT results usually requires use of a relatively low bearing capacity. Use of dilatometer results at the same site has allowed use of significantly higher bearing capacities. Several considerations need to be made, however, in determining when the added cost of the dilatometer is justified. These include the need to make SPT borings, in addition to dilatometer probes, so that soil samples can be obtained for accurate soil classification and other uses. This can double the field costs for a specific study. Another is the expected economic benefit of using a higher bearing capacity when the building loads are relatively low. Specific studies are described and detailed, including one where preloading and settlement monitoring were recommended.

1 WHEN DO WE USE THE DILATOMETER?

Our first use of the dilatometer was in the year 1999 when we were asked to investigate a site for a proposed multi-building self-storage business. The property had previously been used for mining Sand and Gravel which included use of sediment ponds to collect spoil from screening operations. The ponds and overall site were subsequently filled and rough graded to the relatively level condition that existed when we began our study. We were told that none of the backfill was compacted and that the sediment in the ponds was not removed prior to the backfilling. The proposed new grades were generally the same as the existing and the ideal foundation system would be conventional spread footings and slab-on-grade construction supported on the old backfill. We were somewhat familiar with the dilatometer and decided that the existing site conditions could best be evaluated by its use. We performed our study and concluded that conventional foundations could be used. The project was subsequently built and put into use and there have been no known foundation problems since completion several years ago.

Since that study, we have used the dilatometer on over a dozen other projects. Some of these studies are discussed in following sections of this paper. On most studies, we make SPT borings at the usual locations and to the usual depths. If those results indicate potentially excessive settlement, based on the "N" values and visual classification, and the probable recommendation of a low bearing capacity (usually less than 2000 psf) and if the proposed structure is relatively heavy (loads of over about 200 kips), we will contact the Structural Engineer or other affected person and inform them of our preliminary conclusions. At that time, we recommend the addition of dilatometer probes to more accurately evaluate the profile. Most of our dilatometer investigations fall in this category. On some studies, we may have knowledge of the general subsurface conditions at a specific site before we make borings. If we expect that excessive settlement may be a consideration in the study, we may recommend dilatometer probes as part of the initial investigation. A few of our investigations have also been in this category. One of our projects involved apartment building sites where the results of a geotechnical investigation by another firm several years earlier indicated

the use of piles. That study included settlement analyses using laboratory consolidation test results on undisturbed samples. Based on our review of the previous borings, we recommended dilatometer probes at the site and subsequently determined that conventional spread footings could be used after a short period of preloading. A few of the buildings have since been constructed and occupied and there have not been any known foundation problems.

2 FIELD INVESTIGATION PROCEDURES & CONSIDERATIONS

Our soil borings are usually made with a drill rig using hollow stem augers. Split spoon samples are typically obtained at 2.5 to 5-foot intervals of depth by the Standard Penetration Test (SPT) Procedure. A representative portion of each sample is sealed in a glass jar and subsequently inspected and visually classified by our geotechnical staff. The dilatometer soundings are made by hydraulically pushing a dilatometer probe into the ground and recording miscellaneous geotechnical parameters at incremental depths below the surface, usually about 8-inch increments. This provides us with a very complete profile for settlement analysis purposes as compared to other existing methods (SPT borings with a few undisturbed samples and laboratory consolidation tests). We note here that our analysis using SPT data must consider the effects on the "N" values during the sampling process due to liquefaction in Sands and remolding in Clays. These conditions do not develop during the insertion process with the dilatometer. A disadvantage to the dilatometer, however, is that soil samples are not obtained and soil classification is limited accordingly. We also note that dense/hard soils can cause refusal to the penetration of the dilatometer which can be a problem in cases where these conditions are within foundation depth influence and may only be thin layers.

3 DESIGN CONSIDERATIONS

In selecting a foundation bearing capacity magnitude, we consider both the shear strength and compressibility parameters of the soils below the foundation level. The former is related to the shear failure of the subgrade soils under the foundation and the latter to the magnitude of settlement of the foundation both in terms of total amount and relative to adjacent foundations, referred to herein as differential settlement. Based on the subsurface conditions at all sites referenced in this paper, settlement is the governing consideration. Concerning magnitude of settlement, we generally limit the total predicated amount to 1-inch or less. Differential settlements are usually chosen to limit angular distortion to a ratio of about 1/500 or less, or about 0.5-inch over a distance of 20 feet. We usually note in our reports, when applicable, that our computations consider reduction of overburden pressure resulting from excavations to a lower design level and reduction of the applied footing pressure with depth below footing (pressure distribution). We further note that the dilatometer measures the compressibility at depth increments of about 8 inches for the entire depth penetrated and our computations are based on all of those measurements.

4 COMPLETED PROJECT SUMMARIES

Following are descriptions of projects where the dilatometer was used and the results of those studies. It is noted that these descriptions are based on the conditions at the time our investigation was performed. The first project (4.1) was under construction and almost completed at the time this paper was written. The last (4.4) has not been constructed. The other projects are still in design stage.

4.1 *Office Building – Annapolis, Maryland*

This building will have a footprint of about 30,000 sq.ft. and will be five stories above ground and one level below ground when completed. The west portion of the building will be a parking garage and retail space and a restaurant area are planned for the ground floor level of the other portion of the structure. The project site is generally open except for a few trees and bushes. Existing ground surface levels vary from about El 47' to El 42'. The proposed lower level slab grade is El 35.5' and first floor level is El 46'. The garage levels are generally the same. Based on these grades, the entire site will be excavated to a level about 9 to 14 feet below the existing grade. Lateral bracing, possibly solder beams and lagging, will be used to retain the earth outside the excavated area. The proposed column layout for the entire structure was provided. Typical column loads as shown on that plan are summarized below.

Column Load Range

Interior	Exterior
623 kips (max.)	345 kips (max.)
342 kips (min.)	180 kips (min.)

To determine the subsurface conditions, we made eleven soil test borings and four dilatometer soundings. The soil borings extended to depths of between 22 and 40 feet below the existing ground surface and the dilatometer soundings extended to depths of about 40 feet.

The soils at the site are Coastal Plain deposits identified as the Aquia Formation by the Maryland

Geological Survey. They are fine to medium grained Sands that vary from Clayey to Silty (SC-SM) in classification. The condition of the soils in the profile as measured by the Standard Penetration Test (SPT) Procedure was found to be variable. Generally below about El 15' to El 20', the soils were found to be medium dense to dense. The "N" values were generally over 20 below this level indicating relatively low compressibility. Above these soils the "N" values were generally between 5 and 15 with many below 10 indicating loose conditions and generally higher compressibility than the deeper soils. The results of the dilatometer probes generally confirm the profile condition as described above. The groundwater table ranged from about El 22' to El 25' at the time the borings were made (February-March 2002) or about 10 to 13 feet below proposed lower level building slab.

To determine the range of expected settlements under the foundation loadings for this project, we computed settlements using the range of column loads furnished by the Structural Engineer, several assumed bearing capacities and the compressibility parameters at each of the four dilatometer locations. We note here that the results of the dilatometer readings revealed that the "best" conditions relative to settlement exist at the location of D-2 and the "worst" at D-8. They also revealed that the most compressible zone exists generally in the depth range of about El 35' to El 20'. Based on our review of the furnished column loads and our computed settlements, an allowable net bearing capacity of 4000 psf was recommended for preliminary design and cost estimate purposes. The following settlements were predicted using 4.0 ksf bearing.

Column Load	Footing Size	D-2	D-8
623^k (Int.)	12.5' x 12.5'	0.36"	0.64"
342^k (Int.)	9.5' x 9.5'	0.27"	0.51"
345^k (Ext.)	9.5' x 9.5'	0.52"	0.82"
180^k (Ext.)	7' x 7'	0.42"	0.70"

The computed settlement for a column footing is about 0.8-inch and the minimum about 0.3-inch. These numbers are considered within an acceptable range based on the criteria cited above.

We noted in our report that once final column loads and locations are known, an evaluation of each individual pier foundation must be performed to verify that detrimental settlement or differential settlement will not occur. We noted that the bearing capacity of some column footings could probably be increased to 5000 psf and still maintain settlements within acceptable limits.

4.2 *Office Building – Anne Arundel County, Maryland*

This structure will be constructed in an existing building complex on the highest level of a landform that slopes down in all directions from that area. The highest ground surface is at about El 130'; most of the existing complex is at or above El 120'. Most of the land beyond the complex is undisturbed woodlands that slope down to existing roads, a ravine and wetlands. Ground surface levels along one road range from about El 75' to El 100' and along the other from about El 15' to El 20'.

The proposed building will consist of two 11-story towers located at the southwest and southeast corners of a rectangular lower structure consisting of a two to three-level parking garage under a plaza level. The "footprint" of the lowest level garage will be about 720 feet by 168 feet and it will have a slab level at about El 100'. It will be situated generally in the area of the existing office building and immediately north of the main parking lot east of that building. The next level garage above will cover the first level garage and extend south an additional 124 feet where it will be situated under the two towers. This area includes an existing swale south of the existing office building and the existing parking lot. This garage level is proposed at El 110' and will be the lowest level under the two towers and lower structure between. Existing ground surface levels within the proposed lower level garage vary from about El 100' in a small area near the northeast corner to most above El 110' and up to about El 132'. Most of the ground surface levels within the remaining building area range from about El 110' to El 132'. Final grades around the exterior of the structure will generally be the same as existing. Based on information provided by the Structural Engineer, maximum loads for a typical Plaza column will be about 800 kips and for typical interior and exterior Tower columns about 2500 and 2100 kips, respectively.

A total of eight SPT borings were made to depths of 70 to 100 feet below the existing ground surface and nine dilatometer soundings were made to depths of about 66 to 90 feet. The soils at this site are also Coastal Plain deposits identified as the Aquia Formation. The profile is predominated with interbedded layers of Sands that vary in classification from Silty (SM) to Clayey (SC). Isolated layers of Sandy and Silty Clays (CL) and Sandy and Clayey Silts (ML-CL) also exist randomly in the upper profile and pockets and layers of ironstone were also encountered at various locations and depths. Fill and possible fill [Fill?], defined herein as soil that had some visual evidence it might be fill but no positive indicator, were encountered at a few locations to depths of up to as much as about 12 feet. Based on the "N" values the soils were found to be generally loose to medium dense in the upper profile and

dense at the deeper levels. At most boring locations, they were slightly below 10 to the teens to depths of between about El 100' and El 105' and averaged values of over 40 at most locations below those levels. The denser level was below about El 90' at Borings B-2 and B-102 and El 108' at Boring B-13. Groundwater was not encountered in any boring made at this site.

To determine the range of expected settlements under the foundation loadings for this project, we computed settlements using the range of column loads furnished by the Structural Engineer, assumed bearing capacities that ranged from 6,000 to 10,000 psf, and the compressibility parameters at the dilatometer locations.

It was concluded from this investigation that conventional spread footings located in the dense Sands could be used to support the proposed building. Analysis of the compressibility of the profile as determined by the dilatometer data indicates that settlement of spread footings designed for an allowable net bearing capacity of 8000 psf should be within tolerable limits for the proposed structure based on the proposed grades as described above. It was noted that the dense Sands exist below depths that range from about El 90' to El 110' depending on site location that will require relatively deep foundation excavations in some areas.

4.3 *School Building – St. Mary's County, Maryland*

This project site is mostly open and rolling in topography with ground surface levels ranging from about El 34' to El 24'. Surface drainage is generally to the west and southwest. Lower wetlands areas border the site on the north, south and east sides. The proposed building will be situated near the center of the property and will have a first floor level at El 38'. It is understood that the building will be one to two-story without a basement and that the subsurface conditions must be suitable for use of spread footing foundations designed for an allowable net bearing capacity of 2500 psf. Paved parking areas will be located north and west of the building and a new road is proposed west of both parking areas. Based on the proposed and existing grades, fill ranging in thickness from a few feet along the east side of the site to about 12 feet under portions of the building will be required to establish new site grades.

Based on the SPT borings, the subsurface profile was found to be quite variable. Two basic soil types exist, deposits of Sands and lesser deposits of fine-grained Silts and Clays that generally occur as layers within the more predominant Sands. The Sands range in classification from Silty (SM) and Clayey (SC) to Sands with Silt (SP-SM). They vary from very loose to medium dense in condition with "N" values ranging from many below 10 to a few over 20. Most were in the range of 5 to the low teens. The Silts and Clays generally classify as Sandy Clayey Silts (ML) to Silty and Sandy Clays (CL). These deposits exist randomly within the profile and generally vary from soft to stiff in consistency. Soil colors generally range from brown to gray and light gray in the higher levels to gray and dark gray at the deeper elevations. The water table was at a depth range of about 3 to 8 feet below existing grade at the time the borings were made which was in the month of January, a relatively "wet" time of year.

To determine the range of expected settlements under conditions assumed to be similar to final design conditions, reference is made to the following table.

Settlement (inches) Due to Given Loading Condition

Structural Fill to El 38'	Structural Fill & Pier Footing (1)	Structural Fill & Continuous Footing (2)	Preload to El 49' & Structural Fill
0.82	0.97	0.97	1.95+
0.44	0.47	0.48	0.85+
0.23	0.27	0.27	0.49+
0.71	0.73	0.75	1.26+
1.94 (3)	2.04 (3)	2.09 (3)	4.07+ (3)

(1) Assume 150 kip max pier load – Footing dimensions 8 ft. x 8 ft. (2500 psf design soil bearing capacity).

(2) Assume 5 kip/LF max continuous wall load – Footing dimensions 2 ft. wide (2500 psf design soil bearing capacity).

(3) Mud and soft clay layer encountered at 19.5 ft. to 21.5 ft.

We note here that our computations consider pressure increase due to filling the site to achieve final grade (El 38') and reduction of the applied footing pressure with depth below the footing (pressure distribution). As can be seen from these results, the computed total settlement is less than 1 inch at all dilatometer locations except one where it was 2.04 to 2.09 inches. The excessive settlement at this location is believed to be due to the presence of a very soft Clay layer at about 20-foot depth. The magnitude of settlement at all other locations is considered acceptable based on the criteria stated above, however, the settlement at the one is considered exces-

sive. For that reason and assuming that other similar areas may exist within the limits of the site, it is concluded that the site should be preloaded to insure any excessive settlement occurs before building construction.

Concerning consolidation time-rate parameters, the table below summarizes the data obtained from this study.

Test Depth	Coefficient of Consolidation (1)	Time for Settlement to Occur (2)
26.2'	C_h = 6.1 ft.^{2}/day	31.3 days (3)
29.5'	C_h = 6.1 ft.^{2}/day	
32.8'	C_h = 7.2 ft.^{2}/day	
32.2'	C_h = 5.5 ft.^{2}/day	65.6 days (3)
10.5'	C_h = 1.8 ft.^{2}/day	5 days (4)
7.2'	C_h = 1.2 ft.^{2}/day	56.9 days (3)
23.6'	C_h = 8.5 ft.^{2}/day	
5.2'	C_h = 12.7 ft.^{2}/day	0.7 days (4)

NOTES:

1) Computed coefficient of consolidation (square feet/day) based on A-Reading vs. Square Root of Time plot.

2) For general discussion purposes, the computed time is based on dividing the square of the thickness of the compressible layer by the coefficient of consolidation.

3) General profile has deeper Silts & Clays.

4) General profile has shallow Sands.

It was concluded that conventional spread footings could be used to support the proposed building based on preloading the site as recommended. The analysis of the compressibility of the existing profile as determined by the dilatometer data and borings indicated that excessive differential settlement may occur in some areas of the site due to the combined loading of the proposed fill required to establish final grades and additional building loads. However, special site preparation to include placement of a shallow drainage system prior to filling the site and temporary placement of an additional preload fill to El 49' should cause that magnitude of settlement to occur over a computed time period of about 90 days. The preload fill could then be removed and construction of the building proceed. Future building settlements should be minimal. It was recommended that settlement plates be installed prior to fill placement to monitor ground movement and confirm when the preload could be removed.

4.4 *Office Building – Prince Frederick County, Maryland*

The site contains an office building that will be demolished and replace with a new two-story building with a "walk-out" basement in the rear. Development of the project will require only minimal cuts and fills.

The generalized subsurface profile in the building area consists of a surface deposit of fill over deposits of natural Silty and Clayey Sand (SM-SC) and a deeper layer of Sandy Silt (ML). The fill generally classifies as Clayey fine to medium Sand (SC) and was found to be about 2.5 feet thick. Based on an "N" value of 4, the fill is very loose indicating it probably was not compacted when placed. The deeper natural deposits were found to be loose to medium dense with "N" values of 8 to 11.

It was initially recommended that all foundations exposed to outside temperatures be located at least 2.5 feet below final exterior grade for frost protection and that foundations not exposed to outside temperatures could be located as shallow as 1 foot below final grade. Foundations located at these depths and bearing either on approved natural soils or compacted fill could be designed for an allowable net bearing capacity of 1500 psf. It was also recommended that all footings should contain reinforcing steel as designated by a structural engineer.

A supplemental geotechnical study was later made using the dilatometer to determine if a higher bearing capacity could be used. Using the dilatometer results, we made a settlement analysis of the foundation system for the proposed structure using an allowable net bearing capacity of 3000 psf and a foundation layout as provided to us by the project Structural Engineer. That layout showed the bottom of footing elevations, slab level and structural loadings. A tabulation of computed settlements based on this data is given in the table below. As can be seen, the maximum settlement we computed was 0.87-inch (location D-2, continuous footing at El 126', 6' x 6' square). All others were generally in the range of 0.3-inch to 0.7-inch for a differential of about 0.4-inch. This information was presented to the client and Structural Engineer without a recommendation.

Bottom of Footing Elev. Subgrade Elev.	Footing Typing and Dimension*	Computed Settlement
126’	(Col) 7’ x 7’	0.52”
126’	(Cont) 4’ Wide	0.63”
122’	(Col) 7’ x 7’	0.35”
122’	(Cont) 3’ Wide	0.35”
126’	(Col) 7’ x 7’	0.74”
126’	(Cont) 4’ Wide	0.87”
122’	(Col) 7’ x 7’	0.49”
122’	(Cont) 3’ Wide	0.49”
126’	(Col) 7’ x 7’	0.74”
126’	(Cont) 4’ Wide	0.87”
122’	(Col) 7’ x 7’	0.49”
122’	(Cont) 3’ Wide	0.49”
126’	(Col) 7’ x 7’	0.61”
126’	(Cont) 4’ Wide	0.71”
122’	(Col) 7’ x 7’	0.32”
122’	(Col) 6’ x 6’	0.28”
122’	(Cont) 3’ Wide	0.33”

* (Col) = Column
(Cont) = Continuous

5 OTHER DILATOMETER USES

We have also used the dilatometer for purposes other than obtaining data for settlement evaluation and foundation design recommendations as described in the examples above. Some are described briefly below.

5.1 *Retaining Wall – Anne Arundel County, Maryland*

The purpose of this investigation was to determine the in-situ condition of the subsurface profile along the alignment of a proposed 20 to 30 foot high Keystone retaining wall. Two SPT borings and three dilatometer probes were made for this purpose. The results were presented in the form of boring logs, dilatometer printouts and the following table.

Depth	General Soil Classification	Shear Strength	Angle of Internal Friction
0’ – 3’	Clayey Silt	1000 psf*	
3’ – 17’	Layered Silty Clayey Sand and Silty Clay		∅ = 33°*
17’ – 30’	Silty Clay	1200 psf*	
0’ – 8’	Clayey Silt/Silt	1400 psf	
8’ – 15’	Sandy Silt/Silty Sand		∅ = 35°*
15’ – 30’	Clayey Silt/Silty Clay	*1400 psf	
0’ – 25’	Silty Sand/Sandy Silt		∅ = 33°*
25’ - 30’	Clayey Silt	*2400 psf	
0’ – 6’	Clayey Sand		∅ = 33°*
6’ – 30’	Clayey/Silty Sand		∅ = 33°*
0’ – 20’	Silty Sand/Sandy Silt		∅ = 35°*
20’- 30’	Clayey Silt/Silty Clay	*1200 psf	

*Selected by comparison of dilatometer data and visual soil classification of SPT samples and “N” values

5.2 *Existing Building – Annapolis, Maryland*

The purpose of this study was to determine the condition of the subsurface profile under the old portion of a structure with a newer addition relative to the impact of intended subsurface improvements as a result of a recent grouting operation. It was originally planned to perform 3 to 4 tests using a pressuremeter on the assumption that the grouting had densified and solidified the subsurface materials into a stable mass. The bore holes for the tests were made by the wash boring method using a rotary drill rig. A pressuremeter test was attempted at about 5-foot depth in the first boring, however, cave-in of the sides of the bore hole resulted in enlargement of the hole diameter to the extent that the pressuremeter could not reach the sides and that test was terminated. Based on that condition, it was decided to substitute dilatometer probes for the pressuremeter tests. The general procedure consisted of first advancing the hole by wash boring method and setting casing at the top to allow re-circulation of the drill water. Split spoon samples were then obtained continuously by the Standard Penetration Test (SPT) procedure until very soft conditions were encountered at which time testing with the dilatometer probe was begun. It was assumed that effective grouting would result in the creation of a stable mass of soil about 15 feet thick that would be dense-cemented in condition. It was, therefore, not expected that conditions would be encountered in the

borings that included cave-in of the sides of the hole and very loose or soft zones where the split-spoon sampler and dilatometer could easily be hydraulically pushed with the light drill rig. It was also expected that veins of cement grout would be observed throughout the profile.

The Tangent Modulus ("M") obtained by the dilatometer after grouting was selected for comparison to "M" values measured prior to that operation. The "M" value generally reflects the "stiffness" of the profile which relates to both compressibility and strength. For general comparison purposes, a value less than 10 indicates a very low stiffness or high compressibility. A value between 10 and 100 indicates potential problem conditions. The results of this study indicated no significant difference between the stiffness of the profile before and after the grout operation.

It was, therefore, concluded that the subsurface profile under the old portion of the building was not improved to any noticeable degree by the grout operation. It was found that no voids were noted under the slab at any location indicating good contact between the slab and underlying subgrade. However, there was limited evidence of grout penetration and the comparison of the stiffness of the profile as measured by the "M" values from the dilatometer did not indicate any significant change in conditions after the grout operation.

6 COST COMPARISONS

The cost of making a dilatometer sounding, obtaining data and reducing that data to a useful form is somewhat higher than making soil test borings using hollow stem augers and obtaining SPT samples. Based on current prices, an investigation at an arbitrary site where ten SPT borings to 40 feet are to be made would cost about $6700.00 in drilling costs. The cost for making the same number of dilatometer probes to the same depth would be about $7200.00 which includes reduction of the data. As another example, the SPT drilling cost at a site where six 20 foot borings are required would be about $2500.00 compared to $3300.00 using the dilatometer. The cost difference becomes more significant when the dilatometer is used in conjunction with an STB boring program, which is usually the case, due to additional mobilization costs. The difference can be reduced by substituting SPT borings for dilatometer probes which is what we try to do on most projects.

7 CONCLUSIONS

It is our conclusion that the use of the dilatometer provides data and results that are substantially more detailed and accurate than can be obtained from the older methods that have been in use for many years and, therefore, worth the additional cost. Settlement computations using the dilatometer results considers a profile with data available in close increments as compared to wide gaps based on a few undisturbed samples and the results of laboratory consolidation test or SPT results. The in-situ parameters obtained more accurately represent the actual compressibility of the profile than is measured by the other methods. Time is also a positive factor in that the dilatometer data is available immediately whereas several weeks, at least, are lost between the time a boring is made, the undisturbed sample is obtained and consolidation test is completed. The dilatometer does have the disadvantages that samples are not obtained for classification purposes, groundwater information is limited and some subsurface conditions cannot be penetrated.

8 REFERENCES

Marchetti, S., (1980), "In situ tests by flat dilatometer, Journal of the Geotechnical Engineering Division, ASCE, Vol. 106, No. GT3, pages 299-321.

Schmertmann, J. H., (1986), "Dilatometer to compute foundation settlement", Proceedings, ASCE Specialty Conference, In-Situ '86, VPI, Blacksburg, Virginia, pages 303-321.

APPENDIX: UNIT CONVERSIONS

1 foot (ft) = 0.3048 m
1 kip = 4.4482 kN
1 lb/ft^2 (psf) = 0.04788 kPa
1 British ton-force/ft^2 (tsf) = 95.76 kPa

Comparison of DMT and CPTU testing on a deep dynamic compaction project

Heather J. Miller
Department of Civil Engineering, University of Massachusetts, N. Dartmouth, MA, USA

Kevin P. Stetson
Sanborn, Head & Associates, Westford, MA, USA

Jean Benoît
University of New Hampshire, Durham, NH, USA

Edward L. Hajduk
WPC Inc., Mt Pleasant, SC, USA

Peter J. Connors
Massachusetts Highway Department, Boston, MA, USA

Keywords: Marchetti dilatometer, piezocone penetration testing, deep dynamic compaction, cranberry bogs, peat

ABSTRACT: This paper describes Marchetti flat dilatometer testing (DMT) and piezocone penetration testing (CPTU) conducted for site characterization and quality assurance and control QA/QC on a major highway relocation project in Carver, Massachusetts (USA). Stretches of the new highway span existing cranberry bogs with thick peat deposits. Sheet piling was installed along both sides of the new highway alignment, and organic material was dredged from between the sheet pile walls. The area was then backfilled with sands. Since most of the sand was placed in a fairly loose state underwater, subsidence and liquefaction were potential problems. Therefore, deep dynamic compaction (DDC) was used to densify the fill.

An extensive in situ testing program was instituted to characterize site conditions prior to densification, and to assess the sufficiency of the DDC after treatment. The results of this study suggest that both the DMT and the CPTU are excellent tools for providing stratigraphic profiles. Both devices were particularly helpful in identifying pockets of organic soils (i.e., peat) that were not completely removed during the initial dredging operations. In terms of compaction QA/QC, comparisons were conducted between the dilatometer modulus (E_D), DMT horizontal stress index (K_D), DMT constrained modulus (M) and the corrected tip resistance (q_t) values from CPTU testing. The DMT and CPTU parameters showed similar trends regarding the zone of maximum soil improvement. The constrained modulus values determined from the DMT appeared to be the most sensitive indicators of densification effects.

1 INTRODUCTION

The Massachusetts Highway Department (MassHighway) is in the process of relocating a section of US Route 44 from the existing Route 44 in Carver, MA to US Route 3 in Plymouth, MA. The new roadway section will be a four-lane divided highway which will replace the current two-lane highway. The layout of the new highway extends across several existing cranberry bogs with underlying peat deposits. The peat deposits, which extended up to 9.1m (30ft) deep from the existing ground surface, required removal and replacement with on-site soils. Underlying the peat, the in situ soils are glacial outwash deposits consisting of loose to dense, coarse to fine sands with lenses of silt, clay and gravel and occasional cobbles and boulders.

Due to right-of-way considerations which severely restricted the space available for the roadway and environmental concerns regarding the remaining cranberry bog sections, traditional sloped earth embankments could not be used. Therefore, an innovative design incorporating sheet piling and mechanically stabilized earth (MSE) walls was used at the cranberry bog crossings. A typical cross-section of this design is presented in Figure 1.

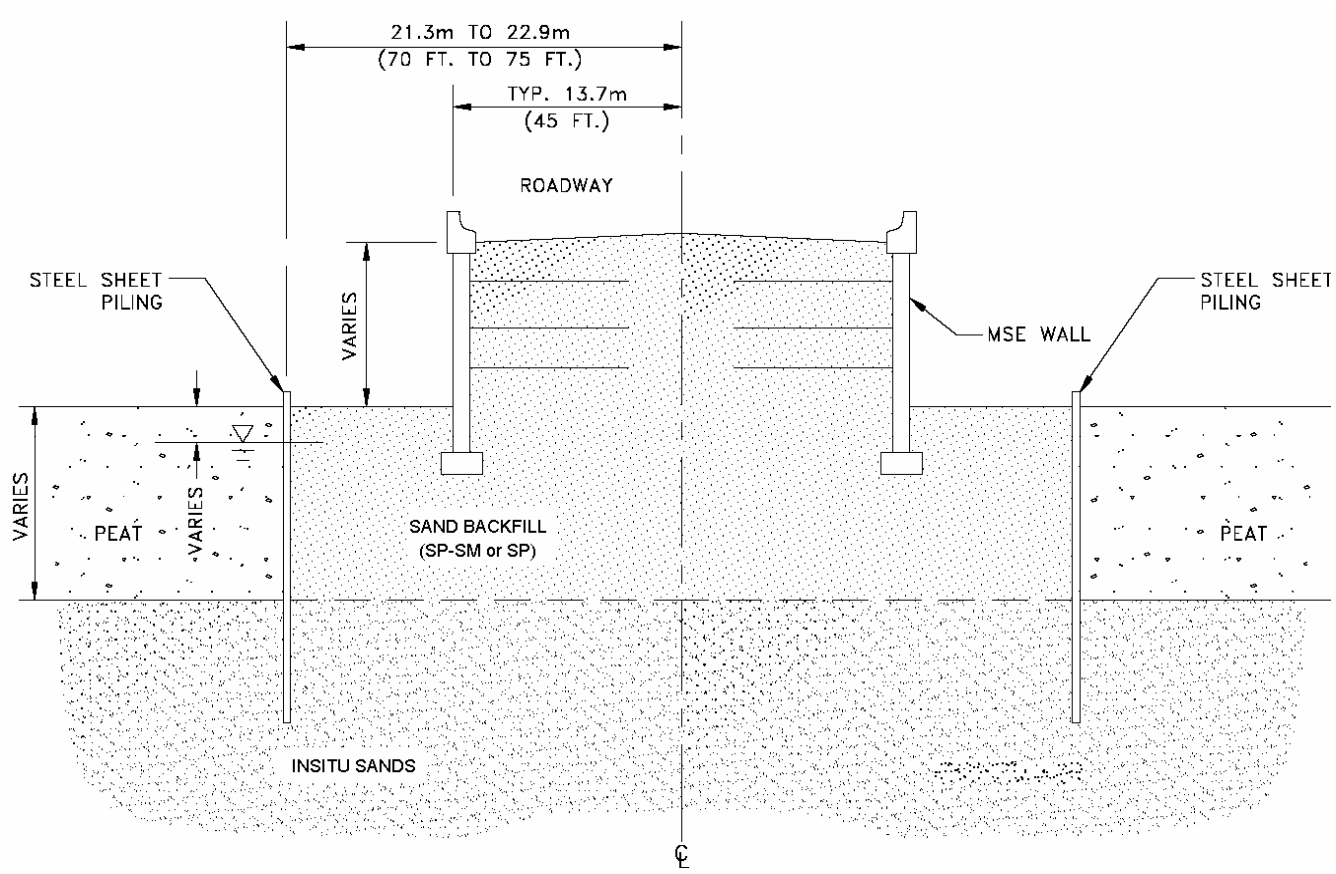

Figure 1. Typical Highway Cross-Section over Peat (Hajduk et al. 2004).

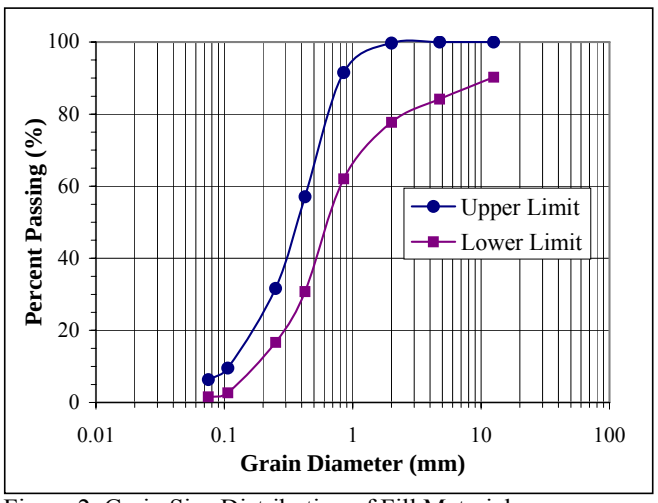

Figure 2. Grain Size Distribution of Fill Material

The construction project started with the installation of steel sheet piling through the pond/bog sections. The sheeting was located about 21.3 to 22.9m (70 to 75ft) off the proposed highway centerline. The removal of the peat between the steel sheeting was accomplished without dewatering using a crane outfitted with a dragline bucket. The thickness of the peat deposits ranged from about 1.52m (5ft) to about 9.1m (30ft). After removal of the peat deposits from within the sheet pile walls, granular fill was placed between the sheet piling by pushing the material forward (from the "land side") with a dozer. Fill was placed from the dredged mudline (which varied widely in elevation) to approximately Elevation 34.5 m (113 ft), which was roughly 1.6 m (5 ft) above the static groundwater table. A typical grain size distribution curve, as well as upper and lower limits of the range of grain size distribution of the fill material is provided in Figure 2. The fill is generally classified as poorly-graded sand (SP or SP-SM) according to the USCS classification system. The mean D_{50} is approximately 0.4 mm.

Since most of the sand was placed in a fairly loose state underwater, the potential for liquefaction was a concern. Therefore, deep dynamic compaction (DDC) was used to densify the fill. In situ testing was conducted before and after compaction to obtain baseline soil parameters and to assess the sufficiency of the DDC treatment.

2 DEEP DYNAMIC COMPACTION PROGRAM

Deep Dynamic Compaction is a process whereby soil is densified by repeatedly dropping a massive weight from a crane to impact the ground. Dynamic energy is applied on a grid pattern over the site, typically using multiple passes with offset grid patterns. The DDC process, described in detail by Lukas (1995), is generally very effective in densifying loose granular deposits. The degree of improvement is a function of the applied energy per unit cross-

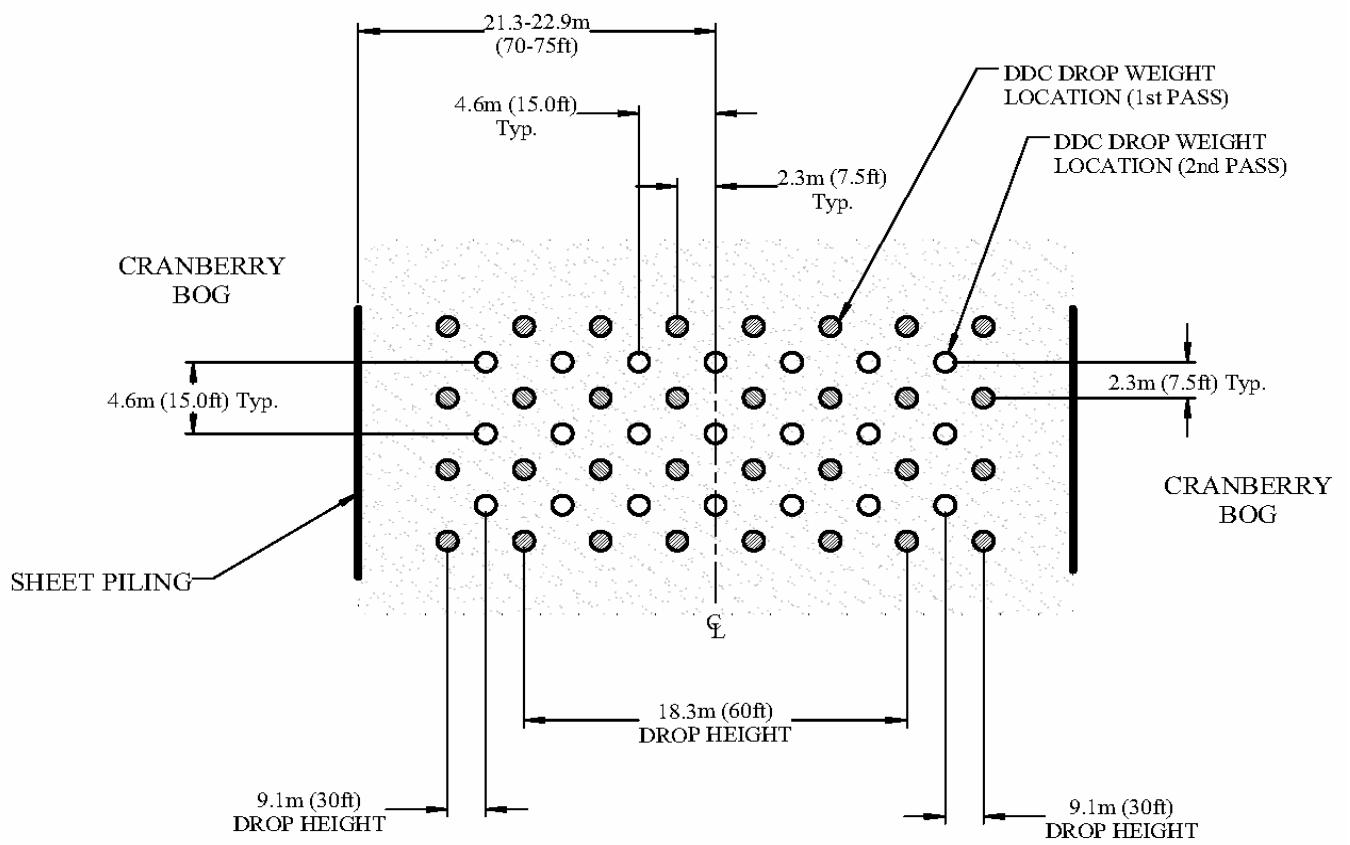

Figure 3. Typical DDC Layout Pattern (Hajduk et al. 2004).

sectional area, which is related to the tamper mass, the drop height, the number of drops and number of passes applied. The depth of improvement can be estimated using an empirical equation developed by Lukas (1995):

$$D = n(WH)^{0.5} \quad (1)$$

where D = depth of improvement in meters; W = mass of tamper in megagrams; H = drop height in meters; and n = empirical coefficient (for pervious soil deposits with a high degree of saturation, a value of 0.5 is recommended; for semi-pervious soils with a high degree of saturation, a value of 0.35 to 0.4 is recommended). The maximum improvement resulting from DDC is likely to occur within the zone from about 1/3 to 1/2 of the depth, D, calculated using equation (1).

The DDC planned for this project consisted of two passes over the site. In situ testing was conducted after the initial two passes of DDC, and additional compaction was applied to any areas where the initial compaction was not deemed sufficient. The layout for each pass consisted of a square pattern with a spacing of 4.6m (15ft). The second pass was offset within the center spacing of the 1st pass. A typical DDC layout for the project is presented in Figure 3. At each grid point location, a maximum of 9 drops were applied, with less drops applied if the depth of the crater exceeded approximately 1.52m (5ft). In some instances, the number of drops applied and/or the drop heights were reduced in response to lateral movement of the sheet pile walls and/or sand boils that occurred over portions of the site.

The DDC was conducted using a tamper weight of 13.15 Mg (14.5 tons). The tamper was a six sided lead weight with an approximate diameter of 1.52m (5ft) and a height of 0.90m (35 inches). Drop heights varied with distance from the roadway centerline. From the roadway centerline to 11.4m (37.5ft) from the roadway centerline, the DDC drop height was 18.3m (60ft). From a distance of 13.7m (45ft) from the roadway centerline and beyond, the drop height was reduced to 9.1m (30ft). The decrease in drop height was implemented to reduce the lateral stresses on the sheet piling from the DDC.

3 IN SITU TESTING PROGRAM

An extensive in situ testing program was carried out to provide baseline conditions of the fill and to assess the degree of compaction resulting from the deep dynamic compaction. The MassHighway construction specifications required an initial round of cone penetration testing to be conducted prior to the DDC, and a verification phase of CPTU after two passes of DDC. WPC conducted

the QC testing under the construction contract with P.A. Landers. Refer to Hajduk et al. (2004) for additional details concerning the initial and verification cone penetration testing for the project. Supplemental in situ testing conducted before and after DDC under a research contract between MassHighway and UMass Dartmouth (UMD) included standard penetration testing (SPT), drive cone penetration testing (DCPT), dilatometer testing (DMT) and instrumented dilatometer testing (IDMT). The University of New Hampshire conducted the DMT and IDMT testing, and Applied Research Associates (ARA) conducted additional cone penetration testing after DDC for the MassHighway/UMD research project. This paper will focus on the results of the DMT and CPTU tests.

3.1 *Cone penetration testing*

The cone penetrometer consists of a steel probe with a conical tip that is pushed at a rate of 2 cm/sec into the soil in accordance with ASTM D5778. Cone penetrometers with a 15cm^2 projected tip area and a 225cm^2 friction sleeve were used throughout the testing. A porous piezoelement saturated in silicon oil is located behind the tip (type 2 for u_2) and detects in-situ penetration pore pressure during cone advancement,

The CPTU data acquisition system records the cone penetration resistance (q_c) and the local sleeve friction (f_s). Typically, CPTU tip resistance values are adjusted to account for porewater pressure effects due to unequal end areas, and the "corrected" values are expressed as q_t. From that information, the friction ratio (FR) can be calculated as equal to the local sleeve friction divided by the corrected tip resistance (f_s/q_t), typically expressed as a percentage.

The CPTU is beneficial in obtaining continuous profiles that provide information concerning soil stratification and variation in soil properties. Under the MassHighway construction specifications, the criterion for ground improvement was based on corrected CPTU tip resistance (q_t) values. The increase of CPTU tip resistance has been widely used to monitor the densification effect of various ground improvement techniques (Dove et al., 2000). Although the use of shear wave velocities measured during seismic testing (SCPT) has gained increased use for determining the degree of ground improvement, specifically the resistance to liquefaction (Andrus and Stokoe, 2000), it was not used for this project.

The ground improvement criterion was set as the minimum q_t value that would prevent liquefaction from the design earthquake. These minimum q_t values were established by WPC using the procedures developed at the 1996 NCEER and 1998 NCEER/NSF Workshops on Evaluation of Liquefaction Resistance of Soils and outlined by Youd and Idriss (2001). The design earthquake for the project has a 2% probability of exceedance in 50 years (i.e. 2,475 return period). According to the WPC liquefaction analysis, the minimum required corrected tip resistance ranged between 5.75 MPa to 7.66 MPa (60 tsf to 80 tsf).

3.2 *Dilatometer testing*

The DMT, introduced by Marchetti in 1975, consists of a stainless steel blade 95 mm wide, 15 mm thick with a 20-degree apex that is statically pushed into the ground for testing. On one face of the blade is a circular flexible steel membrane 60 mm in diameter. At typical test intervals of 15 to 30 cm the penetration is stopped and the membrane is expanded against the soil. Three pressure readings are generally recorded during a test and corrected for membrane stiffness: P_0 the pressure corresponding to the initial movement of the membrane, P_1 the pressure at a displacement of 1.1 mm into the soil and P_2 the pressure at which the membrane recontacts the body of the probe upon deflation. From the corrected pressures, Marchetti introduced the dilatometer indices I_D (material index), K_D (horizontal stress index), and E_D (dilatometer modulus), which can be used to empirically obtain various soil properties. For this project, the tests were carried out according to the ASTM procedure D-6635-01.

The dilatometer has been previously used in monitoring ground improvement by various means including deep dynamic compaction. Schmertmann et al. (1986) and Marchetti et al. (2001) suggest that since most densification work is aimed at reducing settlement, the constrained modulus from the DMT is a better indicator of improvement than relative density. The constrained modulus, M_{DMT} is empirically calculated using the DMT indices I_D, K_D and E_D. Consequently, this modulus inherently takes into account stress history and the state of stress. Their studies have also shown that increases in M_{DMT} are often twice that observed using q_c from the cone penetration test. In addition, settlement calculations based on the M_{DMT} have been in good agreement with observed settlements. The horizontal stress index, K_D is also a good indicator of improvement as densification translates into an increase in the lateral stress coefficient.

3.3 *In situ test results*

As part of the research contract between MassHighway and UMass Dartmouth, extensive testing was performed between stations 156+00 and 159+00 to enable comparison of different in situ test results. Figure 4 shows typical profiles of corrected pressures P_0, P_1 and P_2 for DMT-102 and DMT-104, located near the sheeting at station 156+00 and near the highway centerline at station

159+00, respectively. It should be noted that for most of the DMT soundings, the fill from the ground surface to a depth of about 1.52m (5ft) was pre-bored with a hollow stem auger and then the DMT soundings were initiated at a depth of about 1.83m (6ft). This was done to avoid damage to the DMT blade, since the upper fill material was fairly dense as a result of construction traffic through the area and it also contained some gravel.

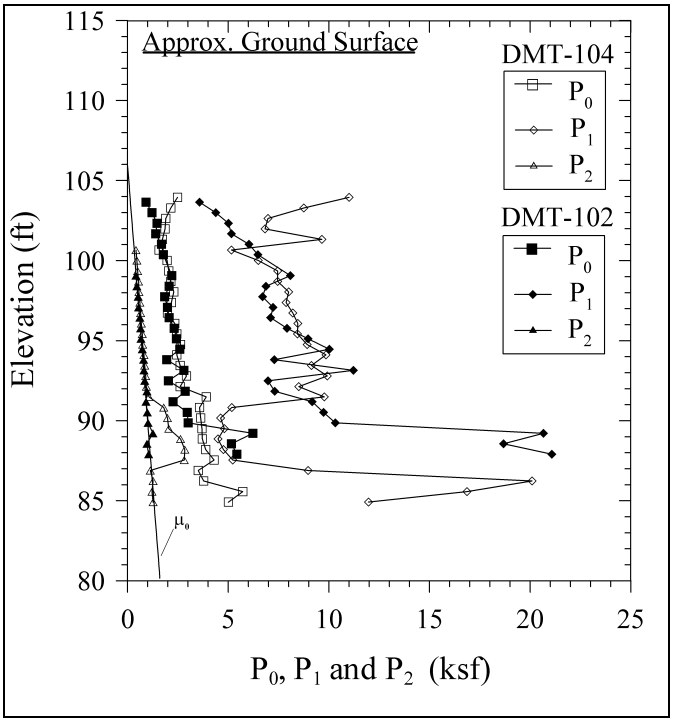

Figure 4. Corrected pressures P_0, P_1 and P_2 for DMT-102 and DMT-104

Below Elevation 92, profile DMT-104 shows a dramatic decrease in P_1 and an increase in P_2 (above hydrostatic conditions) indicating that a 1.22 to 1.52m (4 to 5-foot) layer of soft organic material was left in place prior to filling that area. The material above Elevation 101 appears to be stiffer at DMT-104 than at DMT-102. This is likely due to heavy construction traffic that occurred along the centerline during and after the filling operations. Although the two profiles are approximately 300 feet apart, the results (excluding the deeper soft layer and the upper compacted zone) seem to show that the filling process was minimally variable, especially with respect to P_0.

Profiles of CPTU data from approximately the same location as DMT-104 (station 159+00, centerline) are shown in Figures 5 and 6. The influence of the heavy construction traffic along the centerline is clearly reflected in the high CPTU q_t values within the upper 3.05m (10ft) of fill. Just below Elevation 92, the drop in tip resistance, and increases in pore pressure and friction ratio also suggest that a 1.22 to 1.52m (4 to 5-foot) layer of soft organic material was present below that elevation, just as in DMT-104.

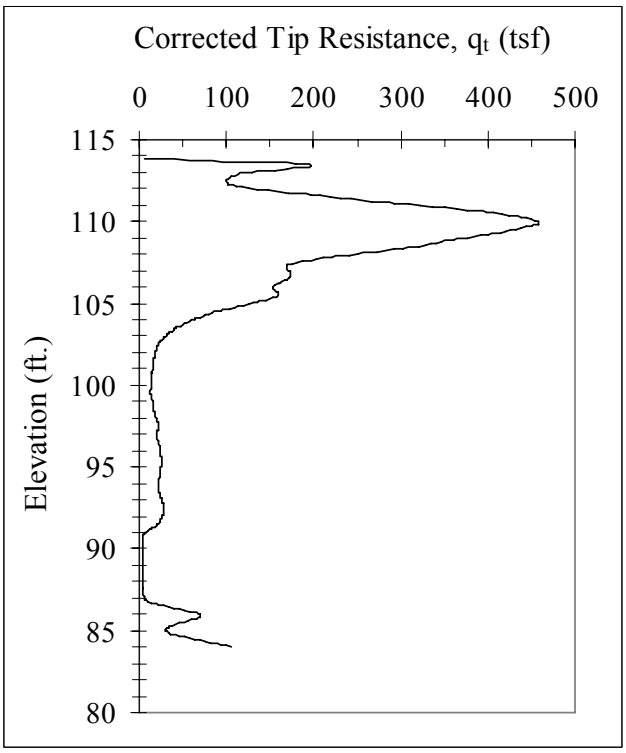

Figure 5. CPTU tip resistance profile at station 159+00

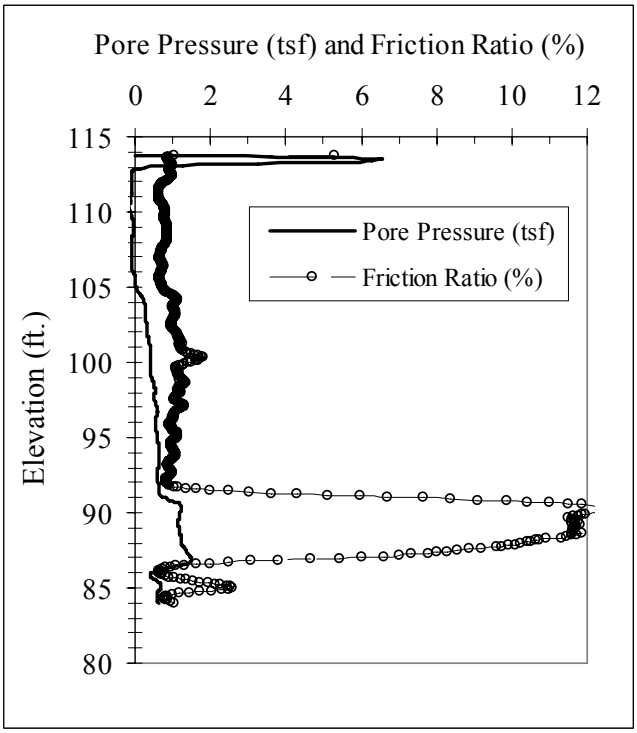

Figure 6. CPTU pore pressure and friction ratio profiles at station 159+00

The locations of DMT and CPTU tests near the sheeting (eastbound lane) at station 156+00 are shown in Figure 7. Figures 8 and 9 show profiles

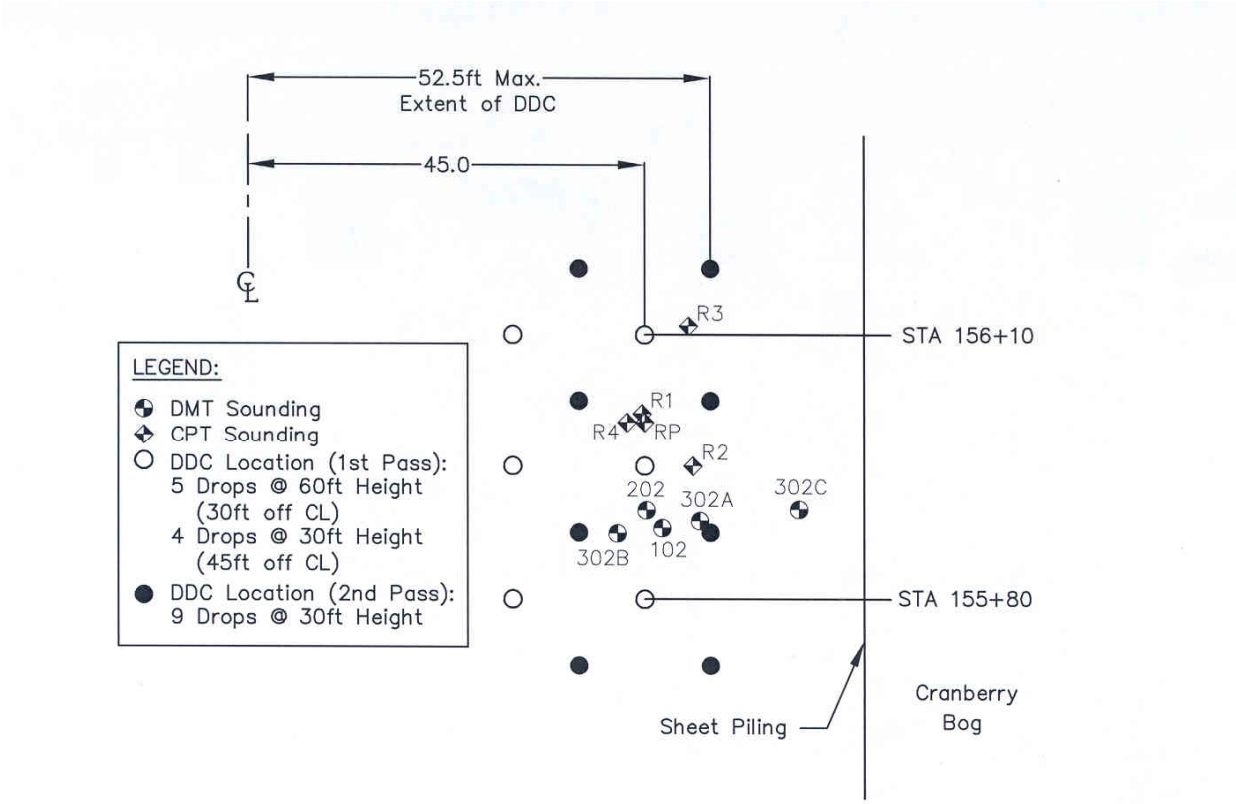

Figure 7. Locations of DMT and CPTU tests near station 156+00

of the horizontal stress index, K_D and the constrained modulus, M_{DMT} for the five DMT soundings; DMT-102 was conducted prior to compaction and the remaining four were conducted after compaction with DDC.

Figure 8 shows expected increases in lateral stress due to compaction with the most significant increases between Elevations 104 and 98. The maximum improvement appears to be approximately between Elevations 100 and 102. Below that depth, the horizontal stress increase attenuates, but still remains higher than the pre-compaction stage except at profile DMT-302C. At that location, it is possible that the lack of increase in horizontal stress resulted from two factors: (1) DMT-302C was located outside of the DDC limits and (2) significant lateral movement of the sheet pile wall occurred during compaction, which likely reduced the horizontal stresses closer to the wall. Inclinometer data obtained at station 156+25 indicated that the sheet pile wall deflected outward about 76 cm (30 inches) near the top of the wall. Outward deflections decreased linearly to about 23 cm (9 inches) at a depth of 8.54m (28ft).

Figure 9 also indicates that the constrained modulus increased substantially between Elevations 104 and 98, especially at DMT-202 and DMT-302B. At those locations, the maximum improvement also appears to be approximately between Elevations 100 and 102, where post-DDC values of constrained modulus are about 15 to 20 times larger than the pre-compaction values. Another trend noted in Figure 9 is that the increase in constrained modulus values is less as one moves farther away from centerline towards the sheet piling.

As illustrated in Figure 7, DMT-302C was located outside of the DDC limits, so the smaller increases in modulus may be due to little direct energy from the DDC being delivered to that area. At profile DMT-302A, however, the applied energy was roughly equivalent to that applied at DMT-302B, and greater than that applied in the vicinity of DMT-202. Since the M_{DMT} values in DMT-302A were lower than those in DMT-202, it is likely that the lateral movement of the sheet pile wall that occurred during compaction had a pronounced effect on the DMT constrained modulus values.

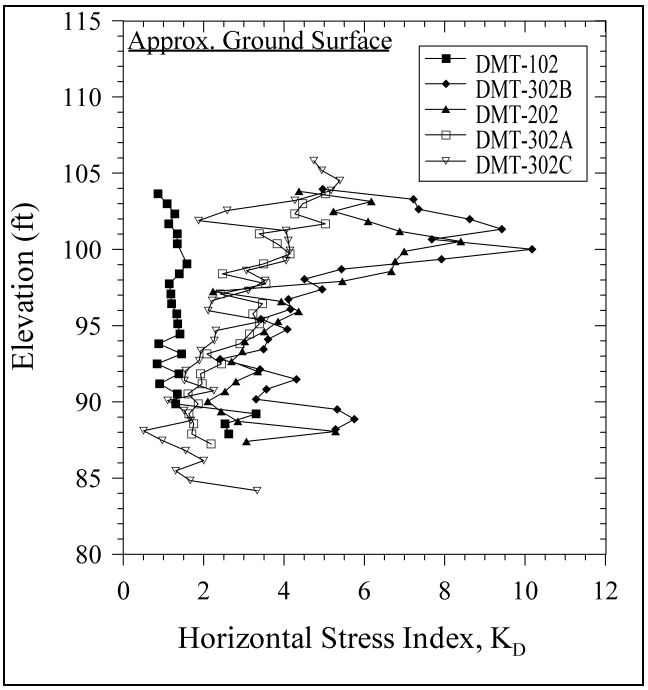

Figure 8. Profiles of horizontal stress index, K_D, near station 156+00

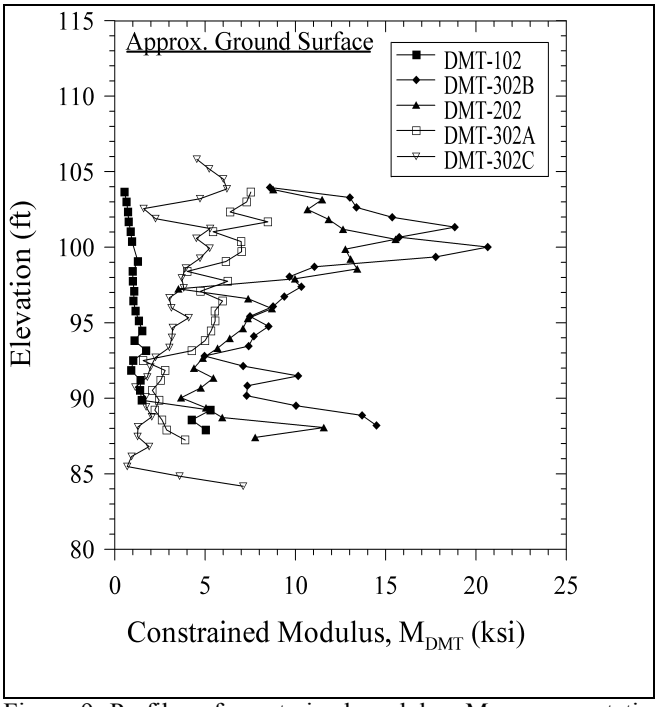

Figure 9. Profiles of constrained modulus, M_{DMT}, near station 156+00

Profiles of tip resistance values in CPTU soundings conducted near the sheeting (eastbound lane) at station 156+00 are shown in Figure 10. Sounding RP was conducted prior to compaction, and the remaining four soundings were conducted after compaction with DDC. It is interesting to note that, within the upper 0.9 to 1.2m (3 to 4 feet) of fill, the post-DDC q_t values shown in Figure 10 are actually less than the pre-DDC values. Ground improvement in this zone was not expected, since DDC severely affects near surface soils, resulting in a looser surface after the process is completed.

Below Elevation 110, Figure 10 shows expected increases in tip resistance due to compaction. The most significant increases are approximately between Elevation 108 and Elevation 98, which is consistent with the DMT data. The maximum improvement zone appears to be approximately between Elevations 103 and 105.5, which is slightly higher than the maximum improvement zone indicated by the DMT data. Within the zone of maximum improvement, the post-DDC q_t values are about 5 to 8 times larger than the pre-compaction values.

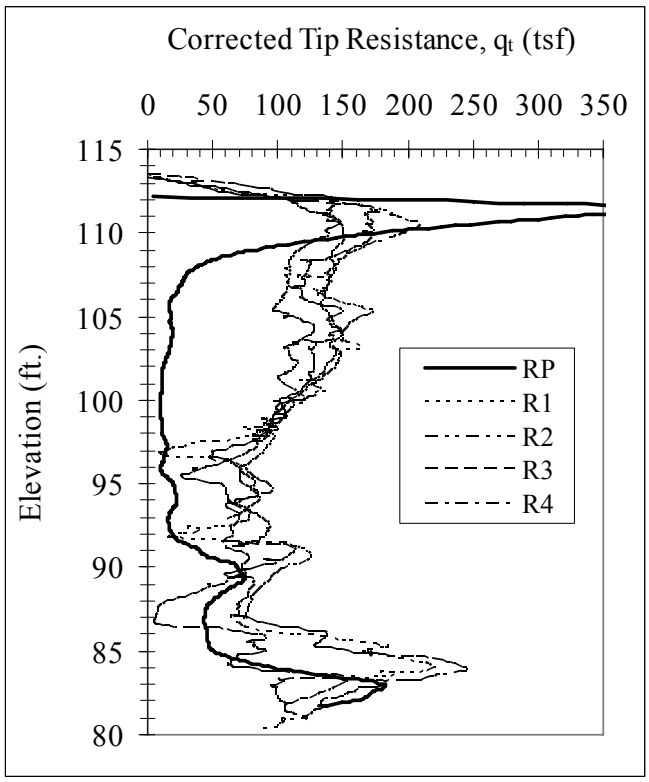

Figure 10. Profiles of CPTU tip resistance, q_t, near station 156+00

Based upon a 13.15 Mg tamper and a 9.1m (30ft) drop height, the depth of improvement computed from equation (1) using a coefficient, n, of 0.5 is 5.5m (18ft). The corresponding maximum improvement would then be predicted to occur within a zone between 1.8 and 2.7m (5.9 and 9.0 feet) below ground surface (i.e., Elevation 107 to 104, respectively). Both the CPTU and DMT data indicate that the depth of improvement extended slightly below that predicted by equation (1), and that the zone of maximum improvement may also be slightly deeper than that predicted using equation (1).

In contrast to the DMT horizontal stress index and constrained modulus data, the CPTU q_t data does not clearly indicate decreases in tip resistance as one moves farther away from centerline towards the sheet piling. This suggests that the DMT horizontal stress index and constrained modulus values

are more directly related to lateral stress conditions than the q_t values measured in CPTU testing. Given the direction of the measurements, it would stand to reason that the DMT readings would be more sensitive than the CPTU to changes in horizontal stresses such as those caused by lateral wall movements.

4 CONCLUSIONS

The results of this study suggest that both the DMT and the CPTU are very useful tools for providing stratigraphic profiles as well as parameters for QA/QC on in situ densification projects. During preliminary site investigations, the DMT and CPTU were particularly helpful in identifying pockets of organic soils (i.e., peat) that were not completely removed during the initial dredging operations. After compaction, the CPTU tip resistance values and the horizontal stress index and constrained modulus values obtained from the DMT were all good indicators of densification effects. The DMT constrained modulus values appeared to be the most sensitive indicators of densification effects.

Data from both the DMT and the CPTU indicate that the depth of improvement resulting from DDC extended slightly beyond the depth predicted using equation (1), and that the zone of maximum improvement may also be slightly deeper than that predicted using equation (1).

And finally, the trends observed in the DMT data presented herein illustrate another interesting phenomenon. This site was somewhat unusual in that DDC was conducted between rows of sheet piling spaced about 46m (150ft) apart, parallel to the highway centerline. Based upon the profiles of constrained modulus shown in Figure 9, it appears that lateral movement of the sheet piling that occurred during compaction reduced effectiveness of the DDC in areas adjacent to the sheet piling.

ACKNOWLEDGMENTS

The writers wish to acknowledge the Massachusetts Highway Department for their financial support for this research. Additionally, several MassHighway personnel provided much assistance in conducting the field testing for this project. Mr. Nabil Hourani, Mr. Edward Mahoney, and the entire staff of the MassHighway Route 44 Field Office in Carver, MA are acknowledged in that regard. And finally, the writers appreciate help provided by Mr. Glenn Stewart at P.A. Landers, Inc., and Mr. John Jones TerraSystems and UMD undergraduate research assistants Nicholas Yafrate and Tracy Willard.

REFERENCES

Andrus R.D., and Stokoe K.H. (2000) Liquefaction Resistance of Soils from Shear-Wave Velocity. Journal of Geotechnical and Geoenvironmental Engineering 126 (11), 1015-1025.

ASTM D6635-01, "Standard Test Method for Performing the Flat Plate Dilatometer".

ASTM D5778-95 (2000) "Standard Test Method for Performing Electronic Friction Cone and Piezocone Penetration Testing of Soils."

Ernst H., Connors P., and Pettis P. (1996). Massachusetts Highway Department Geotechnical Report for Relocated Route 44, Section I Carver, Plympton and Kingston. MHD Geotechnical Section, Boston, MA.

Dove J.E., Boxill L.E.C., and Jarrett J.B. (2000) A CPT-Based Index for Evaluating Ground Improvement. Advances in Grouting and Ground Modification, ASCE Geotechnical Special Publication 104, 296-310.

Hajduk E. L., Connors, P.J., Miller H. J., and Meng, J. (2004), "Verification testing of deep dynamic compaction between sheet piling using cone penetration testing", *Proc. of the 2004 Intern. Symp. on Ground Improvement*, Paris, France.

Lukas, R.G. (1995), Geotechnical Engineering Circular No.1: Dynamic Compaction, Report FHWA-SA-95-037, Federal Highway Administration, Washington, D.C.

Marchetti, S. (1975), "A New In Situ Test for the Measurement of Horizontal Soil Deformability", Proceedings of the Conference on In Situ Measurement of Soil Properties, ASCE Specialty Conference, Raleigh, NC, June, Vol. 2, pp. 255-259.

Marchetti, S., Monaco, P., Totani, G. and Calabrese, M. (2001), "The Flat Dilatometer Test (DMT) in Soil Investigations", a report by the ISSMGE Committee TC16, Proceedings of the International Conference on In Situ Measurements of Soil Properties, Bali, Indonesia, May, 41 p.

Massachusetts Highway Department (1999) Project Specifications for Relocated Route 44, Section I Carver, Plympton and Kingston. Boston, MA.

Schmertmann, J., Baker, W., Gupta, R. and Kessler, K. (1986), "CPT/DMT QC of Ground Modification at a Power Plant", Proceedings of In Situ '86, Blacksburg, Virginia, June, ASCE Geotechnical Special Publication No. 6, pp. 985-1001.

Youd T.L. and Idriss I.M. (2001) Liquefaction Resistance of Soils: Summary Report from the 1996 NCEER and 1998 NCEER/NSF Workshops on Evaluation of Liquefaction Resistance of Soils" Journal of Geotechnical and Geoenvironmental Engineering 127 (4), 297-313.

APPENDIX: UNIT CONVERSIONS

1 foot (ft) = 0.3048 m
1 kip/in^2 (ksi) = 6.895 MPa
1 kip/ft^2 (ksf) = 47.88 kPa
1 British ton-force/ft^2 (tsf) = 95.76 kPa

Suitability of the SDMT method to assess geotechnical parameters of post-flotation sediments.

Zbigniew Młynarek, Sławomir Gogolik
August Cieszkowski Agricultural University of Poznań, Poland
Diego Marchetti
Studio prof. Marchetti, Rome, Italy

ABSTRACT: The paper presents a comparison of results of SDMT, CPTU and SCPTU, which were obtained while investigating post-flotation deposits. Tests were performed at the Żelazny Most mine waste dump near Lubin (Poland). In this location the dump embankments are formed from post-flotation sediments of copper ore. The article contains statistical assessment of differences between geotechnical parameters of the sediments, determined using the above mentioned methods.

1 INTRODUCTION

Post-flotation sediments, which are process wastes in the processing of copper ore, are unconventional materials used in earthen structures. This is the case in the development of one of the biggest tailing waste dumps in the world, i.e. the Żelazny Most Dump near Lubin (Poland). A precise determination of geotechnical parameters of sediments is a crucial issue for the design of the development of this dump. This problem, in the case of the Żelazny Most Dump, needs to be emphasized as at present the embankments are 45 m high, and the planned development forecasts the elevation of the dump embankments to 100 m. For this reason, the most modern in-situ tests are being used to assess parameters of shear strength and constrained moduli. The basic method to investigate properties of sediments is the cone penetration tests i.e. CPTU (Młynarek, Tschuschke, Lunne 1994; Młynarek 2000)
The necessity to evaluate constrained moduli of sediments and subsoil, especially small strain shear modulus G_0, resulted in the undertaking of testing using a Marchetti dilatometer, including its latest version – an SDMT seismic dilatometer. The suitability of the application of this device is evaluated and a comparative analysis of the results with those obtained using other methods is presented in this study.

2 THE OBJECT OF THE STUDY, A CHARACTERISTIC OF POST-FLOTATION SEDIMENTS

Calibration testing for CPTU, SCPTU and DMT was performed on the beach and embankments of the Żelazny Most Dump (Fig. 1). The current volume of accumulated waste is 350 million m^3, and the length of embankments is 14.5 km. Flotation tailings are transported to the dump using the hydrotransport method, and then are spilled onto the dump beach.

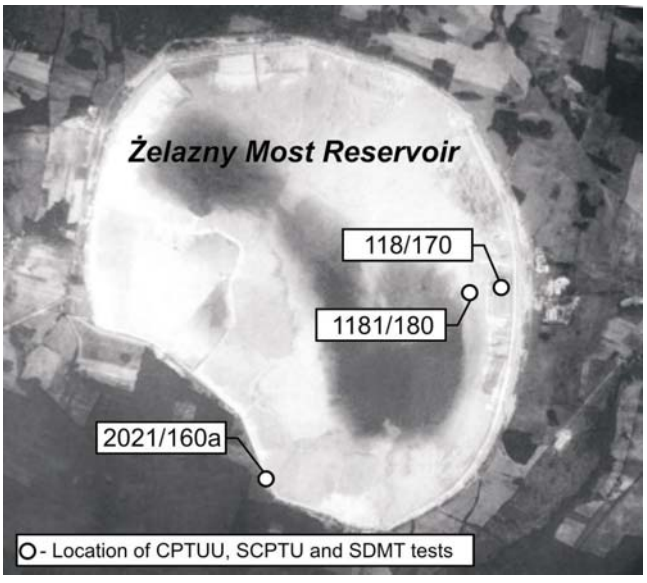

Figure 1. Location of CPTUU, SCPTU and SDMT tests

This type of waste transport and beach formation results in the segregation of sediment grains (Wierzbicki 2000). Embankments are formed from the material found on the beach in a zone approx. 70

m wide. The concentration of the material and the method of its transport to the dump results in the sediments embedded in the embankments exhibiting numerous laminations and considerable anisotropy of the structure (Młynarek 2000). The grain size distribution of sediments classifies them as silty and fine sands. Some sediments exhibit the grain-size distribution of silts and silty clays. This group of sediments is found at the distance ranging from 60 to 300 m from the top of the embankment (Wierzbicki 2000) and generally is not used for the construction of the embankments. Calibration tests were performed at the so-called investigation points, where apart from SCPTU and SDMT also CPTU was conducted along with vane tests, and MOSTAP cores were collected for the purpose of laboratory testing. Calibrations of SCPTU were performed through an analysis of significance of differences between measured values of cone resistance q_c, friction of the frictional sleeve f_s and excess pore pressure, measured in this test and the values recorded in the standard CPTU. The comparison was performed at various levels of geostatic stress σ_{vo}. This analysis showed that mean values of parameters from CPTU – q_c, f_s, u_2, u_1 did not differ statistically from identical parameters obtained from SCPTU. On the basis of this assessment it was assumed that parameters from SCPTU may be used to calibrate parameters from SDMT, and as a result may constitute the basis for an unambiguous assessment of the suitability of a seismic dilatometer to investigate mechanical properties of sediments, embedded in the dump.

3 CHARACTERISTIC CURVES OF SCPTU AND SDMT IN POST-FLOTATION SEDIMENTS

Figure 2 presents characteristic curves of SCPTU and SDMT in one of three investigation points. It may be observed that q_c from SCPTU and P_0, P_1 from SDMT react in a similar way to changes in soil properties, in particular to the sediment macrostructure. Similar trends are also observed (Fig.3) in the D_r (SCPTU) and K_d (SDMT) profiles. Changes in macrostructure, as has been indicated previously, are the effect of numerous and very thin interbeddings in sandy sediments with cohesive soils. The effect is very well documented also by the recorded pore pressures u_1 and u_2.
High consistency is also found for the trend in the recorded seismic wave along with depth (Fig. 2).

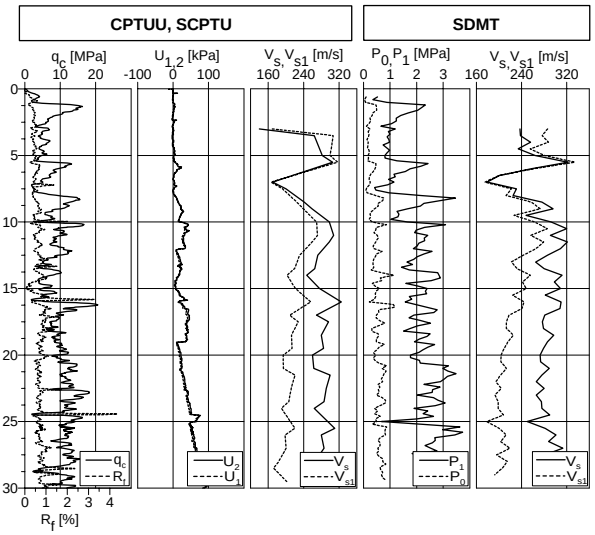

Figure 2. CPTUU, SCPTU and SDMT characteristics at investigation point No. 118/170

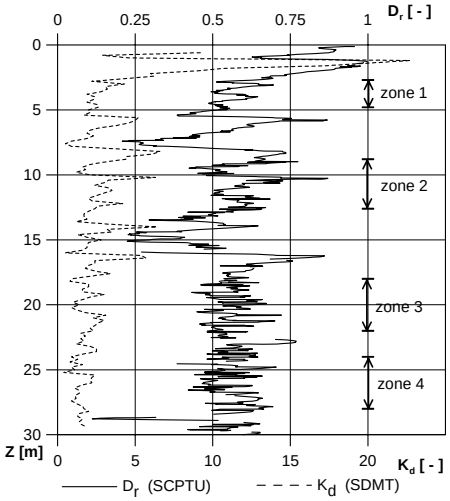

Figure 3. Changes of D_r and K_d with depth

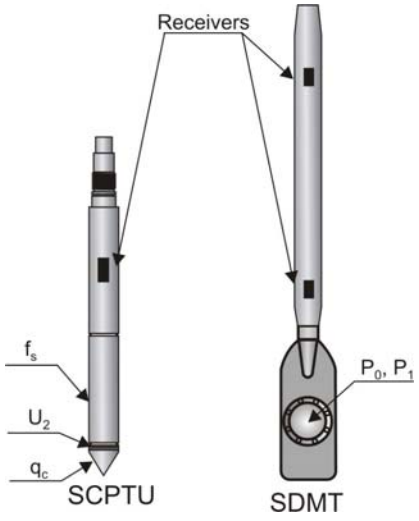

Figure 4. SCPTU cone and SDMT blade

The seismic cone by Ap van den Berg (Holland) used in this study was equipped with one geophone, whereas the seismic dilatometer – with two geophones (Fig. 4). A comprehensive assessment of

the consistency or inconsistency of SCPTU and SDMT may be obtained through a statistical analysis of differences between the geotechnical parameters of sediments estimated with the application of both tests. Such an analysis is presented below.

4 METHODOLOGY OF ASSESSMENT OF COMPATIBILITY OF ESTIMATION FOR GEOTECHNICAL PARAMETERS OF SEDIMENTS USING SCPTU AND SDMT

Four geotechnical parameters of sediments were selected for the analysis, i.e. relative density D_r, effective friction angle ϕ', constrained modulus corresponding to oedometer modulus M and shear modulus G_0. The selection of parameters was based on the inclusion in the analysis of a differing effect of geostatic stresses on measured parameters in both tests. (Jamiolkowski, 2002).

The following procedure algorithm was adopted for statistical assessment of compatibility of estimated geotechnical parameters of sediments. First, homogeneous sediment zones were determined in the embankments using the filtration method, in terms of relative density D_r (Fig. 3), and next in the established zones mean values were calculated for the effective friction angle - ϕ', as well as mean values of constrained moduli M and G_0. Values of relative density were determined from the formula, which was established on the basis of extensive documentation material from sediment testing, (Młynarek, Tschuschke, Lunne 1994):

$$D_r = a \cdot \sigma_{v0}^{b} \cdot \ln(q_c) + c \cdot \ln(\sigma_{v0}) + d \qquad (1)$$

where:

a,b,c,d – constants depended on tailings type

This extensive documentation material made it also possible to adopt formulas to determine constrained modulus from CPTU.

$$M = m(q_c - \sigma_{v0}) \qquad (2)$$

where:

m - constant depended on type of tailings (Młynarek, Tschuschke, Lunne 1994)

The shear modulus G_0 is obtained from V_s by SCPTU with the usual elasticity formula:

$$G_0 = \rho \cdot V_s^2 \qquad (3)$$

where:

ρ – mass density

V_s – shear wave velocity

while the effective friction angle was obtained with the formula:

$$\phi' = 17{,}6 + 11 \cdot \log(q_{c1}) \qquad (4)$$

where:

q_{c1} – normalized cone resistance

$$q_{c1} = \left[\frac{q_c}{p_a}\right] \cdot \left[\frac{p_a}{\sigma'_{v0}}\right]^{0{,}5} \qquad (5)$$

For the purpose of assessment of the analyzed geotechnical parameters of sediments using DMT the relationships were adopted after Marchetti (2001).

A detailed analysis of significance of differences in the assessment of geotechnical parameters of sediments using both methods may be preceded by several interesting observations, namely similar trend was found for all the investigation points. Consistent trend in changes of both parameters (D_r and K_d) shows that coefficient K_d may be used to assess changes in relative density of sediments in embankments.

It results from a comparison of constrained modulus profiles (Fig. 5) that values of moduli obtained from SDMT are higher than those from CPTU. This difference is much higher in the range of small values of σ_{v0} (at shallow depths) and high values of relative density, and the difference between moduli decreases along the depth. Differences in values of constrained moduli are well justified since sediments are characterized by their anisotropic macrostructure, connected with the above mentioned laminations. It results from studies by Muromachi (1981) that the mechanism of the formation of plastic areas under the cone differs from that in the volume of soil facing the Dilatometer membrane (Marchetti 1999).

Moreover, it clearly results from studies by Silva, Bolton (2004) that in case of stratified sands cone resistance and area of destruction zones are affected by laminations found at the distance of 3 cone diameters from the cone base. These elements probably result in different rigidity of sediments in the vertical and horizontal planes and differing values of constrained moduli determined in SDMT and SCPTU. The same factors determined differences in forecasted changes of effective friction angle of sediments along with depth (Fig. 6). Higher assessed values were obtained from CPTU for friction angle ϕ' than it was the case in SDMT, with the trend to increase the difference between friction angles along with an increase of σ_{v0}.

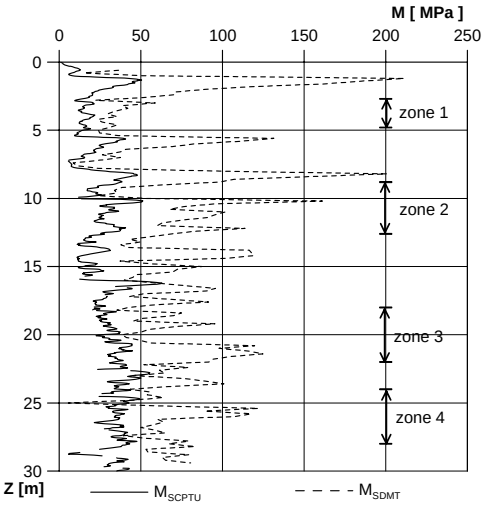

Figure 5. Changes of M_{SDMT} and M_{SCPTU} with depth

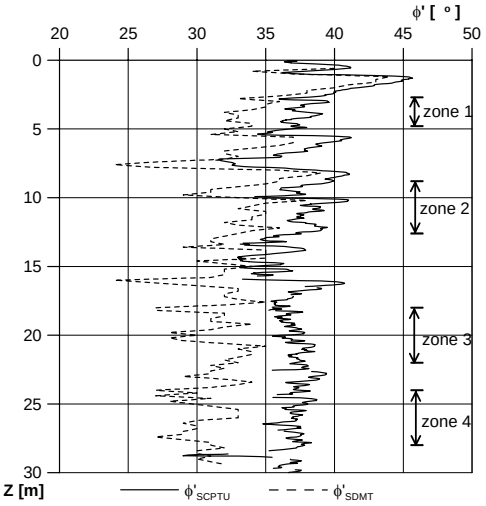

Figure 6. Changes of ϕ' with depth

5 STATISTICAL ASSESSMENT OF SIGNIFICANCE OF DIFFERENCES BETWEEN GEOTECHNICAL PARAMETERS OF SEDIMENTS FROM SCPTU AND SDMT

Statistical assessment of differences in forecasted constrained moduli and internal friction angles ϕ' of sediments was performed for rather "uniform" depth zones. In this way, it was attempted to additionally assess the effect of geostatic stress σ_{v0} on the investigated differences between mean values of M and ϕ' obtained from both tests. The analysis was carried out using the results obtained at investigation point (118/170), while in the other investigation points the results were very similar. It may be observed from Table 1 that mean values of moduli and friction angles from SDMT and SCPTU tests are statistically different at the significance level of α=0.05 in all ranges of σ_{v0} (Fig. 7), whereas comparison of significance of the variance differences proves these values to be non-significant. The latter conclusion shows that the assessment of variation in parameters M and ϕ' measured using both methods in each range of σ_{v0} is very similar. However, confidence intervals differ in size (Fig. 7). This results from differences in sample size from SDMT and SCPTU tests.

Table 1. Results of statistical analysis of significance of differences between M and ϕ' from SDMT and SCPTU

		Mean value (ϕ', M)		p-value*
		SDMT	SCPTU	
zone 1	M_{SDMT} vs. M_{SCPTU}	35,74	15,66	0,000
	ϕ'_{SDMT} vs. ϕ'_{SCPTU}	33,92	37,60	0,000
zone 2	M_{SDMT} vs. M_{SCPTU}	73,81	29,08	0,000
	ϕ'_{SDMT} vs. ϕ'_{SCPTU}	33,58	38,03	0,000
zone 3	M_{SDMT} vs. M_{SCPTU}	72,62	32,11	0,000
	ϕ'_{SDMT} vs. ϕ'_{SCPTU}	31,33	37,05	0,000
zone 4	M_{SDMT} vs. M_{SCPTU}	66,67	36,62	0,000
	ϕ'_{SDMT} vs. ϕ'_{SCPTU}	29,95	37,20	0,000

* statistical significance

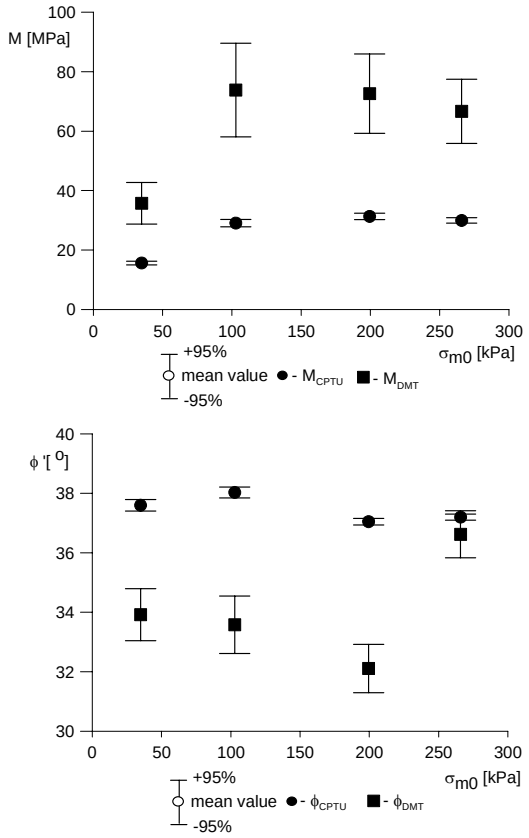

Figure 7. Statistical evaluation of mean values of M modulus and ϕ' from SCPTU i SDMT tests on different levels of σ_{v0}

The result of the analysis of significance of differences in the constrained moduli established using both methods is of paramount importance. The conclusion is consistent with previously given comment on the effect of anisotropy on deformability of sediments in horizontal and vertical direction. On the other hand, a dependence may easily be developed, which on the basis of constrained modulus from SDMT makes it possible to determine compression modulus of sediments

based on CPTU test. Fig. 8 suggests that this dependence is statistically highly significant. The regression coefficient changed in individual investigation points from 0.79 to 0.90, while in the global analysis (Fig. 8) this coefficient was 0.76. It needs to be stressed that the coefficient defining the M_{DMT}/q_c ratio was on average 8.1, while proposed by Marchetti (1999) for NC sands should fall within the range from 5 to 10.

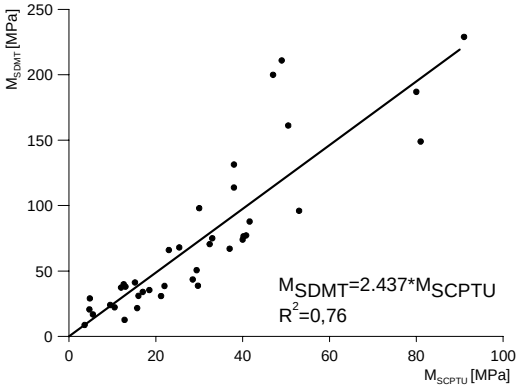

Figure 8. Relationship between the modulus M from SDMT and SCPTU tests

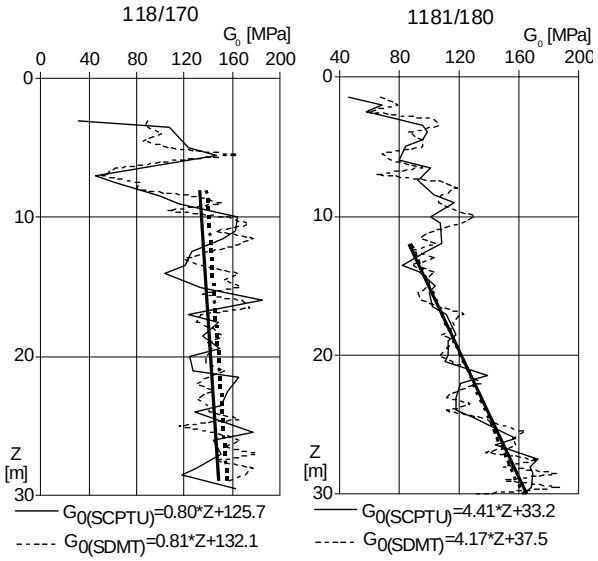

Figure 9. Changes of $G_{0(SCPTU)}$ and $G_{0(SDMT)}$ with depth

The main aim of the investigations was to analyze the suitability of SDMT to assess the G_0 modulus, while - as it has been said previously - the reference point for this analysis was SCPTU. The most unambiguous assessment of differences in the forecasted shear modulus G_0 found using both methods may be obtained by analyzing zones of sediments in subsoil with a uniform parameter D_r. In this way the effect of this factor on this dependence is eliminated, while the effect of the trend of changes in shear modulus G_0 along with a change of σ_{v0} is taken into consideration. Figure 9 shows two extreme case of the effect of the trend in the investigated points. To assess differences in the forecasted modulus G_0 with the use of both methods, the significance of differences between coefficients of regression line was investigated. The conducted analysis (Table 2) showed that the coefficients of regression line in each node do not differ statistically at $\alpha = 0.05$. This conclusion makes it possible to formulate an unambiguous opinion that the assessment of values of modulus G_0 using both methods and its variation along with changes in the state of geostatic stress in subsoil is very similar.

Table 2. Results of statistical analysis for relationship G_0 versus depth

Inv. point	F	p	k(0,05)
118/170	0,040	0,841	3,991
1181/180	0,161	0,689	4,007
2021/160a	0,187	0,669	4,183

k-critical value on significance level α=0,05

6. CONCLUSIONS

On the basis of the conducted investigations a general opinion may be formulated that the seismic dilatometer may be considered a very useful device for the assessment of values of constrained moduli in sediments. An especially crucial conclusion is the finding that the identification of the trend in changes of moduli and effective friction angle along with changes in geostatic stress in the dump embankments using SCPTU, CPTU and SDMT is almost identical. The shown effect of laminations (anisotropy) on the forecasted values of moduli and the effective friction angle of sediments emphasizes the advisability of the application of both tests at the dump. This principle ought to be also applied in geotechnical situations of soils with exposed macrostructure and - connected with it - anisotropy. As shown in Fig. 9, there is practically coincidence between G_0 from SCPTU and G_0 from SDMT tests.

REFERENCES

Jamiolkowski M., Le Presti D.C.F., Manassero M. (2001) Evaluation of relative density and shear strength of sands from CPT and DMT. C.C.Ladd Symposium M. 15 Cambridge Mass.

Marchetti S., Monaco P., Calabrese M. Totani G. (1999) The flat dilatometer test. A report to the ISSMGE Committee TC-16.

Marchetti S. (2001) The flat dilatometer. 18th CGT – Conference Geotecnica Torino.

Mayne P., Martin M. (1999) Small and large strain soil properties from seismic flat dilatometer tests. Proceedings of Conference Pre-failure Deformation Characterization of Geomaterials.

Młynarek Z., Tschuschke W., Lunne T. (1994) Techniques for examining parameters of post flotation sediments accumulated in the pond. Proceedings of the third

International Conference, Re-use of Contaminated Land and Land fills. University of Edinburgh, Press London.

Młynarek Z. (2000) Effectiveness of in-situ tests in evaluation of strength parameters of post-flotation sediments. Proceedings of 2000 Geotechnics. Geotechnical Engineering Conference Bangkok.

Muromachi T. (1981) Cone penetration testing and experience. ASCE. St. Louis.

Silva M.F., Bolton M.D. (2004) Centrifuge penetration tests in saturated layered sands. Proceedings of the seconds International Conference on Site Characterization. Porto

Studio Prof. S. Marchetti & HEBO Poznań Report (2005) Seismic Dilatometer Tests (SDMT) Zelazny Most Dam.

Tschuschke W., Młynarek Z., Wierzbicki J. (1999) Assessing deformation modulus from dilatocone and seismic cone tests results. The 12th European Conference on Soil Mechanics and Foundation Engineering. Amsterdam, Balkema.

Wierzbicki J., Tschuschke W., Pordzik P.(2000), Statistical evaluation of tailings grain size distribution of the Zelazny Most reservoir dams , 12th National Conference on Soil Mechanics and Foundation Engineering, Międzyzdroje

DMT testing for consolidation properties of the Lake Bonneville Clay

A. T. Ozer
Geotechnical Engineer, Ph.D., BCI Engineers and Scientists Inc., 2000 E. Edgewood Drive, Ste. 215 Lakeland, FL 33803

S. F. Bartlett
Assistant Professor, PE., University of Utah, Dept. of Civil and Environmental Engineering 122 South Central Campus Drive,113 EMRO Salt Lake City, Utah 84112-0561

E. C. Lawton
Professor, PE., University of Utah, Dept. of Civil and Environmental Engineering 122 South Central Campus Drive, 109 EMRO Salt Lake City, Utah 84112-0561

Keywords: DMT, CRS consolidation test, Lake Bonneville clay, compressibility, consolidation

ABSTRACT:

This paper discusses the use of the flat dilatometer test (DMT) to estimate the compressibility of the Lake Bonneville clay in Salt Lake City, Utah. The DMT is evaluated regarding its effectiveness in predicting the virgin compression ratio (CR), 1-D constrained modulus (*M*), preconsolidation stress (σ'_p) and overconsolidation ratio (*OCR*). This is accomplished by correlating DMT parameters with results obtained from high quality sampling and laboratory constant rate strain consolidation (CRS) tests. Multiple linear regression (MLR) analyses were carried out to develop correlations of CR, M, and σ'_p with DMT parameters. This study shows that the DMT can be successfully used to predict consolidation properties for soft, clayey deposits. These findings can significantly reduce the amount and cost of conventional sampling and laboratory testing performed by geotechnical consultants in the Salt Lake Valley for settlement evaluations in the Lake Bonneville clay.

1 INTRODUCTION AND RESEARCH SITES

The flat dilatometer test (DMT) was developed in Italy by Marchetti (1980). It was initially introduced in North America and Europe in 1980 and is currently used in over 40 countries. Test procedures are described by Marchetti (1980) and Schmertmann (1986).

The Utah Department of Transportation funded a study to develop in situ methods to predict consolidation properties of the soft to medium stiff clays found in Salt Lake Valley, Utah. The objectives of this research were to correlate high quality CRS laboratory results with DMT results so that the latter can be used in geotechnical evaluations of the Lake Bonneville clay. Evaluation of the effectiveness of the DMT in predicting the virgin compression ratio, CR, and the preconsolidation stress, σ'_p, was accomplished by comparing the field results with CRS laboratory test results.

Undisturbed samples of Lake Bonneville Clay were taken in three locations of the Salt Lake Valley near the I-15 alignment in downtown Salt Lake City. A B-80 mobile drill rig was used for drilling. At the South Temple Street location, two sites were drilled, one underneath the northbound bridge and one in the embankment median of the interstate, just north of the north abutment of the South Temple Street Bridge. At the North Temple Street location, the drilling was done in a vacant lot northeast of the northbound structure. For the North Temple Street site, rotary wash drilling was used and for both South Temple Street sites, hollow stem auger drilling methods were used. The CRS tests were performed on high quality undisturbed samples obtained from piston samples and Shelby tube samples were used for soil classification and determination of index properties purposes. The overlying and underlying Holocene and Pleistocene alluvium, respectively, were not sampled. These units are more granular and not as compressible.

The surficial Holocene alluvium at the research sites consists of about 5 m of interbedded clay, silt, and sand and was not part of the scope of this study. The alluvium is underlain by about 15 m of lacustrine Lake Bonneville deposits. This Pleistocene sequence consists of interbedded clayey silt and silty clay, with thin beds of silt and fine sand found near the middle of the sequence. These interbedded sediments divide the clay into the upper Lake Bonneville clay and the lower Lake Bonneville clay (Figure 1). The upper Lake Bonneville clay is more plastic than

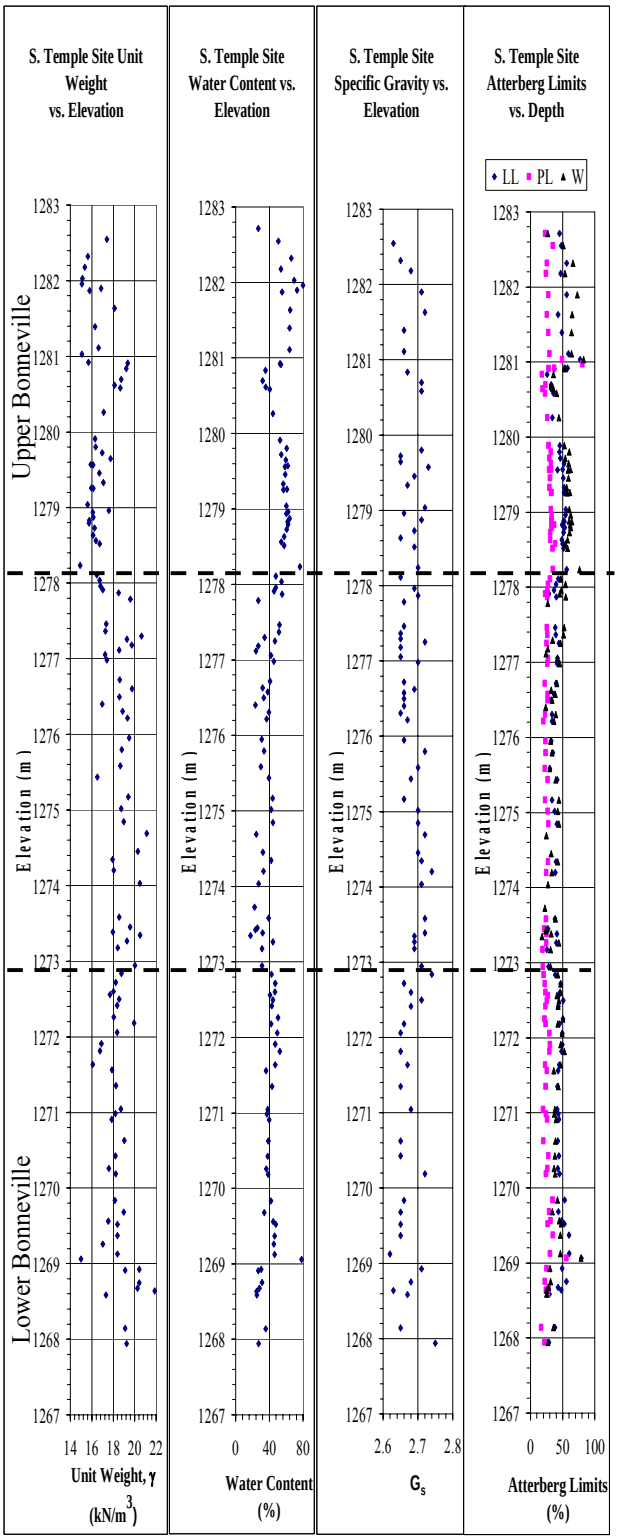

Figure 1. Physical Properties of Lake Bonneville Clay at South Temple Street Research Site

the lower clay and consists of MH, CL, and ML soils. The interbeds represent sediments that were deposited when the lake levels were lower and therefore have more granular soils representing near-shoreline conditions. The interbeds are predominantly silts (ML), with beds of clay (CL) and thin layers of medium dense sand (SC). The lower Lake Bonneville clay is found beneath these interbeds and is mainly CL soils with some silt (ML) layers.

2 DMT RESULTS

The average values of I_D, K_D and E_D for the Lake Bonneville clays at the three different research sites are summarized in Table 1.

Values of P_o and P_1 increase approximately linearly with depth for the upper Lake Bonneville clay, but P_1 did not follow the same trend for the lower Lake Bonneville clay. Also in the upper Lake Bonneville clay, the values of P_o and P_1 are very similar. (This might be attributed to very small values of I_D, which is an index of relative spacing between P_o and P_1. Values of I_D ranged from 0.22 to 0.4 for this zone). The horizontal stress index, K_D, is almost constant both for the upper Lake Bonneville clay with an average value of 3.67 and for the lower Lake Bonneville clay with an average value of 3.05. The dilatometer modulus, E_D, is almost constant for the upper Lake Bonneville clay, except for a silty clay layer at the middle of this zone. Values of E_D increase linearly with depth in the lower Lake Bonneville clay.

3 OCR AND σ'_p CORRELATIONS

A comparison of the calculated values of OCR and preconsolidation stress using Marchetti's method and from the CRS consolidation tests showed that Marchetti's method underestimates values of OCR and σ'_p compared to most of the CRS consolidation tests for the North and South Temple Street sites. However, calculated values of OCR and σ'_p from the DMT at the South Temple Street embankment site were close to those calculated from the CRS consolidation tests. The empirical equation for OCR provided by Marchetti (1980) is given in Equation (1).

$$OCR = (0.5K_D)^{1.56} \text{ for } 0.2\langle I_D \langle 2 \qquad (1)$$

From Equation (1), Marchetti (1980) proposed a functional form to determine the OCR that includes K_D. However, when values of K_D from the DMT were correlated with laboratory determined values of

Table 1. Summary of DMT Results for Bonneville Clay

DMT Test No. and Location	Average I_D		Average K_D		Average E_D	
	Upper Bonneville	Lower Bonneville	Upper Bonneville	Lower Bonneville	Upper Bonneville	Lower Bonneville
DMT – 1 N. T.	0.468	0.249	3.04	3.03	44.1	31.8
DMT -2 S. T.	0.430	0.330	3.67	3.05	43.7	57.5
DMT – 3 S. T. Embankment	0.434	---	1.85	---	110	---

OCR and σ'_p in this study, only modest correlation found. Regression relations correlating OCR and σ'_p with K_D had relatively low R^2 values of 0.458 and 0.526 respectively. To improve the predictive performance of Equation (1), additional regression analyses were carried out to find additional factors that might improve is predictive performance.

In Figure 2, the preconsolidation stress is correlated to the difference between dilatometer contact stress and hydrostatic pore water pressure, $(P_o - u_o)$, and the difference between dilatometer expansion stress and the hydrostatic pore water pressure, $(P_1 - u_o)$. These independent variables are measured by the dilatometer test (DMT) and are related to the total overburden stress, σ_{vo}:

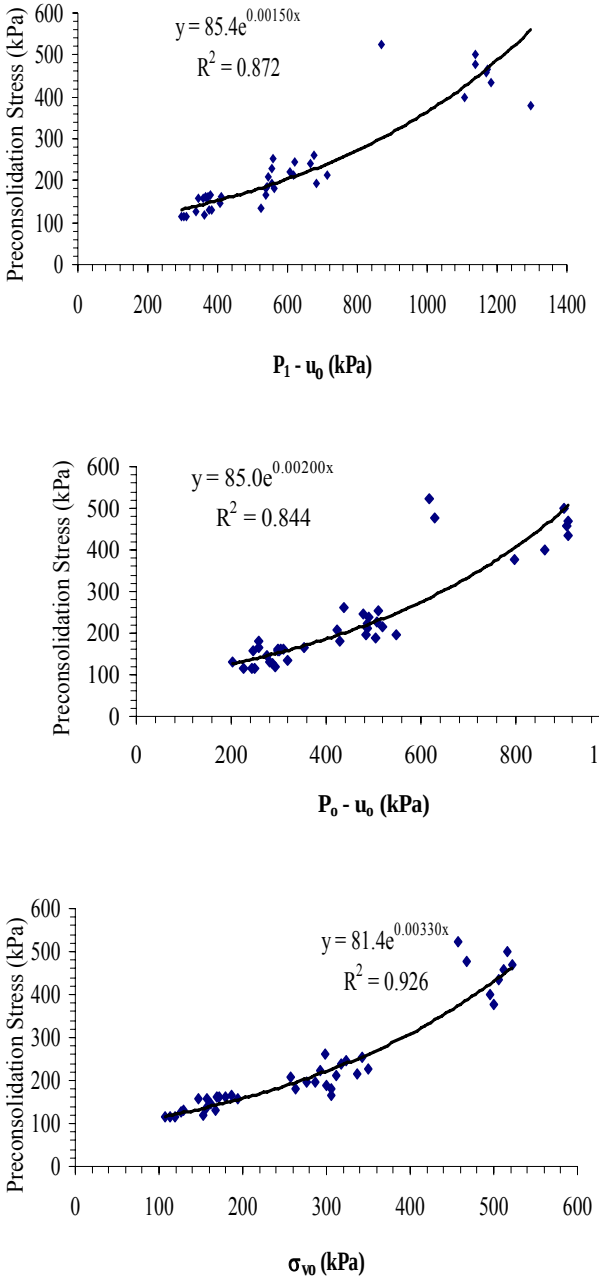

Figure 2. DMT Correlations, Dilatometer $(P_1 - u_o)$ vs. Laboratory Determined σ'_p, Dilatometer $(P_o - u_o)$ vs. Laboratory Determined σ'_p, and Total overburden stress, σ_v vs. σ'_p

$$\cap = \phi[(P_o - u_o),(P_1 - u_o),\sigma_{vo};B_{P_o-u_u},B_{P_1-u_o},B_{\sigma_{vo}}] \quad (2)$$

where:

$\cap$, is the true response, $B_{P_o-u_u}, B_{P_1-u_o}$ and $B_{\sigma_{vo}}$ are unknown regression parameters corresponding to $(P_o - u_o),(P_1 - u_o)$, and σ_{vo}.

As can be seen in Figure 2 the simple linear regression models given in Equation 2 have better R^2 values than Equation (1) for the preconsolidation stress of the Lake Bonneville clay. Thus, a MLR model was set up for σ'_p by dividing those factors correlated with σ'_p into seven different models, which are summarized in Table 2. For an application standpoint, it is preferable that a regression model not be dependent on the stress units, so all variables were divided by atmospheric pressure, P_a ($1\,P_a$ = 101.325 kPa = 1.01325 Bar), to make the variables dimensionless.

Table 2. Data Variables Sets for Preconsolidation Stress

Data Set	Independent Variables	R^2 (%)
A	$\left(\frac{P_1 - u_o}{P_a}\right)$	88.0
B	$\left(\frac{P_o - u_o}{P_a}\right)$	83.6
C	$\left(\frac{\sigma_{vo}}{P_a}\right)$	85.9
D	$\left(\frac{P_1 - u_o}{P_a}\right), \left(\frac{P_o - u_o}{P_a}\right)$	89.0
E	$\left(\frac{P_1 - u_o}{P_a}\right), \left(\frac{\sigma_{vo}}{P_a}\right)$	89.2
F	$\left(\frac{P_o - u_o}{P_a}\right), \left(\frac{\sigma_{vo}}{P_a}\right)$	88.6
G	$\left(\frac{P_1 - u_o}{P_a}\right), \left(\frac{P_o - u_o}{P_a}\right), \left(\frac{\sigma_{vo}}{P_a}\right)$	87.2

It was observed that model E, which has gave the highest R^2 value. This model has the general form:

$$y = \beta_o x_1^{\beta_1} x_2^{\beta_2} \tag{3}$$

Equation (3), can be expressed in a linear form for multiple regression using:

$$\log y = \log \beta_o + \beta_1 \log x_1 + \beta_2 \log x_2 \tag{4}$$

From the above model and the regression output by using Microsoft EXCEL, the linear regression can be back transformed to:

$$\frac{\sigma'_p}{P_a} = 0.528 \left(\frac{P_1 - u_o}{P_a} \right)^{0.609} \left(\frac{\sigma_{vo}}{P_a} \right)^{0.352} \tag{5}$$

From an application standpoint all of the models shown in Table 2 appear to be adequate for use. Based on R^2, Equation (5) has the best correlation, but is only slightly better than the other models attempted. Also, a strong correlation between the preconsolidation stress and the total overburden stress was found. This correlation was even better than the correlation between preconsolidation stress and the effective vertical stress, which was somewhat surprising and may represent a peculiarity of this particular data set.

Regression models were also attempted using the total overburden stress instead of 1 atmospheric pressure in the denominator of Equation (5). The model has the form:

$$\log \left(\frac{\sigma'_p}{\sigma_{vo}} \right) = \log \beta_o + \beta_1 \log \left(\frac{P_1 - u_o}{\sigma_{vo}} \right) \tag{6}$$

The R^2 value of the regression analysis of Equation (6) was only 5.57 % which is considerably lower than 89.2 % for Equation (5). Thus this model was not further considered. The model given in Equation (5) is recommended as the best model to predict preconsolidation stress for the Lake Bonneville clay.

A comparison of the preconsolidation stress predicted from Equation (5) with that of Equation (1) and the laboratory CRS test results can be seen in Figure 3. Equation (5) shows a better prediction of the laboratory values than Marchetti's (1980) model for the Lake Bonneville clay. Thus, Equation (5) is recommended for these deposits.

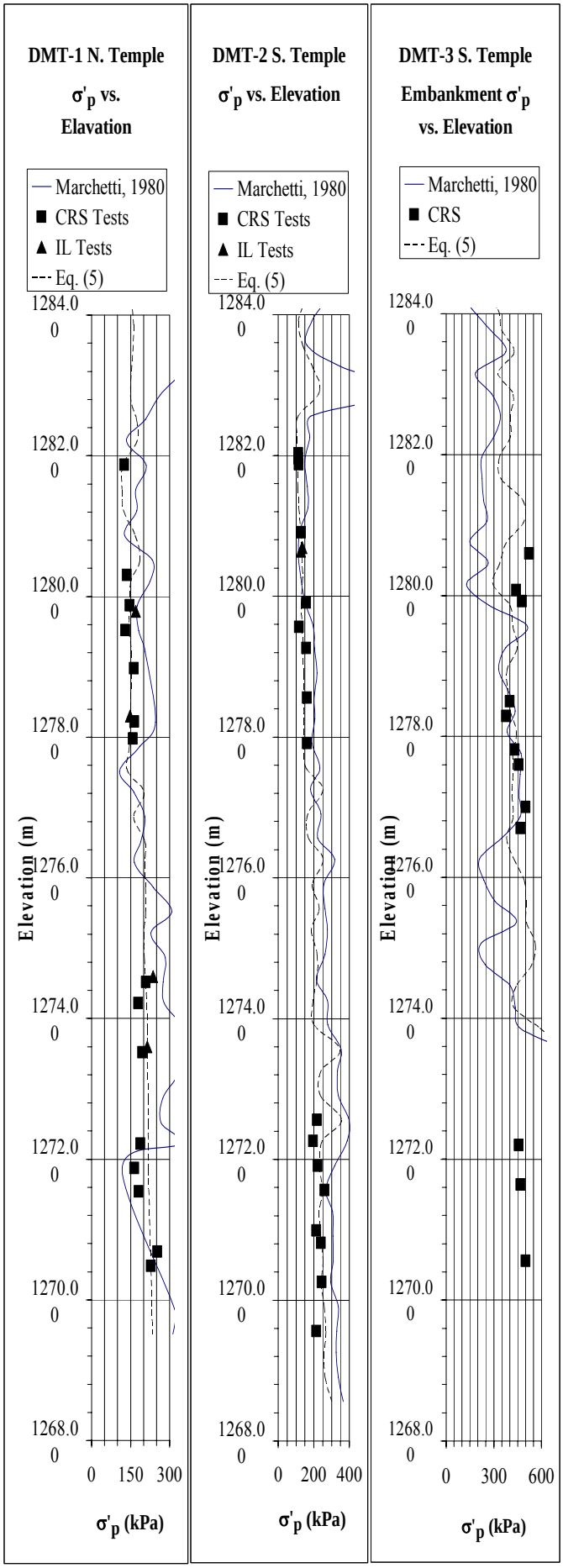

Figure 3. Comparison of Preconsolidation Stress

4 CORRELATIONS FOR COMPRESSION RATIO (CR) AND CONSTRAINED MODULUS (M)

The constrained modulus, M, defined by Marchetti (1980) for the DMT is given in following Equations 7 a, b, c, d, e, and f. From this, Equation (8) can be used to calculate the compression ratio, CR, for virgin compression. Comparison of calculated CR values from DMT results, using the method proposed by Marchetti (1980), with the laboratory CR values is provided in Figure 4. It is obvious that Marchetti's model considerably underestimates CR values for the Lake Bonneville clay.

$$M = R_M E_D \tag{7}$$

where:

$$\text{If } I_D < 0.6 \quad R_M = 0.14 + 2.36 \log K_D \tag{7.a}$$

$$\text{If } I_D > 3.0 \quad R_M = 0.5 + 2 \log K_D \tag{7.b}$$

$$0.6 < I_D < 3.0 \quad R_M = R_{M,o} + \left(2.5 - R_{M,o}\right) \log K_D \tag{7.c}$$

$$R_{M,o} = 0.14 + 0.15\left(I_D - 0.6\right) \tag{7.d}$$

$$\text{If } K_D > 10 \quad R_M = 0.32 + 2.18 \log K_D \tag{7.e}$$

$$\text{Always } R_M > 0.85 \tag{7.f}$$

$$M = \sigma'_p \left(\frac{1 + e_o}{C_c} \right) \ln 10 = \sigma'_p \frac{2.3}{CR} \tag{8}$$

and CR for normally consolidated clays can be estimated from:

$$M = \sigma'_v \left(\frac{1 + e_o}{C_c} \right) \ln 10 = \sigma'_v \frac{2.3}{CR} \tag{9}$$

According to Equations (7), Marchetti proposed a model to determine CR from K_D. The dilatometer K_D results plotted against laboratory determined CR values are shown in Figure 5. As can be seen in this figure, the correlation between laboratory CR values and K_D values is very low (R^2=5.29 %). This result also explains why Marchetti's model does not agree very well with the laboratory determined CR values, as shown in Figure 4.

Additional regression analyses were performed to improve this predictive performance. Laboratory determined CR values were correlated with $(P_0 - u_o)$,$(P_1 - u_o)$ and σ_{vo}. With these newly included variables, the R^2 values improved, but they are still relatively low (i.e., about 20 %).

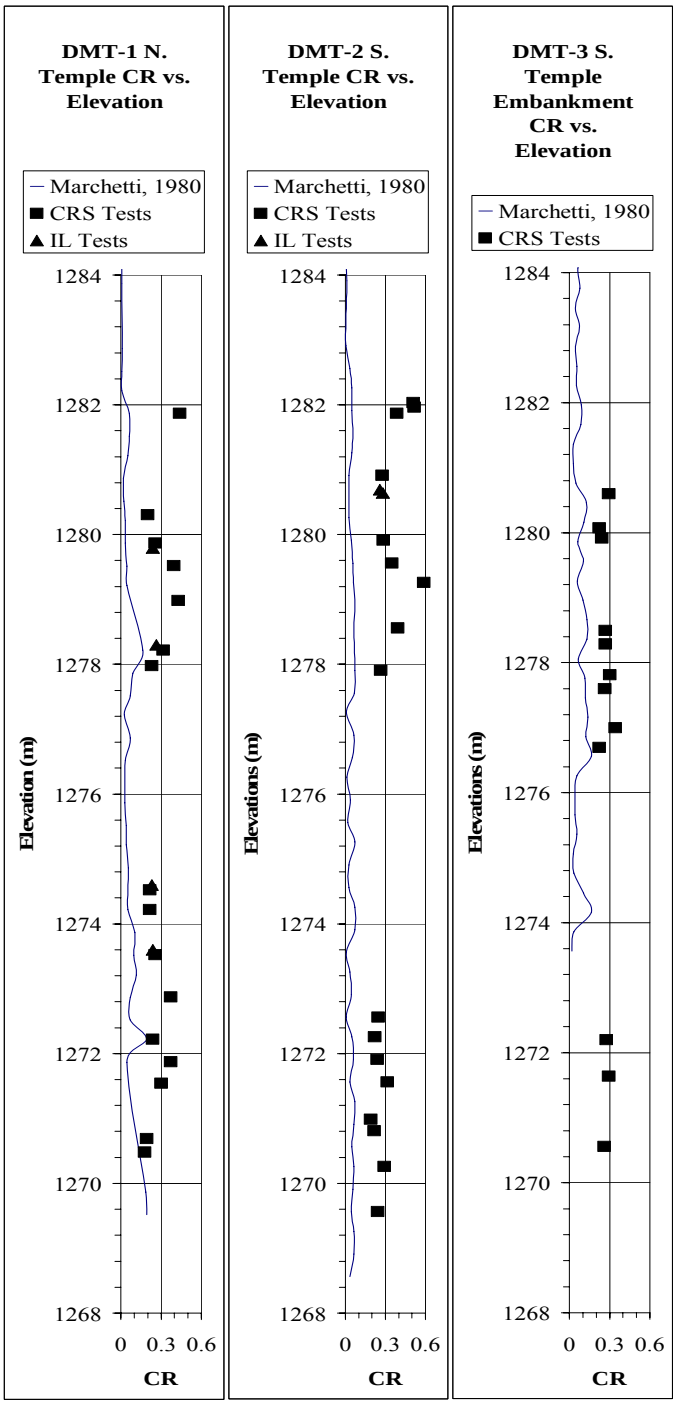

Figure 4. Comparison of laboratory CR values with values determined using Marchetti's (1980) Method

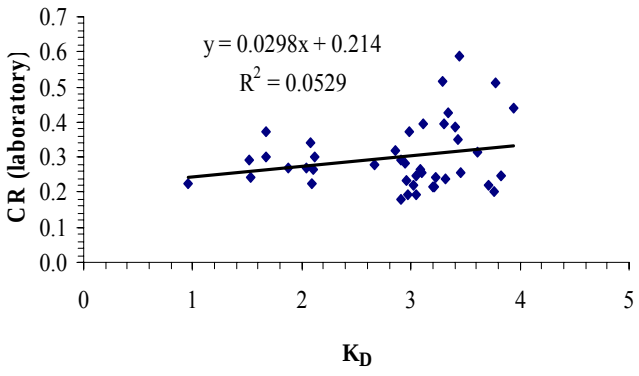

Figure 5. K_D vs. CR

As given in Equations (8) and (9), one can also back-calculate CR values from the 1D constrained modulus, M, for virgin compression. Because very low R^2 values were obtained for the CR correlations, it was decided to investigate possible correlations between the DMT and laboratory determined M values. As seen in Figure 6, laboratory determined M values plotted against values of $(P_0 - u_o)$,$(P_1 - u_o)$, and σ_{vo} produced significantly better correlation. The R^2 values improved to about 77 to 84 %.

As was done for the preconsolidation stress in the previous section, independent variables were divided into seven different models and regression analyses were conducted. Potential MLR models for M are given in Table 3.

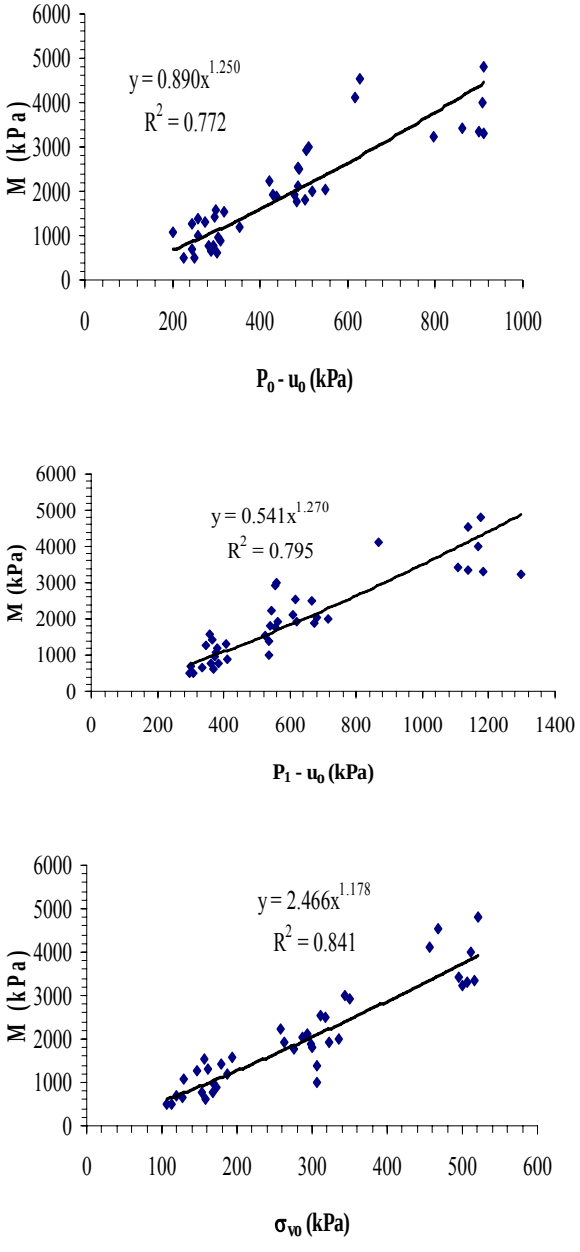

Figure 6. DMT Correlations, Dilatometer $(P_o - u_o)$ vs. Laboratory Determined M, Dilatometer $(P_1 - u_o)$ vs. Laboratory Determined M, and Total Overburden Stress vs. M

Table 3 Data Variables Sets for 1D Constrained Modulus, M

Data Set	Independent Variables	R^2 (%)
A	$\left(\frac{P_1 - u_o}{P_a}\right)$	78.9
B	$\left(\frac{P_o - u_o}{P_a}\right)$	76.6
C	$\left(\frac{\sigma_{vo}}{P_a}\right)$	83.7
D	$\left(\frac{P_1 - u_o}{P_a}\right), \left(\frac{P_o - u_o}{P_a}\right)$	80.2
E	$\left(\frac{P_1 - u_o}{P_a}\right), \left(\frac{\sigma_{vo}}{P_a}\right)$	83.8
F	$\left(\frac{P_o - u_o}{P_a}\right), \left(\frac{\sigma_{vo}}{P_a}\right)$	84.3
G	$\left(\frac{P_1 - u_o}{P_a}\right), \left(\frac{P_o - u_o}{P_a}\right), \left(\frac{\sigma_{vo}}{P_a}\right)$	83.9

Model F produced the highest R^2 value. However, from the analysis of variance (ANOVA) table of model F, it was observed that first independent variable is not significantly contributing to the model (P-value is 11.4 %). The same problem was encountered in models D, E and G. The second independent variable in models D and E was also not significantly contributing to the model, as judged from the ANOVA table, at the 95 percent confidence level. The first two independent variables in model G have also had high P-value of 75.5 and 23.9 %, respectively, which means that these variables are not statistically contributing the models. However, this does not mean that these variables are not correlated with M, it just suggests that this is cross-correlation between the independent variables in a multi variable model.

From a statistical standpoint, Model C, which has the total overburden pressure as an independent variable, is the best one variable model. Thus, for Lake Bonneville clay, M is highly correlated with the total overburden pressure. Correlations were also tried with M and effective vertical stress, but these

had poorer predictive performance for this particular data set.

It should be noted that the constrained modulus, M, is the modulus calculated at the preconsolidation stress (Equation 8). CRS Laboratory tests indicated that OCR values at the research sites have relatively constant behavior over depth. In other words, since the total overburden stress increases with depth, the preconsolidation stress also increases proportion to the total overburden stress. Since the constrained modulus is the modulus at the preconsolidation stress level, it should produce a relatively high correlation. Model C has the general form:

$$y = \beta_o x_1^{\beta_1} \tag{10}$$

This can be expressed in a linear form for multiple linear regression using:

$$\log y = \log \beta_o + \beta_1 \log x_1 \tag{11}$$

From the above equation and the MLR output, the linear model back was transformed to:

$$\frac{M}{P_a} = 5.61\left(\frac{\sigma_{vo}}{P_a}\right)^{1.18} \tag{12}$$

However, Equation (12) does not use any DMT parameters, which it not as desirable from an application standpoint. As an alternative to Equation (12), model A from Table 3, was analyzed to develop a relationship between M and DMT parameters. In short, it was found that model A is almost as good as model C from a statistical standpoint and the analysis of variance suggested that the independent variables of both model A and C are also highly correlated with each other. In other words, model A can be used to predict M as well as the total overburden stress, because of the cross-correlation.

Model A has the same general form as model C and is back transformed to:

$$\frac{M}{P_a} = 1.89\left(\frac{P_1 - u_o}{P_a}\right)^{1.27} \tag{13}$$

Ultimately, one can also back-calculate CR values from M using the definition of M from Equation (8):

$$CR_{DMT} = \frac{2.3\sigma'_p}{M\left(from\ Eq.\ 13\right)} \tag{14}$$

Comparison of M from Equations (12) and (13) and the back-calculated CR from Equation (14) with the CRS laboratory results is shown in Figures 7 and 8, respectively.

As can be seen in these figures, calculated values of M from Equations (12) and (13) and back-calculated CR values from Equation (14) closely approximate the laboratory values.

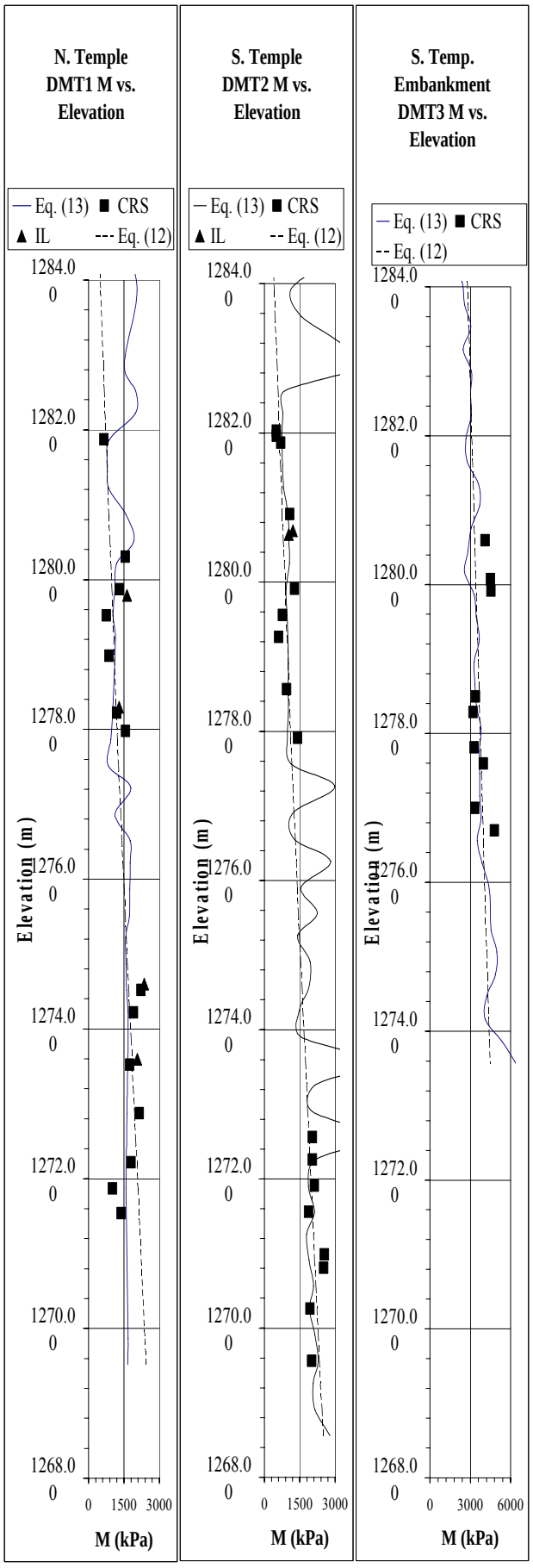

Figure 7. Comparison of constrained modulus

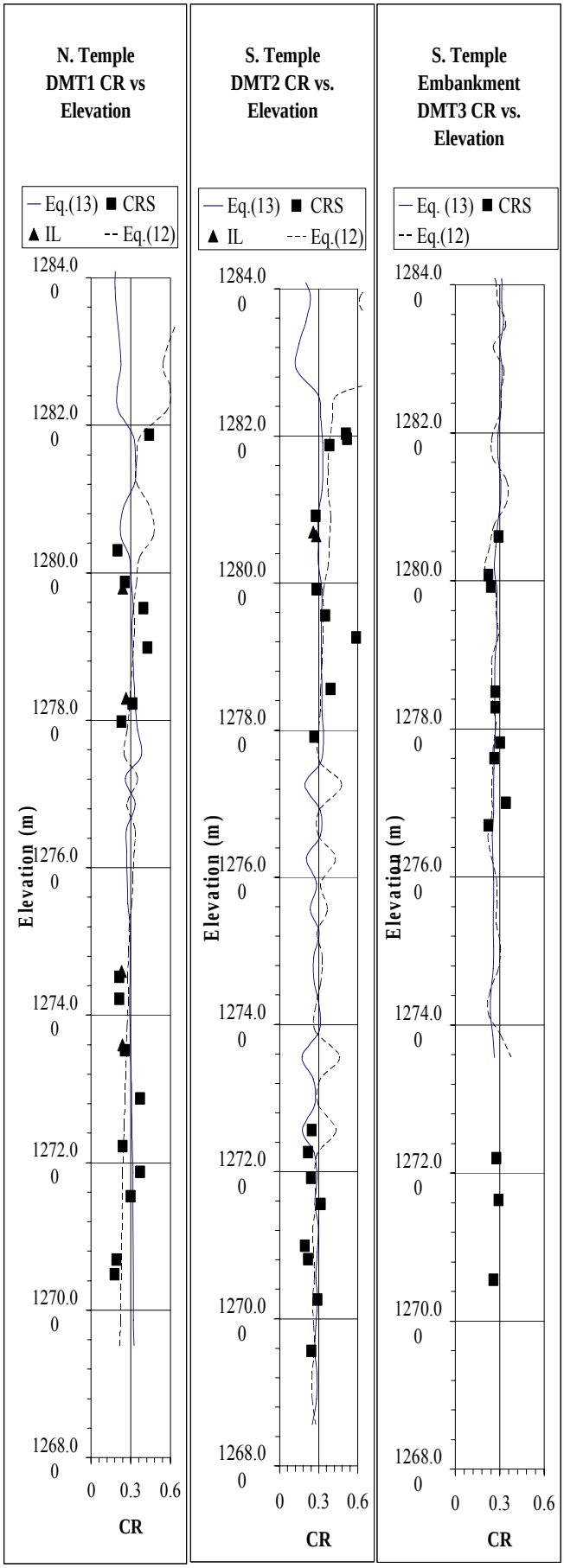

Figure 8. Comparison of compression ratio

5 CONCLUSIONS

The use of the above equations is recommended for geotechnical evaluations for locations underlain by the silty clay and clayey silt sediments of Lake Bonneville. These clayey deposits constitute the "deep water deposits" of Lake Bonneville that are found in the lower elevations of many northern Utah valleys in Salt Lake, Utah, Davis, Weber and Box Elder Counties. Although the recommended correlations were developed specifically for the Salt Lake Valley Lake Bonneville deposits, we expect that the model will have adequate performance for other northern Utah locales where the Lake Bonneville clays is found. This expectation is based on the premise that because these clays have the same geologic origin, they will be reasonably similar in their geotechnical properties, regardless of the specific location. However, it may be prudent in some cases, to perform a limited sampling and laboratory-test program to verify the performance of our models for other Utah locales outside of Salt Lake Valley. Using this approach, we anticipate that the scope of geotechnical laboratory testing can be significantly reduced for many UDOT projects. The reliability of these models from predicting behavior of clay deposits of other origins and locations is unknown, and should be further researched.

REFERENCES

Bartlett, S. F., Ozer, A. T., (2005). Estimation of Consolidation Properties from In-Situ and Laboratory Testing, *Utah Department of Transportation Research, Research Devision Report, In Review.*

Marchetti, S. (1980). In Situ Flat Dilatometer. *Journal of the Geotechnical Engineering Division of ASCE, GT3,* 299-321.

Mayne, P. W., and Kemper, J. B., (1988). "Profiling OCR in stiff clays by CPT and SPT," *Geotechnical Testing Journal*, 11(2), 139-147.

Mayne, P. W., and Frost, D. D., (1990). Dilatometer Experience in Washington, D.C., and Vicinity, *Transportation Research Record,* 1169, 16-23.

Ozer, A. T. (2005). *Estimation of Consolidation and Drainage Properties for Lake Boneville Clays*, Ph.D. Dissertation, University of Utah, SLC, UT.

Schmertmann, J. H. (1986). Suggested Method for Performing the Flat Dilatometer Test. *Geotechnical Testing Journal, GT-JODJ*, 2, 93-101.

Shallow foundations of tall buildings, designed on the basis of DMT results

Prof. Dr. Antônio Sérgio Damasco Penna

Damasco Penna Engenheiros Associados S/C Ltda

Universidade Mackenzie, São Paulo, Brazil

Keywords: Shallow foundations, tall buildings

ABSTRACT: The objective of this paper is to describe the use of DMT in the design of shallow foundations for tall buildings in Sao Paulo / SP, Brazil. This city in Brazil has a well known geologic formation, with a sedimentary basin in its central area, surrounded by residual soils. Shallow foundations are often economical, both for sedimentary over-consolidated clays and sands, and residual silty soils. The design of those shallow foundations, for typical 20–25 floor buildings, is controlled by settlements. Dilatometer tests DMT, performed with SPT and CPT, were used in those settlements evaluations and provided the necessary support for design decisions.

1 GEOLOGICAL CONDITIONS OF SAO PAULO

Sao Paulo is a 1.516 Km^2 (585 mi^2) city, and when including suburbs its area is about 3.000 Km^2 (1,158 mi^2).

The elevations above sea level generally vary between 730 m (2,395 ft) and 830 m (2,723 ft), with a maximum of 1.126 m (3,694 ft) at Jaragua Peak.

During the tertiary geological age, a sedimentary basin was formed, with many layers of clays and sands, reaching elevations of 830 m (2,723 ft) above sea level.

Gradually, the two principal rivers, Tiete and Pinheiros, partially eroded valleys to about elevation 730 m (2,395 ft).

Many mountains of gneissic or granitic residual soils surround this basin.

In this area a large number of tall buildings have been constructed both in the central area (sedimentary basin) and in the contour area (mountains of residual soils).

2 SITE CHARACTERIZATION PRACTICE

Generally, the practice of foundation engineering in Brazil is based on Standard Penetration Test (SPT) results.

The use of additional site characterization, based on field (CPT, DMT, PMT) or laboratory tests is rare.

Since 1997 we have been encouraging the use of DMT as an additional field test.

This practice has been growing slowly in some construction companies. We have demonstrated that a better site characterization can be obtained with DMT. With the more accurate DMT data a better foundation design can occur resulting, in some cases in lower foundation construction costs.

3 BUILDING FOUNDATIONS IN SAO PAULO

The development of building constructions in Sao Paulo started around 1930 - 1940.

Five to fifteen floors were common at that time.

Shallow foundations on spread footings, drilled piers with enlarged base, obtained by manual under reaming and with or without the aid of compressed air, “Franki” piles, precast concrete piles and steel piles, were all used then.

Since 1970 - 1980 slurry method of drilled pier construction and concrete flight auger piles have been used.

Nowadays, most tall buildings in Sao Paulo are constructed on piled foundations.

The number of floors is growing as well as the total weight of the building.

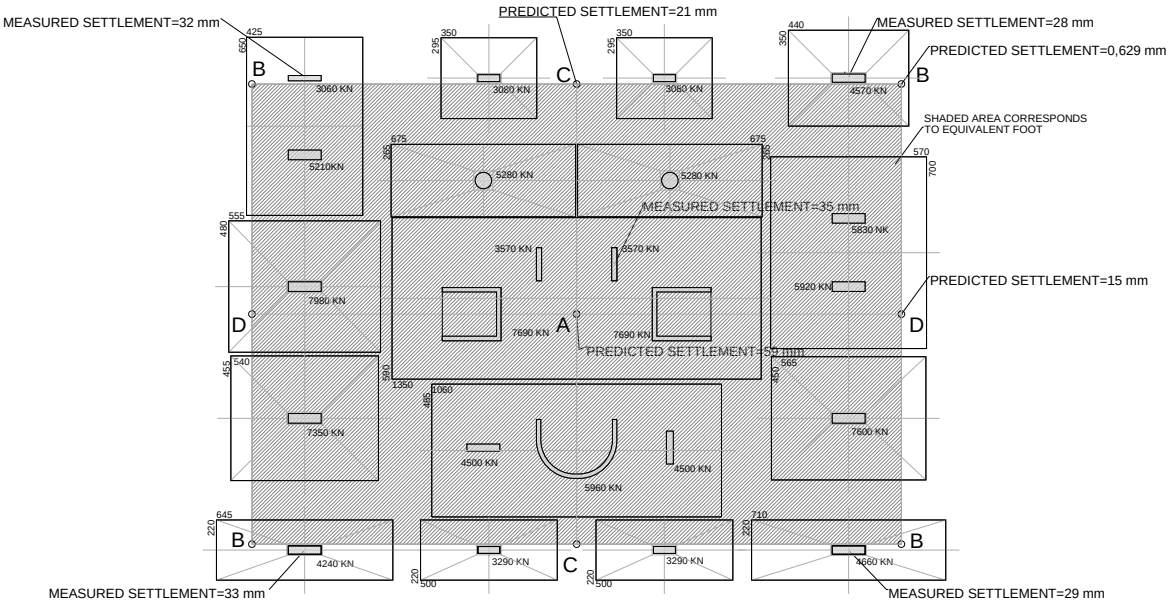

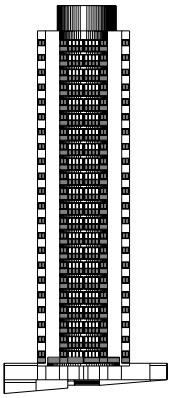

STANDARD PENETRATION TEST (SPT)	MARCHETTI DILATOMETER TEST (DMT)	CONE PENETRATION TEST (CPT)

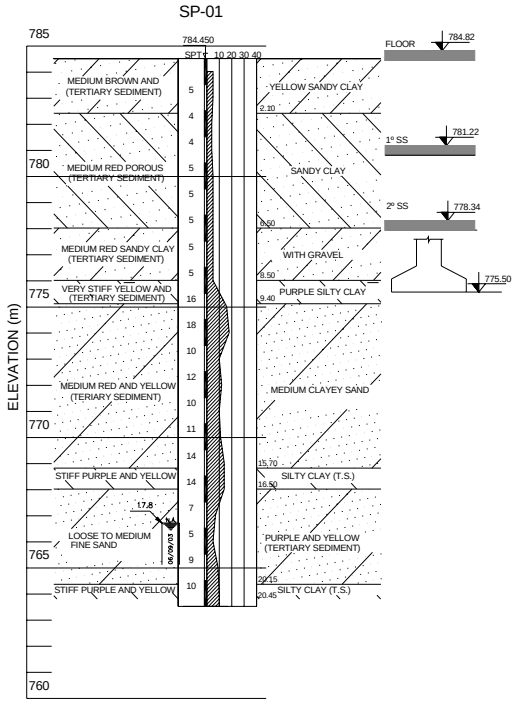

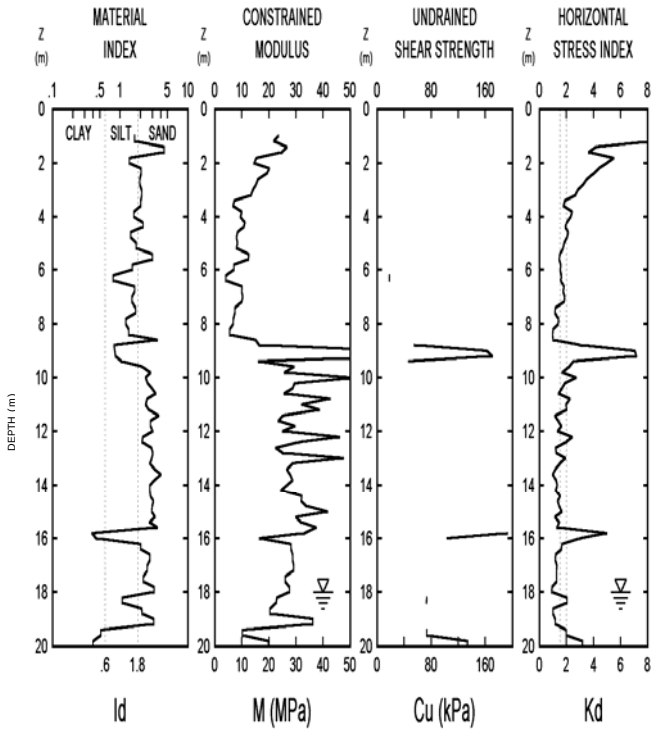

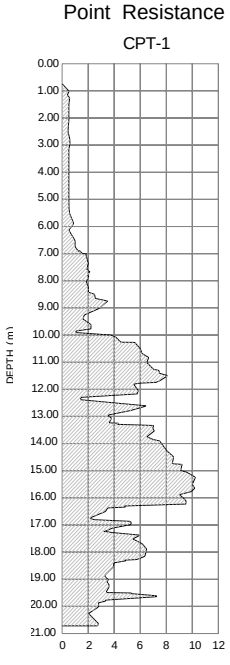

Figure 1. Pompéia building

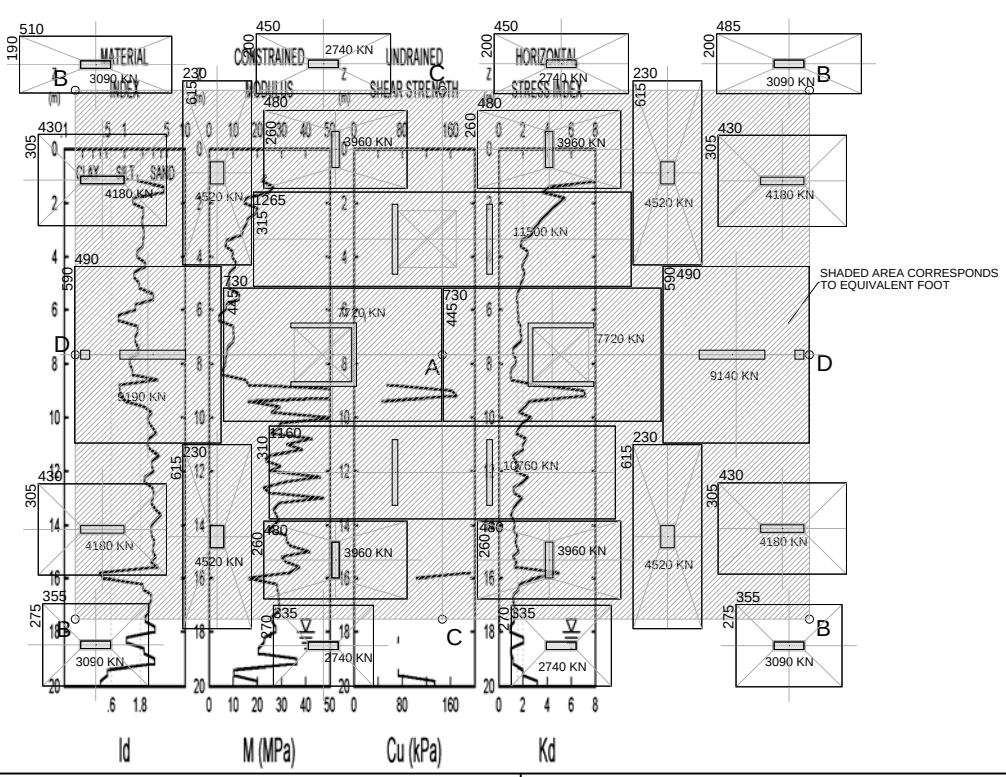

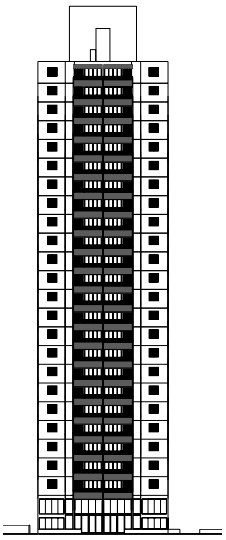

STANDARD PENETRATION TEST (SPT)	MARCHETTI DILATOMETER TEST (DMT)	CONE PENETRATION TEST (CPT)

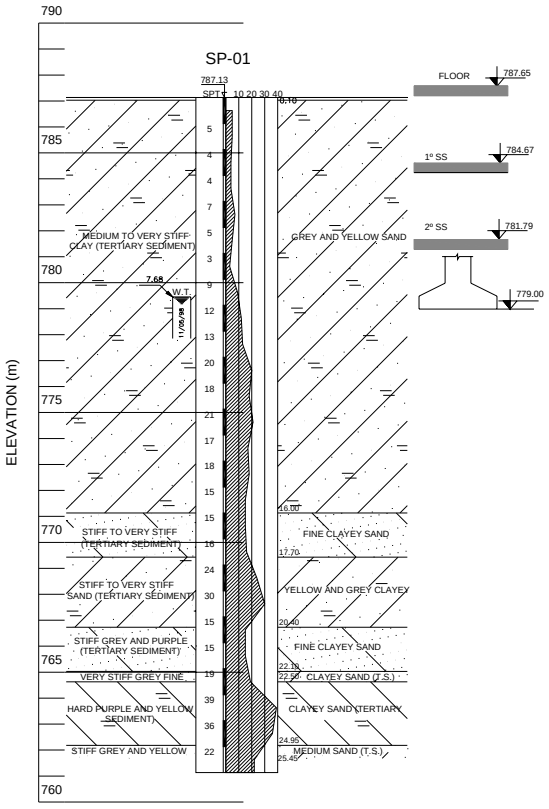

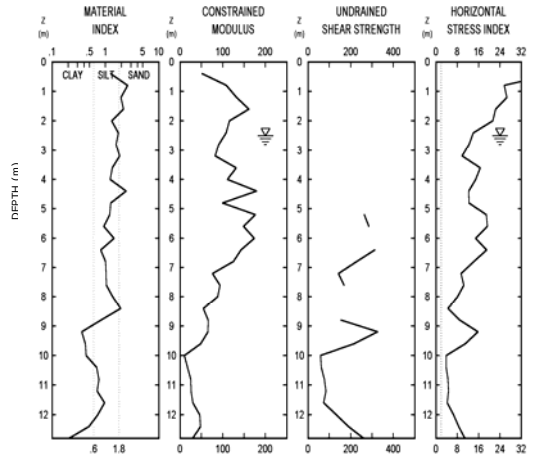

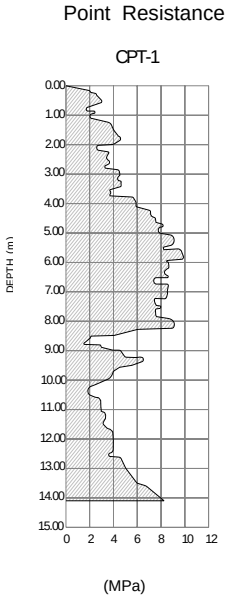

Figure 2.Moóca building

BACK

These conditions combined with a large number of available equipment for different types of piles, and a poor site characterization techniques, lead to the use of pile foundations for most buildings.

Better information about soil properties can change this practice.

The use of DMT, as illustrated in this paper, can give the necessary information for settlement evaluation, allowing in some cases, the use of shallow foundations, with a substantial reduction in costs, when compared with pile foundations.

4 FOUR CASE HISTORIES IN SAO PAULO

This paper presents four case studies of buildings constructed on spread footings.

On Table 1 a summary of those four building cases is presented.

Table 1 – Building characteristics

LOCATION IN SAO PAULO	NUMBER OF FLOORS	DEPTH OF EXCAVATION FOR SUBSOIL FLOORS	LOAD IN EACH COLUMN (KN)	APPLIED STRESS IN SPREAD FOOTING
Pompéia	25	5.5m (18ft)	3,000-8,000	300 KPa
Moóca	25	5.5m (18ft)	3,000-8,000	350 KPa
Água Rasa	20	8.0m (26.2 ft)	1,000-5,000	275 KPa
Morumbi	31	4.0m (13.1 ft)	3,000-10,000	400 KPa

Figures 1 to 4 show the footings of the four buildings and one of the tests results combining SPT, DMT and CPT.

5 FOUR CASE HISTORIES IN SAO PAULO

It is well known that settlement governs foundation design for tall building over spread footings.

That is the reason why when predicted settlements are high pile are preferred, instead of footings, eventhough a pile foundation is usually more expensive than a footing foundation (about 1.3 to 1.6 times).

Using DMT, the design engineer can accurately predict settlement, than with only SPT results.

The DMT method used to compute settlement for those buildings is very simple.

The reduction in stress imposed by the excavation is considered as acting in the whole area and this induces reductions in the layers below the footings. No heaving is considered. The subsoil below the footing is divided in to numerous 20 cm thick layers, each one having a M value determined from the DMT test.

All the footing are considered together, as a large stressed fictitious rectangle, having an area representing the sum of the individual areas of the footings, receiving the total load of the building.

Four points are considered in this fictitious rectangle, the center (A), the corner (B), the middle of the length (C) and the middle of the width (D), as showed in figures 1 to 4.

The stresses induced in the subsoil by the rectangular loaded area are calculated in the centre of each 20 cm thick layer, using Newmark formula.

Thickness reduction in each 20 cm layer is calculated by the expression

$$\Delta\varepsilon_i = \frac{\Delta\sigma'_i}{M_i} \qquad (1)$$

Settlement evaluated using this method does not consider the effect of the building structure, which will reduce the differences at points on the fictitious rectangle.

Results obtained in the predictions based on this method, for those four buildings are shown in Figures 1 to 4.

6 SETTLEMENT MEASUREMENTS

Unfortunately in Brazil, it has been difficult to persuade managers of construction companies to use better quality tests for site characterization to complement the SPT.

With only SPT, settlement predictions have been almost impossible to obtain.

We have been working hard to show the advantages of special field tests, as DMT. For “Moóca” site there were no settlement measurements, and the building is now finished. For the “Pompéia” site the settlement was measured at five columns, with a simple approach, and the building is also finished. For “Água Rasa” and “Morumbi” sites, both are under construction, and a specialized company is measuring settlements monthly.

For “Pompéia Building”, Figure 1 shows the predicted and measured settlements. The mean measured value is 31,4 mm and the mean predicted value is 24,1 mm. This prediction is good enough for design decisions.

For “Morumbi Building”, until now (February, 2006), only 40% of the total loads have been applied. Measured settlements are compared to predicted settlements in Figure 5 (for 40% of the total load).

The mean predicted settlement (13.1 mm) for 40% of the total loads, are compared with the mean measured settlement (8.9 mm) also for 40% of the total loads.

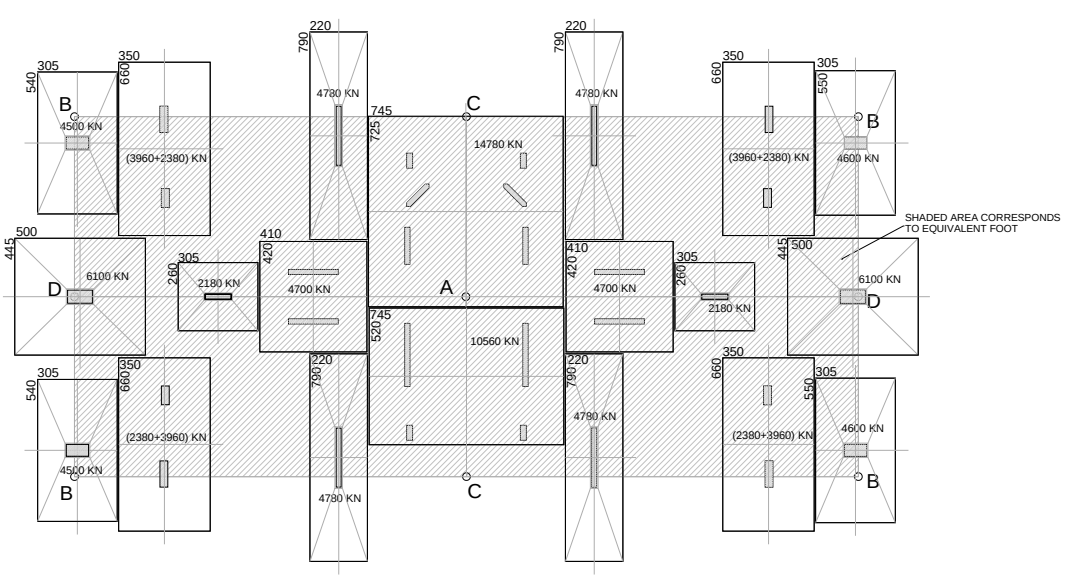

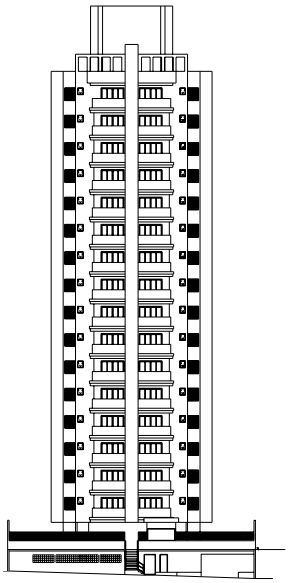

STANDARD PENETRATION TEST (SPT)	MARCHETTI DILATOMETER TEST (DMT)	CONE PENETRATION TEST (CPT)

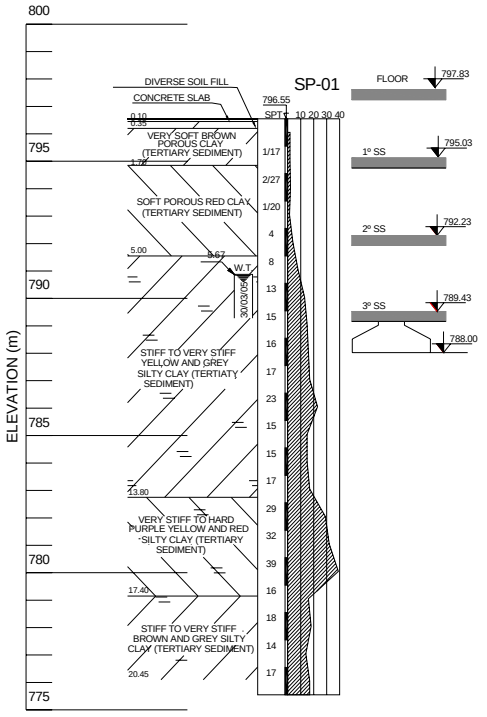

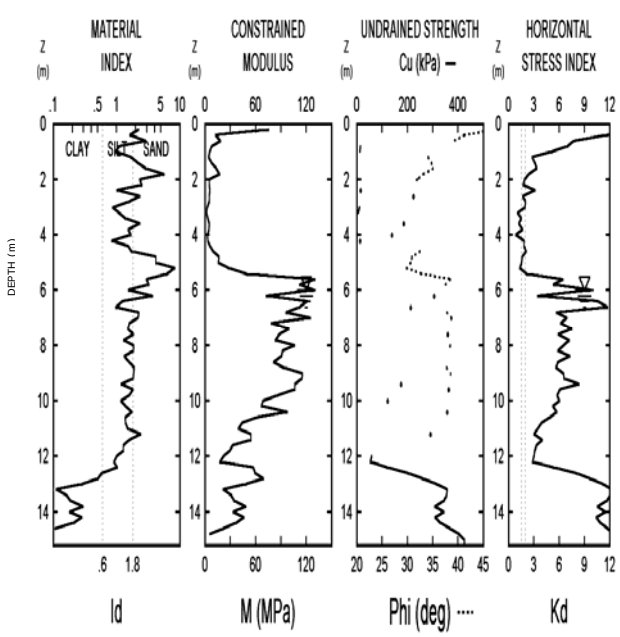

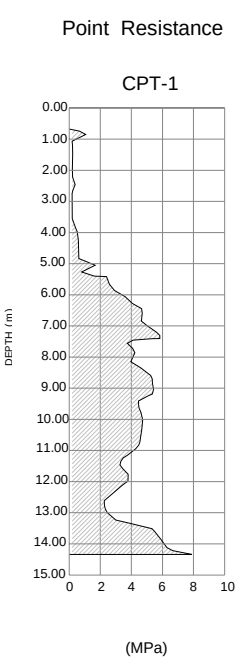

Figure3. Água Rasa building

BACK

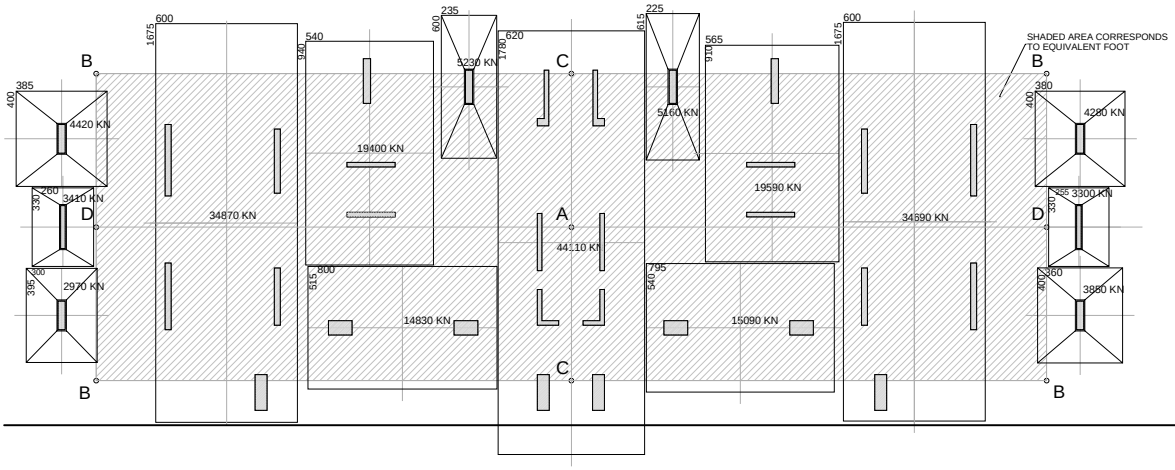

Point Resistance

STANDARD PENETRATION TEST (SPT)

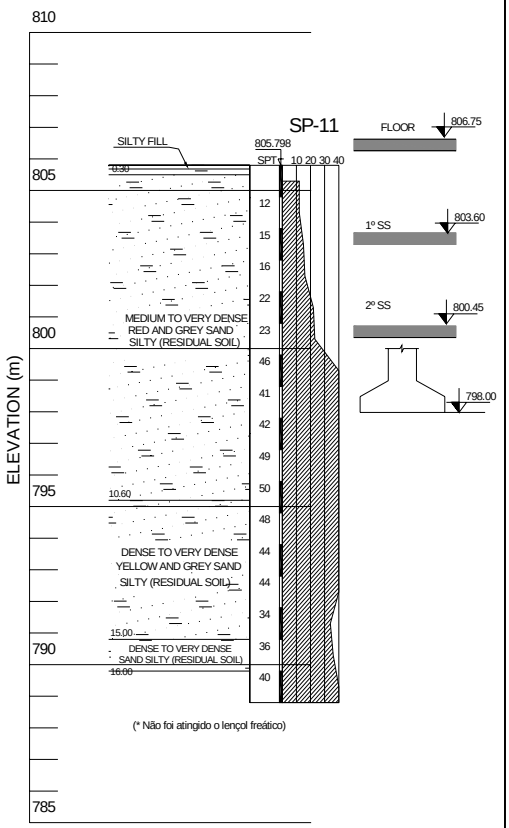

MARCHETTI DILATOMETER TEST (DMT)

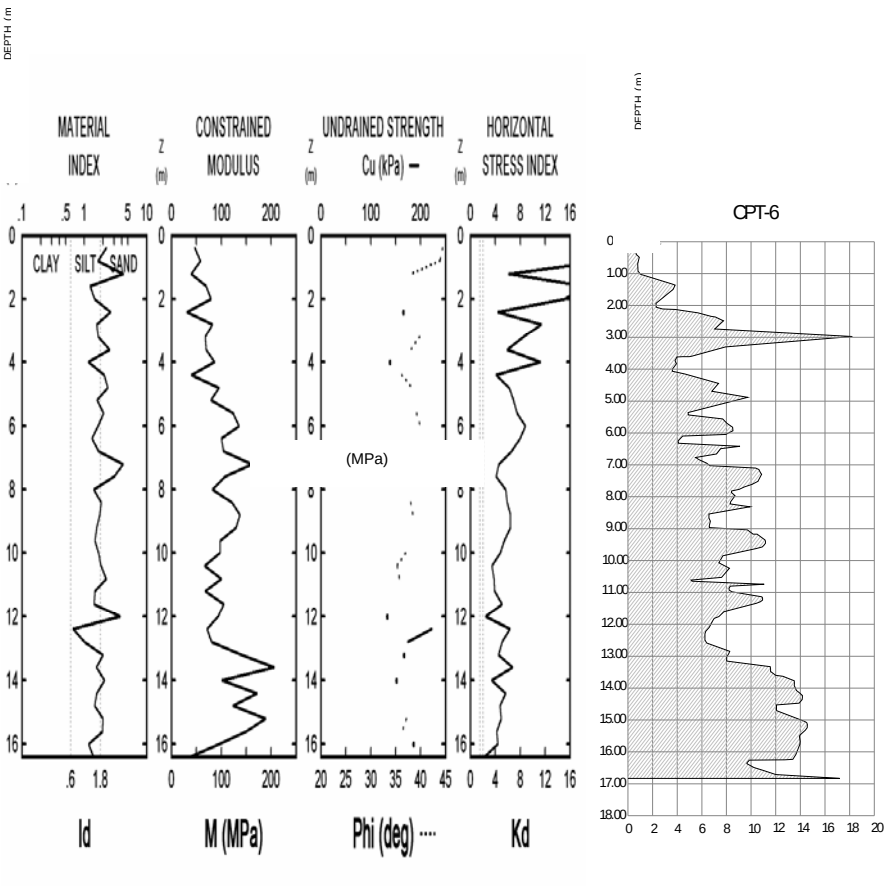

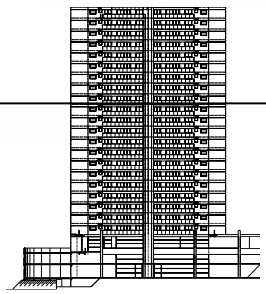

Figure4. Morumbi building

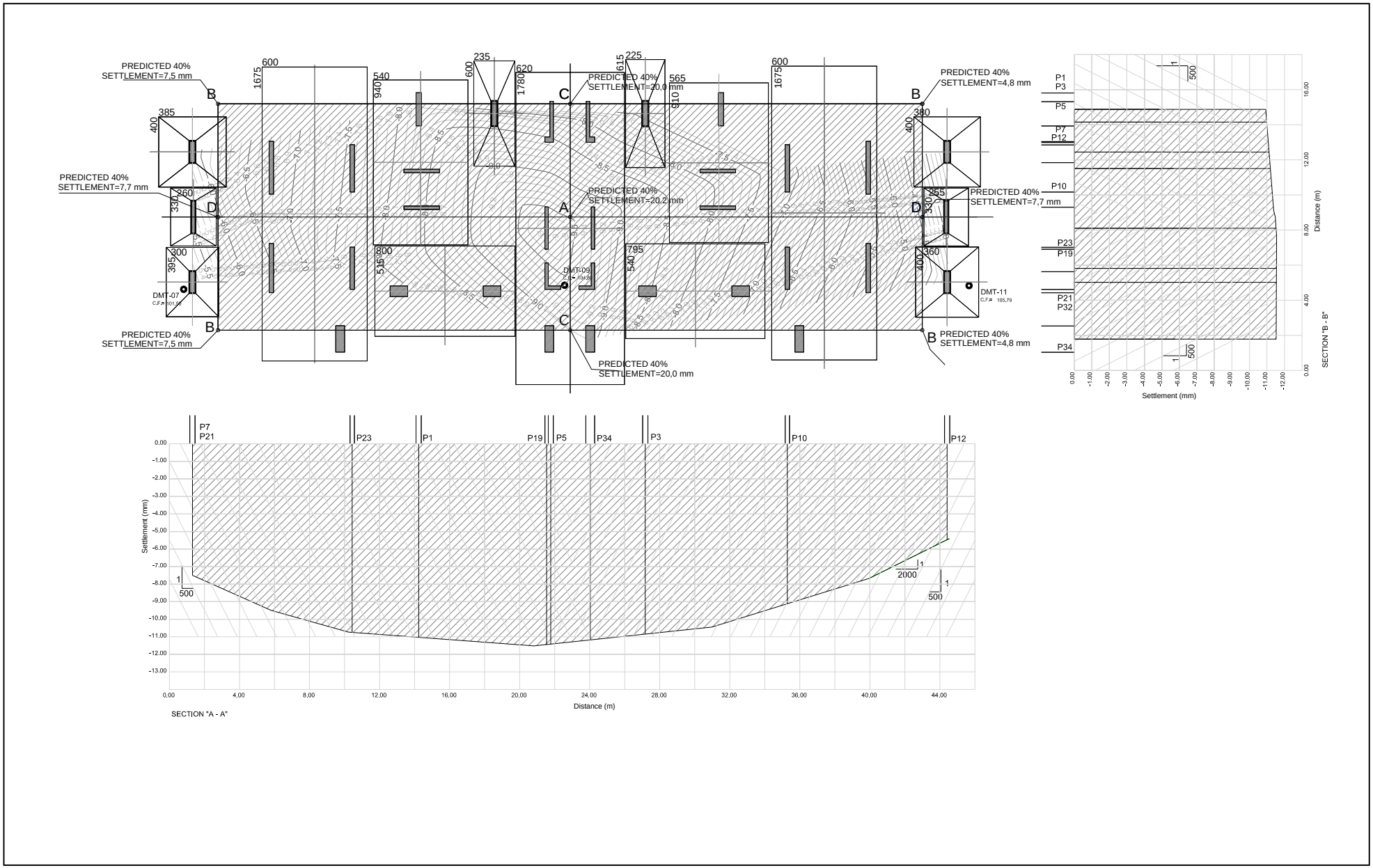

Figure 5." Morumbi building" in constrution, with 40% of the total load

7 CONCLUSIONS

The Marchetti Dilatometer "DMT" is a powerful tool to predict settlements for buildings on spread footings, where no primary or secondary consolidation is involved.

The mean values predicted with dilatometer results, area accurate for design decisions.

The influence of building structure in settlement distribution is somewhat complex. In profile view the predicted settlements give a more curved "dish" shape than what is measured, because of the rigidity of the building frames.

REFERENCES

ASTM D6635-01. *"Standard Test Method for Performing the Flat Plate Dilatometer"*. American Society for Testing and Materials ASTM, 2001.

EUROCODE 7 (1997). *Geotechinical Design - Part 3: Design assisted by field testing, Section 9: "Flat dilatometer Test (DMT) Final Draft",* ENV 1997-3, Apr. 66-73, CEN-European Committee for Stardardization.

MARCHETTI, S. (1975). *"A New In Situ Test for the measurement of horizontal soil deformability"*. Proc. Conf. On In Situ Measurement of Soil Properties, ASCE, Special Conf., Raleigh, Vol. 2, 255-259, June.

BACK

Some recent experience obtained with DMT in Brazilian soils

Prof. Dr. Antônio Sérgio Damasco Penna

Damasco Penna Engenheiros Associados S/C Ltda

Universidade Mackenzie, São Paulo, Brazil

Keywords: Brazilian soils

ABSTRACT: The objective of this paper is to show the use of DMT in Brazilian geotechnical engineering, which is gradually growing, in spite of a country where the practice in site investigations is completely dominated by the Standard Penetration Test SPT. Some Brazilian sites are presented in this paper, with the results of DMT, SPT and/or CPT, in different geological conditions.

1 HISTORICAL REVIEW

The DMT equipament has been used in Brazil for about 10 to 15 years.

It was introduced in some Federal Universities and a few private companies.

Some research at universities was developed based on DMT results, but its practical usage is increasing at a very slow rate because of the unfamiliarity of the geotechnical engineers with the interpretation of test results.

This tendency is changing gradually, with the introduction of DMT test in engineering schools, both in graduate and post graduate courses and with more results, obtained in different geological conditions, as shown in this paper.

2 SOFT SEDIMENTARY CLAY AT ALEMOA – SANTOS/SP

This site represents a sedimentary deposition of clays along the Brazilian coast.

The undrained strength (Cu) increases with depth (Z) in this site as:

$$C_u = 7{,}0+0.89 * Z$$

With C_u (kPa) and Z (m).

The horizontal stress index Kd lies between 1,8 and 2,3 as are normally consolidated clays found worlwide.

3 HYDROMECHANICAL FILL AT SANTANA DE PARNAÍBA/SP

This site represents a fill constituted of fine particles (silts and very fine sands).

The artificial process involves spraying water at the mountain, removing the soil (silt and sand), and filling in a depression, such as a lake, and the coarser sands are separated and removed for construction, leaving behind a hydromechanical fill, constituted by silts and very fine sands, wich are normally consolidated as they settle inside the water.

4 SOFT RESIDUAL SILTY SOILS AT DUQUE DE CAXIAS/RJ

This site represents a gnaissic residual soil constituted of very soft silt and silty sand, situated at the base of a montain chain.

The water table is at the surface, and the use of the area involves a 5,0 m (16,4 ft) thick fill.

5 COMPACTED SILTY FILL AT CAJAMAR/SP

At this site an extensive amount of earthwork was done, to obtain a plain platform with an area of 250.000 m2 (61,7 ac), involving cuts and fills up to 30 m (98,4 ft) high.

The fill was very well compacted in 30 cm (1ft) layers at a minimum of 98% Standard Proctor Compaction.

STANDARD PENETRATION TEST RESULTS (SPT)

MARCHETTI DILATOMETER TEST RESULTS (DMT)

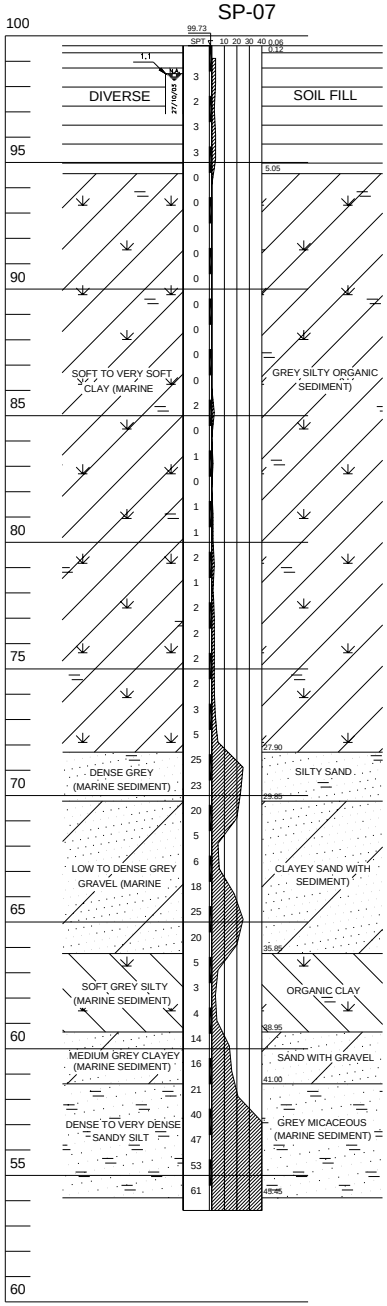

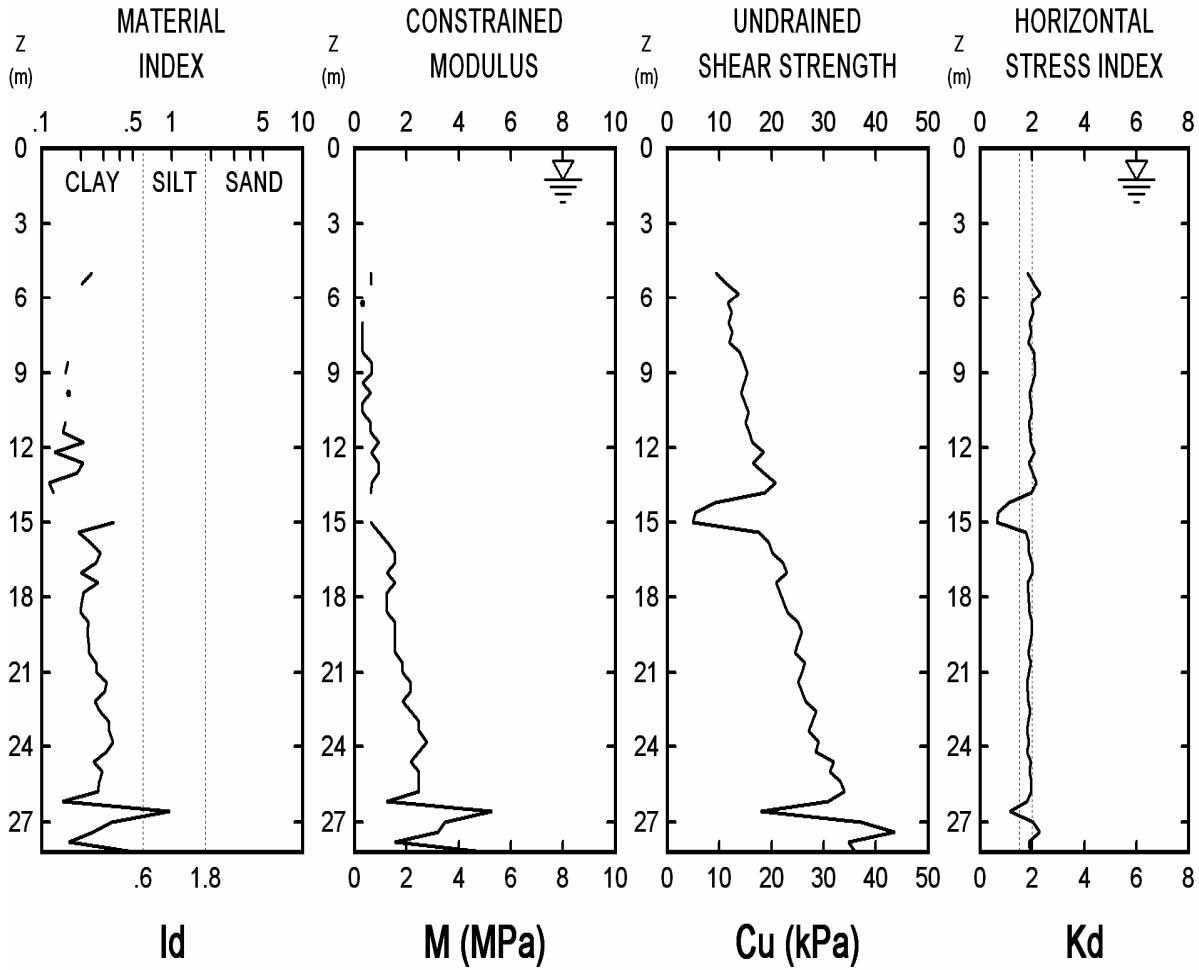

Figure 1. Soft Sedimentary Clay At Alemoa – Santos/SP

BACK

STANDARD PENETRATION TEST RESULTS (SPT)	MARCHETTI DILATOMETER TEST RESULTS (DMT)	CONE PENETRATION TEST RESULTS (CPTU)

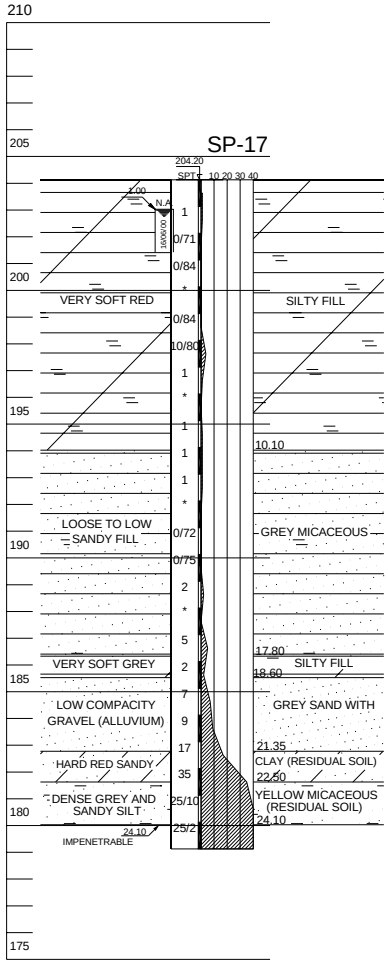

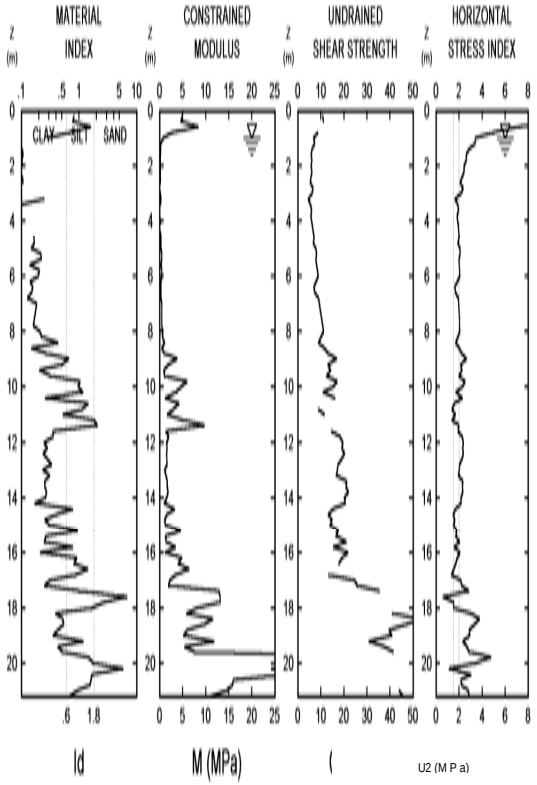

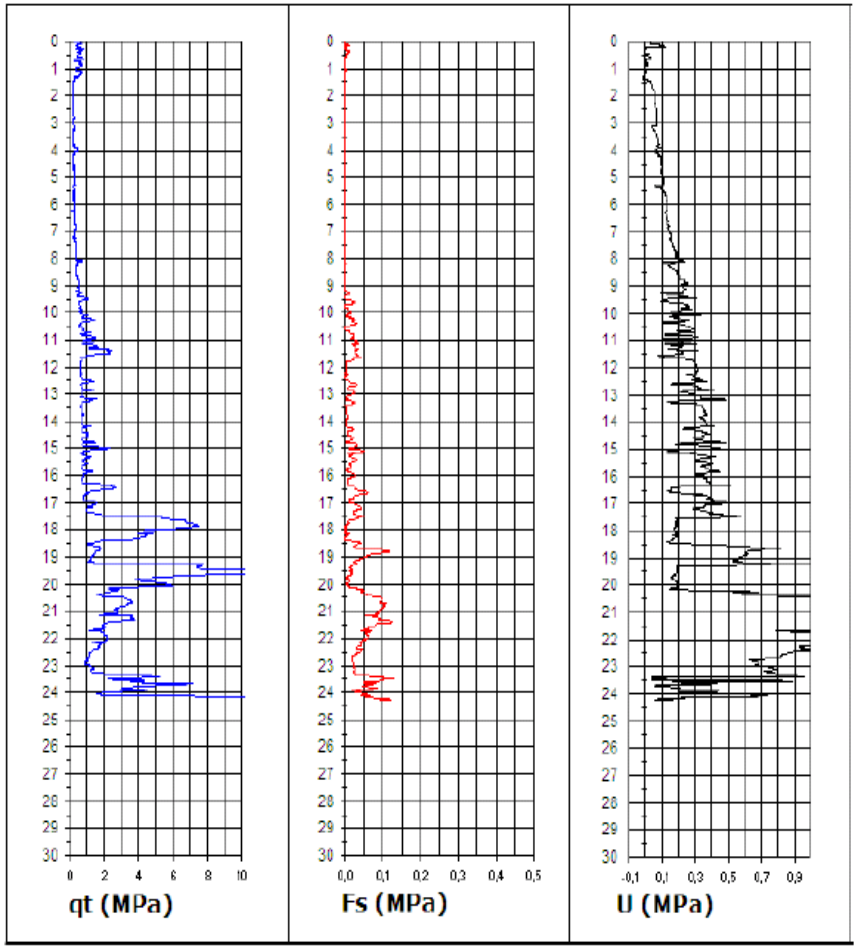

Figure 2.Hydromechanical Fill – Santana de Parnaíba/SP

BACK

STANDARD PENETRATION TEST RESULTS (SPT)

MARCHETTI DILATOMETER TEST RESULTS (DMT)

CONE PENETRATION TEST RESULTS (CPT)

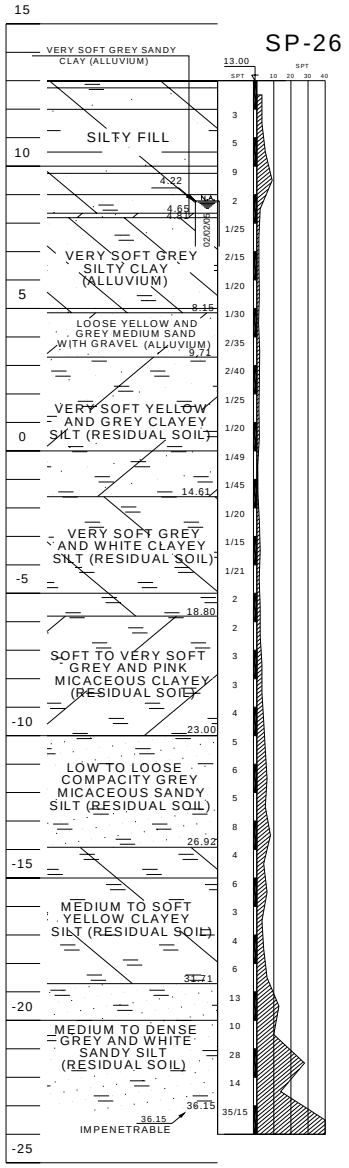

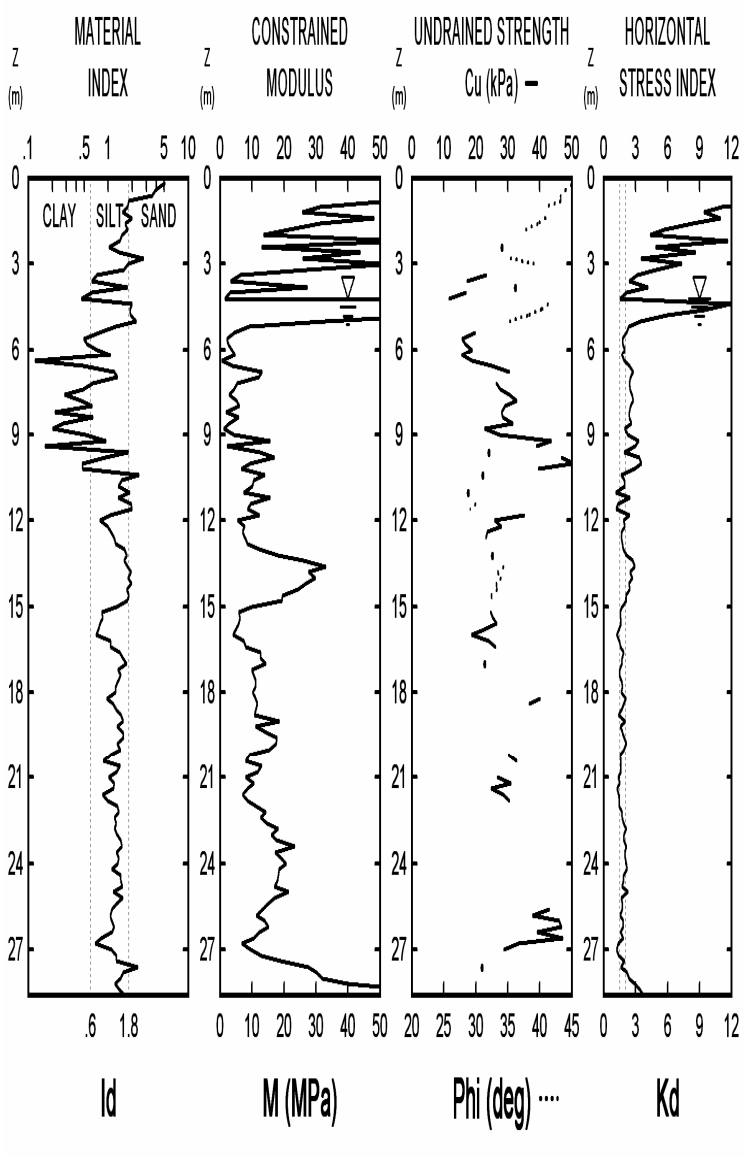

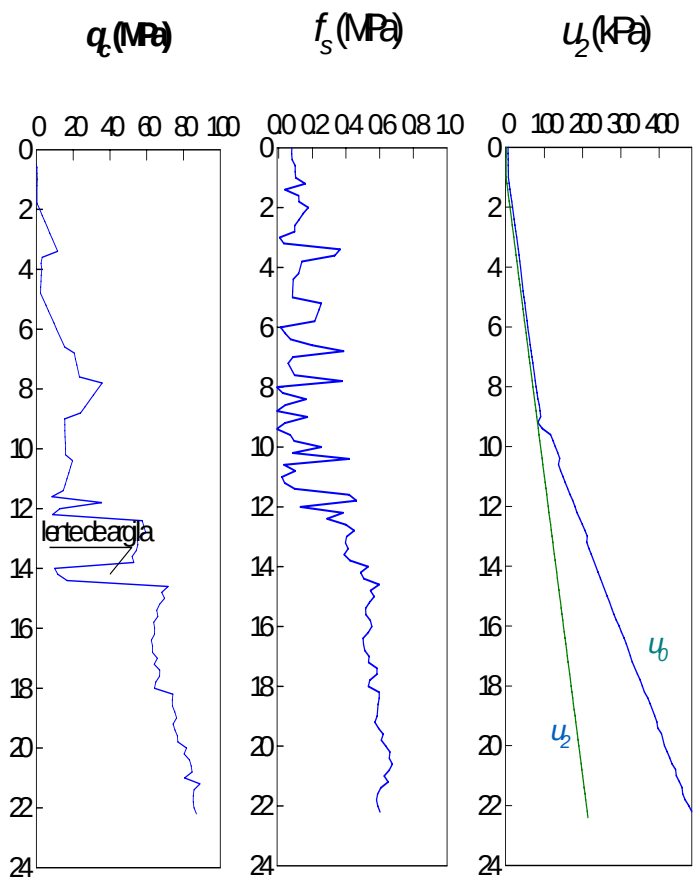

Figure 3. Soft Residual Silty Soils At Duque de Caxias/RJ

BACK

STANDARD PENETRATION TEST RESULTS (SPT)

MARCHETTI DILATOMETER TEST RESULTS (DMT)

CONE PENETRATION TEST RESULTS (CPT)

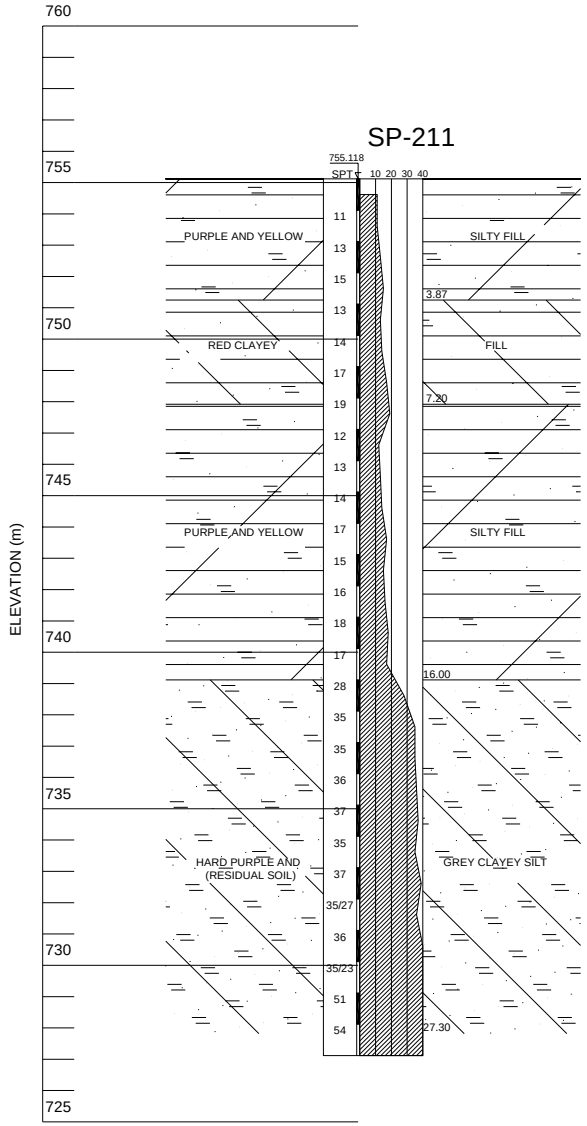

Figure 4. Compacted Silty Fill – Cajamar/SP

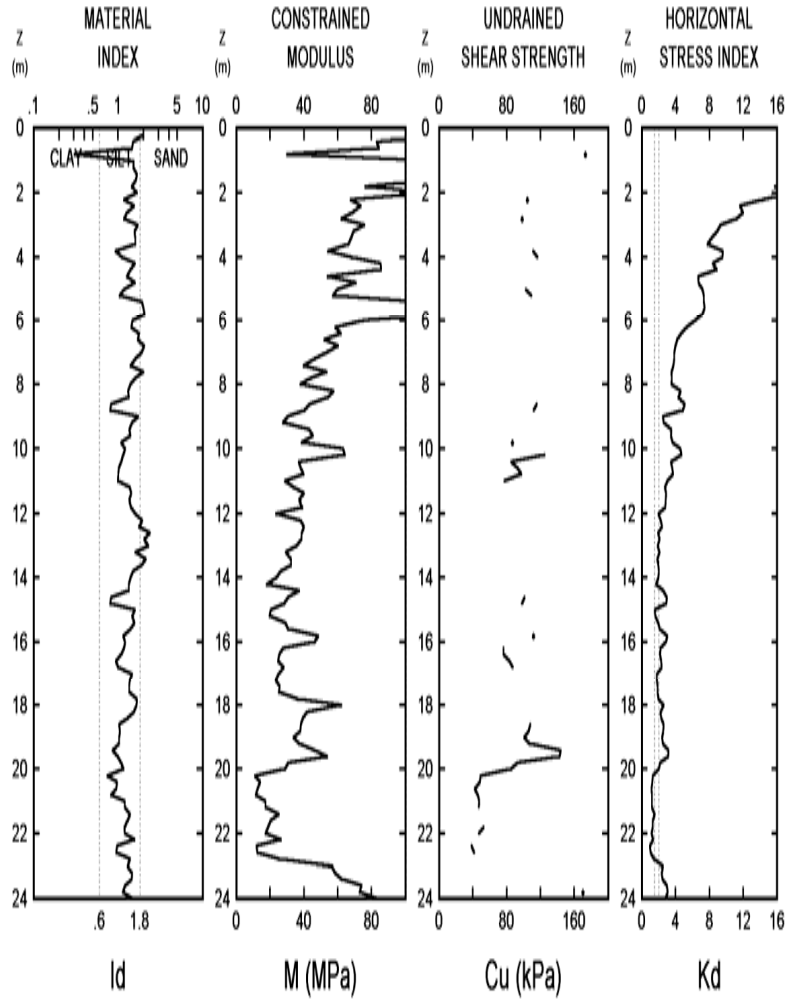

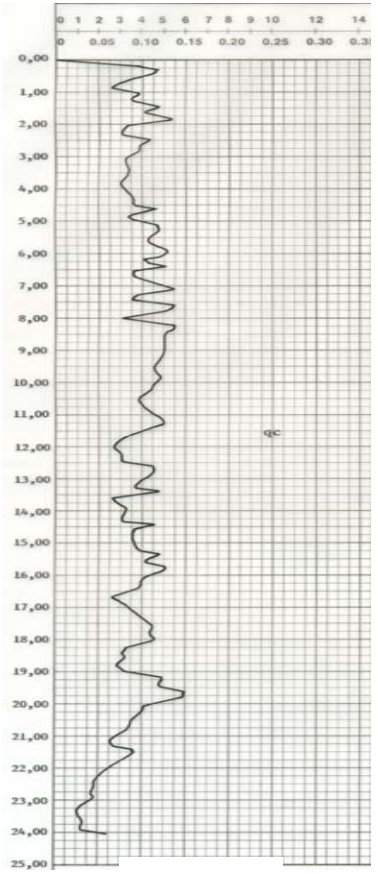

BACK

STANDARD PENETRATION TEST
RESULTS (SPT)

Figure 5. Tertiary Sediment At Sao Paulo/SP MARCHETTI DILATOMETER TEST RESULTS (DMT)

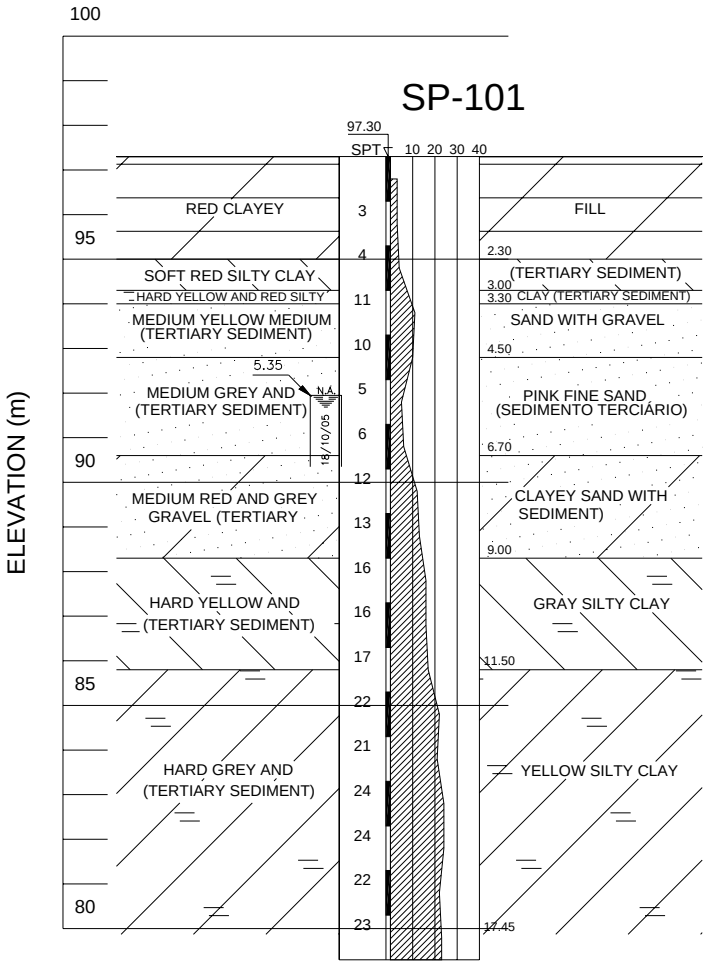

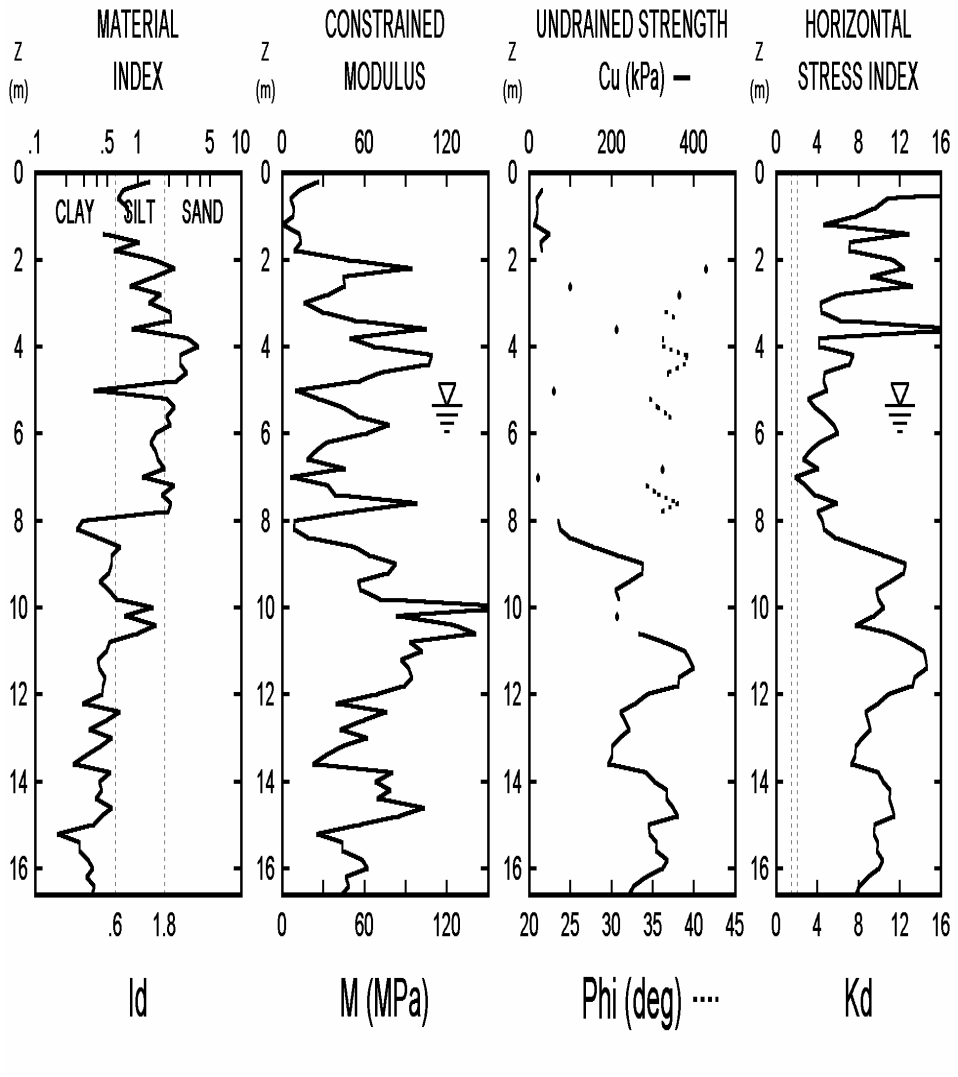

BACK

STANDARD PENETRATION TEST RESULTS (SPT)

Figure 6.Silty Fill – Embu/SP

MARCHETTI DILATOMETER TEST RESULTS (DMT)

CONE PENETRATION TEST RESULTS (CPT)

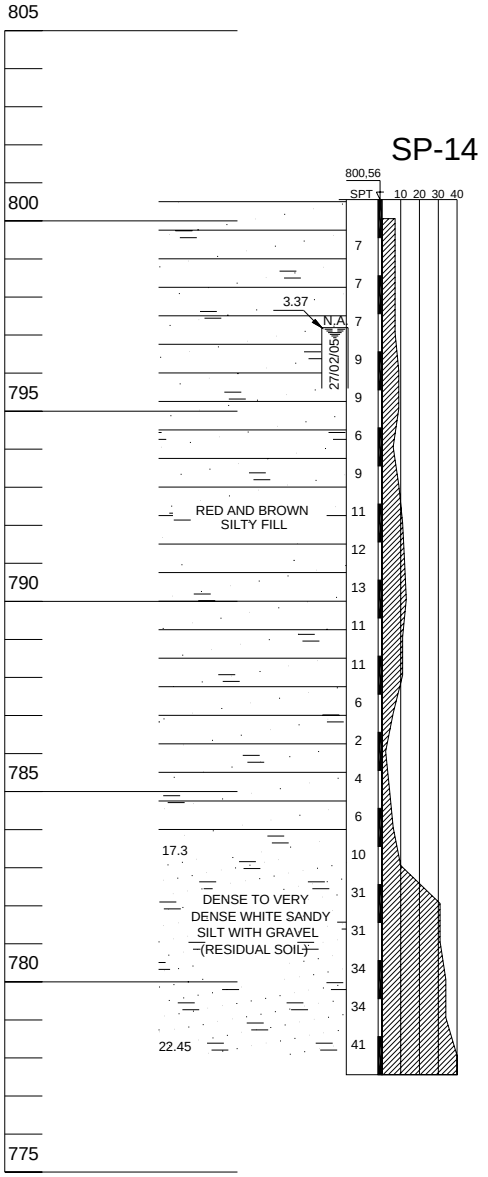

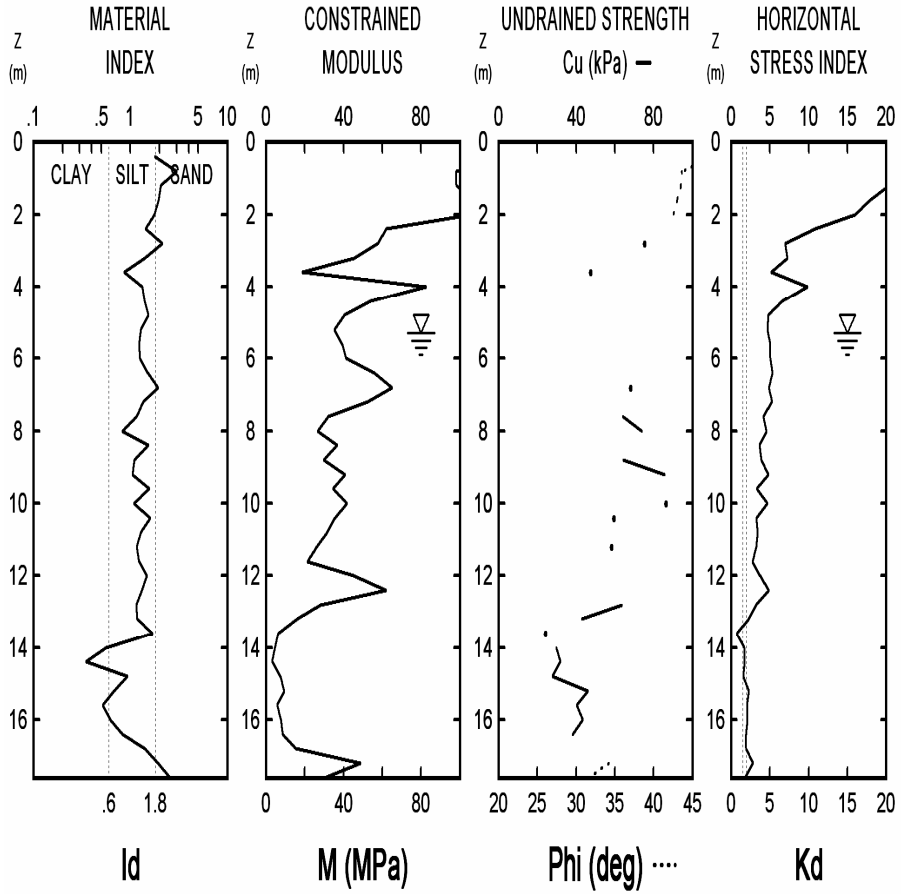

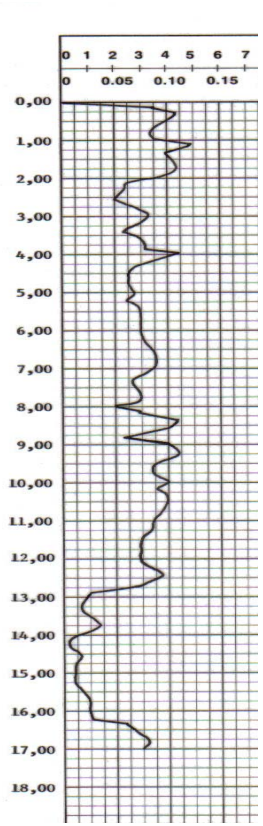

BACK

6 TERTIARY SEDIMENT AT SAO PAULO/SP

This site represents a typical situation of the central area of Sao Paulo city, with tertiary over consolidated sediments.

At the depth about 14 m to 16 m the silty clay is overconsolidated (OCR = 10 to 15), with an estimation of undrained strength about 300 kPa and SPT ranging about 21 to 24 blows/30 cm. (Brazilian SPT energy is about 72%).

This proportion 300 kPa / 23 = 13 is about the same recommended by Décourt (1989) ($Cu = 12{,}5 * N_{72\%}$ kPa).

7 SILT FILL – EMBU/SP

This site represents an area where a distribution centre will be built.

To help the floor slab design, the fill characteristics were studied with SPT, DMT and CPT tests.

8 CONCLUSIONS

The use of DMT as complimentary site characterization is increasing in Brazil.

Its usage in typical Brazilian subsoil conditions, is giving the necessary validation of this test in our soils.

Geotechnical engineers are confidently making design decisions based on DMT correlated parameters.

REFERENCES

ASTM D6635-01. *"Standard Test Method for Performing the Flat Plate Dilatometer"*. American Society for Testing and Materials ASTM, 2001.

EUROCODE 7 (1997). *Geotechinical Design - Part 3: Design assisted by field testing, Section 9: "Flat dilatometer Test (DMT) Final Draft",* ENV 1997-3, Apr. 66-73, CEN-European Committee for Stardardization.

DECOURT L. (1989). "The Standard Penetration Test – State of the Art report". Proc. XII ICSMFE, Vol. IV , pp 2405 – 2416, Rio de Janeiro.

Taxiway Embankment Design Across Wetlands Using Dilatometer Shear Strength Parameters

R.C. Wells, P.E. & X.C. Barrett, P.E.
Trigon Engineering Consultants, Inc.

Keywords: Dilatometer, Slope Stability, Wetlands, Taxiway

ABSTRACT: Reliable shear strength parameters are difficult to estimate in soft soils. Dilatometer results from six test locations were correlated with Standard Penetration Resistances to obtain shear strength and modulus values for slope stability and settlement analysis. Limit equilibrium and finite element analysis are used to verify staged construction of 60 feet (18 meters) high embankment fill over soft wetland soils. The analysis results will be used as construction controls for the instrumentation program during fill placement.

1 Project Background

The Piedmont Triad International Airport (PTIA) located in Greensboro, North Carolina is undergoing an approximate $550 million expansion. This expansion is the result of Federal Express selecting this site for a Mid-Atlantic regional hub, scheduled to open in 2009. The hub will operate up to 63 flights per night at final capacity in 2012. The expansion to the PTIA is shown in Photograph 1 and involves four major components as follows:

- The relocation of Bryan Boulevard which currently provides the main access to the airport. This will include 2.5 miles of multi-lane roadway in addition to a major interchange.
- Preparation of a 170-acre site for the new FedEx hub which includes sorting facilities for airplane and truck delivery access.
- New 9,000-foot (2,744-meter) runway 5L/23R and parallel taxiways.
- The new 3,500-foot (1,067-meter) connector Taxiway Echo between existing runway 5/23 and the new runway 5L/23R which also provides primary access to the new FedEx hub.

Taxiway Echo alignment is controlled both horizontally and vertically by existing and planned improvements at the airport. Its alignment from east to west results in cut sections on the order of 25 feet (8 meters), crossing access roads with a proposed tunnel, grade transition to a 60-foot (18-meter) high fill embankment over wetlands, and a taxiway bridge structure crossing existing Bryan Boulevard which will become the single entrance to the airport facility.

Photograph 1. Piedmont Triad International Airport

The wetland crossing portion is approximately 600 feet (183 meters) in length. The final grades in this area require the construction of a 60-foot (18-meter) earth embankment over the existing soft ground. The wetland area contains existing Brush Creek, which is the headwaters for the City of Greensboro water supply. The wetland areas have been permitted by the Corps of Engineers which require on- and off-site mitigation of over 101 acres that was agreed to by all parties prior to the beginning of design. The footprint of the taxiway alignment is restricted by this agreement and other water quality standards, including wildlife habitat re-

quirements imposed by state agencies. The wetland water quality and flow cannot be impacted by the crossing, which imposes restrictions on design and construction. The flow of Brush Creek will be diverted into a box culvert approximately 525 feet (160 meters) long.

2 PROJECT SCOPE

Thirty-three soil test borings using wash drilling techniques and six dilatometer soundings were performed within the wetland area to depths of between 20 to 50 feet (6 to 10 meters) below the ground surface. The soil types contained within the alluvial materials were highly variable and included micaceous silty medium-to-fine sands or slightly clayey medium-to-fine sandy silts. The Standard Penetration Resistances ranged between Weight of Rod (WOR) to 10 bpf in the alluvial soils. The large variation in density and consistency of the alluvial soils prevented conventional undisturbed sampling and laboratory testing to obtain reliable strength parameters. Figure 1 provides a typical summary of the variability of the subsurface soils. The dilatometer was chosen for in-situ testing since the results would be reliable for undrained shear strength determination or phi (Φ) values for slope stability analysis and would provide information for consolidation properties.

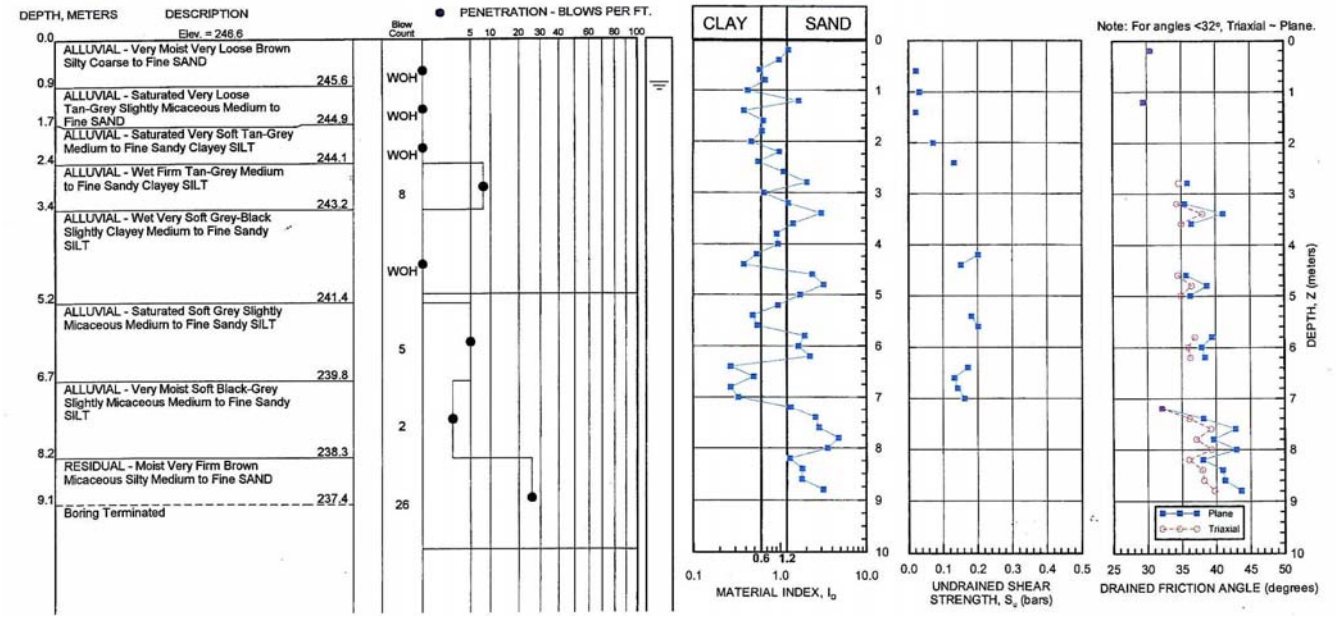

Figure 1. Boring Record

The dilatometer locations were chosen adjacent to six representative soil test borings to correlate the shear strength properties with the Standard Penetration Resistance values. The Weight of Rod (WOR) materials in the upper 10 feet (3 meters) were correlated separately from the Weight of Rod (WOR) material below the 10-foot (3-meter) depth since the undrained shear strength values were apparently higher due to the weight of the rods and hammer. The correlation obtained for the cohesive soils and the micaceous silty medium-to-fine sands with Standard Penetration Resistances are shown in Table A. Less reliability was given for the Φ values versus Standard Penetration Resistances, so this data is not shown. The Φ values appeared greater for these soil types and were not used. The dilatometer modulus values were also used for settlement analysis but not correlated with the Standard Penetration Resistances. Overall, the dilatometer results indicated a significantly larger variation in soil types and density than the soil test borings. Many test values could not differentiate the soil types between silts and sands based on the Material Index since the soil types are generally a combination of Φ-C (phi-cohesive) soils.

Standard Penetration Resistance [blows per foot (bpf)]	Undrained Shear Strength (cohesion) [pounds per square foot (bars)]		
	Average	Range	No. of Readings
WOR (Weight of Rod) Less than 10-foot (3-meter) depth	185(0.1)	62.7(0.03) – 459.5(0.23)	28
WOR* - 4 *Below 10-foot (3-meter) depth	370(0.18)	146.2(0.07) – 793.6(0.40)	54
5 - 10	1204(0.60)	188.0(0.09) – 2130.3(1.06)	27

Table A. Standard Penetration Resistances

3 EXISTING WETLAND CONDITIONS

Site: The wetland area is fairly flat and comprises the flood plain of Brush Creek. General site conditions are shown in Photograph 2. The creek has a very low gradient through this area with the main channel not distinctively defined. The stream has meandered through this area for many years with the flood plain area very prone to flooding after normal rain events resulting in the deposition of sediment.

The wetland area is currently very thickly vegetated with underbrush and isolated small trees. The groundwater table is at or near the surface which results in very soft conditions, particularly below the upper root mat. Access by self-propelled equipment is very difficult. A track drill CME 850 was utilized to collect subsurface information in this area.

Photograph 2. Wetland Area

Site Geology: Below the alluvial materials, a residual profile is present. The residual soil profile is the product of the chemical and mechanical weathering of the underlying bedrock. At this site, the bedrock is a formation of the Carolinas Slate Belt of the Piedmont Physiological Province of North Carolina and generally consists of metamorphosed granitic bedrock.

Subsurface: The subsurface conditions were determined based on 33 soil test borings using a track-mounted CME 850 due to the difficult site access conditions. Because of the softness and variability of the upper alluvial materials, undisturbed sampling and laboratory testing would be questionable due to sampling and testing disturbance. Therefore, Standard Penetration Tests were supplemented utilizing a dilatometer at six locations for density and strength parameters.

The alluvial soils present at the borings within the wetland area extend from 3 to 27 feet (1 to 8 meters) below the existing ground surface. The alluvial soils are highly variable in classification and density due to the depositional history of the Brush Creek floodplain. In general, the alluvial soils consist of either sandy silts or silty sands with varying amounts of mica and clay. Standard Penetration Resistance values obtained in the alluvial soils range from Weight of Rod (WOR) to 10 blows per foot (bpf). Undrained shear strengths in the fine grained soils measured between 20 (0.01) to 1000 pounds per square foot (0.44 bars).

Below the alluvial materials is a relatively thin veneer of residual soils on the order of 7 to 15 feet (2 to 5 meters) in thickness. The residual soils consist of zones of sandy silts and silty sands with mica. Standard Penetration Resistance ranges between 6 and 9 bpf, with the majority being greater than 15 bpf. Undrained shear strengths are generally between 500 (0.22) and 2500 pounds per square foot (1.11 bars).

Partially weathered rock underlies this area at depths between 21 and 34 feet (6 to 10 meters) exhibiting Standard Penetration Resistances greater than 100 bpf. This is a transition between residual soils and unweathered bedrock.

Groundwater within the wetland areas is generally within 2 feet (0.6 meter) of the ground surface.

4 ANALYSIS

The fill placement over the soft alluvial soils presents slope stability issues from the rapid load application and poor drainage properties of the foundation soils. Even with the placement of vertical wick drains, the authors chose the undrained shear strength parameters for the soil types and subsurface conditions present. This would represent the most critical condition for the construction phase since the factor of safety increases with time due to consolidation.

Various slope configurations, including a vertical retaining wall, were analyzed in a value engineering study. This study included settlement and slope stability analyses. Also, various alternatives were investigated to improve the safety factors for slope stability since failures were predicted due to the soft alluvial soils beneath the embankment. These scenarios included complete removal of alluvial material, partial removal of alluvial material, stone column reinforcement of the foundation soils, and the chosen option of using staged construction. The chosen option included the use of vertical wick drains in the alluvial materials to improve drainage for faster consolidation to allow shear strength improvements within the alluvial soils. Temporary rip rap and soil berms were used beyond the toe of the

final slopes in the wetlands to obtain the needed shear strength increases for stability purposes. The berm materials outside the slope toe are to be removed in later stages of filling. The final design cross section is shown in Figure 2.

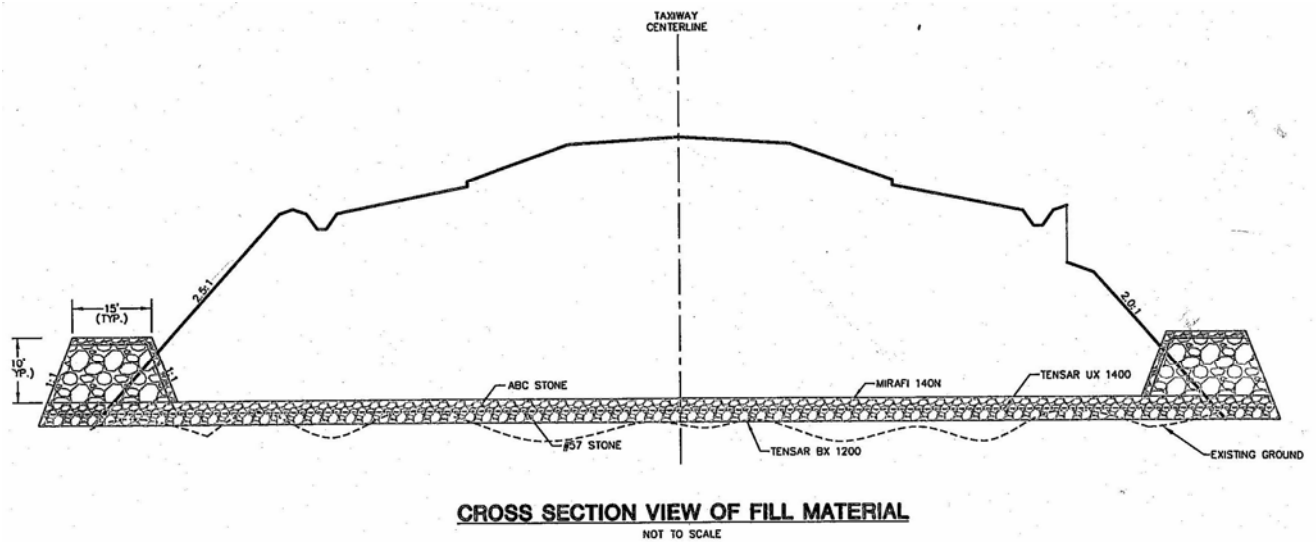

Figure 2. Cross Section View of Fill Material

The settlement potential of the embankments was estimated to range from 3 to 5 feet (1 to 1.5 meters) based on dilatometer data, Schmertmann's method, and finite element analysis using Plaxis. Large deformations were anticipated along the cross section. A high strength uniaxial geogrid was placed near the existing ground surface to produce more uniform deformation and to serve as reinforcing for the outer slope areas. The slope stability analysis was performed using a limit equilibrium method developed by Bishop. Due to the anticipated large deformations, numerical analysis using Plaxis is being performed on the selected cross section. The Plaxis analysis results are being used to confirm the design factor of safety for the different stages of construction. Plaxis also will provide allowable pore pressure increases and allowable horizontal deformation of alluvial soils below the slope toe that will be utilized during construction.

5 CONTROL DURING CONSTRUCTION

The staged construction concept to be utilized for embankment construction will require an instrumentation program during fill placement to prevent slope stability problems. The instrumentation program will consist of pore pressure and settlement monitoring, and slope indicator measurements of the horizontal and vertical deformations. This data will be used to determine the fill placement rate or appropriate waiting periods during fill placement to accommodate consolidation and shear strength increases in the alluvial materials. The horizontal and vertical deformations of the materials will be monitored to prevent slope failures from occurring.

6 CONCLUSIONS

The dilatometer results for undrained shear strength generally correlated with Standard Penetration Resistance in most of the fine grain soils at the site. The micaceous materials generally exhibited Material Indexes that corresponded to silts which are probably more representative of their performance. The Φ-C properties of these soil types have limitations with the interpretation using the dilatometer data. The Φ angles seemed to be overstated for these soil types based on past experience.

Overall, the dilatometer results provided reliable undrained shear strength values used in our analysis. The dilatometer seems to be an excellent application for the undrained shear strength determination for soft fine grained soils.

ACKNOWLEDGEMENTS

Special thanks go to Piedmont Triad International Airport, Baker Associates, and Talbert & Bright personnel who have been involved through the design phase of this project. In addition, thanks to Dr. J. Brian Anderson, P.E., professor of Civil Engineering at the University of North Carolina at Charlotte, and Dr. Manuel Gutiérrez, P.E., with Trigon Engineering Consultants, Inc. for their Plaxis finite element analysis. Mr. Roger Failmezger, P.E. with In-Situ Soil Testing, L.C. provided the dilatometer listing and data reduction.

BACK

REFERENCES

Fell, R., Hunter, G. 2003. *Prediction of impending failure of embankments on soft ground*. NRC Research Press. J. Vol. 40: 209-220.

Han, et al. *Evaluation of Deep-Seated Slope Stability of Embankments over Deep Mixed Foundations*.

Ladd, C.C. 1991. *Stability Evaluation during Staged Construction*. Journal of Geotechnical Engineering Vol. 117 (No. 4): 540-615.

Pelnick, et al. (1999) *Foundation Design Applications of CPTU and DMT Tests in Atlantic Coastal Plain Virginia*. Washington, D.C. Transportation Research Board, 78th Annual Meeting, January 10-14, 1999: Paper No. 990794.

CORRELATIONS AND COMPARISONS WITH OTHER LAB OR INSITU TESTS

DMT Testing for the Estimation of Lateral Earth Pressure in Piedmont Residual Soils

J. B. Anderson
V.O. Ogunro
J.M. Detwiler
J.R. Starnes
Department of Civil Engineering, University of North Carolina Charlotte, Charlotte, NC, USA

Keywords: dilatometer, sheet-piling, retaining structures, residual soils, Piedmont, insitu

ABSTRACT: In this study, two instrumented flexible retaining walls were used to measure the earth pressure in Piedmont residual soil (PRS). A research site was established near Statesville in Iredell County, North Carolina within a major PRS region. The site was characterized with Marchetti Dilatometer tests, cone penetration tests, standard penetration tests, borehole shear tests and a single K_0 stepped blade test. Results of the in-situ tests were used to predict the at-rest and active lateral earth pressure. Two 36.9m long cantilevered sheet-pile retaining walls were constructed using 10.7m long PZ22 sheet piles. The walls were instrumented with strain gages and a slope inclinometer to measure bending moments and displacements, respectively. The soil between the walls was excavated in 1.2m lifts to a depth of 6.1m. The bending moments measured in the walls were used to derive the net earth pressure acting on the walls. The earth pressure calculated for the single well driven pile coincides with predictions made using the DMT.

1 INTRODUCTION

The lateral earth pressure on retaining structures due to Piedmont residual soils (PRS) is difficult to quantify by traditional methods and is often over predicted. Thus, large safety factors are used in retaining structure design that increase conservatism but not necessarily the engineer's confidence. Much of this conservatism can be attributed to the divergence between the behavior of PRS and traditional cohesive and cohesionless soils.

Traditional methods for calculation of lateral earth pressures in residual soils over predict the actual insitu stresses. Much of this conservatism is attributable to the additional strength exhibited by Piedmont residual soils due to the fabric-type nature of the material that is overlooked in traditional soil models (i.e. Mohr-Coulomb limiting equilibrium). Unfortunately, it is difficult if not impossible to obtain *undisturbed* samples of Piedmont residuum for laboratory testing; thus, engineers rely on in-situ tests to gather strength parameters used in retaining structure design. Since these tests are calibrated to laboratory tests on **either** cohesionless **or** cohesive soils, they do not provide a true measurement of the strength of Piedmont soil. Thus, engineers often design these structures based on conservative parameters and apply afore-mentioned conservative factors of safety. Yet, there is no direct increase in the engineer's confidence in the design.

Residual soils, which are found throughout the world, have a significant range in the eastern portion of the United States, as shown in Figure 1. Due to the prevalence of PRS in North Carolina, the North Carolina Department of Transportation (NCDOT) must routinely consider PRS for all types of geotechnical design projects – retaining walls, pile and drilled shaft foundations, shallow foundations, embankments, and roadway bases. Beginning FY2005, NCDOT is supporting research to develop a simple earth pressure model for PRS.

This brief paper presents an overview of the concept, some of the in-situ tests, construction of instrumented full-scale field wall, and data reduction carried out on this study.

2 SELECTION AND CHACTERIZATION OF A PRS RESEARCH SITE

Piedmont residual soils cover about one half of the land area of North Carolina. Figure 2 shows three major regions including the Carolina Slate Belt, the Charlotte Belt, and the Inner Piedmont. North Carolina DOT located a project in Statesville, NC that lies directly on the boundary of the Carolina

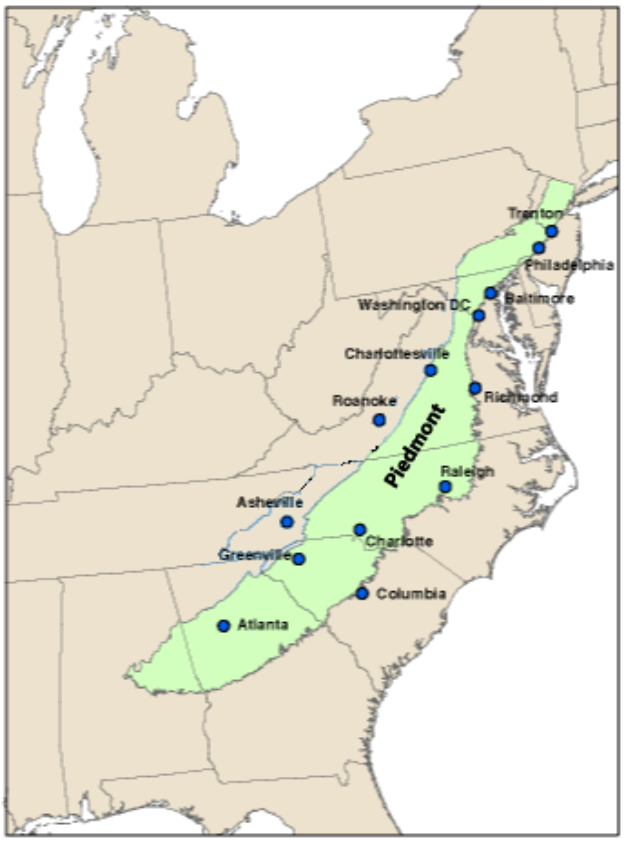

Figure 1. Range of residual soil in the Eastern United States.

Slate Belt and the Charlotte Belt. The site was a borrow pit for the US 70 bypass around Statesville, NC. Initial exploratory investigation revealed thick layers of residual soil with only slight surface disturbance. The site was quickly earmarked for construction of the first set of sheet pile walls.

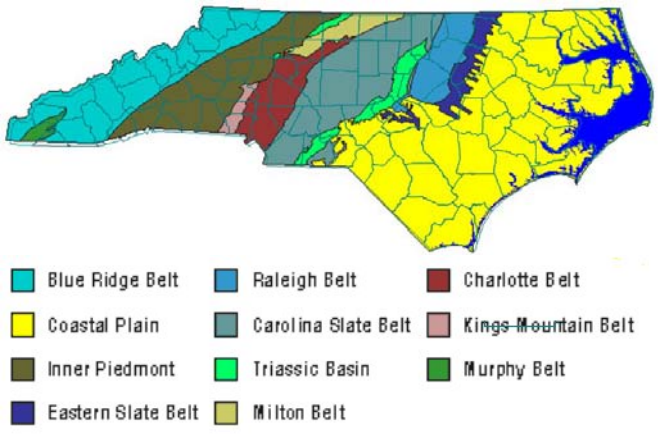

Figure 2 North Carolina Piedmont Residual soils

When the notice-to-proceed work at the site was given, an extensive in-situ testing program was initiated. Tests conducted included standard penetration tests (SPT), cone penetration tests (CPT), dilatometer tests (DMT), borehole shear tests (BST), and K_0 stepped blade tests, all detailed in figure 3

The profiles of SPT-3, CPT-4, and DMT-5 are shown together in figure 4. The SPT boring reported a soil type of residual tan to brown micaceous clayey silt. The CPT classification was OC to NC

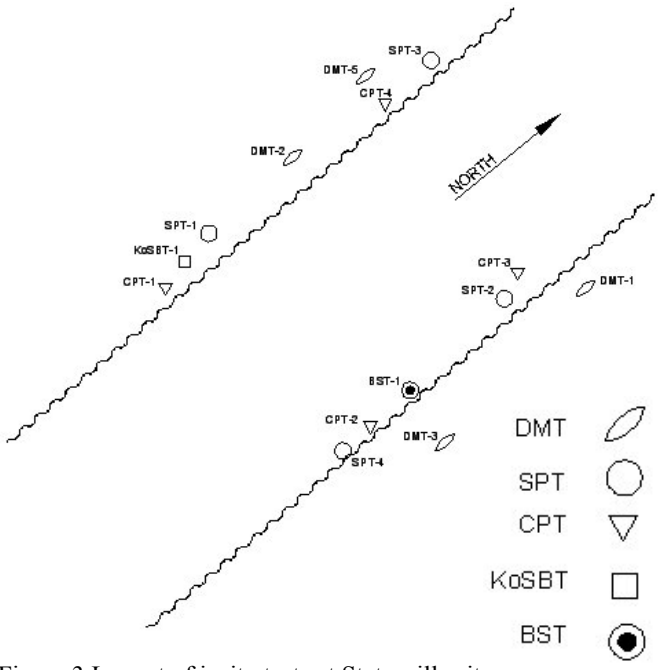

Figure 3 Layout of insitu tests at Statesville site

clay, while the DMT reported silt to clayey silt, much like the SPT. Results of BST hole and K_0 stepped blade are not presented here.

3 PREDICTION OF EARTH PRESSURE BASED ON IN-SITU TESTS

The results of in-situ tests were used to estimate the potential earth pressure on the retaining walls. As the walls would be flexible cantilever, the earth lateral pressure distribution beneath the excavation will be complex consisting of a net active and passive. However, above the base of the excavation should be subject only to at rest or active earth pressure. Therefore, the calculations of at rest and active earth pressures were made. Values of coefficient of lateral earth pressure at-rest, K_0, were estimated from DMT data using correlations developed by Marchetti (1980) and Baladi et al. (1986) presented as equations (1) and (2), respectively.

$$K_0 = \left(\frac{K_D}{1.5}\right)^{0.47} - 0.6 \qquad (1)$$

$$K_0 = 0.376 - 0.095K_D - 0.005\frac{q_c}{\sigma'_v} \qquad (2)$$

The DMT sounding was parsed through the equations with the q_c values to develop profiles of K_0 with depth, that were then used to calculate the at rest earth pressure.

Friction angle was correlated from DMT and CPT soundings and used to determine K_a and K_0 for each sounding. For this analysis, the soil was as-

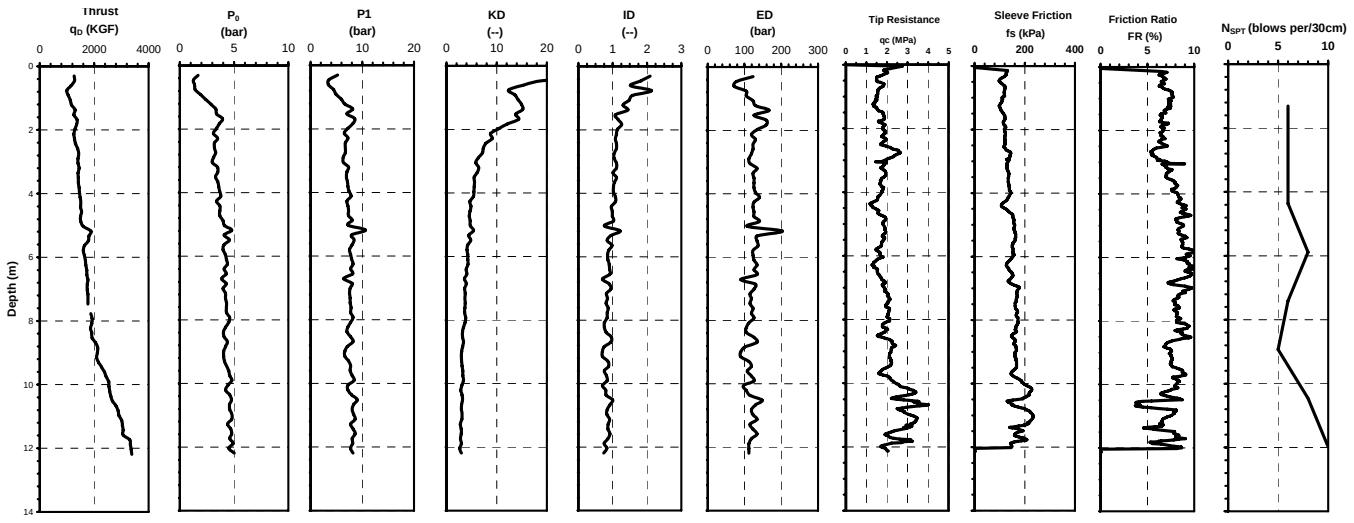

Figure 4 Composite plot of DMT, CPT, and SPT profiles

sumed to be purely frictional. A second set of earth pressures versus depth was developed based upon these coefficients. Figure 5 shows the lateral earth pressures calculated from insitu tests.

4 DEVELOPMENT AND IMPLEMENTATION OF A MECHANISM FOR MEASUREMENT OF EARTH PRESSURE

Measuring earth pressure in-situ is difficult for textbook soils, and even more so for PRS. To measure the lateral stress in place, a device would need to be inserted into the soil profile without the need for excavation, and with a minimum of soil disturbance. These requirements eliminate all but a few possibilities.

With any of the insitu tests, it is likely that any earth pressure measurement would be an estimate at best. Therefore, it was proposed to instrument a full scale retaining structure built in PRS. To meet the criteria of no excavation and minimum soil disturbance, the only choice was sheet piling. Sheet piles could be instrumented, then vibrated or driven into place without excavation. Therefore, it was proposed to construct two sheet-pile retaining walls at each research site in the configuration show in figure 6. After the project was awarded, a plan for the design and instrumentation of the walls was developed. The critical items to be determined were:

1) Section of the sheet pile
2) Total length of sheet piles
3) Minimum separation distance between walls
4) Safe maximum excavation depth
5) Maximum safe deflection of walls
6) Instrumentation type and location

Since the behavior of flexible retaining walls is a soil-structure-interaction problem, the finite element program Plaxis was used to determine the potential earth pressure, shear and bending in the wall, and displacements.

The results of the initial study were that the minimum safe sheet pile section was PZ22. The sheet piles would be 10.7m in length. They would be driven to an embedment of 10.4m. The walls would need to be a minimum of 12.2m apart. The maximum safe excavation depth between the walls would be 6.1m, leaving the sheet piles embedded 4.3m.

Many factors contributed to the instrumentation plan most notably survivability and budget. For survivability concerns, bolt-on vibrating wire strain gages, with weldable mounts, were used. These gages had been widely used in the testing of steel piles in axial and lateral load. Gages were installed in pairs at 1.22m (4 foot) intervals at 8 levels along the sheet piles. The gages were protected from installation damage by a steel angle cover. Additional advantages of the vibrating wire gages were low power consumption and integration with a Campbell Scientific datalogger, tried and true equipment, for long term deployment. Four sheet piles were instrumented with 16 gages each for a total of 64 strain gages.

In case the strain gages did not survive driving, the slope inclinometer was chosen as the backup "low tech" measurement. A box tube steel section with diagonal equal to a slope inclinometer casing was welded to the back side of four sheet piles. Unlike typical slope inclinometer tests, the axes of measurement are skewed at 45^o from direction of wall movement. The measurements would be rotated in the data reduction equations to match the offset angle. A schematic layout of the instrumented sheets is presented in figure 7. Finally, the third level of redundant measurements would be made using surveying equipment to monitor movements of the wall at many points.

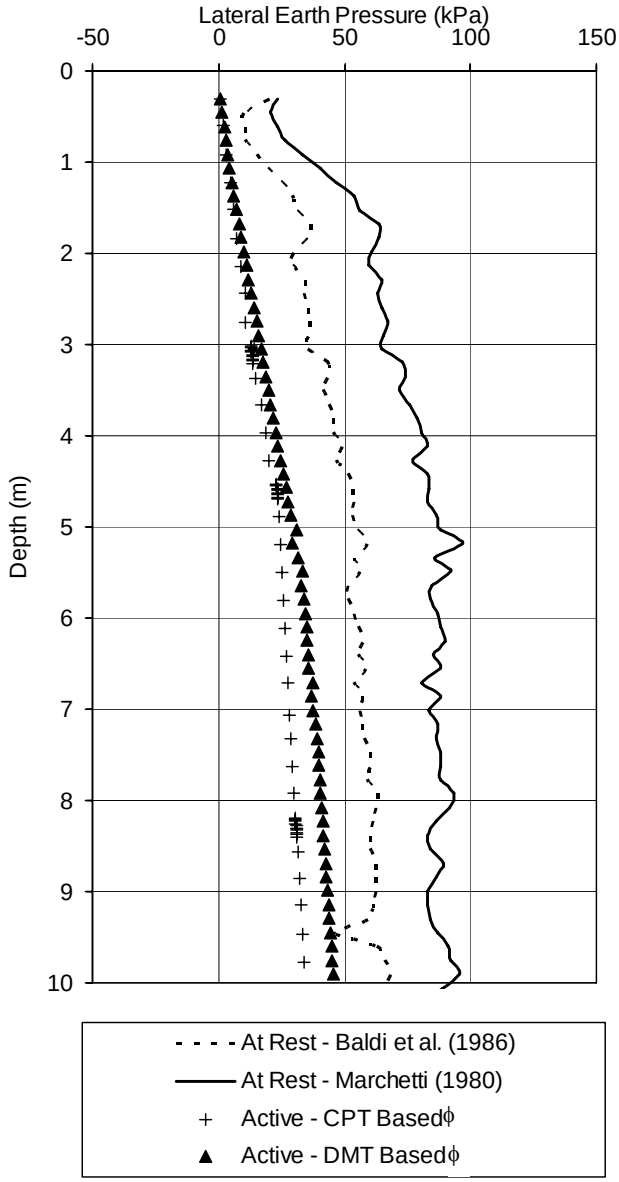

Figure 5 Predicted earth pressure

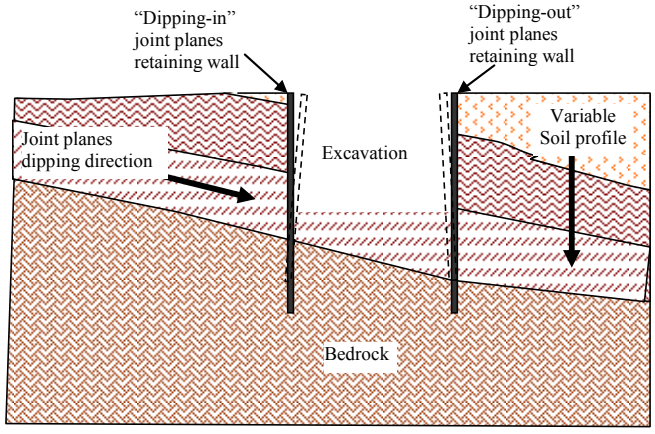

Figure 6. Idealized test wall setup

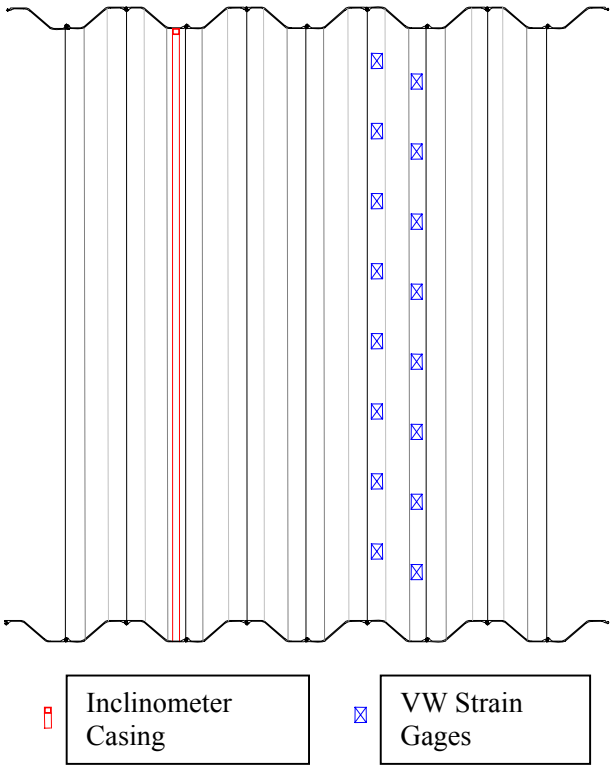

Figure 7. Strain gage and inclinometer layout

The final sheet pile walls at the Statesville site were 36.9m long consisting of 66 sheets per side. The strain gage sheets on the west wall were installed at 17.9m and 22.4m from the north end, and the inclinometer sheets were installed at 2.2m from the strain gage sheets.

The sheet piles were installed beginning September 12, 2005. As mentioned previously, the sheets were to be driven 10.4m leaving 0.3m of exposure. In the northwest corner of the site, this was possible. However, the PRS provided much higher resistance to driving than predicted by the initial tests. As shown in figure 8, the result was that many of the piles were significantly under driven. Additionally, harder driving efforts compromised four gages in the top of the southeast instrumented pile.

The soil between the sheet pile walls was excavated in 5 lifts over a period of ten days between October 17 and October 27 2005. After each excavation step, inclinometer readings were immediately taken. Subsequently, strain gage readings were downloaded from the dataloggers and a survey was conducted on selected points along the sheet pile walls and within the excavation. Figure 9 is a view looking south into the completed excavation.

Due to the driving problems, the only instrumented piles that were installed to the proper depth and completely survived installation were the strain gage-inclinometer pair in the northwest (NW) corner of the site. Subsequent analysis will focus on these piles only.

BACK

Figure 8 Installed sheet piles

Figure 9 Excavation complete at 6.1m

Inclinometer readings for the Northwest pile (NWI) are shown in figure 10. The maximum deflection at the ground surface was just less than 24mm. By the final excavation step, a visible gap developed between the sheet pile and the soil. The gap was far more pronounced at other locations along the walls where the sheets had been under driven. Using a tape measure as a crude feeler gage, the depth of soil separation from the wall was at least 3.0m.

Calculation of the bending moment was based on strain measurement. First, the net strains were determined by taking the difference of the strains at the final excavation step from the strains after the piles were driven, before any excavation. The curvature was determined by subtracting the strain measurements from the pair at any given level then dividing by the distance between gages. Knowing the moment of inertia and stiffness of the sheet pile, the curvatures were used to calculate bending moments. Bending moment profiles for strain gage in northwest pile (NWS) are shown in figure 11.

Inspection of the bending moment curves shows expected behavior. As the excavation proceeds, the sheet piles appear to relax as the maximum bending moment increases and propagates down the pile.

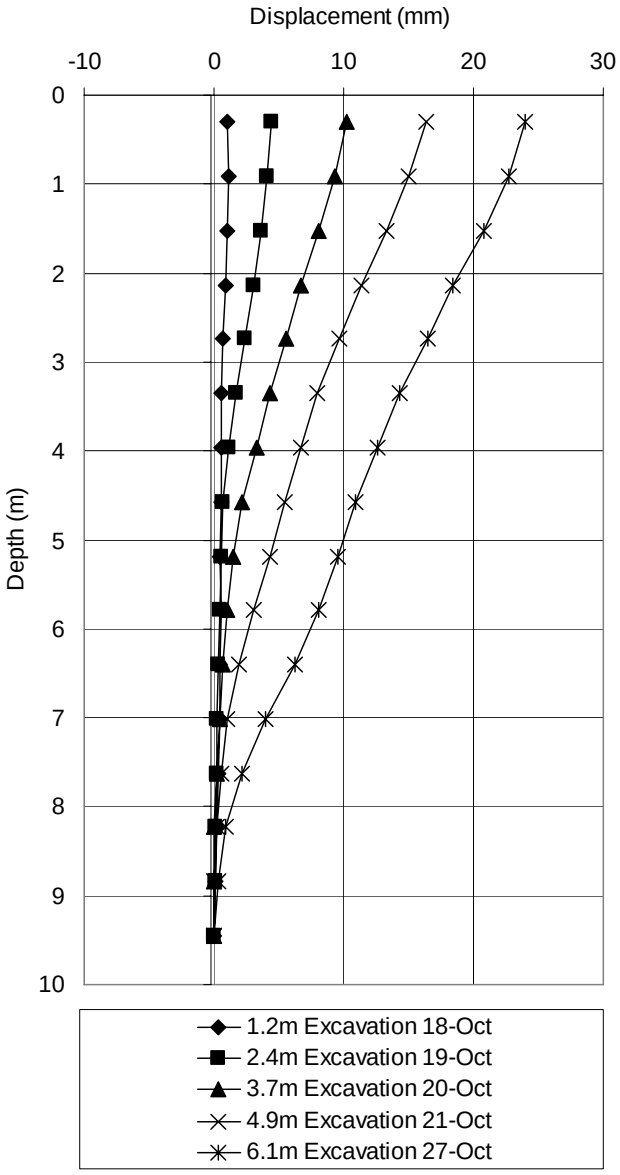

Figure 10 Sheet-pile deflections from inclinometer (NWI)

5 COMPARISON OF PREDICTED AND MEASURED EARTH PRESSURE

Sheet piles were instrumented to measure strain and deflection. Using an analytical model borrowed from laterally loaded piles, the same Winkler model of a beam on an elastic foundation, the functions for bending moment versus depth were generated. Two derivatives of these functions were taken to determine the shear in and soil reaction on the wall, respectively. The resulting earth pressure distribution for the pile NWS is plotted in figure 12 with the earth pressures determined earlier from in-situ tests. The excavation depth was 6.1m and the point of separation was 3.0m or deeper. The calculated distribution of earth pressure fits fairly well into those boundary conditions. Futhermore, the maximum value seems to coincide with active earth pressures estimated based on friction angle measurements from the DMT and CPT.

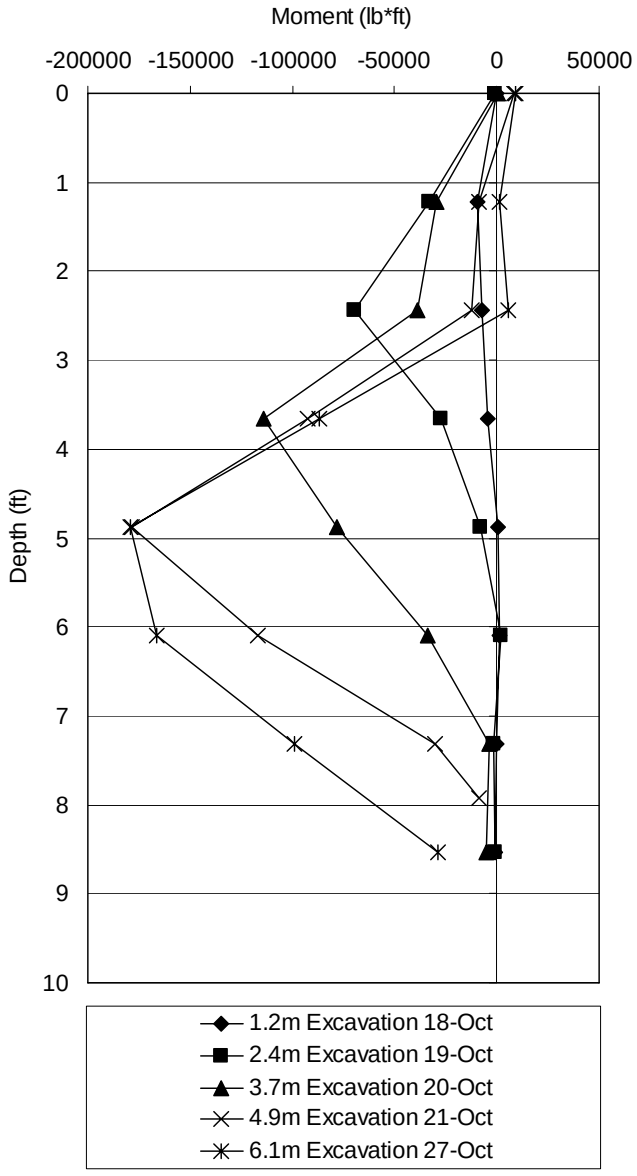

Figure 11 Bending moments from strain gages

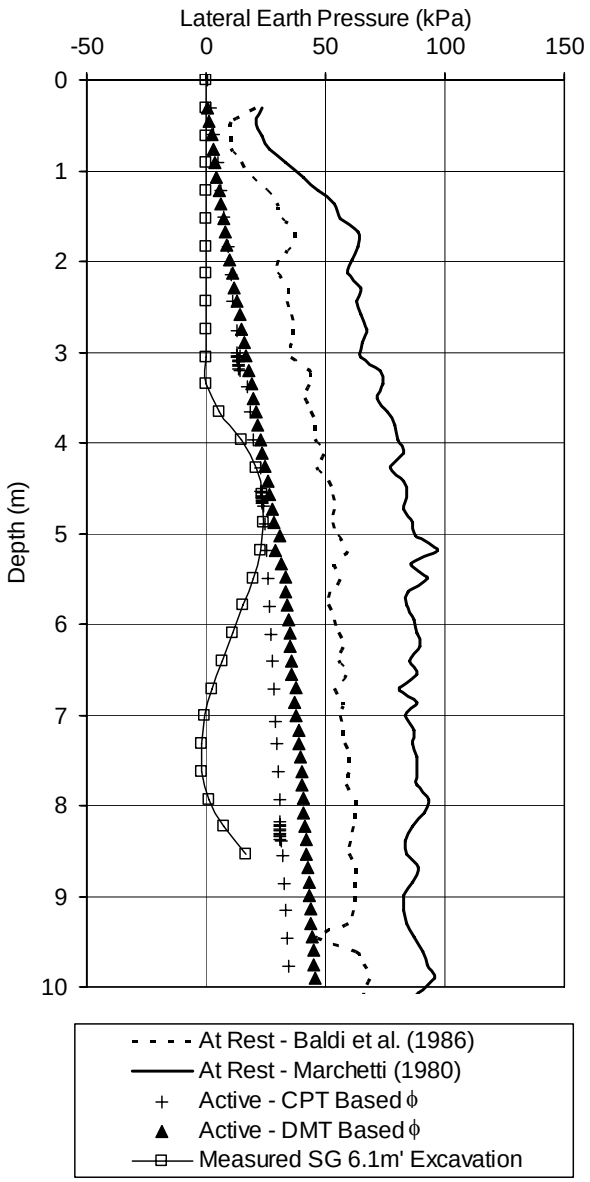

Figure 12 Derived earth pressure versus depth compared to predictions

6 CONCLUSIONS

DMT and CPT are valuable in-situ testing methods for estimating lateral earth pressure in PRS. Back-calculation from bending moment and slope measurements from cantilever sheet pile walls has proved to be viable concept to derive earth pressure distribution in PRS. For the walls excavated to a depth of 6.1m, comparisons of prediction of earth pressure using a non cohesive relationship for PRS based on DMT and CPT leads to a conservative estimate. To predict earth pressure in PRS, the friction angle derived from the DMT should be used with a cohesion value of nearly 9.6 kPa.

ACKNOWLEDGEMENTS

This paper originates from a research project sponsored by NCDOT through research grant 2005-16. The authors would like to acknowledge Tim Cleary and Billy Camp from S&ME Inc. in Charleston, SC for donating four CPT tests at the research site. Mr. Roger Failmezger generously loaned the K_0 stepped blade for use in this study.

REFERENCES

Baldi, G., Bellotti, R., Ghionna, V., Jamiolkowski, M., Marchetti, S. & Pasqualini, E. (1986). "Flat Dilatometer Tests in Calibration Chambers". Proc. In Situ '86, ASCE Spec. Conf. on "Use of In Situ Tests in Geotechn. Engineering", Virginia Tech, Blacksburg, VA, June, ASCE Geotechn. Special Publ. No. 6, 431-446.

Marchetti, S. (1980). "In Situ Tests by Flat Dilatometer." Journal of the Geotechn. Engineering Division, ASCE, Vol. 106, No. GT3, Proc. Paper 15290, pp. 299-321.

The use of DMT data for lateral load analyses

David K. Crapps, Ph.D., P.E.
GPE, Inc., Gainesville, FL, USA

Keywords: DMT, effects of construction, lateral load, p-y curves

Abstract: Several methods have been proposed in the literature to develop p-y curves from DMT data. Dilatometer soundings are often completed before construction begins. Construction may have an important effect upon lateral loads and lateral resistances. Construction may also have an important effect upon the parameters used to develop p-y curves. Therefore, construction effects should be addressed, to the extent practical, when estimating lateral load behavior. This paper reviews likely effects from construction and presents methods to adjust preconstruction DMT results to account for excavation.

1. INTRODUCTION

The dilatometer provides an almost continuous profile of data for lateral load analyses. The equipment and test methods for dilatometer tests (DMT) are described in ASTM D6635. There are a number of methods to estimate lateral loads including those proposed by Gabr and Borden (1988); Robertson, Davies, and Campanella (1989); Marchetti, Totanti, Calabrese and Monaco (1991) and Gabr, Lunne and Powell (1994)). Each of these papers demonstrates a reasonable match between the proposed method and limited load test data.

The practicing engineer often selects a method to compare predicted versus measured lateral load test data. If he or she does not get a good match, another method may be tried before a method of analyses is judged suitable for a given project. Most engineers are hesitant to modify published methods. However, the analysis method may not be the reason for the poor match. The poor match may be due to construction methods and equipment. This paper describes modifications to p-y curves to provide improved correlations between lateral load test data and estimated lateral loads. These modifications may be applied to p-y curves from DMT data at other locations on a project using the same construction procedures.

2. EFFECTS OF CONSTRUCTION ON LATERAL LOADS

The effects of construction upon axial capacity of piles and drilled shafts are now generally recognized. Construction may also have an important effect upon lateral capacity. However, there have been very few studies documenting the effects. Perhaps future research will help to quantify further the effects of construction on lateral capacity. In the meantime, lateral load tests may be used to calibrate a given site and provide correlations between lateral load estimates and load tests to provide confidence in lateral load design considerations.

2.1 *Possible Construction Effects on Pile Lateral Capacity*

The lateral capacity of piles is likely affected by soil type, ground water location, use of pile penetration aids (jetting, predrilling or punching), whether pipe piles or cylinder piles are driven open-ended or closed ended, whether open-ended piles are plugged or unplugged, driving equipment (impact or vibratory hammers), spacing of piles, order of pile installation, nearby fills or excavations, etc. There is some direct evidence documenting construction effects on lateral capacity. However, much of the evidence is indirect.

Schmertmann & Crapps (1993) performed a model study of the effects of jetting upon pile axial capacity. These experiments showed the axial capacity of an existing (previously driven) pile was reduced approximately 50% for piles located 5 pile widths away and the axial capacity was reduced approximately 20% for piles located 12.5 pile widths away. The study estimated the effects of jetting were close to zero at about 25 pile widths. If jetting results in pile penetration under the influence of gravity during jetting and its effect extends out almost 25 pile widths, one can readily surmise that disturbance due to jetting would influence lateral capacity. Vibrations from additional driving reconsolidate non-cohesive

soils to some extent. However, lateral load tests may be required to provide accurate estimates of the effects of jetting or other pile penetration aids (jetting, drilled preformed holes or punched preformed holes, etc.).

Hwang et al (2001) reported the results of a study of ground response during pile driving. Measurements were made during the driving of 800 mm cylinder piles with an inside diameter of 560 mm. The piles were constructed of prestressed concrete and were driven with a closed conical shaped end. Slope inclinometer measurements showed 20 mm average horizontal ground movements 3 diameters from the pile center, movements equal to 2.5% of the pile diameter. They estimated that the horizontal ground movements were insignificant at 12 times the pile diameter. If the initial ground surface was displaced laterally, the ground was horizontally displaced, from the pile centerline, at least 0.5 times the pile diameter (440 mm) at the face of the pile. Measurements made 1.5 times the pile diameter showed vertical ground movements (heave) of 36 mm. They also estimated that horizontal ground movements extended 10 diameters or more below the center of the pile tip. These data show significant ground disturbance for considerable distance around and below a driven pile. This disturbed soil would have different properties than the undisturbed soil and the estimated lateral load behavior would certainly be different for soils data taken before and after pile driving.

Many investigators, including Hwang et al (2001), have measured significant pore pressures during pile driving. Pore pressure induced by pile driving may create permanent changes in the soil strength even after their dissipation. For example, high pore pressures may break down the soil structure and create drainage paths that may affect lateral load behavior.

Huang et al (2001) reported on the effects of construction on laterally load pile and drilled shaft groups. They performed preconstruction and post construction CPT and DMT tests. The post-construction tests were conducted through the cap of the pile group. The authors introduced a p-multiplier to account for group effects from preconstruction DMT data and a p-multiplier to account for group effects from post-construction DMT data. The ratio of the post-construction effect to the preconstruction effect reflects the effects of construction. The authors derived a factor of 0.70 for the driven pile group which indicates that "... the installation of driven piles caused a densifying effect" (or increase in lateral stresses).

2.2 *Possible Construction Effects on Drilled Shaft Lateral Capacity*

Construction methods and equipment likely have more of an effect upon drilled shaft lateral capacity than on piles. Lateral capacity of drilled shafts is likely affected by soil type, ground water location, use of casing or no casing, sidewall relaxation, slurry buildup, nearby fills or excavations etc.

Crapps (2005) presented curves for measured slurry buildup versus time for bentonite and attapulgite. These curves showed 20 mm buildup of attapulgite and 23 mm buildup of bentonite in 2 days. Bentonite buildup was 100 mm in about 16.5 days. The filter cake or gel layer has little strength and could significantly affect lateral capacity if not removed before concrete placement. Note that before construction and after construction DMT testing would not likely detect excessive lateral movements due to slurry buildup. However, the effects of slurry buildup could be indirectly accounted for by adjusting p-y curves (say with a y-offset of the p-y curve) derived from DMT data so that lateral loads match those measured by lateral load tests.

O'Neill (2001, p.11) presented results of shear wave velocity measurements made three hours after a borehole was opened in Beaumont Clay (a stiff clay). The shear wave velocities increased with distance away from the side of the shaft excavation. These measured shear wave velocities indicate that stress relief was felt 2 to 3 borehole radii away from the wall of the shaft. The shear wave velocity was about 70% of the "free field" shear wave velocity away from the shaft. O'Neill estimated that the shear strength of the clay at the eventual concrete/shaft interface was about 50% of the undisturbed strength before excavation. Note that p-y curves estimated from DMT tests performed in undisturbed soil would be stiffer than those estimated from DMT tests performed within the zone of relaxation.

Rhyner (2005) presented a case history that demonstrated differences in lateral capacity of drilled shafts due to a difference in method of casing installation. The initial drilled shafts for the New York City World Trade Center Building 7 were installed using a vibratory hammer while new casings for replacement construction were installed using external flush. Lateral load tests showed that there were dramatic differences in lateral capacity due to different casing installation methods. The lateral load capacity of the shafts with casings installed by external flush was significantly lower than those with

casings installed with a vibratory hammer, especially at low loads. The lateral loads for the external flush shafts were close to zero until lateral deflections of about 12.7 mm (0.5") were reached.

Huang et al (2001) reported on the effects of construction on laterally loaded pile and drilled shaft groups as previously mentioned. They performed preconstruction and post-construction CPT and DMT tests. The post-construction tests were conducted through the cap of the drilled shaft group. The authors introduced a p-multiplier to account for group effects from preconstruction DMT data and a p-multiplier to account for group effects from post-construction DMT data. The ratio of the post-construction effect to the preconstruction effect reflects the effects of construction. The authors derived a factor of 1.19 for the drilled shaft group which indicates that "... the installation of bored piles softened the surrounding soil...".

3. GROUP EFFECTS

The lateral capacity of a pile or drilled shaft group is different than the capacity of a single pile or shaft times the number of piles or shafts in the group because the effects of lateral stresses from each pile or shaft overlap. The capacity depends upon the number of rows and the spacing of the piles or shafts. The "leading" row has the highest lateral capacity and each row behind the leading row has a reduced lateral capacity. Most lateral load programs have p-multipliers to account for group effects (see Ensoft (2005) or Florida Pier (2005)).

4. ESTIMATING LATERAL LOADS USING DMT DATA

The Robertson et al (1989) method is likely the most widely used method to develop p-y curves from DMT data. This method was described in detail by Briaud and Miran (1992) in a manual prepared for the FHWA. This method will be used in this paper.

The Robertson et al method uses a cubic parabola, reproduced as Equation (1) below, to produce p-y curves:

$$\frac{P}{P_u} = 0.5\left(\frac{y}{y_c}\right)^{0.33} \qquad (1)$$

Where: P/P_u = ratio of soil resistance
y/y_c = ratio of pile deflection
P_u = ultimate lateral force
y_c = critical deflection

The method to determine the values of P_u and y_c depend upon the soil type.

4.1 *P-y Curves For Clay*

Equation (2) may be used to determine the value of y_c for clays:

$$y_c = 23.67\frac{S_u D^{0.5}}{F_c E_D} \qquad (2)$$

Where: y_c = critical deflection in cm
D = pile diameter in cm
S_u = undrained shear strength (from DMT)
E_D = dilatometer modulus (same units as S_U)
F_c = ratio of initial tangent modulus to the dilatometer modulus.

Robertson et al assumed a value of 10 for F_c, as a first approximation, for clay soils. The reader should note that the value of F_c is not well established and may vary. Part of the variation may be due to construction effects.

Equation (3) may be used to determine P_u for clay:

$$P_u = N_p S_u D \qquad (3)$$

Where: P_u = ultimate lateral force (same units as S_u)
N_p = nondimensional ultimate resistance coefficient

$$N_p = 3 + \frac{\sigma_v'}{S_u} + \frac{Jx}{D} \qquad (3a)$$

Where: J = empirical coefficient (0.25 for stiff clay and 0.50 for soft clay; stiff clay assumed in this study as $S_u > 0.5$ tsf - values of J interpolated between 0.25 and 0.50)
x = depth
σ_v' = effective vertical stress at depth x

Note that S_u and E_D are required for y_c and S_u is required for P_u. These values are provided by DMT tests.

4.2 *P-y Curves for Sand*

Equation (4) may be used to determine the value of y_c for sand:

$$y_c = \frac{4.17\left(\sin\phi'\right)\sigma_v' D}{F_s E_D\left(1-\sin\phi'\right)} \qquad (4)$$

Where: y_c = critical deflection in cm
D = pile diameter in cm
F_s = empirical stiffness factor
ϕ' = angle of internal friction

Robertson et al (1989) first assumed F_s would be equal to 1 as a first approximation. However, analyses of their data required use of a value of F_s equal to 2 for the best match of their test data. The reader should note that the value of F_s is not well established and may vary. Part of the variation may be due to construction effects.

Equations (5a) and (5b) may be used to determine possible values of P_u for sand. The value of P_u is taken as the minimum from (5a) or (5b).

$$P_u = \sigma_v'\left[D\left(K_p - K_a\right) + xK_p \tan\phi' \tan\beta\right] \qquad (5a)$$

$$P_u = \sigma_v' D\left(K_p^3 + 2K_o K_p^2 \tan\phi' + \tan\phi' - K_a\right) \qquad (5b)$$

Where: P_u = lesser of (5a) or (5b)
K_a = Rankine active coefficient
$= \left(1-\sin\phi'\right)/\left(1+\sin\phi'\right)$
K_p = Rankine passive coefficient = $1/K_a$
K_0 = coefficient of earth pressure at rest
β = $45^o + \varphi'/2$

Note that ϕ' and E_D are required for y_c and that ϕ' and K_0 are required for P_u. These values are provided by DMT tests.

5. ACCOUNTING FOR EXCAVATIONS

The dilatometer is a valuable tool to provide design data for retaining structures. As previously mentioned, soils data, including DMT data, are often obtained before construction. This section provides a method to account for the effects of excavation. Excavations obviously have an important effect upon σ_v' and may have an important effect upon E_D, S_u, K_0, and ϕ' values used to estimate the value of y_c and P_u for p-y curves. The equations to account for excavation are included in Appendix A along with background information concerning the equations. Large projects may justify DMT testing before and after excavation to properly account for site specific changes due to excavation. However, the equations included herein may be used to estimate the effects.

6. RECOMMENDED MODIFIERS FOR P-Y CURVES

The author proposes three modifiers (C_y, C_P and Δ_y) for p-y curves to account for the effects of construction. The first modifier, C_y, adjusts the estimated value of y_c as shown in Equation 6a and the second modifier, C_P adjusts the value of P_u as shown in Equation (6b). The value of Δ_y denotes the y-movement required before the value of P begins to increase from zero.

$$y_c' = C_y y_c \qquad (6a)$$

$$P_u' = C_p P_u \qquad (6b)$$

Equations (1a) and (1b) reflect the changes in Equation (1) after introducing the modifiers.

$$P' = 0 \qquad \text{when } y' \le \Delta_y \qquad (1a)$$

$$\frac{P'}{P_u'} = 0.5\left(\frac{y}{y_c'}\right)^{0.33} \qquad \text{when } y' > \Delta_y \qquad (1b)$$

$$y' = y + \Delta_y \qquad (1c)$$

The intent is to offset the p-y curve by an amount equal to Δ_y to account for conditions that allow lateral movement before lateral resistance is encountered. The modified curves, P' versus y', are used in the lateral load analyses. Note that one may make a p-y curve stiffer by increasing the value of P_u or by decreasing the value of y_c. A value of C_P greater than 1.0 or a value of C_y less than 1.0 makes the p-y curve

stiffer; and, conversely a value of C_P less than 1.0 or a value of C_y greater than 1.0 makes the p-y curve softer (less stiff). One may note that the use of a value of C_y other than 1.0, effectively modifies F_c or F_s which may vary depending upon the effects of construction, as previously noted. One may also note that the use of a value of C_p other than 1.0, effectively modifies S_u, which may also be affected by construction as previously noted. A value of Δ_y greater than zero offsets the entire p-y curve but does not change the stiffness. Also note that the introduction of multipliers for P_u and y_c and the use of an offset, Δ_y , for y may be used for p-y curves generated by any method.

7. CASE HISTORY

This case history is from the Puerto Nuevo Project, a U.S. Army Corps of Engineers Project located in San Juan, Puerto Rico. Rains swell mountainous streams which flow through San Juan to the ocean. The streams are narrow and development in San Juan has reached both sides of the streams at some locations. These existing natural waterways are being widened and/or deepened to improve the drainage in San Juan. At some locations, retaining walls are required to protect existing construction. This case history is from the load test program for this project.

One of the wall designs included 1220 mm (48 inch) diameter pipe “king” piles providing lateral support for steel sheet piles placed between the pipe piles. The plan excavation in front of the wall was to elevation -4880 mm (-16 feet). The elevation of the ground surface at the time the DMT soundings were made was about elevation +1220 mm (+4 feet). Therefore, there would be about 6100 mm (20') of excavation in front of the wall after it was constructed.

The load test program included the lateral testing of two steel 1220 mm piles of different lengths. The pipe piles, with 19 mm (0.75 inch) wall thickness, were driven and a cap constructed on each of the piles at the Contract 2A test site. Two separate static lateral load tests were performed at the site by jacking one cap against the other. Test 1 was conducted before excavation and Test 2 was constructed after a cofferdam was constructed and excavated to approximately the design excavation elevation. Additional details are available in the project report (see Crapps (2000)).

The lateral load test site was moved from its intended location due to a conflict with a fly-over bridge subsequently constructed after the original testing was completed. New DMT tests were completed at the test site by GEOCIM (see GEOCIM (2000) or Crapps (2000)). The DMT data at the test site were adjusted for the effects of excavation (a small excavation primarily to remove construction debris before the first test and a deep excavation before the second lateral load test), p-y curves were developed and appropriate values of C_p were developed by trial and error using LPILE3 (see Reese and Wang (1997)). A value of C_p equal to 1.1 before excavation and 1.2 after excavation provided a good match with the load test results. Note that C_y was set equal to 1.0 and Δ_y was set equal to 0.0. Note that relatively small adjustments (C_p values of 1.1 and 1.2 versus 1.0) were required for a good match between predicted and measured results, after making the adjustments for the effects of excavation.

Anderson et al (2003) used *FloridaPier* (*FLPier*) with p-y curves derived from SPT, CPT, DMT and PMT data to compare predicted versus measured lateral deflections. The Puerto Nuevo Project test program data were included in their analyses. One of their conclusions was that "On the average, DMT derived p-y curves predict well at low lateral loads.” However, they did not have a good correlation between predicted deflections using DMT data and measured deflections at high lateral loads. The differences in the match for lateral load behavior determined by Anderson et al. (2003) and Crapps (2000) are likely due to construction effects. This paper and the Anderson et al. paper demonstrate the need for future research to provide a better understanding of the effects of construction.

8. SUMMARY & CONCLUSIONS

1. Factors, related to construction, which may have an effect upon the lateral load capacity of piles and drilled shafts are summarized.

2. A method to account for excavation (decrease in effective stresses) is presented for DMT data.

3. Modifiers for p and y are proposed to account for the effects of construction upon lateral load behavior.

4. A case history was presented using the methods to account for excavation.

APPENDIX A – ACOUNTING FOR THE EFFECTS OF EXCAVATION

A1. INTRODUCTION

Appendix A provides the background for derivation of equations to estimate the effects of excavation.

A2: CHANGE IN EFFECTIVE STRESS DUE TO EXCAVATION

Elastic methods may be used to estimate the effects of excavation upon effective stress (for example, see Poulos and Davis (1974)).

A3. DEFINITIONS

Marchetti (1980) provided Equations (A1), (A2) and (A3 which define three key DMT variables:

$$E_D = 34.7\left(p_1 - p_0\right) \tag{A1}$$

$$K_D = \frac{p_0 - u_0}{\sigma_0^{'}} \tag{A2}$$

$$I_D = \frac{p_1 - p_0}{p_0 - u_0} \tag{A3}$$

A4. UNDRAINED SHEAR STRENGTH

The undrained shear strength is required for a number of methods to estimate P-y curves for clay. Many sites have clays that are overconsolidated or will be overconsolidated upon excavating in front of the walls. Equation (A4), from Schmertmann (1978) and/or Tang & Tsuchida (1999) provides a method to estimate the effects of overconsolidation ratio on the undrained shear strength of clays:

$$\frac{S_{u1}/\sigma_{01}^{'}}{S_{u2}/\sigma_{02}^{'}} = \left(\frac{OCR_1}{OCR_2}\right)^{\Lambda} = \left(\frac{\sigma_{p1}^{'}/\sigma_{01}^{'}}{\sigma_{p2}^{'}/\sigma_{02}^{'}}\right)^{\Lambda} \tag{A4}$$

Where: S_{u1} = undrained shear strength for cond. 1
S_{u2} = undrained shear strength for cond. 2
OCR_1 = over consolidation ratio for cond. 1
OCR_2 = over consolidation ratio for cond. 2
$\sigma_{p1}^{'}$ = preconsolidation stress for condition 1
$\sigma_{p2}^{'}$ = preconsolidation stress for condition 2
$\sigma_{01}^{'}$ = vertical effective stress for condition 1
$\sigma_{02}^{'}$ = vertical effective stress for condition 2
Λ = coefficient ranging from 0.7 to 0.9

A4.1 *Effect of Excavation on S_u*

Noting that the preconsolidation stress remains the same when there is an excavation ($\sigma_{p1}^{'} = \sigma_{p2}^{'}$) and using the average value of 1-Λ = 0.2 provides equation (A5):

$$S_{u2} = \left(\frac{\sigma_{02}^{'}}{\sigma_{01}^{'}}\right)^{0.2} S_{u1} \tag{A5}$$

A5. EFFECT OF EXCAVATION ON E_D

A5.1 Undrained E_D

Marchetti (1980) presented the Equation (A6) for undrained shear strength (also see Schmertmann (1988) or Briaud and Miran (1992).

$$S_u = 0.22\sigma_o^{'}\left(0.5K_D\right)^{1.25} \tag{A6}$$

Equation (A7a) may be derived from equations (A1), (A2) and (A3).

$$E_D = 34.7\left(K_D I_D\right)\sigma_0^{'} \tag{A7a}$$

Solving Equation (A7a) for K_D and substituting in Equation (A6) provides Equation (A7b).

$$E_D = 233 S_u^{0.8} I_D \left(\sigma_0^{'}\right)^{0.2} \tag{A7b}$$

The value of I_D remains constant with a change in effective stress ($I_{D2} = I_{D1}$). Equation (A8) may be used to estimate the effects of excavation upon undrained values of E_D.

$$\frac{E_{D2}}{E_{D1}} = \left(\frac{S_{u2}}{S_{u1}}\right)^{0.8} \left(\frac{\sigma'_{01}}{\sigma'_{02}}\right)^{0.2} \quad \text{(A8)}$$

A5.2 *Drained E_D*

The drained value of E_D is expected to remain constant with excavation. Therefore, assume $E_{D2} = E_{D1}$.

A6. EFFECT OF EXCAVATION ON ϕ'

A detailed discussion of estimates of ϕ' from DMT test data may be found in Schmertmann (1988). The value of ϕ' for sands is dependent upon effective stress due to the non-linearity of the failure envelope. The values of ϕ' presently reported in the DMT data reduction program provided by GPE, Inc. are based upon a standard reference failure pressure of 2.72 bars as explained in Schmertmann (1983). Schmertmann (1983) and Schmertmann (1984) presented an equation (presented below as Equation (A9)) as well as a figure to estimate ϕ' for other failure pressures. Both the figure and Equation (A9) require an iteration procedure for a solution based upon a change in effective stress. However, Equation (A9) converges rapidly even if the value of ϕ'_2 is set equal to ϕ'_1 for the first trial. Note that the value of ϕ' provided by the DMT is a plane-strain parameter.

$$\phi'_2 = \tan^{-1}\left\{\begin{array}{l}\tan\phi'_1 + 0.0446 - \\ 0.105\log\left((1+\sin\phi'_2)\,\sigma'_{02}\right)\end{array}\right\} \quad \text{(A9)}$$

Where: $\phi'_1 = \phi'$ before excavation
$\phi'_2 = \phi'$ after excavation
$\sigma'_{02} = \sigma'_0$ after excavation

One may note that the effect of excavation typically increases the value of ϕ'_2. In the event that the calculated value of ϕ'_2 is greater than 45 degrees, a value of 45 degrees should be used.

A7. EFFECT OF EXCAVATION UPON K_o FOR SANDS

The value of K_o is required to determine the value of P_u for sands. Schmertmann (1992) derived the following expression relating the *OCR* to K_o.

$$OCR = \left[K_0/(1-\sin\phi'_{ax})\right]^{\left(1/0.8\sin\phi'_{ax}\right)} \quad \text{(A10a)}$$

Where: *OCR* = overconsolidation ratio
ϕ'_{ax} = axisymetric ϕ'

Solving Equation (A10a) for K_o provides Equation (A10b).

$$K_0 = \left(1-\sin\phi'_{ax}\right)OCR^{\left(0.8\sin\phi'_{ax}\right)} \quad \text{(A10b)}$$

Equation (10b) provides Equation (A11).

$$\frac{K_{01}}{K_{02}} = \frac{\left(1-\sin\phi'_{ax1}\right)OCR_1^{\left(0.8\sin\phi'_{ax1}\right)}}{\left(1-\sin\phi'_{ax2}\right)OCR_2^{\left(0.8\sin\phi'_{ax2}\right)}} \quad \text{(A11)}$$

The excavation does not change the value of the preconsolidation stress. Therefore, $\sigma'_{p2} = \sigma'_{p1}$ and Equation (11a) may be derived.

$$\frac{K_{02}}{K_{01}} = \left\{\frac{(1-B)}{(1-A)}\frac{\left(\sigma'_{01}\right)^{0.8A}}{\left(\sigma'_{02}\right)^{0.8B}}\right\}\left(\sigma'_{p1}\right)^{0.8(B-A)} \quad \text{(A11a)}$$

Where: $A = \sin\phi'_{ax1}$ and $B = \sin\phi'_{ax2}$
K_{o1} = before excavation value of K_o
K_{o2} = after excavation value of K_o
ϕ'_{ax1} = before exc. value of axisymetric ϕ'
ϕ'_{ax2} = after exc. value of axisymetric ϕ'

A8. ESTIMATING AXISYMETRIC ϕ' FROM PLANE STRAIN ϕ'

Note that all the values of ϕ' prior to Equation (A10) have been plane-strain parameters provided by the DMT test. One may use Equation (A12) from

Schmertmann (1992) to estimate axisymetric parameters.

$$\phi'_{ax} = \phi'_{ps} \quad \text{for } \phi'_{ps} \leq 32^0 \qquad \text{(A12a)}$$

$$\phi'_{ax} = \phi'_{ps} - \left[\left(\phi'_{ps} - 32\right)/3\right] \text{ for } \phi'_{ps} \rangle 32^0 \qquad \text{(A12b)}$$

Where: ϕ'_{ax} = axisymetric ϕ'

ϕ'_{ps} = plane strain ϕ'

REFERENCES

Anderson, J. B.; Townsend, F. C.; and Grajales, B. (2003), "Case History Evaluation of Laterally Loaded Piles", *Journal of Geotechnical and Geoenvironmental Engineering*, Vol. 129, No. 3, March, pp.187-196.

Briaud, Jean-Louis & Miran, Jerome (1992), The Flat Dilatometer Test, Report No. FHWA-SA-91-044, FHWA Office of Technology Applications, Washington, D.C., February.

Crapps, David K. (2000), PUERTO NUEVO RIVER FLOOD CONTROL PROJECT CONTRACT 2A, LATERAL LOAD TEST REPORT, 2 Volumes, Schmertmann & Crapps, Inc. report to Corps of Engineers, December.

Crapps, David K. (2005), "Effects of Construction Time On Drilled Shaft Capacity", Drilled Shafts: Constructability and its Effect on Capacity, DFI Seminar, Kissimmee, Florida, August 8.

Ensoft, Inc. (1997), "Group 4.0, A Program for the Analyses of Piles In a Group", Austin, Texas.

Ensoft, Inc. (2004), "LPILE Plus v5.0 for Windows", A Program for the Analyses of Piles and Drilled Shafts Under Lateral Loads", Austin, Texas, http.

Gabr, Mohammed A. & Borden, Roy H. (1988), Analyses of load deflection response of laterally loaded piers using DMT, *Proceedings*, Penetration Testing 1988, ISOP-1, De Ruiter (ed.), 1988 Balkema, Rotterdam, ISBN 90 6191 801 4, pp. 513-520.

Gabr, M. A.; Lunne, T.; and Powell, J. J. (1994), Analyses of Laterally Loaded Piles in Clay Using DMT@, Proceedings, *Journal of Geotechnical Engineering*, Vol. 120, No. 5, May, pp. 816-837.

Gabr, M. A.; Lunne, T.; and Powell, J. J. (1995), Closure to Discussion Analyses of Laterally Loaded Piles in Clay Using DMT, *Journal of Geotechnical Engineering*, Vol. 120, No. 9, September, pp. 682-683.

GEOCIM (2000), Report of DMT and SPT Testing, prepared for Jacksonville District of the U. S. Army Corps of Engineers (included in Schmertmann & Crapps, Inc. report to GEOCIM on DMT Testing).

Huang, An-Bin, Hsueth, Chao-Kuang, O'Neill, Michael W., Chern, S. and Chen, C. (2001), "Effects of Construction on Laterally Loaded Pile Groups", *Journal of Geotechnical and Geoenvironmental Engineering*, Vol. 127, No. 5, May, pp.385-397.

Hwang, Jim-Hung, Liang, Neng; and Chen, Cheng-Hsing (2001), "Ground Response During Pile Driving", *Journal of Geotechnical and Geoenvironmental Engineering*, Vol. 127, No. 11, November, pp. 939-949.

Marchetti, S.; Totanti, G; Calabrese, M and Monaco, P. (1991), P-y curves from DMT data for piles driven in clay, *Proceedings*, 4th International Conference on Piling and Deep Foundations, Deep Foundations Institute, Stresa Italy, April 7-12.

Monaco, Paola & Marchetti, Silvano (1995), Discussion to Analyses of Laterally Loaded Piles in Clay Using DMT by Gabr, Lunne, and Powell (1994), *Journal of Geotechnical Engineering*, Vol. 120, No. 9, September, pp. 680-682

O'Neill, Michael W. (2001), "Side Resistance in Piles and Drilled Shafts", 34th Terzaghi Lecture, *Journal of Geotechnical and Geoenvironmental Engineering*, Vol. 127, No. 1, Jan., pp. 3-19.

Poulos, H. G. and Davis, E. H. (1974), *ELASTIC SOLUTIONS FOR SOIL AND ROCK MECHANICS*, John Wiley & Sons, Inc., New York, p.54.

Reese, Lymon C. and Wang, S.T. (1997), *Technical Manual of Documentation of Computer Program LPILE^{PLUS} 3.0 For Windows, Stress-and-Deformation Analysis of Piles Under Lateral Loading With Special Feature of Use of Piles To Stabilize a Slope*, Ensoft, Inc., Austin, Texas, May.

Rhyner, Frederick C. (2005), "Effect of External Flush on Lateral Load Capacity", Drilled Shafts: Constructability and its Effect on Capacity, DFI Seminar, Kissimmee, Florida, August 8.

Robertson, Peter K., Davies, Michael P., and Campanella, Richard G. (1989), Design of Laterally Loaded Driven Piles Using the Flat Dilatometer, *ASTM Geotechnical Testing Journal*, Volume 12, Number 1, March, pp. 30-38.

Schmertmann, John H. (1978), *Guidelines for Cone Penetration Test Performance and Design*, FHWA-TS-78-209, Federal Highway Administration, Implementation Division, Washington, D.C., July 1978.

Schmertmann, John H. (1983), *DMT DIGEST Number 2*, GPE, Inc. publication for DMT Users, Gainesville, Florida, July.

Schmertmann, John H. (1984), *DMT DIGEST Number 3*, GPE, Inc. publication for DMT Users, Gainesville, Florida, February.

Schmertmann, John H. (1988), Guidelines for using the CPT, CPTU and Marchetti DMT for Geotechnical Design, Volume III, DMT Test Methods and Data Reduction, Report to FHWA & Pennsylvania DOT, March, 183 pages.

Schmertmann & Crapps, Inc. (1993), Buckman Bridge (Job 884) Project Records, "Model Pile Jetting Experiments"

Tang, Yi Xin and Tsuchida, Takashi (1999), The Development of other Shear Strength for Sedimentary Soft Clay With Respect To Aging Effect, Japanese Geotechnical Society, *SOILS AND FOUNDATIONS*, Vol. 39, N. 6, 13-24, Dec.

DMT experience in Iberian transported soils

Nuno Cruz
Mota-Engil, SA, Univ. Aveiro, Portugal (www.mota-engil.pt)

Marcelo J. Devincenzi
IgeoTest, S.L., Figueres, Spain (www.igeotest.com)

António Viana da Fonseca
Faculdade de Engenharia da Universidade do Porto, Portugal (www.fe.up.pt)

Keywords: Marchetti Flat Dilatometer, Transported Soils

ABSTRACT: For the last ten years DMT has been used successfully, both in Portugal and Spain, in transported soils characterization, with special emphasis on alluvial deposits. These results have been cross-correlated with those from both in situ and laboratory testing, such as SCPTU, FVT, PMT, triaxial and consolidation tests, to test the efficiency of interpretation models in the soils of both countries. In this paper, the general conclusions of ten years of work will be presented, primarily with stress history, shear strength and stiffness parameters. Some comparisons of p_2 (DMT) and u_2 (CPTU) results are also presented

1 INTRODUCTION

The results presented in this paper are part of an extensive program, composed of 47 experimental sites, first located in Portuguese territory and recently enlarged to Spain.. The main goal was to check the accuracy of DMT tests with regards to the universally accepted correlations established for parametrical derivation, and to study other approaches that are being studied in our group (Cruz, 1995; Cruz et al, 1997). From the total amount of experimental sites, 15 were performed in granitic residual soils whose behaviour is quite different from sedimentary transported one. The research on residual soils is presented in another paper in this conference.

Sedimentary experimental sites covered all types of soils from clays to sands, organic to non-organic, stable to sensitive. Over all, 200 tests were performed (plus identification and physical index tests) including 57 DMT, 50 FVT, 40 CPTU, 4 PMT, 6 SCPTU, 2 cross-hole seismic, 9 triaxial and 37 oedometric consolidation tests.

2 STRATIGRAPHY, UNIT WEIGHT AND PORE PRESSURE

One of the basic important features of DMT is its capacity to give information related to the basic properties (identification and physical index) of soils, thus creating a rare autonomy in the characterization field. Analysing the global data set obtained in this research program, one should be tempted to say that DMT can easily take the place of boreholes in general subsurface investigations. Of course, this is not a suggestion to fully substitute boreholes in investigations, but just some of them (perhaps a maximum of 50%). This consideration is mainly due to the following reasons:

a) DMT identifies with accuracy the type soil and the resulting information is easy to correlate with boreholes, thus allowing to create cross sections with the same level of accuracy;
b) DMT shows even higher accuracy to characterise strata with interbedded thin layers, usually undetected in bore-hole information;
c) It is possible to determine the position of water level, and consequently hydrostatic pore pressure (u_0), in sandy environments;
d) Through U_D parameter information on permeability can be obtained;
e) I_D is a numerical way for classification of soils, easier to use than CPTs, which surely opens a new range of possibilities for data interpretation, with special emphasis in statistical analysis and to basic understanding of mixed soils behaviour.

The data analysis that supports these conclusions is presented in the following paragraphs. In the first place, identification of soils based on Marchetti (1980) original correlation, globally represents the geological environment of the experimental sites, confirming the international recognition of his corre-

lation. In fact, DMT results show good comparisons with borehole information and laboratory identification tests, by means of Triangular and Unified classifications. Additionally, comparisons with CPTU identification results revealed the same level of accuracy for both tests.

The unit weight was evaluated by Marchetti and Crapps (1981) chart and compared with values obtained in laboratory from undisturbed samples. Of course, in sandy soils undisturbed sampling is very difficult, so the results reflect mainly cohesive soils (clays and silts). The final results revealed variations globally less than 1kN/m^3, and only in a few cases differences of $\pm$ 2kN/m^3 (Figure 1). Thus, it can be said that results show good accuracy allowing reasonable vertical effective stresses evaluations which makes the test more independent from external needs.

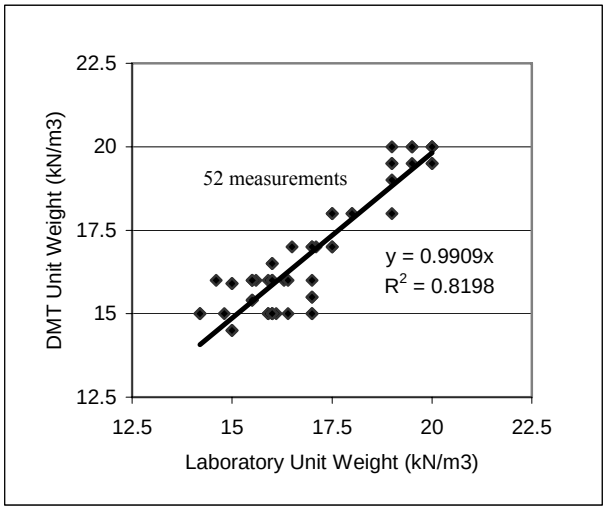

Figure 1 - Unit Weight comparisons

Although DMT cannot measure pore pressure directly, the value of pressure P2 (Luttenegger, 1988) and consequent Pore Pressure Index, U_D, can be used to derive important information of the strata, as pointed out by ISSMGE TC16 report (Marchetti, 2001):

a) Determination of water level in sandy environments;
b) Discerning free from non-free draining layers.

Besides DMT tests, the data collection of this work include piezometric measurements and CPTU (u_2 type) which allowed to outline some conclusions. In fact, direct comparisons of P_2 and u_2 revealed a general parallel increasing pattern, although with some scatter for low values (Figure 2).

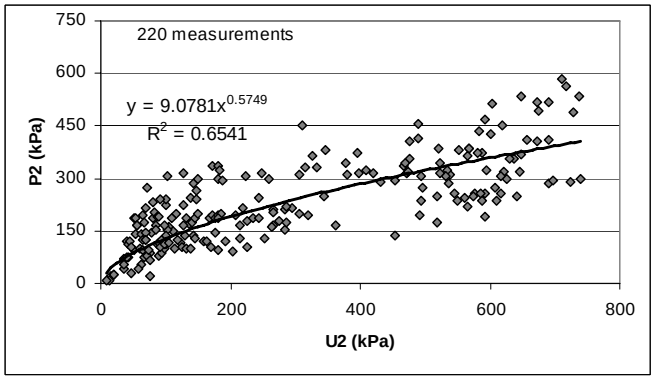

Figure 2 - P_2 (DMT) - u_2 (CPTU) comparing results

In fine grained soils with I_D lower than 0.9, when plotting the ratio P_2/u_2 against I_D reveal a clear drop-down of the ratio with increasing I_D is revealed, approaching gradually a lower level of 0.5 (Figure 3a). In sandy soils, the overlap of P_2 and u_0 profiles can be easily recognized, confirming the efficiency of the parameter to detect the depth of water table. The general plot shows a distribution that could be useful to interchange P_2 and u_2, mostly in silty soils.

.

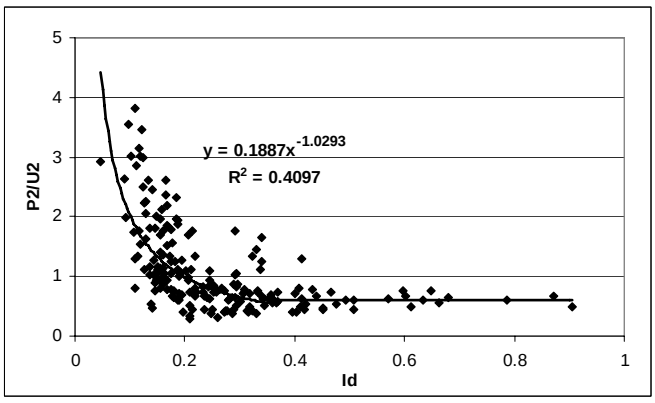

Figure 3a - Variation P_2 / u_2 with I_D in fine grained soils

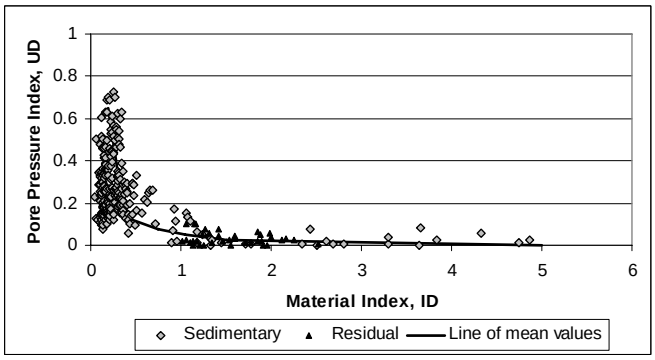

Figure 3b - Variation of U_D with I_D

As for the Pore Pressure Index, U_D, evaluations, Figure 3b presents the globally obtained data, with the black line representing the evolution of mean values for each interval of soils defined by Marchetti (1980) and represented by I_D. From these data the following conclusions can be outlined:

a) Data reflects fully undrained behaviour for soils with I_D < 0.35, meaning clayey soils.

U_D, within this interval decreased globally from a maximum of 0.65 to 0.25.

b) Fully drained behaviour ($U_D = 0$) was identified for soils with $I_D > 1.8$, meaning sands to silty sands

c) Partially undrained behaviour (transition curve) for the intermediate soils, showing U_D decreasing from 0.25 to 0, with increasing I_D.

d) The obtained values fit well with data from Benoit (1989)

3 STATE OF STRESS AND STRESS HISTORY

In the course of this research, it was not possible to experimentally determine K_0, namely through Self-Boring Pressuremeter testing and/or K_0 triaxial testing, so the main comparisons are limited to some empirical correlations applied to fine grained soils. DMT data was derived from Marchetti correlation (1981) and then compared with evaluations proposed by Mayne & Kulhawy (1982), and confirmed, in clays by recent research (Lunne et al., 1990), as refered by Mayne (2001):

$$K_0 = (1 - \sin\phi') \, OCR^{\sin\phi'}$$

The shear strength angle of clays was derived through IP (Kenney, 1967) and OCR derived from dilatometer. The results of the obtained correlations are presented in Figure 4, where the results of K_0 deduced from plasticity index and OCR (Brooker & Ireland, 1965) were included. It results clear that there is no gap between both correlations and showing essentially 1:1 proportion.

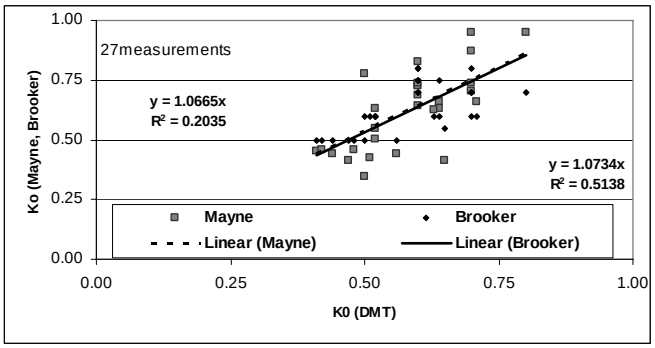

Figure 4 - K_0 comparisons

Stress history was analysed by comparing OCR(DMT) with oedometric consolidation test results, which generally fit together. It should be remembered that the work covered a narrow band of OCR values (1-3), corresponding to normally to slightly overconsolidated soils.

4 ANGLE OF INTERNAL FRICTION, ϕ'

The determination of friction angle throughout DMT is a very difficult task since there is a strong dependency of K_0, whose evaluation in sandy soils is very problematic. Various methods have been proposed, which can be summarized as follows (ISSMGE TC 16):

a) Method 1a - Iterative method (Schmertmann, 1983); it is based on K_D and thrust penetration of the blade (directly determined or through q_c from CPT tests), which can be applied to both K_0 and ϕ'.

b) Method 1b - Based in CPT and DMT tests performed side by side (Marchetti, 1985), the method first derives K_0 from q_c and K_D through Baldi's correlation (1986) and then recours to the theory of Durgonuglu & Mitchell (1975) to estimate ϕ' from K_0 and q_c.

c) Method 2 - Based on the definition of a lower bound (Marchetti, 1997), this method does not procure the precise value of the parameter, but just a safe value; it depends solely on K_D.

The first method is very complex and demands for the measurement of a penetration force which normally is not available, so it hasn't been considered. The second method needs both CPT and DMT results, not always available. The third one, although not so accurate as the other two, has the advantage of being easy to apply. Its expected deviation makes only a small difference in final calculations of bearing capacity for day-to-day problems. The global results obtained by the latter, were plotted against reference ϕ' (CPTU) evaluated by Robertson & Campanella chart (1983) and presented in Figure 5.

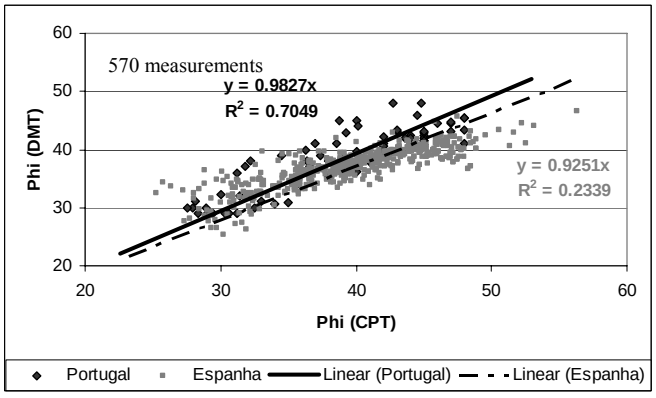

Figure 5 - Marchetti lower bound determination of ϕ' compared with CPTU results

As it can be observed Spanish data shows ratios DMT / CPT lower than the Portuguese and smaller than 1 in both cases. Statistical analysis performed on the ratio ϕ' (DMT) / ϕ' (CPTU) revealed results

expressed by 0.95 $\pm$ 0.1, globally within the interval 0.76 to 1.33.

5 UNDRAINED SHEAR STRENGH

The undrained shear strength of fine grained soils is one of the best correlated parameters from the dilatometer test. In this scope, the calibration of the parameter was strongly based on Field Vane Tests (FVT), as it is the reference test in Portugal and Spain. The final results (with Bjerrum correction to FVT results) revealed some interesting aspects that will be discussed below.

The most often applied correlation to derive undrained shear of fine grained soils is the one established by Marchetti (1980), which is obtained via OCR, derived from K_D as an input parameter. Several researchers concluded that obtained results by this approach correlates well with corrected field vane test values. On the other hand, since s_u determination is dependent on the test type, Lacasse and Lunne (1988) proposed different correlations related to FVT, triaxial and simple shear tests. The differences between this latter and Marchetti's derived values are represented by parallel trends, so they are very similar.

A completely different approach is given by Roque et al. (1988) who have proposed a determination based on load capacity theories. In this case s_u would be dependent of P_1 parameter (instead of P_0, used on K_D determination), horizontal total stress (derived from DMT, through K_0) and a factor (Nc) depending on the plasticity of soils. This latter may be the weakest point of this formulation since its subjectivity can be significant (reference values for this parameter are just 5, 7 and 9, respectively for non-plastic, intermediate and plastic clays).

It is relevant to emphasize that, as concluded by Lutenegger (1988) the gap between reference values and DMT's increases with increasing I_D, which is certainly linked to partial drainage that arise and becomes significant with increasing silt and/or sand components.

The overall results, when first plotted altogether revealed significant scatter, showing difficult interpretation. However, when divided in two groups, organic and non-organic soils, the results showed quite different trends, as it is presented in Figure 6.

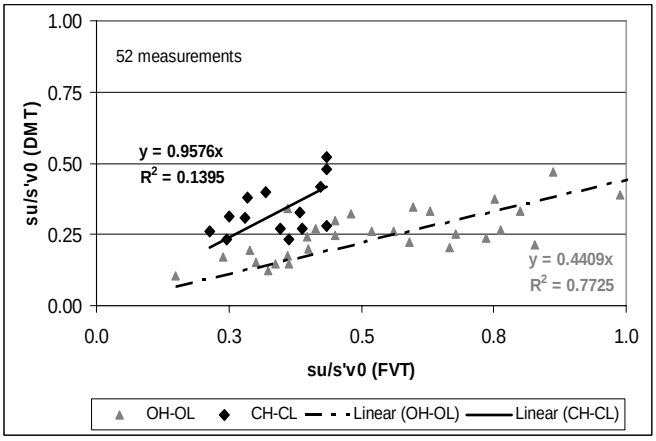

Figure 6 - S_u (DMT) for organic and non-organic soils, compared with FVT

In the non organic cases it is quite clear that results confirm the international experience with the values from Marchetti's correlation being comparable to FVT results. The same conclusion can be applied when the results are compared with those from triaxial tests (Figure 7).

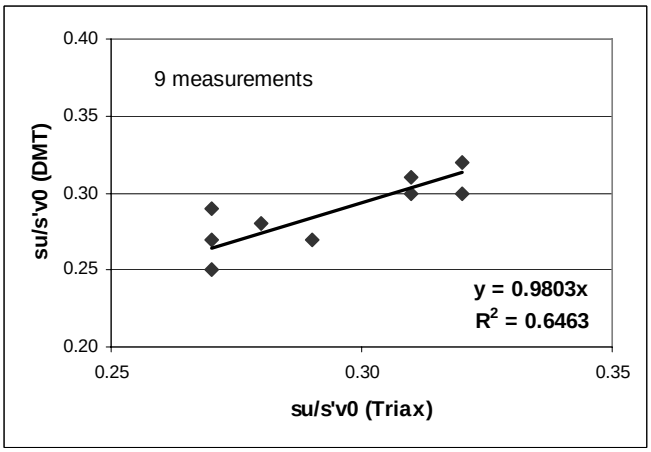

Figure 7 - Results from Marchetti's correlation, compared with triaxial testing

In the case of organic soils, Marchetti´s correlation tends to be too low when according FVT results, while Roque's seem to reproduce them better (Figure 8). More than that, the ratio s_u/σ'_{v0} (DMT) / s_u/σ'_{v0} (FVT) seems to increase with increasing OCR_{DMT} (Figure 9). OCR lower than one, represented in the same Figure, belong to a soft soil layer under an earthfill, whose consolidation was not yet complete. It should be referred that oedometric consolidation tests showed similar values.

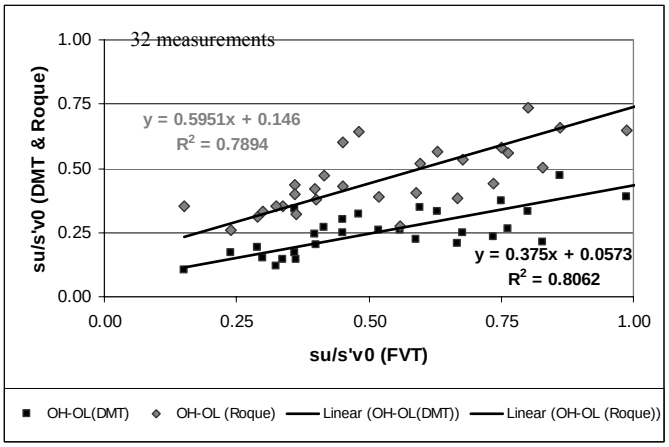

Figure 8 - Results from Marchetti's and Roque's correlation, compared with FVT

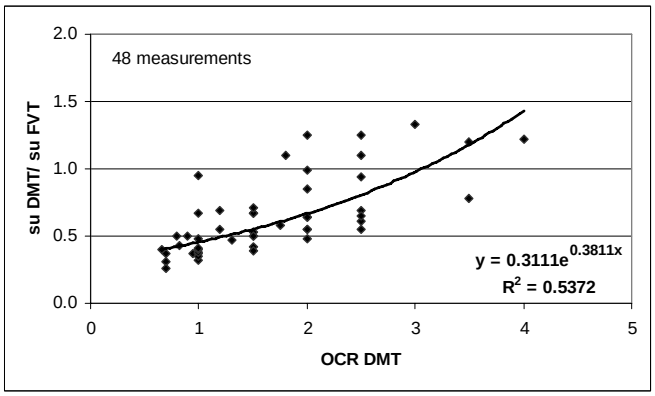

Figure 9 - Ratios S_u (DMT) / S_u (FVT) versus of OCR

The trend expressed in Figure 9 may be a consequence of the different considerations of OCR in each s_u evolution.

6 STIFFNESS PARAMETERS

In terms of stiffness parameters of soils, DMT results are classically interpreted for the purpose of getting constrained modulus, M, (Marchetti, 1980), equivalent to E_{oed} ($1/m_v$), which is based on the 3 intermediate parameters (I_D, E_D, K_D). Thus this calculation not only depends on the stress-strain relationship (E_D) but also the type of soil (I_D) and overconsolitation ratio (K_D). This is, undoubtedly, the main reason for the widely recognized high accuracy of the parameter, when applied to all types of transported soils.

More recently, with the increasing use of seismic measurements to determine small-strain modulus, some attempts have been made to correlate DMT parameters with G_0 through calibrations based in cross-hole tests and seismic SCPTU. Particularly, the works of Jamiolkowski et al (1985) Sully & Campanella (1989), Baldi (1989), Tanaka & Tanaka (1998), and the well documented method by Hryciw (1990) should be pointed out as references..

6.1 *Constrained Modulus, M*

In the present research, 37 oedometer tests were performed to calibrate M_{DMT}, with the results confirming the already known high accuracy of the parameter, as it is shown in Figure 10. Statistical analyses show 1.04 $\pm$ 0.27 for this comparison.

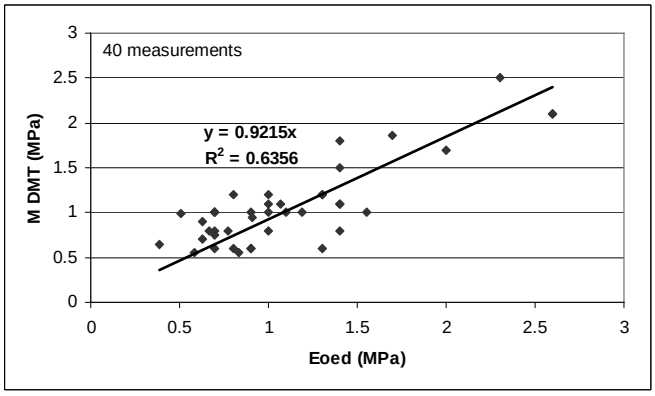

Figure 10 - Comparison between M_{DMT} and E_{oed}

On the other hand, DMT results were also compared with CPTU data, through M and q_t. The resulting correlations are presented in Figure 11.

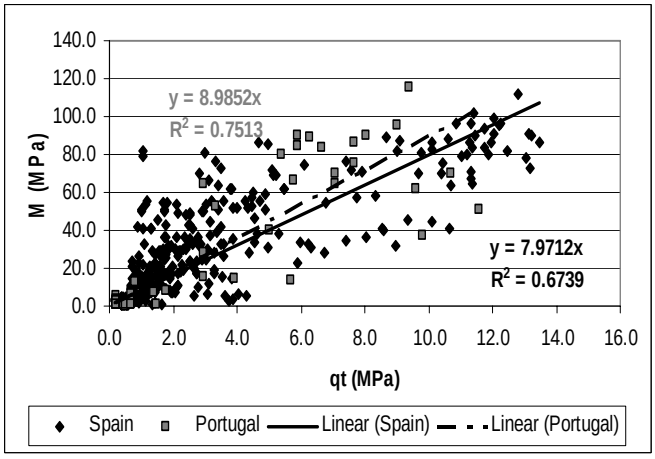

Figure 11 - M/qt correlations

Analysis of data shows a small difference between Portuguese and Spanish ratios of M/q_t, respectively 9 and 8. The M/q_t relation has been as a useful tool for the definition of OCR in granular soils, given the higher sensitivity of M parameter to variations with consistency, when compared to the tip resistance, q_t. Marchetti (1997) suggested that values between 5 and 10 correspond to normally consolidated soils, whereas values between 12 and 24 correspond to overconsolidated soils. Thus, the presented results have only local meaning, which clearly correspond to normally consolidated soils.

6.2 *Initial or Dynamic Shear Modulus, G_0*

The reference work in this subject shows two different approaches for calibration of DMT results in terms of G_0 determination. The first approach correlates E_D with G_0 (Sully & Campanella, 1989, Tanaka & Tanaka, 1998, etc), being E_D the DMT parameter that relates stress and strain. However, Hryciw (1990), pointed out that correlations based on ED would be affected by the strain DMT working level being too high to be related with small-strain behaviour. Thus, he proposed a new method for all types of soils, developed from indirect method of Hardin & Blandford (1989), which substitutes the variables σ'_0 and void ratio (e) for K_0, γ e σ'_{v0}, all derived from DMT.

During the present work, in two cases it was possible to have seismic data together with DMTs. These campaigns were developed in an alluvial deposit (clayey and sandy) where 6 DMT, 6 SCPTU and 2 cross-hole seismic tests were performed, and the analysis was conducted to get comparisons following both approaches.

The results of the first approach show a local trend for G_0 to increase with both E_D and M (and also q_t from CPTU) with the first one showing less scatter (Figure 12). The general ratio G_0/E_D (=R_G) for clays would be around 7.0 which is close to Tanaka & Tanaka's (1998) results (R_G = 7.5), while for sands (silica's) would be around 1.9 ± 0.6, close to Jamiolkowski (1985) and Baldi's (1986) results (2.2 ± 0.7 and 2.7 ± 0.57, respectively). The comparison of R_G with K_D, in turn, was found inconclusive, confirming Hryciw (1990) observations. However, a relationship was found between that ratio and I_D, which indicates its decrease with the presence of silty fraction (or sandy). In fact, a significant drop of R_G is observed as the soil goes from clay to silty clay. The results are shown in Figure 13.

The comparison of Hryciw proposal with seismic data showed a set of results overlapping those presented by the same author, which seems to indicate the adequacy of the method for this particular case (Figure 14). Using the same error definition used by Hryciw ($G_{0predicted} - G_{0observed} / G_{0observed}$) it comes out that 62% of the total data points reveal an error less than 25% and 93% less than 50%, which is very similar to Hryciw's results.

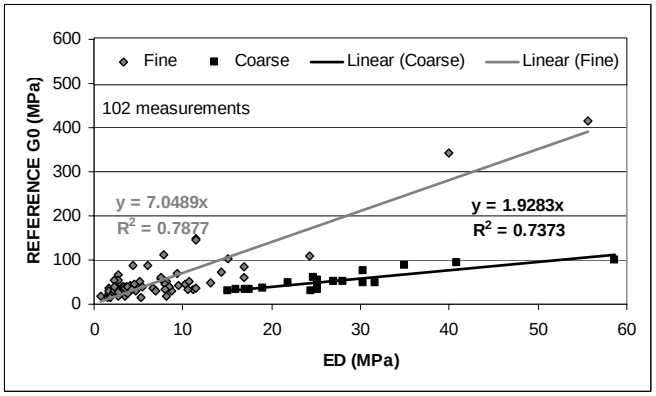

Figure 12 - Comparison between reference G_0 and E_D

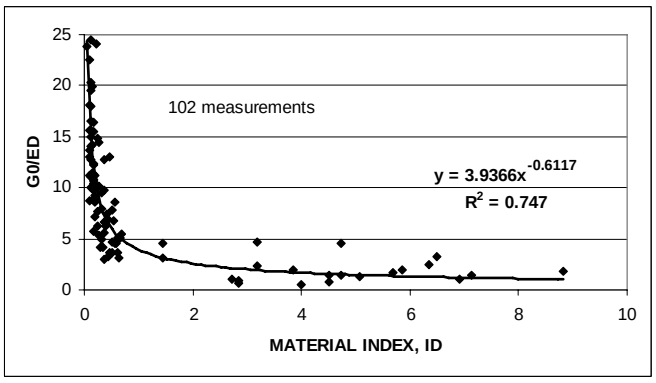

Figure 13 - Comparison between G_0 /E_D and I_D

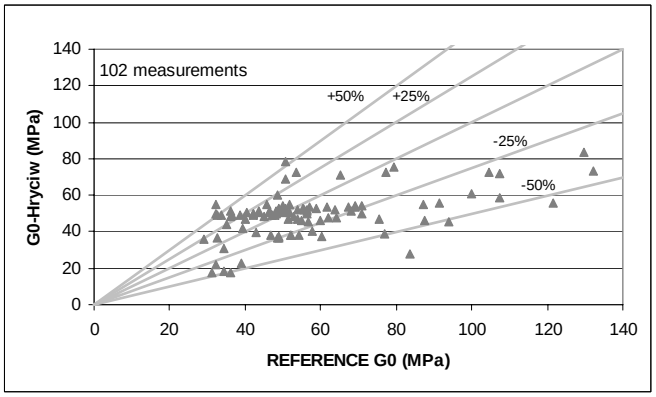

Figure 14 - Comparison between G_{0DMT} (Hryciw method) and Reference G_0

7 CONCLUSIONS

The work presented herein, performed along the last 10 years in Portugal and Spain, involved a great variety of laboratory and in-situ tests and fundamentally aimed to test and improve the quality of DMT correlations to derive geotechnical parameters. Based on the overall analysis the following conclusions are presented below:

a) DMT gives accurate definition of soil stratigraphy, unit weight following the general patterns described in the references.

b) P_2 correlates well with u_2 from CPTU, and the ratio between them seems to decrease with increasing I_D
c) Earth pressure coefficient at rest, K_0, deduced from DMT was confirmed to be reliable both by ϕ' and OCR correlations (Mayne, 2001) and for I_Ps (Brooker & Ireland, 1965).
d) Shear strength angles deduced from DMT (Marchetti, 1997) matches with CPTU solutions (Robertson & Campanella, 1983), with DMTs being slightly lower.
e) Undrained shear strength, showed two patterns, according to the major or minor percentage of organic content, which seem to lower s_u(DMT)/s_u(FVT) ratios; in this case, Roque's data seem to overpredict the peak FVT value, while Marchetti's correlation tends to underpredict residual FVT values.
f) Constrained Modulus, M, derived from DMT reveals its excellency, confirming the international comments on the subject.
g) Small strain modulus, G_0, seems to correlate well with E_D, presenting rates similar to Tanaka & Tanaka's data for clayey soils and to Jamiolkowski and Baldi´s data for silica sands. Nevertheless, it was also clear that G_0/E_D decreases with increasing I_D. Another approach on this subject was evaluated through Hryciw's method, and results confirm previous data.

REFERENCES

Baldi, G., Bellotti, R., Ghionna, V., Jamiolkowski, M., Marchetti, S., Pasqualini, E. 1986. Flat dilatometer tests in calibration chambers. *Proc. of IV conference in use of In situ tests*: 431-446. Blacksburg, Virginia, ASCE

Baldi, G., Bellotti, R., Ghionna, V., Jamiolkowski, M., Lo Presti, D.C.F. 1989. Modulus of sands from CPT's and DMT´s. *Proc. of XI ICSMFE*: vol.1, 165-170.

Cruz, N. 1995. Evaluation of geotechnical parameters by DMT tests (in portuguese). *MSc thesis. Universidade de Coimbra.*

Cruz, N., Viana, A., Coelho, P., Lemos, J. 1997. Evaluation of geotechnical parameters by DMT in Portuguese soils. *XIV Int. Conf. on Soil Mechanics and Foundation Engineering, pp 77-80.*

Hardin, B.O.; Blandford, G.E. 1989. Elasticity of particulate materials. *J. Geotechnical. Eng. Div. ASCE*, 115 (6), 788-805.

Hryciw, R. 1990. Small-Strain-Shear of Soil by Dilatometer. *ASCE Jnl GE, Vol.116, 11, 1700-1716.*

Jamiolkowski, B.M., Ladd, C.C., Jermaine, J.T., Lancelotta, R. 1985. New Developments in Field and Laboratory Testing of soils. *Theme lecture, Session II, XI ISCMFE, Proceedings, Vol.1, S. Francisco, CA 1985, pp.57 a 153.*

Kenney, T.C., Moum, J., and Berre, T. (1967). An experimental study of the bonds in a natural clay, *Proc. Geotech. Conf. on Shear Strength Prop. of Natural Soils and Rocks*, *Oslo, v.1, p.65*.

Lacasse, S., Lunne, T. 1988. Calibration of dilatometer correlations. *Proc. ISOPT-1*: vol.1 539-548. Florida

Lutenegger, A.J.(1988). Current Status of the Marchetti Dilatometer Test. *I Int. Symposium on Penetration Testing, Orlando*.

Marchetti, S. 2001. The Flat Dilatometer Test (DMT) in Soil Investigation. *ISSMGE TC 16 Report*.

Marchetti, S. 1997. The Flat Dilatometer: Design Applications *Proc. 3rd Int. Geotechnical Engennering Conf. Cairo University*.

Marchetti, S. 1980. In-situ tests by flat dilatometer. *J. Geotechnical. Eng. Div. ASCE*, 106, GT3, 299-321.

Marchetti, S. & Crapps, D.K. 1981. Flat Dilatometer Manual. *Internal report of GPE Inc., distributed to purchasers of DMT equipment.*

Mayne, P. 2001. Stress-strain-strengh-flow Parameters from Enhanced In-Situ Tests. *Proc. Int. Conference on In-Situ Measurements of Soil Properties & Case Histories*. Bali, Indonesia.

Robertson, P., Campanella, R. (1983). *Interpretation of cone penetrometer test: Part I – Sand*. Canadian Geotech. J., 20, pp. 718 – 733.

Roque, R.; Janbu, N.; Senneset, K. (1988). "Basic Interpretation Procedures of Falt Dilatometer Tests". Penetration Testing, ISOPT-1. Orlando, 1988.

Sully, J.P.; Campanella, R.G. 1989. Correlation of Maximum Shear Modulus with DMT Test Results in Sands. *Proc. XII ISCMFE, , Vol.1, pp339 - 343 R. Janeiro.*

Tanaka, H.; Tanaka, M. 1998. Characterization of Sandy Soils using CPT and DMT. Soil and Foundations, Japanese Geot. Society, Vol 38, nº 3, pp 55-65.

BACK

Comparative Study of Different In-Situ Tests For Site Investigation

MD Sahadat Hossain, Assistant Professor, Department of Civil and Environmental Engineering, University of Texas at Arlington, TX 76019, email: hossain@uta.edu.
Bill Khouri, Principal, Schnabel Engineering North, Suite 700, Gaithersburg, MD 20878, email: khouri@schnabel-eng.com.
Mohamed A. Haque, Graduate Student, Department of Civil and Environmental Engineering, University of Texas at Arlington, TX 76019, email: msa_889@yahoo.com.

Abstract: In situ testing is rapidly emerging as a viable alternative to the traditional approach of obtaining geotechnical parameters required for prediction of soil bearing capacity and settlement. The diversity of the data obtained during in situ testing enables engineers to obtain a better sense of site conditions and variability, leading to more reliable geotechnical solutions. This paper presents the results of site investigation using in situ tests for a building in northern Virginia. The site investigation included pressuremeter tests, dilatometer tests, Standard Penetration Tests (SPT), cone penetration tests (CPT), and a plate load test. The objective of the current paper is to compare the bearing capacity and settlement predictions based on the different in-situ tests used for the building.

1 INTRODUCTION

The interpretations of initial geostatic stress state and stress-strain-strength-flow characteristics can be obtained with laboratory test data on high-quality samples (Mayne, 2004). However these are often done at high costs, and also the accuracy of geotechnical parameters measured from laboratory testing had been debated extensively over the last three decades. A growing awareness of this fact led to an increasing interest in all forms of in situ testing, where the disturbance of the soil structure is minimal. In situ testing is rapidly emerging as a viable alternative to the traditional approach of obtaining geotechnical parameters for design and analysis (Crawford and Campanella, 1990, Bergado et al., 1991). In recent years, some researchers have indicated the existence of a strong correlation between the predicted results from some of the insitu test methods and the observed results from the field. Bergado et al., (1991) investigated the usefulness of the screw plate and pressuremeter tests to provide meaningful results for the prediction of embankment settlement on soft clays. The settlement predictions were generally in good agreement with the observed field settlement. LeClair et al. (1999) utilized flat dilatometer, piezocone, and screw plate tests to predict consolidation settlements of embankments at Vancouver International Airport. The authors concluded that settlement magnitudes can be predicted with reasonable confidence based on the parameters interpreted from in situ tests. In this paper the results obtained from four insitu tests namely standard penetration test (SPT), cone penetration test (CPT), dilatometer (DMT), and pressuremeter (PMT) on a site for the regional jail located in Fort A. P. Hill, Virginia are presented. The objective of this paper is to compare the bearing capacity and settlement values predicted from the in-situ tests with those of observed from plate load test.

2 SITE AND PROJECT DESCRIPTION

The site for the regional jail is located in Fort A. P. Hill on the west side of U.S. Route 301, midway between the towns of Bowling Green and Port Royal in Caroline County, Virginia. Existing grades vary between EL 216 Ft. (66 m) in the northeast corner of the site to about EL 170 Ft. (52 m) along the south side. Several tributaries are located along the northern and western boundaries of the property. These ravines have relatively step slopes up to about 2.5H: 1V. Most of the site is wooded except in some areas, which were recently cleared and along the existing dirt roads. The proposed construction consisted of three housing facilities, an industries building, a food service building, a recreation center, special housing units, and an employee administration building. These buildings would consist of one to two stories with no below grade levels. In the areas where the upper portion of the natural soils is loose, the footings would be lowered. The estimated highest footing sub-grade elevations for the footings supported on natural soils at the locations of some of the borings are given in Table 1. The lowest levels of these buildings are planned at about EL 203 Ft. (62 m). The column and wall loads are not expected to

exceed 30 kips (133 kN) and 6 kips (27 kN) per linear foot, respectively. Spread footings founded on natural soils of Stratum A are to be designed for a maximum allowable soil bearing pressure of 2000 psf. (96kPa)

Table 1 Estimated highest footing sub-grade elevation

Boring No.	Highest footing sub-grade elevation, ft (m)
B-7	197 (60.0)
B-22	196 (59.7)
B-24	206 (62.8)

3 FIELD INVESTIGATIONS

The field investigations were conducted by using four different in-situ tests at various locations. In order to investigate the surface conditions for the proposed development, 40 Standard Penetration Tests (SPT) were conducted. Based on the test borings and laboratory test results, the following generalized soil profile was developed for the site to the maximum depths of investigation:

Stratum A: (Chesapeake Group)	Below the topsoil to depths of 10 to 50 feet (3 to 15 m), which is the maximum depth of the borings.	Brown clayey sand (SC), silty sand (SM), and poorly graded sand (SP, SP-SM, SP-SC) with silt, clay, and clay layers, trace wood fragments, cemented sand and roots; generally very loose in the upper 6 feet and loose to firm below this depth (N = 1 to 21).
Stratum B: (Chesapeake Group)	Below Stratum A in borings B-7 and B-106 to the maximum depth of these borings.	Brown and gray elastic silt (MH) and lean clay (CL), with sand layers; generally stiff (N = 8 to 11).

In addition to the above strata, the site also contained topsoil depths of 0.1 to 0.4 feet (0.03 to 0.12 m). The soils of Strata A and B are marine deposits from the Chesapeake group of the upper Pliocene to the lower Miocene geologic ages. The site investigation in Stratum A indicated between 7.1 and 29.2 percent fines passing the No. 200 sieve. The samples were classified as clayey sand (SC) and poorly graded sand (SP-SM) per ASTM D-2487. The clayey sand material had liquid limits of 26 and 40, and plasticity indices of 8 and 25. On the basis of available information the poorly graded sand is considered to have an average moist unit weight of 115 lb/ft^3 (18.1 kN/m^3). The natural moisture content of the samples varied between 6.7 and 17.7 percent. Most of the borings indicated dry conditions except for a few borings where the ground water level varied between 3.0 to 33.5 feet (0.9 to 10.2 m) below the existing grades. High ground water was observed only in the low lying areas of the site.

However, only three boring locations were selected for this study, since all the in-situ tests were performed in close proximity to these three borings. Figure 1 shows the site plan and the locations of borings B-7, B-22, and B-24 at which all the four in-situ tests were done, and also B-16 where the plate load test was done. The results from each of these in-situ test methods at each boring location are discussed in the following sections.

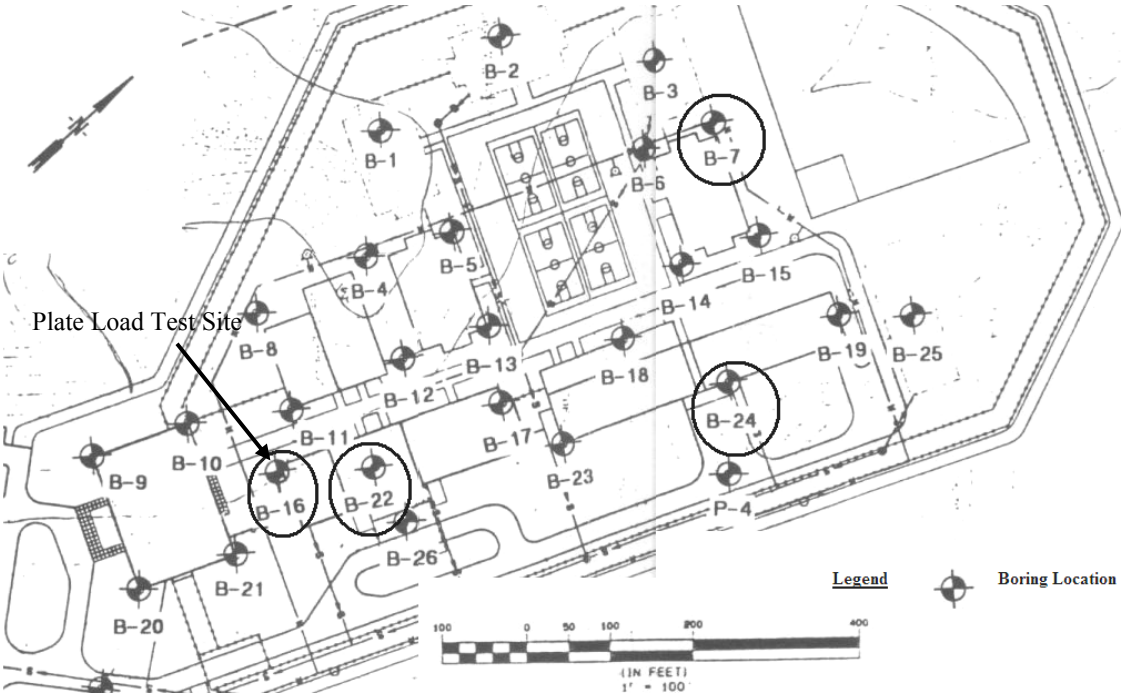

Figure 1 Plan view of A.P.Hill regional jail site, Virginia.

3.1 Standard Penetration Test (SPT)

The SPT -*N* values were obtained using a standard 2-inch (50.8 mm) O.D., 1-3/8-inch (34.9 mm) I.D. sampling spoon driven with a 140 pound (63.5 kg) hammer falling 30 inches (762 mm) as per ASTM D-1586. The soil profile for borings B-7, B-22, and B-24 is shown in Figure 2. Borings B-7 and B-22 were at the same elevation and had almost the same soil profile, whereas B-24 was at a higher elevation, and had an 8 feet (2.4 m) thick layer of clayey sand. The results indicate that the upper surfacial soils in the top six feet are very loose and are underlain by generally firmer soils. The average corrected SPT –*N* values from B-7 and B-22 for the top 8 feet (2.4 m) of the poorly graded sand layer were almost the same; however B-7 indicated a higher *N* value below 8 feet (2.4 m). The poorly graded sand layer in boring B-24 showed a higher *N* value than the other two borings. Friction angles for the different layers at each of these borings were calculated using the Hatanaka and Uchida (1996) relationship by using the corrected SPT –*N* values (Table 2). The SPT –*N* values are corrected using Liao and Whitman's (1986) relationship.

Table 2 SPT –N values and the Computed Average Friction Angles

Boring No.	Depth, ft (m)	SPT-N	Corrected $(N_1)_{60}$	Friction Angle (ϕ^o)
B-7	2 (0.6)	2	6	30
	4.5 (1.4)	2	4	
	7 (2.1)	3	5	
	9.5 (2.9)	12	16	38
	14.5 (4.4)	17	19	
B-22	2 (0.6)	2	6	31
	4.5 (1.4)	3	6	
	7 (2.1)	4	6	
	9.5 (2.9)	5	7	
	14.5 (4.4)	13	14	
B-24	7 (2.1)	6	10	33
	9.5 (2.9)	10	14	
	14.5 (4.4)	5	6	

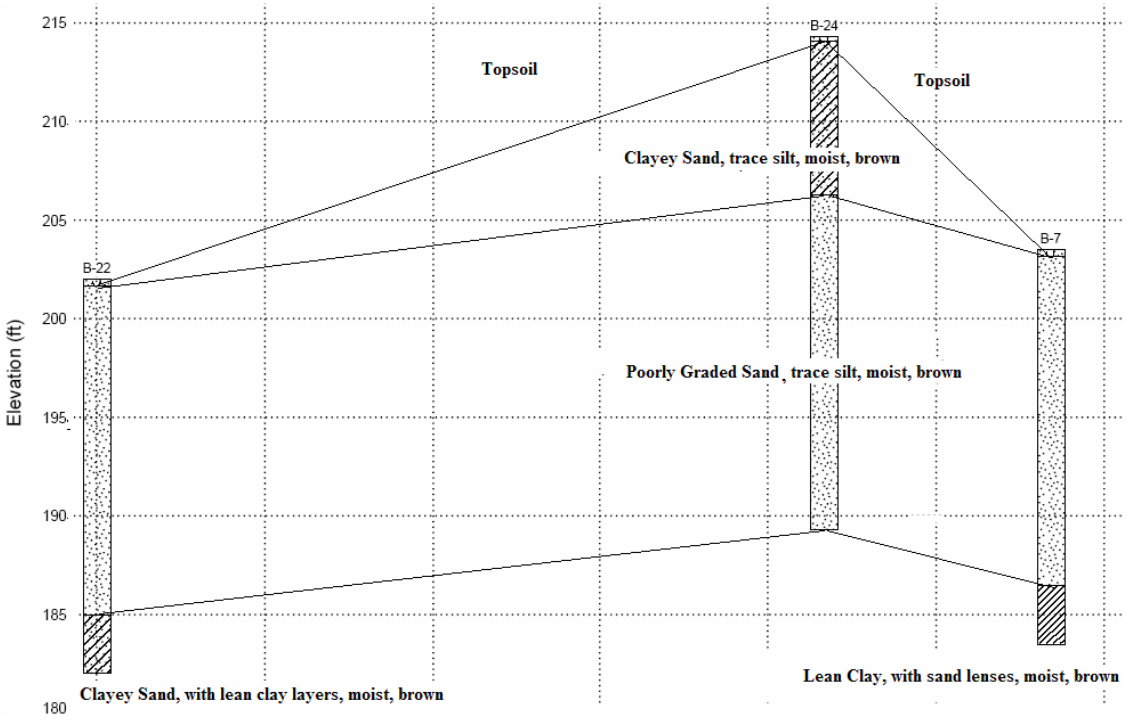

Figure 2 Soil profile for borings B-7, B-22, and B-24

3.2 Cone Penetration Test (CPT)

In-situ cone penetrometer *testing* was performed at seven boring locations to aid in evaluating soil bearing capacity and settlement characteristics. The soil interpreted from the CPT data was similar to that observed from the SPT data in some borings. However, interpretation of CPT data indicated thin clay seams in between the sandy silt layer. Since the SPT was performed only in layers of 18-inch (457 mm) increments, these thin seams may have been missed. The test results for borings B-7, B-22, and B-24 are shown in Figure 3. The results indicate the presence of clayey silt in the upper layers underlain by generally firmer silty sand to sandy silt. Also, interpretations of results from B-22 indicated the presence of sensitive fine grained soils up to a depth of 7 feet. The friction angle (ϕ^o) was calculated using the Robertson and Campanella (1983) charts and is presented in Table 3. Also, the CPT data gave higher strength parameters than those estimated by using SPT.

Table 3 Computed strength parameters from CPT data

Boring No.	Depth, ft (m)	Cohesion (C), tsf (kPa)	Friction Angle (ϕ^o)
B-7	1 – 5 (0.3-1.6)	0.88 (84)	0
	5–13 (1.6-4.0)	0	40
B-22	1 – 7 (0.3-2.1)	0.8 (77)	0
	7–16 (2.1-4.9)	0	41
B-24	1 – 4 (0.3-1.2)	1.1 (105)	0
	4–16 (1.2-4.9)	0	38

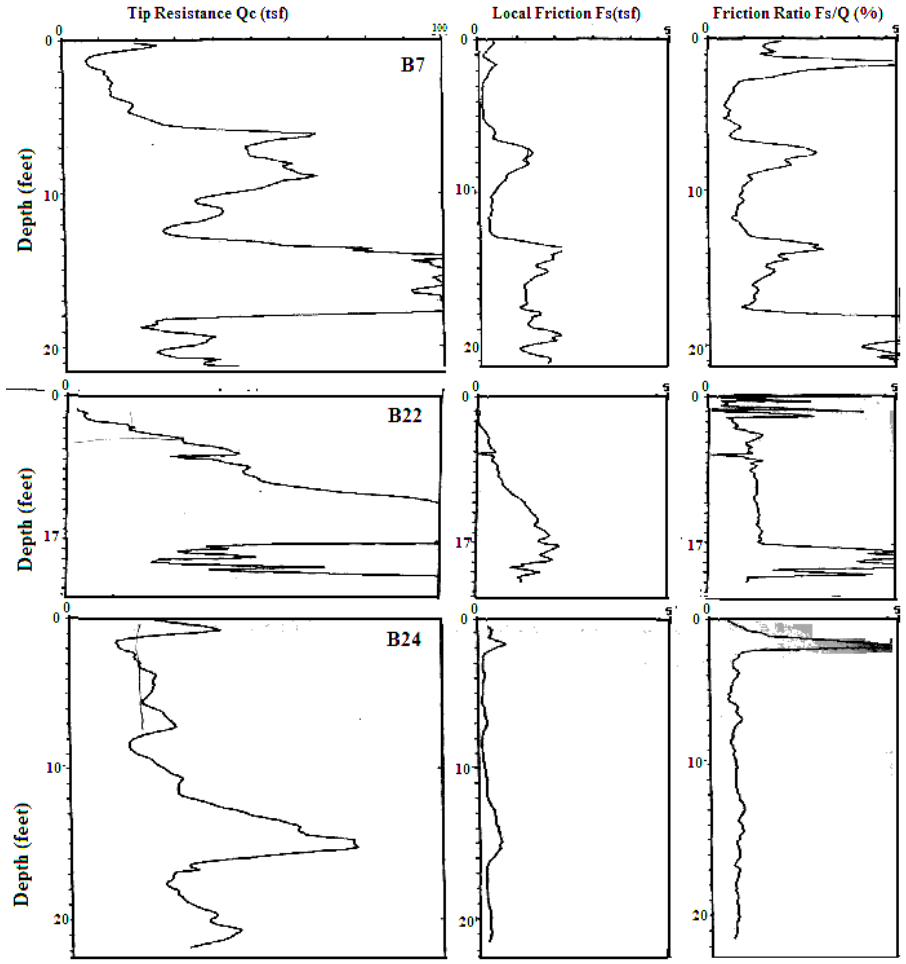

Figure 3 CPT data from borings B-7, B-22, and B-24

3.3 Menard Pressuremeter Test (PMT)

A total of seven in-situ pressuremeter tests were performed at borings B-4A, B-7A, B-11A, B-22A, and B-24A. The pertinent design values obtained from the tests are summarized in Table 4. The limit pressure (P_L) determined using the correlations from the PMT data is the pressure at which failure occurs and the pressuremeter modulus (E_M) estimated from this test is a representation of stiffness of the soil. The PMT produces much more direct measurements of soil compressibility and lateral stresses than the SPT and CPT (Coduto, 2001). The results indicate an increase in limit pressure with depth, demonstrating the presence of stiffer soils below 5 feet (1.6 m). A lowest pressuremeter modulus of 52 tsf (5.0 MPa) was obtained in B-24A, indicating the presence of a weaker sandy clay layer.

Table 4 Results from Pressuremeter Test

Boring Number	Depth, ft (m)	N value	Pressuremeter Modulus, tsf (MPa)	Limit Pressure, tsf (MPa)
4 A	5.0 (1.6)	5	118 (11.3)	9.5 (0.91)
7 A	4.0 (1.2)	4	82 (7.8)	7.5 (0.72)
11 A	6.5 (2.0)	4	118 (11.3)	11.8 (1.13)
22 A	5.0 (1.6)	4	127 (12.2)	11.3 (1.08)
22 A	9.0 (2.7)	5	115 (11.0)	12.4 (1.19)
24 A	5.0 (1.6)	7	52 (5.0)	8.2 (0.79)
24 A	9.5 (2.9)	10	112 (10.7)	13.8 (1.32)

3.3 Dilatometer Test (DMT)

Seven dilatometer tests were performed to evaluate soil bearing capacity and settlement characteristics. The soil resistance measured during insertion of the dilatometer blade is correlated to the strength of granular soils, while the soil modulus, undrained strength and other parameters are determined during dilation of the blade against the

soil. The strength parameters from the DMT test results are computed using Schmertmann (1986) method and the results are shown in Figure 4. The test results predicted a lower strength and stiffness parameter for surfacial soils up to six feet, and generally uniform higher values below this depth.

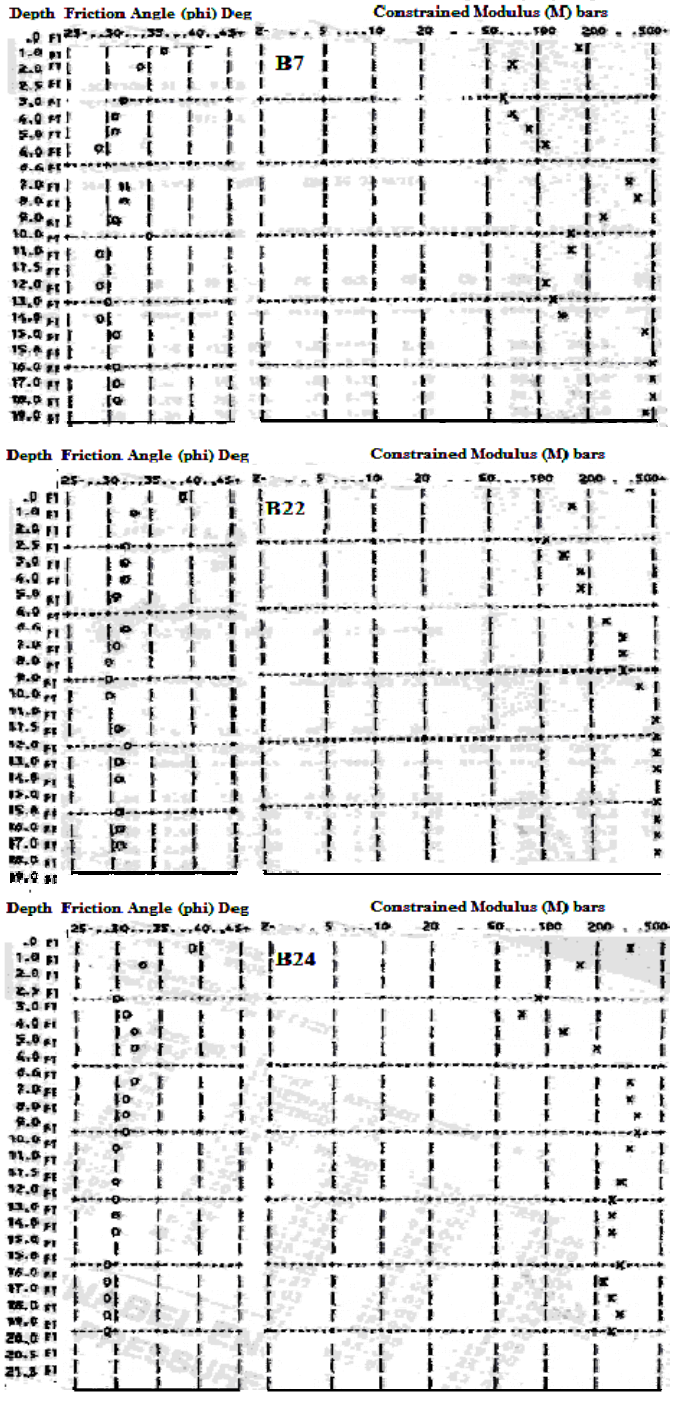

Figure 4 Results from DMT tests.

3.4 Plate Load Test

A plate load test was performed using a 1' × 1' square plate in the area of test boring B-16. Subsoil encountered around this vicinity was considered to be the least favorable for direct support of the footings. The plate load test results shown in Figure 5 are typical of a dense cohesionless soil which does not show any marked sign of shear failure under the loading intensities of the test. The observed cumulative settlement using this method for a bearing pressure of 2000 psf (96 kPa) was 0.21 inches (5.3 mm).

4 SOIL BEARING CAPACITY AND SETTLEMENT FROM IN-SITU TESTS

Bearing capacity and settlement were estimated at three boring locations (B-7, B-22, and B-24) using the data from SPT, CPT, DMT, and PMT. The footings at B-7 and B-22 should be founded six feet below the ground surface, and the footing at B-24 should be eight feet below the ground surface. All three footings would be resting on the sand layer. Meyerhof's (1963) bearing capacity equation was used to estimate the ultimate bearing capacity of the soil by using the data obtained from SPT, CPT, and DMT. Bearing capacity from the PMT data was estimated using the pressuremeter limit pressure (P_L) in the Menards (1975) correlation.

The estimated allowable bearing capacities and settlements at borings B-7, B-22, and B-24 are presented in Figure 6. A factor of safety of 3 was used to estimate the allowable bearing capacity from ultimate bearing capacities. The bearing capacity of the soil varied with each boring, boring B-22 returned higher values of bearing pressure. SPT always underestimated the bearing capacity in comparison to CPT and PMT, regardless of the borings. CPT predicted higher bearing capacities than SPT and DMT, but less than PMT. The pressuremeter test predicted higher values of bearing capacity out of all the methods. It should be noted that the PMT produces much more direct measurements of soil compressibility and lateral stresses than do SPT and CPT (Coduto, 2001).

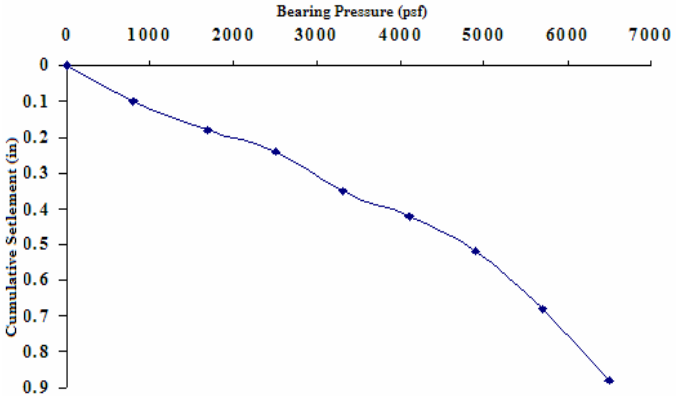

Figure 5 Plate load test results

Schnabel (1990) indicated that the bearing capacity calculations from PMT would generally yield high values of bearing pressure and must be used with an adequate factor of safety. The dilatometer test creates a bearing capacity, or cavity expansion, failure and allows for direct determination of ultimate strength values. Two methods are currently used for estimating ϕ from DMT (Marchetti, 1997). The first method provides simultaneous estimates of ϕ and K_0 derived from the pair K_D and q_D or from the pair K_D and q_c. The second method provides a lower bound estimate of ϕ based only on K_D. Marchetti et al. (2001) indicated that the underestimation of ϕ would be between 2° to 4°. The authors have also suggested that higher values of ϕ could be used if those values are more accurate. In this study the second method is used to estimate the ϕ value, this is the reason for DMT results predicting lower bearing capacity than the other three methods.

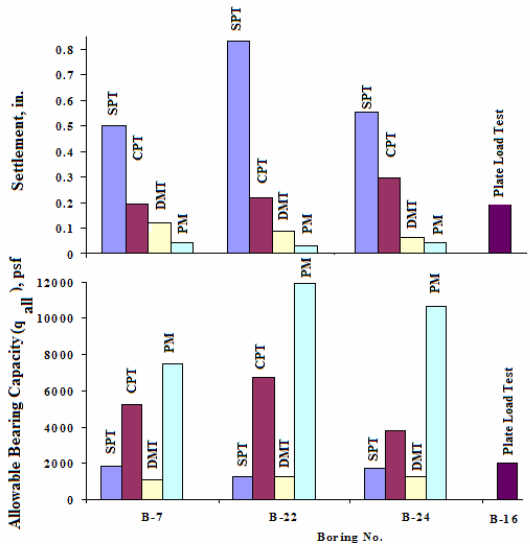

Figure 6 Predicted and measured bearing capacity and settlement

The settlement calculations for settlement in sandy soils from SPT and CPT data were performed using Bowles (1977) and Schmertmann (1978) formulations respectively. A foundation pressure of 2000 psf (96 kPa) was used in all the settlement analysis. DMT modulus (M) was used to predict the settlement from DMT data. The SPT and CPT data predicted a settlement higher than PMT and DMT. The pressuremeter modulus (E_M) estimated from PMT is a representation of stiffness of the soil, and hence used to evaluate the settlement of foundations directly. Generally settlement calculations based on the Menard method indicate low values that may be more accurate than other evaluations, but at the same time represent a lower safety margin and should be handled accordingly (Schnabel, 1990). The settlement calculated using DMT was generally higher than that calculated with the PMT method. The same phenomenon was also noted on a silty sandy soil in Quebec by Geopac (1992).

Borings B-16 and B-22 were closer to each other, therefore it is quite reasonable to compare the predicted and measured settlement from the in-situ tests in those two borings. SPT and CPT predicted a higher settlement than the plate load test in all three borings, whereas the other two methods predicted lower values. These results indicate that SPT and CPT are overestimating the actual settlement. However, the settlement predicted by DMT and PMT in boring B-22 was less than 0.1 in (2.5 mm). The possible reason for the difference in predicted settlement from DMT and PMT, and the measured values from plate load test, might be due to the small size of the plate used in the plate load test. Due to the small size of the plate, the test reflected only the properties of the uppermost soils and thus could be misleading. This is of great concern especially when the soil properties vary with depth (Coduto, 2001). In the case presented here the soil properties varied with depth, the soil profile showed generally weaker soils in the top 6 foot (1.8 m)followed by firmer soils. This might be the reason for the plate load test showing higher settlement values than the DMT and PMT. Though the PMT predicted slightly lower value than DMT, the absolute difference between the two did not exceed more than 2 mm of settlement. From these results it can be concluded that the settlement predicted by DMT

and PMT is almost equal, and could possibly represent actual settlement.

5 SUMMARY AND CONCLUSION

In situ testing is rapidly emerging as a viable alternative to the traditional approach of obtaining geotechnical parameters required in prediction of bearing capacity and settlement. The site investigation for building in northern Virginia included pressuremeter tests (PMT), dilatometer tests (DMT), Standard Penetration Tests (SPT), cone penetration tests (CPT), and plate load test. The bearing capacity and settlement predicted by the four in-situ methods at three boring locations was compared with the observed settlement from the plate load test and summarized as follows:

- The CPT and SPT methods predicated lower bearing capacity and higher settlement than PMT method.
- DMT method predicted bearing capacities of less than 2000 psf (96 kPa), due to underestimation of strength parameters.
- The settlements predicted by DMT and PMT were 0.1 in (2.5 mm). Whereas, CPT and SPT predicted a settlement of more than 0.3 in (7.6 mm). The settlement observed in the field using the plate load test for a bearing pressure of 2000 psf (96 kPa) was 0.21 in (5.3 mm).
- SPT and CPT over estimated the settlement, while DMT and PMT predicted settlements less than those observed in the field by the plate load test.
- The soil profile showed generally weaker soils in the top 6 foot (1.8 m) followed by firmer soils and the plate load test was performed at the least favorable soil conditions for footing. Therefore, it is expected that plate load test would show higher settlement than actual field settlement. This might be the reason for the plate load test showing higher settlement values than the in-situ DMT and PMT.
- From these results it can be concluded that the settlement predicted by DMT and PMT could possibly represent actual settlement.

REFERENCES

Bergado, D. T., Daris, P. M., Sampaco, C. L., and Alfaro, M. C. (1991). “Prediction of Embankment Settlements by In-Situ Tests,” Geotechnical Testing Journal, GTJODJ, Vol. 14, No. 4, pp. 425 – 439.

Bowles, J. E.(1977). “Foundation Analysis and Design,” McGraw-Hill. New York.

Coduto (2001). “Foundation Design: Principles and Practices,” Prentice Hall 2 Edition, CA.

Crawford, C. B., and Campanella, R. G. (1990). "Comparison of Field Consolidation with Laboratory and In-Situ Tests," Canadian Geotechnical Journal, Vol. 28, No. 1.

Geopac (1992) “Comparisons of settlements predicted by PMT and DMT in a silty-sandy soil in Quebec,” Personal communication.http://www.marchettidmt.it/pdffiles/geopac92.pdf

Hatanaka, M. and Uchida, A. (1996). “Empirical correlation between penetration resistance and N of sandy soils,” Soils &Foundations, Vol. 36, No. 4, pp. 1-9.

LeClair, D. G., Robertson, P. K., Campanella, R. G., and Joseph, A. (1989). "Prediction of Embankment Performance at Vancouver International Airport using In-Situ Tests." 42nd Canadian Geotechnical Conference, Winnipeg, Manitoba.

Liao, S. S. C., and Whitman, R. V. (1986). “Overburden Correction Factors for SPT in Sand,” Journal of Geotechnical Engineering, American Society of Civil Engineers, Vol.112, No.3, pp. 373-377.

Marchetti, S. (1997). “The flat dilatometer: design applications,” Proceedings, 3rd Geotechnical Engineering Conference, Cairo University, 1-25.

Marchetti S., Monaco P., Totani G., and Calabrese M. (2001). “The Flat Dilatometer Test (DMT) in soil investigations,” A Report by the ISSMGE Committee TC16, Proc. IN SITU 2001, Intnl. Conf. On In situ Measurement of Soil Properties, Bali, Indonesia, May 2001.

Mayne, Paul W. (2004). “Current Trends and Challenges in In-Situ Testing,” Civil & Environmental Engineering, Georgia Institute of Technology, Atlanta, GA 30332. http://www2.egr.uh.edu/~civeb1/CIGMAT/04_present/5.pdf

Menard, L. (1975). “The Menard Pressuremeter: Interpretation and Application of the Prsssuremeter Test Results to Foundations Design,” Sols-Soils, No. 26, Paris, France.

Meyerhof, G. G. (1963) **“**Some Recent Research on the Bearing Capacity of. Foundations,” Canadian Geotechnical Journal, Vol 1, No. 1, pp 16-26.

Robertson, P.K. and Campanella, R.G. (1983). “Interpretation of cone penetration tests: sands,” Canadian Geotechnical Journal, Vol. 20, No. 4, pp. 719-733.

Schnabel Associates (1990). “Insitu Testing Manual”

Schmertmann, J. H. (1978). “Guidelines for Cone Penetration Test Performnace and Design,” Report No. FHWA-TS-78-209. Available from US Department of Transportation, Federal Highway Adminstration, Office of Research and Development, Washington, DC 20590.

Schmertmann, J. H. (1986). “Suggested method for performing the flat dilatometer test,” ASTM Geotechnical Testing Journal., Vol. 9. No. 2, pp. 93-101.

Use of DMT for subsurface characterization: strengths and weaknesses

Hai-Ming Lim
Burgess Engineering and Testing, Inc., Moore, Oklahoma, USA

Musharraf Zaman
School of Civil Engineering and Environmental Science, University of Oklahoma, Norman, Oklahoma, USA

Kianoosh Hatami
School of Civil Engineering and Environmental Science, University of Oklahoma, Norman, Oklahoma, USA

Keywords: DMT, site characterization, soil properties,

ABSTRACT: In this study, the Marchetti Dilatometer Test (DMT) was used to evaluate the soil type and properties at a site of a highway improvement project in north eastern Oklahoma. The DMT was used to determine the lateral effective stress ratio, strength parameters (i.e. cohesion, angle of internal friction), compressibility, coefficient of consolidation, and coefficient of permeability of the soil at the site. Additional laboratory tests and selected in-situ tests were conducted on the site soil. The properties obtained from the DMT have been compared to those from other laboratory and field tests including standard penetration test (SPT). Using this comparison, the strengths and weaknesses of the DMT in determining soil properties are identified and discussed.

1 INTRODUCTION

A highway improvement project is proposed on State Highway 99 (SH 99), south of Stroud, Oklahoma. The proposed highway improvement project is about one mile in length and includes the construction of a parallel alignment with two bridges across the Deep Fork River and an overflow structure. The proposed project site is located within a valley in between two hills on its north and south sides. An embankment is proposed to be constructed to achieve the desired highway grade. During the construction of the current highway that is in service, the old highway embankment located on the east side of the current highway was abandoned and was left in place. A study was undertaken to examine the feasibility of elevating the abandoned embankment to the same elevation as the current highway. The proposed project involves overcoming some geotechnical challenges: The proposed alignment is located within a flood zone. Moreover, the north part of the proposed alignment is always under water. During the construction of the current highway, both the bridge approaches and the roadway showed some settlements. In addition, the proposed pile foundations for the overflow structure require additional lateral load resistance.

In-situ testing, including several geotechnical test borings, was carried out as part of the subsurface exploration for the proposed alignment site. To obtain a continuous subsurface soil profiles and shorten the time of testing, Marchetti Dilatometer tests (DMT) were performed in several locations at the bridge approaches and roadway embankment sections. The DMT test results provided a detailed profiling of the subsurface materials and the soil parameters needed for the analysis of embankment settlement, slope stability and the lateral load resistance of the embankment foundation.

In this study, the experience of using DMT for the proposed highway improvement project is discussed. The DMT test results are compared to a selection of laboratory and in-situ test results and the accuracy of the DMT testing in determining soil mechanical properties is discussed.

2 COMPARISON OF DMT RESULTS WITH OTHER IN-SITU AND LABORATORY TEST RESULTS AT THE HIGHWAY SITE

The Marchetti Dilatometer Test (DMT) has been used as a rather simple and economical penetration test to measure in-situ soil stresses and modulus values using a series of correlations between the DMT test results and significant soil parameters. These empirical correlations have been developed by comparing the DMT test results with carefully conducted laboratory test data, large-scale chamber tests, in-situ tests (e.g. Cone Penetration Test) and field observations (Schmertmann 1988a).

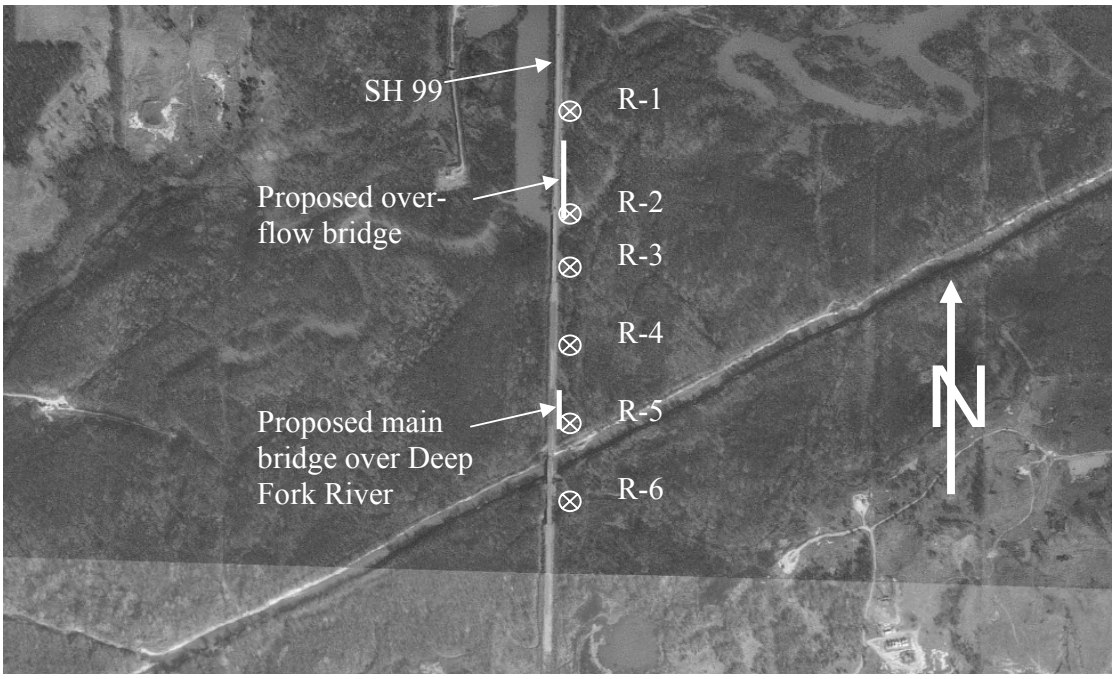

Figure 1. Location of the project site in north eastern Oklahoma and the bore-hole locations map

There are usually four DMT indices that are calculated using the DMT field data. These DMT indices are: (i) material index (I_D); (ii) horizontal strength index (K_D); (iii) dilatometer modulus (E_D); and (iv) pore pressure index (U_D). In general, the DMT indices are not directly used in the engineering design, especially since they represent data from a soil disturbed by insertion of the dilatometer blade. Rather, these DMT indices are used to correlate and interpret the soil engineering properties. For the proposed project on SH 99, the following soil engineering properties are interpreted using the correlations proposed by Marchetti and other researchers (e.g. Schmertmann 1988a): (i) soil type; (ii) lateral effective stress ratio; (iii) strength; (iv) compressibility; (v) coefficient of consolidation; and (vi) coefficient of permeability.

In the SH 99 project, six test borings were drilled on the proposed bridge approaches and roadway sections. The test borings were drilled as deep as 5 ft into the bedrock stratum. The test borings at the proposed bridge piers locations were drilled 30 ft into the bedrock stratum. Locations of the test borings are shown in Fig. 1.

DMT tests were performed adjacent to these six test borings. In addition, three DMT tests were performed at the locations of the test borings of the proposed bridge piers. Standard penetration tests (SPT) were performed in 5 ft intervals at boring locations drilled for the bridge approaches and roadway sections. Shelby tube samples were obtained from test borings R-1, R-2 and R-4 at the depth of 25 ft below the existing ground surface. The Shelby tube samples were used for laboratory testing of the site soils including soil classification tests and unconfined compression tests. SPT tests were carried out on the overburden soils and Texas Cone Penetration tests (CPT) were carried out on the bedrock stratum. The DMT tests were performed to dilatometer blade refusal. The terminal depths of the test borings and DMT tests are shown in Table 1.

Table 1. Borehole and DMT terminal depths

Boring	Borehole depths in meters (ft)	Water table at 72 hours after boring in meters (ft)	DMT terminal depth in meters (ft)
Roadway and bridge approaches			
R-1	15.2 (50.0)	2.9 (9.4)	8.2 (27.0)
R-2	18.3 (60.0)	3.4 (11.3)	14.9 (49.0)
R-3	22.9 (75.0)	3.7 (12.1)	13.1 (43.0)
R-4	25.9 (85.0)	3.5 (11.5)	15.5 (51.0)
R-5	27.4 (90.0)	3.6 (11.8)	16.2 (53.0)
R-6	29.0 (95.0)	2.4 (7.8)	9.8 (32.0)
Bridge piers			
M-5	29.0 (95.0)	5.5 (18.1)	
B-2	29.4 (96.5)	1.1 (3.5)	
B-5	29.7 (97.5)	0.9 (3.0)	

Soil samples from the SPT test sites were also tested for moisture content and soil classification (i.e. gradation and Atterberg limits). Shelby tube samples obtained were tested for unit weight, unconfined compression strength, moisture content and soil classification. Based on the DMT results, other in-situ test results and laboratory test results, the soil type, strength, compressibility, coefficient of consolidation and coefficient of permeability were determined.

2.1 *Soil Classification*

Soil classifications from DMT and the Unified Soil Classification System (USCS) are compared for borehole R-2 as shown in Table 2. The soil types in

the DMT column are determined using the material index (I_D) from the DMT tests.

Table 2. USCS soil classifications and DMT soil descriptions for borehole R-2.

Depth in meters (ft)	DMT Soil Class	USCS Soil Class
4.9 (16)	Sand	Silty Sand
6.1 (20)	Clayey Silt	Sandy Lean Clay
6.4 (21)	Silt	
7.6 (25)	Silt	Sandy Lean Clay
7.9 (26)	Silty Clay	
9.1 (30)	Silty Sand	Silty Sandy Lean Clay
9.4 (31)	Silt	
10.7 (35)	Silty Clay	Silty Sand
11.0 (36)	Silty Sand	
12.2 (40)	Silty Sand	Silty Sand
12.5 (41)	Silty Sand	
13.7 (45)	Silty Sand	Silty Sand
14.0 (46)	Silty Sand	

As shown in Table 2, the soil classifications from the DMT test results and the USCS using the laboratory test results do not exactly match. The soil classification using I_D can be expected to yield different results from the sieve analysis (Schmertmann 1988a). The parameter I_D is an indicator of the soil mechanical behavior, similar to a *rigidity index*. Thus, the DMT results can misidentify silt as clay or vice versa. For example, if a clay soil exhibits a stiff response to the DMT test, it may be interpreted as silt according to its I_D value. However, it has generally been shown that the DMT soil classifications are capable of identifying the basic soil type, such as sandy soils or clayey soils (Schmertmann 1988a). The I_D parameter from DMT was also used to estimate the unit weight of the soils. A comparison of the DMT and laboratory test results is shown in Table 3.

Table 3. Predicted unit weight of soil samples from DMT and laboratory tests.

Borehole	Sample depth in meters (ft)	Laboratory unit weight in kN/m^3 (pcf)	DMT unit weight in kN/m^3 (pcf)
R-1	3.0-3.5 (10-11.5)	14.9 (94.9)	17.6 (112.3)
R-2	6.1-6.6 (20-21.5)	18.1 (115.5)	17.2 (109.2)
R-4	6.1-6.6 (20-21.5)	16.3 (103.6)	17.2 (109.2)
	9.1-9.6 (30-31.5)	16.5 (104.9)	17.2 (109.2)
	15.2-15.7 (50-51.5)	16.4 (104.3)	16.7 (106.1)
R-5	7.6-8.1 (25-26.5)	15.4 (98.0)	17.6 (112.3)
	15.2-15.7 (50-51.5)	16.2 (103.0)	17.6 (112.3)
R-6	7.6-8.1 (25-26.5)	17.0 (108.0)	17.6 (112.3)

As shown in Table 3, the unit weight values from the DMT test results are notably different from the laboratory test results in boreholes R-1 and R-5. For example, the DMT results overestimate the soil unit weight at Borehole 1 by about 18%. In other boreholes, the unit weight values from the DMT results are closer to the laboratory test results. For the most part, the soil unit weight from the interpretation of DMT results can be viewed as a reasonable approximation of the value expected from the more accurate laboratory tests and a preferred alternative to the use of lookup tables. As explained by Marchetti (1980), the unit weight is a soil property that is estimated empirically using the DMT I_D parameter. As a result, similar to soil classification, the estimated soil unit weight from the DMT results could be different from those from laboratory testing of the soil.

2.2 *Soil Strength*

Shelby tube soil samples were procured for clayey soils to perform unconfined compression tests. The values for the cohesion of clayey soils and the friction angle of sandy soils were determined using the data obtained from DMT, unconfined compression tests (clayey soils only) and SPT tests. These properties are presented in Tables 4 and 5.

Table 4. Comparison of cohesion values from laboratory and DMT test results.

Borehole	Depth (ft)	Unconfined compression test cohesion (psf)	DMT cohesion (psf)
R-1	7.6-8.2 (25-27)	32.0 (668)	N/A*
R-2	7.6-8.2 (25-27)	45.1 (941)	26.8 (560)
R-4	7.6-8.2 (25-27)	92.1 (1922)	72.8 (1520)

* N/A: Inconclusive

Table 5. Comparison of friction angle values of sandy soils from SPT and DMT test results.

Borehole	Depth (ft)	SPT Friction Angle (^{o})	DMT(^{o}) (ϕ)	DMT (ϕ)(^{o}) (adjusted**)
R-2	10.7 (35)	30.7	43.6	40
	12.2 (40)	31.1	45.6	41
	13.7 (45)	28.2	OOR*	OOR*
R-5	9.1 (30)	28.1	40.2	37
	10.7 (35)	28.1	40.0	37
R-6	9.1 (30)	29.3	38.3	36
B-5	6.1 (20)	31.7	45.8	41
	9.1 (30)	29.1	47.4	42
	12.2 (40)	30.4	OOR*	OOR*
	13.7 (45)	29.6	OOR*	OOR*
	15.2 (50)	30.2	OOR*	OOR*
	16.8 (55)	32.3	OOR*	OOR*

* OOR: Out of Range ** Equation 1.

As shown in Table 4, in test boring R-1 at a depth of 25-27 ft, DMT yields an inconclusive cohesion value. Based on the interpretation of DMT results, the soil at this depth is classified as clayey silt with the I_D value greater than 0.6 (Marchetti 1980). The data reduction software program developed by Marchetti (1980) to simplify the interpretation of

DMT data appears to be incapable of interpreting the cohesion value for soils with I_D values greater than 0.6. However, the program provides an option to change the default range of values for I_D to predict the soil cohesion value. In this study, the default range of values for I_D was changed in the program (in test boring R-1) and as a result, the clayey soil at 25-27 ft in the test boring R-1 was found to have a cohesion value of 550 psf. Table 4 shows that the DMT test results underestimate the predicted cohesion values for clayey soils by about 400 to 500 psf compared to the values from unconfined compression tests. However, in the absence of more accurate laboratory test results, DMT results could be used as preliminary values for the soil strength properties.

The correlation between the horizontal stress index (K_D) from DMT test results and the undrained shear strength of cohesive soils has been confirmed by several different studies (e.g. Kamei, 1995). However, Powell and Uglow (1988) stated that this correlation is suitable for *young* clay deposits and suggested that for *old* clay deposits, either (a) the existing correlations for that soil type can be used, or (b) if only limited amount of new data is available, a new correlation could be derived by drawing a straight line through the new data parallel to the Marchetti correlation line. Fig. 2 shows the Marchetti correlation line for undrained shear strength of cohesive soils.

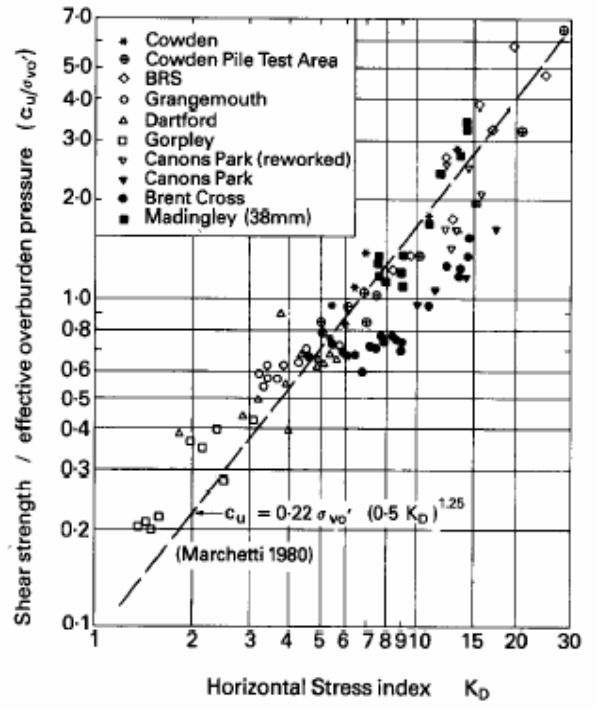

Figure 2. Shear strength/effective overburden pressure vs. horizontal stress Index, K_D (Powell and Uglow, 1988)

In Table 5, the soils internal friction angle values are estimated from the SPT tests using the correlations between the SPT data and the soils friction angle values as given by Peck, Hanson and Thornburn (1974). The SPT results are corrected for the influence of the effective overburden pressure (Liao and Whitman, 1986). The term OOR in Table 5 refers to the fact that the data reduction program provided by Marchetti (1980) is not capable of calculating the soil friction angle value using the available correlation formulae. Once the calculated friction angle value for sandy soils is greater than 50^o, the program automatically terminates the calculation. Hence such case is shown as OOR (i.e. out of range) in the table.

The (plane-strain) DMT friction values in Table 5 have been downward adjusted to determine equivalent traiaxial friction values using the following equation (Schmertmann 1988b):

$$\phi_{tr} = 32 + 2\left(\phi_{ps} - 32\right)/3 \qquad [1]$$

As shown in Table 5, the DMT correlations overpredict the friction angle values for the sandy soils compared to the SPT results. Part of the reason for the difference between the friction angle values determined from the two approaches can be attributed to the difference in the degree of sensitivity of the test results to the test procedures. Overall, DMT test results are perceived to be less sensitive to the test procedure and would require fewer corrections compared to the SPT results. At the same time, it is also possible that the proposed correlations between the DMT results and soil friction angle values are not suitable for the subsurface conditions of the SH 99 project site. Marchetti (1997) noted that the DMT results in a number of earlier studies have overpredicted the friction angle value of sandy soils. Therefore, these values could be non-conservative if used at the site of the proposed SH 99 project.

2.3 *Compressibility*

The consolidation settlement of the highway embankment was predicted using the coefficient of compressibility of the subsurface soils predicted from DMT test results and an empirical formula proposed by Skempton (Das, 1998) using the SPT test data (Table 6)..

The Skempton's empirical approach using SPT results is based on the correlations between the soil shear strength and its stress history (FHWA 2002). From these correlations, the over-consolidation ratio (OCR) of the soils and the magnitudes of the embankment consolidation settlement were estimated using the undrained shear strength values of the soils. The DMT results were used to predict the tangent drained constrained modulus of the soils (M) and the magnitude of the consolidation settlement using Janbu's method (Schmertmann, 1988a).

Table 6. Consolidation settlement underneath the proposed SH99 highway embankment based on DMT test results and Skempton's empirical formula (C_c=0.009*(LL-10)).

	Estimated consolidation settlement in mm (in)	
Borehole	Skempton's empirical formula using SPT data	DMT results
R-1	5 (0.21)	5 (0.18)
R-2	4 (0.17)	15 (0.58)
R-3	35 (1.37)	39 (1.52)
R-4	32 (1.27)	44 (1.73)
R-5	24 (0.93)	23 (0.90)
R-6	15 (0.60)	N/A*
B-2	546 (21.5)	244 (9.59)

* N/A: Not enough information for analysis.

Results shown in Table 6 indicate that the predicted values for the consolidation settlement at boreholes R-1 through R-5 are comparable, with a maximum difference of about 0.5 in. However, the predicted results for the consolidation settlement at borehole B-2 are significantly different. Comparison of the laboratory and in-situ test results indicated that the subsurface soils at locations R-1 through R-6 are much stiffer and stronger than subsurface soils at location B-2. This is because boreholes R-1 through R-6 are located on the abandoned old highway, i.e. on the subsurface soils that had been consolidated due to the weight of the old highway embankment. However, boring B-2 is located in the flooded area and the subsurface soils in that location are extremely soft.

To determine the accuracy of the predicted consolidation settlements, the settlement analysis carried out in this study was compared to the analysis that had been carried out during the construction of the current highway alignment by the Oklahoma Department of Transportation (ODOT). Based on the information provided by ODOT, the predicted consolidation settlement of the current highway built in the flooded zone was about 14 in. Because the height of the proposed embankment is less than the height of embankment placed during the construction of current highway, the expected magnitude of the consolidation settlement underneath the proposed highway embankment is less than the value of 14 in that was predicted for current highway embankment. Therefore, the predicted magnitude of the consolidation settlement for the proposed embankment from DMT test results (Table 6) is considered to be reasonable.

2.4 *Coefficients of Consolidation and Permeability*

The OCR and the pre-consolidation pressure (P_c) values for Borehole B-2 were calculated in order to evaluate the accuracy of the OCR values predicted from DMT results. This borehole was selected because the subsurface soils in this location were softest. The P_c and OCR values for the B-2 location are presented in Fig. 3. The P_c test results shown in Fig. 3 indicate that the subsurface soils (i.e. at shallower depths) at the borehole B-2 location are, for the most part, normally consolidated clayey soils.

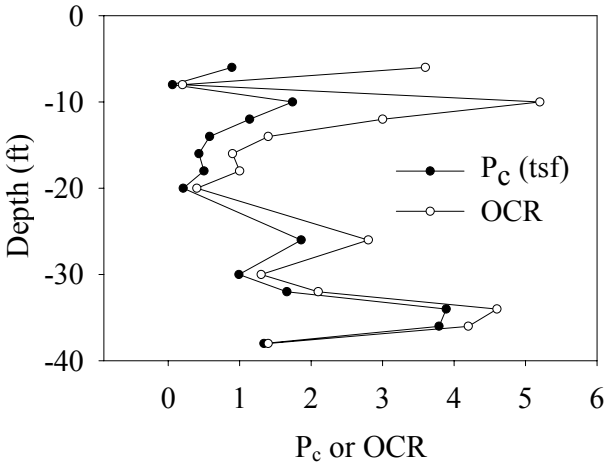

Figure 3. Variations of OCR and P_c with depth in borehole B-2.

However, the OCR values from DMT tests are less than 1 only at isolated depths (e.g. from 15 ft to approximately 22 ft). The predicted OCR values down to the depth of about 15 ft are mainly greater than 1, which is unexpected considering that these soils are very soft and have continuously been under water. Nonetheless, it can be observed in Fig. 3 that the variations of the OCR (from DMT results) and P_c with depth are very similar in shape. This is consistent with the remark made by Marchetti (1997) that DMT results could be used to obtain a reasonable first order approximation of the soil OCR values and their variation with depth. However, it is imperative that engineers interpret the DMT soil information from any site tested very carefully.

In addition to the regular DMT, a DMTC test was carried out (Robertson et al. 1988) by monitoring the dissipation of pore pressure with time to determine the coefficient of consolidation (C_v) of the clayey soils (Table 7). However, due to the lack of laboratory test results, the predicted C_v values could not be compared to the values from other test methods.

Table 7. C_v values predicted from DMTC tests.

Borehole	R-2	R-3	R-4	R-5
C_v m2/day (ft^2/day)	0.132 (1.427)	0.014 (0.156)	Layer 1: 0.063 (0.685) Layer 2: 0.009 (0.100)	(0.01) 0.113

* N/A: Not enough information for analysis.

As shown in Table 7, the predicted C_v values for different boreholes vary over a wide range. Even though these coefficients are not verified using other test methods, they provide a basis to estimate the values for the coefficient of consolidation and coefficient of permeability of the soils. For example, values of coefficient of consolidation for the Chicago Clay vary in the range between 0.085 ft^2/day and 0.428 ft^2/day (Das, 1998). The predicted values

for the coefficient of consolidation in Table 7 are comparable to this range of values.

3 CONCLUSIONS

The use of DMT as an alternative in-situ testing to conventional subsurface drilling, laboratory testing and other in-situ test methods to obtain soil information for engineering analysis and design has been explored. Based on a comparison of the actual field results from a project site on State Highway 99 (SH 99) in northeastern Oklahoma and the available correlations, the following conclusions are drawn about using DMT as an in-situ testing method:

(i) More work is needed to improve the soil density and description charts (Powell and Uglow, 1988). In general, the DMT test results can be used to determine the soil type and unit weight. However, the actual descriptions and values may need some correction and refining. As indicated by Marchetti (1997), DMT results usually provide a reasonable soil description. However, in the range of cohesive soils, DMT sometimes misidentifies silt as clay and vice versa. Such misread was encountered in some of the boreholes of the project site described in this study. It is understood that the parameter I_D from the DMT tests is primarily an indicator of the mechanical behavior of soils, and therefore may not completely yield consistent results with the sieve analysis. For the most part, however, the DMT results yield reasonably accurate soil density values and are a preferred alternative to the use of lookup tables for engineering analysis and design.

(ii) It was found that the DMT results can be used to predict the undrained shear strength of cohesive soils with reasonable accuracy. However, the correlations proposed for the DMT data are valid for soils with I_D values less than 0.6. The data reduction program provided by Marchetti (2002) has an option to modify the range of variation for the I_D parameter to use the correlation. It was found in this study that allowing I_D to assume values as great as 1.0 would provide reasonable results for the undrained shear strength of cohesive soils. However, further study is needed to validate the admissible range of values for the I_D parameter in order to predict the undrained shear strength of the cohesive soils more accurately.

(iii) It was found that the friction angle values for sandy soils using the DMT test results were overestimated compared to the values obtained from the SPT tests. Therefore, the soil friction angle values from the DMT tests would be non-conservative if used for the SH 99 project site.

(iv) The proposed highway embankment consolidation settlement was estimated using the tangent drained constraint modulus (M) and was compared to an empirical formula proposed by Skempton (Das, 1998), which is based on the standard penetration test results. In addition, the predicted consolidation settlement magnitude from previous subsurface exploration during the construction of the current highway was obtained from ODOT. The magnitude of consolidation settlement predicted from DMT results was found to be reasonably close to the value predicted by ODOT. It was found that Skempton's empirical formula using the standard penetration test results tend to over-predict the magnitude of consolidation settlement.

(v) The variations of the OCR (from DMT results) and pre-consolidation pressure values with depth were found to be very similar in shape. It was concluded that the DMT results could be used to obtain a reasonable first order approximation of the soil OCR values and their variation with depth. However, it is imperative that engineers interpret the degree of consolidation of the soil at a given site based on the OCR values from DMT test results very carefully.

ACKNOWLEDGEMENTS

The financial support and field data provided by Burgess Engineering And Testing, Inc. is acknowledged.

REFERENCES

Das, B.M. 1998. *Principles of Geotechnical Engineering.* PWS Publishing Company, Boston, USA

FHWA 2002. *Interpretation of Soil Properties, FHWA-NHI Subsurface Investigation, Lesson 13: Interpretation of Soil Properties*, http://www.nhi.fhwa.dot.gov/crsmaterial.asp?courseno=FHWA-NHI-132070

Kamei T. and Iwasaki K., 1995. *Evaluation of undrained shear strength of cohesive soils using a Flat Dilatometer*, *Soils and Foundations*, 35 (2): 111-116

Liao, S., and Whitman, R.V. 1986. *Overburden Correction Factor for SPT in Sand, Journal of Geotechnical Engineering, ASCE, Vol. 112, No. 3*: 373-377

Marchetti, S. 1980. *Insitu Tests by Flat Dilatometer, Journal of Geotechnical Engineering, ASCE, Vol. 106, No. GT3, Proc. Paper 15290*: 299-321

Marchetti S. 1997. *The Flat Dilatometer: design applications, 3rd Geotechnical Engineering Conference, University of Cairo,* Cairo, January 1997

Marchetti, S., 2002. *WinDMT- DMT Data Reduction Program,* Schmertmann & Crapps, Inc., Gainsville, Florida

Powell, J.J.M. & Uglow, I.M. 1988. *The interpretation of the Marchetti dilatometer tests in UK clays. ICE Proceedings of Penetration Testing in the UK, University of Birmingham, Paper No. 34*: 269-273.

Peck, R.B., Hanson, W.E., and Thornburn, T.H. 1974. *Foundation Engineering, 2nd ed.,* John Wiley & Sons, New York

Robertson, P.K., Campanella, R.G., Gillespie, D., and By, T. 1988. *Excess Pore Pressures in the DMT, Proc. First International Symposium on Penetration testing (ISOPT-1),* Florida, March, 1988

Schmertmann, J.H. 1988a. *Guidelines for using the CPT, CPTU and Marchetti DMT for geotechincal design,* Schmertmann & Crapps, Inc., Gainsville, Florida.

BACK

Schmertmann, J.H. 1988b. Rept. No. FHWA-PA-87-022+84-24 to PennDOT, Office of Research and Special Studies, Harrisburg, PA, in 4 volumes.

Comparison of moduli determined by DMT and backfigured from local strain measurements under a 40 m diameter circular test load in the Venice area

S. Marchetti, P. Monaco, M. Calabrese & G. Totani
University of L'Aquila, Italy

Keywords: Flat dilatometer test, constrained modulus, stiffness decay curves, test embankment, Venice

ABSTRACT: A full-scale instrumented test embankment (40 m diameter, 6.7 m height, applied load 104 kPa) was constructed at the site of Treporti, typical of the highly stratified, predominantly silty deposits of the Venice lagoon. DMT results at Treporti and comparisons of DMT-predicted vs measured settlements, indicating good agreement, have been presented by Marchetti et al. (2004). This paper concentrates mainly on the comparison of moduli obtained by DMT and from back-analysis of the test embankment performance. The moduli comparisons were carried out not only when the load was fully applied, but also at various stages during loading. In this way it was possible to reconstruct the in situ curves of decay of soil stiffness with strain level. Such curves were backfigured from vertical strains measured at 1 m depth intervals under the increasing loads throughout the embankment construction. The comparison of these curves with datapoints corresponding to DMT constrained moduli (M_{DMT}) indicates that M_{DMT} can be possibly associated to a strain range $\varepsilon_v \approx 0.1$ to 1 %, 0.5 % on average. This finding may help for the development of methods for deriving in situ decay curves of soil stiffness with strain level from seismic dilatometer (SDMT).

1 INTRODUCTION

A full-scale instrumented test embankment was recently constructed at the site of Treporti (Venice, Italy) as part of a research project aimed at the characterization/modeling of the Venetian soils, in connection with plans for the protection of Venice and its lagoon against recurrent flooding.

The construction of the sand embankment, of cylindrical shape (40 m diameter) with geogrid-reinforced vertical walls, started on 12 September 2002 and ended on 10 March 2003. It was carried out in 13 steps by placing sand layers of 0.50 m thickness each. When completed, the sand embankment was covered with 0.20 m of gravel, thus reaching a final height of 6.70 m and a load of 104 kPa.

The embankment was heavily instrumented, at the surface and down to 60 m depth, for monitoring total settlements, local vertical strains, pore pressures and horizontal deformations. Data records of measurements are available so far over a period of more than two years after the beginning of the embankment construction.

The site of Treporti, typical of the Venice lagoon, has been carefully characterized by means of numerous in situ and laboratory tests, performed by various research groups.

Relevant results from the research program at Treporti have already been published (Simonini 2004, Marchetti et al. 2004, McGillivray & Mayne 2004, Gottardi & Tonni 2004, 2005, Cola & Simonini 2005).

Results of flat dilatometer tests (DMT) carried out at Treporti were presented by Marchetti et al. (2004), as well as comparisons of settlements predicted by DMT – before the field measurements were available – and measured. The settlement predicted by DMT at the end of construction (net of secondary developed during construction) was found in good agreement with the observed settlement.

This paper concentrates mainly on the comparison of moduli obtained from DMT and from back-analysis of the test embankment performance.

Also shown in this paper are in situ decay curves of soil stiffness with strain level backfigured from vertical strains measured at 1 m depth intervals under various loads throughout the embankment construction. Datapoints corresponding to the DMT constrained moduli (M_{DMT}) are superimposed to the observed decay curves, in order to locate the strain range associated to M_{DMT}, in view of the possible development of methods for deriving in situ decay curves of soil stiffness with strain level from the seismic dilatometer (SDMT).

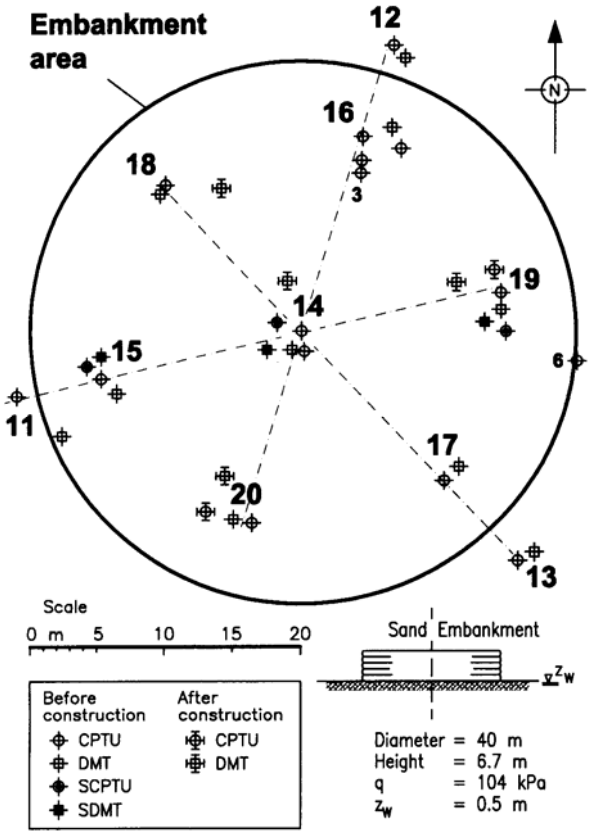

Fig. 1. Treporti test embankment and location of in situ tests

2 BASIC PROPERTIES OF THE VENETIAN SOILS

The soil deposits in the Venice lagoon are composed of a complex system of interbedded sands, silts and silty clays with inclusions of peat. Due to their complex geological history (Ricceri & Butterfield 1974), the sediments exhibit great non-homogeneity even in the horizontal direction. On the other hand, such non-homogeneities, seen on a larger scale, repeat themselves rather "uniformly" (see Fig. 3 later in the paper).

The main characteristic of the Venice lagoon soils is the presence of a predominant silt fraction combined with clay and/or sand, forming a chaotic interbedding of different sediments, whose basic mineralogy varies narrowly, as a result of a unique geological origin and a common depositional environment (Simonini 2004).

The cohesive layers are predominantly silts and very silty clays (ML and CL of the Unified Soil Classification System) of low plasticity. Granular layers are mainly composed of medium-fine sands and fine silty sands (SP-SM). Some thin peat layers are found embedded in the soil profile.

3 SITE INVESTIGATION AT TREPORTI

The site of Treporti was extensively investigated before the embankment construction by means of flat dilatometer tests (DMT), piezocone tests (CPTU), seismic dilatometer tests (SDMT), seismic piezocone tests (SCPTU), boreholes and laboratory tests on samples.

Additional DMTs and CPTUs were performed after construction from the top of the embankment, nearby pre-construction DMTs and CPTUs, in order to detect changes induced in the soil (particularly in stiffness) by the embankment load.

Fig. 1 shows the plan layout of the embankment and the location of all DMT, CPTU, SDMT and SCPTU soundings. Details on DMT results at Treporti are given by Marchetti et al. (2004). Comments on SCPTU and SDMT results are given by McGillivray & Mayne (2004). CPTU results are described by Gottardi & Tonni (2004, 2005). Preliminary laboratory results are presented by Simonini (2004) and Cola & Simonini (2005).

4 DMT RESULTS AT TREPORTI

Ten DMT soundings to ≈ 44-46 m depth (DMT 11 – DMT 20) were performed at various locations (Fig. 1) before the embankment construction.

C readings were taken every 20 cm, besides *A* and *B* readings, to obtain more detailed soil profiles and distinguish layer of different permeability.

A large number of DMTA dissipation tests was carried out to estimate the in situ coefficient of consolidation in the cohesive layers.

Fig. 2 shows the profiles with depth of the main parameters (material index I_D, constrained modulus M, undrained shear strength c_u, horizontal stress index K_D) obtained from the interpretation of DMT 14, located at the center of the embankment.

Fig. 3 shows the superimposed profiles of the above parameters obtained from all the ten pre-construction DMT soundings.

Fig. 4 shows the profiles of p_0 and p_1 (corrected *A* and *B* readings), p_2 (corrected "closing pressure" *C* reading), the pore pressure index $U_D = (p_2 - u_0)/(p_0 - u_0)$ (Lutenegger & Kabir 1988) and the material index $I_D = (p_1 - u_0)/(p_0 - u_0)$ obtained at the center of the embankment (DMT 14). Details on the use of *C* readings and U_D may be found in TC16 (2001).

The DMT investigation indicated the following.

– Stratigraphic profile

The soil at Treporti, typical of the Venice lagoon, is highly stratified and remarkably heterogeneous. The profiles of I_D and U_D indicate that alternating layers of sand, silt and silty clay of variable thickness (rarely > 2 m) are intensely interbedded.

A well-defined layer of sand of significant thickness was found just below the ground surface, in the upper 6-8 m. A thin layer of very soft clay is present at 1.5-2 m depth. The soil between 6-8 m and 20 m

depth is predominantly silt, often interbedded with a variable sand layer between 15 and 18 m.

The "peaks" observed in all K_D and c_u profiles, at about 27-28 m, 34-35 m and 43-44 m depths, are due to the presence of thin stiff peat layers.

– Stress history and OCR

The OCR-K_D correlation commonly used for clay (Marchetti 1980) indicates that the deposit at Treporti is normally consolidated to slightly overconsolidated ($K_D \approx 2.5$, OCR ≈ 1.2-2). These values are in agreement with OCR estimated from oedometer and from observed in situ stress-strain curves (Simonini 2004).

In the upper 6-8 m an overconsolidated "crust" ($K_D > 5$-6), maybe due to desiccation, is present.

– Constrained modulus M_{DMT}

The constrained modulus M determined from DMT (M_{DMT}) is the vertical drained confined (one-dimensional) tangent modulus at σ'_{vo} (same as $E_{oed} = 1/m_v$ obtained by oedometer). The profiles of M_{DMT} at Treporti reflect the vertical and horizontal disuniformity of the deposit. M_{DMT} varies from ≈ 5 MPa in soft clay layers to 100-150 MPa in sand layers.

– Small strain shear modulus G_0

Fig. 5 shows the profiles of the shear wave velocity V_S obtained from three seismic flat dilatometer tests (SDMT) and three seismic piezocone tests (SCPTU) carried out along the cross section 15–14–19 (see Fig. 1). SDMT and SCPTU tests were performed and interpreted by the Georgia Tech research group (McGillivray & Mayne 2004).

Fig. 6 shows the profiles of the small strain shear modulus G_0 obtained from V_S, with soil density ρ estimated from γ_{DMT}.

The profiles of G_0 are more uniform than M_{DMT}. G_0 increases almost linearly with depth from ≈ 30 MPa to ≈ 150 MPa at 40 m depth.

– Coefficient of consolidation and permeability

Figs. 7 and 8 show the values of the horizontal coefficient of consolidation c_h (estimated according to Marchetti & Totani 1989) and the horizontal coefficient of permeability k_h derived from c_h (Schmertmann 1988, see also TC16 2001) obtained from all DMTA dissipations.

The oscillations in the values of c_h and k_h reflect the marked heterogeneity of the deposit. Higher values are influenced by the presence of more permeable silt/sand layers close to the dissipation depths.

The values of c_h are mostly of the order of $1 \cdot 10^{-1}$ cm^2/s. The minimum values of k_h (in silty clay layers) are higher than usually found in most soft clays. The relatively high values of c_h obtained from DMTA suggested rather fast primary consolidation, later confirmed by piezometer readings.

Also, the nearly rectilinear shape of the DMTA dissipation curves, in contrast with the usual "S-shape", was interpreted as a likely indicator of significant creep of the soil skeleton and provided a warning that the secondary settlement could be important, as later confirmed by field measurements.

– Repetitions of DMTs after construction. Observed variation of DMT results

After completion of the embankment, four DMT soundings to ≈ 44 m were performed starting from the top surface of the embankment (Fig. 9), very close (≈ 2 m) to pre-construction DMT soundings.

Fig. 10 shows the profiles of before/after DMT soundings at the center of the embankment. The soil variations due to the embankment load were reflected by the following changes of DMT results:

(a) A reduction in K_D (i.e. in OCR) is particularly evident in the upper OC crust at 6-8 m depth. This "rejuvenation" is due to the fact that the vertical stress increase in the soil under the embankment load approaches the preconsolidation stress, leading the soil to a nearly NC state.

(b) While K_D decreased, the dilatometer modulus E_D increased under the load. Since $M_{DMT} = f(K_D, E_D)$, the two opposite variations approximately compensated each other, so that M_{DMT} remained substantially unchanged. This result, apparently in contradiction with the common notion that M should increase with stress, can be explained observing that, in oedometer tests, M stops to increase as the vertical stress σ'_v approaches the preconsolidation pressure p'_c, or rather, in the case of a pronounced break, M decreases when σ'_v exceeds p'_c. It appears fitting that the DMT correlations have indicated no change in modulus, as the tendency of modulus to increase with stress was compensated by the tendency of modulus to decrease nearing the NC state.

(c) A slight increase in c_u, more evident in the soft clay layer at 1.5-2 m below the ground surface.

(d) An increase in $\sigma'_h = K_0 \sigma'_v$ with K_0 estimated from DMT in clay, similar to the corresponding $\Delta\sigma_h$ calculated by Boussinesq. This is a broad confirmation of the DMT K_0 correlation for clay.

5 OBSERVED PORE PRESSURES AND DEFORMATIONS

The monitoring instrumentation installed at Treporti and the field measurement results are described in detail by Simonini (2004). The most significant indications obtained by field measurements are summarized here below.

– Pore pressures during/after construction

Piezometer readings indicated no detectable excess pore pressure due to consolidation in any layer

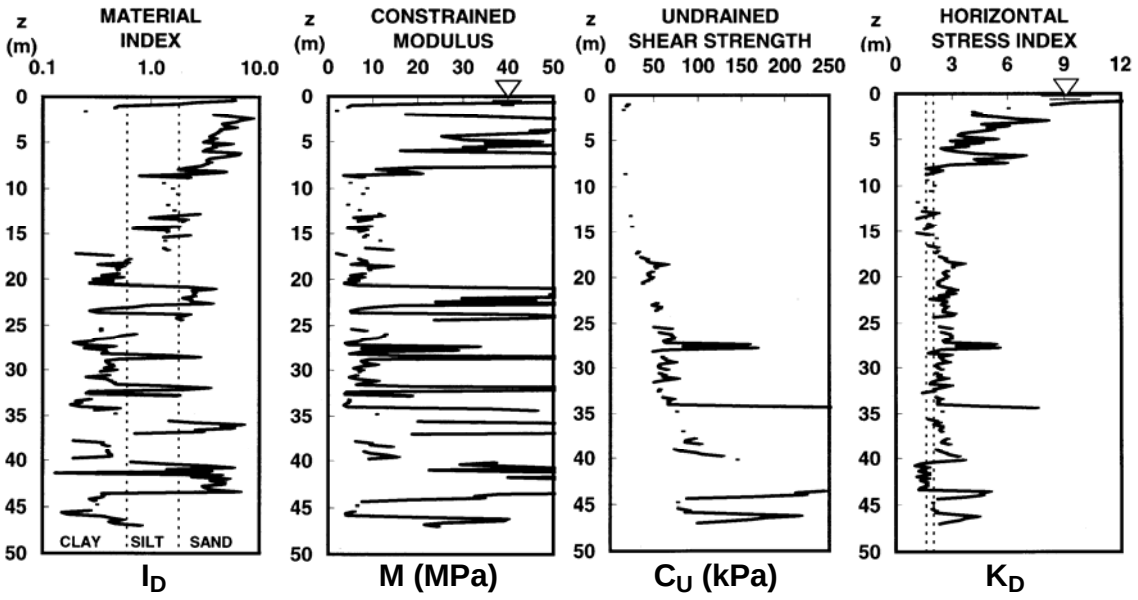

Fig. 2. DMT profiles at the center of the embankment (DMT14)

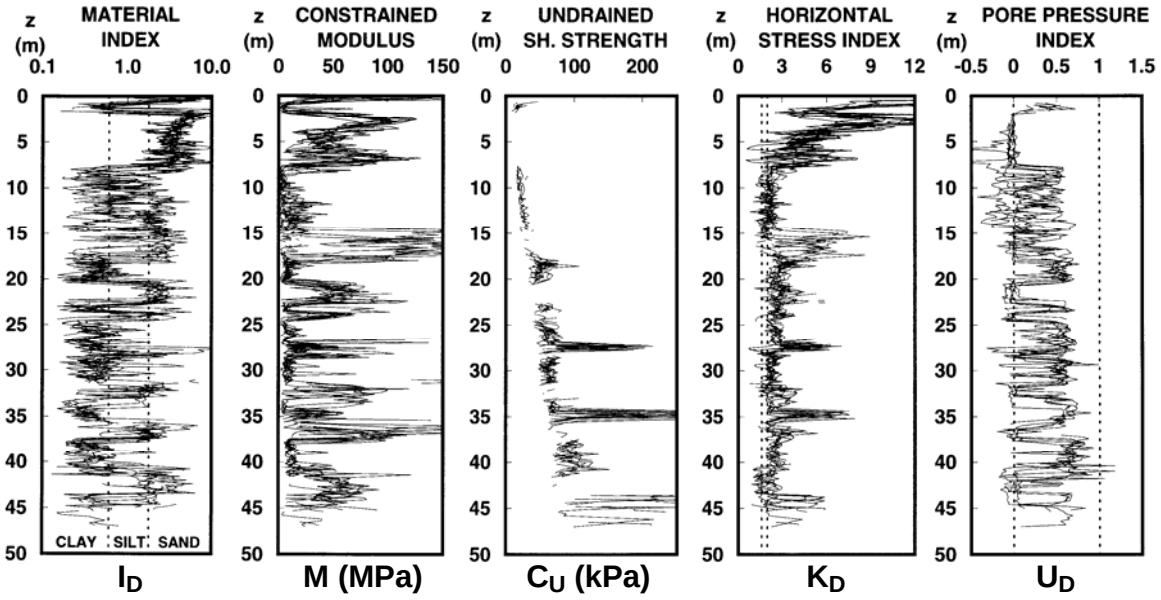

Fig. 3. Superimposed profiles of all DMT soundings (DMT11, 12, …, 20)

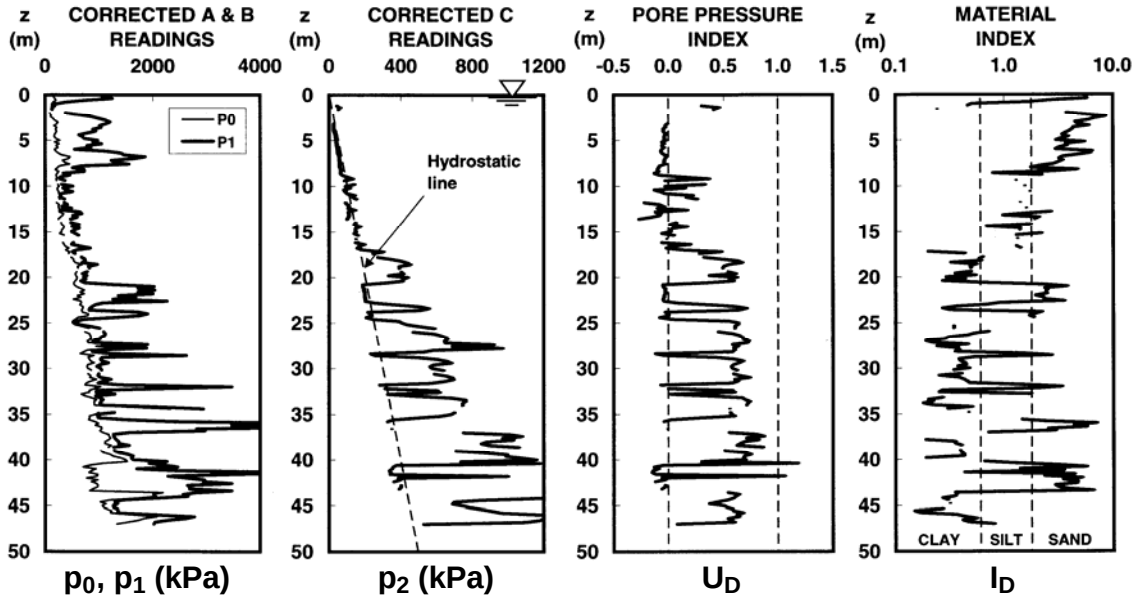

Fig. 4. Profiles of p_0 & p_1, p_2, U_D and I_D at the center of the embankment (DMT14)

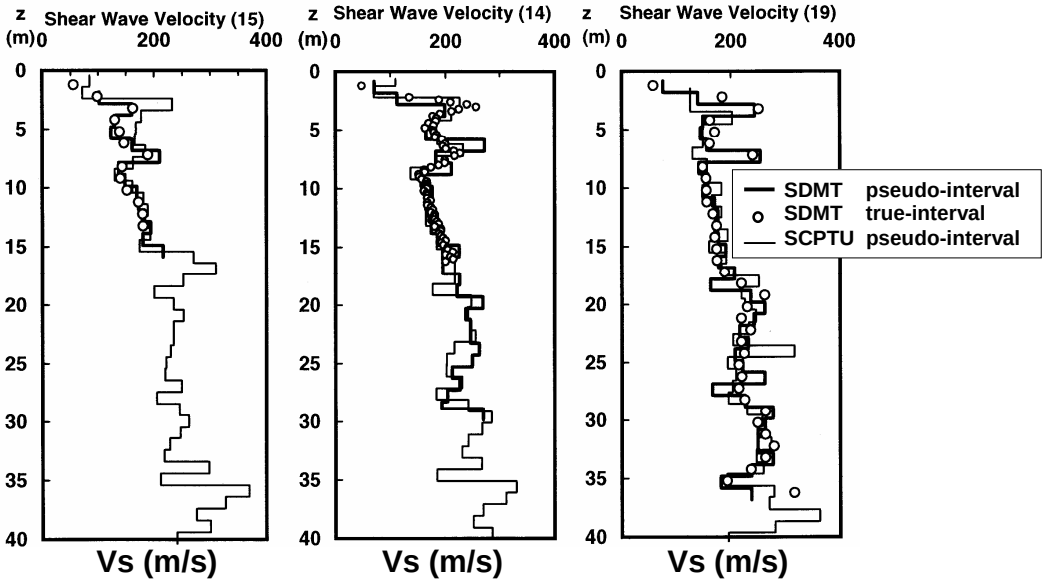

Fig. 5. Profiles of shear wave velocity V_S along the cross section 15–14–19

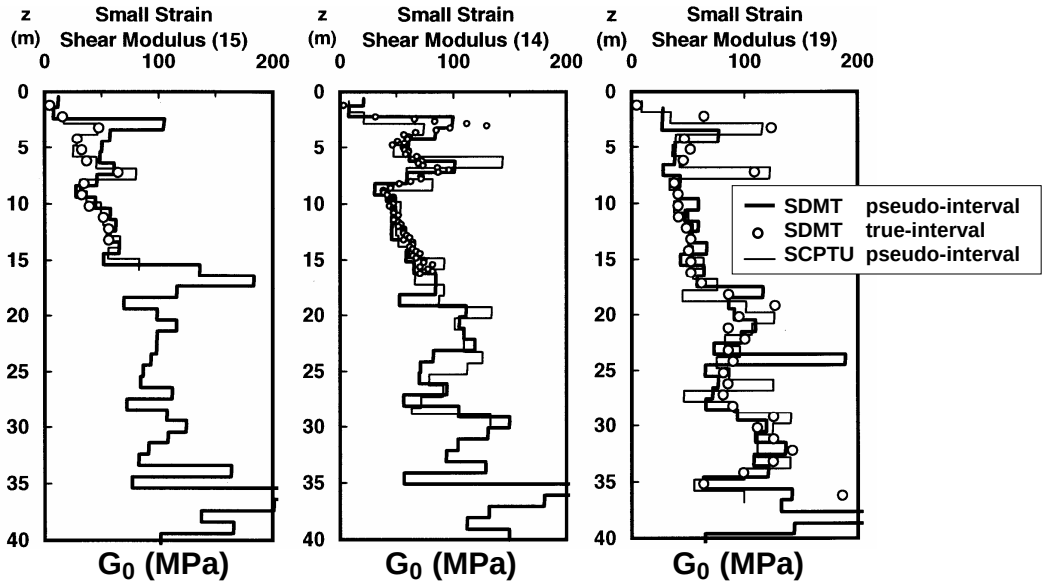

Fig. 6. Profiles of small strain shear modulus G_0 along the cross section 15–14–19

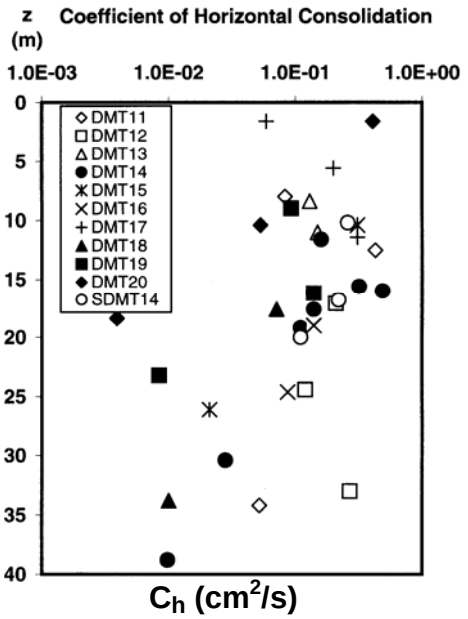

Fig. 7. Coefficient of horizontal consolidation

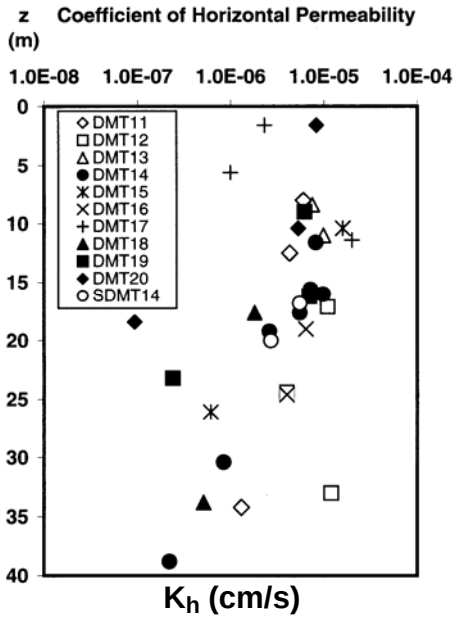

Fig. 8. Coefficient of horizontal permeability

BACK

Fig. 9. Positioning of the penetrometer truck for testing after embankment construction

during and after the embankment construction (fully drained conditions throughout).

Due to the high drainage properties of the soils, primary consolidation was rather fast and contemporary with the six-month embankment construction.

– Settlement-time curve

Fig. 11 shows the evolution with time of the total settlement measured at the center of the embankment, during and after construction.

The total settlement measured under the center the day of embankment completion, i.e. 180 days after the beginning of construction, was ≈ 36 cm. This settlement includes, besides immediate and primary, also the secondary settlement developed in the 180 days of construction, occurred essentially in drained conditions.

Secondary during construction was presumably significant. On 2 September 2004, i.e. 540 days after the end of construction (last reading available to the writers), the total measured settlement was ≈ 48 cm, hence an additional secondary settlement of ≈ 12 cm developed under constant load.

Note that the after-construction secondary settlement alone is about 25 % of the total settlement measured so far.

As remarked by Cola & Simonini (2005), secondary settlements play a key role in the overall time-dependent response of the relatively free draining, predominantly silty Venice lagoon soils. It is difficult to clearly distinguish between the primary and secondary compression, the latter seeming to occur from the very beginning of the compression phase. Consequently, the interpretation of the settlement-time curve, by use of the classic primary-followed-by-secondary model, is not straightforward.

Cola & Simonini (2005) also present values of the secondary compression index C_α obtained from laboratory and from interpretation of the full-scale strain-time curves observed at Treporti (Fig. 12).

– Local vertical strains

Measurements of local vertical strains at 1 m depth intervals, down to 57 m depth, were obtained by use of high-accuracy multiple extensometers (sliding micrometers).

Fig. 13a shows the distribution with depth of local vertical strains ε_v measured at the center of the embankment under various loads throughout the embankment construction (in 180 days) and 540 days after the end of construction, under constant load. The corresponding accumulated settlements S are shown in Fig. 13b.

Fig. 13 clearly shows that vertical strains and settlements are mostly concentrated in the shallow soft clay layer at 1.5-2 m depth and in the silt layer between ≈ 8 and 20 m depth. The maximum vertical strain ε_v measured in these layers at the end of construction is about 3 to 5 %. The contribution of soil layers deeper than 35-40 m appears negligible.

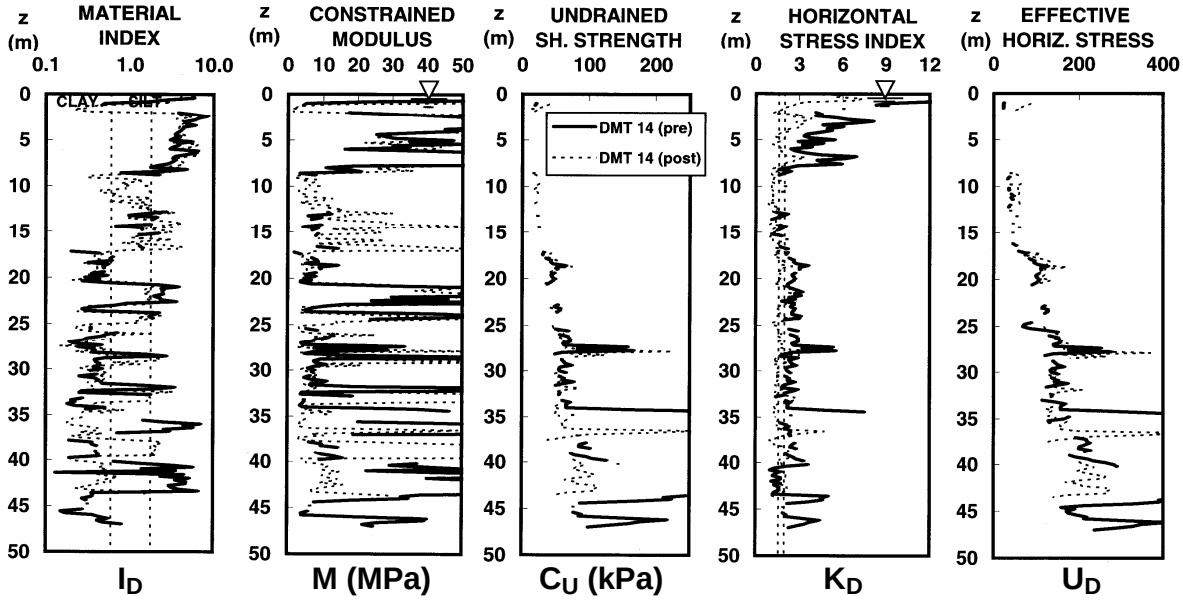

Fig. 10. DMT profiles before/after construction at the center of embankment (DMT 14)

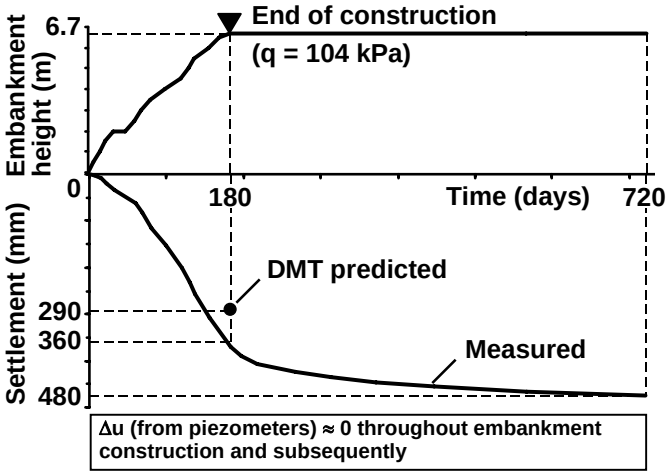

Fig. 11. Settlement-time curve at the center of the embankment and comparison of settlements predicted by DMT and measured at the end of construction

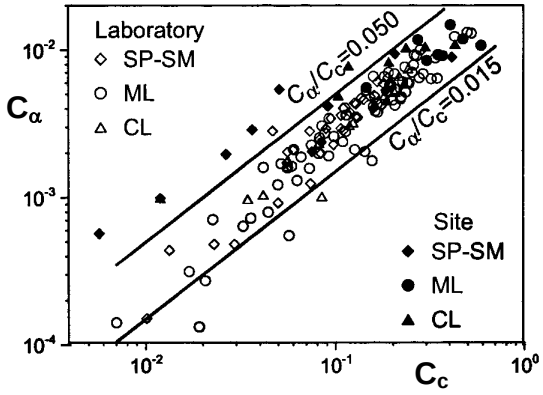

Fig. 12. Ratio between secondary and primary compression indexes C_α/C_c obtained from laboratory and from observed full-scale strain-time curves (Cola & Simonini 2005)

– Horizontal vs vertical deformations

The comparison of vertical and horizontal displacements, measured by inclinometers (Fig. 14), indicated that the total vertical displacement is one order of magnitude greater than the maximum horizontal displacement, i.e. soil compression occurred mostly in the vertical direction, as also shown in Fig. 15.

6 COMPARISON OF DMT-PREDICTED VS OBSERVED SETTLEMENTS

Settlements were predicted by DMT, before the field results were available, by use of the classic 1-D formula $S = \Sigma\,(\Delta\sigma_v / M)\,\Delta z$, assuming $M = M_{DMT}$. Vertical stress increments $\Delta\sigma_v$ were calculated by current linear elasticity solutions for a circular uniform surface load (Poulos & Davies 1974). Details on settlement calculation by DMT at Treporti can be found in Marchetti et al. (2004).

As remarked in TC16 (2001), the settlements calculated by DMT according to the above expression are *primary consolidation* settlements (i.e. net of immediate and secondary). To obtain the total values, the immediate and secondary settlements need to be added.

DMT predicted a primary settlement of 267 mm at the center of the embankment, 101 to 160 mm at the edge. The immediate (undrained) settlement of the sole clay layers at the center of the embankment was estimated as ≈ 20-23 mm Hence the settlement predicted by DMT at the end of construction, net of secondary developed during construction (DMT does not predict secondary), was 29 cm.

The DMT-predicted 29 cm is 7 cm less (20 % less) than the 36 cm measured at the end of

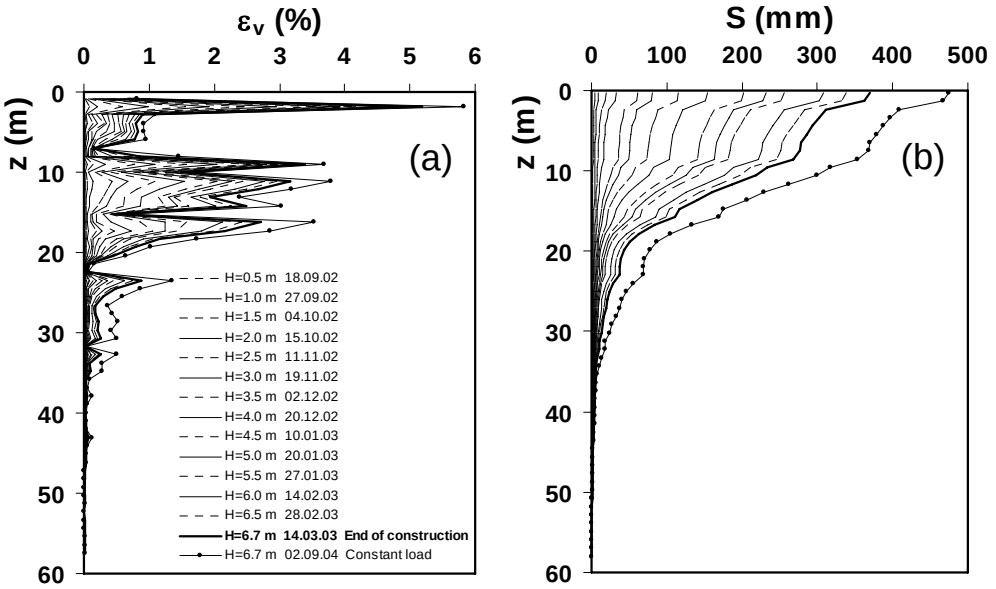

Fig. 13. (a) Vertical strains measured every 1 m depth under the center of the embankment and (b) corresponding accumulated settlements (updated after Simonini 2004)

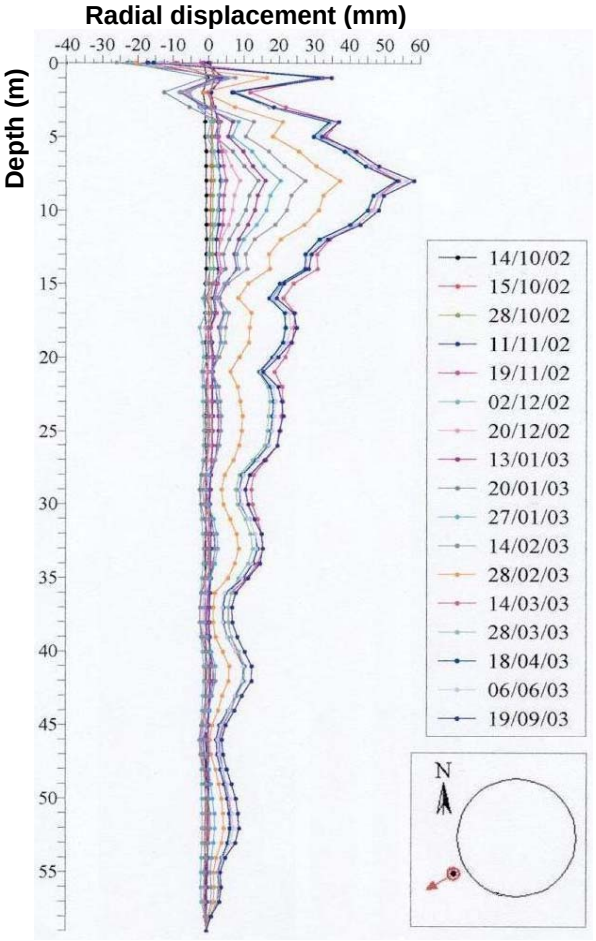

Fig. 14. Radial displacement measured by inclinometer at the edge of the embankment

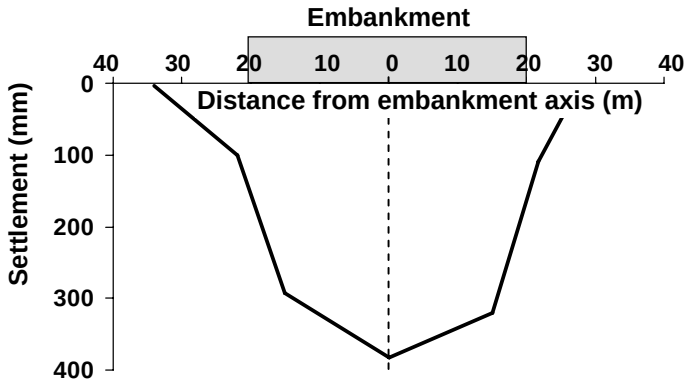

Fig. 15. Settlement profile measured at the end of construction across the embankment cross section SW-NE

construction (Fig. 11). However, if homologous quantities have to be compared, the 36 cm developed during the 180 days of construction should be reduced of the contribution of the secondary during construction. Quantifying such contribution would require a specific analysis separating primary from secondary. Such detraction, however, should end up not very different from the above mentioned difference. If this view is correct, the ability of DMT to predict settlement (net of secondary) proved in this case quite satisfactory.

7 COMPARISON OF *M* BY DMT AND *M* BACKCALCULATED FROM MEASURED LOCAL VERTICAL STRAINS

Fig. 16a shows the comparison of the profiles of the 1-D constrained moduli M_{DMT} obtained by DMT 14 and *M* backcalculated from local vertical strains measured every 1 m depth by the sliding micrometer located at the center of the embankment, at the end of construction.

M values were backcalculated from local vertical strains $\Delta\varepsilon_v$ measured in each 1 m soil layer as $M=\Delta\sigma_v/\Delta\varepsilon_v$, with vertical stress increments $\Delta\sigma_v$ calculated at the mid-height of each layer by linear elasticity formulae (approximation considered acceptable in view of the very low ε_h as in Figs. 14 and 15).

The comparison in Fig. 16a shows that the profile of M_{DMT} (values obtained every 0.2 m depth) is much more variable than the profile of *M* backfigured from measurements. This was expectable, since *M*-backfigured is an "average" over 1 m.

In Fig. 16b the profile of the local vertical strains $\Delta\varepsilon_v$ measured by the sliding micrometer at the center of the embankment, at the end of construction, is compared to the profile of $\Delta\varepsilon_v$ calculated by M_{DMT} (from DMT 14) as $\Delta\varepsilon_v = \Delta\sigma_v/M_{DMT}$. The corresponding profiles of measured and DMT-calculated settlements *S* are compared in Fig. 16c.

Note that the vertical strains/settlements calculated by M_{DMT}, shown in Figs. 16b and c, are due solely to primary consolidation (net of immediate and secondary), while the measured values also include immediate and secondary during construction.

Fig. 16b shows that M_{DMT} slightly underestimates the vertical strains in the upper 15-20 m and slightly overestimates them below this depth. However, these errors partially compensate each other when the local vertical strains are summed up to obtain the accumulated settlement (Fig. 16c).

The comparisons in Fig. 16 indicate an overall satisfactory agreement between M_{DMT} and *M* backcalculated at the end of construction.

8 IN SITU DECAY CURVES OF SOIL STIFFNESS WITH STRAIN LEVEL

The comparisons in the previous section indicate an overall satisfactory ability of M_{DMT} to predict the observed *M* – under the fully applied load.

As a subsequent step, M_{DMT} (one value at a given depth) was compared with the (variable, dependent on the applied load) moduli backcalculated at various stages during construction.

As shown in this section (where the analyses are carried out in terms of Young's modulus *E*), moduli backfigured at small fractions of the final load were much higher than final moduli.

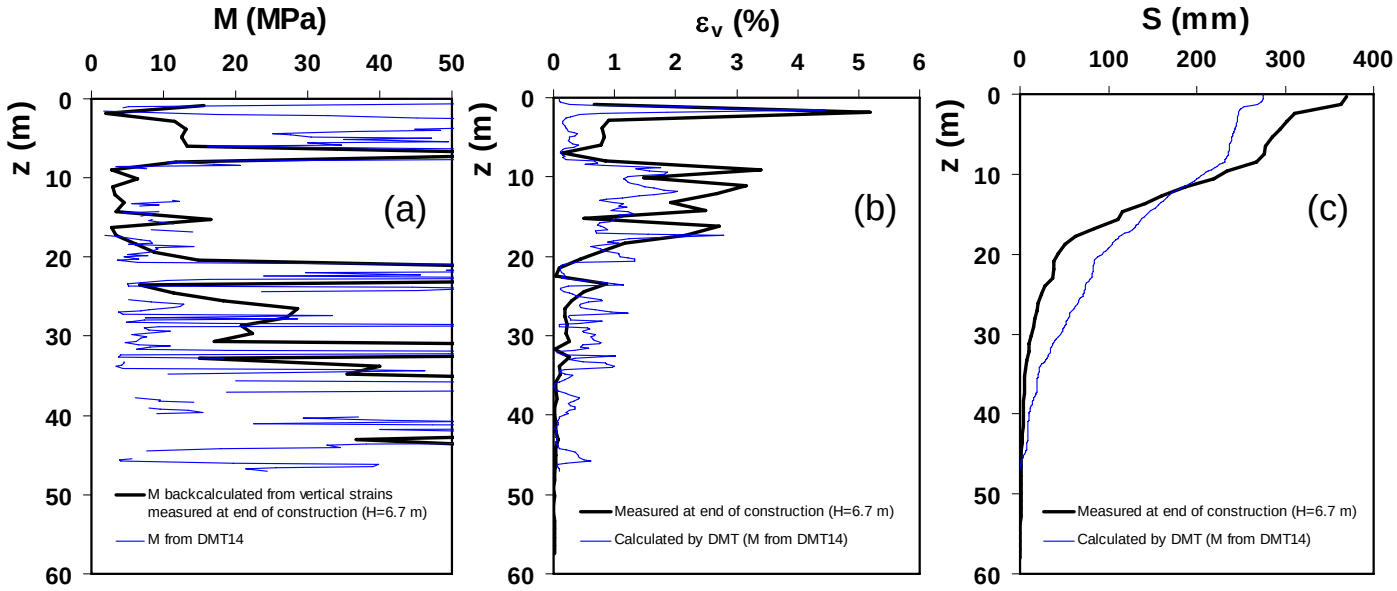

Fig. 16. Comparison of (a) M_{DMT} vs M backcalculated from measurements, (b) vertical strains ε_v and (c) accumulated settlement S measured under the center of the embankment at the end of construction and calculated by M_{DMT}

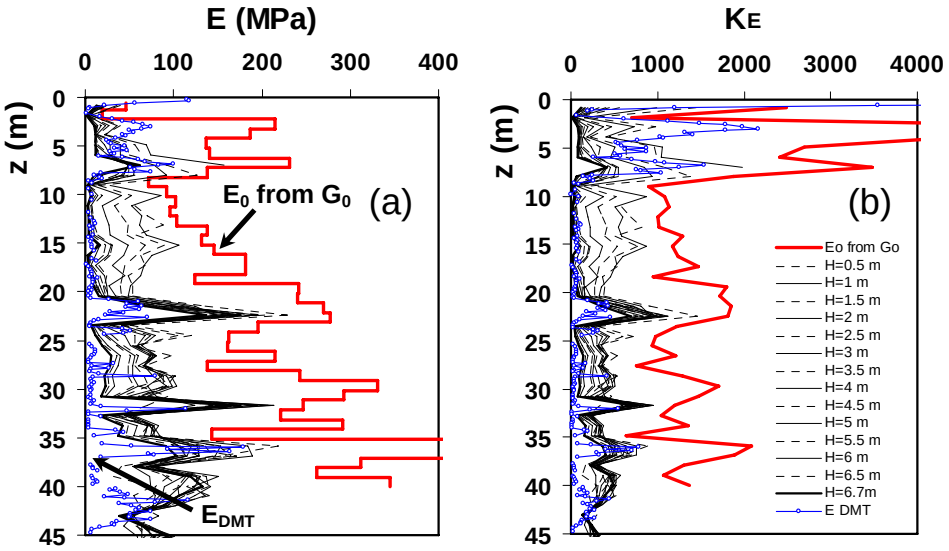

Fig. 17. Variation of (a) secant Young's modulus E backcalculated from vertical strains measured under the center of the embankment under various loads throughout embankment construction and (b) corresponding modulus number K_E

Fig. 17a shows the variation of secant Young's moduli E backcalculated from local vertical strains measured at 1 m depth intervals by the sliding micrometer located at the center of the embankment, under each load increment ($\Delta q \approx 8$ kPa for each 0.50 m thick added sand layer), from the beginning to the end of construction.

The moduli E were calculated at the mid-height of each 1 m soil layer based on linear elasticity formulae. The vertical and radial stress distributions $\Delta\sigma_v$ and $\Delta\sigma_r$ under each load increment were calculated according to current linear elasticity solutions (Poulos & Davies 1974), assuming a Poisson's ratio $\nu = 0.15$.

E values backcalculated at depths greater than 35-40 m may not be dependable, due to the very small measured deformations. Also, a few anomalous "peaks" in the E profiles, derived from uncertain values of strains locally measured under the small initial loads, have been ignored.

The profile of the small strain Young's modulus E_0 (initial modulus) is also shown in Fig. 17a. E_0 was derived from G_0 obtained from Vs measured at the center of the embankment (SCPTU 14) via elasticity theory, assuming $\nu = 0.15$.

Fig. 17a shows the progressive reduction of the backcalculated moduli E under increasing load. Such variation of soil moduli should reflect the combined effects – of opposite sign – of the increase in stress and strain level (stiffness should increase with stress and decrease with strain).

In order to separate the two effects, the dependence of E on current stress level was taken into account, as a first approximation, by use of the classic Janbu's relation $E = K_E\, p_a\, (\sigma'_v / p_a)^n$, where K_E = modulus number, p_a = reference atmospheric

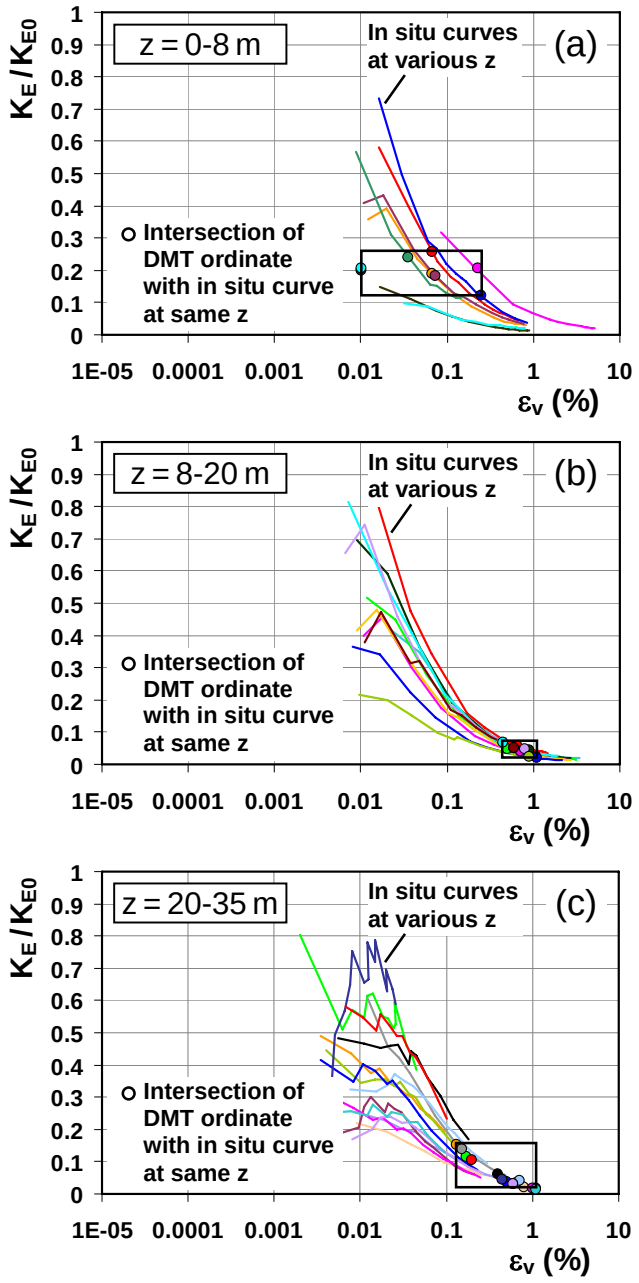

Fig. 18. Curves of decay of soil stiffness with vertical strain backcalculated from measurements (curves labeled "In situ curves") and their intersection with datapoints corresponding to DMT moduli M_{DMT} at the same depth

pressure (100 kPa) and σ'_v = current vertical effective stress. The exponent n was assumed = 0.8, from back-fitting of the observed moduli profiles.

Fig. 17b shows the variation of the modulus number K_E corresponding to the E values backcalculated under each load increment. Fig. 17b clearly shows the decay of soil stiffness with increasing strain level, even purged of the effects of stress increase.

In situ curves of decay of soil stiffness with strain level were reconstructed, at 1 m depth intervals, from local vertical strains measured at the center of the embankment under each load increment, from the very small initial loads up to the final load of 104 kPa.

In order to account for the effect of varying stress level on the backcalculated moduli, these curves, shown in Fig. 18, are expressed in terms of variation of the ratio of the modulus number K_E corresponding to the backcalculated E values to the modulus number K_{E0} corresponding to the initial modulus E_0, obtained by Janbu's expression for $E=E_0$ and $\sigma'_v=\sigma'_{v0}$.

The sets of curves shown in Fig. 18 are representative of different soil layers: (a) the upper sand layer (depth z = 0 to 8 m), (b) the intermediate silt layer (z = 8 to 20 m) – which gave rise to most of the observed settlements, and (c) the silty-sandy layers between z = 20 to 35 m.

As shown in Fig. 18, the smallest detectable values of vertical strains ε_v measured by the sliding micrometer are in the range $\approx 0.5\text{-}1\cdot10^{-2}$ %. Therefore the initial part of the curves, at very small to small strains, is missing.

Research currently in progress investigates the possible use of the seismic dilatometer (SDMT) for deriving in situ decay curves of soil stiffness with strain level (G-γ curves or similar). Such curves could be tentatively constructed by fitting "reference typical-shape" laboratory curves through two points, both obtained by SDMT: (1) the initial shear modulus G_0 from V_S, and (2) a modulus at "operative" strains, corresponding to M_{DMT} – provided the strain range corresponding to M_{DMT} is defined.

Preliminary indications (Mayne 2001, Ishihara 2001) have suggested that the shear strain range corresponding to M_{DMT} is ≈ 0.05-0.1% to 1 %.

To investigate this point, datapoints corresponding to DMT moduli have been superimposed to the observed in situ decay curves in Fig. 18. The rectangular areas in Fig. 18 represent, at each depth interval, the range of values of the ratio K_E/K_{E0} corresponding to E_{DMT}/E_0, where E_{DMT} is the Young's modulus derived from the constrained modulus M_{DMT} (DMT 14) via elasticity theory, for ν = 0.15. The values of E_{DMT} were obtained as average values over 1 m soil layers at each measurement depth.

The comparison of DMT datapoints with the observed in situ decay curves in Fig. 18 indicates that the moduli estimated from DMT (M_{DMT}) are located in a range of vertical strains $\varepsilon_v \approx 0.1$ to 1 %, 0.5 % on average, a result that agrees with the preliminary indications (Mayne 2001, Ishihara 2001).

A note of caution: The vertical strain (ε_v in the abscissas of Fig. 18) appears a legitimate substitute of the shear strain γ, given the "negligible" values of ε_h (it is reminded that $\gamma_{max} = \varepsilon_1 - \varepsilon_3$). Hence the decay curves in Fig. 18 could be regarded as common curves of moduli decay with shear strains.

However the oedometer-like pattern of deformation of the loaded soil (Figs. 14 and 15) would induce to expect an increase – not a decrease – of the modulus with the applied load (as in the oedometer), unless the applied load exceeds the preconsolidation stress, which is probably the case for the studied site.

Then the decreasing trends in Fig. 18 could be due to the combined effect of the two mentioned causes.

9 CONCLUSIONS

A full-scale instrumented test embankment (40 m in diameter, 6.70 m high, applied load 104 kPa) was built at the site of Treporti, typical of the silty deposits in the Venice lagoon area.

The most significant results obtained from comparison of DMT results with the in situ observed embankment behavior, presented in this paper, are:

(a) The settlement predicted by DMT at the end of construction (net of secondary developed during construction) is in good agreement with the measured settlement.

(b) The comparison of the profiles of moduli *M* obtained from DMT and backcalculated from local vertical strains measured every 1 m depth under the center of the embankment, at the end of construction, shows an overall satisfactory agreement.

(c) Field measurements show a progressive reduction of the backcalculated moduli *E* with increasing strain level. In situ full-scale curves of decay of soil stiffness with strain level were reconstructed from local vertical strains measured at the center of the embankment, at 1 m depth intervals, under each load increment throughout the embankment construction. From comparison with the observed in situ decay curves, the moduli estimated from DMT are located in the strain range $\varepsilon_v \approx 0.1$ to 1%, 0.5% on average. This finding may help for the development of methods for deriving in situ decay curves of soil stiffness with strain level from seismic dilatometer (SDMT).

ACKNOWLEDGMENTS

The authors wish to thank for their cooperation P.W. Mayne, Alec McGillivray and the Georgia Tech research group (Atlanta, USA), the Universities of Padova and Bologna (Italy), the Soil Test company (Arezzo, Italy).

This study was funded by the Italian Ministry of University and Scientific Research.

The technical and financial support of Consorzio Venezia Nuova is also acknowledged.

REFERENCES

Cola, S. & Simonini, P. 2005. Relevance of secondary compression in Venice lagoon silts. *Proc. XVI ICSMGE, Osaka,* Vol. 2, 491-494.

Gottardi, G. & Tonni, L. 2004. Use of piezocone tests to characterize the silty soils of the Venetian lagoon (Treporti test site). *Proc. 2nd Int. Conf. on Site Characterization ISC'2, Porto,* Vol. 2, 1643-1650.

Gottardi, G. & Tonni, L. 2005. The Treporti test site: Exploring the behaviour of the silty soils of the Venetian lagoon. *Proc. XVI ICSMGE, Osaka,* Vol. 2, 1037-1040.

Ishihara, K. 2001. Estimate of relative density from in-situ penetration tests. *Proc. Int. Conf. on In Situ Measurement of Soil Properties and Case Histories, Bali,* 17-26.

Lutenegger, A.J. & Kabir, M.G. 1988. Dilatometer C-reading to help determine stratigraphy. *Proc. ISOPT-1, Orlando,* Vol. 1, 549-554.

Marchetti, S. 1980. In Situ Tests by Flat Dilatometer. *ASCE Jnl GED*, 106, GT3, 299-321.

Marchetti, S., Monaco, P., Calabrese, M. & Totani, G. 2004. DMT-predicted vs measured settlements under a full-scale instrumented embankment at Treporti (Venice, Italy). *Proc. 2nd Int. Conf. on Site Characterization ISC'2, Porto,* Vol. 2, 1511-1518.

Marchetti, S. & Totani, G. 1989. Ch Evaluations from DMTA Dissipation Curves. *Proc. XII ICSMFE, Rio de Janeiro,* Vol. 1, 281-286.

Mayne, P.W. 2001. Stress-strain-strength-flow parameters from enhanced in-situ tests. *Proc. Int. Conf. on In Situ Measurement of Soil Properties and Case Histories, Bali,* 27-47.

McGillivray, A. & Mayne, P.W. 2004. Seismic piezocone and seismic flat dilatometer tests at Treporti. *Proc. 2nd Int. Conf. on Site Characterization ISC'2, Porto,* Vol. 2, 1695-1700.

Poulos, H.G. & Davis, E.H. 1974. Elastic Solutions for Soil and Rock Mechanics. John Wiley & Sons.

Ricceri, G. & Butterfield, R. 1974. An analysis of compressibility data from a deep borehole in Venice. *Géotechnique* 24(2), 175-192.

Schmertmann, J.H. 1988. Guidelines for Using the CPT, CPTU and Marchetti DMT for Geotechnical Design. Rept. No. FHWA-PA-87-022+84-24 to PennDOT, Office of Research and Special Studies, Harrisburg, PA.

Simonini, P. 2004. Characterization of the Venice lagoon silts from in-situ tests and the performance of a test embankment. *Proc. 2nd Int. Conf. on Site Characterization ISC'2, Porto,* Vol. 1, 187-207.

TC16 - Marchetti, S., Monaco, P., Totani, G. & Calabrese, M. 2001. The Flat Dilatometer Test (DMT) in Soil Investigations - A Report by the ISSMGE Committee TC16. *Proc. Int. Conf. on In Situ Measurement of Soil Properties and Case Histories, Bali,* 95-131.

Interrelationships of DMT and CPT readings in soft clays

Paul W. Mayne
Civil & Environmental Engineering, Georgia Institute of Technology, Atlanta, GA, USA

Keywords: clays, cone penetration, dilatometer, in-situ tests, porewater readings, pressures

ABSTRACT: Interrelationships between the flat dilatometer readings (lift-off pressure, p_0, and expansion pressure, p_1) and piezocone readings (cone tip stress, q_t, and penetration porewater pressures, u_2) are explored for three soft clay sites. Within the intact regions, the p_0 and u_2 measurements are quite consistently similar in magnitude, whereas q_t is variably larger than both p_0 and p_1, perhaps somewhat dependent on the effective friction angle of the clay. Companion sets of DMT and CPTU at a given site could be used to better define the extent of the crustal zone, degree of fissuring, intact regions, and related permeability characteristics of these substrata within a clay formation.

1 INTRODUCTION

The combined use of flat dilatometer tests (DMT) together with piezocone penetration tests (CPTU) can be a nice complement in defining sublayer zones and general geostratigraphy within the subsurface environment. While many consider each of these in-situ tests to be self-standing by themselves for detailing a soil layer profile, in some instances, the use of CPT soil behavioral charts (e.g., Robertson, 1990) can, in fact, give misleading or erroneous results and/or miss changes in soil strata and substrata (Zhang & Tumay, 1999).

The standard piezocone test provides three separate readings with depth, including: cone tip stress (q_t), sleeve friction (f_s), and penetration porewater pressure at the shoulder (u_2), whereas the flat dilatometer determines two readings: the lift-off or contact pressure (p_0) and expansion pressure (p_1). For the CPT, soil types are often distinguished by use of 2 of the 3 of the readings, as summarized by Kulhawy & Mayne (1990) and Fellenius & Eslami (2000). The earlier CPT classification methods utilized q_t and f_s, yet some measurement difficulties can be found with the sleeve friction because of roughness, wear, porewater presure corrections, and other factors (Lunne, et al. 1986). On the other hand, soil behavior type (SBT) using q_t and u_2 readings will undoubtably be weak in interpretations for situations involving deep water tables, as porewater readings will be zero or change with capillarity effects. Consequently, SBT methods utilizing all 3 readings have been developed (Campanella & Robertson, 1986; Robertson, 1990). In these systems, conflicts can arise as paired readings or normalized parameters from the q_t-f_s and q_t-u_2 charts can provide different evaluations for the same depths.

For the DMT, the soil type is evaluated from the material index: $I_D = (p_1-p_0)/(p_0-u_0)$ per the recommendations of Marchetti (1980), whereby clays are indicated by $I_D < 0.6$ and sands are identified by $I_D > 1.8$. Further distinctions of silty to sandy subcategorizations are available too. The original relationship appears to solidly produce reasonable evaluations of soil types over two decades later (e.g., Marchetti, et al. 2001). An advantage of the DMT over CPTU profiling is the lack of worry over desaturation of a porous element and ability to detail geostratigraphy at sites having a deep groundwater table.

2 INTRA- AND INTER-RELATIONSHIPS

For each test with multiple measurements, intra-relationships between the individual readings can be sought to ascertain trends in the measurements, particularly within a specific geologic formation or soil type. Within that given geotechnical unit, inter-relationships between different test data (lab or field) can be made to develop correlative and statistical trends. Herein, some interrelationships between the DMT and CPT readings in soft clays have been explored.

Intra-relationships between the two DMT readings in different soils have been explored by Garcia

(1991) based on compiled databases from field tests and calibration chamber test series. The successful evaluation of soil type using I_D would corroborate such findings. For the CPT in clays, intra-relations between tip stress (q_t) and penetration porewater pressures on the cone tip (u_1) and shoulder (u_2) have been produced (Mayne, Kulhawy, & Kay, 1990). The presence of fissures, whether from crustal formation and/or desiccation, or from mechanical overconsolidation effects, was shown significant in the q_t-u_2 link, yet much less so in the q_t-u_1 trends.

Interrelationships between the DMT and CPTU readings have been investigated previously by Mayne & Bachus (1989) who showed that, as a first approximation:

$$p_0 \approx u_{max} \quad (1)$$

where u_{max} = peak penetration porewater pressure given by u_2 in intact clays and by u_1 in fissured clays, as shown by Figure 1.

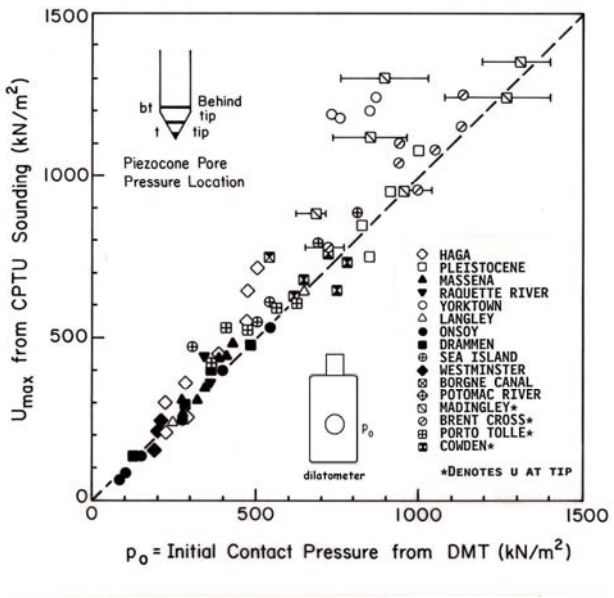

Figure 1. Trend between CPTu porewater pressures and DMT contact pressures in clays (after Mayne & Bachus 1989).

The aforementioned trend was later found applicable for residual silty soils of the Atlantic Piedmont geology by Mayne & Liao (2004).

Direct comparisons of the profiles of the measured cone tip resistance (q_t) with the DMT p_0 and p_1 pressure readings in clays, as well as other readings, have been made at sites in Northwestern Canada (Sully & Campanella, 1990; Sully 1994). Herein, generalized trends are explored between the DMT and CPT measurements at four clays sites tested following the 1989 correlations. These data were obtained from 3 soft clays (two tested by the authors team) and one fissured clay that was overconsolidated by desiccation.

3 CLAY SITES INVESTIGATED

Companion series of DMT and CPTU soundings were obtained in two intact soft clays and one fissured clay by GT field crews, as well data from as one very well-documented intact soft clay site reported in the literature. Table 1 lists the four sites considered for this study.

Table 1. Clay sites with DMT and CPT datafiles.

Site	*Soil Conditions*	*Reference*
Amherst, MA	Soft varved clay	Hegazy (1998)
Bothkennar UK	Soft clay	Nash et al. (1992)
Ford Center, IL	Soft glacial clay	This study
I-10 & 42, LA	Stiff fissured clay	Chen-Mayne (1994)

Recently, tests were performed by the GT field crew in soft clay deposits north of Chicago, Illinois. These in-situ tests were conducted as part of the geotechnical site investigation for the Ford Design Center located on the campus of Northwestern University, in conjunction with an instrumented excavation project. The project is located near the national geotechnical experimentation site (NGES) next to Lake Michigan (Finno, et al. 2000). Subsurface consists of a shallow sandy fill overlying soft silty clays from glacial freshwater lacustrine deposits and a groundwater table located about 3 m deep.

Figure 2 shows the profiles of dilatometer expansion pressure and measured cone tip resistance with depth and Figure 3 presents the dilatometer contact pressure with penetration porewater pressures from two piezocone soundings. The region of intact clay can be interpreted for depths below 9 m, as evidenced by the agreement & similarity of p_0 and u_2 profiles. Above 9 m, less consistency in the readings are observed. For the same depth range, $q_t > p_1$.

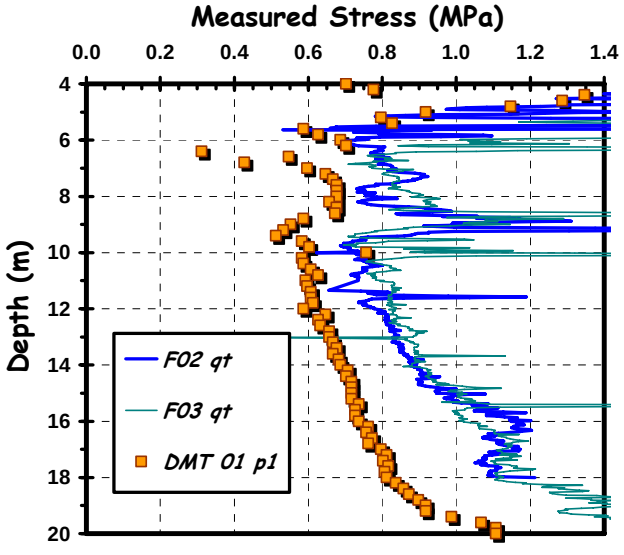

Figure 2. DMT p_1 and CPT q_t at Ford Center Design, IL.

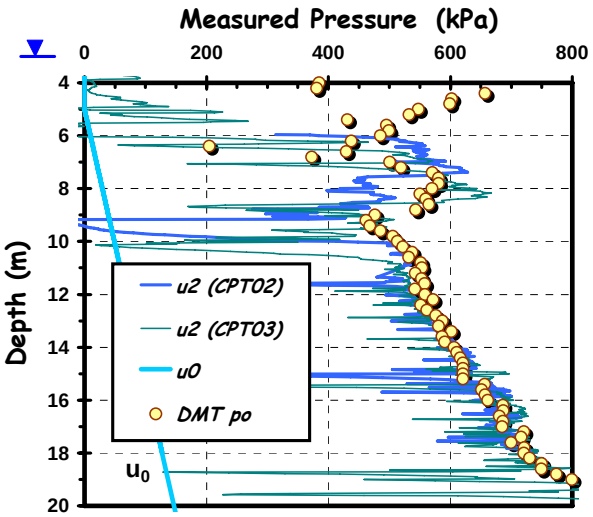

Figure 3. DMT p_0 and CPT u_2 at Ford Design Center, IL.

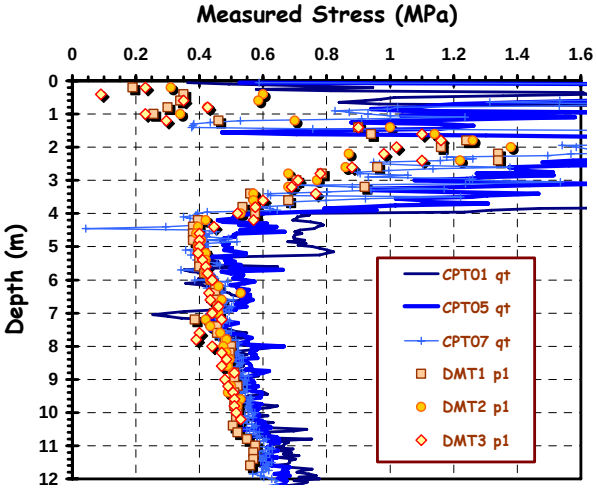

Figure 4. DMT p_1 and CPT q_t at Amherst NGES, MA.

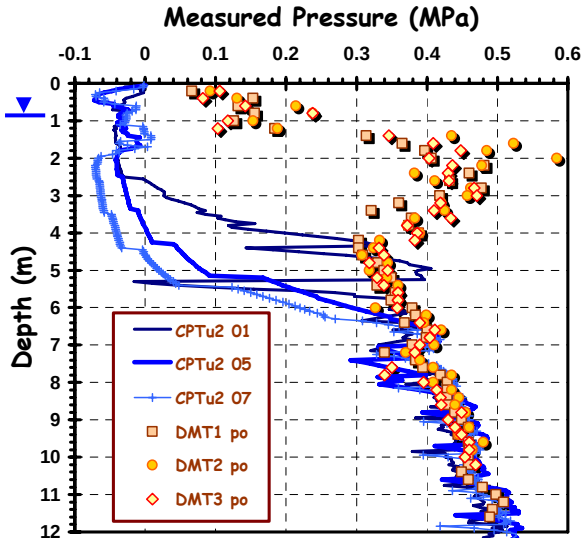

Figure 5. DMT p_0 and CPT u_2 at Amherst NGES, MA.

Series of DMTs and CPTus were conducted by the GT field crew at the Amherst NGES (Martin & Mayne 1997; Hegazy 1998). The soils consist of an upper shallow clay fill and desiccated crust overlying soft varved lacustrine clay. Groundwater lies about 1 m deep. Full details on the testing program and soil properties for the NGES are given by Lutenegger (2000). Figure 4 shows the comparison profiles of three sets of p_1 with three sets of q_t, indicating the intact varved clay below depths of 4 m. Here, the cone tip resistance is just barely greater than the expansion pressures. There is also a parallel profiling of p_1 and q_t in the upper clay fill and desiccated crust, as well.

In Figure 5, the DMT contact p_0 pressures are comparable to the CPT shoulder u_2 porewater pressures. However, it is also apparent that for two of the CPTs, either the porous elements were insufficiently saturated prior to testing, or else became desaturated during advancement through the crust. Only CPTu sounding 01 appears to have properly delineated the transition into the soft intact region below 4 m. In contrast, the p_0 readings clearly and consistently show the change in strata, as well as a relatively uniformity in the underlying soft clay. Thus, the DMT offers an advantage in that the p_0 measurements are not subject to desaturation effects.

In-situ test data from DMTs and CPTs obtained in the soft clay at the British national experimentation test site at Bothkennar (Nash, et al. 1992) were also reviewed and digitized. These data were utilized to provide a reference benchmark in relative comparisons of the data from the Amherst and Evanston sites.

4 DMT-CPT TRENDS IN INTACT CLAYS

Interrelationships between the dilatometer pressures and cone penetrometer measurements can be approximately formulated in terms of cavity expansion theory (e.g., Mayne & Bachus, 1989; Sully 1994). The relationships can be established in terms of total stress parameters: i.e., the undrained shear strength (s_u) and rigidity index ($I_R = G/s_u$), where G = shear modulus. Alternatively, the relationships may be obtained from more fundamental derivations using critical-state soil mechanics to utilize the effective stress friction angle (ϕ') and stress history in terms of overconsolidation ratio (OCR = σ_p'/σ_{vo}'), where σ_p' = preconsolidation stress and σ_{vo}' = current effective overburden stress (Mayne, 2001). In any event, the expressions can only be approximate since neither the flat dilatometer blade nor the cone penetrometer with 60º apex tip are represented by an infinite cylinder nor by a perfect sphere. Instead, empirical relations can be explored.

For the data corresponding to the intact regions of the three soft clays, Figure 6 shows the direct relationships between p_1 and p_0. Best fit lines from regression analyses with forced intercepts equal to zero are shown for each (y = mx with b = 0). As the groundwater tables are rather shallow for these sites, these regressions correspond directly with the individual material indices for each site, including: the Ford Design Center at Evanston, Illinois (I_D = 0.163 ± 0.069), Amherst NGES in Massachusetts (I_D = 0.166 ± 0.044), and Bothkennar test site in Scotland (I_D = 0.291 ± 0.052). All three sites contain lightly overconsolidated clays with 1 < OCRs < 2 in the soft intact zones. Additional index parameters and properties of these clays are summarized in Table 2, including: natural water content (w_n), liquid limit (LL), plasticity index (PI), and effective stress friction angle (ϕ').

Table 2. Mean values of index parameters for soft clay sites.

Clay Site	*Depth (m)*	*w_n (%)*	*LL (%)*	*PI (%)*	*ϕ' (deg)*
Amherst	6 to 12	62	51	21	22º
Evanston	10 to 18	32	33	17	26º
Bothkennar	2 to 16	65	70	45	37º

The notable trends between p_0 and u_2 at each of the sites are shown in Figure 7, substantiating the original correlation represented by equation (1) based on earlier data. Similarly, forced fit best lines (b = 0) are shown with their associated coefficients of determination (R^2). The interrelationship of p_0 and u_2 appears unique and applies to all three intact clays.

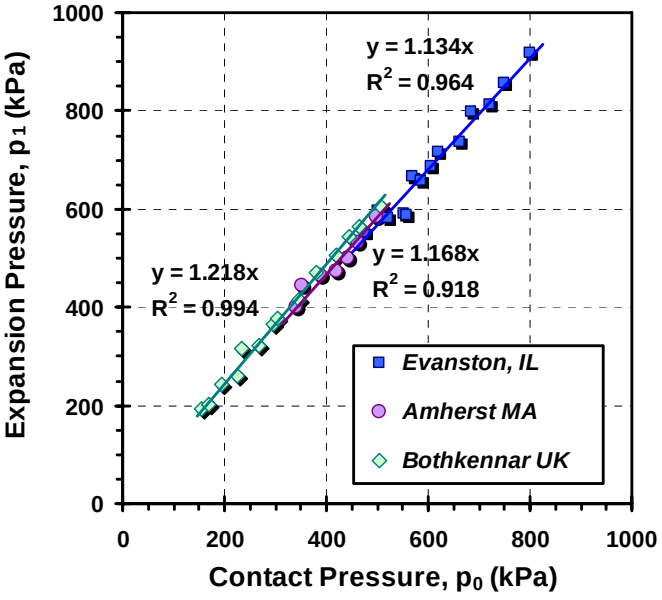

Figure 6. Interrelationships of p_1 with p_0 for intact clays.

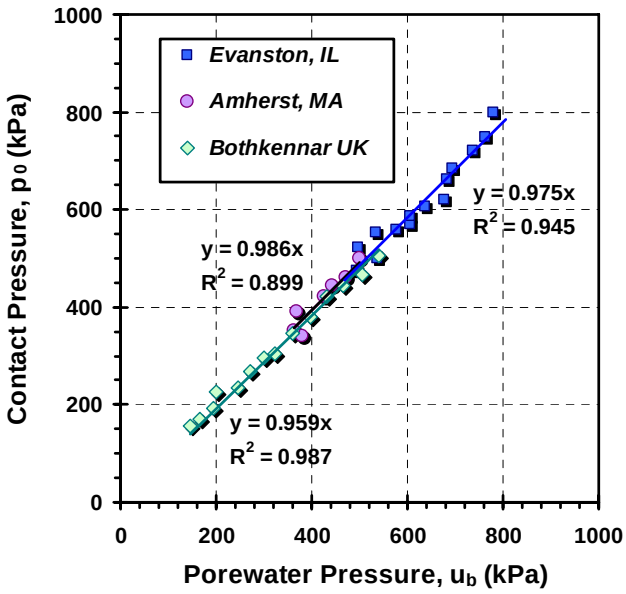

Figure 7. One-to-one relationship between DMT p_0 and CPT u_2 readings in soft intact clays.

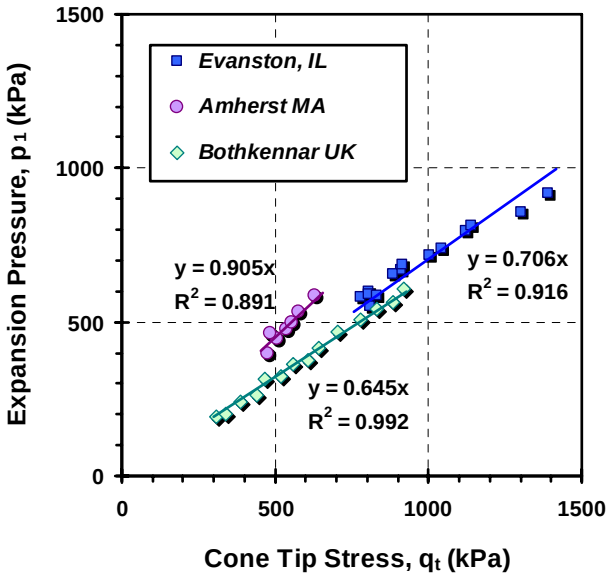

Figure 8. Observed relationship between DMT p_1 and CPT q_t readings in soft intact clays.

For the p_1 trends with q_t, Figure 8 shows that each of the clays shows a distinct and unique interrelationship. In this case, the ratios p_1/q_t appear to decrease with the effective stress friction angle of the clay.

BACK

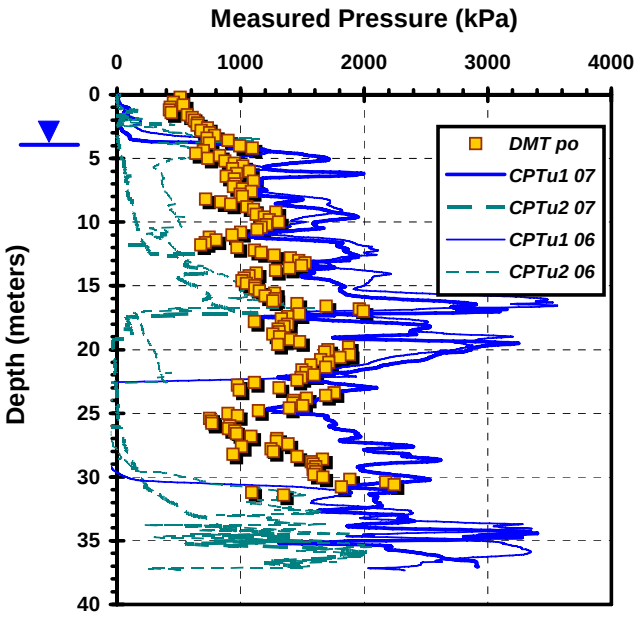

Figure 9. Comparision of p_0 with u_1 and u_2 readings in overconsolidated clay at I-10 and Route 42 near Baton Rouge, LA

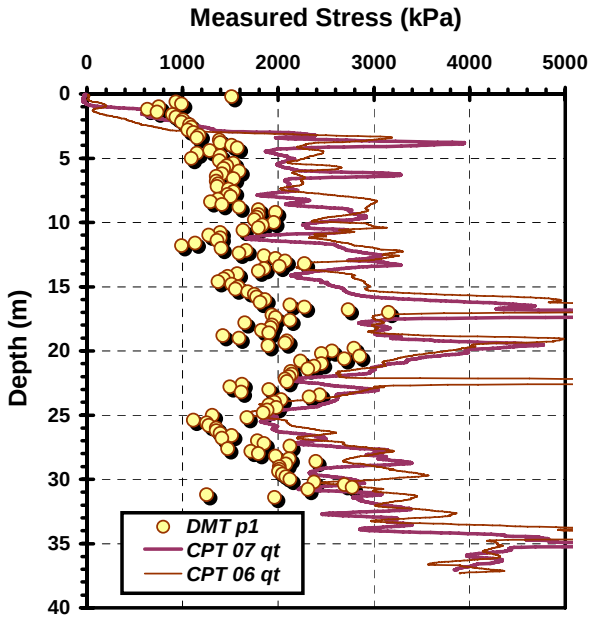

Figure 10. Comparision of p_1 with q_t profiles in OC clay at Baton Rouge, LA.

5 DISCUSSION FOR FISSURED CLAYS

In the case of fissured overconsolidated clays, the piezocone shoulder porewater pressures tend towards zero and even negative values (Mayne, et al. 1990). Thus, since face porewater pressures at the tip or midface (u_1 readings) will remain as positive values, these will better correlate with DMT p_0 readings. Yet, it is likely that $u_1 > p_0$, as shown previously in Figure 1 by fissured London clay at Brent Cross and fissured Gault clay at Madingley (Lunne, et al. 1997).

This facet is illustrated by DMT and CPTU data collected at the I-10 and state route 42 site near Baton Rouge, Louisiana (Chen & Mayne, 1994), as shown in Figure 9. Index parameters for the stiff clay are given in Table 3. At this site, a multi-element piezocone was used and perhaps the water-saturated porous elements were not as responsive as those should glycerine or silicon oils have been used for the saturation process. In any event, the p_0 more closely parallels a profile with the measured face u_1 porewater pressures than with the u_2 readings that are normally used in practice because of the need for porewater corrections on the measured cone tip resistance (Campanella & Robertson, 1988; Lunne et al., 1997).

Table 3. Index parameters of stiff fissured clay from Louisiana

Clay Site	*Depth (m)*	*w_n (%)*	*LL (%)*	*PI (%)*	*ϕ' (deg)*
Baton Rouge	5 to 30	34	61	33	27º

Interestingly, the relative profiles of DMT expansion pressure and CPT tip resistance with depth appear to behave similarly to that noted for the intact clays and the p_1 interrelationship with q_t is not apparently affected by the presence of fissuring.

In the case of fissured crusts overlying soft clays, the DMT can be used to help delineate the extent of the desiccation zone, without fear of desaturation of porous elements or poor element saturation practices associated with piezocone deployment. In companion sets of DMT and CPTU soundings, the results can be used together to better define the zone of intact clays where permeability characteristics are likely to be low. In the upper crustal regions with fissuring, the permeability will be higher and will also reduce the operational undrained shear strength.

6 CONCLUSIONS

Interrelationships between DMT pressures and CPT readings are explored to discern general trends in soft clays. Data from three soft intact clays show that the DMT contact pressure (p_0) is about equal to the CPT shoulder (u_2) penetration porewater pressure and the CPT tip stress (q_t) exceeds the expansion pressure (p_1) by 10 to 50 percent. Companion sets of DMT and CPT can help better define the extent of crustal & desiccated zones. In fissured clays, the profiles of q_t and p_1 appear similar, but p_0 more closely follows the CPT face (u_1) porewater pressures because u_2 readings go negative.

ACKNOWLEDGMENTS

The author appreciates the support of the National Science Foundation (Award No. CMS-0338445) for which Dr. Rick Fragaszy is the program director. Thanks to Professor Richard Finno of Northwestern University who provided access to the Illinois site and to Professor Alan Lutenegger for his help at the Amherst NGES.

REFERENCES

Campanella, R.G. and Robertson, P.K. (1988). Current status of the piezocone. *Penetration Testing 1988*, Vol. 1 (Proc. ISOPT, Orlando), Balkema, Rotterdam: 93-116.

Chen, B.S-Y. and Mayne, P.W. (1994). Profiling the overconsolidation ratio of clays by piezocone tests. Georgia Tech Research Corp. *Report No.GIT-CEEGEO-94-1*submitted to National Science Foundation, 280 pages.

Fellenius, B.H. and Eslami, A. (2000). Soil profile interpreted from CPTu data. *Proceedings Geotechnical Engineering Conference*, Asian Institute of Technology, Bangkok: 1-18.

Finno, R.J., Gassman, S.L. and Calvello, M. (2000). NGES: Northwestern Univ. *National Geotechnical Experimentation Sites* (GSP No. 93), ASCE, Reston/VA: 130-159.

Garcia, S.R. (1991). Interrelationship between the initial lift-off and extended pressure readings of the Marchetti flat blade dilatometer in soils. *Special Research Project*, MS in Civil Engrg., Georgia Inst. of Technology: 119 pages.

Hegazy, Y.A. (1998). Delineating geostratigraphy by cluster analysis. *PhD Thesis*, Civil & Env. Engrg., Georgia Institute of Technology, Atlanta, GA: 464 p.

Kulhawy, F.H. and Mayne, P.W. (1990). Manual on estimating soil properties for foundation design. *Report EL-6800*, Electric Power Research Institute, Palo Alto, 306 p.

Lunne, T., Eidsmoen, T., Gillespie, D. and Howland, J.D. (1986). Laboratory and field evaluation of cone penetrometers. *Use of In-Situ Tests in Geotechnical Engineering* (GSP 6), ASCE, Reston/VA: 714-729.

Lunne, T., Robertson, P.K. and Powell, J.J.M. (1997). *Cone Penetration Testing in Geotechnical Practice*, EF Spon/Blackie Academic, Routledge Publishers, London.

Lutenegger, A.J. (2000). NGES: Univ. of Massachusetts. *National Geotechnical Experimentation Sites* (GSP No. 93), ASCE, Reston/VA: 102-129.

Marchetti, S. (1980). In-situ tests by flat dilatometer. *Journal of Geotechnical Engrg.* 106 (GT3): 299-324.

Marchetti, S., Monaco, P., Totani, G. and Calíbrese, M. (2001). The flat dilatometer (DMT) in soil investigations (ISSMGE TC 16). *Proc. Intl. Conf. on In-Situ Measurement of Soil Properties & Case Histories*, Bali, Indonesia: 95-131.

Martin, G.K. and Mayne, P.W. (1997). Seismic flat dilatometer tests in Connecticut valley varved clay", *ASTM Geotechnical Testing Journal* 20 (3), 357-361.

Mayne, P.W. and Bachus, R.C. (1989). Penetration porewater pressures in clays by CPTU, DMT, and SBP. *Proc. 13th Intl. Conf. Soil Mechanics & Fdn Engrg* (1), Rio: 291-294.

Mayne, P.W., Kulhawy, F.H., and Kay, J.N. (1990). Observations on the development of porewater pressures during piezocone tests in clay. *Canadian Geot. J.* 27 (4): 418-428.

Mayne, P.W. (2001). Stress-strain-strength-flow parameters from enhanced in-Situ tests, *Proceedings, International Conference on In-Situ Measurement of Soil Properties & Case Histories*, Bali, Indonesia: 27-47.

Mayne, P.W. and Liao, T. (2004). CPT-DMT interrelationships in Piedmont residuum. *Geotechnical & Geophysical Site Characterization* (2), Millpress, Rotterdam: 345-350.

Nash, D.F.T., Powell, J.J.M. and Lloyd, I.M. (1992). Initial investigations of the soft clay test site at Bothkennar, U.K. *Geotechnique* 42 (2): 163-181.

Robertson, P.K. (1990). Soil classification using the cone penetration test. *Canadian Geotechnical J.* 27 (1): 141-158.

Sully, J.P. (1994). Measurement of in-situ lateral stress during full-displacement penetration tests. *PhD Dissertation*, Dept. of Civil Engrg., Univ. British Columbia, 485 pages.

Sully, J.P. and Campanella, R.G. (1990). Measurement of lateral stress in cohesive soils by full-displacement in-situ tests. *Transportation Research Record* 1278: 164-171.

Zhang, Z. and Tumay, M.T. (1999). Statistical to fuzzy approach toward CPT soil classification. *Journal of Geotechnical & Geoenvironmental Engineering* 125 (3): 179-186.

Observations from Insitu Testing within a Calcareous Soil

Jiewu Meng, PhD.
Geotechnical Project Manager, WPC Inc., Mt Pleasant, SC, USA

Edward L. Hajduk, PE
Senior Geotechnical Engineer, WPC Inc., Mt Pleasant, SC, USA

Thomas J. Casey, PE
Senior Geotechnical Engineer, WPC Inc., Myrtle Beach, SC, USA

William B. Wright, PE
Senior Geotechnical Engineer and CEO, WPC Inc., Mt. Pleasant, SC, USA

Keywords: marl, calcareous soil, DMT, CPTu, and Osterberg-cell test, side friction

ABSTRACT: Flat Blade Dilatometer Testing (DMT) and Piezocone Penetration Testing (CPTu) within a calcareous soil formation in the Greater Charleston, SC area along with laboratory tests are reviewed. The calcareous soil investigated during the study is typically classified as a young lightly cemented overconsolidated clayey silt, which is known locally as the Cooper Marl Formation, and demonstrates relative uniformity throughout the area. Typical material index (I_D), dilatometer modulus (E_D), and horizontal stress index (K_D), corrected tip resistance (q_t), sleeve friction (f_s), and pore pressure behind the cone tip (U_2) were summarized for the CPTu and DMT, respectively. Due to the difficulty and uncertainty in characterizing the side friction from calcareous soils, the DMT and CPTu along with Osterberg-cell test results from drilled shaft load tests were used to improve the existing understanding of the marl behavior for engineering applications.

1 INTRODUCTION

Calcareous soils have been encountered in many regions around the world. In the last two decades, they have been studied as problematic materials in numerous cases regarding deep foundation design and construction practices. According to Jewell and Khorshid (1999), a very large gas production platform was supported on deep foundations bearing within lightly consolidated calcareous sediments on the North West Shelf of Western Australia. The actual friction capacity of the large open ended driven piles was substantially lower than the design values and after this occurrence many studies were then focused on the friction behavior of calcareous sediments by almost all the major international geotechnical researchers.

Unlike this problematic sediment, the calcareous soil formation in the Charleston, SC region, known locally as the Cooper Marl Formation (CMF), is a primary bearing stratum for supporting deep foundations in the area. The CMF is a relatively homogeneous formation, as determined by local geotechnical experience and a comprehensive examination of data from several project sites in the area (Meng et al., 2005). Unlike other problematic calcareous sediments, experience and testing in the CMF has shown it to a stable formation for deep foundations.

The following paper presents representative DMT testing results within the CMF along with the CPTu findings and some laboratory summaries in the greater Charleston area. Fundamental characteristic parameters of the CMF with the two testing methods are also presented and discussed. In a case study, Osterberg load cell test results were compared to the calculated undrained shear strengths derived from CPTu and DMT tests. The side shear resistance developed along the shaft side was measured with an Osterberg-cell test, which is often used to measure both end bearing and side shear resistance and provides estimates ascribed to each part. Unlike most other studies within the CMF (e.g., Camp, 2004), the drilled shaft was physically detached from the overlying non-marl soils and the test therefore provides a unique advantage of interpreting only the side shear resistance within the marl. Effectiveness of the interpretation of the strength parameters from CPTu and DMT testing results is discussed by using the Osterberg load cell test results.

2 CHARLESTON, SC AREA GEOLOGY

Charleston is located within the Lower Coastal Plain geological province of South Carolina along the Atlantic Coastal terraces, which is approximately 120 km in width. The “overburden” of the area consists of soft and loose Pleistocene and Recent marine de-

posits of the Quaternary Period. The area is primarily underlain by young marine deposits in chronologic age from Upper Cretaceous to Recent, which lie on ancient crystalline rocks (granites, gneisses, and schists such as the Black Mingo Formation). Immediately overlying the rocks is the "Great Carolinian Bed" consisting of Upper Cretaceous limestone (i.e., the Santee Limestone) and Eocene cementious marl (e.g., the Cooper Marl Formation). Figure 1 shows the typical geological strata underlying the Greater Charleston area.

3 GEOTECHNICAL CHARACTERIZATION OF THE COOPER MARL

A large quantity of testing results within the CMF is available from consulting projects across the area. Laboratory testing results including the index properties (i.e., natural water content, gradation, and Atterberg Limits), calcium carbonate content, and undrained shear strength are summarized in Table 1. The reviewed data were arbitrarily divided into the downtown Charleston and the Inland Charleston groups according to their geographic closeness and locations of the samples origin. According to the Unified Soil Classification System (USCS) (ASTM D2487), the CMF is classified as silt (ML) to elastic silt (MH) by using the averages in Table 1. In addition, the CMF has calcium carbonate contents between 60% to 70% and undrained shear strengths between 0.21 MPa and 0.25 MPa. In terms of statistics, there appears little difference between the two groups regarding the considered parameters and the CMF may be considered relatively uniform in the area. This conclusion matches experience by local practicing geotechnical engineers.

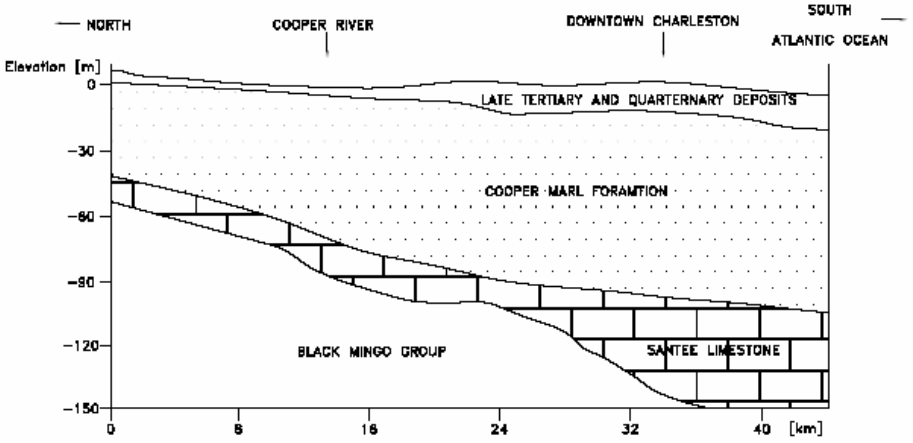

Figure 1. Geological profile of the Charleston area (Modified after Klecan et al., 2001).

Table 1. Summary of Laboratory Results of the Cooper Marl.

Location	Statistic	Wn (%)	FC <#200 (%)	Atterberg Limits		$CaCO_3$ (%)	S_u (UU) (MPa)	Reference
				LL	PI			
Downtown Charleston	# of Tests	23	14	21	21	6	22	Klecan et al. (2001)
	Average	46	75	49	20	67	0.25	
	Stdev	5	13	5	6	9	0.05	
	Max	58	94	58	35	77	0.34	
	Min	32	49	40	12	57	0.17	
Inland	# of Tests	8	4	18	17	13	42	Unpublished Test Results
	Average	42	74	62	29	66	0.21	
	Stdev	6	6	22	14	4	0.16	
	Max	48	79	146	79	71	0.72	
	Min	30	65	44	13	60	0.02	

BACK

From insitu tests, the CMF is typically identified by uniform testing parameters such a dilatometer modulus (E_D) for the DMT and corrected tip resistance (q_t) for the CPTu. For piezocone CPTu testing (i.e. CPTu), the CMF is also distinctly noted by the sharp increase in penetration pore pressure after encountering the marl. This pore pressure increase typically ranges from 1 MPa to 4 MPa regardless of embedment depth. This pore pressure increase phenomenon has been consistently observed in CPTu data within the CMF in the area and therefore serves as a signature of identification. Figure 3 shows typical DMT and CPTu results from adjacent testing (i.e. within 3 m) for a site in downtown Charleston, South Carolina. The material index (I_D), dilatometer modulus (E_D), corrected tip resistance (q_t) and sleeve friction (f_s) within the CMF are relatively uniform at values of 0.2 to 0.4, 150 to 200 bar, 3 to 5 MPa and 20 to 50 kPa, respectively. As shown in Figure 3, occasionally seams of increasing sand content in the CMF are encountered as observed at depths of 27 m and 33 m. These increased sand content seams typically increase the measurements of E_D and q_t.

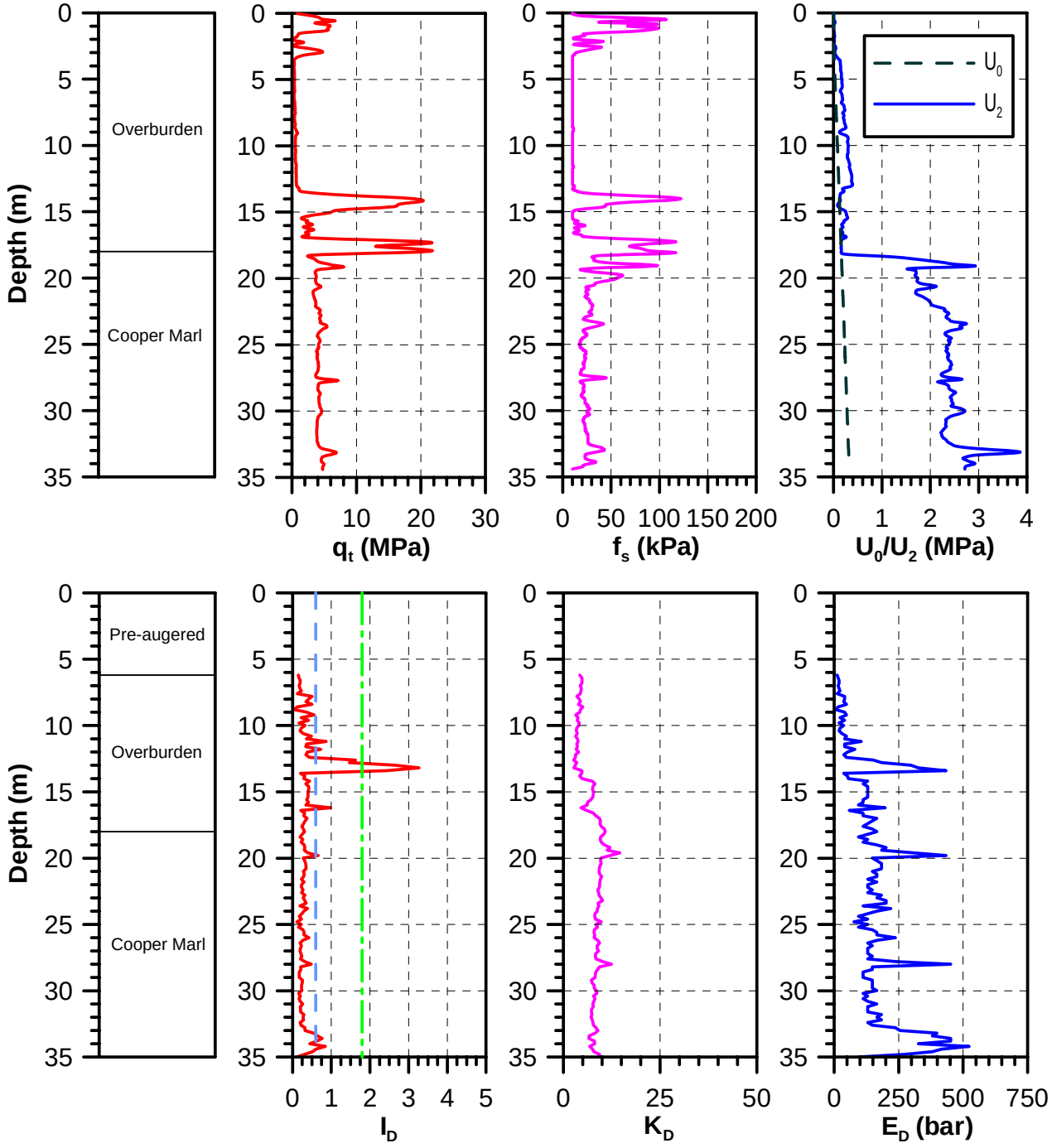

Figure 3. Representative soil profile from CPTU and DMT from downtown Charleston, SC site.

Given the noticeable increase in U_2 to delineate the CMF and the lack of a comparable parameter for the DMT, the DMT is often used as a complementary means of insitu testing for deeper subsurface investigations. Therefore, the DMT is used less frequently by local engineers for deep foundation designs.

Although there in no unique feature (i.e. signature) that identifies the CMF in the three "intermediate" DMT parameters, it is evident that the parameters are as effective in characterizing the CMF as a uniform silty clay to clayey silt. The material index (I_D) for the CMF ranges between 0.2 and 0.4 identifies it as clay to silty clay, which deviates from the typical laboratory classification based on the index properties. The original classification system by Marchetti (1980) was based on experience from normal soils instead of calcareous soils. It is very likely the CMF behaves more like clay to silty clay due to the cementation between the silt particles of the marl. Therefore, the CMF behaves more like a clay than silt and since the identification of the soil type from the DMT material index is based on soil behavior rather than the index properties, the DMT classification shows how the soil behaves insitu. The horizontal stress index (K_D) of the CMF ranges between 6 and 10 and demonstrates a modest decreasing trend versus the embedment depth.

4 O-CELL TESTING ON A DRILLED SHAFT

For a parking garage project in Charleston, SC, DMT and CPTu tests were predominantly used for the geotechnical exploration. Given the high structural loadings, the structure was founded on drilled shafts embedded within the CMF, which was located approximately 6 m below the existing ground surface. Figure 4 presents the location of the project relative to the downtown Charleston, SC area.

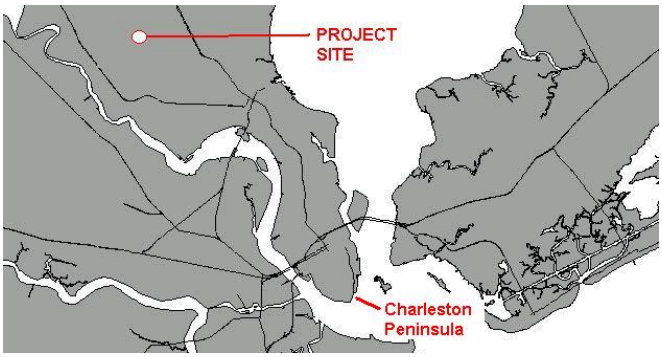

Figure 4. Drilled Shaft Testing Site relative to Charleston.

To verify the design and production procedures, a test drilled shaft was installed at a non-production location. The test shaft had a nominal diameter of approximately 1.4 m and a total length of 10 m. The test shaft was embedded 5 m into the CMF. The shaft was constructed such that the overburden soils above the CMF were not in contact with the shaft. An Osterberg Load Cell (i.e. O-Cell) was installed at the base of the shaft. Refer to Osterberg (1995) for additional details of the O-Cell. DMT and CPTu results adjacent to the test drilled shaft are presented in Figure 5.

Nine days after concrete placement, static load testing was conducted using the O-Cell. During the test, load was applied to the shaft stepwise through a hydraulic pump and was maintained at the load level for a minimum of 8 minutes before a next step load was added. Each load step was uniformly set at 177 kN. When the total load reached approximately 2.8 MN, the test shaft was pushed upward approximately 76.2 mm, which was considered a sign of side friction failure. At the time, the end bearing of the shaft had a downward displacement of approximately 8.6 mm. The results of the static load testing using the O-Cell are presented in Figure 6.

The side friction from the O-Cell static load testing was determined by the following formula:

$$Q_s = f_s \cdot A_s \qquad (1)$$

where Q_s is the side friction capacity around the shaft, f_s is the side friction along the shaft, and A_s is the contact area between the shaft and its surrounding soils. For Q_s = 2.8 MN and A_s = 22 m² (based on a shaft diameter of 1.4 m in the CMF), f_s was determined to be 127 kPa. It was therefore concluded that design side friction of 127 kPa can be used for production shafts for the CMF on this site. This result agrees closely with typical values for skin friction in the CMF for drilled shafts based on local experience (e.g., Wagoner et al., 1984).

The results of the DMT and CPTu were analyzed to evaluate the use of undrained shear strength values from these tests in determining the design skin friction within the CMF. These calculated CMF skin friction values were then compared to the results of the O-Cell test.

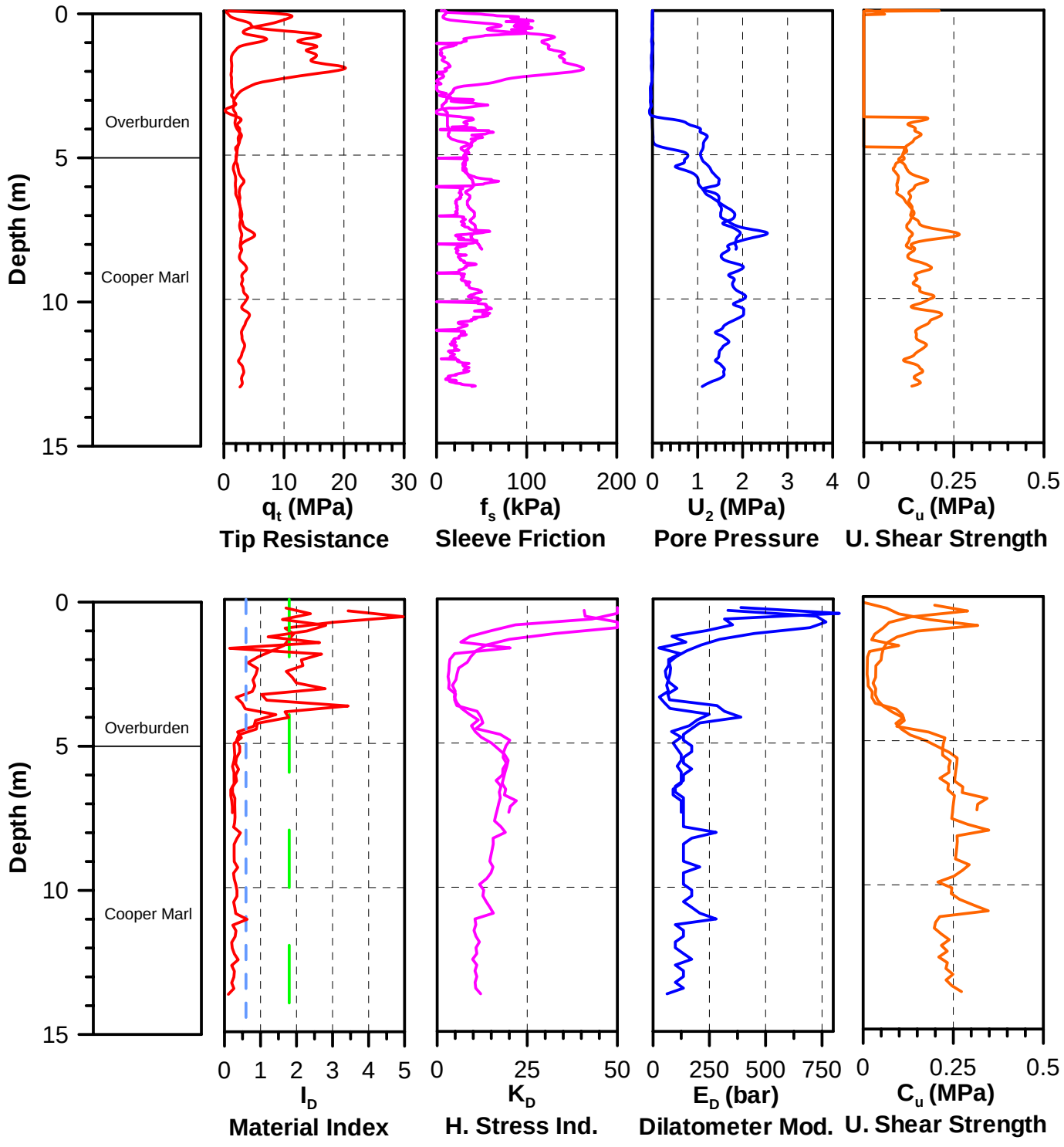

Figure 5. CPTu and DMT adjacent to the test shaft location

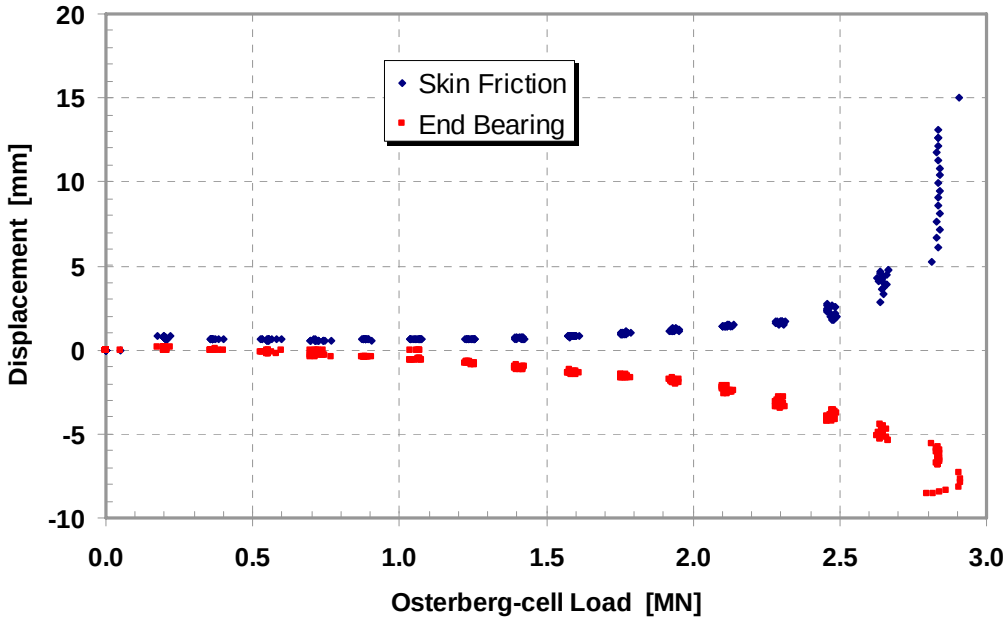

Figure 6. Osterberg-cell test results showing the shaft side and end displacement versus the applied load.

Correlations between CPTu results and soil strength parameters have been well established for common soils, whereas there is little information available for the fine-grained calcareous soils (Lunne et al., 1997). A correlation between the undrained shear strength and cone tip resistance from Beringen et al. (1982) for calcareous clays is presented in the following equation:

$$C_{u\_CPT} = \frac{q_c}{N_k} \qquad (2)$$

where q_c is the uncorrected cone tip resistance and N_k is a regression coefficient between 15 and 20 based on study of offshore Bombay and North Sea clays. In this study, N_k was determined to be 15 based on the authors' local experience and the corrected tip resistance (q_t) was used in place of the uncorrected tip resistance (q_c). The estimated undrained shear strength based on the cone tip resistance was between 0.1 to 0.2 MPa as shown in Figure 5.

From the DMT results presented in Figure 5, it is evident that the CMF has a uniform material index (I_D) between 0.1 and 0.6 and therefore is expected to behave as a clay. The horizontal stress index (K_D) is in a range between 10 and 20, which has a decreasing trend with the embedment depth. In addition, the dilatometer modulus was calculated to be approximately 100 to 120 bars, except for the values distorted by denser sand seams. These three "intermediate" DMT parameters indicate that the CMF is a lightly cemented calcareous soil that should still be characterized as a normal soil without significant deviation. However, it is noted by the authors of this paper that most of the available empirical formula for calculating DMT parameters are based on general cohesive soils without previous verification for use on the cemented materials such as calcareous soils. The undrained shear strength is interpreted by using the horizontal stress index, K_D, in the following formula proposed by Marchetti (1980):

$$C_{u\_DMT} = 0.22\sigma'_{v0}(0.5K_D)^{1.25} \qquad (3)$$

where σ'_{v0} is effective stress. The undrained shear strength of the CMF is between 0.2 and 0.3 MPa as shown in Figure 5.

The data indicates that the estimated undrained shear strength of the CMF from the DMT is approximately 50% higher than that from the CPTu. Although the undrained shear strength from the DMT compares better to the averages of the reviewed laboratory results as shown in Table 1, it is difficult by large to claim a better estimate regarding the uncertainties of each individual correlation.

Poulos (1999) proposed a correlation between the unconfined compressive strength and skin friction for moderately to well-cemented calcareous sediments as Equation (4) below:

$$f_s = A(q_u)^{0.5} \text{ kPa} \qquad (4)$$

where q_u is the unconfined compressive strength in MPa and A is 200. The unconfined compressive strengths from CPTu and DMT are determined to be between 0.2 to 0.4 and 0.4 to 0.6 MPa, respectively. By using Eq. 4, the side frictions from CPTu and DMT are estimated to be approximately 89 to 126 kPa and 126 to 155 kPa, respectively. When these estimated side frictions are compared with the O-Cell test result, it appears that the estimate from the DMT is closer to the side friction of 127 kPa determined from the O-Cell test.

5 CONCLUSIONS – RECCOMENDATIONS

Insitu testing including Flat Blade Dilatometer Testing (DMT) and Piezocone Penetration Testing (CPTu) was primarily used to characterize the geotechnical behavior of a calcareous soil formation in the Greater Charleston, SC area. The calcareous soil investigated during the study was a young lightly cemented clayey silt, which is known locally as the Cooper Marl Formation (CMF). Previous testing experience in this formation has shown that it is a relatively uniform soil deposit. Typical material index (I_D), dilatometer modulus (E_D), and horizontal stress index (K_D), corrected tip resistance (q_t), sleeve friction (f_s), and penetration pore pressure behind the cone tip (U_2) were summarized for the DMT and CPTu, respectively. Due to the difficulty and uncertainty in characterizing the side friction from calcareous soils, Osterberg-Cell test results from a test drilled shaft were used to improve the existing understanding of the CMF behavior for engineering applications.

Our study concluded that design side friction of 127 kPa between the marl and drilled shaft can be established. This result agrees closely with typical values for skin friction in the CMF for drilled shafts based on local experience. When these estimated side frictions from CPTu and DMT are compared with the O-Cell test result, it appears that the estimate from DMT is closer to the estimated side friction from the O-Cell test.

ACKNOWLEDGEMENT

The authors thank WPC, Inc. for providing the raw data for this study. However, the opinions and conclusions presented herein are those of the authors and do not necessarily reflect the views of WPC, Inc. The authors are also grateful to the anonymous reviewers' comments that help improve the quality of the paper.

REFERENCES

ASTM D2487, (2000). Standard Practice for Classification of Soils for Engineering Purposes (Unified Soil Classification System), ASTM International.

Beringen, F.L., H.J., Kolk, and H.J. Windle, (1982). Cone Penetration and Laboratory Testing in Marine Calcareous Sediments. Geotechnical Properties, Behavior and Performance of Calcareous Soils, ASTM Special technical publication, STP 777, 179-209.

Camp, W.M., III. (2004). Drilled and Driven Foundation Behavior in a Calcareous Clay, GeoSupport 2004, Drilled Shafts, Micropiling, Deep Mixing, Remedial Methods, and Specialty Foundation Systems (GSP No. 124)

Jewell, R.J. and M.S. Khorshid, (1999). A Historical Prespective, 1988 to 1999. Engineering for Calcareous Sediments, Proceedings of the Second International Conference on Engineering for Calcareous Sediments, Bahrain. Volume 2, p305-312.

Klecan, W.F., R.L. Horner, and M.J. Robison. (2001). Tunneling in the Cooper Marl of Charleston, South Carolina. Proceeding of Rapid Excavation and Tunneling Conference, San Diego, CA.

Lunne, T., P.K. Robertson, and J.J.M. Powell, (1997). Cone Penetration Testing in Geotechnical Practice, E&FN Spon, London.

Marchetti, S. (1980). In Situ Tests by Flat Dilatometer, ASCE Journal of Geotechnical Engineering Division, Vol. 106, No. GT3, 299-321.

Meng, J., E.L. Hajduk, and W.B. Wright. (2005). Geotechnical Review of Back River Tunnel, WPC Report CHS-05-409.

Osterberg, J.O., (1995). "The Osterberg Cell for Load Testing Drilled Shafts and Driven Piles", U.S. Department of Transportation, Federal Highway Administration, Publication No. FHWA-SA-94-035.

Poulos, H.G. (1999). Some Aspects of Pile Skin Friction in Calcareous Sediments, Engineering for Calcareous Sediments, Proceedings of the Second International Conference on Engineering for Calcareous Sediments, Bahrain. Volume 2, p457-471.

Wagoner, L., Calsing, R., and W.B. Wright, (1984). Test Pile Program at North Charleston Test Site, I-526 Bridges, North Charleston, South Carolina, Soil & Material Engineers, Inc., 061-83-020D.

DMT-predicted vs observed settlements: a review of the available experience

Monaco P., Totani G. & Calabrese M.
University of L'Aquila, Italy

Keywords: DMT, settlements, shallow foundations, operative modulus

ABSTRACT: This paper presents a compilation of documented case histories to include comparisons of DMT-predicted vs observed settlements, to review the available experience on the use of DMT for settlement calculations and to evaluate the accuracy of settlement predictions based on DMT. The available data indicate that, in general, the constrained modulus obtained by DMT (M_{DMT}) can be considered a reasonable "operative modulus" (relevant to foundations in "working conditions") for settlement predictions based on the traditional linear elastic approach. Attention is also given to the determination of the strain range appropriate to M_{DMT}, in view of the possible use of M_{DMT} for settlement predictions based on non linear methods by taking into account the decay of soil stiffness with strain level.

1 INTRODUCTION

Predicting settlements of shallow foundations is probably the No. 1 application of the DMT, especially in sands, where undisturbed sampling and estimating compressibility are particularly difficult.

This paper presents a compilation of documented case histories (available to the writers) including comparisons of DMT-calculated vs observed settlements, in order to evaluate the accuracy of settlement predictions based on DMT. The database includes several contributions, ranging from well-documented cases to semi-qualitative assessments of DMT-predicted vs observed behavior or simple comparisons between moduli/settlements obtained by DMT and by other methods. The data are critically reviewed and summarized.

The available experience, reviewed in this paper, indicates, in general, satisfactory agreement between DMT-predicted and observed settlements. In most cases the constrained modulus obtained by DMT (M_{DMT}) proved to be a reasonable "operative modulus" (relevant to foundations in "working conditions") for settlement predictions based on the traditional linear elasticity approach.

2 CONSTRAINED MODULUS *M* FROM DMT

The most significant stiffness parameter for settlement analyses obtained from DMT is the constrained modulus M (often designated as M_{DMT}), defined as the vertical drained confined (1-D) tangent modulus at σ'_{vo} (same as $E_{oed} = 1/m_v$ obtained by oedometer).

M_{DMT} is obtained by applying to the dilatometer modulus $E_D = 34.7\,(p_1 - p_0)$ – "intermediate" modulus derived from the DMT readings p_0 and p_1 by simple theory of elasticity – the correction factor R_M, according to the expression $M_{DMT} = R_M\, E_D$. The equations defining R_M as a function of the material index I_D and the horizontal stress index K_D were established by Marchetti (1980). $R_M = f\,(I_D, K_D)$ is not a unique proportionality constant relating M_{DMT} to E_D. The value of R_M varies mostly in the range 1 to 3 and increases with K_D (major influence).

The reasons for applying the correction R_M to E_D are listed in TC16 (2001). In general, the "uncorrected" modulus E_D should not be used as such in deformation analyses, but only in combination with I_D, K_D by use of M_{DMT}, primarily because E_D lacks information on stress history and lateral stresses, reflected to some extent by K_D. The necessity of stress history for a realistic assessment of settlements has been emphasized by many researchers (e.g. Leonards & Frost 1988, Massarsch 1994).

M_{DMT} is to be used in the same way as if it was obtained by oedometer and introduced in one of the available procedures for calculating settlements. If required, the Young's modulus E (not to be confused with the dilatometer modulus E_D) can be derived from M_{DMT} using the theory of elasticity, that, e.g. for a Poisson's ratio $\nu = 0.2$, provides $E = 0.9\,M$,

BACK

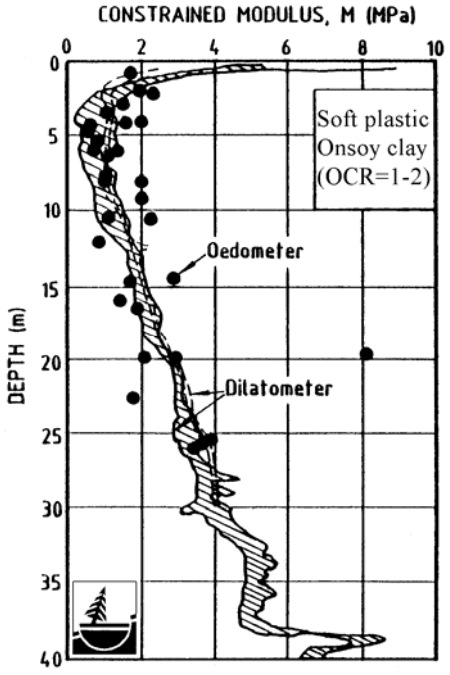

Fig. 1. Comparison between M determined by DMT and by high quality oedometers, Onsøy clay, Norway (Lacasse 1986)

a factor not very far from 1. (Indeed M and E are often used interchangeably in view of the involved approximation).

Experience has shown that M_{DMT} is highly reproducible and in most sites variable in the range 0.4 to 400 MPa. Comparisons both in terms of M_{DMT} vs reference M (e.g. M from high quality oedometers, see example in Fig. 1, Lacasse 1986) and in terms of predicted vs measured settlements have shown that, in general, M_{DMT} is reasonably accurate and dependable for everyday design practice.

3 PREDICTING SETTLEMENTS OF SHALLOW FOUNDATIONS BY DMT

Settlements of shallow foundations using DMT are generally calculated by means of the traditional linear elastic approach (1-D or 3-D formulae), with stress increments $\Delta\sigma$ calculated by elasticity theory (Boussinesq) and soil moduli determined from DMT (constrained modulus M_{DMT} or Young's modulus E derived from M_{DMT} via elasticity theory). This approach, being based on linear elasticity, provides a settlement proportional to the load and is unable to provide non linear predictions. The calculated settlement is meant to be the settlement in "working conditions", i.e. for a safety factor Fs ≈ 2.5 to 3.5.

Marchetti (1997) (see also TC16 2001) recommended to calculate settlements of shallow foundations by DMT by means of the classic 1-D method:

$$S_{1-DMT} = \sum \frac{\Delta\sigma_v}{M_{DMT}} \Delta z \qquad (1)$$

with $\Delta\sigma_v$ calculated e.g. by Boussinesq (Fig. 2).

Settlements in sand are generally calculated using the 1-D formula (large rafts) or the 3-D formula (small isolated footings). However, Marchetti (1991) observed that, since the 1-D and the 3-D formulae give generally similar answers (in most cases the 1-D settlements are within 10 % of the 3-D calculated settlements), it appears preferable to use the 1-D formula in all cases, as being simpler and "engineer independent" (no need of subjective guesses of ν or horizontal stresses as required by the 3-D formula). On the other hand, Burland et al. (1977) had observed that errors introduced by simple classical methods are small compared with errors in deformation parameters. Hence, the emphasis should be on the accurate determination of simple parameters, such as the one-dimensional compressibility coupled with simple calculations. Similarly, Poulos et al. (2001) emphasized that simple elasticity-based methods appear capable of providing reasonable estimates of settlements, and the key to success lies more in the appropriate choice of soil moduli than in the details of the method of analysis used.

The 1-D method (Eq. 1) is also used for predicting settlements in clay. It should be noted that the calculated settlement is the primary settlement (i.e. does not include immediate and secondary), and M_{DMT} is to be treated as the average E_{oed} derived from the oedometer curve in the expected stress range.

As noted by Marchetti (1997), in some highly structured clays, whose oedometer curves exhibit a sharp break and a dramatic reduction in slope across the preconsolidation pressure p'_c, M_{DMT} could be an inadequate average if the loading straddles p'_c. However in many common clays (and probably in most sands) the M fluctuation across p'_c is mild, and M_{DMT} can be considered an adequate average modulus.

$S_{1\text{-}DMT}$ calculated by Eq. 1 should still be corrected for rigidity, depth, Skempton-Bjerrum correction. In 3-D problems in OC clays the Skempton-Bjerrum correction is often in the range 0.2 to 0.5. However, considering that (a) the application of the Skempton-Bjerrum correction is equivalent to

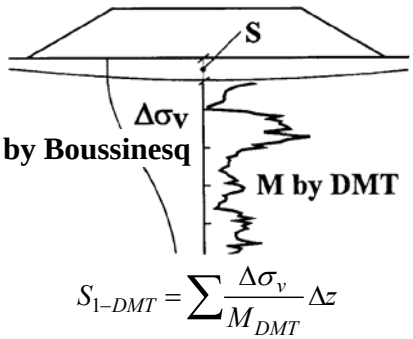

Fig. 2. Recommended method for settlement calculation using DMT (Marchetti 1997, TC16 2001)

reducing $S_{1\text{-}DMT}$ by a factor 2 to 5, and (b) in OC clays "the modulus from even good oedometers may be 2 to 5 times smaller than the in situ modulus (Terzaghi & Peck 1967)", Marchetti (1997) observed that these two factors approximately cancel out, and suggested to adopt as primary settlement (even in 3-D problems in OC clays) directly $S_{1\text{-}DMT}$ from Eq. 1, without the Skempton-Bjerrum correction (while adopting, if applicable, the rigidity and depth corrections, typically ≈ 0.8 to 1).

Methods for settlement calculations using DMT had been presented by other Authors. Schmertmann (1986) suggested to calculate settlements using the classic 1-D method, assuming $M = M_{DMT}$ (Ordinary Method). (This method coincides, in practice, with the method recommended by Marchetti 1997). Schmertmann (1986) also introduced a procedure (Special Method) for adjusting M_{DMT} (1-D tangent modulus at σ'_{vo}) with varying effective vertical stress during loading, in the virgin compression or recompression range. However, Schmertmann (1986) observed that the Ordinary Method, with no adjustment of M_{DMT}, is adequate in most cases.

Leonards & Frost (1988) proposed a procedure for estimating settlements of footings on granular soils that takes into account the effects of overconsolidation on compressibility. The procedure uses a combination of DMT and CPT results to identify the preconsolidation pressure, while soil moduli (E or M) are obtained from DMT. However, the method by Leonards & Frost (1988) is less used than the other mentioned DMT-based methods.

4 COMPARISON OF DMT-CALCULATED VS OBSERVED SETTLEMENTS

This section presents a compilation of documented case histories (available to the writers) including comparisons of DMT-calculated vs observed settlements. The database includes both Class-A and Class-C predictions. Contributions by various authors (listed in chronological order) range from well-documented cases, with detailed description of soil properties, foundation characteristics and measurements, to semi-qualitative assessments of DMT-predicted vs observed behavior, with no quantitative data, or simple comparisons between moduli/settlements obtained by DMT and by other methods.

Lacasse & Lunne (1986)

Lacasse & Lunne (1986) report very good agreement between constrained moduli obtained from DMT and moduli backfigured from measured settlements of silos and determined from screw plate and cone penetration tests in Drammen sand (Norway), a 40 m deposit of medium to medium coarse loose sand with occasional silty and organic layers (Fig. 3).

Schmertmann (1986)

Schmertmann (1986) reports 16 case histories at various locations and for various soil types, including sands, silts, clays and organic soils, with measured settlements ranging from 3 to 2850 mm (Table 1). In most of the cases settlements from DMT were calculated using the Ordinary 1-D Method. The average ratio DMT-calculated/observed settlement was 1.18, with the value of the ratio mostly in the range ≈ 0.7 to 1.3 and a standard deviation of 0.38.

Hayes (1990)

Fig. 4 by Hayes (1990), including the datapoints by Schmertmann (1986) in Table 1 and additional datapoints, shows a remarkably good agreement between observed and DMT-calculated settlements for a wide settlement range.

Dumas (1992)

Dumas (1992) reports good agreement between settlements calculated by pressuremeter (PMT) and DMT in a silty-sandy soil in Quebec, Canada. However, Dumas (1992) notes that the time for PMT testing was about 4 times the time for DMT testing. Similar remarks have been expressed by other authors. Sawada & Sugawara (1995) observed that the self-boring pressuremeter (SBPM) and the DMT are both valuable for estimating soil parameters in sands, but the SBPM is much more time-consuming and too expensive. Schnaid et al. (2000) compared parameters from SBPM and DMT in a granite

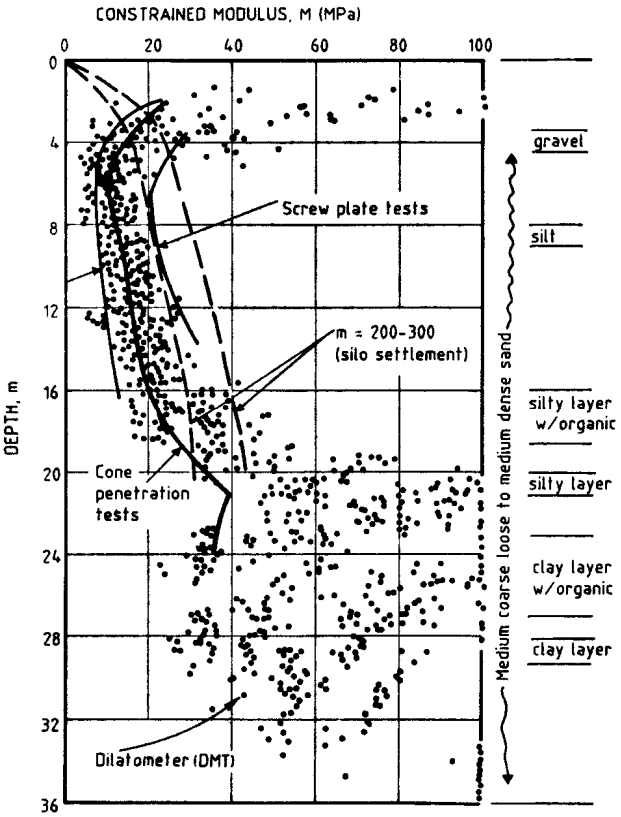

Fig. 3. Comparison of constrained moduli M from DMT and from other methods in Drammen sand (Lacasse & Lunne 1986)

Table 1 – Comparison of DMT-calculated vs measured settlements from 16 case histories (Schmertmann 1986)

No.	Location	Structure	Compressible soil	Settlement (mm)			Ratio DMT/Measured Settlement
				DMT	**	Measured	
1	Tampa	Bridge pier	Highly OC clay	*25	b, d	15	1.67
2	Jacksonville	Power plant (3 structures)	Compacted sand	*15	b, o	14	1.07
3	Lynn Haven	Factory	Peaty sand	188	a	185	1.02
4	British Columbia	Test embankment	Peat & organic soils	2030	a	2850	0.71
5 a	Fredricton	Surcharge	Sand	*11	a	15	0.73
5 b	"	3' plate load test	Sand	*22	a	28	0.79
5 c	"	Building (raft foundation)	Quick clayey silt	*78	a	35	2.23
6 a	Ontario	Road embankment	Peat	*300	a, o	275	1.09
6 b	"	Building	Peat	*262	a, o	270	0.97
7	Miami	4' plate load test	Peat	93	b	71	1.31
8 a	Peterborough	Apartment building	Sand & silt	*58	a, o	48	1.21
8 b	"	Factory	Sand & silt	*20	a, o	17	1.18
9	Peterborough	Water tank	Silty clay	*30	b, o	31	0.97
10 a	Linkoping	2×3 m plate	Silty sand	*9	a, o	6.7	1.34
10 b	"	1.1×1.3 m plate	Silty sand	*4	a, o	3	1.33
11	Sunne	House	Silt & sand	*10	b, o	8	1.25

* Ordinary Method used (1-D settlement, no adjustment of M for vertical effective stress during loading)

** b Settlements calculated before the event
a Settlements calculated after the event
o Settlements calculated by other than the Author
d Dilatometer advanced by driving with SPT hammer

saprolite (Kowloon Bay, Hong Kong) and concluded that the DMT proved to be a reliable tool that yielded good soil parameters at a fraction of the cost of other tests.

Woodward & McIntosh (1993)

Woodward & McIntosh (1993) report the case of a 4-story steel-framed office building in Jacksonville, Florida, supported on a shallow foundation. The soil was made by an upper ≈ 3-4 m thick layer of loose to firm clean sand overlying a ≈ 2-6 m thick layer of compressible very loose silty fine sand (N_{SPT} = 0 to 5). Total settlements (up to 5 cm) and differential settlements (up to 2.5 cm) estimated using SPT data were considered intolerable. DMT tests were then performed to refine settlement estimates. Total and differential settlements re-evaluated using DMT data (up to 3.2 cm and 1.9 cm, respectively) were considered acceptable to the structural engineer. Settlements measured during construction were slightly less than predicted by DMT, in general with reasonably good agreement. Use of the DMT at this site enabled the structure to be constructed on a conventional shallow foundation system, avoiding costly and time consuming soil improvement techniques.

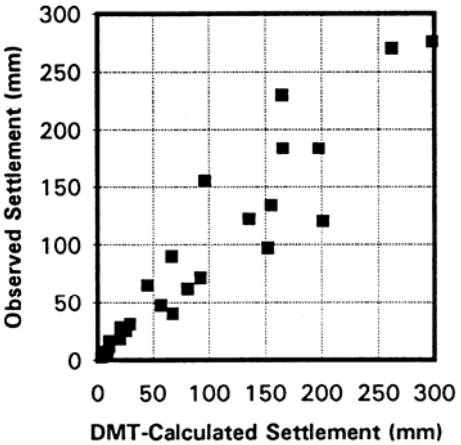

Fig. 4. Observed vs DMT-calculated settlements (Hayes 1990)

Skiles & Townsend (1994)

Skiles & Townsend (1994) report comparisons of settlements predicted by DMT and measured in 11 load tests conducted in a controlled test pit filled with a uniformly graded subangular sand. The load tests and the DMT tests were conducted at four separate times, corresponding to different densities of the sand. Square concrete footings of various sizes (12, 18, 24 and 36 in.) were pushed into the sand and the full load-settlements curves were recorded and compared to the predicted settlements at the allowable bearing capacity and near failure. Settlements predicted by DMT were generally in good agreement with measured settlements at "working loads" of about 1/3 of the ultimate bearing capacity (Table 2). The ratio DMT-predicted/measured settlement was 1.87 on average, with values mostly in the range ≈ 1 to 2.5. The predictions appeared more conservative for low sand density and small footing size. A trend towards unconservative predictions was noted as the footing size and the sand density increased.

Spread Footing Prediction Symposium at Texas A&M University (1994)

A well-known documented case is the Spread Footing Prediction Symposium held in June 1994 at Texas A&M University, as part of the ASCE Conference Settlement '94 (ASCE, Briaud & Gibbens 1994). Five square footings, ranging in size from 1 to 3 m, were constructed at the Texas A&M University test site. The soil profile at this site consists of 11 m of medium dense (D_R = 50-60 %) silty fine sand underlain by a very hard clay layer.

Table 2 – Comparison of settlements predicted by DMT (using Schmertmann's Ordinary Method) and measured at allowable bearing capacity in 11 load tests on square footings in sand (modified from Skiles & Townsend 1994)

Series	Sand density	Footing size (m)	Allowable bearing capacity (kPa)	Settlement (mm)		Ratio DMT/Measured Settlement
				DMT	Measured	
Sept 1990	very loose	0.61	35	18.3	3.3	5.54
		0.91	53	40.4	30.2	1.34
May 1991	medium dense	0.30	39	1.3	0.5	2.50
		0.46	59	2.5	1.0	2.50
		0.61	78	3.8	3.0	1.25
		0.91	117	6.6	6.4	1.04
June 1992	loose to medium dense	0.30	20	1.3	0.8	1.67
		0.46	30	2.8	1.3	2.20
		0.61	40	4.1	3.0	1.33
		0.91	61	7.9	11.4	0.69
July 1992	heavily compacted	0.91	169	2.3	4.3	0.53

Based on the results of a large amount of laboratory and in situ tests (including DMT) carried out at the site, the predictors were asked to formulate a Class-A prediction of the load-settlement behavior of all the five footings.

Various predictors used DMT data for estimating Q_{25} (load measured in the load test curve at a settlement of 25 mm on the 30 minute load-settlement curve of each footing), using in general the methods by Schmertmann (1986) and by Leonards & Frost (1988). Fig. 5 shows the comparison of DMT-predicted vs measured values of Q_{25} for Footing 1 (North) of size 3×3 m. The average ratio DMT-predicted/measured Q_{25} for all the five footings was generally between ≈ 0.7 to 1.2, i.e. within ± 30 % from the measured value. (Note that the "benchmark" settlement S = 25 mm, for a footing size B = 1 to 3 m, corresponds to a ratio S/B = 0.8 to 2.5 %).

Subsequently Marchetti (1997) formulated a Class-C prediction using the 1-D method (Eq. 1). For the footing 3×3 m he calculated a load of 3519 kN to cause a "working conditions" settlement S = 0.5 % B, equal to 15 mm. For this load, $S_{observed}$ (Fig. 5) was 12 mm, while $S_{1\text{-}DMT}$ = 15 mm, with a DMT overprediction of +25 %. Similarly, for the footing 1.5×1.5 m the calculated load to cause the settlement S = 0.5 % B (7.5 mm) was 844 kN, while $S_{observed}$ = 6.5 mm, with a DMT overprediction of + 15 %.

Steiner (1994)

Steiner (1994) reports the case of a backfilled retaining wall of an avalanche protection gallery in the Swiss Alps, founded on a strip footing on loose silty-sandy soil. The observed settlements were substantially higher than anticipated based on soil borings. An additional boring was then drilled to detect the exact depth of the bedrock at the wall position and DMT tests were performed. Settlements re-evaluated using DMT moduli agreed well with monitored settlements of the wall.

Didaskalou (1999)

Didaskalou (1999) reports good agreement between DMT-predicted and observed settlements of the Hyatt Regency Hotel in Thessaloniki (Greece), supported on a shallow foundation on a very compressible silt. The maximum settlement predicted by DMT was 105 mm, while the settlement measured near the hotel inauguration (probably including some secondary) was ≈ 120 mm.

Failmezger et al. (1999)

Failmezger et al. (1999) present 5 case histories with comparisons of settlements predicted by DMT and by SPT. At Route 460 Bypass, Blacksburg, Virginia, SPT predicted 100 mm settlements, while DMT predicted 27 mm (confirmed by oedometer), leading to change in design and cost savings. Generally SPT overpredicted settlements (in one case by a factor 10).

Pelnik et al. (1999)

Pelnik et al. (1999) present examples of use of CPTU and DMT in the sedimentary soils in the

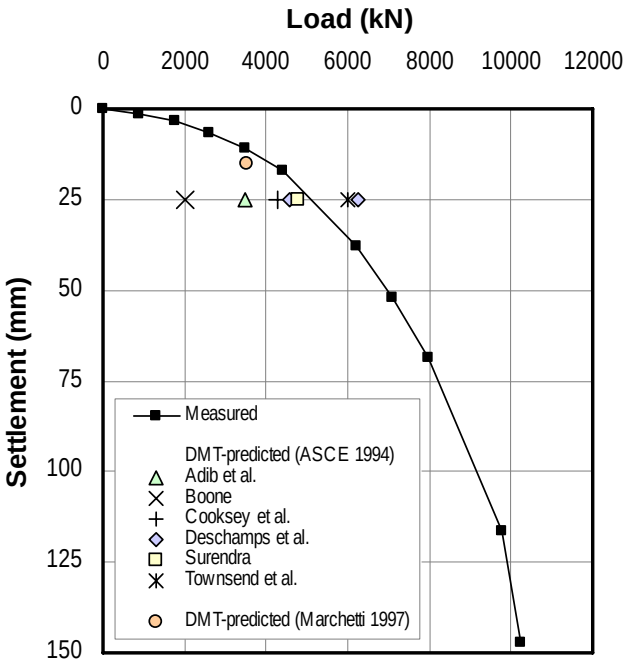

Fig. 5. ASCE Settlement '94 Spread Footing Prediction Symposium. Measured load-settlement curve for Footing 1 (3×3 m) vs values of load Q_{25} predicted by DMT by various Authors (ASCE 1994) and additional prediction by Marchetti (1997)

Atlantic Coastal Plain region of Virginia, with a subjective rating of the relative value of CPTU and DMT for several design applications in these soils. The DMT is rated as "excellent" for evaluating settlements in sands and soft clays. At Hoskins Creek (New bridge at US Route 17), a very soft NC clay site, Pelnik et al. (1999) report good agreement of M_{DMT} with oedometer moduli. Also, settlements estimated by DMT were in agreement with presumed settlements of the road leading to the existing bridge.

Tice & Knott (2000)

Tice & Knott (2000) describe the case of moving the Cape Hatteras Lighthouse about 900 m from its original location to protect it from a receding coastline. Tice & Knott (2000) found that DMT data provided reliable settlement estimates in the predominantly sandy soils along the path and at the final destination of the lighthouse.

Failmezger (2001)

Failmezger (2001), in a discussion on probability analysis of settlement predictions of footings in sand, analyzed the standard deviation of settlement predictions by SPT and DMT. According to Failmezger (2001), the overall standard deviation is a combination of three independent sources of uncertainty: model uncertainty, measurement noise (test repeatability) and spatial variability of the site. Various studies have indicated that the uncertainty from measurement noise for the SPT can be as high as 45-100 %, while the measurement noise for the DMT is much less (6%). Failmezger (2001) analyzed the different probability distributions and the test and analysis methods to determine their effects on the probability of unsatisfactory performance of exceeding a threshold settlement. Assuming the standard deviation from spatial variability equal to 20 % of the average settlement for both SPT and DMT, the standard deviations from measurement noise and model uncertainty from SPT were much larger than those from DMT. The overall standard deviation for the SPT was 86 % of the average value, as compared with only 29 % for the DMT. Failmezger (2001) questioned the value of using the SPT as a method to compute settlements altogether and concluded that, in view of the above high SPT variability, the engineer should select for design the best available test and analysis method and attempt to minimize model uncertainty and measurement noise, then focus on the spatial variability of the site, e.g. by use of probabilistic methods.

Marchetti et al. (2004)

Marchetti et al. (2004) present the comparison of DMT-predicted vs measured settlements under a full-scale instrumented test embankment (40 m diameter, 6.7 m height, applied load 104 kPa) at the research site of Treporti (Venice, Italy). The site, typical of the Venice lagoon, consists of highly

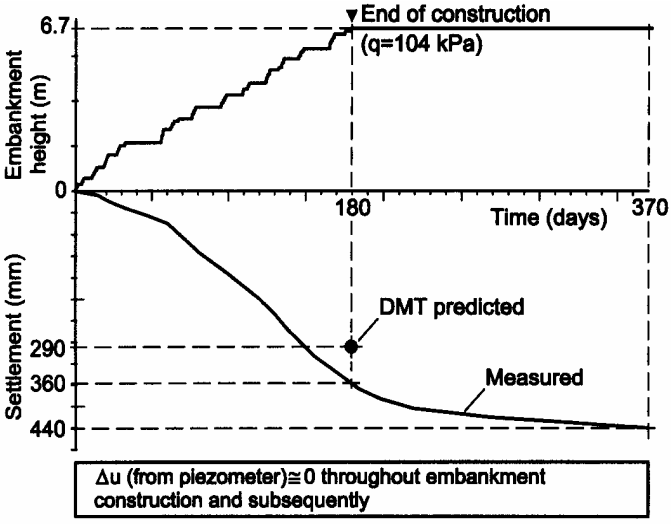

Fig. 6. DMT-predicted vs measured settlement under the center of Treporti test embankment (Marchetti et al. 2004)

stratified silts or silty clays and sands, remarkably heterogeneous even in the horizontal direction. Moduli M_{DMT} are highly variable, from ≈ 5 MPa in soft clay layers to ≈ 150 MPa in sand layers.

The total settlement measured under the center of the embankment at the end of construction (180 days) was ≈ 36 cm (Fig. 6). Significant additional settlements were measured after the end of construction (≈ 44 cm at 370 days), hence the 36 cm settlement measured at the end of construction presumably includes, besides immediate and primary, also a significant amount of secondary developed during construction (occurred essentially in drained conditions, as indicated by ≈ zero excess pore pressure measured by piezometers). The settlement predicted by M_{DMT} using the 1-D approach (Eq. 1), before the field measurements were available, was 29 cm net of secondary, i.e. 7 cm less (- 20 %) than the 36 cm measured (also including secondary during construction). Hence the settlement predicted by DMT (net of secondary) was in good agreement with the observed settlement.

Mayne (2005)

Mayne (2005) presents the case of a large mat foundation (104×18 m size, 1.1 m thickness) constructed to support a 13-story dormitory building on Piedmont residual silty soils in Atlanta, Georgia. The maximum expected settlement of the mat estimated prior to construction was 46 mm, while the building proceeded to deflect as much as 250 mm at the center and 100 to 140 mm at the corners near the end of construction. Mayne (2005) attributes such incorrect settlement prediction to an over-reliance on SPT data, coupled with a poor choice of the model for analysis and other bad judgments, and shows that simple elastic continuum solutions with input moduli derived from DMT tests (conducted by the independent engineering firm) and finite layer

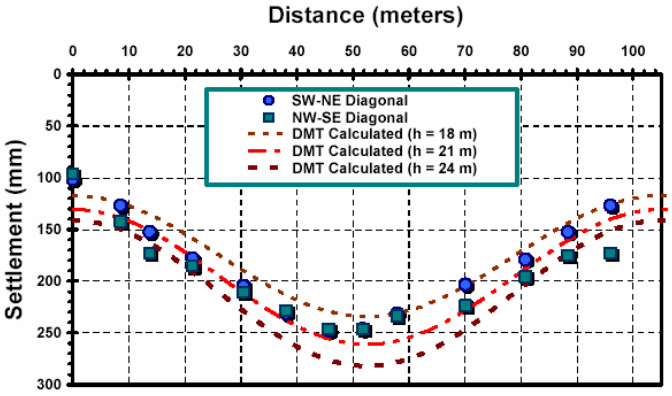

Fig. 7. Measured vs DMT-calculated settlement profiles along the diagonal axes of the mat foundation of a 13-story dormitory building in Atlanta, Georgia (Mayne 2005)

thicknesses are in excellent agreement with measured settlement profiles (Fig. 7). If carried out before, such calculations would have given essentially the correct answer and warned the designers of excessive displacements.

5 SUMMARY OF AVAILABLE EXPERIENCE ON DMT-CALCULATED VS OBSERVED SETTLEMENTS

Fig. 8 summarizes the available comparisons of DMT-calculated vs observed settlements. The over 40 datapoints in Fig. 8 are representative of the case histories previously described, limited to the cases reporting numerical values of DMT-calculated and measured settlements.

Fig. 8 shows that settlements predicted by DMT are generally in good agreement with observed settlements for a wide range of soil types (including sands, silts, clays and organic soils), settlements (from a few mm to over 300 mm) and footing sizes (from small footings to large rafts and embankments). The average ratio DMT-calculated/observed settlement for all the case histories summarized in Fig. 8 is ≈ 1.3. The band amplitude (ratio between maximum and minimum) of the datapoints in Fig. 8 is less than 2, i.e. the observed settlement is within ± 50 % from the DMT-predicted settlement.

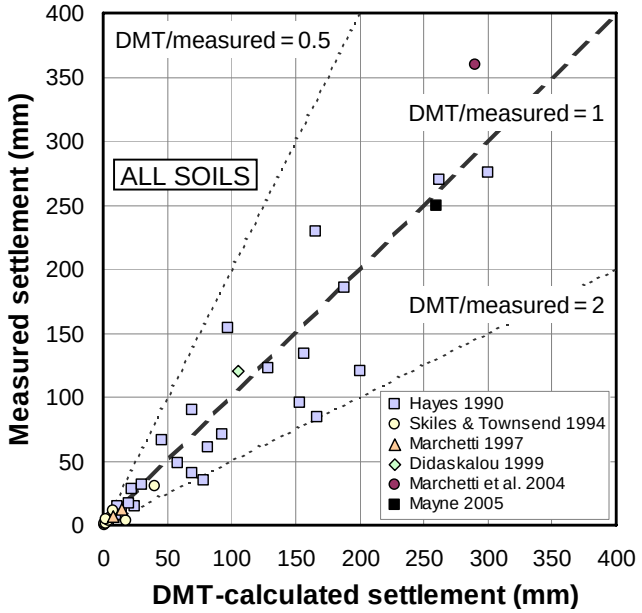

Fig. 8. Summary of available comparisons of DMT-predicted vs observed settlements

6 M_{DMT} AS "OPERATIVE MODULUS" AND POSSIBLE USE OF M_{DMT} FOR NON LINEAR SETTLEMENT PREDICTIONS

The global experience from several case histories reviewed in this paper indicates that M_{DMT} can be considered a reasonable "operative modulus", i.e. a modulus that, introduced into the linear elasticity theory formulae, provides reasonably accurate settlement predictions for foundations in "working conditions" (say for a safety factor Fs ≈ 2.5 to 3.5).

In the linear elasticity approach, soil moduli are assumed as constant (not dependent on variations in stress and strain level). Research currently in progress investigates the possible use of M_{DMT} for settlement predictions based on non linear methods taking into account the decay of soil stiffness with strain level. The objective is to develop methods for evaluating "in situ" the decay curves of soil stiffness with strain level (G-γ curves or similar). This approach should permit to bypass the effect of sample disturbance on G_0 and G-γ curves determined in the laboratory. In situ G-γ curves could be tentatively derived by use of the seismic dilatometer (SDMT), recently entered into current practice, by fitting "reference" laboratory curves through 2 points: (1) the initial shear modulus G_0 obtained from shear wave velocity V_S measurements, and (2) a modulus at "operative" strains, corresponding to M_{DMT} – provided the strain range appropriate to M_{DMT} is defined. This approach is expected to provide more realistic estimates compared to other methods proposed for deriving in situ G-γ curves (e.g. Mayne et al. 1999), since the second point for the curve-fitting (given the first point G_0) is not located "at failure", but in the range of "operative" strains (i.e. the strain range of "well designed foundations").

Yamashita et al. (2000) have shown that OCR significantly influences soil moduli mostly in the strain range ≈ 0.05 to 0.1 % (Fig. 9), where the ratio E_{OC}/E_{NC} (secant Young's moduli from triaxial tests on NC and OC sand specimens) was found as high as ≈ 4 to 7 (for K_0 consolidation), while at very small and at very large strains the ratio E_{OC}/E_{NC} is ≈ 1, i.e. moduli are much less influenced by OCR.

Yet, as it is well known, OCR has a strong influence on settlements. Hence G_0, scarcely sensitive to OCR, appears inadequate, if used alone, to correctly

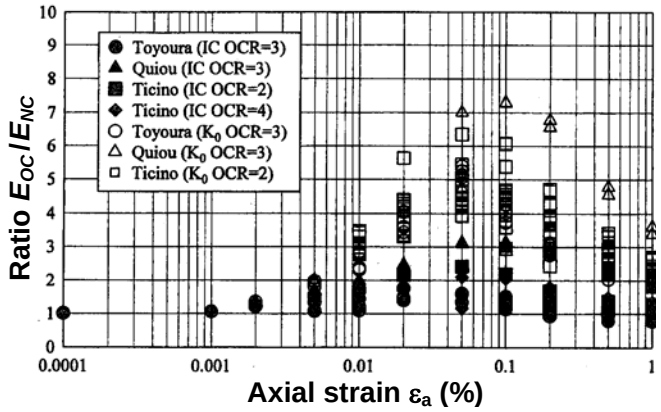

Fig. 9. Effect of OCR on *secant* Young's modulus from triaxial tests on NC and OC sand specimens (Yamashita et al. 2000)

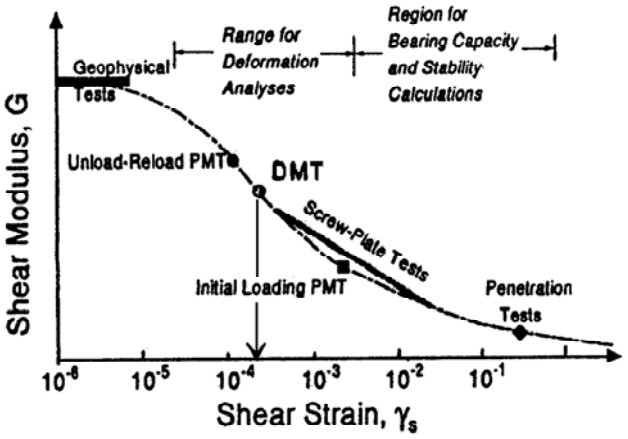

Fig. 10. Decay of shear modulus with strain level and possible strain range of moduli from various in situ tests (Mayne 2001)

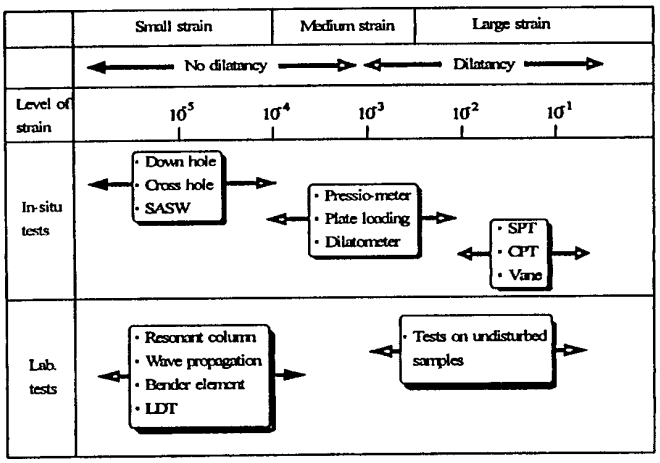

Fig. 11. Classification of methods of measurement of soil deformation characteristics according to the strain level involved (Ishihara 2001)

predict settlements.

In order to use M_{DMT} for locating the second point of the G-γ curve, it is necessary to know at least approximately the shear strain – i.e. the abscissa – corresponding to M_{DMT}. The following indications have been advanced so far.

Mayne (2001) observed that correlations, developed between some in situ tests (e.g. PMT, DMT) and performance monitored data of full-scale structures or reference laboratory values, provide a modulus "somewhere along the stress-strain-strength curve" (Fig. 10), generally at an "intermediate" level of strain (≈ 0.05-0.1% in Fig. 10). A similar indication is given in Fig. 11 (Ishihara 2001), where the DMT is classified within the group of methods of measurement of soil deformation characteristics involving an intermediate level of strain (0.01-1%).

In most of the cases reviewed in this paper M_{DMT} predicted well settlements for values of the ratio S/B (measured settlement/width of footing) mostly in the range ≈ 0.5-1%. This observation, supplemented by further investigations, could possibly help develop criteria for deriving in situ curves of decay of soil stiffness with strain level from SDMT, to be used for non linear settlement predictions. Such curves could be expressed e.g. in form of decay of Young's modulus E/E_0 vs foundation settlement to width ratio S/B (as proposed e.g. by Atkinson 2000).

7 CONCLUSIONS

Many researchers, practitioners and investigation firms have presented case histories comparing observed vs DMT-predicted settlements, reporting generally satisfactory agreement.

The available experience indicates that the constrained modulus M_{DMT} can be considered a reasonable "operative modulus", i.e. introduced into the traditional elasticity theory formulae predicts settlements with reasonably good accuracy for foundations in "working conditions" (say for a safety factor Fs ≈ 2.5 to 3.5).

The accuracy of settlement predictions by M_{DMT} is believed to be due mostly to the fact that M_{DMT} routinely takes into account overconsolidation and possible existence of high lateral stresses (incorporated via the stress history parameter K_D), that reduce considerably soil compressibility.

According to Poulos et al. (2001), methods for estimating footing settlements can be evaluated in terms of: (1) accuracy (ratio of calculated/measured settlement), (2) reliability (percentage of cases in which the calculated settlement was equal or greater than the measured settlement), and (3) ease of use (length of time required to apply the method). Based on the available data, the ability of the DMT to predict settlements proved in general quite satisfactory from all the above points of view.

REFERENCES

ASCE. 1994. Predicted and Measured Behavior of Five Spread Footings on Sand. *Proc. Spread Footing Prediction Symposium at ASCE Spec. Conf. Settlement '94, Texas A&M Univ., Edited by Briaud, J.L. & Gibbens, R.M. ASCE Geotech. Spec. Publ. No. 41.*

Atkinson, J.H. 2000. Non-linear soil stiffness in routine design. *Géotechnique,* 50, No. 5, 487-508.

Burland, J.B., Broms, B.B. & De Mello, V.F.B. 1977. Behavior of foundations and structures. *Proc. IX ICSMFE, Tokyo,* Vol. 2, 495-546.

Didaskalou, G. 1999. Personal communication to S. Marchetti.

Dumas, J.C. 1992. Personal communication to S. Marchetti.

Failmezger, R.A. 2001. Discussion to Duncan, J.M. 2000. "Factor of Safety and Reliability in Geotechnical Engineering" (in ASCE Jnl GGE, Vol. 126, No. 4). *ASCE Jnl GGE,* Vol. 127, No. 8, 703-704.

Failmezger, R.A., Rom, D. & Ziegler, S.B. 1999. SPT? A better approach to site characterization of residual soils using other in-situ tests. *Behavioral characteristics of residual soils, ASCE Geotech. Spec. Publ. No. 92,* 158-175.

Hayes, J.A. 1990. The Marchetti Dilatometer and Compressibility. *Seminar on In Situ Testing and Monitoring, Southern Ontario Section of Canad. Geotech. Society, Sept.,* 21 pp.

Ishihara K. 2001. Estimate of relative density from in-situ penetration tests. *Proc. Int. Conf. on In Situ Measurement of Soil Properties and Case Histories, Bali,* 17-26.

Lacasse, S. 1986. In Situ Site Investigation Techniques and Interpretation for Offshore Practice. *Norwegian Geotechnical Institute, Report 40019-28.*

Lacasse, S. & Lunne, T. 1986. Dilatometer Tests in Sand. *Proc. ASCE Spec. Conf. on Use of In Situ Tests in Geotechnical Engineering In Situ '86, Virginia Tech, Blacksburg. ASCE Geotech. Spec. Publ. No. 6,* 686-699.

Leonards, G.A. & Frost, J.D. 1988. Settlements of Shallow Foundations on Granular Soils. *ASCE Jnl GE,* Vol. 114, No. 7, 791-809.

Marchetti, S. 1980. In Situ Tests by Flat Dilatometer. *ASCE Jnl GED,* Vol. 106, GT3, 299-321.

Marchetti, S. 1991. Discussion to Leonards, G.A. & Frost, J.D. 1988. "Settlements of Shallow Foundations on Granular Soils" (in ASCE Jnl GE, Vol. 114, No. 7). *ASCE Jnl GE,* Vol. 117, No. 1, 174-179.

Marchetti, S. 1997. The Flat Dilatometer: Design Applications. *Keynote Lecture, Proc. 3rd Int. Geotech. Engineering Conference,* Cairo, 421-448.

Marchetti, S., Monaco, P., Calabrese, M. & Totani, G. 2004. DMT-predicted vs measured settlements under a full-scale instrumented embankment at Treporti (Venice, Italy). *Proc. 2nd Int. Conf. on Site Characterization ISC'2, Porto,* Vol. 2, 1511-1518.

Massarsch, K.R. 1994. Settlement Analysis of Compacted Granular Fill. *Proc. XIII ICSMFE, New Delhi,* Vol. 1, 325-328.

Mayne P.W. 2001. Stress-strain-strength-flow parameters from enhanced in-situ tests. *Proc. Int. Conf. on In Situ Measurement of Soil Properties and Case Histories, Bali,* 27-47.

Mayne, P.W. 2005. Unexpected but foreseeable mat settlements of Piedmont residuum. Int. Jnl of Geoengineering Case Histories, http://casehistories.geoengineer.org, Vol. 1, Issue 1, 5-17.

Mayne P.W., Schneider J.A. & Martin G.K. 1999. Small- and large-strain soil properties from seismic flat dilatometer tests. *Proc. 2nd Int. Symp. on Pre-Failure Deformation Characteristics of Geomaterials, Torino,* Vol. 1, 419-427.

Pelnik, T.W., III, Fromme, C.L., Gibbons, Y.R. & Failmezger, R.A. 1999. Foundation Design Applications of CPTU and DMT Tests in Atlantic Coastal Plain Virginia. *Transp. Res. Board, 78th Annual Meeting, Jan., Washington, D.C.*

Poulos, H.G., Carter, J.P. & Small, J.C. 2001. Foundations and retaining structures – Research and practice. *Proc. XV ICSMGE, Istanbul,* Vol. 4, 2527-2606.

Sawada, S. & Sugawara, N. 1995. Evaluation of densification of loose sand by SBP and DMT. *Proc. 4th Int. Symp. Pressuremeter and its New Avenues, Sherbrooke, Canada,* 101-107.

Schmertmann, J.H. 1986. Dilatometer to compute Foundation Settlement. *Proc. ASCE Spec. Conf. on Use of In Situ Tests in Geotechnical Engineering In Situ '86, Virginia Tech, Blacksburg. ASCE Geotech. Spec. Publ. No. 6,* 303-321.

Schnaid, F., Ortigao, J.A.R., Mántaras, F.M, Cunha, R.P. & MacGregor, I. 2000. Analysis of self-boring pressuremeter (SBPM) and Marchetti dilatometer (DMT) tests in granite saprolites. *Canad. Geotech. Jnl,* Vol. 37, 4, 796-810.

Skiles, D.L. & Townsend, F.C. 1994. Predicting Shallow Foundation Settlement in Sands from DMT. *Proc. ASCE Spec. Conf. Settlement '94, Texas A&M Univ., ASCE Geotech. Spec. Publ. No. 40,* Vol. 1, 132-142.

Steiner, W. 1994. Settlement Behavior of an Avalanche Protection Gallery Founded on Loose Sandy Silt. *Proc. ASCE Spec. Conf. Settlement '94, Texas A&M Univ., ASCE Geotech. Spec. Publ. No. 40,* Vol. 1, 207-221.

TC16 - Marchetti, S., Monaco, P., Totani, G. & Calabrese, M. 2001. The Flat Dilatometer Test (DMT) in Soil Investigations - A Report by the ISSMGE Committee TC16. *Proc. Int. Conf. on In Situ Measurement of Soil Properties and Case Histories, Bali,* 95-131.

Terzaghi, K. & Peck, R.B. 1967. Soil mechanics in engineering practice. 2nd Ed., John Wiley & Sons, New York.

Tice, J.A. & Knott, R.A. 2000. Geotechnical Planning, Design, and Construction for the Cape Hatteras Light Station Relocation. *Geo-Strata-Geo Institute of ASCE,* Vol. 3, No. 4, 18-23.

Woodward, M.B. & McIntosh, K.A. 1993. Case history: Shallow Foundation Settlement Prediction Using the Marchetti Dilatometer. *ASCE Annual Florida Section Meeting.*

Yamashita, S., Jamiolkowski, M. & Lo Presti, D.C.F. 2000. Stiffness nonlinearity of three sands. *ASCE Jnl GGE,* Vol. 126, No. 10, 929-938.

NEW TESTING DEVELOPMENTS (SEISMIC AND OTHER INSTRUMENTATION)

The Newcastle Dilatometer Testing in Pakistani Sandy Subsoils

A. Akbar
Professor, Civil Engineering Department, University of Engineering and Technology, Lahore Pakistan

H. Nawaz
Research Student, Civil Engineering Department, University of Engineering and Technology, Lahore

B.G. Clarke
Professor of Geotechnical Engineering, Newcastle University, UK

Keywords: dilatometer, sand, shear strength, stiffness

ABSTRACT: The Newcastle Flat Rigid Dilatometer (*NDMT*) is a new in-situ soil testing device developed in 2001 for direct measurement of the in-situ characteristics of soils such as strength, stiffness, deformation etc. It is quite simple and robust and produces repeatable calibration data with no hysteresis. The *NDMT* loads the soil with a relatively rigid piston of 3 mm thickness so that it can be used in all soils including those containing gravel. The *NDMT* rigid plate is instrumented so that pressure and displacement can be measured directly.

This paper is based on the *NDMT* testing in the typical alluvial deposits of the Punjab province of Pakistan which consist of silty sand/fine sand. In order to correlate the *NDMT* test results with those of other conventional methods, Standard Penetration Tests (SPTs) were carried out at locations close to the *NDMT* testing locations. The disturbed soil samples recovered in the split spoon sampler were used to determine the grain size distribution and direct shear strength parameters.

The *NDMT* indices viz. material index (I_D), dilatometer modulus (E_D), and horizontal stress index (K_D) have been evaluated from the corrected load – deformation curves of each *NDMT* test. Subsequently, new correlations for the dilatometer indices have been developed with conventional soil characteristics such as drained shear strength (ϕ') and elastic modulus (E) for the Punjab sandy subsoils.

1 INTRODUCTION

The evaluation of strength and deformation characteristics of soil deposits has always been an area of key interest for design engineers. A host of techniques have been developed, over the years, for representative sampling, laboratory testing and in-situ testing. While it is possible to sample all soils the quality of the samples depends on the type of soil and the sampling technique. This means that it is often difficult to obtain representative samples for laboratory testing. This is one reason that in situ tests are used.

Ever since the appearance of the first in situ test, the penetration test, engineers and scientists have continuously endeavored to improve the equipment, the test protocol and the interpretation to obtain more representative values of in-situ strength, stiffness and stress. This has led to an improvement in the analyses required for the design of foundations and cut slopes.

Like other engineering techniques used in the evaluation of geotechnical design parameters, intrusive in-situ testing does disturb the ground to some extent creating difficulties in interpreting tests to obtain intrinsic design parameters. This difficulty in the interpretation of test results is primarily due to the complex behaviour of soils, together with the lack of control and choice of the boundary conditions in any field test. Therefore the results of many in situ tests are interpreted using empirical correlations with results of laboratory tests.

One such test is the Marchetti dilatometer test. The original Marchetti dilatometer (*MDMT*) is a simple device that can be used to determine in-situ stress, stiffness and strength of a soil with some degree of confidence. However, the *MDMT* is not robust enough to test stony soils such as residual soils and glacial till, as the membrane can tear. It is for this reason that a new blade has been developed that can be used in a greater variety of soils. The new dilatometer, the *NDMT* has been found to be more robust than the *MDMT* as it has been used in a variety of difficult soils. Akbar (2001) presents the design of the *NDMT* together with in-situ testing procedures, data analysis techniques and comparison of the results with those from the *MDMT*.

This paper describes the results of testing the non-cohesive soils with the *NDMT* at a site near Jaranawala city of Pakistan to improve correlations

between the *NDMT* indices and soil properties and geotechnical design parameters.

2 THE NEWCASTLE FLAT DILATOMETER (*NDMT*)

The *NDMT* blade is shown as (i) in Fig. 1 where the piston that loads the soil during a test is shown as (ii). Fig. 2 shows the components in the piston assembly. The use of the wave spring washer (iii in Fig. 2) between the piston flange (ii) and the retaining ring (iv) keeps the piston flush with the blade until the piston is pressurized using dry N_2 gas and returns the piston to its at rest position when depressurized. Two O-rings are incorporated in the *NDMT* to keep the assembly air and water-tight. The applied gas pressure is recorded using a pressure transducer.

A Hall Effect Transducer (*HET*) is used to measure the displacement of the piston. The magnet is fixed at the center of moving piston while the *HET* is fixed to the body of the blade in front of the magnet. When the piston moves by internally pressurizing the blade, the *HET* produces a change in its output according to the flux intensity. This output is non-linear but non-hysteretic and a second-degree curve fits the data as shown in Fig. 3. Access to the connections between the *HET* and the cable is via steel cover plate (iii in Fig. 1). The output of the pressure transducer and the *HET* are read and recorded by a computer. The blade is either jacked or pushed to the test level.

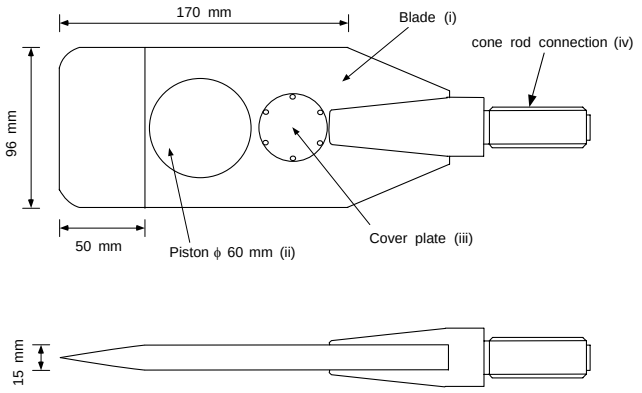

Figure 1 The Newcastle flat rigid dilatometer (*NDMT*)

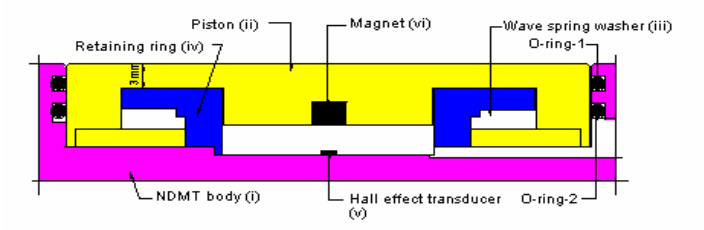

Figure 2 Piston assembly of the *NDMT*.

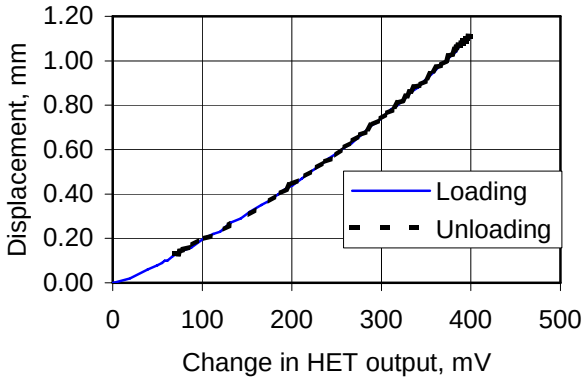

Figure 3 A typical data plot for the *HET* in the *NDMT*.

3 SITE OPERATIONS

The Newcastle dilatometer testing was carried out at a site near Jaranwala, district Faisalabad, Pakistan. The *NDMT* equipment was assembled on-site as shown in Figure 4. The system compliance calibration needed to correct for the pressure required to overcome the stiffness of the wave spring was carried out by increasing the gas pressure at a constant rate i.e. similar to that for the Marchetti *DMT*. Figure 5 shows a typical plot for system compliance calibration. The maximum pressure required to move the piston by 1.1 mm is less than 90 kPa. This is comparable with that required to inflate the *MDMT* membrane.

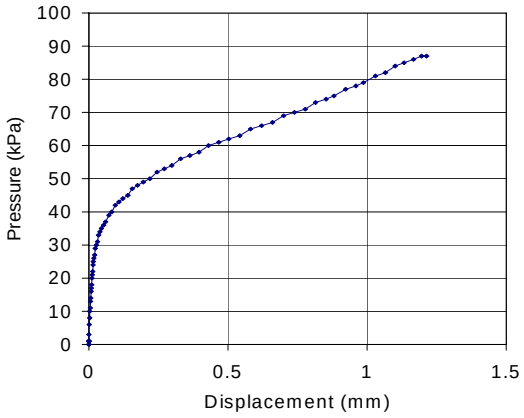

Figure 5 A typical calibration data plot for the *NDMT* system compliance

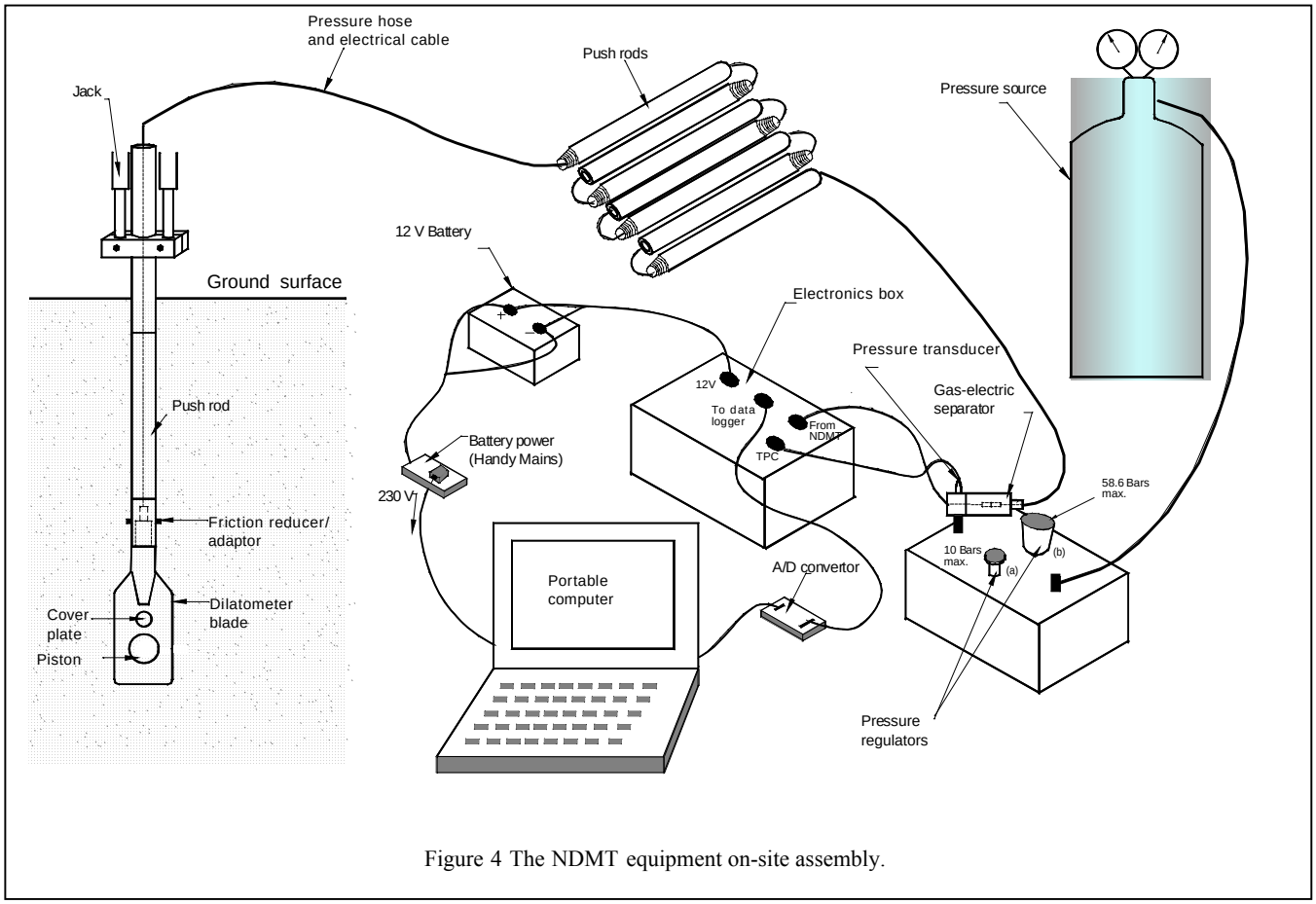

Figure 4 The NDMT equipment on-site assembly.

After the calibration, the probe was pushed into the ground using a hydraulic jack. The reaction force was obtained through a heavy-duty frame loaded with sand bags. During the testing, the pressure was applied through a needle valve pressure regulator. After attaining 1.1 mm movement of the piston, the pressure was vented off. Each test took between 1 and 3 minutes. No unload-reload cycles during tests were included in this study. At the end of testing at each location, the instrument was withdrawn and calibrated for system compliance. The calibrations before and after the in-situ testing were averaged. The in-situ pressure deformation curves were then corrected for system compliance

The *NDMT* tests were carried out at every 20 cm interval as recommended by Marchetti (1980) at three locations to depths varying between 6 m and 9 m below the existing surface level. In all, 84 tests were performed in the three holes.

In order to correlate the *NDMT* data with other techniques, *SPT* testing was also carried out adjacent to the *NDMT* test locations on the same site. Fig. 6 shows plots of SPT blows (N-values) against depth for the three test locations. Subsoil samples were recovered from the *SPT* for determining various properties in the laboratory.

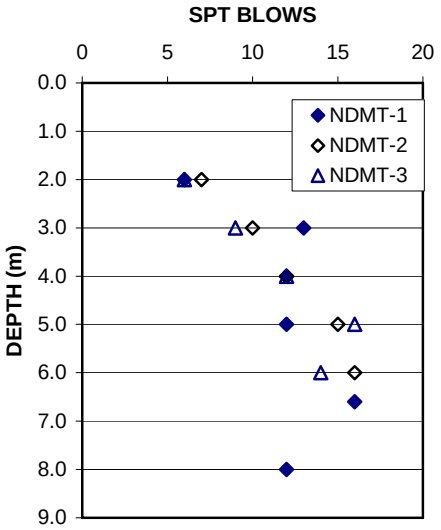

Fig. 6 Plot of SPT blows against depth.

4 INTERPRETATION OF TEST DATA

The field test records and the laboratory testing results have revealed that the subsoils comprise fine sand with varying amounts of silt content and are in loose to medium dense state within the depth explored. The ground water table was encountered at 3.50 m depth below the existing ground level.

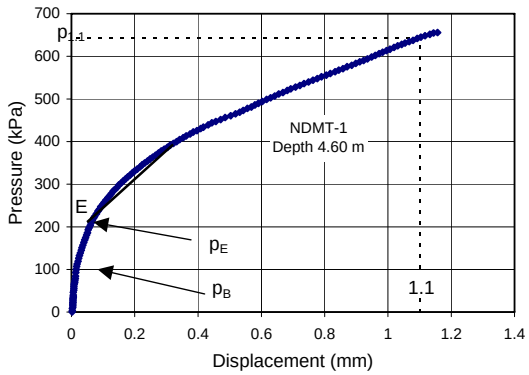

Figure 7 A typical *NDMT* test curve

the blade into the soil causes the soil to yield, which implies the initial pressure on the piston should be p_E. The fact that the initial pressure (p_B) is less than p_E is a result of unloading that occurs; as the soil is unloaded as it moves past the shoulder of the blade.

The piston is forced to move by at least 1.1 mm and the pressure corresponding to this displacement is recorded as $p_{1.1}$, which is an equivalent to Marchetti *DMT* p_1 pressure.

The three pressures (p_B, p_E and $p_{1.1}$) together with the effective overburden pressure and in-situ static pore water pressure at the test depth were

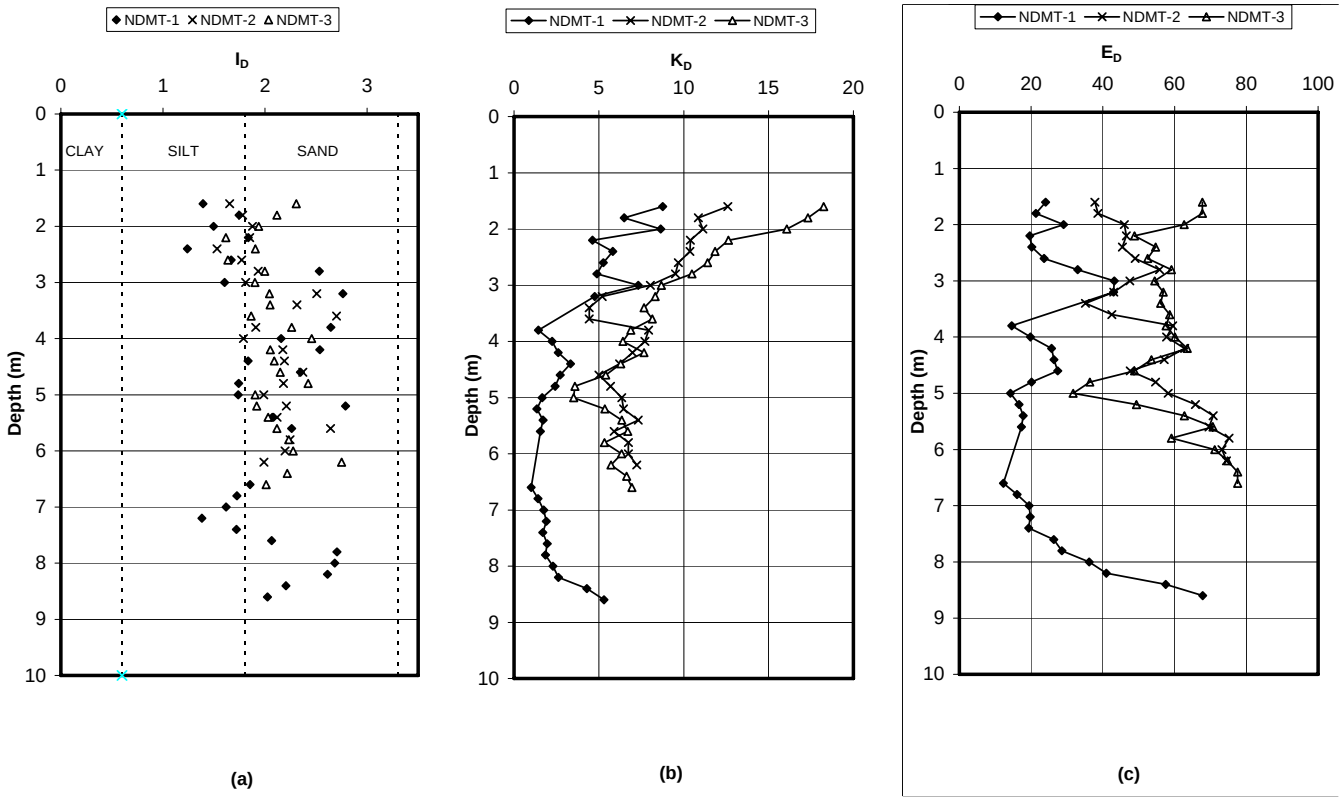

Fig. 8 Plot of dilatometer indices vs. depth for the three NDMT locations

The data points for each *NDMT* test were plotted after being corrected for system compliance. Fig. 7 shows a typical corrected test curve. The corrected load-deformation curves of each *NDMT* test have been analyzed to find the representative pressures (p_B, p_E and $p_{1.1}$) and the appropriate indices (I_D, K_D and E_D), as discussed in the following sections.

p_B, (Fig. 7) represents that pressure on the load-displacement curve where the piston just starts to move. This can also be termed the take-off pressure. The yield pressure p_E (equivalent to Marchetti *DMT* p_o pressure) has been determined by tracing back the trend of (or tangent to) the initial part of the loading curve to intercept the pressure axis at point *E*. This pressure corresponds to zero displacement of the piston, that is when the piston is flush with the blade. Note that pushing

converted to horizontal stress index (K_D), material index (I_D) and dilatometer modulus (E_D), using the following equations:

$$K_D = \frac{p_E - u_o}{\sigma'_v} \tag{1}$$

$$I_D = \frac{p_{1.1} - p_E}{p_E - u_o} \tag{2}$$

$$E_D = 42.8(p_{1.1} - p_B) \tag{3}$$

These indices are plotted against depth in Fig. 8. The interpretation of these indices for the soils of this site is briefly discussed as below:

4.1 *Material Index, I_D*

The particle size distribution analyses performed in the laboratory indicate that the soils are predominantly fine sands with fines varying between 3 and

40 % within the *NDMT* test depths (Fig. 9). The I_D values determined using eq. 2 show close agreement to soil classification established from the sieve analyses. The I_D values for all the three *NDMT* soundings are plotted against depth and shown in Fig. 8(a). These values range between 1.3 and 2.8 indicating the subsoils to vary from sandy silt to silty sand using the classification chart of Marchetti and Crapps (1981).

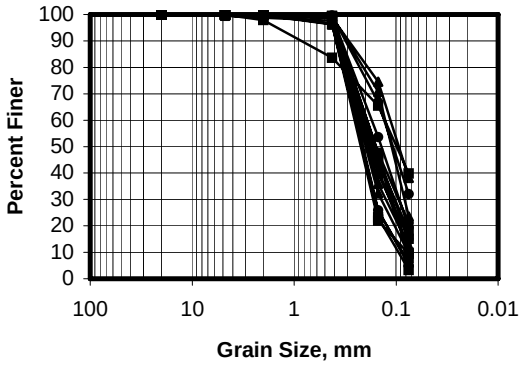

Fig. 9 Particle size distribution curves for the subsoils at the site.

4.2 *Horizontal Stress Index*

K_D gradually decreases with depth, becoming nearly constant below a depth of 3.5m as shown in Fig. 8(b). This trend may be due to the desiccation effects near the ground surface. The K_D values at the three locations vary between 8.8 and 1.0, 12.6 and 4.4, 18.3 and 3.5 respectively.

4.3 *Dilatometer Modulus*

The dilatometer modulus values have been determined using eq. (3) and are plotted in Fig. 8(c). The E_D values for the three locations range from 12 to 68, 35 to 75 and 32 to 78 (MPa). In general, the E_D values are increasing with depth indicating an increase in stiffness of soil though there are a few inter bedded weak layers giving lower values.

The correlations developed using the data obtained from the field and laboratory tests are discussed in the following sections:

4.4 *Soil Identification and Unit Weight*

The data obtained from this research are plotted on the Marchetti and Crapps (1981) chart, Fig. 10(a, b) and the following conclusions have been drawn.

- The I_D values plot in silty sand zone with a few values in sandy silt zone. This agrees with the sieve analysis results (Fig. 10a).
- The E_D values for borehole *NDMT*-1 are lower than those for the other boreholes. This is due to weak subsoil conditions at this location. The fact that it was easier to jack the *NDMT* blade into the ground at *NDMT*-1 location compared to the other two locations supports this finding.
- Plot of E_D and I_D values on the Marchetti and Crapps (1981) chart shows unit weight values higher than those obtained from correlations based on SPT blow count (Bowles, 1988). Settlement predictions based on the assumption that a foundation is flexible are adjusted by a factor of 0.8 to allow for the actual rigid behaviour. Thus a coefficient of 0.8 has been used to produce Figure 10b which gives a better fit the Marchetti and Crapps (1981) soil classification chart.

4.5 *Drained Friction Angle, ϕ'*

The angle of friction is related to the soil type and density of the soil which, in the case of dilatometer tests is a function of I_D and K_D. Fig 11 shows the dilatometer data plotted against the angle of friction obtained from laboratory tests. There appears to be two trend lines which suggests that there may be a correlation between the dilatometer data and angle of friction. This is reinforced when the empirical ϕ' values derived from the SPT tests are included. Further, these lines are parallel with a slope of 0.173. This suggests that there may be a relationship between the indices and the angle of friction of the form:

$$\phi' = 0.173\ (I_D \times K_D) + \text{constant}$$

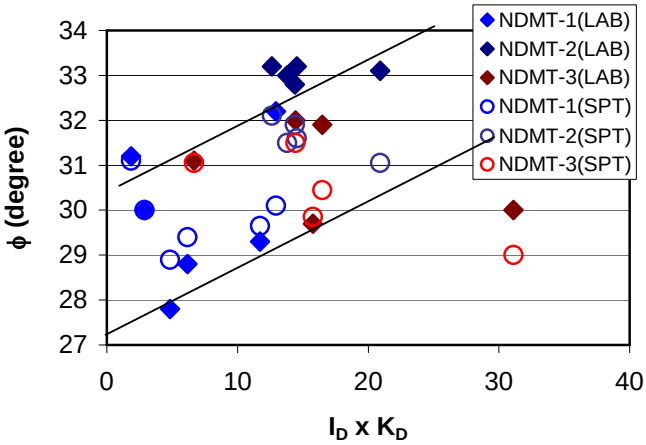

Fig. 11 dilatometer data plotted against the angle of friction obtained from laboratory tests

Note that this relationship does not take into account the density of the soil. However, the constant may be a function of density given that the data clustered about the lower line are either tests at shallow depths or in soil that has a low stiffness (see Fig. 8). Further data are needed to validate this model.

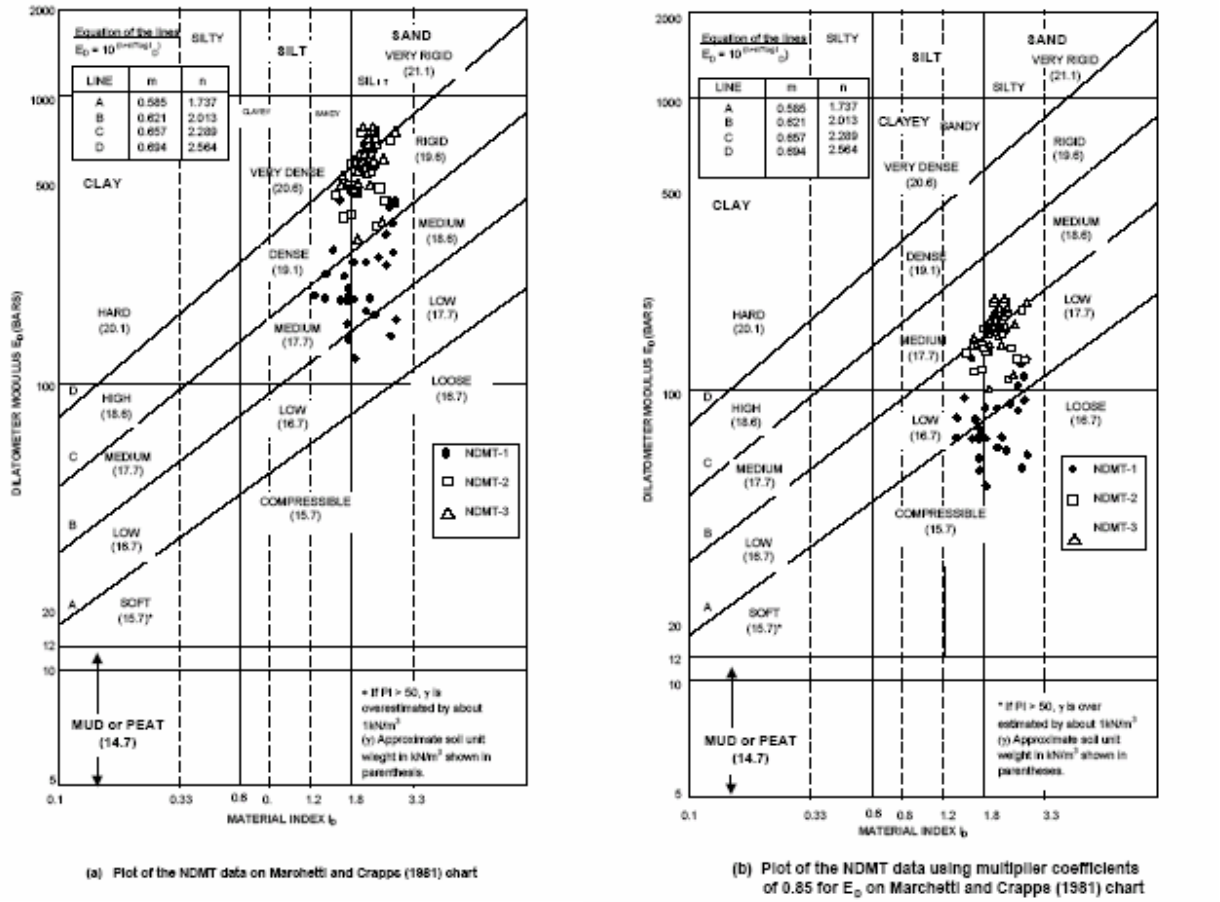

Fig. 10 Plot of NDMT data on the Marchetti and Crapps (1981) chart

4.6 *Elastic Modulus*

The modulus of elasticity E and the Dilatometer Modulus E_D are related by the following formula (Marchetti, 1980).

$$E = (1-\nu^2)E_D \quad (4)$$

For silty sands taking $\nu = 0.4$ (Bowles, 1988) then

$$E = 0.84E_D \quad (5)$$

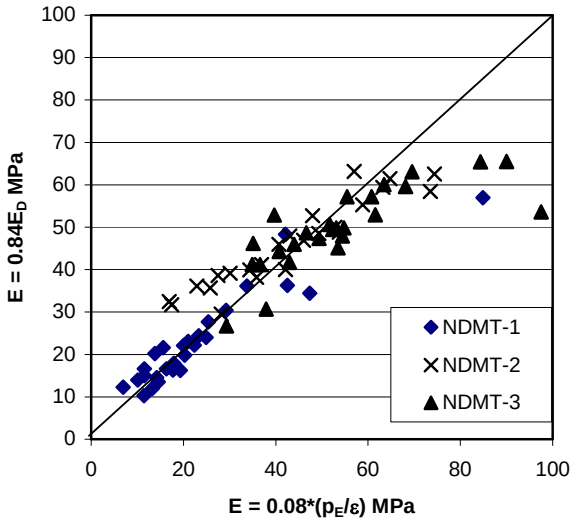

Figure 12 Comparison of Elastic Moduli values

The initial part of the loading curve corresponds to reloading of the soil that has been unloaded during installation. Therefore it is an elastic response. The values of E calculated using eq. (5) are plotted in Fig. 12 against the ratio between the yield pressure, p_E, and the strain defined as the displacement corresponding to p_E divided by half the thickness of the *NDMT* blade. A good agreement between the two approaches suggests using the following relation to determine modulus of elasticity from the initial part of the *NDMT* curve.

$$E = 0.08(p_E/\varepsilon) \quad (6)$$

where, ε = (displacement) ÷7.5

This relationship needs to be validated against results of other types of tests and observations of soil behaviour and be extended to cover other soil types.

5 OTHER SALIENT FEATURES OF NDMT

There are a number of features of the *NDMT* that enable repeatable and consistent results to be obtained:

- The *HET* output is stable and unaffected by any change in temperature.

- The *NDMT* piston assembly is relatively straightforward.
- The movement if the piston is monitored during a test which produces a pressure displacement curve that may be analyzed using cavity expansion theory.
- Unload reload cycles can be included to provide further information on the elastic response of the ground.

6 CONCLUSIONS

The following conclusions are drawn from the analysis of *NDMT* tests in silty sand in conjunction with results from the SPT and laboratory tests.

1. The soil classification chart of Marchetti and Crapps (1981) can be used to classify and estimate the unit weight of the soil after applying a correction of 0.80 to E_D.
2. There is a relationship between the angle of friction obtained from laboratory tests and the material and horizontal stress indices. This is supported by the angles of friction derived from SPT data which suggests that the indices are appropriate.
3. The initial loading portion of the *NDMT* test is the elastic response of the ground. The value of stiffness derived from this portion compares favorably with that derived using the Marchetti formula.

Further tests on different soil types are needed to establish whether these correlations are site specific or generic.

REFERENCES

Akbar, A. (2001): Development of Low Cost In-situ Testing Devices, *Ph.D. Thesis*, Civil Engineering Department, University of Newcastle, UK.

Akbar, A. and Clarke, B.G. (2001): A Flat Dilatometer to Operate in Glacial Tills, *Geotech. Testing Journal*, GTJODJ, Vol. 24, No.1, pp. 51-60.

Akbar, A. and Clarke, B.G. (2002): A New Robust Device for the Identification of Potential Slip Surfaces, 3rd Int. Conf. On Land Slides, Slope Stability and the Safety of Infra Structures, July 11-12, 2002, Singapore.

Bowles, J.E. (1988). Foundation analysis and Design, 4th ed. McGraw Hill International edition

Campanella, R.G. and Robertson, P.K. (1991*)*: Use and Interpretation of a Research Dilatometer, *Canad. Geotechn. Journal*, Vol. 28: 113-126.

Marchetti, S. (1980): In Situ Tests by Flat Dilatometer, *J. Geotech. Engng. Div., ASCE,* Vol. 106, No. GT 3, pp.299-321.

Marchetti, S. and Crapps, D.K. (1981), "Flat Dilatometer Manual," *GPE Inc., USA*.

Marchetti, S. (1997): The Flat Dilatometer Design Applications, *Proceedings, Third Geotechnical Engng. Conference, Cairo University, Egypt*, pp. 1-25.

Clay Soil Characterization by the New Seismic Dilatometer Marchetti Test (SDMT)

Cavallaro A.
CNR – IBAM, Catania, Italy

Grasso S. & Maugeri M.
Department of Civil and Environmental Engineering, University of Catania, Italy

Keywords: small shear modulus, in situ tests, non linearity.

ABSTRACT: This paper describes and compares the results of in situ laboratory investigations performed on Catania soil that were carried out to determine the variation of shear modulus with depth and strain level by Seismic Dilatometer Marchetti Test (SDMT), Down-Hole (DH) Test and Resonant Column Tests (RCT). Some considerations on shear modulus degradation evaluation by SDMT are proposed. The available data also enabled one to compare the shear modulus profile obtained by empirical correlations based on CPT or laboratory results with Down Hole Test and Seismic Dilatometer Marchetti Test.

1 INTRODUCTION

Soil stiffness, at small strains, is a relevant parameter in solving boundary value problems such as:
- seismic response of soil deposits to earthquakes;
- dynamic interaction between soils and foundations;
- design of special foundations for which the serviceability limit allows only very small displacements.

However, it was been pointed out by many researchers that the strain level which often occurs in geotechnical problems is quite small even under the static loading condition and the case of conventional foundations (Jardine et al. 1986, Battaglio and Jamiolkowski 1987, Burland 1989, Berardi and Lancellotta 1991, Maugeri et al. 1998).

On the other hand, the hypotheses of homogeneity, elasticity and isotropy are unrealistic for soils. In reality soil behaviour is non linear (non linear elasticity or plasticity) and anisotropic. In particular, some researchers (Hardin 1978, Jardine et al. 1984, 1986) have postulated that an elastic or apparently elastic soil response occurs only at small strains (i. e. less than 0.001 %).

In this paper the seismic flat dilatometer test (SDMT) was used to provide shear wave velocity (V_s) measurements to supplement conventional inflation readings (p_o and p_1).

Soil stratigraphy and soil parameters are evaluated from the pressure readings while the small strain stiffness (G_o) is obtained from in situ V_s profiles.

A comprehensive in situ and laboratory investigation has been carried out to study the STM M6 test site in the city of Catania.

The results obtained by SDMT were compared with those evaluated by in situ and laboratory tests during the seismic microzonation study performed in the city of Catania.

2 INVESTIGATION PROGRAM AND BASIC SOIL PROPERTIES

The investigated STM M6 area, located in the South zone of the city, has plane dimensions of 212400 mq and a maximum depth of 100 m. The area pertaining to the investigation program and the locations of the boreholes and field tests are shown in Figure 1.

The STM M6 site consists of fine alluvial deposits. Undisturbed samples were retrieved by means of Osterberg (1973) piston sampler and an 86 mm Shelby tube sampler.

In the Catania STM M6 area, the clay fraction (CF) is predominantly in the range of 2 - 54 %. This percentage decreases to 0 - 2 % at the depth of 95 m where a sand fraction of 4 - 9 % is observed. The gravel fraction is always zero. The silt fraction is in the range of about 50 - 100 %. The values of the natural moisture content, w_n, range from between 22 and 56 %.

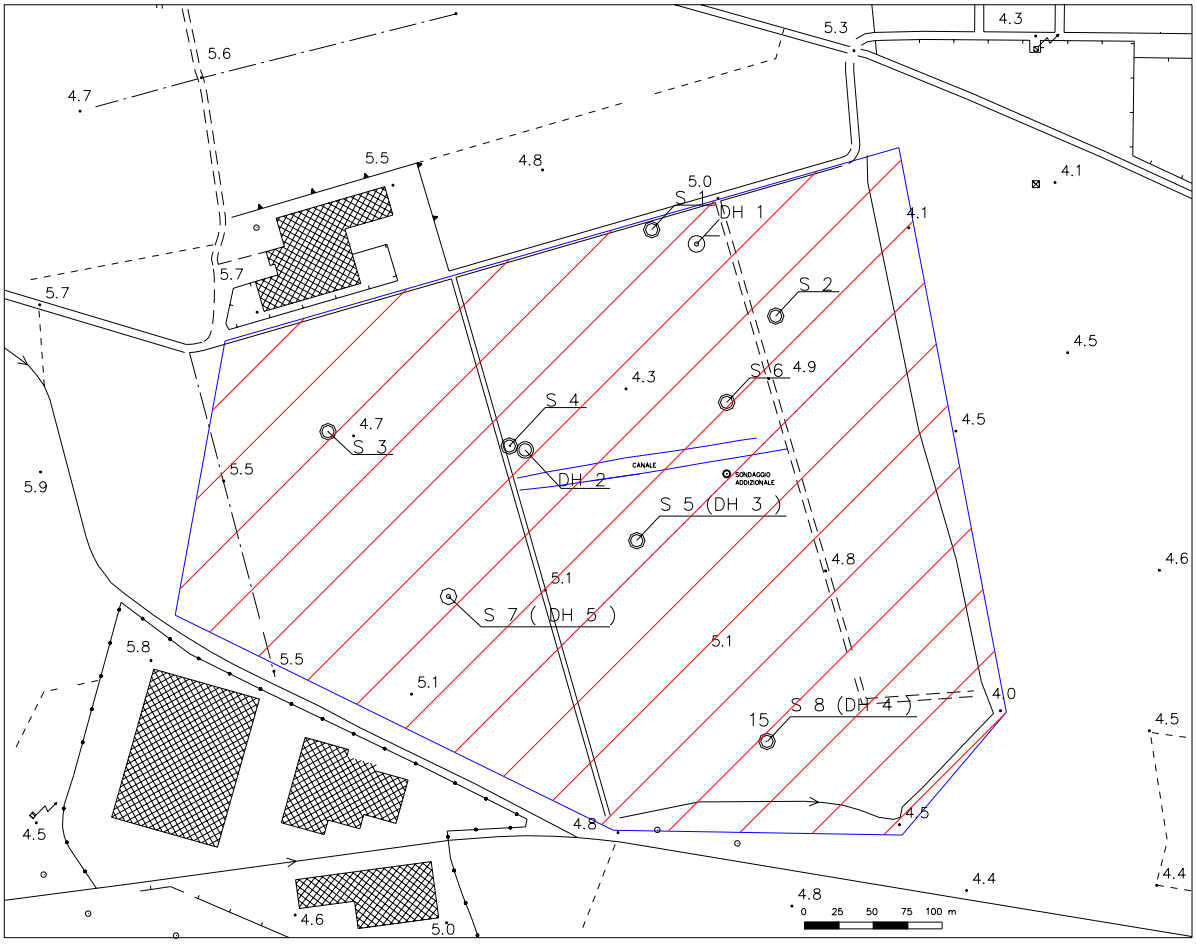

Figure 1. Layout of investigation area with locations of the boreholes and of field tests.

Characteristic values for the Atterberg limits are: w_L = 54 - 84 % and w_p = 27 - 46 %, with a plasticity index of PI = 22 - 41 %.

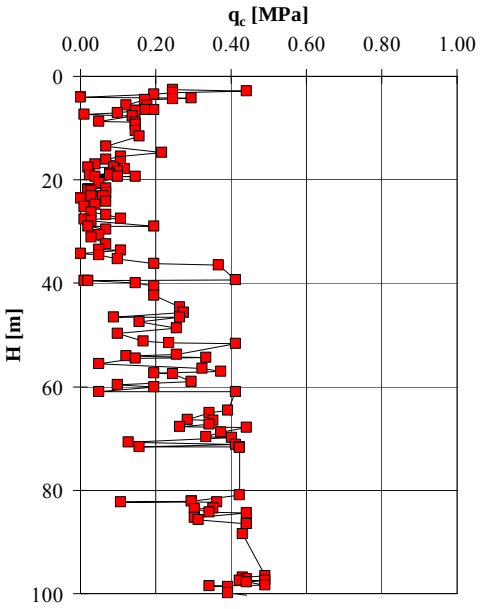

Figure 2. Static cone penetration test results.

The good degree of homogeneity of the deposit is confirmed by comparing the penetration resistance q_c from mechanical cone penetration tests (CPT) performed at different locations over the investigated area (Figure 2). The variation of q_c with depth clearly shows the very poor mechanical characteristics of soil. Typical values of q_c are in the range of 0.01 to 0.49 MPa. The soil deposits can be classified as inorganic silt of high compressibility and organic clay.

Typical range of physical characteristics, index properties and strength parameters of the deposit are reported in Table 1.

Table 1. Mechanical characteristics for Catania STM M6 area.

Site	γ [kN/m^3]	e	c_u [kPa]	c' [kPa]	ϕ' [°]
STM M6	16.6-20.2	0.56-1.51	28.75-203.61	2.41-21.7	16-18

where: c_u (Undrained shear strength), c' (Cohesion) and ϕ' (Angle of shear resistance) were calculated from and C-U and C-D Triaxial Tests.

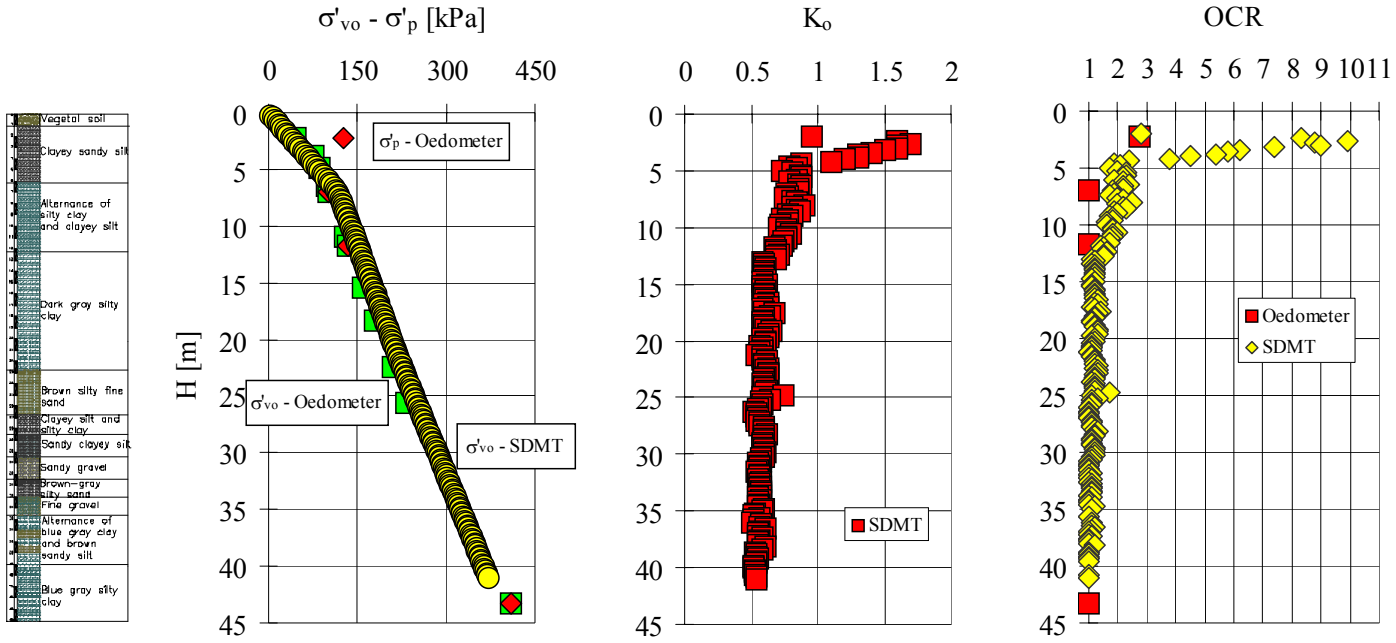

Figure 3. Stress history from in situ and laboratory tests.

The preconsolidation pressure σ'_p and the over-consolidation ratio OCR = σ'_p/σ'_{vo} were evaluated from the 24^h compression curves of 5 incremental loading (IL) oedometer tests. Moreover, a SDMT was used to assess OCR and the coefficient of earth pressure at rest K_o following the procedure suggested by Marchetti (1980).

The information obtained from laboratory and in situ tests is summarized in Figure 3.The OCR values obtained from SDMT range from 1 to 10 (K_o = 0.5 to 1) with an average value equal to 1.2 up to about 10 for the 40 m deep sounding. The OCR values inferred from oedometer tests are lower than those obtained from in situ tests.

One possible explanation of these differences could be that lower values of the preconsolidation pressure σ'_p are obtained in the laboratory because of sample disturbance.

3 SHEAR MODULUS

The small strain ($\gamma \leq 0.001$ %) shear modulus, G_o, was determined from SDMT and a Down Hole (DH) test. The equivalent shear modulus (G_{eq}) was determined in the laboratory by means of a Resonant Column test (RCT) performed on Shelby tube specimens by means of a Resonant Column. Moreover it was attempted to assess G_o by means of empirical correlations, based either on penetration test results or on laboratory test results (Jamiolkowski et al. 1995).

3.1 *Small strain shear modulus G_o: in situ vs. laboratory measurements*

The SDMT provides a simple means for determining the initial elastic stiffness at very small strains and in situ shear strength parameters at high strains in natural soil deposits.

Source waves are generated by striking a horizontal plank at the surface that is oriented parallel to the axis of a geophone connects by a co-axial cable with an oscilloscope (Martin & Mayne, 1997, 1998). The measured arrival times at successive depths provide pseudo interval V_s profiles for horizontally polarized vertically propagating shear waves (Figure 4).

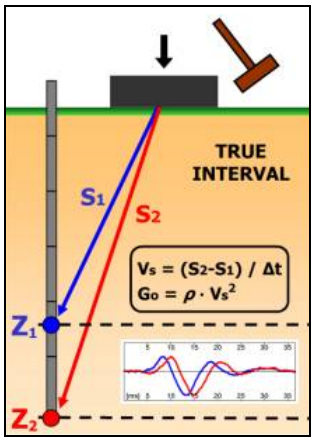

Figure 4. SDMT scheme for the measure of V_s.

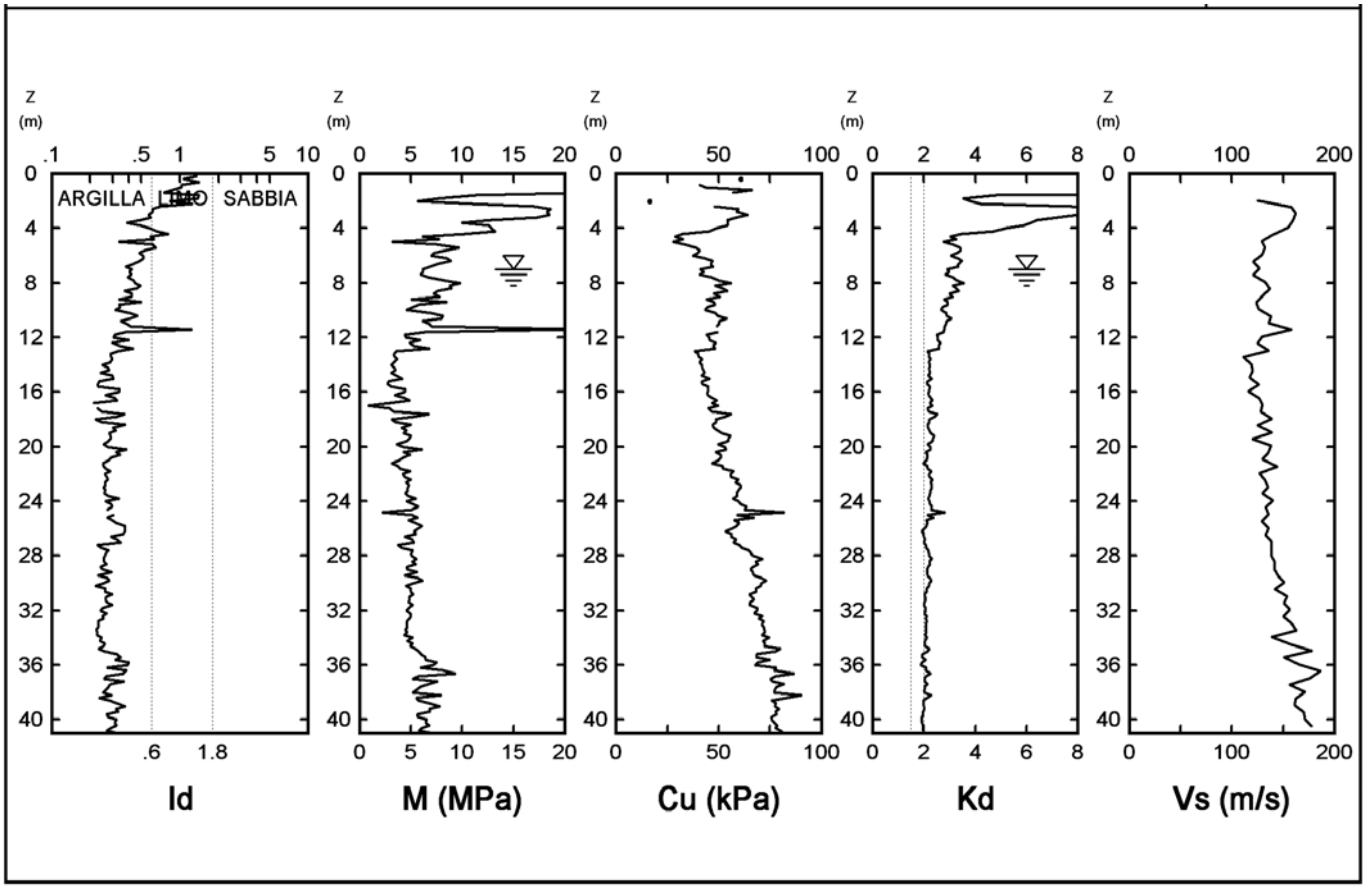

Figure 5. Summary of SDMTs in Catania STM M6 area.

The small strain shear modulus G_o is determined by the theory of elasticity by the well known relationships:

$$G_o = \rho V_s^2 \quad (1)$$

where: ρ = mass density.

A summary of SDMT parameters are shown in Figure 5 where:
- I_d: Material Index; gives information on soil type (sand, silt, clay);
- M: Vertical Drained Constrained Modulus;
- C_u: Undrained Shear Strength;
- K_d: Horizontal Stress Index; the profile of K_d is similar in shape to the profile of the overconsolidation ratio OCR. $K_d = 2$ indicates in clays OCR = 1, KD > 2 indicates overconsolidation. A first glance at the K_d profile is helpful to "understand" the deposit;
- V_s: Shear Waves Velocity.

Figure 6 shows the values of G_o obtained in situ from a DH test and SDMT and those measured in the laboratory from RCT performed on undisturbed solid cylindrical specimens which were isotropically reconsolidated to the best estimate of the in situ mean effective stress.

The G_o values are plotted in Figure 6 against depth (Carrubba & Maugeri 1988). In the case of laboratory tests, the G_o values are determined at shear strain levels of less than 0.001 %.

Quite a good agreement exists between the laboratory and in situ test results. On average the ratio of G_o (Lab) to G_o (Field) by SDMT and DH was equal to about 0.90 at the depth of 29.5 m.

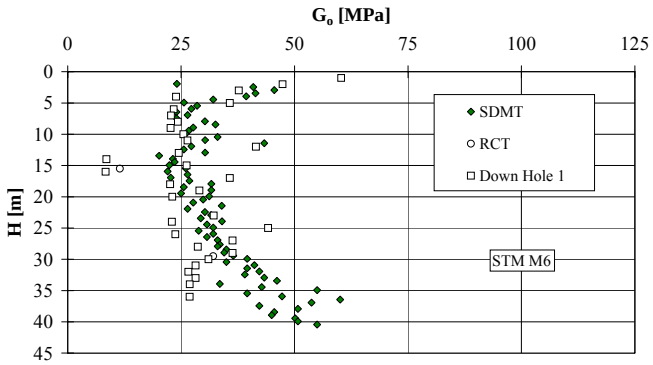

Figure 6. G_o from laboratory and in situ tests.

In the superficial strata G_o by SDMT assumed the value of 45 MPa. In the medium Holocene strata G_o values are between 20 and 35 MPa. In the

lower Holocene soil G_o increases with depth to 55 MPa.

3.2 *Shear modulus degradation from SDMT*

G is the unload-reload shear modulus evaluated from RCT, while G_o is the maximum value or also "plateau" value as observed in the G-log(γ) plot. Generally G is constant until a certain strain limit is exceeded. This limit is called elastic threshold shear strain (γ_t^e) and it is believed that soils behave elastically at strains smaller than γ_t^e. The elastic stiffness at $\gamma<\gamma_t^e$ is thus the already defined G_o. At strains greater than γ_t^e some plastic deformation occurs and the stress-strain relationship becomes non-linear. When a certain limit strain is exceeded, degradation phenomena are observed. This limit strain is called volumetric threshold shear strain (γ_t^v) and is rate dependent. For shear at a strain rate of about 0.4%/min γ_t^v ranges between 0.05 and 0.1 % and increases for increasing strain rates (Lo Presti 1989, Vucetic 1994).

A key feature distinguishing SDMT from other seismic tests is that in adition to G_o, a "working strain" shear modulus, G_{ws} is determined. The availability of two datapoints (G_o and G_{ws}) may help in selecting the G-γ decay curve, important in soil dynamics.

G_{ws} can be evaluated by the following equation based on M_{DMT} values:

$$G_{ws} = \frac{(1-2\cdot\nu)}{2\cdot(1-\nu)}\cdot M_{DMT} \qquad (2)$$

where ν (Figure 7) is the Poisson ratio, obtained from Down Hole (DH) test.

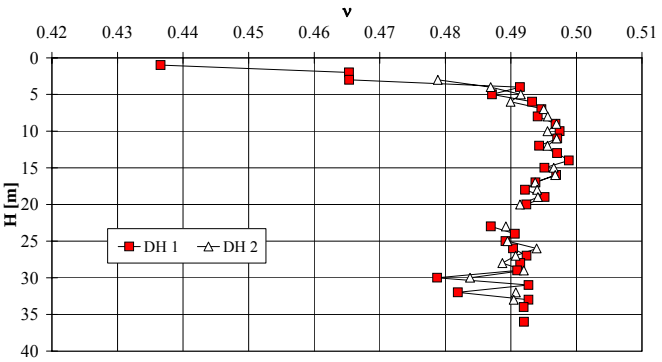

Figure 7. Poisson ratio from Down Hole (DH) test.

As regard the evaluation of "working strain" γ_{ws}, we must distinguish the settlements predicted during the analysis of case histories (γ = 0.05 to 0.1 %) and the real strain investigated by SDMT to measure the dilatometer modulus E_D.

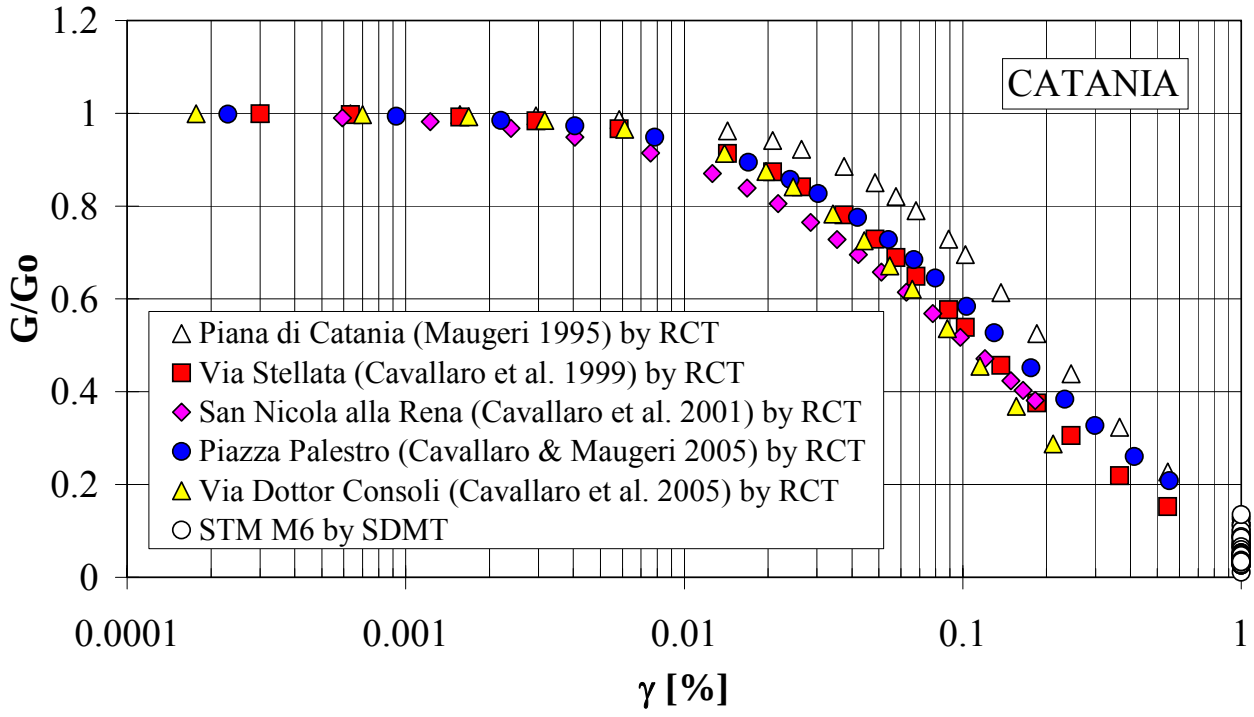

Figure 8. G/G_o vs shear strain for Catania area.

In the vicinity of the probe, the flat dilatometer blade is expected to produce shear similar to the cylindrical probes of the piezocone and smaller than the push-in pressuremeter (Lacasse & Lunne, 1988). Tentatively reported in Figure 8 is the comparison between RCT for different Catania site and SDMT results at large strain for STM M6 area.

3.3 *Evaluation of* G_o *from empirical correlations*

It was also attempted to evaluate the small strain shear modulus by means of the following empirical correlations based on penetration tests results or laboratory results available in literature.

a) Hryciw (1990):

$$G_o = \frac{530}{(\sigma'_v/p_a)^{0.25}} \frac{\gamma_D/\gamma_w - 1}{2.7 - \gamma_D/\gamma_w} K_o^{0.25} \cdot (\sigma'_v \cdot p_a)^{0.5} \quad (3)$$

where: G_o, σ'_v and p_a are expressed in the same unit; p_a = 1 bar is a reference pressure; γ_D and K_o are respectively the unit weight and the coefficient of earth pressure at rest, as inferred from SDMT results according to Marchetti (1980);

b) Mayne and Rix (1993):

$$G_o = \frac{406 \cdot q_c^{0.696}}{e^{1.13}} \quad (4)$$

where: G_o and q_c are both expressed in [kPa] and e is the void ratio. Eq. (4) is applicable to clay deposits only;

c) Jamiolkowski et. al. (1995):

$$G_o = \frac{600 \cdot \sigma'^{0.5}_m p_a^{0.5}}{e^{1.3}} \quad (5)$$

where: $\sigma'_m = (\sigma'_v + 2 \cdot \sigma'_h)/3$; p_a = 1 bar is a reference pressure; G_o, σ'_m and p_a are expressed in the same unit. The values for parameters which appear in equation (5) are equal to the average values that result from laboratory tests performed on quaternary Italian clays and reconstituted sands. A similar equation was proposed by Shibuya and Tanaka (1996) for Holocene clay deposits.

Equation (5) incorporates a term which expresses the void ratio; the coefficient of earth pressure at rest only appear in equation (3). However only equation (3) tries to obtain all the input data from the SDMT results.

The G_o values obtained with the methods above indicated are plotted against depth in Figure 9. The method by Jamiolkowski et al. (1995) was applied considering a given profile of void ratio. The coefficient of earth pressure at rest was inferred from SDMT.

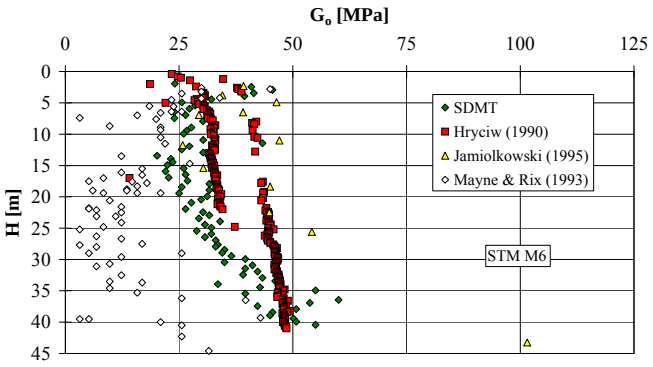

Figure 9. G_o from different empirical correlations.

All the considered methods show very different G_o values of the Holocene soil. On the whole, equation (3) and (5) seems to provide the most accurate trend of G_o with depth, as can be seen in Figure 9. It is worthwhile to point out that equation (5) overestimated G_o for depths greater than 25 m.

4 CONCLUSIONS

A site characterization for seismic response analysis has been presented in this paper. On the basis of the data shown it is possible to draw the following conclusions:

- SDMT were performed up to a depth of 42 meters. The results show a very detailed and stable shear wave profile. The shear wave profiles obtained by SDMT compare well with laboratory tests;
- the small strain shear modulus measured in the laboratory is on average 0.90 of that measured in situ by means of SDMT and DH tests;
- empirical correlations between the small strain shear modulus and penetration test results were used to infer G_o from CPT and SDMT. The values of G_o were compared to those measured with SDMT and DH tests. This comparison indicates that some agreement exists between empirical correlations and SDMT and DH test;

- moreover SDMT measurements are much more stable and repeatable than DH test, so the SDMT is a powerful investigation tool.

- SDMT, because of three independent measurements of p_o, p_1 and V_s, gives shear modulus at small strain and large strain for detecting soil non linearity.

ACKNOWLEDGMENTS

The authors wish to thank the geotechnical engineer Alessio Carbonaro for his contribution to the work.

REFERENCES

Battaglio, M. & Jamiolkowski, M. 1987. Analisi delle Deformazioni. *XII CGT*, Politecnico di Torino.

Berardi, R. & Lancellotta, R. 1991. Stiffness of Granular Soils from Field Performance. *Geotechnique* Vol. 41, N°. 1: 149-157.

Burland, J.B. 1989. Small is Beatiful - The stiffness of Soil at Small Strains. *Proceedings of the 9th Laurits Bjerrum Memorial Lecture, Canadian Geotechnical Journal*, Vol. 26, N°. 4: 499-516.

Carrubba, P. & Maugeri, M. 1988. Determinazione delle Proprietà Dinamiche di un'Argilla Mediante Prove di Colonna Risonante. *Rivista Italiana di Geotecnica*, N°. 2, Aprile-Giugno1988: 101-113.

Cavallaro, A., Maugeri, M., Lo Presti, D.C.F. & Pallara O. 1999. Characterising Shear Modulus and Damping from in Situ and Laboratory Tests for the Seismic Area of Catania. *Proceedings of the 2nd International Symposium on Pre-failure Deformation Characteristics of Geomaterials*, Torino, 28 - 30 September 1999: 51-58.

Cavallaro, A., Grasso, S. & Maugeri, M. 2001. A Dynamic Geotechnical Characterization of Soil at Saint Nicolò alla Rena Church Damaged by the South Eastern Sicily Earthquake of 13 December 1990. *Proceeding of the 15th International Conference on Soil Mechanics and Geotechnical Engineering, Satellite Conference "Lessons Learned from Recent Strong Earthquakes"*, Istanbul, 25 August 2001: 243-248.

Cavallaro, A. & Maugeri, M. 2005. Non Linear Behaviour of Sandy Soil for the City of Catania. *Seismic Prevention of Damage: A Case Study in a Mediterranean City*, Wit Press Publishers, Editor: Maugeri M.: 115-132.

Cavallaro, A., Grasso, S. & Maugeri, M. 2005. Site Characterisation and Site Response for a Cohesive Soil in the City of Catania. *Proceedings of the Satellite Conference on Recent Developments in Earthquake Geotechnical Engineering*, Osaka, 10 September 2005: 167-174.

Hardin, B.O. 1978. The Nature of Stress-Strain Behaviour of Soils. *Earthquake Engineering and Soil Dynamics*, Vol. 1, Pasadena, CA, ASCE, New York: 3-90.

Hryciw, R.D. 1990. Small Strain Shear Modulus of Soil by Dilatometer. *JGED, ASCE*, Vo. 116, N°. 11: 1700-1715.

Jamiolkowski, M., Lo Presti, D.C.F. & Pallara, O. 1995. Role of In-Situ Testing in Geotechnical earthquake Engineering. *Proceedings of 3rd International Conference on Recent Advances in Geotechnical Earthquake Engineering and Soil Dynamic*, State of the Art 7, St. Louis, Missouri, April 2-7, 1995, vol. II: 1523-1546.

Jardine, R.J., Symes M.J. & Burland J.B. 1984. The Measurement of Soil Stiffness in the Triaxial Apparatus. *Geotechnique*, Vol. 34, N°. 3 : 323-340.

Jardine, R.J., Potts, D.M., Fourie, A. & Burland, J.B. 1986. Studies of the Influence of Non-Linear Stress-Strain Characteristics in Soil-Structure Interaction. *Geotechnique*, Vol. 36, N°.3 : 377-396.

Lacasse S. & Lunne T. 1988. Calibration of Dilatometer Correlations. *Proceedings of 1st International Symposium on Penetration Testing*, ISOPT-1, Orlando: 539-548.

Lo Presti, D.C.F. 1989. Proprietà Dinamiche dei Terreni. *XIV C.G.T.* Torino.

Marchetti, S. 1980. In Situ Tests by Flat Dilatometer. *Journal of the Geotechnical Engineering Division*, ASCE, Vol. 106, N°. GT3, March, 1980: 299-321.

Martin, G.K. & Mayne, P.W. 1997. Seismic Flat Dilatometers Tests in Connecticut Valley Vaeved Clay. *ASTM Geotechnical Testing Jornal*, 20 (3): 357-361.

Martin, G.K. & Mayne, P.W. 1998. Seismic Flat Dilatometers Tests in Piedmont Residual Soils. *Geotecnical Site Characterization*, Vol. 2, Balkema, Rotterdam: 837-843.

Maugeri, M. 1995. Discussions and Replies Session IX. *Proceedings of International Conference on Recent Advances in Geotechnical Earthquake Engineering and Soil Dynamics*, St. Louis, 2 – 7 April 1995: 1323-1327.

Maugeri, M., Castelli, F., Massimino, M.R. & Verona, G. 1998. Observed and Computed Settlements of Two Shallow Foundations on Sand. *Journal of the Geotechnical and Geonvironmental Engineering*, ASCE, Vol. 124, N°. 7, July, 1998: 595-605.

Mayne, P.W. & Rix, G.J. 1993. G_{max}-q_c Relationships for Clays. *Geotechnical Testing Journal,* Vol. 16, N°. 1: 54-60.

Osterberg J.O. 1973. An Improved Hydraulic Piston Sampler. *Proceedings of 8th ICSMFE,* Moscow. Vol 1.2.

Shibuya, S. & Tanaka, H. 1996. Estimate of Elastic Shear Modulus in Holocene Soil Deposits. *Soils and Foundations*, Vol. 36, N°. 4: 45-55.

Vucetic M. 1994. Cyclic threshold shear strains in soils. *Journal of Geotechnical Engineering, ASCE*, Vol. 120, N°. 12: 2208-2228.

Modifications to the Control Unit to Enable a Computer to Control and Take Readings

Roger A. Failmezger, P.E.
In-Situ Soil Testing, L.C., 173 Dillin Drive, Lancaster, Virginia 22503, email: insitusoil@prodigy.net
Peter Nolan
Hogentogler and Company, Inc., 9515 Gerwig Lane, Suite 109, Columbia, Maryland 21046, email: peter@hogentogler.com

Keywords: Dilatometer, Control Unit

ABSTRACT: The manual version of the dilatometer control unit has been used successfully for over 25 years. The advancement in computers since its development enables a computer program to perform the same steps that have been done by hand. A computer program can use the previously recorded "A" and "B" reading data to estimate what the current pair will be. The nitrogen flow rate is slowed down when the pressure gets near the anticipated readings and the time lag for the pressure at the control unit to be the same as the pressure inside the blade is minimized. The computer records the data saving data entry time later.

1 INTRODUCTION

The dilatometer control unit was modified so that a computer can regulate the flow control valve and record the data. After the computer records at least five dilatometer tests with thrust, "A" and "B" readings, a database is established to predict the next "A" and "B" readings. The "A" reading is predicted from the thrust reading, and the "B" reading is predicted from a combination of thrust and "A" reading. The computer controls the flow rate so that it is slow near the anticipated "A" and "B" readings so that the lag for the pressure inside the blade to be the same as in the control unit will be minimized. Manual readings using the gauges can also be used as a check or manually recorded. The more homogeneous the soil is, the better the computer will predict "A" and "B" readings and thereby more accurately collect and record the data.

2 HARDWARE MODIFICATIONS

An auxiliary computer-controlled unit was manufactured to do the above tasks. With this unit, the nitrogen source connects to a quick fitting; the computer turns a motor, which turns the needle valve regulating the nitrogen flow; and the nitrogen exits back to the standard control unit.

For the initial readings needed to establish the database, the operator controls the flow using the computer's mouse and a slide bar. Afterwards, the Auto DMT program computer communicates to a purposefully built microcontroller over another serial line. The microcontroller opens / closes the flow valve by controlling a stepper motor. The Auto DMT program, based on operator input or feedback from the pressure transducer, sends commands the microcontroller which then turns the stepper motor.

It is possible for the nitrogen to exit directly to the blade, but we chose to make use of the existing dial gauges. A short male-to-male quick-connect cable connects the computer-controlled unit to the standard control unit. A short ground cable also connects the two control units. On one end it has a male and female banana plug. The dilatometer cable plugs into a female quick-connect fitting on the computer-control unit. A photo of the computer-control unit is shown below in Figure 1.

A pressure transducer is connected to a "T" near where the dilatometer cable exits the computer-control unit. The transducer has a calibrated maximum pressure of 100 bars with an accuracy of $\pm$0.01 bars.

A 9-pin serial port is connected to the pressure transducer, step-motor flow control valve, and the dilatometer signal. The switch in the blade is connected, via a pull-up resistor, to the Data Set Ready (DSR) line in the serial port connecting the computer to the microcontroller. When the switch opens or closes, the change in state of the DSR line is de

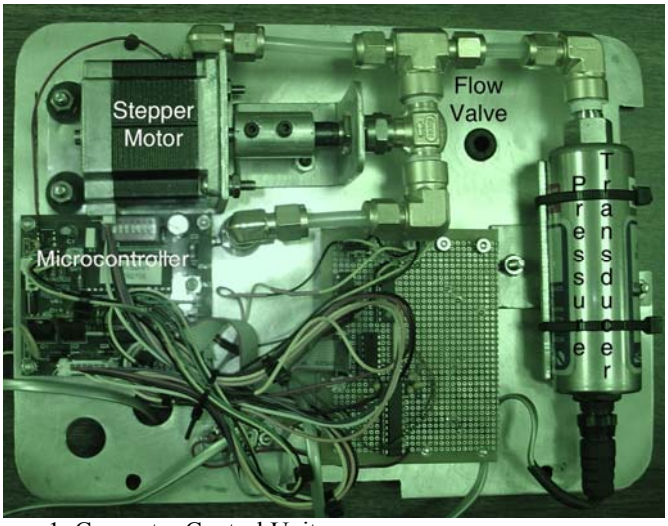

Figure 1: Computer Control Unit

tected by the computer. The computer polls the dilatometer signal to determine the "A" reading, which occurs when the electrical continuity is lost (switch goes from closed to open) and later for the "B" reading, when electrical continuity returns (switch goes from open to closed). If the switch is closed, an indicator on the screen of the computer is set to red. When the switch is open, the indicator is set to white. The pressure is read from the transducer and outputted to the computer through the serial port. The computer records the "A" and "B" readings, saving the operator data entry time.

3 OPERATION

There are two modes of operation.

3.1 *Manual Mode*

Manual mode requires the operator to open or close the valve by using the scroll bar. This is akin to the operator manually opening the valve on a traditional DMT readout box. Also, the operator has to monitor the indicator on the screen to determine whether the A or B reading had been reached. The steps required to perform the test in manual mode are:

1. Advance to the desired depth.
2. Enter the thrust. After the operator has performed five previous readings, then the computer estimates the A and B readings when the thrust is entered.
3. Open the valve. The valve is adjusted using the scroll bar on the screen. When the slider is positioned to the far left of the scroll bar, the valve is closed. When the slider is positioned to the far right of the scroll bar, the valve is opened by two rotations. The valve may be adjusted any time during the test at that depth.
4. Press "Take A reading" to record the A reading when the indicator changes from red to white. At this point, the switch in the blade is open. This is similar to the buzzer going silent on the old DMT unit. After the operator has performed five previous readings, then the computer predicts the B reading after the A reading is recorded.
5. Press "Take B reading" to record the B reading when the indicator changes from white to red. At this point, the switch in the blade is closed. This is similar to the buzzer indicating that the B reading has been reached on the old DMT unit. Once the B reading is recorded the unit closes the valve, and the computer is ready to collect data for the next depth.
6. The operator vents nitrogen from the system or takes a "C" reading.

3.2 *Automatic Mode*

Automatic mode, which is available only after five readings have been performed, requires no input / control from the operator after the thrust is entered. In automatic mode, the unit estimates the A reading based on the thrust and controls the valve based on feedback from the pressure transducer. The goal is to reach the percentages listed in Table 2 at the specified time intervals. The computer will automatically take the A reading when the switch in the blade is opened. The computer then estimates the B reading, adjusts the valve, and records the B reading when the switch is closed.

A computer screen of the automatic mode is shown in Figure 2.

4 COMPUTER ESTIMATES OF "A" AND "B" READINGS

The first five readings of a sounding need to be taken manually to start to establish the computer's database. From the database a best fit linear relationship is found between thrust and the "A" reading. The thrust is measured at the test depth and entered into the computer. The computer estimates the "A" reading based on that best fit linear relationship.

From each prior test the I_D is computed. Plots of I_D versus thrust and "A" reading are created and the linear best fit relationships are generated for each plot. The operator can choose what percentages to assign the thrust and "A" reading components when determining the overall I_D prediction. The predicted overall I_D value is computed as:

$$I_D = (A\ I_D)(\%A) + (\text{Thrust } I_D)(\%\text{Thrust}),$$

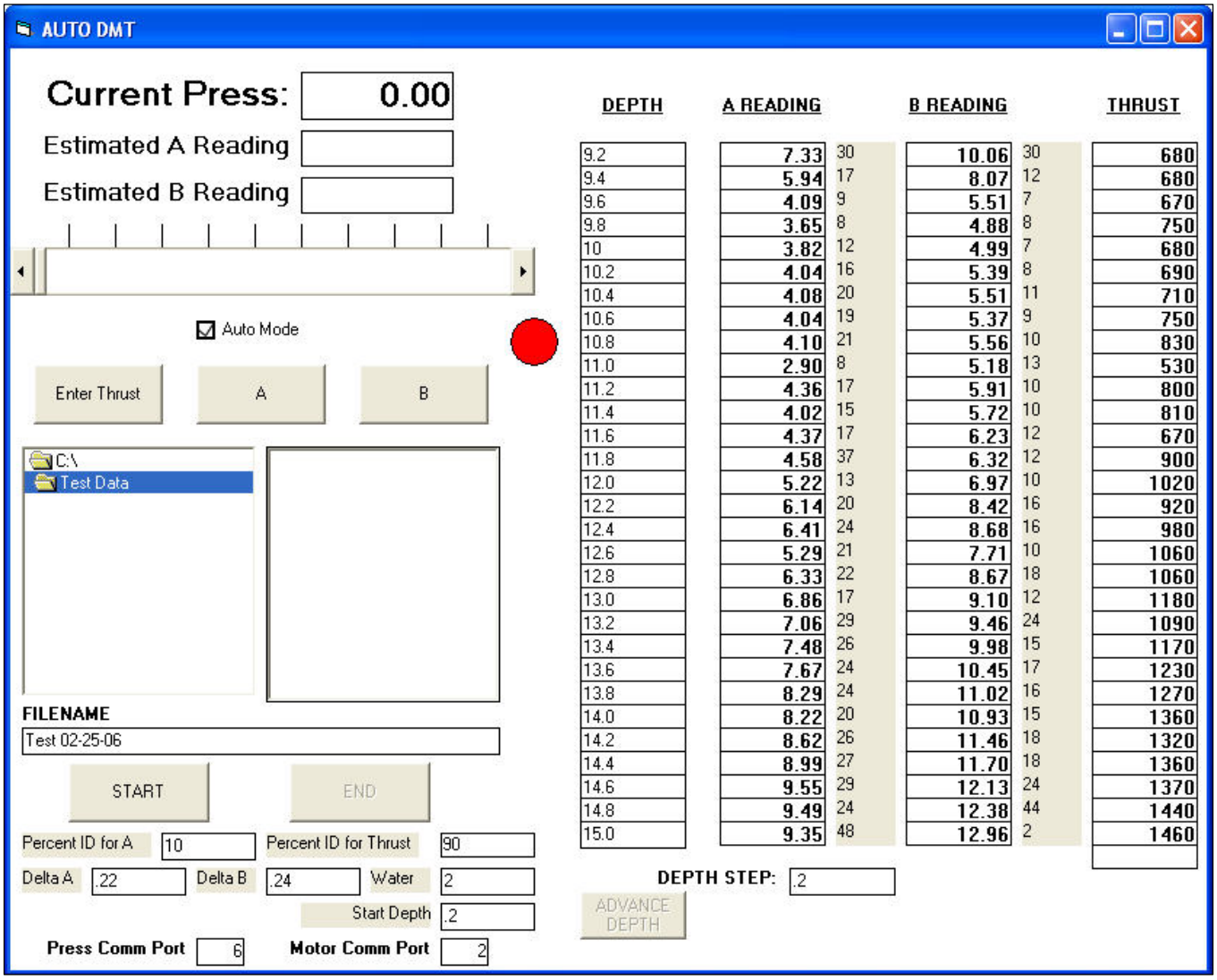

Figure 2: Screen shot of AutoDMT program

where A I_D is the predicted I_D based on the A reading, %A is the weighted percentage attributed to the A reading, Thrust I_D is the predicted I_D based on the thrust measurement, and %Thrust is the weighted percentage attributed to the thrust measurement. The sum of %A and %Thrust must equal 1.0. Based on the predicted overall I_D value, the predicted "B" reading is computed from the following:

$$B=\frac{I_D(1.05(A+\Delta A)+0.05\Delta B-U_0)+1.05(\Delta B+A+\Delta A)}{1.05+0.05I_D}$$

5 REVIEW OF EXISTING DATA

We analyzed five soundings with different geologic conditions to determine how many data points were needed to establish linear relationships for predicting the "A" and "B" readings. When determining the best linear fits, we reviewed the previous 5, 6, 7, 8, 9, 10 readings and all the previous readings. We found that the worst fits were when all the previous data were considered because the soil type and geostatic vertical and horizontal stresses change throughout the sounding. For predicting the "A" and "B" readings, the following table providing a summary of the review analyses:

Number of Previous Readings Used to Establish Best Fit	Number of Test Sites with Best "A" Reading Prediction	Number of Test Sites with Best "B" Reading Prediction
5	1	2
6	0	0
7	0	0
8	1	0
9	0	1
10	3	2
ALL	0	0

Table 1: Number of test soundings that had the best fit for the "A" and "B" reading predictions

Based on the review, we made additional adjustments to our method for predictions. For the thrust

reading prediction of "A" and "B" readings, the best fit slope should not be negative. For the same type of soil, for higher thrust readings one should get higher "A" and "B" readings. We accepted negative slopes for predicting I_D based on "A" readings because a hard clay can have a higher "A" reading and a lower I_D value than a sand. The minimum value of I_D that we allowed for predicting the "B" reading was 0.1.

We also found that the "A" reading was a better predictor of the "B" reading than the thrust. We preliminarily suggest using 70 to 80% of the "A" reading prediction and 20 to 30% of the thrust prediction when making the overall I_D prediction.

6 FLOW VALVE CONTROL

To get accurate data from the dilatometer tests, the engineer must accurately measure the pressure in the blade at the "A" and "B" signals. It takes some time for the pressure that is applied and measured at the surface to travel to the dilatometer blade. However, when the rate of flow is slow when the signals occur, these lag effects are minimized. With good programming a computer can do a better job at controlling the flow rate than an engineer.

We developed a program that uses the estimates of the "A" and "B" readings, described in the above sections, to determine flow rates. The following table contains the default inflation rates used by the computer:

Percent of Estimated "A" or "B" Reading	Elapsed Time (seconds)
50	3
60	4
70	5.5
80	8
90	11
100	15
>100	Same rate as from 90 to 100%

Table 2: Programmed flow rate for "A" and "B" readings

The default elapsed times are based on using an 18-meter long cable. For longer cable lengths the elapsed time factor should be changed (default value is 1.0). We suggest using a factor equal to the cable length divided by 18.

If the reading occurs in less than 3 seconds, the program considers the data to be poor and does not record them. The next test depth will have a default value of 0.1 meters more than the current depth.

After the "B" reading is obtained, the computer stops flow to the dilatometer blade. The operator has the choice of either venting the system with the toggle valve or deflating slowly and manually measuring the "C" reading. The "C" can then be input into the computer.

7 PROGRAM OPTIONS

The initial depth is assumed to be 0.2 meters and the initial test depth increment for the next test is assumed to be 0.2 meters. The actual test depth can be overwritten by the operator. The test depth interval for the next test will be the current test depth minus the previous test depth.

The groundwater depth in meters is input. The hydrostatic groundwater level, U_0, is used to predict the "B" reading and it is computed in bars as follows:

$$U_0 = (\text{test depth} - \text{groundwater depth})/10.2 \geq 0$$

The thrust measurement is manually read and input by the engineer. We chose this simplistic approach because of the variety of readout boxes for load cells. The computer always records the "A" and "B" readings. The data file is saved after each test.

The engineer can choose how many of the previous readings will be used for computing the estimated "A" and "B" readings. The default and suggested minimum value is 5. When the soil type changes, the engineer can reduce the number of readings to include only those readings from that soil type. This new number of readings now becomes the default value. The engineer can decide what percentage will come from the correlation with thrust and what remaining percentage will come from the "A" reading correlation. The values for the current test become the default value for the next test.

Before and after each sounding, the engineer is asked to input the ΔA and ΔB calibration readings. The program will then average the readings using the rounding down procedure (Marchetti, 1999) and save these values. If the membrane is torn while performing the sounding, the new values for ΔA and ΔB can be input if the sounding is continued. The initial ΔA and ΔB are used up to that depth; the new ΔA and ΔB readings are used below that depth.

8 INTERFACING WITH WINDMT PROGRAM

The final saved file will be an ASCII file that can be read by "WinDMT". At the start of the sounding the user is asked to input the heading information and analyses parameters. The information from the last sounding is used as the default values for the current sounding. The user may change any of these values. The file name is the job number plus sounding name. The file name can only be used once.

9 FIELD TEST

At the GeoService's test sites, which is the location of the conference's field exercise, we performed one dilatometer sounding using the manual control unit and one dilatometer sounding using the computer control unit. The soundings were 1.5 meter apart. The results of those sounding are presented in Figure 3.

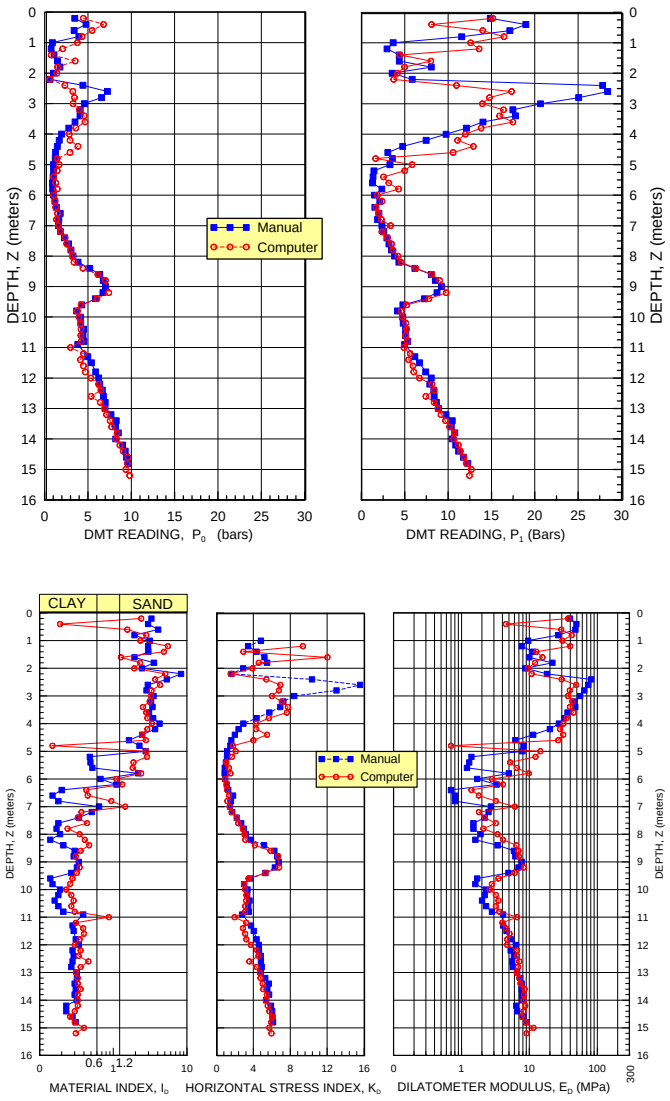

Figure 3: Dilatometer results from field tests

10 FUTURE UPGRADES:

1. Solenoid valve. The current setup of using a stepper motor closing and opening a valve worked well. However, there was still some flow with the valve fully closed, ie the stepper motor lacked the torque to completely close off the valve. For most soils the amount of flow was minimal enough to not pose a problem. However, in very soft soils it is conceivable that the flow could cause the A reading to trip before the program was able to detect it. A solenoid valve in conjunction with the stepper motor controlled valve would solve this potential problem. The solenoid valve would allow "C" readings to be taken automatically by the computer.

2. Microstepping motor. It was determined through field testing that a microstepping motor is better suited to various soil types than the current stepper motor. A microstepping motor with approximately 2000 steps / revolution would allow tighter control of the flow than the current motor which had 200 steps / revolution. This is especially true in soft soils where even minute changes in the flow can cause a percentage increase in the pressure that is beyond the desired speed.

3. Offloading of the stepper motor control to the microcontroller. In the current setup, the stepper motor is controlled by the PC reading the pressure every 100 ms. Based on the change in pressure, the computer sends a command specifying the motor position to the microcontroller. The microcontroller then advances the motor in the specified direction. If the pressure were to be read by the microcontroller, the lag time between reading the pressure and adjusting the motor could be reduced.

4. Replacing the digital pressure transducer with an analog pressure transducer. Coupled with #3 above, the microcontroller could read the analog output of a pressure transducer and convert it to digital in a fraction of the time required to read the pressure over the serial line. This would further reduce the lag time between reading the pressure and adjusting the motor. Furthermore, it would reduce the overall cost of the system.

5. Interfacing the thrust transducer to the unit. This will eliminate the requirement of the operator entering the thrust manually.

6. Adding sound to the program. While the indicator functions well enough to alert the operator to the change in state of the switch in the blade, an audible indicator may provide added "comfort" to operators familiar with the traditional DMT unit.

11 CONCLUSIONS

- The computer controlled dilatometer unit makes it easier to take and record the data. The test is less operator dependent and more accurate.
- Data processing time is reduced.
- Data comparisons between the computer control unit and the manual control unit from an experienced operator were excellent as was anticipated.

12 REFERENCES

GPE, Inc., "WinDMT Version 1.1 – Marchetti Dilatometer Test Data Reduction Program", Gainesville, FL, 2002

Marchetti, S., "On the Calibration of the DMT Membrane", L'Aquila University, International Technical Note, March 1999

Interpretation of SDMT tests in a transversely isotropic medium

S. Foti, R. Lancellotta
Politecnico di Torino, Italy

D. Marchetti
Studio Prof. Marchetti, Rome, Italy

P. Monaco, G. Totani
University of L'Aquila, Italy

Keywords: wave propagation, transversely isotropic medium, seismic dilatometer SDMT

ABSTRACT: This paper presents theoretical aspects of wave propagation in a transversely isotropic medium, aimed at providing a framework within which cross-hole (CH), down-hole (DH) and seismic dilatometer tests (SDMT) can be correctly interpreted. In particular, as an example, tests performed at the well documented Fucino site, with the source located at various distances from the sounding, indicate the capability of SDMT to detect the ratio G_{HH}/G_{VH}.

1 INTRODUCTION

The use of seismic methods for geotechnical site characterization is strongly motivated by the non invasive character of these tests, which preserve the initial structure of soil deposits and the major influence of all diagenetic phenomena (sutured contacts of grains, overgrowth of quartz grains, precipitation of calcite cements and authigenesis) contributing to a stiffer mechanical response, mainly at low strains (Jamiolkowski et al., 1985).

In addition, by noting that during depositional processes, soils usually experience one-dimensional deformation and the so-called initial anisotropy reflects this depositional history, it follows that a rather realistic model is, in this case, the cross-anisotropic body: the soil response is different if the loading direction changes from vertical to horizontal, but it is the same when changes occur in the horizontal plane (Hardin and Black, 1966). Seismic waves have been used to study soil anisotropy in the lab (Stokoe et al., 1980; Kuwano and Jardine, 2002). The velocity of propagation of seismic waves is influenced by both intrinsic and stress-induced anisotropy (Knox et al., 1982).

Starting from these remarks, this paper is aimed at presenting a consistent interpretation of SDMT tests, in order to detect the ratio of G_{HH}/G_{VH}.

Research currently in progress investigates the possible use of the SDMT for deriving "in situ" decay curves of soil stiffness with strain level (G-γ curves or similar). Such curves could be tentatively constructed by fitting "reference typical-shape" laboratory curves through two points, both obtained from SDMT: (1) the initial shear modulus G_0 from V_S, and (2) a modulus at "operative" strains, corresponding to the DMT constrained modulus M_{DMT} – provided the strain range corresponding to M_{DMT} is defined. Preliminary indications suggest that the shear strain range corresponding to M_{DMT} is ≈ 0.05-0.1% to 1 %.

Further developments are associated to the possibility of estimating soil porosity from combined measurements of compressional and shear wave velocities (Foti et al., 2002; Foti and Lancellotta, 2004).

2 A REMAINDER ON WAVE PROPAGATION

A wave can be seen as a perturbation propagating with a finite speed depending on the properties of the medium, and, for this reason, within the context of continuum mechanics, a wave can be considered as a singular surface for some fields.

By considering the constitutive equation

$$\sigma_{ik} = C_{iklm}\varepsilon_{lm} \tag{1}$$

where the small strain tensor ε_{lm} is defined as the symmetric part of the displacement gradient

$$\varepsilon_{lm} = \frac{1}{2}\left(\frac{\partial u_l}{\partial x_m} + \frac{\partial u_m}{\partial x_l}\right) \tag{2}$$

and the equation of the motion

$$\rho\ddot{u}_i = \rho b_i + \sigma_{ik,k} \tag{3}$$

(ρ is the soil density and b_i is the vector field representing the body forces per unit mass), it can be

proved, by applying the jump operator and by taking into account the continuity of the fields $\rho, u_i, u_{i,j}, b_i$, that the following equation is obtained

$$\left(C_{iklm} n_k n_l - \rho c^2 \delta_{im}\right) a_m = 0 \tag{4}$$

Equation (4) shows that the squared speed of the propagation are the eingenvalues of the acoustic tensor:

$$A_{im} = C_{iklm} n_k n_l \tag{5}$$

where n_i is the vector normal to the wavefront and a_m is the amplitude of particle motion, or polarization vector.

To analyse the geometrical character of wave propagation, let indicate, according to Love (1944), the non vanishing components of the stiffness tensor C_{ijhk} as

$$\begin{aligned} &C_{1111} = C_{2222} = A \\ &C_{3333} = C \\ &C_{3311} = C_{3322} = F \\ &C_{2323} = C_{1313} = L \\ &C_{1212} = N \\ &C_{1122} = C_{2211} = A - 2N \end{aligned} \tag{6}$$

To give the above elastic constant a physical meaning, we write the constitutive law (1) in the following form:

$$\begin{aligned} &\sigma_{xx} = A\varepsilon_{xx} + (A-2N)\varepsilon_{yy} + F\varepsilon_{zz} \\ &\sigma_{yy} = (A-2N)\varepsilon_{xx} + A\varepsilon_{yy} + F\varepsilon_{zz} \\ &\sigma_{zz} = F\varepsilon_{xx} + F\varepsilon_{yy} + C\varepsilon_{zz} \\ &\sigma_{xy} = 2N\varepsilon_{xy}; \quad \sigma_{yz} = 2L\varepsilon_{yz}; \quad \sigma_{xz} = 2L\varepsilon_{xz} \end{aligned} \tag{7}$$

so that it appears that N represents the shear modulus in the horizontal plane, i.e. G_{HH}, and L is the shear modulus in the vertical plane, i.e. G_{VH}.

Let now consider the case where the normal to the plane wavefront (direction of propagation) belongs to the vertical plane (x_1, x_3), i.e. $n_2 = 0$, the x_3 direction assumed to be the vertical one. In addition, suppose that the particle motion (direction of polarization) is given by the vector $\mathbf{a}(0,1,0)$. Then equation (4) reduces to

$$(C_{2112} n_1 n_1 + C_{2332} n_3 n_3 - \rho c^2) a_2 = 0 \tag{8}$$

If α is the angle between the direction of propagation and the vertical one, $n_1 = sin\alpha$ and $n_3 = \cos\alpha$, so that, by accounting for (6) and (7), the wave front propagates with a velocity equal to

$$c = \sqrt{\frac{G_{HH} sin^2\alpha + G_{VH} \cos^2\alpha}{\rho}} \tag{9}$$

In particular, if the direction of propagation is coincident with the x_1 axis, then the above results gives

$$c = \sqrt{\frac{G_{HH}}{\rho}} \tag{10}$$

a result which applies to cross-hole tests, when the induced shear waves is polarized in the horizontal plane (Stokoe and Woods, 1972; Ballard, 1976; Hoar and Stokoe, 1978).

On the contrary, if the direction of propagation is coincident with the x_3 axis, then

$$c = \sqrt{\frac{G_{VH}}{\rho}} \tag{11}$$

Now we observe that when dealing with down-hole tests or with SMDT tests (Auld, 1977; Hepton, 1988), the measured velocity of propagation is the one given by equation (9), i.e. it depends on both shear moduli in the vertical plane and the horizontal plane. Presumed that the direction of propagation has a negligible deviation from the vertical, the velocity of propagation can be assumed to depend mainly on G_{VH}. But even in this case, the relevant aspect to be outlined is that the direction of polarization must be coincident with the x_2 axis. If this is not the case, by using similar arguments, it can be proved that the velocity of propagation is a rather complicate function of 4 elastic constants, so that it is not easy to relate the measured wave velocity to soil parameters.

However, it is also apparent from equation (9) that, by performing tests at conveniently different distance between the source and the receiver, in order to change the direction of propagation, i.e. of the angle α, the obtained measurements allow to obtain values of G_{VH} and G_{HH}, as it is shown in the sequel.

3 SEISMIC DILATOMETER TESTS AT THE FUCINO SITE

The seismic dilatometer (SDMT) is a combination of the standard flat dilatometer (DMT) equipment with a seismic module for the downhole measurement of the shear wave velocity V_S.

First introduced by Hepton (1988), the SDMT was subsequently improved at Georgia Tech, Atlanta, USA (Martin and Mayne, 1997, 1998; Mayne et al., 1999). The test is conceptually similar to the seismic cone (SCPT) (Robertson et al., 1985).

Figure 1 shows a schematic layout of the SDMT equipment used in this study.

The seismic module (Figure 1a) is a cylindrical element placed above the DMT blade, equipped with two receivers located at 0.5 m distance.

The signal is amplified and digitized at depth.

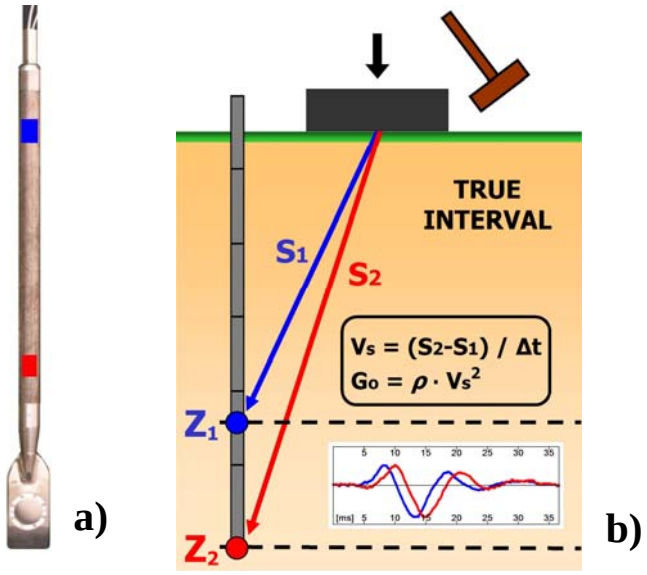

Figure 1. (a) DMT blade and seismic module. (b) Schematic layout of the seismic dilatometer test.

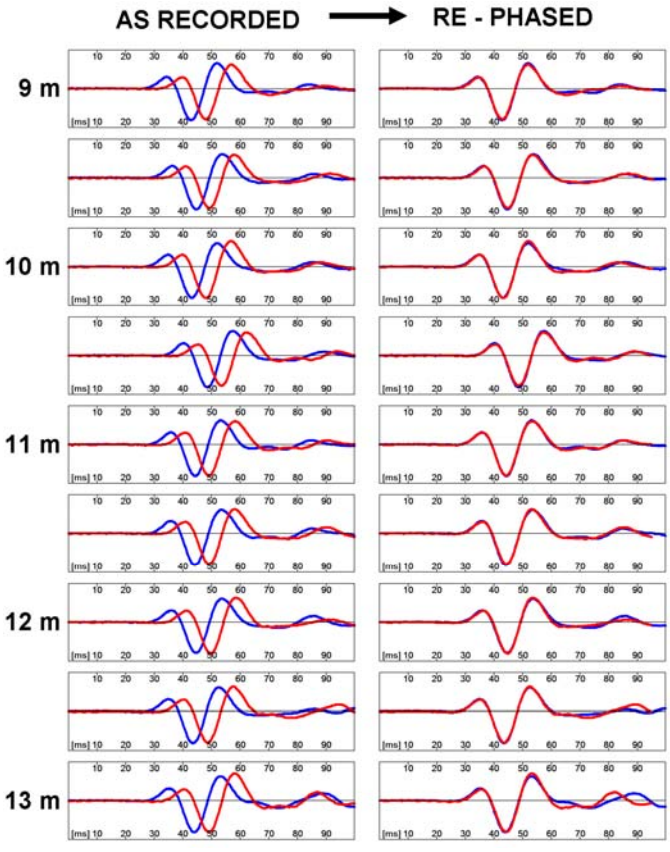

Figure 2. Example of seismograms obtained by SDMT at various test depths at the Fucino site (as recorded and re-phased according to the calculated delay)

The shear wave source at the surface is a pendulum hammer, of approximately 10 kg weight, which hits horizontally a steel rectangular base pressed vertically against the soil and oriented with its long axis (≈ 0.8 m) parallel to the axis of the receivers, so that they can offer the highest sensitivity to the generated shear wave.

The "true-interval" test configuration with two receivers avoids possible inaccuracy in the determination of the "zero time" at the hammer impact, sometimes observed in the "pseudo-interval" one-receiver configuration. Moreover, the couple of seismograms recorded by the two receivers at a given test depth (Figure 2) corresponds to the same hammer blow and not to different blows in sequence, not necessarily identical. Hence the repeatability of V_S measurements is considerably improved – observed V_S repeatability about 1 m/s.

The shear wave velocity V_S (Figure 1b) is obtained as the ratio between the difference in distance between the source and the two receivers (S_2 - S_1) and the delay of the arrival of the impulse from the first to the second receiver (Δt).

V_S measurements are obtained every 0.5 m of depth.

Seismic dilatometer tests were performed in 2004-2005 at the site of Fucino (Italy), a well-documented research test site, extensively investigated at the end of the '80s by means of several in situ and laboratory tests carried out by various research groups. Results of this investigation and a detailed characterization of the site can be found in AGI (1991).

The soil is constituted by a thick deposit of soft, homogeneous highly structured $CaCO_3$ cemented lacustrine clay of high plasticity.

The clay deposit is lightly overconsolidated. Based on geological evidence, this overconsolidation is most likely due to structure/aging, in particular to secondary consolidation and post-depositional diagenetic bonds caused by $CaCO_3$ cementation. In the upper few meters of the deposit, overconsolidation may be due in part also to groundwater level fluctuation (the water table is about 1 m below the ground surface).

The significant diagenetic bonds due to $CaCO_3$ cementation have a strong influence on most of the soil parameters obtained from the interpretation of in situ and laboratory tests in the Fucino clay (AGI, 1991). E.g. oedometer tests suggested a quantitative link between $CaCO_3$ content and OCR. A dependence of the undrained shear strength c_u on $CaCO_3$ content was evidentiated in particular by UU triaxial compression tests.

The values of the small strain shear modulus G_0 resulting from both laboratory and in situ seismic tests also appeared to be influenced by the $CaCO_3$ content.

Figure 3 shows the most significant profiles obtained by SDMT at the Fucino site.

The basic DMT parameters – material index I_D (soil type), constrained modulus M, undrained shear strength c_u and horizontal stress index K_D (related to stress history) – were obtained using current correlations (Marchetti, 1980).

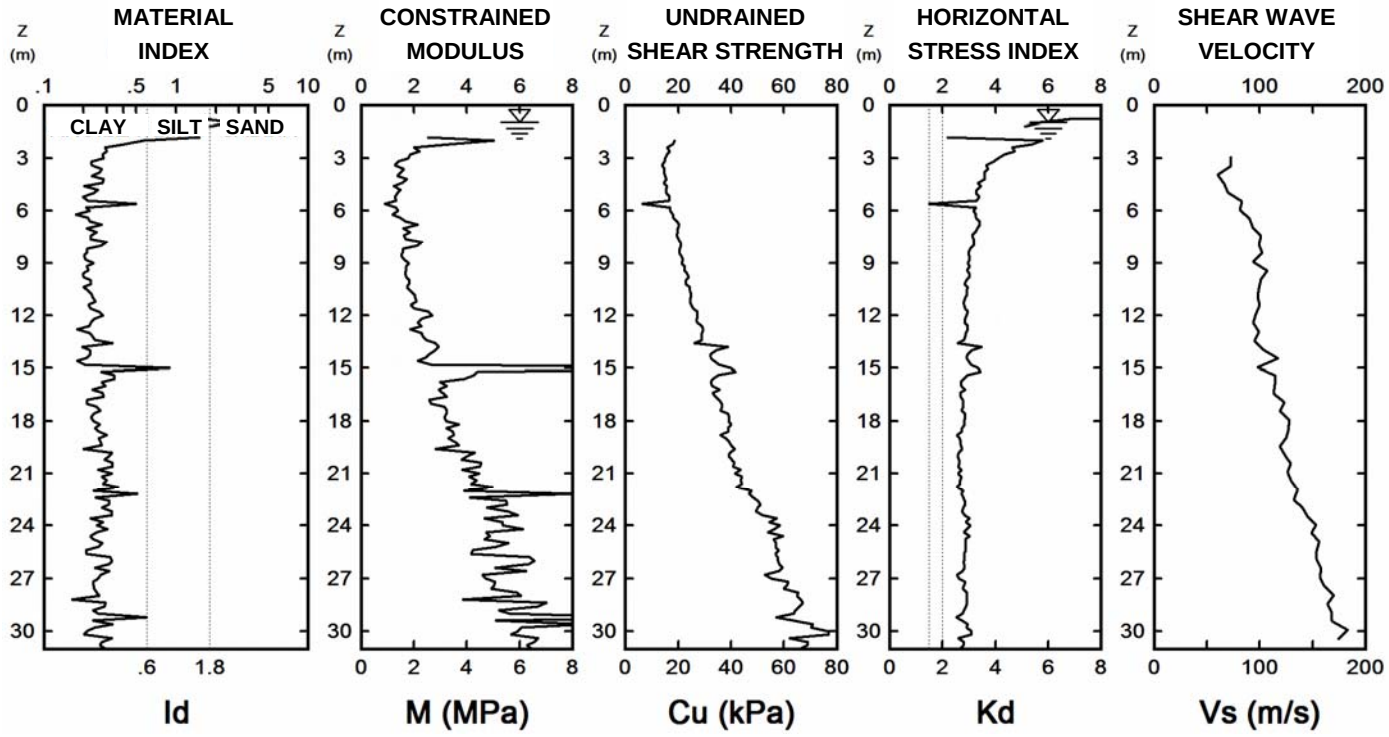

Figure 3. SDMT profiles at the Fucino site

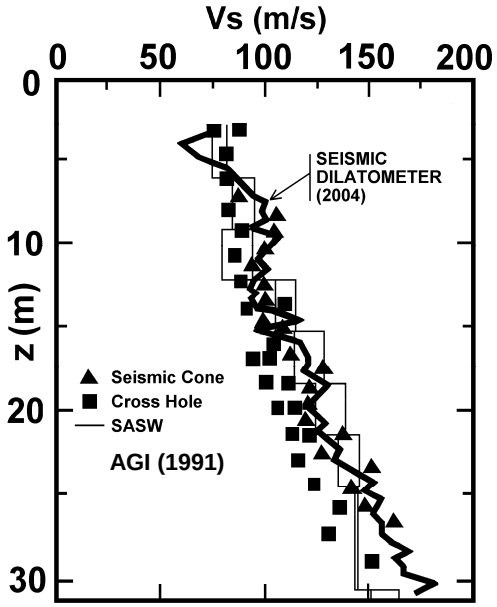

Figure 4. Comparison of V_S profiles obtained by SDMT and by other in situ seismic tests at the Fucino site (AGI, 1991)

The values of the horizontal stress index K_D (Figure 3) are ≈ 3 to 4, constant with depth. As indicated in TC16 (2001), if a geologically NC clay has $K_D > 2$, any excess of K_D above the value $K_D \approx 2$ (lower bound value for genuinely NC clays) indicates the likely existence of cementation/structure/aging. However the NC condition can be easily recognized, despite $K_D > 2$, because K_D does not decrease with depth as in OC deposits.

The profile of the shear wave velocity V_S obtained by SDMT, plotted in Figure 3, is also shown in Figure 4, superimposed to profiles of V_S obtained by seismic cone penetration tests (SCPT), cross-hole and SASW in previous investigations (AGI, 1991). The comparison in Figure 4 shows that V_S obtained by SDMT is in good agreement with V_S obtained by other methods.

4 ANISOTROPY RATIO FROM RESULTS AT THE FUCINO SITE

In order to explore the possibility of using Equation 9 to obtain G_{HH} and G_{VH} in anisotropic media a testing campaign has been planned at Fucino test site. To determine the two shear moduli, at least two independent evaluations of shear wave velocity are needed with different angle of incidence with respect to the receivers.

The experimental data have been collected using the usual SDMT configuration, repeating then the test for two additional shot locations as shown in Figure 5. The sources are placed along a straight line starting from the position of the SDMT probe and are orientated perpendicular to the line itself in order to detect primarily horizontally polarized shear waves (Figure 5a). The shear wave velocity obtained in each testing configuration has been associated to the angle of incidence corresponding to the hammer position and to the intermediate point in between the two receivers (Figure 5b).

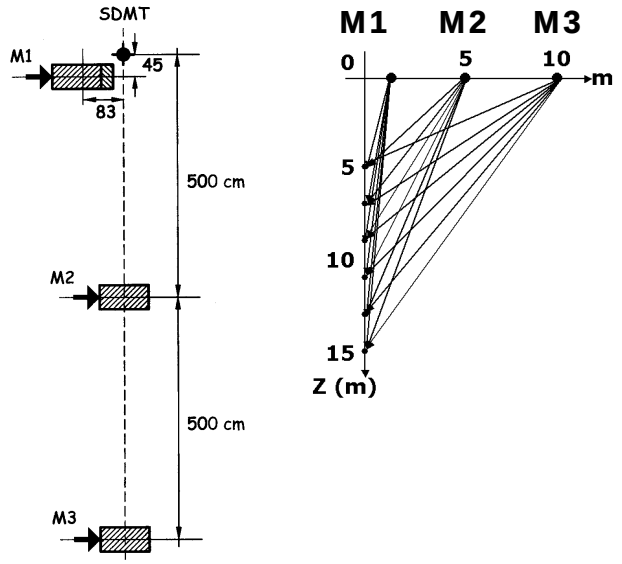

Figure 5. Test setup: a) Plan view b) Ray paths

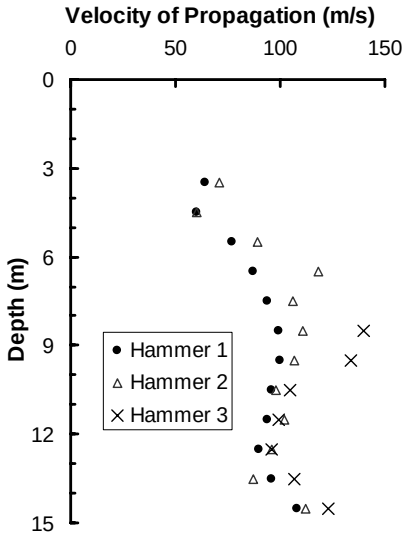

Figure 6. Shear wave velocity profiles

Shear wave velocity measurements have been performed at 1m interval from 3.5 to 14.5m, but the data for depth 3.5m to 7.5m for the third hammer (M3) are not used in the following because they showed unusual results.

The shear wave velocity profile obtained using a true interval interpretation of experimental data is reported in Figure 6. As explained in the previous section, these velocities have to be regarded as intermediate values between those pertinent to vertically traveling-horizontally polarized shear waves and horizontally traveling-horizontally polarized shear waves. Hence, assuming homogeneity of the medium in between the receiver position, in the case of an isotropic medium, the three velocities should coincide. The detected differences can be interpreted in the framework of anisotropic linear elasticity.

For depths from 3.5m to 7.5m only two measurements of V_S were available (from hammers M1 and M2), hence the shear moduli have been obtained directly by using Equation 9 and solving the system of 2 equations in two unknowns for each depth. For depths 8.5m to 14.5m, since three measurements were available for the determination of two parameters, an optimization procedure has been adopted, selecting the two values of the moduli at each depth such that the minimum difference in the least square sense was obtained between the experimental values and the velocities predicted with Equation 9 for the three available measurements.

The values of the shear moduli and their ratio are reported in Figure 7. Most of the results show a ratio of the two moduli ranging between 1 and 2, that seems reasonable for the site characteristics. Two values out of trend ranging between 3 and 4 are obtained for depth of 6.5m and 8.5m. There seem to be no coherent explanation for these values, which have been considered as experimental scatter.

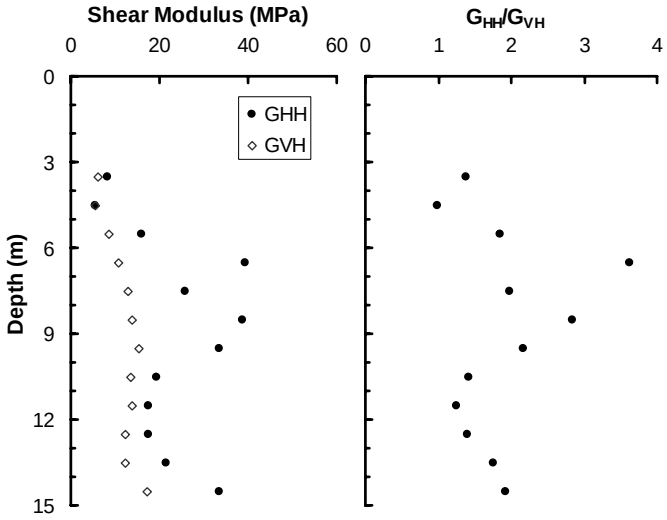

Figure 7. Shear Moduli obtained from measured V_S

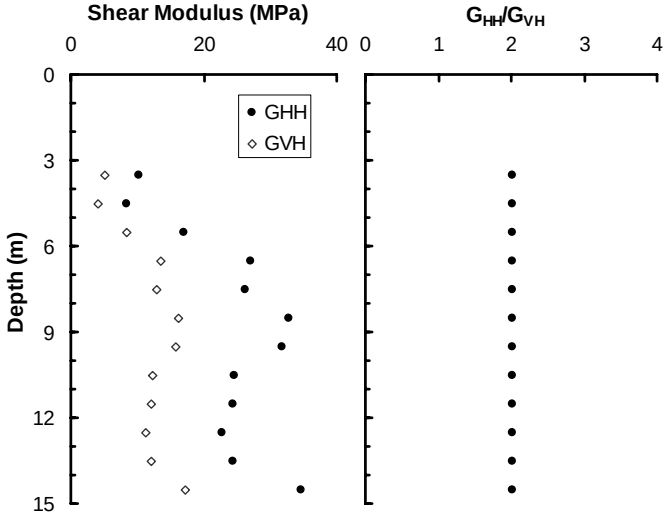

Figure 8. Shear Moduli obtained from measured V_S with the constraint G_{HH}/G_{VH} = constant

Considering the peculiarity of the experimental site, consisting of a very homogeneous soft clay, a second interpretation was attempted, imposing the condition of constant ratio between the shear moduli (G_{HH}/G_{VH} = constant). The ratio was one of the parameters in the optimization procedure together with one of the two moduli at each depth. The results are reported in Figure 8 and show a global value of G_{HH}/G_{VH} equal to 2.0.

5 CONCLUSIONS

From the operative viewpoint the described investigation has evidenced the following features of the seismic dilatometer:

- Simplicity of operation.
- High quality of the signals.
- Accurate determination of the shear wave velocity V_S.
- High repeatability.

From the interpretation viewpoint the investigation has shown that, if the SDMT is performed by placing the source, for each probe depth, both adjacent to the sounding and at conveniently different distances, the obtained SDMT measurements allow, on the basis of wave propagation theory for anisotropic media, to evaluate anisotropy, in particular to obtain values of G_{VH} and G_{HH}.

REFERENCES

AGI - Burghignoli A., Cavalera L., Chieppa V., Jamiolkowski M., Mancuso C., Marchetti S., Pane V., Paoliani P., Silvestri F., Vinale F. and Vittori E. 1991. Geotechnical Characterization of Fucino Clay. *Proc. X ECSMFE, Firenze,* 1, 27-40.

Auld B. 1977. Cross-Hole and Down-Hole Vs by Mechanical Impulse. *Journal of Geotechnical Engineering Division, ASCE,* 103, 12, 1381-1398.

Ballard R.F. Jr 1976. Method of Cross-Hole Seismic Testing. *Journal of Geotechnical Engineering Division, ASCE,* 102, 12, 1261-1273.

Foti S., Lai C. and Lancellotta R. 2002. Porosity of fluid-saturated porous media from measured seismic wave velocity. *Géotechnique,* 52, 5, 359-373.

Foti S. and Lancellotta R. 2004. Soil porosity from seismic velocities. *Géotechnique,* Technical Note, 54, 8, 551-554.

Hardin B.O. and Black W.L. 1966. Sand Stiffness Under Various Triaxial Stresses. *Journal of Soil Mechanics and Foundation Division, ASCE,* 92, 2, 27-42.

Hepton P. 1988. Shear wave velocity measurements during penetration testing. *Proc. Penetration Testing in the UK, ICE,* 275-278.

Hoar R.J. and Stokoe K.H. II 1978. Generation and Measurement of Shear Waves In Situ. *Dynamical Geotechnical Testing,* ASTM STP 654, 3-29.

Jamiolkowski M., Ladd C.C., Germain J.T. and Lancellotta R. 1985. New developments in field and laboratory testing of soils. *Theme Lecture, Proc. 11th ICSMFE, San Francisco,* 1, 57-152.

Knox D.P., Stokoe K.H. II and Kopperman S.E. 1982. Effect of state of stress on velocity of low-amplitude shear wave propagating along principal stress directions in dry sand. *Geotechnical Engineering Report GR 82-83,* Un. Texas, Austin.

Kuwano R. and Jardine R.J. 2002. On the applicability of cross-anisotropic elasticity to granular materials at very small strains. *Géotechnique,* 52, 10, 727-749.

Love A.E.H. 1944. A treatise on the mathematical theory of elasticity. Dover, New York. 644 pp.

Marchetti S. 1980. In Situ Tests by Flat Dilatometer. *ASCE Jnl GED,* 106, GT3, 299-321.

Martin G.K. and Mayne P.W. 1997. Seismic Flat Dilatometer Tests in Connecticut Valley Varved Clay. *ASTM Geotech. Testing Jnl,* 20(3), 357-361.

Martin G.K. and Mayne P.W. 1998. Seismic flat dilatometer in Piedmont residual soils. *Proc. 1st Int. Conf. on Site Characterization ISC'98, Atlanta,* 2, 837-843.

Mayne P.W., Schneider J.A. and Martin G.K. 1999. Small- and large-strain soil properties from seismic flat dilatometer tests. *Proc. 2nd Int. Symp. on Pre-Failure Deformation Characteristics of Geomaterials, Torino,* 1, 419-427.

Robertson P.K., Campanella R.G., Gillespie D. and Rice A. 1985. Seismic CPT to measure in situ shear wave velocity. *Proc. of Geotechnical Engineering Division Session on Measurement and Use of Shear Wave Velocity, Denver ASCE Convention,* 34-48.

Stokoe K.H. II, Roesset J.M., Knox D.P., Kopperman S.E. and Sudhiprakarn C. 1980. Development of a large scale triaxial testing device for wave propagation studies. *Geotechnical Engineering Report GR 80-10,* Un. Texas, Austin.

Stokoe K.H. II and Woods R.D. 1972. In situ wave velocity by cross-hole method. *Journal of Soil Mechanics and Foundation Division, ASCE,* 98, 5, 443-460.

TC16 - Marchetti S., Monaco P., Totani G. and Calabrese M. 2001. The Flat Dilatometer Test (DMT) in Soil Investigations - A Report by the ISSMGE Committee TC16. *Proc. Int. Conf. on In Situ Measurement of Soil Properties and Case Histories, Bali,* 95-131.

Using K_D and V_S from Seismic Dilatometer (SDMT) for evaluating soil liquefaction

Grasso S.
Department of Civil and Environmental Engineering, University of Catania, Italy

Maugeri M.
Department of Civil and Environmental Engineering, University of Catania, Italy

Keywords: Liquefaction; Seismic Dilatometer (SDMT); Horizontal Stress Index K_D; Shear Waves Velocity.

ABSTRACT: The Authors have collected in the recent years a large amount of data from site investigations in the city of Catania, which was struck in the past by severe earthquakes. At San Giuseppe La Rena, measurements of SPT, CPT and K_D and *Vs* using SDMT have been made in a saturated sandy soil. This paper presents K_D and *Vs* recommended relationships for sandy soils for potential liquefaction evaluation. When using semi-empirical procedures for evaluating liquefaction potential during earthquakes, it is important to use redundant correlations. The SDMT has the advantage, in comparison with CPT and SPT tests, by measuring independent parameters, K_D and *Vs*. CPT and SPT based correlations are supported by large databases, while SDMT correlations are based on a limited database. Based on the San Giuseppe La Rena SDMT measurements recent data, a re-evaluation of K_D and *Vs* correlations have been made.
The results show that *Vs* is less sensitive to potential liquefaction behaviour than K_D, which is, in contrast, very sensitive. The plotted correlations with critical values of K_D and *Vs* are suitable and very simple to use for detecting liquefaction potential.

1 INTRODUCTION

The coastal plain of the city of Catania (Sicily, Italy), which is recognized as a typical Mediterranean city at high seismic risk, was investigated by SDMT. Seismic liquefaction phenomena were reported by historical sources following the 1693 (M_s = 7.0-7.3, I_o = X-XI MCS) and 1818 (M_s = 6.2, I_o = IX MCS) Sicilian strong earthquakes. The most significant liquefaction features seem to have occurred in the Catania area, situated in the meisoseismal region of both events. These effects are significant for the implications on hazard assessment mainly for the alluvial flood plain just south of the city, where most industry and facilities are located.

For a new commercial building, deep site investigations have been performed, which included borings, SPT and CPT. More recently, at the same site, SDMT has been performed. The locations of the SPT, CPT and SDMT are reported in Fig. 1. SPT and CPT were located in the area where the commercial building has been built. The SDMT was performed after the construction of the building, and was located outside the construction area.

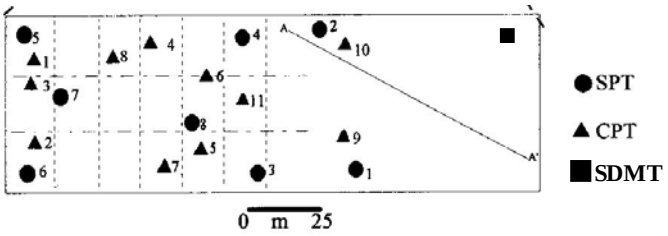

Fig. 1. Location of SPT, CPT and SDMT tests.

When using semi-empirical procedures for evaluation liquefaction potential during earthquakes, it is important to use redundant correlations. The SDMT has the advantage, in comparison with CPT and SPT, to measure independent parameters, such as K_D and V_S. Hence "matched" independent evaluations of liquefaction resistance can be obtained from K_D and from V_S according to recommended CRR-K_D and CRR-V_S correlations. CPT- and SPT-based correlations are supported by large databases, while SDMT correlations are based on a smaller database.

The liquefaction potential has been evaluated using empirical correlations with SPT and CPT, as well as by *Vs* and K_D measured by SDMT. From the comparison of the results, re-evaluations of K_D correlations have been made.

2 CURRENT METHODS FOR EVALUATING LIQUEFACTION POTENTIAL USING SPT AND CPT MEASUREMENTS

The traditional procedure, introduced by Seed & Idriss (1971), has been applied for evaluating the liquefaction resistance of San Giuseppe La Rena sandy soil. This method requires the calculation of the cyclic stress ratio CSR, and cyclic resistance ratio CRR. If CSR is greater than CRR, liquefaction can occur. The cyclic stress ratio CSR is calculated by the following equation (Seed & Idriss 1971):

$$CSR = \tau_{av}/\sigma'_{vo} = 0.65\,(a_{max}/g)\,(\sigma_{vo}/\sigma'_{vo})\,r_d \qquad (1)$$

where τ_{av} = average cyclic shear stress, a_{max} = peak horizontal acceleration at the ground surface generated by the earthquake, g = acceleration of gravity, σ_{vo} and σ'_{vo} = total and effective overburden stresses and r_d = stress reduction coefficient depending on depth. The r_d has been evaluated according to Liao and Whitman (1986).

The procedures used herein for the computation of the cyclic resistance ratio CRR are from Iwasaki et al.(1978) for SPT data and from Robertson and Wride (1997) for SPT and CPT.

The results of the SPT are reported in Fig. 2. $(N_1)_{60cs}$ according to Skempton (1986) assuming Ks= 1.5 according to Robertson and Wride (1997) are reported in Fig. 3.

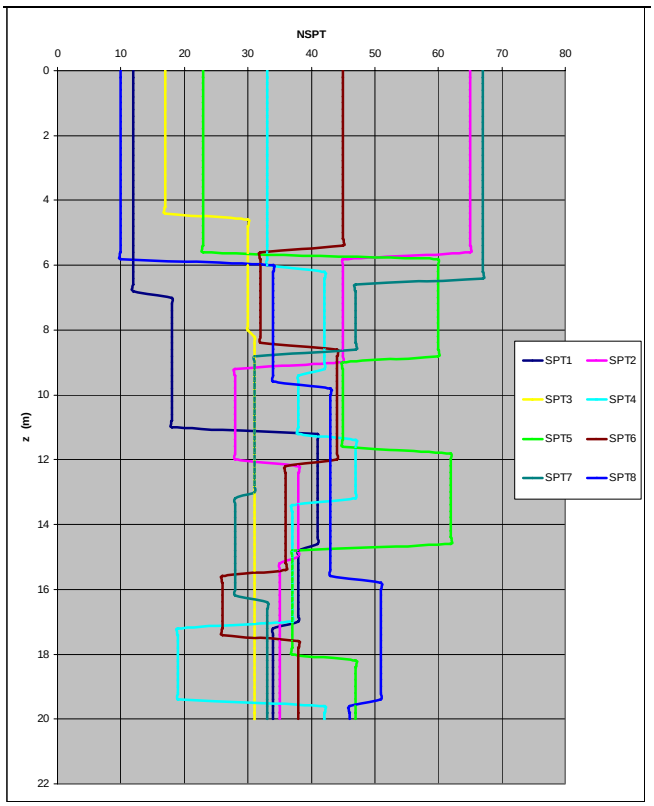

Fig. 2. N_{SPT} test results versus depth (8 profiles).

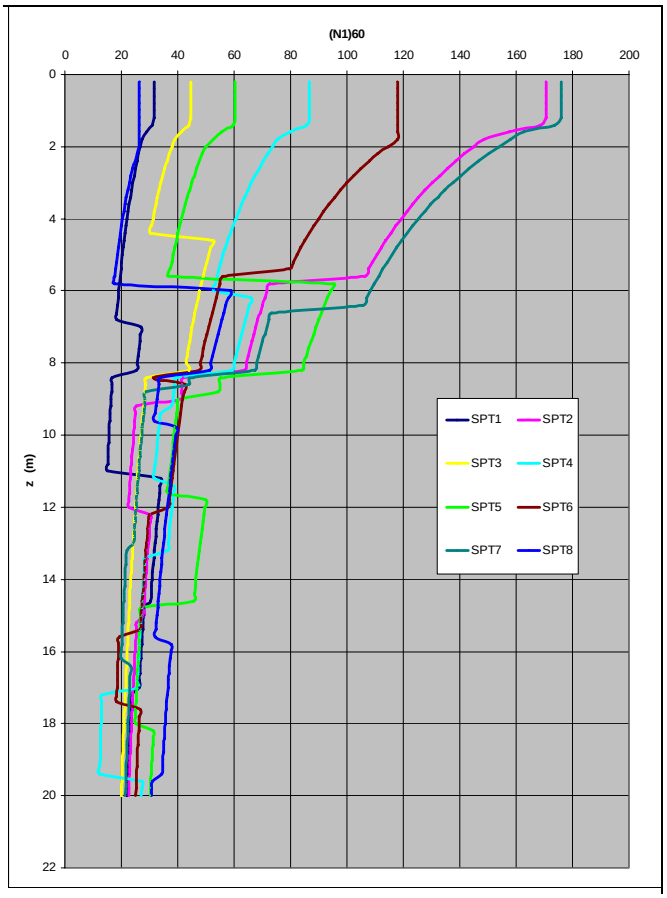

Fig. 3. $(N_1)_{60cs}$ test results versus depth assuming Ks= 1.5.

The results of CPT tests are reported in Fig. 4, and. $(qc_{1N})_{cs}$ according to Robertson and Wride (1997) are reported in Fig. 5.

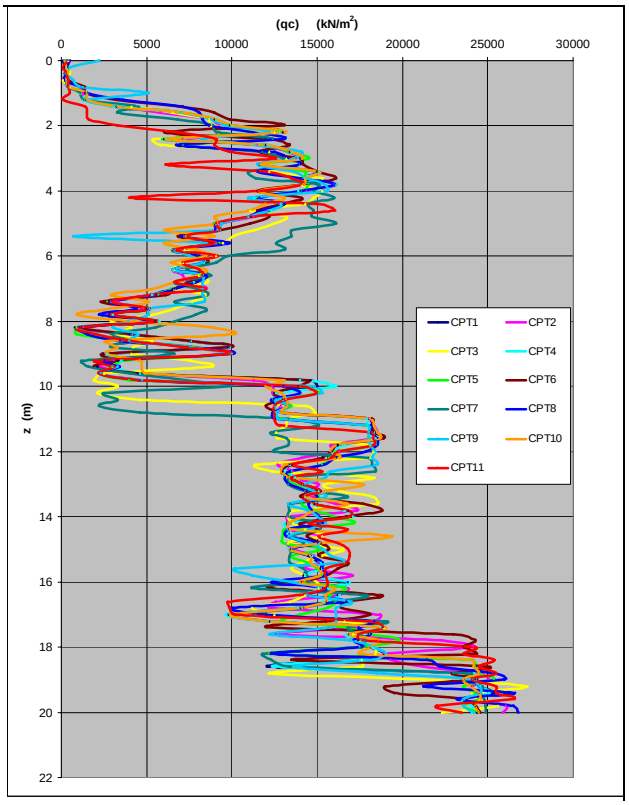

Fig. 4. q_c test results versus depth (11 profiles).

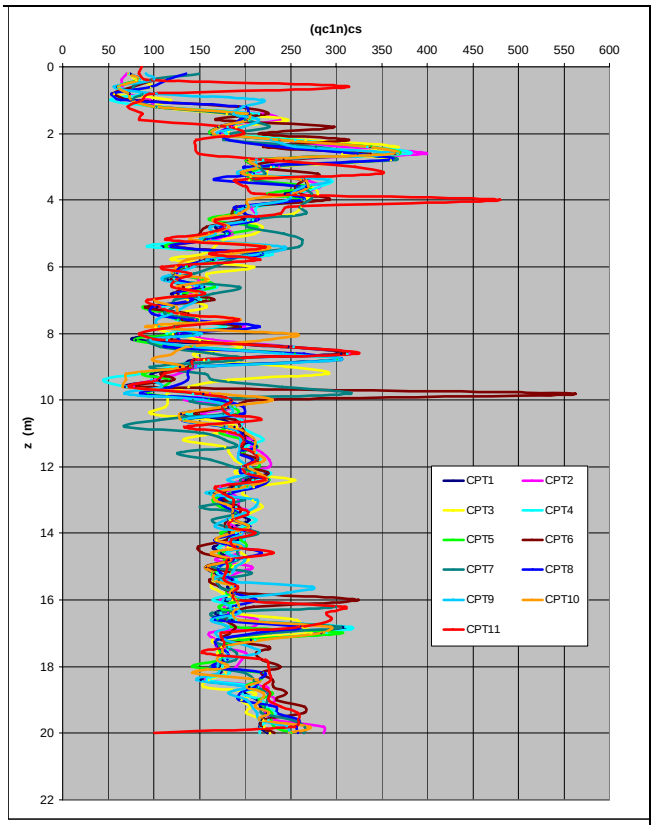

Fig. 5. $(qc_{1N})_{cs}$ test results versus depth.

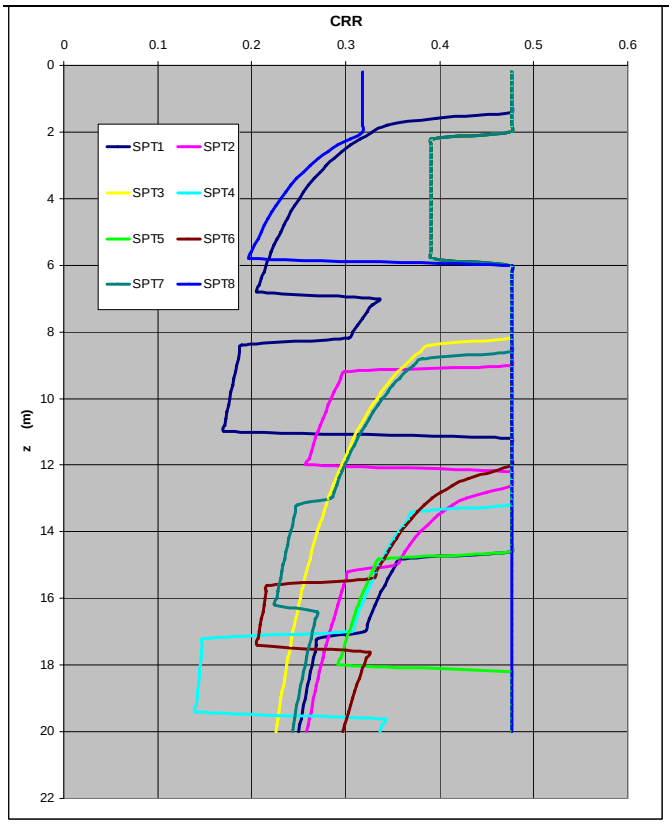

Fig. 6. $CRR_{7.3}$ for SPT data versus depth (8 profiles).

CRR for SPT data of Fig. 3 has been evaluated according to Robertson and Wride (1997) by the expression:

$$CRR_{7.5}=[a+cx+ex^2+gx^3]/[1+bx+dx^2+fx^3+hx^4] \quad (2)$$

CRR for CPT data of Fig. 5 has been evaluated according to Robertson and Wride (1997) by the expression:

$$CRR_{7.5} = 93\,[(qc_{1N})_{cs}/1000]3 + 0.08 \quad (3)$$

for $50 \le (qc_{1N})_{cs} < 160$.

The values of $CRR_{7.5}$ for SPT data and CPT data have been scaled to a magnitude of M= 7.3 according to Idriss (1985) by the following expression:

$$MSF = 10^{2.24}/M^{2.56} \quad (4)$$

The values of $CRR_{7.3}$ for SPT data, are reported in Fig. 6, and the values of $CRR_{7.3}$ for CPT data are reported in Fig. 7. CSR has been evaluated assuming in equation (1) a_{max} = 0.50g. The ratio CSR to CRR is called the liquefaction resistance factor (F_{SL}). Then is possible to evaluate the liquefaction potential index P_L (Iwasaki et al., 1978), given by the following expression:

$$P_L = \int_0^{20} F(z)w(z)dz \quad (5)$$

where w(z)= 10 – 0.5z and F(z) is a function of the liquefaction resistance factor (F_{SL}) and its values are: F(z)= 0 for $F_{SL} \ge 1$ and F(z)= 1 - F_{SL} for $F_{SL} < 1$. The liquefaction potential index, P_L, for the SPT test No. 1 is reported in Fig. 8.

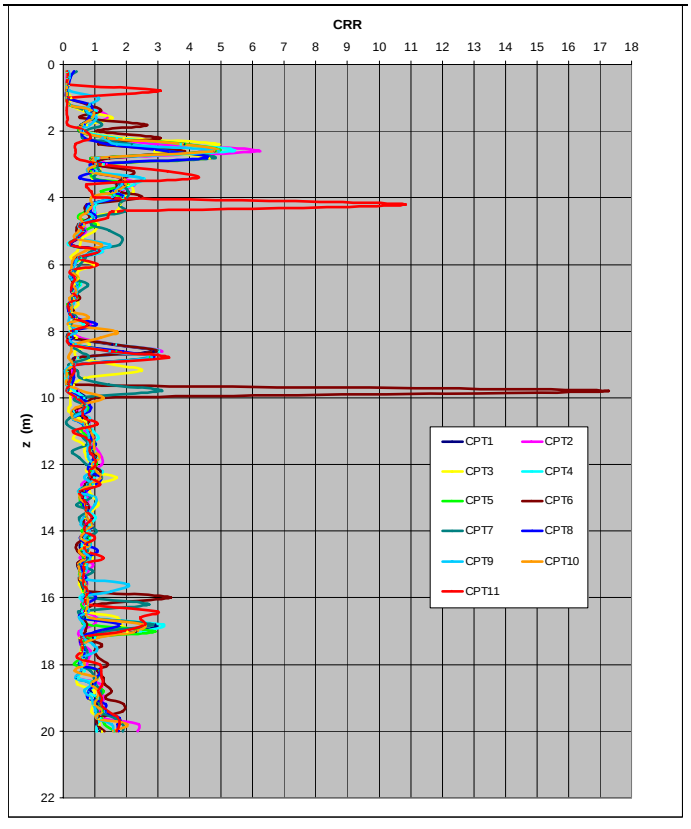

Fig. 7. $CRR_{7.3}$ for CPT data versus depth (11 profiles).

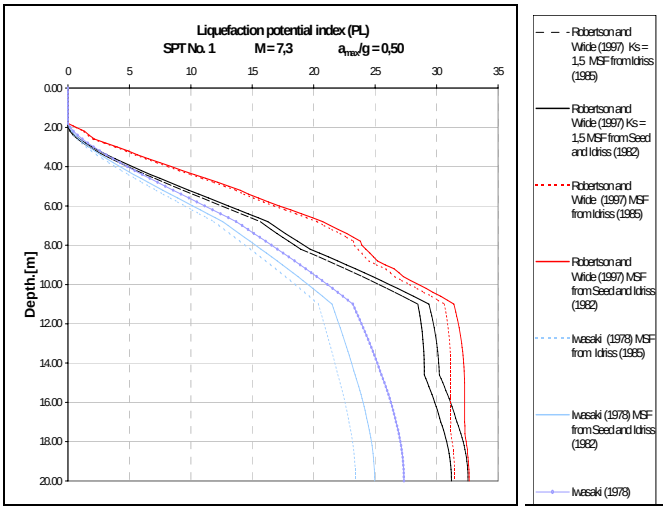

Fig. 8. P_L evaluation from SPT versus depth, for test No. 1.

From this figure the evaluation according to Robertson and Wride (1997), according to MSF given by Seed and Idriss (1982), is more conservative. In Fig. 9 is reported the evaluation of P_L for all the SPT tests assuming this most conservative evaluation criterion.

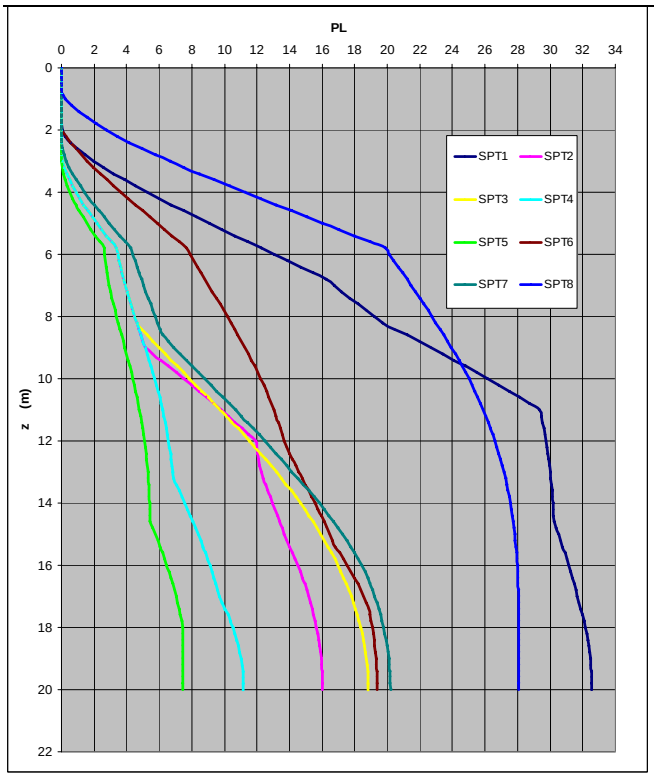

Fig. 9. The conservative P_L evaluation from SPT versus depth (8 profiles).

The liquefaction potential index, P_L, for the CPT test No. 1 is reported in Fig. 10. From this figure the evaluation according to Robertson and Wride (1997) and according to MSF given by Seed and Idriss (1982) is more conservative. In Fig. 11 is reported the evaluation of P_L for all the CPT tests assuming this most conservative evaluation criterion. From comparison of Fig. 9 with Fig. 11 the liquefaction potential index, P_L, is more conservative for SPT data. which reaches the average value of 30 than the CPT data, which reaches the average value of 15. From these values the liquefaction potential is very high for SPT data and high for CPT data (Maugeri and Vannucchi, 1999).

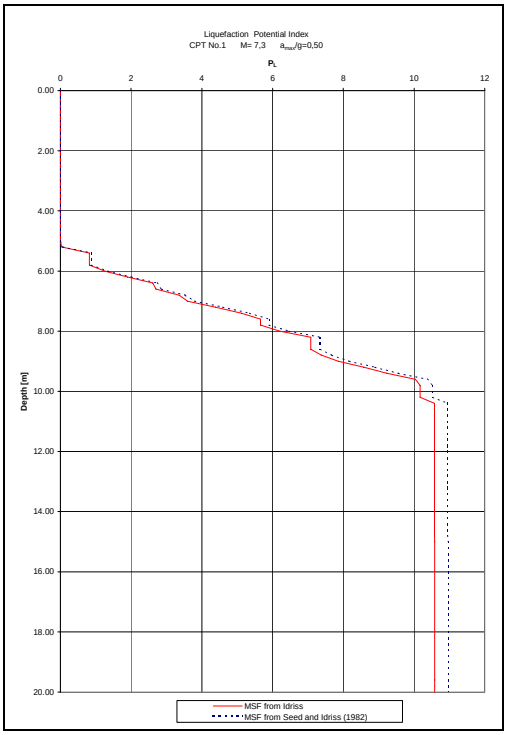

Fig. 10. P_L evaluation from CPT versus depth, for test No. 1.

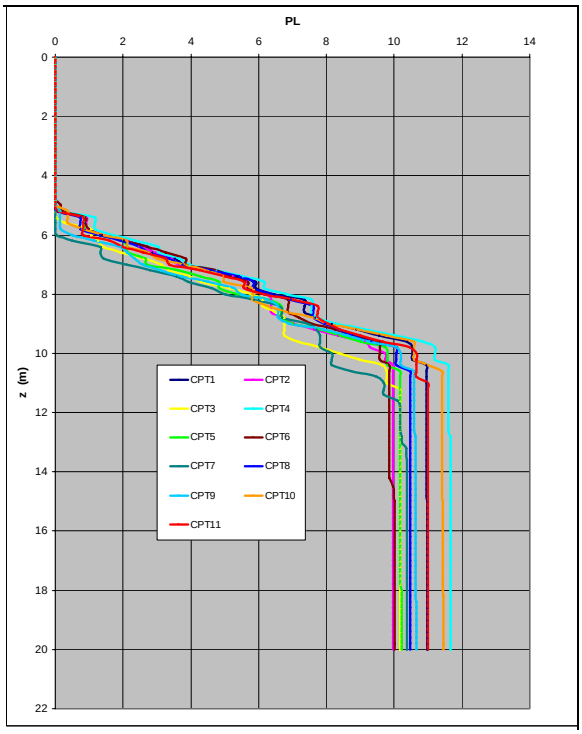

Fig. 11. The conservative P_L evaluation from CPT versus depth (11 profiles).

3 EVALUATION OF CRR FROM SHEAR WAVES VELOCITY V_S MEASURED BY SDMT

The use of the shear wave velocity, V_S, as an index of liquefaction resistance has been illustrated by several authors (Tokimatsu and Uchida, 1990; Kayen et al., 1992, Robertson et al., 1992, Lodge, 1994, Andrus and Stokoe, 1997, 2000; Robertson & Wride 1997; Andrus et al., 1999). The V_S based procedure for evaluating CRR has advanced significantly in recent years, and is included by the '96 and '98 NCEER workshops (Youd & Idriss 2001) in the list of the recommended methods for routine evaluation of liquefaction resistance. A comparison of some relationships between liquefaction resistance and overburden stress-corrected shear wave velocity for granular soils is reported in Fig. 12.

The correlation between V_S and CRR given by Andrus & Stokoe (1997, 2000) is:

$$\mathrm{CRR} = a\left(\frac{V_{S1}}{100}\right)^2 + b\left(\frac{1}{(V^*_{S1} - V_{S1})} - \frac{1}{V^*_{S1}}\right) \qquad (6)$$

Where: V^*_{s1} = limiting upper value of V_{s1} for liquefaction occurrence; $V_{S1} = V_S\,(p_a/\sigma'_{vo})^{0.25}$ is corrected shear wave velocity for overburden-stress; a and b are curve fitting parameters.

This correlation has been improved by Andrus et al. (2004). CRR is plotted as a function of an overburden-stress corrected shear wave velocity $V_{S1} = V_S\,(p_a/\sigma'_{vo})^{0.25}$, where V_S = measured shear wave velocity, p_a = atmospheric pressure (≈ 100 kPa), σ'_{vo} = initial effective vertical stress in the same units as p_a.

The relationship CRR-V_{S1} is approximated by the equation for $M_w = 7.5$:

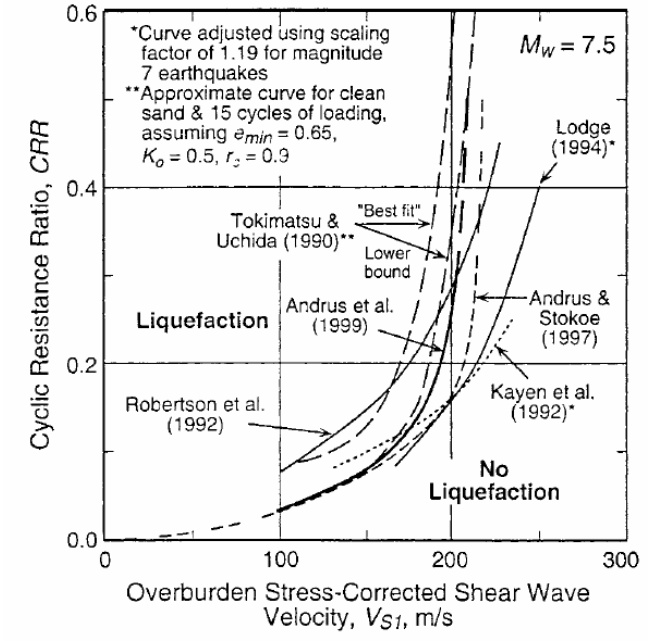

Fig. 12. Comparison of some Relationships between Liquefaction Resistance and Overburden Stress-Corrected Shear Wave Velocity for Granular Soils (Youd & Idriss 2001).

$$\mathrm{CRR}_{7.5} = \left[0.022\left(\frac{K_{a1}V_{S1}}{100}\right)^2 + 2.8\left(\frac{1}{V^*_{S1} - (K_{a1}V_{S1})} - \frac{1}{V^*_{S1}}\right)\right]K_{a2} \qquad (7)$$

where V^*_{S1} = limiting upper value of V_{S1} for liquefaction occurrence, assumed to vary linearly from 200 m/s for soils with fines content of 35% to 215 m/s for soils with fines content of 5% or less. K_{a1} is a factor to correct for high V_{S1} values caused by aging, K_{a2} is a factor to correct for influence of age on CRR. Both K_{a1} and K_{a2} are 1.0 for uncemented soils of Holocene age. For older soils the SPT- V_{S1} equations by Ohta & Goto (1978) and Rollins et al. (1998) suggest average K_{a1} values of 0.76 and 0.61, respectively, for Pleistocene soils (10,000 years to 1.8 million years). Lower-bound values of K_{a2} are based on the study by Arango et al. (2000).

Shear wave velocity can be measured in-situ by down-hole, cross-hole and the new SDMT. The profile of shear wave velocity measured by SDMT at the San Giuseppe La Rena sandy site is reported in Fig. 13. The evaluation of CRR according to equation 6 (Andrus & Stokoe, 2000) and equation 7 (Andrus et al., 2004), at San Giuseppe La Rena site is reported in Fig. 14. From Fig. 14 the CRR values given by equation 7 are lower than those given by equation 6, so therefore the evaluation given by equation 7 according to Andrus et al., 2004 is more conservative. Fig. 15 shows the evaluation of liquefaction potential index, P_L, according to Iwasaki et al., 1978, which shows that the liquefaction potential index, P_L, is more conservative for Vs data than SPT and CPT data. For Vs data P_L reaches the average value of 70 according to the evaluation of CRR given by Andrus et al., 2004 and the value of 40 according to the evaluation of CRR given by Andrus & Stokoe (1997). For these values of P_L the liquefaction potential is very high. If we plot the CRR

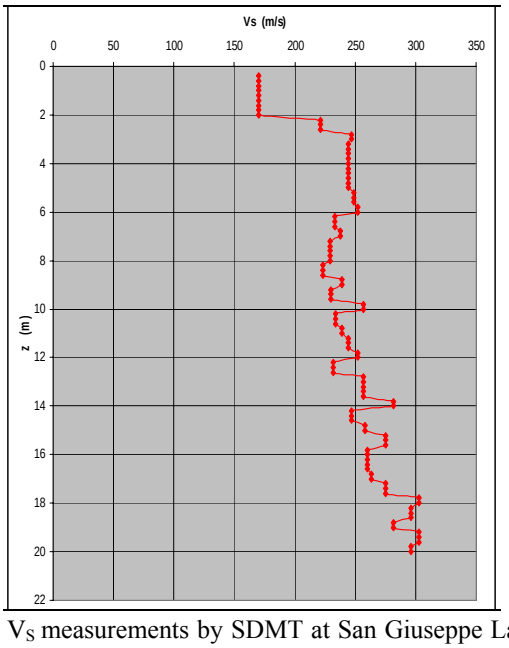

Fig. 13. V_S measurements by SDMT at San Giuseppe La Rena sandy site.

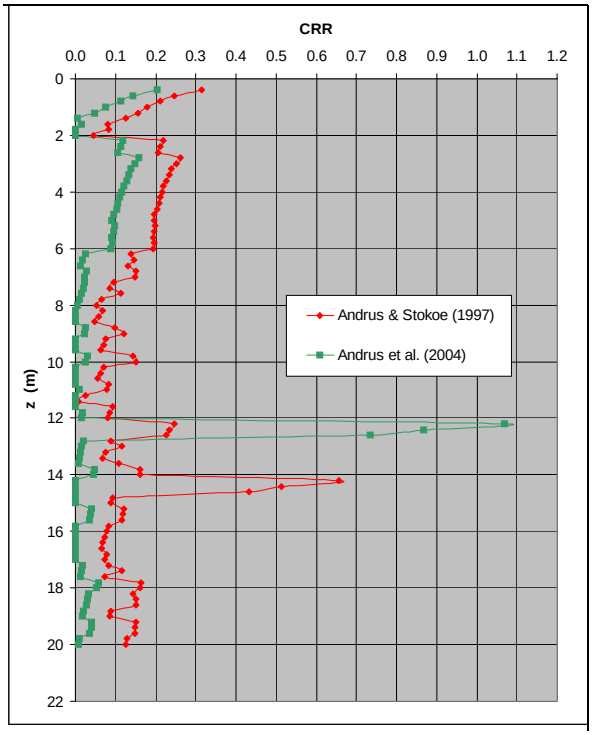

Fig. 14. Evaluation of CRR at San Giuseppe La Rena sandy site according to equation 6 and equation 7.

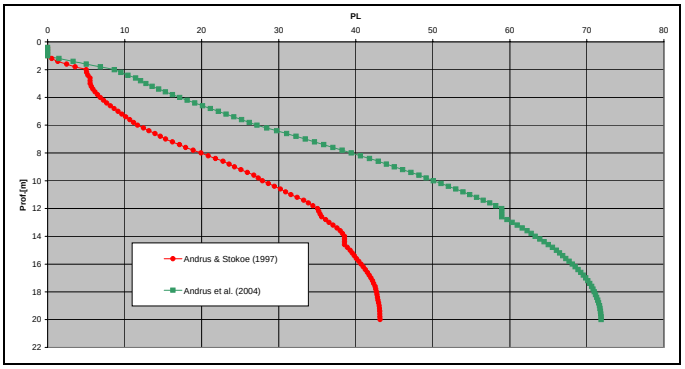

Fig. 15. Evaluation of Liquefaction potential Index P_L from V_s data at San Giuseppe La Rena sandy site.

results in the graphs of Fig. 12, the representative points lie on the border line between the liquefaction and non-liquefaction areas.

4 EVALUATION OF CRR FROM THE DMT HORIZONTAL STRESS INDEX K_D

Marchetti (1982) and later studies (Robertson & Campanella 1986, Reyna & Chameau 1991) suggested that the horizontal stress index K_D from DMT ($K_D = (p_o - u_o)/\sigma'_{vo}$) is a suitable parameter to evaluate the liquefaction resistance of sands.

Fig. 16 (Monaco et al. 2005) summarizes the various correlations developed to estimate CRR from K_D, expressed in form of CRR-K_D boundary curves separating possible "liquefaction" and "no liquefaction" regions.

Previous CRR-K_D curves were formulated by Marchetti (1982), Robertson & Campanella (1986) and Reyna & Chameau (1991) – the last one including liquefaction field performance data-points (Imperial Valley, South California).

A new tentative correlation for evaluating CRR from K_D, to be used according to the Seed & Idriss (1971) "simplified procedure", was formulated by Monaco et al. (2005) by combining previous CRR-K_D correlations with the vast experience incorporated in current methods based on CPT and SPT (supported by extensive field performance databases), translated using the relative density D_R as intermediate parameter.

Additional CRR-K_D curves were derived by translating current CRR-CPT and CRR-SPT curves (namely the "Clean Sand Base Curves" recommended by the '96 and '98 NCEER workshops, Youd & Idriss 2001) into "equivalent" CRR-K_D curves via relative density. D_R values corresponding to the normalized penetration resistance in the CRR-CPT and CRR-SPT curves, evaluated using current correlations (D_R -q_c by Baldi et al. 1986 and Jamiolkowski et al. 1985, D_R -N_{SPT} by Gibbs & Holtz 1957), were converted into K_D values using the K_D - D_R correlation by Reyna & Chameau (1991).

The "equivalent" CRR-K_D curves derived in this way from CPT and SPT (dashed lines in Fig. 16) plot in a relatively narrow range, very close to the Reyna & Chameau (1991) curve.

A new tentative CRR-K_D curve (bold line in Fig. 16), approximated by the equation:

$$\mathrm{CRR} = 0.0107\,K_D^3 - 0.0741\,K_D^2 + 0.2169\,K_D - 0.1306 \quad (8)$$

was proposed by Monaco et al. (2005) as "conservative average" interpolation of the curves derived from CPT and SPT.

Additional CRR-K_D curves for San Giuseppe La Rena coastal plain area were derived by translating current CRR-CPT and CRR-SPT curves into "equivalent" CRR-K_D curves via relative density.

D_R values, corresponding to the normalized penetration resistance in the CRR-CPT and CRR-SPT

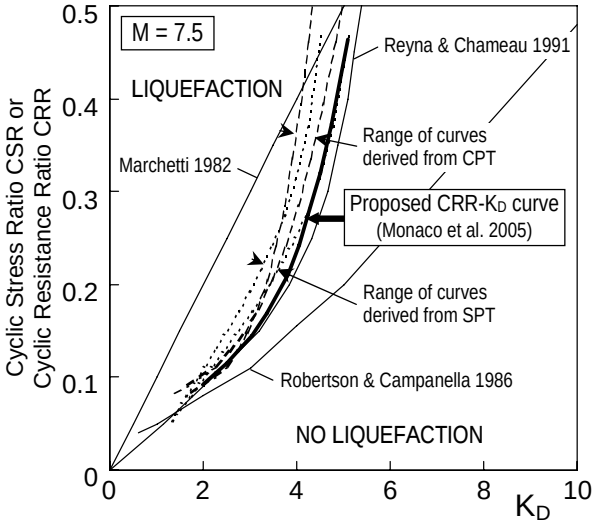

Fig. 16. CRR-K_D curves for evaluating liquefaction resistance from DMT (after Monaco et al. 2005).

curves, evaluated using current correlations (D_R -q_c by Baldi et al. 1986 and Jamiolkowski et al. 1985, D_R -N_{SPT} by Gibbs & Holtz 1957), were converted into K_D values using the K_D - D_R correlation by Reyna & Chameau (1991). Three new tentative CRR-K_D curves approximated by the equations:

$$CRR = 0.0908\,K_D^3 - 1.0174\,K_D^2 + 3.8466\,K_D - 4.5369 \quad (9)$$

$$CRR = 0.0308\,e^{(0.6054K_D)} \quad (10)$$

$$CRR = 0.0111\,K_D^{2.5307} \quad (11)$$

have been proposed by the authors as interpolation of the K_D curves derived from SPT and CPT.

Fig. 17 shows the variation with depth of K_D measured by SDMT and K_D obtained by empirical correlations for SPT and CPT data. The discrepancy of K_D results for top layers are due mainly to different location of SPT and CPT tests (located in the area before the construction of the industrial building) and SDMT located about 55 m from the constructed building. It is important to stress that the upper rigid crust (probably due to the increasing of clay content and to the presence of cemented layer) evidenced by K_D (Fig. 17) is not felt by V_s (see Fig. 13).

Fig. 18 shows the evaluation of CRR, for CPT No. 1, according to different correlations given by equations (8), (9), (10) and (11). Equation (8), given by Monaco et al. (2005) is the less conservative than the proposed equations (9), (10) and (11).

Fig. 19 shows the variation with depth of CRR given by correlation with SPT No. 1 and CPT No. 1 tests, performed at San Giuseppe La Rena test site. The CRR obtained by correlations with Vs, according to Andrus & Stokoe (1997) and to Andrus et al. (2004), show that the correlations with Vs give lower and more conservative CRR values.

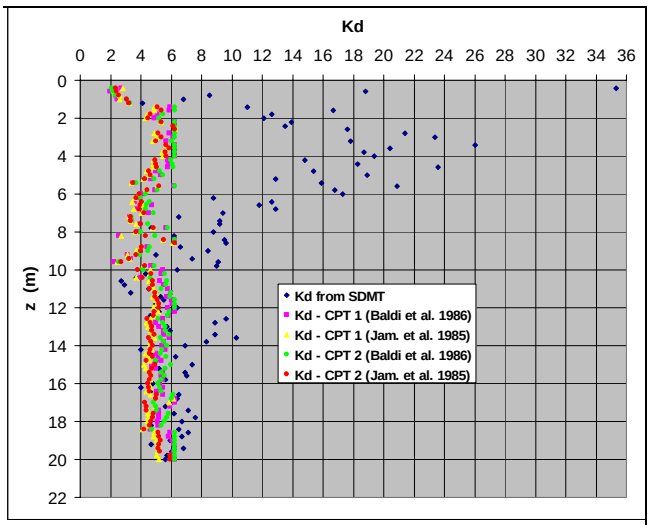

Fig. 17. K_D versus depth from SDMT and from empirical correlations for CPT test No. 1 and test No. 2 data.

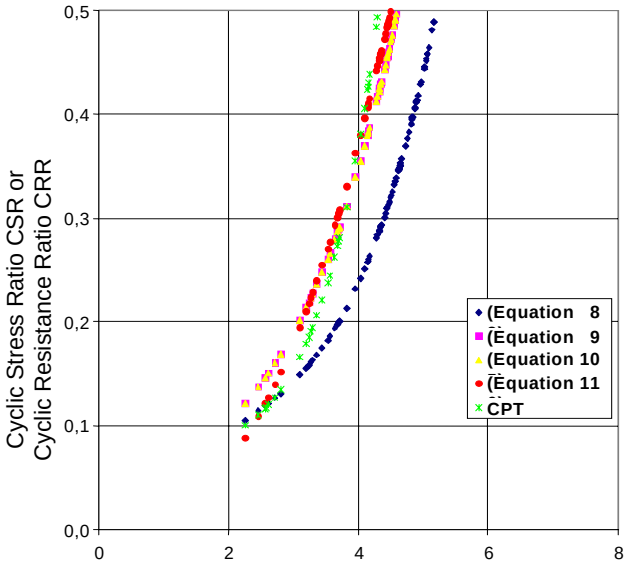

Fig. 18. CRR-K_D curves given by different correlations for CPT test No. 1.

For the evaluation of liquefaction potential index, P_L, (Iwasaki et al., 1978), the correlations given by equations (8), (9), (10) and (11) use the K_D values measured by SDMT instead of the correlations by SPT and CPT because of the presence of the upper rigid crust was not measured by Vs or by SPT and CPT.

Fig. 20 shows that the evaluation of the liquefaction potential index, P_L, is less than 5 because this method took into consideration the presence of the rigid upper crust. Therefore, the liquefaction potential is low for K_D data, according to Fig. 16 (representative point CRR=0.4 and K_D=10), while it was high for CPT data and very high for SPT and Vs data.

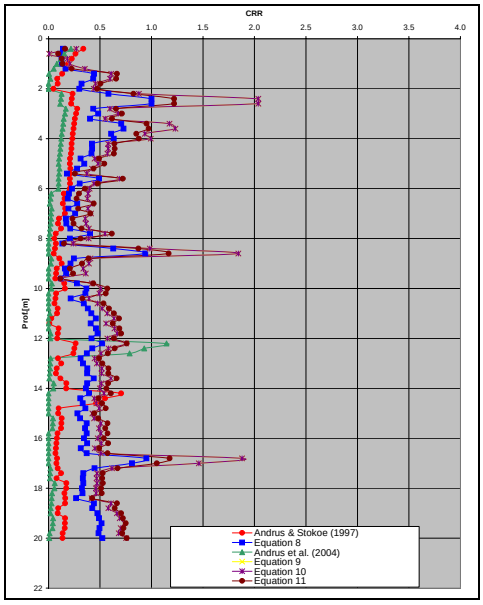

Fig. 19. CRR. with depth, from CPT, K_D and V_S data from SDMT, at San Giuseppe la Rena test site.

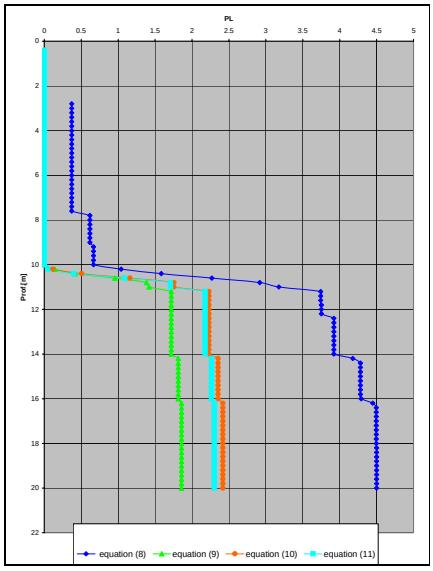

Fig. 20. Evaluation of Liquefaction potential Index P_L from K_D data at San Giuseppe La Rena sandy site.

5 CONCLUSIONS

SDMT gives the possibility to use two independent measurements V_s and K_D for evaluating soil liquefaction. The test performed at San Giuseppe La Rena, Catania, Italy, gave some contrasting results. When using the V_s or SPT data, the liquefaction potential index, P_L, is very high, and P_L is high for the CPT data. When using K_D data, however, P_L is low because K_D detected the upper rigid crust, which was overlooked by V_s, SPT and CPT measurements.

REFERENCES

Andrus, R.D. & Stokoe, K.H., II. 1997. Liquefaction resistance based on shear wave velocity. *Proc. NCEER Workshop on Evaluation of Liquefaction Resistance of Soils*, *Technical Report NCEER-97-0022*, T.L. Youd & I.M. Idriss, eds., National Center for Earthquake Engineering Research, Buffalo, 89-128.

Andrus, R.D. & Stokoe, K.H., II. 2000. Liquefaction resistance of soils from shear-wave velocity. *Jnl GGE*, ASCE, 126(11), 1015-1025.

Andrus, R.D., Stokoe, K.H., II, & Juang, C.H. 2004. Guide for Shear-Wave-Based Liquefaction Potential Evaluation. *Earthquake Spectra*, 20(2), 285-305.

Arango, I., Lewis, M. R. & Kramer, C. 2000. Updated liquefaction potential analysis eliminates foundation retrofitting of two critical structures. *Soil Dyn. Earthquake Eng.* 20, 17–25.

Baldi, G., Bellotti, R., Ghionna, V., Jamiolkowski, M. & Pasqualini, E. 1986. Interpretation of CPT and CPTUs. 2nd part: Drained penetration of sands. *Proc. 4th Int. Geotech. Seminar*, Singapore, 143-156.

Gibbs, K.J. & Holtz, W.G. 1957. Research on determining the density of sands by spoon penetration testing. *Proc. IV ICSMFE*, 1, 35-39.

Iwasaki, T., Tatsuoka, F., Tokida, K. & Yasuda, S. 1978. A practical method for assessing soil liquefaction potential based on case studies at various sites in Japan. *Proc 2nd Int Conf on Microzonation for Safer Construction, Research and Application*, San Francisco, California, 2, 885-896.

Jamiolkowski, M., Baldi, G., Bellotti, R., Ghionna, V., & Pasqualini, E. 1985. Penetration resistance and liquefaction of sands. *Proc. XI ICSMFE*, San Francisco, 4, 1891-1896.

Kayen, R. E., Mitchell, J. K., Seed, R. B., Lodge, A., Nishio, S., and Coutinho, R. 1992. Evaluation of SPT-, CPT-, and shear wave-based methods for liquefaction potential assessment using Loma Prieta data. Proc., 4th Japan-U.S. Workshop: Earthquake-Resistant Des. of Lifeline Fac. and Countermeasures for Soil Liquefaction, Vol.1, 177–204.

Liao, S. S. C., and Whitman, R. V. 1986. Catalogue of liquefaction and non-liquefaction occurrences during earthquakes.Res. Rep., Dept. of Civ. Engrg., Massachusetts Institute of Technology, Cambridge, Mass.

Lodge, A. L. 1994. Shear wave velocity measurements for subsurface characterization. PhD thesis, Univ. of Berkeley.

Marchetti, S. 1982. Detection of liquefiable sand layers by means of quasi-static penetration tests. *Proc. 2nd European Symp. on Penetration Testing*, Amsterdam, 2, 689-695.

Maugeri M., Vannucchi G. 1999. Liquefaction risk analysis at S.G. La Rena, Catania, (Italy). *Earthquake Resistant Engineering Structures*, Catania, 15-17 June, 1999, 301-310.

Monaco, P., Marchetti, S., Totani, G. & Calabrese, M. 2005. Sand liquefiability assessment by Flat Dilatometer Test (DMT). *Proc. XVI ICSMGE*, Osaka, 4, 2693-2697.

Ohta,Y., & Goto, N. 1978. Empirical shear wave velocity equations in terms of characteristic soil indexes. *Earthquake Eng. Struct. Dyn.* 6, 167–187.

Reyna, F. & Chameau, J.L. 1991. Dilatometer Based Liquefaction Potential of Sites in the Imperial Valley. *Proc. 2nd Int. Conf. on Recent Adv. in Geot. Earthquake Engrg. and Soil Dyn.*, St. Louis, 385-392.

Robertson, P.K. & Campanella, R.G. 1986. Estimating Liquefaction Potential of Sands Using the Flat Plate Dilatometer. *ASTM Geotechn. Testing Journal*, 9(1), 38-40.

Robertson, P.K., Woeller, D.J. & Finn, W.D.L. 1992. Seismic cone penetration test for evaluating liquefaction potential under cyclic loading. *Canadian Geotech. Jnl*, 29, 686-695.

Robertson, P.K. & Wride, C.E. 1997. Cyclic liquefaction and its evaluation based on SPT and CPT. *Proc. NCEER Workshop on Evaluation of Liquefaction Resistance of Soils*, *Technical Report NCEER-97-0022*, T.L. Youd & I.M. Idriss, eds., National Center for Earthquake Engineering Research, Buffalo, 41-88.

Rollins, K. M., Diehl, N. B., & Weaver, T. J. 1998. Implications of V_S-BPT $(N_1)_{60}$ correlations for liquefaction assessment in gravels. *Geotechnical Earthquake Engineering and Soil Dynamics III*, Geotech. Special Pub. No. 75, P. Dakoulas, M. Yegian, and B. Holtz, eds., ASCE, I, 506–517.

Seed, H.B. & Idriss, I.M. 1971. Simplified procedure for evaluating soil liquefaction potential. *Jnl GED*, ASCE, 97(9), 1249-1273.

Seed, H. B., and Idriss, I. M. 1982. Ground motions and soil liquefaction during earthquakes. Earthquake Engineering Research Institute Monograph, Oakland, Calif.

Skempton, A. K. 1986. Standard penetration test procedures and the effects in sands of overburden pressure, relative density, particle size, aging, and overconsolidation. Geotechnique, London, 36(3), 425–447.

Tokimatsu, K., and Uchida, A. 1990. Correlation between liquefaction resistance and shear wave velocity. Soils and Found., Tokyo, 30(2), 33–42.

Youd, T.L. & Idriss, I.M. 2001. Liquefaction Resistance of Soils: Summary Report from the 1996 NCEER and 1998 NCEER/NSF Workshops on Evaluation of Liquefaction Resistance of Soils. *Jnl GGE* ASCE, 127(4), 297-313.

BACK

TDR/DMT Characterization of a Reservoir Sediment under Water

An-Bin Huang and Chih-Ping Lin
Department of Civil Engineering, National Chiao Tung University, Hsin Chu, TAIWAN

Keywords: DMT, time domain reflectometry, sediment, in situ density, stress state

ABSTRACT: The Shihmen Reservoir, completed in early 1960's, has been an important hydro project in Northern Taiwan. Soil erosion and sediment have been a major concern for the longevity of the reservoir. After a series of typhoons in 2004, the intake valve of the hydro power plant was covered by 10m of sediment. The power generation has been halted since then. The intake valve was originally designed to be operated in clean water. In order to evaluate the feasibility of re-opening the power plant intake valve, it was necessary to know the density state of the sediment (referred to locally as the bottom mud) and the lateral pressure exerted on the intake valve. The center of the intake valve was at approximately 70m below water. A testing device that consisted of a time domain reflectometry (TDR) probe placed on top of the Marchetti dilatometer (DMT) was developed by the authors to determine simultaneously, the solid concentration, stiffness and stress state of the bottom mud. The TDR/DMT probe was attached to a string of 90m long drill rods. A skid mount drill rig bolted to a barge was used to control the drill rods. The weight of the drill rods was sufficient to push the TDR/DMT probe into the bottom mud. TDR and DMT readings were taken from 60 to 80m below water. The conductivity measurement from the TDR probe was used to determine the solid concentration. The lateral stress was inferred from the DMT P_o readings. The difference between p_o and p_1 was used to determine the density state of the bottom mud. Ten DMT profiles were taken, five of them had TDR readings. The paper describes field set up of the TDR/DMT probe, its test procedure and interpretation of the test results.

1 INTRODUCTION

Shihmen Reservoir is a multi-purpose water resources project, for irrigation, power generation, water supply, flood control and tourism. The Shihmen Dam is an earth-filled dam situated at approximately 50 km south east of Taipei. Since plugging of the diversion tunnel in May, 1963, the hydro-project has made significant contributions to northern Taiwan in agricultural production, industrial and economic developments, as well as alleviating flood or drought losses. The watershed of Shihmen Reservoir has characteristics of being steep in slopes and weak in geologic formations. As a result, during heavy storms, severe surface erosions coupled with land slides often occur. Since its completion in 1963, reservoir siltation has gradually increased, in spite of measures taken on dredging and construction of silt retention structures. The reservoir was designed to have a total storage of 309 million m^3 (volume of water that can be stored in the reservoir) and an effective storage of 252 million m^3 (volume of water above the intake level). As of March of 2004, the total storage had been reduced to 253 million m^3 and the effective storage was 238 million m^3. Aere Typhoon invaded northern Taiwan in August, 2004. The event caused an average rainfall of 973mm in the watershed which resulted in a total landslide area of 854 hectares, and an estimated inflow of approximately 28 million m^3 of sediments into the Reservoir. This has caused severe impacts on normal operation and useful life of the Reservoir. One of the immediate impacts was that the intake valve of the hydro power plant was covered by 10m of sediment. The power generation has been halted since then. The intake valve with its center at approximately 70m below water, was originally designed to be operated in clean water. In order to evaluate if the control mechanism had sufficient power to safely lift the intake valve, it was necessary to know the density state of the sediment (referred to locally as the bottom mud) and the lateral pressure exerted on the intake valve. A premature pulling of the mechanism could cause severe damage to the

BACK

forty year old intake valve. Because of the significant amount of revenue involved in power generation, the reservoir operator was eager to obtain the necessary parameters for their decision making.

The bottom mud was expected to have consistencies ranging from close to liquid to as stiff as medium dense silt. The Marchetti dilatometer (DMT) (Marchetti, 1980) with its pointed blade can easily penetrate into the bottom mud, using the weight of the drill rods. The material density, γ and its ratio to that of water, γ_w or γ / γ_w can be inferred through DMT modulus (E_D) and material index, I_D as shown in Figure 1. However, this empirical procedure is limited to γ / γ_w greater than 1.5. The time domain reflectometry (TDR) on the other hand, can be used to estimate the concentration of sediment (or density of the bottom mud) through dielectric constant and electrical conductivity measurements. The correlation between TDR readings and concentration of sediment is most desirable when γ / γ_w is less than 1.5. Thus, a combination of DMT and TDR should compliment each other and serve the purpose as a hybrid testing device.

After a brief description on the principles of TDR, the paper presents field set up of the TDR/DMT probe, the test results and their interpretation.

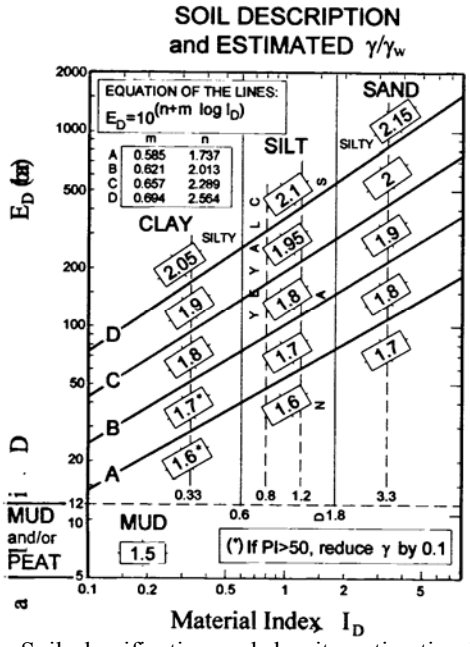

Figure 1. Soil classification and density estimation based on DMT (Marchetti and Crapps, 1981).

2 PRINCIPLES OF THE TDR

The basic principle of time domain reflectometry (TDR) is the same as radar. Instead of transmitting a 3-D wave front, the electromagnetic wave in a TDR system is confined in a waveguide. Figure 2 shows a typical TDR measurement setup composed of a TDR device and a transmission line system. A TDR device generally consists of a pulse generator, a sampler, and an oscilloscope; the transmission line system consists of a leading coaxial cable and a measurement waveguide. The pulse generator sends an electromagnetic pulse along a transmission line and the oscilloscope is used to observe the returning reflections from the measurement waveguide due to impedance mismatches. The electromagnetic pulse is reflected at the beginning and end of the probe. The TDR waveform recorded by the sampling oscilloscope is a result of multiple reflections and dielectric dispersion. A typical TDR output waveform is shown in Figure 3. Electrical properties of the material surrounding the sensing waveguide can be determined from the TDR waveform and geometry of the waveguide (Giese and Tiemann 1975; Topp et al. 1980; Heimovaara 1994; Lin 2003).

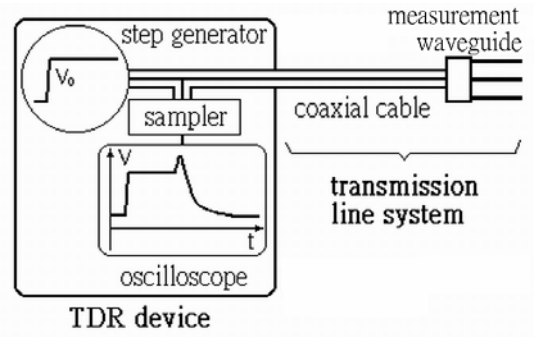

Figure 2. Typical configuration of a TDR measurement system.

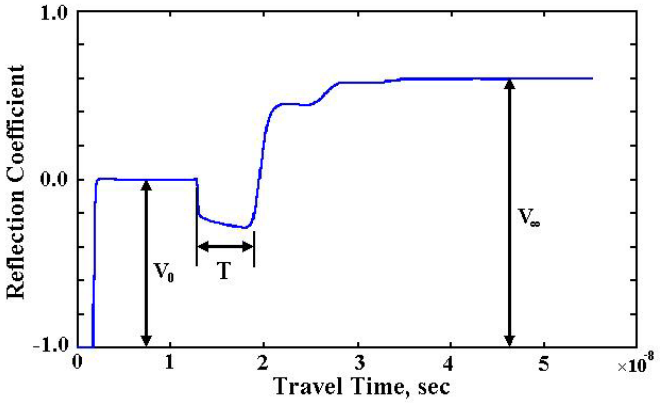

Figure 3. Determination of apparent dielectric constant and electrical conductivity from TDR signal.

The electrical properties of a material include frequency-dependent dielectric permittivity (ε) and electrical conductivity (σ). A travel time analysis of the two reflections can determine the apparent dielectric constant (K_a) as

$$\sqrt{K_a} = \frac{cT}{2L} \qquad (1)$$

in which c is the speed of light , T is the time difference between the arrivals of the two reflections (as shown in Figure. 3) and L is the length of the sensing waveguide. The electrical conductivity (σ) can be measured using the steady-state response as

$$\sigma = \left(\frac{\varepsilon_0 c}{L}\right)\left(\frac{Z_p}{R_s}\right)\left(\frac{2V_0}{V_\infty} - 1\right) = \alpha\left(\frac{2}{V_{r,\infty}} - 1\right) \quad (2)$$

where ε_0 is the dielectric permittivity of free space, c is the speed of light, L is the length of the probe, Z_p is the impedance of the probe filled with air (called geometric impedance), R_S is the output impedance of the TDR device (typically 50 ohm), V_0 is the amplitude of the step input, and V_∞ is the asymptotic value of the reflected signal. To simplify the expression, $V_{r,\infty} = V_\infty/V_0$ is defined as the asymptotic value of the voltage relative to input and α is a lumped parameter accounting for geometric factors (Z_p and L) and instrument parameter (R_s). The geometric factor Z_p may be calculated theoretically from probe dimensions for probes with special configurations (Ramo et al., 1994). In practice, it is easier to calibrate the lumped parameter α with measurements in solutions of known electrical conductivity.

3 CORRELATING TDR SIGNALS TO SEDIMENT CONCENTRATION

Sediment concentration may be measured electrically based on the relationship between the sediment concentration and electrical properties. Because of the permanent dipole of the water molecule, the dielectric constant of water is very high (≈80 at frequencies below the water relaxation frequency). Dry soil is only polarizable by atomic and electronic polarization, leading to a low dielectric constant (typically it is less than 5). This difference makes it possible to measure the sediment concentration by determining the dielectric constant of the soil-water mixture. Sediment samples were taken from the Shihmen reservoir to conduct calibration tests for sediment concentration. Figure 4 shows the relationship between the apparent dielectric constant and sediment concentration in ppm (parts per million). The dielectric constant method is more suitable for determining high sediment concentration. When the sediment concentration is below 0.2×10^5 ppm, the dielectric constant readings tend to fluctuate significantly. A more sensitive and consistent relationship between the electrical conductivity and sediment concentration can be found, but the relationship is affected by water salinity. The experimental results reveal a unique relationship between the electrical conductivity and sediment concentration if the electrical conductivity of water phase (σ_w) is subtracted from the electrical conductivity of the soil-water mixture (σ), as shown in Figure. 5. For better sensitivity, the sediment concentration is determined from electrical conductivity in this study. As shown in Figure 5, however, when sediment concentration exceeds 10×10^5 ppm, the correlation between sediment concentration and electrical conductivity curves downward and loses its linearity.

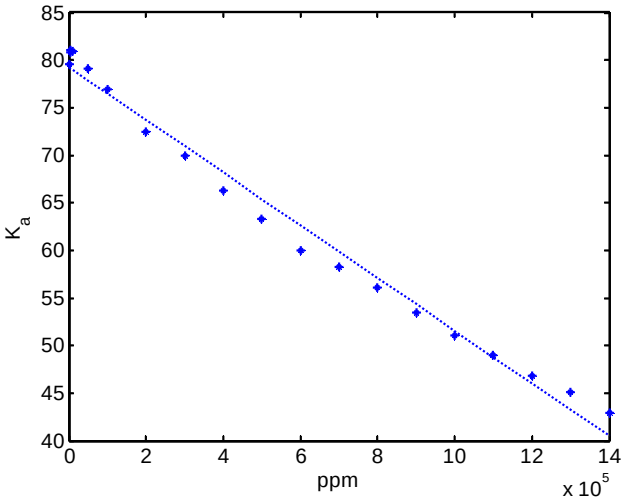

Figure 4. Relationship between dielectric constant and sediment concentration.

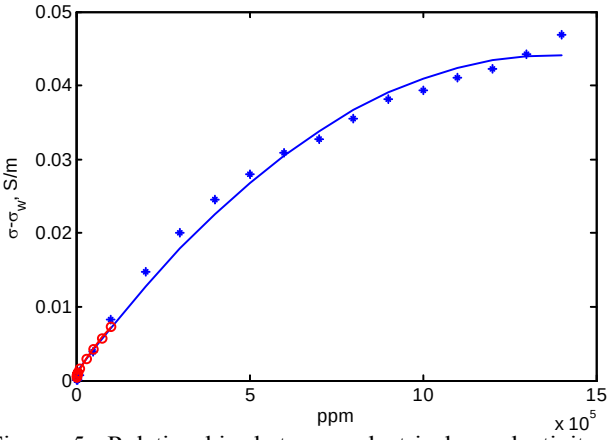

Figure 5. Relationship between electrical conductivity and sediment concentration.

4 THE TDR/DMT PROBE

A TDR penetrometer is a multi-conductor waveguide placed around a non-conductive cylindrical shaft (Lin et al., 2005a and 2005b). In this study, the TDR penetrometer module used is 800 mm long, in which the main part is a 2-conductor, 300 mm long sensing waveguide configured into a hollow, cylindrical shape as shown in Figure 6. With an outside diameter of 35.6 mm, it was designed to be used in conjunction with CPT or DMT so that the TDR waveguide can be inserted into soil at greater depths. The TDR penetrometer waveguide allows simultaneous measurement of dielectric permittivity and electrical conductivity during penetration. Unlike the conventional multi-conductor waveguide in which the conductors are fully embedded in the soil near ground surface, the TDR penetrometer waveguide is placed in between the non-conducting shaft and the surrounding soils at depths. Therefore, the TDR waveform responds not only to the surrounding material of interest but also the non-conducting shaft. The apparent dielectric constant and electrical conductivity calculated by Eqs 1 and 2 represent a weighted average of the two materials. Lin et al. (2005a and 2005b) derived a new calibra-

tion procedure for determining the electrical properties of the surrounding material. The apparent dielectric constant of the material (in this case, soil) can be written as

$$K_{a,soil} = \left(\frac{\left(\frac{cT}{2L}\right)^{2n} - b}{a} \right)^{1/n} \quad (3)$$

where n, a and b are calibration parameters for the measurement of apparent dielectric constant using the TDR penetrometer waveguide. The constants (n, a, and b) for dielectric measurements can be calibrated from TDR measurements in a few materials of known dielectric constant. Similarly, the electrical conductivity can be written as

$$\sigma_{soil} = \beta \left(\frac{2}{V_{r,\infty}} - 1 \right) \quad (4)$$

where β is the calibration parameter for measurement of electrical conductivity using the TDR penetrometer waveguide. The constant β can be calibrated from TDR measurements in a few NaCl solutions of known electrical conductivity.

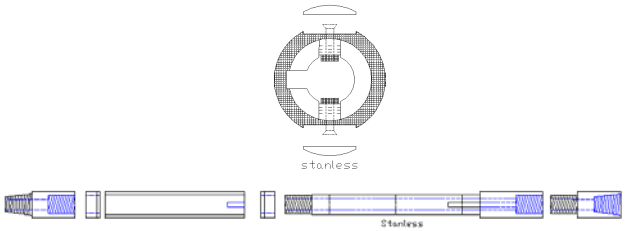

Figure 6. Schematic views of the TDR penetrometer waveguide.

In this study the TDR penetrometer waveguide was fitted immediately behind the DMT blade as shown in Figure 7. The DMT electric/pneumatic tubing passed through the inside of the hollow TDR penetrometer waveguide.

Figure 7. The TDR/DMT probe.

5 FIELD OPERATION OF TDR/DMT

The TDR/DMT probe was attached to 90 m long A rods. The A rods had a total weight of approximately 900 kg, enough to offset the buoyancy and provide reaction force to penetrate the TDR/DMT probe 10 m into the sediment. A portable drill rig mounted on a barge was used to hold the drill rods from the water surface as shown in Figure 8. The DMT tubing along with the TDR co-axial cable were threaded to the outside of the A rods through an adaptor and then connected to their respective control unit on the barge. The function of the drill rig was to hang the drill rods and passively let them be lowered instead of pushing the drill rods. Thus, the arrangement should avoid the potential problem of buckling the drill rods. The relative position of the drill rig in relation to a reference point on the dam crest was determined with a total station. The barge was fixed to a rather massive dredging boat which was in turn fixed to the shore with cables. All drainage tunnels of the reservoir were shut down during TDR/DMT tests to prevent fluctuation of the water surface elevation. With these arrangements, the barge vertical movement during a single DMT is expected to be less than 30 mm.

Figure 8. Operation of TDR/DMT from a barge.

The water surface was at an elevation of 244 m at the time of field testing. A total of 10 profiles were conducted, five of them used the TDR/DMT probe (numbered TDR/DMT-1 to TDR/DMT-5), and the other five profiles used DMT only (numbered DMT-1 to DMT-5). Figure 9 presents a location diagram of all the DMT and TDR/DMT operations. In plan view and at water surface level, the test locations were at 50 to as much as 130 m from the shore line. The power plant inlet was located on the surface of a natural rock formation with a slope of approximately 2 (vertical):1 (horizontal). The DMT readings started at elevation 185 m, TDR tests began at elevation 215, all tests ended at elevation 160 m. Thus, the bottom of the penetration could be as close as 10 m from the rock surface. The test interval varied

from 5 m in clean water to 20 cm in dense sediment. The DMT was inflated to just below A reading at all times when underwater. This arrangement prevented any possibility of water leakage and provided an opportunity to calibrate the DMT p_o readings against the hydrostatic pressure (u_o) in clean water while lowering the DMT.

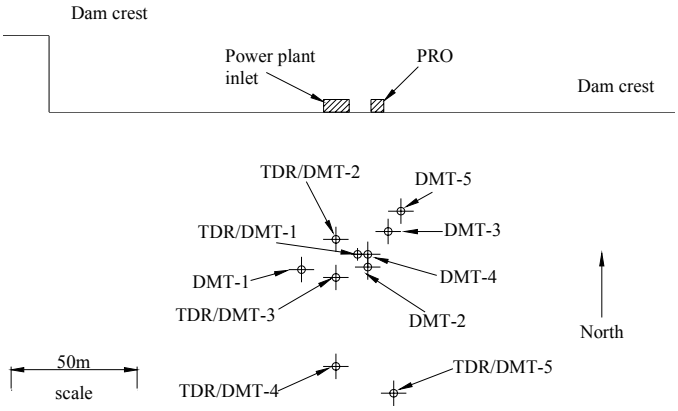

Figure 9. The test locations.

6 INTERPRETATION OF TEST RESULTS

Figure 10 shows a series of waveforms recorded in TDR/DMT-3, of reflection coefficient versus the sequential number of data points. At elevation 212.5, TDR was in clean water, the waveform at elevation 182.5 m indicated that the TDR had entered bottom mud. The depth or elevation of all the TDR and DMT was referred to the center of the DMT blade. The reflection coefficient towards the end of the record where the reading had reached a stable value was referred to as the terminal value, $V_{r,\infty}$. A laboratory calibration between $V_{r,\infty}$ and $(\sigma - \sigma_w)$ at various sediment concentrations was conducted using the sediment and water collected from the test location. With the $V_{r,\infty}$ - $(\sigma - \sigma_w)$ correlation and relationship between $(\sigma - \sigma_w)$ and sediment concetration as shown in Figure 5, the sediment concentration in terms of ppm is inferred from $V_{r,\infty}$. The solid concentration by volume (θ_s) and thus the density ratio of bottom mud over water (γ_t/γ_w) can then be calculated based on the specific gravity of the solid.

Figure 11 shows the results from the interpretation of all the TDR readings. Except for TDR/DMT-1, the tests indicated a water/mud interface at elevation 183 m where solid concentration had a significant increase to $4x10^5$ ppm. At elevation 171 m, the γ_t/γ_w reached approximately 1.4. From below elevation 171 m, the TDR readings became unstable. This is likely due to the fact that the bottom mud had become solid below that elevation, and the inevitable waving of the barge caused disturbance or cavitations within the solid mud around the TDR waveguides.

The original plan of using the chart Marchetti and Crapps (1981) to determine the bottom mud density could not materialize as in most cases, p_o was very close to u_o, and that resulted in unreasonable material index, I_D. Thus, the interpretation of DMT results was mostly based on p_o and p_1. In diluted bottom mud, where the strength was close to zero, p_o should represent the ambient total stress. Thus a comparison between the increase of p_o and that of hydrostatic pressure with depth should reveal the presence of mud. As the solid content continued to increase and the mud turned into solid, there should be significant differences between p_o and p_1 and thus the E_D values can be inferred. The results of DMT-1 to DMT-5, following the above concept are shown in Figure 12. Significant differences between p_o and u_o could not be identified until elevation 176 m which was 7 m lower than the TDR prediction.

From below elevation 173 m, the E_D became consistently larger than zero, indicating that the bottom mud was dense enough to behave like solid. As in the case of TDR, below elevation 171 m, the E_D became erratic likely due to the solid nature of the material and wave motion of the barge.

The DMT results from TDR/DMT-1 to TDR/DMT-5 are more or less consistent with those of DMT-1 to DMT-5. Figure 13 shows the variation of DMT p_o with elevation, based on results from TDR/DMT-1 to TDR/DMT-5 from below elevation 185 m. The total vertical stress based on γ_t of 1.1 γ_w from below elevation 176 m is also included in Figure 13. This γ_t is much lower than that suggested by TDR. The total stress based on γ_t of 1.1 γ_w fits most of the DMT p_o data reasonably well, up to elevation 173 m. From below elevation 173 m, most of the DMT p_o readings showed a sharp decrease. This is again likely due to the solid nature of the material and wave motion of the barge.

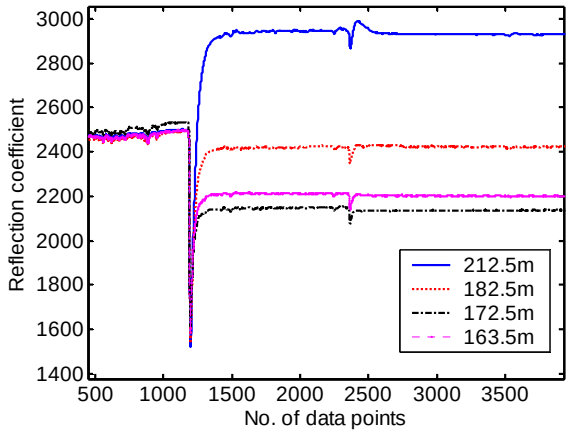

Figure 10. TDR waveforms from TDR/DMT-3.

7 CONCLUSIONS

In this project, a combination of TDR and DMT was used to investigate the interface between the clean

water and sediment as well as the density state of the sediment. Because of the diluted nature of the sediment, the TDR complimented DMT well. The experience gained in this project showed that TDR had much higher sensitivity in detecting the change of sediment or solid concentration. As a result, the interface between clean water and sediment or bottom mud according to TDR was much higher than that predicted by DMT. Also, the bottom mud density according to the change in DMT p_o and its relationship with total vertical stress was lower than that predicted by TDR. Unless good quality samples can be taken, it is not possible to ascertain which method was more accurate. It is believed however, that much improvement in the use of DMT for similar applications can be made, if the p_o and p_1 readings are converted into differential readings against u_o. In this case, the interior of the DMT blade would have to be filled with water under a pressure of u_o. The DMT has the advantage of simplicity over TDR plus the fact that DMT readings are more directly related to the stress state of the surrounding material than TDR.

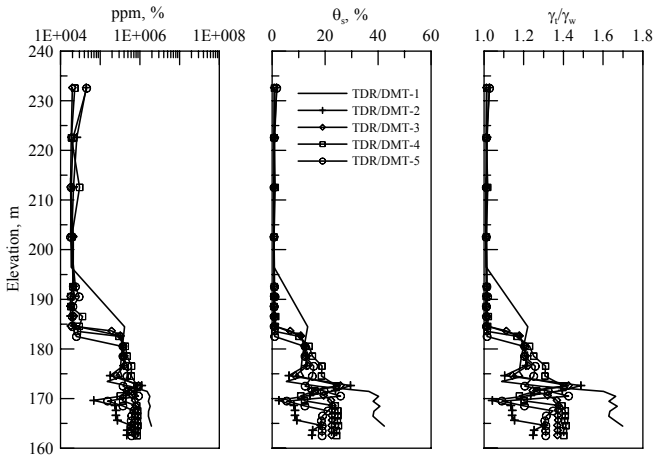

Figure 11. The interpreted TDR test results

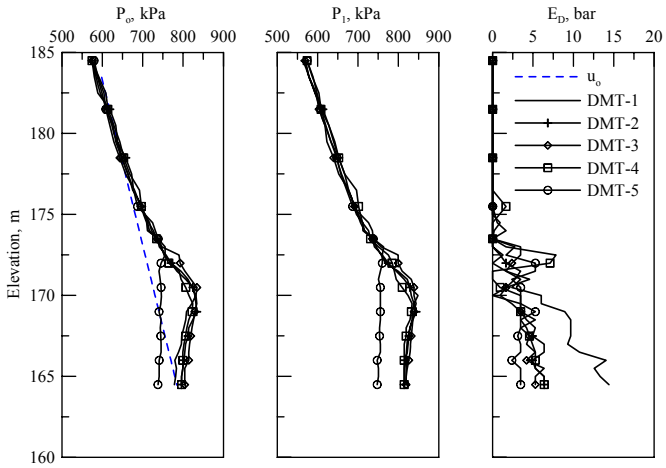

Figure 12. The DMT test results.

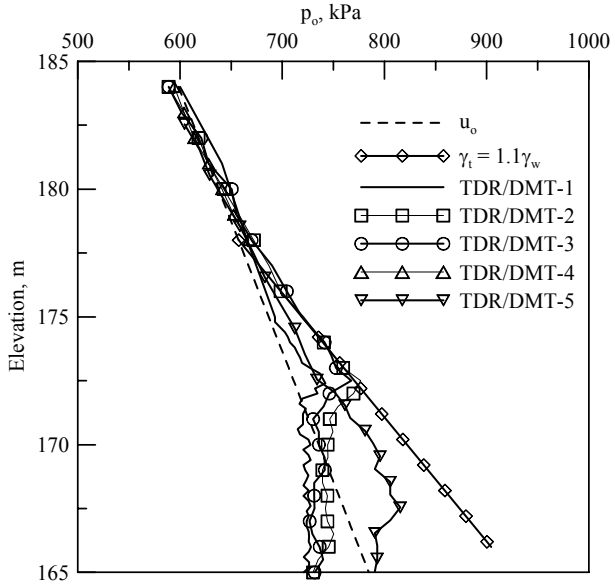

Figure 13. DMT p_o versus elevation.

REFERENCES

Giese, K., and Tiemann, R., 1975, "Determination of the complex permittivity from thin-sample time domain reflectometry: Improved analysis of the step response wave form," Adv. Mol. Relax. Processes, Vol. 7, pp. 45-59.

Heimovaara, T. J., 1994, "Frequency Domain Analysis of Time Domain Reflectormetry Waveforms: 1 Measurement of the Complex Dielectric Permittivity of Soils," Water Resources Research, Vol. 30, No. 2, pp. 189-199.

Kamey, T., and Iawasaki, K. (1995) "Evaluation of Undrained Shear Strength of Cohesive Soils Using a Flat Dilatometer," Soils and Foundations, Vol.35, No.2, pp.111-116.

Lin, C.-P. (2003a) "Analysis of a Non-uniform and Dispersive TDR Measurement System with Application to Dielectric Spectroscopy of Soils," *Water Resources Research*, Vol. 39, art. no. 1012.

Lin, C.-P. (2003b) "Frequency Domain versus Traveltime analyses of TDR Waveforms for Soil Moisture Measurements," *Soil Sci. Soc. Am. J.*, Vol. 67, pp.720-729.

Lin, C.-P., Chung, C.-C, and Tang, S.-H., 2005a, "Development of TDR Penetrometer through Laboratory Investigations: 1. Measurement of Soil Dielectric Permittivity," *Geotechnical Testing Journal*, submitted.

Lin, C.-P., Tang, S.-H., and Chung, C.-C, 2005b, "Development of TDR Penetrometer through Laboratory Investigations: 2. Measurement of Soil Electrical Conductivity," *Geotechnical Testing Journal*, submitted.

Marchetti, S. (1980) "In Situ Tests by Flat Dilatometer," Journal of Geotechnical Engineering Division, ASCE, Vol.106, No.GT3, pp.299-321.

Marchetti, S. and Crapps, D.K. (1981) "Flat Dilatometer Manual," Internal Report of G.P.E. Inc.

Ramo, S., Whinnery, J. R., and Duzer, T. V., 1994, *Fields and Waves in Communication Electromagnetics, 3rd edition,* Jown Wiley & Sons.

Topp, G. C., Davis, J. L., and Annan, A. P., 1980, "Electromagnetic Determination of Soil Water Content and Electrical Conductivity Measurement Using Time Domain Reflectometry," Water Resources Research, Vol. 16, pp. 574-582.

Liquefaction Potential Evaluation by SDMT

M. Maugeri
University of Catania, Italy

P. Monaco
University of L'Aquila, Italy

Keywords: Liquefaction, Seismic Dilatometer (SDMT), Horizontal Stress Index, Shear Wave Velocity

ABSTRACT: The seismic dilatometer (SDMT) permits to obtain parallel independent evaluations of liquefaction resistance CRR from the horizontal stress index K_D and from the shear wave velocity V_S. The use of V_S for evaluating CRR is well known. Correlations CRR-K_D have also been developed in the last two decades, stimulated by the recognized sensitivity of K_D to a number of factors which are known to increase liquefaction resistance – such as stress state/history, prestraining, aging, cementation, structure – and its correlation to relative density and state parameter. The authors have collected in the recent years, using SDMT, a large amount of parallel measurements of K_D and V_S in different saturated sandy soils. Using such data an evaluation has been made of the CRR-K_D and CRR-V_S correlations. Additional verification, supported by more real-life liquefaction case histories where V_S and K_D are known, is desirable.

1 INTRODUCTION

The seismic dilatometer (SDMT), a tool initially conceived for research, is gradually entering into use in routine geotechnical investigations, allowing the parallel accumulation of numerous data.

SDMT provides, among other measurements, two parameters that previous experience has indicated as bearing a significant relationship with the liquefaction resistance of sands. Such parameters are the horizontal stress index K_D, whose use for liquefaction studies was summarized by Monaco et al. (2005), and the shear wave velocity V_S, whose relationship with liquefaction resistance has been illustrated by several Authors (Robertson et al. 1992, Robertson & Wride 1997, Andrus & Stokoe 1997, 2000, Andrus et al. 2003, 2004).

For evaluating liquefaction potential during earthquakes, within the framework of the simplified penetration tests vs case histories based approach (Seed & Idriss 1971 procedure), it is important to use redundant correlations and more than one test.

The SDMT has the advantage, in comparison with the standard penetration test SPT and the cone penetration test CPT (in its basic non-seismic configuration without V_S measurement), to measure two independent parameters, such as K_D and V_S. Hence independent evaluations of liquefaction resistance at each test depth can be obtained from K_D and from V_S according to recommended CRR-K_D and CRR-V_S correlations. On the other hand, CPT- and SPT-based correlations are supported by large databases, while SDMT correlations are based on a smaller database.

The writers have collected in the recent years, using SDMT, a large amount of parallel measurements of K_D and V_S in different sandy soils. Taking into account such data, an evaluation of the CRR-K_D and CRR-V_S correlations has been made.

2 CURRENT METHODS FOR EVALUATING LIQUEFACTION POTENTIAL USING THE SIMPLIFIED PROCEDURE

The "simplified procedure", introduced by Seed & Idriss (1971), is currently used as a standard of practice for evaluating the liquefaction resistance of soils. This method requires the calculation of two terms: (1) the seismic demand on a soil layer generated by the earthquake, or cyclic stress ratio CSR, and (2) the capacity of the soil to resist liquefaction, or cyclic resistance ratio CRR. If CSR is greater than CRR, liquefaction can occur.

The cyclic stress ratio CSR is calculated by the following equation (Seed & Idriss 1971):

$$CSR = \tau_{av}/\sigma'_{vo} = 0.65\,(a_{max}/g)\,(\sigma_{vo}/\sigma'_{vo})\,r_d \qquad (1)$$

where τ_{av} = average cyclic shear stress, a_{max} = peak horizontal acceleration at ground surface generated

by the earthquake, g = acceleration of gravity, σ_{vo} and σ'_{vo} = total and effective overburden stresses and r_d = stress reduction coefficient dependent on depth, generally in the range ≈ 0.8 to 1.

The liquefaction resistance CRR is generally evaluated from in situ tests. The 1996 NCEER and 1998 NCEER/NSF workshops (summary report by Youd & Idriss 2001) reviewed the state-of-the-art of the Seed & Idriss (1971) "simplified procedure" and recommended revised criteria for routine evaluation of CRR from various in situ tests, including the cone penetration test CPT, the standard penetration test SPT (both widely popular, because of the extensive databases and past experience) and shear wave velocity V_S measurements.

Further contributions on CRR from CPT-SPT were recently provided by Seed et al. (2003) and Idriss & Boulanger (2004).

According to the various methods, CRR is evaluated from in situ measurements by use of charts where CRR is plotted as a function of a normalized penetration resistance or shear wave velocity. The CRR curve separates two regions of the plot – "liquefaction" and "no liquefaction" – including data obtained at sites where surface effects of liquefaction were or were not observed in past earthquakes.

Several Authors have pointed out the importance of using redundant correlations for evaluating liquefaction potential. Robertson & Wride (1998) warned that CRR evaluated by CPT (preferred over SPT, due to its poor repeatability) may be adequate for low-risk, small-scale projects, while for medium- to high-risk projects they recommended to estimate CRR by more than one method. Accordingly, the '96 and '98 NCEER workshops (Youd & Idriss 2001) concluded that, where possible, two or more tests should be used for a more reliable evaluation of CRR.

Idriss & Boulanger (2004) observed that the reliability of any liquefaction evaluation depends directly on the quality of the site characterization, and it is often the synthesis of findings from several different procedures that provides the most insight and confidence in making final decisions. For this reason, the practice of using a number of in situ testing methods should continue to be the basis for standard practice, and the allure of relying on a single approach (e.g. CPT-only procedures) should be avoided.

As to evaluating CRR from laboratory or calibration chamber (CC) testing, the major obstacle is to obtain undisturbed samples, unless non-routine sampling techniques (e.g. ground freezing) are used. The adequacy of using reconstituted sand specimens, even "exactly" at the same "in situ density", is questionable (in situ fabric/cementation/aging affect significantly CRR), as noted e.g. by Porcino & Ghionna 2002.

3 EVALUATION OF CRR FROM THE DMT HORIZONTAL STRESS INDEX K_D

3.1 *Theoretical/experimental basis of the correlation CRR-K_D*

Marchetti (1982) and later studies (Robertson & Campanella 1986, Reyna & Chameau 1991) suggested that the horizontal stress index K_D from DMT ($K_D = (p_o - u_o)/\sigma'_{vo}$) is a suitable parameter to evaluate the liquefaction resistance of sands. Comparative studies have indicated that K_D is noticeably reactive to factors such as stress state/history (σ_h, OCR), pure prestraining, aging, cementation, structure – all factors increasing liquefaction resistance. Such factors are scarcely felt e.g. by q_c from CPT (see e.g. Huang & Ma 1994) and, in general, by cylindrical-conical probes.

As noted by Robertson & Campanella (1986), it is not possible to separate the individual contribution of each factor on K_D. On the other hand, a low K_D signals that none of the above factors is high, i.e. the sand is loose, uncemented, in a low K_0 environment and has little stress history. A sand under these conditions may liquefy or develop large strains under cyclic loading.

The most significant factors supporting the use of K_D as an index of liquefaction resistance, listed by Monaco et al. (2005), are:

– Sensitivity of DMT in monitoring soil densification

The high sensitivity of the DMT in monitoring densification, demonstrated by several studies (e.g. Schmertmann et al. (1986) and Jendeby (1992) found DMT ≈ twice more sensitive than CPT to densification), suggests that the DMT may also sense sand liquefiability. In fact a liquefiable sand may be regarded as a sort of "negatively compacted" sand, and it appears plausible that the DMT sensitivity holds both in the positive and in the negative range.

– Sensitivity of DMT to prestraining

CC research on Ticino sand (Jamiolkowski & Lo Presti 1998, Fig. 1) has shown that K_D is much more sensitive to prestraining – one of the most difficult effects to detect by any method – than the penetration resistance (the increase in K_D caused by prestraining was found ≈ 3 to 7 times the increase in penetration resistance q_D). On the other hand, Jamiolkowski et al. (1985 a) had already observed that reliable predictions of liquefaction resistance of sand deposits of complex stress-strain history require the development of some new in situ device (other than CPT or SPT), more sensitive to the effects of past stress-strain histories.

– Correlation K_D - Relative density

In NC uncemented sands, the relative density D_R can be derived from K_D according to the correlation by Reyna & Chameau (1991) shown in Fig. 2. This correlation has been strongly confirmed by datapoints

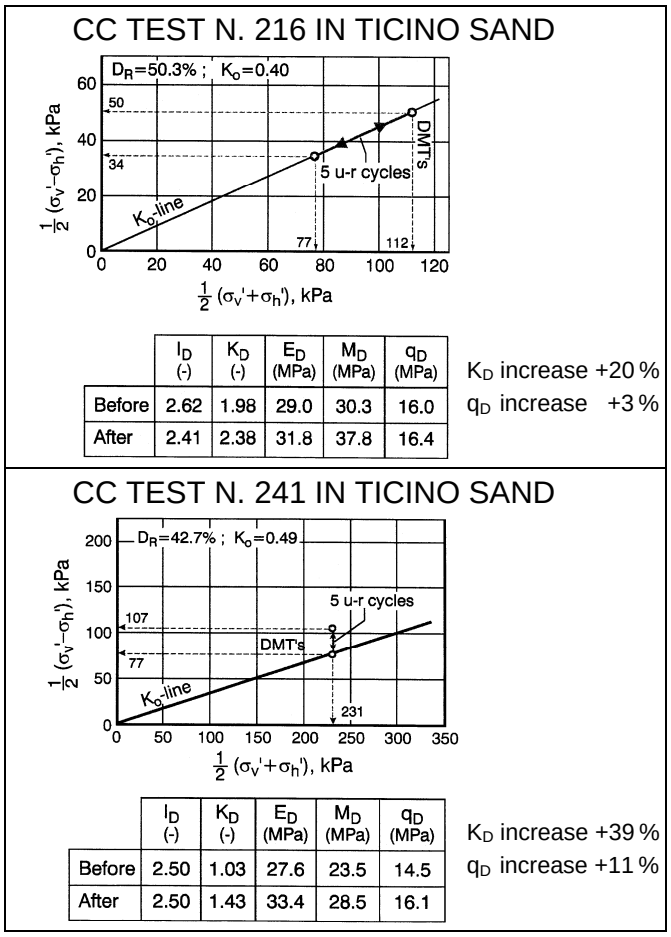

	I_D (-)	K_D (-)	E_D (MPa)	M_D (MPa)	q_D (MPa)	
Before	2.62	1.98	29.0	30.3	16.0	K_D increase +20 %
After	2.41	2.38	31.8	37.8	16.4	q_D increase +3 %

	I_D (-)	K_D (-)	E_D (MPa)	M_D (MPa)	q_D (MPa)	
Before	2.50	1.03	27.6	23.5	14.5	K_D increase +39 %
After	2.50	1.43	33.4	28.5	16.1	q_D increase +11 %

Fig. 1. Results of CC testing (prestraining cycles) showing the higher sensitivity of K_D to prestraining than penetration resistance q_D (Jamiolkowski & Lo Presti 1998)

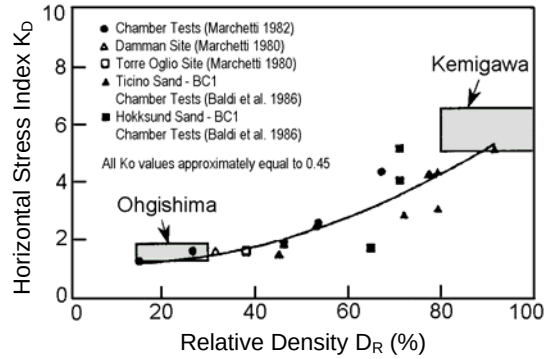

Fig. 2. Correlation K_D-D_R for NC uncemented sands (Reyna & Chameau 1991), also including Ohgishima and Kemigawa datapoints obtained by Tanaka & Tanaka (1998) on high quality frozen samples

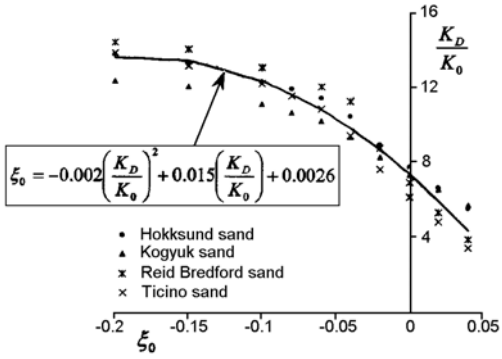

Fig. 3. Average correlation K_D - in situ state parameter ξ_o (Yu 2004)

added by subsequent research, in particular by additional K_D-D_R datapoints (shaded areas in Fig. 2) obtained by Tanaka & Tanaka (1998) at the sites of Ohgishima and Kemigawa, where D_R was determined on high quality frozen samples.

– Correlation K_D - In situ state parameter

The state parameter concept is an important step forward from the conventional relative density concept in characterizing soil behavior, combining the effects of both relative density and stress level in a rational way. The state parameter (vertical distance between the current state and the critical state line in the usual e-ln p' plot) governs the tendency of a sand to increase or decrease in volume when sheared, hence it is strongly related to liquefaction resistance. More rational methods for evaluating CRR would require the use of the state parameter (see e.g. studies by Boulanger 2003 and Boulanger & Idriss 2004, incorporating critical state concepts into the analytical framework used to evaluate liquefaction potential). Recent research supports viewing K_D from DMT as an index reflecting the in situ state parameter ξ_o. Yu (2004) identified the average correlation K_D - ξ_o shown in Fig. 3 (study on four well-known reference sands). Clearly relations K_D - ξ_o as the one shown by Yu (2004) strongly encourage efforts to develop methods to assess liquefiability by DMT.

– Physical meaning of K_D

Despite the complexity of the phenomena involved in the blade penetration, the reaction of the soil against the face of the blade could be seen as an indicator of the soil *reluctance* to a volume reduction. Clearly a loose collapsible soil will not strongly contrast a volume reduction and will oppose a low σ'_h (hence a low K_D) to the insertion of the blade. Moreover such *reluctance* is determined at the existing ambient stresses increasing with depth (apart an alteration of the stress pattern in the vicinity of the blade). Thus, at least at an intuitive level, a connection is expectable between K_D and the state parameter.

3.2 *CRR-K_D curves*

Fig. 4 (Monaco et al. 2005) summarizes the various correlations developed to estimate CRR from K_D, expressed in form of CRR-K_D boundary curves separating possible "liquefaction" and "no liquefaction" regions.

Previous CRR-K_D curves were formulated by Marchetti (1982), Robertson & Campanella (1986) and Reyna & Chameau (1991) – the last one including liquefaction field performance datapoints (Imperial Valley, South California). Coutinho & Mitchell (1992), based on Loma Prieta (San Francisco Bay) 1989 earthquake liquefaction datapoints, proposed a slight correction to the Reyna & Chameau (1991) correlation.

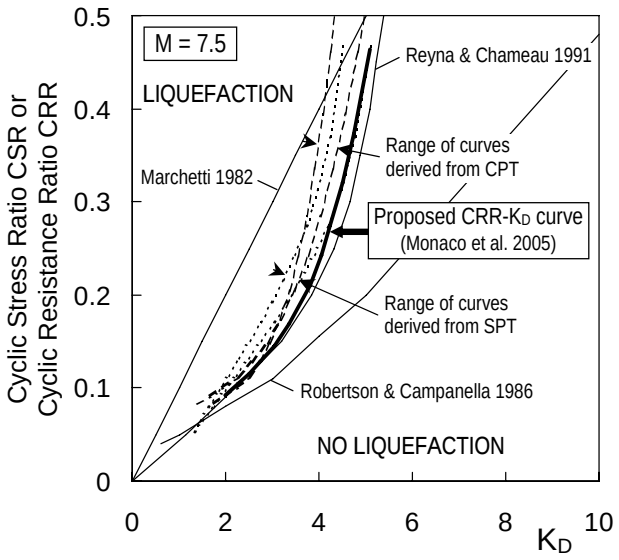

Fig. 4. CRR-K_D curves for evaluating liquefaction resistance from DMT (Monaco et al. 2005)

A new tentative correlation for evaluating CRR from K_D, to be used according to the Seed & Idriss (1971) "simplified procedure", was formulated by Monaco et al. (2005) by combining previous CRR-K_D correlations with the vast experience incorporated in current methods based on CPT and SPT (supported by extensive field performance databases), translated using the relative density D_R as intermediate parameter.

Additional CRR-K_D curves were derived by translating current CRR-CPT and CRR-SPT curves (namely the "Clean Sand Base Curves" recommended by the '96 and '98 NCEER workshops, Youd & Idriss 2001) into "equivalent" CRR-K_D curves via relative density. D_R values corresponding to the normalized penetration resistance in the CRR-CPT and CRR-SPT curves, evaluated using current correlations (D_R-q_c by Baldi et al. 1986 and Jamiolkowski et al. 1985 b, D_R-N_{SPT} by Gibbs & Holtz 1957), were converted into K_D values using the K_D-D_R correlation by Reyna & Chameau (1991) in Fig. 2. The "equivalent" CRR-K_D curves derived in this way from CPT and SPT (dashed lines in Fig. 4) plot in a relatively narrow range, very close to the Reyna & Chameau (1991) curve.

A new tentative CRR-K_D curve (bold line in Fig. 4), approximated by the equation:

$$\mathrm{CRR} = 0.0107\,K_D^3 - 0.0741\,K_D^2 + 0.2169\,K_D - 0.1306 \quad (2)$$

was proposed by Monaco et al. (2005) as "slightly conservative average" interpolation of the curves derived from CPT and SPT.

The proposed CRR-K_D curve should be used in the same way as other methods based on the Seed & Idriss (1971) procedure: (1) Enter K_D in Fig. 4 (or Eq. 2) to evaluate CRR. (2) Compare CRR with the cyclic stress ratio CSR generated by the earthquake calculated by Eq. 1.

This CRR-K_D curve (Eq. 2) applies to magnitude M = 7.5 earthquakes, as the CRR curves for CPT and SPT from which it was derived. For magnitudes other than 7.5, magnitude scaling factors (e.g. Youd & Idriss 2001, Idriss & Boulanger 2004) should be applied.

Also, the proposed CRR-K_D curve applies properly to "clean sand" (fines content ≤ 5%), as its "parent" CRR-CPT and CRR-SPT curves. No further investigation on the effects of higher fines content has been carried out so far, also due to the lack of reference field performance liquefaction data.

Of course, the method is affected by the same restrictions which apply, in general, to the Seed & Idriss (1971) procedure (level to gently sloping ground, limited depth range).

4 EVALUATION OF CRR FROM SHEAR WAVE VELOCITY V_S

The use of the shear wave velocity V_S as an index of liquefaction resistance has been illustrated by several Authors (Robertson et al. 1992, Robertson & Wride 1997, Andrus & Stokoe 1997, 2000, Andrus et al. 2003, 2004).

The V_S based procedure for evaluating CRR, which follows the general format of the Seed & Idriss (1971) "simplified procedure", has advanced significantly in recent years, with improved correlations and more complete databases, and is included by the '96 and '98 NCEER workshops (Youd & Idriss 2001) in the list of the recommended methods for routine evaluation of liquefaction resistance.

According to Andrus & Stokoe (2000), the use of V_S as a field index of liquefaction resistance is soundly based, because both V_S and CRR are similarly influenced by many of the same factors (e.g. void ratio, effective confining stresses, stress history and geologic age).

As today, the V_S based correlation currently recommended is the one formulated by Andrus et al. (2004) shown in Fig. 5, modified after the correlation obtained Andrus & Stokoe (2000) for uncemented Holocene-age soils with various fines contents, based on a database including 26 earthquakes and more than 70 measurement sites. CRR is plotted as a function of an overburden-stress corrected shear wave velocity $V_{S1} = V_S\,(p_a/\sigma'_{vo})^{0.25}$, where V_S = measured shear wave velocity, p_a = atmospheric pressure (≈ 100 kPa), σ'_{vo} = initial effective vertical stress in the same units as p_a.

The relationship CRR-V_{S1} in Fig. 5, for magnitude $M_w = 7.5$, is approximated by the equation:

$$\mathrm{CRR}_{7.5} = \left[0.022\left(\frac{K_{a1}V_{S1}}{100}\right)^2 + 2.8\left(\frac{1}{V^*_{S1} - K_{a1}V_{s1}} - \frac{1}{V^*_{S1}}\right)\right]K_{a2} \quad (3)$$

BACK

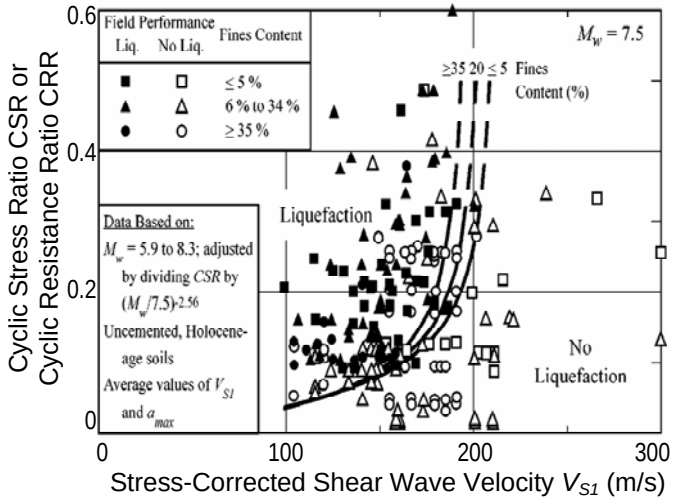

Fig. 5. Recommended curves for evaluating CRR from shear wave velocity V_S for clean, uncemented soils with liquefaction data from compiled case histories (Andrus et al. 2004)

where V^*_{S1} = limiting upper value of V_{S1} for liquefaction occurrence, assumed to vary linearly from 200 m/s for soils with fines content of 35 % to 215 m/s for soils with fines content of 5 % or less, K_{a1} = factor to correct for high V_{S1} values caused by aging, K_{a2} = factor to correct for influence of age on CRR.

Both K_{a1} and K_{a2} are 1 for uncemented soils of Holocene age. For older soils the SPT-V_{S1} equations by Ohta & Goto (1978) and Rollins et al. (1998) suggest average K_{a1} values of 0.76 and 0.61, respectively, for Pleistocene soils (10,000 years to 1.8 million years). Lower-bound values of K_{a2} are based on the study by Arango et al. (2000).

The CRR curves in Fig. 5 apply to magnitude M_w = 7.5 earthquakes and should be scaled to other magnitude values through use of magnitude scaling factors.

5 MINIMUM "NO LIQUEFACTION" K_D AND V_{S1} VALUES

In many everyday problems, a full seismic liquefaction analysis can be avoided if the soil is clearly liquefiable or non liquefiable. Guidelines of this type would be practically helpful to engineers.

A tentative identification of minimum values of K_D for which a clean sand (natural or sandfill) is safe against liquefaction (M = 7.5 earthquakes) is indicated in TC16 (2001):

– Non seismic areas, i.e. very low seismic: $K_D > 1.7$
– Low seismicity areas ($a_{max}/g = 0.15$): $K_D > 4.2$
– Medium seismicity areas ($a_{max}/g = 0.25$): $K_D > 5.0$
– High seismicity areas ($a_{max}/g = 0.35$): $K_D > 5.5$

The above K_D values are marginal values, to be factorized by an adequate safety factor.

Such K_D values were identified based on the Reyna & Chameau (1991) CRR-K_D curve and on indications given by Marchetti (1997) for non seismic areas, and were substantially confirmed by the CRR-K_D curve by Monaco et al. (2005) in Fig. 4.

Limiting upper values of V_{S1} for liquefaction occurrence for areas of different seismicity could be correspondingly derived from the CRR-V_{S1} curve (for clean sand) in Fig. 5.

6 COMPARISON OF CRR FROM K_D AND CRR FROM V_S OBTAINED BY SDMT AT VARIOUS SAND SITES

6.1 *SDMT K_D-V_S database in sands*

The authors have collected in the recent years a large amount of parallel measurements of K_D and V_S in sands by use of the seismic dilatometer SDMT.

The first check that the authors found natural to carry out was to see if V_S and K_D are correlated, considering the intended use of both for predicting CRR. (Such check is independent from liquefaction occurrence). Several V_{S1}-K_D data pairs obtained by SDMT in sand layers/deposits (having material index $I_D > 2$) at various sites recently investigated in Italy and Europe are plotted in Fig. 6. The data shown in Fig. 6 suggest the following observations.

– *Site-specific trend of the relationship V_{S1}-K_D*

Fig. 6 shows a significant scatter of the V_{S1}-K_D datapoints. Based on these data, no evident correlation – not even site specific – seems to exist between V_S and K_D in sands. The "trend" of the possible relationship between V_{S1} and K_D varies from one site to another.

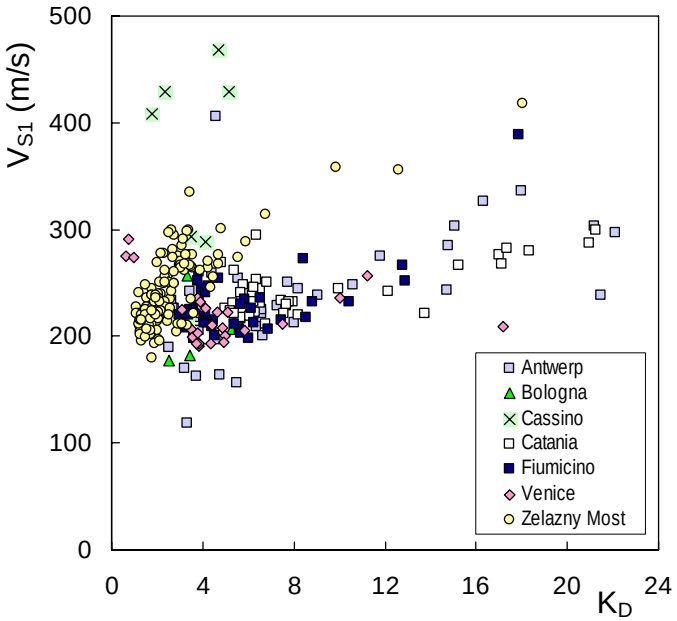

Fig. 6. V_{S1}-K_D data pairs obtained by SDMT in sands ($I_D > 2$) at various sites

E.g. at Zelazny Most, while V_{S1} varies in the range 200 to 300 m/s, K_D varies in a relatively narrow range, mostly ≈ 2 to 2.5. On the contrary at Catania, while V_{S1} is moderately variable (≈ 250-300 m/s), K_D varies in a much larger range (≈ 5 to 20).

The high dispersion in Fig. 6 indicates that V_S and K_D reflect, besides possibly CRR, other properties, so V_S and K_D are not interchangeable for predicting CRR. Therefore different CRR estimates are to be expected.

– *OCR and K_D crusts in sand*

"Crust-like" K_D profiles – very similar to the typical K_D profiles found in OC desiccation crusts in clay – have been found at the top of most of the sand deposits investigated by SDMT. An example of K_D crusts (Catania) is shown in Fig. 7.

OCR in sand is often the result of a complex history of preloading or desiccation or other effects. Apart from quantitative estimates of OCR, the K_D profile generally shows some ability to reflect OCR in sand. Shallow K_D crusts may be also (in part) a consequence of their vicinity to ground surface, i.e. dilatancy effects. On the other hand, the K_D-D_R correlation by Reyna & Chameau (1991) shown in Fig. 2, developed for NC uncemented sands, provides D_R = 100 % for a value of K_D ≈ 6-7. Values of K_D well above 6-7 have been observed in the shallow K_D crusts in most of the investigated sandy sites. This confirms that part of K_D is due to overconsolidation or cementation, rather than to D_R.

In the example shown in Fig. 7 it should be noted that, while the existence of a shallow desiccation crust in the upper ≈ 8 m is well highlighted by the K_D profile, the profile of V_S, moderately increasing with depth, is much more uniform and does not appear to reflect the shallow crust at all. A similar behavior has been observed at several of the investigated sites (e.g. Venice, Fig. 8). The fact that OCR crusts such as the one in Fig. 7 (believed by far not liquefiable) are unequivocally depicted by the high K_Ds, but are almost unfelt by V_S, suggests a lesser ability of V_S to profile liquefiability.

– *Role of the interparticle bonding*

Fig. 6 shows that the Cassino data (top of Fig. 6) are somehow anomalous, in that high V_{S1} coexist with low K_Ds. Many of the sands in that area are known to be volcanic and active in developing interparticle bonding (pozzolana).

A possible explanation could be the following: The shear wave travels fast in those sands thanks to the interparticle bonding, that is preserved because the strains are small. K_D, by contrast, is "low" because it reflects a different material, where the interparticle bonding has been at least partly destroyed by the strains produced by the blade penetration. On the other hand, pore-pressure build up and liquefaction are medium- to high-strain phenomena. Thus, for liquefiability evaluations, the K_D indications could possibly be more relevant.

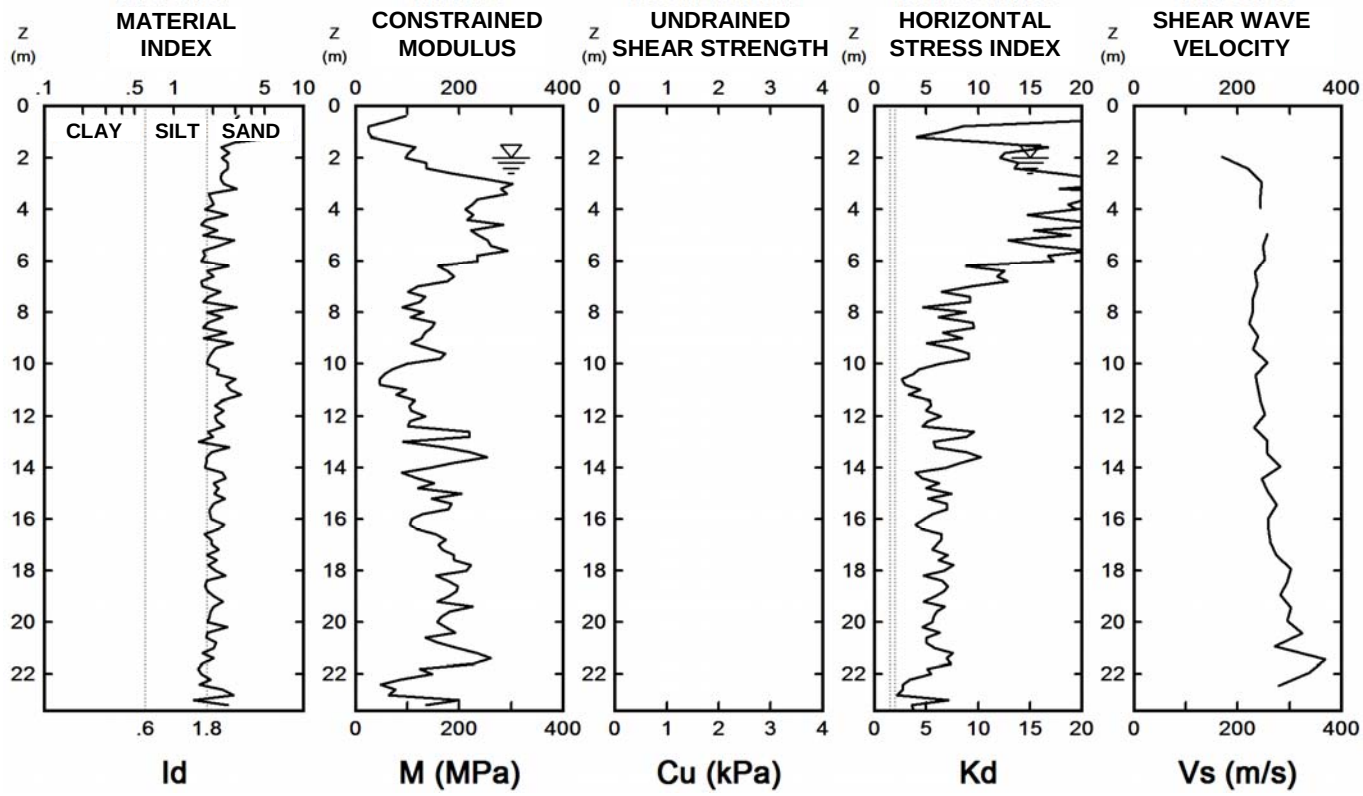

Fig. 7. SDMT results at the site of Catania (San Giuseppe La Rena), Italy

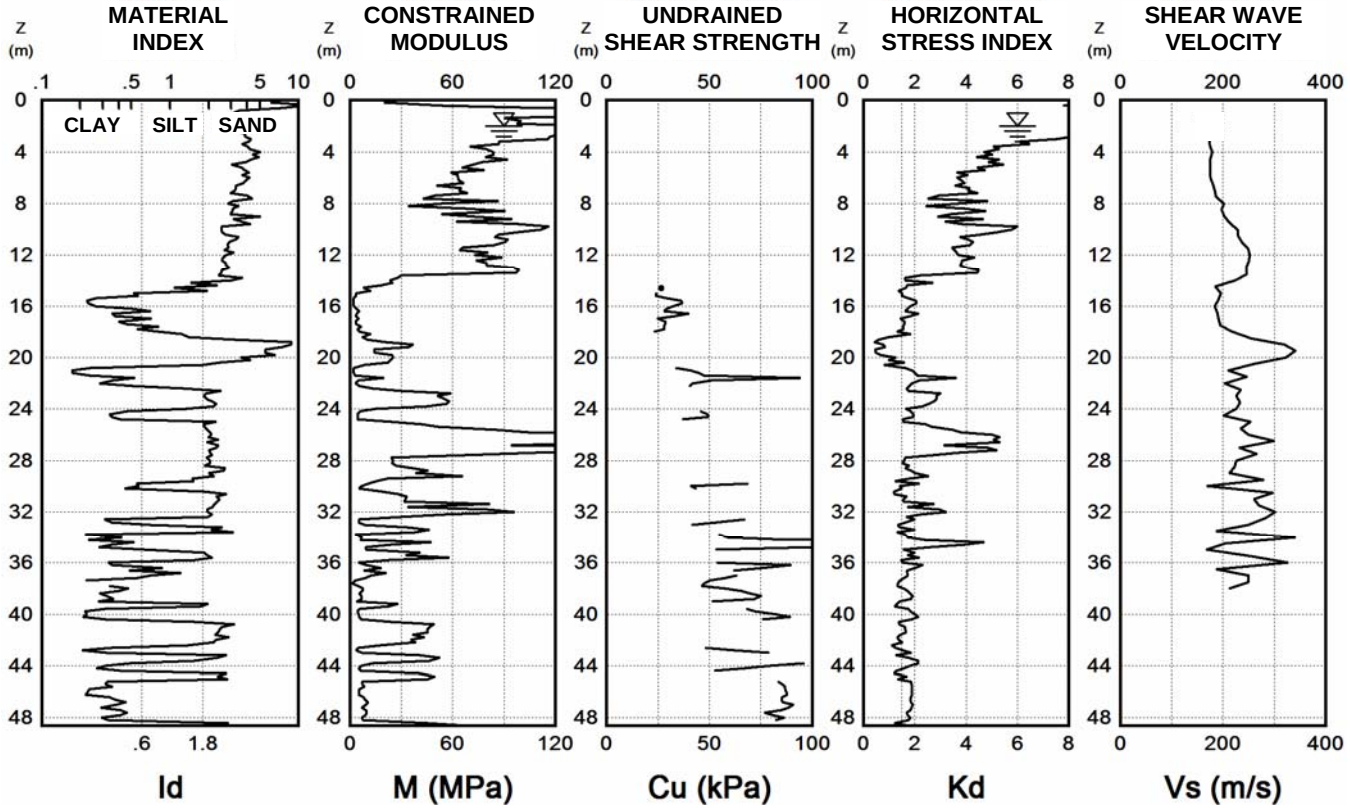

Fig. 8. SDMT results at the site of Venice, Italy

6.2 *Comparison of CRR predicted by V_S and by K_D*

In order to evaluate the consistency of liquefaction resistance predicted by V_S and by K_D for a given sand, the CRR-V_S method by Andrus et al. (2004) and the CRR-K_D method by Monaco et al. (2005), previously described, have been compared (indirectly) by constructing a relationship between V_{S1} and K_D implied by the CRR-V_{S1} curve for FC ≤ 5% in Fig. 5 (assuming both aging correction factors K_{a1} and K_{a2} = 1) and the CRR-K_D curve in Fig. 4. Both curves apply to magnitude M_w = 7.5 earthquakes and clean sands. This CRR-equivalence curve was obtained by combining Eqns. 2 and 3 and then eliminating CRR.

The advantage of studying such V_{S1}-K_D relationship is that it provides a comparison of the two liquefaction evaluation methods without needing to calculate CSR. Hence data from sites not shaken by earthquakes can also be used to assess the consistency between the two methods. This option is particular helpful, in view of the lack of documented liquefaction case histories including DMT data.

Note that a similar procedure was adopted by Andrus & Stokoe (2000) for comparing CRR from V_S vs CRR from SPT. In that case, however, the database consisted of V_S and SPT data from various sites where liquefaction had actually occurred during past earthquakes.

The CRR-equivalence curve is shown in Fig. 9. Also shown in Fig. 9, superimposed to the curve, are field V_{S1}-K_D data pairs obtained by SDMT at several sandy sites. Such V_{S1}-K_D data pairs are those plotted in Fig. 6, excluding the V_{S1}-K_D data pairs belonging to shallow (OC) K_D crusts, where it is often found K_D > 10. Also, the datapoints shown in Fig. 9 are limited to a maximum depth of 15 m (usual depth range for liquefaction occurrence), also to take into account the limits of applicability of the Seed & Idriss (1971) simplified procedure.

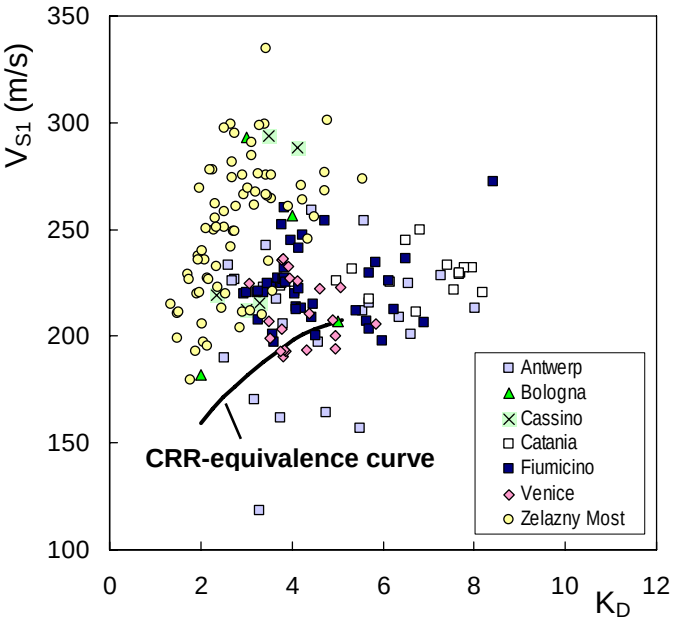

Fig. 9. CRR-equivalence curve between the correlations CRR-V_{S1} (Andrus et al. 2004) and CRR-K_D (Monaco et al. 2005) for clean sands and M_w = 7.5

In practice, the comparison is limited to the sand layers "more likely to liquefy", i.e. excluding OC crusts and deep layers. In this way, the scatter of the V_{S1}-K_D datapoints is somewhat reduced (though not substantially), if compared to Fig. 6.

The meaning of Fig. 9 is the following. When the V_{S1} -K_D data point lies on the CRR-equivalence curve, both the CRR-V_{S1} and the CRR-K_D methods provide similar predictions of liquefaction resistance. When the data point plots below this curve, the V_{S1} method provides the more conservative prediction. When the data point plots above the curve, the K_D method provides the more conservative prediction.

Fig. 9 shows that the two methods here considered for evaluating CRR from V_S and from K_D would provide substantially different predictions of CRR. In general, the V_{S1} method predicts CRR values less conservative than the K_D method.

Another inconsistency observed between the two methods concerns the limiting values of V_{S1} and K_D for which liquefaction occurrence can be definitely excluded (asymptotes of the CRR-V_{S1} curve in Fig. 5 and of the CRR-K_D curve in Fig. 4). Such values are respectively V^*_{S1} = 215 m/s and K^*_D = 5.5 (for clean sands and M_w = 7.5). E.g. at Zelazny Most (see Fig. 9), while V_{S1} values (mostly > 215 m/s) suggest "no liquefaction" in any case, K_D values (≈ 2-2.5) indicate that liquefaction may occur above a certain seismic stress level.

7 CRR-K_D VS CRR-V_S AT LOMA PRIETA 1989 EARTHQUAKE LIQUEFACTION SITES

A preliminary validation of the proposed CRR-K_D curve (Fig. 10) was obtained by Monaco et al. (2005) from comparison with field performance liquefaction datapoints from various sites investigated after the Loma Prieta 1989 earthquake (M_w = 7), in the San Francisco Bay region (to the authors' knowledge, one of the few documented liquefaction cases with DMT data).

The CSR-K_D datapoints in Fig. 10 were calculated based on data contained in the report by Mitchell et al. (1994), which includes the results of DMTs performed after the earthquake at several locations where soil liquefaction had occurred (mostly in hydraulic sandfills), along with data on soil stratigraphy, water table, depths of soil layers likely to have liquefied, a_{max} estimated or measured from strong motions recordings.

A detailed description of the DMT investigation and an assessment of liquefaction potential based on previous CRR-K_D correlations for the Loma Prieta 1989 earthquake had been presented by Coutinho & Mitchell (1992).

Fig. 10 shows that the datapoints obtained at sites where liquefaction had occurred are correctly located in the "liquefaction" side of the plot. One datapoint relevant to a site non classified as "liquefaction" or "non-liquefaction" site by Mitchell et al. (1994) plots very close to the proposed CRR-K_D boundary curve (scaled for M_w = 7).

V_S measurements at the liquefaction sites investigated after the Loma Prieta 1989 earthquake, reported by Mitchell et al. (1994), were obtained by seismic cone SCPT, SASW, cross-hole and up-hole tests. (The seismic dilatometer had not been developed yet at the time of the investigation).

V_S data obtained by the above methods were used to calculate the CSR-V_{S1} datapoints shown in Fig. 11. Like the corresponding CSR-K_D datapoints in Fig. 10, all the CSR-V_{S1} datapoints are located on the "liquefaction" side, on the left of the CRR-V_{S1} curve (Andrus et al. 2004), scaled for M_w = 7.

In this case the liquefaction potential evaluations by K_D (Fig. 10) and by V_{S1} (Fig. 11) are in reasonably good agreement, as also indicated by the "indirect" comparison shown in Fig. 12.

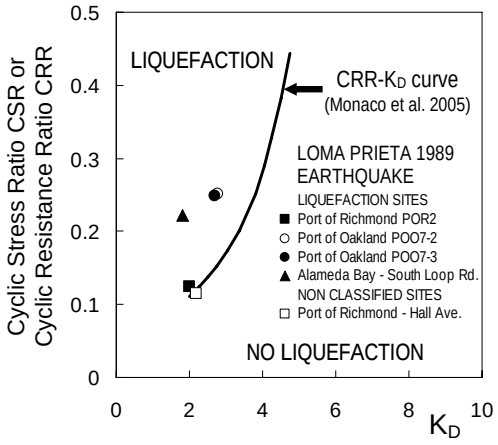

Fig. 10. Comparison of CRR-K_D curve by Monaco et al. (2005) and Loma Prieta 1989 earthquake liquefaction datapoints (after Mitchell et al. 1994)

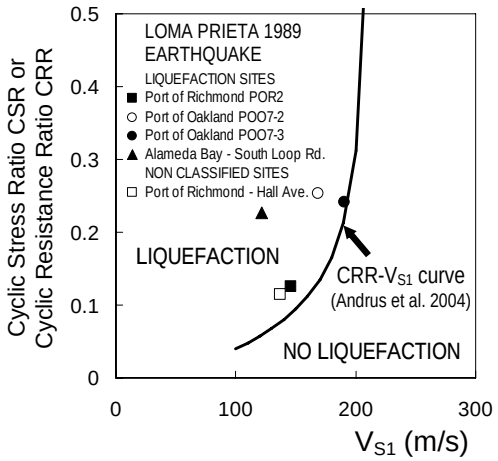

Fig. 11. Comparison of CRR-V_{S1} curve by Andrus et al. (2004) and Loma Prieta 1989 earthquake liquefaction datapoints (after Mitchell et al. 1994)

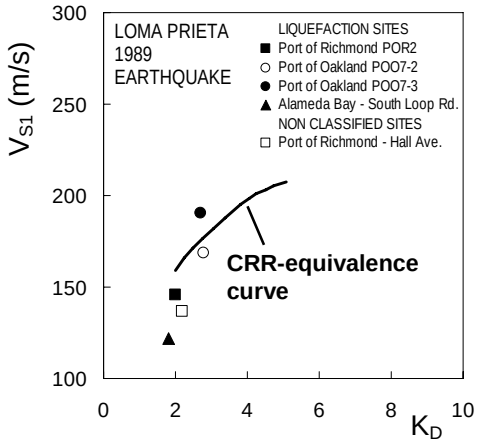

Fig. 12. Loma Prieta 1989 earthquake liquefaction V_{S1}-K_D data pairs superimposed to the CRR-equivalence curve

8 COMMENTS ON EVALUATION OF CRR FROM V_S AND K_D VS CRR FROM OTHER METHODS

The reliability of CRR evaluated from V_S compared to CRR evaluated by other methods has been discussed by various Authors.

According to Seed et al. (2003), V_S based CRR correlations provide less reliable estimates than SPT and CPT based correlations, not only because the V_S based field case history database is considerably smaller than that available for SPT and CPT correlation development, but also because V_S is a very small-strain measurement and correlates poorly with a much "larger-strain" phenomenon such as liquefaction. Seed et al. (2003) conclude that current V_S based CRR correlations are best employed either conservatively or as preliminary rapid screening tools to be supplemented by other methods.

According to Idriss & Boulanger (2004), V_S based liquefaction correlations provide a valuable tool that ideally should be used in conjunction with SPT or CPT, if possible. An interesting question, however, is which method should be given greater weight when parallel analyses by SPT, CPT, and/or V_S procedures produce contradictory results. A particularly important point to consider is the respective sensitivity of SPT, CPT and V_S measurements to the relative density of the soil. E.g. changing D_R of a clean sand from 30% to 80% would be expected to increase the SPT blowcount by a factor of ≈ 7.1 and the CPT tip resistance by a factor of ≈ 3.3 (using D_R correlations proposed by Idriss & Boulanger 2004). In contrast, the same change in D_R would be expected to change V_S only by a factor of ≈ 1.4 based on available correlations. Given that D_R is known to have a strong effect on the cyclic and post-cyclic loading behavior of a saturated sand, it appears that V_S measurements would be the least sensitive for distinguishing among different types of behavior. For this reason, Idriss & Boulanger (2004) conclude that it may be more appropriate to view the V_S case history database as providing bounds that identify conditions where liquefaction is potentially highly likely, highly unlikely and where it is uncertain whether or not liquefaction should be expected. As such, there is still a need for an improved understanding of V_S based correlations and an assessment of their accuracy relative to SPT and CPT based correlations. In the mean time, Idriss & Boulanger (2004) recommend that greater weight be given to the results of SPT or CPT based liquefaction evaluations (for materials without large particle sizes).

The considerations expressed by Idriss & Boulanger (2004) for CRR from CPT/SPT vs CRR from V_S could be extended to CRR from K_D. According to the K_D-D_R correlation by Reyna & Chameau (1991) in Fig. 2, a change in D_R from 30% to 80% would increase K_D from ≈ 1.5 to ≈ 4.2, i.e. a factor of ≈ 2.8, indicating a higher sensitivity of K_D than V_S to relative density.

Moreover, research has shown that K_D is more sensitive than V_S to factors such as stress history, aging, cementation, structure, which greatly increase, for a given D_R, liquefaction resistance and, incidentally, are felt considerably more than by penetration resistance.

Particularly relevant to this point is the discussion by Pyke (2003). The Author recalled that Seed (1979) had listed five factors which were known, or could be reasonably assumed, to have a similar effect on penetration resistance and liquefaction potential, but these were never intended to be equalities. In particular, two of these factors – overconsolidation and aging – are likely to have a much greater effect on increasing liquefaction resistance than they do on penetration resistance. Thus soils that are even lightly OC or more than several decades old may have a greater resistance to liquefaction than indicated by the current correlations, which are heavily weighted by data from hydraulic fills and very recent streambed deposits.

Hence, in the authors' opinion, when using V_S and K_D from SDMT for parallel evaluations of liquefaction resistance, the CRR-K_D method should be given greater weight – in principle – than the V_S based method, in case of contradictory CRR predictions from the two methods. However, since the CRR-K_D correlation is based on a limited liquefaction case history database, considerable additional verification is needed.

9 CONCLUSIONS

The seismic dilatometer SDMT offers an alternative or integration to current methods for evaluating the liquefaction resistance of sands based on CPT or SPT, within the framework of the simplified penetration tests vs case histories based approach (Seed & Idriss 1971 procedure).

This opportunity appears attractive, since "redundancy" in the evaluation of CRR by more than one method is generally recommended.

Parallel independent evaluations of liquefaction resistance can be obtained from the horizontal stress index K_D and from the shear wave velocity V_S according to recommended CRR-K_D and CRR-V_S correlations. The use of V_S as an index of liquefaction resistance is well known. The basis for correlating liquefaction resistance to K_D, illustrated in detail in this paper, includes the sensitivity of K_D to a number of factors which are known to increase liquefaction resistance – such as stress state/history, prestraining, aging, cementation, structure – and its correlation to relative density and state parameter.

A preliminary validation of the recommended CRR-K_D method was obtained from comparison with field performance datapoints obtained at liquefaction sites investigated after the Loma Prieta 1989 earthquake. In that case the CRR-K_D and CRR-V_S correlations provided similar estimates.

In general, however, estimates of CRR by V_S have been found to be less conservative than by K_D, leaving open the question which CRR should be given greater weight. The authors would propend to give greater weight to CRR by K_D for the following reasons:

- OCR crusts, believed to be very unlikely to liquefy, are unequivocally depicted by the high K_Ds, but are almost unfelt by V_S. This suggests a lesser ability of V_S to profile liquefiability.
- V_S measurements are made at small strains, whereas pore-pressure build up and liquefaction are medium- to high-strain phenomena. Thus in cemented soils V_S can be "misleadingly" high thanks to interparticle bonding, that is eliminated at medium and high strains. By contrast, K_D is measured at considerably higher strains than V_S.
- Many indications suggest at least some link between K_D and state parameter, which is probably one of the closest proxy of liquefiability.
- K_D is sensitive not only to D_R but also to factors such as stress history, aging, cementation, structure, that greatly increase liquefaction resistance.

The above obviously deserves considerable additional verification, supported by more well documented real-life liquefaction case histories where V_S and K_D are known.

ACKNOWLEDGMENTS

The authors wish to thank Roberto Quental Coutinho for kindly providing the Loma Prieta DMT liquefaction data report.

Diego Marchetti is also acknowledged for providing the SDMT data at various sites.

REFERENCES

Andrus, R.D. & Stokoe, K.H., II. 1997. Liquefaction resistance based on shear wave velocity. *Proc. NCEER Workshop on Evaluation of Liquefaction Resistance of Soils*, *Technical Report NCEER-97-0022*, T.L. Youd & I.M. Idriss, eds., National Center for Earthquake Engineering Research, Buffalo, 89-128.

Andrus, R.D. & Stokoe, K.H., II. 2000. Liquefaction resistance of soils from shear-wave velocity. *Jnl GGE*, ASCE, 126(11), 1015-1025.

Andrus, R.D., Stokoe, K.H., II, Chung, R.M. & Juang, C.H. 2003. Guidelines for evaluating liquefaction resistance using shear wave velocity measurements and simplified procedures. *NIST GCR 03-854*, National Institute of Standards and Technologies, Gaithersburg.

Andrus, R.D., Stokoe, K.H., II & Juang, C.H. 2004. Guide for Shear-Wave-Based Liquefaction Potential Evaluation. *Earthquake Spectra*, 20(2), 285-305.

Arango, I., Lewis, M.R. & Kramer, C. 2000. Updated liquefaction potential analysis eliminates foundation retrofitting of two critical structures. *Soil Dyn. Earthquake Eng*., 20, 17–25.

Baldi, G., Bellotti, R., Ghionna, V., Jamiolkowski, M. & Pasqualini, E. 1986. Interpretation of CPT and CPTUs. 2nd part: Drained penetration of sands. *Proc. 4th Int. Geotech. Seminar*, Singapore, 143-156.

Boulanger, R.W. 2003. High overburden stress effects in liquefaction analysis. *Jnl GGE*, ASCE, 129(12), 1071-1082.

Boulanger, R.W. & Idriss, I.M. 2004. State normalization of penetration resistance and the effect of overburden stress on liquefaction resistance. *Proc. 11th Int. Conf. on Soil Dynamics & Earthquake Engineering & 3d Int. Conf. on Earthquake Geotechnical Engineering*, Berkeley, 484-491.

Coutinho, R.Q. & Mitchell, J.K. 1992. Evaluation of Dilatometer Based Methods for Liquefaction Potential Assessment Using Loma Prieta Earthquake Data. Internal Report of Research Project (unpublished).

Gibbs, K.J. & Holtz, W.G. 1957. Research on determining the density of sands by spoon penetration testing. *Proc. IV ICSMFE*, 1, 35-39.

Huang, A.B. & Ma, M.Y. 1994. An analytical study of cone penetration tests in granular material. *Canadian Geotech. Jnl*, 31(1), 91-103.

Idriss, I.M. & Boulanger, R.W. 2004. Semi-empirical procedures for evaluating liquefaction potential during earthquakes. *Proc. 11th Int. Conf. on Soil Dynamics & Earthquake Engineering & 3d Int. Conf. on Earthquake Geotechnical Engineering*, Berkeley, 32-56.

Jamiolkowski, M., Baldi, G., Bellotti, R., Ghionna, V. & Pasqualini, E. 1985 a. Penetration resistance and liquefaction of sands. *Proc. XI ICSMFE*, San Francisco, 4, 1891-1896.

Jamiolkowski, M., Ladd, C.C., Germaine, J.T. & Lancellotta, R. 1985 b. New developments in field and laboratory testing of soils. SOA Report, *Proc. XI ICSMFE*, San Francisco, 1, 57-153.

Jamiolkowski, M. & Lo Presti, D.C.F. 1998. Oral presentation. *1st Int. Conf. on Site Characterization ISC'98*, Atlanta.

Jendeby, L. 1992. Deep Compaction by Vibrowing. *Proc. Nordic Geotechnical Meeting NGM-92*, 1, 19-24.

Marchetti, S. 1982. Detection of liquefiable sand layers by means of quasi-static penetration tests. *Proc. 2nd European Symp. on Penetration Testing*, Amsterdam, 2, 689-695.

Marchetti, S. 1997. The Flat Dilatometer: Design Applications. Keynote Lecture, *Proc. 3rd Int. Geotech. Engrg. Conference*, Cairo, 421-448.

Monaco, P., Marchetti, S., Totani, G. & Calabrese, M. 2005. Sand liquefiability assessment by Flat Dilatometer Test (DMT). *Proc. XVI ICSMGE*, Osaka, 4, 2693-2697.

Mitchell, J.K., Lodge, A.L., Coutinho, R.Q., Kayen, R.E., Seed, R.B., Nishio, S. & Stokoe, K.H. 1994. Insitu test results from four Loma Prieta earthquake liquefaction sites: SPT, CPT, DMT and shear wave velocity. *Report No. UCB/EERC-94/04*, Earthquake Engineering Research Center, Univ. of California, Berkeley.

Ohta, Y. & Goto, N. 1978. Empirical shear wave velocity equations in terms of characteristic soil indexes. *Earthquake Eng. Struct. Dyn*., 6, 167-187.

Pike, R. 2003. Discussion of "Liquefaction Resistance of Soils: Summary Report from the 1996 NCEER and 1998 NCEER/NSF Workshops on Evaluation of Liquefaction Resistance of Soils" by Youd, T.L. et al. (in *Jnl GGE* ASCE, 2001, 127(10), 817-833). *Jnl GGE* ASCE, 129(3), 283-284.

Porcino, D. & Ghionna, V.N. 2002. Liquefaction of coarse grained sands by laboratory testing on undisturbed frozen samples (in Italian). *Proc. Annual Meeting Italian Geot. Res. IARG 2002*, Naples.

Reyna, F. & Chameau, J.L. 1991. Dilatometer Based Liquefaction Potential of Sites in the Imperial Valley. *Proc. 2nd Int. Conf. on Recent Adv. in Geot. Earthquake Engrg. and Soil Dyn.*, St. Louis, 385-392.

Robertson, P.K. & Campanella, R.G. 1986. Estimating Liquefaction Potential of Sands Using the Flat Plate Dilatometer. *ASTM Geotechn. Testing Journal*, 9(1), 38-40.

Robertson, P.K., Woeller, D.J. & Finn, W.D.L. 1992. Seismic cone penetration test for evaluating liquefaction potential under cyclic loading. *Canadian Geotech. Jnl*, 29, 686-695.

Robertson, P.K. & Wride, C.E. 1997. Cyclic liquefaction and its evaluation based on SPT and CPT. *Proc. NCEER Workshop on Evaluation of Liquefaction Resistance of Soils*, *Technical Report NCEER-97-0022*, T.L. Youd & I.M. Idriss, eds., National Center for Earthquake Engineering Research, Buffalo, 41-88.

Robertson, P.K. & Wride, C.E. 1998. Evaluating cyclic liquefaction potential using the cone penetration test. *Canadian Geotech. Jnl*, 35(3), 442-459.

Rollins, K.M., Diehl, N.B. & Weaver, T.J. 1998. Implications of V_S-BPT $(N_1)_{60}$ correlations for liquefaction assessment in gravels. *Geotechnical Earthquake Engineering and Soil Dynamics III*, Geotech. Special Pub. No. 75, P. Dakoulas, M. Yegian & B. Holtz, eds., ASCE, I, 506-517.

Schmertmann, J.H., Baker, W., Gupta, R. & Kessler, K. 1986. CPT/DMT Quality Control of Ground Modification at a Power Plant. *Proc. In Situ '86, ASCE Spec. Conf. on "Use of In Situ Tests in Geotechn. Engineering"*, Virginia Tech, Blacksburg, ASCE Geotechn. Special Publ. No. 6, 985-1001.

Seed, H.B. 1979. Soil liquefaction and cyclic mobility evaluation for level ground during earthquakes. *Jnl GED*, ASCE, 105(2), 201-255.

Seed, R.B., Cetin, K.O., Moss, R.E.S., Kammerer, A.M., Wu, J., Pestana, J.M., Riemer, M.F., Sancio, R.B., Bray, J.D., Kayen, R.E. & Faris, A. 2003. Recent advances in soil liquefaction engineering: a unified and consistent framework. *Keynote Presentation 26th Annual ASCE Los Angeles Geotechnical Spring Seminar, Long Beach*. Report No. EERC 2003-06.

Seed, H.B. & Idriss, I.M. 1971. Simplified procedure for evaluating soil liquefaction potential. *Jnl GED*, ASCE, 97(9), 1249-1273.

Tanaka, H. & Tanaka, M. 1998. Characterization of Sandy Soils using CPT and DMT. *Soils and Foundations*, 38(3), 55-65.

TC16 - Marchetti, S., Monaco, P., Totani, G. & Calabrese, M. 2001. The Flat Dilatometer Test (DMT) in Soil Investigations - A Report by the ISSMGE Committee TC16. *Proc. Int. Conf. on In Situ Measurement of Soil Properties and Case Histories, Bali,* 95-131.

Youd, T.L. & Idriss, I.M. 2001. Liquefaction Resistance of Soils: Summary Report from the 1996 NCEER and 1998 NCEER/NSF Workshops on Evaluation of Liquefaction Resistance of Soils. *Jnl GGE* ASCE, 127(4), 297-313.

Yu, H.S. 2004. In situ soil testing: from mechanics to interpretation. *Proc. 2nd Int. Conf. on Site Characterization ISC-2*, Porto, 1, 3-38.

THEORETICAL AND NUMERICAL EVALUATIONS OF THE DMT

Analysis of dilatometer test in calibration chamber

Lech Bałachowski
Gdańsk University of Technology, Poland

Keywords: calibration chamber, DMT, quartz sand, FEM

ABSTRACT: Because DMT in calibration test chamber is two parameter test performed in well defined boundary conditions with a homogeneous soil mass, it presents an interesting possibility for numerical simulations. Insertion of the blade followed by membrane inflation was modeled. Dilatometer tests performed in calibration chamber at Gdańsk UT were modeled with finite element methods using Mohr-Coulomb and Hardening Soil Models. Soil data from triaxial tests were used to define model parameters. The tests made in loose and dense sand at different stress levels were modeled. The influence of BC1 and BC3 conditions and size effect in the calibration chamber was studied numerically. *A* and *B* values measured in dilatometer tests were compared to the calculated mean contact normal stress acting on the dilatometer membrane after the blade insertion and after the inflation of the membrane, respectively. Two modes for membrane inflation were applied: uniform horizontal stress and volumetric strain imposed. A more realistic shape of the membrane displacement and a better correlation with calibration chamber data were obtained with volumetric strain imposed. A good correlation was found between *A* and *B* values measured in calibration chamber and the calculated mean normal contact stress on the membrane.

1 DMT TESTS IN CALIBRATION CHAMBER

A series of dilatometer tests in the calibration chamber were performed for confining pressures ranging from 50 to 400 kPa with either loose or dense sands. The soil specimen was 53 cm in diameter and 100 cm high. The detailed description of the calibration chamber is given in Bałachowski and Dembicki (2000). Soil mass in the calibration chamber is prepared with sand raining. Dense soil mass (I_D=0,8) is obtained with stationary device. Soil mass with I_D=0,4 is formed using small traveling sieves and small falling height of grains. The sand mass is consolidated with K_0 conditions. Predominantly quartz uniform (U=1,4) fine sand (d_{50}=0,21 mm) from the Baltic beach in Lubiatowo is used. The sand parameters were obtained from triaxial CID tests for loose, medium dense and dense sand specimens. Maximum angle of internal friction ϕ_{max} (Fig. 1), modulus of deformation E_{50} at the half of deviatoric stress at failure (Fig. 2) and dilatancy angle ψ were determined. These parameters at given consolidation stress (here 50 kPa) are used (Table 1) to model the soil behavior using Mohr-Coulomb (M-C) and Hardening Soil Model (HSM).

A boundary condition with constant lateral stress (BC1) was maintained during blade insertion. At the end of each 5 cm step of penetration the membrane was inflated and *A* and *B* measurements were read. An example of readings taken at a vertical stress of 100 kPa applied to the upper membrane in the calibration chamber is given for loose and dense sand (Fig. 3). Quite uniform distribution of readings with depth is observed. Derived *A/B* ratio, up to 10, is typical for clean quartz sand.

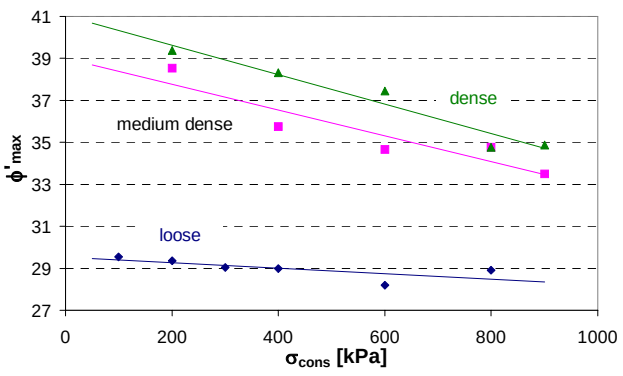

Figure 1. Angle of internal friction.

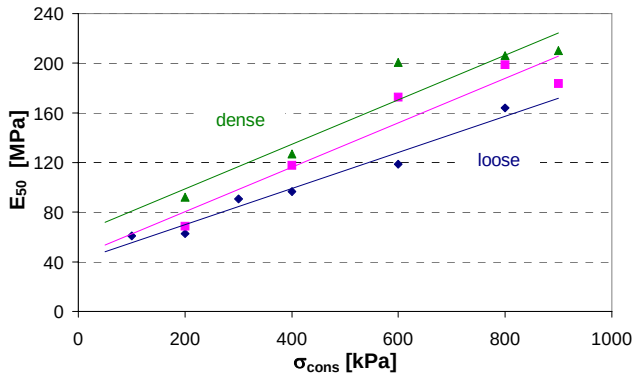

Figure 2. Modulus of deformation E_{50}.

Table 1. Soil parameters from triaxial tests.

I_D [-]	ϕ [°]	ψ [°]	E_{50} [MPa]
0,4	35	5	40
0,8	42	15	70

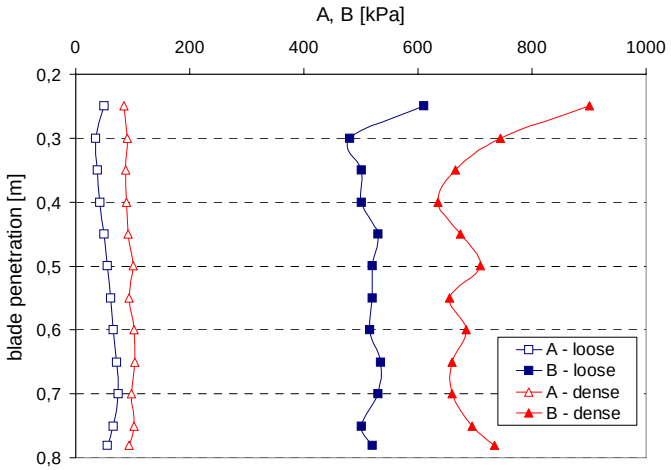

Figure 3. Profiles of A, B measurements in calibration chamber with σ'_v = 100 kPa.

2 NUMERICAL ANALYSIS

2.1 *Plain strain vs. axisymetric problem*

The penetration of dilatometer and the inflation of the membrane are very complex, truly three dimensional phenomena. The penetration of the dilatometer blade, being almost flat, can be considered in simplified manner as 2D problem. The inflation of the circular membrane is, however, a truly 3D phenomena.

Two schemes for membrane inflation analysis in elastic conditions can be considered (Fig. 4). In a first one – corresponding to plane strain conditions - membrane can be treated as a simple beam with free supports. In the second scheme circular plate with free supports on the circumference is considered.

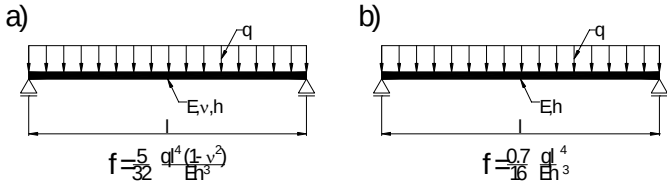

Figure 4. Schemes for membrane deflection: a) simple beam in plane strain conditions, b) circular plate

The formula for membrane deflection under uniform load for both schemes (Fig. 4) are given for :
- simple beam with v=0,3 as :

$$f = 0{,}1422\frac{ql^4}{Eh^3} \quad (1)$$

- circular plate as :

$$f = 0{,}0437\frac{ql^4}{Eh^3} \quad (2)$$

For the same load, the membrane deflection will be thus about 3,5 times more important in plane strain conditions than in axisymetric ones. In order to model properly the inflation of circular membrane one should increase 3,5 times the imposed deflection of the membrane center for the calculation under plane strain conditions. The problem is however more complex as the soil is elasto-plastic and we should include not only the imposed pressure, but the soil response as well.

Some numerical analyses were done to verify the membrane response in plane strain and axisymetric conditions. The calculations were performed using PLAXIS v.8.2 code and Mohr-Coulomb (M-C) and Hardening Soil Model (HSM). A fine mesh, additionally refined near the blade and the membrane, with 15 nodes elements was used. The blade was placed horizontally on the surface of the box filled with sand. Due to symmetry only a half of the membrane was modeled. Vertical stress of 40 kPa was applied on the box surface to simulate lateral stress in the calibration chamber σ'_v = 100 kPa. Then the membrane was inflated by imposing volumetric strain in the cluster just behind the membrane. A numerical response corresponding to *B* reading was evaluated for plane strain (beam) and axisymetric conditions (circular plate). The computed contact normal stress distribution on the half of the membrane is given in Figure 5. Considerably higher contact normal stress is obtained for axisymetric conditions than for plane strain ones. Normal stress distribution is also given for the 1,1 mm displacement multiplied by 3,5 in plane strain conditions. Due to soil plasticity the contact normal stress in axisymetric case is higher than in plane strain conditions with 3,85 mm deflection at the membrane center.

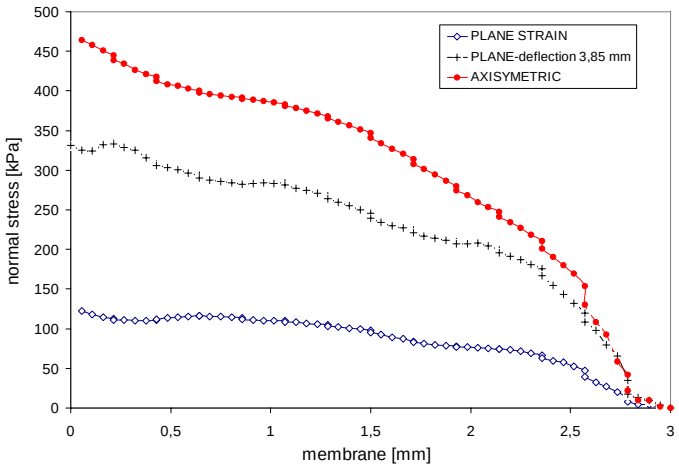

Figure 5. Calculated contact normal stress distribution on the dilatometer membrane.

2.2 *Modeling of blade insertion*

As a first approximation the real chamber dimensions were assumed for calculation mesh. The DMT blade was placed in the middle of the chamber. Stage calculations were made. Gravity was applied in addition to the boundary stresses and conditions. The blade shape was reproduced with the membrane 6 cm in diameter. An interface was introduced between the membrane and the soil. The penetration of the blade was stopped in the calculation when penetration resistance approaches asymptotic value. At this moment the normal stress distribution in the membrane interface was registered, which corresponds to *A* measurement. A series of preliminary calculations show that a considerable chamber size effect was observed during insertion phase (Fig. 6). Horizontal displacement fields after the blade insertion for the chamber of 53 cm and 200 cm in diameter are presented. For further analysis a chamber 200 cm in diameter was assumed.

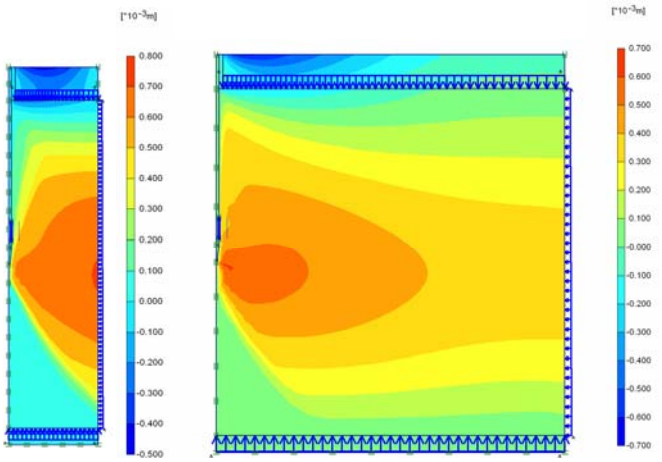

Figure 6. Horizontal displacement fields after the blade insertion for different diameter of the chamber.

2.3 *Modeling of blade inflation*

The membrane inflation was modeled in two manners (Fig. 7). According to the first one a cluster behind the membrane was inactivated and the lateral uniform stress was applied behind the membrane until its center was displaced 1,1 mm, corresponding to *B* measurement. Larger displacements at the edges of the membrane, related to the stress concentration, are observed than in the center (Fig. 8). Such a form of the membrane deflection is however unrealistic, so a different solicitation mode was considered. Moreover, as the membrane inflates the applied stress remains horizontal.

The membrane inflation was modeled with volumetric strain imposed in the cluster behind the membrane. The stress exerted on the membrane is not horizontal, but it is perpendicular to the membrane, which simulates the gas pressure. The maximum deflection of the membrane is observed in its center (Fig. 8). This mode of solicitation was chosen for further analysis.

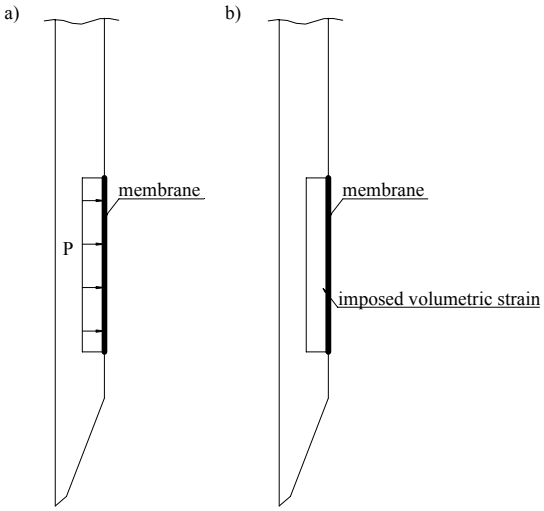

Figure 7. Two modes for membrane inflation.

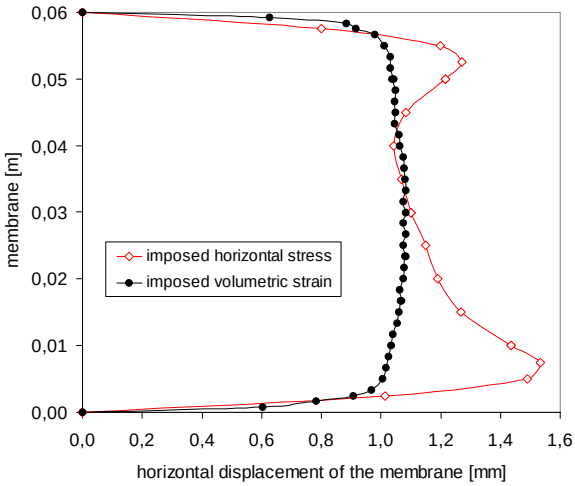

Figure 8. Shape of the inflated membrane with imposed horizontal stress and volumetric strain.

A considerable influence of chamber size effect can be found (Fig. 9) for the *B* measurement (inflated membrane). Chamber size effect in numerical analysis of normal stress distribution along the membrane corresponding to *A* and *B* measurements is given for dense sand (Fig. 10) and for loose sand (Fig. 11). Chamber radius of 100 cm minimizes the influence of the chamber size effect in the calculation. A calibration chamber 200 cm in diameter was used for further parametric studies.

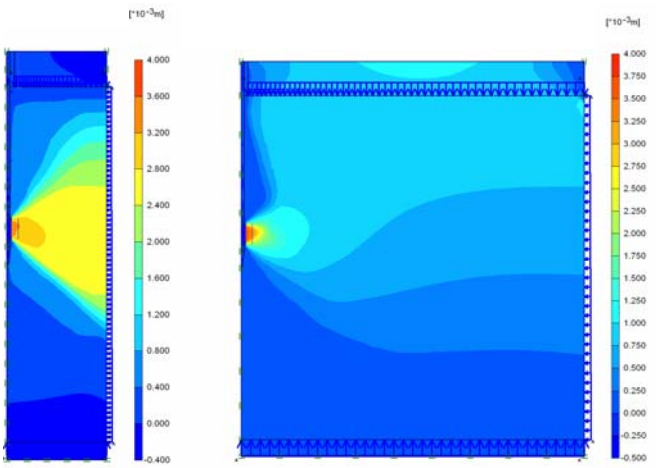

Figure 9. Horizontal displacement fields with inflated membrane.

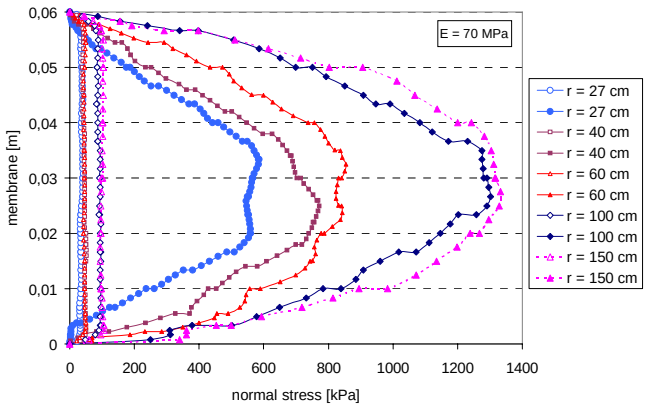

Figure 10. Normal contact stress on the membrane - chamber size effect for dense sand.

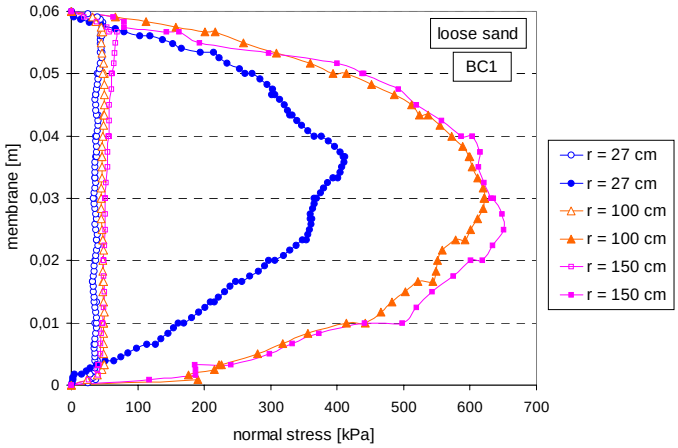

Figure 11. Normal contact stress on the membrane - chamber size effect for loose sand.

An influence of the soil modulus of deformation E_{50} on the calculated normal stress for *A* and *B* measurements was studied (Fig. 12). Calculations were performed for the angle of internal friction equal to 42. The calculated normal contact stress distribution on the membrane for *A* and *B* measurements is insensitive to soil modulus of deformation E_{50} higher than 70 MPa.

The contribution of the angle of internal friction was studied (Fig. 13) for dense sand with E_{50}=70 MPa. Contact normal stress to the membrane corresponding to *A* and *B* measurements is sensitive to the internal friction angle, especially for its high values.

The distribution of contact normal stress on the membrane for loose and dense sand is presented (Fig. 14) for the calculations performed with the soil parameters derived from triaxial tests. Mean contact normal stress on the membrane for loose and dense sand calculated with assumed soil parameters (Table 1) is given for dense sand (Table 2) and loose sand (Table 3). The evaluated mean contact stresses corresponding to both *A* and *B* measurements are close to the values measured in DMT test in calibration chamber (Table 2, Table 3).

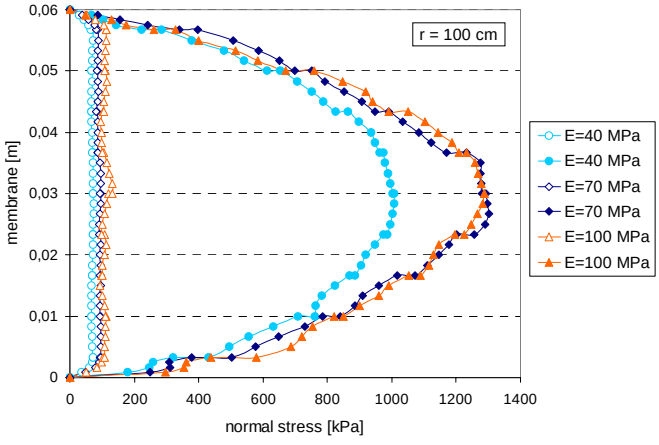

Figure 12. Normal contact stress on the membrane - influence of deformation modulus.

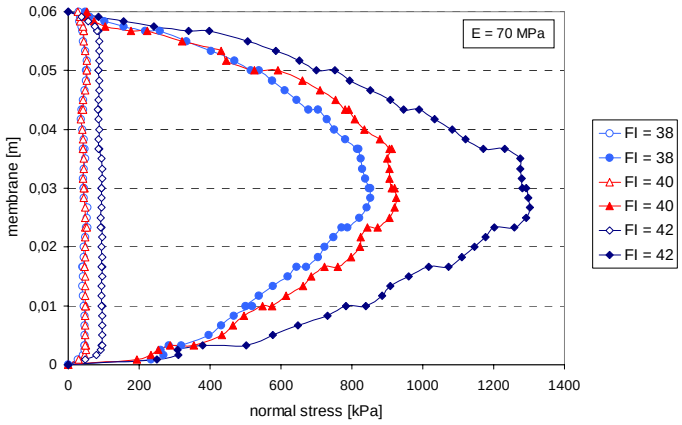

Figure 13. Normal contact stress on the membrane – influence of angle of international friction.

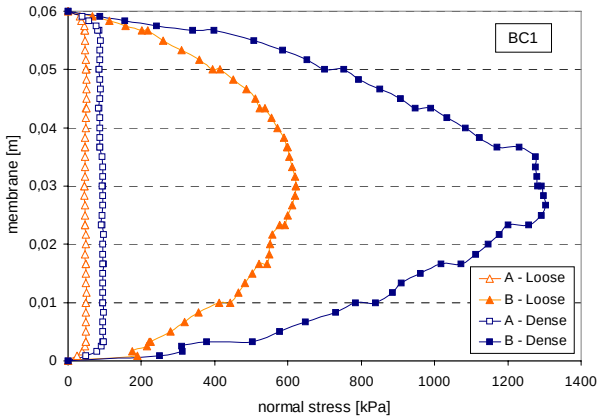

Figure 14. Normal contact stress on the membrane for loose and dense sand for *A* and *B* measurements.

Comparative analyses with M-C and HSM Soil Models were performed for dense sand using the same values of internal friction angle ϕ and modulus of deformation E_{50}. For *A* measurements the numerical analysis gives a similar response for both soil models. For membrane deflection analysis, HSM gives smaller normal contact stress than M-C (Fig. 15).

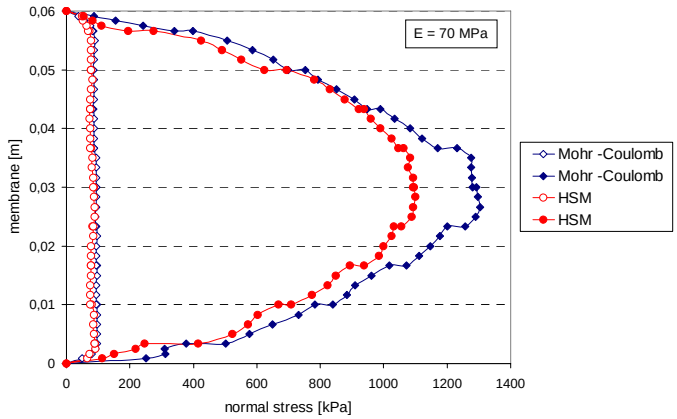

Figure 15. Normal contact stress on the membrane calculated for M-C and HSM soil models.

Table 2. Calculated mean normal contact stress to the membrane for dense sand.

E_{50} [MPa]	ϕ [°]	M-C A [kPa]	M-C B [kPa]	HSM A [kPa]	HSM B [kPa]
40	42	65	679	78	662
70	38	42	558		
	40	44	608		
	42*	85	831	76	721
100	42	101	858		

* A=92 kPa, B=670 kPa for DMT in calibration chamber

Table 3. Calculated mean normal contact stress to the membrane for loose sand.

E_{50} [MPa]	ϕ [°]	M-C A [kPa]	M-C B [kPa]
30	35	41	402
40	35#	45	427
	38	50	518
70	35	43	475

A=62 kPa, B=520 kPa for DMT in calibration chamber

2.4 *Influence of boundary conditions*

The comparison of the calculated distribution of normal contact stress at BC1 and BC3 boundary conditions is given for dense (Fig. 16) and loose sand (Fig. 17). Higher normal stress is calculated for no lateral strain condition (BC3) than at constant lateral stress (BC1) condition. The contribution of the boundary condition is more evident for dense sand.

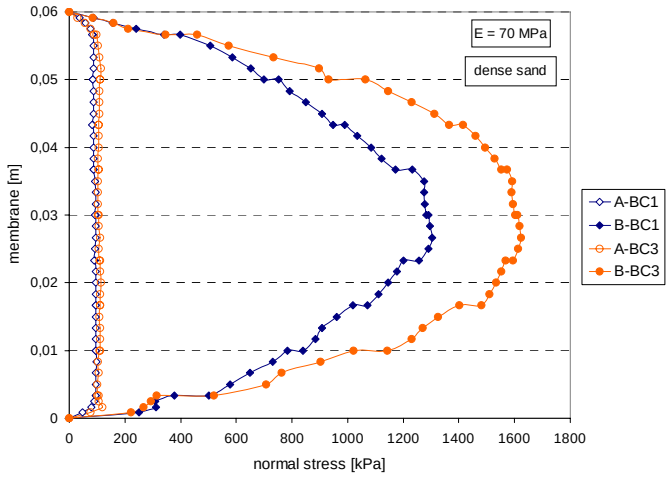

Figure 16. Normal contact stress on the membrane for BC1 and BC3 conditions for *A* and *B* measurements.

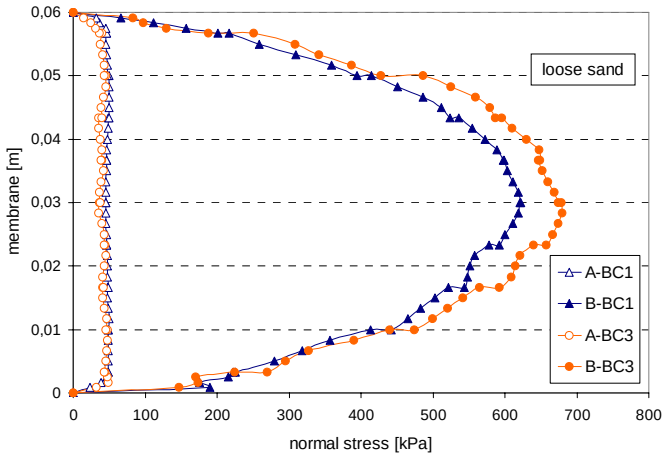

Figure 17. Normal contact stress to the membrane for BC1 and BC3 conditions for *A* and *B* measurements.

3 CONCLUSIONS

DMT model test with well defined boundary conditions in a reference sand was studied with FEM. Simplified two dimensional analysis in plane strain conditions were used to model 3D problem of blade insertion and membrane inflation. Larger deflection of the dilatometer membrane was applied in numerical analysis in order to adjust and approximate axisymetric response of circular membrane. A quite good approximation of DMT model tests was obtained in numerical modeling of two pressures (*A, B*), independently.

The parametric studies were performed and the analysis shows that the calculation performed with the soil parameters derived from triaxial tests fits well the measurements in calibration chamber. The results are sensitive to the internal friction angle and less to the modulus of deformation.

Sensitivity analysis shows that the chamber with at least 200 cm in diameter is necessary to minimize chamber size effect in numerical calculation. In reality the blade insertion induces less soil disturbance than in 2D case. Inflation of circular membrane generates less soil deformation than in plane strain conditions. It is generally considered that classical chamber 120 cm in diameter permits to avoid size effect in dilatometer tests. With the calibration chamber 53 cm in diameter some size effects could be however observed, especially for dense specimen.

Additional analyses are necessary to model the blade insertion with large deformation analysis. Analysis with PLAXIS code, even with updated mesh procedure, does not permit to reach large displacement during dilatometer blade insertion. Further research with 3D analysis is necessary.

ACKNOWLEDGEMENTS

I express my gratitude to prof. Silvano Marchetti for his suggestions and for supplying DMT equipment used in the calibration chamber tests.

REFERENCES

Baldi, G. Bellotti, R. Ghionna, V. Jamiolkowski, M. Marchetti, S. & Pasqualini, E. 1986. Flat dilatometer tests in calibration chambers. Proc. In Situ'86, GT Div., ASCE, June 23-25, Blacksburg, VA : 431-446.

Bałachowski, L. & Dembicki, E. 2003. La construction d'une chambre d'étalonnage à l'Université Technique de Gdańsk. Studia Geotechnica et Mechanica, Vol. XXV, No. 1-2.

Jamiolkowski, M. Lo Presti, D. C. F., Manassero, M. 2001. Evaluation of relative density and shear strength of sand from CPT and DMT. LADD Symposium, October 2001.

Marchetti, S. 1980. In situ tests by flat dilatometer, Journal of the Geotechnical Engineering Division, ASCE, Vol. 106, No. GT3.

Marchetti, S. Monaco, P. Totani, G. & Calabrese, M. 2001. The flat dilatometer test (DMT) in soil investigations. A report by the ISSMGE Committee TC16. Proc. IN SITU 2001, Bali, May 21.

PLAXIS v.8.2 manual

DMT dissipation analysis using an equivalent radius and optimization technique

Young-Sang Kim
Ocean Engineering Program, Division of Marine Technology, Chonnam National University, Jeonnam, Korea
Sewhan Paik
Dohwa Geotechnical Engineering Co., Ltd, Seoul, Korea

Keywords: DMT, Coefficient of consolidation, Dissipation test, Equivalent radius, Optimization technique

ABSTRACT: The worldwide spread of the DMT lies on its simplicity, cost effectiveness, rapid and repetitive use for geotechnical engineering practice. Despite of the simple equipment and operation, various soil parameters – e.g., K_o, OCR, s_u, ϕ, c_h, k_h, γ, M, u_o – can be obtained and have been successfully applied to geotechnical design practice. However, most of those parameters were obtained from the calibrated relationship between the real soil parameter and indices from DMT test. Among them, the estimation of horizontal coefficient of consolidation is more complex due to the inherent difficulty on analyzing a plane strain deformation of the soil around DMT blade during its penetration. Therefore, empirical and semi-empirical methods that use the theoretical solution developed for piezocone with some assumptions have been used to estimate the coefficient of consolidation from dilatometer dissipation test.
In this paper, a new method is proposed which uses an optimization technique and an equivalent radius that is same area with the DMT blade to estimate the coefficient of consolidation from the dilatometer p_2-value dissipation test. Using the BFGS optimization technique, the horizontal coefficient of consolidation that minimizes the differences between the predicted excess pore pressures and measured excess pore pressures (p_2) is determined. Validity of the proposed method was confirmed by comparing the obtained horizontal coefficients of consolidation with those of other interpretation methods and oedometer for the Yang-san site. It has been known that proposed method can give more precise horizontal coefficient of consolidation than other methods do. In addition, the possible determination of representative coefficient of consolidation corresponding to entire dissipation process was also shown from the good agreements between measured and predicted excess pore pressures over whole dissipation stage.

1 INTRODUCTION

In-situ dissipation tests are increasingly conducted in recent years to evaluate a horizontal coefficient of consolidation (c_h) of soft clay layer. Nevertheless, the dissipation tests by flat Dilatometer have not been carried out so frequently. Some researchers have proposed empirical analysis procedures to interpret the dissipation curve obtained from the flat DMT test. Even though it does not have a porous element for measuring the dissipation characteristics of excess pore water pressure induced by the penetration of Dilatometer blade, it has some advantages over piezocone test. The most favorable aspect of flat DMT dissipation test is believed to be the absence of problems concerning the filter element such as smearing, loss of saturation, clogging, etc. Besides, the horizontal coefficient of consolidation obtained by flat DMT is the representative of an average value of steel membrane contact areas (radius = 60mm), while the piezocone measures the dissipation of pore pressure through the very narrow 5mm band element.

However, DMT methods empirically use theoretical solutions developed for the piezocone dissipation analysis. The present three methods are two DMTC methods [p_2-log t method proposed by Robertson et al. (1988) and C-$\sqrt{t}$ method suggested by Schmertmann (1988)] and one DMTA method developed by Marchetti & Totani (1989). The in-situ determination of horizontal coefficient of consolidation by Piezocone dissipation test has been studied from the early 1970s'. A number of researchers have proposed several available theoretical time factors since then. Presently, it has been well known that the c_h obtained from CPTU dissipation test represents relatively well the in-situ consolidation characteristics, better than those determined by laboratory tests. Among those theoretical solutions for the CPTU dissipation analysis, Torstensson's solution (1977) and Gupta's solution (1983) have been used to interpret the dissipation characteristics of flat DMT in p_2-log t method and C-$\sqrt{t}$ method, respectively.

Totani et al. (1998) compared the coefficient of consolidation results obtained by DMTC (especially p_2-log t method) and DMTA dissipation tests with laboratory results. They pointed out that it is not possible to comparatively evaluate the quality of two methods. Therefore, the validity of those methods has to be verified before using under specific local site characteristics.

In this study, a new interpretation method for DMT dissipation test is proposed using an equivalent radius and optimization technique. Validity of the proposed method was confirmed by interpreting the flat DMT dissipation tests carried in Yangsan site of Korea and comparing the estimated coefficients of consolidation with reference values. For the purpose of comparison, undisturbed samples were taken and oedometer tests were carried out.

2 INTERPRETATION METHODS FOR DMT DISSIPATION TEST RESULTS

2.1 *DMTC method*

In this method, there are two types of interpretation. One is the p_2-log t method developed by Robertson et al. (1988) and the other is the C-$\sqrt{t}$ method suggested by Schmertmann (1988). This method consists of stopping the blade at a given depth and taking a sequence of readings A-B-C at different times. The p_2-log t method uses a dissipation curve of p_2, which is an adjusted C-reading for the membrane stiffness, while the C-$\sqrt{t}$ method uses the uncorrected C-reading. The p_2-log t method was developed upon the basic fact that the value of p_2 is essentially the penetration pore pressure of DMT blade and the final p_2 value in a complete dissipation represents the static pore pressure u_o. This fact has been verified by several researchers for NC and slightly OC clays. Other difference between those two methods is determination of the elapsed time t_{50} for estimating the c_h. The p_2-log t method uses logarithmic time scale plot, while the C-$\sqrt{t}$ method uses $\sqrt{time}$ scale plot.

The equation that is used for evaluating the c_h in both methods is as follows:

$$c_h = \frac{R^2 \cdot T_{50}}{t_{50}} \qquad (1)$$

where R = equivalent radius, T_{50} = theoretical time factor for 50% degree of dissipation, t_{50} = elapsed time for 50% degree of dissipation.

2.2 *Equivalent radius and theoretical time factor T*

To use equation (1), Robertson et al. (1988) and Schmertmann (1988) had proposed different equivalent radius and used different theoretical time factor as shown in table 1.

Table 1. Summary of equivalent radius and time factor of DMTC method

	p_2-log t method	C-$\sqrt{t}$ method	Remark
Equivalent Radius	20.57mm considering the section area of DMT blade	24.5mm R^2=600mm^2	DMT blade dimension (95mm ×14mm)
Theoretical time factor T_{50}	Torstensson (1977) Cylindrical Cavity Expansion solution	Gupta (1983) Successive Spherical Cavity Expansion solution	C-$\sqrt{t}$ method can consider the location of pore pressure measurement

2.2.1 *Equivalent radius*

The p_2-log t method uses the equivalent radius of R=20.57mm which has the same section area as DMT blade, while C-$\sqrt{t}$ method proposed R^2=600mm^2, which results in the enlarged equivalent radius R=24.5mm. However, comparison between maximum volumetric and shear strains developed by insertion of DMT blade and cone shows that the maximum volumetric strain of cone is 3 times larger than that of DMT (Schmertmann, 1988). This kind phenomenon has been also found theoretically by Baligh & Scott (1975).

2.2.2 *Theoretical solution*

As summarized above in Table 1, p_2-log t method uses Torstensson's (1977) cylindrical cavity expansion solution and C-$\sqrt{t}$ method uses Gupta's (1983) successive spherical cavity expansion solution. Major difference between those two theoretical solutions is whether it can consider the measuring point of pore pressure which is developed by penetration of dilatometer or not. Schmertmann (1988) used the Gupta's theoretical solution, which was obtained 4 times behind of equivalent radius from the tip, to consider the location of measuring pore pressures.

Figure 1 shows the comparisons between penetration pore pressures measured from the three different locations of piezocone - u_1, u_2, and u_3 – and measured from the porous stone located at center of steel membrane of DMT blade (Robertson et al., 1988). From the figure, it was found that the penetration pore pressures measured from the DMT blade are similar to those measured at the u_3 location (behind the sleeve fiction) than the location u_2. It was also known that initial excess pore pressure magnitude decreases from the tip to the sleeve friction but the dissipation time becomes longer (Baligh & Levadoux, 1980). From these facts, it is more appropriate to use theoretical solution that can consider the pore pressure measurement point of DMT blade.

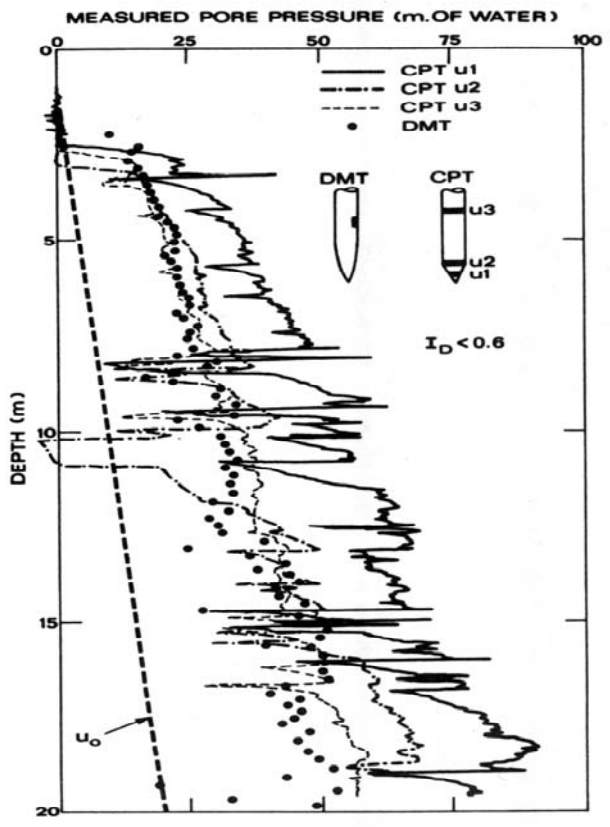

Figure 1. Comparison of penetration pore pressure measured by DMT and Piezocone (Robertson et al., 1988)

3 DETERMINATION OF HORIZONTAL COEFFICIENT OF CONSOLIDATION USING OPTIMIZATION TECHNIQUE

In this research, a direct optimization technique that determines unknown soil parameters by minimizing the objective function defined as the sum of squares of differences between calculated and measured quantities [Eqn (2)] is adopted. It is implemented in the program which can simulate the penetration process of the DMT simulated with equivalent radius and the linear-uncoupled consolidation process. By introducing an optimization technique to dissipation analysis, horizontal coefficient of consolidation, which reflects the dissipation trend, can be obtained (Kim & Lee, 2000).

$$f(\mathbf{x}) = \sum_{n=1}^{ntime} (u^n - U^n)^2 \qquad (2)$$

where ntime = number of measuring time steps; u^n = calculated pore pressure at time n; U^n = measured pore pressure at time n, and $\mathbf{x}$ = vector of design variables.

Based on research results (Robertson et al., 1988; Lutenegger, 1988; Schmertmann, 1988), it is assumed that dissipation process around the DMT blade is predominantly horizontal, therefore, horizontal coefficient of consolidation has been considered as design variable [Eqn (3)].

$$\mathbf{x} = (c_h) \qquad (3a)$$

$$\mathbf{x}_{lower} \le \mathbf{x} \le \mathbf{x}_{upper} \qquad (3b)$$

In Eqn (3), $\mathbf{X}_{lower}$ and $\mathbf{X}_{upper}$ are lower and upper bound values for the variables, respectively. The values of $\mathbf{X}$, $\mathbf{X}_{lower}$, and $\mathbf{X}_{upper}$ can be reasonably estimated by either laboratory tests, in-situ tests, or engineering judgments.

To consider the measuring point of pore pressure, excess pore pressures calculated 4 times behind of equivalent radius from the tip were used as the calculated pore pressures u^n shown in equation (2). Equivalent radius was selected as 20.57mm, which has the same section area with DMT blade. To solve the formulated unconstrained optimization problem, the BFGS (Broyden-Fletcher-Goldfarb-Shanno) technique (Arora, 1989), which is the most popular and has been proven to be the most effective in application to unconstrained optimization problems, was used. The gradient vector of the objective function was calculated by the finite difference scheme because of the highly implicit nature of the objective function.

4 APPLICATION OF THE PROPOSED METHOD

4.1 *Comparison of the horizontal coefficient of consolidation*

To validate the proposed method, 6 DMT dissipation test results, which were carried at the Yangsan siteof Korea, were analyzed. Coefficients of consolidation determined from the proposed method are compared with those calculated from other DMTC interpretation methods and laboratory test results. Basic soil properties, rigidity indices, and soil classification results for the sample obtained from the test site are summarized in Table 2.

Table 2. Basic soil properties of Yangsan site (Lee et al., 2001)

Borehole	Depth (m)	Undrained shear strength s_u (kPa)	E/s_u	Liquid limit	Plastic index	USCS
YS -1	15	60.8	110	56.3	28.9	CH
YS -1	18	68.6	85	47.3	24.9	CL
YS -2	12	52.0	110	54.1	30.8	CH
YS -2	15	60.8	90	55.4	30.1	CH
YS -3	19	86.3	85	47.3	24.0	CL
YS -3	24	127.5	70	43.3	19.2	CL

Figure 2 shows the dissipation test results that were carried by Lee et al. (2001). The early phase up to around 50% degree of dissipation is used as an input degree of dissipation data. An arrow on each dissipation curve points 50% degree of dissipation which is a half of initial excess pore pressure.

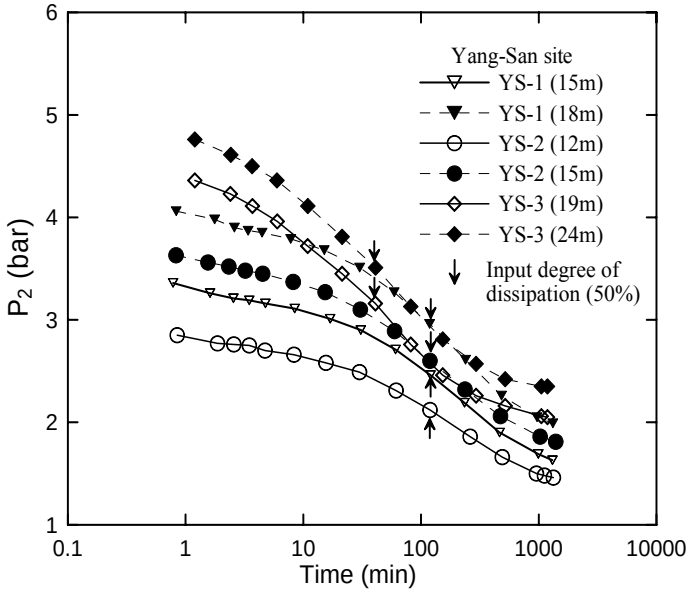

Figure 2. DMT p_2 dissipation curves measured at Yangsan site (Lee et al., 2001)

Coefficients of consolidation are compared in Table 3 and Figure 3. In Figure 3, x–axis shows the coefficient of consolidation estimated from p_2-log t method. As a reference value, coefficient of consolidation obtained from oedometer test for the undisturbed sample was used. It has been known that the horizontal coefficient of consolidation is generally larger than vertical coefficient of consolidation. Lacerda et al. (1977) proposed a correlation between vertical and horizontal permeability considering the void ratio based on the laboratory permeability test results. Although little experimental information exists on the ratio of horizontal to vertical compressibility, this ratio has been believed to be close to unity for OCR ≈ 1 and, in practice, the compressibility of clays is generally considered isotropic (Parry & Wroth, 1977). Therefore, the ratio of c_h/c_v can be obtained from the ratio k_h/k_v proposed by Lacerda et al. (1977) based on the void ratio of Yangsan site. In this study, horizontal coefficient of consolidation were obtained from the following equation (4) using the ratio of k_h/k_v as 2.2.

$$c_h = \left(\frac{k_h}{k_v}\right) \cdot c_v = 2.2 \cdot c_v \qquad (4)$$

where c_h = horizontal coefficient of consolidation, c_v = vertical coefficient of consolidation, k_h = horizontal coefficient of permeability, k_v = vertical coefficient of permeability

As shown in the Figure 3, horizontal coefficients of consolidation determined from the proposed method were obtained consistently with r^2=0.99 and magnitude of those values are similar with those determined from the oedometer except one point, which is indicated by dot circle and might be affected by sample disturbance.

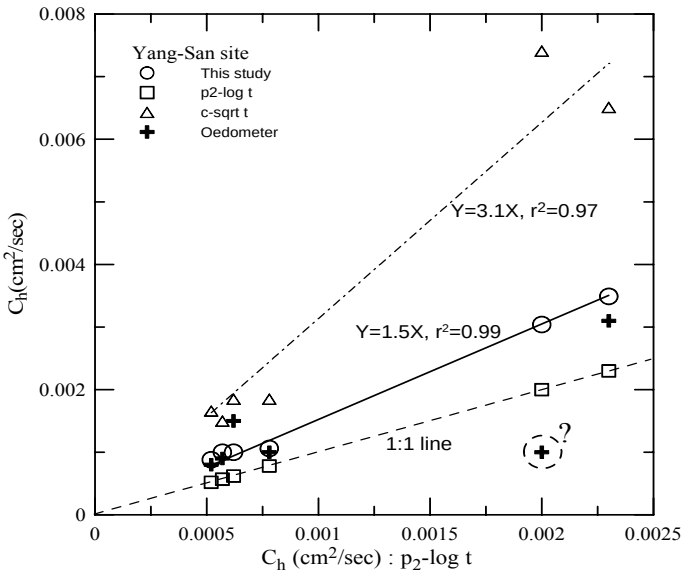

Figure 3. Comparisons of coefficients of consolidation

Table 3. Comparisons of the coefficient of consolidation

Location	This study	P_2-log t method	C-$\sqrt{t}$ method	Oedometer*
	($c_h \times 10^{-3}$ cm^2 / sec)			
YS-1(15m)	1.0	0.6	1.9	1.5
YS-1(18m)	1.1	0.8	1.9	1.0
YS-2(12m)	0.9	0.5	1.7	0.8
YS-2(15m)	1.0	0.6	1.5	0.9
YS-3(19m)	3.0	2.0	7.4	1.0
YS-3(24m)	3.5	2.3	6.5	3.1

* calculated using Eq. (4)

Coefficients of consolidation determined from the proposed method fall between those determined by p_2-log t method and C-$\sqrt{t}$ method. Comparing coefficients of consolidation determined from the laboratory with those determined from p_2-log t and C-$\sqrt{t}$ method, p_2-log t method underestimates while C-$\sqrt{t}$ method over-estimates. It supports that equivalent radius and theoretical solution integrated with optimization technique is effective to model the penetration and dissipation procedure of dilatometer test.

4.2 *Prediction of dissipation behavior over the entire dissipation range*

Present interpretation methods – i.e., p_2-log t method and C-$\sqrt{t}$ method – determine the coefficient of consolidation from the particular degree of dissipa-

tion (or particular elapsed time t_{50}) using equation (1). Therefore, back calculated dissipation curve using those coefficients of consolidation would match exactly at one point t_{50}. However, the proposed method uses dissipation trend by introducing the optimization technique. Figure 4 shows the effectiveness of optimization technique and dissipation trend by comparing between measured and predicted dissipation curve over the entire dissipation range. Predicted dissipation curve is calculated by simulating the penetration of DMT blade and dissipation behavior of excess pore pressure around DMT blade with coefficient of consolidation determined from the proposed method. Predicted dissipation curves coincide well with measured dissipation curves. From the result shown in the Figure 4, it can be concluded that the proposed method can evaluate the representative coefficient of consolidation over the various stress levels which were experienced during entire dissipation range.

5 CONCLUSIONS

A new method, which uses an equivalent radius (R=20.57mm) and integrates the theoretical solution that can consider the measuring point of penetration pore pressure and optimization algorithm, was proposed to estimate the coefficient of consolidation from the DMT p_2 dissipation data. The proposed method estimates with higher precision than other interpretation methods (such as p_2-log t or C-$\sqrt{t}$ methods) the coefficients of consolidation determined in-situ, particularly when compared with laboratory test results. Dissipation curve calculated with coefficient of consolidation determined from the proposed method coincide well with measured dissipation curve over the entire dissipation range. It can be concluded that the optimization technique can evaluate with good representativeness the coefficient of consolidation over the various stress levels experienced during entire dissipation range, by reflecting the early phase of dissipation trend.

REFERENCES

Arora, J. S. 1989. *Introduction of Optimum Design*, McGraw-Hill Series.

Baligh, M.M. & Levadoux, J.N. 1980. Pore Pressure Dissipation after cone penetration. *MIT. Dept. of Civil Engineering, Report R.80-1*, Cambridge, MA, 367 pp.

Baligh, M.M. & Scott 1975. Quasi-Static Deep Penetration in Clay. *Journal of ASCE*, Geotechnical Division.

Gupta, R.C. 1983. Determination of the in situ coefficient of consolidation and permeability of submerged soil using electrical piezoprobe sounding. *Ph.D. Dissertation, Univ. of Florida*.

Kim, Y.S. & Lee, S.R. 2000. Prediction of long-term pore pressure dissipation behavior by short-term piezocone dissipation test, *Computers and Geotechnics*, Vol.27, No.4: 273~287.

Lacerda, W.A., Costa-Filho, L.M., & Duarte, A.E.R. 1977. Consolidation characteristics of Rio de Janeiro soft clay. *Proceedings of International Symposium on Soft Clay,* Bangkok: 231~243.

Lee, S.R., Kim, Y.S., & Seong, J.H. 2001. Evaluation of applicability of Dilatometer dissipation test method estimating horizontal coefficient of consolidation in Korean soft deposits. *KGS*, Vol. 17, No 4: 153-160.(in Korean)

Lutenegger, A.J. 1988. Current status of Marchetti dilatometer test. *1-ISOPT*: 137~155.

Marchetti, S. & Totani, G. 1989. C_h evaluations from DMTA dissipation curves. *XII ICSMFE*: 281~286.

Parry, R.H.G. & Wroth, C.P. 1977. Shear properties of soft calys. *Report presented at the Symposium on Soft Clay*, Bangkok, Thailand.

Roberton, P.K., Campanella, R.G., Gillespie, D., & By, T. 1988. Excess pore pressures and the flat dilatometer test. *1-ISOPT*: 567~576.

Schmertmann, J.H. 1988. Guidelines for Using the CPT, CPTU and Marchetti DMT for geotechnical design. *Report No. FHWA-PA-87-024+84-24* to PennDOT, Vol. III – DMT.

Totani, G., Calabrese, M. & Monaco, P. 1998. In situ determination of Ch by Flat Dilatometer (DMT), Proc. First Intnl Conf. On Site Characterization ISC '98, Atlanta, Georgia (USA), Apr 1998, Vol. 2, 883-888.

Torstensson, B.A. 1977. The pore pressure probe. Nordiske Geotekniske M ϕ te, Oslo, Paper No. 34. 1-34.15.

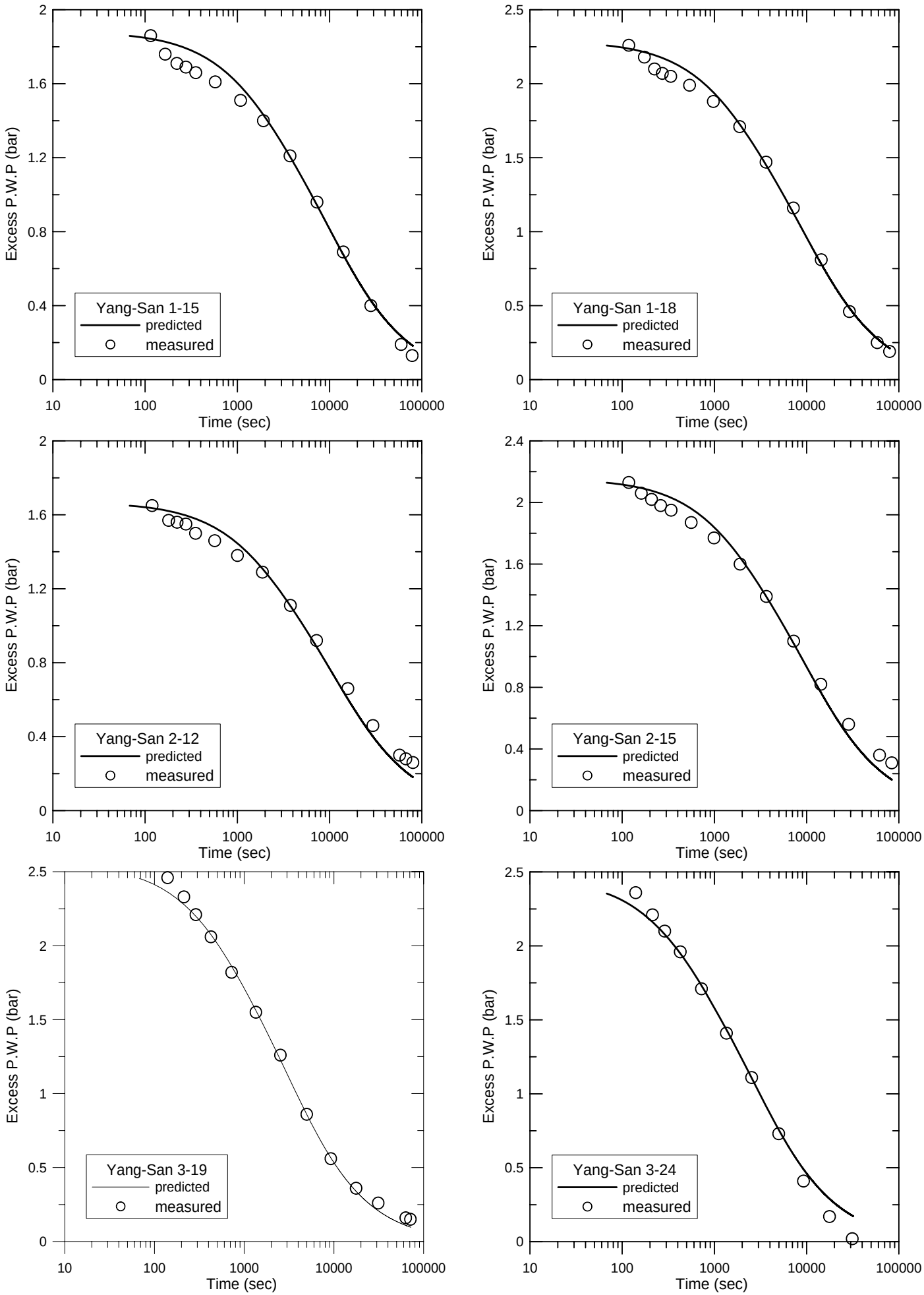

Figure 4. Comparisons of the entire dissipation behavior between calculated and measured dissipation curve

Cavity expansion model to estimate undrained shear strength in soft clay from Dilatometer

Alan J. Lutenegger
University of Massachusetts, Amherst, Massachusetts, USA

Keywords: Dilatometer, clays, undrained strength

ABSTRACT: The Dilatometer has rapidly become a common in situ test for evaluating geotechnical properties of clays. In general, current empirical correlations for most engineering properties are in part site specific and considerable scatter between estimated and measured values of soil properties has been reported. At the present time there are at least seven different empirical methods available for estimating undrained shear strength in clays from Dilatometer results. In this paper, a technique based on a simple cylindrical cavity expansion theory is proposed for predicting the undrained shear strength of soft and medium stiff saturated clays using the results of flat Dilatometer tests. The method uses an estimate of the excess pore water pressures generated by an advancing full-displacement probe to predict the penetration effective stress at the probe face. An estimate of the penetration effective stress on the face of the blade after penetration is obtained from (P_o - P_2). A comparison between values estimated using this approach and undrained strength obtained by field vane tests at a several clay sites are presented and show excellent results. The proposed method appears to be superior to existing empirical methods for evaluating undrained strength from the DMT and is generally independent of the site.

1 INTRODUCTION

The Flat Dilatometer has become a common in situ test used by a growing number of geotechnical engineers throughout the world for routine site investigations. The test is also seeing increased usage in a variety of soils and applications (Marchetti, 1980; Lutenegger, 1988). Apart from its use as a profiling tool in which individual pressure measurements may be used to indicate relative changes in stratigraphy, the test has excellent potential for use in estimating several specific soil properties; provided proper interpretation techniques are employed. As suggested by Wroth (1984), such techniques should be well founded in soil mechanics and should be checked against other well established data and/or well documented case histories in which soil behavior can be reliably deduced.

One of the specific uses for the DMT has been to provide an estimate of the undrained shear strength of saturated clays. Generally, comparisons of the predicted strength have been reasonably accurate and generally on the conservative side in softer soils but are less accurate in stiffer soils which exhibit "overconsolidated" behavior. The current procedure for predicting undrained shear strength of clays as proposed by Marchetti (1981) has been shown to be unreliable in some cases and as a result may often require extensive local correlation to develop site specific correlations and a sense of reliability.

This paper presents the results of a field investigation performed to compare the results of the DMT with undrained shear strength in clay obtained with the field vane test. A simple cylindrical cavity expansion model is presented and is proposed as an initial theoretical basis to serve as a framework for interpreting the DMT for undrained shear strength. Issues relating to values of undrained strength obtained from either laboratory tests or other in situ tests are not addressed.

2 BACKGROUND – EVALUATING UNDRAINED STRENGTH FROM DMT

The DMT represents an in situ soil test which has seen rapid growth in use, partly because of its robust construction, simple deployment and operation, and

general applicability in a wide range of materials. In fine-grained soil deposits, the DMT is particularly attractive over other in situ tests that might be used; it is faster than a field vane, easier to deploy than a piezocone; and generally makes more sense than a Standard Penetration Test. A specific application of the DMT in these materials is in the evaluation of the undrained shear strength. A number of methods have been suggested for evaluating undrained shear strength from DMT measurements.

2.1 *Marchetti(1980)*

Marchetti (1980) had suggested that a simple empirical relationship could be used to predict the normalized undrained strength of cohesive soils from the DMT lift-off pressure, P_o, according to the expression:

$$s_u/\sigma'_{vo} = 0.22\ (0.5\ K_D)^{1.25} \qquad (1)$$

where: s_u = undrained shear strength, σ'_{vo} = initial vertical effective stress, K_D = DMT Lateral Stress Index = $(P_o - u_o)/\sigma'_{vo}$, and u_o = in situ pore water pressure. This correlation was developed based on the observed comparison between soil overconsolidation ratio (OCR) determined from oedometer tests and K_D and the SHANSEP concept presented by Ladd et al. (1977) in which:

$$(s_u/\sigma'_{vo})_{OC} = (s_u/\sigma'_{vo})_{NC} OCR^m \qquad (2)$$

Using a value of $(s_u/\sigma'_{vo})_{NC}$ equal to 0.22 as suggested by Mesri (1975) based on his observations of Bjerrum's (1972) field vane correction chart and a value of m = 0.8 as suggested by Ladd et al. (1977), Marchetti obtained Eq.1. Marchetti (1980) presented a comparison between Eq.1 and the results of undrained shear strength measurements obtained from laboratory unconfined compression tests, triaxial compression tests, and in situ field vane tests which provided reasonable accuracy for the soils investigated. This technique has been used by a number of investigators to compare with a local data base for individual soil types and it appears from more recent investigations that there is a need for site specific verification (e.g., Chang 1988; Lacasse and Lunne 1988; Powell and Uglow 1988). In some cases, Eq.1 tends to overpredict strength obtained by other lab or field techniques, but more generally, it tends to underpredict strength which would be on the conservative side of design.

It may be useful to consider several points about the application of Eq.1 which may contribute to errors in its use:

(1) The normally consolidated value of normalized strength $(s_u/\sigma'_{vo})_{NC}$ = 0.22 was obtained by Mesri (1975) by combining the results of the variation in field shear strength for "young" and "aged" clays with Bjerrum's (1972) field vane correction, and therefore the strength predicted by eq.1 is apparently a "corrected" field vane shear strength. Recall that this correction factor was obtained from back-calculated embankment failures and was developed to force the factors of safety to 1.0 and then applied to the field vane strength. Bjerrum's correction factor may be considered inappropriate in certain design situations by some engineers since variations in vane testing techniques, determination of plasticity index, analytical procedures, etc., are unknown. It may be more appropriate to obtain a measure of the "uncorrected" strength and let the engineer decide if corrections are appropriate to the given design situation, e.g., embankment stability vs. pile skin friction.

(2) The normalized undrained shear strength parameter of 0.22 σ'_{vo} for normally consolidated clays may provide an appropriate initial approximation but does not appear to accurately depict the laboratory derived strength of all clay soils. Available strength data from direct simple shear tests and reported in the open literature, suggest that normalized undrained strength of NC clays increases slightly with increasing plasticity index. Values of $(s_u/\sigma'_{vo})_{NC}$ range from about 0.19 to 0.50 over the range in P.I. from 5 to 90. Some of this variation may be because of difference in test procedures and equipment used even within the same type of test however the results suggest a significant source of error when applying Eq.1. Similar observations have been suggested by other investigators (e.g., Larrsson 1982).

(3) Some engineers may argue that the use of Eq.2 is not generally appropriate for describing the relationship between normalized undrained strength and OCR in other than artificially sedimented soils prepared in the laboratory or very soft young deposits which have not developed any substantial structure. Natural soil deposits which have developed an overconsolidated crust from mechanisms other than simple unloading may have a shear strength relationship which deviates considerably from that described by Eq.2.

(4) In a summary of a large number of available test results, Mayne (1980) showed that the value of m in Eq.2 varied considerably for different clays, ranging from 0.20 to 0.95. The value of m = 0.8 presented by Ladd et al. (1977) was for direct simple shear results, and there is evidence (Mayne 1980) that the value of m varies depending on test conditions for the same soil, e.g., simple shear vs. triaxial CK_oUE vs. triaxial CK_oUC. Additionally, m may

vary with strain rate and other factors which are as yet unknown.

(5) The reference data which were used as the basis for comparison for the results given by Eq.1 were obtained from a number of different laboratory and field tests yet P_o is obviously obtained from the same technique. More appropriately, since undrained shear strength in clays is a function of test technique and other factors, a single test procedure would be desirable for developing a correlation. It should be recognized that even within a single reference test, such as the field vane test, variations in test equipment such as vane length-to-diameter ratio, vane geometry, blade thickness, torque measurement technique, etc. and test procedures such as strain rate, waiting time, etc., may produce different results.

As indicated, comparisons between Eq.1 and measurements of undrained strength using some reference value show a wide variation. Several investigators have presented comparisons with field vane strength and laboratory or other field strength tests. Naturally one would suspect variations because of the reasons previously described. Additionally, it should be remembered that the correlation presented by Marchetti (1980) was developed on a relatively small database and as the base has expanded to other soils variations in accuracy should be expected. Figure 1 shows a comparison of a number of reported correlations between K_D and normalized undrained shear strength illustrating this variation.

The writer (Lutenegger 1988) previously had shown that the accuracy of Eq.1 in predicting the uncorrected field vane strength in clays was related to the DMT material index, I_D, $(= (P_1 - P_o)/(P_o-U_o))$ which generally describes the drainage characteristics of the test; i.e., low I_D indicates undrained while high I_D indicated drained. As I_D increases, it appears that the error in the estimated strength increases. These results may help explain some of the variations obtained by other investigators.

2.2 *Roque et al. (1988)*

An alternative approach to estimating the undrained shear strength was presented by Roque et al. (1988) using a simple bearing capacity approach as:

$$s_u = (P_1 - \sigma_{HO})/N_c \qquad (3)$$

where: P_1 = DMT 1 mm expansion pressure; σ_{HO} = in situ total horizontal stress = $K_o\sigma'_{vo} + u_o$; N_c = bearing capacity factor. Values of N_c varying from 5 to 9 were suggested by Roque et al. (1988) as:

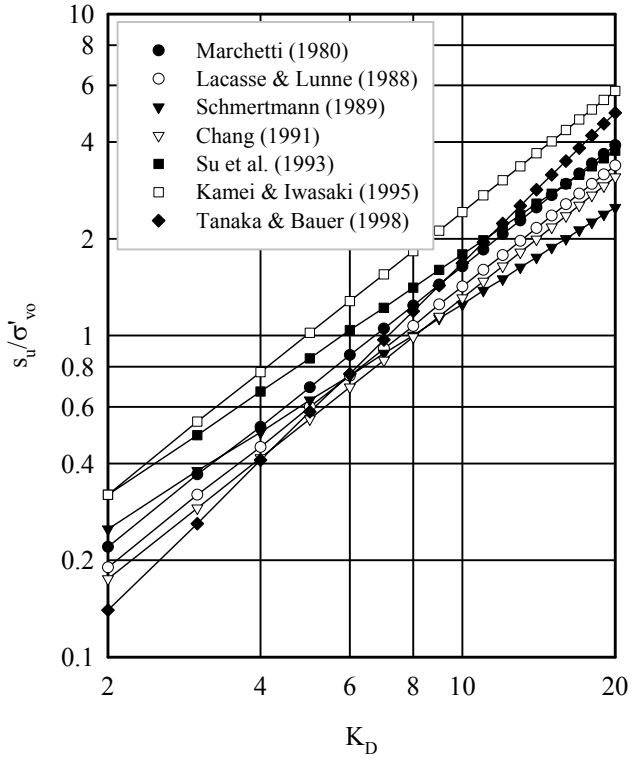

Figure 1. Comparison of several proposed DMT undrained strength correlations.

Soil	N_c
Brittle clay & silt	5
Medium clay	7
Nonsensitive plastic clay	9

This procedure is similar to the semi-empirical approach used to predict undrained shear strength from a prebored (Menard type) pressuremeter using the limit pressure, P_L, where:

$$s_u = (P_L - \sigma_{HO})/N_p \qquad (4)$$

In Eqs. 3 and 4, it is assumed that a limit pressure is obtained during the expansion phase of the test such that $P_1 = P_L$. For the pressuremeter, values of N_p from the literature are often in the range of 5 to 7 which compares well with values of N_c suggested by Roque et al. (1988). This technique requires a value of the in situ horizontal stress and some assumption of the soil type to estimate the bearing capacity factor, N_C. One could estimate K_o from the DMT K_D, however this may introduce an additional source of unknown error.

2.3 Schmertmann (1989)

Schmertmann (1989) presented an explanation for an expected trend between K_D and the undrained

strength based on the limit pressure from cylindrical cavity expansion. For an ideal elastic-plastic, cylindrical expansion in saturated clay with Poisson's ratio = 0.5, the undrained strength may be obtained from:

$$s_u = P_L^*/[1+1n(E/3s_u)] \quad (5)$$

where: P_L^* = net limit pressure = $P_L - (K_o\sigma'v_o + u_o)$. The denominator of Eq.5 may be replaced with:

$$\lambda = 1 + 1n\,(E/3\,s_u) = 5.2 \text{ to } 7.5 \quad (6)$$
$$\text{for } 200 < E/s_u < 2000$$

The normalized undrained strength may then be written as:

$$s_u/\sigma'_{vo} = [(P_L-u_o)/(\sigma'_{vo} - K_o)]/\lambda \quad (7)$$

In soft clays, (i.e., OCR < 2.5) it has been noted that the DMT lift-off pressure, P_o, is approximately equal to the limit pressure obtained from a pressuremeter (Lutenegger 1988), therefore one can reasonably substitute the value of P_o for P_L in Eq.7. Noting that by definition:

$$K_D = (P_o-u_o)/\sigma'_{vo} \quad (8)$$

gives:

$$s_u/\sigma'_{vo} = (K_D - K_o)/\lambda \quad (9)$$

Schmertmann (1989) suggested that since K_o may be expressed in terms of K_D using the empirical equation presented by Marchetti (1980) and using a reasonable value of $\lambda = 6$ from pressuremeter tests, that a good approximation for predicting the normalized undrained strength would be:

$$s_u/\sigma'_{vo} = K_D/8 = (P_o-u_o)/(8\,\sigma'_{vo}) \quad (10)$$

While this technique derives from initially sound theoretical basis from cylindrical cavity expansion, it may suffer from at least two potential sources of error:

(1) Experimental data presented by Lutenegger and Blanchard (1990) have shown that the limit pressure from a full-displacement pressuremeter, which is installed in a manner similar to the DMT, is more accurately predicted by the DMT 1 mm expansion pressure, P_1, for a wide range of clays. This means that it may be more appropriate to substitute P_1 for P_L in Eq.7. Dividing through by the vertical effective stress, this expression becomes identical to Eq.3. Use of Eq.10 then would result in a conservative estimate of undrained strength since $P_o < P_1$. The error will be least for soft clays since P_1 will be close to P_o and greatest for stiff clays where P_1 is much greater than P_o.

(2) The use of Eq.10 indirectly uses an empirical correlation between K_D and K_o, which may also introduce an unknown error.

2.4 Yu et al. (1993)

Yu et al. (1993) performed a numerical study of the undrained penetration mechanics of the DMT by modeling the penetration of the blade as the expansion of a flat cavity. An elastoplastic soil model was used and a plane strain condition was assumed so that no strain was permitted in the vertical direction. The results of this study indicated that the lift-off pressure is a function of the initial horizontal stress, the undrained shear strength, and the rigidity index of the soil. It was found that the normalized lift-off pressure, defined as:

$$N_{po} = (P_o - \sigma_{HO})/s_u \quad (11)$$

N_{po} was not a constant, but increases with the rigidity index of the soil as:

$$N_{po} = -1.75 + 1.57\,\ln(G/s_u) \quad (12)$$

For typical values of rigidity index for clays, the normalized lift-off pressure would range from about 3.6 to 8.3. Rearranging Eq. 12 and solving for s_u would give:

$$s_u = (P_o - \sigma_{HO})/N_{po} \quad (13)$$

2.5 Kamei and Iwasaki (1995)

A suggestion was made by Kamei and Iwasaki (1995) that for soft clays and peat, a correlation could be established between the undrained shear strength obtained from laboratory UU triaxial compression tests and unconfined compression tests and the DMT elastic modulus, E_D, as:

$$s_u = 0.018\,E_D \quad (14)$$

The correlation was based on results of tests conducted in Holocene deposits, all of which have undrained strengths less than 100 kPa. It may be reasonable to expect such a correlation in very soft soils since the value of P_1 is only slightly higher than P_o, giving very low values of I_D. Since E_D reflects the

difference in going from P_o to P_1 it is reasonable to expect that as strength increases E_D also increases.

3 PROPOSED MODEL FOR ESTIMATING UNDRAINED STRENGTH

It may be possible to use a different approach to predicting the undrained strength in saturated soft clays from the DMT by evaluating the installation effective stress acting on the face of a full-displacement (closed-end) probe. Soil movements during the installation of a full-displacement driven cylindrical pile have been described by Carter et al. (1979) as involving purely radial straining. The use of undrained cavity expansion theory provides analytical and numerical methods to predict the installation stresses in the soil adjacent to the pile face. These studies have been summarized by Randolph et al. (1979), Wroth et al.(1979), and Carter et al. (1979).

From cylindrical cavity expansion theory, the installation radial effective stress acting at the face of a cylindrical probe or pile may be given as:

$$\sigma'_r = [1 + (3/M)^{0.5}]\, s_u \qquad (15)$$

where: s_u = initial (in situ) undrained shear strength prior to installation; M = critical state line gradient. This prediction of effective radial stress resulting from full-displacement installation assumes that the soil adjacent to the shaft of the pile is at critical state under plane strain conditions with a radial major principal stress. The plane strain value of the critical state line gradient, M, may be obtained from:

$$M = 3 \sin \varphi'_{ps} \qquad (16)$$

where: φ'_{ps} = plane strain friction angle. By rearranging terms, eq.15 may be rewritten in terms of the undrained strength as:

$$s_u = \sigma'_r/\alpha \qquad (17)$$

where: $\alpha = [1 + (3/M)^{0.5}]$. For most clays, reasonable values of φ'_{ps} range from about 20^o to 30^o, and from Eq.17, it follows that α only varies from 2.56 to 2.72. This represents a maximum difference of only about 6%. Therefore, a reasonable estimate of the undrained strength from the initial installation effective stress for a cylindrical cavity expansion may be obtained as:

$$s_u = \sigma'_r/2.65 \qquad (18)$$

Eq.18 suggests that an estimate of the in situ undrained shear strength may be obtained from full-displacement probes provided that an evaluation of the installation radial effective stress at the soil/probe interface may be made. In most situations this would require a measurement of both the installation radial total stress and total (excess + in situ) pore water pressure at the face of the probe. For most in situ tests, this is not done. Usually, one or the other is measured, but not both. A comparison between predicted and measured installation stresses on a small diameter model pile using this theory was presented by Coop and Wroth (1989) and showed very good results.

4 INSTALLATION EFFECTIVE STRESS ON DMT

The DMT is an instrument which is designed to provide measurements of total stress and has only been equipped to measure pore water pressures as a research tool (Robertson et al., 1988; Campanella and Robertson, 1991). A tool designed to investigate pore water pressures generated by the DMT blade has also been described as the Piezoblade (Boghrat and Davidson, 1983; Lutenegger and Kabir, 1988). It has been shown by several investigators that the total stress value obtained from the DMT lift-off pressure, P_o, is nearly identical to the initial penetration stress from a cylindrical probe (e.g., Full-Displacement Pressuremeter or Lateral Stress Cone).

Robertson et al. (1988) and Lutenegger and Kabir (1988) have shown that the recontact pressure, P_2, obtained from the DMT, is essentially a pore water pressure measurement. Since the P_2 reading is obtained about 1 min after penetration because of the time to inflate the probe to obtain P_o and P_1 and then deflate to obtain in P_2, one would expect this value to be slightly lower than the pore pressure obtained from the Piezoblade which is obtained on installation. It appears that during penetration, at least in soft and medium stiff clays, the effective stress conditions around a cylindrical probe and the DMT do not differ that much. This is probably related to the fact that the aspect ratio of the DMT blade (width/thickness) is not all that far removed from an axisymetric condition and is far from plane strain conditions. In terms of the measurements taken with the DMT, Eq.18 may be rewritten as:

$$s_u = (P_o - P_2)/2.65 \qquad (19)$$

Therefore, it may be that a simple cavity expansion approach may be used to obtain an estimate of the undrained shear strength from the DMT using

two pressure readings. The author recommends that the P_2 measurement be taken routinely as a part of the test and therefore this approach does not require any significant modification to the equipment or procedure. The pressure must be released from the blade after the P_1 reading is obtained before the blade can be advanced to the next test depth anyway; the only difference being that the C-Reading requires slow controlled rather than rapid deflation. Unlike the method presented by Marchetti (1980) the proposed technique does not require estimates of the vertical effective stress or the in situ pore water pressure, both of which may introduce errors.

5 RESULTS

In order to evaluate the accuracy of applying Eq.19 to predict the undrained shear strength of natural clays, a field testing program was conducted at several test sites using both the DMT and field vane test. The approach is illustrated herein using results obtained at four test sites. Table 1 presents a summary of the sites presented. In most of the cases, the sites have a weathered surficial crust which exhibits stiffer overconsolidated behavior.

Table 1. Sites Used to Illustrate Method.

Site	Soil
UMass	Lacustrine soft clay with stiff clay crust
IDA	Marine clay - moderately sensitive
St. Albans	Marine clay - highly sensitive
Bothkennar	Marine clay - sensitive

Dilatometer tests were performed using a standard DMT blade. At each test depth (generally intervals of 0.3 m) the three pressure readings corresponding to P_o, P_1, and P_2 were obtained. The DMT and vane profiles were generally performed within a distance of about 1.5 m. At sites investigated by the author, field vane tests were conducted using a Nilcon Vane Borer with a self-recording torque head. Tests were performed using a 65 mm diameter rectangular vane with a height to diameter ratio of 2 and a blade thickness of 1.5 mm. Tests were performed within one minute of the vane insertion.

The first two test sites (UMass and IDA) were tested by the author. Field vane results from St. Albans were taken from the literature (LaRochelle et al. 1974). Dilatometer and field vane results from Bothkennar were taken from the literature (Nash et al. 1992). These four sites were selected to illustrate the accuracy of the proposed method. To date, the method has been applied to 18 different sites with similar results.

5.1 UMass

Figure 2 shows test results obtained in the Connecticut Valley Varved clay at the UMass site in western Massachusetts.

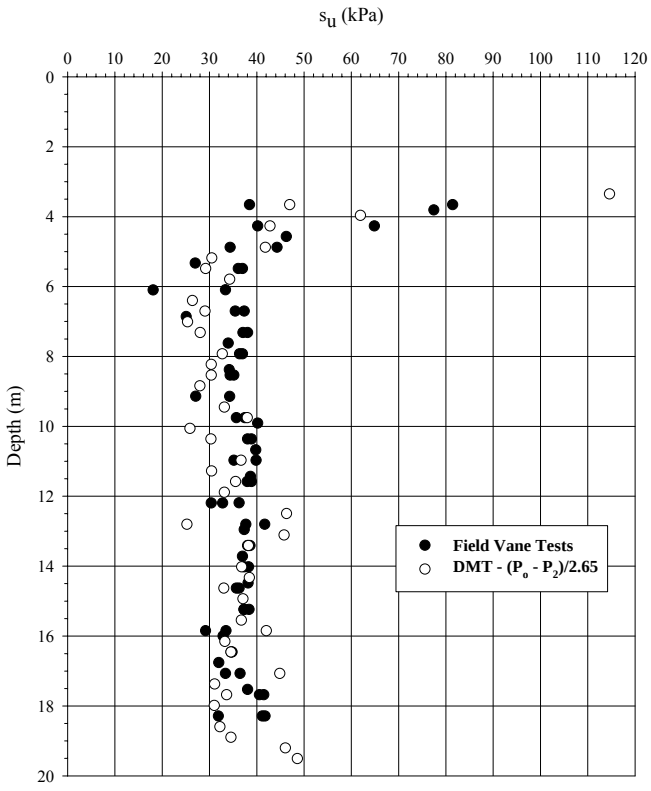

Figure 2. DMT Results at UMass.

5.2 IDA

Figure 3 shows test results obtained in the marine clay at the IDA site in northern New York.

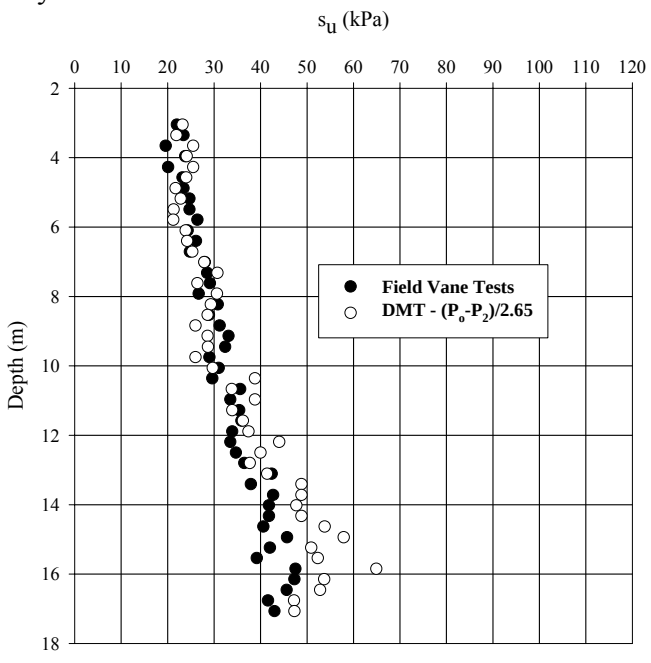

Figure 3. DMT Results at IDA.

5.3 St. Albans

Figure 4 shows test results obtained in the marine clay at the St. Albans site in southern Ontario.

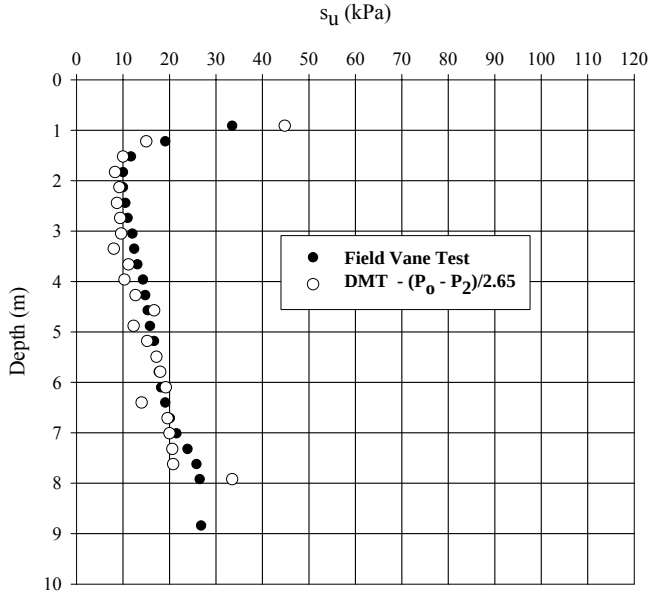

Figure 4. DMT Results at St. Albans.

5.4 Bothkennar

Figure 5 shows test results obtained in the marine clay at the Bothkennar site in Scotland.

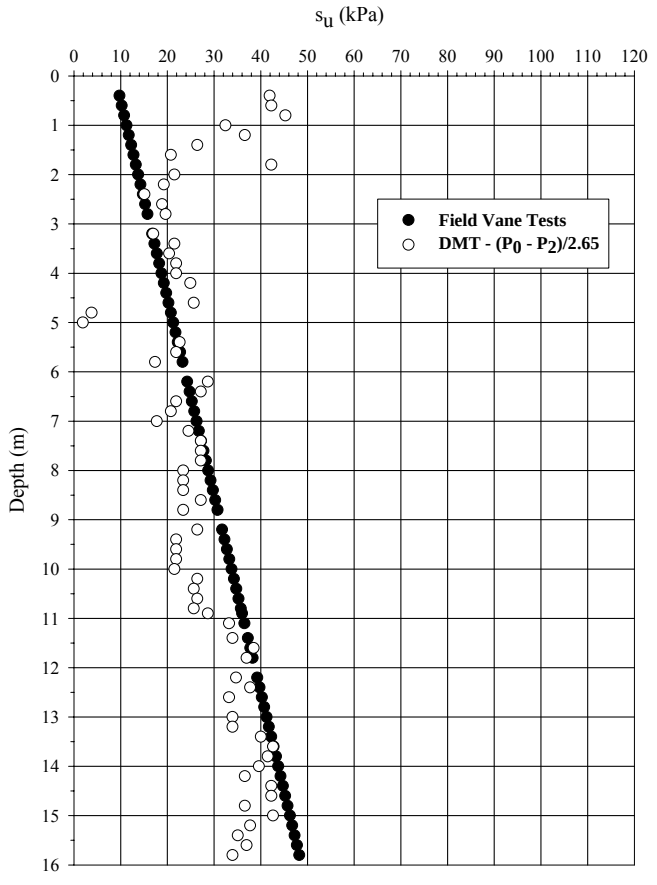

Figure 5. DMT Results at Bothkennar.

A comparison using the method proposed in this paper and expressed by Eq. 19, for all of the results obtained by the author from the field vane and DMT tests shows the results to be grouped between α = 2.0 to 3.0 which fits well with Eq.18. The correlation does not appear to be site specific. Additional examination of the test results is needed to investigate the dependence of α on other specific soil characteristics, such as Plasticity Index (P.I.) and the stress history (OCR) as data become available.

6 DISCUSSION

There are both advantages and disadvantages to the method presented in this paper. These may also be considered in regard to the correct application and potential limitations of the method.

6.1 Disadvantages/Limitations

1. The proposed method often requires the subtraction of two numbers which are relatively close to each other; i.e., the difference between two large numbers. This means that there may be some question about the precision of the resulting number. In order to obtain reliable values for the lift-off (A) and recontact (C) pressure readings operators should be instructed to be careful in performing the test.

2. The method requires an additional pressure reading to be obtained over the two pressure readings originally presented by Marchetti (1980). The author considers this pressure reading of significant importance to the test; some engineers may consider this an unnecessary complication of the test and one which just can lead to confusion for the operator.

3. In order to accurately obtain the recontact pressure reading, a modification to the control console may be necessary by incorporating a flow control needle valve in the deflation pressure circuit.

4. The method is limited by the applicability of Eq. 15. The interpretation assumes that the soil adjacent to the blade is at critical state which may not always be true, especially for overconsolidated soils.

5. It is assumed that the recontact pressure is an accurate representation of the total pore water pressure acting on the face of the blade. As previously shown, this assumption appears to be adequately justified in softer materials (lightly overconsolidated to near normally consolidated) but will certainly be incorrect in the case that negative shear induced pore water pressures are generated. This is because it is not possible to measure a value less than zero on the control console.

6. The test procedure may adversely influence the results. Data presented by Powell and Uglow (1986)

have shown that the recontact pressure may increase if the diaphragm is inflated past the 1 mm pressure (B-reading). Therefore it is important that the operator shut off the inflation valve and begin deflation immediately when the B-Reading is obtained.

6.2 Advantages

1. The proposed method makes use of two pressure measurements obtained from the test to make a prediction of a single soil behavioral property. This means that the correlation should be stronger than methods which use only a single measurement to predict a property.

2. The method makes use of a theory which provides a direct connection from the measurements to the predicted property. There is no required assumption of normalized behavior or normally consolidated behavior or consolidated state.

3. Unlike the method of Marchetti (1980) in which the in situ total stress and in situ pore water pressure at the test depth must be known in order to evaluate the strength, the proposed method does not require input of either total stress or in situ pore pressures. This may be especially advantageous in situations where the in situ pore water pressures are not known or are not hydrostatic and in situations where the vertical stress is difficult to evaluate, such as below fills or adjacent to structures.

4. The method does not appear to be site specific, requiring a new correlation to be developed with each new geologic material or area tested and appears to be reasonably successful in a number of different materials representing a wide range of geologies, plasticity, OCR, sensitivity, etc. Since a single concept based on soil behavior and single reference strength is used, this may be expected.

7 CONCLUSIONS

The results presented in this paper have shown that there is a sound theoretical basis by which the results of Dilatometer Tests may be used to estimate the undrained field vane strength of soft clays. The method requires the measurement of the recontact pressure, P_2. On the basis of comparisons with field vane strengths obtained at several sites, the test results suggest that the approach is sound. It is suggested however, that since the data base presented was obtained using a field vane as the basis for comparison, any precautions which an engineer might normally take when using field vane data because of uncertainties in its application to design should still be applied.

8 REFERENCES

Bjerrum, L. 1972 Embankments on Soft Ground, *Proc. Conf. on Performance of Earth and Earth-Supported Structures, ASCE*, Vol. 2: 1-54.

Carter, J.P., Randolph, M.F., and Wroth, C.P., 1979. Stress and Pore Pressure Changes in Clay During and After the Expansion of a Cylindrical Cavity. *Int. Jour. Numer. and Analyt. Methods in Geomechanics*, Vol. 3: 305-322.

Chang, M.F., 1988. Some Experience with the Dilatometer Test in Singapore, *Proc. 1st Int. Symp. on Penetration Testing*, Vol. 1: 489-496.

Coop, M.R. and Wroth, C.P., 1989. Field Studied of an Instrumented Model Pile in Clay. *Geotechnique*, Vol. 39 (No. 4): 679-696.

Lacasse, S. and Lunne, T., 1988. Calibration of Dilatometer Correlations, *Proc. 1st Int. Symp. on Penetration Testing*, Vol. 1: 539-548.

Ladd, C.C., Foott, R., Ishiharg, K., Scholosser, F. and Poules, H.G., 1977. Stress-Deformation and Strength Characteristics, *Proc. 9th Int. Conf. on Soil Mech. and Found. Engr.*, Vol. 2: 421-494.

LaRochelle, P., Trak, B., Tavenas, F. and Roy, M., 1974. Failure of a Test Embankment on a Sensitive Champlain Sea Clay Deposit. *Canadian Geotechnical Journal*, Vol. 11 (No. 1): 142-164.

Lutenegger, A.J., 1988. Current Status of the Marchetti Dilatometer Test, *Proc. 1st Int. Symp. on Penetration Testing,* Vol. 1: 137-155.

Lutenegger, A.J. and Kabir, M.G., 1988. Dilatometer C-Reading to Help Determine Stratigraphy, *Proc. 1st Int. Symp. on Penetration Testing*, Vol. 1: 549-554.

Marchetti, S., 1980. In Situ Tests by Flat Dilatometer, *Jour. Geotech. Engr. Div., ASCE*, Vol. 106: 229-231.

Mayne, P.W., 1980. Cam-Clay Predictions of Undrained Strength, *Jour. Geotech. Engr. Div., ASCE*, Vol. 106: 1219-1242.

Mesri, G., 1975. Discussion of New Design Procedure for Stability of Soft Clays, *Jour. Geotech. Engr. Div., ASCE*, Vol. 101: 409-412.

Mesri, G., 1989. A Reevaluation of $s_{u\,(MOB)} = 0.22\ \sigma'_p$ Using Laboratory Shear Tests, *Can. Geotech. Jour.*, Vol. 26: 162-164.

Nash, D.F.T., Powell, J.J.M. and Lloyd, I.M., 1992. Initial investigations of the soft clay test site at *Bothkennar. Geotechnique*, Vol. 42 (No. 2): 163-181.

Powell, J.J.M. and Uglow, I.M., 1988. Marchetti Dilatometer Testing in U.K. Soils, Proc. 1st Int. Symp. on Penetration Testing, Vol. 1, pp. 555-562.

Randolph, M.F., Carter, J.P. and Wroth, C.P., 1979. Driven Piles in Clay - the Effects of Installation and Subsequent Consolidation. *Geotechnique*, Vol. 29(No. 4): 361-393.

Schmertmann, J.H., 1986. Suggested Method for Performing the Flat Dilatometer Test, *Geotech. Testing Jour.*, ASTM, Vol. 9: 93-101.

Wroth, C.P., Carter, J.P. and Randolph, M.F., 1979. Stress Changes Around a Pile Driven into Cohesive Soil. *Recent Developments in the Design and Construction of Piles*: 255-264.

Wroth, C.P. 1984. The Interpretation of In Situ Soil Test. *Geotechnique*, Vol. 34 (No. 4): 449-489.

Consolidation lateral stress ratios in clay from flat Dilatometer tests

Alan J. Lutenegger
University of Massachusetts, Amherst, Massachusetts, USA

Keywords: stress ratio, clay, consolidation, Dilatometer

ABSTRACT: The Flat Dilatometer may be used as a push-in earth pressure spade cell to obtain a measure of the reconsolidated lateral stress after penetration excess pore pressures have dissipated. In this procedure, a DMT A-Dissipation test is performed until a constant equilibrium value is obtained and the DMT acts as a total stress cell. Results obtained at several test sites ranging in consistency from very soft to very stiff fine-grained soils are presented. The test data show that the value of $K_C = (\sigma_c - u_o)/\sigma'_{vo}$, the reconsolidation coefficient of lateral stress, obtained after allowing installation effects to stabilize and the lateral stress to reach equilibrium, may be related to the initial state of stress and the stress history (OCR) of the soil. The results demonstrate that the value of K_C is very close to estimated values of K_o in soft and very soft clays but that there is a potential error associated with using the test results directly to infer the at-rest coefficient of lateral stress in stiff clays. The results also give some insight into the magnitude of effective lateral stresses acting on the face of driven piles in clay for use in an effective stress analysis of axial pile skin friction capacity. The results also show that K_C is related to both the initial lateral stress ratio, $K_i = (P_o - P_2)/\sigma'_{vo}$ and the Dilatometer lateral stress index, $K_D = (P_o - u_o)/\sigma'_{vo}$. This eliminates the need to wait until all of the penetration effects have dissipated to make an initial estimate of K_c.

1 INTRODUCTION

Engineers often need to estimate horizontal stresses acting in the ground either under at-rest conditions or on the face of driven piles for using an effective stress design approach. The Dilatometer may be useful in providing a measure of the effective lateral stress by conducting a reconsolidation test. In this way the DMT is used much like a push-in spade cell. Results presented in this paper illustrate this procedure and test results show that K_C is related to K_D.

2 LATERAL STRESS RATIOS IN CLAY

It is useful to consider some basic definitions of lateral stress ratios in clay soils for the purpose of considering possible interrelationships.

2.1 At-Rest Lateral Stress Ratio

Most engineers are familiar with the in situ lateral stress ratio under at-rest conditions which is defined as:

$$K_o = \sigma'_{Ho}/\sigma'_{vo} \quad (1)$$

where σ'_{Ho} = effective in situ at-rest lateral stress and σ'_{vo} = effective in situ vertical stress. The value of K_o is an important parameter for a number of design problems and for clays having undergone simple unloading K_o has been shown to be related to the oedometric yield stress, σ'_p, through the overconsolidation ratio, OCR ($= \sigma'_p/\sigma'_{vo}$) (e.g., Brooker and Ireland 1965; Mayne and Kulhawy 1982); i.e.,

$$K_o = f(OCR) \quad (2)$$

2.2 Dilatometer Lateral Stress Ratio

The Dilatometer provides a determination of a lateral stress ratio through the lift-off pressure, P_o, defined by Marchetti (1979) as the Dilatometer Lateral Stress Index; K_D, in which:

$$K_D = (P_o - u_o)/\sigma'_{vo} \quad (3)$$

where: P_o = DMT lift-off pressure; u_o = in situ pore water pressure. Note that u_o is used in the definition of K_D as a matter of convenience, since the actual pore water pressure at the time P_o is obtained is un-

known and not determined routinely. The value of P_o reflects the lateral stresses prior to installation and any changes that may occur as a result of the blade penetration:

$$P_o = \sigma'_{Ho} + u_o + \Delta\sigma'_H + \Delta u \quad (4)$$

Marchetti (1979) and many others have shown that in clays and other fine-grained soils an empirical relationship may be established between K_D and the stress history (OCR) such that:

$$OCR = f(K_D) \quad (5)$$

2.3 Initial Lateral Stress Ratio

We may also find it convenient to define the Initial Lateral Stress Ratio which may be used to reflect the effective stress ratio immediately after insertion of a probe or a driven pile:

$$K_i = (\sigma_{Ho} - u_i)/\sigma'_{vo} \quad (6)$$

where: u_i is the total pore water pressure ($u_o + \Delta u$) immediately after insertion of the probe. Values of K_i were shown by Baligh et al. using the Piezolateral Stress Cell (Baligh et al. 1985).

In the case of the Dilatometer, the value of u_i is not measured directly, may be estimated from the recontact pressure P_2 which is obtained after the DMT lift off pressure (P_o) and 1 mm expansion pressure, (P_1). Therefore, Eq. 6 may be rewritten as:

$$K_{i(DMT)} = (P_o - P_2)/\sigma'_{vo} \quad (7)$$

K_i may be a useful reference parameter for evaluating soil behavior such as soil type, strength, stress history and drainage characteristics.

2.4 Reconsolidation Lateral Stress Ratio

In the past twenty years, some researchers have shown that it is possible to use special probes such as push-in earth pressure cells or instrumented model piles to obtain a measurement of the lateral stress in the ground after the effects of installation have dissipated. Essentially this is achieved by taking long term measurements of total stress until a stable value is obtained. In this way, any excess pore water pressures, which are difficult to measure, are no longer present and only the in situ pore water pressure, u_o, remains. In this case, the Reconsolidation Lateral Stress Ratio may be defined as:

$$K_C = (\sigma_C - u_o)/\sigma'_{vo} = \sigma'_C/\sigma'_{vo} \quad (8)$$

where: σ'_C is equal to the final effective lateral stress (corrected for u_o) acting on the probe. Naturally, the final effective lateral stress is composed of the initial at-rest effective lateral stress (prior to probe insertion) and any change in effective stress as a result of the probe insertion and reconsolidation; i.e.

$$\sigma'_{C=(\sigma C - u_{o)} = \sigma'_{Ho} + \Delta\sigma'_H} \quad (9)$$

It should be expected that in very soft clays the value of $\Delta\sigma'_H$ will be very small; in very stiff clays $\Delta\sigma'_H$ may be very large.

In the case of the Dilatometer, the value of σ_C may be estimated from a reconsolidation test and Eq. 8 may be rewritten as:

$$K_{C\,(DMT)} = (P_{of} - u_o)/\sigma'_{vo} \quad (10)$$

The value of P_{of} is obtained by observing the change in P_o with time until a stable value is obtained as described in the next section. Previous results (Marchetti et al. 1986; Lutenegger and Miller 1993) have shown that these tests are simple to perform and give reliable results in clays.

3 DETERMINING THE DILATOMETER RECONSOLIDATION STRESS

The Dilatometer may be used in much the same way that push-in earth pressure cells are used to obtain a direct measure of the reconsolidation lateral stress after the effects of installation have come to equilibrium. The test is performed by taking only A-Readings without expanding the diaphragm further to obtain the B-Reading. This procedure is similar to the procedure sometimes referred to as an "A-Dissipation" test. The diaphragm is expanded to obtain the lift-off pressure (A-Reading) but no B-Reading is taken. In this way, the soil remains in contact with the face of the blade and the flexible diaphragm throughout the test. As soon as the DMT penetration is stopped, a stopwatch is started so that the elapsed time between blade penetration and the A-Readings may be obtained.

Successive A-Readings are then taken over time in order to track the decrease in A with time until a stable value is obtained, indicating that the insertion effects, i.e., excess pore water pressure, have dissipated. Depending on the soil conditions, this may require a waiting period ranging from several hours to several days. Since the A-Reading (or P_o) is a total stress measurement, this procedure provides a record of the decay of total horizontal stress with time and is essentially the same as using a push-in total earth pressure cell as previously reported (e.g., Massarch 1975; Tavenas et al. 1975; Tedd and Charles 1981). Once a stable condition is reached and the final A-Reading is taken, the test is performed as in

any other DMT test, i.e., a B-Reading (1 mm expansion) and C-Reading (re-contact) are obtained.

4 RESULTS

DMT reconsolidation tests have been conducted at a number of sites consisting of medium stiff and soft clays. Figure 1 gives results of a typical reconsolidation curve showing the change in total stress (Po) with time. These results were obtained in a soft clay and show the characteristic "S" shaped curve that is similar to results obtained from push-in spade cells and from pore pressure dissipation tests, such as from a Piezocone or Piezoblade. In this case however, Figure 1 represents the change in total horizontal stress with time. The stable value thus becomes the final total horizontal stress, σ_C, and since the pore water pressure has returned to in situ conditions, i.e., prior to blade insertion, the final effective horizontal stress may be obtained from $\sigma'_C = (\sigma_C - u_o)$. Figure 2 shows a set of reconsolidation curves obtained from a single DMT sounding in a deposit of Connecticut Valley Varved Clay (CVVC) at the NGES at the University of Massachusetts in Amherst.

The results obtained from seven soundings at this site show the variation in σ'_C with depth, Figure 2. These results clearly show the sharp decrease in σ'_C through the stiff overconsolidated crust, down to a

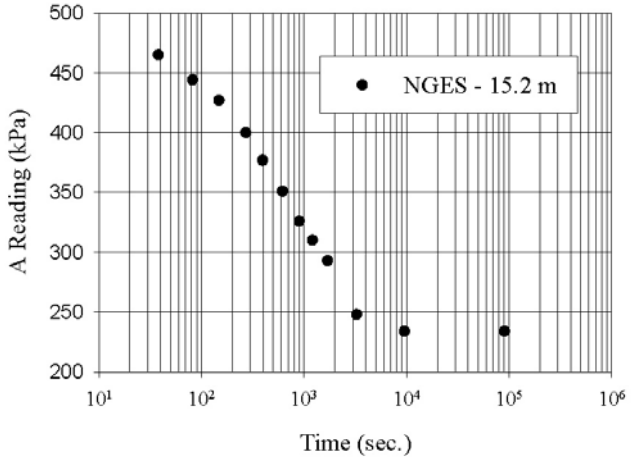

Figure 1. Typical DMT reconsolidation test results.

depth of about 6 m and then a more gradual decrease throughout the remainder of the profile in the softer, near normally consolidated zone. Figure 3 shows the variation in K_C (Eq. 10) at the site using the results from Figure 2. Again it can be seen that in the upper 6m K_C decreases rapidly. In the lower 6m, the value approaches a constant of about $K_C = 0.8$.

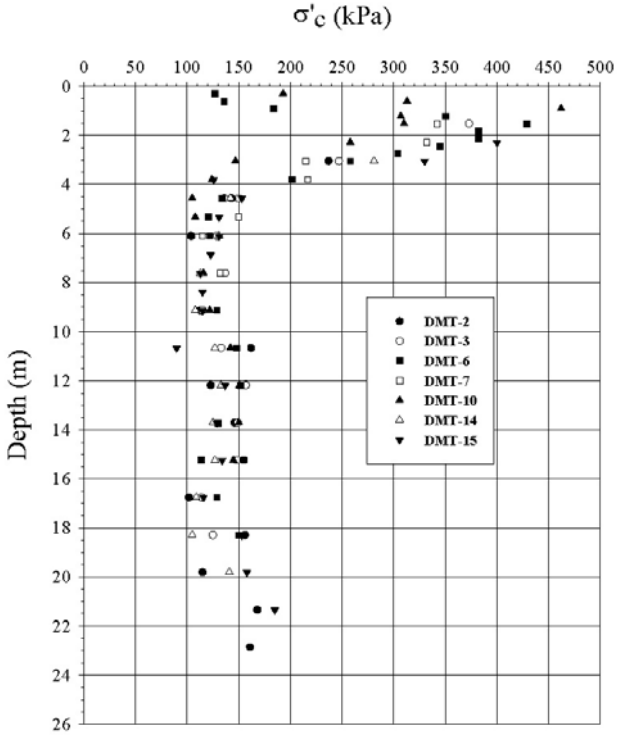

Figure 2. Variation in σ'_C with depth at UMass-Amherst.

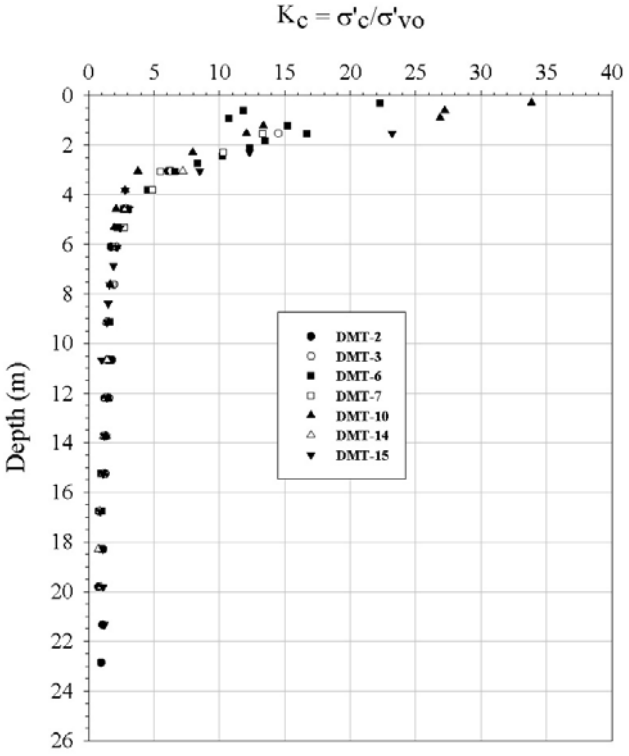

Figure 3. Variation in DMT K_C with depth at UMass-Amherst.

Values of K_C may be related to the stress history of the soil through OCR using the results of laboratory oedometer tests on undisturbed samples obtained at the site. These data are shown in Figure 4.

It can be seen that the reconsolidation lateral stress ratio, K_C, from the DMT is a function of the stress history of the soil, an observation that has been made by others using instrumented model-scale and full-scale piles in clays. This suggests that a first order estimate of K_C for use in pile design might be initially made using OCR if laboratory oedometer test results are available.

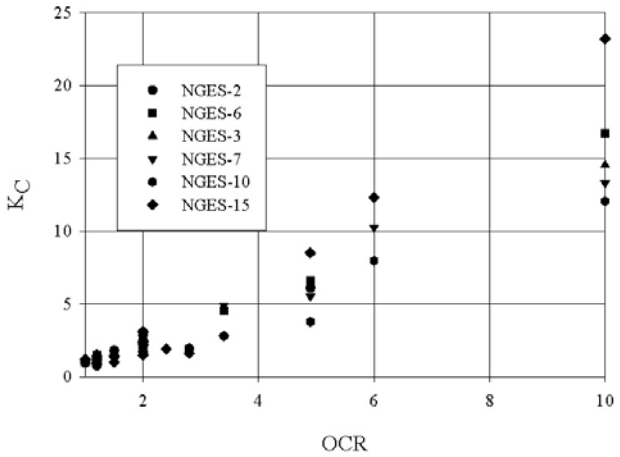

Figure 4. Relationship between DMT K_C and OCR. – UMass.

Figure 5 shows additional DMT results obtained by the author at several other sites, confirming the observations presented in Figure 4 for a wider range of clays. The scatter in the results is likely related to the fact that not all of the sites developed overconsolidation by simple unloading, which will tend to complicate a single straightforward relationship between OCR and K_C for all clays.

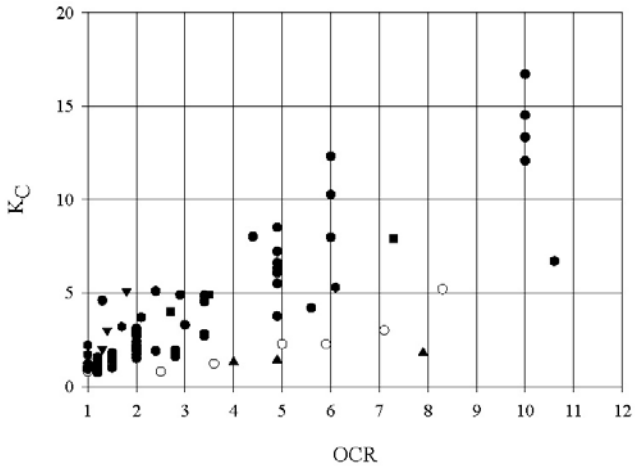

Figure 5. Variation in DMT K_C with OCR for several sites.

The data shown in Figure 5 are supported by additional test results obtained by the author and available in the literature from push-in earth pressure cells ("spade cells") at sites with OCR measured from oedometer tests. These data are shown in Figure 6 and show scatter similar to DMT results. Some of the scatter from the spade cell data may also result from the fact that not all of the spade cells used had the same geometry, whereas the data presented in Figure 5 are all from a probe of constant geometry. The data in Figure 6 support the observation that K_C is generally related to OCR.

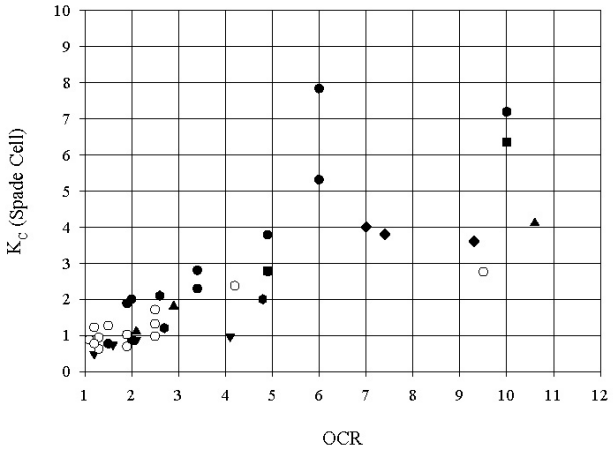

Figure 6. Variation in K_C with OCR from push-in spade cells.

5 INTERRELATIONSHIPS

Naturally, one problem with determining K_C from a full DMT or spade cell reconsolidation test is the long time period required to obtain a stable reading. To investigate a more expedient approach, the relationships between K_C and K_D and between K_C and K_i were explored. The rationale behind this approach is that for clays having undergone simple unloading:

$K_C = f(OCR)$ and $K_D = f(OCR)$

therefore it can be expected that: $K_C = f(K_D)$

Figure 7 presents a summary of available DMT results showing the relationship between K_D and K_C. Additional results obtained by the author and from the literature from push-in spade cells is shown in Figure 8. Again it can be seen that K_C may be related to K_D (where K_D is obtained from spade cell data rather that the DMT). With the exception of one site, the scatter is not all that great, again considering that the geometry of the spades was not the same at all sites.

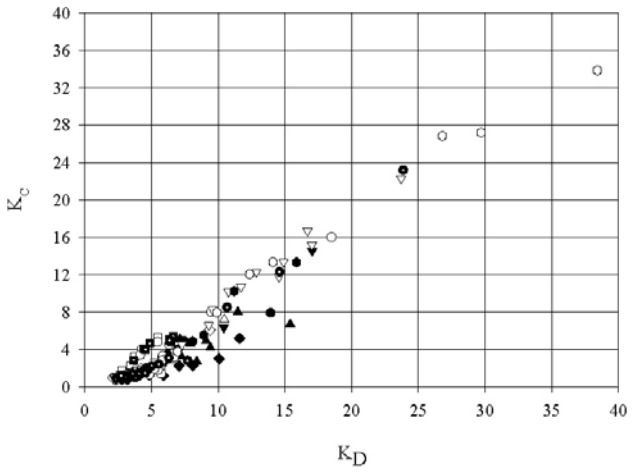

Figure 7. Observed relationship between K_D and K_C from DMT reconsolidation tests.

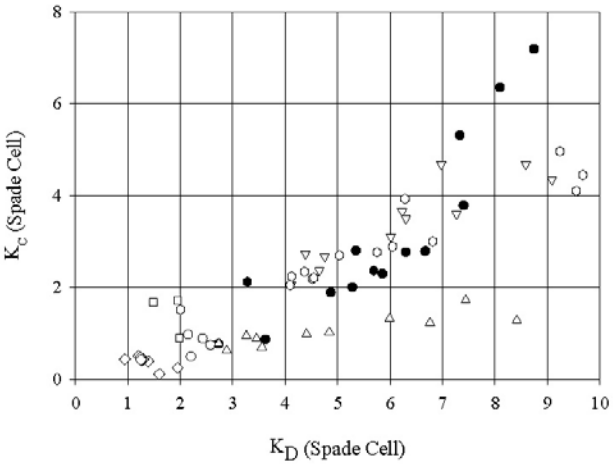

Figure 8. Relationship between K_D and K_C from push-in spade cell reconsolidation tests.

In very soft clay, it may be expected that K_C will be very near K_o and the soil will be somewhat "forgiving" for the intrusion of inserting the blade. This is not to be expected in stiffer clays however, and there will be an "overstress" resulting from the blade insertion, the $K_C > K_o$. The "overstress" is a component of effective stress and/or soil tensile strength that remains in place after the excess pore water pressure produced from blade insertion dissipates and reconsolidation is complete. This is illustrated from a comparison of between K_C and K_o for the CVVC at the UMass site shown in Figure 9. K_o data were obtained from tests on undisturbed samples using an instrumented oedometer capable of measuring lateral stress at known OCR produced by simple unloading. The "overstress" indicated in Figure 9 clearly increases as the initial stress or K_o increases and as OCR increases.

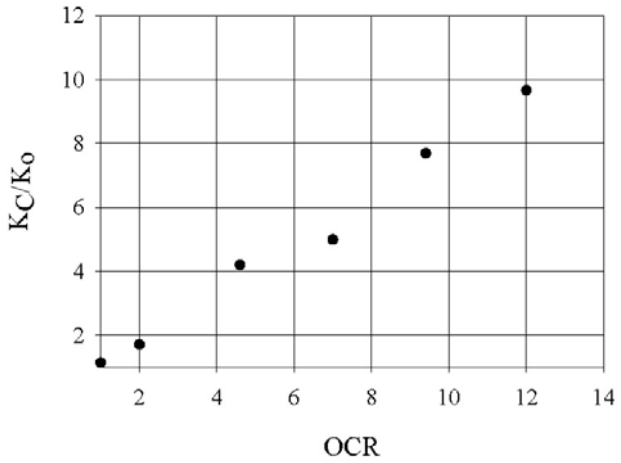

Figure 9. Variation in DMT K_C and laboratory K_o with OCR for CVVC.

Tedd and Charles (1981) suggested that in stiff clays the "overstress" acting on a push-in spade cell could be related to the undrained shear strength and that the final reconsolidation stress measured in the test might be adjusted to obtain a value closer to the true value. Intuitively, one could argue that the overstress is related to the normalized undrained shear strength or, as shown in Figure 9, the OCR.

The initial lateral stress ratio, K_i, may be related to stress history as shown in Figure 10, which shows results obtained by the author in Champlain Sea Clays. Additionally, K_i should be expected to relate to both K_C and K_D. The ratio K_D/K_i will be close to unity in very stiff clays where u_o and P_2 are very low or zero.

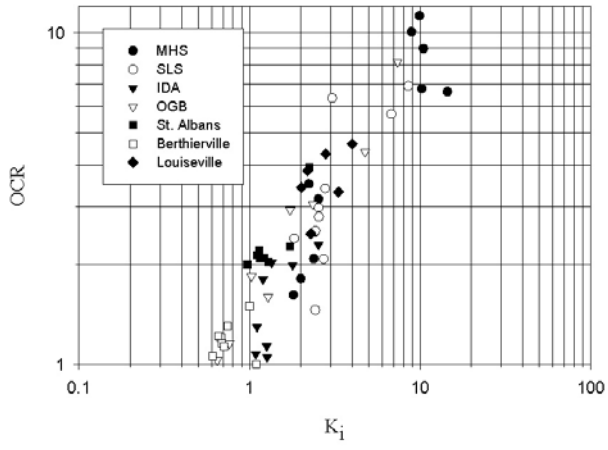

Figure 10. Variation in K_i with OCR.

One expects that if K_o, K_D, K_C , and K_i are all related to OCR then they are all related to each other. Figure 11 shows a comparison between K_C and K_i obtained at several clay sites. Of course, any relationship between K_D or K_i and OCR may also be used to de-

velop a direct relationship between (P_o - u_o) or (P_o - P_2) and σ'_p.

If the soil exhibits normalized behavior and the normalized undrained shear strength is related to stress history via OCR, then K_D, K_C and K_i will in turn be related to undrained shear strength. This argues that one should expect the DMT to provide a fairly reliable estimate of OCR, undrained strength and K_o through K_D, provided there has been sufficient reference calibration.

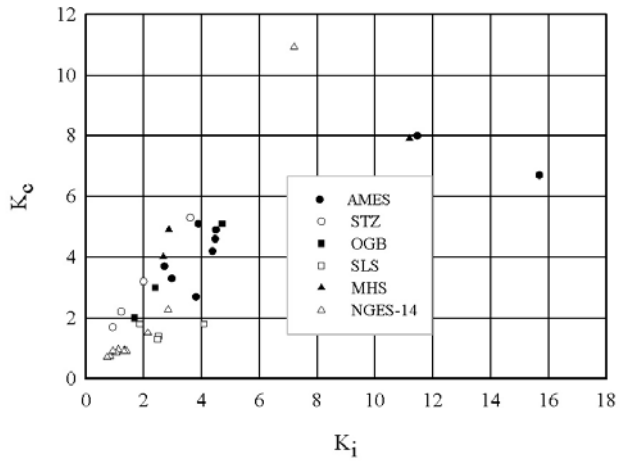

Figure 11. Comparison between K_C and K_i at several clay sites.

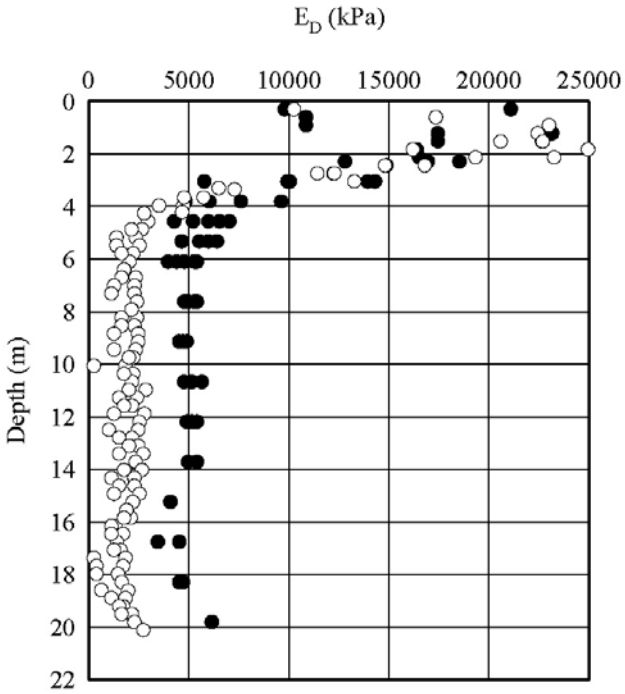

Figure 12. Comparison between DMT E_D and $E_{D(Consol)}$.

Since a regular DMT (i.e., with both A- and B-Readings) is performed after installation effects have dissipated, reconsolidation tests may also be used to obtain a measure of the consolidated DMT Modulus. In soft clays $E_{D(Consol)}$ will be higher than E_D. An example from the UMass Site is shown in Figure 12 where the open symbols represent regular tests and the closed symbols represent consolidated tests.

6 CONCLUSIONS

A measure of the reconsolidation lateral stress may be obtained in clays using the Dilatometer. The reconsolidation Lateral Stress Ratio, K_C, which may be useful for design of driven piles or for estimating at-rest lateral stresses in soft clays is seen to be related to the soil stress history. The test data presented indicate that in clays the Initial Lateral Stress Ratio, K_i, the DMT Lateral Stress Index, K_D, and the Reconsolidation Lateral Stress Ratio, K_C are all interrelated and related to OCR. The DMT Lateral Stress Index, K_D, may be used to make an initial estimate of K_C in the absence of a full reconsolidation test. However, when possible, it may be necessary to perform reconsolidation tests in order to obtain additional test data for use in design. In addition to obtaining a measure of soil behavior after reconsolidation, the time rate of dissipation may be useful as has been previously noted by others.

7 REFERENCES

Baligh, M.M., Martin, R.T., Azzouz, A.S., and Morrison, M., 1985. The Piezo-Lateral Stress Cell. *Proceedings of the 11th International Conference on Soil Mechanics and Foundation Engineering*, Vol. 2: 841-844.

Brooker, E. and Ireland, H., 1965. Earth pressures at rest related to stress history. *Canadian Geotechnical Journal*, Vol. 1 (No. 1): 1-15.

Lutenegger, A. J. and Miller, G.A., 1993. Evaluation of Dilatometer method to determine axial capacity of driven pipe piles in clay. *Design and Performance of Deep Foundations: Pioles and Piers in Soil and Soft Rock, ASCE*: 40-63.

Marchetti, S. 1980. In situ tests by flat dilatometer. *Journal of the Geotechnical Engineering Division, ASCE*, Vol. 106 (No. GT3): 299-321.

Marchetti, S., Totani, G., Campanella, R.G., Robertson, P.K., and Taddei, B. 1986. The DMT-σ_{HC} method for piles driven in clay. *Use of in situ tests in geotechnical engineering, ASCE*, 765-779.

Massarch, K. R., 1975. New method for measurement of lateral earth pressures in cohesive soils. *Canadian Geotechnical Journal*, Vol. 12 (No. 1):142-146

Massarch, K.R., Holtz, R.D., Holm, B.G., and Fredriksson, A., 1975. Measurement of horizontal in situ stresses. *Proceedings of the Conference on In Situ Measurement of Soil Properties, ASCE*, Vol. 1: 266-286.

Mayne, P.W. and Kulhawy, F.H., 1982. K_o-OCR relationships in soil. *Journal of the Geotechnical Engineering Division, ASCE*, VOl. 108 (No. GT6): 851-872.

Tavenas, F., Blanchete, G., Leroueil, S., Roy, M. and La-Rochelle, P., 1975. Difficulties in the in situ measurement of K_o in soft sensitive clays. *Proceedings of the Conference on*

In Situ Measurement of Soil Properties, ASCE, Vol. 1: 450-476.

Tedd, P. and Charles, J.A., 1981. In situ measurement of horizontal stress in overconsolidated clay using push-in spade-shaped pressure cells. *Geotechnique*, Vol. 31 (No.4): 554-558.

Flat Dilatometer method for estimating bearing capacity of shallow foundations on sand

Alan J. Lutenegger
University of Massachusetts, Amherst, Massachusetts, USA
Michael T. Adams
Federal Highway Administration, McLean, Virginia, USA

Keywords: Dilatometer, bearing capacity, shallow foundations, design, footings, sand

ABSTRACT: A design method is presented for estimating the ultimate bearing capacity of shallow foundations on granular soils using the results from the Dilatometer Test. The method is developed using results obtained from prototype-scale footing load tests performed on compacted sand at the FHWA Turner-Fairbank Highway Research Center and full-scale footing load tests performed on natural sand at the National Geotechnical Experimentation Site at Texas A& M University. The method uses the DMT lift-off and 1mm expansion pressures directly and is similar to the empirical design approach currently in use with the prebored Menard Pressuremeter test. The method incorporates an empirical bearing capacity factor which, much like the Pressuremeter method, is shown to be related to the embedment ratio (D/B) of the footing.

1 INTRODUCTION

Estimating the ultimate bearing capacity of shallow foundations on granular soils is a routine exercise performed by practicing geotechnical engineers throughout the world. Engineers need to evaluate the ultimate bearing capacity in order to insure that a sufficient factor of safety is provided against bearing capacity under the proposed design allowable pressure. The bearing capacity and settlement behavior of shallow foundations are uniquely interrelated. That is, at higher factors of safety, footings experience smaller settlements.

The ultimate bearing capacity of footings on sands may be evaluated using traditional bearing capacity equations (e.g., Terzaghi, Meyerhof, Hansen, etc.) in which superposition of terms is assumed and bearing capacity factors are evaluated as a function of the internal friction angle of the soil or by empirical equations using the results obtained from different in situ tests. Alternatively, empirical allowable bearing capacity charts may be used which provide a limit on settlement. The use of traditional bearing capacity equations is an indirect design approach that requires an estimate of the internal friction angle of the soil, often obtained from empirical correlations to penetration tests such as the SPT or CPT.

This paper presents an alternative direct design method for determining the ultimate bearing capacity of shallow foundations resting on granular soils using results obtained from Dilatometer tests. The method uses the Dilatometer lift-off and 1 mm expansion pressure readings directly without any additional interpretation of test results and is developed based on the observed ultimate bearing capacity of Prototype-Scale and Full-Scale footing load tests performed on concrete footings on compacted and natural sand.

2 DETERMINING BEARING CAPACITY FROM IN SITU TESTS

Engineers have a number of options for estimating the ultimate bearing capacity of shallow foundations using the results obtained from in situ tests. This approach is attractive for granular soils since it is difficult to obtain undisturbed samples for laboratory testing. The more common methods rely on the results of penetration tests, such as the Standard Penetration Test (SPT), the Cone Penetration Test (CPT) or Dynamic Drive Cone Tests (DCPT). For the current study, the design methods based on the pressure expansion curve of the Pressuremeter Test and the tip resistance from the Cone Penetration Test are most applicable.

3.1 *Bearing Capacity of Footings from the Pressuremeter*

Menard (1963) had suggested that the ultimate bearing capacity of shallow foundations, q_{ult}, could be evaluated from the results of prebored pressuremeter tests as:

$$q_{ult} = K P^*_L + \sigma_{vo} \quad (1)$$

where P^*_L is defined as the net limit pressure which equals $P_L - \sigma_{Ho}$, where P_L is equal to the PMT limit pressure extrapolated from the actual test data and σ_{Ho} equals the in situ total horizontal stress at the test depth, K equals an empirical bearing capacity factor that depends on soil type, soil stiffness, and equivalent footing embedment ratio, H_e/B, and σ_{vo} is the total vertical stress at the base of the foundation. In many cases, the expansion of the pressuremeter in sands does not give a limiting pressure and therefore, the value of P_L may be interpreted by a graphical extrapolation procedure as described in ASTM Test Method D4719 or by other means. The value of σ_{Ho} is often taken directly from the PMT curve as P_o or alternatively from an estimate of the in situ lateral stress ratio, K_o, and soil unit weight. A potential drawback to this technique is that a reliable estimate of K_o is needed.

A detailed design procedure using Equation 1 is described by Baguelin et al. (1978) and Briaud (1992). It should be noted that for this method the recommended value of P^*_L for use in design is taken at depths between 1.5 B below and 1.5 B above the base of the footing. Charts for choosing appropriate values of K are provided by Menard (1963) Baguelin et al. (1978) and Briaud (1992). There is only a slight increase in K with increasing footing embedment within the range of H_e /B from 0 to 1.

2.2 *Bearing Capacity of Footings from the Cone Penetration Test*

Meyerhof (1956; 1965) suggested that the ultimate bearing capacity of shallow foundations on granular soils could be estimated from the CPT tip resistance, q_c. Charts for estimating the allowable bearing capacity of shallow foundations from q_c and taking into account the relative footing embedment have been presented in the Canadian Foundation Engineering Manual (1975; 1985; 1992). In general this approach assumes that q_{ult} is directly related to q_c and is supported by Briaud and Jeanjean (1994) Tand et al. (1995) and Eslaamizaad and Robertson (1996) as:

$$q_{ult} = Kq_c \quad (2)$$

The factor K is dependent on the relative footing embedment D/B. For square footings and D/B in the range of 0 to 1, the factor K varies from about 0.22 to 0.30, depending on the sand density.

3 INVESTIGATION

The principal focus of the work presented in this paper was to investigate the use of the Dilatometer test for estimating the ultimate bearing capacity of shallow foundations on sands. Results from a number of Prototype-Scale footing load tests performed on compacted sand in conjunction with the Shallow Foundations Research Program at the Federal Highway Administration were used. Additional footing load test results available from Full-Scale footings performed on a natural sand deposit at Texas A&M University for the Federal Highway Administration were also used to supplement the Prototype-Scale tests.

3.1 *Prototype-Scale Footing Tests*

Prototype-Scale footing load tests were conducted at the Federal Highway Administration Turner-Fairbank Highway Research Center at McLean, Virginia. Tests were performed in a 3.5 m x 7.1 m x 6.5 m deep test pit on compacted sand beds prepared at different relative densities. Sand placement in the test pit was by 0.3 m loose lifts using a vibratory plate compactor to achieve the required relative density. In place density tests were performed using a nuclear moisture-density gauge at several locations around the pit for each lift to verify the density achieved with each pit fill. The sand used for the testing was uniform fine mortar sand having a mean grain size of 0.75 mm and a uniformity coefficient of 2.6. There is a small amount of fines present in this material, generally less than 5%. Minimum unit weight is 1.41 Mg/m^3 and maximum unit weight is 1.70 Mg/m^3. Tests were conducted on sand beds with relative densities ranging from 13.1% to 75.0%. Load tests were performed with the sand in a moist (M) condition (i.e., as compacted with no water table present), and with the water table located at the surface (S).

Footings were constructed of reinforced concrete and had widths ranging from 0.30 m to 1.22 m. Footings were placed at different depths in the sand to provide varying embedment ratios (D/B) ranging from 0 to 1. Incremental load tests were performed on each footing using a hydraulic ram loading system with the central vertical load measured using an

electronic load cell and the vertical displacement measured at the four corners of the footing using LVDT's. Data from each of the load tests were recorded automatically on a data acquisition system as the test progressed. All but two of the footings tested in the facility were square. A summary of the square footing tests performed at the FHWA facility is presented in Table 1.

Table 1. Prototype-scale footing tests.

Series	D_r (%)	Moisture	Width (m)	D/B
90	13.1	M	0.30	0
			0.46	0
			0.61	0
			0.91	0
95	38.8	M	0.30	0
			0.46	0
			0.61	0
			0.91	0
95GA1	46.0	S	0.30	0
			0.61	0
			0.91	0
95GA2	42.4	S	0.30	1
			0.61	1
			0.91	1
95GA3	38.8	M	0.30	1
			0.61	1
			0.91	1
95SD1	35.2	M	0.61	0
			0.61	0.25
			0.61	0.5
			0.61	1
			0.91	1
95SD2	38.8	M	0.61	0
			0.91	0.5
95SD3	38.8	M	0.61	0
			1.22	0.5
95SD4	38.8	M	0.30	0
			0.30	0.5
			0.61	0
			0.61	1
			1.22	0
97SD1	54.5	M	0.30	0.5
			0.61	0
			0.61	0.25
			0.61	0.5
			0.61	1
			0.91	0.5
100SD1	75.0	M	0.30	0.5
			0.61	0
			0.61	0.25
			0.61	0.5
			0.61	1
			0.91	0.5

The Dilatometer test provides a measure of the lift-off and 1 mm expansion pressure of a flexible, circular diaphragm on the face of a flat blade after quasi-static penetration into the soil. Dilatometer tests were performed in each of the test pit fills at FHWA using the procedure recommended by Schmertmann (1986). Two DMT profiles were performed in each pit fill at intervals of 0.3 m beginning alternatively at a depth of 0.3 m and 0.45 m at two locations and were continued to a depth of 4 m below the sand surface.

3.2 *Full-Scale Footing Tests*

In order to provide a comparison between the Prototype-Scale footing load tests performed at FHWA on compacted sand and Full-Scale production size footings placed on a natural sand, test results from the footing load tests performed at the National Geotechnical Experimentation Site at Texas A&M University for the ASCE Specialty Conference Settlement '94 were also used. The sand at this site is a natural deposit which can be described as medium dense fine silty sand. Grain-size and other characteristics of this sand are given by Gibbens and Briaud (1994). The in situ relative density of the sand was estimated to be on the order of 55% based on the results of Standard Penetration and Cone Penetration Tests. Footing load test results and DMT test data for this site are reported by Briaud and Gibbens (1994). All footings tested in this field program were square and ranged in size from 1 m to 3 m. The embedment ratio (D/B) ranged from 0.27 to 0.70. A summary of these footing tests is given in Table 2.

Table 2. Full-scale footing tests.

Footing No.	Width (m)	Depth (m)	D/B
1	3.0	0.8	0.27
2	1.5	0.8	0.53
3	3.0	0.9	0.30
4	2.5	0.8	0.32
5	1.0	0.7	0.70

3.3 *Determining Ultimate Bearing Capacity*

In order to develop a bearing capacity design method, it was important to determine the ultimate bearing capacity from each of the load tests in a consistent manner. In the absence of a well-defined plunging failure which identifies the ultimate capacity, there are a number of methods that can be used to interpret either the "allowable" or the ultimate bearing capacity of foundations from footing load

tests. In many cases, an "allowable" bearing pressure is used to design footings, where the footing stress corresponding to a limiting absolute settlement value, e.g., 25.4 mm, is used to define the "allowable" bearing capacity. This approach typically is used with any one of a number of design charts.

When actual footing load test data are available, the ultimate bearing pressure may be interpreted using one of the following approaches: 1) choosing the footing stress corresponding to a limiting *relative* settlement value, e.g., s/B = 10% (Briaud and Jeanjean 1994); 2) choosing the footing stress corresponding to a marked change in the settlement, e.g., the intersection of the initial and final tangent slope of the stress vs. settlement curve (Trautman and Kulhawy 1988); 3) manipulating the stress vs. settlement data and then selecting the footing stress corresponding to an intersection point e.g., log stress vs. log settlement (DeBeer 1970); or 4) choosing a reasonable model to fit the stress vs. settlement data and extrapolating to the asymptotic value corresponding to an upper limit of stress, e.g., hyperbolic model (Chin 1983; Wrench and Nowatzki 1986; Ghionna et al. 1991; Wiseman and Zeitlan 1994; Thomas 1994). Each of these interpretation methods may give a different value of bearing capacity and therefore in the development of a design method it is important to select a single interpretation approach in order to be consistent.

In this study the ultimate bearing capacity for all footings (Prototype-Scale and Full-Scale) was determined as the stress producing a relative displacement of 10% of the footing width, hereafter referred to as the 0.1B Method.

4 PROPOSED DESIGN METHOD

Using the results of the footing load tests and the Dilatometer tests performed, an approach similar to that used with the Pressuremeter was investigated for using the DMT results to estimate ultimate bearing capacity as:

$$q_{ult} = N_D (P_1 - P_o) + \sigma_{vo} \qquad (3)$$

In this case, P_o represents the DMT lift-off pressure and P_1 represents the DMT 1mm expansion pressure taken directly from the DMT test results. Since the DMT blade is of fixed dimensions, the use of P_o and P_1 represent pressure values that are repeatable from any DMT equipment and which are not subject to arbitrary graphical interpretation. The value of N_D is a DMT "bearing capacity factor" that should depend only on soil stiffness and the geometry of the loading and is analogous to the factors K used in the PMT and CPT design methods and given in Equations 1 and 2.

In sands, it has been well documented that the pressure-expansion curve of the DMT membrane closely follows a linear shape as the membrane is expanded from P_o to P_1 (Campanella and Robertson 1991; Bellotti et al 1997). The slope of the curve is dependent on OCR and relative density. Therefore, the pressure difference $P_1 - P_o$ represents a measure of the stiffness of the soil and was used by Marchetti (1980) to define the "Dilatometer Modulus", E_D. The value of P_o is related to the initial in situ horizontal stress, but also reflects the influence of stress history and relative density, all of which influence bearing capacity of shallow foundations on granular soil. Therefore, the analogy between the PMT approach and the DMT approach is very strong. In Equations 1 and 3, the vertical stress at the base of the foundation typically represents a relatively small contribution to the bearing capacity for D/B in the range of 0 to 1 and therefore a reasonable estimate of soil unit weight is be considered adequate.

Houlsby and Wroth (1989) showed that in clean sands, the thrust required to advance the DMT blade was related to the lift-off pressure P_o. This has been confirmed by others (e.g., Campanella and Robertson; Bellotti et al. 1994). Additionally, it has been shown that the DMT thrust also relates to the 1 mm expansion pressure P_1 (Campanella and Robertson 1991). It has also been shown that the DMT thrust and the tip resistance from a CPT are strongly correlated in the same sand deposit (Campanella and Robertson 1991). Therefore, it is intuitive that a correlation may be established between the CPT q_c and the DMT pressure difference ($P_1 - P_o$). This means that it should be expected that if q_c may be related to q_{ult} (i.e., Equation 2) then ($P_1 - P_o$) may also similarly be related to q_{ult}.

The DMT and the PMT are in situ tests that measure soil response principally in the horizontal direction. One may question the use of such tests to provide useful results for predicting the response of vertically loaded foundations. The bearing capacity of square and circular footings can actually be modeled as a spherical cavity expansion in soil, which obtains a large degree of expansion resistance from the horizontal support of the soil immediately under the footing. This is also consistent with basic Rankine theory for bearing capacity of shallow foundations.

5 RESULTS

Since q_{ult} was determined for each of the footing load tests and σ_{vo} may be calculated from total unit

weight that was measured during each pit fill, values of N_D were back calculated for all of the tests by re-arranging Equation 3 to solve for N_D. In this procedure, since footing tests represent embedment ratios less than 1, the DMT results within a zone between the base of the footing and a depth of 1.5B below the footing were used. A comparison using the DMT results in a zone of 2B above and 2B below the footing indicated no significant change in the results. Typical DMT results obtained on compacted sand pit fills at FHWA showed that the values P_o and P_1 increased with depth as would be expected in a uniform sand of constant Relative Density.

5.1 *Prototype Footing Tests*

The results of interpreted ultimate bearing capacity from the footing load tests in Table 1 are given in Table 3 along with back calculated values of N_D. The variation in N_D with relative footing embedment from the prototype-scale footing tests are shown in Figure 1. It can be seen that N_D increases slightly with increasing D/B as is expected and is similar in magnitude to values of K suggested for the PMT.

Table3. Results of prototype-scale tests.

Series	D_r (%)	Moisture	Q_{ult} (kPa)	N_D
90	13.1	M	121	0.89
			138	0.90
			180	1.16
			197	1.14
95	38.8	M	245	0.63
			260	1.29
			300	1.53
			380	1.52
95GA1	46.0	S	65	0.63
			87	0.70
			140	0.88
95GA2	42.4	S	197	1.72
			350	2.11
			490	2.27
95GA3	38.8	M	480	1.25
			655	1.23
			770	1.34
95SD1	35.2	M	240	1.19
			345	1.16
			405	1.35
			525	1.57
			280	0.88
95SD2	38.8	M	237	0.58
			448	0.97
95SD3	38.8	M	230	0.89
			620	1.52
95SD4	38.8	M	280	0.92
			400	1.13
			355	0.79
			785	1.36
			580	1.04
97SD1	54.5	M	755	2.29
			508	0.77
			800	1.16
			1110	1.50
			1320	1.48
			1350	1.47
100SD1	75.0	M	1510	2.06
			1000	1.10
			1175	1.22
			1160	1.10
			1350	1.01
			2325	1.68

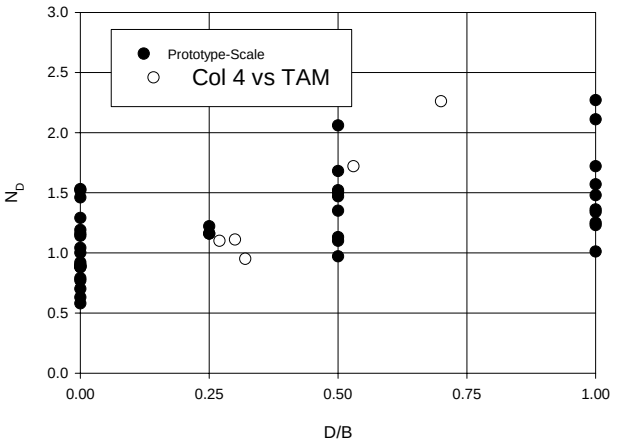

Figure 1. Test results.

The test data of Figure 1 suggest a more or less linear increase in N_D with increasing embedment over the range of D/B from 0 to 1. Beyond an embedment ratio of 1 it is likely that an increase in N_D occurs at a much lower rate and becomes negligible beyond D/B greater than about 4. This would be consistent with observations of PMT results and other general bearing capacity observations as a transition from shallow to deep behavior occurs and bearing capacity increases. The results shown in Figure 1 also suggest that the value of N_D is generally independent of footing size for a given D/B, at least in the range of footings included in this study (B = 0.3 m to 3.0 m).

For the same size footing and footing embedment and for similar same water table conditions, the results indicate that the value of N_D is independent of the relative density of the sand. Variations in the relative density and other soil conditions e.g., water table, appear to be automatically reflected in the DMT results through P_o and P_1. The influence of footing size is accounted for by using the DMT results over an appropriate zone of influence for indi-

vidual footings. The observed variation in bearing capacity factors at a given D/B value indicated in Figure 1 is likely the result of variations in the DMT results and variations in interpreting the load test results. It should be noted that the scatter indicated in Figure 1 for any given value of D/B is similar to the observed scatter in K values reported for the PMT.

Prototype-Scale tests were also performed on two rectangular footings having length/width ratios (L/B) equal to 2 and 4 to provide a comparison with results obtained from square footings having the same width. The results of these tests indicated that the back calculated values of N_D were less than for square footings of the same width and embedment, and on average represented values of N_D on the order of 70% of the value for a square footing. This is also consistent with the PMT design procedure and with general bearing capacity theory. Therefore, the bearing capacity factors in Figure 1 are recommended for use with square footings only and an adjustment factor of 0.7 should be applied for use with rectangular footings.

5.2 *Full-Scale Footing Tests*

The results of the full-scale footing tests conducted at Texas A&M are given in Table 4 and are also shown on Figure 1. These results fall within the band of test results obtained from the prototype-scale tests and confirm that the value of N_D depends primarily on relative embedment. The results indicated in Figure 1 are also intuitively reasonable.

Table 4. Results of Full-Scale Footing Tests.

Footing No.	q_{ult} (kPa)	N_D
1	1820	1.10
2	1560	1.72
3	1210	1.11
4	1280	0.95
5	1060	2.26

In a uniform, normally consolidated sand deposit with a constant relative density, one would expect the values of P_o and P_1 to increase linearly with depth, but with P_1 increasing at a faster rate. This would produce a higher modulus with increasing depth because of the effect of increasing confining pressure. This would in turn produce higher N_D values for larger D/B ratios for a constant footing width B. Since the ultimate bearing capacity factors obtained using Equation 3 and presented in Figure 1 are based on defining the ultimate bearing capacity as 10% of the footing width, there is no provision for settlement limitations in the design procedure presented.

Using a global factor of safety of 3, which is common in routine shallow foundation design practice, the recommended approach gave "allowable" footing bearing stresses which all produced settlements of less than 25.4 mm. Therefore, the authors suggest that provisionally, a factor of safety of 3 be applied to this procedure to obtain an allowable bearing capacity. As always, the permissible settlement criteria must be checked to provide an adequate foundation design since a fixed settlement criterion of 25.4 mm represents different *relative* displacement for different size footings. At the present time, no recommended design curve for evaluating N_D is given in Figure1. A conservative approach would be to use the lower bound data for a given D/B.

One could argue that an alternative approach to the one presented could be to correlate q_{ult} to the DMT Modulus, E_D, however, this is less direct than the approach presented and implies a certain level of confidence in the use of the Modulus value.

6 CONCLUSIONS

An empirical design procedure for estimating the ultimate bearing capacity of shallow foundations on granular soils based on the results obtained from the Flat Dilatometer test has been presented. The proposed method is simple to use and similar to a procedure that has previously been suggested and used with Pressuremeter results. The procedure makes use of the two pressure readings routinely obtained from the Dilatometer test and requires no additional interpretation of test results. Unlike the PMT method, no estimate of K_o is required.

An empirical bearing capacity factor, N_D, is introduced. Bearing capacity factors for use with this method have been presented for square footings for different values of the footing embedment ratio, D/B. An adjustment factor of 0.7 is suggested for use with rectangular footings. The value of N_D may be dependent on the method used in interpreting the ultimate bearing capacity, which in the present study was the stress producing a relative settlement of 10% of the footing width.

In sands, the use of the Dilatometer allows a more rapid testing approach than the Pressuremeter test, allows for more test data to be obtained within the zone of interest, does not usually require a borehole, and requires less time for data reduction. The proposed method may provide a more cost effective direct design method for shallow foundations and

would also be more attractive than using the results of the SPT, which can be subject to large variations.

Additionally work is currently underway to determine if this approach may be extended to other soil types and to determine if other variables can be identified which influence the value of N_D.

ACKNOWLEDGEMENTS

This work was supported by the Federal Highway Administration as a part of the Shallow Foundation Research Program on the bearing capacity and settlement behavior of shallow foundations. The authors wish to acknowledge the continuing encouragement and support of Al DiMillio in the work on shallow foundations.

REFERENCES

Baguelin, F., Jezequel, J.F., and Shields, D.H., 1978. *The Pressuremeter and Foundation Engineering*. Trans Tech Publications, 617 pp.

Bellotti, R., Benoit, J., Fretti, C., and Jamiolkowski, M., 1997. Stiffness of Toyoura Sand from Dilatometer Tests. *Journal of Geotechnical and Geoenvironmental Engineeering*, ASCE, Vol. 123 (No. 9): 836-846.

Briaud, J.-L., 1992. *The Pressuremeter*. A.A. Balkema Publishers, Rotterdam, 322 p.

Briaud, J.-L. and Gibbens, R.M., 1994. Test and Prediction Results for Five Spread Footings on Sand. Predicted and Measured Behavior of Five Spread Footings on Sand, ASCE: 92-128.

Briaud, J.-L. and Jeanjean, P., 1994. Load Settlement Curve Method for Spread Footings on Sand. *Vertical and Horizontal Deformations of Foundations and Embankments, ASCE*, Vol.2: 1774-1804.

Campanella, R.G. and Robertson, P.K., 1991. Use and Interpretation of a Research Dilatometer. *Canadian Geotechnical Journal,* Vol. 28 (No. 1): 113-126.

Canadian Foundation Engineering Manual, 1975, 1985, 1992. 1st, 2nd, and 3rd Editions, Canadian Geotechnical Society.

Chin, F.K., 1983. Bilateral Plate Bearing Tests. *Proceedings of the International Symposium on In Situ Testing in Soil and Rock,* Vol.2: 37-41.

DeBeer, E.E., 1970. Experimental Determination of the Shape Factors and the Bearing Capacity Factors of Sand. *Geotechnique*, Vol. 20 (No. 4): 387-411.

Eslaamizaad S. and Robertson, P.K., 1996. Cone Penetration Test to Evaluate Bearing Capacity of Foundations on Sand. *Proceedings of the 49th Canadian Geotechnical Conference:* 429-438.

Gibbens, R.M. and Briaud, J.-L., 1994. Data and Prediction Requests for the Spread Footing Prediction Event. Predicted and Measured Behavior of Five Spread Footings on Sand, ASCE: 1-85.

Gionna, V.N., Manassero, M., and Peisino, V., 1991. Settlements of Large Shallow Foundations on a Partially Cemented Gravelly Sand Deposit Using PLT Data. *Proceedings of the 10th European Conference on Soil Mechanics and Foundation Engineering,* Vol.1: 417-422.

Houlsby, G.T. and Wroth, C.P., 1989. The Influence of Soil Stiffness and Lateral Stress on the Results of In Situ Soil Tests. *Proceedings of the 12th International Conference on Soil Mechanics and Foundation Engineering*, Vol. 1: 227-232.

Menard, L., 1963. Calcul de la Force Portante des Fondations sur la Base des Resultants des Essais Pressiometriques. *Sols-Soils*, Vol.2 ,(Nos. 5 and 6).

Meyerhof, G.G., 1956. Penetration Tests and Bearing Capacity of Cohesionless Soils. *Journal of the Soil Mechanics Division, ASCE*, Vol. 82 (No. SM1): 1-12.

Meyerhof, G.G., 1965. Shallow Foundations. *Journal of the Soil Mechanics and Foundation Division, ASCE*, Vol. 91 (No. SM2): 21-31.

Schmertmann, J.H., 1986. Recommended Method for Performing the Flat Dilatometer Test. *Geotechnical Testing Journal, ASTM*, Vol.9: 93-101.

Tand, K.E., Funegard, E.G., and Warden, P.E., 1995. Predicted/Measured Bearing Capacity of Shallow Footings on Sand. *Proceedings of the International Symposium on Cone Penetration Testing*, Vol. 2: 589-594.

Thomas, D., 1994. Spread Footing Prediction Event at the National Geotechnical Experimentation Site on the Texas A&M University Riverside Campus. *Predicted and Measured Behavior of Five Spread Footings on Sand, ASCE*: 149-152.

Trautmann, C.H. and Kulhawy, F.H., 1988. Uplift Load-Displacement Behavior of Spread Foundations. *Journal of Geotechnical Engineering, ASCE*, Vol.114 (No.2): 168-183.

Wrench, B.P. and Nowatzki, E.A., 1986. A Relationship Between Deformation Modulus and SPT N for Gravels. *Use of In Situ Tests in Geotechnical Engineering, ASCE:* 1163-1177.

Wiseman, G. and Zeitlen, J.G., 1994. Predicting the Settlement of the Texas A&M Spread Footings on Sand. *Predicted and Measured Behavior of Five Spread Footings on Sand, ASCE:* 129-132.

APPLICATIONS IN DIFFICULT GEOMATERIALS

Seashore sand parameters with DMT and CPTU tests

Lech Bałachowski
Gdańsk University of Technology

Keywords: CPTU, DMT, quartz sand, fills, constrained modulus

ABSTRACT: An extensive study was performed on the characterization of sand deposits on the Polish seashore including triaxial tests, penetration testing in-situ and calibration chamber tests. Fine to medium quartz sand from Baltic beach was used. A series of CPTU and DMT tests were performed in fresh deposits of hydraulic sand fills. Stress history of the deposits was established on the basis of CPT and DMT. There is considerable difference in strength and deformation parameters for hydraulic sand fills formed by subaerial and subaqueous placement methods. In a first case the sand is dense and often overconsolidated with high cone resistance and K_D, E_D and M values. In case of subaqueous hydraulic fills loose to medium dense sand was found in NC state. Some correlations between strength parameters from CPT and deformation moduli from DMT were established. Linear relationship between cone resistance and constrained modulus were proposed for Baltic sand.

1 INTRODUCTION

Sand fills placed with pipelines are frequently used in port and reclamation works in Poland. Two examples of hydraulic deposition are described. The first one concerns the sand fill formed by subaqueous placement method at the back of the harbour in Gdynia Port. The sand fill was placed in the period of port construction about 75 years ago. Some new construction projects are planned on this fill just behind the existing harbour. In the second example the reclamation works on The Hel peninsula are discussed. The sand fill is regularly transported with the pipeline along the coast to supply the beach material and to protect the peninsula against the erosion and material transport induced by maritime currents and waves.

Hydraulic sand fills are the unaged fresh sediments of fine to medium predominantly quartz sands. Their properties can be described with CPTU and DMT tests and the correlations elaborated on calibration chamber tests for the unaged and uncemented sands. Standard CPTU and DMT tests were performed in parallel at the harbour and at the Baltic beach at The Hel Peninsula to determine the stress state and history, relative density and modulus of deformation for different placement methods of hydraulic sand fills.

2 INTERPRETATION OF CPTU AND DMT TESTS IN SAND FILLS

Interpretation of CPTU tests was made assuming medium compressibility of the sand and relative density evaluated for normally consolidated and overconsolidated sands according to Baldi et al. (1986). Relative density of the sand can also be determined from DMT correlations based on calibration chamber tests – Reyna & Chameau (1991) and Jamiolkowski et al. (2001). These correlations were established for medium and high overburden stress exceeding 50 kPa. For small penetration depth, exceeding critical depth but not larger than 3 m, it can be considered that the effect of the overburden on the rate of increase of the cone resistance below the critical depth can be neglected Puech & Foray (2002). The quasi-stationary cone resistance at small penetration depths q_{st} can be considered as dependent only on relative density D_R. Such a correlation is presented (Fig. 1) for the laboratory sand fills - Puech & Foray (2002):

$$D_R = 0{,}209 \ln(q_{st}) + 0{,}25 \quad (1)$$

It can be used to evaluate relative density at small depth in the unaged hydraulic sand fills.

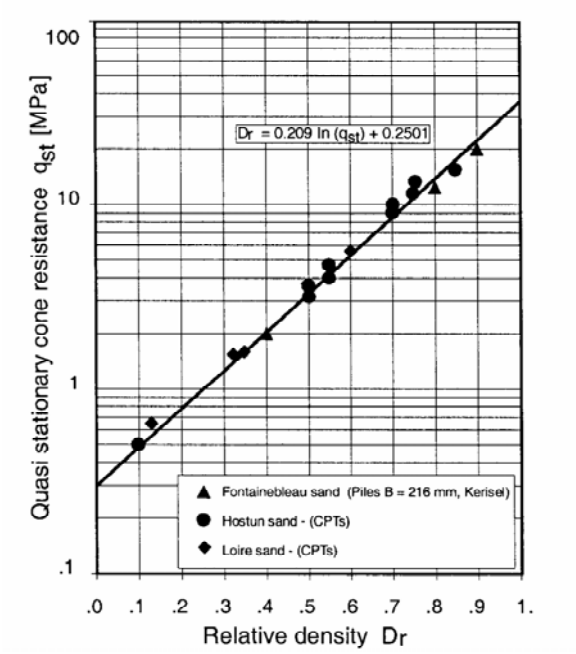

Figure 1. Correlation between quasi-stationary cone resistance and relative density

Overconsolidation ratio was determined with the formula of Mayne (2001):

$$OCR = \left[\frac{1{,}33}{K_{0NC}} \frac{q_T^{0,22}}{\left(\sigma'_{v0}\right)^{0,31}} \right]^{1/(\alpha - 0{,}27)} \quad (2)$$

where:
Corrected cone resistance q_T in MPa can be assumed equal to q_c in sands. K_{0NC}= *1-sinϕ'*, α= *sinϕ'* and σ'_{v0} is the effective overburden stress in kPa. The angle of internal friction was determined with DMT test according to Marchetti (1980) formula.

The earth pressure coefficient at rest K_0 was determined with the CPTU data – Mayne (2001) or CPTU/DMT data – Baldi et al. (1986) for the "seasoned" sand:

$$K_0 = 1{,}33(q_T)^{0,22}\left(\sigma'_{v0}\right)^{-0,31} OCR^{0,27} \quad (3)$$

$$K_0 = 0{,}376 + 0{,}095 K_D - 0{,}0046 q_c / \sigma'_{v0} \quad (4)$$

The stress state in the sand can be also described with the ratio $\alpha = M_{DMT}/q_c$. Marchetti et al. (2001) suggest that:
α=5 to 10 for NC sand and
α=12 to 24 for OC sand.

3 ANALYSIS OF IN-SITU TESTS

3.1 *Harbour backfill*

CPTU profile in hydraulic fill at the back of the massive harbour in Gdynia port is given (Fig. 2). The water table is about 2 m below ground level. Relatively dense and overconsolidated sand (see Figs. 3 and 4) was found in the surface layer and confirmed with DMT horizontal stress index and OCR evaluated with Eq. 2. This is related to crust phenomena and densification/ overconsolidation of the superficial layers with small storage facilities and traffic. Below, a medium dense normally consolidated or lightly overconsolidated sand is found. Some loose sand with silt and mud inclusions was detected from 11 to 12 m. The roof of a very dense Pleistocene sands is located at the depth of 12 m. The properties of this layer and the surface layer are outside the scope of this paper. Relative density of the sand fill was determined (Fig. 5) from CPTU according to Baldi et al. (1986). Two methods for the determination of the earth pressure coefficient at rest give a very similar results (Fig. 6). The constrained modulus from DMT (Fig. 7) and calculated M_{DMT}/q_c ratio are presented (Fig. 8) in the profile. Values of this ratio from 2 to 8 correspond to NC sands.

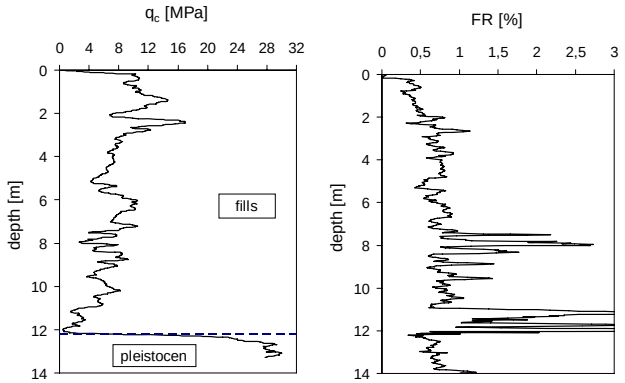

Figure 2. Profile of cone resistance and friction ratio.

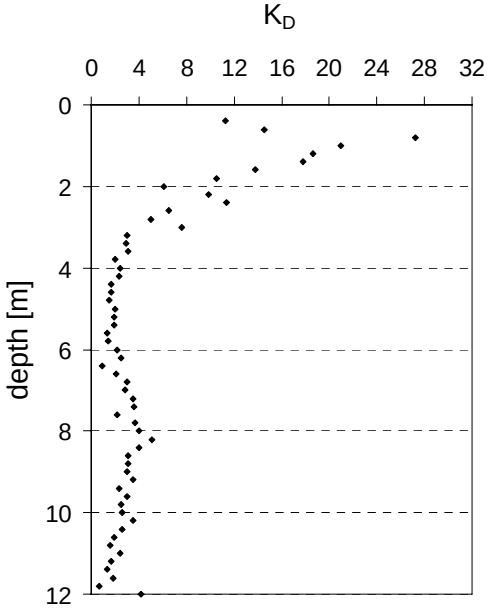

Figure 3. Profile of K_D.

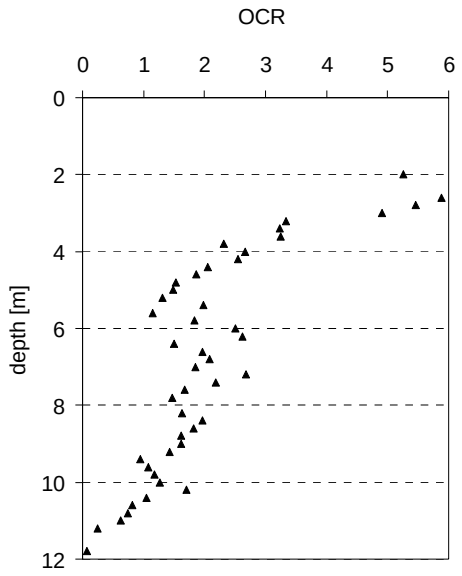

Figure 4. *OCR* profile.

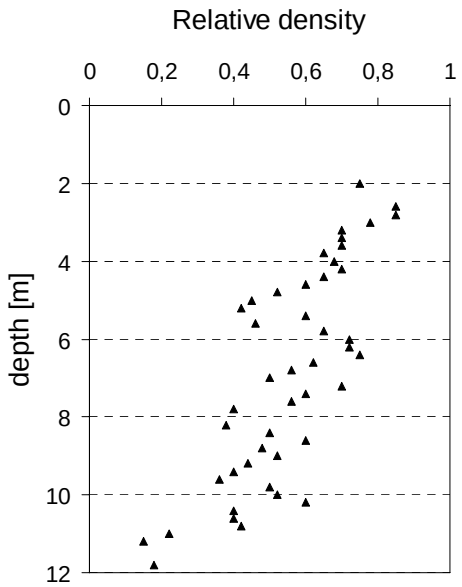

Figure 5. Relative density profile.

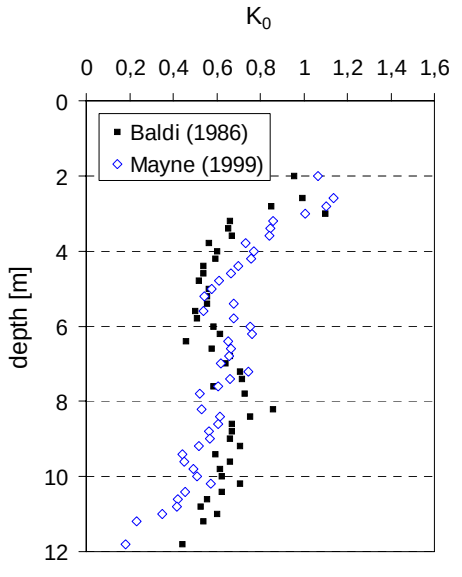

Figure 6. Earth pressure coefficient at rest.

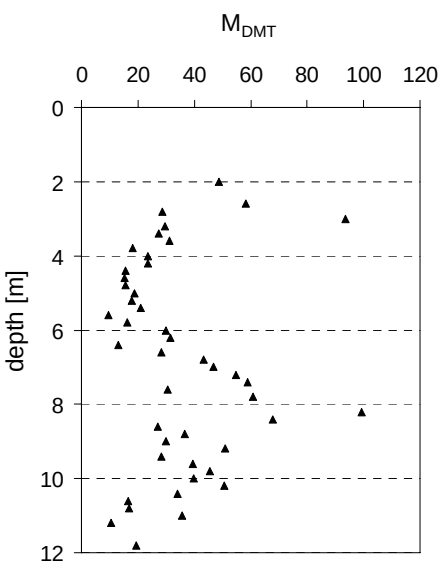

Figure 7. Constrained modulus M_{DMT}.

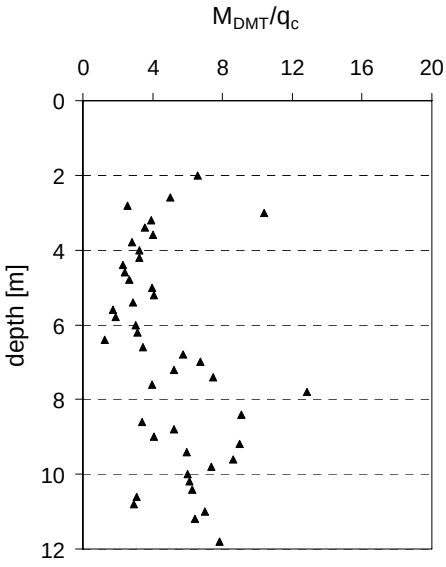

Figure 8. Profile of M_{DMT}/q_c ratio.

Linear correlation between constrained modulus from DMT and cone resistance (Fig. 9) slightly overpredicts the proposition of Lunne & Christophersen (1983).

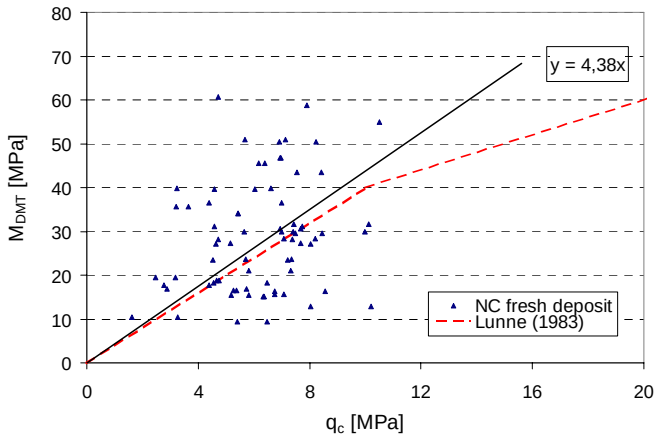

Figure 9. Constrained modulus vs. cone resistance in NC sand.

BACK

3.2 *Sand fills on the Baltic coast*

CPTU and DMT tests were performed in the fresh sand fills placed a few weeks before. These fills were discharged above sea level and densified with a flow of water. Downward seepage flow can induce overconsolidation of the sand fill. Leveling operations of bulldozer contribute to mechanical compaction and to the overconsolidation of the sand fill. Flat sandy beach (Fig. 10) has a width of about 20 to 30 m. The tests were performed with Geotech rig 220 (Fig. 11). The total thickness of the sand fills placed during a few placement periods was about 3 m (Fig. 12). A very steep mobilization of cone resistance is observed in this layer. The estimation of relative density from CPTU tests at small depths is subject to high uncertainty. A rough estimation of relative density (Eq. 1) gives D_R close to 1 in saturated sand fills. The water table is about 1,5 m under ground level. Some aged Holocene sands with a high density is found under the sand fill layer. A very high, close to 18, lateral stress index K_D is obtained in the fully saturated fills (Fig. 13). It is considerably higher than K_D which was - close to 6 at maximum relative density - found for the NC sands in the calibration chamber - Reyna & Chameau (1991). K_D values derived in partially saturated soils are even more important due to capillary forces, which will affect the effective stress state. It signifies that the sand fill is not only close to the maximum relative density, but is highly overconsolidated as well (see Fig. 14).

Figure 10. Pipeline for sand fill transport.

Figure 11. The anchoraged rig.

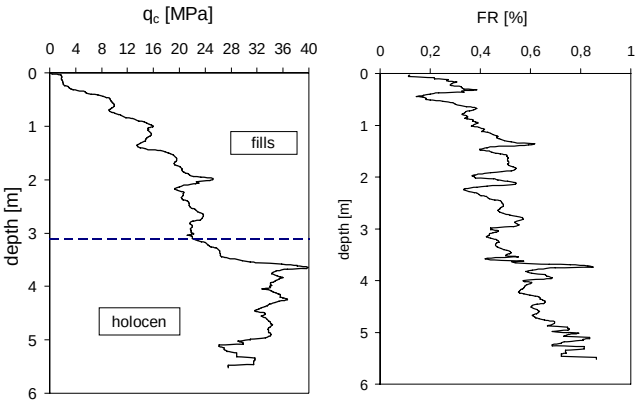

Figure 12. Profile of cone resistance and friction ratio.

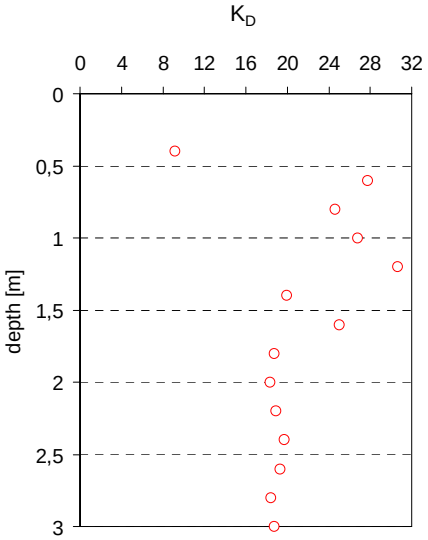

Figure 13. Profile of K_D.

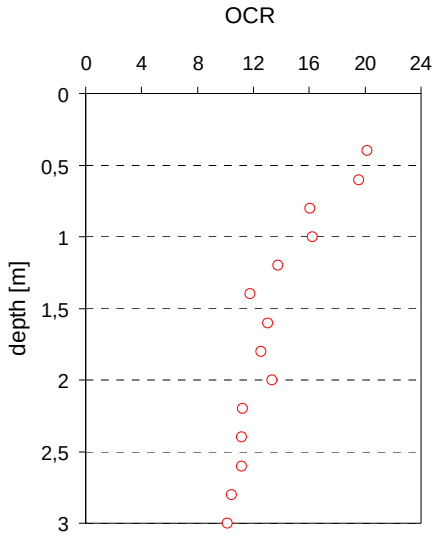

Figure 14. *OCR* profile.

To account for the overconsolidation effect in subaerial beaching by the pipeline discharge method, Lee (2001) suggests to take the coefficient of earth pressure at rest K_0 equal 1. The earth pressure coefficient at rest (Fig. 15) calculated with both methods (Eqs. 3, 4) is however considerably higher (about 2). Moreover, in partially saturated soil the capillary effect additionally increases the K_0 coefficient near the ground level.

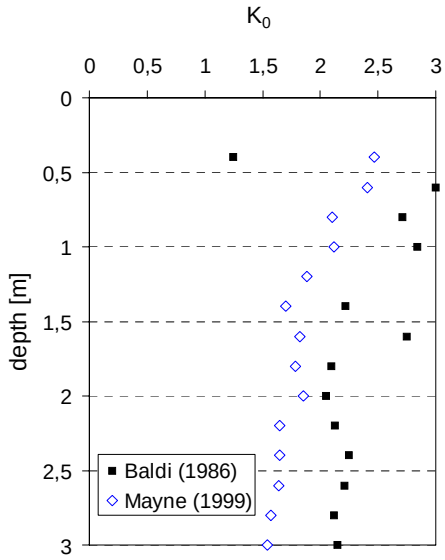

Figure 15. Earth pressure at rest coefficient.

A very high constrained modulus was found (Fig. 16) for the sand fill placed with subaerial hydraulic method. A ratio M_{DMT}/q_c from 8 to 10 was obtained in the saturated sand fills (Fig. 17). It is less than typically accepted for OC sand. Linear correlation between constrained modulus from DMT and cone resistance (Fig. 18) considerably overpredicts the Lunne & Christophersen (1983) correlation from CPTU tests. The dilatometer test is thus more sensible to stress state and history than the cone penetration test. This correlation was established for small penetration depths. Further research is necessary to expand this kind of relationship to higher depths/ confining pressures.

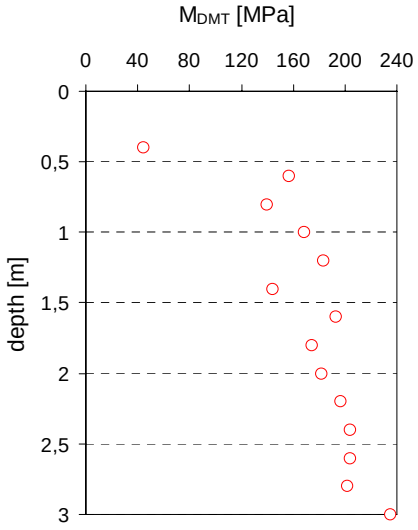

Figure 16. Constrained modulus M_{DMT}.

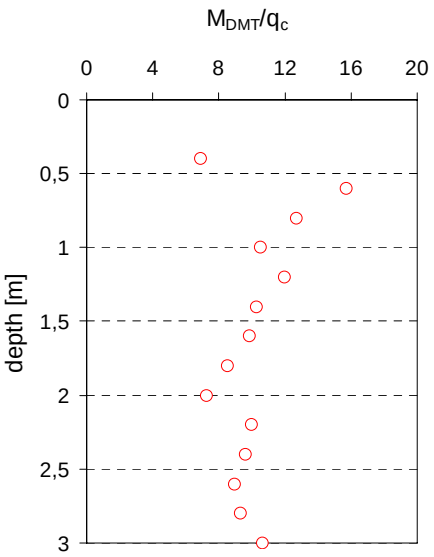

Figure 17. Profile of M_{DMT}/q_c ratio.

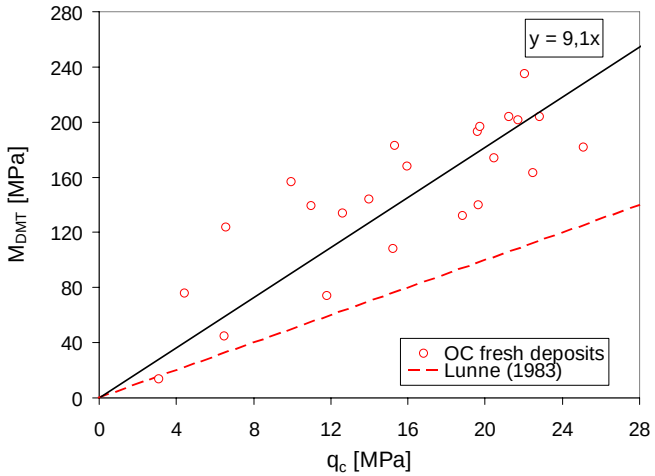

Figure 18. Constrained modulus vs. cone resistance for OC sand fills.

4 CONCLUSIONS

Strength and deformation parameters of hydraulic sand fills are essentially dependent on the placement method. Coupled CPTU and DMT tests permit a better description of sand fills including stress state and history. Sand fill at the back of harbour formed by subaqueous placement method is in normally consolidated or slightly overconsolidated state and has medium density. The constrained modulus derived from DMT tests is similar to Lunne's & Christophersen's CPTU correlation for NC sands. A very dense and overconsolidated sand was found in the hydraulically formed subaerial beach on The Hel peninsula. For OC sands the constrained modulus from DMT is significantly higher than the CPTU correlation. The dilatometer test is more sensible to stress state and history than the cone penetration test.

ACKNOWLEDGEMENTS

A part of in-situ tests was financed with a grant of Polish Scientific Research Committee No. 8 T07E 00 121. I express my gratitude to prof. Silvano Marchetti for supplying DMT equipment used during in-situ tests. I wish to thank Mrs. Anna Stelmaszyk from Maritime Office in Gdynia for her assistance during in-situ tests on the Hel peninsula. I would like to thank my colleagues from the research group for their contribution during in-situ tests.

REFERENCES

Baldi, G. Bellotti, R. Ghionna, V. Jamiolkowski, M. Marchetti, S. & Pasqualini, E. 1986. Flat dilatometer tests in calibration chambers. Proc. In Situ'86, GT Div., ASCE, June 23-25, Blacksburg, VA : 431-446.

Lee, K.M. 2001. Influence of placement method on the cone penetration resistance of hydraulically placed sand fills. Canadian Geotechnical Journal, 38 : 592-607.

Lunne, T. Christophersen, H.P. 1983. Interpretation of cone penetrometer data for offshore sands. Proc. Offshore Technology Conference, Richardson, Texas U.S.A., Paper No. 4464.

Jamiolkowski, M. Lo Presti, D. C. F., Manassero, M. 2001. Evaluation of relative density and shear strength of sand from CPT and DMT. LADD Symposium, October 2001.

Marchetti, S. 1980. In situ tests by flat dilatometer, Journal of the Geotechnical Engineering Division, ASCE, Vol. 106, No. GT3.

Marchetti, S. Monaco, P. Totani, G. & Calabrese, M. 2001. The flat dilatometer test (DMT) in soil investigations. A report by the ISSMGE Committee TC16. Proc. In-situ 2001, Bali, May 21.

Mayne, P.W. 2001. Stress-strain-strength-flow parameters from enhanced in-situ tests. Proc. In-situ 2001, Bali, May 21.

Puech, A. & Foray P. 2002. Refined model for interpreting shallow penetration CPTs in sands. Proc. Offshore Technology Conference, Houston, Texas U.S.A., 6-9 May. Paper No. 14275.

Reyna, F. & Chameau, J.L. 1991. Dilatometer based liquefaction potential of sites in the imperial valley. 2nd Int. Conf. on recent advances in geot. earthquake engrg. and soil dynamics. St. Louis, May.

Geotechnical Investigation of the Recife Soft Clays by Dilatometer Tests

R. Q. Coutinho;
Federal University of Pernambuco, Recife, Brazil

M. I. M. C. Bello
Federal University of Pernambuco, UFPE, Brazil

A. C. Pereira;
Federal University of Pernambuco, UFPE, Brazil

Keywords: Geotechnical Investigation, Dilatometer, Soft Clay, Steel Pile Under Lateral Loading.

ABSTRACT: The presence of soft clay deposits requires careful evaluation of soil parameters to analyze the performance of foundations. Due to its high compressibility and low strength, soft clays usually present serious problems. Laboratory and in situ tests are usually used to obtain the soil properties. Comprehensive research has been carried out in Recife soft clay deposits in northeastern Brazil by the Geotechnical Group of the Federal University of Pernambuco, Brazil (Coutinho et al., 1997; 1999; 2002). This paper presents an evaluation of the geotechnical information from Recife soft clays (two research sites) using the dilatometer test (DMT). Classification of types of soils, stress history and in situ horizontal stress, compressibility and strength parameters are obtained and discussed with the literature results. Comparisons are also made with laboratory and in situ reference tests results. In general, the results obtained confirm the potential of the dilatometer to obtain good predictions of geotechnical parameters in these soft clay deposits. In one of the sites investigated, the research was prompted by the general failure of a concrete structure caused by buckling of steel pile foundations in 1995. A lateral load test was performed in two steel piles, and the field results were compared to those predicted using linear and nonlinear finite element analysis. In a nonlinear analysis, lateral displacements reduce drastically the vertical loading capacity of the steel pile in soft clay deposits. DMT testing turned out to be a sufficiently viable technique for obtaining data needed for generating p-y curves in very soft soils (Coutinho et al., 2005).

1. INTRODUCTION

More than 50% of the plain area of the city of Recife is underlain by soft ground deposits. Due to its high compressibility and low resistance, the presence of soft clay deposit requires careful evaluation of soil parameters to analyze the performance of the foundations. Laboratory and in situ tests are usually used to obtain the soil properties. The flat dilatometer test (DMT) was developed in Italy (Marchetti, 1980) and has become a routine site investigation tool in more than 40 countries over the world. A general overview of the dilatometer and its design applications, guidelines for the proper execution, basic interpretation methods and recent findings and practical developments are given by Marchetti et al (2001) in a report under the auspices of the ISSMGE Technical Committee TC16.

Since 1980 the Geotechnical Group of the Department of Civil Engineering of the Federal University of Pernambuco has developed a research program in the Recife soft clays deposits performing laboratory and in situ tests for many sites of the plain area (Coutinho et al 1997, 1998, 1999, 2002). The primary goals of the research program include evaluating the applicability in the Recife soil deposits of the tests developed in other countries, developing of advanced operational techniques or equipment better suited to our natural conditions, publishing the results for use by the Profession, comparing of the results with references laboratory and in situ tests and the formation and continually expanding the knowledge data base.

This paper presents an evaluation of the geotechnical information from Recife soft clays (two research sites) using the DMT. Classification of soil types, stress history and in situ horizontal stress, compressibility and strength parameters are obtained and discussed with results from the literature and from laboratory and in situ reference tests. In one of the sites investigated, the research was prompted by the general failure of a concrete structure caused by bucking of steel pile foundations. A lateral load test was performed on two steel piles, the field results being compared to those predicted by linear and

nonlinear finite element analysis. The influence of lateral displacement on the vertical loading capacity of a steel pile in soft clay deposit is also investigated (Coutinho et al., 2005).

2. CHARACTERISTICS OF THE EXPERIMENTAL FIELD

Figure 1 shows the location of Recife city and the investigated soft clays sites in the lowland area (Coutinho et al., 1998). Recife has two soft clays research sites being studied by the Geotechnical Group of the Federal University of Pernambuco: RRS1 (International Club) and RRS2 (SESI-Ibura). The RRS1 is located near the center of the city and the RRS2 is located near the Recife Airport. In the later one, a geotechnical accident occurred, in 1995, causing total destruction of an one-floor structure on steel pile foundation.

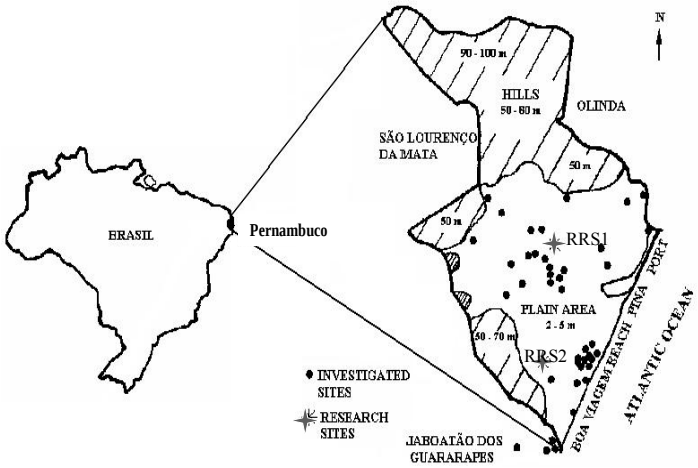

Figure 1. Location of Recife – Pernambuco / Brazil and the Research Sites (RRS1 and RRS2)

Figure 2 presents the soil profile and results of the characterization tests from the RRS1 and RRS2. The soil profile of the RRS1 consists of 6-7 meters of clayey sand and sandy clay, underlain by a soft organic clay with a thickness of about 20 meters. This organic clay can be subdivided into two layers, with the lower layer having lower plasticity. SPT (N-value) varying from 1 to 4, and are usually between 2 and 3. Underneath this, there are alternate layers of sand and clay with the SPT N-values increasing in depth. The water table level is between 1 and 2 meters deep depending on the season. The results of the characterization tests were usually quite different from each soft clay layer. The natural water content is usually presented slightly below the liquid limit in both layers, showing values in the range of 65-100% in layer 1 (6–16m) and in the range of 45-65% in layer 2 (16-26m). The plasticity index of the first soft layer is 70.4 ± 12.4%, while in the second soft layer the values are 33.0 ± 5.7%. The organic content is also higher in layer 1 (7.0 ± 1.5%) than in layer 2 (3.7 ± 1.7%). The grain size distribution for both layers can be described as 65% clay, 25% silt, and 10% sand.

The soil profile of the RRS2 consists of about 3 meters of old embankment, underlain by a clayey peat layer with thickness of about 1 meter and a very soft organic clay deposit (SPT: 0/200) with a thickness of 17 meters, subdivided into two layers. Below the organic clay, a clayey sand layer is observed. The water table level is 0 to 1 meter deep.

Artesian pressure and gas pressure also were observed showing higher pore water pressure than the hydrostatic conditions, inside of the very soft clay layers, reducing the overburden effective stress.

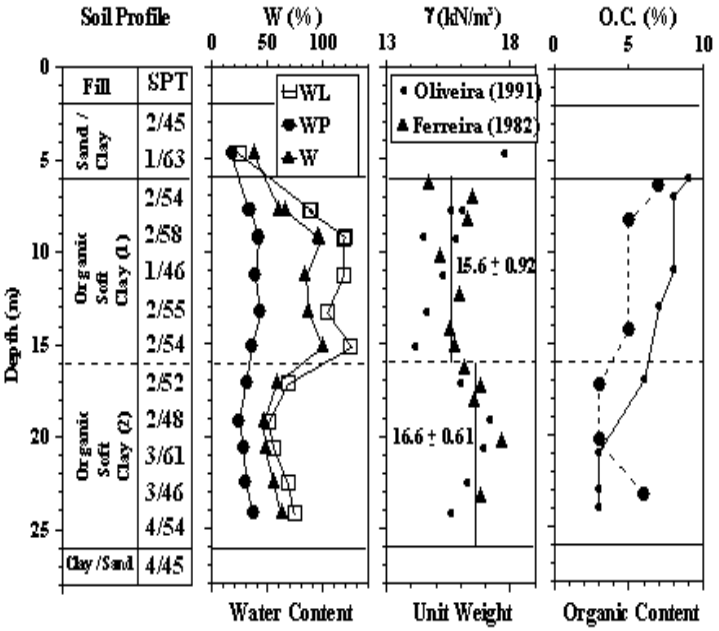

a) RRS1

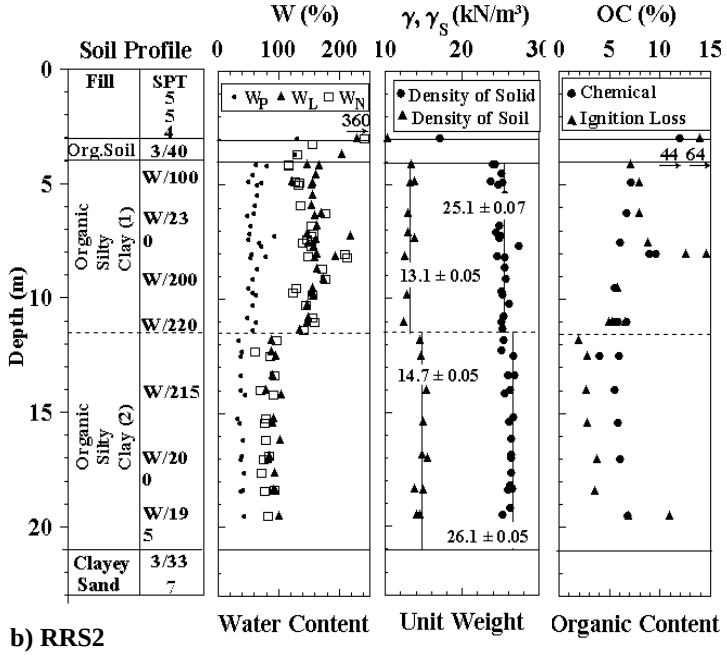

b) RRS2

Figure 2. Results of Characterization Tests vs Depth: (a) Research Site 1; (b) Research Site 2 (Coutinho & Oliveira, 1997; Coutinho et al., 1999).

The natural water content is close to the liquid limit in both soft clay layers, being 149.7 ± 23.7% in first layer, and 84.2 ± 15.5% for the second layer. The plasticity index of the first soft layer (4-11.5m) is 97.5 ± 13.6%, while in the second soft layer (11.5-21m) the values are 53.1 ± 5.9%. The organic content is usually between 3 and 10%, with the first layer generally having slightly higher values. The grain size distribution for both layers can be described as 72% clay, 20% silt, and 8% sand.

3. DILATOMETER TESTS

Three dilatometer test soundings (D_1, D_2 and D_3) were performed at each research site. The dilatometer blade and membrane were standard as defined by Marchetti (1980). The dilatometer control unit was a 1985 model. The procedures used were in accordance with what is suggested in the literature (e.g. ASTM, 1986; Schmertmann, 1988; Campanella and Robertson, 1991). The corrected pressures and intermediate DMT parameters were obtained using Equations 1 - 3 and Equations 4 - 7, respectively.

Corrected pressures:

$$p_0 = 1.05\ (A - Z_M - \Delta A) - 0.05\ (B - Z_M - \Delta B) \quad (1)$$

$$p_1 = (B - Z_M - \Delta B) \quad (2)$$

$$p_2 = (C - Z_M + \Delta A) \quad (3)$$

Intermediate DMT parameters:

$$I_D \text{ (material index)} = (p_1 - p_0) / (p_1 - u_0) \quad (4)$$

$$E_D \text{ (dilatometer modulus)} = 34.7\ (p_1 - p_0) \quad (5)$$

$$K_D \text{ (horizontal stress index)} = (p_0 - u_0) / \sigma'_{v0} \quad (6)$$

$$U_D \text{ (pore-pressure index)} = (p_2 - u_0) / (p_0 - u_0) \quad (7)$$

Figure 3 presents the results of the intermediate DMT parameters for the three DMT test soundings performed in each research site. This figure shows a repeatable and continuous profile of the measured parameters.

4. DERIVATION OF GEOTECHINICAL PARAMETERS

4.1. Stress History / State Parameters

(a) Soil type

According to Marchetti (1980) the soil type can be identified as follows: clay ($0.1<I_D<0.6$), silt ($0.6<I_D<1.8$) and sand ($1.8<I_D<10$).

Figure 4 summarizes the positions of the soils tested by NGI on the dilatometer soils classification chart proposed by Marchetti & Crapps (1981) and modified by Lacasse & Lunne (1988). The newer information enables one to illustrate qualitatively the effects of overburden, overconsolidation ratio and density on the dilatometer modulus. For Norwegian soils, material indices between 0.05 and 0.1 have been obtained. The original chart was therefore extended in this direction.

The positions of the Recife soft clays deposits are superimposed on that classification chart in Figure 4 and they agree with the soil sample descriptions shown on Figure 2.

(b) Unit Weight

Figure 5 presents comparisons of the unit weight predicted by the Marchetti and Crapps (1981) dilatometer soil classification chart (Figure 4) and reference unit weights measured in the laboratory for the both Recife Research Sites (RRS1 and RRS2).

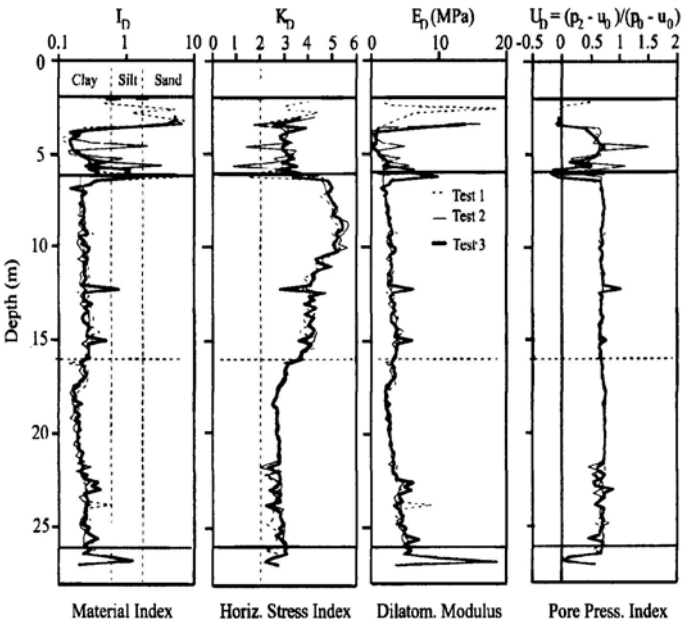

a) RRS1

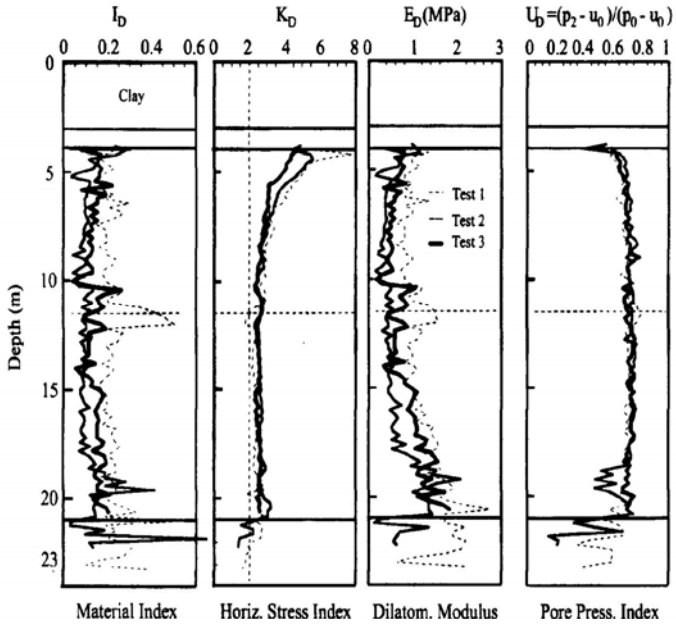

b) RRS2

Figure 3. Dilatometer test results – I_D, K_D, E_D, U_D vs Depth: (a) Research Site 1; (b) Research Site 2 (Coutinho & Oliveira, 1997; Coutinho et al., 1999).

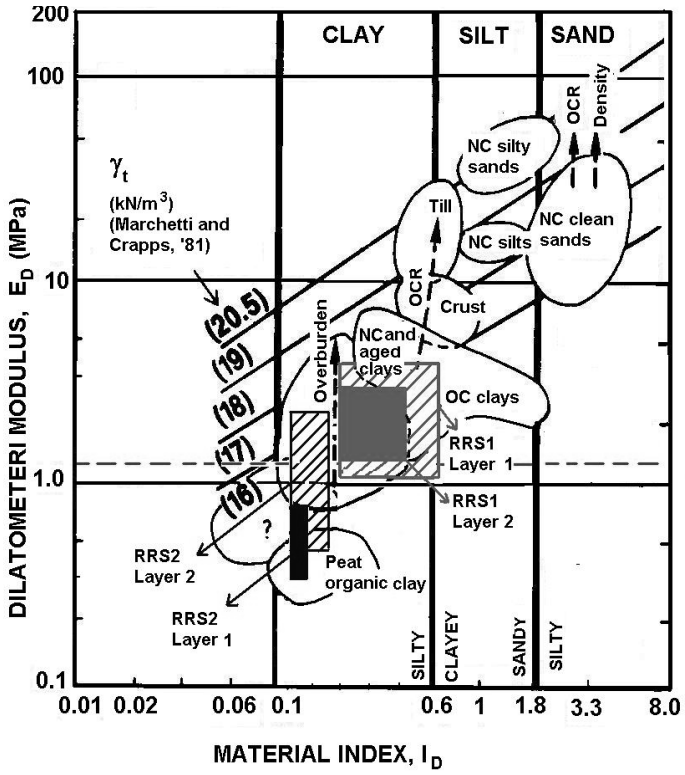

Figure 4. Classification chart for soils test. Effects of overburden, overconsolidation ratio and density (Lacasse & Lunne, 1988) with results of Recife Soft clay deposits.

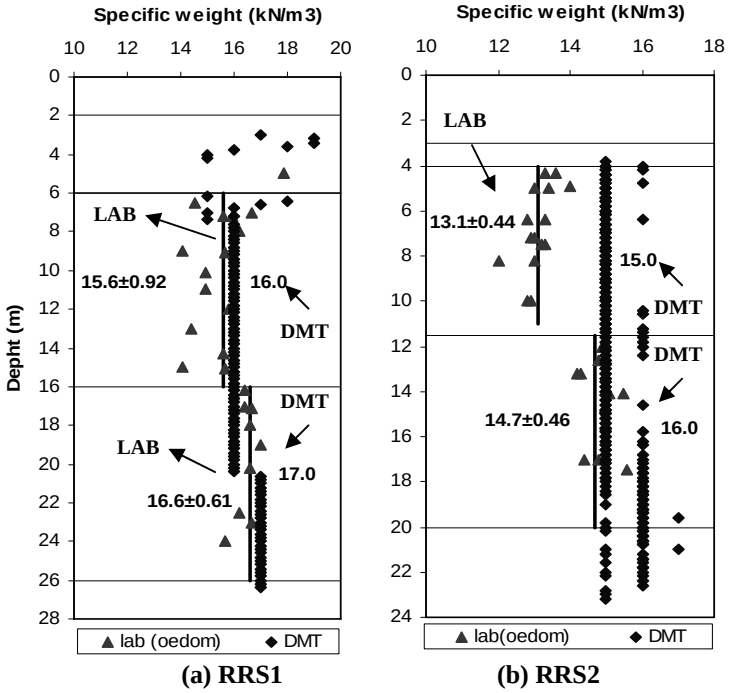

Figure 5. Comparison between γ_{DMT} vs. $\gamma_{lab.}$: (a) Research Site 1; (b) Research Site 2.

Lacasse & Lunne (1988) observed that the chart tends to underpredict the unit weight in soft clays. Marchetti et al. (2001) comment that the main scope of the chart is not the accurate estimation of unit weight, but the possibility of constructing an approximate profile of σ'_{vo}, needed in correlations.

In Figure 5a (RRS1) can be seen that in general the estimated results agree with the laboratory results, in both layers of the deposit. For the RRS2 (Figure 5b) it can be seen that, in the layer 2 the estimated results are close to the laboratory; however, in the layer 1, where the clay is in a very soft consistency (E_D<1000kPa), with presence of organic content and high percent of natural water content (149.7 ± 23.7%), the values of unit weights obtained from the chart are higher than the laboratory. These results are different from that observed by Lacasse & Lunne (1988).

(c) Coefficient of earth pressure at rest K_0

The effective in situ horizontal stress, σ'_{h0} (or coefficient of earth pressure at rest K_0) is an important geotechnical parameter but very difficult to obtain accurately with any device. In general, there is an uncertain reability, because of the scarcity of reference values (Lunne et al, 1990).

In this research the Equations 8 to 10 were used for obtaining the K_0 values from correlation proposal in the literature.

$$K_0 = (K_D/1.5)^{0.47} - 0.6\,;\text{(Marchetti, 1980)} \qquad (8)$$

$$K_0 = 0.34\ K_D^{0.54}\,;\text{(Lunne et al., 1990)} \qquad (9)$$

$$K_0 = (1 - \sin\phi')\ OCR^{\sin\phi'}\,; \qquad (10)$$

(Mayne & Kulhawy, 1982).

Figure 6 presents the average values of K_0 that were obtained using Equation (9) and (10) considered, showing that the DMT results (Lunne et al., 1990) were close to the "laboratory" correlation (Mayne & Kulhawy, 1982). Lunne et al. (1990) estimated that for the "young" clays the uncertainty associated with K_0 from DMT is about 20%.

Figure 7 confirms this result and shows that the Marchetti (1980) K_0 correlation presents significant higher values than the reference values considered in this research.

Numerical studies (Yu, 2004) which assume that the insertion of the dilatometer is a flat cavity expansion process enabled a theoretical relationship between K_D and K_0 (also K_D and OCR) to be obtained. The numerical estimative of K_0 for three different clays compared to predictions obtained directly from Equation 8 showed that the Marchetti (1980) proposal can be used with reasonable confidence for the soils investigated.

(d) Overconsolidation ratio OCR

The overconsolidation ratio OCR has been usually defined as the ratio of the "maximum" past

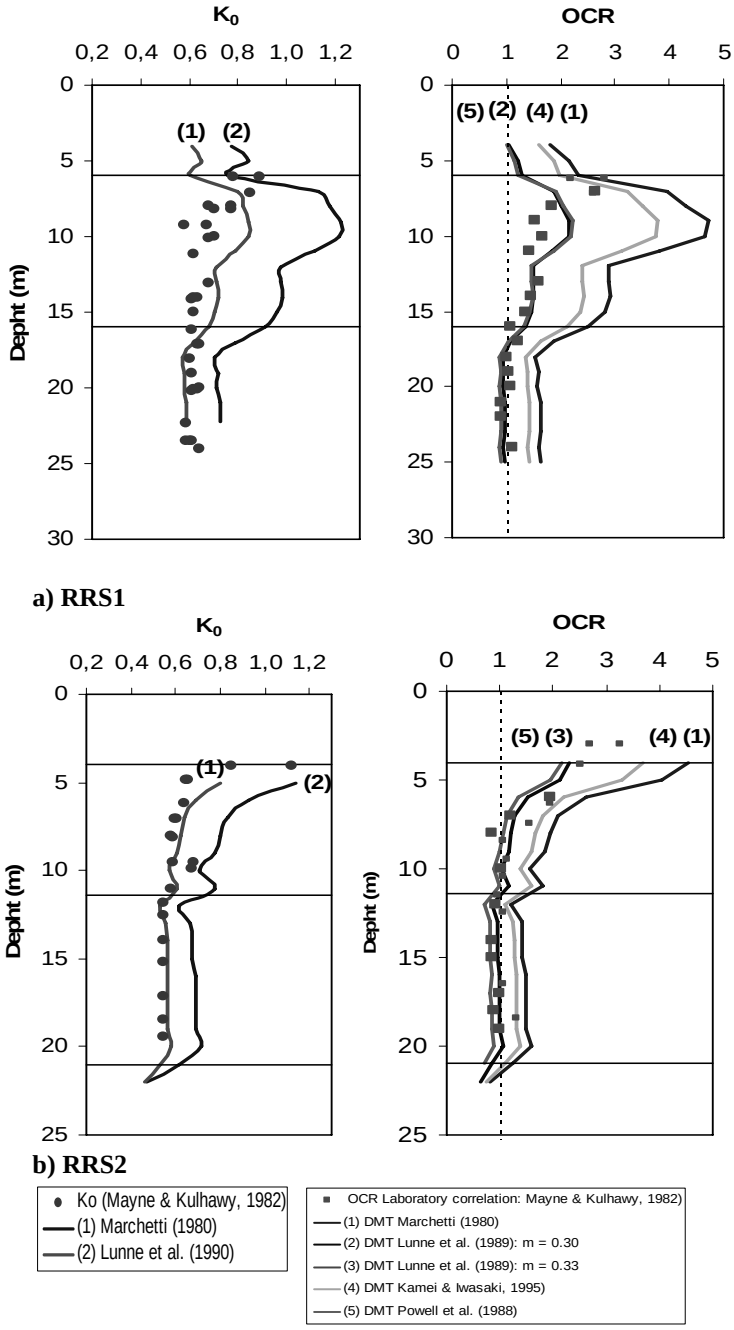

Figure 6. Stress history and in situ horizontal stress parameters: (a) Research Site 1; (b) Research Site 2.

effective stress and the currently vertically applied stress.

Marchetti (1980) pointed out the similarity between the K_D and OCR profiles and later confirmed by several authors (e.g. Jamiolkowski et al, 1988). In the present research this similarity is also very well observed with the "exception" of the upper part of the first soft clay layer in the RRS1.

For uncemented clays OCR can be simply predicted as:

$$OCR = (0.5K_D)^{1.56} \text{ (Marchetti, 1980)} \quad (11)$$

Equation 11 has built-in the assumption that K_D=2 for OCR=1. This assumption has been confirmed in many genuinely NC (no cementation,

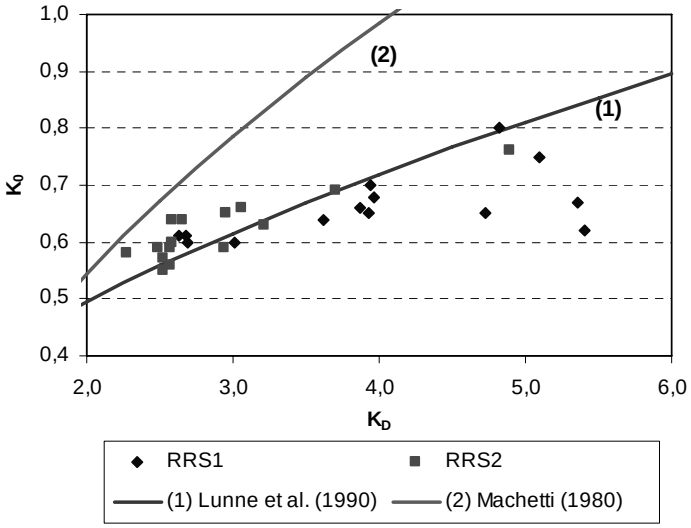

Figure 7. Coefficient of earth pressure at rest K_0 stress parameters: (a) Research Site 1; (b) Research Site 2.

aging, structure) clay deposits (Marchetti et al.,2001). In the present research OCR values were also predicted from other correlations proposed in the literature.

$$OCR = m\ K_D^{1.17};\ m=0.30 - 0.33 \text{ (Lunne et al 1989) (for young clays: < 60,000 years)} \quad (12)$$

$$OCR = (0.34\ K_D)^{1.43} \text{ (Kamei \& Iwasaki, 1995)} \quad (13)$$

$$OCR = 0.24K_D^{1.32} \text{ (Powell \& Uglow, 1988)} \quad (14)$$

Figure 6 presents results of OCR profiles from the Recife research sites obtained using oedometer tests. Predictions of OCR from DMT correlations are shown in Figures 6 and 8.

Figure 6a, for RRS1, shows a small overconsolidated upper crust (OCR values decreasing from a value of about 3.0 to 1.3), and remaining approximately 1.3 until reaching layer 2 which is normally consolidated (OCR≈1.0). The OCR data distinguishes layer 1, which is generally overconsolidated, from layer 2, which is generally normally consolidated.

Figure 6b, for RRRS2, shows a similar pattern to that of Figure 6a for RRS1 with layer 1 having an overconsolidated crust. However, the OCR values decrease more rapidly at RRS2 (from an OCR of about 3 to a value of 1) than at RRS1. Layer 2 at both sites is normally consolidated (OCR≈1.0).

From the K_D profile (Figure 3) in both research sites the NC layer 2 (Figure 6) has $K_D \approx 2.0$ to 3.0 indicating some level of cementation/structure/aging (Marchetti et al., 2001). The values of K_D are lower at RRS2 than RRS1 indicating that the level of cementation/structure/aging at RRS2 is likely less than at RRS1.

Figures 6 and 8 show that the correlations for OCR proposed by Lunne et al. (1989) using m = 0.30–0.33 and Powell et al. (1988) can be used with reasonable confidence in Recife soft clays. The Marchetti (1980) and Kamei & Iwasaki (1995) OCR correlations present significant higher values than the reference values considered in this research.

Numerical estimates of OCR from the theoretical relationship between K_D and OCR developed by Yu (2004) (see also Schnaid, 2005) for three different clays showed that the Marchetti correlation can be used with reasonable confidence for the clays investigated with OCR<8.

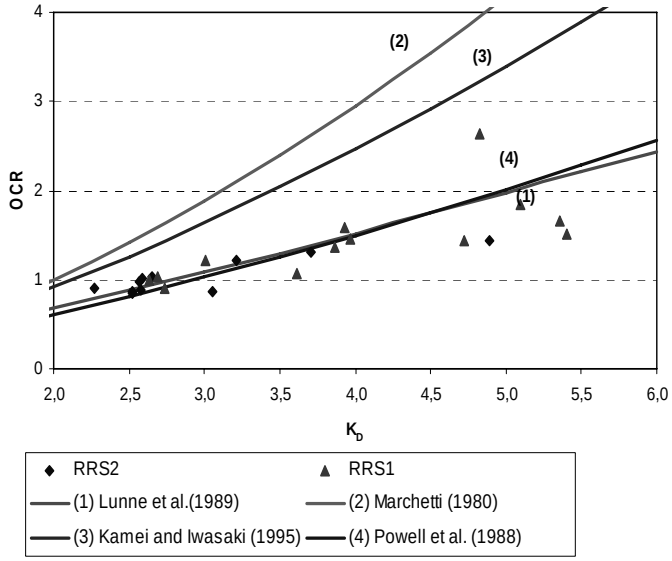

Figure 8. Stress history and in situ horizontal stress parameters: (a) Research Site 1; (b) Research Site 2.

4.2. Characteristics of Deformation

Figure 9 shows the results obtained in the research sites for the compressibility parameters from oedometer tests: void ratio (e_0), compression index (C_{C1}), swell index (C_S). They are basically constant in each soft layer with higher values in layer 1.

Constrained tangent modulus values (M) from laboratory tests and DMT tests are compared in Figure 9 at the same in situ overburden stress. The Marchetti (1980) correlation for clays ($I_D < 0.6$) was used:

$$M_{DMT} = R_M.E_D; \quad (15)$$

$$\text{Where } R_M = 0.14+2.36 \log K_D \quad (16)$$

The results show a very reasonable agreement in the soft layer 2 – RRS1. In the other layers, in general, M_{DMT} were slightly higher (0 - 20%) than oedometer results (RRS2 – layer 1 and 2; RRS1 – layer 1).

Lunne et al. (1989) stated that, for clays, it was recommended to use the Marchetti (1980) correlation.

Experience has shown that M_{DMT} is highly reproducible and in most cases varies between from about 0.4 MPa to 400 MPa. Comparisons both in terms of $M_{DMT} - M_{reference}$ and in terms of predicted vs. measured settlements have shown that, in general, M_{DMT} is reasonably accurate and dependable for everyday design practice (Marchetti et al., 2001).

4.3 Characteristics of flow

(a) Coefficient of horizontal consolidation

The method used in the present research for deriving C_h from DMT dissipations was the DMT-C (Schertmann, 1988; Robertson, 1989) considering a time factor (T_{30}) corresponding to t_{30} determined from the C-decay dissipation curve (Pereira, 1997).

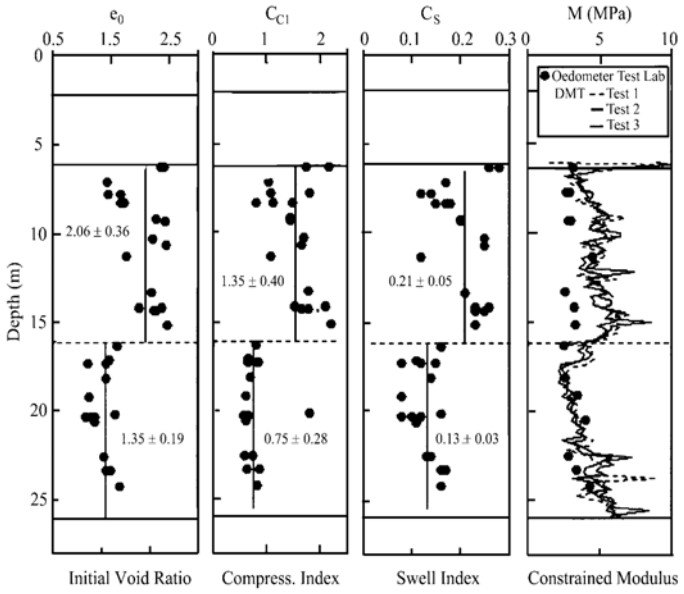

a) RRS1

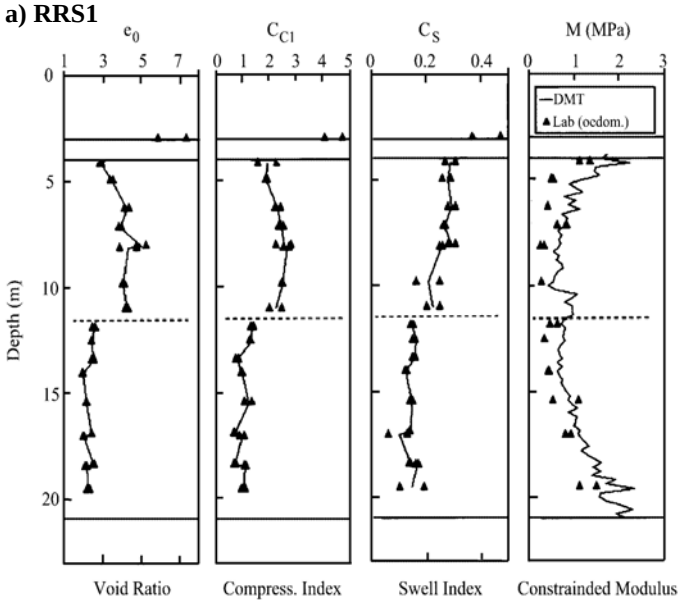

b) RRS2

Figure 9. Compressibility parameters – oedometer tests and DMT: (a) Research Site 1; (b) Research Site 2 (Coutinho & Oliveira, 1997; Coutinho et al., 1999).

BACK

Table 1 presents the C_h values that were obtained in the RSS2. Figure 10 shows the comparison with C_v values from laboratory oedometer tests, for the depth of 7.40 m.

The DMT C_h values obtained in soundings D-1 and D-2 showed some differences at 12.4 and 17.4 meters but were similar at the depth of 7.40 m (Table 1). In general, the DMT C_h values were higher than the C_v (C_h/C_v = 1 to 3) laboratory results as was expected (Figure 10).

The method recommended by Marchetti el al (2001) for deriving C_h from DMT dissipations is the DMT-A method. Another accepted method is DMT-A_2 method that is considered basically an evolution of the DMT-C method.

Case histories indicated that the C_h from DMT-A are in good agreement (or "lower" by a factor 1 to 3) with C_h backfigured from field observed behavior (Marchetti et al., 2001).

The DMT-A_2 method (and the DMT-C method) rely on the assumption that the contact pressure A_2 (or C), after the correction, is approximately equal to the pore pressure in the soil facing the membrane. Such assumption is generally valid for soft clays, but dubious in more consistent clays. The DMT-A method does not rely on that assumption (Marchetti et al., 2001).

(b) Coefficient of horizontal permeability

Schmertmann (1988) proposes the following procedure for deriving k_h from C_h:

- Estimate M_h using $M_h = K_0 M_{DMT}$, i.e. assuming M proportional to the effective stress in the desired direction.
- Obtained $k_h = C_h \gamma_w / M_h$. (17)

4.4. Undrained shear strength (S_u)

In the present research the DMT Su values were predicted from the following correlations:

$$S_u = 0.22\ \sigma'_{V0}\ (0.5\ K_D)^{1.25}\ ; \quad (18)$$
(Marchetti, 1980)

$$S_u = 0.20\ \sigma'_{V0}\ (0.5\ K_D)^{1.25}\ ; \quad (19)$$
(Lacasse & Lunne, 1988)

$$S_u = 0.350\ \sigma'_{V0}\ (0.47\ K_D)^{1.14}; \quad (20)$$
(Kamei & Iwasaki, 1995)

Figure 11 presents the S_u values from both research sites (RRS1 and RRS2) obtained through the dilatometer and the references tests – Vane and triaxial compression tests (UU-C and CIU-C, with $\sigma'_C \cong \sigma'_{OCT\ in\ situ}$).

Table 1. Coefficient of horizontal consolidation values from DMT – RRS2 (Pereira, 1997).

	Depth (m)	C_h (x10^{-4} cm^2/s)
Test D-1	7.40	3.737
	12.40	12.279
	17.40	6.121
Test D-2	7.40	3.336
	12.40	4.198
	17.40	1.954

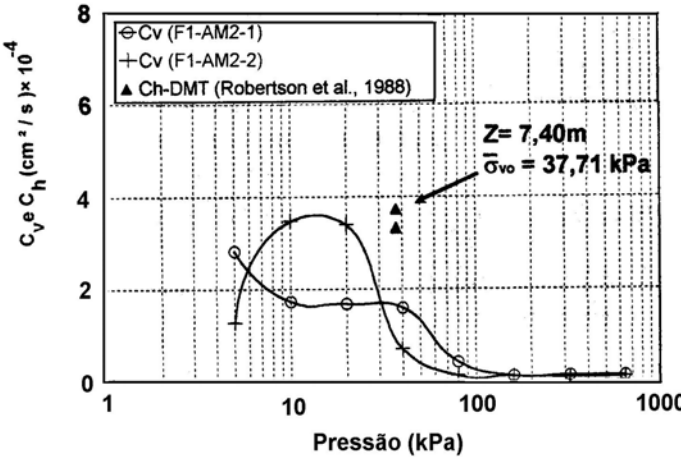

Figure 10. Coefficient of horizontal consolidation - DMT and Oedometer results - RRS2 (Pereira, 1997).

In Recife Research Site 1 (Figure 11a and 12) the Marchetti's correlation S_u values in general are close or slightly higher than the vane tests and the laboratory triaxial results. The Lacasse & Lunne (1988) correlation S_u values were in general close to the laboratory triaxial tests and lower or close to the vane tests results. The Kamei & Iwasaki (1995) correlation gave higher S_u values than both tests (Figure 12). In the Recife Research Site 2 (Figure 11b and 12) the Marchetti's correlation Su values in general are close or slightly lower than the vane tests and close or slightly higher than the laboratory tests results. The Lacasse & Lunne (1988) correlation S_u values were close or slightly lower than the triaxial compression tests and lower than the vane tests results. The Kamei & Iwasaki (1995) correlation in general presented S_u values close to the vane tests and higher than the laboratory triaxial tests results.

Marchetti et al. (2001) comments that the correlation $S_u = 0.22\ \sigma'_{V0}\ (0.5\ K_D)^{1.25}$ has generally been found to be in an intermediate position between subsequent datapoints presented by various researchers (e.g. Lacasse & Lunne, 1988; Powell & Uglow, 1988). Experience has shown that, in general, Su_{DMT} is quite accurate and dependable for design, at least for everyday practice.

Numerical analysis of the installation of flat dilatometers reported by some authors have provided useful insights of the dilatometer test and

BACK

generally support the Marchetti (1980) empirical correlation for S_u (Schnaid, 2005).

Considering both research sites, an estimation of S_u for the Recife soft clays deposits can be obtained with reasonable confidence for practical purposes. S_u compares favorably with the vane test using the original correlation (Marchetti, 1980) and with triaxial compression test results using the correlation proposed by Lacasse & Lunne (1988).

5. Comparative study – laboratory x DMT

Table 2 shows a summary of the correlations used in the present research to obtain from DMT results for some important geotechnical parameters, OCR, K_0, S_u and M. Values of the geotechnical parameters from DMT were compared with that obtained by reference tests.

Column 5 of the Table 2 (Recife Experience) shows the results from the quantitative comparative study between the geotechnical parameters values predicted from the DMT and the results from the reference tests. In can be observed that for the Recife soft clay the estimation of geotechnical parameters is quite accurate for practical purpose from results of DMT using correlations from the literature. Column 6 presents the DMT correlations recommended to be used in the Recife soft clays deposits and the uncertainty associated with the prediction of the geotechnical parameters.

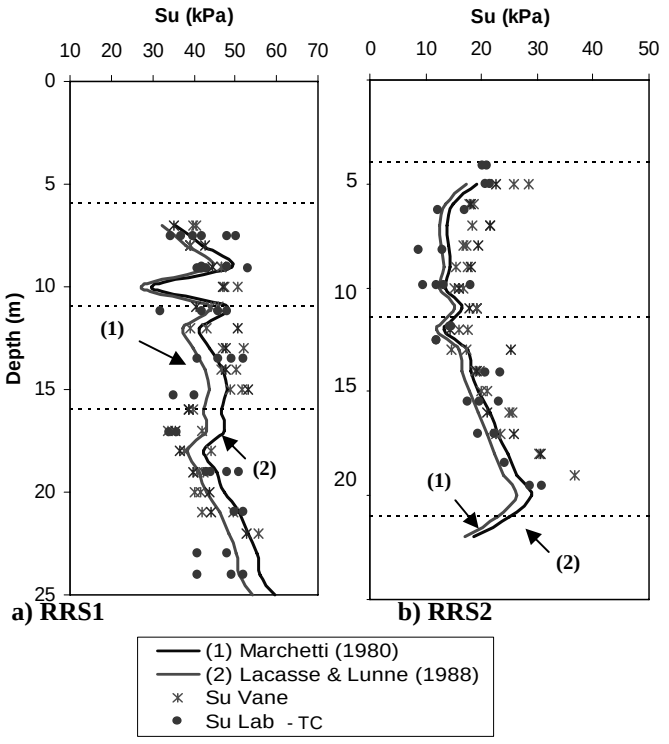

Figure 11. Su vs. depth: DMT, triaxial compression tests, and uncorrected field vane tests; (a) Research Site 1 (b) Research Site 2 (Coutinho et al., 1999).

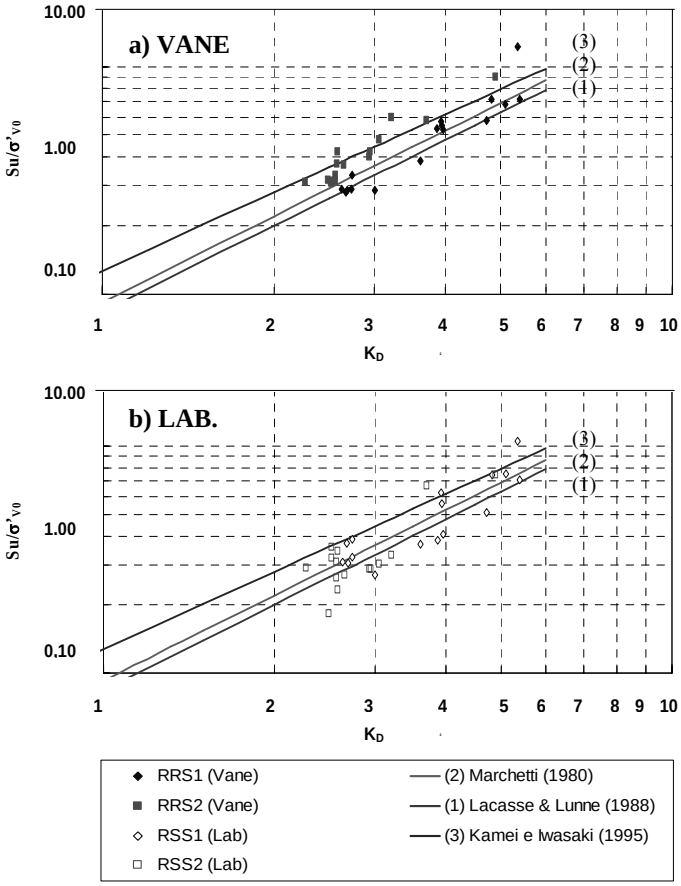

Figure 12. S_u vs. K_D parameters: (a) Vane Test; (b) Laboratory test – TC.

6. Practical application – Steel Pile Under Lateral Loading in a Very Soft Clay Deposit

In 1995, a thorough rupture in a reinforced concrete structure of a floor supported on steel piles embedded in a 17 meters thick soft clay layer in Recife, Brazil, occurred 21 years after it had been built, with no warning of potential failure.

Figure 13 presents the geotechnical profile of a cross section of the area and the hypothesis proposed for the accident. A slow lateral movement of the organic clay layer provoked lateral displacement of the piles which were supporting the total vertical load (structure self weight + negative friction) causing a buckling failure. This case demonstrates the importance of a buckling study in steel piles caused by lateral displacement in soft soil.

Afterwards, the Geotechnical Group of the Federal University of Pernambuco, Brazil, has performed extensive geotechnical research program in the area (UFPE - RRS2).

A study was developed on the behavior of laterally loaded steel piles in thick layers of soft clay, consisting of analytical and experimental stages (Coutinho et al, 2005). In the experimental stage, lateral loading tests in steel piles driven into the organic clay deposit were carried out where the aforementioned accident took place.

In the analytical stage, predictions on the horizontal displacements of piles top and also for the buckling load of a steel pile in very soft clay were made from linear and non-linear analyses through the finite element method.

The soil was modeled with p-y curves obtained from dilatometer (DMT) and Ménard pressuremeter (PMT) testing results performed at the site of the accident and near the damaged structure that bear deforming-power element. The following assumptions were considered: the steel pile was perfectly vertical and steel pile had vertical load eccentricity, that is, with initial lateral deformation. The p-y curves were found through the semi-empirical method proposed by Robertson et al. (1989), which uses data from dilatometer tests, and for the semi-empirical method proposed by Ménard (1969), which uses data from pressumeter tests.

Table 2. Comparative study – DMT correlations versus reference tests

PARA-METER	CORRELATIONS - DMT	EQUATIONS	REFERENCE TEST	RECIFE EXPERIENCE	CORRELATION RECOMENDED
OCR	**Lunne et al.(1989)**	$OCR = m\ K_D^{1.17}$; m = 0.3-0.33 (young clays: < 60.000 years)	**oedometer**	± 10%	**Lunne et al (1989)** $OCR = 0.3\ K_D^{1.17}$ m = 0.30-0.33 ±10%
	Marchetti (1980)	$OCR = (0.5\ K_D)^{1.56}$ (uncemented clays) ($I_D \leq 1.2$)		40 – 160% (average) 80% (higher)	
	Kamei & Iwasaki (1995)	$OCR = (0.34\ K_D)^{1.43}$		10 – 120% - average 55% (higher)	
	Powell et al. (1988)	$OCR = 0.24\ K_D^{1.32}$		± 15%	
K_0	**Lunne et al.(1990)**	$K_0 = 0.34\ K_D^{0.54}$ (young clays: < 60.000 years)	$K_0 = (1 - \text{sen}\ \phi')\ OCR^{\text{sen}\ \phi'}$ **(Mayne & Kulhavy, 1982)**	± 10%	**Lunne et al (1989)** $K_0 = 0.34\ K_D^{0.54}$ ± 10%
	Marchetti (1980)	$K_0 = (K_D / 1{,}5)^{0.47} - 0.6$		40% (higher)	
Su	**Marchetti (1980)**	$Su = 0.22\ \sigma'_{V0}\ (0.5\ K_D)^{1.25}$	**(Triaxial) UU-C / CIU-C**	± 20%	**VANE TESTS Marchetti (1980)** $Su = m\ \sigma'_{V0}\ (0.5\ K_D)^{1.25}$ m = 0.22 ± 0.03 ± 15% **TRIAXIAL TESTS Lacasse & Lunne (1988)** $Su=0.20\sigma'_{V0}(0.5\ K_D)^{1.25}$ ± 15%
			(Vane)	± 15%	
	Lacasse & Lunne (1988)	$Su = 0.20\ \sigma'_{V0}\ (0.5\ K_D)^{1.25}$	**(Triaxial) UU-C / CIU-C**	± 15%	
			(Vane)	± 18%	
	Kamei & Iwasaki (1995)	$Su = 0.350\ \sigma'_{V0}\ (0.47\ K_D)^{1.14}$	**(Triaxial)**	± 30%	
M	**Marchetti (1980)**	$M = R_M\ .\ E_D$; with $R_M = 0.14 + 2.36 \log K_D$; ($I_D < 0.6$)	**oedometer**	0 - 20% (higher)	**Marchetti (1980)** 20% (higher)

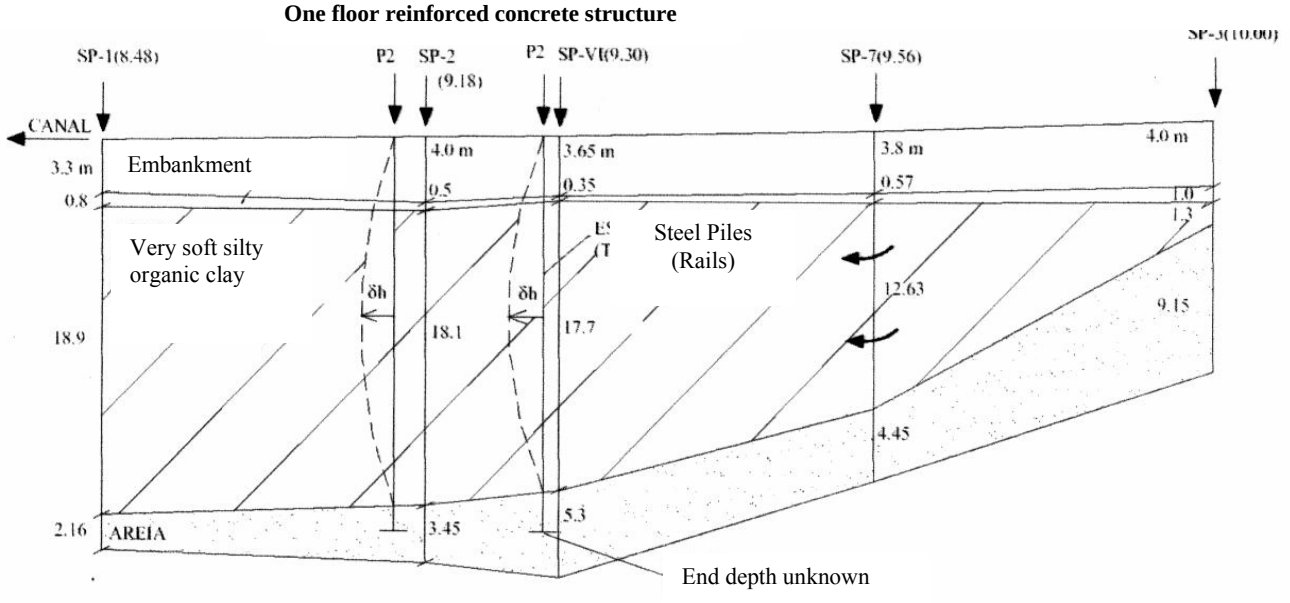

Figure 13. Geotecnical profile – horizontal pull

The horizontal displacements were measured (inclinometer) and predicted with linear and nonlinear FEM analyses for level land grades and after fill excavation. Figure 14 and Table 3 presents the results obtained versus the applied loads. It can be noted that the nonlinear analyses (DMT and PMT) results are very close to the values measured showing, in general, differences ranging from 1 % to 20 %.

In the analysis for the collapse of the steel piles, two important facts must be taken into consideration: a) whether the steel pile was completely vertical and; b) whether there was any eccentricity in the vertical load.

It was assumed that the steel pile suffered horizontal displacements and showed a second degree parabola form. These displacements were triggered by lateral nodal loads at the scores 1, 2, 3, 4, 5, and 10 cm in L / 2. The analysis results of critical loading due to accidental displacements performed according to ANSYS (1989) are summarized in Table 4.

Table 3. Predicted and measured displacements (Coutinho et al., 2005)

H = (kN)	2.5	5.0	7.5	10.05
	Horizontal Displacements (mm)			
Anál. Linear	25.95	51.9	77.85	103.81
DMT	9.22	27.09	56.85	108.56
PMT	10.32	33.52	63.27	106.74
Measured	18.59	27.86	68.71	109.65

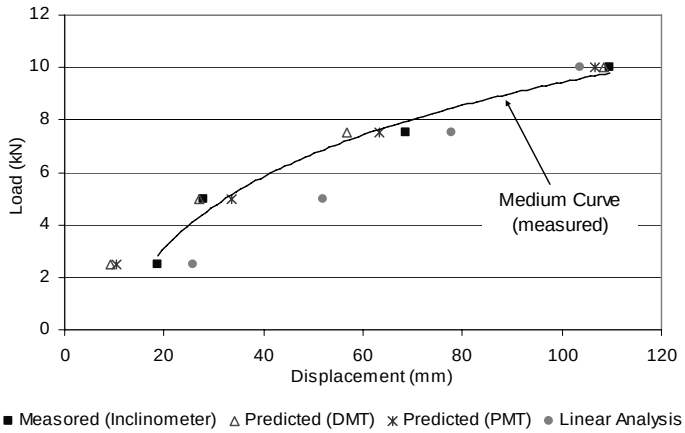

Figure 14. Predicted and measured displacements (Coutinho et al., 2005)

It can be observed that the critical load is considerably sensitive to the effect of accidental displacements which rapidly decreases its value.

The loading capacity of the steel pile under analysis was calculated through the Aoki-Velloso method (1975) using data from SPT performed at the accident site. As shown in Table 4 the working load for the steel pile would be 186.5kN and was within the interval which determines the occurrence of failure corresponding to an accidental displacement between 30 and 50cm.

Table 4. Critical loading due to accidental displacements (Coutinho et al., 2005)

Defor-rmattion (mm)	Critical Loading (kN)	
	Curves P-Y (DMT)	Curves P-Y (PMT)
	Free / Labeled Top	Free / Labeled Top
0	2,988.64	1,925.11
10	1,738.18	1,877.44
20	1,183.99	510.21
30	360.29	98.86
50	58.19	70.89
100	46.25	56.90

7. CONCLUSIONS

The flat dilatometer test has been extensively used and calibrated in soil deposits all over the world. An extensive and carefully planned investigation performed in Recife soft clays confirms the important potential of the DMT in the determination of soil type, geotechnical parameters and application for laterally loaded steel pile analyses.

The DMT correlations are recommended to be used in Recife soft clays deposits for geotechnical design parameters (uncertainty associated ≤ 20%).

The predicted lateral displacements obtained from the nonlinear analysis by using p-y curves obtained from DMT tests closely match the results measured with the lateral load test.

Lateral displacements drastically reduce the vertical loading capacity of a steel pile in soft clay deposits, as can be observed through the nonlinear analysis, making possible the occurrence of a buckling failure.

ACKNOWLEDGEMENTS

The authors are grateful to the CNPq – Brazilian Research Council for the financial support given to the research project and for the civil engineering Juliana Lemos who have contributed to this paper.

REFERENCES

ANSYS (1989), User's Manual, Swanson Analysis System Inc.,.

ASTM, Subcommittee D18.02.10 (1986).J.H. Schmertmann, Chairnan, suggested method for performing the flat dilatometer test, ASTM GT Journal, 9(2): 93-101. June.

Campanella, R. G. & Robertson, P. K. (1991). "Use and Interpretation of a Research Dilatometer". Canad. Geotechn. Journal, Vol. 28, 113-126.

Coutinho, R. Q. & Oliveira, J. T. R. (2002). Behaviour of the Recife Soft Clays. Workshop Foundation Eng.in Difficult

Soft Soil Conditions, TC 36 Meeting, Edited buy G. Y. Auvimet – SMMS, 2004, V.1, pp. 49-77.

Coutinho, R. Q. & Oliveira, J. T. R. 1997. Geotechnical Characterization of a Recife Soft Clay - Laboratory and In Situ Tests. Proceedings of 14th Int. Conf. on Soil Mech. and Found. Eng., Hamburg , 1: 69-72, Germany.

Coutinho, R. Q.; Oliveira, J. T. R. & Oliveira, A.T.J. 1998a. Geotechnical Site Characterization of Recife Soft Clays. 1st International Symposium on Site Characterization, 2: 1001-1006, Atlanta, USA.

Coutinho, R. Q., Oliveira, J. T. R., Pereira, A.C. & Oliveira, A. T. J. (1999). Geotechnical Characterization of a Recife very Soft Organic Clay – RRS2. XI PCSMGE., Foz de Iguassu, Brasil, 1: 275-282.

Jamiolkowiski, M., Ghionna, V.N., Lancellotta, R. & Pasqualine, E. (1988). New Correlations of Penetration Testting for Design Practice. In: Proceding ISOPOT-1, Orlando, Flórida, V.1, 236-296.

Kamei, T. & Iwasaki, K (1995). Evaluation of Undrained Shear Strength of Cohesive Soils Using a Flat Dilatometer. Journal of JSSMFE, V. 35, 2, 111-116.

Lacasse, S. & Lunne, T. (1988). Calibration of dilatometer correlations. Penetration Testing 1988, ISOPOT-1. A.A. Balkema, Rotterdam V.1,539-548

Lunne, T.; Powell, J.J.M.; Hange, E.A.; Uglow, I.M. & Mokkelbost, K.H. (1990). Correlation of Dilatometer Reading to lateral Stress. Specially Session on Measurement of Lateral Stress. Annual Meeting of the Transportation Research Board 69, Washington, D.C.

Lunne, T. Lacasse, S. & Rad, N.S. (1989). Pressuremeter Testing and Recent Developments – Part I : All Tests Except SPT, General Report, Session 2. 12ICSMGE, V.4, 2339-2403, Rio de Janeiro.

Marchetti, S. (1975). A New In-Situ Test for the Measurement of Horizontal Soil Deformability. Proc. Conf. on In-Situ Measurement of Soil Properties. ASCE Speciality Conference, V.2, pp. 255-259.

Marchetti, S. (1980). In situ tests by flat dilatometer – ASCE, GE Journal, 106(3): 299-321.

Marchetti, S. & D. K. Crapps (1981). Flat Dilatometer Manual. GPE, Inc., Gainesville, Florida, USA.

Marchetti, S., Monaco P., Totani G. & Calabrese M (2001). The Flat Dilatometer Test (DMT) in soil investigations – A Report by the ISSMGE Committee TC16

Mayne, P. & Kulhawy, F.H. (1982). K_0 – OCR Relationship in Soil, ASCE, JGED, V.108. GT6, 851-872.

Ménad, J.L., Durdon, G., & Gambin, M.P. (1969). Methode Generale de Calcul d'un Rideau ou Pieu sollicite Horiz. en Function des Resultats Pressiometriques. *Soils-Soils, nº22/23.*

Pereira, A. C. (1997). Ensaios dilatométricos em um depósito de argila mole do Bairro do Ibura, Recife, PE. MSc Thesis. Federal University of Pernambuco, Brazil (in Portuguese), 226 p.

Powell, J.J.M & Uglow, J.M (1988). Marchetti Dilatometer Testing in UK Soils. In: Proceding ISOPOT-1, Orlando, Flórida, V.1, 555-562.

Robertson, P.K. (1989). Design of Laterally Loaded Drivin Piles Using the Flat Dilatometer, Geotechnical Testing Journal, *12: 30-38.*

Schnaid, F. (2005). Geocharacterisation and properties of natural soils by in situ tests. 16ICSMGE, Osaka,1, 3-46.

Schmertmann, J.H. (1988). Guideline for using the CPT, CPTU and Marchetti DMT for geotechnical design. V. 3: DMT test methods and data reduction. Department of Transportation, Washington, D.C., USA. Report FHWA-PA-024+84-24, 183pp.

Yu, H.S. (2004). The James K. Mitchell Lectuce: In situ testing: from mechanics to prediction. 2nd Int. Conf. on Site Characterisation, Milpress, Porto, 1: 3-38.

BACK

Portuguese experience in residual soil characterization by DMT tests

Nuno Cruz
Mota-Engil, SA, Univ. Aveiro, Portugal (www.mota-engil.pt)

António Viana da Fonseca
Faculdade de Engenharia da Universidade do Porto, Portugal (www.fe.up.pt)

Keywords: Marcheti Flat Dilatometer, Residual Soils

ABSTRACT: The mechanical behaviour of residual soils, products of rock weathering have significant deviations from conventional transported soils, for which Classical Soil Mechanics models have been developed. In situ tests are very useful for deriving geomechanical parameters, both for stiffness and strength property evaluations, and of these DMT test has been proving very useful for the characterisation of these soils. For the last decade the dilatometer test has been systematically incorporated in research programs for residual soils, which are very common in the North of Portugal.

In this paper, the at rest earth pressure coefficient (K_0), shear strength parameters (c' and ϕ') and stiffness parameters (G_0, E and M) of these soils will be evaluated. A first approach to the interpretation of an alternative dynamic insertion procedure of the blade for the most compacted or less weathered horizons of these residual soils will also be described.

1 INTRODUCTION

The first campaign of DMT tests performed in Portugal, 10 years ago, in the context of a MSc thesis (Cruz, 1995), had the main goal to evaluate the adequacy of international established correlations, in Portuguese soils. From the geological point of view, the Center and South of Portugal are dominated by sedimentary environments, while North region lies on residual soil massifs with special emphasis on granitic type. The collected data for residual soil will be presented herein, while of another paper presented elsewhere in this conference discusses sedimentary soils for this region.

Due to the presence of a cemented structure, residual soils show a quite different behaviour from sedimentary soils and thus classical soil mechanic theories have some limitations in the interpretation of geotechnical parameters. Being aware of that, the authors establish a large scale research work in order to adapt DMT evaluations to residual soils, which included 15 site experimental programmes carried out between Porto and Braga, with a total of 40 drillings with SPT tests, 36 DMT tests, 22 CPT(U) tests, 4 PMT tests, 5 DPSH tests, and 10 triaxial tests.

2 GENERAL IDENTIFICATION

Granitic residual soils (saprolitic) of North region of Portugal are the result of mechanical and chemical weathering, by means of arenization and hydrolysis of feldspar minerals, respectively. The resulting soils can be globally characterized as non-plastic sandy silts to silty sands, systematically classified as SM or SC, according to Unified Classification. In the context of this work, these soils had 15 to 35% of non-plastic fines, void ratios varying from 0.5 to 0.8, and saturation degrees ranging from 50 to 100%.

3 ANALYSIS OF RESULTS

3.1 *Stratigraphy and unit weight*

One of the basic important features of DMT is its ability to give information related to the basic properties (identification and physical index) of soils, thus creating a rare autonomy in the field characterization. In the course of this research, the overall data set have shown the same level of accuracy of that found in Portuguese sedimentary soils (Cruz et al, 2005) and thus, revealing no need for specific approaches for residual soils.

.

3.2 *Strength properties*

As previously described, residual soil behaviour are deeply marked by the presence of a cemented structure, represented by the development of both cohesive intercept (c') and shear strength angle (ϕ'), according to Mohr – Coulomb criterion. This reality takes the following implications for deducing the strength parameters by DMT:

i. Cohesion intercept it is not considered in the basic DMT data reduction.
ii. Shear strength angle derived with recourse to the formulae considered for sedimentary soils, represents the overall strength instead of the parameter on its own, and thus giving higher values than reality.

However, as DMT is a two-parameter test, it is reasonable to expect the possibility of deriving both c' and ϕ', and so it was tried by Cruz et al (2004) as explained in the following paragraphs. According to basic DMT reference (Marchetti, 1980), K_D profiles follow the classical shape of OCR profiles and present typical patterns as function of typified behaviours:

i. Normally consolidated (NC) soils tend to present values around 2.
ii. Low to medium over-consolidated (OC) soils show K_D higher than 2, and generally decreasing with depth until reaching the NC value.
iii. NC soils affected by cementation or aging show K_D profiles stable with depth and higher than 2.

The K_D profiles within the present study show a general tendency to remain stable with depth, showing values significantly higher than 2, namely ranging from 5 to 15. Thus, following the above mentioned assumptions, Cruz et al (2004) concluded that K_D clearly reflects the effects of cementation, although the range of results was too narrow to feel c' variations. However, OCR (which is a numerical amplification of K_D) can be taken as reference parameter, since it represents the cemented structure, as it is presented in the following paragraph.

Even tough the concept of overconsolidation ratio does not have the same meaning for sedimentary and residual soils, the presence of a naturally cemented structure gives rise to similar behaviour. In fact, preconsolidation stress (designated as virtual preconsolidation stress) now represents not the maximum past stress, but the break of cementation yeld locus, and the ratio with vertical rest stress is called 'virtual over-consolidation degree (vOCR)', thus differentiating it from the one physically sustained in the process of sedimentary soils generation with 'stress memory'. This concept, as previously designated, has the same meaning as the established terminology: "vertical yield stress = σ'_{vy}"; which corresponds to other established more general concept: "yield stress ratio = YSR". Thus, the OCR derived from the DMT test on residual soils (vOCR) reflects the strength resulting from the cemented structure, normalised in relation to the effective vertical stress. Moreover, it should be pointed out that OCR evaluation is I_D and K_D dependent (that is P_0 and P_1 dependent), allowing to be confident on the determination of both angle of shear resistance and effective cohesive intercept.

In soils with the mechanical complexity of residual soils it is useful to get information from distinct sources. Thus, the pair DMT+CPT(U) tests has been adopted frequently. Following the same pattern as for OCR, another approach was also considered to deduce c' based on this combination, since M/q_c ratios has been used with success to determine OCR in granular soils (Marchetti, 1997). The available data show M/q_c values situated in the frontier NC/OC (10-12), frequently tending to OC (12 to 15), which must be interpreted as an effect of the matricial cementated structure. It is also clear that the increase with depth is substantially higher with M than with q_c.

Figure 1 illustrates representative evolution of K_D, vOCR and M/q_c with depth, obtained in the present study. The results clearly show the sensitivity of vOCR and M/q_c to variations in soil condition and the lack of it with K_D.

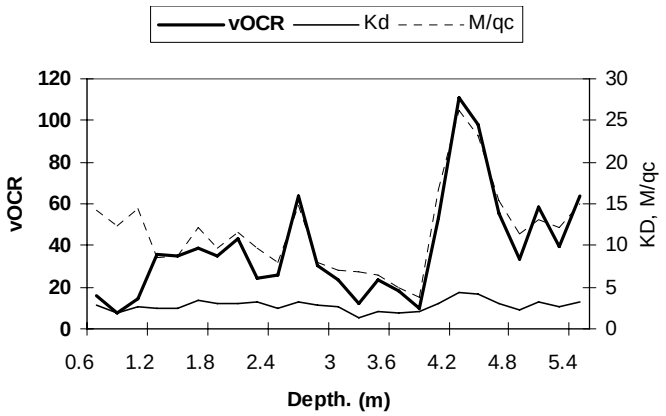

Figure 1. Representative K_D, vOCR, and M/q_c profiles.

The comparisons of these 3 parameters with triaxial testing confirmed that convergence with c' is greater with vOCR (DMT) and M/q_c than with K_D (Figures 2, 3 and 4), as it was expected. In the same figures it is also represented the correlations with c'/σ'_{v0} (true values of this latter multiplied by 100 to be represented in the same scale).

On the other hand, comparing c' with preconsolidation pressure, σ'_p, obtained via DMT, the relation between them is represented by 0,011, which is lower of those pointed out by Mayne & Stewart

(1988) and Mesri et al (1993), for overconsolidated clays (0.03 to 0.06 and 0.024, respectively), which could be explained by a stronger overconsolidation effect.

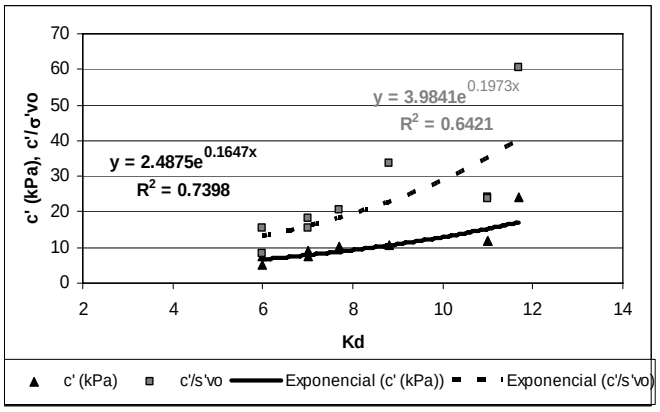

Figure 2 c' and c'/σ'vo (x100) - K_D correlations

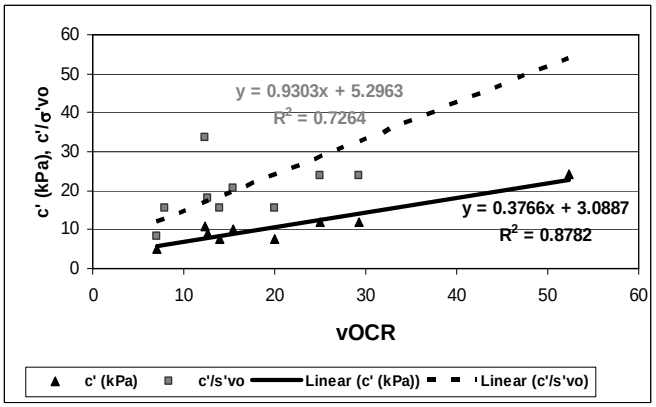

Figure 3 c' and c'/σ'vo (x100) - vOCR correlations

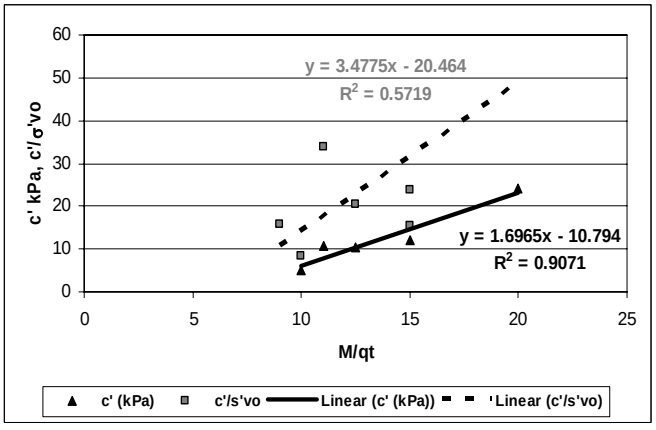

Figure 4 c' and c'/σ'vo (x100) - M/q_t correlations

Once c' is obtained, it is reasonable to expect that it can be used to correct the over-evaluation of ϕ', when sedimentary formulae is considered. Thus, taking the difference between ϕ'_{DMT} (represents the global strength) and $\phi'_{triaxial}$ (represents ϕ', uniquely) and comparing it with c', it becomes clear (Figure 5) the good correlation between them (Cruz et al, 2004). Of course, the data is not enough to validate a proper correlation, but it seems to indicate the adequacy of the method for these evaluations.

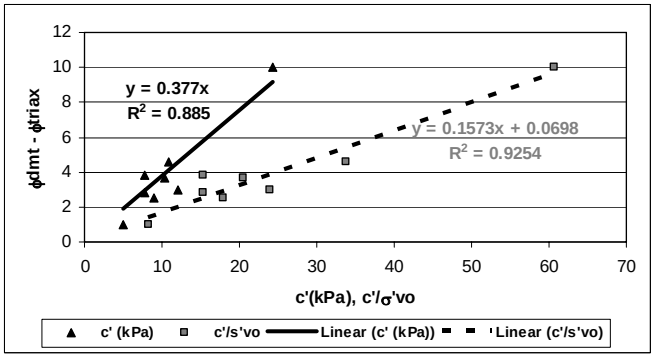

Figure 5 (ϕ'_{DMT} - ϕ'_{TRIAX}) - c' and c'/σ'vo (x100) correlations

4 STIFFNESS PARAMETERS

The determination of stiffness parameters in sedimentary soils has been obtained with considerable success with M (Marchetti, 1980), mainly because of the following reasons:

i. M is a parameter that includes information on soil type (I_D), overconsolidation ratio (K_D), as well as dilatometer modulus (E_D). Note that in residual soils cementation structure is also represented by K_D, as explained before.
ii. E_D represents a ratio between applied stress and resulting displacement.
iii. DMT insertion creates a lower level of disturbance than usual penetrometers (Baligh & Scott, 1975).

In this context, M_{DMT} was cross checked with $M_{0(CPTU)}$ (Lunne and Christophersen, 1983), whose results showed respectively values generally between 10 and 70 MPa (DMT) and lower than 40 MPa (CPTU). This is probably justified by the smaller disturbance degree caused by DMT insertion and also because its known higher sensitivity (than q_c) to stiffness variations. Finally, the triaxial tests performed clearly converge with the DMT test.

A different approach was established by Viana da Fonseca et al. (2001), based on studies performed in two of the locations within the scope of this paper, where the dilatometer modulus, E_D, was correlated with the maximum shear modulus, G_0, and deformation modulus at 10% of shear strain, $E_{s10\%}$. The respective relations are represented as follows:

$$G_0 / E_D = 16.7 - 16.3 \log (P_{0N}) \quad (1)$$

$$E_{s10\%} / E_D = 2.35 - 2.21 \log (P_{0N}) \quad (2)$$

These relations are higher than the ones proposed by Baldi et al. (1989) for sedimentary soils. In addition, the second correlation was between the correlations defined by these authors for the NC and OC behaviours of sedimentary soils.

5 COEFFICIENT OF EARTH PRESSURE AT REST, K_0

Even though the evaluation of coefficient of earth pressure at rest through in situ or laboratory testing is very controversial, due to the level of disturbance induced by penetration/installation of equipments and sampling processes, the fact is that this parameter is often needed for design purposes, and so even a rough experimental estimation is better than only an empirical one. Once more, the usefulness of combining CPT(U)+DMT became evident.

Baldi (1986) proposed the following correlation to derive K_0 in granular sedimentary soils, which was taken as a starting point for this purpose:

$$K_0 = C_1 + C_2 \cdot K_D + C_3 \cdot q_c/\sigma'_v \qquad (3)$$

where:

$$C_1 = 0.376,\ C_2 = 0.095,\ C_3 = -0.00172$$

q_c represents the CPT tip resistance and σ'_v stands for the effective vertical stress, which can be derived from DMT results.

Taking into consideration the q_c/σ'_v relation equal to 33 K_D, established by Campanella & Robertson (1991) for non-cemented sandy soils, it is clear that this ratio is not representative of the studied soils. Thus, Cruz et al. (1997) and Viana da Fonseca et al. (2001) proposed to correct C_2 constant of expression (3) as follows:

$$C_2 = 0.095 * [(q_c/\sigma'_v) / K_D] / 33 \qquad (4)$$

Although available data on K_0 is very rare, the analysed data reflects the local experiment (0,35 – 0,5). It should be noted that direct application of Baldi's correlation would lead to much higher values, usually greater than 1.

6 DMT WITH DYNAMIC INSERTION

The static insertion of DMT blade can be a significant limitation testing heterogeneous grounds as it is the case of rock weathering profiles where residual soils are presented. Deriving stiffness parameters of compacted soils have had to rely on dynamic penetrometers which are not suited for this type of determination. Taking into consideration that DMT induces a horizontal deformation (while the penetration is vertical) it can be expected, at least, some preservation of the intrinsic characteristics of natural soils. In that sense, a specific research is going on, to find out the real efficiency of parameter evaluation under dynamic insertion. The research work consists in performing pairs of dynamic and static push in DMT tests (1.0 to 1.5 m apart), both in granitic residual soils and reference earthfill made by soils of the same nature. SPT and DPSH tests were also performed to create some basic reference.

The available data (3 sites, which include ISC'2 experimental site – www.fe.up/isc-2) are discussed in the following paragraphs.

The mechanical behaviour of the tested soils can be summarized by the results of SPT, DPSH and PMT tests. Table 1 shows the basic data obtained, including the data related to the number of blows (SPT hammer) needed to penetrate the soil with DMT blade. This results show a very similar strength profile in the case of V.Conde and Gaia's sites, while the ISC'2 site is clearly weaker.

Table 1 – Mechanical characterization of test sites

Site	N(60)	$N_1(60)$	N_{20DPSH}	N(60)/pl	$N_1(60)$/ Epm	N_{20DMT}
ISC2	8 - 25	10 - 25	5 - 15	5 - 15	0.5 - 1.5	12 - 20
V.Conde	20 - 35	25 - 35	---	10 - 15	1.5 - 2.5	15 - 30
Gaia	25 - 30	20 - 35	---	10 - 20	1.5 - 3.0	20 - 30

Typical profiles. The superficial level of ISC2 experimental site (1.5-2.0m) is characterized by an earthfill composed by identical grain size distribution of the granitic residual soils involved in this work (sandy silt to silty sand). As it will be explained below, results from the earthfill showed completely different behaviours, although there was an insufficient amount of data to be relied on for correlations. Therefore, another pair of tests was performed in a silty-sand to sandy silt reference earthfill (10m high) with insufficient level of compaction which allowed both dynamic and static insertion.

Tables 2 and 3 include a representation of analyzed data, through the mean values of parametrical ratios (always static/dynamic), in terms of basic, intermediate and derived geotechnical parameters.

Table 2 – Statistics on basic and intermediate parameters

Site	P_{0S}/P_{0D}	P_{1S}/P_{1D}	I_{DS}/I_{DD}	E_{DS}/E_{DD}	K_{DS}/K_{DD}
ISC'2	1.42	1.24	0.85	1.20	1.42
V. Conde	1.26	1.10	0.86	1.10	1.23
Gaia	1.28	1.15	0.89	1.13	1.25
ISC'2 earthfill	0.84	0.77	0.85	0.74	0.84
Reference earthfill	0.79	0.75	0.82	0.71	0.80

Table 3 – Statistics on geotechnical derived parameters

Site	γ_S/γ_D	ϕ'_S/ϕ'_D	M_S/M_D	OCR_S/OCR_D
ISC'2	1.01	1.04	1.37	1.74
V. Conde	1.00	1.02	1.15	1.40
Gaia	1.02	1.03	1.18	1.48
ISC'2 earthfill	0.95	0.98	0.71	0.68
Reference earthfill	0.97	0.97	0.71	0.69

The main considerations that can be outlined from these analyses are the following:

i. Dynamic insertion of DMT blade is responsible for an important loss of bonding in residual soils which leads to decreasing stiffness and strength properties. With the exception of I_D, all DMT parameters analysed have presented smaller values for the tests performed with dynamic insertion.
ii. The opposite behaviour is found in earthfills. Dynamic insertion seems to create a densification of the soil, since all DMT parameters analysed have shown higher values with dynamic insertion.
iii. I_D intermediate parameter increases with dynamic insertion, both in residual and earthfill soils, which means that soil type will be classified coarser than reality.
iv. The rates of variation of unit weight (Marchetti and Crapps, 1981) and angle shear resistance (Marchetti, 1997) are very small, thus showing the low sensitivity of these two parameters to dynamic insertion.
v. M and OCR work as an amplification of E_D and K_D, inducing higher sensitivity to variations. The respective results confirm the conclusions presented before where it was shown that the cemented structure could be assessed with OCR.
vi. There is a clear tendency of correlation between N_{20DMT}, N_{20DPSH} and N_{60}. The trends in these three parameters can be expressed by the following ratios:

$$N_{20}\,(DPSH) = 0.58\ N_{60}$$
$$N_{20}\,(DMT) = 1.58\ N_{20}\,(DPSH)$$
$$N_{20}\,(DMT) = 0.88\ N_{60}$$

These results suggest that N_{DMT} could be used as a control parameter after applying some normalization to friction reducers.

For what we expressed in preliminary considerations, the possibility of using dynamic insertion in DMT seems to enlarge its field of application making it easier to overcome rigid layers interbedded in soft soils, and increases the range in depth of in situ characterization. In fact, the data suggest that DMT could be used as a static and dynamic testing tool.

7 CONCLUSIONS

Ten years of practice with DMT in residual soils showed a very high standard which can be defined by the following conclusions:

i. Information on stratigraphy and unit weight evaluations revealed itself accurate enough for test and design needs to similar levels of confidence as in sedimentary soils.
ii. The results of the test detect the presence of cementation structures, typical of residual soils
iii. When performed together with CPT(U) tests, it makes possible cross-checking and access to some parameters that would be impossible to get from each of the tests on their own. In this context, DMT + CPT(U) tests have provided reasonable estimations of lateral earth pressure coefficient in the regional granitic complexes.
iv. Being a 2-parameter test, strength parameters (c' and ϕ') can be derived. A method for that evaluation was proposed, needing further research for accurate correlations.
v. Because DMT is a loaddisplacement test, and also can represent numerically both type of soil and cemented structure, it can provide better quality results of stiffness parameters than those obtained by other current in-situ tests, such as penetration tests.
vi. Because the DMT deforms the soil horizontally, it is reasonable to expect some quality of results, even with dynamic insertion. In fact, some research performed on the subject showed interesting possibilities of exploring it as a dynamic tool, enlarging the field of application to compacted soils (N_{SPT}<50, as reference). This may create some chances of using the test in compaction control.

As a final comment, DMT has proven to be very versatile, providing accurate data for design applications, both in residual and sedimentary soils. Dynamic insertion may also provide reasonable quality in results, since the first signs seem to point out that it can be used over a wide range of soils.

REFERENCES

Baldi, G., Bellotti, R., Ghionna, V., Jamiolkowski, M., Marchetti, S., Pasqualini, E. 1986. Flat dilatometer tests in calibration chambers. *Proc. of IV conference in use of In situ tests*: 431-446. Blacksburg, Virginia, ASCE

Baligh & Scott 1975. Quasi static deep penetration in clays. ASCE Geotech. J., Vol. 101, GT11, 1119-1133.

Campanella, R.G., Robertson P.K. 1991. Use and interpretation of a research dilatometer. *Canadianan Geot. Journal*: 28, 113-126.

Cruz, N. 1995. Evaluation of geotechnical parameters by DMT tests (in portuguese). *MSc thesis. Universidade de Coimbra.*

Cruz, N., Viana, A., Coelho, P., Lemos, J. 1997. Evaluation of geotechnical parameters by DMT in Portuguese soils. *XIV Int. Conf. on Soil Mechanics and Foundation Engineering, pp 77-80.*

Cruz, N., Viana da Fonseca, A., Neves, E. 2004. Evaluation of effective cohesive intercept on residual soils by DMT data. *Geotechnical Site Characterization. Proc. of ISC2. Ed. Viana da Fonseca & Mayne. Milpress Pub. Netherlands.*

Lunne, T., Christophersen, H. 1983. Interpretation of cone penetrometer data for offshore sands. *Proc. of the Offshore Tech. Conf., Richardson, Texas.*

Marchetti, S. 2001. The Flat Dilatometer Test (DMT) in Soil Investigation. *ISSMGE TC 16 Report*.

Marchetti, S. 1997. The Flat Dilatometer: Design Applications *Proc. 3rd Int. Geotechnical Engennering Conf. Cairo University*.

Marchetti, S. 1980. In-situ tests by flat dilatometer. *J. Geotechnical. Eng. Div. ASCE*, 106, GT3, 299-321.

Marchetti, S. & Crapps,D.K. 1981. Flat Dilatometer Manual. *Internal report of GPE Inc., distributed to purchasers of DMT equipment.*

Robertson, P., Campanella, R. (1983). *Interpretation of cone penetrometer test: Part I – Sand*. Canadian Geotech. J., 20, pp. 718 – 733.

Viana da Fonseca, A., Vieira, F., Cruz, N. 2001. Correlations between SPT, CPT, DP, DMT, CH and PLT Tests Results on Typical Profiles of Saprolitic Soils from Granite. *International Conference on In Situ Measurement of Soil Properties and Case Histories. Bali, Indonesia.*

Strength Determination of "Tooth-Paste" Like Sand and Gravel Washing Fines Using DMT

David L. Knott, P.E. and James M. Sheahan, P.E.
HDR Engineering, Inc.
3 Gateway Center
Pittsburgh, PA 15222-1074
Phone: (412) 497-6000; E-mail: dave.knott@hdrinc.com
jim.sheahan@hdrinc.com

Susan L. Young, CPG
HDR Engineering, Inc.
4480 Cox Road, Suite 103
Glen Allen, VA 23060-6751
Phone: (804) 648-6630; E-mail: sue.young@hdrinc.com

Keywords: dilatometer, undrained shear strength, drained shear strength, confined dike facility (CDF), borehole shear test, settlement, short-term stability, long-term stability, sand and gravel washings

ABSTRACT: An approximately 18 acre (0.1 km^2) site was proposed for a Confined Dike Facility (CDF) for the disposal of dredged materials. Based on available information the site was believed to be located on natural ground. During the initial investigation, the site was found to be located on top of a slurry pond that had been covered with fill. The slurry pond was previously used for the disposal of slurried fines "washings" from sand and gravel processing. The washings had the consistency of "toothpaste", even after having been covered with fill for at least 14 years. The initial investigation used Standard Penetration Tests (SPTs) and Shelby tubes to obtain samples, since the materials at the site were expected to be a natural deposit. Two types of washings were encountered – "clayey washings," which were primarily clay; and "sandy washings," generally consisting of sand with various amounts of clay, gravel and silt. The clayey washings were an almost pure clay and had pocket penetrometer values of 0 tsf (0 kPa) even with the special foot attachment for very soft soils. Laboratory strength tests were not able to be performed on the Shelby tubes samples, since the sample of the washings deformed upon opening the tube due to lack of confinement. To obtain strength parameters for design, in situ techniques were assessed for a supplemental investigation. DMT testing was selected to determine the undrained shear strength of the washings, which varied from 83.5 to 355 psf (4 to 17 kPa) over a depth of 31.5 feet (9.6 m) in an area without surface fill and was higher in areas where fill had been placed. Borehole shear testing of the washings was selected to provide drained strength parameters, which varied from 15.9º and 1.1 psf (0.1 kPa) to 27º and 9 psf (0.4 kPa). The investigation indicated that washings up to 36.5 feet (11.1 m) thick were present beneath the entire site to depths varying from 21 to 36.5 feet (6.4 to 11.1 m). The data was then used to design the CDF.

1 BACKGROUND

The work described in this paper was performed as part of a project to dredge Lake Accotink, a county-owned lake in Fairfax County, Virginia, in a highly developed suburban area. The materials dredged from the lake are to be pumped through a slurry line to a disposal facility for sedimentation. The proposed disposal facility consists of a Confined Dike Facility (CDF) with a height of 12 feet (3.7 m) and a capacity of 53.3 acre-feet (65,745 m^3). The CDF capacity was subsequently reduced to 33.5 acre-feet (41,322 m^3). The site and current CDF configuration are shown on

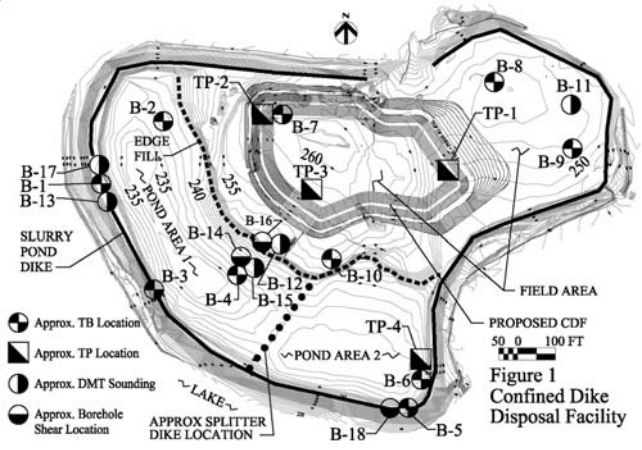

Figure 1. Confined Dike Disposal Facility

Figure 1. This approach results in significant savings for the client in lieu of hauling the dredged material from the lake which required high dewatering and trucking costs.

The site location was initially determined to be suitable and was to have been "natural ground." However, during the initial investigation, the site was found to have been a slurry pond for "washings" from a sand and gravel processing operation that had been subsequently covered with fill. No other suitable sites were available, so work progressed even after the presence of the poor soil conditions was determined.

The history of the site was determined using

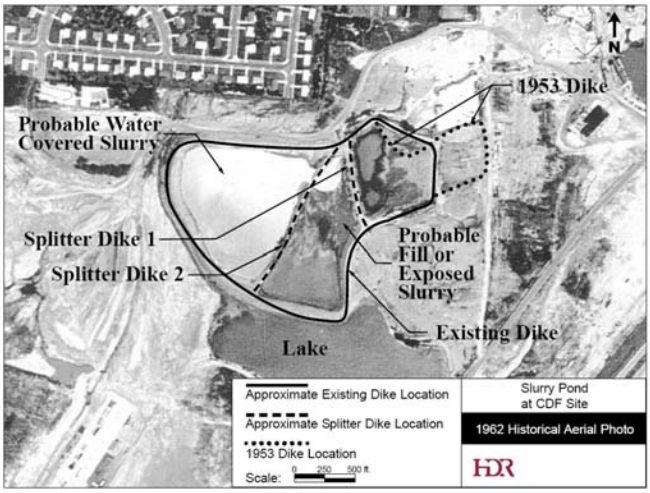

Figure 2A. Slurry Pond at CDF Site in 1962

aerial photography, since no other information was available. The photos indicated that the site was surface mined for sand and gravel, probably prior to 1940, and the slurry pond is visible on a 1953 photo. Aerial photography indicated that the pond configuration changed over time with the expansion of the dike system, including the use of "splitter dikes" (dikes to divide the facility into cells) as shown on Figure 2A. The historical photos show that the area within the slurry pond was filled with washings and then covered with fill. The fill consists of soil and materials from concrete truck washout. The site appears to have been in its current configuration since 1988 (Figure 2B). An active concrete plant is located adjacent to the site, and a portion of the site is used for the storage of precast concrete products. The current site elevation ranges from 250 to 260 feet (76.2 to 79.2 m) mean sea level (msl).

The sand and gravel mined at the site belonged to the Pliocene epoch, which consisted of varying amounts of sand and gravel, and lesser amounts of clay and silt. This material is underlain by the Potomac Formation of the Cretaceous Age, which generally consisted of clay with sand and silt.

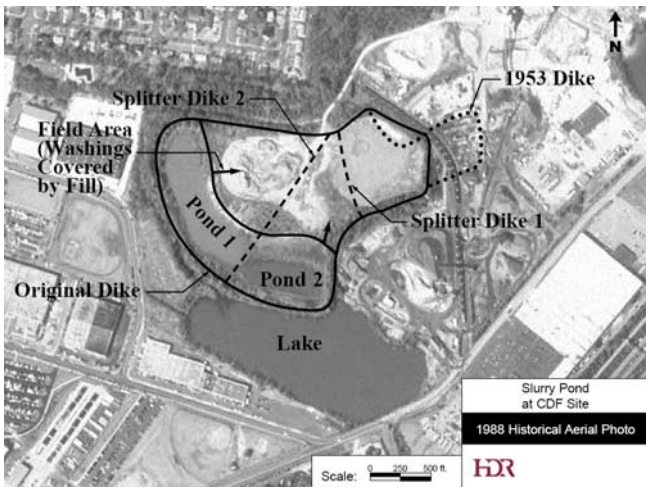

Figure 2B. Slurry Pond at CDF Site in 1988

2 INITIAL SUBSURFACE INVESTIGATION

Ten borings, in which Standard Penetration Tests (SPTs) were performed, were drilled as shown in Figure 1. The borings were advanced using hollow stem augers. In addition, four test pits (TPs) were excavated with a large track backhoe. A typical subsurface section with the proposed CDF dike is shown on Figure 3. Generally, the site could be subdivided into two areas, the field area and the pond area, as shown on Figure 1. The conditions in each are described below.

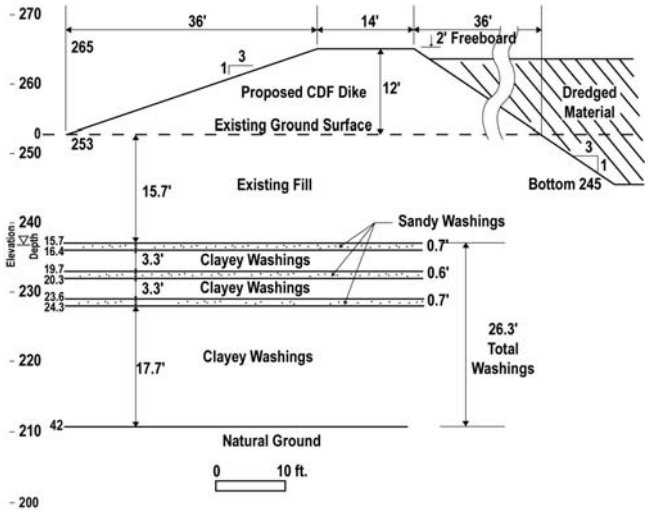

Figure 3. Typical CDF Section at Dilatometer Sounding B-12

2.1 *Field Area*

The field area consisted of a relatively level area that had been created by filling over the washings in the slurry pond. Part of the area had been used as a baseball field. The borings in the field area, B-7, B-8, B-9, and B-10, generally encountered fill, varying in thickness from 11.5 to 21.5 feet (3.5 to 6.6 m), overlying very soft clay (clayey washings) or loose sand (sandy washings). The fill was also encountered in Test Pits (TPs) 1, 2, and 3. It varied from clayey silty sand to "concrete truck washout" that was so hard it could not be excavated with a medium-sized trackhoe. Washings up to 34 feet (10.4 m) thick were encountered beneath the fill in borings that penetrated their full thickness.

A groundwater observation well was installed in one of the borings, and the depth to groundwater was found to vary from 3.5 feet (1.1 m) (winter) to 9 feet (2.7 m) (summer) below the surface. The shallow depth to groundwater is probably due to the precipitation being confined to this area as a result of the slurry pond dikes.

2.2 *Pond Area*

The pond area consists of two low-lying areas in which surface water is present to varying depths during the year—Ponds 1 and 2 (see Figure 1). The ground surfaces of the ponds are the remains of the top of the original slurry pond surface, and the sides are the interior of the slurry pond dike and the edge of fill (Figure 4). The washings

Figure 4. Desiccation cracks in Pond 1 area looking toward slurry pond dike.

could be walked on where a crust was established or where vegetation had developed.

Desiccation cracks extended to depths of several feet in the Pond 2 area. Borings B-2, B-4, and B-6 were drilled around the perimeter of

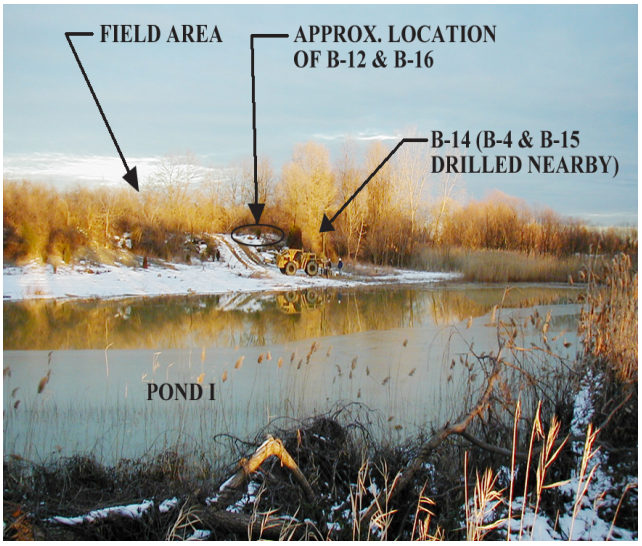

Figure 5. Approximate boring locations in Pond 1 area. View from slurry pond dike.

Ponds 1 and 2 where access was possible to obtain samples of the washings (Figure 5). Shelby tubes were taken in the washings in several borings.

Generally, the borings encountered several feet of fill underlain by very soft clay (washings). Borings B-2 and B-4 encountered natural ground at depths of 36.5 feet (11.1 m) (elevation 201.5 feet msl (61.4 m)) and 35 feet (10.7 m) (elevation 208 feet msl (63.4 m)), respectively. The natural ground consisted of dense to very dense bluish/greenish gray fine sandy silt. Boring B-6 encountered very soft clay (washings) to 25 feet (7.6 m) (elevation 213 feet msl (64.9 m)); at which point the interior side of the slurry pond dike was encountered. The slurry pond dike material consisted of hard silty clay. Natural material, similar to that from the other borings, was encountered beneath the slurry pond dike at a depth of 30 feet (9.1 m) (elevation 208 feet msl) (63.4 m).

Figure 6. Hard, desiccated and soft, wet clayey washings at Test Pit 4

Test pit TP–4 was excavated at the edge of Pond 2. It encountered clay washings, which were hard and blocky due to desiccation in the upper 2 feet (0.6 m) and became softer with depth to 5 feet (1.5 m), where it became very soft (Figure 6). The moisture content increased with depth and was wet at 5 feet (1.5 m).

2.2.1 Southern and Western Dike

Borings B-1, B-3, and B-5 were drilled in the slurry pond dike, since it was originally anticipated that this area would be used as part of the CDF. Soft soils were encountered beneath the slurry pond dike. Aerial photographs also showed the slurry pond dike being constructed over the washings. The presence of the underlying washings beneath the dike was confirmed by subsequent DMT testing. The location of the CDF was modified to exclude this area due to the presence of these soft soils.

2.3 Lab Testing

Representative samples of the various on-site soils were tested to provide classification data. However, classification test data will only be provided for the washings as summarized in Table 1.

Strength testing was attempted on undisturbed samples of clayey washings obtained in the initial investigation, but the sample started to expand and crack as it was being taken out of the tube as it was opened and was, therefore, not suitable for testing (Figure 7). Consolidation tests were performed on two undisturbed samples of the washings obtained in the initial investigation. The testing indicated that the Compression Index (c_c), was 1.1; the Coefficient of Consolidation (c_v) varied from 0.0213 to 0.0568 in^2/min (13.7 to 36.6 mm^2/min), the Initial Void ratio, e_0, was 3.1077, the wet unit weight was 93.5 pcf (1500 kg/m^3), and the preconsolidation pressure was 575 psf (27.5 KP_a at a depth of 11 feet (3.4 m), indicating normal consolidation. (Note: a DMT reading in B-14 at 11.2 feet (3.4 m) indicated a preconsolidation pressure of 501.3 psf and an OCR of 1.2.)

Figure 7. Sample of clayey washings expanding due to lack of confinement during extrusion from Shelby Tube.

Gradation and hydrometer tests on the clayey washings indicate that 100 percent of the material passed the No. 200 sieve, and they consisted of 81.9 to 93.4 percent clay-sized material. The moisture content of the clayey washings generally decreased with depth from 84.2 to 43.3 percent from a depth of 6 to 31.5 feet (1.8 to 9.6 m) for borings in the pond area where the washings had been covered by several feet of fill. The composition of the sandy washings varied significantly, as indicated in Table 1. This may be the result of the proximity of the sampled location to the slurry discharge location.

The data from classification tests on the fill material from the field area indicated that it was generally sandy with varying amounts of clay, silt, and gravel.

Table 1. ***Summary of Laboratory Test Data for Washings***

Material Type	Description	Unified Class	Atterberg Limits			Natural Moisture Content (%)	Grain Size (%)		
			LL	PL	PI		Gravel	Sand	Silt & Clay
Clayey washings	Clay	CH	72 to 81	31 to 32	41 to 49	84.2* to 43.3	0	0.1	99.9 to 100
Sandy washings	Clayey silt to Clayey/silty gravel	MH to GC/GM SC	24 to 52	19 to 24	5 to 28	15.9 to 23.2	3.0 to 30.3	29.8 to 71.9	21.8 to 39.9

* decreasing with depth from 6 to 31.5 feet

BACK

3 SUPPLEMENTAL INVESTIGATIONS

A supplemental investigation was performed to obtain further data on the site due to the variable conditions encountered and to obtain strength data for the washings. Dilatometer soundings (DMT) and borehole shear testing were performed by In-Situ Testing, L.C.

The dilatometer data was reduced using the WinDMT program from GPE, Inc. (GPE). The reduced data includes soil type, total unit weight, pore water pressure, preconsolidation pressure, strength, and over-consolidation ratio.

Since the DMT test is performed in about two-minute intervals at a given depth, excess pore water pressures cannot dissipate in fine-grained soils, and the undrained shear strength, Su, is determined. In sandy soils, it is assumed that drainage can occur and a drained plane strain friction angle (ø') is calculated. Dilatometer soundings were performed in five additional borings (B-11 through B-14 and B-17) to provide undrained shear strength values for the washings encountered in the pond area (B-12 and B-14), eastern field area (B-11), and western dike (B-13 and B-17). A track-mounted rig was used due to soft site conditions (Figure 8). Standard Penetration tests were performed in the harder fill materials

Figure 8. Track-mounted DMT rig.

above the washings to advance the hole, since the dilatometer would be damaged by those materials. Starting near the base of the fill, dilatometer soundings were performed at about every 8 inches (20.3 cm) of depth in the washings until harder natural ground or gravel was encountered. The dilatometer soundings confirmed that the washings were generally clayey and contained thin sandy or silty zones. Figure 9 shows all of the dilatometer data for the washings and natural soils in borings

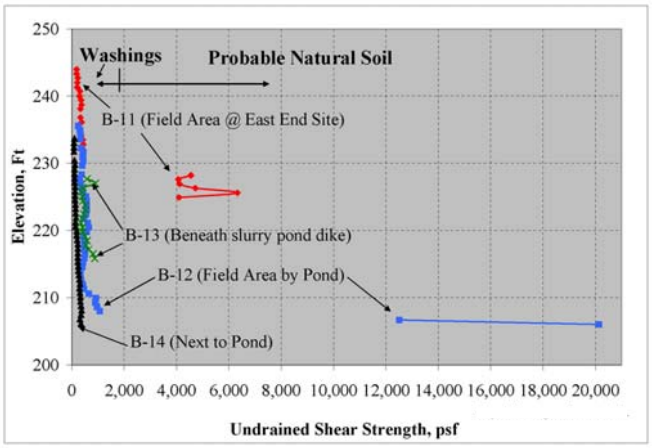

Figure 9. In-place undrained shear strength of all soils by DMT. (Note: Gaps in data indicate granular material)

B-11, B-12, B-13, and B-14, while Figure 10 only provides data on the washings, since their strength is much lower than that of the natural soils. Figure 10 indicates that higher strengths are present in washings that have been covered by fill or underlie the dike (B-11, B-12, and B-13) than the washings with minimal overlying fill (B-14). The figure also indicates that there is generally some strength gain with depth, which is likely due to normal consolidation. DMT results for Boring B-14, in particular, exhibit this trend.

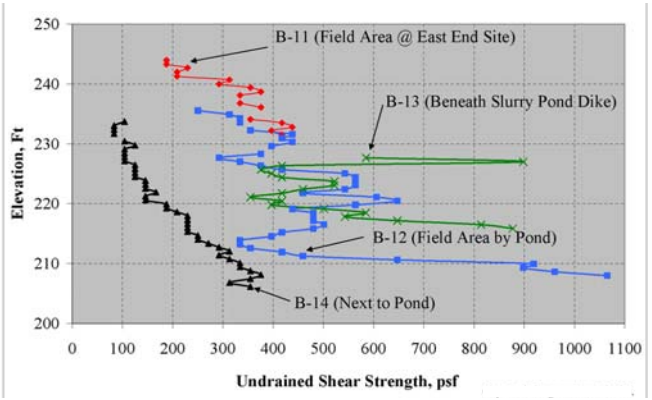

Figure 10. In-place undrained shear strength of washings by DMT. (Note: Gaps in data indicate granular material)

Borehole shear tests were performed in borings to obtain drained shear strength design parameters for the washings. The borehole shear device was manufactured by Handy Geotechnical Instruments, Inc. (Handy 2002) Those borings were advanced using hollow stem augers to just above the test

sampling interval, at which point a cutting head and drilling mud were used to advance the borings.

The borehole shear test is performed in a vertical orientation along the sides of the borehole at a specific depth. The test is performed by inserting a shear head into the borehole to the desired depth. Gas is then injected under pressure (normal stress) to expand the shear plates on the side of the shear head so that the plates are in contact with the sides of the borehole (Figure 11).

Figure 11. View of borehole shear head with shear plate in expanded position

When contact is achieved, the soil being pressed against by the shear plates is allowed to consolidate for 15 minutes. Then the shear head is pulled upward at a rate of about 0.002 inches per second (0.05 mm/sec) until failure occurs, which is usually at a total movement about 0.5 inches (1.3cm) (Figure 12). The shear (resistance) stress to pulling of the shear head is measured, and the confining pressure and resistance force are then plotted on a shear versus normal stress diagram. The process is repeated for a range of higher normal stresses, with a consolidation time of ten minutes between each test, until maximum expansion of the shear plates occurs.

Borehole shear testing was performed in three borings to provide drained shear strength values for some of the softer materials encountered in the pond area (B-15 and B-16) and the western dike

Figure 12. View of borehole shear head being raised.

(B-18). The test depths were based on materials encountered in the test borings and DMT soundings. Two tests were performed in both B-15 and B-16 at different depths and one test in B-18.

The results are provided in Figure 13. The strength envelopes for B-15 at 5.8 feet (1.8 m), B-15 at 20 feet (6.1 m); and B-16 at 26 feet (7.9 m)

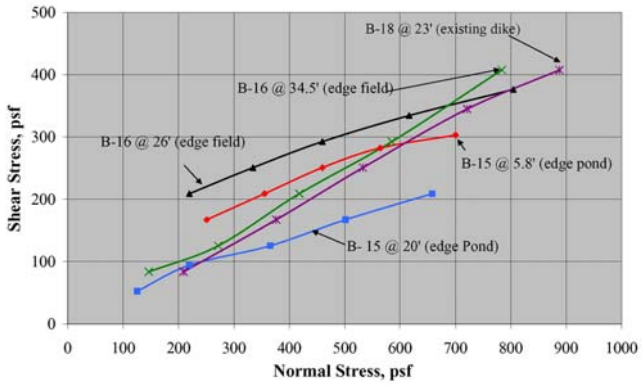

Figure 13. In-place drained shear strength of washings determined by borehole shear test.

are generally parallel to each other but are not parallel to the envelopes for B-16 at 34.5 feet (10.5m) and B-18 at 23 feet (7.0 m). This may be due to variations of the washing materials since the first group exhibit cohesion and the second group has no cohesion. Curvature of the strength envelopes of B-15 at 5.8 feet (1.8 m) and B-16 at 26 feet (7.9 m) are also present at higher loadings. Strength parameters adopted for design are indicated in Table 2.

Table 2. Borehole Shear Test Drained Strength Values Selected for Design

Boring	Depth (feet)	Material	Drained Shear Strength Φ (°)	c (psf)
B-15	5.8	Clayey washings	20.3	77.3
B-15	20.0	Clayey washings	15.9	1.1
B-16	26.0	Clayey washings	17.5	142.0
B-16	34.5	Clayey washings	27.0	0.0
B-18	23.0	Washings under slurry pond dike	24.9	0.0

4. ANALYSIS

4.1 Slope Stability

The stability of the CDF was assessed at several locations using the STABL6H computer program. Analyses were performed for the new CDF dike at the boundary between the field and pond areas, the southeastern side of the CDF, and the eastern side of the CDF. The locations for the analyses were selected based on being representative and/or being a more critical location. Both drained and undrained analyses were performed and seepage through the CDF dike was considered as appropriate based on whether or not dredged material would be impounded for the condition being analyzed. The washings were divided into zones based on strength data from the testing and estimated at intermediate locations. The typical dike configuration was about 100 feet (30.5 m) wide at its base, has 3H:1V interior and exterior slopes, and top width of 14 feet (4.3 m). Minimum factor of safety requirements were in accordance with USCOE guidelines (USCOE 1987 and 2000).

Stability analyses for rapid filling and rapid drawdown were not made, since inflow and outflow to the CDF is controlled.

Due to the low strength of the materials underlying the CDF, the results of the analyses indicated that the dike needed to be constructed in stages to achieve the targeted minimum factor of safety and set back from the edge of the pond area. The first stage dike was made to be approximately half the size of the full dike. The analyses also indicated that a geogrid-reinforced buttress was needed in the pond area prior to construction of the full dike. Construction of the first stage dike would allow some strength gain in the materials underlying the dike due to consolidation. Staging of dike construction also allowed for dredging operations to begin so that sand could be generated for use as a buttress in the pond area prior to constructing the Stage 2 dike. In a portion of the field area, the interior dike slopes had to be flattened to 6H:1V and the floor of the CDF raised due to the presence of washings at shallow depths.

4.2 Settlement

An assessment of the long-term settlement of the full CDF dike section at the edge of the field/pond area was performed using boring and laboratory data. The stratigraphy was based on Boring B-12, in which dilatometer soundings were taken at 8-inch (20.3 cm) intervals, resulting in a complete profile of the washings, as shown in Figure 3. The fill overlying the washings was considered relatively incompressible under the CDF dike load, based on its being a dense granular material. The underlying washings were about 26 feet (7.9 m) thick. As shown in Figure 3, the washings consisted of clayey washing separated by several layers of sandy washings. Relatively incompressible natural soils, consisting of clayey silt, were encountered below the washings. Long-term settlement was estimated for each of the clayey washings layers. Consolidation settlement was estimated to be about 15 inches (38.1 cm) at this location. However, the magnitude of settlement across the site could vary due to variations in the thickness and pre-loading of the washings and other factors such as dike staging and rate of construction. Immediate settlement due to compression of the sandy layers in the washings should occur during construction. In addition, some additional long-term settlement could occur due to the weight of the dredged materials.

The time for 90 percent of the new dike settlement to occur was also estimated to assess the impact of settlement on dike freeboard requirements. The time for 90 percent settlement to occur could vary from less than a year to several years, depending on the number and persistence of the sandy washings resulting in either single or double drainage of the clayey washings. Therefore, raising of the dike is to be performed as needed to provide adequate free-board while the facility is operating.

5 CONCLUSIONS

The DMT soundings allowed the strength of very soft clay, which could not otherwise be determined by SPT; pocket penetrometer, even with the

special foot attachment; and laboratory testing, to be determined. The DMT data also provided a detailed subsurface profile of material types and strengths, which was not possible to obtain with SPT tests due to the softness of the material. The project also showed how DMT and conventional boring techniques can complement each other.

After evaluating the data from the investigations, it was determined that the site could be used for final disposal of dredged material. This allowed the use of a very poor site and saving the client a significant amount of money over hauling dredged material to another site.

REFERENCES

GPE, WinDMT, Version 1.1, "Marchetti Dilatometer Test Data Reduction Program."

Handy Geotechnical Instruments, Inc., 2002, "Borehole Shear Test Instructions", Madrid, Iowa.

U.S. Army Corps of Engineers, 1987, *Engineering and Design – Confined Disposal of Dredged Material*

U.S. Army Corps of Engineers, 2000, *Design and Construction of Levees.*

First experiences with flat dilatometer test in Slovenia

Janko LOGAR, Alenka ROBAS, Bojan MAJES
University of Ljubljana, Faculty of Civil and Geodetic Engineering, Jamova 2, 1000 Ljubljana, Slovenia, janko.logar@fgg.uni-lj.si

Keywords: DMT, flat dilatometer test, comparison of soil properties, marine clay

ABSTRACT: In Slovenia first DMT tests were performed in the beginning of 2003. Slovenia is a small country, covering only 20 500 km^2, but with very complex geology. The assessment of ground properties is therefore a demanding task and methods that provide profiles of material properties rather than individual material data are very important. A CPT test with pore pressure measurements has been extensively used in the past. Ménard pressuremeter tests have also been used to complement CPT. Marchetti flat dilatometer tests have proven to be a fast and reliable tool when material properties are required for the assessment of stability and settlements for different geotechnical structures. The paper presents some first comparisons of DMT results with other soil investigation techniques, including laboratory and in situ tests, such as vane test, CPT and Ménard pressuremeter. Measured and predicted settlements are compared at three locations. During the first three years of the use of DMT test in Slovenia, it has become highly popular and is regularly used to test soft soil deposits.

1 INTRODUCTION

In geologically heterogeneous Slovenia, in-situ ground testing gained popularity during intensive motorway construction that began in 1994. Traditionally only SPT and vane tests had been used. The CPT(U) was first introduced in the mid 1980s and was not readily accepted by the local geotechnical community. Ménard pressuremeter followed in 1996 and Marchetti flat dilatometer in 2003. These two in-situ test methods were soon accepted due to their versatility, rapid evaluation of test results, and high reliability of evaluated soil parameters. Papers by Logar et al (2001), Kuder and Robas (2003), Robas et al (2005), Gaberc et al (2004) presented some comparative analysis of geotechnical predictions with DMT and PMT, which contributed to the wide acceptance of both tests in Slovenian geotechnical practice.

There are two DMTs operating in Slovenia. Only the results obtained and analyzed by the Geotechnical department of the University of Ljubljana are presented in the paper. The University performed 1511 m of dilatometer soundings between 2003 and 2005. At most locations DMT tests were complemented with other in-situ and/or laboratory tests. The results of selected flat dilatometer tests performed at different locations in Slovenia with different soil types are presented with other available test results at the same locations. Figure 1 shows the map of Slovenia with locations where most of DMT tests were performed. The numbers indicate the quantity of DMT tests in meters performed at those locations.

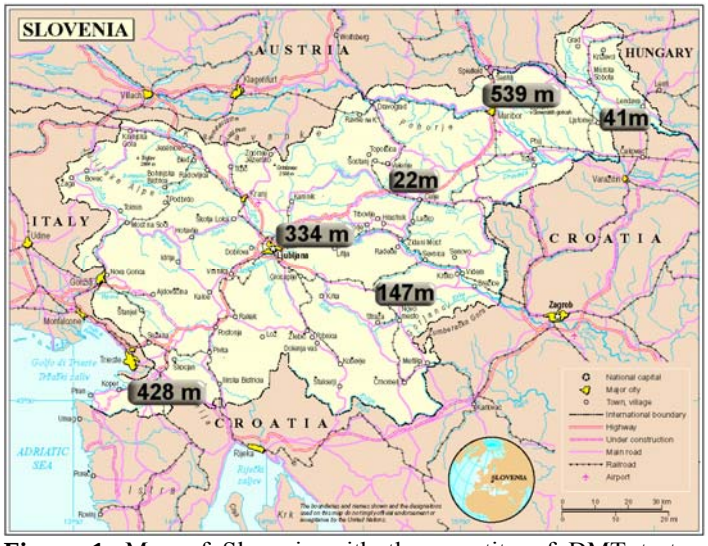

Figure 1. Map of Slovenia with the quantity of DMT tests performed from 2003 to 2005

2 SOIL CLASSIFICATION

Generally a fairly good insight into soil classification is provided from material index, I_d. Three selected profiles are plotted in Fig. 2 together with borehole logs. The main discrepancy in the classification is regularly observed in dry clayey or silty crust layers where the material index is normally greater than 1.8 indicating sandy soils (e.g. Fig 2c). The important benefit of material index obtained from DMT results is in identifying thin layers of different soil types within the tested formations (e.g. Fig. 2a).

BACK

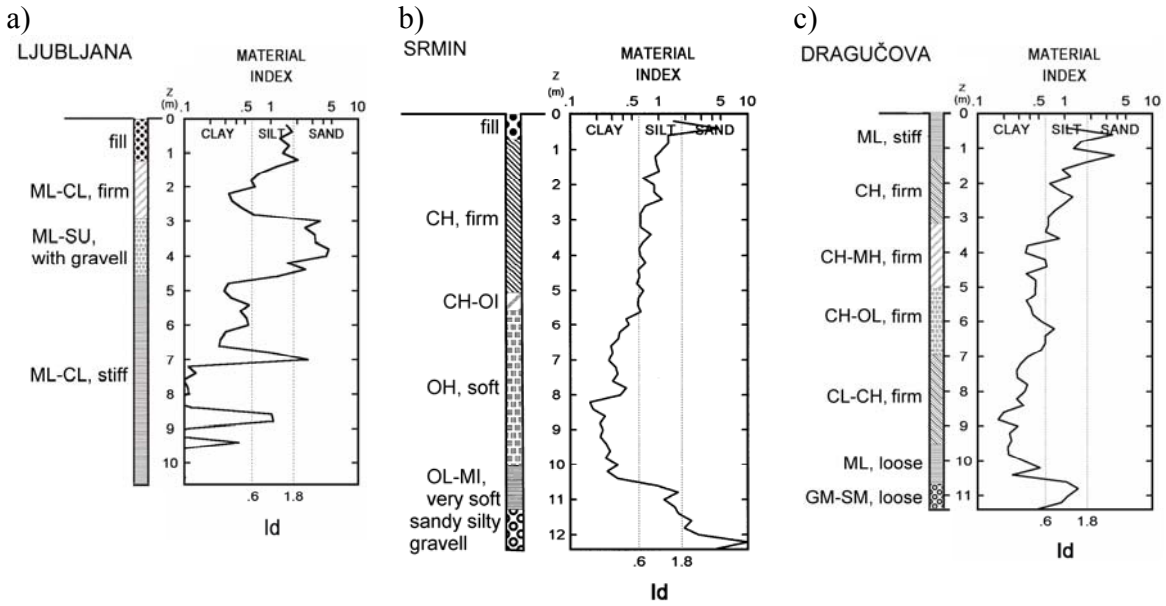

Figure 2. Comparison of selected borehole logs with DMT profiles for three different locations

3 OEDOMETER MODULI

The first analyses compared oedometer (constrained) moduli and undrained shear strength. Oedometer moduli (E_{oed}) were traditionally measured only in laboratories. CPT results were rarely used for settlement predictions or were used with caution and possibly together with laboratory results. The following examples show that constrained moduli obtained from flat dilatometer tests are comparable to the laboratory results. Comparisons with CPT results show that moduli derived from cone resistance can be either too large or too small. Moreover, we observed that thin layers of sand found in soft soil deposits do not provide significantly increased cone resistance and hence give similar moduli as soft cohesive soils. Due to different directions of penetration and membrane expansion, DMT provides reliable moduli estimates for such soil deposits (Figures 5 and 6).

Figures 3 to 9 show comparisons of oedometer moduli obtained by DMT, CPT and/or by laboratory oedometer tests in. Figure 8 shows the results for a site with up to 6 m thick layer of unsaturated clay on the top of soil profile. All other profiles are obtained within saturated soil layers, except for thin dry crust. DMT gives unusually high moduli for the unsaturated layer from Fig. 8, predominantly over 30 MPa. This value is significantly greater than laboratory values. Also the settlement measurements at the same location (see paragraph 5) indicate that moduli obtained within unsaturated soil layer are probably too high. Such cases are regularly observed for relatively thin (and therefore less significant) dry crust layers on the top of many soil profiles (see Figures 3, 5, 6, 7).

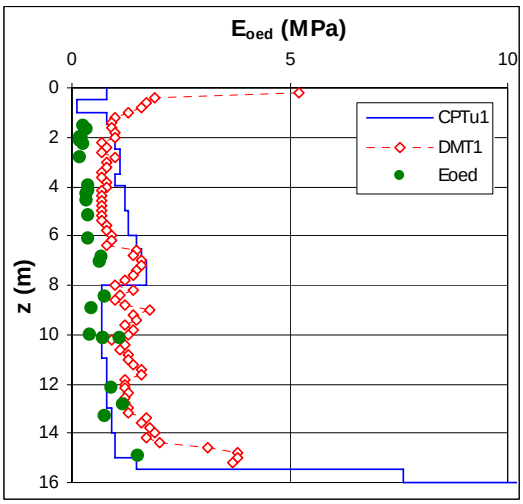

Figure 3. E_{oed} at crossover Peruzzijeva, Ljubljana

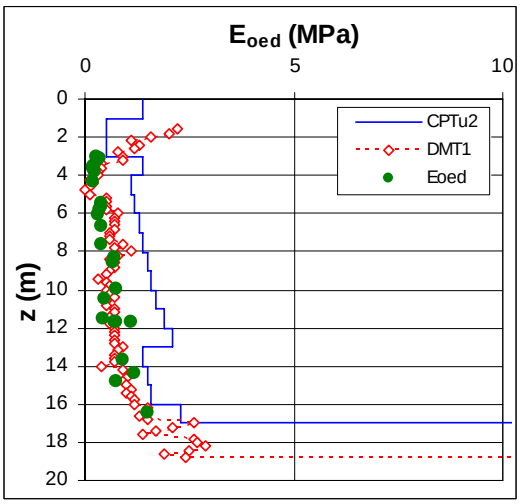

Figure 4. E_{oed} at Lidl, Ljubljana

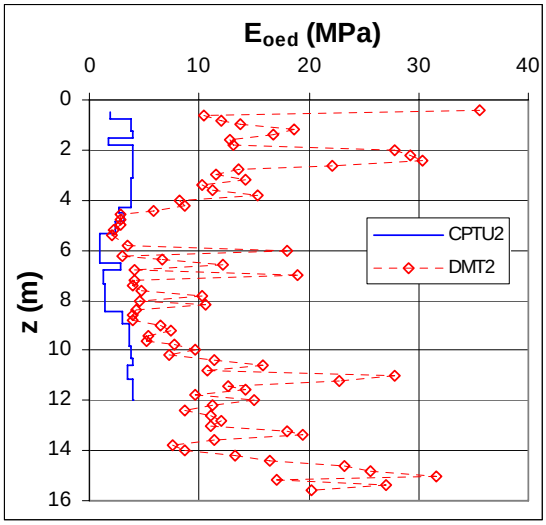

Figure 5. E_{oed} at Dolenjska

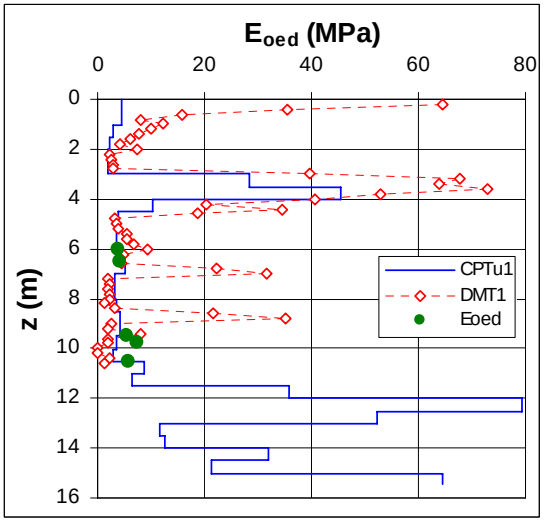

Figure 6. E_{oed} at veterinary faculty, Ljubljana

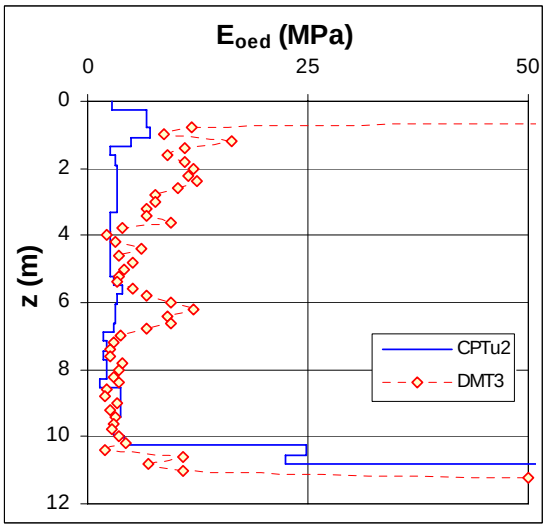

Figure 7. E_{oed} at Dragučova

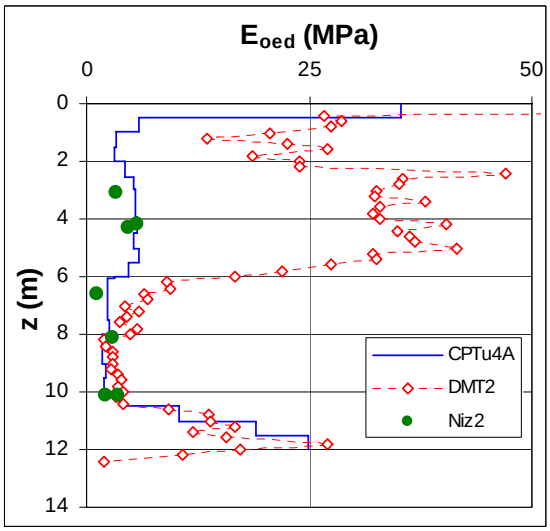

Figure 8. E_{oed} at Srmin

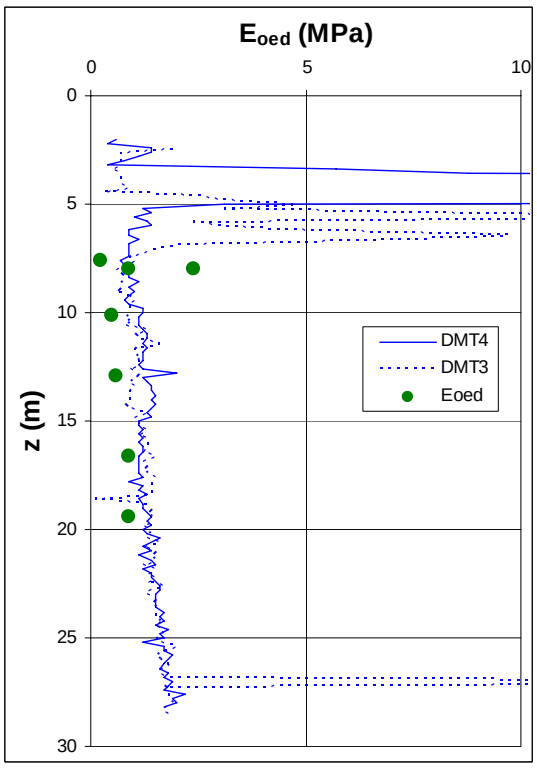

Figure 9. E_{oed} at Port of Koper

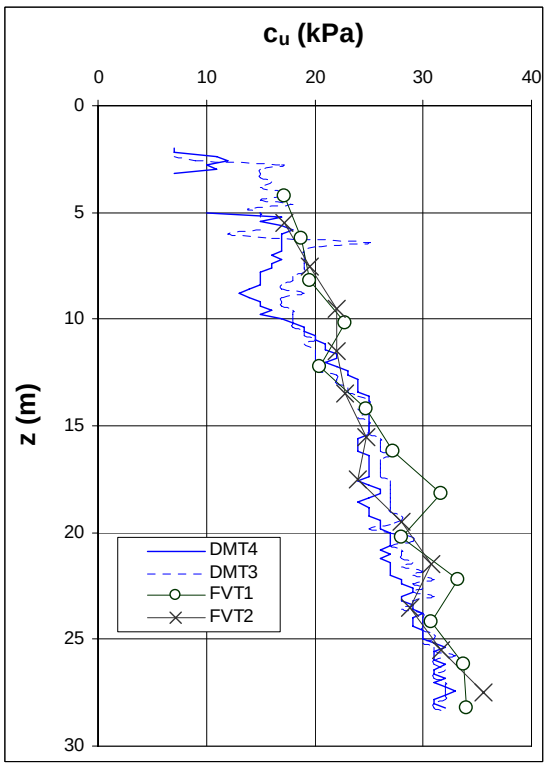

Figure 10. c_u at Port of Koper

4 UNDRAINED SHEAR STRENGTH

Undrained shear strength was measured or derived from field vane test, CPT test and Ménard pressuremeter test and compared to values obtained by the interpretation of DMT results.

Figures 10 to 16 show comparisons of undrained shear strength profiles for the same locations where oedometer moduli were previously studied.

Generally, fair to good agreement can be seen. The differences are partly due to variations in natural ground and partly due to different test methods and tools.

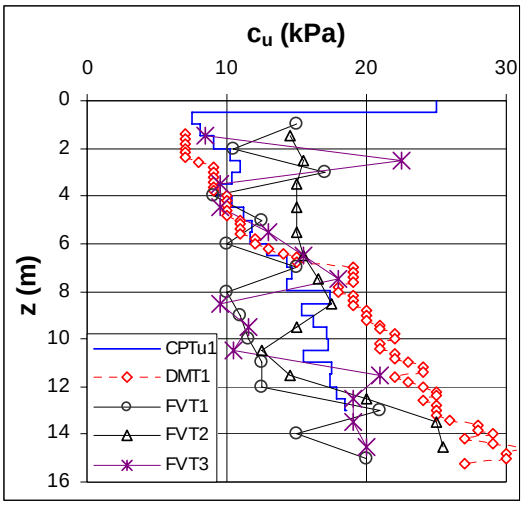

Figure 11. c_u at crossover Peruzzijeva, LJ.

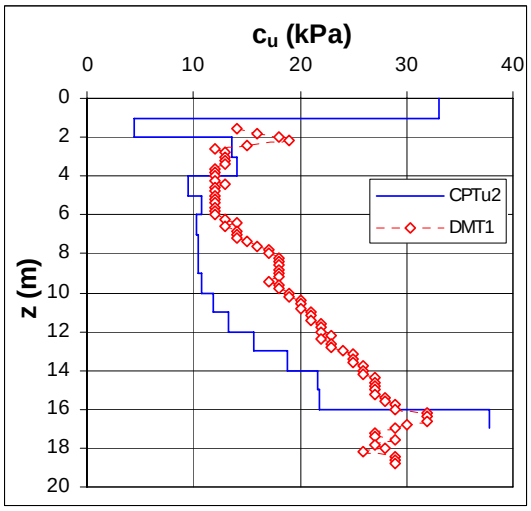

Figure 12. c_u at Lidl, Ljubljana

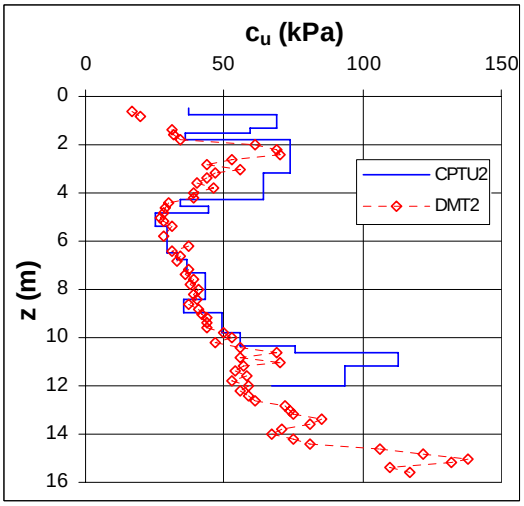

Figure 13. c_u at Dolenjska

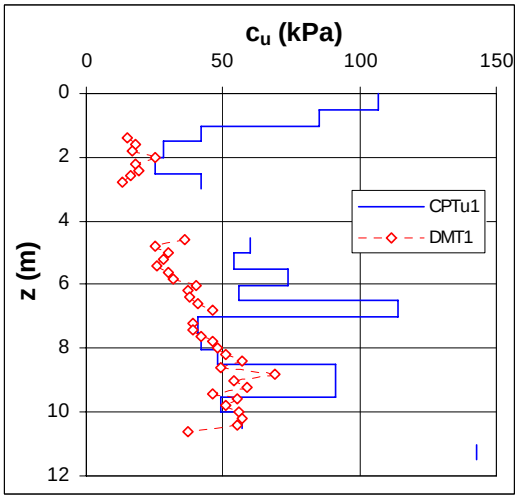

Figure 14. c_u at veterinary faculty, Ljubljana

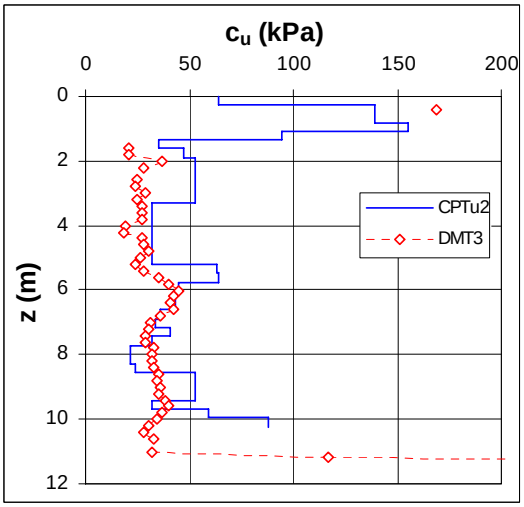

Figure 15. c_u at Dragučova

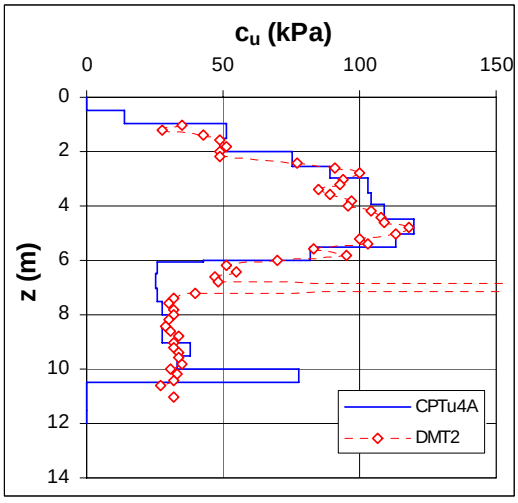

Figure 16. c_u at Srmin

Figure 17 presents the comparison of undrained shear strength for soft marine clay made after the extensive site investigation program at Pier II of Port of Koper. 4 DMT and 3 CPTU profiles were recorded. Only average values are presented in Fig. 17 together with the results of field vane test and pressuremeter results.

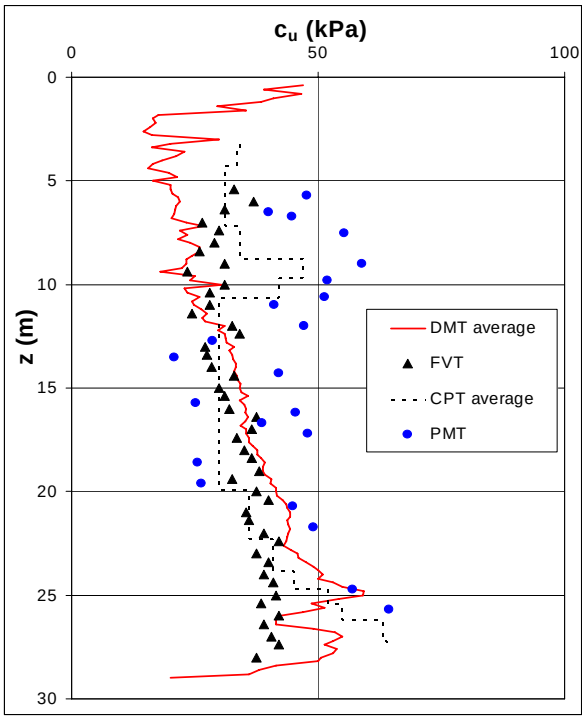

Figure 17. c_u at Pier II, Port of Koper

5 SETTLEMENTS

Three cases with settlement prediction based on DMT results and subsequent settlement measurements have been are documented so far. In all cases the settlements are caused by motorway embankments.

In the first case a 11.5 m high embankment was constructed on the soil profile presented above in Figures 8 and 16. Complete DMT results are given in Fig. 18. The main characteristics of this profile are the unsaturated top clayey layer, which is up to 6 m thick, and a soft layer below the first one having undrained shear strength c_u=20 kPa and even lower local values. Due to high load imposed by the embankment, the ground was improved by the installation of stone columns 60 cm in diameter at a spacing of 2.25 m. The estimated settlement reduction factor for such pattern of stone columns was β=0.8.

Table 1 shows the predicted and the measured values of settlements. Three DMT soundings were made and all three gave essentially the same settlement prediction, even though the profiles of the moduli were not equal.

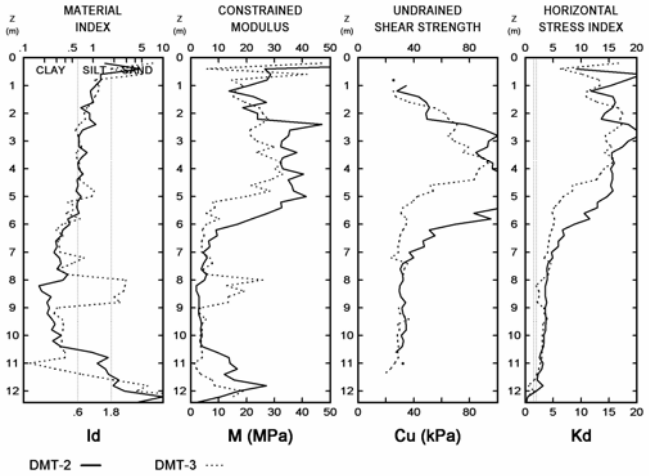

Figure 18. DMT results for the Srmin embankment

Table 1. Predicted and measured settlements for the Srmin motorway embankment (first case history)

	u_z
DMT prediction without stone columns	40 cm
DMT prediction with stone columns	32 cm
Measured total settlement	68 cm

The significant difference between the predicted and the measured values can be attributed to several reasons:

- DMT tests were performed at the toe of the embankment when the embankment was nearly completed and the ground was partly consolidated. One test was made farther away, but a thick layer of sand was encountered, again leading to lower settlements.
- Part of the settlement was deviatoric settlement.
- The moduli determined from DMT results for the upper unsaturated layer were too high.

In the second case a 7 m high motorway embankment near Smednik was constructed over 15 m thick deposit of soft soil resting on a stiffer sandy layer. The profile of oedometer modulus is given in Fig. 19. Table 2 gives the predicted and the measured settlement. In this case, the class A prediction of settlements under the embankment is in excellent agreement with later measurements.

Table 2. Comparison of the measured settlements with class A prediction based on DMT results (second case history)

Settlement at	Center	Edge
Class A DMT prediction	23.5 cm	13.6 cm
Last measured	20.6 cm	11.6 cm
Estimated end settlement by the Asaoka method	23.6 cm	13.5 cm

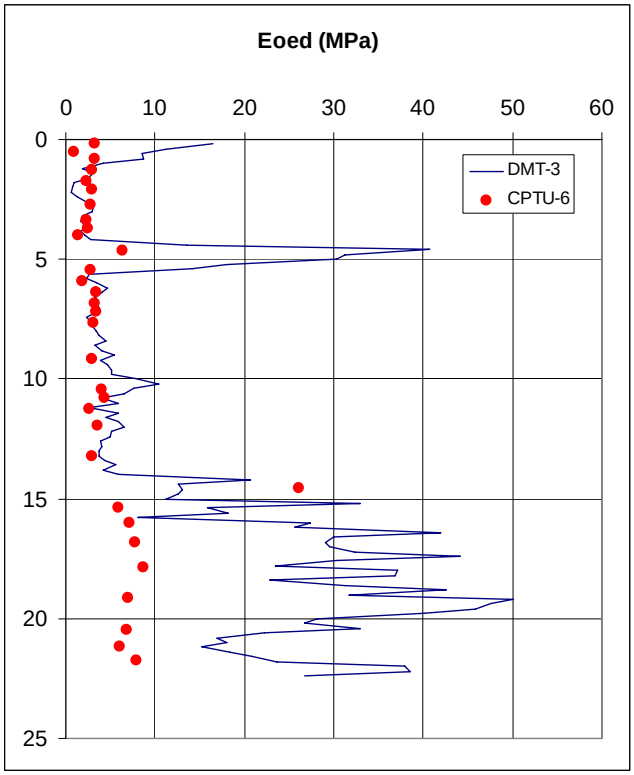

Figure 19. Profile of oedometer modulus (2nd case history)

The third case consists of two embankments constructed at two opposite ends of a motorway viaduct. The ground consists mainly of clayey and silty soils and was investigated by CPT and laboratory tests. The northern embankment was 6.6 m high and the southern 4.3 m high. Shortly before the construction began, the dilatometer had become available and two tests were made, one within the area of each embankment. The results are given in Figures 20 and 21.

The design prediction of settlement was based on previously available results. The settlements were measured by horizontal inclinometers and settlement plates. The comparison of the calculated and the measured settlement is given in Table 3. The measured settlements are given in a range, since slightly different values were obtained at individual measuring points.

Table 3. Comparison of the measured and the calculated settlements (third case history)

	Northern embankment	Southern embankment
Design prediction	39 cm	40 cm
DMT prediction	27 cm	17 cm
Last measured	41 cm	19 cm

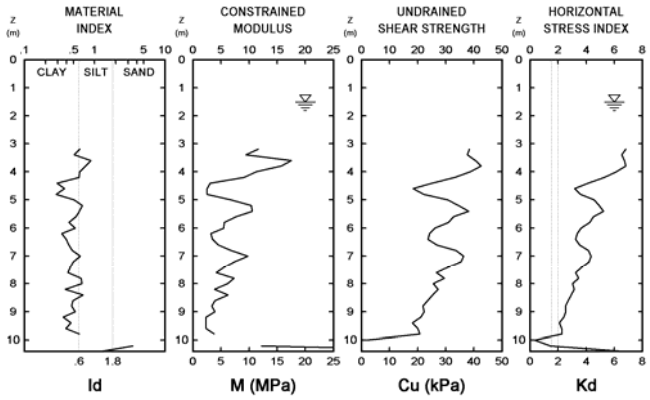

Figure 20. The DMT results for the northern embankment (third case history)

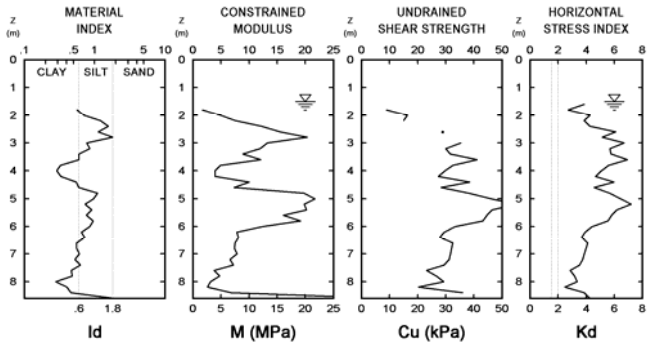

Figure 21. The DMT results for the southern embankment (third case history)

It is evident that the calculated settlements do not agree very well with the measurements. However, much more consistent agreement with the measured values is obtained by DMT prediction.

6 CONCLUSIONS

First experiences with flat dilatometer test in Slovenia were presented. This easy to use and versatile tool has proven to be competitive with other in-situ test procedures. Until now, it has mainly been used for the analysis of safety and settlements of ground under fills and embankments. Reliable results for undrained shear strength were obtained. The main advantage of DMT was found to be in stiffness data. The profile of constrained modulus is much more realistic compared with CPT moduli, and the resulting settlements are in fairly good agreement with the measured settlements.

The differences between the DMT predictions and the observed behavior were mainly found in cases where layers of unsaturated soil layers were present.

DMT has been well accepted in Slovenia. In three years University of Ljubljana has carried out over 1500 m of DMT soundings. Many projects where DMT was used are still in preparatory stage or under construction. Further research is in progress.

REFERENCES

Gaberc, A., Ajdič, I., Vogrinčič, G. (1995). Experimental study of compression moduli obtained by the CPT. Proc. 11th Eur. Conf. Soil mech. Fndn. Eng., Copenhagen, 28 May – 1 June. Danish geotechnical Society, Bulletin 11, Vol, pp. 1.121 – 1.126

Gaberc, A., Logar, J., Robas, A., Majes, B. First experiences with dilatometer tests in Slovenia. Proceedings of 4th conference of the Slovenian geotechnical society, *Rogaška Slatina, June 2004*, 165-174

Geotechnical investigation and testing - Field testing - Part 11: Flat dilatometer test (ISO/DTS 22476-11:2004), Final draft, April 2004

Kuder, S., Robas, A., The comparison between behaviour of axially loaded piles during load tests and prediction of behaviour based on pressuremeter tests. The 2nd International Young Geotechnical Engineer's Conference, September 2003, Constantza – Mamaia, Romania, 10 Pages.

Logar, J., Robas, A., Kuder, S., Gaberc, A., The use of pressuremeter test results in geotechnical design. Proceedings DRC, Gornja Radgona, Slovenia, 2001, 55-64 (in Slovene).

Marchetti S., et al, 2002. The Flat Dilatometer Test (DMT) in soil investigations. A Report by the ISSMGE Committee TC 16. Proceedings of the 3rd Croatian conference on soil mechanics and geotechnical engineering, Hvar, 79-120.

Robas, A., Gaberc, A., Kuder, S., Report on the use of pressuremeter tests in Slovenia, Symposium International ISP5/Prressio 2005, Paris, 2005 (in print).

The assessment of variability of CPTU and DMT parameters in organic soils

Zbigniew Młynarek, Wojciech Tschuschke, Jędrzej Wierzbicki
August Cieszkowski Agricultural University of Poznań, Poland

ABSTRACT: Organic soils differ from mineral subsoil in terms of physical and strength properties. A characteristic feature of these soils is their non-homogenous macrostructure, anisotropy and considerable deformations. These factors may also have a significant effect on the variation of parameters measured in CPTU and DMT, i.e. tests which are used to assess shear strength and constrained moduli of these soils. The article presents an analysis of variability of CPTU and DMT testing data, concerning layers of peat, gyttja, and marginal lake silty clay. The analysis contains statistical assessment of differences in the variability of tests parameters and the effect of this variability on forecasting undrained shear strength and constrained moduli.

1 INTRODUCTION

The application of empirical relationships to determine shear strength parameters and constrained modulus of soils is presently the most frequently applied method in case of CPTU and DMT (Lunne et al. 1997, Marchetti 1980). Relationships of this type may be used with special efficiency when they are supported by the interpretation, which includes the strength model of the subsoil (Jamiołkowski 2001) and takes into consideration a verification of the solution, which is obtained in tests conducted in calibration chambers (non-cohesive soils). Achievements in this respect in case of CPTU and DMT are considerable, but pertain primarily to mineral subsoil. A key issue in developing a correlation is the introduction of representative measurement data. It is true of both discussed tests. A commonly applied technique to obtain representative parameters is to use filtration methods (Harder and Bloh 1988, Tschuschke and Młynarek 1992, Hagazy and Mayne 2002). The application of these methods in mineral subsoil is well-known. In case of organic subsoil there is limited information on the variability of parameters measured in CPTU and DMT and its effect on forecasted shear strength parameters and constrained moduli. This article discusses this problem.

2 METHODS AND THE OBJECT OF THE STUDY

Cone penetration tests (CPTU), dilatometer and field vane tests were performed in the valley of the Bogdanka River in the city of Poznań. In this area the foundation for a sanitary sewer with the diameter of 1400 mm was planned. Designing the foundation of a collecting pipe requires detailed knowledge about soil bearing capacity and about the magnitude and heterogeneity of the settlements. The soil profile is composed of a surfical layer of embankments, followed by a layer of peats and marginal lake deposits represented by silts, mud and gyttjas, as well as silty clays. These deposits lay on fluvial sands (Fig. 1).

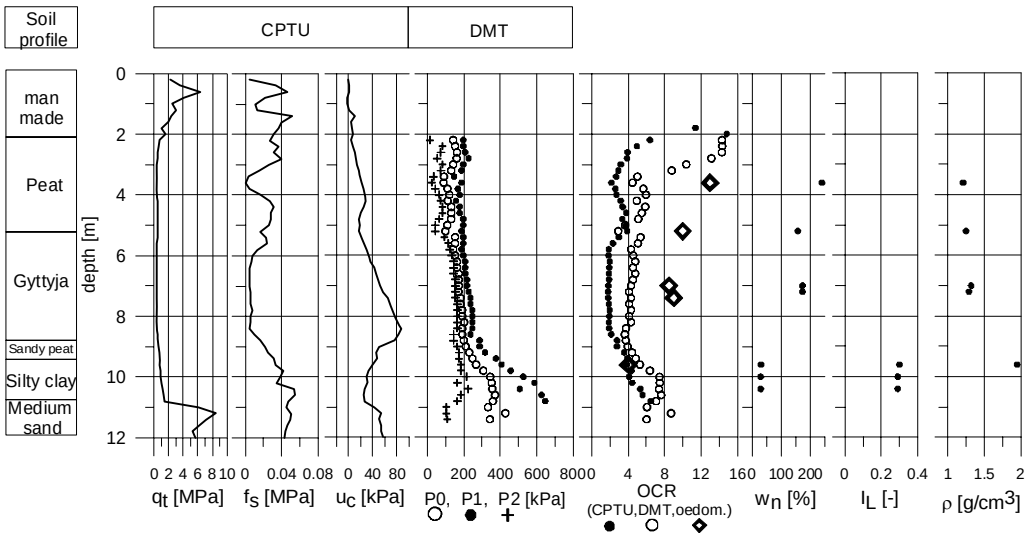

Figure 1. The soil profile at the testing point, based on CPTU, DMT and sampling (after Młynarek et al. 2006).

Piezocone penetration tests were performed using a HYSON 200 kN penetrometer by A. P. van den Berg (Holland). Testing was conducted according to the International Test Procedure for Cone Penetration Test (1999). Dilatometer tests were conducted using an original Marchetti dilatometer. Measurements were recorded according to the International Test Procedure for DMT Test (Monaco et al. 1999). For the field vane a gauging point was applied with the height of 80 mm and width of 40 mm The velocity of the gauging point rotation was 25 rpm. Soil cores for laboratory testing were collected using a Mostap sampler. The procedure of the oedometer test was of the "end of primary" (EOP) type. For each load increment an arbitrary stabilization of sample deformation was assumed at 0.01 mm within 48 hours. On the basis of oedometer tests constrained modulus were determined for the load range from 0.0 to 150 kPa and from 0.0 to σ'_{vo}, and tangential moduli: tan σ'_{vo} and tan σ' = 100kPa.

3 ASSESSMENT OF VARIABILITY OF CPTU AND DMT PARAMETERS

The F-Snedecor test (Gouri and Johnson 1977) was used to analyze the significance of differences between variability observed in individual testing samples. Data originating from one geotechnical layer were assumed to constitute one testing sample. The analysis covered three groups of samples: a layer of peats, gyttjas and silty clays.

Testing parameters for which differences were studied included: q_n (CPTU) and E_D (DMT), as parameters standardized by subtracting the value of the vertical geostatic stress, and Q_t (CPTU) and K_D (DMT) – as parameters normalized by the division of direct testing results by the vertical geostatic stress. The obtained values of testing probability "p" (defining the probability of no error being committed at the assumption of a zero hypothesis on a lack of differences) are listed in Table 1, along with mean values, standard deviations (σ) and coefficients of variation (CV) for individual parameters.

As shown on the results of Table 1 that in each analyzed case there are statistically significant differences in the variability of recorded parameters. The size of the variability may be inferred on the basis of the determined coefficient of variation. While comparing parameters q_n and E_D, it needs to be stated that in each tested soil lower variability is observed for parameters from CPTU. However, in the case of parameters Q_t and K_D, in gyttjas and firm sandy clays parameters from DMT are more homogenous.

Soil layer	Compared parameters	p	Mean [MPa]	σ [MPa]	CV
Peat	qn	0.000	0.404	0.103	0.255
	ED		2.032	0.570	0.281
	Qt	0.000	10.474	3.038	0.290
	KD		2.357	1.060	0.450
Gyttja	qn	0.000	0.284	0.048	0.169
	ED		1.772	0.398	0.225
	Qt	0.000	5.952	0.714	0.120
	KD		1.478	0.101	0.068
Silty clay	qn	0.000	0.887	0.238	0.268
	ED		6.622	2.074	0.313
	Qt	0.000	14.439	2.835	0.196
	KD		2.170	0.302	0.139

Table 1 Results of statistical analysis of the significance of differences between parameters from DMT and CPTU

Soil layer	Compared parameters	n	Mean [MPa]	- 95%	+95%	Size of confidence interval as % of mean
Peat	qn	18	0.404	0.356	0.451	23.7
	ED	18	2.032	1.769	2.296	25.9
	Qt	18	10.474	9.070	11.877	26.8
	KD	18	2.357	1.868	2.847	41.6
Gyttja	qn	16	0.284	0.262	0.306	15.5
	ED	16	1.772	1.588	1.956	20.8
	Qt	16	5.952	5.623	6.282	11.1
	KD	16	1.478	1.432	1.525	6.3
Silty clay	qn	8	0.887	0.777	0.997	24.8
	ED	8	6.622	5.664	7.580	28.9
	Qt	8	14.439	13.129	15.748	18.1
	KD	8	2.170	2.030	2.309	12.9

Table 2 95% confidence intervals for parameters q_n, KD, Q_t and ED and their size in relation to the mean value of the parameter

Significant information is also supplied by Table 2. Results presented in this table confirm a considerably lower range of variation in parameters from both tests in the layer of gyttjas and silty clay than it was the case in the layer of peat. The peat layer, apart from its complex macrostructure and anisotropic properties, will thus require a higher number of replications for in situ tests in order to obtain representative data, which would make it possible to assess strength and deformation parameters for this layer. This conclusion is confirmed by the results of studies on the non-homogeneity of a peat deposit by Młynarek and Niedzielski (1983).

4 VARIABILITY AND THE ESTIMATIVE F UNDRAINED SHEAR STRENGTH

Undrained shear strength s_u on individual levels σ_{v0} of CPTU was determined from a formula, in which coefficient N_{kt} was applied (Lunne et al., 1997). Coefficient N_{kt} was corrected on the basis of a field vane test. In the case of DMT shear strength s_u was calculated from relationships given by Marchetti (1980), Larson and Eskilson (1989) and Rabarijoely (1999).

Compressibility modulus of individual soil layers was referred to the constrained and oedometric moduli, while the variation of the moduli with depth for CPTU was obtained by determining the modulus from the Kulhawy and Mayne relationship (1990), assuming coefficients α at 1.3 for peat, 1.6 for gyttja and 8.25 for silty clay, respectively. For DMT compressibility moduli were determined from relationships given by Marchetti (1980) and Rabarijoely (1999). Figure 2 presents changes in undrained shear strength, determined using the above mentioned methods, whereas Fig. 3 shows changes in compressibility moduli along with depth.

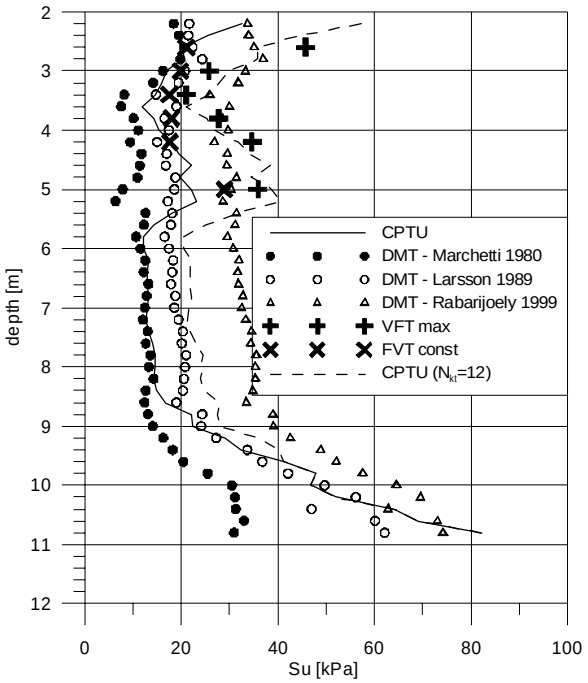

Figure 2. Values of undrained shear strength s_u determined on the basis of different tests.

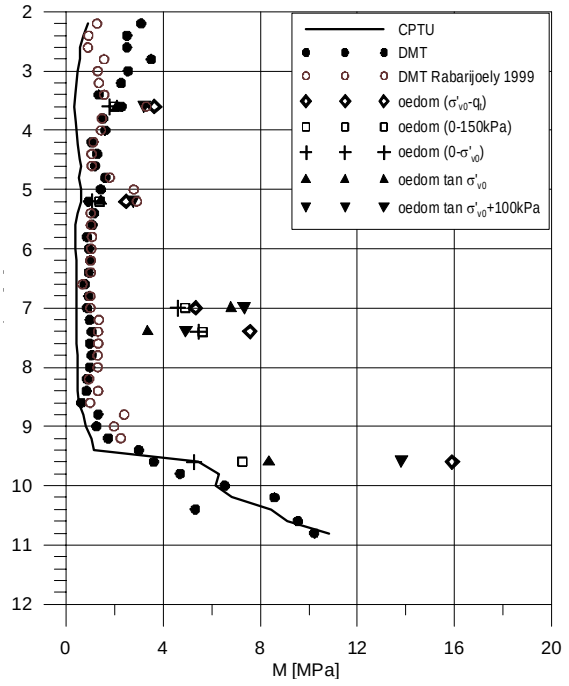

Figure 3. Changes in constrained modulus along with depth, determined using different methods.

The significance of differences between mean values of shear strength s_u was assessed statistically in two stages. In the first stage s_u(CPTU) and s_u(DMT)

were compared – the latter defined according to the Larsson formula (Larson and Eskilson, 1989). In the second stage differences were analyzed in the values of undrained shear strength defined from CPTU and DMT, as well as FVT. The analysis of results in case of CPTU was conducted both for the originally adopted value N_{kt}=21, and the one corrected on the basis of FVT, i.e. N_{kt}=12. Results of the analysis, supplemented with the analysis of significance of differences between means, are given in Table 3.

Results from Table 3 confirm a known relationship for mineral soils between s_u(CPTU) and $s_{u\ max}$(FVT). The introduced correction of coefficient N_{kt} resulted in the differences in mean strength values for these layers, determined on the basis of both tests, being statistically non-significant. Results based on DMT in turn show a similarity (both in terms of means and variability) to stabilized values of undrained shear strength from FVT.

It may also be observed from Table 3 that discrepancies in the assessment of undrained shear strength between DMT and the field vane test are much larger if they pertain to the maximum value of shear resistance in the field vane test than the determined value. A consequence of the determined dispersion of parameters from CPTU and DMT is the differing probability of the forecast concerning the mean value of undrained shear strength for individual subsoil layers.

Soil layer	Compared parameters	p		Mean [MPa]	σ [MPa]	CV
		For dispe-rsion of data	For means			
Peat	Su(CPTU, Nkt=21)	0.011	0.711	19.21	4.92	0.26
	Su(DMT)			18.73	2.56	0.14
	Su(CPTU, Nkt=21)	0.065	0.000	19.21	4.92	0.26
	Su max(FVT)			31.79	8.79	0.28
	Su(CPTU, Nkt=12)	0.851	0.658	33.63	8.61	0.26
	Su max(FVT)			31.79	8.79	0.28
	Su(DMT)	0.000	0.000	18.73	2.56	0.14
	Su max(FVT)			31.79	8.79	0.28
	Su(DMT)	0.093	0.230	18.73	2.56	0.14
	Su const(FVT)			20.51	4.34	0.21

Table 3 Results of statistical analysis of significance of differences between undrained shear strength s_u from DMT, CPTU and FVT.

Soil layer	Compared parameters	n	Mean [MPa]	- 95%	+95%	Size of confidence interval as % of mean
Peat	Su(CPTU, Nkt=12)	18	33.63	29.65	37.61	23.7
	Su (DMT-Lars.)	18	18.73	17.55	19.91	12.6
Gyttja	Su (CPTU)	16	23.07	22.03	24.11	9.0
	Su (DMT-Lars.)	16	19.47	18.62	20.32	8.7
Silty clay	Su (CPTU)	8	55.41	48.54	62.28	24.8
	Su (DMT-Lars.)	8	48.44	43.57	53.32	20.1

Table 4 95% confidence intervals of undrained shear strength and their size in relation to the mean value of parameter

Table 4 shows that in the peat layer, at the assumed normal distribution for the analyzed data, the 95% range of confidence intervals for the assessment of the mean value determined using the CPTU method is smaller than it is the case in the DMT approach. In contrast, in the gyttja and silty clay layers this assessment is similar.

Variation in compressibility moduli assessed using CPTU and DMT is presented in Table 5, while the forecast of probability for the assessment of mean values of moduli is shown in Table 6.

It may be generally observed from the assessment of variability for compressibility moduli obtained using CPTU and DMT according to the Marchetti formula (Marchetti 1980) that in organic soils the stated differences are statistically significant in contrast to the firm silty clay layer. In the layer of gyttja and silty clay the precision of assessment for the mean value of compressibility modulus using CPTU and DMT is

Soil layer	Compared parameters	p	Mean [MPa]	σ [MPa]	CV
Peat	M(CPTU)	0.000	0.525	0.134	0.255
	M(DMT-March.)		1.832	0.764	0.417
	M(CPTU)	0.000	0.525	0.134	0.255
	M(DMT-Rabar.)		1.551	0.718	0.463
Gyttja	M(CPTU)	0.013	0.454	0.076	0.167
	M(DMT-March.)		0.939	0.149	0.159
	M(CPTU)	0.000	0.454	0.076	0.167
	M(DMT-Rabar.)		1.193	0.373	0.313
Silty clay	M(CPTU)	0.890	6.794	2.897	0.426
	M(DMT-March.)		6.439	2.744	0.426

Table 5 Results of statistical analysis of significance of differences between constrained moduli from DMT and CPTU

Soil layer	compared parameters	n	mean [MPa]	- 95%	+95%	Size of confidence interval as % of mean
peat	M(CPTU)	18	0.525	0.463	0.587	23.7
	M(DMT-March.)	18	1.832	1.479	2.184	38.5
	M(DMT-Rabar.)	18	1.551	1.219	1.883	42.8
gyttja	M(CPTU)	16	0.454	0.419	0.489	15.5
	M(DMT-March.)	16	0.939	0.870	1.008	14.7
	M(DMT-Rabar.)	16	1.193	1.020	1.365	28.9
silty clay	M(CPTU)	8	6.794	5.456	8.132	39.4
	M(DMT-March.)	8	6.439	5.171	7.706	39.4

Table 6 95% confidence intervals of compressibility modulus and their size in relation to the mean value of parameter

similar (coefficients of variation are similar in value and confidence intervals have similar percentage range). In contrast, in the peat layer the accuracy of the assessment for the mean value of compressibility modulus using CPTU is much higher than in case of DMT. However, it needs to be stressed that values of means for compressibility moduli in layers of peats and gyttjas obtained with the use of CPTU and DMT differ statistically, while they are completely consistent in the layer of silty clay. The problem of the assessment of these differences and the consistency of in situ methods with oedometer testing was discussed in a study by Młynarek et al (2006).

5 CONCLUSIONS

On the basis of the conducted analysis several generalizations may be formulated as follows:

- The variability of CPTU and DMT testing data as well as estimated geotechnical soil parameters is significantly dependent from the type of organic soil. Higher variability was observed in peat than in gyttja layers for both CPTU and DMT testing.
- A consequence of this variability in parameters from CPTU and DMT is the different precision of assessment in case of undrained shear strength and tangential constrained modulus obtained using both tests in peat and gyttja.
- Due to the diverse variation in parameters of CPTU and DMT it is highly recommended to use both methods to assess strength and deformation parameters especially for organic soils. Such an approach makes it possible to obtain a continuous picture of changes in geotechnical parameters of the subsoil along with depth and it allows conducting a mutual correction for the assessment of numerical values of these parameters.
- Adaptation on correlations to estimate geotechnical soil parameters commonly used for mineral soils, onto organic subsoil is another aspect that has to be considered for organic soil. The conducted investigations showed that correlations have to be modified considering the differences between peats and gyttjas.

REFERENCES

De Groot D.J, Baecher G.B. (1993). Extimating autocovariance of in situ soil properties. ASCE, Journal of Geotechnical Engineering, Vol. 119, No. 1, pp. 147-167.

Gouri K. Bhattacharyya and Richard A. Johnson (1977). Statistical concepts and methods, John Wiley & Sons.

Harder H., von Bloh G. (1988). Determination of representative CPT-parameters. Proc. of Penetration Testing in U.K., Geotechnology Conference Birmingham, pp. 237-240.

Hegazy Y.A., Mayne P.W. (2002). Objective Site Characterization Using Clustering of Piezocone Data. Journal of Geotechnical and Geoenvironmental Engineering. Vol. 12; s. 986-996.

International Test Procedure for Cone Penetration Test (CPT) and Cone Penetration Test with pore pressure (CPTU) (1999). Report of TC-16, ISSMGE.

Jamiolkowski M. (2001). Evaluation of Relative Density and Shear Strength of Sands from CPT and DMT. Proc. of C.C. Ladd Symposium, October 2001, M.I.T., Cambridge, Mass.

Kulhawy F., Mayne P.W. (1990). Manual on estimating soil properties for foundation design. Electric Power Research Institute, EPRI, August 1990.

Larsson R., Eskilson S. (1989). DMT Investigations in Organic Soils. Swedish Geotechnical Institute, Publ. No. 248. Aug., 1989.

Lunne T., Robertson P.K., Powell J.J.M. (1997). Cone Penetration Testing in geotechnical practice. Reprint by E & FN Spon, London, 1997.

Marchetti S. (1980). In situ tests by flat dilatometer. ASCE, JGED, V. 106, No. GT3, pp. 299-321, 1980.

Młynarek Z., Niedzielski A., Tschuschke W. (1983). Variability of shear strength and physical parameters of peat. Proc. of 7th Danube European Conference on Soil Mechanics and Foundation Engineering, vol. 1.

Młynarek Z., Tschuschke W., Pordzik P. (1983). Variability of cone resistance in the process of static penetration of clay. Proceedings of 4th International Conference on Application of Statistics and Probability in Soil and Structural Engineering. Universita di Firenze

Młynarek Z., Tschuschke W., Wierzbicki J., Marchetti S. (2006). An interrelationship between shear and deformation parameters of gyttja and peat from CPT and

DMT tests. Proc. of 13th Danube-European Conference on Geotechnical Engineering, Ljubljana.

Monaco P., Marchetti S., Calabrese M., Totani G. (1999). The Flat Dilatometer Test. Draft of the Report to the ISSMGE Committee TC-16.

Mortensen J.K., Hansen G., Sorensen B. (1991). Correlation of CPT and field vane test for clay fills. Danish Geotechnical Society, Bulletin No. 7

Nadim F. (1988). Geotechnical site description using stochastic interpolation. 10th NGM-Conf, Oslo, pp. 158-162.

Rabarijoely S. (1999). Wykorzystanie badań dylatometrycznych do wyznaczania parametrów gruntów organicznych obciążonych nasypem. PhD Thesis, SGGW University of Warsaw.

Tschuschke W., Młynarek Zb., Werno M. (1992). Assessment of subsoil variability with the cone penetration test. Proc. of Conference on Probabilistic Methods in Geotechnical Engineering. Canbera, Australia. Balkema, Rotterdam, pp. 215-220.

AUTHOR INDEX

BACK